Advances in **Green and Sustainable Chemistry**

Green Approaches in Medicinal Chemistry for Sustainable Drug Design

Edited by
Bimal Krishna Banik

ELSEVIER

Green Approaches in Medicinal Chemistry for Sustainable Drug Design

Edited by

Bimal Krishna Banik
Department of Mathematics and Natural Sciences, College of Sciences and Human Studies, Deanship of Research, Prince Mohammad Bin Fahd University, Al Khobar, Kingdom of Saudi Arabia

Elsevier
Radarweg 29, PO Box 211, 1000 AE Amsterdam, Netherlands
The Boulevard, Langford Lane, Kidlington, Oxford OX5 1GB, United Kingdom
50 Hampshire Street, 5th Floor, Cambridge, MA 02139, United States

© 2020 Elsevier Inc. All rights reserved.

No part of this publication may be reproduced or transmitted in any form or by any means, electronic or mechanical, including photocopying, recording, or any information storage and retrieval system, without permission in writing from the publisher. Details on how to seek permission, further information about the Publisher's permissions policies and our arrangements with organizations such as the Copyright Clearance Center and the Copyright Licensing Agency, can be found at our website: www.elsevier.com/permissions.

This book and the individual contributions contained in it are protected under copyright by the Publisher (other than as may be noted herein).

Notices
Knowledge and best practice in this field are constantly changing. As new research and experience broaden our understanding, changes in research methods, professional practices, or medical treatment may become necessary.

Practitioners and researchers must always rely on their own experience and knowledge in evaluating and using any information, methods, compounds, or experiments described herein. In using such information or methods they should be mindful of their own safety and the safety of others, including parties for whom they have a professional responsibility.

To the fullest extent of the law, neither the Publisher nor the authors, contributors, or editors, assume any liability for any injury and/or damage to persons or property as a matter of products liability, negligence or otherwise, or from any use or operation of any methods, products, instructions, or ideas contained in the material herein.

Library of Congress Cataloging-in-Publication Data
A catalog record for this book is available from the Library of Congress

British Library Cataloguing-in-Publication Data
A catalogue record for this book is available from the British Library

ISBN: 978-0-12-817592-7

For information on all Elsevier publications
visit our website at https://www.elsevier.com/books-and-journals

Publisher: Susan Dennis
Acquisitions Editor: Anneka Hess
Editorial Project Manager: Laura Okidi
Production Project Manager: Prem Kumar Kaliamoorthi
Cover Designer: Alan Studholme

Typeset by SPi Global, India

Contributors

Bimal Krishna Banik Department of Mathematics and Natural Sciences, College of Sciences and Human Studies, Deanship of Research Development, Prince Mohammad Bin Fahd University, Al Khobar, Kingdom of Saudi Arabia

Ajoy Basak Pathology and Laboratory Medicine; Ottawa Hospital Research Institute, The Ottawa Hospital, Ottawa, ON, Canada

Sarmistha Basak Formerly of Kidney Research Center, Ottawa Hospital Research Institute, Ottawa, ON, Canada

Baburaj Baskar Department of Chemistry, Faculty of Engineering Technology, SRM Institute of Science and Technology, Kattankulathur, Kancheepuram (Dt), Tamilnadu, India

Basudeb Basu Department of Chemistry, North Bengal University, Darjeeling; Department of Chemistry, Raiganj University, Raiganj, India

Shibani Basu Department of Chemistry and Biochemistry, Boise State University, Boise, ID, United States

Preetismita Borah CSIR-Central Scientific Instruments Organization, Chandigarh, India

Arindam Chatterjee Saint Louis University, School of Medicine, Department of Pharmacology and Physiology, St. Louis, MO, United States

Aroni Chatterjee Virus Research Laboratory, National Institute of Cholera and Enteric Diseases, ID & BG Hospital Campus, Kolkata, India

Dhrubajyoti Chattopadhyay Amity Institute of Biotechnology, Amity University, New Town, Kolkata, West Bengal, India

Prasun Choudhury Department of Chemistry, North Bengal University, Darjeeling, India

Aparna Das Department of Mathematics and Natural Sciences, College of Sciences and Human Studies, Prince Mohammad Bin Fahd University, Al Khobar, Kingdom of Saudi Arabia

Muhammad Faisal Department of Chemistry, Quaid-i-Azam University, Islamabad, Pakistan

Jhuma Ganguly Department of Chemistry, Indian Institute of Engineering Science and Technology, Shibpur, Howrah, India

Arkajit Ghosh Indian Institute of Engineering Science and Technology, Shibpur, India

Manojit Ghosh Indian Institute of Engineering Science and Technology, Shibpur, India

K. Ilango Department of Pharmaceutical Chemistry, SRM College of Pharmacy, SRM Institute of Science and Technology, Kattankulathur, Kancheepuram (Dt), Tamilnadu, India

Adya Jain School of Studies in Chemistry, Jiwaji University, Gwalior, India

Dripta De Joarder Department of Chemistry, University of Calcutta, Kolkata, India

Sarita Khandelwal Department of Chemistry, University of Rajasthan, Jaipur, India

Anjan Kumar Roland Institute of Pharmaceutical Sciences, Berhampur, India

Hritwik Kumar Indian Institute of Engineering Science and Technology, Shibpur, India

Mahendra Kumar Department of Chemistry, University of Rajasthan, Jaipur, India

Arun Kumar Mahato Department of Pharmaceutical Sciences, Sardar Bhagwan Singh University, Dehradun, India

Dilip K. Maiti Department of Chemistry, University of Calcutta, Kolkata, India

Santu Maity Department of Chemistry, Indian Institute of Engineering Science and Technology, Shibpur, Howrah, India

Bibhash C. Mohantad Seemanta Institute of Pharmaceutical Sciences, Mayurbhanj, Odisha, India

Chhanda Mukhopadhyay Department of Chemistry, University of Calcutta, Kolkata, India

Sankaranarayanan Murugesan Medicinal Chemistry Research Laboratory, Department of Pharmacy, Birla Institute of Technology & Science, Pilani Campus, Pilani, India

Jnyanaranjan Panda Roland Institute of Pharmaceutical Sciences, Berhampur, India

Ch. Niranjan Patra Roland Institute of Pharmaceutical Sciences, Berhampur, India

Prasun Patra Amity Institute of Biotechnology, Amity University, New Town, Kolkata, West Bengal, India

B.V.V. Ravi Kumar Roland Institute of Pharmaceutical Sciences, Berhampur, India

Gildardo Rivera Laboratory of Pharmaceutical Biotechnology, Center for Genomic Biotechnology, National Polytechnic Institute, Reynosa, Mexico

Avinava Roy Indian Institute of Engineering Science and Technology, Shibpur, India

Esha Rushell Department of Chemistry, University of Rajasthan, Jaipur, India

Aamer Saeed Department of Chemistry, Quaid-i-Azam University, Islamabad, Pakistan

Gourab Saha Tampere University of Technology, Tampere, Finland

Biswa Mohan Sahoo Roland Institute of Pharmaceutical Sciences, Berhampur, India

Rajarshi Sarkar Narsee Monjee Institute of Management Studies, Indore, India

C. Nithya Shanthi Department of Pharmaceutical Sciences, Sardar Bhagwan Singh University, Dehradun, India

Ashok Kumar Srivastava Department of Chemistry, Faculty of Engineering & Technology, Veer Bahadur Singh Purvanchal University, Jaunpur, India

Yogesh Kumar Tailor Department of Chemistry, University of Rajasthan, Jaipur, India

Ram Naresh Yadav Department of Chemistry, Faculty of Engineering & Technology, Veer Bahadur Singh Purvanchal University, Jaunpur, India

Editor's biography

Bimal Krishna Banik conducted postdoctoral research at Case Western Reserve University (United States) and Stevens Institute of Technology (United States). He is an FRSC, CChem, and FICS. Dr. Banik was a tenured full professor in chemistry and First President's Endowed Professor in Science & Engineering at the University of Texas-Pan American and the Vice President of Research & Education Development of the Community Health Systems of South Texas. At present, Dr. Banik is a professor and senior researcher of the Deanship of Research Development & College of Natural Sciences at the Prince Mohammed Bin Fahd University in Kingdom of Saudi Arabia.

Professor Banik has taught organic and medicinal chemistry to BS, MS, and PhD students in US universities for many years. His teaching skills are exceptionally strong and these are proved by several thousand students' and peer's evaluations. He has mentored approximately 450 students, 20 postdoctoral fellows, and 7 PhD research scientists and has advised 20 university faculties. Professor Banik has acted as the advisor of 2 students' organizations and societies that have 1400 students.

Professor Banik has conducted synthetic chemistry and chemical biology research on ovary, colon, breast, blood, prostate, brain, pancreas and skin cancers (also on NCI 60 cancer cell lines); antibiotics; hormones; catalysis; green chemistry; natural products; and microwave-induced reactions. As the principal investigator (PI), he has been awarded $7.25 million in grants from NIH, United States and NCI, United States. Importantly, he has peer-reviewed 402 publications along with 491 presentation abstracts. The number of citations of his publications is close to 6550. His research has been exposed in media approximately 200 times. Professor Banik has served as the PI of a joint green chemistry symposium between United States and India. He

has presided 20 symposiums at the American Chemical Society (ACS) National Meetings and over 2-dozen conferences at the State, National, and International level, including 1 at the Nobel Prize celebration in Germany. In the capacity of chair, he has introduced more than 300 speakers. He is a reviewer of 93, editorial board member of 28, editor-in-chief of 14, founder of 4, associate editor of 4, and guest editor of 6 journals. As the editor-in-chief, he has recruited approximately 200 associate editors, regional editors, and editorial board members from different countries. He is an examiner of NSF, NCI, NRC, DOE, ACS, and international grant applications; reviewer of promotion and tenure of faculty of national and international universities; examiner of doctoral theses; panel member of NSF and NCI/NIH grant sections. Over the years, he has served as the chair/member of more than 100 scientific committees. Professor Banik has served as the chair of the University of Texas M.D. Anderson Cancer Center's drug discovery symposiums and directed the NCI funded analytical chemistry Core research laboratory.

Professor Banik has received the Indian Chemical Society's (ICS) Life-Time Achievement Award in 2018; Mahatma Gandhi Pravasi Honor gold medal from the UK Parliament; ICS's Professor P.K. Bose endowment medal; Dr. M.N. Ghosh gold medal; University of Texas Board of Regents' Outstanding Teaching award; 5 top-cited papers awards by Elsevier Journals; approximately 50 certificates of excellence in his profession; Indian Association Community Service award; ACS Member Service award; NCI webpage recognition; best researcher and mentor award by the UTPA; chosen as one of the World's Most Influential People on Earth in Year-2016 by US News Corporation; Burdwan University Eminent Alumnus recognition; First President's Endowed Professorship at the UTPA in its 87 year of history; UTPA's award for excellence in international studies. Some of his international research presentations are considered as keynote, plenary, inaugural and award-winning lectures. Dr. Banik has received more than 200 invitations to deliver lectures in United States, India, United Kingdom, Germany, China, Hong Kong, Greece, Italy, France, Jamaica, Sweden, Japan, Singapore, Pakistan, Norway, Bangladesh, Canada, Mexico, Vietnam, South Korea, Thailand, Saudi Arabia, United Arab Emirates, Argentina, Portugal, Switzerland, Venezuela, Brazil, Spain, New Zealand, Egypt, Austria, Australia and Turkey. He is also invited to write research and textbooks by major publishers, including Wiley, Elsevier, Springer, Springer Nature, Taylor & Francis, Thompson, Linus, Nova, Pearson, Cengage, Houghton Mifflin and PMU Press.

Preface

Green approaches in medicinal chemistry for sustainable drug design is based on the knowledge of a team of reputable scientists. This group integrates and encourages the growth of medicinal chemistry, organic chemistry, and drug discovery efforts. This book offers numerous green and sustainable approaches toward medicinal chemistry through the synthesis of molecules by environmentally benign methods (in water, in the absence of solvents, nonconventional reaction media, one-pot method, and ionic liquid), catalysis, microwave-induced reactions, natural edible materials, nanotechnology, engineering, biochemical and computer-assisted methods. A number of test results of medicinally active molecules with respect to specific diseases are provided in this context. The use of natural and nonharmful resources (spices, vegetables, clay, and sugar) is shown as one of the sustainable methods for obtaining useful structures.

This book reveals how green approaches are used in medicinal chemistry for human's life improvement. Various important points are made: adoption of sustainable and green chemistry pathways in the preparation of useful molecules, risks of using hazardous materials, and identifies cost-effective simple processes. I believe this book will be useful for diverse chemists, biologists, pharmacologists, pharmacists, biotechnologists, clinicians, and engineers working in both academia and industry; undergraduate and graduate students, and postdoctoral fellows; scientists/faculty members working in government, industry, and academics.

This book has 27 chapters written by the scientists of diverse background and experience. These chapters are divided in accordance with the principal aims described. Illango et al. explored green synthesis of natural and synthetic compounds as anticancer agents. Ghosh et al. studied antibacterial and antimicrobial coatings on metal substrates by cold spray method. Choudhury and Basu synthesized medicinally important heterocycles using graphene oxide as a sustainable catalyst. Mukhopadhyay et al. investigated green methods for the synthesis of potentials drugs against tropical diseases. Jain and Banik studied clay-mediated synthesis of biologically active compounds. Faisal and Saeed explored the role of ionic liquid in medicinal chemistry. De Joarder and Maiti described synthesis of heterocycles inside nanoreactors. Jain and Banik investigated the medicinal aspects of nanoparticles and nanocomposites.

Kumar et al. developed sustainable organic transformations in the construction of heterocycles. Yadav and Banik investigated the one-pot synthesis of medicinally active molecules. Banik et al. studied organocatalytic cycloaddition reactions toward the synthesis of complex compounds. Borah and Banik explored the synthesis of diverse steroids as biologically active molecules. Sahoo et al. investigated numerous reactions in water. Sahoo and Banik explored important reactions in the absence of any solvents toward the synthesis of medicinally important compounds. Das and Banik investigated the application of thiosugars in organic synthesis.

Basak and Basak reported a green chemistry approach for the synthesis of crucial cholesterol-lowering drugs. Patra and Chattopadhyay described the release of nanodrugs through biosafe process. Ganguly et al. demonstrated an approach in cancer biology using sugar-derived hydrogels. Banik and Sahoo studied green synthesis and biological evaluation of anticancer drugs. Sahoo et al. explored green chemistry approaches in the development of antidepressant and antipsychotic agents.

Basu and Banik studied the properties and benefits of natural spices on health. Borah and Banik investigated a few medicinal plants with compounds that have anticancer activities.

Sahoo et al. described microwave-assisted synthesis of several antitubercular agents. Borah and Banik studied microwave-assisted synthesis of steroids. Sahoo et al. investigated microwave-mediated synthesis of antiinflammatory compounds.

Das and Banik demonstrated a correlation between dipole moment and medicinal properties of diverse molecules. Chatterjee explored computer-assisted method in the drug discovery process.

This book would not have been possible without the significant contributions of scientists working in different countries on diverse projects related to green approaches in medicinal chemistry for sustainable drug design. I sincerely thank all the authors for their valuable book chapters. Finally, I thank the management of Elsevier publisher and particularly to Ms. Anneka Hess and Ms. Laura Okidi for their active participation with me.

Thank you, ALL.

Bimal Krishna Banik
Department of Mathematics and Natural Sciences, College of Sciences and Human Studies, Deanship of Research Development, Prince Mohammad Bin Fahd University, Al Khobar, Kingdom of Saudi Arabia

Green chemistry assisted synthesis of natural and synthetic compounds as anticancer agents

1

K. Ilango[a,*], *Baburaj Baskar*[b], *Sankaranarayanan Murugesan*[c]
[a]Department of Pharmaceutical Chemistry, SRM College of Pharmacy, SRM Institute of Science and Technology, Kattankulathur, Kancheepuram (Dt), Tamilnadu, India, [b]Department of Chemistry, Faculty of Engineering Technology, SRM Institute of Science and Technology, Kattankulathur, Kancheepuram (Dt), Tamilnadu, India, [c]Medicinal Chemistry Research Laboratory, Department of Pharmacy, Birla Institute of Technology & Science, Pilani Campus, Pilani, India
[*]Corresponding author. e-mail address: ilangok67@gmail.com

1.1 Introduction

Green chemistry mediated synthesis of nanoparticles is a budding technology, which has received substantial attention among the researchers in the present decade due to their wide applications in various fields such as medicine, biotechnology, chemistry, physics, catalysis, electronics, and material science due to their attractive physicochemical properties and stability [1]. Among the metallic nanoparticles, silver nanoparticles (AgNPs) in particular are known for their versatile biological applications in the fields of medicine and biotechnology [2, 3]. Several studies have been reported on the synthesis of AgNPs using physical and chemical methods [4–7]. Moreover, the chemical-based synthesis of AgNPs has been reported to pollute the ecosystem [8]. Recently, biological methods for the synthesis of AgNPs have been developed because they are eco-friendly and cost effective. With advances in the green chemistry approach, biological synthesis of AgNPs has been focused on as a substitute to physical and chemical processes and offers budding opportunities for the synthesis of AgNPs. Several biological materials such as microorganisms, plant extracts and milk have been used for the synthesis of AgNPs [3, 9, 10]. Synthesis of AgNPs using plant extracts is potentially advantageous over microorganisms because of its easy scale-up operations [11].

Natural compounds/drugs obtained from the plant sources are highly safe and easily metabolized when compared to other synthetic medicinal compounds [12]. The secondary metabolites obtained from the plant materials lead towards the development of drugs [13]. Nearly one-fourth of the total medicinal compounds used by the developed countries are obtained from natural resources [14].

In recent years, microwave heating has been used in many organic reactions leading cleaner reaction products and the use of environmentally more benign conditions compared with classical heating. Because of easy operation, safety, shorter reaction

Green Approaches in Medicinal Chemistry for Sustainable Drug Design. https://doi.org/10.1016/B978-0-12-817592-7.00001-0
© 2020 Elsevier Inc. All rights reserved.

times, high yields and environmental benignity, microwave irradiation is an alternative to conventional synthesis [15, 16].

Cancer is a group of diseases characterized by uncontrolled growth/proliferation and spread of abnormal cells. It is a fatal disease that leads to the second most common cause of death worldwide and has posed a serious threat to human health due to ever-increasing nature [17]. There is about 25 million new cases/year has been reported as per World Cancer Report from World Health Organization [18]. Because of its low cure rate and high mortality, tumor has become one of the most terrible diseases around the world. Apoptosis or programmed cell death, is a major control mechanism by which cells die if DNA damage exceeds the capacity of repair mechanisms. As part of normal development, apoptosis plays an important role in controlling cell number and proliferation. Defects in apoptotic responses are considered as a major contributor in different human diseases including cancer. The resistance to apoptosis is a hallmark of cancer cells, the crucial approach to anticancer drug discovery is the activation/restoration of normal apoptotic pathway/cascades [19]. But, a large number of anticancer drugs have been found to induce the apoptotic process in cancerous cells [20]. However, undue toxicity, side effects and resistance of the available medicines reduce their efficacy and utility [21–23]. Despite recent advances made in anticancer drug development, the presence of resistance to existing chemotherapeutic agents is a major obstacle to the effective treatment of cancer [24]. Consequently, discovering novel, puissant molecular entities as potential anticancer drugs with improved efficacy and resistance to complement the present chemotherapeutic strategies is highly desired. Interestingly, natural products provide a healthy source for such compounds. Apart from that, nearly one-half of all cancers that are diagnosed results in the death of the patient. Therefore, identification of novel potent, safe, and selective anticancer drugs remains one of the most pressing health problems.

1.2 Natural products as anticancer agents

In 2017, Anu et al. [25] reported the green synthesis of selenium nanoparticles using Garlic Cloves (*Allium sativum*), its biophysical characterization and cytotoxicity evaluation on vero cells. They found that biologically green synthesized selenium nanoparticles showed eco-friendly biocompatible features and limited cytotoxicity when compared with conventional chemically synthesized selenium nanoparticles.

Recently, in 2018, Akter et al. [26] reported *Brassica rapa* var. *japonica* leaf extract mediated green synthesis of crystalline AgNPs and evaluation of their cytotoxicity and antibacterial activity using in vitro $PC1_2$ cell model, disk diffusion method, respectively. They found that commercial AgNPs reduced cell viability to 23% (control 97%) and increased lactate dehydrogenase activity at a concentration of 3 ppm, whereas, *Brassica* AgNPs did not show any effects on both of the cytotoxicity parameters up to 10 ppm in $PC1_2$ cells. Moreover, *Brassica* AgNPs exhibited higher antibacterial activity against Gram-negative *Escherichia coli* (11.1 ± 0.5 mm, ZOI) and *Enterobacter* sp. (15 ± 0.5 mm, ZOI) than some previously reported green-synthesized AgNPs.

In 2016, Sengottaiyan et al. [27] reported green synthesis of AgNPs using *Solanumindicum L.* and their antibacterial, splenocyte cytotoxic potentials. They found that the green synthesized AgNPs at the concentration of 1–4 mM, extensively inhibited the growth of the tested pathogens *Staphylococcus* sp., *Klebsiella* sp. and the percentage of viable rat splenocyte cells were also diminished while increasing the concentration of AgNPs.

In 2017, Alishah et al. [28] reported green synthesis of starch extracted from *Solanum tuberosum* mediated CuO nanoparticles and evaluated their antimicrobial (micro dilution method) and antibreast cancer activity (MTT assay method) against *Bacillus cereus*, *Shigellasonnei*, *Staphylococcus epidermidis*, *Enterococcus*, *Pseudomonas aeruginosa*, *Escherichia coli*, and Michigan Cancer Foundation-7 (MCF-7) cell lines, respectively.

In 2014, Arun et al. [29] reported green synthesis of AgNPs using the mushroom fungus *Schizophyllum commune* and screened their antibacterial (against *Escherichia coli*, *Bacillus subtilis*, *Klebsiell apneumoniae*, *Pseudomonas fluorescens*), antifungal (against *Trichophyton simii*, *Trichophyton mentagrophytes*, *Trichophyton rubrum*) and anticancer (against Human Epidermoid Larynx Carcinoma (HEP-2) cell lines) activity.

In 2013, Geetha et al. [30] reported green synthesis of gold nanoparticles using flowers of *Couroupita guianensis* and their antileukemic cancer activity against HL-60 cells.

In 2013, Sujin Jeba Kumar et al. [31] reported green synthesis of AgNPs by aqueous extract of *Plumbago indica* and its antitumor activity against Dalton's Lymphoma Ascites Model (DLA cells).

Recently, in 2018, Soleimani et al. [32] reported green synthesis of AgNPs and evaluation of their antibacterial (measurement of minimum inhibitory concentrations (MICs) activity against Gram-positive (*Staphylococcus aureus* and *B. subtilis*) and Gram-negative (*Pseudomonas. aeruginosa* and *Escherichia coli*) bacteria) and antibreast cancer activity against MCF-7 cells.

In 2017, Yugandhar et al. [33] reported bioinspired green synthesis of copper oxide nanoparticles using *Syzygium alternifolium* stem bark and evaluation of its synergistic antimicrobial (against *Escherichia coli* and *Trichoderma harzianum*) and anticancer activity against MDA-MB-231 human breast cancer cell lines.

In 2014, Sivaraj et al. [34] reported biosynthesis and characterization of aqueous extract of *Acalypha indica* leaf mediated copper oxide nanoparticles and evaluation of its antimicrobial activity against *Escherichia coli, Pseudomonas fluorescens*, *Candida albicans* and anticancer activity against MCF-7 (breast cancer) cell lines.

In 2017, Nagajyothi et al. [35] reported green synthesis using an aqueous black bean (*Phaseolus vulgaris*) extract and anticancer activity of copper oxide nanoparticles against human cervical carcinoma (HeLa cells). They also observed that CuO NPs induced intracellular reactive oxygen species (ROS) generation in a dose-dependent manner and significantly reduced cervical carcinoma colonies.

In 2013, Sankar et al. [36] reported aqueous extract of *Origanum vulgare* mediated biosynthesis of AgNPs for its antibacterial activity against *Aeromonas hydrophilla*,

Bacillus sps., *Escherichia coli* (*Enteropathogenic–EP*), *Klebsiella* sps., *Salmonella* sps., *Salmonella paratyphi*, *Shigella dysenteriae*, *Shigella sonnei*, and anticancer activity against human lung cancer (A549) cell lines (LD_{50} at 100 μg/mL). They also proposed that, the improved cytotoxic effects of *O. vulgare* may be due to the presence of bioactive compounds such as carvacrol, terpinen, thymol, sabinine, linolool, terpinolene, quercetin, apigenin as capping agents in green synthesis of AgNPs.

In 2014, Vasanth et al. [37] reported anticancer activity of *Moringa oleifera* stem bark extract mediated AgNPs on human cervical carcinoma (HeLa) cells by apoptosis induction through ROS generation and its subsequent action on inhibiting cell replication in HeLa cells.

In 2015, Nayak et al. [38] reported biologically synthesized AgNPs of plant extracts of *Cucurbita maxima* (petals), *M. oleifera* (leaves), *Acorus calamus* (rhizome), and their anticancer activity against epidermoid carcinoma (A431) cells. Among the three synthesized nanoparticles, the rhizome extract generated AgNPs were significantly superior to the petal and leaves extract generated AgNPs in relation to their antimicrobial activity against *B. subtilis, Escherichia coli, P. aeruginosa* and *Vibrio cholerae*.

In 2017, Gnanavel et al. [39] reported the biosynthesis and characterization of copper oxide nanoparticles from the leaves of *Ormocarpum cochinchinense* and its anticancer activity on human colon cancer (HCT-116) cell lines with IC_{50} value of 40 μg/mL.

In 2013, Suman et al. [40] reported biosynthesis, characterization, and cytotoxic effect of AgNPs using *Morinda citrifolia* root extract against human cervical carcinoma (HeLa) cells. They also proposed that the cytotoxicity of the AgNPs via the generation of ROS or increases in intracellular oxidative stress and trigger cell death process including apoptosis and necrosis.

In 2015, Ramar et al. [41] reported biosynthesis of AgNPs using ethanolic petals extract of *Rosa indica* and its antibacterial, anticancer, and antiinflammatory activities. They found that the prepared AgNPs showed an effective antibacterial activity against Gram-negative (*Escherichia coli*, *Klebsiella pneumoniae*) than Gram-positive (*Streptococcus mutans*, *Enterococcus faecalis*) bacteria. The AgNPs also showed potential anticancer activity against human colon adeno carcinoma cancer (HCT 15) cell lines as well as in vitro antiinflammatory activity.

In 2013, Inbathamizh et al. [42] reported in vitro evaluation of antioxidant and anticancer potential of the aqueous leaf extract of *Morinda pubescens* synthesized AgNPs against human epithelium liver cancer (HEP G2) cells.

In 2012, Harne et al. [43] reported novel route for rapid biosynthesis of copper nanoparticles using aqueous extract of *Calotropisprocera L.* latex and their cytotoxicity on tumor (human cervical carcinoma-HeLa, human lung cancer-A549 and Baby hamster kidney-BHK21) cell lines at 120 μM concentration.

In 2014, Kathiravan et al. [44] reported the synthesis of AgNPs from *Meliadubia* leaf extract and their in vitro anticancer activity against human breast cancer (MCF-7) cell lines (IC_{50} 31.20 μg/mL).

1.3 Synthetic compounds as anticancer agents

In 2016, Ding et al. [45] reported green synthesis using microwave irradiation technique and antitumor evaluation of 15 novel series of 3-[4-bi-(4-fluorophenyl)methyl-piperazinyl]-4-amino-5-thione-1,2,4-triazole Schiff bases against cell division cycle 25 homolog B (CDC25B) cells from *Schizosaccharomyces pombe*. Among these, around 14 compounds (**6a–n**) showed significant inhibitory activity (83%–99%) against CDC25B.

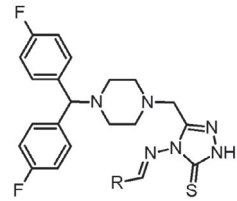

6(a–n)

Comp. code	R
6a	C_6H_5
6b	2-ClC_6H_4
6c	4-ClC_6H_4
6d	2-$NO_2C_6H_4$
6e	4-$NO_2C_6H_4$
6f	4-$CH_3OC_6H_4$
6g	3-$NO_2C_6H_4$
6h	4-BrC_6H_4
6i	2,4-$Cl_2C_6H_4$
6j	3-$CH_3OC_6H_4$
6k	4-$CF_3C_6H_4$
6l	2-Furyl
6m	2-Thiophenyl
6n	2-Pyridinyl

In 2017, Reddy et al. [46] reported heterogeneous catalysis such as chitosan mediated one-pot green synthesis using microwave irradiation under neat conditions and cytotoxicity evaluation of 15 novel α-aminophosphonates containing trifluoromethylaniline moiety against PC-3 (prostate cancer), MCF-7 (breast cancer), HeLa (Cervix Cancer), U973, K562, and HL60 (human Leukemia cell lines). Among these compounds, compound **4k** with pyrene moiety showed higher cytotoxic potency against breast cancer, U973, K562, HL60 cancer cell lines while compound **4g** with trifluoromethyl group exhibited promising cytotoxicity against U973, K562, and

HL60 cancer cell lines. They also proposed that the significant activity exhibited by the above-mentioned compounds may be due to strong inhibition of the topoisomerase-II enzyme of cancer cells.

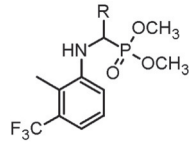

Comp. code	R
4g	2-SH,5-$NO_2C_6H_3$
4k	$C_{16}H_9$

Recently, in 2018, Dofe et al. [47] reported green synthesis under ultrasound irradiation and inhibitory effect of novel 16 quinoline-based thiazolidinones on the growth of MCF-7 human breast cancer cell lines by G2/M cell cycle arrest. Among the titled compounds, analogues **2c**, **2d**, and **2f** (IC_{50} values 5.38, 5.12, and 0.73 μM, respectively) showed significant anticancer activity against human breast cancer cell lines (MCF-7) and were considered as a potential lead. They also observed the induction of G2/M cell arrest within 24 h via flow cytometry analysis by the above-mentioned significantly active compounds.

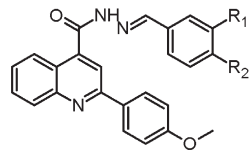

Comp. code	R_1	R_2
2c	H	Cl
2d	H	Br
2f	H	NO_2

In 2018, Mohan et al. [48] reported one-pot solvent-free green synthesis using β-cyclodextrin as a biomimetic catalyst and anticancer activity of novel 15 pyrazolyl phosphonates against breast cancer (MCF-7), prostate cancer (DU-145), and lung cancer (A-549) cell lines by sulfarodamine-B (SRB) assay. Among the synthesized compounds, compounds **4o** (IC_{50} 7.854, 6.753, 5.967), **4n** (IC_{50} 9.187, 7.672, 6.483), and **4m** (IC_{50} 9.867, 9.839, 8.113) exhibited excellent cell growth inhibitory effects on MCF-7, DU-145, and A-549 cell lines when compared to the doxorubicin (IC_{50} 9.652, 7.114, 8.340) standard used.

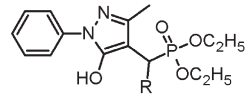

Comp. code	R
4o	Pyrene
4n	Anthracene
4m	Naphthalene

In 2010, Sharma et al. [49] reported microwave-assisted, solvent-free, parallel synthesis of 20 novel substituted imidazoles and evaluated their antibacterial, anthelmintic, short-term anticancer, and antitubercular activity. All the synthesized substituted imidazoles have shown good antibacterial activity against Gram-negative bacterial strains (*Klebsiella pneumoniae* and *Escherichia coli*) and moderate to good anthelmintic activity (against earthworms *Megascolex konkanensis*, *Pontoscolex corethruses*). The synthesized imidazole derivative (compounds **5b**, **7b**, **12b**, **15b**, **16b**) possessed significant cytotoxic activity (CC_{50} 31.25, 91.61, 50.32, 50.00, 94.63 μg/mL, respectively) against Ehrlich's ascites carcinoma (EAC) cell lines.

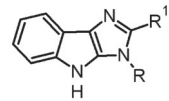

Comp. code	R	R^1
5b	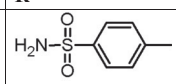	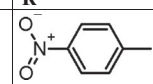
7b	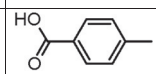	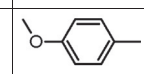
12b	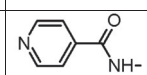	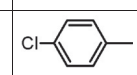
15b	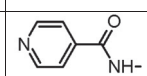	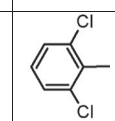
16b	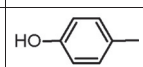	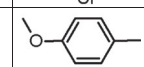

In 2010, Kidwai et al. [50] reported environment friendly synthesis and anticancer evaluation of 10 novel 2-oxo/thioxooctahydroquinazolin-5-one derivatives using ceric ammonium nitrate (CAN) as catalyst and polyethylene glycol (PEG) as solvent. Among the titled analogues, compounds **4c**, **4d**, and **4e** were found to exhibit excellent activity at a concentration as low as 0.06 μg/mL against U87 human glioma cells.

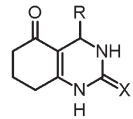

Comp. code	X	R
4c	S	C_2H_5
4d	O	C_3H_8
4e	S	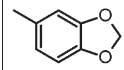

In 2012, Mungara et al. [51] reported green synthesis using (PEG-400) as a green reaction media and antiproliferative activity of 14 novel α-aminophosphonates against A549 (human lung cancer), MCF-7 (human breast cancer) and NCI-N87 (human stomach cancer) cells. Among these, compounds **4c**, **4e**, and **4m** exhibited good antiproliferative activity against the above-mentioned three cancer cells.

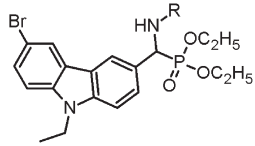

Comp. code	R
4c	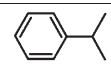
4e	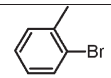
4m	

1.4 Conclusion

In conclusion, the authors have successfully compiled the recently published findings in the area of green chemistry assisted synthesis of natural and synthetic heterocyclic organic compounds that are effective against various cancer cell lines. This detailed review work will definitely give an meaningful insight for the readers who will be working in the area of green chemistry assisted cancer chemotherapeutics.

References

[1] P. Raveendran, J. Fu, S.L. Wallen, Completely "green" synthesis and stabilization of metal nanoparticles, J. Am. Chem. Soc. 125 (2003) 13940–13941.
[2] V. Venkatpurwar, V. Pokharkar, Green synthesis of silver nanoparticles using marine polysaccharide: study of in-vitro antibacterial activity, Mater. Lett. 65 (2011) 999–1002.
[3] S.A. Babu, G. Prabu, Synthesis of AgNPs using the extract of Calotropis procera flower at room temperature, Mater. Lett. 65 (2011) 1675–1677.
[4] S. Iravani, H. Korbekandi, S.V. Mirmohammadi, B. Zolfaghari, Synthesis of silver nanoparticles: Chemical, physical and biological methods, Res. Pharm. Sci. **9** (2014) 385–406.
[5] K. Gudikandula, S.C. Maringanti, Synthesis of silver nanoparticles by chemical and biologicalmethods and their antimicrobial properties, J. Exp. Nanomed. 9 (2016) 714–721.
[6] F. Mafune, J. Kohno, Y. Takeda, T. Kondow, H. Sawabe, Structure and stability of silver nanoparticles in aqueous solution produced by laser ablation, J. Phys. Chem. B 104 (2000) 8333–8337.
[7] H. Huang, Y. Yang, Preparation of silver nanoparticles in inorganic clay suspensions, Compos. Sci. Technol. 68 (2008) 2948–2953.
[8] T.Y. Suman, S.R. Radhika Rajasree, A. Kanchana, E. Beena, Biosynthesis, characterization and cytotoxic effect of plant mediated silver nanoparticles using *Morinda citrifolia* root extract, Colloid Surf. B 106 (2013) 74–78.
[9] K.J. Lee, S.H. Park, M. Govarthanan, P.H. Wang, Y.S. Seo, M. Cho, W.H. Lee, J.Y. Lee, S. Kamala-Kannan, B.T. Oh, Synthesis of silver nanoparticles using cow milk and their antifungal activity against phytopathogens, Mater. Lett. 105 (2013) 128–131.
[10] S.V. Otari, R.M. Patil, N.H. Nadaf, S.J. Ghosh, S.H. Pawar, Green biosynthesis of silver nanoparticles from an actinobacteria Rhodococcus sp, Mater. Lett. 72 (2012) 92–94.
[11] M.F. Zayed, W.H. Eisa, A.A. Shabaka, Malva parviflora extract assisted green synthesis of silver nanoparticles, Spectrochim. Acta A 98 (2012) 423–428.
[12] S.M. Roopan, G. Elango, Exploitation of Cocos nucifera a non-food toward the biological and nanobiotechnology field, Ind. Crop. Prod. 67 (2015) 130–136.
[13] G. Madhumitha, S.M. Roopan, Devastated crops: Multifunctional efficacy for the production of nanoparticles, J. Nanomater. 2013 (2013) 1–12.
[14] G. Elango, S.M. Kumaran, S.S. Kumar, S. Muthuraja, S.M. Roopan, Green synthesis of SnO_2 nanoparticles and its photocatalytic activity of phenolsulfonphthalein dye, Spectrochim. Acta A 145 (2015) 176–180.
[15] B.A. Roberts, C.R. Strauss, Toward rapid, "green", predictable microwave-assisted synthesis, Acc. Chem. Res. 38 (2005) 653–661.
[16] V. Polshettiwar, R.S. Varma, Greener and rapid access to bioactive heterocycles: One-pot solvent-free synthesis of 1,3,4-oxadiazoles and 1,3,4-thiadiazoles, Tetrahedron Lett. 49 (2008) 879–883.

[17] A. Jemal, T. Murray, E. Ward, A. Smuels, R.C. Tiwari, A. Ghafoor, E.J. Feuer, M.J. Thun, Cancer statistics, CA Cancer J. Clin. 55 (2005) 10–30.
[18] B. Stewart, C.P. Wild, World Cancer Report 2014, International Agency for Research on Cancer World Health Organization, Lyon, France, 2014. ISBN 978-92-832-0429-9. Available online, http://www.iarc.fr/en/publications/books/wcr/wcr-order.php.
[19] S.W. Lowe, A.W. Lin, Apoptosis in cancer, Carcinogenesis 21 (2000) 485–495.
[20] S.W. Fesik, Promoting apoptosis as a strategy for cancer drug discovery, Nat. Rev. Cancer 5 (2005) 876–885.
[21] G. Yang, S. Nowsheen, A. Khaled, A. Georgakilas, Toxicity and adverse effects of tamoxifen and other anti-estrogen drugs, Pharmacol. Ther. 139 (2013) 392–404.
[22] A. Monnier, Long-term efficacy and safety of letrozole for the adjuvant treatment of early breast cancer in postmenopausal women: a review, Ther. Clin. Risk Manag. 5 (2009) 725–738.
[23] K.A. Lyseng-Williamson, C. Fenton, Docetaxel: a review of its use in metastatic breast cancer, Drugs 65 (2011) 2513–2531.
[24] K. Kelly, L.P.J. Lovato, R.B. Livingston, J. Zangmeister, S.A. Taylor, D. Roychowdhury, J.J. Crowley, D.R. Gandara, Cisplatin, etoposide and paclitaxel with granulocyte colony-stimulating factor in untreated patients with extensive-stage small cell lung cancer: a phase II trial of the southwest oncology group, Clin. Cancer Res. 7 (2001) 2325–2329.
[25] K. Anu, G. Singaravelu, K. Murugan, G. Benelli, Green-synthesis of selenium nanoparticles using garlic cloves (*Allium sativum*): biophysical characterization and cytotoxicity on Vero cells, J. Clust. Sci. 28 (2017) 551–563.
[26] M. Akter, M.M. Rahman, A.K.M.A. Ullah, M.T. Sikder, T. Hosokawa, T. Saito, M. Kurasaki, *Brassica rapa var. japonica* leaf extract mediated green synthesis of crystalline silver nanoparticles and evaluation of their stability, cytotoxicity and antibacterial activity. J. Inorg. Organomet. Polym. Mater. (2018), https://doi.org/10.1007/s10904-018-0818-7.
[27] A. Sengottaiyan, R. Mythili, T. Selvankumar, A. Aravinthan, S. Kamala-Kannan, K. Manoharan, P. Thiyagarajan, M. Govarthanan, J.-H. Kim, Green synthesis of silver nanoparticles using Solanum indicum L. and their antibacterial, splenocyte cytotoxic potentials, Res. Chem. Intermed. 42 (2016) 3095–3103.
[28] H. Alishah, S. Pourseyedi, S.Y. Ebrahimipour, S.E. Mahani, N. Rafiei, Green synthesis of starch-mediated CuO nanoparticles: preparation, characterization, antimicrobial activities and in vitro MTT assay against MCF-7 cell line, Rend. Fis. Acc. Lincei 28 (2017) 65–71.
[29] G. Arun, M. Eyini, P. Gunasekaran, Green synthesis of silver nanoparticles using the mushroom fungus *Schizophyllum commune* and its biomedical applications, Biotechnol. Bioprocess Eng. 19 (2014) 1083–1090.
[30] R. Geetha, T. Ashokkumar, S. Tamilselvan, K. Govindaraju, M. Sadiq, G. Singaravelu, Green synthesis of gold nanoparticles and their anticancer activity, Cancer Nanotechnol. 4 (2013) 91–98.
[31] T. Sujin Jeba Kumar, C.K. Balavigneswaran, R. Moses Packiaraj, A. Veeraraj, S. Prakash, Y. Natheer Hassan, K.P. Srinivasakumar, Green synthesis of silver nanoparticles by *Plumbago indica* and its antitumor activity against Dalton's lymphoma ascites model, BioNanoScience 3 (2013) 394–402.
[32] F.F. Soleimani, T. Saleh, S.A. Shojaosadati, R. Poursalehi, Green synthesis of different shapes of silver nanostructures and evaluation of their antibacterial and cytotoxic activity, BioNanoScience 8 (2018) 72–80.
[33] P. Yugandhar, T. Vasavi, P. Uma Maheswari Devi, N. Savithramma, Bioinspired green synthesis of copper oxide nanoparticles from Syzygium alternifolium (Wt.) Walp:

Characterization and evaluation of its synergistic antimicrobial and anticancer activity, Appl. Nano. Sci. 7 (2017) 417–427.
[34] R. Sivaraj, P.K.S.M. Rahman, S.N. Rajiv, R. Venckatesh, Biosynthesis and characterization of *Acalypha indica* mediated copper oxide nanoparticles and evaluation of its antimicrobial and anticancer activity, Spectrochim. Acta A Mol. Biomol. Spectrosc. 129 (2014) 255–258.
[35] P.C. Nagajyothi, P. Muthuraman, T.V.M. Sreekanth, D.H. Kim, J. Shim, Green synthesis: in-vitro anticancer activity of copper oxide nanoparticles against human cervical carcinoma cells, Arab. J. Chem. 10 (2017) 215–225.
[36] R. Sankar, A. Karthik, A. Prabu, S. Karthik, K.S. Shivashangari, V. Ravikumar, *Origanum vulgare* mediated biosynthesis of silver nanoparticles for its antibacterial and anticancer activity, Colloids Surf. B: Biointerfaces 108 (2013) 80–84.
[37] K. Vasanth, K. Ilango, R. Mohan Kumar, A. Agrawal, G.P. Dubey, Anticancer activity of *Moringa oleifera* mediated silver nanoparticleson human cervical carcinoma cells by apoptosis induction, Colloids Surf. B: Biointerfaces 117 (2014) 354–359.
[38] D. Nayak, S. Pradhan, S. Ashe, P.R. Rauta, B. Nayak, Biologically synthesized silver nanoparticles from three diverse family of plant extracts and their anticancer activity against epidermoid A431 carcinoma, J. Colloid Interface Sci. 457 (2015) 329–338.
[39] V. Gnanavel, V. Palanichamy, S.M. Roopan, Biosynthesis and characterization of copper oxide nanoparticles and its anticancer activity on human colon cancer cell lines (HCT-116), J. Photochem. Photobiol. B Biol. 171 (2017) 133–138.
[40] T.Y. Suman, S.R. Radhika Rajasree, A. Kanchana, S.B. Elizabeth, Biosynthesis, characterization and cytotoxic effect of plant mediated silver nanoparticles using *Morinda citrifolia* root extract, Colloids Surf. B: Biointerfaces 106 (2013) 74–78.
[41] R. Manikandan, B. Manikandan, T. Raman, K. Arunagirinathan, N.M. Prabhu, M. Jothi Basu, M. Perumal, S. Palanisamy, A. Munusamy, Biosynthesis of silver nanoparticles using ethanolic petals extract of *Rosa indica* and characterization of its antibacterial, anticancer and anti-inflammatory activities, Spectrochim. Acta A Mol. Biomol. Spectrosc. 138 (2015) 120–129.
[42] L. Inbathamizh, T. Mekalai Ponnu, E. Jancy Mary, *In vitro* evaluation of antioxidant and anticancer potential of Morinda pubescens synthesized silver nanoparticles, J. Pharm. Res. 6 (2013) 32–38.
[43] S. Harne, A. Sharma, M. Dhaygude, S. Joglekar, K. Kodam, M. Hudlikar, Novel route for rapid biosynthesis of copper nanoparticles using aqueous extract of *Calotropis procera* L. latex and their cytotoxicity on tumor cells, Colloids Surf. B: Biointerfaces 95 (2012) 284–288.
[44] V. Kathiravan, S. Ravi, S. Ashokkumar, Synthesis of silver nanoparticles from *Melia dubia* leaf extract and their *in vitro* anticancer activity, Spectrochim. Acta A Mol. Biomol. Spectrosc. 130 (2014) 116–121.
[45] Y. Ding, Z. Zhang, G. Zhang, S. Mo, Q. Li, Z. Zhao, Green synthesis and evaluation of the antitumor activity of a novel series of 3-[4-bi-(4-fluorophenyl)methyl-piperazinyl]-4-amino-5-thione-1,2,4-triazole Schiff bases, Res. Chem. Intermed. 42 (2016) 3105–3116.
[46] K.M.K. Reddy, S.M. Sadik, N. Saichaithanya, K. Peddanna, N.B. Reddy, G. Sravya, Z. Grigory, C.S. Reddy, One-pot green synthesis and cytotoxicity of new α-aminophosphonates, Res. Chem. Intermed. 43 (2017) 7087–7103.
[47] V.S. Dofe, A.P. Sarkate, R. Azad, C.H. Gill, Green synthesis and inhibitory effect of novel quinoline based thiazolidinones on the growth of MCF-7 human breast cancer cell line by G2/M cell cycle arrest, Res. Chem. Intermed. 44 (2018) 1149–1160.

[48] G. Mohan, S. Santhisudha, S. Murali, N.B. Reddy, G. Sravya, G.V. Zyryanov, C.S. Reddy, One-pot green synthesis and bio-assay of pyrazolylphosphonates. Res. Chem. Intermed. (2018), https://doi.org/10.1007/s11164-018-3319-y.

[49] G.K. Sharma, D. Pathak, Microwave-assisted, solvent-free and parallel synthesis of some novel substituted Imidazoles of biological interest, Chem. Pharm. Bull. 58 (2010) 375–380.

[50] M. Kidwai, D. Bhatnagar, R. Kumar, P.M. Luthra, Synthesis of 2-Oxo/Thioxooctahydroquinazolin-5-one derivatives and their evaluation as anticancer agents, Chem. Pharm. Bull. 58 (2010) 1320–1323.

[51] A.K. Mungara, Y.-K. Park, K.D. Lee, Synthesis and antiproliferative activity of novel α-Aminophosphonates, Chem. Pharm. Bull. 60 (2012) 1531–1537.

Antibacterial and antimicrobial coatings on metal substrates by cold spray technique: Present and future perspectives

2

Manojit Ghosh[a,*], *Avinava Roy*[a], *Arkajit Ghosh*[a], *Hritwik Kumar*[a], *Gourab Saha*[b]
[a]Indian Institute of Engineering Science and Technology, Shibpur, India, [b]Tampere University of Technology, Tampere, Finland
[*]Corresponding author. e-mail address: mghosh@metal.iiests.ac.in

Nomenclature

ALP	alkaline phosphatase activity is determined by quantifying the amount of -p-nitrophenol, the end product hydrolyzed of paranitrophenyl phosphate.
Bioactivity	the ability of material to bring out response in living tissue.
Biodegradable	gets resorbed when one placed in the human body.
Bioinert	does not initiate a reaction with host when introduced to body.
BMG	bulk metallic glasses are formed at very low critical cooling rates in order to suppress the nucleation of crystalline phases.
HA	hydroxyapatite ($Ca_{10}(PO_4)_6(OH)_2$) is ceramic material which is widely used in biomedical applications due to its low release of antibiotics and simulates the bone ingrowth between implant and bone.
hBMSC	human bone marrow stromal cells are used to study osteogenesis in vitro and got applications in bone tissue engineering.
HPCS	high-pressure cold spray refers to the system in which there is axial injection of powders and utilization of 25–30 bars pressure gas.
LPCS	low-pressure cold spray system refers to the system in which there is radial injection of powders and utilization of 5–10 bars pressure gas.
MRSA	methicillin-resistant *Staphylococcus aureus* is the Gram-positive infectious bacteria that is resistance to many antibiotics and accounts for 8% hospital infections in the United States.
MTS	it is the colorimetric method for assessing cell metabolic activity used in the field of cancer biology, immunology, and drug delivery pharmacy.
PEEK	poly-ether-ether-ketone [$(C_6H_4\text{-}O\text{-}C_6H_4\text{-}O\text{-}C_6H_4\text{-}CO\text{-})_n$] is popular implant material because of having excellent properties such as excellent thermal stability, friction reduction and mechanical properties similar to human bone.
VCS	vacuum cold spray refers to the process in which specimen is placed in the vacuum tank and nanoparticles are sprayed into using a propellant flow of gas especially helium or air.

Green Approaches in Medicinal Chemistry for Sustainable Drug Design. https://doi.org/10.1016/B978-0-12-817592-7.00002-2
© 2020 Elsevier Inc. All rights reserved.

2.1 Introduction

The interest in the evolution of substrates with antibacterial properties for different biomedical applications is of growing concern as so many microorganisms are antibiotic-resistant. This subject has helped in designing innovative biomaterials. Possible microbe-controlling strategies include using biomedical devices and implants. Highly fascinating paths are either used or under the research stage, involving the deposition of bactericidal agents upon the biomaterial surface to prevent the attachment of bacteria to the surface and also to arrest the growth of any biofilm. Products found in nature, as well as certain bioactive metals like Ag, Cu, and Zn, provide viable options for advanced biomaterials for antibacterial agents. Cold spray (CS) simply explained as acceleration through Laval Nozzle and deposition of solid composite powders on a suitable substrate. Particles undergo plastic deformation only when the bombarding speed is in excess of a certain value—the threshold value. The close link existing between the fundamental understanding of bonding mechanisms and fluid dynamics of CS makes it a powerful tool for various applications and different from other traditional consolidation processes. CS has emerged as a promising candidate for depositing biocompatible and antimicrobial coatings over the past decades. It offers many advantages as compared to the thermal spray process as it involves kinetic energy instead of thermal energy for spray. Since it is a low-temperature deposition process, undesired tensile residual stresses, oxidation, and chemical reactions can be avoided. Due to the plasticity of coatings, it is possible to deposit different antimicrobial biocompatible coatings of metallic materials and polymers. In addition, it is cost effective and environmentally green. The following write-up provides a comprehensive idea about the latest advancements in the field of modified biomaterials along with an account of the most interesting processes used to deposit antibacterial coatings on particular surfaces to be used in the field of biomedical implant applications. Further, it describes the present status of antimicrobial coatings using CS and its future applications and investigations are suggested in the field of antibacterial coatings and orthopedics industry.

2.2 The need for the development of antibacterial and antimicrobial coatings

The meaning of the term "biomaterial" is recently proposed by Williams et al. [1] in 1987 as "a nonviable material used in a medical device and intended to interact with biological systems". For over the last 60–70 years, this field has always been under progressive development and experienced many changes till date. The field of biomaterials has evolved through three generations each with clear-cut and definitive objective starting from the first-generation bio-inert materials in the late 1960s to third-generation biomimetic biomaterials (Fig. 2.1). The two major problems in biomaterials are biocompatibility and structural compatibility. Biocompatibility can be perceived as "material's ability

to perform with an appropriate host response in a particular application." It indirectly expresses two terms, namely, biosafety and biostability, where the material does not have to evoke long-term persisting infection which may yield death of a cell or produce a malfunctioning of the cell or tissue matrix.

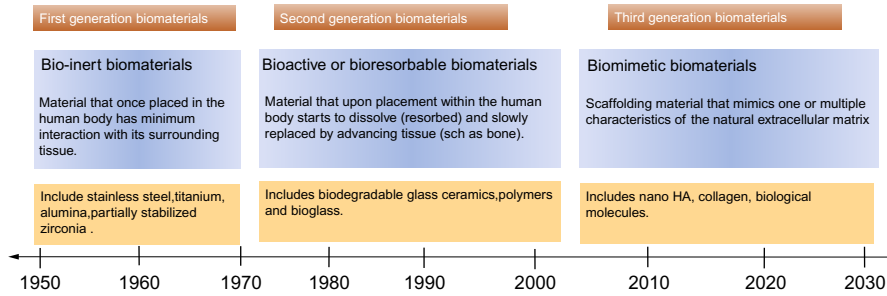

Fig. 2.1 Evolution of biomaterials science.

However, the section of implant tissue interactions in biomedical science can be better comprehended by surface engineering. The ideal medical implant is one that owns both antibacterial function and excellent cell biocompatibility. Medical implants on the basis of applications can be categorized into groups namely Sensory and neurological, cardiovascular, Orthopedic, contraception, cosmetic, and other organs and systems. Other organs and systems include treatment of acid reflux disease, respiratory failure, sleep apnoea, involuntary urination, and anal incontinence and erectile dysfunction.

Titanium alloys are broadly used in biomedical applications mainly in dental and orthopedic implants [2]. However, at the tissue and implant interface of titanium, there is the formation of surface biofilm which makes implant surface susceptible to infection. Hence, there is a requirement of potential methods of surface modifications, with the capability to coat the biomaterials with antibacterial substances like copper, tin, and zinc to fulfill the specific demands of particular applications. Formation of biofilms can only be tackled by the development of antibacterial coatings which will prevent initial adhesion of bacteria to the surface of Ti. For the coatings of biomedical surfaces such as catheters [3], polymeric nanocomposites of silver are used successfully. Similarly, peptide-based [4] antimicrobial coatings were useful for medical implants. In addition, oil-based coating is a natural process to prepare antimicrobial essential oils. Carvacrol [5], the chief component of thyme oil is introduced into waterborne polyurethane coatings, prevents the formation of biofilm by lowering the bacterial attachment.

Surface characteristics of medical implants play a key role in initial adherence and growth of bacteria on the implant surface and subsequent cell action and response. These characteristics generally include roughness, surface free energy, surface potential, conductivity, wettability, etc. [2]. Bacteria resistant interface can be obtained by altering physical and chemical surface properties [2] and development of antiadhesive polymer coatings.

2.3 The coating techniques

There is a wide range of surface treatment techniques for the development of antimicrobial coating like ultraviolet (UV) radiation, chemical and plasma grafting, ion implantation, and plasma immersion ion implantation and deposition.

As far as metal coatings are concerned, rough and porous Ti coatings are prepared through vacuum plasma spraying (VPS). Earlier, Yang et al. [6] obtained Ti coatings on Ti substrates containing an outer layer full of macropores which are beneficial for tissue ingrowth into the coating. Such macropores have a surface roughness of approximately Ra = 100 μm. However, Borsari et al. [7] produced the dense VPS-Ti coatings with the purpose to avoid the depletion in the density of bone, also known as "stress shielding" and thus increasing the prosthesis life span. VPS coating provided a good biological response in vitro and it behaved the same as the coatings used in orthopedics.

Copper and copper-based alloys are widely used as coatings which are thermally sprayed on the top of the construction elements such as steel which preserves its necessary strength. One of the advantages of the thermally sprayed coatings is a possibility to generate coatings made of materials of different compositions including composite materials. It also finds its usage in hospital equipment as it is very much effective in fighting pathogenic microorganisms. Michels et al. [8] showed that there is an increase in antimicrobial effectiveness with increasing content of copper in alloys. Fig. 2.2 shows that the decrease in bacteria count of *Listeria monocytogenes* is more rapid in the higher content of copper in alloys. The formation of biofilms is not possible because of rapid contact killing [9] and the formation of radicals in Cu complexes makes the viruses idle and inactive [10]. Although the inhibitory effect of Cu on biofilm is not well known, it is believed that the cupric ion is responsible for the antimicrobial action of copper [8]. The research revealed that the equipment with

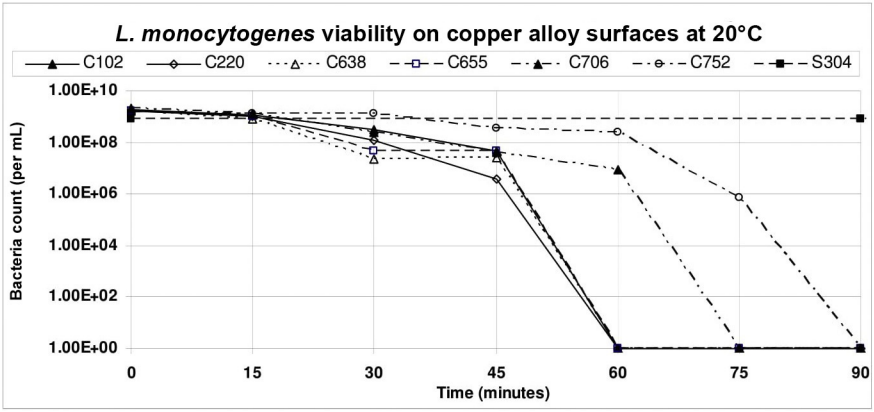

Fig. 2.2 The viability of *L. monocytogenes* on the surfaces of alloys UNS C10200, C22000, C63800, C70600, C75200, and S30400 at 20°C.

copper-containing surfaces, the chances for bacterial infections is decreased by 90%–100% as compared to the same made from conventional materials such as steel or plastic. There are various ways of depositing copper coatings such as electrodeposition, plasma spraying, arc spraying, and cold spraying. In the study of different spraying methods to deposit copper coatings, their antimicrobial properties were also examined. Jing et al. [11] prepared Cu porous materials by electrodeposition on a precursor of conventional polyamide foam. The antibacterial effect of Cu was also investigated against *Escherichia coli*. The results showed that Cu porous materials exhibited very strong antibacterial activity and persistent antibacterial activity against *Escherichia coli*. The percentage of dead cells reached 100% on *Escherichia coli* after a 40-min incubation. Nie et al. [9] evaluated the effectiveness of Cu-plate and superhydrophilic Cu-dotted oxide coating surface in the inactivation of *Escherichia coli* ATCC 25922, MRSA ATCC 43300 and *Enterococcus faecium* ATCC 51299. In this work, electrolytic plasma oxidation of Al was used to produce an oxide surface followed by electroplating of Cu metal on the top of the oxide layer. The results indicated that the antibacterial performance of Cu-dotted oxide surface was even better than the Cu plate surface and it is effective in even a moist or wet environment. According to Wrona et al. [12] copper, copper alloys (CuNi35, CuSn10), and Cu-$TiO_2$10 copper composite coatings were deposited on stainless steel substrates by plasma spraying. It has been confirmed that all coatings show sufficient antibacterial activity, especially toward Gram-negative bacteria strains and on surfaces with a satin finish. However, other than microbiological testing, there is no other significant material characterization that could indicate material-behavior toward bacteria properly.

On the other hand, Ag has its importance since ancient times for its antibacterial, antifungal, and antiviral properties. It has been in use for the treatment of different chronic wounds and burns for centuries. Its compounds like silver nitrate ($AgNO_3$) and silver sulfadiazine ($C_{10}H_9AgN_4O_2S$) have been used for the treatment of fresh burns [13], wounds, and several bacterial infections. Around AD 1700, Ag-based compound, silver nitrate has been used for the treatment of venereal diseases, including gonorrhea, fistulae from salivary glands, and bone and perianal abscesses [14]. In 1881, silver nitrate was used as eye drops to cure opthalmia neonatorum by Carl S.F Crede [13, 15]. With the introduction of silver in penicillin, bacterial infections could be minimized. Silver sulfadiazine (AgSD) consists of Ag and sulfadiazine. It possesses antifungal, antiviral properties and is well effective against some bacteria like *Escherichia coli*, *Staphylococcus aureus*, *Klebsiella* spp., *Pseudomonas* sp. [16] Currently, Ag nanoparticles are considered to be the most effective antimicrobial agent as it prevents bacteria colonization and possesses good antimicrobial efficacy against bacteria, viruses, and other eukaryotic microorganisms [17]. It has better wound healing capacity, better cosmic appearance, and scareless when tested using an animal model [18]. The antimicrobial efficacy also depends on the shape of nanoparticles. Different shapes have different effects on the bacterial cell. Pal et al. [19] discovered that rod-shaped particles need a total of 50–100 μg of Ag content while spherical-shaped nanoparticles need a total Ag content of 12.5 μg. Truncated triangular nanoparticles show bacterial inhibition with Ag content of 1 μg. In recent decades,

Ag nanoparticles are used in different textile fabrics as Ag is nontoxic and it also possesses antimicrobial properties. According to Yeo et al. [20] from scanning electron microscopic study, it was concluded that antibacterial property possessed by Ag nanoparticles incorporated inside the sheath part of fabrics is more significant as compared to the fabrics incorporated with Ag nanoparticles in the core part. It is due to the good dispersibility of silver nanoparticles in fabrics. Co-deposition of Ag has also been documented [21] with many other materials using the thermal spray method. For example, the silver-containing hydroxyapatite (HA) coatings have been obtained by depositing a titanium substrate by VPS proved to have both antibacterial and bioactivity properties. Yikai et al. [22] concluded that HA coatings exhibited a remarkable antibacterial effect against *Escherichia coli*, *Pseudomonas aeruginosa*, and *Staphylococcus aureus*. Recently, Meininger et al. [23] electrochemically deposited $Ca(OH)_2$ (Portlandite) coatings on titanium surfaces. The addition of Ag^+ and Cu^{2+} ions led to the reduction of bacterial growth of the hydroxide against *Staphylococcus epidermidis*. There can be further improvement in $Ca(OH)_2$ coating systems and coatings can also be possible on titanium alloys, Co—Cr alloys or stainless steel.

Plasma-sprayed alumina and zirconia are in clinical use due to high wear resistance than Titania in ceramic coatings [24]. One of the limitations of using them in hard tissue is that their coatings cannot be bound directly to bone tissues as they are bioinert in nature. The use of bioactive coatings produced by plasma spraying as well as the flame spray was a very successful achievement. The HA-coated prosthesis is a good alternative to a cemented prosthesis which has high rates of loosening as it maximizes fixation and decreases the migration of microparticles along with the prostheses [25]. Nanocrystalline ceramics yield better biocompatibilities. HA particles are needle shaped which promote the inflammatory reaction, spherically shaped particles show increased inhibition with time and spherically shaped particles have less response than irregularly shaped particles. That's why they have a high influence on cell performance. In recent studies, polymer composite materials [26] have been proposed as an alternative choice to get rid of the failures of metals and ceramics. For example, polyether ether ketone (PEEK) resembles bone in terms of biocompatibility, bio inertness, and elastic modulus and it also has good mechanical properties for hard tissue applications, for example, hip and knee replacements.

2.4 Thermal spraying: Processes and techniques

Thermal spraying refers to the family of coating processes in which feedstock is sprayed in molten or semimolten state onto a prepared substrate [27]. Thermal spray techniques can be classified into three broad categories: flame spray, electric arc spray, and plasma arc spray. Table 2.1 shows the classification of various thermal processes. The energy sources (flame spray, electric arc spray, and plasma arc spray) are used to heat the coating material to molten or semimolten state. The hot energetic particles are given sufficient kinetic and thermal energy using process jets to propel the molten particulates toward a prepared surface. The most common heat sources for producing thermal energy for spraying are the combustion of fuels with oxygen or air or through electrical heating of industrial gases. Kinetic energy can be produced through

gas jets which are able to accelerate the droplets through the nozzle. The droplets impact and form bonds with the surface causing the formation of lamellar microstructure on the surface (Fig. 2.3). The thin splats are formed that finally build up and adhere to the surface of the substrate. These undergo very high cooling rates, typically 10^6 K/s for metals.

Table 2.1 Classification of thermal spray process.

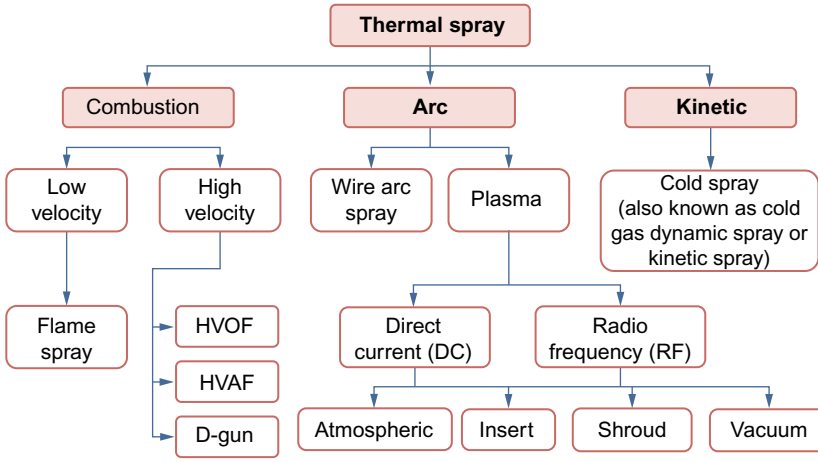

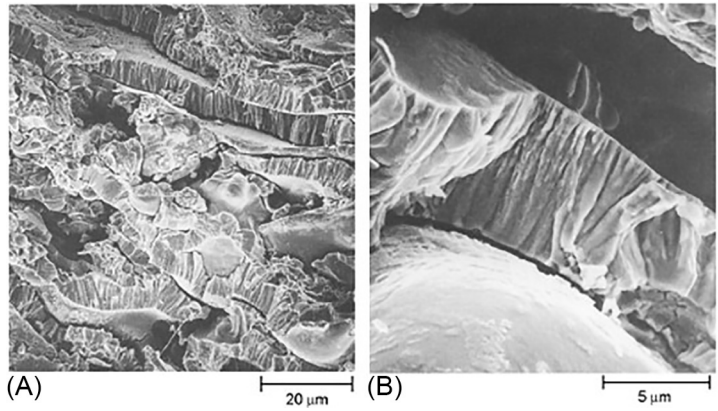

Fig. 2.3 Scanning electron micrographs of fracture cross sections of an air plasma-sprayed tungsten coating: (A) lamellar microstructure and (B) the presence of a columnar grain structure within the splats.

Fig. 2.4 gives the graphical representation between gas temperature and particle velocity of various thermal processes. The flame spray can be divided into low-velocity powder flame, wire flame and high-velocity oxy-fuel (HVOF) [29] on the basis of gas temperature and particle velocities. Flame spray propels molten particles

into the substrate with the addition of high-velocity stream. It uses the basic principles of a welding torch. In HVOF, combustion jet at temperatures of 2500–3100°C is created by a combination of oxygen and fuels such as hydrogen, propane, or propylene [24]. The combustion takes place at very high chamber pressures and the process results in extremely dense well-bonded coatings [24]. Electric wire arc processes are very cost effective and are applied for pure metals (pure aluminum, zinc, copper, and metal alloys such as stainless steel). Compared to the flame spray process, the velocity of the particles is low and the temperature is higher. It involves two consumable electrodes which are connected direct-current source and are fed into the gun and meet. It establishes an arc between them that melts the tips of wires [30]. In the plasma arc process, the powder heating region ranges from 2500°C to 14,000°C [25], much higher than the melting point of any material. To generate the plasma, argon or argon-hydrogen mixture is heated by a dc arc to produce plasma [24].

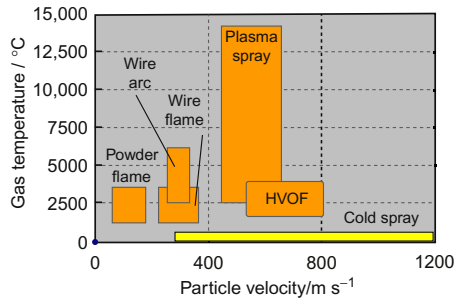

Fig. 2.4 Temperature vs velocity profile for thermal and cold spray processes [28].

One of the major advantages and unique ability of thermal spray processes is that it can be used to deposit a wide range of materials [31]. Any spraying material whose molten phase is stable can be deposited and even some materials like graphite or boride ceramics can be co-deposited with other sprayable material to form the composite coating material [24]. Another major advantage is that it offers high deposition rates at low cost as compared to other coating processes. In most of the thermal processes, there is no need for significant heat input and hence it has higher efficiency. That's why the material's mechanical properties do not get affected and there is no excessive thermal distortion of the part. Hence, it is possible to strip off and recoat worn or damaged coatings without a change in significant dimensions of the material.

Although the thermal spraying technique is a widely accepted commercial technique, there is the formation of oxide inclusions as well as degradation of oxide sensitive materials. Oxide inclusions in limited amount are beneficial as it improves mechanical properties of the material but excessive presence at interplay regions leads to cohesive failure and wear debris [32]. The maximum thickness of coatings also reduced due to the introduction of residual stresses. Another disadvantage is that it can coat only a limited amount of portion, i.e., it can coat only what the torch or gun can see.

2.5 Cold spray: The process and its advantages

CS is one of the emerging spray coating technologies which comes under the family of thermal spraying technologies. It was developed in the mid-1980s by Papyrin et al. [33] at the Institute of Theoretical and Applied Mechanics, part of the Siberian Division of the Russian Academy of Science in Novosibirsk while studying particle flow in wind tunnels. They deposited a wide range of pure metal alloys and composites on substrate metals. It has a variety of applications for manufacturing of wear and corrosion-resistant coatings, for repairing of damaged parts. It has got its application in power generation plant where it is applied on the boiler tubes to provide resistance from cavitation wear of turbine blades, resistance from high-temperature corrosion, and the water pump housing, impeller fins and wear rings [34]. Also, the fabrication of the Al-tube heat exchanger in air conditioning equipment for all types of vehicles is done by CS technique. According to Yoon et al. [35], a high-quality coating is obtained by CS process which is having high corrosion resistance as well as good braze ability and also with low manufacturing cost. Gas dynamics, nozzle design, physics of high-speed particle impact, powder materials, novel application methods, and the development of specific applications are some of the key areas of research within the CS. In addition, it is an eco-friendly spraying process since it is easy to dispose of its wastes and the process is noncombustive.

Generally, there are two types of CS process—high-pressure cold spray (HPCS) and low-pressure cold spray (LPCS). Figs. 2.5 and 2.6 show the schematic diagram of HPCS and LPCS, respectively. The basic difference between these two is the utilization of pressures and the injection of powder. The spray particles are injected prior to the spray nozzle throat from a high-pressure gas supply [36] in HPCS, and LPCS powders are injected in the diverging section of the spray nozzle from a low-pressure gas supply [37]. Lower weight gases such as nitrogen or helium, are the preferred propellant gases for HPCS. In HPCS, the pressure utilized is 5–10 bars and there is a radial injection of powder whereas the pressure utilized is 25–30 bars and powder injection is axial in the case of LPCS [38]. The spray efficiency of HPCS system is more, reaching up to 90% as compared to 50% in LPCS process. However, both types of processes have some limitations. For HPCS, a high-pressure powder feeder running

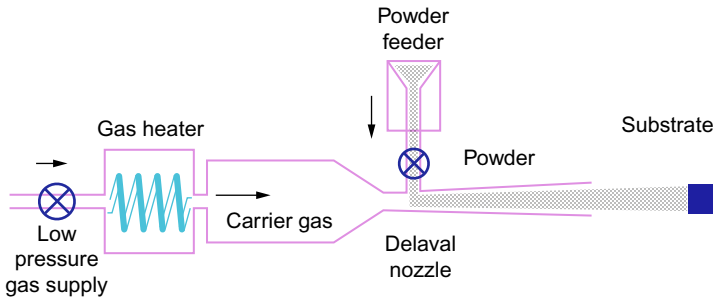

Fig. 2.5 Low-pressure cold spray [35].

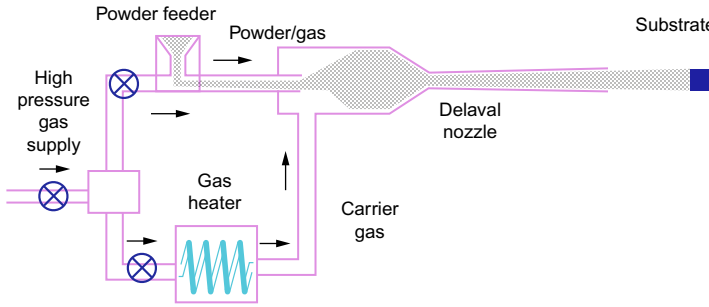

Fig. 2.6 High-pressure cold spray [35].

at a higher pressure compared to that of the main gas stream has to be used to avoid backflow of powder [39]. Also, the high-pressure powder feeders are big expensive. Another limitation of HPCS includes severe wear of nozzle throat and clogging of the nozzle. This becomes worse when particle velocity and temperature are increased and hard particles are being sprayed. However, the LPCS system is more flexible considering automation and is portable due to the elimination of the high-pressure delivery system requirement. In addition, a LPCS system is more compatible due to the number of system modifications.

In CS process, relatively smaller particles which have approximately diameter ranging from 1 to 50 μm in solid state and they are accelerated to high velocities, i.e., 300–1200 m/s which impart high kinetic energies. The plastic deformation of solid particles takes place on impact which produces bonded splats on the surface. In this process, there is a temperature-dependent critical velocity which is responsible for bonding and it varies with particle and substrate material. When the particle velocity (V_p) is less than the critical velocity (V_{crit}), they bounce off and erode the surface, hence, not forming the contiguous deposits or coating. When $V_p > V_{crit}$, the first thin layer is formed and particles begin to plastically deform, adhere to surface, and form an overlay coating. This process has the ability to produce coatings with preheated gas temperatures in the range of 0–700°C, which is much lower than the melting point of coating particle materials. It ultimately leads to the elimination of the detrimental effects of high-temperature oxidation, evaporation, melting, recrystallization, residual stresses and other concerns that cannot be resolved with thermal spray methods.

In the CS process, nozzle design influences on particle velocity which basically depends on the nozzle inlet diameter, throat diameter, exit diameter, the entrance convergent section length (upstream length), divergent exit length (downstream length) and expansion ratio (the ratio of the area of exit of the throat). There are basically three types of the nozzle—convergent-barrel, convergent-divergent, and convergent-divergent barrel nozzle. The nozzle which achieves high particle velocity is CDB nozzle, also known as Laval Nozzle (Fig. 2.7) due to its conical geometry. In de' Laval-type nozzle, the coating material is injected into the gas stream in powder form at the inlet of the nozzle, accelerated by a gas in the nozzle and propelled toward the substrate to be coated. In the Laval nozzle, the velocity of the gas at the throat is a function of temperature. It is given

by equation, $V_t = \sqrt{\gamma R T_t}$ [41]. γ is the ratio of gas specific heats, R is specific gas constant, and T_t is the temperature of the gas at throat, respectively. The use of preheated gas is beneficial as it provides higher particle velocity but at the same time, it raises the risk of oxidation and nitridation which can damage the design functionality of applied coatings [42]. Nitrogen gas is mostly used as a preheated gas for a wide diversity of materials. But it requires high velocity and hence hard materials cannot be deposited. Yoon et al. [43] enhanced the deposition efficiency by changing process gas nitrogen to helium during cold spraying of NiTiZrSiSn amorphous powder. Since helium is inert, it eliminates the problem and allows reaching the particle gas to the highest velocity. However, helium is almost 10 times more expensive than nitrogen and its use is limited to many applications unless recycled. In many applications, the mixture of He and N_2 gas [44] is used as a diatomic gas. Since N_2 is a diatomic gas, it increases the enthalpy of the carrier gas and better heat transfer with spray particles. But there is a decrease in particle velocity due to heavier atomic mass which leads to a decrease in density and hardness of applied coatings.

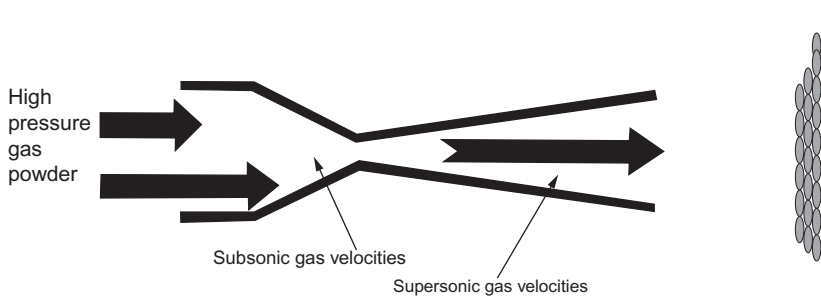

Fig. 2.7 Schematics of a cold gas dynamic spray de Laval nozzle [40].

The chief advantage of using CS process is that the particles remain in solid state and the coating formation takes place due to the kinetic energy of particles during impact. The temperatures of gas and particle remain well below the melting point of the spray materials [25].

2.6 Present status of the antibacterial and antimicrobial coating by cold spray

There exist well-defined approaches determining the eligibility of materials, suitable for CS process. Hardness of the particular material along with its melting point, density, and particle velocity [45] are the various physical factors on which the ability of the material to be used in CS technique depends on. Those materials which have lower melting points than others, as well as low mechanical strength, are the best suited materials for this process (e.g., zinc, aluminum, and copper) as they have relatively low melting points and low mechanical strength. Contrastingly, in the case of materials having relatively higher strengths, i.e., materials having iron and nickel as their bases, the low processing temperatures are insufficient for successful deposition [39].

The risk of infection increases drastically in the case of bacterial accumulation on the touch surfaces. In the last few decades, a significant amount of time and money has been dedicated to exploring and improving the antimicrobial properties of metals and its alloys (titanium, copper, silver, etc.) to be used for combating numerous threatening microorganisms. In addition to significant hikes in medical costs, the infection also causes serious damage to the parents. The initial attachment of the bacteria and thereby inactivation of any cell connected to the surface is prevented by the antibacterial surface formed. The antibacterial surface can be classified as antibiofouling surfaces and bactericidal surfaces [24]. The former may resist the cellular attachment of bacteria owing to the presence of unfavorable surface topography whereas, on the other hand, bactericidal surfaces rupture the cell contact, resulting in cell apoptosis. The CS process provides solutions to both problems by functionalizing surfaces in that way.

Initially, the biocompatible metals were tested and sprayed via the CS process. Efficient coatings were achieved owing to the high plasticity of metals. Stainless steel and titanium were the first metal coatings used for biomedical applications. It is possible to reach different porosity levels by modifications in the spraying method. According to Li et al. [46], the porosity of titanium (Ti) and Ti6Al4V coatings onto Ti6AL4V substrates has increased by the effect of heat treatment. The possible reason behind this is the healing of incomplete interfaces through the atom diffusion annealing treatment. Fig. 2.8 represents the different degrees of porosity via a wide range of modifications in spraying conditions [47]. Additionally, the tamping effect

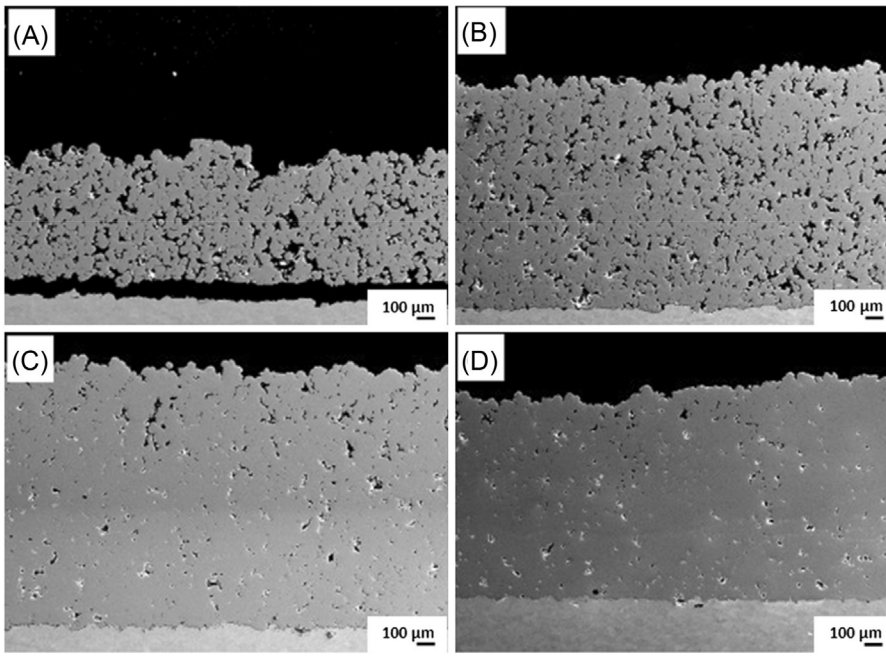

Fig. 2.8 Porous Ti coatings by cold spray from less to high energetic conditions [47].

affects the density of microstructures. This effect leads to more porous structures on the top rather than near the interface with the interface due to successive impacting particles [48]. Choudhuri et al. [49] showed the deposition characteristics of vacuum atomized Cp-Ti powder (Fig. 2.9). There is an increase in coating density and porosity levels with increasing gas pressures and decreasing transverse speed. Increasing coating structures lead to gradient coating structures which is beneficial for biomedical

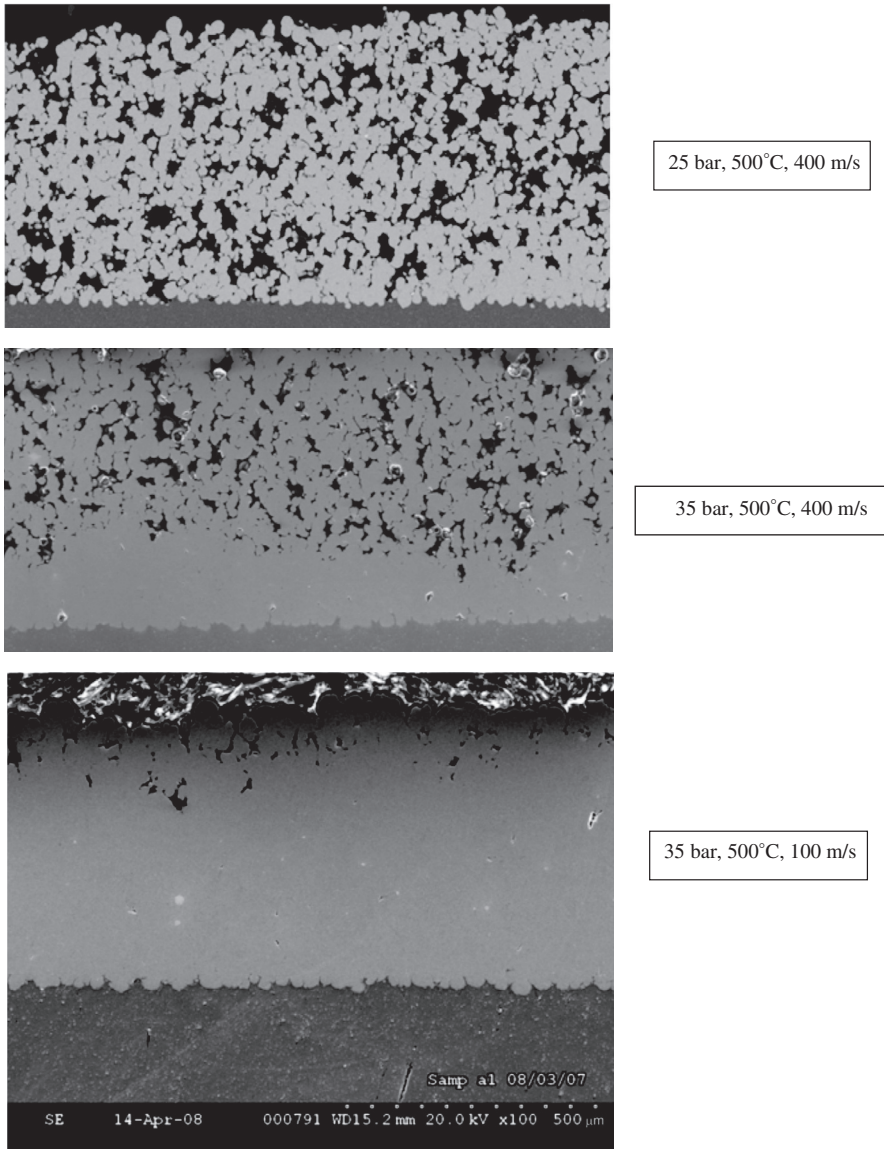

Fig. 2.9 Cross-sectional view of Cp-Ti sprayed at different conditions [49].

applications as bone tissues can grow into these open pores creating a mechanical hinge and eliminating the need for cement.

The titanium coatings sprayed, have irregular porosity when sprayed by plasma. Consequently, the pores are also not properly connected with one another. Sun et al. [50] proposed using porous titanium coatings having Mg + Ti powders integrated into titanium, where the Mg would hold as the constituents together and can also be removed by the process of vacuum sintering. Obtained average porosity was of 48.6% and pore sizes −70 to 150 μm. Furthermore, Gardon et al. [51] deposited Ti onto PEEK (C_6H_4-O-C_6H_4-O-C_6H_4-CO-)$_n$ substrates using CS technology. Viscous, homogeneous, and adhesive coatings were obtained on PEEK without its degradation. This investigation evolved PEEK as a highly suitable biomedical implant.

CS technique has also found its usage as an alternative to plasma-sprayed technique which is used to deposit bioceramics such as hydroxyapatite ($Ca_{10}(PO_4)_6(OH)_2$) [52]. HA has been widely used in dental and orthopedic implants due to its chemical and crystallographic similarity with bone minerals. HA coatings promote rapid fixation and stronger bonding between host bone and implant. In addition, there is increased uniform bone ingrowth and on-growth at bone/implant surface. However, long-term stability is still a challenge using earlier thermal spray techniques due to a high-temperature deposition process. Thermal spraying technique has limitations such as phase alteration, evaporation, deboning, residual stresses, etc. Also, when HA is plasma-sprayed, the formation of phases of calcium phosphate [49] deteriorates the novel bioactive properties of HA and adhesion to the bone implant. That's why CS has been proposed as an alternative to producing HA coatings with high density and controlled crystallinity. There are also other low-temperature techniques such as sol-gel, biomimetic deposition, solution deposition, electrochemical deposition and atomic layer deposition [24], but HA coatings produced via CS technique is a simple and economical process as compared to other low-temperature range processes. Choudhuri et al. [49] presented a novel approach to deposit bioceramic coatings, i.e., composite powders of titanium and HA on Ti and Al substrate using HPCS system. Dense composite coatings, containing up to 30% HA have been deposited by this technique. The coatings density further increased by using sponge powder and nitrogen process gas. Furthermore, Zhou et al. [53] evaluated the electrochemical behavior of cold sprayed 20 and 50 wt% HA/Ti composite coatings. A 20 wt% HA/Ti composite coating exhibited higher corrosion current and lower corrosion resistance which was improved by postspray heat treatment. The CS and postspray heat treatment provided an effective approach to manufacture HA/Ti composite coatings with good corrosion and mechanical properties which is much needed for biomedical implant applications. Some attempts have been made to improve the ductility and impart high fracture toughness of HA. In recent years, graphene [54] has got a lot of attention in the field of biomedical applications due to its exceptional mechanical, thermal, and electrical properties. It has been found that the addition of graphene as additives in HA could enhance load-bearing biomedical applications. Studies of graphene as biosensors [55], nanoprobe [56], and drug delivery [57] have denoted its superior biocompatibility and biostability. Liu et al. [58] studied HA-GN (Graphene Nanosheet) composite coatings onto Ti substrates at room temperature by VCS. It has been found that HA-GN composite coatings retained nanostructural features of both HA and GN.

Upon using HA-GN coatings, the adhesive and the multiplicative nature of osteoblast cells increased significantly. This significant increase can be attributed to the rapid take-up of key serum proteins fibronectin, having elongated stretching conformation on GN. Moreover, Zeng et al. [59] reported that the addition of Graphene oxide as an additive of HA enhanced both the crystallinity of deposited apatite particles and the bonding strength of the synthesized composite coatings. More recently, Li et al. [60] successfully synthesized and deposited HA-gentamicin sulfate (GS) composite powder onto titanium substrates by vacuum cold spraying at room temperature. It was done by dispersing synthesized HA powders in GS PBS solution and then dried. Gram-negative bacterium *Escherichia coli* was used to evaluate the antibacterial properties of the samples whereas titanium substrate was used as controls. It has been found that antibacterial rates of GS coatings showed the highest antibacterial rate. However, HA-GS (R) coating (HA-GS coating immersed in PBS solution for 31 days) showed a slight decrease (Fig. 2.10), but still, favorable antibacterial property was observed. It confirmed that gentamicin released was still bioactive. Moreover, the coating fabrication by VCS of HA-GS composite with antibacterial agent-incorporated HA composite might open a new window for producing antimicrobial biomedical materials.

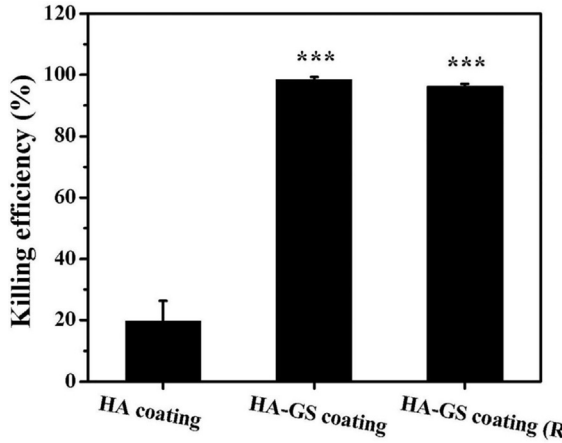

Fig. 2.10 Killing efficiency of HA coatings [60].

Sanpo et al. [61] studied the deposition characteristics of Al/ZnO coatings at room temperature by examining deposits caused by CS processes using different ratios of Al/ZnO powder. There has been a significant increase in the antibacterial activity with increasing ZnO nanopowder concentration in the composite powder feedstock and CS coating. Similarly, the antibacterial behavior of CS-Cu (chitosan-copper complex) [62] powder and its depositions are tested against *Escherichia coli*. These results showed how the antibacterial activity rose with mounting CS Cu/Al powder concentrations in the composite powder feedstock and CS coating. Moreover, it has also been demonstrated cold spraying a biopolymer complex is a possibility. Another recent paper in this series has investigated the effect of different transition metals such as silver, nickel, zinc, and copper-substituted HA/PEEK coatings [63] on the antimicrobial properties against *Staphylococcus aureus*. Preheating air temperatures (150–160)°C and

pressure conditioning to 10–14 bar (parameters suitable to CS) resulted in successful depositions by the CS process. Fig. 2.11 depicts the killing effect of all cold sprayed samples when observed against the control solution. The HA-Ag PEEK is shown to have the maximum antibacterial tendency as it had the least surviving population of the bacteria.

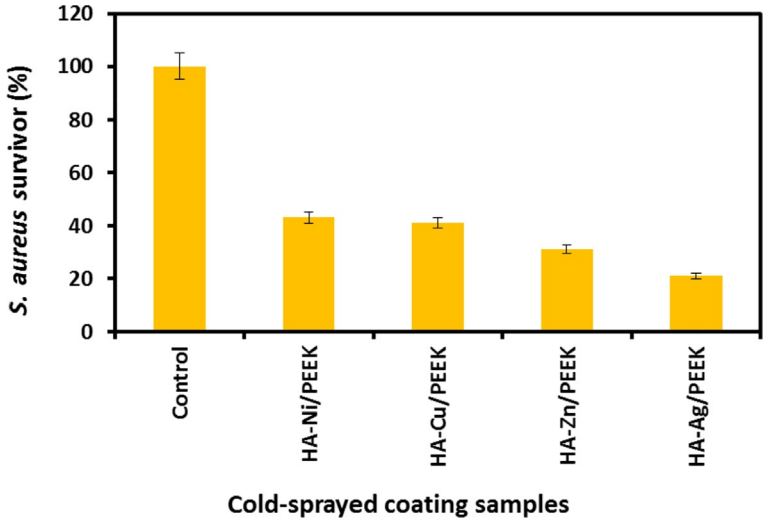

Fig. 2.11 Analysis of antibacterial properties of cold-sprayed coating samples compared with control solution [63].

Mangour et al. [64] studied the microstructural, mechanical properties and corrosion behavior of CS SS 316L-L605 mixture coatings onto mild steel substrate in as-sprayed conditions. It has been found that CS process is an efficient technique to produce coatings from various chemical compositions of powders with fine-grained structure. Table 2.2 shows the deposition efficiency, coating thickness, and porosity of different vol% of Co alloy in powder mixture. The heat treatments improved the densification and porosity reduction as well as a significant increase in ductility. In addition, it has been concluded that SS material mixed with Co alloys have better corrosion and mechanical characteristics and is ideal for the development of a new class of metallic biomaterials. Furthermore, Jin et al. [65] studied Ti-Cu-coated layer on 316 L Stainless Steel. It was obtained by using a Closed Field Unbalanced Magnetron Sputtering (CFUMS) system to improve antimicrobial and corrosion properties. Nearly all bacteria overlaid on Ti-Cu-coated on AISI316L killed within 6 h. The results concluded that coatings exhibited excellent antibacterial abilities with the modified surface due to the release of copper ions.

Alternatively, metallic glassy $Cu_{50}Ti_{30}Ni_{20}$ fine powders [66] were synthesized as a new class of antibacterial powders proposed for coating of 304 Stainless Steel using CS technology. The coatings were fabricated at 400°C under helium gas at atmospheric pressure. Fig. 2.12 shows the antimicrobial effect of coated substrates against *Escherichia coli* biofilm formation. These were incubated for 24, 48, and 72 h. No

Table 2.2 Microstructural parameters and micro-hardness of the cold sprayed coatings.

Vol% of Co alloy in powder mixture	Retained volume % of Co alloy in as-sprayed coating	Deposition efficiency (%)	Number of spray passes	Coating thickness (mm)	Porosity (%)	Matrix Vickers hardness (HV)
25	23.45	77	60	3.4	1.2	432.8
33.3	30.67	50	35	2.5	0.81	440.3
50	33.11	9	50	0.47	4.45	301

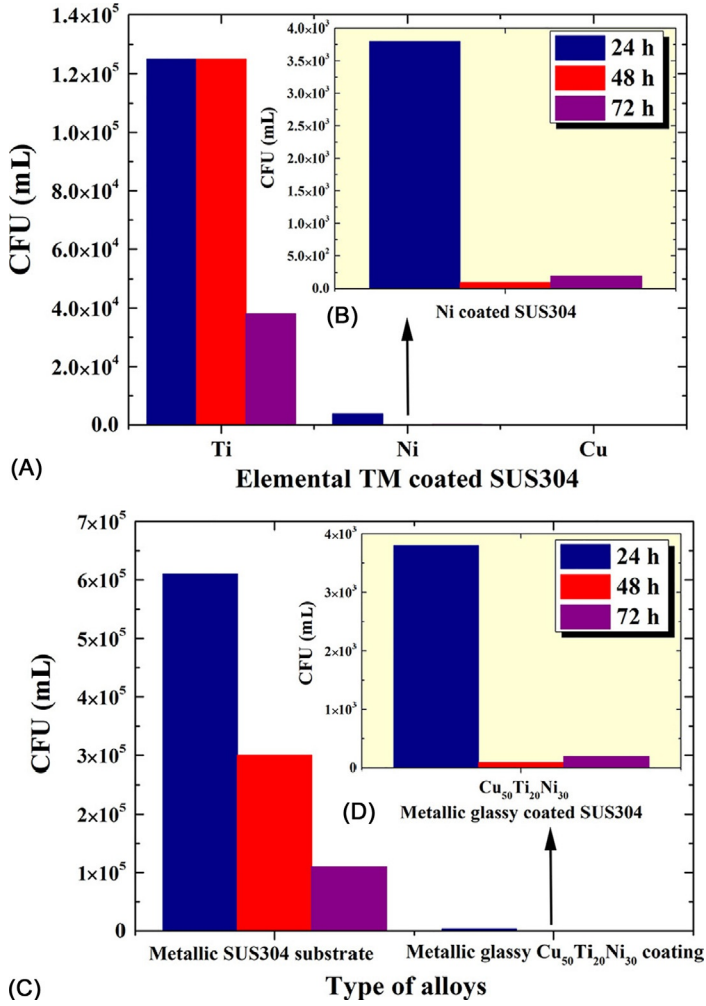

Fig. 2.12 Effect of (A, B) elemental metal, and (C, D) metallic alloys CS coatings on biofilm formation by *Escherichia coli* (ATCC 25922) after 24, 48, and 72 h.

biofilm formation was there in Cu-coated substrate as compared to negative control substrate SUS304 in which high bacteria count was observed. Furthermore, $Cu_{50}Ti_{30}Ni_{20}$ – coated substrate was more effective against biofilm formation when Ni was combined with Cu and Ti. This method, however, did not result in crystallization of the metallic glassy phase but it might provide a possible path to control the creation of biofilm.

Copper (Cu) has been already highlighted as an antibacterial material. The antibacterial activity of copper does not come from itself but rather than the utilized technique. CS processes are able to directly deposit copper on touch surfaces as coatings. Champagne et al. [67] produced the deposition of copper by three TS methods: plasma spray, wire arc spray, and CS. Surfaces were treated with *Staphylococcus aureus* (MRSA) having resistance to meticillin. Then those samples were kept at room temperature for nearly 130 min. Fig. 2.13 shows the amount of MRSA living after being exposed to different copper coatings. CS resulted in the least amount of MRSA surviving 2 h exposure as compared to other methods because it involves high strain rates which lead to extreme work hardening and high dislocation density than any other coating. However, there is less research existing on the use of copper as an antiviral agent and on the effects of nanomaterial copper surfaces in contact killing of viruses. Sundberg et al. [68] evaluated the use of conventional and nanocopper CS particles toward the antivirus contact killing of the Influenza A virus. The results showed that the nanocopper surface was more effective at the percent reduction of Influenza A virus than that of conventional copper. However, nanocopper was less effective than the study of antimicrobial killing of MRSA on copper surfaces [59]. The superiority of nano-agglomerate was due to an increase in grain boundaries at the nano-level. Surface roughness is also determined to be a major contributing factor to higher contact killing of the Influenza A virus.

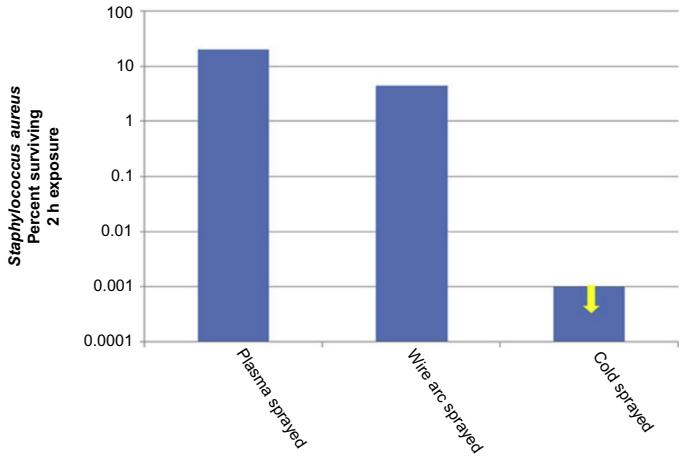

Fig. 2.13 Percent MRSA surviving after exposure to various copper deposits [67].

On the other hand, investigations and studies have also been carried out on biodegradable implants and biocompatible coatings for implant material. The most

reputable material for implant applications has been Mg-based alloys [69] due to their good biocompatibility, biodegradability, and acceptable mechanical properties. These are lightweight materials with densities similar to those of human critical bone. However, rapid degradation of Mg inside the human body has always been a stumbling block for its use in the clinic. For any biodegradable implant material, it is important that the rate of implant degradation matches the rate of healing of bone tissue. AZ series alloys, mainly AZ31 (3% Al, 1% Zn) and AZ91 (9% Al, 1% Zn) alloy corrosion behavior have been extensively studied in Hanks solution. However, some efforts have been made to deposit cold sprayed coatings on Mg-based alloys to control its localized corrosion behavior. In the recent study done on AZ91D alloy substrate, Wang et al. [70] observed how CS and DS affected the microstructural aspects and other properties of Al-Al_2O_3 composite coatings. It has been found that both depositions provided better resistance to corrosion. However, the cold sprayed process produced more dense coatings as compared to DS coatings due to the bombardment of particles at a very high speed during the solid state. Al-based Noorkama et al. [71] deposited HAP coatings of the order 25 μm on AZ51 (5% Al, 1% Zn) samples by using a pressurized spray of cold air through a nozzle-like structure. SBF tests showed that HAP-coated samples began to dissolve after a day of holding. The samples started to regenerate on nearly the 10th day of observation (Fig. 2.14) confirming that coating is bioactive. However, the ones without any coatings degraded heavily from the

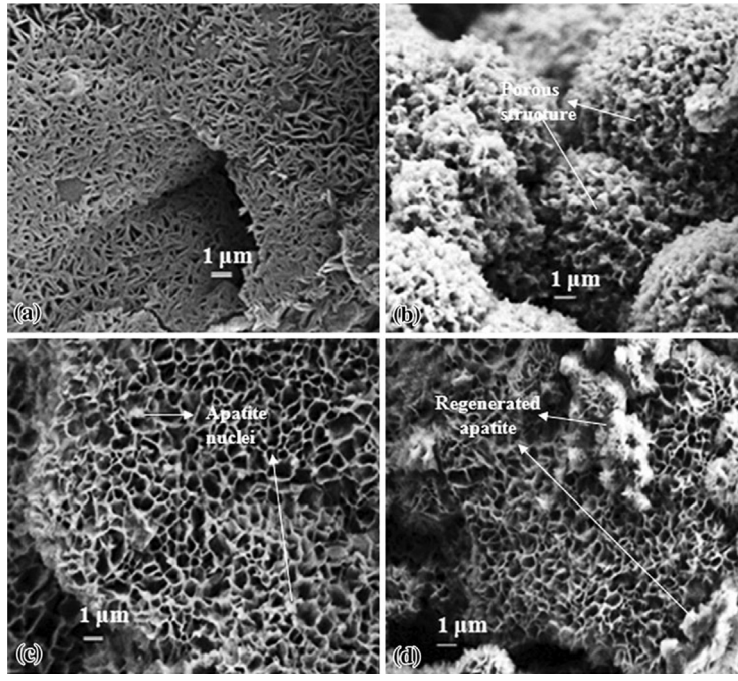

Fig. 2.14 Surface morphology of HAP-coated samples (A) after 1 day, (B) after 4 days, (C) after 10 days, and (D) after 14 days of immersion in SBF. Initial degradation (A, B) and isolated re-precipitation (C, D) of apatite is visible [71].

beginning. The results thereby proved how the alloys having coatings were biodegradable as well as biocompatible and thus suited to be implanted orthopedically.

Similarly, PEEK has been already highlighted as a novel implant material due to its mechanical properties' resemblance with the human bone. Lee et al. [72] tested the biocompatibility of HA coating on PEEK implant added with CS method in vitro and in vivo. The MTS assay, ALP assay, calcium assay was performed. The cell proliferation index, ALP activity of cultured hBMCS as well as calcium concentration of cultured hBMCS was significantly higher in cells on HA-coated PEEK disks (Fig. 2.15). It is due to rough surfaces of the HA coating layer which provides a larger interfacial contact area as compared to the smooth surface of bare PEEK. In addition, the hydrophilic and biocompatible nature by HA-coated layers modified the surface of PEEK and thus making it suitable for cells to grow on. The coatings promoted the differentiation and proliferation of cultured hBMSCs and promoted bone fusion with surrounding iliac bone.

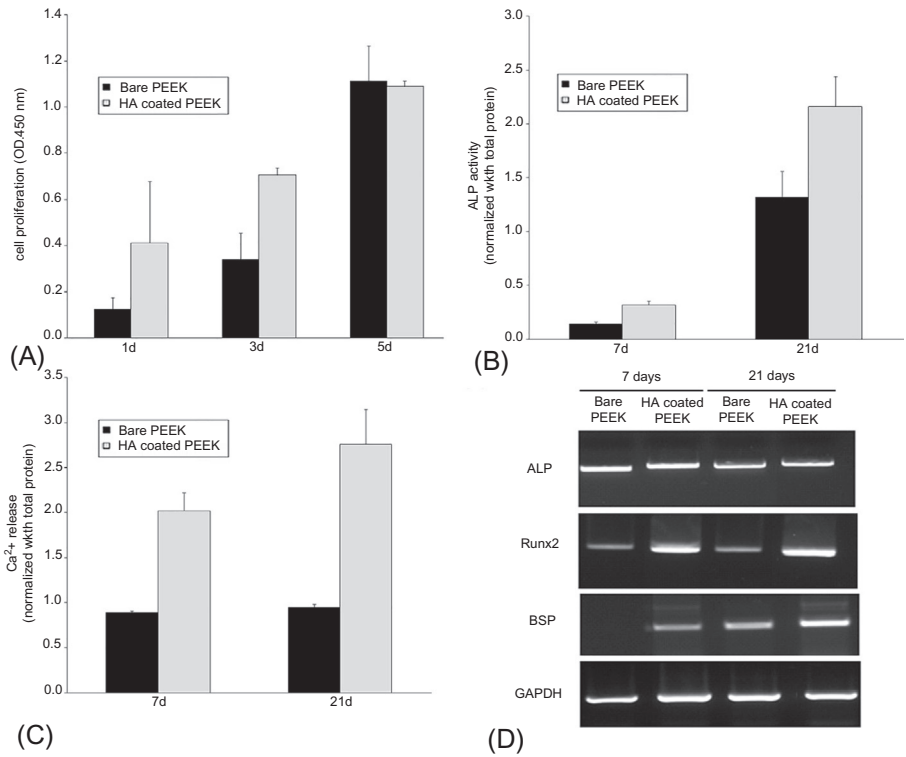

Fig. 2.15 (A) Cell proliferation by MTS assay, (B) ALP activity, (C) calcium assay, and (D) The RT-PCR results of osteoblast differentiation [72].

Gardon et al. [73] applied nanostructured anatase coatings onto biocompatible PEEK by cold gas spray. He studied cell proliferation, cell viability and cell differentiation on PEEK, and CGS Ti layer and CGS nano TiO_2 coatings. In terms of cell

viability and cell proliferation, Ti surfaces showed better biological responses from 3 days of cell culture than PEEK. In addition, PEEK coated with nanostructure titanium oxide showed optimal results in osteoblast differentiation (Fig. 2.16).

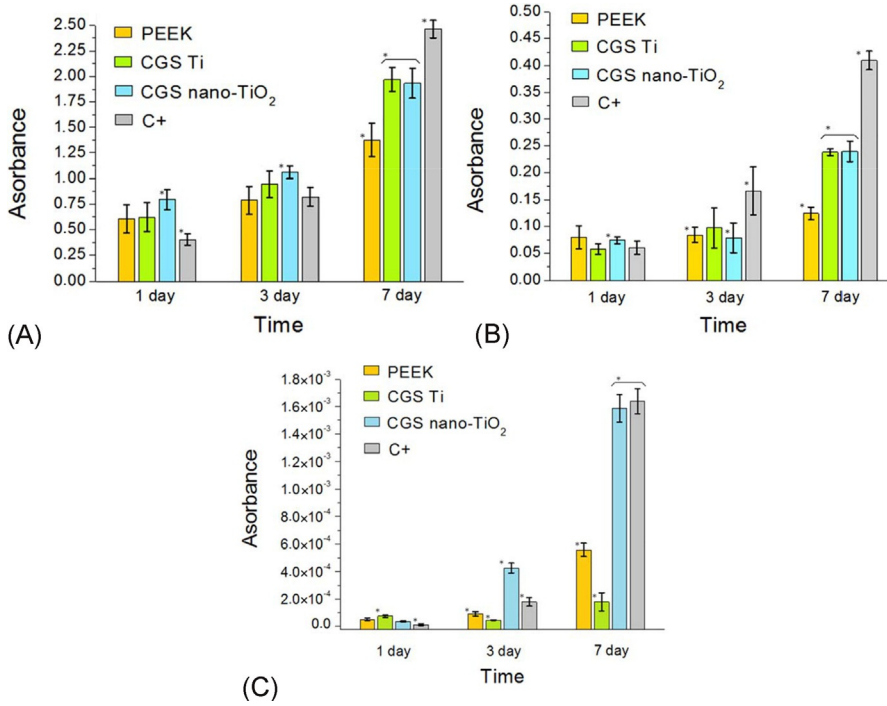

Fig. 2.16 (A) Cell proliferation, (B) cell viability, and (C) cell differentiation results on PEEK, CGS Ti, CGS nano-TiO_2 [73].

Lee et al. [74] performed similar in vitro and in vivo studies on the surface of three dimensionally shaped HA-PEEK substrates by CS. A homogeneous coating regardless of the height difference and gradient level was formed on the surface of PEEK implants. Fig. 2.17 depicts the both ridged and flat surfaces of HA-coated PEEK implant interacted with surrounding bone tissue while fibrous tissue interaction was observed in the case of implant and bone in bare PEEK implant. HA-coated implant enhanced the fusion rate with bone and achieved better stability for bone recovery. Further, in vitro tests concluded that HA-coated PEEK implants demonstrated enhanced ALP activity.

Another recent paper in this series is slightly different from previous studies. Vilardell et al. [75] studied the differences in cell proliferation and differentiation up to 10 days of nanotextured samples taking into consideration factors like topography and composition. The anatase hierarchal structures were achieved upon using nanotexturing surface treatments like (i) anodic oxidation (ii) alkaline treatment onto roughly as-sprayed CGS Cp-Ti coatings. In the anodic oxidation, due to organized

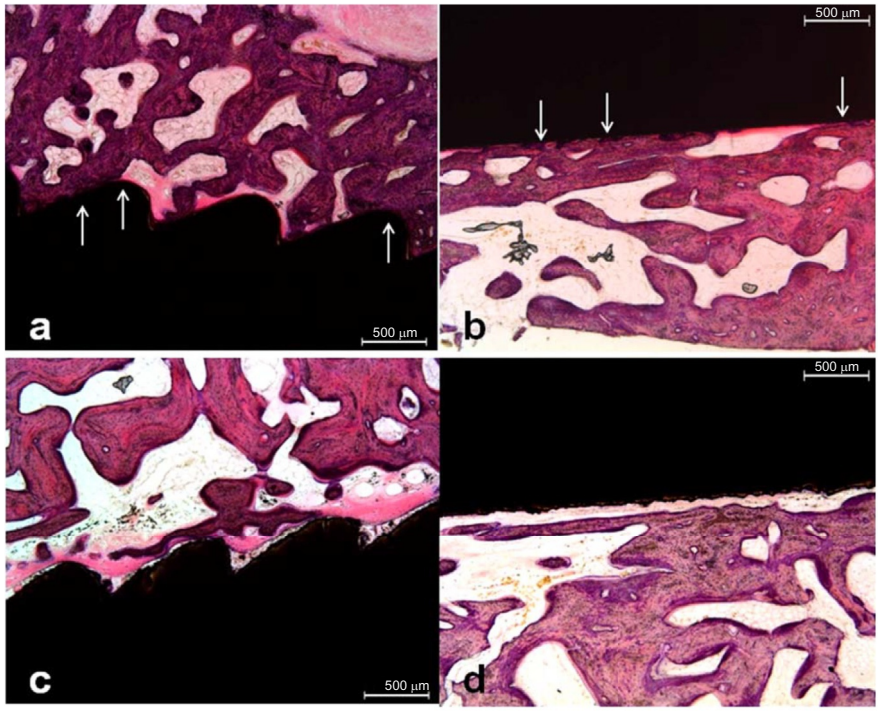

Fig. 2.17 In vivo evaluation of HA-coated PEEK implant, both the (A) ridged and flat, (B) noncoated PEEK implant, (C) ridged, and (D) flat surface.

porous structures which facilitate the cell attachment favoring cell proliferation. It led to the highest cell proliferation values whereas the best surface nanostructure was obtained after the alkaline heat treatment.

2.7 Sustainability and cold spray technique

From the sustainability viewpoint, CS technique has the following features:

Table 2.3 Characteristics parameters of cold spray and some thermal spray techniques [76].

	Wire arc	Plasma	HVOF	Cold spray
Jet temperature (K)	6000	13,000	5500	300–900
Jet velocity (m/s)	50–100	800–1500	1000–2000	1000–2500
Gas	Air, N_2, Ar	Ar, H_2, N_2, He	CH_4, C_3H_6,H_2	Air, N_2, He
Gas flow rates (N/m)	500–3000	40–150	400–1100	1000–3300
Power (kW)	2–5	40–200	150–300	5–10
Feedstock (g/mn)	150–2000	10–80	15–50	20–80
Deposit density (%)	80–95	90–95	>95	>95

- No requirement of high temperature at the beginning of the process. However, temperature increases due to conversion of the kinetic energy to heat.
- The composition of initial phases can be retained.
- Very little amount of oxidation.
- Elimination of solidification stresses that enables the formation of thicker coatings.
- Contains lower defects density.
- Recyclability of this process makes it cost-effective although costly Helium gas is used.

Generally, CS processes are advantageous (see Table 2.3) considering so many aspects, like high deposition efficiency, high deposition rate, high denseness, minimal thermal input to the substrate, no oxidation, and no phase changes. This process enables the production of overall dense coatings with porosity free and pure (without oxidation) coating structures. Furthermore, cold sprayed coatings with impermeable structures have high potential to be used in corrosion protection. Spatial density improvement can be done by optimized powder spraying parameters combination, by optimized powder feedstock (e.g., by adding hard particles to metallic powder) and by assisting or posttreatments (e.g., laser assistance or heat treatments).

Cold spraying has proven to be an optimal thermal spray method in order to prepare fully dense or low-porosity coatings from metallic or composite powder feedstock (e.g., Al, Zn, Cu, Ta, Ti, stainless steel, Ni, and Ni alloys). This opens new possibilities to use cold sprayed coatings as real corrosion barrier coatings in the applications where high corrosion resistance is needed.

2.8 Green aspects of cold spray

CS is considered as a "green" technology. It creates no harmful emissions and consequently has no appreciable environmental impact, and is a powerful tool for sustainability across a wide range of industries by repairing rather than replacing components.

CS can even perform "spot" repairs on components coated with other plating and thermal spray processes which would normally have to be entirely removed and recoated to repair a damaged area. Thus, CS supports sustainable manufacturing in the following ways:

(1) Relatively lower environmental impact.
(2) Supports repair rather than replacement.
(3) High performance extending the shelf life of components.
(4) Replacement of more polluting or less sustainable alternatives.

- Environmental concerns

Overall, CS technology has a low environmental impact as an industrial process [77]. There are no toxic fumes or harmful emissions from the process, metal powders, and inert gases such as helium are recyclable, and the powders can be deposited with very high efficiencies.

- Repair over replacement

Probably the most obvious way that CS technology enhances the sustainability of manufacturing and manufactured systems is through repairing rather than replacing components. The decision to repair or replace is also highly driven by both repair cost and repair frequency. With CS, there is the opportunity to both maintain reasonable repair costs and reduce the frequency of repair.

- Increment in shelf life with the use of advanced coatings [78]

CS offers increased sustainability in a way by replacing less sustainable practices like improving upon the material used in spraying in order to reduce chances of corrosion or wear or instance, ceramics and carbide powders can be easily incorporated into CS deposits, providing significant wear benefits. Furthermore, materials with different electrochemical corrosion potentials can be deposited, such that the CS zone corrodes preferentially (anodic), at a similar rate to the substrate (matching), or is protected from corrosion (cathodic), or because it generally resists chemical corrosion in that environment.

- Replacement of more polluting or less sustainable options

In particular, chrome plating, which releases hexavalent chrome, Cr(VI), and is a genotoxic carcinogen, has been targeted for replacement due to its low exposure limits set by governing bodies such as Occupational Safety and Health Agency (OSHA) [79] in the United States. CS offers an attractive alternative, as no hexavalent chrome or metal fumes are produced during the process. CS also boasts very high deposition efficiencies under optimum conditions. These efficiencies are 2–3 times higher compared to the typical values observed in the thermal spray technique. This increased efficiency can lower the cost and reduce the waste generation compared to the other processes.

2.9 Future prospects and concluding remarks

CS is the solid-state material process, where particles of the order of micron size bond to substrate due to high sonic velocity impact and associate with severe plastic deformation. In the earlier stages, it was only possible to deposit metallic materials to understand its adhesion mechanism. But in recent decades, new advanced materials can be used for coatings for specific applications and hence reducing the excess material consumption. For example, it is now possible to deposit brittle materials such as cermet, metals composites, and metallic glasses in a ductile matrix. However, there are still some open discussions about the cold spraying behavior of brittle materials. For instance, there is a possibility of deposition between two limiting impact velocities using molecular dynamics [80] (Fig. 2.18). Further, there is a certain degree of mechanical shock to the surface due to the particle impact and thermal shock due to the high temperature. In the case of bulk metallic glasses, there is no standard way to characterize the deposition of BMG coatings. The adhesion mechanism of BMG is complex and is yet to be understood. Ceramics and cermet may be classified as intrinsically brittle materials. Small particles agglomerates with a certain level of

porosity were used. But there is very little information available regarding deformation and mechanism of such agglomerates [81]. Further, Shear instability and mechanism of coating buildup in a ceramic deposition is still in the initial stage and more fundamental studies are needed to perform for this phase. Deposition of polymer substrates is new and in the development stage by the cold spraying process. Polymers have got a wide range of applications [39] in the field of electrical device, composites, biomedical devices, and many newly developed high-tech ceramics. The main difference between polymer and metal depositing is the critical velocity and temperature of deposition. Polymers need much lower velocities as compared to metallic deposition. In addition, they have lower melting temperatures. In regard, modifications have been done in the initial design of nozzle, i.e., using cylindrical nozzle [39] instead of de-Laval nozzle. Similarly, the cold spraying technique has gained considerable attention in the field of metal matrix composites. It has improved the mechanical properties, corrosion behavior as well as wear resistance. There have been several studies and all show that there is no alloying, phase transformation, and the onset of thermite reaction during CS deposition. There are lot of questions regarding the effect of granulometry, the mass ratio of powders, and powder characteristics of coatings to the substrate which are needed to be addressed in a systematic way.

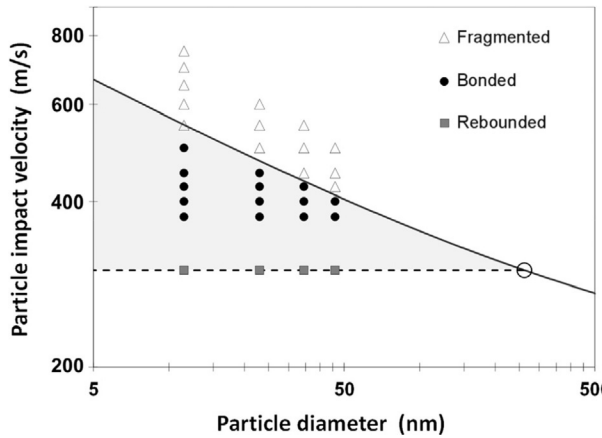

Fig. 2.18 Window of deposition for simulation of the impact of brittle materials [76].

CS is considered one of the most effective and promising technology for producing antibacterial and antimicrobial coatings in biomaterials. It has inhibited the bacterial activity and improved the biocompatibility of implants. However, fundamental studies on the deposition of substrates have not been quantitatively conducted. Results from limited experiments are not adequate to form a concrete conclusion regarding the antibacterial properties of CS depositions. Still, more tests are needed to be carried out using various strains of bacteria, in the future. The killing mechanisms by different transition metals [63] such as silver, nickel, and zinc against *Staphylococcus aureus* has not been explained and a valid mechanism can be suggested by performing a

greater number of experiments with other transition metals. In the study of cold sprayed SS-33.3% Co [64], it has shown the formation of novel metallic biomaterials with improved mechanical and corrosion properties. More in vivo and in vitro tests are required in the upcoming future to assess its antibacterial property. The study of HA coating on PEEK substrate [72] by cold spraying confirmed its clinical applicability in the near future for quicker recovery. Further, 3D PEEK implants having HA deposited on them [74] can have applications in treating degenerative spinal disorders. Further, this new coating technique shall help in strategizing the formation of coatings on 3D layers of inert implant materials in the near future. On the other hand, limited number of investigations exists on the use of nano-material copper [68] as antimicrobial surface. More research needs to be carried out to assess its surface morphology on micron and nanoscale to determine its effect on contact killing of Influenza A Virus. It can be predicted in the near future that new antibacterial coatings produced by CS will exhibit the best compatibility with biomaterials and the new surfaces developed, will kill the bacteria effectively.

2.10 Summary

Thereby we can infer that antiviral agents, e.g., Cu, Ag, and Zn have been thoroughly studied and their uses have increased rapidly for the purpose of combating infections and also to reduce wastage. CS is a new promising technology that has attracted considerable attention in the field of coatings and additive manufacturing like intermetallics, metallic glasses, ceramics, and composites in recent years. It can deposit thick coatings cold with high deposition efficiency as compared to other thermal spraying techniques. It has got unique characteristics like low-temperature processing due to which no oxidation happens and the microstructure of the coatings is the same as that of feedstock material. There has been much interest in research on the development of antimicrobial coatings cold spraying within the past few decades. These cold sprayed coatings can be used for the prevention of transfer of bacteria from the contact surfaces to healthy people.

However, a lot of work still needs to be done to convert the theoretical studies and experimental investigations to the commercial level. More experiments needed to be performed aided by tests on animals and also by other clinical trials in order to accurately interpret the antimicrobial properties that these agents have. There are many material systems left in which the mechanism of deposition by CS and feedstock powders for producing antimicrobial is still not well explored and extensively discussed. More in vitro and in vivo studies are needed to be carried out. These coatings possess huge potential for the development of contact surfaces in many places like hospitals, restaurants, trains, theaters, cash machines, schools, and other objects in the near future. Here, we tried to sketch a strategic present and future perspective of bacteria resistant coatings on metals and polymers substrates using CS. We hope that ideas and proposals presented in this review will help researchers in moving forward and pushing the limits of CS technique toward their clinical antimicrobial applications.

References

[1] D.F. William, Consensus and definitions in biomaterials, in: C. de Potter, K. de Lange, K. de Groot, A.J.C. Lee (Eds.), Advancesin Biomaterials, Elsevier, Amsterdam, 1987, pp. 11–16.

[2] L. Zhao, P.K. Chu, Y. Zhang, Z. Wu, Antibacterial coatings on titanium implants, J. Biomed. Res. (2009) 470–479.

[3] M. Agarwala, T. Barman, D. Gogoi, B. Choudhury, A.R. Pal, R.N.S. Yadav, Highly effective antibiofilm coating of silver-polymer nanocomposite on polymeric medical devices deposited by one step plasma process, J. Biomed. Mater. Res. B Appl. Biomater. 102 (6) (2014) 1223–1235.

[4] G. Xu, D. Pranantyo, B. Zhang, L. Xu, K.-G. Neoh, E.-T. Kang, Tannic acid anchored layer-by-layer covalent deposition of Parasin I peptide for antifouling and antimicrobial coatings, RSC Adv. 6 (18) (2016) 14809–14818.

[5] H. Saman, E. Billur Sevinis, S. Unal, F. Cebeci, Y.Z. Menceloglu, H. Unal, Antibacterial sustained-release coatings from halloysite nanotubes/waterborne polyurethanes, Prog. Org. Coatings 101 (2016) 253–261.

[6] Y.Z. Yang, J.M. Tian, J.T. Tian, Z.Q. Chen, X.J. Deng, D.H. Zhang, Preparation of graded porous titanium coatings on titanium implant materials by plasma spraying, J. Biomed. Mater. Res. 52 (2000) 333–337.

[7] V. Borsari, G. Giavaresi, M. Fini, P. Torricelli, M. Tschon, R. Chiesa, Comparative in vitro study on a ultra-high roughness and dense titanium coating, Biomaterials 26 (2005) 4948–4955.

[8] H. Michels, S. Wilks, J. Noyce, C. Keevil, Copper Alloys for Human Infectious Disease Control, Proceedings of the Materials Science and Technology Conference, Pittsburgh, PA, 2005.

[9] Y. Nie, C. Kalapos, X. Nie, M. Murphy, R. Hussein, J. Zhang, Superhydrophilicity and antibacterial property of a Cu-dotted oxide coating surface, Ann. Clin. Microbiol. Antimicrob. 9 (2010) 25.

[10] A. Lewis, C.W. Keevil, Antibacterial Properties of Alloys and its Alloys in HVAC&R Systems, International Copper Association, Inc, New York, 2004.

[11] H. Jing, Z. Yu, L. Li, Antibacterial properties and corrosion resistance of Cu and Ag/Cu porous materials, Wiley InterScience, 2007, pp. 33–37.

[12] A. Wrona, K. Bilewska, M. Lis, M. Kamińska, T. Olszewski, P. Pajzderski, G. Więcław, M. Jaśkiewicz, W. Kamysz, Antimicrobial properties of protective coatings produced by plasma spraying technique, Surf. Coat. Technol. 318 (2017) 332–340.

[13] H.J.A. Klasen, Historical review of the use of silver in the treatment of burns. Part I early uses, Burns 30 (2000) 1–9.

[14] J.J. Castellano, S.M. Shafii, F. Ko, G. Donate, T.E. Wright, R.J. Mannari, et al., Comparative evaluation of silver-containing antimicrobial dressings and drugs, Int. Wound J. 4 (2) (2007) 114–122.

[15] A.B.G. Landsdown, Silver I: its antibacterial properties and mechanism of action, J. Wound Care 11 (2002) 125–138.

[16] C.L. Fox, S.M. Modak, Mechanism of silver sulfadiazine action on burn wound infections, Antimicrob. Agents Chemother. 5 (6) (1974) 582–588.

[17] P. Gong, H. Li, X. He, K. Wang, J. Hu, W. Tan, et al., Preparation and antibacterial activity of Fe3O4@Ag nanoparticles, Nanotechnology 18 (2007) 604–611.

[18] J. Tian, K.K.Y. Wong, C.M. Ho, C.N. Lok, W.Y. Yu, C.M. Che, J.F. Chiu, P.K.H. Tam, Topical delivery of Silver nanoparticles promotes wound healing, ChemMedChem 00 (2006) 171–180.
[19] S. Pal, Y.K. Tak, J.M. Song, Does the antibacterial activity of silver nanoparticles depend on the shape of the nanoparticle? A study of the gram-negative bacterium *Escherichia coli*, Appl. Environ. Microbiol. 27 (6) (2007) 1712–1720.
[20] S.Y. Yeo, J.S.H. Preparation, Characterization of polypropylene/silver nanocomposite fibres, Polym. Int. 52 (2003) 1053.
[21] B. Li, X. Liu, C. Cao, F. Meng, Y. Dong, T. Cui, et al., Preparation and antibacterial effect of plasma sprayed wollastonite coatings loading silver, Appl. Surf. Sci. 255 (2008) 452–454.
[22] Anti-bacterial and cytotoxic properties of plasma sprayed silver-containing HA coatings, J. Mater. Sci. Mater. Med. 19 (12) (2008) 3603–3609.
[23] M. Meininger, S. Meininger, J. Groll, U. Gbureck, C. Moseke, Silver and copper addition enhances the antimicrobial activity of calcium hydroxide coatings on titanium, J. Mater. Sci. Mater. Med. 29 (2018) 61.
[24] A.M. Vilardell, N. Cinca, A. Concustell, S. Dosta, I.G. Cano, J.M. Guilemany, Cold spray as an emerging technology for biocompatible and antibacterial coatings: state of art, J. Mater. Sci. 50 (2015) 4441–4462.
[25] M. Pajares Lo'pez, P. Herna'ndez Corte's, M. Peregrinaf Palomares, M.A. Herna'ndez Herna'ndez, Va'stagos cementados y no cementados en artroplastias totales de cadera por coxopatı'as meca'nicas, Rev. Esp. Cir. Osteoart. 33 (1998) 59–65.
[26] S. Ramakrishna, J. Mayer, E. Wintermantel, K.W. Leong, Biomedical applications of polymer-composite materials: a review, Compos. Sci. Technol. 61 (2001) 1189–1224.
[27] J.R. Davis, Introduction to thermal spray processing, in: J.R. Davis (Ed.), Handbook of Thermal Spray Technology, ASM International, Materials Park, 2004, pp. 3–13.
[28] R.C. McCune, J.N. Hall, A.N. Papyrin, W.L. Riggs II, P.H. Zajchowski, An exploration of the cold gas-dynamic spray method for several materials system, in: C.C. Berndt, S. Sampath (Eds.), Advances in Therma Spray Science and Technology, ASM International, Houston, TX, 1995, pp. 1–5.
[29] T. Hussain, Cold spraying of titanium: a review of bonding mechanisms, microstructure and properties, Key Eng. Mater. 533 (2012) 53–90. ISSN: 1662-9795.
[30] M.L. Thorpe, T. Spray, Industry in transition, Adv. Mater. Process. 143 (5) (1993) 50–56.
[31] R.C. Tucker Jr., Thermal spray coatings, surface engineering, vol. 5, ASM Handbook, ASM International, 1994, pp. 497–509.
[32] M. Villa, S. Dosta, J. Ferna'ndez, J.M. Guilemany, Laproyeccio'nfrı'a (CGS): Una alternativa a las tecnologı'asconvencionales de deposición, Rev. Metal. 48 (2012) 175–191.
[33] A. Alkhimov, A. Papyrin, V. Kosarev, et al., Gas-dynamic spraying method for applying a coating, [cited 2018 Apr 18]. Available from: http://www.google.com/patents/US5302414, 1994.
[34] T. Goyal, T.S. Sidhu, R.S. Walia, National Conference on Advancements and Futuristic Trends in Mechanical and Materials Engineering, 2010, p. 364.
[35] S. Yoon, H. Kim, C. Lee, Fabrication of automotive heat exchanger using kinetic spraying process, Surf. Coat. Technol. 201 (2007) 9524.
[36] A. P. Alkhimov, A. N. Papyrin, V. F. Kosarev, N. I. Nesterovich and M. M. Shushpanov, Gas-dynamic spraying method for applying a coating, US Patent 5302414, 1994.
[37] A. I. Kashirin, O. F. Klyuev and T. V. Buzdygar, Apparatus for gas-dynamic coating, US Patent 6402050, 2002.

[38] V. Julio, Current and future applications of cold spray technology, Met. Finish. 108 (1) (2010) 37–39.
[39] A. Moridi, S.M. Hassani-Gangaraj, M. Guagliano, M. Dao, Cold spray coating: review of material systems and future perspectives, Surf. Eng. 36 (2014) 369–395.
[40] T.S. Price, Cold Gas Dynamic Spraying of Titanium Coatings, University of Nottingham, 2008.
[41] R.S. Lima, A. Kucuk, C.C. Berndt, J. Karthikeyan, C.M. Kay, J. Lindemann, J. Mater. Sci. Lett. 21 (2002) 1687.
[42] S. Desaulniers, Polycontrols, 2010.
[43] S. Yoon, C. Lee, H. Choi, H. Jo, Kinetic spraying deposition behavior of bulk amorphous NiTiZrSiSn feedstock, Mater. Sci. Eng. 415 (2006) 45.
[44] K. Balani, A. Agarwal, S. Seal, J. Karthikeyan, Transmission electron microscopy of cold sprayed 1100 aluminum coating, Scr. Mater. 53 (2005) 845.
[45] J. Vlcek, L. Gimeno, H. Huber, E. Lugscheider, A systematic approach to material eligibility for the cold-spray process, J. Thermal Spray Technol. 14 (2005) 125–133.
[46] W.-Y. Li, C. Zhang, X. Guo, J. Xu, C.-J. Li, H. Liao, et al., Ti and Ti-6Al-4V coatings by cold spraying and microstructure modification by heat treatment, Adv. Eng. Mater. 9 (2007) 418–423.
[47] Lozier A, Popoola OO, Mason JJ, Forstein M (2009) Bone fracture fixation system. US Patent 0198286 A1, August 6, 2009.
[48] C.-J. Li, W.-Y. Li, Deposition characteristics of titanium coating in cold spraying, Surf. Coat. Technol. 167 (2003) 278–283.
[49] A. Choudhuri, P.S. Mohanty, J. Karthikeyan, Bio-ceramic composite coatings by cold spray technology, Proc. Int. Thermal Spray Conf. (2009) 391–396.
[50] J. Sun, Y. Han, K. Cui, Innovative fabrication of porous titanium coating on titanium by cold spraying and vacuum sintering, Mater. Lett. 62 (2008) 3623–3625.
[51] M. Gardon, A. Latorre, M. Torrell, S. Dosta, J. Ferna'ndez, J.M. Guilemany, Cold gas spray titanium coatings onto a biocompatible polymer, Mater. Lett. 106 (2013) 97–99.
[52] L. Sun, C.C. Berndt, K.A. Gross, A. Kucuk, Material fundamentals and clinical performance of plasma-sprayed hydroxyapatite coatings: a review, J. Biomed. Mater. Res. 58 (2001) 570–592.
[53] X. Zhou, P. Mohanty, Electrochemical behavior of cold sprayed hydroxyapatite/titanium composite in Hanks' solution, Electrochim. Acta 65 (2012) 134–140.
[54] C. Chung, Y.K. Kim, D. Shin, S.R. Ryoo, B.H. Hong, D.H. Min, Biomedical applications of graphene and graphene oxide, Acc. Chem. Res. (2013), https://doi.org/10.1021/ar300159f.
[55] L. Feng, Y. Chen, J. Ren, X. Qu, A graphene functionalized electrochemical aptasensor for selective label-free detection of cancer cells, Biomaterials 32 (2011) 2930–2937.
[56] S. He, B. Song, D. Li, C. Zhu, W. Qi, Y. Wen, L. Wang, S. Song, H. Fang, C. Fan, A graphene nanoprobe for rapid, sensitive, and multicolor fluorescent DNA analysis, Adv. Funct. Mater. 20 (2010) 453–459.
[57] X. Sun, Z. Liu, K. Welsher, J.T. Robinson, A. Goodwin, S. Zaric, H. Dai, Nano-graphene oxide for cellular imaging and drug delivery, Nano Res. 1 (2008) 203–212.
[58] Y. Liu, Z. Dang, Y. Wang, J. Huang, H. Li, Hydroxyapatite/graphene-nanosheet composite coatings deposited by vacuum cold spraying for biomedical applications: inherited nanostructures and enhanced properties, Carbon 67 (2014) 250–259.
[59] Y. Zeng, X. Pei, S. Yang, H. Qin, C. He, S. Hu, L. Sui, Q. Wan, J. Wang, Graphene oxide/hydroxyapatite composite coatings fabricated by electrochemical deposition, Surf. Coat. Technol. 286 (2016) 72–79.

[60] D. Li, Y. Gong, X. Chen, B. Zhang, H. Zhang, P. Jin, H. Li, Room-temperature deposition of hydroxyapatite/antibiotic composite coatings by vacuum cold spraying for antibacterial applications, Surf. Coat. Technol. 330 (2017) 87–91.
[61] N. Sanpo, T. Saraswati, T.M. Lu, P. Cheang, Anti-bacterial property of cold sprayed ZnO-Al coating, in: 2008 International Conference on BioMedical Engineering and Informatics, vol. 1, 2008, pp. 488–491.
[62] N. Sanpo, S.M. Ang, P. Cheang, K.A. Khor, Antibacterial property of cold sprayed chitosan-Cu/Al coating, J. Thermal Spray Technol. 18 (2009) 600–608.
[63] N. Sanpo, J. Tharajak, Antimicrobial property of cold-sprayed transition metals-substituted hydroxyapatite/PEEK coating, Appl. Mech. Mater. 866 (2017) 77–80.
[64] B. Al-Mangour, R. Mongrain, E. Irissou, S. Yue, Improving the strength and corrosion resistance of 316L stainless steel for biomedical applications using cold spray, Surf. Coat. Technol. 216 (2013) 297–307.
[65] X. Jin, L. Gao, E. Liu, F. Yu, X. Shu, H. Wang, Microstructure, corrosion and tribological and antibacterial properties of Ti–Cu coated stainless steel, J. Mech. Behav. Biomed. Mater. 50 (2015) 23–32.
[66] M.S. El-Eskandranya, A. Al-Azmi, Potential applications of cold sprayed Cu50Ti20Ni30 metallic glassy alloy powders for antibacterial protective coating in medical and food sectors, J. Mech. Behav. Biomed. Mater. 56 (2016) 183–194.
[67] V.K. Champagne, D.J. Helfritch, A demonstration of the antimicrobial effectiveness of various copper surfaces, J. Biol. Eng. 7 (2013) 8. http://www.jbioleng.org/content/7/1/8.
[68] K. Sundberg, V. Champagne, B. McNally, D. Helfritch, R. Sisson, Effectiveness of nanomaterial copper cold Spray surfaces on inactivation of influenza a virus. J. Biotechnol. Biomater. 5 (2015) 205, https://doi.org/10.4172/2155-952X.1000205.
[69] D. Persaud-Sharma, A. McGoron, Biodegradable magnesium alloys: a review of material development and applications, J. Biomim. Biomater. Tissue Eng. 12 (1) (2011) 25–39.
[70] Q. Wang, Q. Sun, M.-X. Zhang, W.-J. Niu, C.-B. Tang, K.-S. Wang, X. Rui, L. Zhai, L. Wang, The influence of cold and detonation thermal spraying processes on the microstructure and properties of Al-based composite coatings on Mg alloy, Surf. Coat. Technol. 352 (2018) 627–633.
[71] A.W. Noorakma, H. Zuhailawati, V. Aishvarya, B.K. Dhindaw, Hydroxyapatite-coated magnesium-based biodegradable alloy: Cold spray deposition and simulated body fluid studies, J. Mater. Eng. Perform. 22 (2013) 2997–3004.
[72] J.H. Lee, H.L. Jang, K.M. Lee, H.-R. Baek, K. Jin, K.S. Hong, et al., In vitro and in vivo evaluation of the bioactivity of hydroxyapatite-coated polyetheretherketone biocomposites created by cold spray technology, Acta Biomater. 9 (2013) 6177–6187.
[73] M. Gardon, H. Melero, N. Garcia-Giralt, S. Dosta, I.G. Cano, J.M. Guilemany, Enhancing the bioactivity of polymeric implants by means of cold gas spray coatings, J. Biomed. Mater. Res. B Appl. Biomater. 2014 (102B) (2014) 1537–1543.
[74] J.H. Lee, H.L. Jang, K.M. Lee, H.-R. Baek, K. Jin, J.H. Noh, Cold-spray coating of hydroxyapatite on a three-dimensional polyetheretherketone implant and its biocompatibility evaluated by in vitro and in vivo minipig model, J. Biomed. Mater. Res. B Appl. Biomater. 105 (2017) 647–657.
[75] A.M. Vilardell, N. Cinca, N. Garcia-Giralt, C. Muller, S. Dosta, M. Sarret, I.G. Cano, X. Nogués, J.M. Guilemany, In-vitro study of hierarchical structures: Anodic oxidation and alkaline treatments onto highly rough titanium cold gas spray coatings for biomedical applications, Mater. Sci. Eng. C Mater. Biol. Appl. (2017), https://doi.org/10.1016/j.msec.2018.05.071.

[76] F. Raletz, M. Vardelle, G. Ezo'o, Critical particle velocity under cold spray conditions. Surf. Coat. Technol. 201 (2006) 1942–1947, https://doi.org/10.1016/j.surfcoat.2006.04.061.
[77] V. Champagne Jr., M. West, M. Rokni, T. Curtis, V. Champagne III, B. McNally, Joining of cast ZE41A Mg to wrought 6061 Al by the cold spray process and friction stir welding, J. Therm. Spray Technol. 25 (1–2) (2016) 143–159.
[78] C.P. Hodges, A facility manager's approach to sustainability, J. Facil. Manag. 3 (4) (2005) 312–324.
[79] "Standard on the Fundamentals of Combustible Dust," NFPA 652, 2016.
[80] B. Daneshian, H. Assadi, Impact behavior of intrinsically brittle nanoparticles: a molecular dynamics perspective, J. Therm. Spray Technol. 23 (2014) 541e550.
[81] H. Assadi, et al., Coldspraying—a materials perspective, Acta Mater. (2016), https://doi.org/10.1016/j.actamat.2016.06.034.

Graphene oxide nanosheets as sustainable carbocatalysts: Synthesis of medicinally important heterocycles

3

Prasun Choudhury[a], *Basudeb Basu*[a,b,*]
[a]Department of Chemistry, North Bengal University, Darjeeling, India, [b]Department of Chemistry, Raiganj University, Raiganj, India
[*]Corresponding author. e-mail address: basudeb.basu@gmail.com

3.1 Introduction

Graphene belonging to a new generation of 2D carbon nanomaterials made up entirely of sp^2-C spread endlessly in a honeycomb fashion [1]. Its oxidized form, that is, graphene oxide (GO) and other chemically modified graphenes (CMGs) are often used as heterogeneous catalysts because of their vast potential in catalysis under environmentally benign conditions [2, 3]. Owing to its oxidative and acidic properties, GO has become one of the fundamental carbocatalysts for the synthesis of heterocyclic compounds with a pursuit of biological relevance. The most common method for the preparation of GO dates back to 1958 [4] when Hummers and Offeman presented a safer method for the oxidation of graphite powder into GO (Fig. 3.1). Recently, in 2010, Tour's modified the Hummers method, which claimed to generate a more oxidized form of GO [5].

The oxidative and acidic properties of pristine GO are suitably modified resulting in the formation of new nanocomposite materials with different catalytic properties [2]. These nanocomposites are then used as heterogeneous catalysts for multifarious purposes including the synthesis of diverse complex organic molecules [2].

Heterocyclic scaffolds like benzothiazines, quinoxalines, imidazopyridines, pyridines, and pyrimidones possess extensive medicinal properties [6–9]. Functionalized benzothiazines, quinoxalines, pyridines, and congeners are the key structural units in numerous bioactive molecules. Several clinical drugs and bioactive molecules like amlodipine (calcium channel blockers), zolpidem (for treating insomnia), varenicline (for treating nicotine addiction), omeprazole (proton pump inhibitor), nolatrexed (thymidylate synthase inhibitor), etc. contain privileged heterocyclic scaffolds as their core unit (Fig. 3.2).

Green Approaches in Medicinal Chemistry for Sustainable Drug Design. https://doi.org/10.1016/B978-0-12-817592-7.00003-4
© 2020 Elsevier Inc. All rights reserved.

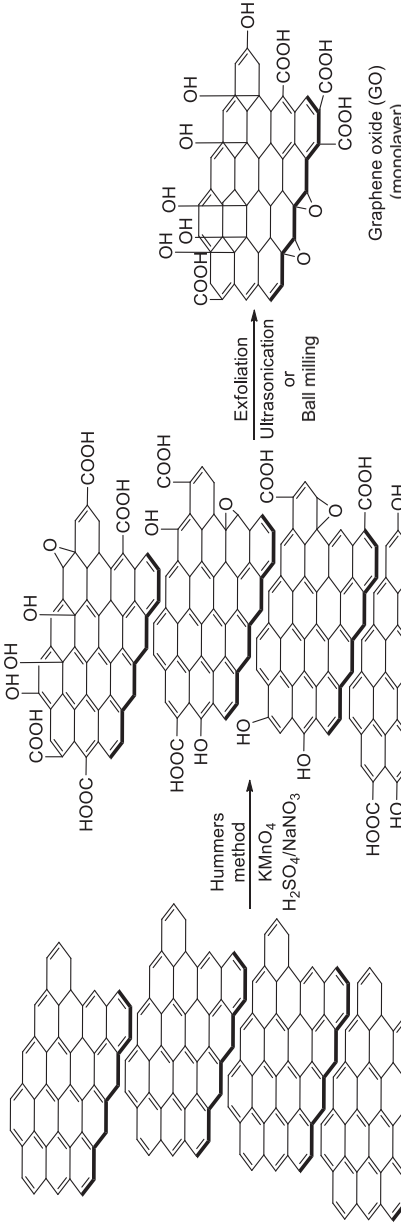

Fig. 3.1 Representation for the preparation of graphene oxide by Hummers method.

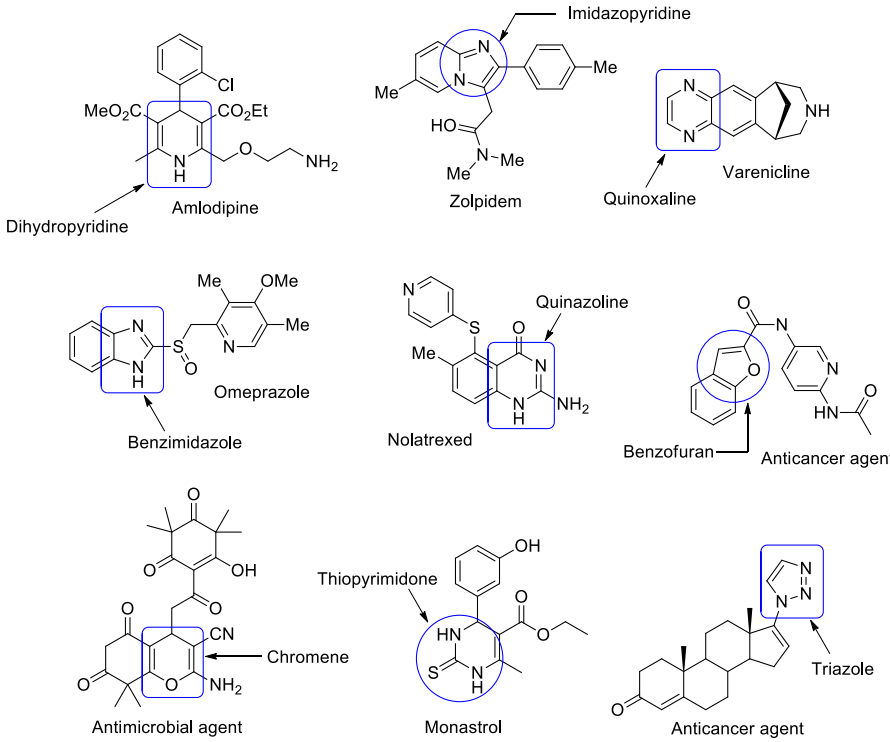

Fig. 3.2 Medicinally important heterocyclic compounds.

3.2 Strategies for the synthesis of medicinally important heterocyclic scaffolds using GO and CMGs

In 2010, Bielawaski and coworkers used GO as a heterogeneous catalyst for oxidation and hydration reactions [10]. Since, then the concept of carbocatalysis using GO has been widely explored for facilitating a number of synthetically useful transformations [11, 12]. The acidic and oxidative functionalities of GO has been suitably exploited in reactions involving aerobic conditions. Besides, there are numerous reports where the surface of graphene/GO has been modified suitably giving rise to chemically modified graphenes (CMGs) [2, 3]. Metal nanoparticles (NPs) are immobilized on to the surface of these materials giving rise to myriads of new nanocomposites with enhanced catalytic activity [2]. Thus, catalysis using GO and CMGs has emerged as an intriguing new direction in contemporary organic synthesis.

In the following section, we attempt to highlight the diverse strategies involved in the synthesis of numerous heterocyclic scaffolds by employing pristine GO or CMGs as heterogeneous catalyst.

3.2.1 Synthesis of substituted pyrroles and related heterocycles using GO nanosheets

Five-membered heterocycles containing N, O, and S are prevalent in nature. A wide range of bioactive natural products like cotinine (tobacco alkaloid) and doxapram (respiratory stimulant) contains 2-pyrrolidinone core as the structural unit [13–15]. Various substituted 2-pyrrolidinone are used in antibacterial [16], antiinflammatory [17], and antimicrobial treatments [18]. Benzofuran which is another important heterocyclic compound contains oxygen as heteroatom. Various bioactive compounds and organic materials possess benzofuran moiety as their core unit [19].

Das et al. have achieved the synthesis of diverse 2-pyrrolidinones, 3,4,5-substituted furanones, and 2-oxo dihydropyrroles using GO nanosheets as catalyst (Scheme 3.1). In the synthesis of 2-pyrrolidinones **1**, a variety of primary amines, aldehydes, and diethyl acetylenedicarboxylate were stirred at room temperature in water for 50–80 min. The same reaction when carried out without any solvent afforded 3,4,5-substituted furanones **2**. Furthermore, the solvent-free variant in the presence of the same or different amine in an equivalent amount resulted in the formation of a different heterocyclic compound, 2-oxo dihydropyrrole **3**. Thus, in the formation of such closely related heterocyclic compounds, solvent played a prominent role by altering the course of the reaction [20].

A series of 2-oxo dihydropyrroles **4** were synthesized by Niknam et al., from three-component reaction among formaldehyde, amines, and dimethyl acetylenedicarboxylate (Scheme 3.2) using GO as catalyst in ethanol at room temperature [21].

Balakrishna and coworkers synthesized diverse 2-substituted indoles **5** and 2-substituted benzofurans **6** using graphene oxide grafted aminobisphosphine-Pd(II) complex (Scheme 3.3) as a heterogeneous catalyst (GO@PNP-Pd). A tandem coupling and cyclization reaction of 2-iodoanilines/2-iodophenols and terminal alkynes results in the formation of indole and benzofuran derivatives in good to excellent yields [22].

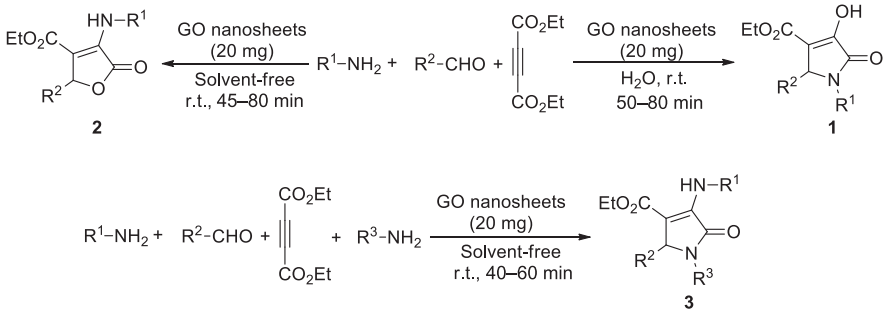

Scheme 3.1 Synthesis of 2-pyrrolidinones, 3,4,5-substituted furanones, and 2-oxo dihydropyrroles.

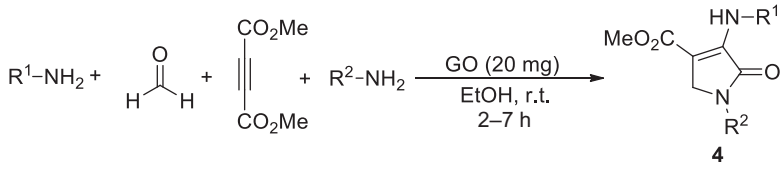

Scheme 3.2 Synthesis of 2-oxo dihydropyrroles.

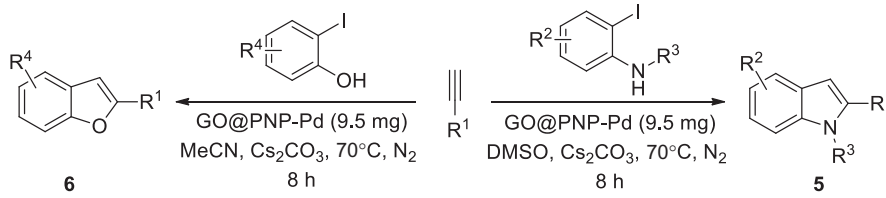

Scheme 3.3 Synthesis of 2-substituted indoles and 2-substituted benzofurans.

3.2.2 Synthetic approaches for quinazoline derivatives

Owing to the diverse application in the field of medicinal chemistry, the synthesis of quinazoline derivatives is a challenging area of research [23, 24]. Several quinazoline derivatives are used as antihypertensive [25], anticancer [26], antitubercular [27], antiinflammation [28], and antitumor agents [29]. Besides, some quinazolinone-based compounds like albaconazole, febrifugine, and isofebrifugine possess a significant biological activity [30].

Recently, Pramanik and his group have developed a facile and convenient protocol for a one-pot synthesis of pharmaceutically interesting diverse quinazoline derivatives using GO as a carbocatalyst (Scheme 3.4). A library of isoindolo[2,1-*a*]quinazoline-5,11-diones **7** were synthesized from 2-carboxybenzaldehyde and 2-aminobenzohydrazides/2-aminobenzamides via domino condensations under solvent-free conditions [31].

Kumari and coworkers accomplished the synthesis of quinazolinones employing DMSO as one carbon synthon in the presence of GO catalyst (Scheme 3.5). A wide range of 3-substituted quinazolinones **8** were synthesized by three-component reaction of isatoic anhydride, substituted methyl amines, and DMSO (one carbon source) [30].

An efficient on-water reaction of 2-aminobenzamide and aldehyde/ketone in the presence of GO leading to the formation of 2,3-dihydroquinazolinones and quinazolin-4(3*H*)-ones has been reported by Das and coworkers (Scheme 3.6). It is noteworthy to mention that during the synthesis of quinazolin-4(3*H*)-ones, oxone has been used as a co-oxidant in combination with graphene oxide catalyst [32].

Mahdavi et al. have developed a novel magnetic copper(II) supported polyethylenimine-functionalized graphene oxide catalyst (Cu@PEI-MGO) for the synthesis of quinazolinones **10** from 2-aminobenzamide and benzylacetamide (Scheme 3.7) in the presence of *N*-hydroxyphthalimide (NHPI) and O_2 as oxidant [33].

Quinazolin-4(3*H*)-ones **11** have been synthesized by Pd-supported magnetic graphene oxide (Pd@MGO) as a heterogeneous catalyst (Scheme 3.8). The methodology involves carbonylation-cyclization of *N*-(2-bromoaryl) benzimidamides, where $Mo(CO)_6$ acts as the CO source [34].

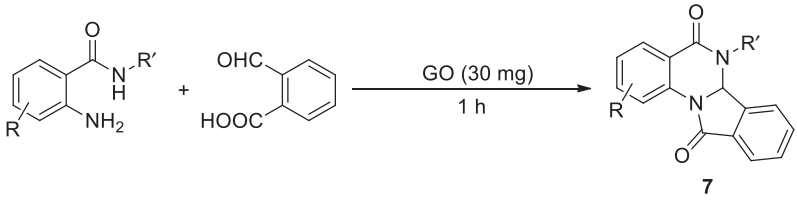

Scheme 3.4 Synthesis of isoindolo[2,1-*a*]quinazolinones.

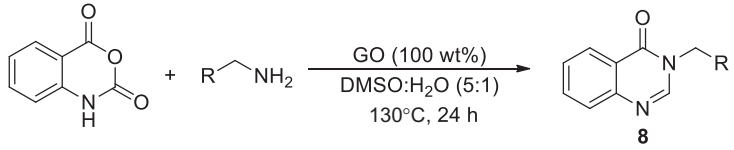

Scheme 3.5 Synthesis of 3-substituted quinazolinones.

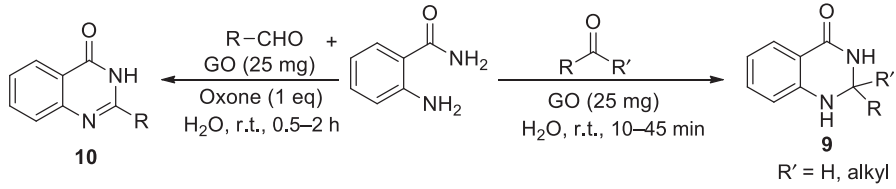

Scheme 3.6 Synthesis of 2,3-dihydroquinazolinones and quinazolin-4(3*H*)-ones.

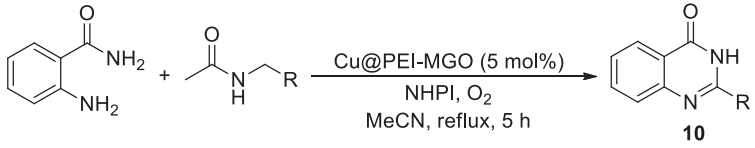

Scheme 3.7 Synthesis of quinazolin-4(3*H*)-ones.

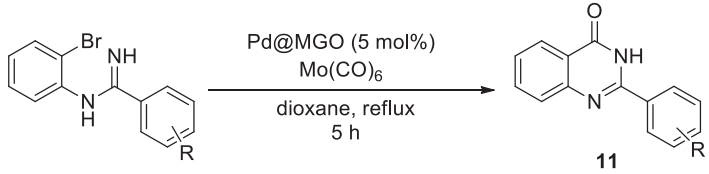

Scheme 3.8 Synthesis of quinazolin-4(3*H*)-ones using Pd-supported magnetic GO.

3.2.3 Multicomponent approach for the synthesis of substituted pyridine derivatives

Among the six-membered nitrogen heterocycles, the entity that has by far received the most attention is pyridine. Another important analog, 1,4-dihydropyridine (1,4-DHP) has attracted much attention owing to its diverse pharmaceutical and biological profile [35–37]. Pyridine and substituted pyridines are privileged pharmacophores for multifarious marketed drugs like amlodipine, nifedipine, etc. [38–41].

Kapoor et al. have developed a one-pot multicomponent strategy for the synthesis of functionalized tetrahydropyridines (Scheme 3.9). A library of diverse polysubstituted tetrahydropyridines **12** was synthesized using β-ketoester, aldehyde, and aniline. The authors also proposed a plausible mechanistic pathway and tested the recyclability of GO for five consecutive runs [42].

Another efficient protocol for the synthesis of 2-amino-3-cyanopyridines **13** has been demonstrated by Khalili (Scheme 3.10). A simple multicomponent reaction among aldehyde, ketone, malononitrile, and ammonium acetate using GO in water under air, formed corresponding pyridine derivatives in good to excellent yields [43].

Sen et al. reported the synthesis of 1,8-dioxoacridine derivatives **14**, which is an essential heterocyclic scaffold for numerous bioactive compounds. Aromatic aldehydes, anilines, and dimedone were reacted (Scheme 3.11) in the presence of DMF as solvent via a multicomponent approach [44].

Recently, Basu and coworkers have reported the synthesis of diverse 1,4-dihydropyridines **15**, 1,8-dioxoacridines **16**, and polyhydroquinolines **17** using amine-functionalized graphene oxide nanosheets (AFGONs) as a heterogeneous and recyclable catalyst (Scheme 3.12). Using pristine GO as catalyst results in the formation of oxidized pyridine derivatives. Further functionalization of the surface of GO limits its oxidizing property and consequently prevents oxidation of 1,4-dihydropyridines to pyridines. The reaction conditions are facile, and a plausible mechanism based on some control experiments has been demonstrated [45].

Kilbas et al. have developed monodispersed Pd, Ru, and Ni NPs embedded on graphene oxide nanosheets by using double solvent reduction method under ultrasonication. The as-prepared material (PdRuNi@GO) has been used for the synthesis of 1,4-dihydropyridines **18** (Scheme 3.13). The same catalyst was also used for the synthesis of hexahydroquinolines **19** based on a multicomponent approach [46].

Hexahydroquinoline derivatives **19** were also synthesized by the research group of Skibsted, using a novel multifunctional heterogeneous catalyst (Scheme 3.13). They prepared ionic liquid grafted graphene oxide (IL@GO) catalyst and characterized it through spectroscopic, microscopic, and MAS-NMR techniques [47].

The synthesis of 1,8-dioxoacridines **20** has been accomplished by using 5-sulfobenzoic acid-functionalized graphene oxide catalyst (SBGO) under solvent-free conditions (Scheme 3.14) [48].

Dandia et al. synthesized pyrroloacridines by using Ag NPs immobilized on reduced graphene oxide surface (Ag NPs/RGO). A three-component approach

involving isatin, anilines, and dimedone in the presence of Ag NPs/RGO (Scheme 3.15) selectively forms pyrrolo[2,3,4-*kl*]acridin-1-ones **21** under microwave irradiation (400 W). The mechanism of the reaction involves the cleavage of amidic C—N bond of isatin followed by cyclization to form the desired pyrroloacridines [49].

Magnetic graphene oxide anchored sulfonic acid ($CoFe_2O_4$/GO-SO_3H) has been prepared and employed in the synthesis of pyrazolopyridines **22** in deep eutectic solvent under microwave irradiation (700 W). Three-component reaction in choline chloride/glycerol as a green solvent furnished the desired products in 84%–95% yield (Scheme 3.16). The reusability of the catalyst and a plausible mechanism has also been demonstrated [50].

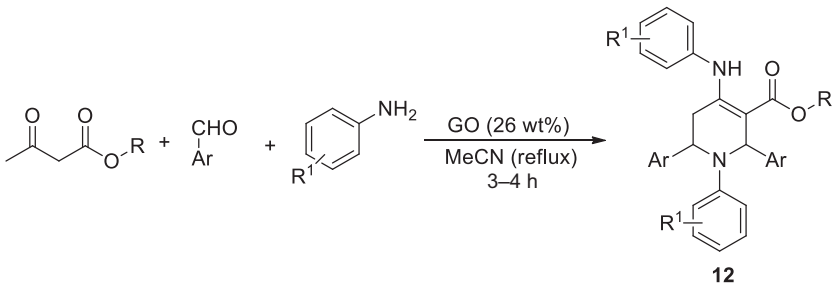

Scheme 3.9 Synthesis of polysubstituted tetrahydropyridines.

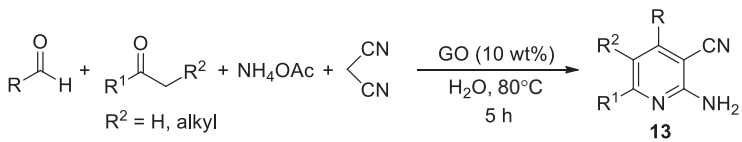

Scheme 3.10 Synthesis of 2-amino-3-cyanopyridines.

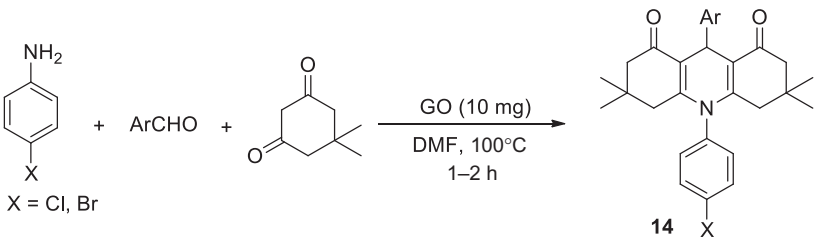

Scheme 3.11 Synthesis of 1,8-dioxoacridine derivatives.

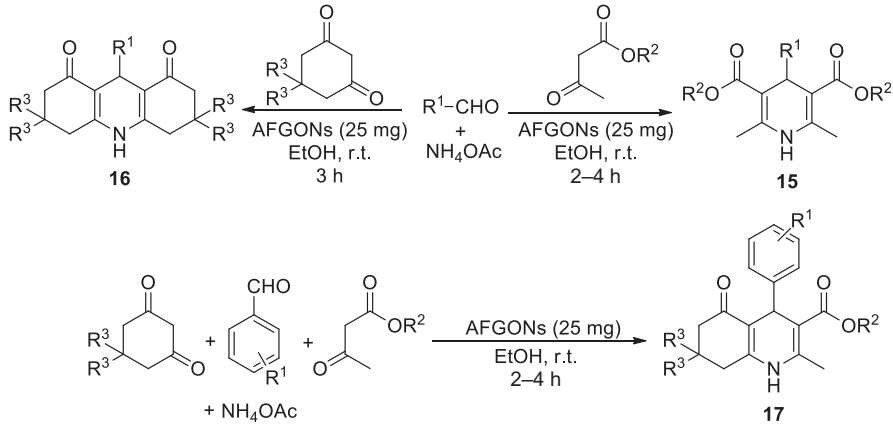

Scheme 3.12 Synthesis of 1,4-dihydropyridines, 1,8-dioxoacridines, and polyhydroquinolines.

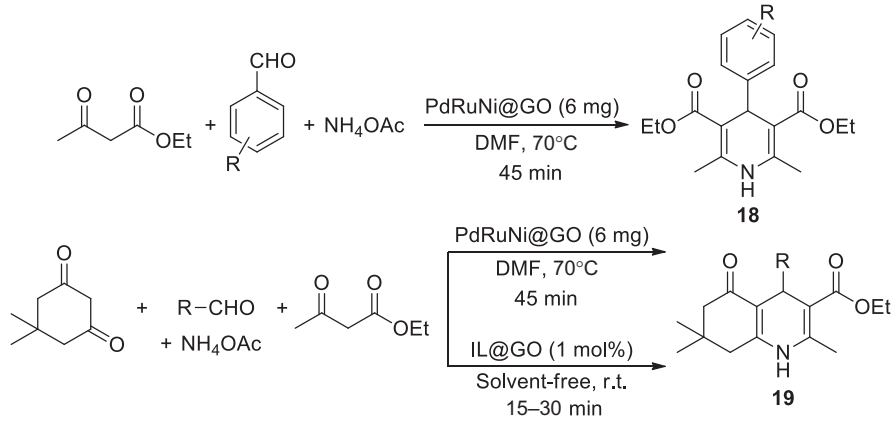

Scheme 3.13 Synthesis of dihydropyridines and hexahydroquinolines.

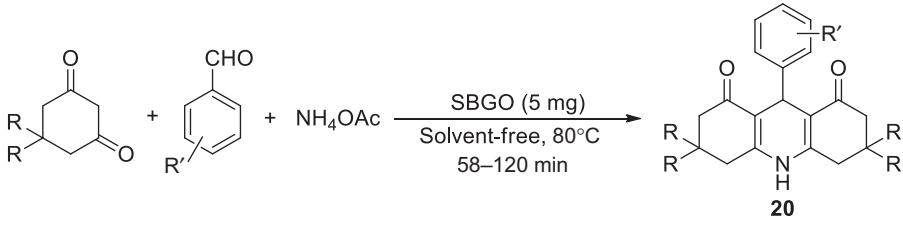

Scheme 3.14 Synthesis of 1,8-dioxoacridines using SBGO catalyst.

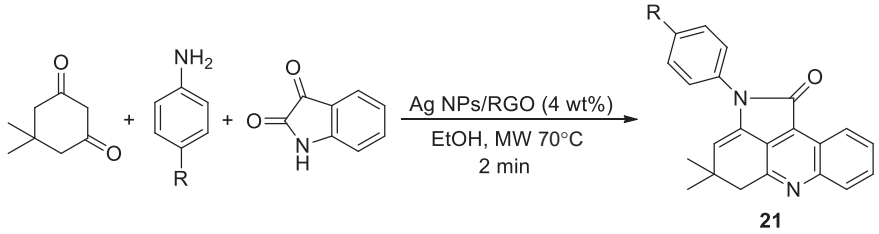

Scheme 3.15 Synthesis of pyrroloacridines.

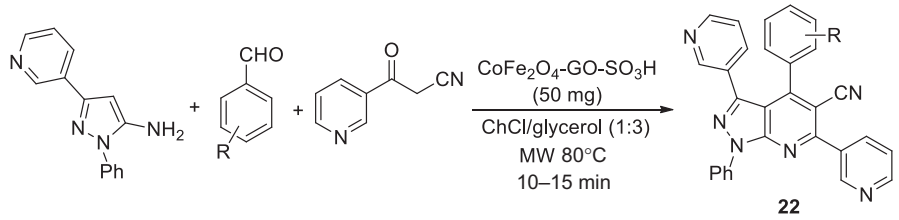

Scheme 3.16 Synthesis of pyrazolopyridines.

Imidazopyridines are another essential class of structural motifs present in a wide variety of clinical drugs like zolpidem, miroprofen, olprinone, etc. [51–61]. Basu et al. have used catalytic graphene oxide in combination with sodium iodide for the facile synthesis of imidazo[1,2-*a*]pyridines **23** and 3-sulfenylimidazo[1,2-*a*]pyridines **24** based on a multicomponent approach (Scheme 3.17). They have also recycled the catalyst and proposed a plausible mechanism involving Ortoleva-king-type intermediate [62].

Artemkina and coworkers have prepared different RGO and boron nitride supported copper nanocomposite catalysts for the synthesis of imidazo[1,2-*a*]pyridines **25**. Among them, copper oxide supported RGO nanocomposite (CuO/RGO) was found to be efficient for the synthesis of substituted imidazopyridines (Scheme 3.18). A three-component reaction of 2-aminopyridines, aldehydes, and terminal alkynes resulted in the formation of **25** in 86%–95% yield [63].

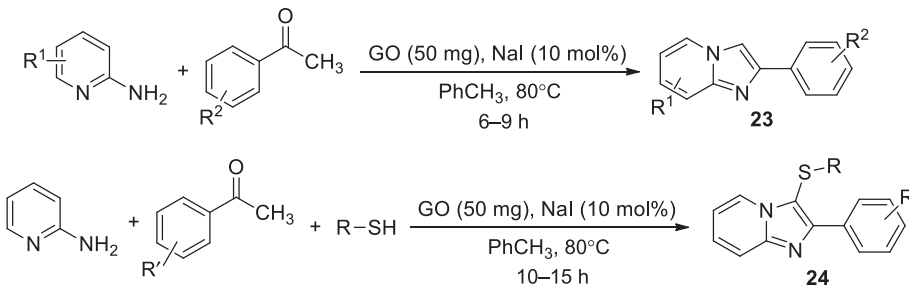

Scheme 3.17 Synthesis of imidazo[1,2-*a*]pyridines and 3-sulfenylimidazo[1,2-*a*]pyridines.

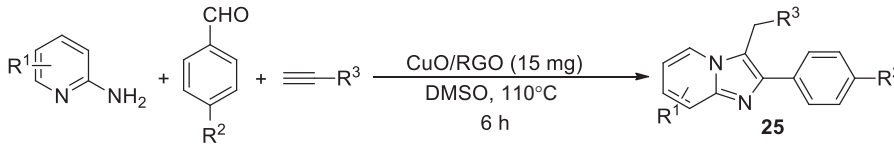

Scheme 3.18 Synthesis of imidazo[1,2-*a*]pyridines.

3.2.4 Synthesis of benzothiazines, benzothiazoles, imidazoles, and benzimidazoles

Functionalized benzothiazines **26** exhibits multifarious biological properties related to HIV, malaria, cardiovascular ailments, etc. [64, 65]. GO as a catalyst displays chemoselectivity in the reaction of 2-aminothiophenol and 1,3-dicarbonyl compounds. The reaction when carried out using *p*-toluenesulfonic acid (*p*-TSA) forms substituted benzothiazoles. However, the same reaction when conducted using GO as catalyst (Scheme 3.19) selectively forms functionalized benzothiazines [66].

Nemade and his groups have synthesized 2-substituted benzothiazoles and benzimidazoles **27** by reacting various aldehydes and 1,2-diaminobenzene/2-aminothiophenol in the presence of GO catalyst (Scheme 3.20) under conventional heating at 60°C, as well as by ultrasonic irradiation at 35°C. The yield of products enhanced when the reaction was performed under ultrasonic irradiation [67].

Sulfonic acid-functionalized magnetic graphene oxide (Fe_3O_4@GO-Pr-SO_3H) was prepared and used in the synthesis tetrasubstituted imidazoles **28**. A four-component methodology using benzil, aromatic aldehydes, primary amines, and ammonium acetate (Scheme 3.21) furnished the desired imidazoles in 89%–95% yield [68].

Zandi et al. have used covalently functionalized fluorinated graphene oxide (A-MFGO) as an efficient catalyst for the synthesis of 2,4,5-trisubstituted imidazoles **29**. The reaction conditions involve a three-component strategy using benzil, aromatic aldehydes, and ammonium acetate (Scheme 3.21) in the presence of A-MFGO (accompanied with H_2SO_4) in EtOH [69].

Graphene oxide-chitosan bionanocomposite has been prepared by Paydar and coworkers. This polysaccharide grafted GO composite was used for the synthesis of 2,4,5-trisubstituted imidazoles **30** through a one-pot three-component reaction of benzoin or benzil, benzaldehydes, and NH_4OAc (Scheme 3.22). Moreover, GO-chitosan composite also exhibits good biocompatibility and biodegradability [70].

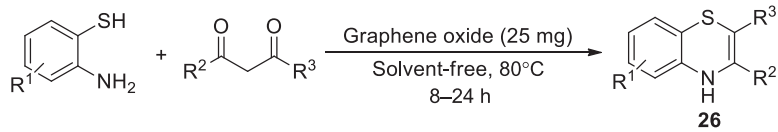

Scheme 3.19 Synthesis of functionalized benzothiazines.

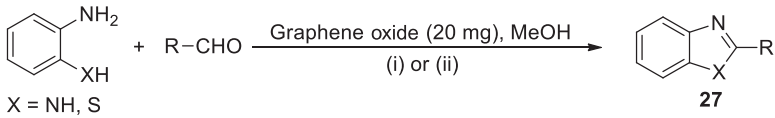

Reaction conditions: (i) conventional heating at 60°C, 3–5.5 h; product yield: 70%–82%
(ii) ultrasonic irradiation at 35°C, 1–2 h; product yield: 42%–89%

Scheme 3.20 Synthesis of benzothiazoles and benzimidazoles.

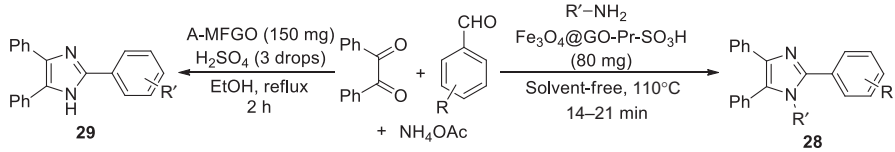

Scheme 3.21 Synthesis of tri- and tetra-substituted imidazoles.

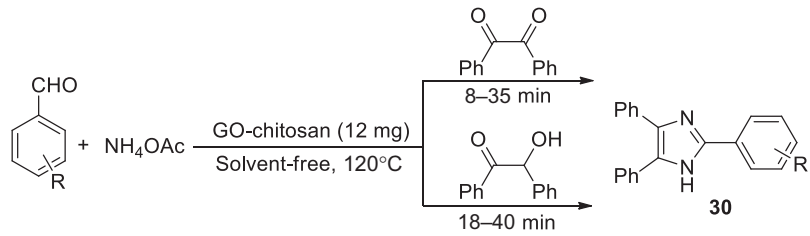

Scheme 3.22 Synthesis of 2,4,5-trisubstituted imidazoles.

3.2.5 Synthesis of functionalized quinoxalines

Quinoxalines are another important class of heterocyclic compounds, associated with wider pharmacological applications [71–73]. They are used in the treatment of bacterial, cancer, and HIV infections [74–77]. Moreover, varenicline, a clinical drug is used for treating nicotine addiction, also contains quinoxaline moiety [78].

A one-pot tandem reduction and condensation of 2-nitroanilines with 1,2-diketo compounds or α-hydroxyketones for the synthesis of quinoxalines **31** has been reported by Basu and his group (Scheme 3.23). Initially, reduction of nitroanilines with hydrazine hydrate takes place in the surface of graphene oxide (GO) or reduced graphene oxide (RGO), which then undergoes condensation reaction to afford diversely functionalized quinoxalines in good to excellent yields [79].

In another method, Chowhan et al. have synthesized spiro compounds, via azomethine ylid-mediated 1,3-dipolar cycloaddition reaction using GO catalyst (Scheme 3.24). A vast array of spiro indenoquinoxaline pyrrolizidines **32** and spiro

oxindoles pyrrolizidines **33** were synthesized with excellent regio- and diastereoselectivity [80].

Shingare et al. have synthesized diverse quinoxalines **34** from *o*-phenylene diamines and 1,2-doketo/substituted phenacyl bromide by using silica-graphene oxide nanocomposite catalyst (SiO_2-GO). A comparison between SiO_2, GO, and SiO_2-GO nanocomposite, with respect to product yield, showed that the yield of the desired product substantially increased when SiO_2-GO was used as catalyst (Scheme 3.25). A cooperative effect between silica and GO was suggested for the enhanced catalytic activity of SiO_2-GO [81].

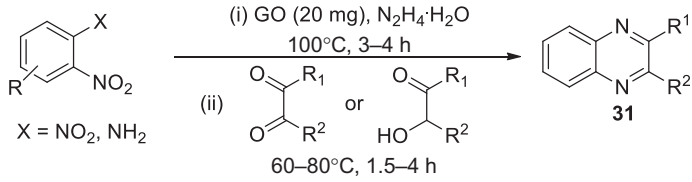

Scheme 3.23 Synthesis of quinoxalines.

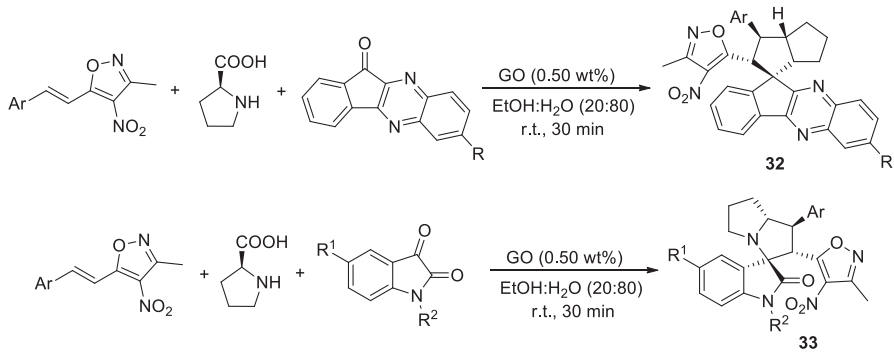

Scheme 3.24 Synthesis of spiro compounds via azomethine ylids.

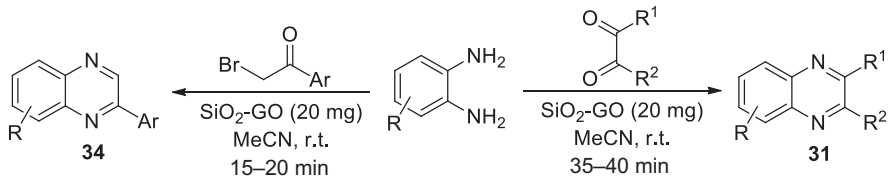

Scheme 3.25 Synthesis of quinoxalines using SiO_2-GO nanocomposite.

3.2.6 Synthesis of 4H-pyrans, coumarins, chromenes, flavones, and xanthenes

The synthesis of pyrans, chromenes, flavones, and other oxygen-heterocycles are an important area of research owing to their diverse application in medicinal chemistry [82–87]. Pyrans and chromenes are widely distributed in natural products and shows antifungal, insecticidal, anti-HIV, antiinflammatory, and antibacterial activities [88–92].

A library of pyranopyrans **35** and pyranoquinolines **36** was synthesized from chalcones and 4-hydroxycoumarin/4-hydroxy-1-methylquinolinone/4-hydroxypyrane (Scheme 3.26) in water using catalytic amount of GO [93].

A simple methodology for the synthesis of substituted pyranocoumarins **37** has been reported by Abbasabadi et al. (Scheme 3.27). A three-component protocol using aldehydes, 4-hydroxycoumarin, and malononitrile using GO under reflux in aqueous EtOH furnished the desired pyranocoumarins [94].

Krishnan et al. have described the synthesis of aryl-substituted 4*H*-chromenes **38** by using potassium-functionalized graphitic carbon nitride supported on reduced graphene oxide (KGCN-RGO) as a heterogeneous recyclable catalyst (Scheme 3.28). Based on a three-component reaction, diverse chromene derivatives were synthesized with high atom economy and shorter reaction time [95].

Gold NPs supported on thiol-functionalized reduced graphene oxide (AuNPs@RGO-SH) catalytic system was utilized for the synthesis of tetrahydro-4*H*-chromenes **39** in aqueous media (Scheme 3.29). The reaction mechanism involves knoevenagel condensation between aldehyde and malononitrile, where Au NPs aids in the polarization of carbonyl moieties [96].

In another report, Sen et al. have also synthesized similar 2-amino-4*H*-chromenes **40** by using bimetallic Pd—Ru NPs immobilized on GO (Scheme 3.30). A three-component reaction of resorcinol, aromatic aldehydes, and malononitrile resulted in the formation of **40** in excellent yields [97].

Badri and his group have synthesized **40** by using sulfonated reduced graphene oxide (RGO-SO_3H) as catalyst (Scheme 3.30). A similar three-component approach was employed in the presence of RGO-SO_3H, which furnished the desired chromenes in 86%–97% yields [98].

A magnetically separable nanocatalyst supported on GO [Fe_3O_4@GO-*N*-(pyridine-4-amine)] was prepared by Abbasabadi and coworkers and used it for on-water synthesis of 4*H*-chromenes **41** and pyrano[2,3-*c*]pyrazoles **42** (Scheme 3.31). Initially, graphene oxide was functionalized with 4-aminopyridine and then Fe_3O_4 NPs, generated in situ from iron salts were grafted onto the amine-functionalized GO [99].

Dandia et al. have developed a green method for the synthesis of pyranopyrazolones via Ag NPs immobilized on graphene oxide nanocomposite (Ag NPs/GO). The catalyst exhibited superior activity for on-water chemoselective synthesis of pyrano[2,3-*c*:6,5-*c*′]dipyrazol-2-ones **43** under ambient temperature (Scheme 3.32) [100].

Copper oxide-reduced graphene oxide (CuO-RGO) has been employed as a heterogeneous catalyst for the synthesis of flavanones **44** via cyclization of a variety of chalcone derivatives (Scheme 3.33). As an application to the methodology, the same catalyst was used in the reaction between the flavanones and aromatic azides for the construction of hybrid triazole derivatives **45** [101].

Yaghoubi et al. have synthesized xanthenediones **46** by using ZnO nanorods embedded on graphene oxide catalyst under solvent-free conditions (Scheme 3.34). The GO/ZnO nanocomposite catalyst exhibits excellent catalytic activity for this

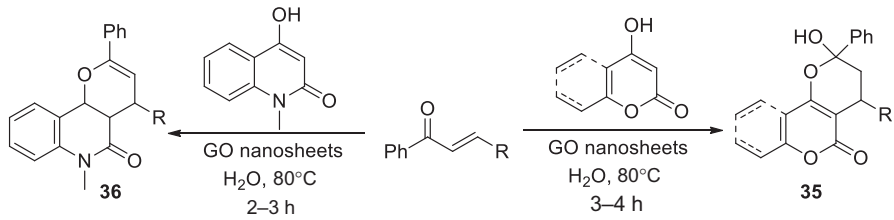

Scheme 3.26 Synthesis of pyranopyrans and pyranoquinolines.

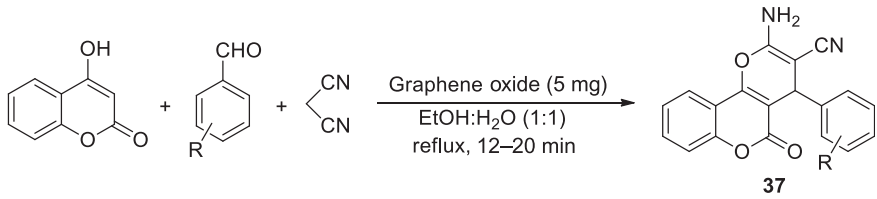

Scheme 3.27 Synthesis of pyranocoumarins.

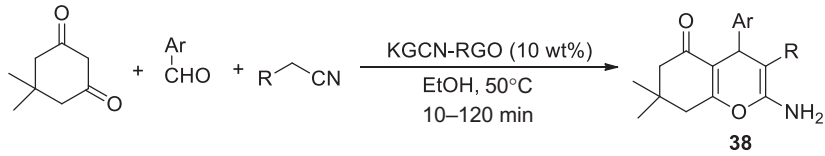

Scheme 3.28 Synthesis of 4*H*-chromenes.

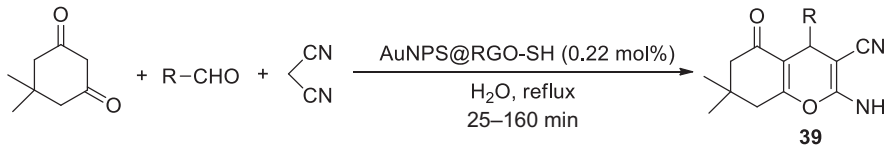

Scheme 3.29 Synthesis of tetrahydro-4*H*-chromenes.

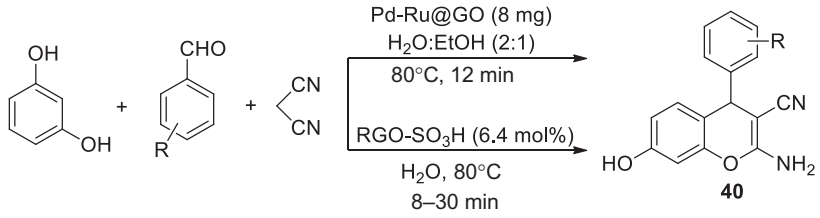

Scheme 3.30 Synthesis of 2-amino-4*H*-chromenes.

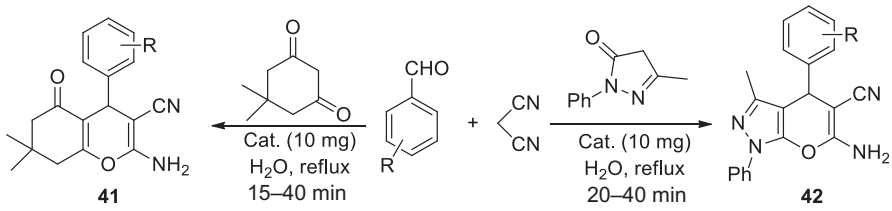

Scheme 3.31 Synthesis of 4*H*-chromenes and pyrano[2,3-*c*]pyrazoles.

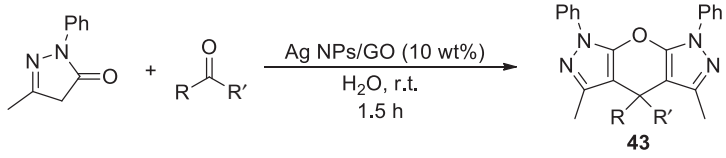

Scheme 3.32 Synthesis of pyranopyrazolones.

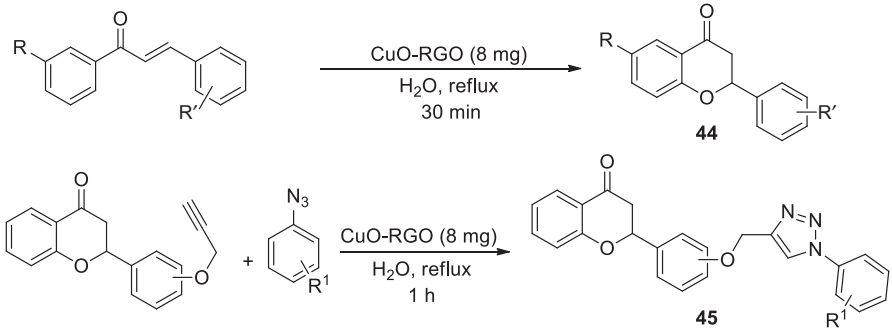

Scheme 3.33 Synthesis of flavanones.

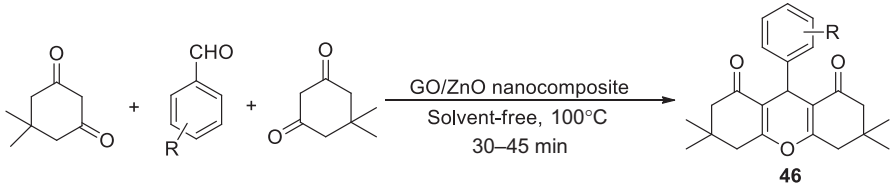

Scheme 3.34 Synthesis of xanthenediones.

pseudo three-component reaction and the corresponding xanthene derivatives were obtained in 89%–99% yield [102].

3.2.7 Synthesis of pyrimidones

Pyrimidines are a well-known structural moiety present in numerous bioactive compounds and in three of the five major bases of nucleic acids (thymine, cytosine, and uracil) [103, 104]. 3,4-Dihydropyrimidone, another important heterocyclic scaffold is also present in several pharmacological agents possessing antibacterial, antimalarial, anticancer, and anticonvulsant properties [105–107]. A multicomponent reaction among aldehydes, urea, and 1,3-dikeoesters, also known as Biginelli reaction is the most efficient method for the synthesis of 3,4-dihydropyrimidone derivatives.

Ashiri et al. have prepared organosilane sulfonated graphene oxide (SSi-GO) and used it as a heterogeneous catalyst (Scheme 3.35) for the synthesis of 3,4-dihydropyrimidones **47** and diarylpyrimidin-2(1*H*)-ones **48**. The reaction conditions are mild affording the desired products in good to excellent yields using ethanol as a green solvent [108].

Sulfonated graphene oxide nanosheet catalyst (GO-SO_3H) was also used for on-water synthesis of 3,4-dihydropyrimidones at ambient temperature (Scheme 3.35). Diverse 3,4-dihydropyrimidin-2(1*H*)-ones/thiones **47** were synthesized from 1,3-dikeoesters, aldehydes, and urea (or thiourea) in 83%–93%. Moreover, the yields of the products increased when GO-SO_3H was used in the place of pristine GO as a catalyst [109].

$BiFeO_3$ nanowires decorated reduced graphene oxide has been prepared by following a hydrothermal method. The nanocomposite material was then employed for several organic reactions including Biginelli reaction for the synthesis of **47** [110].

Recently, Narayanan and coworkers have developed rice husk ash—reduced graphene oxide nanocomposite catalyst (RHA-G10) for the one-pot synthesis of 3,4-dihydropyrimidones **49** under solvent-free conditions (Scheme 3.36) [111]. The same group has developed an efficacious method for the preparation of clay-graphene oxide nanocomposite catalyst, characterized by microscopic and X-ray techniques. The nanocomposite material was employed in the Biginelli reaction for the synthesis of **49** [112].

The research group of Yaghoubi also reported the synthesis of diverse 3,4-dihydropyrimidones **49** by using 1,3,5-tris(2-hydroxyethyl)isocyanurate-functionalized graphene oxide (GO-THEIC) as a heterogeneous catalyst (Scheme 3.36). A probable mechanism involving the role of catalyst has also been demonstrated [113].

Functionalized graphene oxide where the surface of GO was modified by using [3-(2-aminoethylamino)propyl]trimethoxysilane has been prepared by Jonnalagadda et al. After characterization, the prepared nanocomposite was used for the one-pot four-component synthesis of pyrazolo-pyranopyrimidine derivatives **50** under green reaction conditions (Scheme 3.37) [114].

A facile one-pot strategy for the synthesis of pyrido[2,3-*d*]pyrimidine has been reported by Mohebat et al. (Scheme 3.38). Multicomponent reaction of

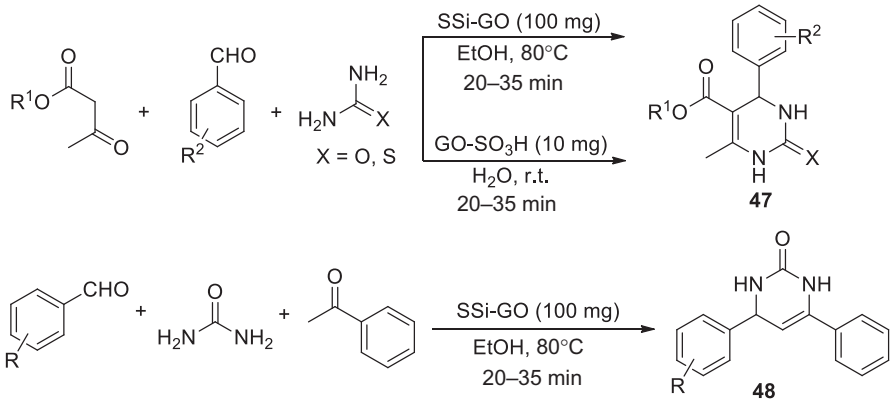

Scheme 3.35 Synthesis of 3,4-dihydropyrimidones and diarylpyrimidin-2(1*H*)-ones.

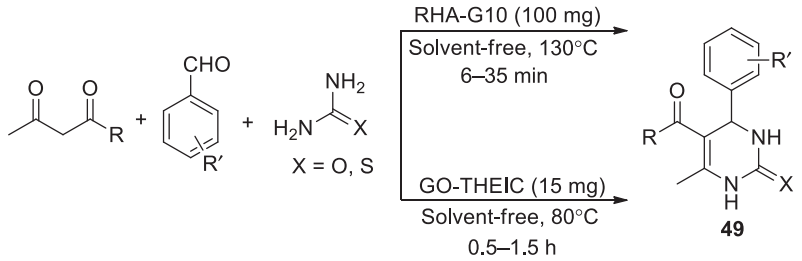

Scheme 3.36 Synthesis of 3,4-dihydropyrimidones.

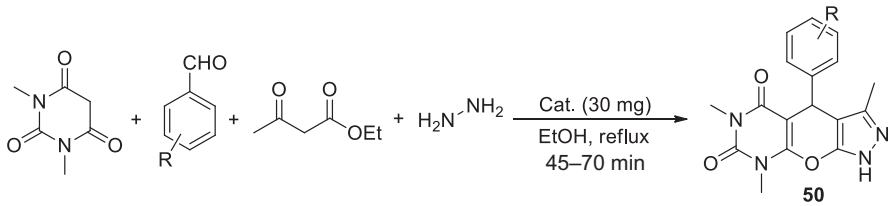

Scheme 3.37 Synthesis of pyrazolo-pyranopyrimidines.

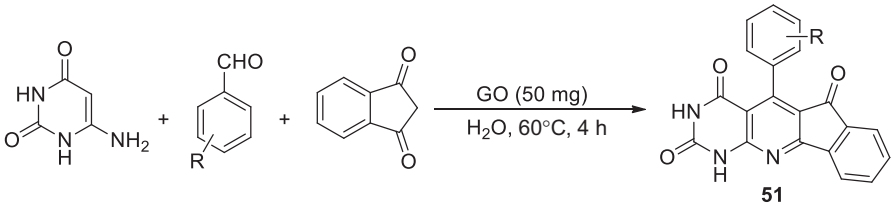

Scheme 3.38 Synthesis of pyrido[2,3-*d*]pyrimidines.

indane-1,3-dione, aromatic aldehydes, and 6-aminopyrimidin-2,4(1*H*,3*H*)-dione using GO in water resulted in the formation of 5-aryl-1*H*-indeno[2′,1′:5,6]pyrido [2,3-*d*]pyrimidine-2,4,6(3*H*)-trione **51** in good to excellent yields [115].

3.2.8 Catalytic processes for the synthesis of 1,2,3-triazoles

Triazoles represent an important class of five-membered heterocycles and constitute the basic skeleton of various medicinal compounds possessing antibacterial [116], antimicrobial [117], anticancer [118], and anti-HIV properties [119]. In 2002, Sharpless and Meldal group have independently reported the most popular way for the synthesis of 1,2,3-triazoles based on Huisgen 1,3-dipolar cycloaddition reaction [120, 121]. A copper-catalyzed reaction between azide and alkynes results in the formation of 1,2,3-triazoles, which is also known as click reaction. The following section enumerates the use of carbonaceous materials based on graphene as a heterogeneous catalyst for the synthesis of triazoles.

Reddy et al. have synthesized 1,4-disubstituted-1,2,3-triazole **52** by using copper oxide supported graphene oxide (CuO-GO) as a heterogeneous catalyst (Scheme 3.39) in water at ambient temperature [122].

A photoinduced protocol for azide-alkyne-cycloaddition reaction has been developed by Yagci and coworkers (Scheme 3.39). The catalytic system comprises mesoporous graphitic carbon nitride (mpg-C_3N_4) and $CuCl_2$/*N*,*N*,*N*′,*N*′,*N*″-pentamethyldiethylenetriamine (PMDETA). The mechanism of the reaction involve in situ reduction of Cu(II) to Cu(I) photochemically (UV light irradiation) on the surface of mpg-C_3N_4. The corresponding triazoles **52** are obtained from 68% to 99% yield [123].

Cu(I) NPs immobilized on to graphene nanosheets (TRGO/Cu) have been prepared and characterized. The nanocomposite has been used for the click synthesis of 1,4-disubstitutes-1,2,3-triazoles **53** in good to excellent yields (Scheme 3.40). Moreover, the TRGO/Cu catalyst shows an excellent activity for bulk click reaction [124].

Bennet et al. have immobilized copper ions on graphene oxide/poly(vinyl imidazole) nanocomposite and used it as heterogeneous catalyst (GO/Pim/Cu) for the synthesis of 1,2,3-triazoles **53** via multicomponent reaction (Scheme 3.41) in the presence of sodium ascorbate as reducing agent [125].

Reduced graphene oxide-cuprous oxide (RGO/Cu_2O) has been used as a recyclable heterogeneous catalyst (Scheme 3.41) for the synthesis of **53** from phenyl acetylene, substituted benzyl bromides, and sodium azide in water [126].

Jiang et al. reported the synthesis of CuBr supported on graphene oxide/Fe_3O_4 as a superparamagnetic nanocatalyst (GO/Fe_3O_4-CuBr). The catalyst has been characterized in detail by spectroscopic and gravimetric analyses and employed in the three-component synthesis of **53** under microwave irradiation (480 W). Diverse 1,4-disubstitutes-1,2,3-triazoles (Scheme 3.41) were prepared in 88%–98% isolated yields [127].

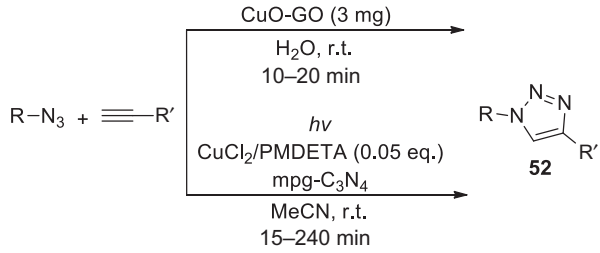

Scheme 3.39 Synthesis of 1,2,3-triazoles.

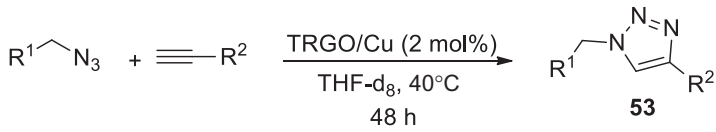

Scheme 3.40 Synthesis of 1,2,3-triazoles using TRGO/Cu.

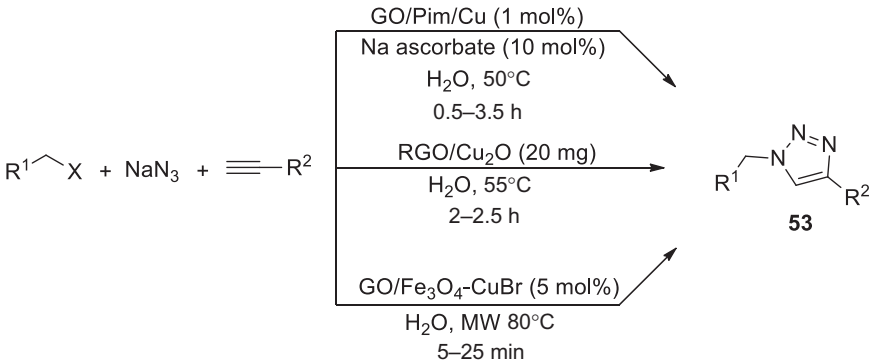

Scheme 3.41 Synthesis of 1,4-disubstituted-1,2,3-triazoles using different catalysts.

References

[1] D.R. Dreyer, R.S. Ruoff, C.W. Bielawski, From conception to realization: an historial account of graphene and some perspectives for its future, Angew. Chem. Int. Ed. 49 (2010) 9336–9344.

[2] B. Qiu, M. Xing, J. Zhang, Recent advances in three-dimensional graphene based materials for catalysis applications, Chem. Soc. Rev. 47 (2018) 2165–2216.

[3] D.R. Dreyer, S. Park, C.W. Bielawski, R.S. Ruoff, The chemistry of graphene oxide, Chem. Soc. Rev. 39 (2010) 228–240.

[4] W.S. Hummers Jr., R.E. Offeman, Preparation of graphitic oxide, J. Am. Chem. Soc. 80 (1958) 1339.

[5] D.C. Marcano, D.V. Kosynkin, J.M. Berlin, A. Sinitskii, Z. Sun, A. Slesarev, L. B. Alemany, W. Lu, J.M. Tour, Improved synthesis of graphene oxide, ACS Nano 4 (2010) 4806–4814.

[6] G. Brahmachari, Green Synthetic Approaches for Biologically Relevant Heterocycles, Elsevier, Oxford, 2014, p. 632.
[7] F. Couty, G. Evano, in: A.R. Katritzky, C.A. Ramsden, E.F.V. Scriven, R.J.K. Taylor (Eds.), Comprehensive Heterocyclic Chemistry, third ed., 11, Elsevier, Oxford, 2008, pp. 409–499.
[8] M. Baumann, I.R. Baxendale, An overview of the synthetic routes to the best selling drugs containing 6-membered heterocycles, Beilstein J. Org. Chem. 9 (2013) 2265–2319.
[9] T.N. Akhaja, J.P. Raval, 1, 3-Dihydro-2*H*-indol-2-ones derivatives: design, synthesis, in vitro antibacterial, antifungal and antitubercular study, Eur. J. Med. Chem. 46 (2011) 5573–5579.
[10] D.R. Dreyer, H.P. Jia, C.W. Bielawski, Graphene oxide: a convenient carbocatalyst for facilitating oxidation and hydration reactions, Angew. Chem. Int. Ed. 49 (2010) 6813–6816.
[11] H.P. Jia, D.R. Dreyer, C.W. Bielawski, Graphite oxide as an auto-tandem oxidation–hydration–aldol coupling catalyst, Adv. Synth. Catal. 353 (2011) 528–532.
[12] D. Sengupta, S. Ghosh, B. Basu, Advances and prospects of Graphene oxide (GO) as heterogeneous 'Carbocatalyst', Curr. Org. Chem. 21 (2017) 834–854.
[13] L.P. Dwoskin, L. Teng, S.T. Buxton, P.A. Crooks, (S)-(−)-cotinine, the major brain metabolite of nicotine, stimulates nicotinic receptors to evoke [3*H*] dopamine release from rat striatal slices in a calcium-dependent manner, J. Pharmacol. Exp. Ther. 288 (1999) 905–911.
[14] P. Singh, V. Dimitriou, R. Mahajan, A. Crossley, Double-blind comparison between doxapram and pethidine in the treatment of postanaesthetic shivering, Br. J. Anaesth. 71 (1993) 685–688.
[15] V. Koz'minykh, N. Igidov, S. Zykova, V. Kolla, N. Shuklina, T. Odegova, Synthesis and pharmacological activity of 3-hydroxy-1,5-diaryl-4-pivaloyl-2,5-dihydro-2-pyrrolones, Pharm. Chem. J. 36 (2002) 188–191.
[16] V. Gein, V. Mihalev, N. Kasimova, E. Voronina, M. Vakhrin, E. Babushkina, Synthesis and antibacterial activity of 1-alkoxyalkyl-5-aryl-4-acyl-3-hydroxy-3-pyrrolin-2-ones, Pharm. Chem. J. 41 (2007) 208–210.
[17] V. Gein, V. Yushkov, N. Kasimova, N. Shuklina, M.Y. Vasil'eva, M. Gubanova, Synthesis and Antiinflammatory and analgesic activity of 1-(2-aminoethyl)-5-aryl-4-acyl-3-hydroxy-3-pyrrolin-2-ones, Pharm. Chem. J. 39 (2005) 484–487.
[18] V. Gein, M. Armisheva, N. Rassudikhina, M. Vakhrin, E. Voronina, Synthesis and antimicrobial activity of 1-(4-hydroxyphenyl)-4-acyl-5-aryl-3-hydroxy-3-pyrrolin-2-ones, Pharm. Chem. J. 45 (2011) 162.
[19] H. Khanam, Bioactive Benzofuran derivatives: a review, Eur. J. Med. Chem. 97 (2015) 483–504.
[20] M. Saha, A.R. Das, Access of diverse 2-Pyrrolidinone, 3, 4, 5-substituted Furanone and 2-Oxo-dihydropyrroles applying Graphene oxide Nanosheet: Unraveling of solvent selectivity, ChemistrySelect 2 (2017) 10249–10260.
[21] M. Bavadi, K. Niknam, Synthesis of functionalized dihydro-2-oxopyrroles using graphene oxide as heterogeneous catalyst, Mol. Div. 22 (2018) 561–573.
[22] D. Sengupta, L. Radhakrishna, M.S. Balakrishna, Synthesis of indoles and benzofurans using a graphene oxide-grafted aminobisphosphine–Pd^{II} complex, ACS Omega 3 (2018) 15018–15023.
[23] D.A. Horton, G.T. Bourne, M.L. Smythe, The combinatorial synthesis of bicyclic privileged structures or privileged substructures, Chem. Rev. 103 (2003) 893–930.

[24] S.B. Mhaske, N.P. Argade, The chemistry of recently isolated naturally occurring quinazolinone alkaloids, Tetrahedron 62 (2006) 9787–9826.
[25] V. Alagarsamy, U.S. Pathak, Synthesis and antihypertensive activity of novel 3-benzyl-2-substituted-3*H*-[1,2,4]triazolo[5,1-*b*]quinazolin-9-ones, Bioorg. Med. Chem. 15 (2007) 3457–3462.
[26] E.A. Henderson, V. Bavetsias, D.S. Theti, S.C. Wilson, R. Clauss, A.L. Jackman, Targeting the α-folate receptor with cyclopenta [g] quinazoline-based inhibitors of thymidylate synthase, Bioorg. Med. Chem. 14 (2006) 5020–5042.
[27] K. Waisser, J. Gregor, H. Dostál, J. Kuneš, L. Kubicová, V. Klimešová, J. Kaustová, Influence of the replacement of the oxo function with the thioxo group on the antimycobacterial activity of 3-aryl-6,8-dichloro-2*H*-1,3-benzoxazine-2,4-(3*H*)-diones and 3-arylquinazoline-2,4-(1*H*, 3*H*)-diones, Farmaco 56 (2001) 803–807.
[28] V. Alagarsamy, V.R. Solomon, K. Dhanabal, Synthesis and pharmacological evaluation of some 3-phenyl-2-substituted-3*H*-quinazolin-4-one as analgesic, anti-inflammatory agents, Bioorg. Med. Chem. 15 (2007) 235–241.
[29] V. Chandregowda, A. Kush, G.C. Reddy, Synthesis and in vitro antitumor activities of novel 4-anilinoquinazoline derivatives, Eur. J. Med. Chem. 44 (2009) 3046–3055.
[30] S. Hada, M.S. Khan Zai, P. Roat, V.P. Verma, A.K. Shah, D.K. Yadav, N. Kumari, Metal-free Graphene oxide promoted a novel multicomponent reaction for the synthesis of 3-substituted Quinazolinones using DMSO as one carbon Synthon, ChemistrySelect 4 (2019) 1176–1179.
[31] C. Bodhak, S. Hazra, A. Pramanik, Graphene oxide: An efficient Carbocatalyst for the facile synthesis of Isoindolo[2,1-*a*]quinazoline-5,11-diones via domino condensation under solvent-free conditions, ChemistrySelect 3 (2018) 7707–7712.
[32] N. Kausar, I. Roy, D. Chattopadhyay, A.R. Das, Synthesis of 2,3-dihydroquinazolinones and quinazolin-4-(3*H*)-ones catalyzed by graphene oxide nanosheets in an aqueous medium: "on-water" synthesis accompanied by carbocatalysis and selective C–C bond cleavage, RSC Adv. 6 (2016) 22320–22330.
[33] M.H. Sayahi, S. Bahadorikhalili, S.J. Saghanezhad, M. Mahdavi, Copper (II)-supported polyethylenimine-functionalized magnetic graphene oxide as a catalyst for the green synthesis of 2-arylquinazolin-4-(3*H*)-ones, Res. Chem. Intermed. 44 (2018) 5241–5253.
[34] S. Bahadorikhalili, S. Ansari, H. Hamedifar, L. Ma'mani, M. Babaei, R. Eqra, M. Mahdavi, $Mo(CO)_6$-assisted Pd-supported magnetic graphene oxide-catalyzed carbonylation-cyclization as an efficient way for the synthesis of 4-(3*H*)-quinazolinones, Appl. Organometal. Chem. (2019) e4769.
[35] R. Mannhold, B. Jablonka, W. Voigt, K. Schönafinger, E. Schraven, Calcium- and calmodulin-antagonism of elnadipine derivatives: Comparative SAR, Eur. J. Med. Chem. 27 (1992) 229–235.
[36] R. Bansal, G. Narang, C. Calle, R. Carron, K. Pemberton, A.L. Harvey, Synthesis of 4-(carbonyloxyphenyl)-1,4-dihydropyridines as potential antihypertensive agents, Drug Dev. Res. 74 (2013) 50–61.
[37] R. Boer, R. Gekeler, Chemosensitizer in tumor therapy: new compounds promise better efficacy, Drugs Future 20 (1995) 499–509.
[38] R.A. Janis, D.J. Triggle, 1, 4-Dihydropyridine Ca^{2+} channel antagonists and activators: A comparison of binding characteristics with pharmacology, Drug Dev. Res. 4 (1984) 257–274.
[39] B. Loev, M.M. Goodman, K.M. Snader, R. Tedeschi, E. Macko, Hantzsch-type dihydropyridine hypotensive agents, J. Med. Chem. 17 (1974) 956–965.
[40] F. Bossert, H. Meyer, E. Wehinger, 4-Aryldihydropyridines, a new class of highly active calcium antagonists, Angew. Chem. Int. Ed. 20 (1981) 762–769.

[41] B.J. Epstein, K. Vogel, B.F. Palmer, Dihydropyridine calcium channel antagonists in the management of hypertension, Drugs 67 (2007) 1309–1327.
[42] A. Gupta, R. Kaur, D. Singh, K.K. Kapoor, Graphene oxide: a carbocatalyst for the one-pot multicomponent synthesis of highly functionalized tetrahydropyridines, Tetrahedron Lett. 58 (2017) 2583–2587.
[43] D. Khalili, Graphene oxide: a reusable and metal-free carbocatalyst for the one-pot synthesis of 2-amino-3-cyanopyridines in water, Tetrahedron Lett. 57 (2016) 1721–1723.
[44] B. Aday, H. Pamuk, M. Kaya, F. Sen, Graphene oxide as highly effective and readily recyclable catalyst using for the one-pot synthesis of 1,8-dioxoacridine derivatives, J. Nanosci. Nanotechnol. 16 (2016) 6498–6504.
[45] P. Choudhury, P. Ghosh, B. Basu, Amine-functionalized graphene oxide nanosheets (AFGONs): an efficient bifunctional catalyst for selective formation of 1,4-dihydropyridines, acridinediones and polyhydroquinolines, Mol. Divers. (2019), https://doi.org/10.1007/s11030-019-09949-0.
[46] T. Demirci, B. Çelik, Y. Yıldız, S. Eriş, M. Arslan, F. Sen, B. Kilbas, One-pot synthesis of Hantzsch dihydropyridines using a highly efficient and stable PdRuNi@ GO catalyst, RSC Adv. 6 (2016) 76948–76956.
[47] S. Sobhani, F. Zarifi, J. Skibsted, Ionic liquids grafted onto graphene oxide as a new multifunctional heterogeneous catalyst and its application in the one-pot multicomponent synthesis of hexahydroquinolines, New J. Chem. 41 (2017) 6219–6225.
[48] M. Mohammadipour, A. Amoozadeh, The synthesis of polyhydroacridines by covalent 5-sulfobenzoic acid-functionalized graphene oxide as a novel, green, efficient, and heterogeneous catalyst, Monatsh. Chem. 148 (2017) 1075–1084.
[49] A. Dandia, A. Sharma, V. Parewa, B. Kumawat, K.S. Rathore, Amidic C–N bond cleavage of isatin: chemoselective synthesis of pyrrolo[2, 3,4-*kl*] acridin-1-ones using Ag NPs decorated rGO composite as an efficient and recoverable catalyst under microwave irradiation, RSC Adv. 5 (2015) 91888–91902.
[50] M. Zhang, P. Liu, Y.-H. Liu, Z.-R. Shang, H.-C. Hu, Z.-H. Zhang, Magnetically separable graphene oxide anchored sulfonic acid: a novel, highly efficient and recyclable catalyst for one-pot synthesis of 3,6-di(pyridin-3-yl)-1*H*-pyrazolo[3,4-*b*] pyridine-5-carbonitriles in deep eutectic solvent under microwave irradiation, RSC Adv. 6 (2016) 106160–106170.
[51] T. Okubo, R. Yoshikawa, S. Chaki, S. Okuyama, A. Nakazato, Design, synthesis and structure–affinity relationships of aryloxyanilide derivatives as novel peripheral benzodiazepine receptor ligands, Bioorg. Med. Chem. 12 (2004) 423–438.
[52] A.N. Jain, Ligand-based structural hypotheses for virtual screening, J. Med. Chem. 47 (2004) 947–961.
[53] M.H. Wiegand, Antidepressants for the treatment of insomnia, Drugs 68 (2008) 2411–2417.
[54] S.M. Hanson, E.V. Morlock, K.A. Satyshur, C. Czajkowski, Structural requirements for eszopiclone and zolpidem binding to the γ-aminobutyric acid type-A (GABAA) receptor are different, J. Med. Chem. 51 (2008) 7243–7252.
[55] J.-B. Véron, H. Allouchi, C. Enguehard-Gueiffier, R. Snoeck, G. Andrei, E. De Clercq, A. Gueiffier, Influence of 6-or 8-substitution on the antiviral activity of 3-arylalkylthiomethylimidazo[1,2-*a*] pyridine against human cytomegalovirus (CMV) and varicella-zoster virus (VZV): part II, Bioorg. Med. Chem. 16 (2008) 9536–9545.
[56] C. Hamdouchi, J. de Blas, M. del Prado, J. Gruber, B.A. Heinz, L. Vance, 2-Amino-3-substituted-6-[(*E*)-1-phenyl-2-(*N*-methylcarbamoyl)vinyl]imidazo[1,2-*a*]pyridines as a novel class of inhibitors of human rhinovirus: stereospecific synthesis and antiviral activity, J. Med. Chem. 42 (1999) 50–59.

[57] A. Gueiffier, S. Mavel, M. Lhassani, A. Elhakmaoui, R. Snoeck, G. Andrei, O. Chavignon, J.-C. Teulade, M. Witvrouw, J. Balzarini, Synthesis of imidazo[1,2-*a*] pyridines as antiviral agents, J. Med. Chem. 41 (1998) 5108–5112.
[58] M. Lhassani, O. Chavignon, J.-M. Chezal, J.-C. Teulade, J.-P. Chapat, R. Snoeck, G. Andrei, J. Balzarini, E. De Clercq, A. Gueiffier, Synthesis and antiviral activity of imidazo [1,2-*a*] pyridines, Eur. J. Med. Chem. 34 (1999) 271–274.
[59] J.T. Starr, R.J. Sciotti, D.L. Hanna, M.D. Huband, L.M. Mullins, H. Cai, J.W. Gage, M. Lockard, M.R. Rauckhorst, R.M. Owen, 5-(2-Pyrimidinyl)-imidazo[1,2-*a*] pyridines are antibacterial agents targeting the ATPase domains of DNA gyrase and topoisomerase IV, Bioorg. Med. Chem. Lett. 19 (2009) 5302–5306.
[60] C. Hamdouchi, J. Ezquerra, J.A. Vega, J.J. Vaquero, J. Alvarez-Builla, B.A. Heinz, Short synthesis and anti-rhinoviral activity of imidazo [1,2-*a*]pyridines: the effect of acyl groups at 3-position, Bioorg. Med. Chem. Lett. 9 (1999) 1391–1394.
[61] J.E. Starrett Jr., T.A. Montzka, A.R. Crosswell, R.L. Cavanagh, Synthesis and biological activity of 3-substituted imidazo[1,2-*a*] pyridines as antiulcer agents, J. Med. Chem. 32 (1989) 2204–2210.
[62] S. Kundu, B. Basu, Graphene oxide (GO)-catalyzed multi-component reactions: green synthesis of library of pharmacophore 3-sulfenylimidazo[1,2-*a*]pyridines, RSC Adv. 5 (2015) 50178–50185.
[63] N. Hussain, P. Gogoi, M.R. Das, P. Sengupta, V.E. Fedorov, I.P. Asanov, M.N. Kozlova, S.B. Artemkina, Development of novel efficient 2D nanocomposite catalyst towards the three-component coupling reaction for the synthesis of imidazo [1,2-*a*] pyridines, Appl. Catal. A 542 (2017) 368–379.
[64] A.E. Sonawane, Y.A. Pawar, P.S. Nagle, P.P. Mahulikar, D.H. More, Synthesis of 1, 4-Benzothiazine compounds containing Isatin Hydrazone moiety as antimicrobial agent, Chin. J. Chem. 27 (2009) 2049–2054.
[65] H. Li, G. Dryhurst, Irreversible inhibition of mitochondrial complex I by 7-(2-aminoethyl)-3,4-dihydro-5-hydroxy-2*H*-1,4-benzothiazine-3-carboxylic acid (DHBT-1): A putative nigral endotoxin of relevance to Parkinson's disease, J. Neurochem. 69 (1997) 1530–1541.
[66] S. Bhattacharya, P. Ghosh, B. Basu, Graphene oxide (GO): An efficient carbocatalyst for the benign synthesis of functionalized 1, 4-benzothiazines, Tetrahedron Lett. 58 (2017) 926–931.
[67] K.B. Dhopte, R.S. Zambare, A.V. Patwardhan, P.R. Nemade, Role of graphene oxide as a heterogeneous acid catalyst and benign oxidant for synthesis of benzimidazoles and benzothiazoles, RSC Adv. 6 (2016) 8164–8172.
[68] A. Nakhaei, Covalently bonded sulfonic acid magnetic graphene oxide promoted synthesis of 1,2,3,4-tetrasubstituted benzimidazoles, Heterocycl. Lett. 7 (2017) 967–973.
[69] H. Hanoon, E. Kowsari, M. Abdouss, M. Ghasemi, H. Zandi, Highly efficient and simple protocol for synthesis of 2,4,5-triarylimidazole derivatives from benzil using fluorinated graphene oxide as effective and reusable catalyst, Res. Chem. Intermed. 43 (2017) 4023–4041.
[70] A. Maleki, R. Paydar, Graphene oxide–chitosan bionanocomposite: a highly efficient nanocatalyst for the one-pot three-component synthesis of trisubstituted imidazoles under solvent-free conditions, RSC Adv. 5 (2015) 33177–33184.
[71] F.A. Rodrigues, I.d.S. Bomfim, B.C. Cavalcanti, C.d.Ó. Pessoa, J.L. Wardell, S. M. Wardell, A.C. Pinheiro, C.R. Kaiser, T.C. Nogueira, J.N. Low, Design, synthesis and biological evaluation of (*E*)-2-(2-arylhydrazinyl)quinoxalines, a promising and potent new class of anticancer agents, Bioorg. Med. Chem. Lett. 24 (2014) 934–939.

[72] A.K. Parhi, Y. Zhang, K.W. Saionz, P. Pradhan, M. Kaul, K. Trivedi, D.S. Pilch, E.J. LaVoie, Antibacterial activity of quinoxalines, quinazolines, and 1,5-naphthyridines, Bioorg. Med. Chem. Lett. 23 (2013) 4968–4974.
[73] R.A. Smits, H.D. Lim, A. Hanzer, O.P. Zuiderveld, E. Guaita, M. Adami, G. Coruzzi, R. Leurs, I.J. de Esch, Fragment based design of new H4 receptor-ligands with anti-inflammatory properties in vivo, J. Med. Chem. 51 (2008) 2457–2467.
[74] F. Rong, S. Chow, S. Yan, G. Larson, Z. Hong, J. Wu, Structure–activity relationship (SAR) studies of quinoxalines as novel HCV NS5B RNA-dependent RNA polymerase inhibitors, Bioorg. Med. Chem. Lett. 17 (2007) 1663–1666.
[75] X. Hui, J. Desrivot, C. Bories, P.M. Loiseau, X. Franck, R. Hocquemiller, B. Figadere, Synthesis and antiprotozoal activity of some new synthetic substituted quinoxalines, Bioorg. Med. Chem. Lett. 16 (2006) 815–820.
[76] Y.B. Kim, Y.H. Kim, J.Y. Park, S.K. Kim, Synthesis and biological activity of new quinoxaline antibiotics of echinomycin analogues, Bioorg. Med. Chem. Lett. 14 (2004) 541–544.
[77] S.T. Hazeldine, L. Polin, J. Kushner, J. Paluch, K. White, M. Edelstein, E. Palomino, T.H. Corbett, J.P. Horwitz, Design, synthesis, and biological evaluation of analogues of the antitumor agent, 2-{4-[(7-chloro-2-quinoxalinyl) oxy] phenoxy}propionic acid (XK469), J. Med. Chem. 44 (2001) 1758–1776.
[78] R. Sarges, H.R. Howard, R.G. Browne, L.A. Lebel, P.A. Seymour, B.K. Koe, 4-Amino[1,2,4]triazolo [4, 3-*a*]quinoxalines. A novel class of potent adenosine receptor antagonists and potential rapid-onset antidepressants, J. Med. Chem. 33 (1990) 2240–2254.
[79] B. Roy, S. Ghosh, P. Ghosh, B. Basu, Graphene oxide (GO) or reduced graphene oxide (rGO): efficient catalysts for one-pot metal-free synthesis of quinoxalines from 2-nitroaniline, Tetrahedron Lett. 56 (2015) 6762–6767.
[80] M.S. Reddy, N.S. Kumar, L.R. Chowhan, Heterogeneous graphene oxide as recyclable catalyst for azomethine ylide mediated 1,3 dipolar cycloaddition reaction in aqueous medium, RSC Adv. 8 (2018) 35587–35593.
[81] P.V. Shitre, R.R. Harale, B.R. Sathe, M.S. Shingare, Silica nanosphere–graphene oxide (SiO_2–GO) hybrid catalyzed facile synthesis of functionalized quinoxaline derivatives, Res. Chem. Intermed. 43 (2017) 829–841.
[82] R.S. Mali, P.P. Joshi, P.K. Sandhu, A. Manekar-Tilve, Efficient syntheses of 6-prenylcoumarins and linear pyranocoumarins: total synthesis of suberosin, toddaculin, O-methylapigravin (O-methylbrosiperin), O-methylbalsamiferone, dihydroxanthyletin, xanthyletin and luvangetin, J. Chem. Soc. Perkin Trans. 1 (2002) 371–376.
[83] Y.-C. Shen, L.-T. Wang, C.-Y. Chen, Chemical transformation of inocalophyllins, preparation of novel pyranocoumarines inocalocyclides, Tetrahedron Lett. 45 (2004) 187–189.
[84] W.-F. Fong, X.-L. Shen, C. Globisch, M. Wiese, G.-Y. Chen, G.-Y. Zhu, Z.-L. Yu, A.K.-W. Tse, Y.-J. Hu, Methoxylation of 3′,4′-aromatic side chains improves P-glycoprotein inhibitory and multidrug resistance reversal activities of 7, 8-pyranocoumarin against cancer cells, Bioorg. Med. Chem. 16 (2008) 3694–3703.
[85] D.L. Galinis, R.W. Fuller, T.C. McKee, J.H. Cardellina, R.J. Gulakowski, J.B. McMahon, M.R. Boyd, Structure-activity modifications of the HIV-1 inhibitors (+)-Calanolide A and (−)-Calanolide B, J. Med. Chem. 39 (1996) 4507–4510.
[86] D.N. Nicolaides, D.R. Gautam, K.E. Litinas, D.J. Hadjipavlou-Litina, K.C. Fylaktakidou, Synthesis and evaluation of the antioxidant and antiinflammatory activities of some benzo [l] khellactone derivatives and analogues, Eur. J. Med. Chem. 39 (2004) 323–332.

[87] C.-R. Su, S.F. Yeh, C.M. Liu, A.G. Damu, T.-H. Kuo, P.-C. Chiang, K.F. Bastow, K.-H. Lee, T.-S. Wu, Anti-HBV and cytotoxic activities of pyranocoumarin derivatives, Bioorg. Med. Chem. 17 (2009) 6137–6143.
[88] L. Bonsignore, A. De Logu, G. Loy, S. Lavagna, D. Secci, Synthesis and antimicrobial activity of coumarin and benzodioxazepine-, diazazepine-and benzoxazepine-substituted penicillins, Eur. J. Med. Chem. 29 (1994) 479–485.
[89] N. Hazeri, M.T. Maghsoodlou, F. Mir, M. Kangani, H. Saravani, E. Molashahi, An efficient one-pot three-component synthesis of tetrahydrobenzo[*b*]pyran and 3,4-dihydropyrano[*c*]chromene derivatives using starch solution as catalyst, Chin. J. Catal. 35 (2014) 391–395.
[90] A. Saini, S. Kumar, J.S. Sandhu, A new LiBr-catalyzed, facile and efficient method for the synthesis of 14-alkyl or aryl-14*H*-dibenzo [*a*,*j*] xanthenes and tetrahydrobenzo[b] pyrans under solvent-free conventional and microwave heating, Synlett 2006 (2006) 1928–1932.
[91] L. Tang, J. Yu, Y. Leng, Y. Feng, Y. Yang, R. Ji, Synthesis and insulin-sensitizing activity of a novel kind of benzopyran derivative, Bioorg. Med. Chem. Lett. 13 (2003) 3437–3440.
[92] R. Thompson, S. Doggrell, J.O. Hoberg, Potassium channel activators based on the benzopyran substructure: synthesis and activity of the C-8 substituent, Bioorg. Med. Chem. 11 (2003) 1663–1668.
[93] N. Kausar, P.P. Ghosh, G. Pal, A.R. Das, Graphene oxide nanosheets: a highly efficient and reusable carbocatalyst catalyzes the Michael-cyclization reactions of 4-hydroxycoumarins, 4-hydroxypyrone and 4-hydroxy-1-methylquinolinone with chalcone derivatives in aqueous media, RSC Adv. 5 (2015) 60199–60207.
[94] S. Khodabakhshi, F. Marahel, A. Rashidi, M.K. Abbasabadi, A green synthesis of substituted coumarins using nano graphene oxide as recyclable catalyst, J. Chin. Chem. Soc. 62 (2015) 389–392.
[95] A. Bahuguna, A. Kumar, T. Chhabra, A. Kumar, V. Krishnan, Potassium-functionalized graphitic carbon nitride supported on reduced Graphene oxide as a sustainable catalyst for Knoevenagel condensation, ACS Appl. Nano Mater. 1 (2018) 6711–6723.
[96] H. Naeimi, M. Farahnak Zarabi, Gold nanoparticles supported on thiol-functionalized reduced graphene oxide as effective recyclable catalyst for synthesis of tetrahydro-4*H*-chromenes in aqueous media, Appl. Organometal. Chem. 32 (2018) e4225.
[97] B. Şen, N. Lolak, Ö. Paralı, M. Koca, A. Şavk, S. Akocak, F. Şen, Bimetallic PdRu/graphene oxide based catalysts for one-pot three-component synthesis of 2-amino-4*H*-chromene derivatives, Nano-Struct. Nano-Objects 12 (2017) 33–40.
[98] S. Behravesh, R. Fareghi-Alamdari, R. Badri, Sulfonated reduced graphene oxide (RGO-SO_3H): as an efficient nanocatalyst for one-pot synthesis of 2-amino-3-cyano-7-hydroxy-4*H*-chromenes
derivatives in water, Polycycl. Aromat. Compd. 38 (2018) 51–65.
[99] D. Azarifar, M. Khaleghi-Abbasabadi, Fe_3O_4-supported *N*-pyridin-4-amine-grafted graphene oxide as efficient and magnetically separable novel nanocatalyst for green synthesis of 4*H*-chromenes and dihydropyrano[2,3-*c*]pyrazole derivatives in water, Res. Chem. Intermed. 45 (2019) 199–222.
[100] A. Dandia, S.L. Gupta, A. Indora, P. Saini, V. Parewa, K.S. Rathore, Ag NPs decked GO composite as a competent and reusable catalyst for 'ON WATER' chemoselective synthesis of pyrano[2,3-*c*:6,5-*c*′]dipyrazol-2-ones, Tetrahedron Lett. 58 (2017) 1170–1175.

[101] A. Gupta, R. Jamatia, R.A. Patil, Y.-R. Ma, A.K. Pal, Copper oxide/reduced graphene oxide nanocomposite-catalyzed synthesis of flavanones and flavanones with triazole hybrid molecules in one pot: a green and sustainable approach, ACS Omega 3 (2018) 7288–7299.
[102] S.H. Banakar, M.G. Dekamin, A. Yaghoubi, Selective and highly efficient synthesis of xanthenedione or tetraketone derivatives catalyzed by ZnO nanorod-decorated graphene oxide, New J. Chem. 42 (2018) 14246–14262.
[103] M. Etienne, S. Cheradame, J. Fischel, P. Formento, O. Dassonville, N. Renee, M. Schneider, A. Thyss, F. Demard, G. Milano, Response to fluorouracil therapy in cancer patients: the role of tumoral dihydropyrimidine dehydrogenase activity, J. Clin. Oncol. 13 (1995) 1663–1670.
[104] V. Saloutin, Y.V. Burgart, O. Kuzueva, C. Kappe, O. Chupakhin, Biginelli condensations of fluorinated 3-oxo esters and 1,3-diketones, J. Fluor. Chem. 103 (2000) 17–23.
[105] M. Ashok, B.S. Holla, N.S. Kumari, Convenient one pot synthesis of some novel derivatives of thiazolo [2,3-*b*] dihydropyrimidinone possessing 4-methylthiophenyl moiety and evaluation of their antibacterial and antifungal activities, Eur. J. Med. Chem. 42 (2007) 380–385.
[106] C.O. Kappe, Biologically active dihydropyrimidones of the Biginelli-type-a literature survey, Eur. J. Med. Chem. 35 (2000) 1043–1052.
[107] G.C. Rovnyak, S.D. Kimball, B. Beyer, G. Cucinotta, J.D. DiMarco, J. Gougoutas, A. Hedberg, M. Malley, J.P. McCarthy, Calcium entry blockers and activators: Conformational and structural determinants of dihydropyrimidine calcium channel modulators, J. Med. Chem. 38 (1995) 119–129.
[108] J. Safari, S. Gandomi-Ravandi, S. Ashiri, Organosilane sulfonated graphene oxide in the Biginelli and Biginelli-like reactions, New J. Chem. 40 (2016) 512–520.
[109] E. Vessally, A. Hassanpour, R. Hosseinzadeh-Khanmiri, M. Babazadeh, J. Abolhasani, Green and recyclable sulfonated graphene and graphene oxide nanosheet catalysts for the syntheses of 3,4-dihydropyrimidinones, Monatsh. Chem. 148 (2017) 321–326.
[110] D. Moitra, B.K. Ghosh, M. Chandel, N.N. Ghosh, Synthesis of a $BiFeO_3$ nanowire-reduced graphene oxide based magnetically separable nanocatalyst and its versatile catalytic activity towards multiple organic reactions, RSC Adv. 6 (2016) 97941–97952.
[111] D.P. Narayanan, S. Sankaran, B.N. Narayanan, Novel rice husk ash - reduced graphene oxide nanocomposite catalysts for solvent free Biginelli reaction with a statistical approach for the optimization of reaction parameters, Mater. Chem. Phys. 222 (2019) 63–74.
[112] D.P. Narayanan, A. Gopalakrishnan, Z. Yaakob, S. Sugunan, B.N. Narayanan, A facile synthesis of clay-graphene oxide nanocomposite catalysts for solvent free multicomponent Biginelli reaction, Arab. J. Chem. 10 (2017) 1–17, https://doi.org/10.1016j.arabjc.2017.04.011.
[113] M.G. Dekamin, F. Mehdipoor, A. Yaghoubi, 1,3,5-Tris(2-hydroxyethyl)isocyanurate functionalized graphene oxide: a novel and efficient nanocatalyst for the one-pot synthesis of 3,4-dihydropyrimidin-2(1*H*)-ones, New J. Chem. 41 (2017) 6893–6901.
[114] S. Rana, S. Maddila, K. Yalagala, S. Maddila, S.B. Jonnalagadda, Covalent modification of organo-functionalized graphene oxide and its scope as catalyst for one-pot pyrazolopyranopyrimidine derivatives, ChemistryOpen 4 (2015) 703–707.
[115] H.R. Dehghanpour, M.H. Mosslemin, R. Mohebat, Graphene oxide: a carbocatalyst for the one-pot multicomponent synthesis of 5-aryl-1*H*-indeno[2′,1′:5,6] pyrido [2,3-*d*] pyrimidine-2,4,6 (3*H*)-trione, J. Chem. Res. 42 (2018) 35–39.
[116] M.J. Genin, D.A. Allwine, D.J. Anderson, M.R. Barbachyn, D.E. Emmert, S.A. Garmon, D.R. Graber, K.C. Grega, J.B. Hester, D.K. Hutchinson, Substituent effects on the

antibacterial activity of nitrogen-carbon-linked (azolylphenyl) oxazolidinones with expanded activity against the fastidious gram-negative organisms Haemophilus influenzae and Moraxella catarrhalis, J. Med. Chem. 43 (2000) 953–970.
[117] D. Dheer, V. Singh, R. Shankar, Medicinal attributes of 1, 2, 3-triazoles: current developments, Bioorg. Chem. 71 (2017) 30–54.
[118] A. Lauria, R. Delisi, F. Mingoia, A. Terenzi, A. Martorana, G. Barone, A.M. Almerico, 1,2,3-Triazole in heterocyclic compounds, endowed with biological activity, through 1, 3-dipolar cycloadditions, Eur. J. Org. Chem. 2014 (2014) 3289–3306.
[119] R. Alvarez, S. Velazquez, A. San-Felix, S. Aquaro, E.D. Clercq, C.-F. Perno, A. Karlsson, J. Balzarini, M.J. Camarasa, 1,2,3-Triazole-[2,5-Bis-O-(*tert*-butyldimethylsilyl)-β-D-ribofuranosyl]-3′-spiro-5″-(4″-amino-1″, 2″-oxathiole 2″, 2″-dioxide) (TSAO) analogs: synthesis and anti-HIV-1 activity, J. Med. Chem. 37 (1994) 4185–4194.
[120] V.V. Rostovtsev, L.G. Green, V.V. Fokin, K.B. Sharpless, A stepwise huisgen cycloaddition process: copper (I)-catalyzed regioselective "ligation" of azides and terminal alkynes, Angew. Chem. 114 (2002) 2708–2711.
[121] C.W. Tornøe, C. Christensen, M. Meldal, Peptidotriazoles on solid phase:[1,2,3]-triazoles by regiospecific copper (I)-catalyzed 1, 3-dipolar cycloadditions of terminal alkynes to azides, J. Org. Chem. 67 (2002) 3057–3064.
[122] V. Reddy, Y. Reddy, B. Sridhar, B. Reddy, Green catalytic process for click synthesis promoted by copper oxide nanocomposite supported on graphene oxide, Adv. Synth. Catal. 358 (2016) 1088–1092.
[123] S. Dadashi-Silab, B. Kiskan, M. Antonietti, Y. Yagci, Mesoporous graphitic carbon nitride as a heterogeneous catalyst for photoinduced copper (I)-catalyzed azide–alkyne cycloaddition, RSC Adv. 4 (2014) 52170–52173.
[124] A.S. Nia, S. Rana, D. Döhler, X. Noirfalise, A. Belfiore, W.H. Binder, Click chemistry promoted by graphene supported copper nanomaterials, Chem. Commun. 50 (2014) 15374–15377.
[125] A. Pourjavadi, N. Safaie, S.H. Hosseini, C. Bennett, Graphene oxide/poly (vinyl imidazole) nanocomposite: an effective support for preparation of highly loaded heterogeneous copper catalyst, Appl. Organometal. Chem. 29 (2015) 601–607.
[126] I. Roy, A. Bhattacharyya, G. Sarkar, N.R. Saha, D. Rana, P.P. Ghosh, M. Palit, A.R. Das, D. Chattopadhyay, In situ synthesis of a reduced graphene oxide/cuprous oxide nanocomposite: a reusable catalyst, RSC Adv. 4 (2014) 52044–52052.
[127] X. Xiong, H. Chen, Z. Tang, Y. Jiang, Supported CuBr on graphene oxide/Fe_3O_4: a highly efficient, magnetically separable catalyst for the multi-gram scale synthesis of 1,2,3-triazoles, RSC Adv. 4 (2014) 9830–9837.

Sustainable green technologies for synthesis of potential drugs targeted toward tropical diseases

4

Dripta De Joarder[a], *Rajarshi Sarkar*[b], *Chhanda Mukhopadhyay*[a,*]
[a]Department of Chemistry, University of Calcutta, Kolkata, India, [b]Narsee Monjee Institute of Management Studies, Indore, India
[*]Corresponding author. e-mail address: cmukhop@yahoo.co.in

4.1 Introduction

With the emergence of green chemistry and green technology, it is imperative to recognize that its usefulness is a "double-edged sword." Terminologies such as "green," "environmentally friendly," and "sustainable" have become hackneyed and lost their true meaning because of their unrestrained usage in the media, advertisements, and scientific discourse. As a matter of fact, there is a palpable mistrust and skepticism among consumers about "green" products and in some cases it is viewed as mere marketing gimmicks. Therefore, it has become extremely crucial that the criticism of widespread misuses of these terms do not become impediment to green chemistry. Moral and ethical ramification of the objective and scope of green chemistry resulted in plentiful discussions. Although, these discussions are important and fruitful but we must be cautious not to lose sight of the ultimate goals of green chemistry to create an infrastructure to enable the innovation of new technologies that decrease or exclude both generation of hazardous substances or methodologies [1–5].

Unfortunately, these misrepresentations are probably the biggest barrier for embracing of green technology at industry and academia. Two most common misperceptions about this field are: (a) green chemistry is a myth and it is propagated by industry as a marketing tool to continue to sell and profit from potentially harmful products and (b) green chemistry is an environmental movement with vested interest forcing expensive yet poor performing products onto customers. Although these views are furthest from the reality, however, for green chemistry to accomplish its goals of preventing pollution, saving the environment from harmful chemical wastes, it must by definition, be successful commercially. For a product to be successful in the market, it should have superior performance at a lower cost. Consumers will not buy a substandard product simply because it is "green." Moreover, very few consumers will be willing to spend too much of a premium for a product because it is "green." Hence, in order for a green technology to have a real impact on the environment and society use, it must be sustainable from both performance and cost perspective [6–10].

Green Approaches in Medicinal Chemistry for Sustainable Drug Design. https://doi.org/10.1016/B978-0-12-817592-7.00004-6
© 2020 Elsevier Inc. All rights reserved.

On the other hand, thousands of people die every day of treatable infectious diseases in the developing world, despite significant advancements in the treatment of infectious diseases [10–15]. Although the cost of treatment of these infectious diseases is not the only barrier to treatment, however, costs do limit access to medicines in the developing countries [16–18]. Meeting the huge demand of affordable medicines and following the principles of green chemistry does not always go hand in hand. But this apparent conflict—the demand to reduce the chemical waste generated and released to the environment during drug synthesis, versus a desire to increase the production of pharmaceutically active drugs that are made and used every year—can also be looked at as an opportunity for green chemistry. Market's demand of lowering prices for drugs can drive discovery of more efficient processes to make and deliver these products. Careful examination of cost factor to the price of pharmaceutical products, ways to reduce both the cost of those products and the environmental footprint associated with their use can be identified. This chapter will focus on the improvements which reduce the cost of active pharmaceutical ingredient (API) for antiretroviral (ARV) drugs, as well as better synthetic methodologies for the most prevalent tropical disease malaria.

In order to devise methods for reduction of the cost of ARV or other drugs, it is critical to understand the underlying relationship between the cost of the product and the market price at first. For a regular drug which is highly commercialized with a dose of 100 mg or more, the price can be broken down into three following categories [19–21]:

- API: contributes about 65%–75% to the market price.
- Formulation and packaging cost: contributes about 10%–20% to the market price.
- Profit: contributes about 5%–15% to the market price.

This cost breakup gives rise to myriad of possibilities for interventions that can bring down cost and can be divided into two interrelated categories:

- Reduction of the cost of the API.
- Finding optimum API dose for maximum effect.

In the clinical development stage of a new drug, often the simplest composition that delivers a clinically effective dose of drug in blood plasma effectively is selected for the development in order to save time, cost, and complexity in the drug development process. The amount of drug present in blood plasma after injecting intravenously, in human subjects is known as 100% bioavailability for any given drug. On the other hand, the amount of drug present in blood plasma after exposure to a specific dose form is called relative bioavailability of that drug-delivery form. Many drugs exhibit relatively low bioavailability after oral dosing, and most essential medicines are delivered orally in the developing countries. The remainder of the drug gets out of the system through excretion (either as "parent" drug or as metabolites) without interacting with the molecular target to provide a positive therapeutic effect. The excretion of "parent" APIs has an environmental impact as well. So to find an optimum dosage of a drug that is safe, convenient, and yet increases the bioavailability can be viewed as a progress in human dosing as well as having a green impact.

4.2 Dose reduction through improved drug composition

A variety of protease inhibitor (PI) drugs for treatment of HIV also have blood levels that are "boosted" by co-dosing in combination with the PI drug ritonavir. This phenomenon is known as "pharmacokinetic enhancement" and is achieved by the inhibition of the cytochrome enzyme CYP 450 isoform 3A4. The metabolism of ritonavir as well as other PIs slows down as its binding to CYP 3A4 isoform results in a down-regulation. This in turn increases the bioavailability of several PI drugs significantly that are primarily metabolized by this enzyme. Extended release mechanism can also open the door for more efficient yet effective dosing. In case of treating infectious diseases, the most important dosing consideration becomes the determination of the minimum inhibitory concentration (MIC) required for effective drug action. Then, it is to establish a dose (amount and frequency) that produces drug exposures that exceed the MIC. With an immediate-release mechanism, a disproportionate peak concentration (C_{max}) often observed immediately after dosing. This apparent unappealing feature of immediate-release delivery becomes necessary in order to maintain the drug concentration in blood stream above the MIC for a long enough period of time so that the frequency of dosing is not exorbitant. Studies found that patients also preferred anti-infective drugs when delivered once or twice daily, rather than three or four times per day. The use of extended release drugs has multiple benefits: lowering the peak concentration (C_{max}) and "smoothing" the curve that describes blood concentrations of the drug with time. This is often correlated to a lowered incidence of adverse side effects. Furthermore to its advantage decreased dosing frequency reduced the release of metabolized drug into the environment considerably. Advances in drug-delivery technology allow selective delivery of drugs into specific tissues, organs, or cell types in the body that need it most, paving ways for even lower doses overall and reducing side effects for patients as well as the harmful effect in the environment [22–25].

4.3 Green dose setting

The clinical processes for setting the dose of an under trial new drug are time consuming and expensive. Proper selection of dose is often achieved on the basis of a few crucial Phase II clinical studies that may span a broad range of dosages. This crude and random design and interpretation of these studies is often driven by the identified maximum tolerated dose and the minimum ineffective dose. For a new drug, exhibiting efficacy often boils down to equivalent or superior to existing drugs in the market, while the need to select a dose that minimizes nonsevere side effects gets ignored. This scenario is most prevalent in case of drugs intended to treat infectious diseases, where the primary consideration in early clinical trials is to dose patients to the maximum tolerated dose in order to achieve maximum inhibition of the infectious agent. But in the process what gets sacrificed or often overlooked is the relation between a certain drug's tolerability and effect of that drug on a particular patient, with poor adherence being a major driver of treatment failure and drug resistance

[26–27]. Additional clinical studies to better select the truly optimal doses of certain drugs may add to cost and time. However, existing data supports that it can produce improved efficacy for improving patient outcomes. Dose optimization studies also provide improved drug tolerability and reduced adverse clinical events. In addition, this reduces the amount of drug required per dose and, in turn, the amount of drug excreted into the environment as well. Hence, studies to find optimum dose in great details can clearly be in the patient's best interest and the reduced environmental impact of drug excretion is aligned with this purpose.

In the area of HIV treatment, there have been multiple precedents for an effective dose optimization strategy, along with the results of dose reduction studies on stavudine (d4T) [28,29], where dosing was decreased from 40 to 30 mg BID (twice daily). As anticipated dose optimization trials produced reduced side effects along with improved tolerability. In case of antiretroviral drug zidovudine (AZT), dosing was reduced from the originally approved dose of 400 mg every 4 h (six times daily) to the current recommended dose of 300 mg BID. A number of other opportunities have been identified for dose optimization. These opportunities include reformulation to reduce the dose of efavirenz (EFV), tenofovir, and multiple other PIs [30,31].

4.4 Reduction of cost through green chemistry

The most simplistic methods for cost reduction of drugs are to reduce the cost of the most expensive component of drugs: the API. At its elemental form, the process for making any APIs comprises of converting commercially available raw materials, which are simpler, into the APIs through a series of chemical conversions. Hence, the cost of this process is primarily dependent on the cost of the raw materials and the efficiency of the chemical process that converts those materials into the API. These same factors—choice of raw materials, number of synthetic steps, and the efficiency of the process for API production—also dictate the amount and nature of waste produced during the manufacture of the drug.

The manufacturing process for an API is generally fixed and well-defined in advance prior to manufacturing the supplies for Phase III clinical trials. The starting materials, synthetic protocols, catalysts (if required), solvents, reaction and isolation conditions, etc. are fixed. Thus, the information about related substances present, residual solvent levels, and physicochemical characteristics of the API are well defined within the specifications prior to process validation in the context of the regulatory filing. Because of the time constraint present in getting a drug through the clinical trial and approval process, these manufacturing processes are locked well before peak efficiency can be reached through process research. At or after receiving the approval, it is disadvantageous to change the manufacturing process mentioned in the regulatory filing for market approval, because of the risk, expense, and time involved. Changes to a manufacturing process, if significant, may require additional toxicology studies or a bioequivalence study in order to obtain regulatory approval; such changes must deliver substantial advantages in terms of time and cost to justify the new process.

However, through process optimization the manufacturing pharmaceutical company of the drug can often improve efficiency with which the raw materials are converted into the API. With judicious employment of the improvement along with the regulatory approval, the cost and environmental impact of making the API are reduced significantly. In some cases, a more drastic change of the process can be undertaken, in the form of introducing a wholly or substantially new synthetic approach or starting materials.

4.5 Green chemistry in ARV therapy

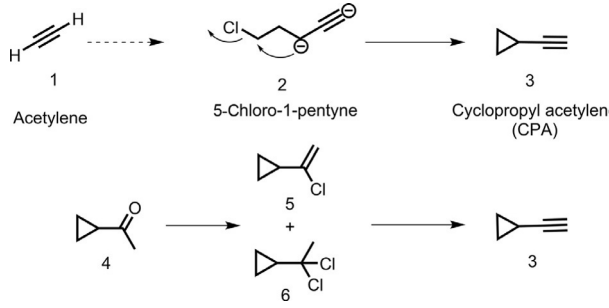

Scheme 4.1 Preparation of cyclopropyl acetylene.

Efavirenz **9**, commercialized as EFV is a well-known nonnucleoside inhibitor of HIV-1 reverse transcriptase drug developed by Dupont Pharmaceuticals, was approved by the US FDA in September 1998. EFV is the key part of the ARV cocktails such as efavirenz/lamivudine/tenofovirdisoproxilfumarate (EFV/LMV/TDF) and efavirenz/emtricitabine/tenofovirdisoproxilfumarate (EFV/FTC/TDF) that are highly recommended for the first-line management of HIV/AIDS in many countries. The demand for EFV in the developing nations (including Brazil and South Africa) in 2011 was estimated at approximately 500 metric tons. EFV is generally prescribed to adults as once daily, 600 mg dose. Under President's Emergency Plan for AIDS Relief (PEPFAR) program, several Indian companies have been approved by the US FDA for generic production of EFV for less-developed countries. API of EFV is, therefore, synthesized by several distinct processes derived from a common route of synthesis. Originally, EFV was introduced to the market at a manufacturing cost of roughly $1600/kg. However, with the advancement of process methods and high demand from the market brought the cost of EFV API down to US$130/kg in 2011. The reduction in cost of EFV was accompanied by the increasing "greenness" of chemical transformations. Two critical sets of improvements played a pivotal role in substantially increasing the "greenness" of EFV manufacturing overtime. The first of these is change in the production of the key building-block cyclopropylacetylene (CPA, **3**; Scheme 4.1); while the second one being the improvements in the asymmetric addition of CPA, **3** to the trifluoromethylketone, **7** to generate

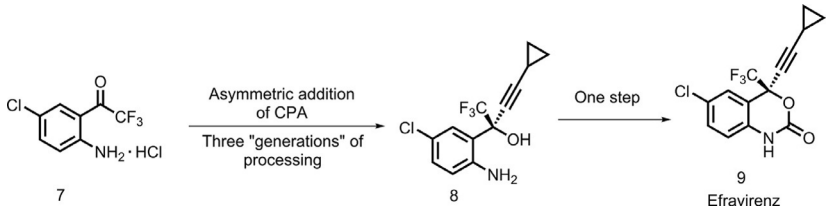

Scheme 4.2 Preparation of efravirenz.

8 (Scheme 4.2). Multiple manufacturers have prepared 5-chloro-1-pentyne, **2** via reaction of sodium acetylide, with 1-bromo-3-chloropropane in liquid ammonia. The laboratory-scale conversion of 5-chloro-1-pentyne to CPA via its dianion using >2 equiv. of *n*-butyllithium as base was first published by Zhao et al. [32]

The by-product of this procedure is large amount of butane, and hence the CPA produced in this method must be purified by fractional distillation in order to produce material of adequate purity for use in the following asymmetric addition step. Although this procedure has been redesigned in a later patent [33], this method still suffers from the use of 2 mol equiv. of a very strong alkyllithium base. In an alternative approach, cyclopropyl methyl ketone, **4** was reacted with phosphorous (V) pentachloride in quinoline to prepare a mixture of vinyl chloride and geminal dichloride [34]. Elimination of the chlorides to CPA followed by distillation gives a viable synthesis from inexpensive starting materials. However, the industrial synthesis of CPA from cyclopropanecarboxaldehyde, **11** is proven to be at least 70% more efficient to either of these approaches in terms of *E*-factor (Scheme 4.3). Although the conversion of aldehyde to acetylene does not take place with a high *E*-factor, but the usage of the aldehyde as a starting material for a one-pot reaction sequence makes the overall process significantly "greener." Cyclopropanecarboxaldehyde is easily derived from 2,3-dihydrofuran, **10** (2,3-DHF) by a thermal rearrangement reaction. 2,3-DHF is obtained from butadiene by way of butadiene monoxide. Butadiene and the butadiene monoxide are used in thousands of ton scale for many commercial products, such as synthetic rubber and THF; this amounts to a one-pot synthesis of CPA from a very high *E*-factor starting material [35].

Scheme 4.3 Preparation of CPA from dihydrofuran.

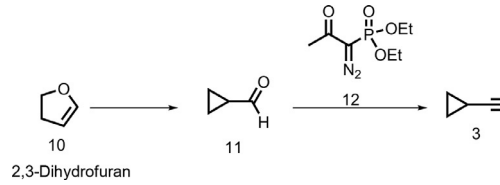

In the first-generation synthesis of EFV (Scheme 4.4) protection of the aniline nitrogen with a *p*-methoxybenzyl (PMB) group was installed in order to achieve high enantioselectivity in the addition of lithium CPA to the aryl trifluoromethyl ketone, **12**. Seminal work of David Collum et al. provided much needed spectroscopic

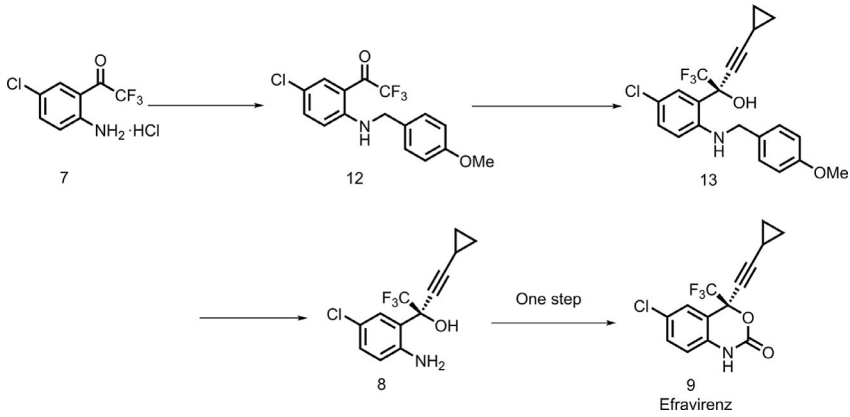

Scheme 4.4 First-generation synthesis of efravirenz.

evidence for the likely structure of the solution-state aggregate of lithium cyclopropylacetylide, **13** and the chiral ligand pyrrolidinyl (norephedrine) which facilitate the high enantioselectivity of addition of LiCPA [36]. However, removal of the PMB group is a two-step procedure [37]. The conversion of **8** to EFV was found to be best carried out with phosgene for various reasons such as less impurity, volume efficiency, and ease of purification through crystallization. Many companies are not equipped to use highly toxic phosgene in pharmaceutical production. Among many alternatives to phosgene, the best option has been described by Bristol-Myers Squibb [38]. The focus of the next generations of this synthesis was direct conversion of **7** to **8** without the protection of the aniline moiety (Scheme 4.5). One-step conversion to **8** was first reported by Tan et al. [39]. They used stoichiometric dialkylzinc reagents along with the chloromagnesium Grignard reagent of CPA. This process is evidently more efficient than the first-generation synthesis as it reduces the number of steps, and has been used in different forms. This method was significantly further improved by multiple Indian producers of generic EFV.

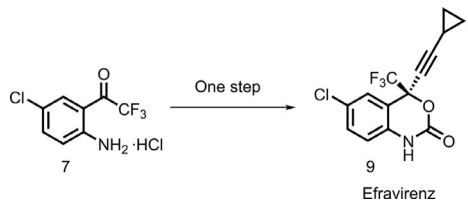

Scheme 4.5 Second-generation synthesis of efravirenz.

Lonza Corp., the producer of API for high-income countries made significant improvements to this conversion. Synthetic procedures involving stoichiometric dialkylzinc reagents still, however, suffer from the inefficiency of generating 2 mol of gaseous hydrocarbon (methane or ethane) per mol of zinc reagent. Along with the problems manufacturer has to face in transportation, and handling, and working with

highly pyrophoric reagents. In addition, a full mole equivalent of corrosive zinc(II) hydroxide is produced as solid waste in this step. An alternate method of this asymmetric addition has been described by Carriera et al. and authors from Lonza Corp. Their method utilizes asymmetric autocatalysis and substoichiometric dialkylzinc reagent [40]. Carreira and coworkers earlier work in utilizing inorganic zinc(II) salts for asymmetric alkynylation reactions has also been utilized in this regard [41,42]. The subsequent generation of improvement bypassed these dialkylzinc reagents. The use of zinc chloride/triethylamine for the addition of CPA to provide racemic **8** [43] was reported by Jiang and Si. This work was further improved by use of zinc(II) triflate and zinc(II) diflate to effect this addition with greater enantiomeric control, giving commercially useful degrees of enantioselectivity [44]. These processes effectively eliminated over 90% of the chemical waste generated in the conversion of **7–8** in the first-generation synthetic methods. Also, inclusion of inorganic zinc(II) salts into the synthetic procedure made the production "greener" as it (a) eliminated the use of pyrophoric dialkylzinc reagents, (b) the reaction can be run at closer to room temperature than other additions, and (c) does not generate volatile organic gases. Moreover, usage of inorganic zinc(II) improved *E*-factor by roughly 40% over the use of dialkylzinc reagents. It is also worth noting that the replacement of zinc(II) triflate with the corresponding zinc(II) diflate brings down the cost of synthesis significantly. The peculiar phase diagram for **8** as a free base is such that a very high chiral purity (roughly 97% ee) is necessary to upgrade the enantiomeric purity by crystallization. The addition of CPA-lithium to the trifluoromethyl ketone **7** using the chiral ligand (pyrrolidinyl)norephedrine proceeds through high enantioselectivity and are generally in the range of 96%–99% [45]. In the first generation, synthesis of EFVAPI was contaminated with <0.1% of the wrong enantiomer, which was dealt with crystallization at intermediate stages. The second generation of this synthesis involving dialkylzinc reagents also utilized the same chiral ligand. The chiral purity of this intermediate was improved by use of the methanesulfonate salt of **8**, with minimal losses of desired product in the mother liquors. In the third generation of this synthesis use of a diamino-alcohol chiral ligand derived from a chloramphenicol precursor [33] provided small yet significant improvements in enantioselectivity.

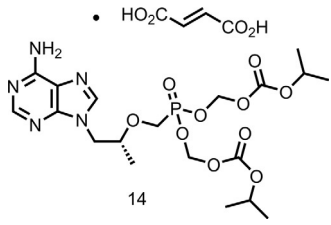

Fig. 4.1 Tenofovir disoproxil fumarate.

Another important component of ARV cocktails is TDF, **14** which received FDA approval in 2001 (Fig. 4.1), was developed at Gilead Laboratories. Usually, TDF is administered into adults as a once daily 300 mg dose. TDF serves as a prodrug of

the molecule tenofovir, 9-[9(*R*)-2-(phosphonomethoxy)propyl]-adenine, or PMPA. The poorly soluble PMPA is absorbed into the bloodstream as the precursor ester; the isopropylmethoxy carbonate (isoproxil) protecting groups are rapidly hydrolyzed by intracellular enzymes. The limited stability of these isoproxil groups (even in aqueous solution) is ideal for its use as a prodrug, however, this aqueous instability makes synthesis, isolation, purification, and scaling up of the molecule rather challenging. Generic production of TDF began in 2006 and the cost of treatment per patient every year was $207 for the TDF drug component (API) alone. Reducing this cost became absolutely essential to market this drug on the preferred first-line regimen in the developing world. As per the initially patented process [46], the overall yield for the three-step synthesis was only about 15% (Scheme 4.6). Although the first step proceeds in reasonably good yield (approximately 80%), the subsequent stages were found to be quite challenging.

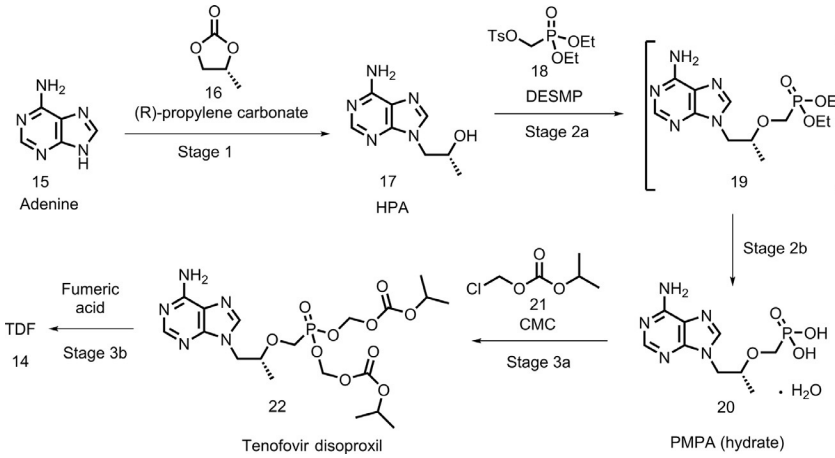

Scheme 4.6 Synthesis of TDF.

Efforts were made to improve the efficiency of these steps, and overall yield reached to a somewhat satisfactory 25% [47]. In Step 2a, 9-[9(*R*)-2-hydroxyprop-1-yl]adenine (HPA), **17** was reacted with a base and the diethyl ester of tosyloxymethylphosphonic acid, **18** (DESMP), and the intermediate diethyl ester, **19** was hydrolyzed under acidic conditions to provide PMPA, **20**. The patented procedure reported lithium *tert*-butoxide as the base, however, subsequent research proved that magnesium *tert*-butoxide was superior [48]. The reported procedure for hydrolysis required a significant molar excess of trimethylsilyl bromide, an expensive pyrophoric material. Alternatively, aqueous HBr [49], was tried for hydrolysis but such conditions required exhaustive distillation of organic solvents used in stage 2a, resulting in long processing times. In a remarkable improvement, it was discovered that an in situ combination of sodium bromide and trimethylsilyl chloride was highly effective [50]. This method produced PMPA, **20** in an excellent yield of 77%, a significant improvement over the 50% yield typical for the original, more costly, process.

Additional improvements in the process were possible in the final step, conversion of PMPA to the prodrug tenofovirdisoproxil. PMPA was reacted with chloromethyl isopropyl carbonate (CMIC) in the presence of an amine base such as triethylamine in a polar aprotic solvent. The procedure as originally reported provided modest yield of 35% yield. However, monitoring the reaction progress by high-performance liquid chromatography (HPLC) provided a maximum yield of about 50% product along with starting material, intermediate monoester, and various degradants. Two distinct pathways exist for degradation: the amine functional group on the purine ring can react to form acylated or alkylated by-products, and the isoproxil functions may be (a) incompletely incorporated or (b) partially cleaved, likely due to participation of the chloride ion released in the reaction.

Further process improvement was made by converting PMPA hydrate starting material to an anhydrous state. The dehydration process was accomplished either through rigorous solid-state drying under high heat and vacuum or by heating a suspension of the solid with distillation of a water azeotrope using a solvent such as cyclohexane. Low water content in the PMPA starting material ensured the reaction at the purine amine were minimized, and isolated yields improved to 50%–55% [51]. However, it was still difficult to drive the reaction to completion, as experiments suggested that the tenofovirdisoproxil would slowly hydrolyze to the monoester under the reaction conditions. Then, the goal became to reach maximum reaction conversion in a short time in order to maximize product recovery. As mentioned above, the solubility of PMPA solid is very poor including in the reaction solvent *N*-methylpyrrolidinone (NMP). To get around this problem, phase transfer catalyst tetrabutylammonium bromide was utilized and that resulted in significant improvement in reaction rate; the reaction reached maximum completion in about 4 h rather than about 10 h. Conversion also reached 75%. As the further refinements discussed here are being implemented, the cost of treatment of HIV/AIDS is dropping significantly.

4.6 Green technology in malaria treatment

Malaria is a global health epidemic that threatens 300–500 million people and takes away more than one million lives every year [52–54]. Occurrence of multidrug-resistant strains of the malaria parasite *Plasmodium falciparum* makes disease control even more challenging. Various antimalarial drugs and malarial vaccines are currently being developed; however, their potency against malaria is yet to be confirmed by clinical testing. Artemisinin, a sesquiterpene lactone endoperoxide is extracted and purified from the herb *Artemisia annua* L. (family Asteraceae; commonly known as sweet wormwood), is highly effective against multidrug-resistant Plasmodium spp., but at present, the environmental and economic costs of its semisynthetic production are relatively high and unaffordable to most malaria sufferers. In this section, we will address different synthetic approaches that have been undertaken to increase the production, reduce the cost and harmful waste.

Although artemisinin **23**, is being used in treating malaria since ages [55], however, semisynthetic derivatives exhibit improved clinical efficacy (Fig. 4.2).

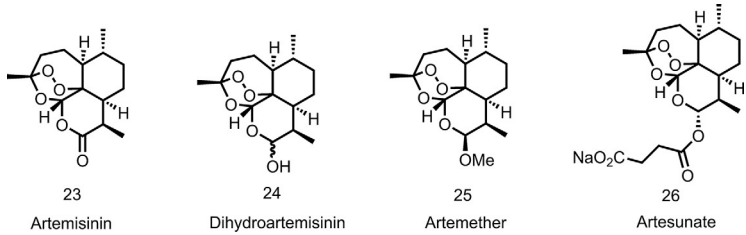

Fig. 4.2 Artemisinin and artemisinin-derived antimalarial compounds.

Artemisinin is reduced to dihydroatemisinin, **24** (DHA) with sodium or potassium borohydride [56] which can be further converted into both artemether, **25** (DHA methyl ether) and artesunate [57], **26** (DHA succinate ester) through one additional synthetic step [58,59]. The cost of artemisinin derivatives depends largely on the price of artemisinin. At present, the costs of artemether and artesunate are about $600/kg. The World Health Organization (WHO) recommends artemisinin combination therapies (ACTs) for the treatment of uncomplicated malaria for all patients who can endure artemisinin therapy. The artemisinin-derived component of an ACT can clear circulating blood schizonts quickly, but short half-life of only a few hours limits its utility. On the other hand, synthetic variant of an ACT has a much longer half-life (usually several days) and gets distributed into tissues significantly owing to its high lipophilicity. Hence, the synthetic derivatives of an ACT provide for a long-lasting antiparasitic effect and prevent recurrence. Most popular ACT combinations used in the developing countries are: (1) artemether, **25**/lumefantrine, **29**; (2) artesunate, **26**/amodiaquine, **27**; and, more recently, (3) dihydroartemisinin, **24**/piperaquine, **28** (Fig. 4.3).

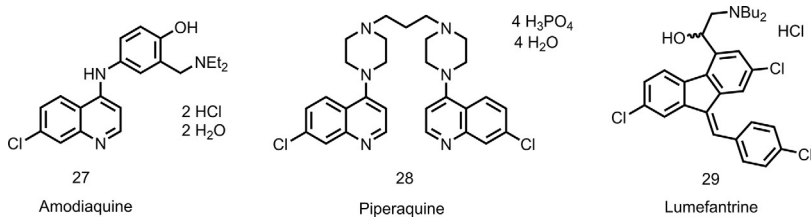

Fig. 4.3 Synthetic antimalarial compounds for ACT.

Although antimalarial activity of amodiaquine was first reported over 60 years ago by Burckhalter [55], its use as component in artesunate:amodiaquine has greatly revived interest in this molecule. Amodiaquine, **27** is synthesized commercially from 4-aminophenol and 4,7-dichloroquinoline in a four-step process (Scheme 4.7). Reaction of 4-aminophenol, **30** with acetic anhydride produced the most common and inexpensive analgesic paracetamol, **31**. Then, paracetamol is treated under a Mannich reaction condition (formaldehyde, diethylamine) followed by a hydrolytic removal of the acetyl group to forge the substituted 4-aminophenol **32**. The substituted aminophenol derivative is then reacted with 4,7-dichloroquinoline **33** to give desired

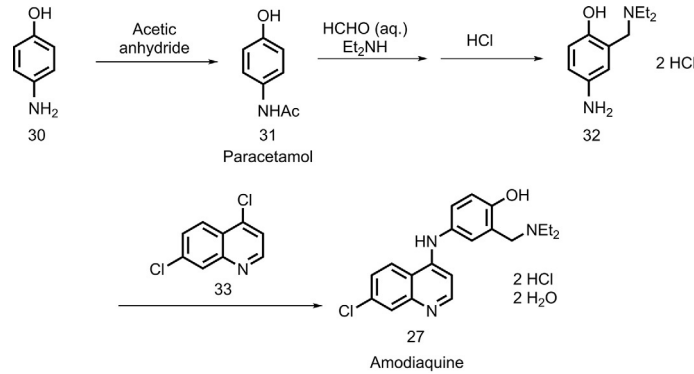

Scheme 4.7 Commercial synthesis of amodiaquine.

amodiaquine, **27** with overall yield 60%–65%. API can be purchased for prices in the range of $20–30/kg on metric ton scale.

Fortunak et al. have developed a simpler synthesis of amodiaquine [60], involving only two of steps thus eliminating over 80% of the waste generated in the commercial synthesis. Reaction of 4,7-dichloroquinoline **33** with 4-aminophenol, **33** in aqueous hydrochloric acid (reflux) produced **34** in near quantitative yield (Scheme 4.8). Mannich reaction of **34** (ethanolic HCl, aqueous formaldehyde, diethylamine) generates amodiaquine in overall yields of 90%–92% from 4,7-dichloroquinoline. The overall *E*-factor for this synthesis is roughly 7 [61].

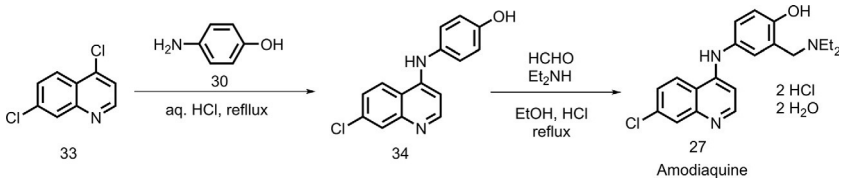

Scheme 4.8 Two-step synthesis of amodiaquine.

Following similar protocol commercial synthesis of piperaquine, **28** has been developed [60]. These processes differ mainly in the solvents used for Step 2 along with the isolation method for intermediate **35**, and the choice of base used in each step (Scheme 4.9).

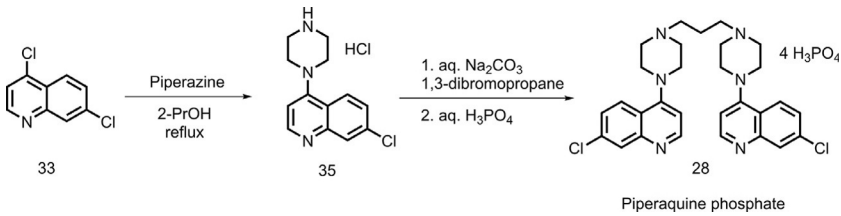

Scheme 4.9 Green synthesis of piperaquine.

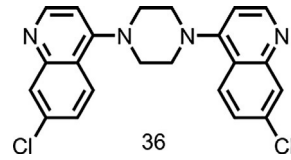

36

Fig. 4.4 Piperaquine dimeric impurity.

The general procedure for Step 1 is quite similar; piperazine (3 mol equiv.) and 4,7-dichloroquinoline **33**, are refluxed in 2-propanol (7–10 vol; *w*/*v*) with potassium carbonate as base. An excess of piperazine is used to minimize the formation of the unwanted dimeric side product **36** (Fig. 4.4). After the completion of the reaction, 2-propanol is distilled off and exchanged with dichloromethane (10 vol). Excess piperazine is extracted with water and a second aqueous extraction with hydrochloric acid is used to prepare the salt of intermediate **35**. The solid product 3**5** is obtained by concentration of the aqueous layer and crystallization from acetonitrile (10 vol). Thus, the usage of solvent, time- and energy-consuming several solvent exchange processes make this method inefficient. The isolated intermediate is converted into piperaquine, **28** in an additional two operations: heating 1-bromo-3-chloropropane with intermediate **35** in aqueous sodium carbonate produces piperaquine free base. The free base is then converted into piperaquine phosphate, **28** (the API) by addition of 4 equiv. of phosphoric acid in an aqueous suspension. It was observed that Step 1 reaction in piperaquine synthesis works best by refluxing dichloroquinoline and piperazine in 2-propanol in the absence of any additional base, giving approximately 97% yield of material that is >99.8% pure by HPLC analysis. Then, addition of ethyl acetate (5 vol) causes much of the excess piperazine to crystallize (largely as its hydrochloride salt), which can be removed by filtration. Remaining piperazine is removed by washing with water followed by concentration and solvent exchange to water (6 vol). This mixture is converted directly to piperaquine free base by heating to reflux with 1 mol equiv. of sodium carbonate and 0.5 mol equiv. of 1,3-dibromopropane. The isolated yield of material that is >99% pure by HPLC is 92%–93% over two steps.

The quinoline moiety is prevalent in a variety of pharmacologically active synthetic and natural compounds and is historically among the most important antimalarial drugs ever used. Taran et al. developed an efficient one-pot three-component synthesis of novel α-(acyloxy)-α-(quinolin-4-yl)acetamides **40–42**, by reacting isocyanides **37**, quinoline-4-carbaldehyde **38**, and arylcarboxylic acids **39** at room temperature in aqueous medium involving the formation of both C—C and C—O bonds (Scheme 4.10) [62]. Operational simplicity, mild reaction conditions, ease of isolation of products, cleaner reaction profiles, and excellent yields are the key advantages of this protocol.

A possible mechanism for the formation of product **40–42** was suggested by the authors (Scheme 4.11). First, carboxylic acid **39** protonates the aldehydic carbonyl oxygen generating an electron-deficient species **43**. Then, isocyanide **37** attacks on the carbonyl carbon through its electron-rich carbon center to form intermediate **44**. The carboxylate ion **45** adds to the intermediate **44** in the next step via nucleophilic

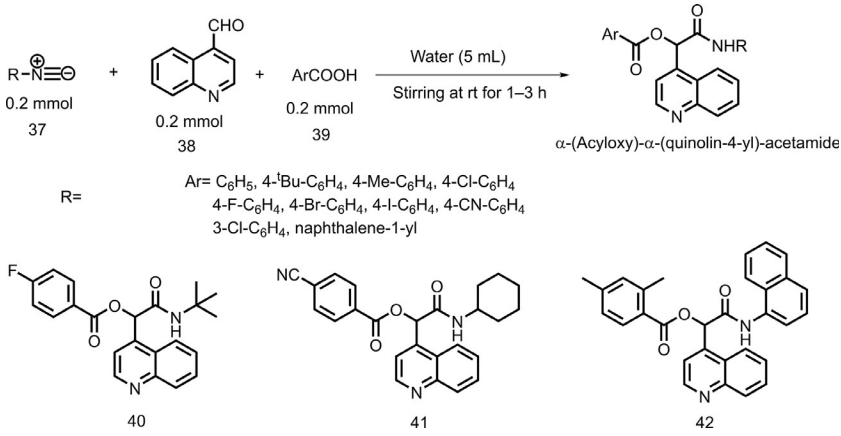

Scheme 4.10 One-pot three-component synthesis of α-(acyloxy)-α-(quinolin-4-yl)-acetamides.

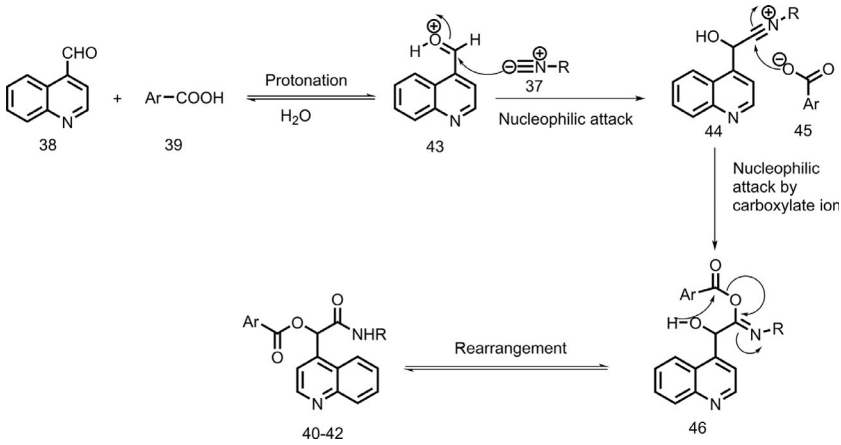

Scheme 4.11 Plausible mechanism for the construction of α-(acyloxy)-α-(quinolin-4-yl)-acetamide moiety.

attack leading to the formation of intermediate **46** that subsequently undergoes a rearrangement reaction to ultimately produce the desired products **40–42**.

Heterocyclic hydrazones recently found to be useful as antimalaria drugs. Microwave synthesis of these heterocyclic hydrazones using PSSA as a catalyst has been developed by Varma and coworkers (Scheme 4.12), which proceeds efficiently in the absence of any organic solvent and involves basic filtration as the product isolation step [63].

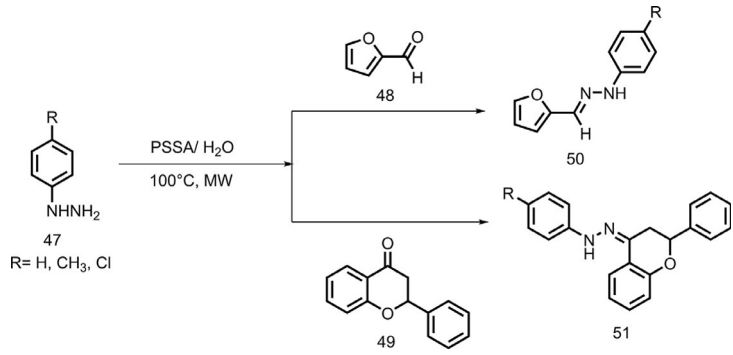

Scheme 4.12 Synthesis of hydrazone derivatives of furaldehyde and flavanone in water.

Indenoquinoline derivatives, **55** are important heterocyclic compounds in drug discovery, which exhibit an antimalarial activity. Tu et al. reported synthesis of these molecules via a three-component reaction between aldehydes, **53**, 1,3-indanedione, **52,** and enaminones, **54** (Scheme 4.13) in aqueous medium. This reaction is catalyzed by *p*-toluene sulfonic acid (*p*-TsOH) under microwave conditions, with high yield of product in 3–7 min.

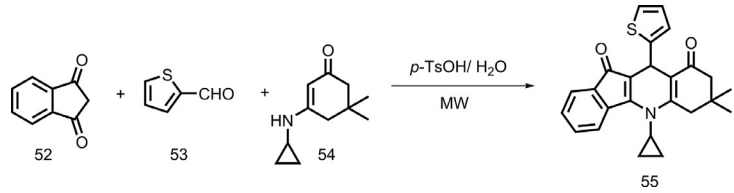

Scheme 4.13 Aqueous protocol for indenoquinoline derivatives.

4.7 Conclusion

The United Nations Millennium Development Program mentions Goal 6 as: "combat HIV/AIDS, malaria, and other diseases." In 2005, the Progress Report toward these goals revealed that the richest 15% of the world's population consumed 91% of medicines. It also indicated that the number of low- to middle-income people worldwide with access to medicines for the treatment of HIV/AIDS, malaria, and other infectious diseases has increased enormously since 2001. Innovation in synthetic chemistry to reduce the cost of APIs for the treatment of these diseases has played a major role in increasing access to needed medicines. However, a lot still remains to be done, although it can be optimistically concluded that much more progress toward increased access to medicines is achievable through the application of new chemistry, reformulation, and dose optimization studies.

References

[1] R. Sheldon, Green and sustainable chemistry: challenges and perspectives, Green Chem. 10 (2008) 359–360.
[2] P. Tundo, A. Perosa, F. Zechhini (Eds.), Methods and Reagents for Green Chemistry, first ed., Wiley Interscience, 2007.
[3] A.S. Matlack, Introduction to Green Chemistry, second ed., CRC Press, 2010.
[4] P.T. Anastas, J.C. Warner, Green Chemistry: Theory and practice, first ed., Oxford University Press, 2000.
[5] C. Jiménez-González, D.J.C. Constable, Green Chemistry and Engineering: A Practical Design Approach, John Wiley & Sons, 2011.
[6] United Nations, Report of the World Commission on Environment and Development: Our Common Future, http://www.un-documents.net/wced-ocf.htm, 1987. (Accessed 1 August 2011).
[7] M. Redclift, Sustainable development (1987–2005): an oxymoron comes of age, Sustain. Dev. 13 (2005) 212–227.
[8] M.S. Carolan, M.M. Bell, An Invitation to Environmental Sociology, Sage Publications, 2012.
[9] M. Taylor, Public Policy in the Community, second ed., Palgrave Macmillan, 2011.
[10] G. Chichilnisky, An axiomatic approach to sustainable development, Soc. Choice Welfare 13 (1996) 231–257.
[11] Department of Commerce and Labor, Bureau of the Census, Mortality Statistics, 1900 to 1904, US Department of Commerce and Labor, Washington, DC, 1906.
[12] D.L. Hoyert, K.D. Kochanek, S.L. Murphy, Deaths: Final Data for 1997, US Department of Health and Human Services, Public Health Service, CDC, National Center for Health Statistics, Hyattsville, Maryland, 1999 (National vital statistics reports, vol 47, no. 19).
[13] A.W. Crosby Jr., Epidemic and Peace, 1918, Greenwood Press, Westport, Connecticut, 1976, p.311.
[14] J. Lederberg, R.E. Shope, S.C. Oaks Jr. (Eds.), Microbial Threats to Health in the United States, National Academy Press, Washington, DC, 1992.
[15] R. Montesano, P. Hainaut, C.P. Wild, Hepatocellular carcinoma: from gene to public health, J. Natl. Cancer Inst. 89 (1997) 1844–1851.
[16] T.P. Van Boeckel, S. Gandra, A. Ashok, Q. Caudron, B.T. Grenfell, S.A. Levin, R. Laxminarayan, Global antibiotic consumption 2000 to 2010: an analysis of national pharmaceutical sales data, Lancet Infect Dis. 14 (8) (2014) 742–750.
[17] A. Wright, N. Desai, B. Samb, F. Adshead, K. Patel, F. Celletti, S. Nishtar, Prevention and management of chronic disease: a litmus test for health-systems strengthening in low-income and middle-income countries, Lancet 376 (9754) (2010) 1785–1797.
[18] A.A. Abdullahi, Trends and challenges of traditional medicine in Africa, Afr. J. Tradit. Complement Altern. Med. 8 (5 Suppl) (2011) 115–123.
[19] E.d.S. Pinheiro, O.A.C. Antunes, J.M.D. Fortunak, A survey of the syntheses of active pharmaceutical ingredients for antiretroviral drug combinations critical to access in emerging nations, Antivir. Res. 79 (2008) 143–165.
[20] A. Falco, E. Barrajón-Catalán, M.P. Menéndez-Gutiérrez, J. Coll, V. Micol, A. Estepa, Melittin-loaded immunoliposomes against viral surface proteins, a new approach to antiviral therapy, Antivir. Res. 97 (2013) 218–221.
[21] V. Mas, A. Falco, I. Brocal, L. Perez, J.M. Coll, A. Estepa, Identification of selective inhibitors of VHSV from biased combinatorial libraries of N,N'-disubstituted 2,5-piperazinediones, Antivir. Res. 2 (2006) 107–115.

[22] P.V. Hoogevest, X. Liu, A. Fahr, Drug delivery strategies for poorly water-soluble drugs: the industrial perspective, Expert Opin. Drug Deliv. 8 (2011) 1481–1500.
[23] A. Fahr, X. Liu, Drug delivery strategies for poorly water-soluble drugs, Expert Opin. Drug Deliv. 4 (2007) 403–416.
[24] Y. Kawabata, K. Wada, M. Nakatani, S. Yamada, S. Onoue, Formulation design for poorly water-soluble drugs based on biopharmaceutics classification system: basic approaches and practical applications, Int. J. Pharm. 420 (2011) 1–10.
[25] T. Loftsson, M.E. Brewster, Pharmaceutical applications of cyclodextrins: basic science and product development, J. Pharm. Pharmacol. 62 (2010) 1607–1621.
[26] H.F. Günthard, M.S. Saag, C.A. Benson, C. del Rio, J. Eron, J.E. Gallant, J.F. Hoy, M.J. Mugavero, P.E. Sax, M.A. Thompson, R.T. Gandhi, R.J. Landovitz, D.M. Smith, D.M. Jacobsen, P.A. Volberding, Antiretroviral drugs for treatment and prevention of HIV infection in adults 2016 recommendations of the international antiviral society–USA panel, JAMA 316 (2016) 191–210.
[27] M.S. Saag, C.A. Benson, R.T. Gandhi, J.F. Hoy, R.J. Landovitz, M.J. Mugavero, P.E. Sax, D.M. Smith, M.A. Thompson, S.P. Buchbinder, C. Del Rio, J.J. Eron Jr., G. Fätkenheuer, H.F. Günthard, J.M. Molina, D.M. Jacobsen, P.A. Volberding, Antiretroviral drugs for treatment and prevention of HIV infection in adults: 2018 recommendations of the international antiviral society-USA panel, JAMA 320 (2018) 379–396.
[28] H. Ait-Mohand, M. Bonmarchand, M. Guiguet, L. Slama, F. Marguet, A. Behin, B. Amellal, Y. Bennai, G. Peytavin, V. Calvez, G. Pialoux, R. Murphy, C. Katlama, Viral efficacy maintained and safety parameters improved with a reduced dose of stavudine: a pilot study, HIV Med. 9 (2008) 738–746.
[29] P.Z. Sinxadi, J.-S. van der Walt, H.M. McIlleron, M. Badri, P.J. Smith, J.A. Dave, N.S. Levitt, G. Maartens, Lack of association between stavudine exposure and lipoatrophy, dysglycaemia, hyperlactataemia and hypertriglyceridaemia: a prospective cross sectional study, AIDS Res. Ther. 7 (2010) 23.
[30] S.P. Yang, W.C. Liu, K.Y. Lee, B.R. Wu, Y.C. Su, P.Y. Wu, J.Y. Zhang, Y.Z. Luo, H.Y. Sun, S.Y. Chang, S.W. Lin, C.C. Hung, Effectiveness of a reduced dose of efavirenz plus 2 NRTIs as maintenance antiretroviral therapy with the guidance of therapeutic drug monitoring, J. Int. AIDS Soc. 17 (2014) 19524.
[31] A. Fayet Mello, T. Buclin, L.A. Decosterd, C. Delhumeau, J. di Iulio, A. Fleurent, M.P. Schneider, M. Cavassini, A. Telenti, B. Hirschel, A. Calmy, Successful efavirenz dose reduction guided by therapeutic drug monitoring, Antivir. Ther. 16 (2011) 189–197.
[32] D. Zhao, C.-Y. Chen, F. Xu, et al., Org. Synth. Coll. 10 (2004) 456–461.
[33] R.L. Parsons Jr., US Patent 6,028,237, 2000.
[34] A. Choudhury, US Patent 6,235,957, 2001.
[35] K.M.J. Brands, US Patent 6,552,239, 2003.
[36] A. Thompson, E.G. Corley, M.F. Huntington, E.J.J. Grabowski, J.F. Remenar, D.B. Collum, Lithium ephedrate-mediated addition of a lithium acetylide to a ketone: solution structures and relative reactivities of mixed aggregates underlying the high enantioselectivities, J. Am. Chem. Soc. 120 (1998) 2028–2038.
[37] M.E. Pierce, R.L. Parsons, L.A. Radesca, Y.S. Lo, S. Silverman, J.R. Moore, Q. Islam, A. Choudhury, J.M.D. Fortunak, D. Nguyen, C. Luo, S.J. Morgan, W.P. Davis, P.N. Confalone, C.-y. Chen, R.D. Tillyer, L. Frey, L. Tan, F. Xu, D. Zhao, A.S. Thompson, E.G. Corley, E.J.J. Grabowski, R. Reamer, P.J. Reider, Practical asymmetric synthesis of Efavirenz (DMP 266), an HIV-1 reverse transcriptase inhibitor, J. Org. Chem. 63 (1998) 8536–8543.
[38] P. Vemishetti, S.T. Chadwick, C.A. Costello, US Patent 7,205,402, 2007.

[39] L. Tan, C.-Y. Chen, R.D. Tillyer, E.J.J. Grabowski, P.J. Reider, A novel, highly enantioselective ketone alkynylation reaction mediated by chiral zinc aminoalkoxides, Angew. Chem. Int. Ed. Engl. 38 (2000) 711–713.
[40] N. Chinkov, A. Warm, E.M. Carreira, Asymmetric autocatalysis enables an improved synthesis of efavirenz, Angew. Chem. Int. Ed. Engl. 49 (2011) 2957–2961.
[41] D.E. Frantz, R. Fassler, E.M. Carreira, Facile enantioselective synthesis of propargylic alcohols by direct addition of terminal alkynes to aldehydes, J. Am. Chem. Soc. 122 (2000) 1806–1807.
[42] N.K. Anand, E.M. Carreira, A simple, mild, catalytic, enantioselective addition of terminal acetylenes to aldehydes, J. Am. Chem. Soc. 123 (2001) 9687–9688.
[43] B. Jiang, Y.-G. Si, Alkynylation of carbonyl compounds with terminal acetylenes promoted by ZnCl2 and Et3N: simple, mild and efficient preparation of propargylic alcohols, Tetrahedron Lett. 43 (2002) 8323–8325.
[44] B. Jiang, Y.-G. Si, US Patent 7,439,400 B2, 2008.
[45] D. Zhao, C.-Y. Chen, F. Xu, et al., Org. Synth. Coll. 10 (2004) 556–564.
[46] M.N. Arimilli, K.C. Cundy, J.P. Dougherty, US Patent 5,922,695, 1998.
[47] D.H. Brown Ripin, D.S. Teager, J. Fortunak, S.M. Basha, N. Bivins, C.N. Boddy, S. Byrn, K.K. Catlin, S.R. Houghton, S.T. Jagadeesh, K.A. Kumar, J. Melton, S. Muneer, L.N. Rao, R.V. Rao, P.C. Ray, N.G. Reddy, R.M. Reddy, K. Chandra Shekar, T. Silverton, D.T. Smith, R.W. Stringham, G.V. Subbaraju, F. Talley, A. Williams, Process improvements for the manufacture of Tenofovir Disoproxil Fumarate at commercial scale, Org. Process. Res. Dev. 14 (2010) 1194–1201.
[48] M.W. Becker, H.H. Chapman, T. Cihlar, PCT Intl. WO/0208241 A3, 2002.
[49] U.M.R. Vasireddy, S.R.P. Vellanki, R.B. Balusu, N.D.R. Bandi, P.K. Jujjavarapu, S.R. Ginjupalli, R.K. Pilli, PCT Intl. WO2008/007392 A2, 2008.
[50] S.R. Houghton, J. Melton, J. Fortunak, D.H. Brown Ripin, C.N. Boddy, Rapid, mild method for phosphonate diester hydrolysis: Development of a one-pot synthesis of tenofovir disoproxil fumarate from tenofovir diethyl ester, Tetrahedron 66 (2010) 8137–8144.
[51] M.N. Arimilli, C.U. Kim, J. Dougherty, A. Mulato, R. Oliyai, J.P. Shaw, K.C. Cundy, N. Bischofberger, Synthesis, in vitro biological evaluation and oral bioavailability of 9-[2-(phosphonomethoxy)propyl]adenine (PMPA) prodrugs, Antivir. Chem. Chemother. 8 (1997) 557–564.
[52] C. Goldsmith, Battling Malaria: On the Front Lines Against a Global Killer, Twenty-First Century Books, 2011.
[53] M.W. Service, Demography and Vector Borne Diseases, CRC Press, Inc., 1989.
[54] World Health Organization (Ed.), Guidelines for the Treatment of Malaria, second ed., 2010.
[55] J.H. Burckhalter, F.H. Tendick, E.M. Jones, P.A. Jones, W.A. Holcomb, A.L. Rawlins, Aminoalkylphenols as antimalarials. II.1 (heterocyclic-amino)-α-amino-o-cresols. The synthesis of Camoquin, J. Am. Chem. Soc. 70 (1948) 1363–1373.
[56] M. Boehm, P.C. Funfschilling, M. Krieger, E. Kuesters, F. Struber, An improved manufacturing process for the Antimalaria drug Coartem. Part I, Org. Process Res. Dev. 11 (2011) 336–340.
[57] Y. Zhao, W.K. Hanton, K.-H. Lee, Antimalarial agents, 2. Artesunate, an inhibitor of cytochrome oxidase activity in Plasmodium berghei, J. Nat. Prod. 49 (1986) 139–142.
[58] Y. Suputtamongkol, P.N. Newton, B. Angus, P. Teja-Isavadharm, D. Keeratithakul, M. Rasameesoraj, S. Pukrittayakamee, N.J. White, A comparison of oral artesunate and artemether antimalarial bioactivities in acute falciparum malaria, Br. J. Clin. Pharmacol. 52 (2001) 655–661.

[59] R.N. Price, N.M. Douglas, Artemisinin combination therapy for Malaria: beyond good efficacy, Clin. Infect. Dis. 49 (2009) 1638–1640.
[60] J.M.D. Fortunak, S.R. Byrn, B. Dyson, Z. Ekeocha, T. Ellison, C.L. King, A.A. Kulkarni, M. Lee, C. Conrad, K. Thompson, An efficient, green chemical synthesis of the Malaria drug, Piperaquine, Trop. J. Pharm. Res. 12 (2013) 791–798.
[61] J.M. Fortunak, n.d., Green Chemistry Synthesis of the Malaria Drug Amodiaquine and Analogs thereof, WO2013/138200.
[62] J. Taran, A. Ramazani, S.W. Joo, K. S'lepokura, T. Lis, Synthesis of novel α-(Acyloxy)-α-(quinolin-4-yl)acetamides by a three-component reaction between an Isocyanide, quinoline-4-carbaldehyde, and arenecarboxylic acids, Helv. Chim. Acta 97 (2014) 1088–1094.
[63] V. Polshettiwar, R.S. Varma, Aqueous microwave chemistry: a clean and green synthetic tool for rapiddrug discovery, Chem. Soc. Rev. 37 (2008) 1546–1557.

Clay-mediated synthesis of biologically active molecules: Green and sustainable approaches

5

Adya Jain[a], *Bimal Krishna Banik*[b,*]
[a]School of Studies in Chemistry, Jiwaji University, Gwalior, India, [b]Department of Mathematics and Natural Sciences, College of Sciences and Human Studies, Deanship of Research Development, Prince Mohammad Bin Fahd University, Al Khobar, Kingdom of Saudi Arabia
[*]Corresponding author. e-mail address: bimalbanik10@gmail.com; bbanik@pmu.edu.sa

5.1 Introduction

5.1.1 Green and sustainable approach

Green chemistry is one of the most fundamental areas of active research. The ideas of green chemistry focus environmental problems in an economically profitable manner. Green chemistry is highly essential for the industries to identify appropriate starting compounds and conditions to avoid less or no hazardous by-product generation. This method aims to eliminate the hazard synthesis [1]. It has gained tremendous attention in medical research. The idea of green chemistry was first introduced by Anastas in 1991 [2]. However, green chemistry was started in 1960s following the contribution of Carson. A book, Silent Spring, authored by Carson in 1962, was the first that focuses on the development of pollution-free environment. The originality of Silent Spring has continued and green chemistry became an inseparable item from our lives and society. In general, many authors have described green chemistry as "Sustainable Chemistry" or "Benign Chemistry." This method allows synthesis of compounds in a safe, nonpolluting, and sustainable way. In addition, this procedure in some examples consumes lesser amounts of substrates and energy during the preparation of molecules [3, 4].

5.1.1.1 Basic principles of green chemistry

Anastas and Warner have advanced 12 principles of green chemistry [5, 6]. Scientifically, these are categorized as prevention of waste, designing safer chemicals, less hazardous chemical synthesis, use of renewable feed stocks, catalysts [7], reduce rerivatives, atom economy, safer solvents and auxiliaries [8], design for energy efficiency, design for degradation, real-time analysis for pollution prevention, and inherently safer chemistry for accident prevention [9]. Probably, among these the most crucial principles are less hazardous synthesis and the use of catalysts in chemical reactions.

Green Approaches in Medicinal Chemistry for Sustainable Drug Design. https://doi.org/10.1016/B978-0-12-817592-7.00005-8
© 2020 Elsevier Inc. All rights reserved.

5.1.1.2 Basic green methods for chemical synthesis

Several aims of green chemistry principles are maintained using methods described below.

Microwave-induced method

Microwave-induced reactions proceed through selective absorption of electromagnetic radiation by polar molecules (reactants, solvents, or both) only. In contrast, nonpolar molecules do not absorb microwave irradiation. Molecules with dipoles are aligned under microwave irradiation. Under microwave field oscillation and orientation of the molecules change rapidly and repetition of this process occurs. As a result, internal heating of the system starts. Microwave heating is homogeneous in nature but classical heating takes place because of preheated molecules [10].

Sonication method

Sonicating a reaction mixture that generates ultrasound waves through electrochemical transductors and piezoelectric effect. Ultrasound waves are capable of passing through a solution and the attractive forces of molecules become high generating bubbles [11]. High internal forces can collapse these bubbles and this process creates high temperature and pressure within the system. Therefore, reactions are accelerated under sonication method due to high temperature and pressure.

Biosynthetic method

This procedure is particularly used for the preparation of nanoparticles. Plant-derived material [12], fungi [13], and bacteria are used as reducer or precursor in this method [14]. Metallic nanoparticles are prepared using mostly toxic chemicals. An environmentally friendly or chemical-free biosynthetic method is also used in their preparation [15].

5.1.2 Clay minerals

The word "clay" originates from a Greek word *argilla*, the root of which, *argos*, means "white," [16]. Clay are mineral particles of size <2 μm. The additional parts along with clay are generally called clay minerals. Clay minerals are in particular thin-grained hydrous crystalline phyllosilicates that give plastic and hard properties. Moreover, clay may have a number of associated minerals. For examples, silicates like quartz and feldspar; carbonates like calcite; oxides and hydrated oxides of iron and aluminum like hematite, goethite, and gibbsite; amorphous materials; and quasiamorphous materials like opal A and ferrihydrite are very common materials found in clay.

Clay minerals are formed based on the physicochemical conditions of the immediate, weather, composition of the starting materials, and a few other factors. Therefore, the use of clay mineral depends on its chemical constituents, structural properties, and some inherent characteristics [17]. Secondary minerals are formed

through the alteration of the primary mineral source (incongruent reaction) or neoformation method by precipitation and recrystallization of soluble components into a stabilized form (congruent reaction). Secondary minerals are sometimes called phyllosilicates. Clays are different aluminum silicate species composed of layers of SiO_4^{4-} connected through three corners to form a specific structure hexagonal in nature that are joined with numerous layers of T-O-OH octahedral. In this instance, 'T' is the trivalent or bivalent cations (for examples, Al, Mg, and Fe) which provide the overall positive charge to the system. The charge is, however, balanced by loosely bonded alkali ions (Na^+ and K^+) that are exchanged with other ions present in the surroundings, if necessary. This cation exchange with surrounding environment is a crucial property which is determined through the capability of the ion to attract other ions.

The aluminum silicates are configured in tetrahedral and octahedral systems (i.e., 1:1 in Kaolinite and 2:1 in montmorillonite, illinite, and vermiculite group) connected through the apical oxygens [18]. The overall negative charges of nanoclays within their surface favors the electrostatic orientation process. This leads to a strong bond formation within the oriented multilayers and the preformed systems [19]. Brucite, $Mg(OH)_2$, and gibbsite $Al(OH)_3$ are found to be similar in structure with numerous clay minerals. But, in these examples, the phyllosilicates have different coordinating anions, not the hydroxyls. If the cations are bivalent (Mg^{2+} and Fe^{2+}), the orientation exhibits a geometrical pattern like brucite. A single bivalent cations bind to two oxygens and predictable cation sites in the structure are filled. The configuration formed from such a system is called trioctahedral. If the cations are trivalent (Al^{3+} and Fe^{3+}), the charge is neutralized by arranging one of the every three octahedral cation sites unfilled. Trivalent cations are bound to oxygens in a proportion of 1:3 and the system adopts a gibbsite-like dioctahedral structure. The tetrahedral and di- or trioctahedral systems connected to oxygen atoms form aluminosilicates which are phyllosilicates. Sheet arrangement in the aluminosilicates may alter which produce different clay minerals with diverse physical and chemical properties [20]. It is understandable that numerous factors determine the composition of a mineral such as chemical array, geometrical arrangement of the components, ions and above all the electrical forces within the system.

5.1.2.1 Classification of clay

Clay is classified into seven classes [21] based on the composition available in it as follows:

Class 1. Allopane group (comprises hisingerite)
Class 2. Aolinite group
Class 3. Montmorillonite group
Class 4. Illinite group
Class 5. Vermiculite group
Class 6. Chlorite group (including septechlorites)
Class 7. Sepiolite and palygorskite group

Crystalline clays are divided into two main categories: chain lattices which are present in polygorskite and sepiolite; and layer lattices which constitute diphormic, triphormic, and tetraphormic.

Depending on the number and arrangement of tetrahedral and octahedral arrays [22] in their fundamental compositions, clay minerals are grouped into five categories as illustrated in Table 5.1.

Table 5.1 Five groups of clay materials along with their properties.

S. No.	Group	Layer type	Net negative charge	Surface area	Basal spacing
1.	Kaolinite	1:1	2–5	10–30	0.7
2.	Fine-grained mica	2:1	15–40	70–100	1.0
3.	Smectite	2:1	80–120	600–800	1.0–2.0
4.	Vermiculite	2:1	100–180	550–700	1.0–1.5
5.	Chlorite	2:2:1	15–40	70–100	1.4

Kaolinite is composed of kaolinite, hallosite, nacrite, and dickite. Silica and alumina are the principal constituents of this group and this is formed through advanced weathering alterations and hydrothermal changes of feldspars and aluminosilicates. The chemical composition of kaolinite is $Al_2O_3{\cdot}2SiO_2{\cdot}2H_2O$ (39% Al_2O_3, 46.5% SiO_2, and 14.0% H_2O) and is a packed structure with strong forces between the layers. The cation interchange power of kaolinite is lower than that of montmorillonite clay because of its low surface volume and isomorphous substitution. In addition, this clay has low plasticity, cohesion, shrinkage, and swelling activities. But it can adsorb lecithin, quinolone, paraquat, diaquat polyacrylonitrite, proteins, bacteria, and viruses. Kaolinite is used to manufacture a number of substances which include paper, paint, rubber, ceramic, plastic, pharmaceutical, catalyst, cosmetic, and pigment. Moreover, kaolin is an anti-cracking agent used in the production of fertilizer. It is used for pesticides, white cement, glass fiber, plant metabolites, microorganisms, and heavy metals.

Smectite is a clay mineral formed from soils, rocks, and volcanic ashes which include montmorillonite, beidellite, nantronite, saponite, and hectorite. These are mainly hydroxyl aluminosilicates. Smectite include quartz, zeolites, calcite, cristobalite, feldspars, volcanic glass, and kaolinite. The groups of smectite have Al^{3+} or Fe^{3+} for Si^{4+} in the tetrahedral cation sites and Fe^{2+}, Mg^{2+}, or Mn^{2+} for Al^{3+} in the octahedral cation sites. Smectites are composed of thin layers of small particles responsible for high surface area and a high degree of adsorption power. Importantly, smectites have cation exchange power and swelling/shrinkage activities better than other common clays. The overall negative charge on the structure of smectites attracts water into the interlayer portion readily. This has effect on expansion although the amount of swelling depends on interlayer cation [23].

5.2 Clay-mediated synthesis of biologically active molecules

5.2.1 Natural clay

Shaikh et al. have investigated *N*-acetylation of aniline derivatives using clay as catalyst. Natural clay is collected and purified by a special method [24]. Clay was crushed and washed with distilled water and 0.1 M H_2SO_4 to remove organic impurities. After filtration and further washing and drying, the mixture was heated at 110°C in oven. The catalyst was characterized using analytical techniques such as X-ray powder diffraction (XRD), energy-dispersive X-ray spectroscopy (EDS), and field emission scanning electron microscope (FESEM). The crystalline products obtained from this reaction were identified by FTIR and NMR spectroscopy. *N*-acetylation of aniline derivatives was performed using a mixture of aromatic amines and clay (0.10) g in acetic acid as shown in Scheme 5.1. The white crystals of products were obtained in 80%–95% yield. This method demonstrates a clean and simple procedure with cost-effectiveness that matches very well with the principles of green and sustainable method. Some of these derivatives have diverse medicinal properties.

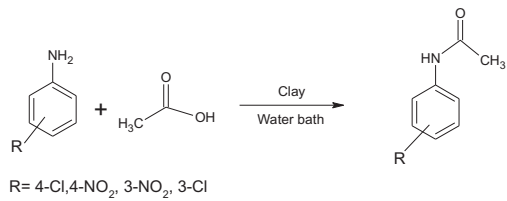

Scheme 5.1 *N*-Acetylation of aniline over clay.

5.2.2 Montmorillonite K-10 clay

Lole et al. have reported clay-mediated (K-10 Montmorillonite) single-step synthesis of azo dye, i.e., 4-(1,3-benzoxazol-2-yl)-anilines using substituted phenols [25]. Azo dyes have diverse pharmacological and medical properties [26]. For example, they are involved in a number of biological processes such as the inhibition of DNA, RNA, protein synthesis, nitrogen fixation, and carcinogenesis [27]. The structures of the products were confirmed by IR, mass spectrometry, ^{1}H NMR, and ^{13}C-NMR spectroscopy. Azo dyes were prepared by mixing 4-(1,3-benzoxazol-2-yl) aniline (5 mmol) in water and montmorillonite K-10 clay and phenol (Scheme 5.2). This is a simple sustainable clay-mediated method for the preparation of drug candidates.

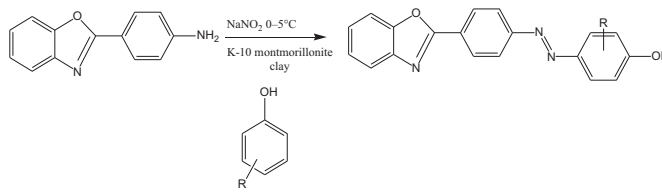

Scheme 5.2 Preparation of azo dyes over montmorillonite K-10 clay.

Mechanistically, diazotization and azo coupling reaction are initiated through the activation of clay. Clay help lose water to retain acidic and basic sites and in the second step $NaNO_2$ is adsorbed over the surface of the clay. Electron pair on nitrogen initiated nucleophilic addition reaction and subsequent dehydration produced diazonium salt and then the salt coupled. These azo compounds have potent antimicrobial activity against *Staphylococcus aureus*, *Escherichia coli* (bacterial strain), and *Aspergillus niger* (fungal strain). The azo compounds as prepared following a green route have greater promise in synthesizing medicinally potent antimicrobial agents.

Chakrabarty et al. have explored the clay-mediated synthesis of 3,3-diindolyl-2-indolinones from isatins (Scheme 5.3) [28]. 2-Indolinones (oxindoles) [29] and 3,3-diaryl-2-indolinones have demonstrated numerous biological activities, e.g., antibacterial, antiprotozoal, antiinflammatory, laxative, and antiproliferative properties [30, 31]. Moreover, a number of diindolylindolinones were formed by the reaction of isatin or *N*-methyl isatin with indoles in the presence of acetic acid [32]. The conversion of 2-indolinone into its 3,3-dibromo derivative was performed by treatment with indoles in the presence of silver carbonate [33]. Alum-catalyzed reaction of indole [34] and 2-methylindole with isatins was performed at room temperature as well as under microwave irradiation [35–37]. A mixture of isatin (**3a**) and excess of indole (**4a**) in methanol/ethyl acetate (1, 1) was adsorbed on montmorillonite K-10 clay and the solvent was allowed to evaporate. On filtration, the crude product **1a** was isolated and crystallized with 87% yield. The autoxidation of skatole (**4f**) on montmorillonite K-10 clay produced two indole derivatives: indolinone **1g** (55%) and 3-methyl-3-(3′-methyl-2′-indolyl)-2-indolinone (**5**). The reactions were extremely rapid and involved simple isolation method, the present procedure was efficient for the one-step synthesis of biologically active 3,3-diindolyl-2-indolinones. This successful method was developed using environmentally benign montmorillonite K-10 clay with enough acidities and a large surface area (Table 5.2).

Table 5.2 Preparation of bis(indolyl)indolinones (**1a–g**) from isatins (**3a,b**) and indoles (**4a–f**) on montmorillonite K-10 clay.

Isatin (3a/3b)	Indole				Reaction time (min)	Product	Yield (%)
		R1	R2	R3			
3a	4a	H	H	H	5	1a	87
3a	4b	H	Me	H	5	1b	92
3a	4c	H	H	Br	5	1c	85
3a	4d	Me	H	H	5	1d	90
3a	4e	Et	H	H	5	1e	75
3b	4d	Me	H	H	5	1f	89
3a	4f	24	H	–	5	1g	55

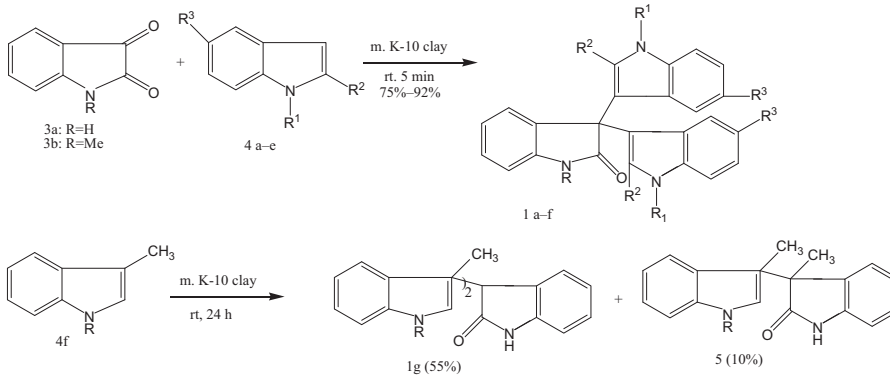

Scheme 5.3 Preparation of 3,3-diindolyl-2-indolinones over montmorillonite K-10 clay.

Yildirim et al. have investigated the montmorillonite K-10-catalyzed synthesis of α-aminonitriles in the presence of dicationic phosphonium salt in water using ultrasound [38]. These compounds are important acyl anion and iminium ion equivalents and suitable intermediates for the preparation of α-amino acids, 1,2-diamines, and numerous nitrogen-containing heterocycles. For example, imidazoles, pyrroles, quinolones, and pyrazinones were prepared from them [39–42].

Acid catalysts [43] such as $NiCl_2$ [44], $Cu(OTf)_2$ [45], $RuCl_3$ [46], iodine [47] $La(NO_3)_3{\cdot}6H_2O$, $GdCl_3{\cdot}6H_2O$, [48], $InCl_3$ [49], and Fe_3O_4 [50] were used successfully in this method. Silica-supported heteropolyacids [51], cellulose sulfuric acid [52], and mesoporous aluminosilicates [53] promoted these reactions in organic solvents or in the absence of solvents. Dicationic salts were prepared from a mixture of dihaloalkane (1.0 mmol) and triphenylphosphine (2.0 mmol) or *N*, *N*-dimethyldodecylamine (2.0 mmol) in absolute ethanol (10 mL) as shown in Scheme 5.4. α-Aminonitriles were synthesized starting from aldehyde (1.0 mmol), (*S*)-α-phenylethylamine (1.0 mmol), montmorillonite K-10 (0.25 g), P-6-P (10 mol%), and NaCN (1.0 mmol) in water. The crude product was washed with diethyl ether and purified by column chromatography over silica gel. Mono- and dicationic phase-transfer catalysts were used for this study. For example, benzyltriethylammonium bromide (TEBAB), 1,6-bis (hexadecyldimethylamino)hexane dibromide (16-6-16), 1,6-bis(triphenylphosphonium) hexane dibromide (P-6-P), 1,12-bis(dodecyldimethylamino)dodecane dibromide (12-12-12), and 1,12-bis(triphenylphosphonium)dodecane dibromide (P-12-P) were tested. Among these six dicationic catalysts, best yield was obtained with P-6-P (85%) as presented in Table 5.3.

Table 5.3 Comparative study of dicationic catalysts.

PTC	Yield (%)	d.r.
–	60	28:72
TEBAB	65	28:72
16-6-16	73	27:73
12-12-12	76	28:72
P-6-P	85	27:73
P-12-P	84	27:73

Phosphonium salts are valuable phase-transfer catalysts due to the fact that they can be prepared from economical and readily available starting materials. This new method used water as solvent and clay as environmentally benign catalyst. It was a fast reaction under ultrasonic method.

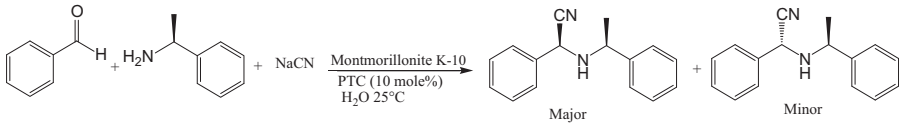

Scheme 5.4 Synthesis of α-aminonitriles over montmorillonite K-10.

Lambat et al. have studied the synthesis of trazodone hydrochloride in the presence of montmorillonite K-10 as catalyst [54]. "Trazodone hydrochloride" [55] is an important medicine with psychoactive properties. These triazolopyridine classes of compounds have also antidepressant, anxiolytic, and hypnotic activities [56]. The preparation of new benzofluorenone derivatives and their HIV-reverse transcriptase inhibitory activity were investigated [57]. A one-pot preparation of *N*, *N*-alkylidene bisamide compounds under solvent-free method by montmorillonite K-10 [58] as well as the preparation of trazodone hydrochloride by sulfamic acid were performed [59]. The pharmacological value of trazodone hydrochloride is because of the inhibition of serotonin uptake and a less affinity for the serotonin transporter than other medicines used for this purpose [60]. Condensation of 1-(3-chlorophenyl)-4-(3-chloropropyl) piperazine and 1,2,4-triazolo [4,3-a] pyridine-3-(2H)-one in acetonitrile under reflux at 90°C for 5 h is shown in Scheme 5.5. The principal advantages of this method were numerous: efficiency, fast and clean reaction, catalytic recyclability, and reusability without the loss of catalytic activity.

Zonouz et al. have studied the synthesis of 1,4-dihydropyridines over montmorillonite K-10 clay-catalyzed reaction [61]. 4-Aryl-2,6-dimethyl-1,4-dihydropyridine-3,5-dicarboxylates (1,4-DHP) are used extensively for the treatment of cardiovascular diseases, for example, hypertension, angina pectoris, and infarction [62]. Studies toward a set of antihypertensive and antianginal drugs were performed [63]. However, they were not related to calcium antagonist properties: neurotropic (antiamnestic, anticonvulsant, neuroregulatory), antidiabetic, anticancer, and anti-inflammatory [64–68]. The main

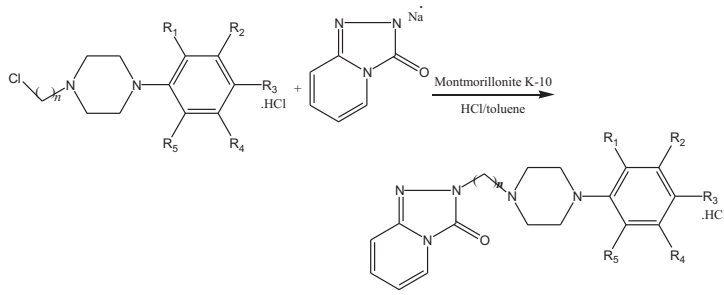

Scheme 5.5 Synthesis of trazodone hydrochloride over montmorillonite K-10.

advantages of this procedure are rapid reactions with high yield of the products. Importantly, montmorillonite K-10 is inexpensive and is reused repeatedly that makes the procedure feasible and sustainable (Scheme 5.6).

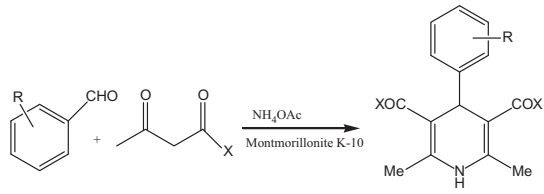

Scheme 5.6 Synthesis of 1,4-dihydropyridine derivatives over montmorillonite K-10 clay.

Song et al. have reported an efficient synthesis of polyhydroquinoline compounds over montmorillonite K-10 clay [69]. 1,4-Dihydropyridines (1,4-DHPs) work well as Ca2þ channel blockers [70, 71] and serve as vasodilator, bronchodilator, antiatherosclerotic, antitumor, geroprotective, hepatoprotective, and antidiabetic molecules [72, 73].

Numerous methods for the synthesis of polyhydroquinoline compounds were investigated. Conventional heating [74], refluxing the reaction mixture in acetic acid, [75], ionic liquids-mediated reaction [76], microwave irradiation method, and ultrasound exposure were studied [77, 78]. These methods required short reaction time but produced products with high yields. The clay used for this study was inexpensive and was recycled many times (Scheme 5.7).

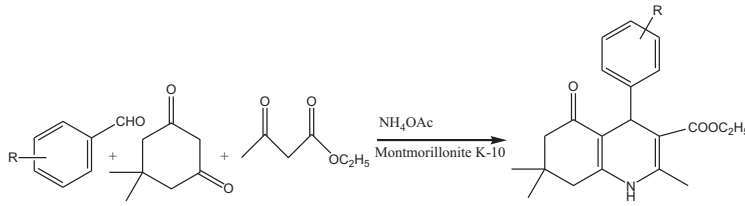

Scheme 5.7 Synthesis of polyhydroquinoline derivatives over montmorillonite K-10 clay.

Marvi et al. have reported the preparation of 5-substituted 1*H*-tetrazoles using montmorillonite K-10 [79]. Tetrazoles have received considerable attention in drug discovery science [80, 81]. 5-Substituted 1*H*-tetrazoles have an acidic hydrogen atom at the *N*-1 and were used as carboxylic acid bioisosteres. These types of compounds demonstrated better cell permeability, bioavailability, and metabolic stability although these have similar pK_a values like carboxylic acids. Substitution of the *N*-1 to produce 1,5-disubstituted tetrazoles was proven helpful in drug discovery as cisamide isosteres [82–86]. Tetrazoles were also used in the preparation of imidoyl azides [87–89].

Considerable work on the preparation of tetrazoles was carried out for material sciences, pharmaceuticals, explosives, and photography research [90–94]. Sharpless et al. have reported an excellent method for the synthesis of 5-substituted 1*H*-tetrazoles by reaction of cnitriles with NaN_3 in the presence of Zn(II) salts [95–98]. Pizzo et al. have studied a new method for the preparation of tetrazoles from nitriles and $TMSN_3$ using TBAF as catalyst [99]. Lakshmi Kantam et al. have efficiently prepared tetrazoles from nitriles and NaN_3 in the presence of nanocrystalline ZnO or zinc hydroxyapatite as the catalyst [100]. Yamamoto et al. have designed a [3+2] cycloaddition reaction between nitriles and trimethylsilyl in the presence of a CuI catalyst to afford 5-substituted 1*H*-tetrazoles [101]. In addition, Zn/Al hydrotalcite-modified montmorillonite K-10 with Cu^{2+}, Fe^{3+}, Ni^{2+}, and Zn^{2+} ions were used in the preparation of terrazoles [102, 103]. The usual method of synthesizing tetrazoles consisted of adding of azide ions to organic nitriles or cyanamides [104–107] mixed with *p*-nitrobenzonitrile, sodium azide, and montmorillonite K-10 clay under microwave irradiation (Scheme 5.8). The catalyst used for this investigation was inexpensive and nontoxic and therefore this method is environmentally benign.

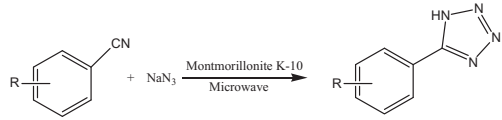

Scheme 5.8 Synthesis of 5-substituted 1*H*-tetrazoles over montmorillonite K-10 clay.

Kannan et al. have reported the preparation of 2,4,6-tri-substituted pyridine using montmorillonite K-10 clay [108]. Multiaryl-substituted pyridines derivatives can serve as electron transporter [109]. The highly substituted 2-amino-4-aryl-3, 5-dicyano-6-sulfanylpyridines have outstanding significant and numerous medicinal properties. For example, these compounds were used as high-potent agonists for human adenosine receptors and act as therapeutic agents against a number of medical disorders: Creutzfeldt-Jacob disease, Parkinson dysfunction, hypoxia, asthma, cancer, kidney problems, and prion disease [110–112].

Some methods for the preparation of 2,4,6-triaryl pyridines were reported. For example, a reaction of α-ketoketene dithioacetals with methyl ketones in the presence of ammonium acetate [113] afforded pyridines. Similarly, a reaction of *N*-phosphinylethanimines with aldehydes [114]; a reaction of lithiated β-enaminophosphonates with chalcones

[115]; condensation of acetophenone derivatives, benzaldehydes, and NH_4OAc in NaOH [116]; one-pot reaction between acetophenones, benzaldehydes, and NH_4OAc in the absence of any catalyst under microwave irradiation method produced substituted pyridines [117]. Because of their π-stacking characteristic properties, some pyridines were used in supramolecular science [118–120]. To overcome some of the limitations of the existing methods, a mild and environmentally friendly procedure in the presence of montmorillonite K-10 clay was developed. Interestingly, the trisubstituted pyridines were obtained with 100% selectivity and without forming any other molecules (Scheme 5.9).

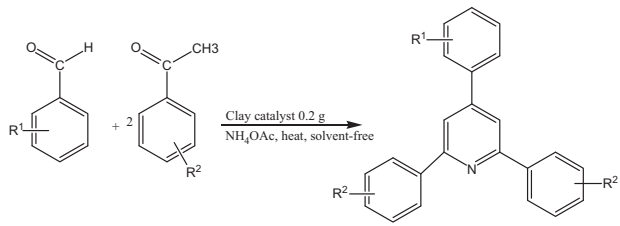

Scheme 5.9 Synthesis of 2,4,6-trisubstituted pyridine over montmorillonite K-10 clay.

Reddy et al. have developed the synthesis of pyranopyrazoles using montmorillonite K-10 as the environmentally benign catalyst [121]. Pyranopyrazoles are crucial heterocycles because they have applications as pharmaceuticals and agrochemicals [122]. The pyranopyrazole was first prepared by reacting 3-methyl-1-phenylpyrazolin-5-one with tetracyanoethylene [123]. A number of 6-amino-5-cyano-4-aryl-4H-pyrazolo[3,4-b] pyrans were made by the reaction of arylidienemalononitrile with 3-methylpyrazoline-5-ones and by the condensation of 4-arylidienepyrazoline-5-one with malononitrile [124–126]. Dihydropyrano[2,3-c]pyrazoles have crucial medicinal properties that include antimicrobial [127], insecticidal [128], and anti-inflammatory [129]. Moreover, dihydropyrano[2,3-c]pyrazoles demonstrated molluscicidal properties [130, 131]. Some of the compounds showed good antioxidant and antibacterial activity (Scheme 5.10).

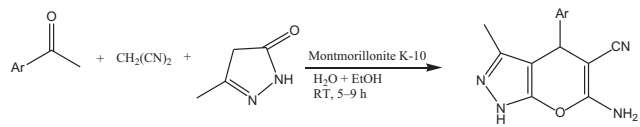

Scheme 5.10 Synthesis of pyranopyrazoles over eco-friendly montmorillonite K-10.

5.2.3 Modified montmorillonite clay

Aslya et al. [132] have studied the polymerization of DL-lactide using protonated montmorillonite [132]. Poly(D,L-lactide) (PLA) is degradable and compatible polymer under biological conditions. The biomedical applications of PLA as drug release

substrate, scaffolds for tissue engineering, and for constructing medical equipment are known [133–135]. This reaction was in general induced by metallic or organometallic catalysts, for example, organo-stannous reagents [136]. Although these catalysts worked well, they had limitations. Most of them were corrosives and preparation of pure products was difficult. To improve the method, a few studies were performed with solid acids, for example, with "Keggin-type heteropolycompounds" [137–140] or clay catalysts [141–143]. These new methods offered some advantages because they were conducted following green chemistry under milder conditions and the products were comparatively easy to purify. This investigation demonstrated the active role of Brønsted/Lewis acids on the clay interface so that D,L-lactide polymerization occurs (Scheme 5.11).

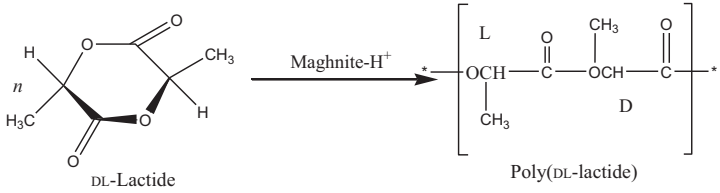

Scheme 5.11 Polymerization of DL-lactide over protonated montmorillonite clay.

Bhaskar et al. have identified an esterification method of phenyl acetic acid with *p*-cresol catalyzed by montmorillonite nanoclay [144]. Esters are important molecules with dierse applications in the preparation of perfumes, flavors, plasticizers, cosmetics, and pharmaceuticals [145]. It was observed that Al^{3+}-montnanoclay has the best catalytic properties. The recyclability of these solid catalysts renders these processes economical. These solid catalysts were recycled and therefor, this method was simple and economical (Scheme 5.12).

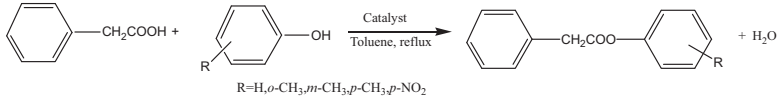

Scheme 5.12 Esterification of phenyl acetic acid (PA) with *p*-cresol (*p*-C) over montmorillonite nanoclay.

Sayyahi et al. have investigated the synthesis of 3,4-dihydropyrimidin-2(1*H*)-ones using ammonium salt-modified clay as catalyst in aqueous medium [146]. The preparation of dihydropyrimidines through multicomponent reactions [147–149] created special recognition due to its ability to synthesize biologically and pharmaceutically active molecules. Cetyltrimethylammonium bromide-modified organoclay was used for the preparation of 3,4-dihydropyrimidin-2(1*H*)-ones by reacting aromatic aldehyde, acetylacetone, or ethyl acetoacetate with urea. This environmentally benign method was rapid, cost effective, and produced products in high yields (Scheme 5.13).

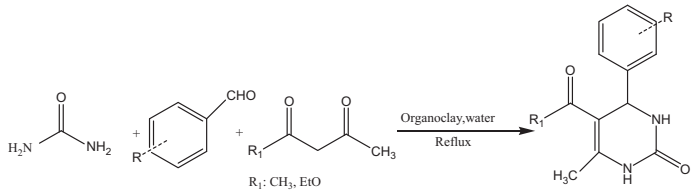

Scheme 5.13 Synthesis of 3,4-dihydropyrimidin-2(1*H*)-ones over quaternary ammonium-treated clay.

Borah et al. have developed azide-alkyne cycloaddition reaction through Cu(0)-nanoparticles in the nanopores of montmorillonite clay [150]. 1,2,3-Triazoles are nitrogen-containing heterocycles that have anti-HIV, antiallergic, antifungal, and antimicrobial properties [151]. These are also used as photostabilizers, agricultural products, optical brighteners, and corrosion preventing materials [152]. Triazoles were commonly prepared by the cycloaddition reaction of azides with different types of alkynes [153, 154]. These were also prepared using azides that are bound to polymer, zeolite or resin, and alkynes, enamines or β-ketoamides [155–157] (Scheme 5.14).

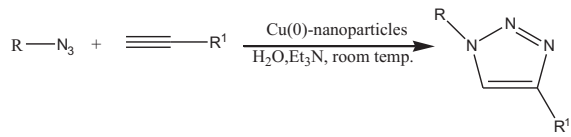

Scheme 5.14 Cycloaddition of azide-alkyne over Cu(0)-nanoparticles@montmorillonite.

5.2.4 Modified montmorillonite K-10 clay

Zeynizadeh et al. investigated the preparation of biscoumarins catalyzed by nickel nanoparticles immobilized on montmorillonite K-10 followed by a reduction method [158]. Biscoumarins (dicoumarols) are crucial intermediates for the preparation of acridinediones and heterocycles [159–162]. In addition, coumarins and dicoumarols demonstrated diverse medicinal properties that include antiinflammatory, antibacterial, antiviral, anticancer, and anti-HIV [160, 163]. Dicoumarols were prepared by refluxing 4-hydroxy-coumarins and aldehydes in suitable solvents [164] in the presence of catalytic amounts of molecular iodine [165], piperidine [166], DBU [167], *n*-dodecylbenzene sulfonic acid [168], lithium perchlorate [169], sodium dodecyl sulfate [170], Zn-proline complex [171], ammonium salt [172], ionic liquids [173], and nano silica [174] (Scheme 5.15).

Wang et al. have prepared neoflavonoid derivatives using sulfated montmorillonite K-10 [175]. Neoflavonoids (4-arylcoumarins) are distributed in nature and have medicinal properties. For example, some them have antioxidant [176], antidiabetic [177], anticancer [178], antimicrobial [179], antiinflammatory [180], antiprotozoal [181], and hormonal [182] properties. The synthesized compounds had antioxidant

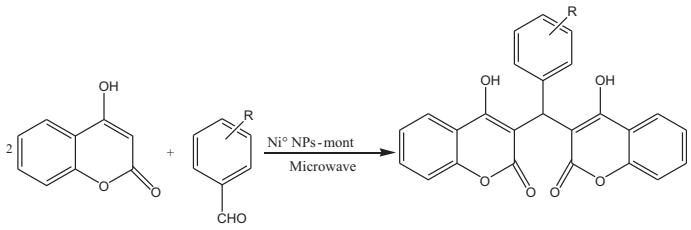

Scheme 5.15 Synthesis of biscoumarins over acid-activated montmorillonite K-10 (Ni-Mont).

and potent hydroxyl radical scavenging activity. Some of the compounds have proven excellent in controlling diabetes. Some compounds in this series were similar to that of the glibenclamide (Scheme 5.16).

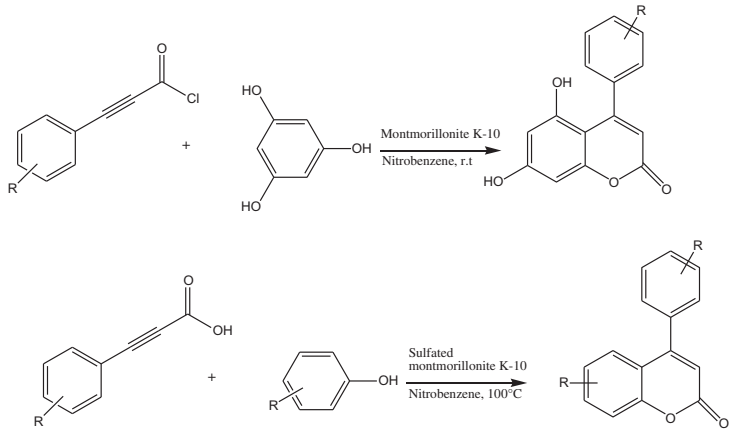

Scheme 5.16 Synthesis of neoflavonoid derivatives over sulfated montmorillonite K-10.

5.2.5 Natural bentonite clay

Vartooni et al. have investigated the solvent-free preparation of 1*H*-1,2,3,4-tetrazoles and reduction of 4-nitrophenol using bentonite-supported copper nanoparticles [183]. Tetrazoles are important medicinal agents. Some of them are isosteric for carboxylic acids [83] and used as analytical reagents with biological activities [184]. The catalyst was highly promising and recyclable for the synthesis of substituted tetrazoles following mild conditions. The Cu nanoparticles/bentonite system were found to be stable (Scheme 5.17).

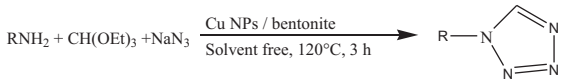

Scheme 5.17 Synthesis of 1-substituted 1*H*-1,2,3,4-tetrazoles over natural bentonite-supported copper nanoparticles.

Salmón et al. have studied the synthesis of dihydropyrimidones through Biginelli reaction in the presence of bentonitic clay as a Lewis catalyst [185]. β-Dicarbonyl compounds demonstrated pharmacological activities as calcium channel blockers and antihypertensive agents [186, 187] (Scheme 5.18).

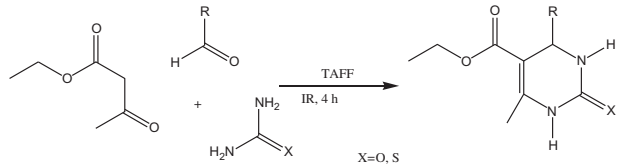

Scheme 5.18 Synthesis of dihydropyrimidones (DHPMs) via Biginelli reaction over bentonitic clay.

5.2.6 Modified bentonite clay

Surendra et al. have identified a route for the preparation of Schiff's bases using bentonite clay as the solid support [188]. Schiff bases are important molecules with a wide spectrum of applications and activities such as ligand synthesis [189], synthesis of organic structures [190] and has antibiotics, antifungal [191], anticancer, antiviral, anti-HIV, antiproliferative, herbicidal, and antiinfluenza A virus activities [192–194]. The preparation of Schiff base under microwave irradiation in the absence of solvent using clay catalyst was an attractive method. A condensation of primary amine with aromatic aldehyde reacted to form an intermediate which on dehydration formed the Schiff base [195]. The Schiff base synthesis was extended with various catalysts under microwave irradiation method [196–198]. This study indicated that a catalytic amount or small quantity of the catalyst is necessary for the preparation of the Schiff bases in the absence of solvent under microwave-induced reaction (Scheme 5.19).

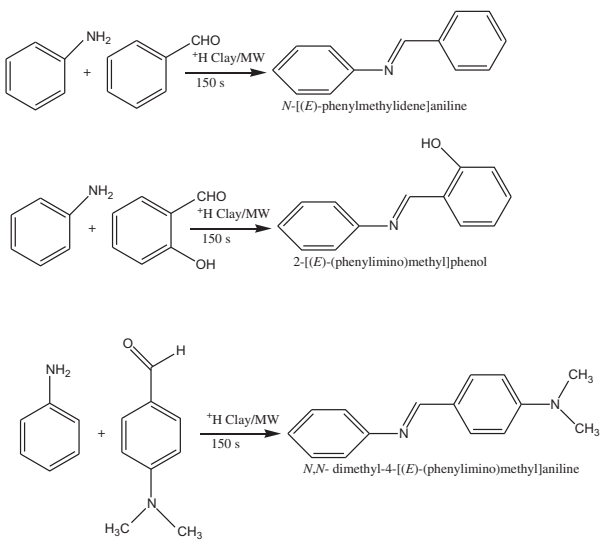

Scheme 5.19 Synthesis of Schiff's bases over modified bentonite clay

5.2.7 Montmorillonite KSF clay

Ballini et al. have achieved the preparation of *trans*-chalcones using catalytic amounts of montmorillonite KSF clay [199]. *trans*-Chalcones are used for their promising antineoplastic, spasmolytic, antibacterial, bacteriostatic, and bactericidal activities [200]. They are also used for the synthesis of five- and six-membered ring compounds due to their flexibility in structures [201]. Various acidic and basic solid catalysts were investigated to prepare *trans*-chalcones. But, ion-exchanged mesoporous materials [202], boric acid [203] and potassium hydroxide [204] bound silica gel, sulfonated carbon [205], and hydrotalcites were more common [206]. Microwave irradiation method with a solid catalyst was also studied for this purpose [207]. For example, montmorillonite KSF, benzaldehyde, and acetophenone at high temperature produced the product (Scheme 5.20). These molecules were synthesized in good yield and selectivity in the presence of montmorillonite KSF as catalyst in the absence of solvent. In addition, the catalyst was used five times without the loss of its power and the yields of the products remained unchanged.

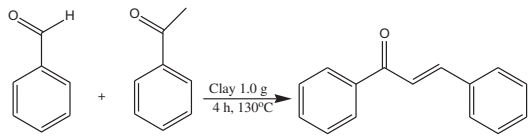

Scheme 5.20 Synthesis of *trans*-chalcones over montmorillonite KSF catalyst.

Reddy et al. have prepared 5-hydroxyindole derivatives using montmorillonite KSF clay as catalyst following the method developed by Nenitzescu [208]. Indoles are naturally abundant and present in many medicinally active molecules [209–218]. Specifically, 5-hydroxyindole systems are present in serotonin, a neurotransmitter and indomethacin, and an antiinflammatory compound. Moreover, 5-hydroxyindoles are active as new 5-lipoxygenase inhibitors [219–221]. Therefore, numerous ideas were forwarded for the preparation of these types of derivatives [222–224]. A ring construction by reacting quinones with enamines, obtained from 1,3-diketones and aromatic amines (Nenitzescu reaction), was the direct procedure to obtain 5-hydroxyindoles [225–229]. Zinc iodide and ceric ammonium nitrate were also found to be good catalysts for this reaction. The method with clay produced products in high yields and proceeded well with different types of dikeones and amines (Scheme 5.21).

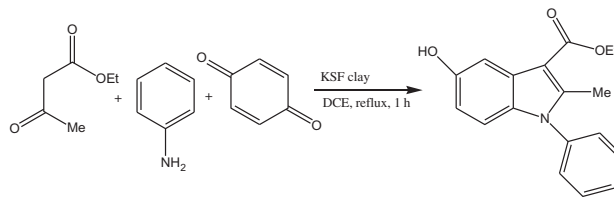

Scheme 5.21 Synthesis of 5-hydroxyindole over montmorillonite KSF clay.

Mitra et al. have investigated the microwave-induced montmorillonite KSF clay-catalyzed reactions for the preparation of dihydropyrimidinones under solvent-free method [230]. Some dihydropyrimidinones [231, 232] are medicinally active. For example, they are used as calcium channel blockers, antihypertensive agents, and neuropeptide Y antagonists [233]. Importantly, a few marine alkaloids have dihydropyrimidinone-5-carboxylate group in their compositions [234]. Batzelladine alkaloids are good HIV gp-120-CD4 inhibitors and they also have these types of structures [235–237].

Biginelli reaction has some limitation. It required corrosive acids in some examples. Moreover, aromatic and aliphatic aldehydes yielded products with low yields [186, 238]. Other Biginelli methods were discovered for the preparation of dihydropyrimidinones [239]. However, some of these nonenvironmentally benign methods had additional disadvantages because they used strong protic acids [240], corrosive Lewis acids [241, 242], and lanthanide reagents [243–247]. The clay-mediated Biginelli reaction is certainly an improved method because this is green and environmentally friendly method and proceeded very fast in the absence of any solvents (Scheme 5.22).

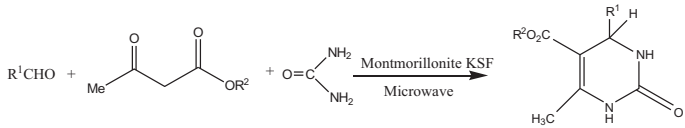

Scheme 5.22 Synthesis of dihydropyrimidinones over montmorillonite KSF clay.

5.2.8 Modified montmorillonite KSF clay

Rafiee et al. have studied a one-pot preparation of α-aminonitriles under catalytic conditions with KSF-supported heteropoly acids (HPAs) that include $H_3PW_{12}O_{40}$, $H_3PMo_{12}O_{40}$, and $H_3SiW_{12}O_{40}$ [248]. α-Aminonitriles are crucial molecules for the synthesis of α-amino acids, biologically active compounds [249], imidazoles, and thiadiazoles [250]. Some improved procedures of the Strecker reaction used for their synthesis were developed [44, 47, 49, 50, 251–259]. The most important improvement was the replacement of cyanide ion generation method [260–263]. For example, trimethylsilyl cyanide (TMSCN) was used as a safer nucleophile compared to hydrogen cyanide, sodium cyanide, or potassium cyanide. At the beginning heteropoly acid-supported clay was prepared under different conditions. This method produced products in excellent yields through easy work-up and mild conditions. The solid support was nontoxic, reusable, highly stable, and economical (Scheme 5.23).

Scheme 5.23 Synthesis of α-aminonitriles over KSF-supported heteropoly acids (HPAs).

Narayanan et al. have developed the preparation of amidoalkyl naphthols using phosphotungstic acid encapsulated montmorillonite clay-catalyzed reaction [264]. Some compounds with 1,3-amino oxygenated groups are known. They are present in natural products, nucleoside antibiotics, and HIV protease inhibitors [265, 266]. 1-Amidoalkyl-2-naphthols were converted to 1-aminomethyl-2-naphthols by hydrolysis and the amino derivatives demonstrate depressor effects and bradycardia [267]. Numerous catalysts including montmorillonite K-10 clay [268], $K_5CoW_{12}O_{40}.3H_2O$ [269], iodine [270], $H_4SiW_{12}O_{40}$ [271], $Ce(SO_4)_2$ [272], dodecylphosphonic acid [273], $Fe(HSO_4)_3$ [274], and $HClO_4$-SiO_2 [275] were used for the preparation of amidoalkyl naphthols. But, most of these methods have limitations: long reaction time, poor yield, use of toxic materials, and solvents (Table 5.4).

Table 5.4 Comparison of 10% PTA/Mont. KSF with reported catalysts in the synthesis of 1-amidoalkyl-2-napthols.

Catalyst	Benzaldehyde:2-naphthol: benzamide (catalyst mol%), reaction conditions	Time	Yield (%)	Ref
Montmorillonite K-10 clay	1:1:1.1 (0.1 g), 125°C	1.5 h	78	[268]
$K_5CoW_{12}O_{40}{\cdot}3H_2O$	1:1:1.3 (1 mol%), 125°C	2 h	80	[269]
Iodine	1:1:1.3 (5 mol%), 125°C	5.5 h	85	[270]
$H_4SiW_{12}O_{40}$	1:1;1.2 (5 mol%), 110°C	20 min	88	[271]
$Ce(SO_4)_2$	1:1:1 (1 mmol), CH_3CN, reflux	36 h	72	[272]
Dodecylphosphonic acid	1:1:1.2 (10 mmol), 90°C	20 min	90	[273]
10% PTA/Mont. KSF	1:1:1.1 (0.075 g), 120°C	6 min	96	–

Different amounts of montmorillonite KSF clay was encapsulated with tungstophosphoric acid (PTA) through sonication method. The catalytic activity of these solid substances for the synthesis of 1-amidoalkyl-2-napthols was compared in the absence of any solvents. Notably, the reaction was highly efficient and the catalyst was repeatedly used many times (Scheme 5.24).

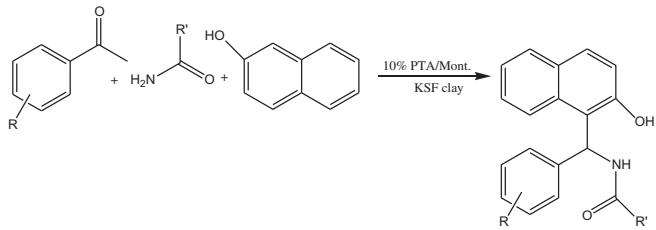

Scheme 5.24 Synthesis of amidoalkyl naphthols over PTA encapsulated montmorillonite clay.

Mahmoodi et al. have demonstrated the synthesis of thiazolidinones using KSF@Ni as catalyst following microwave-induced reaction [276]. Thiazolidinones are very important because of their medicinal properties. They have excellent anticancer [277], antiproliferative and tumor inhibitory [278], antihyperglycemic [279], antifungal [280], antitoxoplasma gondii [281], antibacterial [282], antiurease [283], antiviral [284], antischistosomal [285], antimalarial [286], herbicidal [287], antidiabetic [288], anticandida, and antioxidant values [289]. In the current method, the reaction was completed very fast with (60%–97%) yields [290, 291] (Scheme 5.25).

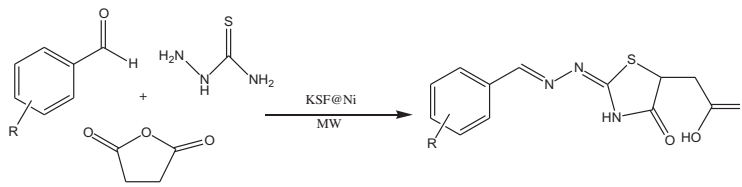

Scheme 5.25 Synthesis of thiazolidinones over KSF@Ni.

Yin et al. have studied the catalytic nitration of substituted phenols by salt-impregnated montmorillonite KSF [292]. Nitration of aromatics is a significant process [293–299]. Several metal salts (Mo and Yb)-impregnated KSF clays were prepared. The catalysts were recycled many times (Scheme 5.26).

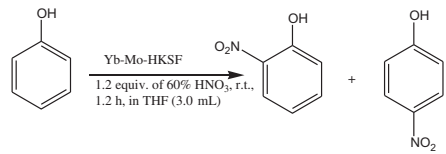

Scheme 5.26 Nitration of substituted phenols over metal salts impregnated Yb-Mo-montmorillonite KSF.

5.2.9 Kaolin

Khaleghi et al. have studied the kaolin-catalyzed synthesis of 5-alkoxycarbonyl-4-aryl-3,4-dihydropyrimidin-2(1*H*)-ones [300]. The dihydropyrimidinone systems are valuable biologically active molecules. Many of these have interesting medicinal values [301, 302]. Some compounds in this series have worked as calcium channel blocker and antihypertensive antagonist [303] (Table 5.5).

Better yield and fast reaction were observed with kaolin compared to other available catalysts. Therefore, this is a green method for the preparation dihydropyrimidinones using economical and reusable catalyst (Scheme 5.27).

Table 5.5 Synthesis of 5-ethoxycarbonyl-4-phenyl-6-methyl-3,4-dihydropyrimidin-2(1*H*)-one by different catalysts.

S. No.	Catalyst	Time (h)	Yield (%)	Ref.
1.	Montmorilonit KSF	48	82	[304]
2.	Sulfuric acid	18	71	[305]
3.	Zeolit	12	80	[306]
4.	Silica sulfuric acid	6	91	[307]
5.	Haulendite	4–5	75	[308]
6.	$BF_3{\cdot}OEt_2$/CuCl	18	71	[239]
7.	Kaolin	2.5	82	[300]

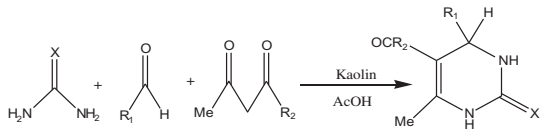

Scheme 5.27 Preparation of substituted dihydropyrimidinones over kaolin.

5.2.10 Modified kaolin

Srihari et al. have developed the preparation of 3-hydroxy-substituted 3-indolyl oxindoles using kaolin/KOH as catalyst [309]. Oxindole derivatives are biologically active in numerous areas [310–312]. In particular, 3,3-diaryl-oxindoles are active against bacteria, protozoa, and inflammation [30, 313–316]. 3-Aryl-3-hydroxy-2-oxindoles are also useful as drug candidates [317, 318] (Table 5.6).

Table 5.6 Catalyst optimization in methanol.

S.No.	Base	Time (h)	Yield (%)
1.	NaOH	3	70
2.	Cs_2CO_3	3.5	70
3.	K_2CO_3	3.5	67
4.	Pyrrolidine	4	35
5.	Piperidine	4	35
6.	Imidazole	3	30
7.	Benzimidazole	4	30
8.	1,2,4-Triazole	4	25
9.	Kaolin/KOH	2.5	90

This procedure is suitable for large-scale synthesis because of its convenient nature (Scheme 5.28).

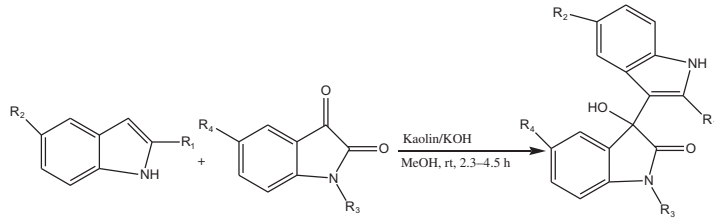

Scheme 5.28 Synthesis of 3-hydroxy-3-indolyl oxindoles over kaolin/KOH.

Sadeghi et al. have synthesized spirooxindoles through a three-component catalytic procedure by nano-Ag/kaolin [319]. Spirooxindoles are valuable compounds used as biopharmaceutical [320–325]. The preparation of spirooxindoles with fused chromenes was performed by three-component reaction between isatins, activated methylene compounds, and 1,3-dicarbonyl molecules. A number of catalysts were used for this purpose. Some of these were triethylbenzyl ammonium chloride [326], $InCl_3$ [327], NEt_3 [328], NaBr/ROH [329], β-cyclodextrin [330], $[BMIm]BF_4$ [331], L-proline [332, 333], MgO [334], surfactant metal carboxylates [335], ethylenediaminediacetate [336], Carbon-SO_3H [337], and ZnS nanoparticle [338]. However, method by kaolin was proved to be the best (Scheme 5.29).

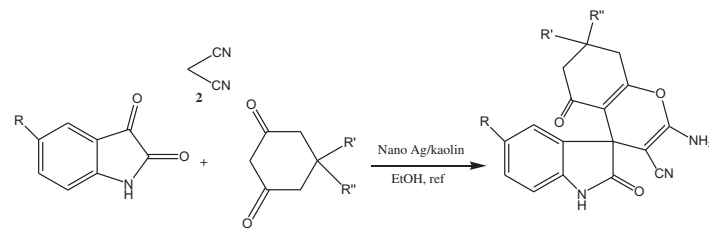

Scheme 5.29 Synthesis of spirooxindoles over nano Ag/kaolin.

5.2.11 Pillared clay

Sharma et al. have synthesized bisindolylmethanes using substituted indoles and carbonyl compounds in the presence of Fe/Al pillared clay [339]. Bis(indolyl)alkanes are isolated from marine sponge alkaloids [340]. These types of compounds have antibacterial and antitumor properties [341] (Table 5.7).

Many other synthetic routes were performed by Bronsted acids [345], Lewis acids [346], ionic liquids [347–350], resins [351], and metals [352] for the synthesis of these types of compounds. But, clay-mediated synthesis was the choice because it was environmentally friendly and more effective, and the entire process was convenient compared to the other methods [342, 344, 353, 354] (Scheme 5.30).

Table 5.7 The effects of Fe/Al pillared clay and other catalysts on the reaction of indole with benzaldehyde.

Entry	Reaction condition/time	Catalyst content	Yield (%)	Ref.
1.	Zeokarb-225/CH_3CN 7.5 h	0.5 g	95	[342]
2.	ZrO_2 (400°C) 1 h	–	70	[343]
3.	$ZrOCl_2 \cdot 8H_2O$, solvent-free, 50°C/40 min	5 mol%	84	[344]
4.	SO_4^{-2}/ZrO_2 (500°C)/50 min	1.5 N	89	[343]
5.	PO_4^{-3}/ZrO_2 (500°C)/20 min	1.5 N	92	[343]
6.	Fe/Al pillared clay (425°C)/ solvent free, 15 min	0.5 mol%	94	[339]

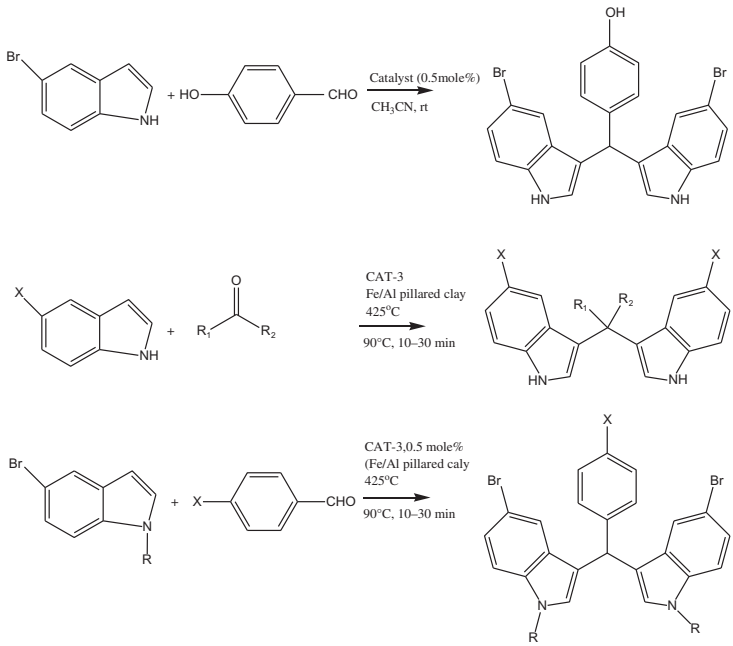

Scheme 5.30 Synthesis of bisindolylmethanes over diversely substituted indoles.

5.2.12 Super acid clays

Guerrero et al. have studied the preparation of 1,3,5-triphenylbenzenes, β-methylchalcones, and 2,4,6-triphenyl pyrylium salts in the presence of super acid triflouromethane sulfonic clay [355]. The pyrylium salts are used in lasers [356, 357], liquid crystalline substrates [358], phototherapeutic compounds [359] and in light-induced electron transfer processes [360]. 2,4,6-Triphenyl pyrylium derivatives have unique photophysical charateristics [361] (Scheme 5.31).

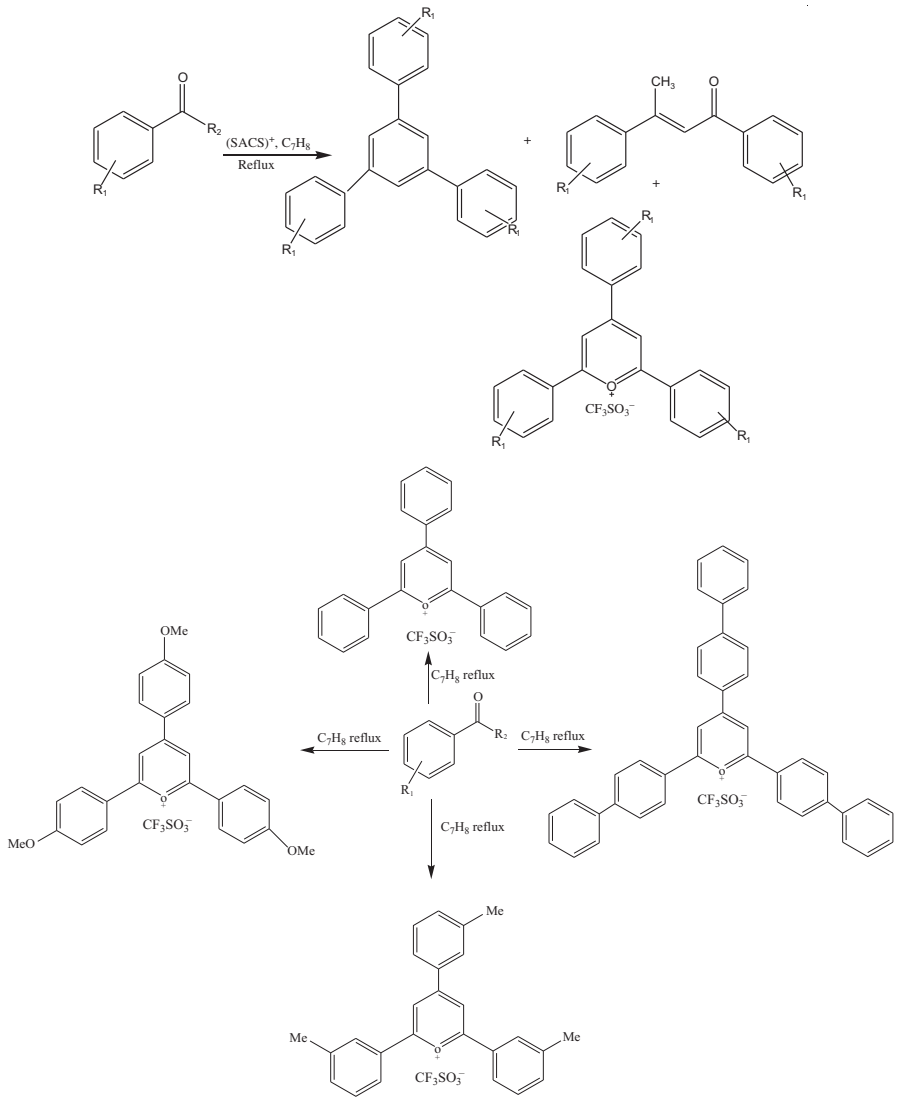

Scheme 5.31 Preparation of triphenylbenzenes, β-methylchalcones, and triphenyl pyrylium salts with super acid triflouromethane sulfonic clay.

5.2.13 Comparative study of montmorillonite-KSF and K-10 clays

Habibi et al. have investigated montmorillonite-KSF and montmorillonite K-10 clay-mediated solventless synthesis of bismaleimides and bisphthalimides [362]. Maleimides are used in biological, synthetic, and polymer chemistry. Maleimides are used as probes of protein structure because they react very fast with cysteines residues. They are also used as linkers for the conjugation of organic compounds to proteins.

They serve as immunoconjugates for cancer treatment or haptens for antibodies [363–366]. The functional groups present in maleimide work like Michael acceptor and are dienophilic in nature. The available methods for the preparation of these important compounds are not satisfactory [367–377]. Synthesis of maleimides by condensation and acid-induced cyclization procedures did not produce products in good yields. Therefore, it was necessary to identify a clean method avoiding strong acids or bases. The clay-induced method was performed under solvent-free conditions and focused to develop these important classes compounds following sustainable conditions (Scheme 5.32).

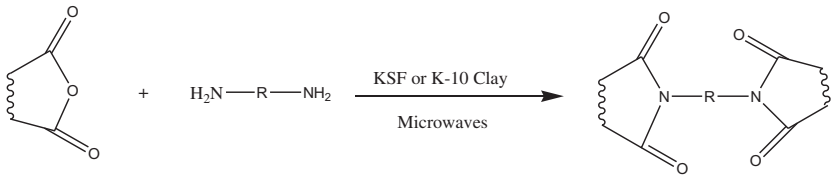

Scheme 5.32 Synthesis of bismaleimides and bisphthalimides in the presence of montmorillonite KSF and montmorillonite K-10 clays.

Naeem et al. have developed the synthesis of 4-thiazolidinones under microwave-induced reaction in the presence of montmorillonite clays (K-10 and KSF) [378]. 4-Thiazolidinones are valuable precursors with numerous medicinal applications [379, 380]. The molecules prepared by this showed excellent antibacterial activities compared with drugs available in the market. The current method was advantageous from the point of view of green chemistry (Scheme 5.33).

Venkatesha et al. have synthesized cyclic imides in the presence of acidic montmorillonite clays [381]. Cyclic imides are used as medicine, polymer, and dyes and for the manufacture of fine chemicals. These types of compounds were prepared through a condensation reaction of dicarboxylic acids with amines. The condensation were performed by H_2SO_4, HCl, *p*-TSA, [382–384], silica sulfuric acid, niobic acid, ZSM-5, heteropoly acid, Al_2O_3 [385], $TaCl_2$ on SiO_2, $FeCl_3$, and $AlCl_3$ [386–388]. Specifically cyclic imides served as intermediates in the synthesis of several medicinally active molecules: floxacin [389], aminopeptidase *N*-inhibitors [390], fungicides [391], herbicides [392], bactericidal [393], antimalarial [394], antitumor, and leprosy [395]. These acid-washed clays were used a number of times without deactivation because of their enhanced pore availability (Table 5.8, Scheme 5.34).

Marvi et al. have identified clay-catalyzed Cannizzaro process in the presence of 1,4-diazabicyclo[2.2.2]octane (DABCO) following microwave and solvent-free methods [396]. The redox disproportion of aldehydes into alcohols and carboxylic acids represent Cannizzaro reaction [397, 398]. This is usually performed at high temperature using excess strong bases. The superiority of K-10 clay was seen as compared

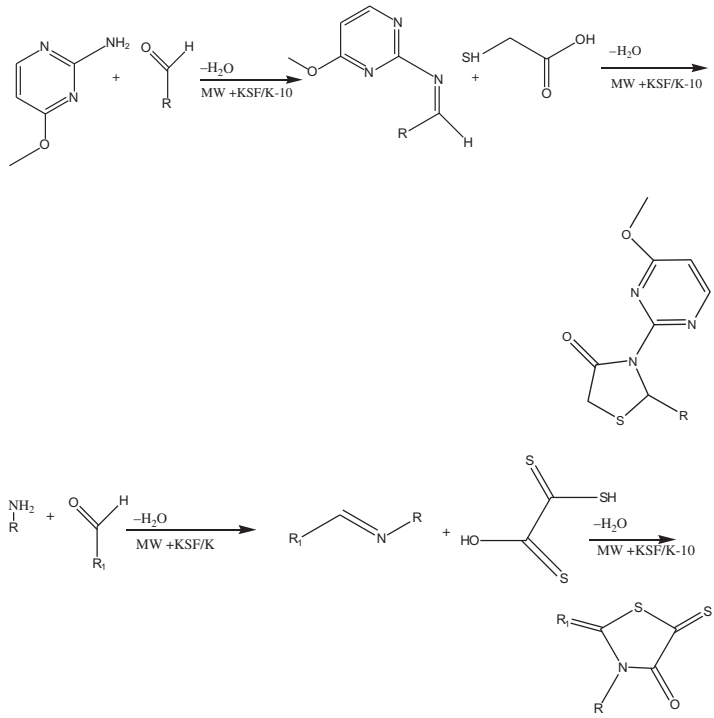

Scheme 5.33 Synthesis of 4-thiazolidinone derivatives over montmorillonite clays (K-10 and KSF).

Table 5.8 Comparison of different catalysts for the conversion of benzene dicarboxylic acid and yield of cyclic imide

S.No.	Catalysts	BDC conversion	% yield of cyclic imides
1.	Al-clay	49	13
2.	Al-pillared clay	56	16
3.	Fe-pillared clay	50	12
4.	Zr-pillared clay	54	10
5.	K-10	54	18
6.	KSF	33	06
7.	ZrO_2	51	22
8.	SnO_2	62	26
9.	Al_2O_3	53	18
10.	ZSM-5	44	20
11.	HBEA	78	78
12.	H-Y	80	76
13.	*p*-TSA clay	80	80
14.	MSA clay	80	80
15.	PDSA clay	80	80

Scheme 5.34 Synthesis of cyclic imides by amidation.

to KSF because K-10 has higher surface area (250 $m^2\ g^{-1}$) compared to KSF (10 $m^2\ g^{-1}$). The combination of montmorillonites and microwave irradiation demonstrated rate acceleration and high yields of the products. The solventless reaction with heterogeneous system media under microwave irradiation method was highly efficient and useful from ecological points of view [399–403] (Scheme 5.35).

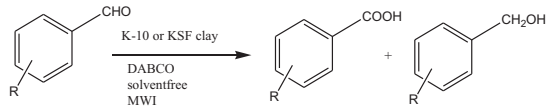

Scheme 5.35 Clay catalyzed Cannizzaro reaction over 1,4-diazabicyclo[2.2.2]octane (DABCO).

5.3 Conclusions

Different clay-catalyzed reactions for the preparation of pharmaceutically relevant organic molecules were investigated. Numerous treated forms of clays played a significant role in increasing the yield of the products. These reactions were investigated under different conditions: in the absence of solvents, microwave, and ultrasound method, at different temperature, by changing molar ratios of the reactants and under various concentrations of clays. The availability of both the Bronsted and Lewis acid sites in the acid-treated clays were found to be more effective in diverse reactions. Most of the reactions produced medicinally important products in excellent yield. The clays were found to be reusable without causing deactivation. The experimental and product isolation procedures were simple and therefore, these methods played an important role in the development of environmentally benign method [9]. Based on the available literature, we believe that clay-mediated reactions would continue to play a major role in drug discovery process following the principles of green chemistry.

Acknowledgment

Bimal Krishna Banik is grateful to Prince Mohammad Bin Fahd University.

References

[1] A. Valavanidis, T. Vlachogianni, Green Chemistry and Green Engineering from Theory to Practice for the Protection of the Environment and Sustainable Development, Synchrona Themata, Athens, 2012.

[2] P.T. Anastas, T.C. Williamson, Green Chemistry: Designing Chemistry for the Environment, ACS Publications, Washington, DC, 1996.
[3] R.A. Sheldon, I. Arends, U. Hanefeld, Green Chemistry and Catalysis, fourteenth ed., Weinheim, Wiley-VCH Verlag, 2007.
[4] S.E. Manahan, Green Chemistry and the Ten Commandments of Sustainability, second ed., Chemchar Research, Inc., Columbia, MO, 2006.
[5] P.T. Anastas, J.C. Warner, Green Chemistry: Theory and Practice, Oxford University Press Inc, New York, 1998.
[6] V.K. Ahluwalia, M. Kidwai, New Trends in Green Chemistry, second ed., Anamaya Publishers, New Delhi, 2004.
[7] K. Cavell, S. Golunski, D. Miller, Handbook of green chemistry–green catalysis, Platin. Met. Rev. 54 (4) (2010) 233–238.
[8] E.J. Beckman, Supercritical and near-critical CO_2 in green chemical synthesis and processing, J. Supercrit. Fluids 28 (2004) 121–191.
[9] W. Wardencki, J. Curylo, J. Namiesnik, Green chemistry–current and future issues, Pol. J. Environ. Stud. 14 (4) (2005) 389–395.
[10] V. Kumar, An Introduction to Green Chemistry, first ed., Vishal Publishing Co., Jalandhar, 2010.
[11] C. Gong, D.P. Hart, Ultrasound induced cavitation and sonochemical yields, J. Acoust. Soc. Am. 104 (1998) 1–16.
[12] M. Pattanayak, P.L. Nayak, Ecofriendly green synthesis of iron nanoparticles from various plants and spices extract, Int. J. Plant Anim. and Environ. Sci. 3 (1) (2013) 68–78.
[13] N. Durán, R. Cuevas, L. Cordi, O. Rubilar, M.C. Diez, Biogenic silver nanoparticles associated with silver chloride nanoparticles (Ag@AgCl) produced by laccase from Trametes versicolor, SpringerPlus 3 (645) (2014) 1–7.
[14] A.G. Ingale, A.N. Chaudhari, Biogenic synthesis of nanoparticles and potential applications: an eco-friendly approach, J. Nanomed. Nanotechol. 4 (2) (2013) 1–7.
[15] J.K. Andeani, S. Mohsenzadeh, Phytosynthesis of cadmium oxide nanoparticles from Achillea wilhelmsii flowers, J. Chem. 2013 (2012) 1–4.
[16] M. Rautureau, Clay and clay mineral definition, in: Clays and Health, Springer International Publishing AG, 2017.
[17] O. Landoulsi, A. Megriche, R. Calvet, F. Espitalier, J.M.F. Ferreira, A. Mgaidi, Effect of heating and acid activation on the structure and surface properties of a kaolinite-illite-Smectite clayey mixture, Miner. Process. J. 6 (2013) 13–20.
[18] Madejova, FT-IR techniques in clay mineral structures: review, Vib. Spectrosc. 31 (1) (2003) 1–10.
[19] H. Chen, G. Zhang, K. Richardson, J. Luo, Synthesis of nanostructured nanoclay-zirconia multilayers: a feasibility study, J. Nanomater. (2008) 1–8.
[20] A.A. Aja, G.J. Randy, Physical properties of kaolin used in soap production in Nigeria, Int. J. Eng. Sci. 2 (10) (2013) 10–15.
[21] R.C. Mackenzie, The classification and nomenclature of clay minerals, Clay Min. Bull (1959) 52–66.
[22] C.D. Barton, A.D. Karathanasis, Clay minerals, in: Encyclopedia of Soil Science, Marcel Dekker, 2002, pp. 187–192.
[23] O. Ombaka, Characterization and classification of clay minerals for potential applications in Rugi Ward, Kenya, Afr. J. Environ. Sci. Technol. 10 (11) (2016) 415–431.
[24] I. Shaikh, S. Pawar, M. Shaikh, S. Abed, A novel clay catalyst: N-acetylation of aniline, J. Chem. Pharm. Res. 8 (5) (2016) 725–729.
[25] B.A. Lole, P.B. Piste, Clay mediated one step synthesis of azo dyes with 1,3-benzoxazole moiety, J. Chem. Pharm. Res. 9 (12) (2017) 53–58.

[26] A.Z. Sayed, M.S.A. Fetouh, H.S. Nassar, Synthesis, biological activity and dyeing performance of some novel azo disperse dyes incorporating pyrazolo[1,5-a]pyrimidines for dyeing of polyester fabrics, J. Mol. Struct. (2012) 146–151.
[27] H. Xu, X. Zeng, Synthesis of diaryl-azo derivatives as potential antifungal agents, Bioorg. Med. Chem. Lett. 20 (4) (2010) 4193–4195.
[28] M. Chakrabarty, S. Sarkar, Y. Harigaya, A facile clay-mediated synthesis of 3,3-diindolyl-2-indolinones from isatins, J. Chem. Res. 2005 (2005) 540–542.
[29] M.H. Hubacher, S. Doernberg, A. Horner, Laxatives: chemical structure and potency of phthaleins and hydroxyanthraquinones, J. Am. Pharm. Assoc. 42 (1) (1953) 23–30.
[30] K.C. Joshi, V.N. Pathak, S.K. Jain, Studies of potential organo-fluorine antibacterial agents. Part 5: Synthesis and antibacterial activity of some new fluorine-containing indole-2,3-dione derivatives, Pharmazie 35 (11) (1980) 677–679.
[31] F. Garrido, J. Ibanez, E. Gonalons, A. Giraldez, Synthesis and laxative properties of some derivative esters of 3,3 bis (4 hydroxyphenyl) 2 indolinone, Eur. J. Med. Chem. 10 (1975) 143–146.
[32] J. Bergman, N. Eklund, Synthesis and studies of tris-indolobenzenes and related compounds, Tetrahedron 36 (10) (1980) 1445–1450.
[33] M. Kobayashi, S. Aoki, K. Gato, K. Matsunami, M. Kurosho, I. Kitagawa, Marine natural products. XXXIV. Trisindoline, a new antibiotic indole trimer, produced by a bacterium of Vibrio sp. separated from the marine sponge Hyrtios altum, Chem. Pharm. Bull. 42 (12) (1994) 2449–2451.
[34] J. Azizian, A.A. Mohammadi, A.R. Karimi, M.R. Mohammadizadeh, $KAl(SO_4)_2.12H_2O$ as a recyclable Lewis acid catalyst for synthesis of some new oxindoles in aqueous media, J. Chem. Res. (2004) 424–426.
[35] M. Chakrabarty, S. Sarkar, Novel clay-mediated, tandem addition–elimination-(Michael) addition reactions of indoles with 3-formylindole: an eco-friendly route to symmetrical and unsymmetrical triindolylmethanes, Tetrahedron Lett. 43 (7) (2002) 1351–1353.
[36] M. Chakrabarty, N. Ghosh, R. Basak, Y. Harigaya, Dry reaction of indoles with carbonyl compounds on montmorillonite K10 clay: a mild, expedient synthesis of diindolylalkanes and vibrindole A, Tetrahedron Lett. 43 (2002) 4075–4078.
[37] M. Chakrabarty, S. Sarkar, A clay-mediated eco-friendly thiocyanation of indoles and carbazoles, Tetrahedron Lett. 44 (2003) 8131–8133.
[38] C. Yildirim, C. Yolacan, F. Aydogan, Synthesis of α-aminonitriles catalyzed by montmorillonite K10 in the presence of dicationic phosphonium salt in water under ultrasonic effect, Turk. J. Chem. 36 (2012) 101–109.
[39] A.J. Davies, M.S. Ashwood, I.F. Cottrell, A Facile Synthesis of Substituted Phenylglycines, Synth. Commun. 30 (6) (2000) 1095–1102.
[40] E. Leclerc, P. Mangency, V. Henryon, Enhancement of the diastereoselectivity in the addition of trimethylsilyl cyanide to chiral aldimines by catalysis with a chiral 1,2-diamine: unexpected mechanistic results, Tetrahedron Asymmetry 11 (2000) 3471–3474.
[41] L.M. Weinstock, P. Davis, B. Handelsman, R.J. Tull, General synthetic system for 1,2,5-thiadiazoles, J. Org. Chem. 32 (9) (1967) 2823–2829.
[42] F. Louafi, J.P. Hurvois, A. Chibani, T. Roisnel, Synthesis of tetrahydroisoquinoline alkaloids via anodic cyanation as the key step, J. Org. Chem. 75 (16) (2010) 5721–5724.
[43] A.R. Hajipour, Y. Ghayeb, N. Sheikhan, $Zr(HSO_4)_4$ catalyzed one-pot strecker synthesis of α-amino nitriles from aldehydes and ketones under solvent-free conditions, J. Iran. Chem. Soc. 7 (2010) 447–454.

[44] S.K. De, Nickel(II) chloride catalyzed one-pot synthesis of α-aminonitriles, J. Mol. Catal. A Chem. 225 (2) (2005) 169–171.
[45] S. Paraskar, A. Sudalai, Cu(OTf)$_2$ or Et$_3$N-catalyzed three-component condensation of aldehydes, amines and cyanides: a high yielding synthesis of a-aminonitriles, Tetrahedron Lett. 47 (2006) 5759–5762.
[46] S.K. De, R.K. Gibbs, Ruthenium(III) chloride–catalyzed ring opening of epoxides with aromatic amines, Synth. Commun. 35 (20) (2005) 2675–2680.
[47] L. Royer, S.K. De, R.A. Gibbs, Iodine as a novel and efficient reagent for the synthesis of α-aminonitriles by a three-component condensation of carbonyl compounds, amines, and trimethylsilyl cyanide, Tetrahedron Lett. 46 (2005) 4595–4597.
[48] M. Narasimhulu, T.S. Reddy, K.C. Mahesh, S.M. Reddy, A.V. Reddy, Y. Venkateswarlu, Lanthanum(III) nitrate hexahydrate or gadolinium(III) chloride hexahydrate catalyzed one-pot synthesis of α-amino nitriles, J. Mol. Catal. A Chem. 264 (1–2) (2007) 288–292.
[49] B.C. Ranu, S.S. Dey, A. Hajra, Indium trichloride catalyzed one-step synthesis of α-amino nitriles by a three-component condensation of carbonyl compounds, amines and potassium cyanide, Tetrahedron 58 (13) (2002) 2529–2532.
[50] M. Mojtahedi, M.S. Abaee, T. Alishiri, Superparamagnetic iron oxide as an efficient catalyst for the one-pot, solvent-free synthesis of α-aminonitriles, Tetrahedron Lett. 50 (20) (2009) 2322–2325.
[51] E. Rafiee, S. Rashidzadeh, A. Azad, Silica supported heteropol acids: Highl efficient catalyst for the synthesis of α-aminonitriles, using trimethylsilyl canide or potassium cyanide, J. Mol. Catal. A Chem. 261 (2007) 49–52.
[52] A. Shaabani, A. Maleki, Cellulose sulfuric acid as a bio-supported and recyclable solid acid catalyst for the one-pot three-component synthesis of α-amino nitriles, Appl. Catal. A Gen. 331 (2007) 149–151.
[53] K. Iwanami, H. Seo, J.C. Choi, T. Sakakura, H. Yasuda, Al-MCM-41 catalyzed three-component strecker-type synthesis of α-aminonitriles, Tetrahedron 66 (10) (2010) 1898–1901.
[54] T.L. Lambat, S.S. Deo, Montmorillonite K10 catalysed condensation of 1-(3-chlorophenyl)-4-(3-chloropropyl) piperazine and 1,2,4-triazolo [4,3-a]pyridine-3-(2H)-one: a proficient and green synthesis of trazodone hydrochloride and its analogues, Synth. Catal. 1 (2016) 1.
[55] N.R. Pai, D.S. Dubhashi, Studies of antipsychotic drugs as potential schizophrenia agents, J. Chem. Pharm. Res. 2 (2010) 458–472.
[56] M. Tatsumi, K. Groshan, R.D. Blakely, E. Richelson, Pharmacological profile of antidepressants and related compounds at human monoamine transporters, Eur. J. Pharmacol. 340 (1997) 249–258.
[57] T.L. Lambat, S.S. Deo, Synthesis of Novel Benzofluorenone Derivatives and their HIV-Reverse Transcriptase Inhibitory Activity, J. Chinese Adv. Mater. Soc. 5 (1) (2017) 20–32.
[58] T.L. Lambat, S.S. Deo, F.S. Inam, T.B. Deshmukh, A.R. Bhat, Montmorillonite K10: an efficient organo heterogeneous catalyst for one-pot synthesis of new N,N′-alkylidene bisamide derivatives under solvent free condition, Karbala Int. J. Mod. Sci. 2 (2016) 63–68.
[59] T.L. Lambat, S.S. Deo, Sulphamic acid: an efficient and green synthesis of 2-[3-{4-(3-chlorophenyl)-1-piperazinyl} propyl]-1, 2, 4-triazolo [4, 3-a] pyridine-3-(2H)-one hydrochloride and its derivatives, Der Pharmacia Lett. 6 (2014) 218–224.
[60] G.J. Marek, C.J. McDougle, L.H. Price, L.S. Seiden, A comparison of trazodone and fluoxetine: implications for a serotonergic mechanism of antidepressant action, Psychopharmacology (Berl) 109 (1992) 2–11.

[61] A.M. Zonouz, S.B. Hosseini, Montmorillonite K10 clay: an efficient catalyst for hantzsch synthesis of 1, 4-dihydropyridine derivatives, Synth. Commun. 38 (2008) 290–296.
[62] G.J. Dubur, M.M. Veveris, G. Weinheimer, E.A. Bisenieks, N.R. Makarova, A.A. Kimenis, J.R. Uldrikis, E.J. Lukevics, D. Dooley, H. Osswald, Synthesis and selective vasodilating properties of esters of 2,6-dimethyl-4-(2-difluoromethoxyphenyl)-1,4-dihydropyridine-3,5-dicarboxylic acid, Arzneimittelforschung 39 (10) (1989) 1185–1189.
[63] R. Peri, S. Padmanabhan, A. Rutledge, S. Singh, D.J. Triggle, Permanently charged chiral 1,4-dihydropyridines: molecular probes of L-type calcium channels. Synthesis and pharmacological characterization of methyl (ω-trimethylalkylammonium)1,4-dihydro-2,6-dimethyl-4-(3-nitrophenyl)-3,5 pyridinedicarboxylate iodide, calcium channel antagonists, J. Med. Chem. 43 (15) (2000) 2906–2914.
[64] I. Misane, V. Klusa, M. Dambrova, S. Germane, G. Duburs, E. Bisenieks, R. Rimondini, S.O. Ogren, A typical neuromodulaotry profile of glutapyrone, a representative of a novel class of amino acid-containing dipeptide-mimicking 1,4-dihydropyridine (DHP) compounds in vitro and in vivo studies, Eur. Neuropsychopharmacol. 8 (1998) 329–347.
[65] A. Krauze, S. Germane, O. Eberlins, I. Sturms, V. Klusa, G. Duburs, Derivatives of 3-cyano-6-phenyl-4-(3'-pyridyl)-pyridine-2(1H)-thione and their neurotropic activity, Eur. J. Med. Chem. 34 (1999) 301–310.
[66] J. Briede, D. Daija, M. Stivrina, G. Duburs, Effect of cerebrocrast on the lymphocyte blast transformation activity in normal and streptozotocin-induced diabetic rats, Cell Biochem. Funct. 17 (2) (1999) 89–96.
[67] L.M. Tarasenko, K.S. Neporada, V. Klusha, Stress-protective effect of glutapyrone belonging to a new type of amino acid-containing 1,4-dihyropyridines on periodontal tissues and stomach in rats with different resistance to stress, Bull. Exp. Bio. Med. 133 (4) (2002) 369–371.
[68] A. Klegeris, E. Liutkevicius, G. Mikalauskiene, G. Duburs, P.L. McGeer, V. Klusa, Anti-inflammatory effects of cerebrocrast in a model of rat paw edema and on mononuclear THP-1 cells, Eur. J. Pharmacol. 441 (3) (2002) 203–208.
[69] G. Song, B. Wang, X. Wu, Y. Kang, L. Yang, Montmorillonite K10 clay: an effective solid catalyst for one-pot synthesis of polyhydroquinoline derivatives, Synth. Commun. 35 (2005) 2875–2880.
[70] T. Godfraid, R. Miller, M. Wibo, Calcium antagonism and calcium entry blockade, Pharmacol. Rev. 38 (1986) 321–416.
[71] R. Mannhold, B. Jablonka, W. Voigdt, K. Schoenafinger, K. Schravan, Calcium- and calmodulinantagonism of elnadipine derivatives: Comparative SAR, Eur. J. Med. Chem. 27 (1992) 229–235.
[72] F. Bossert, H. Meyer, E. Wehinger, 4-Aryldihydropyridines, a new class of highly active calcium antagonists, Angew. Chem., Int. Ed. Engl. 20 (1981) 762–769.
[73] H. Nakayama, Y. Kasoaka, Chemical identification of binding sites for calcium channel antagonists, Heterocycles 42 (1996) 901–909.
[74] J.B. Sainani, A.C. Shah, Synthesis of 4-aryl-1,4,5,6,7,8-hexahydro-5-oxo-2,7,7-trimethylquinoline-3-carboxylate and amides, Indian J. Chem. Sect. B. 33 (1994) 526–531.
[75] M. Sufirez, E. Ochoa, Y. Verdecia, B. Verdecia, L. Moran, N. Martin, M. Quinteiro, C. Seoane, J.L. Soto, H. Novoa, N. Blaton, O.M. Peters, A joint experimental and theoretical structural study of novel substituted 2,5-dioxo-l,2,3,4,5,6,7,8-octahydroquinolines, Tetrahedron 55 (1999) 875–884.
[76] S.J. Ji, Z.Q. Jiang, J. Lu, T.P. Loh, Facile ionic liquids-promoted one-pot synthesis of polyhydroquinoline derivatives under solvent-free conditions, Synlett 5 (2004) 831–835.

[77] V.K. Ahluwalia, B. Goyal, U. Das, One-pot synthesis of 5-oxo-1,4,5,6,7, 8-hexahydroquinolines and pyrimido[4,5-b] quinolines using microwave irradiation and ultrasound, J. Chem. Res. Synop. (1997) 226.
[78] S.J. Tu, J.F. Zhou, X. Deng, P.J. Cai, H. Wang, J.C. Feng, One-step synthesis of 4-arylpolyhydroquinoline derivatives using microwave irradiation, Chinese J. Org. Chem. 21 (2001) 313–316.
[79] O. Marvi, A. Alizadeh, S. Zarrabi, Montmorillonite K-10 clay as an efficient reusable heterogeneous catalyst for the solvent-free microwave mediated synthesis of 5-substituted 1H-tetrazoles, Bull. Korean Chem. Soc. 32 (11) (2011) 4001–4004.
[80] A.J. Zych, R.J. Herr, Tetrazoles as carboxylic acid bioisosteres in drug discovery, PharmaChem 6 (4) (2007) 21–24.
[81] L.V. Myznikov, A. Hrabalek, G.I. Koldobskii, Drugs in the tetrazole series, Chem. Heterocycl. Compd. 43 (1) (2007) 1–9.
[82] B.C.H. May, A.D. Abell, The synthesis and crystal structure of alpha-keto tetrazole-based dipeptide mimics, Tetrahedron Lett. 42 (33) (2001) 5641–5644.
[83] R.J. Herr, 5-Substituted-1H-tetrazoles as carboxylic acid isosteres: medicinal chemistry and synthetic methods, Bioorg. Med. Chem. 10 (11) (2002) 3379–3393.
[84] G.F. Holland, J.N. Pereira, Heterocyclic tetrazoles, a new class of lipolysis inhibitors, J. Med. Chem. 10 (2) (1967) 149–154.
[85] S.K. Figdor, M.S. von Wittenau, Metabolism of 5-(3-Pyridyl)tetrazole, J. Med. Chem. 10 (6) (1967) 1158–1159.
[86] D.W. Esplin, D.M. Woodbury, The fate and excretion of C14-labeled pentylenetetrazol in the rat, with comments on analytical methods for pentylenetetrazol, J. Pharmacol. Exp. Ther. 118 (2) (1956) 129–138.
[87] A.R. Modarresi-Alam, H. Keykha, F. Khamooshi, H.A. Dabbagh, Dynamic 1H NMR study of 4-methylphenoxyimidoyl azides: conformational or configurational isomerisation? Tetrahedron 60 (7) (2004) 1525–1530.
[88] A.R. Modarresi-Alam, F. Khamooshi, M. Rostamizadeh, H. Keykha, M. Nasrollahzadeh, H.R. Bijanzadeh, E. Kleinpeter, Dynamic 1H NMR spectroscopic study of the restricted SN rotation in aryl-N-(arylsulfonyl)-N-(triphenylphosphoranylidene) imidocarbamates, J. Mol. Struct. 841 (1–3) (2007) 61–66.
[89] P.K. Kadaba, Role of protic and diprotic solvents in heterocyclic syntheses via 1,3-dipolar cycloaddition reaction, Synthesis 1973 (2) (1973) 71–84.
[90] H.R. Meier, H. Heimgarther, in: E. Schumann (Ed.), Methoden der Organischen Chemie (Houben-Weyl), Georg Thieme, Stuttgart, 1994. E8d, 664.
[91] R.N. Bulter, Tetrazoles, in: A.R. Katritzky, C.W. Rees (Eds.), Comprehensive Heterocyclic Chemistry, vol. 5, Pergamon, Oxford, 1984, pp. 791–838.
[92] H. Singh, A.S. Chawla, V.K. Kapoor, D. Paul, R.K. Malhotra, Medicinal chemistry of tetrazoles, Prog. Med. Chem. 17 (1980) 151–183.
[93] V.A. Ostrovskii, M.S. Pevznert, T.P. Kofmna, M.B. Shcherbinin, I.V. Tselinskii, Reviews and accounts on heterocyclic chemistry, Targets Heterocycl. Syst. 3 (1999) 467–526.
[94] G.I. Koldobskii, V.A. Ostrovskii, Tetrazoles, Usp. Khim. 63 (10) (1994) 847–865.
[95] Z.P. Demko, K.B. Sharpless, Preparation of 5-substituted 1H-tetrazoles from nitriles in water, J. Org. Chem. 66 (24) (2001) 7945–7950.
[96] Z.P. Demko, K.B. Sharpless, An expedient route to the tetrazole analogues of α-amino acids, Org. Lett. 4 (15) (2002) 2525–2527.
[97] F. Himo, Z.P. Demko, L. Noodleman, K.B. Sharpless, Mechanisms of tetrazole formation by addition of azide to nitriles, J. Am. Chem. Soc. 124 (41) (2002) 12210–12216.

[98] F. Himo, Z.P. Demko, L. Noodleman, K.B. Sharpless, Why is tetrazole formation by addition of azide to organic nitriles catalyzed by zinc(II) salts? J. Am. Chem. Soc. 125 (33) (2003) 9983–9987.
[99] D. Amantini, R. Beleggia, F. Fringuelli, F. Pizzo, L. Vaccoro, TBAF-catalyzed synthesis of 5-substituted 1H-tetrazoles under solventless conditions, J. Org. Chem. 69 (8) (2004) 2896–2898.
[100] M. Lakshmi Kantam, K.B. Shiva Kumar, C. Sridhar, Nanocrystalline ZnO as an efficient heterogeneous catalyst for the synthesis of 5-substituted 1H-tetrazoles, Adv. Synth. Catal. 347 (9) (2005) 1212–1214.
[101] T. Jin, F. Kitahara, S. Kamijo, Y. Yamamoto, Copper-catalyzed synthesis of 5-substituted 1H-tetrazoles via the [3+2] cycloaddition of nitriles and trimethylsilyl azide, Tetrahedron Lett. 49 (17) (2008) 2824–2827.
[102] M.L. Kantam, K.B. Shiva Kumar, K. Phani Raja, An efficient synthesis of 5-substituted 1H-tetrazoles using Zn/Al hydrotalcite catalyst, J. Mol. Catal. A Chem. 247 (1–2) (2006) 186–188.
[103] H.A. Dabbagh, A. Najafi Chermahini, A. Teimouri, Aryloxy tetrazoles with axial chirality: synthesis and partial resolution of 5-(1-(2-methoxynaphthalen-1-yl)naphthalen-2-yloxy)-1H-tetrazole, Heteroatom Chem. 17 (5) (2006) 416–419.
[104] S. Wittenberger, Recent developments in tetrazole chemistry. A review, J. Org. Prep. Proced. Int. 26 (1994) 499–531.
[105] D.P. Curran, S. Hadida, S.Y. Kim, Tris(2-perfluorohexylethyl)tin azide: a new reagent for preparation of 5-substituted tetrazoles from nitriles with purification by fluorous/organic liquid–liquid extraction, Tetrahedron 55 (1999) 8997–9006.
[106] B.E. Huff, M.A. Staszak, A new method for the preparation of tetrazoles from nitriles using trimethylsilylazide/trimethylaluminum, Tetrahedron Lett. 34 (50) (1993) 8011–8014.
[107] A.R. Modarresi-Alam, M. Nasrollahzadeh, Synthesis of 5-arylamino-1H (2H)-tetrazoles and 5-amino-1-aryl-1H-tetrazoles from secondary arylcyanamides in glacial acetic acid: a simple and efficient method, Turk. J. Chem. 33 (2) (2009) 267–280.
[108] V. Kannan, K. Sreekumar, Montmorillonite K10 clay catalyzed one pot synthesis of 2, 4, 6-tri substituted pyridine under solvent free condition, Mod. Res. Catal. 2 (2013) 42–46.
[109] N. Li, P. Wang, S.L. Lai, W. Liu, C.S. Lee, S.T. Lee, Z. Liu, Synthesis of multiaryl-substituted pyridine derivatives and applications in non-doped deep-blue oleds as electron-transporting layer with high hole-blocking ability, Adv. Mater. 22 (4) (2010) 527–530.
[110] L.C.W. Chang, J.K. Von Frijtag, D. Kunzel, T.M. Mulder-Kriegger, R.F. Spangersberg, S.F. Roerink, G. Hout, M.W. Beukers, J. Brussee, A.P. Ijzerman, A series of ligands displaying a remarkable agonistic-antagonistic profile at the adenosine A1 receptor, J. Med. Chem. 48 (6) (2005) 2045–2053.
[111] M.W. Beukers, L.W. Chang, J.K. von Frijtag, D. Künzel, T. Mulder-Krieger, R.F. Spanjersberg, J. Brussee, A.P.I. Jzerman, New, non-adenosine, high-potency agonists for the human adenosine A2B receptor with an improved selectivity profile compared to the reference agonist N-ethylcarboxamidoadenosine, J. Med. Chem. 47 (15) (2004) 3707–3709.
[112] A.D. Pillai, P.D. Rathod, P.X.F.M. Patel, M. Nivsarkar, K.K. Vasu, H. Padh, V. Sudarsanam, Novel drug de-signing approach for dual inhibitors as anti-inflammatory agents: implication of pyridine template, Biochem. Biophys. Res. Commun. 301 (1) (2003) 183–186.
[113] K.T. Potts, M.J. Cipullo, P. Ralli, G. Theodoridis, Ketenedithioacetals as synthetic intermediates. A versatile synthesis of pyridenes, polypyridinyls, and pyrylium salts, J. Am. Chem. Soc. 103 (12) (1981) 3584–3585.

[114] T. Kobayashi, H. Kakiuchi, H. Kato, On the reaction of *N*-(diphenylphosphinyl)-1-phenylethanimine with aromatic aldehydes giving 4-Aryl-2,6-diphenylpyridine derivatives, Bull. Chem. Soc. Jpn 64 (2) (1991) 392–395.
[115] F. Palacios, A.O. Retana, J.A. Oyarzabal, A 'one pot' synthesis of polysubstituted pyridines from metallated alkylphosphonates, nitriles and α,β-unsaturated ketones, Tetrahedron Lett. 37 (26) (1996) 4577–4580.
[116] G.W.V. Cave, C.L. Raston, Towards benign synthesis of pyridines involving sequential solvent free aldol and michael addition reactions, Chem. Commun. 22 (2000) 2199–2200.
[117] S. Tu, T. Li, F. Shi, F. Fang, S. Zhu, X. Wei, Z. Zong, An efficient improve for the kröhnke reaction: one-pot synthesis of 2,4,6-triarylpyridines using raw materials under microwave irradiation, Chem. Lett. 34 (5) (2005) 732–733.
[118] G.W. Cave, M.J. Hardie, B.A. Roberts, C.L. Raston, A versatile six-component molecular capsule based on benign synthons—selective confinement of a heterogeneous molecular aggregate, Eur. J. Org. Chem. 2001 (17) (2001) 3227–3231.
[119] R.R. Jetti, A. Nagia, F. Xue, T.C.W. Mak, Polar host-guest assembly mediated by halogen…π interaction: inclusion complexes of 2,4,6-tris (4-halophenoxy)-1,3,5- triazine (halo = chloro, bromo) with trihalobenzene (halo = bromo, iodo), Chem. Commun. 10 (2001) 919–920.
[120] Z.C. Watson, N. Bampos, J.M. Sanders, Mixed cyclic trimers of porphyrins and dioxoporphyrins: geometry vs. electronics in ligand recognition, New J. Chem. 22 (11) (1998) 1135–1138.
[121] G.R. Reddy, V.H. Reddy, T.V. Reddy, K. Naresh, Synthesis of pyranopyrazoles by using eco-friendly montmorillonite K-10 catalyst-their antioxidant and antimicrobial assays, Der Pharma Chemica 8 (19) (2016) 371–383.
[122] Y.A. Sharanin, L.G. Sharanina, V.V. Puzanova, Cheminform abstract: nitrile cyclization reactions. Vii. synthesis Of 6-amino-4-aryl-3-methyl-5-cyano-1h,4h-pyrazolo(3,4-B) pyrans, Zh. Org. Khim. 19 (12) (1983) 2609–2615.
[123] H. Junek, H. Aigner, Synthesen mit nitrilen, XXXV. Reaktionen von tetracyanäthylen mit heterocyclen, Chem. Ber. 106 (3) (1973) 914–921.
[124] H. Wamhoff, E. Kroth, K. Strauch, Dihalogentriphenylphosphorane in der heterocyclensynthese; 271: heterokondensierte 1,2,4-triazolo[1,5-c]pyrimidine aus enaminonitrilen via O-ethylformimide, Synthesis 11 (1993) 1129–1132.
[125] G. Tacconi, G. Gatti, G. Desimoni, A new route to 4H-pyrano[2,3-c]pyrazoles, J. Prakt. Chem. 322 (5) (1980) 831–834.
[126] G. Sharanina, V.P. Marshtupa, A.S. Yu, Synthesis of 6-amino-5-cyano-1H,4H-pyrazolo[3,4-b]pyrans, Khim. Geterosikl. Soedin. 10 (1980) 1420–1424.
[127] E.S. El-Tamany, F.A. El-Shahed, B.H. Mohamed, Synthesis and biological activity of some pyrazole derivatives, J. Serb. Chem. Soc. 64 (1999) 8–9.
[128] Z.H. Ismail, G.M. Aly, M.S. El-Degwi, H.I. Heiba, M.M. Ghorab, Synthesis and insecticidal activity of some new pyranopyrazoles, pyrazolopyranopyrimidines, andpyrazolopyranopyridines, Egypt J. Biotechnol 13 (2003) 73–82.
[129] M.E.A. Zaki, H.A. Soliman, O.A. Hiekal, A.E.Z. Rashad, pyrazolopyranopyrimidines as a class of anti-inflammatory agents, Z. Naturforsch. C 61 (2006) 1–5.
[130] F.M. Abdelrazek, P. Metz, N.H. Metwally, S.F. El-Mahrouky, Synthesis and molluscicidal activity of new cinnoline and pyrano [2,3-c]pyrazole derivatives, Arch. Pharm. 339 (8) (2006) 456–460.
[131] P. FM Abdelrazek, O. Metz, A.J. Kataeva, SF El-Mahrouky, synthesis and molluscicidal activity of new chromene and pyrano[2,3-c]pyrazole derivatives, Arch. Pharm. 340 (10) (2007) 543–548.

[132] E. Aslya, A. Harrane, M. Belbachir, Polymerization of DL-lactide induced by protonated montmorillonite clay as a solid catalyst: mechanism study, Mater. Res. 19 (1) (2016) 132–137.
[133] A. Sodergard, M. Stolt, Properties of lactic acid based polymers and their correlation with composition, Prog. Polym. Sci. 27 (6) (2002) 1123–1163.
[134] M. Okada, Chemical syntheses of biodegradable polymers, Prog. Polym. Sci. 27 (1) (2002) 87–133.
[135] H. Nishida, M. Yamashita, T. Endo, Y. Tokiwa, Equilibrium polymerization behavior of 1,4-dioxan-2-one in bulk, Macromolecules 33 (19) (2000) 6982–6986.
[136] K. Van de Velde, P. Kiekens, Biopolymers: overview of several properties and consequences on their applications, Polym. Test. 21 (4) (2002) 433–442.
[137] H.R. Kricheldorf, I.K. Saunders, A. Stricker, Polylactones $SnOct_2$-initiated polymerizations of lactide: a mechanistic study, Macromolecules 33 (2000) 702–709.
[138] H. Kaplan, One step process of acid activating mineral clays and alkylating phenolic compounds with an alkene hydrocarbon, US Patent 3287422, 1966.
[139] M. Kunioka, Y. Wang, S. Onozawa, Poly(lactic acid) polymerized by aluminum triflate, Macromol. Symp. 224 (1) (2005) 167–180.
[140] Y. Yingmin, L. Ruying, L. Qingsong, Alkylation of thiophenic compounds with 1-hexene over sulfonated solid acid catalysts, Prog. React. Kinet. Mec. 4 (2013) 425–430.
[141] A.R. Nascimento, J.A. Alves, M.A. Melo, D.M. Melo, M.J. Souza, A.M. Pedrosa, Effect of the acid treatment of montmorillonite clay in the oleic acid esterification reaction, Mater. Res. 18 (2) (2015) 283–287.
[142] A. Harrane, R. Meghabar, M. Belbachir, A Proton exchanged montmorillonite clay as an efficient catalyst for the reaction of isobutylene polymerization, Int. J. Mol. Sci. 3 (2002) 790–800.
[143] A. Harrane, M.A. Belaouej, R. Meghabar, M. Belbachir, Cationic ring-opening polymerization of (d,l-lactide) using Maghnite-H^+, a non-toxic catalyst, React. Funct. Polym. 71 (2) (2011) 126–130.
[144] M. Bhaskar, M. Surekha, N. Suma, Esterification of phenyl acetic acid with p-cresol using metal cation exchanged montmorillonite nanoclay catalysts, R. Soc. Open Sci. 5 (2) (2018) 171378.
[145] O. Secondini, Handbook of Perfumes and Flavors, Chemical Publishing Company, New York, NY, 1998.
[146] S. Sayyahi, S. Jahanbakhshi, Z. Dehghani, A green and efficient method for the preparation of 3,4-dihydropyrimidin-2(1H)-ones using quaternary ammonium-treated clay in water, J. Chem. (2013), Article ID 605324 1–5.
[147] C.O. Kappe, Recent advances in the Biginelli dihydropyrimidine synthesis. New tricks from an old dog, Acc. Chem. Res. 33 (12) (2000) 879–888.
[148] M.A. Kolosov, V.D. Orlov, D.A. Beloborodov, V.V. Dotsenko, A chemical placebo: NaCl as an effective, cheapest, non-acidic and greener catalyst for Biginelli-type 3,4-dihydropyrimidin-2(1H)-ones (-thiones) synthesis, Mol. Divers. 13 (1) (2009) 5–25.
[149] J.P. Wan, Y. Liu, Synthesis of dihydropyrimidinones and thiones by multicomponent reactions: strategies beyond the classical Biginelli reaction, Synthesis 23 (2010) 3943–3953.
[150] B.J. Borah, D. Dutta, P.P. Saikia, N.C. Barua, D.K. Dutta, Stabilization of Cu(0)-nanoparticles into the nanopores of modified montmorillonite: an implication on the catalytic approach for “click” reaction between azides and terminal alkynes, Green Chem. 13 (2011) 3453–3460.

[151] V.V. Rostovtsev, L.G. Green, V.V. Fokin, K.B. Sharpless, A stepwise huisgen cycloaddition process: copper(I)-catalyzed regioselective "ligation" of azides and terminal alkynes, Angew. Chem. Int. Ed. Engl. 41 (14) (2002) 2596–2599.
[152] D. Kumar, V.B. Reddy, R.S. Varma, A facile and regioselective synthesis of 1, 4-disubstituted 1, 2, 3-triazoles using click chemistry, Tetrahedron Lett. 50 (18) (2009) 2065–2068.
[153] G.A. Romeiro, L.O.R. Pereira, M.C.B.V. de Souza, V.F. Ferreira, A.C. Cunha, A new and efficient procedure for preparing 1,2,3-triazoles, Tetrahedron Lett. 38 (29) (1997) 5103–5106.
[154] P.K. Kadaba, B. Stanovnik, M. Tisler, Δ^2-1,2,3-Triazolines, Adv. Heterocycl. Chem. 37 (1984) 217–349.
[155] L. Garanti, G. Molteni, MeOPEG-bounded azide cycloadditions to alkynyl dipolarophiles, Tetrahedron Lett. 44 (6) (2003) 1133–1135.
[156] M. Moore, P. Norris, Dipolar cycloaddition reactions on a soluble polymer-supported dipolarophile: synthesis of sugar-derived triazoles, Tetrahedron Lett. 39 (39) (1998) 7027–7030.
[157] F. Zaragoza, S.V. Petersen, Solid-phase synthesis of substituted 1,2,3-triazoles, Tetrahedron 52 (1996) 10823–10826.
[158] B. Zeynizadeh, S. Rahmani, Synthesis and characterization of Ni0 NPs immobilized on acid activated montmorillonite (Ni°-Mont) as an efficient and reusable heterogeneous catalyst for one-pot synthesis of biscoumarins under microwave irradiation, ARXIV (2017).
[159] I. Manolov, C. Maichle-Moessmer, N. Danchev, Synthesis, structure, toxicological and pharmacological investigations of 4-hydroxycoumarin derivatives, Eur. J. Med. Chem. 41 (7) (2006) 882–890.
[160] Z.H. Chohan, A.U. Shaikh, A. Rauf, C.T. Supuran, Antibacterial, antifungal and cytotoxic properties of novel N-substituted sulfonamides from 4-hydroxycoumarin, J. Enzyme Inhib. Med. Chem. 21 (6) (2006) 741–748.
[161] N. Hamdi, M.C. Puerta, P. Valerga, Synthesis, structure, antimicrobial and antioxidant investigations of dicoumarol and related compounds, Eur. J. Med. Chem. 43 (11) (2008) 2541–2548.
[162] A.C. Luchini, P. Rodrigues-Orsi, S.H. Cestari, L.N. Seito, A. Witaicenis, C.H. Pellizzon, L.C. Di Stasi, Intestinal anti-inflammatory activity of coumarin and 4-hydroxycoumarin in the trinitrobenzenesulphonic acid model of rat colitis, Biol. Pharm. Bull. 31 (7) (2008) 1343–1350.
[163] M. Gersch, J. Kreuzer, S.A. Sieber, Electrophilic natural products and their biological targets, Nat. Prod. Rep. 29 (6) (2012) 659–682.
[164] D. Završnik, S. Muratović, D. Makuc, J. Plavec, M. Cetina, A. Nagl, E.D. Clercq, J. Balzarini, M. Mintas, Benzylidene-bis-(4-hydroxycoumarin) and benzopyranocoumarin derivatives: synthesis, $^{1}H/^{13}C$-NMR conformational and X-ray crystal structure studies and in vitro antiviral activity evaluations, Molecules 16 (7) (2011) 6023–6040.
[165] M. Kidwai, V. Bansal, P. Mothsra, S. Saxena, R.K. Somvanshi, S. Dey, T.P. Singh, Molecular iodine: a versatile catalyst for the synthesis of bis(4-hydroxycoumarin) methanes in water, J. Mol. Catal. A Chem. 268 (2007) 76–81.
[166] K. Khan, S. Iqbal, M. Lodhi, G. Maharvi, Z. Ullah, M. Choudhary, P. Atta-ur-Rahman, Biscoumarin: new class of urease inhibitors; economical synthesis and activity, Bioorg. Med. Chem. 12 (2004) 1963–1968.
[167] H. Hagiwara, N. Fujimoto, T. Suzuki, M. Ando, Synthesis of methylenebis(4-hydroxy-2-pyrone) or methylenebis(4-hydroxycoumarin) derivatives by organic solid state reaction, Heterocycles Sendai Institute of Heterocyclic Chemistry, 53 (3) (2000) 549–552.

[168] A. Shamsaddini, E. Sheikhhosseini, Synthesis of 3,3-arylidene bis(4-hydroxycoumarin) catalyzed by p-dodecylbenzenesulfonic acid (DBSA) in aqueous media and microwave irradiation, Int. J. Org. Chem. 4 (2014) 135–141.
[169] E. Sheikhhosseini, Synthesis of 3,3-arylidene bis(4-hydroxycoumarin) catalyzed by $LiClO_4$, Trend Mod. Chem. 3 (2012) 34–37.
[170] H. Mehrabi, H. Abusaidi, Synthesis of biscoumarin and 3, 4-dihydropyrano [c] chromene derivatives catalysed by sodium dodecyl sulfate (SDS) in neat water, J. Iran. Chem. Soc. 7 (4) (2010) 890–894.
[171] Z.N. Siddiqui, F. Farooq, $Zn(Proline)_2$: a novel catalyst for the synthesis of dicoumarols, Catal. Sci. Technol. 1 (2011) 810–816.
[172] J.M. Khurana, S. Kumar, Tetrabutylammonium bromide (TBAB): a neutral and efficient catalyst for the synthesis of biscoumarin and 3,4-dihydropyrano[c] chromene derivatives in water and solvent-free conditions, Tetrahedron Lett. 50 (28) (2009) 4125–4127.
[173] A. Tzani, A. Douka, A. Papadopoulos, E.A. Pavlatou, E. Voutsas, A. Detsi, Synthesis of biscoumarins using recyclable and biodegradable task-specific ionic liquids, ACS Sustain. Chem. Eng. 1 (9) (2013) 1180–1185.
[174] R. Karimian, F. Piri, A.A. Safari, S.J. Davarpanah, One-pot and chemoselective synthesis of bis(4-hydroxycoumarin) derivatives catalyzed by nano silica chloride, J. Nanostruct. Chem. 3 (52) (2013) 1–6.
[175] B. Wang, N. Li, T. Liu, J. Sun, X. Wang, Synthesis and biological evaluation of novel neoflavonoid derivatives as potential antidiabetic agents, RSC Adv. 7 (2017) 34448–34460.
[176] M.H. Lin, Y.S. Chou, Y.J. Tsai, D.S. Chou, Antioxidant properties of 5,7-dihydroxycoumarin derivatives in in vitro cell-free and cell-containing systems, J. Exp. Clin. Med. 3 (3) (2011) 126–131.
[177] R. Korec, M. Korecova, K.H. Sensch, T. Zoukas, Antidiabetic effect of neoflavonoid coutareagenin in STZ diabetic rats and diabetic menopausal women, Diabetes Res. Clin. Pract. 50 (1) (2000) 42.
[178] C. Billard, F. Menasria, C. Quiney, A.M. Faussat, J.P. Finet, S. Combes, J.P. Kolb, 4-arylcoumarin analogues of combretastatins stimulate apoptosis of leukemic cells from chronic lymphocytic leukemia patients, Exp. Hematol. 36 (12) (2008) 1625–1633.
[179] S.K. Roy, N. Kumari, S. Pahwa, U.C. Agrahari, K.K. Bhutani, S.M. Jachak, H. Nandanwar, NorA efflux pump inhibitory activity of coumarins from Mesua ferrea, Fitoterapia 90 (2013) 140–150.
[180] T. Taechowisan, C. Lu, Y. Shen, S. Lumyong, Secondary metabolites from endophytic Streptomyces aureofaciens CMUAc130 and their antifungal activity, Microbiology 151 (2005) 1691–1695.
[181] J.T. Pierson, A. Dumetre, S. Hutter, F. Delmas, M. Laget, J.P. Finet, N. Azas, S. Combes, Synthesis and antiprotozoal activity of 4-arylcoumarins, Eur. J. Med. Chem. 45 (2010) 864–869.
[182] S. Nishimura, M. Taki, S. Takaishi, Y. Iijima, T. Akiyama, Structures of 4-aryl-coumarin (Neoflavone) dimmers isolated from pistacia chinensis BUNGE and their estrogen- like activity, Chem. Pharm. Bull. 48 (4) (2000) 505–508.
[183] A.R. Vartooni, M. Alizadeh, M. Bagherzadeh, Green synthesis, characterization and catalytic activity of natural bentonite-supported copper nanoparticles for the solvent-free synthesis of 1-substituted 1H-1,2,3,4-tetrazoles and reduction of 4-nitrophenol, Beilstein J. Nanotechnol. 6 (2015) 2300–2309.
[184] A. Burger, Isosterism and bioisosterism in drug design, in: E. Jucker (Ed.), Progress in Drug Research, vol. 12, Birkhäuser, Basel, Switzerland, 1991, pp. 287–371.

[185] M. Salmón, R. Osnaya, L. Gómez, G. Arroyo, F. Delgado, R. Miranda, Contribution to the Biginelli Reaction, using a bentonitic clay as catalyst and a solventless procedure, Revista de la Sociedad Química de México 45 (4) (2001) 206–207.
[186] K.S. Atwal, G.O. Rovnyak, B.C. O'Reilly, J. Schwartz, Substituted 1,4-dihydropyrimidines. 3. Synthesis of selectively functionalized 2-hetero-1, 4-dihydropyrimidines, J. Org. Chem. 54 (25) (1989) 5898–5907.
[187] C.O. Kappe, W.M.F. Fabian, M.A. Semones, Conformational analysis of 4-aryl-dihydropyrimidine calcium channel modulators. A comparison of ab initio, semi-empirical and X-ray crystallographic studies, Tetrahedron 53 (8) (1997) 2803–2816.
[188] B.S. Surendra, M. Veerabhadraswamy, Microwave assisted modification of bentonite clay: characterization and solvent free synthesis of Schiff's bases, J. Org. Inorg. Chem. 3 (1) (2017) 1–7.
[189] A. Saxena, Synthesis and characterization of schiff base salicylaldehyde and thiohydrazones and its metal complexes, Adv. Appl. Sci. Res. 4 (2013) 152–154.
[190] W. Qin, S. Long, M. Panunzio, S. Biondi, Schiff bases: a short survey on an evergreen chemistry tool, Molecules 18 (2013) 12264–12289.
[191] R. Sahu, D.S. Thakur, P. Kashyap, Schiff base: an overview of its medicinal chemistry potential for new drug molecules, Int. J Pham Sci. Nanotech. 5 (2012) 1757–1764.
[192] M. Zarei, A. Jarrahpour, Green and efficient synthesis of azo Schiff bases, Iran. J. Sci. Tech. 35 (2011) 235–242.
[193] S.S. S Rahimullah, T.T. Nida, Dipak eco-friendly synthesis of Schiff bases, Int. J. Pharm. Pharm. Sci. Res. 3 (2013) 100–102.
[194] R. Arora, A. Kapoor, N.S. Gill, A.C. Rana, Synthesis of novel Schiff base of 5- amino-salicylic acid by grindig technique and its evaluation for anti-inflammatory and analgesic activities, Int. Res. J. Pharm. 3 (2012) 185–188.
[195] A. Adabiardakani, H.H. Mohammad, H. Kargar, Cinnamaldehyde schiff base derivatives: a short review, World Appl. Prog. 2 (2012) 472–476.
[196] Y. Bekdemir, K. Efil, Microwave assisted solvent-free synthesis of some imine derivatives, Org. Chem. Int. 1 (2014) 1–5.
[197] S. Patil, S.D. Jadhav, M.B. Deshmukh, U.P. Patil Natural, Acid catalyzed synthesis of Schiff under solvent-free condition: as a green approach, Int. J. Org. Chem. 2 (2012) 166–171.
[198] S. Miglani, M. Mishra, P. Chawla, The rapid synthesis of schiff bases without solvent under microwave irradiation and their antimicrobial activity, Der Pharma Chemica 4 (2012) 2265–2269.
[199] R. Ballini, G. Bosica, R. Maggi, M. Ricciutelli, P. Righi, G. Sartori, R. Sartorio, Clay-catalyzed solventless synthesis of trans-chalcones, Green Chem. 3 (2001) 178–180.
[200] K. Yamaguchi, Y. Sakurai, H. Kurumi, Jap. Pat., 1972. 7247016.
[201] D.G. Powers, D.S. Casebier, D. Fokas, W.J. Ryan, J.R. Troth, D.L. Coffen, Automated parallel synthesis of chalcone-based screening libraries, Tetrahedron 54 (16) (1998) 4085–4096.
[202] K.R. Kloetstra, H. van Bekkum, Base and acid catalysis by the alkali-containing MCM-41 mesoporous molecular sieve, J. Chem. Soc., Chem. Commun. (1995) 1005–1006.
[203] W.H. Zhang, W.L. Chan, Y.H. Lin, Y.S. Szeto, Y.C. Lin, C.H. Yeung, Synthesis of hydroxyflavanones from substituted acetophenones and benzaldehydes in the presence of silica gel, boric acid and piperidine, Heterocycles 45 (1997) 71–75.
[204] R.S. Natekar, S.D. Samant, Gel entrapped base-catalyzed (Gebc) aldol reaction of acetophenones with benzaldehydes, Indian J. Chem. Sec. B 35 (12) (1996) 1347–1348.

[205] V.M. Kazantseva, S.P. Korshunov, The Claisen-Schmidt condensation in aprotic solvents, Zh. Org. Khim. 30 (1994) 313.
[206] M.J. Climent, A. Corma, S. Iborra, J. Primo, Base catalysis for fine chemicals production: Claisen-Schmidt condensation on zeolites and hydrotalcites for the production of chalcones and flavanones of pharmaceutical interest, J. Catal. 151 (1) (1995) 60–66.
[207] E.L. Gall, F. Texier-Boullet, J. Hamelin, Simple access to α, β unsaturated ketones by acid-catalyzed solvent-free reactions, Synth. Commun. 29 (20) (1999) 3651–3657.
[208] B.V.S. Reddy, P.S. Reddy, Y.J. Reddy, N. Bhaskar, B.C.O. Reddy, Montmorillonite clay catalyzed three component, one-pot synthesis of 5-hydroxyindole derivatives, Bull. Korean Chem. Soc. 34 (10) (2013) 2968–2972.
[209] (a) S.M. Li, Prenylated indole derivatives from fungi: structure diversity, biological activities, biosynthesis and chemoenzymatic synthesis, Nat. Prod. Rep. 27 (1) (2010) 57–78. (b) J. Landwehr, S. George, E.M. Karg, D. Poeckel, D. Steinhilber, R. Troschuetz, O. Werz, Design and synthesis of novel 2-amino-5-hydroxyindole derivatives that inhibit human 5-lipoxygenase, J. Med. Chem. 49 (14) (2006) 4327–4332.
[210] J.R. Weng, C.H. Tsai, S.K. Kulp, C.S. Chen, Indole-3-carbinol as a chemopreventive and anti-cancer agent, Cancer Lett. 262 (2) (2008) 153–163.
[211] G.C. Rieck, A.N. Fiander, Human papillomavirus, cervical carcinogenesis and chemoprevention with indole derivates—a review of pathomechanisms, Mol. Nutr. Food Res. 52 (1) (2008) 105–113.
[212] (a) A. Brancale, R. Silvestri, Indole, a core nucleus for potent inhibitors of tubulin polymerization, Med. Res. Rev. 27 (2) (2007) 209–238. (b) M. Somei, F. Yamada, Simple indole alkaloids and those with a non-rearranged monoterpenoid unit, Nat. Prod. Rep. 22 (1) (2005) 73–103.
[213] M.J. McKay, A.R. Carroll, R.J. Quinn, J.N.A. Hooper, 1,2-Bis(1H-indol-3-yl)ethane-1,2-dione, an indole alkaloid from the marine sponge smenospongia sp., J. Nat. Prod. 65 (4) (2002) 595–597.
[214] J.A. Joule, K. Mills, Heterocyclic Chemistry, fourth ed., Blackwell Science, Oxford, 2000.
[215] (a) R.J. Sundberg, Indoles, Academic Press, London, 1996. (b) M. Ishikura, K. Yamada, T. Abe, Simple indole alkaloids and those with a nonrearranged monoterpenoid unit, Nat. Prod. Rep. 27 (2009) 1630–1680.
[216] K. Higuchi, T. Kawasaki, Simple indole alkaloids and those with a nonrearranged monoterpenoid unit, Nat. Prod. Rep. 24 (4) (2007) 843–868.
[217] T. Kawasaki, K. Higuchi, Simple indole alkaloids and those with a nonrearranged monoterpenoid unit, Nat. Prod. Rep. 22 (6) (2005) 761–793.
[218] S.R. Walker, E.J. Carter, B.C. Huff, J.C. Morris, Variolins and related alkaloids, Chem. Rev. 109 (7) (2009) 3080–3098.
[219] Y. Leblanc, W.C. Black, C.C. Chan, S. Charleson, D. Delorme, D. Denis, C. Bayly, J.Y. Gauthier, R. Grimm, R. Gordon, D. Guay, P. Hamel, S. Kargman, C.K. Lau, J. Mancini, M. Ouellet, D. Percival, P. Roy, K. Skorey, P. Tagari, P. Vickers, E. Wong, L. Xu, P. Prasit, Synthesis and biological evaluation of both enantiomers of L-761,000 as inhibitors of cyclooxygenase 1 and 2, Bioorg. Med. Chem. Lett. 6 (6) (1996) 731–736.
[220] J.M. Pawlak, V.V. Khau, D.R. Hutchinson, M. Martinelli, A. Practical, Nenitzescu-based synthesis of LY311727, the first potent and selective s-PLA2 inhibitor, J. Org. Chem. 61 (25) (1996) 9055–9059.
[221] S. Shefali, S.K. Srivastava, S.M. Husbands, J.W. Lewis, Extension of the Nenitzescu reaction to simple ketones provides an efficient route to 1'-alkyl-5'-hydroxynaltrindole

analogues, potent and selective delta-opioid receptor antagonists, J. Med. Chem. 48 (2) (2005) 635–638.
[222] G.W. Gribble, Recent developments in indole ring synthesis—methodology and applications, J. Chem. Soc., Perkin Trans. 1 (2000) 1045–1075.
[223] G.R. Humphrey, J.T. Kuethe, Practical methodologies for the synthesis of indoles, Chem. Rev. 106 (7) (2006) 2875–2911.
[224] N.R. Candeias, L.C. Branco, P.M.P. Gois, C.A.M. Afonso, A.F. Trindade, More sustainable approaches for the synthesis of N-based heterocycles, Chem. Rev. 109 (6) (2009) 2703–2802.
[225] C. Nenitzescu, New indole synthesis, Chem. Zentralbl. (1929) 2331–2332.
[226] R.W. Parr, J.A. Reiss, An application of the Nenitszescu reaction to the synthesis of 1,2-annulated indoles and Benz[g]indoles, Aust. J. Chem. 37 (6) (1984) 1263–1270.
[227] J.M. Pawlak, V.V. Khau, D.R. Hutchison, M.J. Martinelli, A practical, Nenitzescu-based synthesis of LY311727, the first potent and selective s-PLA2 inhibitor, J. Org. Chem. 61 (25) (1996) 9055–9059.
[228] D.M. Ketcha, L.J. Wilson, D.E. Portlock, The solid-phase Nenitzescu indole synthesis, Tetrahedron Lett. 41 (33) (2000) 6253–6257.
[229] J.J. Neumann, S. Rakshit, T. Drçge, S. Wurtz, F. Glorius, Exploring the oxidative cyclization of substituted N-aryl enamines: Pd-catalyzed formation of indoles from anilines, Chem. Eur. J. 17 (26) (2011) 7298–7303.
[230] A.K. Mitra, K. Banerjee, Clay catalysed synthesis of dihydropyrimidinones under solvent-free conditions, Synlett 10 (2003) 1509–1511.
[231] C.O. Kappe, 100 Years of the Biginelli dihydropyridine synthesis, Tetrahedron 49 (32) (1993) 6937–6963.
[232] C.O. Kappe, A reexamination of the mechanism of the Biginelli dihydropyrimidine synthesis. Support for an N-acyliminium ion intermediate, J. Org. Chem. 62 (21) (1997) 7201–7204.
[233] G.C. Rovnyak, S.D. Kimball, B. Beyer, G. Cucinotta, J.D. Marco, J. Gougoutas, A. Hedberg, M. Malley, J.P. McCarthy, R. Zhang, S. Moreland, Calcium entry blockers and activators: conformational and structural determinants of dihydropyrimidine calcium channel modulators, J. Med. Chem. 38 (1) (1995) 119–129.
[234] B.B. Snider, Z. Shi, Biomimetic synthesis of (.+-.)-crambines A, B, C1, and C2. Revision of the structure of crambines B and C1, J. Org. Chem. 58 (15) (1993) 3828–3839.
[235] A.D. Patil, N.V. Kumar, W.C. Kokke, M.F. Bean, A.J. Freyer, C. DeBrosse, S. Mai, A. Truneh, D.J. Faulkner, B. Carte, A.L. Breen, R.P. Hertzberg, R.K. Johnson, J. W. Westley, B.C.M. Potts, Novel alkaloids from the sponge Batzella sp.: inhibitors of HIV gp120-human CD4 binding, J. Org. Chem. 60 (5) (1995) 1182–1188.
[236] A.V. RamaRao, M.K. Gurjar, J. Vasudevan, An enantiospecific synthesis of the tricyclic guanidine segment of the anti-HIV marine alkaloid batzelladine A, J. Chem. Soc., Chem. Commun. (1995) 1369–1370.
[237] B.B. Snider, J. Chen, A.D. Patil, A. Freyer, Synthesis of the tricyclic portions of batzelladines A, B and D. Revision of the stereochemistry of batzelladines A and D, Tetrahedron Lett. 37 (39) (1996) 6977–6980.
[238] J. Barluenga, M. Tomas, A. Ballesteros, L.A. Lopez, 1,4-Cycloaddition of 1,3-diazabutadienes with enamines: An efficient route to the pyrimidine ring, Tetrahedron Lett. 30 (34) (1989) 4573–4576.
[239] E.H. Hu, D.R. Sidler, U.H. Dolling, Unprecedented catalytic three component one-pot condensation reaction: an efficient synthesis of 5-alkoxycarbonyl-4-aryl-3,4-dihydropyrimidin-2 (1H)-ones, J. Org. Chem. 63 (10) (1998) 3454–3457.

[240] J. Lu, H.R. Ma, Iron(III)-catalyzed synthesis of dihydropyrimidinones. Improved conditions for the Biginelli reaction, Synlett 2000 (1) (2000) 63–64.
[241] B.C. Ranu, A. Hajra, U. Jana, Indium(III) chloride-catalyzed one-pot synthesis of dihydropyrimidinones by a three-component coupling of 1,3-dicarbonyl compounds, aldehydes, and urea: an improved procedure for the Biginelli reaction, J. Org. Chem. 65 (19) (2000) 6270–6272.
[242] K. Ramalinga, P. Vijayalakshmi, T.N.B. Kaimal, Bismuth(III)-catalyzed synthesis of dihydropyrimidinones: improved protocol conditions for the Biginelli reaction, Synlett 2001 (6) (2001) 863–865.
[243] J. Lu, Y. Bai, Z. Wang, B. Yang, H.R. Ma, One-pot synthesis of 3,4-dihydropyrimidin-2 (1H)-ones using lanthanum chloride as a catalyst, Tetrahedron Lett. 41 (47) (2000) 9075–9078.
[244] Y. Ma, C. Qian, L. Wang, M. Yang, Lanthanide triflate catalyzed Biginelli reaction. One-pot synthesis of dihydropyrimidinones under solvent-free conditions, J. Org. Chem. 65 (12) (2000) 3864–3868.
[245] H. Robert, B. Ganigues, J. Dubac, The carbonyl-diels-alder reaction catalyzed by bismuth (III) chloride, Tetrahedron Lett. 39 (10) (1998) 1161–1164.
[246] J. Lu, Y. Bai, Catalysis of the Biginelli reaction by ferric and nickel chloride hexahydrates. One-pot synthesis of 3,4-dihydropyrimidin-2(1H)-ones, Synthesis (2002) 466–470.
[247] M.W. Toussaint, A.B. Rosencrance, L.M. Brennan, J.R. Beaman, M.J. Wolfe, F. J. Hoffmann, H.S. Gardner Jr., Chronic toxicity of chloroform to Japanese medaka fish, Environ. Health Perspect. 109 (1) (2001) 35–40.
[248] E. Rafiee, S. Rashidzadeh, S. Eavani, M. Joshaghani, KSF-supported heteropoly acids catalyzed one-pot synthesis of α-aminonitriles, Bull. Chem. Soc. Ethiop. 24 (2) (2010) 209–215.
[249] R.O. Duthaler, Recent developments in the stereoselective synthesis of alpha-amino acids, Tetrahedron 50 (6) (1994) 1539–1650.
[250] W.L. Matier, D.A. Owens, W.T. Comer, D. Deitchman, H.C. Ferguson, R.J. Seidehamel, J.R. Young, Antihypertensive agents. Synthesis and biological properties of 2-amino-4-aryl-2-imidazolines, J. Med. Chem. 16 (8) (1973) 901–908.
[251] J.S. Yadav, B.V. Subba Reddy, B. Eshwaraiah, M. Srinvias, Montmorillonite KSF clay catalyzed one-pot synthesis of α-aminonitriles, Tetrahedron 60 (2004) 1767–1771.
[252] B.M. Fetterly, N.K. Jana, J.G. Verkade, $[HP(HN_CH_2CH_2)_3N]NO_3$: an efficient homogeneous and solid supported promoter for aza and thia- Michael reactions and for Strecker reactions, Tetrahedron 61 (2005) 1.
[253] J.S. Yadav, B.V.S. Reddy, B. Eshwaraiah, M. Srinivas, P. Vishnumurthy, Three-component coupling reactions in ionic liquids: a facile synthesis of α-aminonitriles, New J. Chem. 27 (2003) 462–465.
[254] S.K. De, R.A. Gibbs, Bismuth trichloride catalyzed synthesis of α-aminonitriles, Tetrahedron Lett. 45 (2004) 7407–7408.
[255] S.K. De, RuCl3 catalyzed one-pot synthesis of α-aminonitriles, Synth. Commun. 35 (2005) 653–656.
[256] G.K.S. Prakash, T.E. Thomas, I. Bychinskaya, A.G. Prakash, C. Panja, H. Vaghoo, G. A. Olah, Efficient green synthesis of α-aminonitriles, precursors of α-amino acids, Green Chem. 10 (2008) 1105–1110.
[257] C. Wiles, P. Watts, Evaluation of the heterogeneously catalyzed strecker reaction conducted under continuous flow, Eur. J. Org. Chem. 2008 (33) (2008) 5597–5613.
[258] J. Jarusiewicz, Y. Choe, K.S. Yoo, C.P. Park, K.W. Jung, Efficient three-component strecker reaction of aldehydes/ketones via NHC-amidate palladium(II) complex catalysis, J. Org. Chem. 74 (7) (2009) 2873–2876.

[259] A. Heydari, S. Khaksar, M. Tajbakhsh, Trifluoroethanol as a metal-free, homogeneous and recyclable medium for the efficient one-pot synthesis of α-amino nitriles and α-amino phosphonates, Tetrahedron Lett. 50 (1) (2009) 77–80.
[260] R. Martínez, D.J. Ramón, M. Yus, Catalyst-free multicomponent Strecker reaction in acetonitrile, Tetrahedron Lett. 46 (49) (2005) 8471–8474.
[261] H.A. Oskooie, M.M. Heravi, K. Bakhtiari, V. Zadsirjan, F.F. Bamoharram, $H_{14}[NaP_5W_{30}O_{110}]$ as an efficient catalyst for the one-pot synthesis of α-amino nitriles, Synlett 2006 (11) (2006) 1768–1770.
[262] M.S. Sigman, E.N. Jacobsen, Enantioselective addition of hydrogen cyanide to imines catalyzed by a chiral (salen)Al(III) complex, J. Am. Chem. Soc. 120 (21) (1998) 5315–5316.
[263] M. Takamura, Y. Hamashima, H. Usuda, M. Kanai, M. Shibasaki, A. Catalytic Asymmetric, Strecker-type reaction: interesting reactivity difference between TMSCN and HCN, Angew. Chem., Int. Ed. Engl. 39 (9) (2000) 1650–1652.
[264] D.P. Narayanan, R.M. Ramakrishnan, S. Sugunan, B.N. Narayanan, Solvent free one pot synthesis of amidoalkyl naphthols over phosphotungstic acid encapsulated montmorillonite clay catalysts, J. Saudi Chem. Soc. (2015).
[265] Y.F. Wang, T. Izawa, S. Kobayashi, M. Ohno, Stereocontrolled synthesis of (+)-negamycin from an acyclic homoallylamine by 1,3-asymmetric induction, J. Am. Chem. Soc. 104 (23) (1982) 6465–6466.
[266] S. Knapp, Synthesis of complex nucleoside antibiotics, Chem. Rev. 95 (6) (1995) 1859–1876.
[267] A.Y. Shen, C.T. Tsai, C.L. Chen, Synthesis and cardiovascular evaluation of N-substituted 1-aminomethyl-2-naphthols, Eur. J. Med. Chem. 34 (1999) 877–882.
[268] S. Kantevari, S.V.N. Vuppalapati, L. Nagarapu, Montmorillonite K10 catalyzed efficient synthesis of amidoalkyl naphthols under solvent free conditions, Catal. Commun. 8 (2007) 1857–1862.
[269] L. Nagarapu, M. Baseeruddin, S. Apuri, S. Kantevari, Potassium dodecatungstocobaltate trihydrate ($K_5CoW_{12}O_{40}.3H_2O$): a mild and efficient reusable catalyst for the synthesis of amidoalkyl naphthols in solution and under solvent-free conditions, Catal. Commun. 8 (2007) 1729–1734.
[270] B. Das, K. Laxminarayana, B. Ravikanth, B.R. Rao, Iodine catalyzed preparation of amidoalkyl naphthols in solution and under solvent-free conditions, J. Mol. Catal. A Chem. 261 (2007) 180–183.
[271] A.R. Supale, G.S. Gokavi, An environmentally benign three component one-pot synthesis of amidoalkyl naphthols using $H_4SiW_{12}O_{40}$ as a recyclable catalyst, J. Chem. Sci. 122 (2010) 189–192.
[272] N.P. Selvam, P.T. Perumal, A new synthesis of acetamido phenols promoted by $Ce(SO_4)_2$, Tetrahedron Lett. 47 (2006) 7481–7483.
[273] M. Zandi, A.R. Sardarian, Eco-friendly and efficient multicomponent method for preparation of 1-amidoalkyl-2- naphthols under solvent-free conditions by dodecylphosphonic acid (DPA), C.R. Chim. 15 (2012) 365–369.
[274] H.R. Shaterian, H. Yarahmadi, M. Ghashang, An efficient, simple and expedition synthesis of 1-amidoalkyl-2-naphthols as 'drug like' molecules for biological screening, Bioorg. Med. Chem. Lett. 18 (2008) 788–792.
[275] R. Shaterian, A. Hosseinian, M. Ghashang, Silica-supported perchloric acid ($HClO_4$-SiO_2): an efficient catalyst for the preparation of β-amido carbonyl compounds using multicomponent reactions, Synth. Commun. 38 (2008) 3766–3777.
[276] N.O. Mahmoodi, S. Mohammadgholipour, F.G. Pirbasti, Microwave-assisted one-pot three-component synthesis of thiazolidinones using KSF@Ni as an efficient heterogeneous catalyst, J. Sulfur Chem. 38 (6) (2017) 668–678.

[277] C. De Monte, S. Carradori, B. Bizzarri, et al., Anti-candida activity and cytotoxicity of a large library of new N-substituted-1,3-thiazolidin-4-one derivatives, Eur. J. Med. Chem. 107 (2016) 82–96.
[278] K.S.S. Kumar, A. Hanumappa, M. Vetrivel, et al., Antiproliferative and tumor inhibitory studies of 2,3 disubstituted 4-thiazolidinone derivatives, Bioorg. Med. Chem. Lett. 25 (17) (2015) 3616–3620.
[279] M.R. Bhosle, J.R. Mali, S. Pal, et al., Synthesis and antihyperglycemic evaluation of new 2-hydrazolyl-4-thiazolidinone-5-carboxylic acids having pyrazolyl pharmacophores, Bioorg. Med. Chem. Lett. 24 (2014) 2651–2654.
[280] A. Kunzler, P.D. Neuenfeldt, A.M. das Neves, et al., Synthesis, antifungal and cytotoxic activities of 2-aryl-3-((piperidin-1-yl)ethyl)thiazolidinones, Eur. J. Med. Chem. 64 (2013) 74–80.
[281] R.P. Tenório, C.S. Carvalho, C.S. Pessanha, et al., Synthesis of thiosemicarbazone and 4-thiazolidinone derivatives and their in vitro anti-toxoplasma gondii activity, Bioorg. Med. Chem. Lett. 15 (2005) 2575–2578.
[282] K. Omar, A. Geronikaki, P. Zoumpoulakis, et al., Novel 4-thiazolidinone derivatives as potential antifungal and antibacterial drugs, Bioorg. Med. Chem. 18 (2010) 426–432.
[283] F. Rahim, K. Zaman, H. Ullah, et al., Synthesis of 4-thiazolidinone analogs as potent in vitro anti-urease agents, Bioorg. Chem. 63 (2015) 123–131.
[284] A. Rao, A. Chimirri, S. Ferro, et al., Microwave-assisted synthesis of benzimidazole and thiazolidinone derivatives as HIV-1 RT inhibitors, Arkivoc 5 (2004) 147–155.
[285] H.A. Taha, M.I. Soliman, Antischistosomal activity of 3-substituted-5-(2-aryl-2-oxoethyl)-2,4-dioxo-1,3-thiazolidine, Int. J. Agri. Biol. 1 (2007) 87–93.
[286] M.O. Kristina, R.M. Melissa, H. Gutierrez-de-Teran, et al., α-Substituted norstatines as the transition-state mimic in inhibitors of multiple digestive vacuole malaria aspartic proteases, Bioorg. Med. Chem. 17 (2009) 5933–5949.
[287] Y. Sanemitsu, S. Kawamura, J. Satoh, et al., Synthesis and herbicidal activity of 2-acylimino-3-phenyl-1,3-thiazolines—a new family of bleaching herbicides, J. Pestic. Sci. 31 (3) (2006) 305–310.
[288] R. Murugan, S. Anbazhagan, S.S. Narayanan, Synthesis and in vivo antidiabetic activity of novel dispiropyrrolidines through [3 + 2] cycloaddition reactions with thiazolidinedione and rhodanine derivatives, Eur. J. Med. Chem. 44 (2009) 3272–3279.
[289] D. Secci, S. Carradori, B. Bizzarri, et al., Novel 1,3-thiazolidin-4-one derivatives as promising anti-candida agents endowed with anti-oxidant and chelating properties, Eur. J. Med. Chem. 117 (2016) 144–156.
[290] C. Pizzo, C. Saiz, A. Talevi, et al., Synthesis of 2-hydrazolyl-4-thiazolidinones based on multicomponent reactions and biological evaluation against Trypanosoma Cruzi, Chem. Biol. Drug. Des. 77 (2011) 166–172.
[291] C. Saiz, C. Pizzo, E. Manta, et al., Microwave-assisted tandem reactions for the synthesis of 2- hydrazolyl-4-thiazolidinones, Tetrahedron Lett. 50 (2009) 901–904.
[292] W.P. Yin, M. Shi, Nitration of substituted phenols by metal salts impregnated Yb-Mo-montmorillonite KSF, Arkivoc (v) (2009) 6–16.
[293] G.A. Olah, R. Malhotra, S.C. Narang, in: H. Feuer (Ed.), Nitration: Methods and Mechanism, VCH, New York, 1989.
[294] C.K. Ingold, Structure and Mechanism in Organic Chemistry, second ed., Cornell University Press, Ithaca, New York, 1969.
[295] G.A. Olah, S.J. Kuhn, in: G.A. Olah (Ed.), Friedel-Crafts and Related Reactions, vol. 2, Wiley-Interscience, New York, 1964.

[296] G.A. Olah, S.C. Narang, J.A. Olah, K. Lammertsma, Recent aspects of nitration: New preparative methods and mechanistic studies (a review), Proc. Natl. Acad. Sci. 79 (1982) 4487–4494.
[297] M.J. Thompson, P.J. Zeeger, Two-phase nitration of phenols, part 3: the nitration of anisole, Tetrahedron 47 (41) (1991) 8787–8790.
[298] S.C. Bisarya, S.K. Joshi, A.G. Holker, Calcium nitrate—a new nitrating agent for nuclear nitration of substituted phenols, Synth. Commun. 23 (8) (1993) 1125–1137.
[299] J.A.R. Robrgues, A.P. Oliveira, P.J.S. Moran, R. Custodio, Regioselectivity of the nitration of phenol by acetyl nitrate adsorbed on silica gel, Tetrahedron 55 (22) (1999) 6733–6738.
[300] S. Khaleghi, F. Derikvand, M.M. Heravi, Kaolin: an efficient, reusable and inexpensive catalyst for the one-pot synthesis of 5-alkoxycarbonyl-4-aryl-3,4-dihydropyrimidin-2 (1H)-ones, Iran. J. Org. Chem. 3 (2009) 194–197.
[301] G.C. Rovnyak, S.D. Kimball, B. Beyer, G. Cucinotta, J.D. DiMarco, A. Gougoutas, A. Hedberg, M. Malley, J.P. McCarthy, R. Zhang, S. Moreland, Calcium entry blockers and activators: conformational and structural determinants of dihydro-pyrimidine calcium channel modulators, J. Med. Chem. 38 (1) (1995) 119–129.
[302] K.S. Atwal, G.C. Rovnyak, S.D. Kimball, D.M. Floyd, S. Moreland, B.N. Swanson, J. Z. Gougouta, J. Schwartz, K.M. Smillie, M.F. Malley, Dihydropyrimidine calcium channel blockers. II. 3-substituted-4-aryl-1,4-dihydro-6-methyl-5-pyrimidinecarboxylic acid esters as potent mimics of dihydropyridines, J. Med. Chem. 33 (9) (1990) 2629–2635.
[303] J.J. Baldwin, D.A. Claremon, D.E. McClure, Chem. Abstr. 107, 1987. 242619d (Merck and Co., Inc.) US (1987) 4 675 321.
[304] F. Bigi, S. Carloni, B. Frullanti, R. Maggi, G. Sartori, A revision of the Biginelli reaction under solid acid catalysis. Solvent-free synthesis of dihydropyrimidines over montmorillonite KSF, Tetrahedron Lett. 40 (17) (1999) 3465–3468.
[305] P. Biginelli, P. Gazz, Synthesis of 3,4-dihydropyrimidin-2(1H)-ones, Chim. Ital. 23 (1893) 360–416.
[306] V.R. Rani, N. Srinivas, M.R. Kishan, S.J. Kulkarni, K.V. Raghavan, Zeolite-catalyzed cyclocondensation reaction for the selective synthesis of 3,4-dihydropyrimidin-2(1H)-ones, Green Chem. 3 (2001) 305–306.
[307] P. Salehi, M. Dabiri, M.A. Zolfigol, M.A. Bodaghi Fard, Silica sulfuric acid: an efficient and reusable catalyst for the one-pot synthesis of 3, 4-dihydropyrimidin-2 (1H)-ones, Tetrahedron Lett. 44 (14) (2003) 2889–2891.
[308] M. Tajbakhsh, B. Mohajerani, M.M. Heravi, A.N. Ahmadi, Natural HEU type zeolite catalyzed Biginelli reaction for the synthesis of 3, 4-dihydropyrimidin-2 (1H) one derivatives, J. Mol. Catal. 236 (1–2) (2005) 216–219.
[309] G. Srihari, M. Marthanda Murthy, Kaolin/KOH is an efficient heterogeneous catalyst for the synthesis of 3-hydroxy-3-indolyl oxindoles, Synth. Commun. 41 (18) (2011) 2684–2692.
[310] A. Gazit, N. Osherov, I. Posner, P. Yaish, E. Poradosu, C. Gilon, A. Levitzki, Tyrphostins, II: heterocyclic and a-substituted benzylidenemalononitrile tyrphostins as potent inhibitors of EGF receptor and ErbB2 = neu tyrosine kinases, J. Med. Chem. 34 (1991) 1896–1907.
[311] S. Dilber, M. Saban, J. Jelaca, A. Gelineo, L. Arsenijevic, M. Bogavac, Investigation of antimicrobial activity of some isatin derivatives, Pharmazie 44 (9) (1989) 649–650.
[312] V.J. Ram, L. Mishra, H.N. Pandey, A.J. Vlietnick, Pesticidal Mannich bases derived from isatinimines, J. Heterocycl. Chem. 23 (5) (1986) 1367–1369.
[313] H. Pajaoshesh, R. Parson, F.D. Popp, Potential anticonvulsant, VI: condensation of isatins with cyclohexanone and other cyclic ketones, J. Pharm. Sci. 72 (1983) 318–321.
[314] D. Sundberg, The Chemistry of Indoles, Academic, New York, 1996.

[315] M. Somei, F. Yamada, Simple indole alkaloids and those with a nonrearranged monoterpenoid unit, Nat. Prod. Rep. 22 (1) (2005) 73–103.
[316] Y. Koguchi, J. Kohno, M. Nishio, K. Takahashi, T. Okuda, T. Ohnuki, S. Komatsubara, TMC-95 A, B, C, and D; novel proteasome inhibitors produced by apiospora montagnei Sacc. TC 1093: taxonomy, production, isolation, and biological activities, J. Antibiot. 53 (2) (2000) 105–109.
[317] T. Tokunaga, W.E. Hume, T. Umezome, K. Okazaki, Y. Ueki, K. Kumagai, S. Hourai, J. Nagamine, H. Seki, M. Taiji, H. Noguchi, R. Nagata, Oxindole derivatives as orally active potent growth hormone secretagogues, J. Med. Chem. 44 (26) (2001) 4641–4649.
[318] J. Nagamine, R. Nagata, H. Seki, N. Nomura-Akimaru, Y. Ueki, K. Kumagai, M. Taiji, H. Noguchi, Pharmacological profile of a new orally active growth hormone secretagogue, SM-130686, J. Endocrinol. 171 (3) (2001) 481–489.
[319] B. Sadeghi, Z. Lasemi, R. Azimi, One-pot three-component synthesis of spirooxindoles catalyzed by nano Ag/kaolin, Orient. J. Chem. 31 (2) (2015) 1175–1179.
[320] C.V. Galliford, K.A. Scheidt, Pyrrolidinyl-spirooxindole natural products as inspirations for the development of potential therapeutic agents, Angew. Chem. Int. Ed. Engl. 46 (46) (2007) 8748–8758.
[321] A.H.A. Rahman, E.M. Keshk, M.A. Hanna, S.M. El-Bady, Synthesis and evaluation of some new spiro indoline-based heterocycles as potentially active antimicrobial agents, Bioorg. Med. Chem. 12 (9) (2004) 2483–2488.
[322] A. Dandia, R. Singh, S. Khaturia, C. Merienne, G. Morgant, A. Loupy, Efficient microwave enhanced regioselective synthesis of a series of benzimidazolyl/triazolyl spiro [indole-thiazolidinones] as potent antifungal agents and crystal structure of spiro[3H-indole-3,2'-thiazolidine]-3'(1,2,4-triazol-3-yl)-2,4'(1H)-dione, Bioorg. Med. Chem. 14 (7) (2006) 2409–2417.
[323] J.J. Badillo, N.V. Hanhan, A.K. Franz, Enantioselective synthesis of substituted oxindoles and spirooxindoles with applications in drug discovery, Curr. Opin. Drug. Discov. Dev. 13 (6) (2010) 758–776.
[324] K. Ding, Y.P. Lu, Z. Nikolovska-Coleska, G.P. Wang, S. Qiu, S. Shangary, W. Gao, D.G. J. QinStuckey, K. Krajewski, P.P. Roller, S.M. Wang, Structure-based design of spirooxindoles as potent, specific small-molecule inhibitors of the MDM2-p53 interaction, J. Med. Chem. 49 (12) (2006) 3432–3435.
[325] A.P. Antonchick, C. Gerding-Reimers, M. Catarinella, M. Schurmann, H. Preut, S. Ziegler, D. Rauh, H. Waldmann, Highly enantioselective synthesis and cellular evaluation of spirooxindoles inspired by natural products, Nat. Chem. 2 (9) (2010) 735–740.
[326] S.L. Zhu, S.I. Ji, Y.A. Zhang, A simple and clean procedure for three component synthesis of spirooxindoles in aqueous media, Tetrahedron 63 (2007) 9365–9372.
[327] G. Shanthi, G. Subbulakshmi, P.T. Perumal, A new $InCl_3$-catalyzed, facile and efficient method for the synthesis of spirooxindoles under conventional and solvent-free microwave conditions, Tetrahedron 63 (2007) 2057–2063.
[328] Y.M. Litvinov, V.Y. Mortikov, A.M. Shestopalov, Versatile three-component procedure for combinatorial synthesis of 2-aminospiro[(3′H)-indol-3′,4-(4H)-pyrans], J. Comb. Chem. 10 (2008) 741–745.
[329] M.N. Elinson, A.I. Ilovaisky, V.M. Merkulova, D.V. Demchuk, P.A. Belyakov, Y.N.G. I. Ogibin Nikishin, The electrocatalytic cascade assembling of isatins, malononitrile and N-alkyl barbiturates: An efficient multicomponent approach to the spiro[indole-3,5′-pyrano[2,3-d]pyrimidine] framework, Electrochim. Acta 53 (2008) 8346–8350.
[330] R. Sridhar, B. Srinivas, B. Madhav, V.P. Reddy, Y.V.D.K.R. Nageswar Rao, Multicomponent supramolecular synthesis of spirooxindoles catalyzed by β-cyclodextrin in water, Can. J. Chem. 87 (2009) 1704–1707.

[331] K. Rad-Moghadam, L. Youseftabar-Miri, Ambient synthesis of spiro[4H-pyran-oxindole] derivatives under [BMIm]BF_4 catalysis, Tetrahedron 67 (31) (2011) 5693–5699.
[332] Y. Li, H. Chen, C. Shi, D. Shi, S. Jin, Efficient one pot synthesis of spirooxindole derivatives catalyzed by I-proline in aqueous medium, J. Comb. Chem. 12 (2) (2010) 231–237.
[333] D.S. Raghuvanshi, K.N. Singh, An efficient protocol for multicomponent synthesis of spirooxindoles employing L-proline as catalyst at room temperature, J. Heterocycl. Chem. 47 (6) (2010) 1323–1327.
[334] B. Karmakar, A. Nayak, J. Banerji, A clean and expedient synthesis of spirooxindoles in aqueous media catalyzed over nanocrystalline MgO, Tetrahedron Lett. 53 (37) (2012) 5004–5007.
[335] L.M. Wang, N. Jio, J. Qiu, J.J. Yu, J.Q. Liu, F.L. Guo, Y. Liu, Sodium stearate-catalyzed multicomponent reactions for efficient synthesis of spirooxindoles in aqueous micellar media, Tetrahedron 66 (2010) 339–343.
[336] G.S. Hari, Y.R. Lee, Efficient one-pot synthesis of spirooxindole derivatives by ethylenediamine diacetate catalyzed reactions in water, Synthesis 2010 (3) (2010) 453–464.
[337] B. Maheshwar Rao, G. Niranjan Reddy, T. Vijaikumar Reddy, B.L.A. Prabhavathi Devi, R.B.N. Prasad, J.S. Yadav, B.V. Subba Reddy, Carbon–SO_3H: a novel and recyclable solid acid catalyst for the synthesis of spiro[4H-pyran-3,3′-oxindoles], Tetrahedron Lett. 54 (20) (2013) 2466–2471.
[338] A. Dandia, V. Parewa, A. Kumar Jain, K.S. Rathore, Step-economic, efficient, ZnS nanoparticle-catalyzed synthesis of spirooxindole derivatives in aqueous medium viaKnoevenagel condensation followed by Michael addition, Green Chem. 13 (2011) 2135–2145.
[339] D.K. Sharma, A. Hussain, M.R. Lambu, S.K. Yousuf, S. Maiety, B. Singh, D. Mukherjee, Fe/Al pillared clay catalyzed solvent-free synthesis of bisindolylmethanes using diversly substituted indoles and carbonyl compounds, RSC Adv. 3 (7) (2013) 2211–2215.
[340] K.B. Oh, W. Mar, S. Kim, J.Y. Kim, T.H. Lee, J.G. Kim, D. Shin, C.J. Sim, J. Shin, Antimicrobial activity and cytotoxicity of Bis(indole) alkaloids from the sponge spongosorites sp, Biol. Pharm. Bull. 29 (3) (2006) 570–573.
[341] A. Kamal, M. Naseer, A. Khan, K.S. Reddy, Y.V.V. Srikanth, S.K. Ahmed, K.P. Kumar, U.S.N. Murthy, An efficient synthesis of bis(indolyl)methanes and evaluation of their antimicrobial activities, J. Enzyme Inhib. Med. Chem. 24 (2) (2009) 559–565.
[342] C.J. Magesh, R. Nagarajan, M. Karthik, P.T. Perumal, Synthesis and characterization of bis(indolyl)methanes, tris(indolyl)methanes and new diindolylcarbazolylmethanes mediated by Zeokarb-225, a novel, recyclable, eco-benign heterogenous catalyst, Appl. Catal. A Gen. 266 (1) (2004) 1–10.
[343] S.V. Nadkarni, M.B. Gawande, R.V. Jayaram, J.M. Nagarkar, Synthesis of bis(indolyl) methanes catalyzed by surface modified zirconia, Catal. Commun. 9 (2008) 1728–1733.
[344] H. Firouzabadi, N. Iranpoor, M. Jafarpour, A. Ghaderi, $ZrOCl_2 \cdot 8H_2O$/silica gel as a new efficient and a highly water–tolerant catalyst system for facile condensation of indoles with carbonyl compounds under solvent-free conditions, J. Mol. Catal. A Chem. 253 (1–2) (2006) 249–251.
[345] K. Niknam, M.A. Zolfigol, T. Sadabadi, A. Nejati, Preparation of indolylmethanes catalyzed by metal hydrogen sulfates, J. Iran. Chem. Soc. 3 (4) (2006) 318–322.
[346] V. Murugesan, K.K. Cheralathan, M. Karthik, Catalysis of materials for fine chemicals production, Bull. Catal. Soc. India 3 (2004) 23.
[347] J.S. Yadav, B.V.S. Reddy, S. Sunitha, Three-component one-pot synthesis of α-hydroxylamino phosphonates using ionic liquids, Adv. Synth. Catal. 345 (5) (2003) 564–567.
[348] S.J. Ji, M.F. Zhou, D.G. Gu, S.Y. Wang, T.P. Loh, Efficient synthesis of bis(indolyl) methanes catalyzed by Lewis acids in ionic liquids, Synlett 13 (2003) 2077–2079.

[349] S.J. Ji, M.F. Zhou, D.G. Gu, Z.Q. Jiang, T.P. Loh, Efficient FeIII-catalyzed synthesis of bis(indolyl)methanes in ionic liquids, Eur. J. Org. Chem. 7 (2004) 1584–1587.
[350] S.A. Sadaphal, S.S. Sonar, M.S. Shingare, Ionic liquid promoted synthesis of bis(indolyl) methanes, Cent. Eur. J. Chem. 6 (4) (2008) 622–626.
[351] X.L. Feng, C.J. Guan, C.X. Zhao, Ion exchange resin catalyzed condensation of indole and carbonyl compounds—synthesis of bis-indolylmethanes, Synth. Commun. 34 (3) (2004) 487–492.
[352] L.M. Wang, J.W. Han, H. Tian, J. Sheng, Z.Y. Fan, X.P. Tang, Rare earth perfluorooctanoate [RE(PFO)3]-catalyzed condensations of indole with carbonyl compounds, Synlett 2 (2005) 337–339.
[353] M. Luo, D. Bowden, P. Brimblecombe, Catalytic property of Fe-Al pillared clay for Fenton oxidation of phenol by H_2O_2, Appl. Catal. B: Environ. 85 (3–4) (2009) 201–206.
[354] A.K. Ladavos, P.N. Trikalitis, P.J. Pomonis, Surface characteristics and catalytic activity of Al-pillared (AZA) and Fe·Al-pillared (FAZA) clays for isopropanol decomposition, J. Mol. Catal. A: Chem. 106 (3) (1996) 241–254.
[355] R.R. Guerrero, J. Cárdenas, L. Bautista, M. Vargas, E.V. Labastida, M. Salmón, Catalytic synthesis of 1,3,5-triphenylbenzenes, β-methylchalcones and 2,4,6-triphenyl pyrylium salts, promoted by a super acid triflouromethane sulfonic clay from acetophenones, J. Mex. Chem. Soc. 50 (3) (2006) 114–118.
[356] D. Basting, F.P. Schaefer, B. Steyer, New laser dyes, Appl. Phys. 3 (1) (1974) 81–88.
[357] B. Kopainsky, W. Kaiser, K.H. Drexhage, New ultrafast saturable absorbers for Nd: lasers, Opt. Commun. 32 (1980) 451–455.
[358] D. Markovitsi, I. Lecuyer, B. Clergeot, C. Jallabert, H. Strzelecka, M. Veber, Photophysical properties of discogenic triaryl pyrylium salts excimer migration in columnar liquid crystals, Liq. Cryst. 6 (1) (1989) 83–92.
[359] M.R. Detty, P.B. Merkel, S.L. Gibson, R. Hilf, Chalcogenapyrylium dyes as dual-action sensitizers for photodynamic therapy, Oncol. Res. 4 (8–9) (1992) 367–373.
[360] M.A. Miranda, H. García, 2,4,6-triphenylpyrylium tetrafluoroborate as an electron-transfer photosensitizer, Chem. Rev. 94 (4) (1994) 1063–1089.
[361] Y. Chen, S.K. Wu, A study of the photophysical properties of 2,4,6-triphenyl pyrylium salts with rigid and non-rigid structures, J. Photochem. Photobio. A Chem. 102 (2–3) (1997) 203–206.
[362] D. Habibi, O. Marvi, Montmorillonite KSF and montmorillonite K-10 clays as efficient catalysts for the solventless synthesis of bismaleimides and bisphthalimides using microwave irradiation, Arkivoc (xiii) (2006) 8–15.
[363] A. Da Settimo, G. Primofiore, F. Da Settimo, F. Simorini, C. La Motta, A. Martinelli, E. Boldrini, Synthesis of pyrrolo[3,4-c]pyridine derivatives possessing an acid group and their in vitro and in vivo evaluation as aldose reductase inhibitors, Eur. J. Med. Chem. 31 (1) (1996) 49–58.
[364] M. Ohkubo, T. Nishimura, H. Jona, T. Honma, H. Morishima, Practical synthesis of indolopyrrolocarbazoles, Tetrahedron 52 (1996) 8099–8112.
[365] T. Iijima, N. Suzuki, W. Fukuda, M. Tomoi, Toughening of aromatic diamine-cured epoxy resins by modification with N-phenylmaleimide-styrene-p-hydroxystyrene terpolymers, J. Eur. Polym. 31 (8) (1995) 775–783.
[366] K.D. Janda, J.A. Ashley, T.M. Jones, D.A. McLeod, S.D.M. Chloeder, M.I. Weinhouse, Immobilized catalytic antibodies in aqueous and organic solvents, J. Am. Chem. Soc. 112 (1990) 8886–8888.
[367] R. Grigg, S. Surendrakumar, S. Thianpatanagul, D. Vipond, J. Chem. Soc. Perkin Trans. 1 (1988) 2693–2701.

[368] P.N. Preston, V.K. Shah, S.W. Simpson, I. Souter, N.J. Stewart, Studies on Bismaleimides and related materials. 4. Synthesis and characterization of new Bismaleimides based on terphenyl, tetraphenylketazine, and bisphenol A: "reactive building blocks" for bismaleimides, Macromolecules 27 (5) (1994) 1147–1153.
[369] M.A. Walker, A high yielding synthesis of N-alkyl maleimides using a novel modification of the Mitsunobu reaction, J. Org. Chem. 60 (16) (1995) 5352–5355.
[370] J.E.T. Corrie, Thiol-reactive fluorescent probes for protein labeling, J. Chem. Soc. Perkin Trans. 1 (20) (1994) 2975–2982.
[371] G.B. Gill, G.D. James, K.V. Oates, G. Pattenden, The synthesis of 5-ylidenepyrrol-2 (5H)-ones from maleimides and from pyrrol-2-(5H)-ones, J. Chem. Soc. Perkin Trans. 1 (21) (1993) 2567–2579.
[372] T.F. Braish, D.E. Fox, A practical synthesis of N-substituted maleimides, Synlett 1992 (12) (1992) 979–980.
[373] R.L. Dorta, C.G. Francisco, E. Suarez, Triphenylbismuth dibromide-iodine: An efficient reagent for the dehydration of alcohols, Tetrahedron Lett. 35 (28) (1994) 5035–5038.
[374] O. Nielsen, O. Buchardt, Facile synthesis of reagents containing a terminal maleimido ligand linked to an active ester, Synthesis 1991 (10) (1991) 819–821.
[375] V.M. Rangnekar, R.P. Bharmaria, B.G. Khadse, Synthesis of N-aryl/heteroaryl/-substituted-methyl alpha-(p-substituted anilino) succinimides as antituberculosis agents, Indian J. Chem. 25B (1986) 342.
[376] A.L. Schwartz, L.M. Lerner, Preparation of N-substituted maleimides by direct coupling of alkyl or aralkyl halides with heavy metal salts of maleimide, J. Org. Chem. 39 (1) (1974) 21–23.
[377] N.B. Mehta, A.P. Phillips, F.F. Lui, R.E. Brooks, Maleamic and citraconamic acids, methyl esters, and imides, J. Org. Chem. 25 (6) (1960) 1012–1015.
[378] M. Naeem, M. Nawaz, S. Rehaman, R. Amjad, One pot synthesis of potentially biologically active novel 4-thiazolidinone derivatives, Asian J. Chem. 24 (10) (2012) 4317–4323.
[379] M.L. Barreca, A. Chimirri, L.D. Luca, A.M. Monforte, P. Monforte, A. Rao, M. Zappalà, J. Balzarini, E.D. Clercq, C. Pannecouque, M. Witvrouw, Discovery of 2,3-diaryl-1,3-thiazolidin-4-ones as potent anti-HIV-1 agents, Bioorg. Med. Chem. Lett. 11 (13) (2001) 1793–1796.
[380] P.S. Allen, A.W.K. Khanzada, C.A. McDowell, Nuclear magnetic resonance absorption and relaxation study of tert-butylamine and tert-butylamine clathrate deuterate, J. Chem. Phys. 59 (1) (1973) 470–474.
[381] N.J. Venkatesha, Green synthesis of cyclic imides by amidation and cyclisation using Bronsted-Lewis acidic montmorillonite clays, ChemistrySelect 6 (2016) 1225–1231.
[382] J.A. Seijas, M.P. Va zquez-Tato, M.M. Martinez, G.N. Corredoira, Direct synthesis of imides from di-carboxylic acids using microwaves, J. Chem. Res. (1999) 420–425.
[383] J. Selvakumar, C.R. Ramanathan, Brønsted acid assisted activation of imide carbonyl group: regioselective synthesis of isoindoloisoquinolinone alkaloid (±)-nuevamine, Org. Biomol. Chem. 9 (22) (2011) 7643–7646.
[384] N.P. Shetgiri, B.K. Nayak, Synthesis and antimicrobial activity of some succinimides, Indian J. Chem. 44 (2005) 1933–1936.
[385] M.A. Ali, S.M.A.H. Siddiki, K. Kon, J. Hasegawa, K. Shimizu, Versatile and sustainable synthesis of cyclic imides from dicarboxylic acids and amines by Nb_2O_5 as a base-tolerant heterogeneous Lewis acid catalyst, Chem. Eur. J. 20 (44) (2014) 14256–14260.
[386] E. Benjamin, Y. Hijj, The synthesis of unsubstituted cyclic imides using hydroxylamine under microwave irradiation, Molecules 13 (1) (2008) 157–169.

[387] G.W. Muller, W.E. Konnecke, A.M. Smith, V.D.A. Khetani, A concise two-step synthesis of thalidomide, Org. Process Res. Dev. 3 (2) (1999) 139–140.
[388] E. Bon, R. Reau, G. Bertand, D.C.H. Bigg, Aluminum trichloride-promoted aminolysis of cyclic imides and oxazolidinones, Tetrahedron Lett. 37 (1996) 1217–1220.
[389] O. Alekseeva, M. Konstantinova, S. Rasumovskii, Efficient method of cyclic imides synthesis under ozone influence by the example of ε-caprolactam oxidation reaction, Heteroatom Chem. 19 (7) (2008) 661–667.
[390] N.R. Conley, R.J. Hung, C.G. Willson, A new synthetic route to authentic N-substituted aminomaleimides, J. Org. Chem. 70 (11) (2005) 4553–4555.
[391] P.J. Rosenthal, J.E. Olson, G.K. Lee, Antimalarial effects of vinyl sulfone cysteine proteinase inhibitors, Antimicrob. Agents Chemother. 40 (7) (1996) 1600–1603.
[392] J.J. D'Amico, (Monsanto Co.), 2-Substituted-1,3(2H,4H)-isoquinolinediones as plant growth regulants, U.S. Pat. 4097260, 1978.
[393] F. Zentz, A. Valla, R. Le Guillou, R. Labia, A.G. Mathot, D. Sirot, Synthesis and antimicrobial activities of N-substituted imides, Farmaco 57 (5) (2002) 421–426.
[394] F. Zentz, C. Hellio, A. Valla, D. de la Broise, G. Bremer, R. Labia, Antifouling activities of N-substituted imides: antimicrobial activities and inhibition of mytilus edulis phenoloxidase, Mar. Biotechnol. 4 (4) (2002) 431–440.
[395] J.A. Seijas, M.P. Vazquez-Tato, C. Gonzalez-Bande, M.M. Martinez, B. Pacios-Lopez, Microwave promoted synthesis of a rehabilitate drug: thalidomide, Synthesis 7 (2001) 999–1000.
[396] O. Marvi, M. Talakoubi, K-10 and KSF clays as green and recyclable heterogeneous catalysts for the Cannizzaro reaction using DABCO under MWI and solvent-free conditions, Orient. J. Chem. 32 (1) (2016) 359–365.
[397] S. Cannizzaro, Ueber den der Benzoësäure entsprechenden Alkohol, J. Liebigs Ann. Chem. Pharm. 88 (1) (1853) 129–130.
[398] T.A. Geissman, The Cannizzaro reaction, Org. React. 2 (1944) 94–113.
[399] P. Lidström, J. Tierney, B. Wathey, J. Westman, Microwave assisted organic synthesis—a review, Tetrahedron 57 (2001) 9225–9283.
[400] M.E.F. Braibante, H.T.S. Braibante, A.F. Morel, C.C. Costa, M.G. Lima, The solvent free preparation of beta-amino esters alpha, beta-unsaturated ketones and esters with domestic microwave oven, J. Braz. Chem. Soc. 17 (2006) 184–188.
[401] P. Lidstrom, J.P. Tierney, Microwave-Assisted Organic Synthesis, Blackwell, Oxford, 2005.
[402] M. Larhed, K. Olofsson, Microwave Methods in Organic Synthesis, Springer, Berlin, 2006.
[403] D. Dallinger, C.O. Kappe, Microwave-Assisted Synthesis in Water as Solvent, Chem. Rev. 107 (6) (2007) 2563–2591.

Further reading

[404] L.J. Krstic, S. Sukdolak, S. Solujic, An efficient synthesis of warfarin acetals on montmorillonite clay K-10 with microwaves, J. Serb. Chem. Soc. 67 (5) (2002) 325–329.

The role of ionic liquid in medicinal chemistry

6

*Muhammad Faisal, Aamer Saeed**
Department of Chemistry, Quaid-i-Azam University, Islamabad, Pakistan
*Corresponding author. e-mail address: aamersaeed@yahoo.com

6.1 Introduction

6.1.1 Green chemistry and its requirements

For over two decades, the concept of green chemistry has been extensively acknowledged as the future over traditional chemistry. Previously, chemistry has been established to reach the most productivity and the greatest economical advantage with little consciousness on the impact of chemical courses to the sustainability and environment. As society experiences the impact in the form of global warming, air pollution, polluted water, etc., researchers have started to realize that these disasters resulted from nonsustainable chemical courses. The concepts of green chemistry were first set forth in the early 1990s with initial leading programs in Italy, the United Kingdom, and the United States. They have received international recognition over the past 20 years [1, 2].

Warner and Anastas in 1998 first introduced the 12 principles of green chemistry which focused on the whole chemical process from starting material design to management of waste. In all, 12 principles of green chemistry are a skeleton of the green chemistry idea, which can generate a better understanding and can simply be applied to the design of chemical courses. Moreover, the well-known definition of green chemistry by Anastas and Warner in the book "Green Chemistry-Theory and Practice," defines that "green chemistry is the utilization of a set of principles that eliminates or reduces the generation or use of dangerous substances in the design, production and applications of chemical products." Since the 12 principles of green chemistry were formulated in 1998, environment-friendly synthetic approaches, reaction conditions, and chemical compounds have been disclosed [3, 4].

6.1.2 Green and alternative solvents in organic synthesis

Green chemistry is highly depended on solvent. Solvents employed by chemists are usually utilized as a reaction media, in purification or in separation techniques. The suitability and quality appropriateness of chemical processes and reactions are highly dependent on the solvent used. Most of the common solvents (for instance, benzene, toluene, dichloromethane, etc.) that are frequently utilized are dangerous. Benzene is popular for causing cancer, toluene causes kidney, liver, and brain problems, and halogenated solvents (methylene chloride, chloroform, and carbon tetrachloride) have

Green Approaches in Medicinal Chemistry for Sustainable Drug Design. https://doi.org/10.1016/B978-0-12-817592-7.00006-X
© 2020 Elsevier Inc. All rights reserved.

been recognized as human carcinogens. Volatility is also one of the key issues with several organic solvents that may damage health of human and environment [5, 6].

All of these harmful effects have made scientist seek alternative solvents that can be a replacement for classical petrochemical solvents. There are numerous solvents which have been inspected and utilized in the organic reactions to move to more environmentally benign and innocuous conditions for nature and human health [7, 8]. Following are the most utilized and researched solvents in attendance as well as the solvent-free conditions: (i) water; (ii) supercritical fluids (widely carbon dioxide and water); (iii) ethanol, aqueous surfactant micelles, and polymers [9]; (iv) fluorous solvents; and (v) ionic liquids (ILs).

6.1.3 ILs and their synthesis

ILs are family of molten organic salts, typically comprised of inorganic/organic anions and unsymmetrical organic cations with melting points (MP) at or below 100°C. Ones which are liquid under ambient conditions are termed room temperature ionic liquids (RTILs). The reduced coordination between the ions that form the ILs (attributed to the asymmetry of the cations with respect to the anions) decreases the lattice energy of the crystalline phase of the salt, and it is responsible for the significantly low melting point of these substances compared to conventional salts [10, 11]. The ILs often comprise unsymmetrical and large organic cations and inorganic or organic anions. As these ILs may contain a reduced proportion of molecular species, their vapor pressure is not as negligible as in the case of aprotic ILs [12, 13]. Within the broad range of cations present in ILs, the most important are those created by phosphorus or nitrogen-containing entities with different alkyl chains. In the case of anions, they can be reduced-size entities, for instance, halides, but also greater and more complex structures. Fig. 6.1 displays the most frequent cations and anions, respectively, that form part of the structure of the ILs [14].

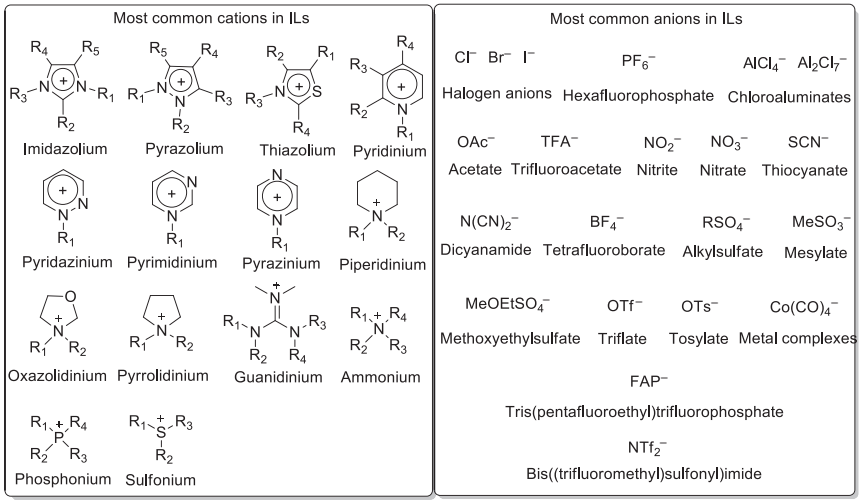

Fig. 6.1 Most common anions and cations in ILs.

Owing to all of the possible combinations of different ions, the potential for research and synthesis of new ILs is almost limitless [14]. Usually, ILs can be synthesized from phosphines, sulfonates, or amines in two key steps. For example, there are two main steps in the formation of imidazolium-mediated ILs: the development of the preferred cation and subsequent exchange (metathesis) of the anion with the required anionic partner to yield the final IL (Scheme 6.1) [14]. During the anion exchange reaction, there are two possible routes, which can be followed. One is the development of complex anions by the direct reaction of a strong Lewis acid with a halide salt and the other is the construction of the IL through introduction of a metal salt so as to precipitate the undesired anion. There are numerous other techniques which have been established for the preparation of ILs, for instance, halide and solvent-free routes, microwave or sono-chemical procedures, or using very cheap industrial products (e.g., H_2SO_4) as regents [15, 16]. Depending on the approaches used in the preparation of the ILs, common impurities include tertiary amines, alkyl sulfates, alkyl halides or other side-reaction moieties and, after metathesis, residual halide and sulfate. There are numerous purification procedures, which can be used after the preparation of the ILs, for example, treatment of the IL with activated charcoal, extraction of the IL with a polar solvent, or extraction of the aqueous solution of the IL with an immiscible organic solvent [17, 18].

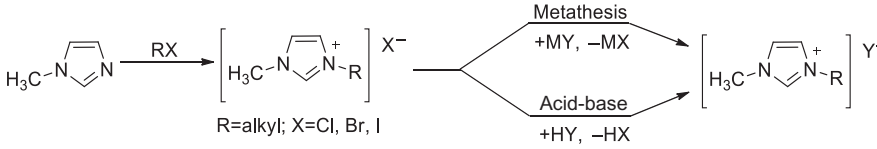

Scheme 6.1 Synthesis pathway for the formation of imidazolium ILs.

6.1.4 Properties of ILs and their applications in green chemistry

There are some properties which are common to many ILs. For instance, ILs with quaternary nitrogen cations are not flammable and considered to display insignificant vapor pressure. These features create a great proportion of attention in ILs from the green chemistry point of view. As nonvolatile solvents, air pollution is avoided and the upper limit of their liquid range is measured by their temperature at which thermal decomposition takes place [19–21]. The insignificant vapor pressure of ILs also improves their reusing contributing to their classification as "green solvents." Generally, ILs are usually thermally stable compounds. This means that ILs can be employed at high operating temperatures without solvent degradation. Also, ILs present high conductivity values and a broad electrochemical window. Moreover, ILs can dissolve compound of different natures. The presence of nonpolar and polar domains in the molecule of the IL is responsible for diverse range of molecular interactions, depending on the nature of the chemical species dissolved in such medium [22–24]. Depending on the requirements of an application, the characteristics of ILs can be straightforwardly modified using simple chemical reactions. For instance,

1-alkyl-3-methylimidazolium-based ILs with halide anions possess appropriate solubility in aqueous solutions and show tremendous solvent properties for the dissolution of complex bioactive molecules [25]. However, these ILs are not appropriate for high-temperature gas chromatography (GC) applications on account of their low thermal stabilities. The replacement of halides with the bis[(trifluoromethyl)sulfonyl]imide ($[NTf_2^-]$) anion via ion-exchange metathesis reaction delivers ILs with large thermal stabilities and are consequently employed as GC stationary phases [26]. In addition, ILs can be custom designed through the incorporation of task-specific functional groups within the cationic or anionic portion of the IL. Lewis acids [27], chiral amino acids [28], and metal chelators [29] are a few examples of task-specific functional groups that are appended to ILs. Hence, attributed to their versatile nature and structural tunability, ILs are frequently described as "designer solvents" [30]. Furthermore, ILs are usually costly chemical compounds and, therefore, their recyclability must be taken into account after their application. Several research reports have showed the successful recycling of ILs after their utilization and numerous techniques for recycling ILs have been disclosed [31, 32]. Following properties of ILs are also reported in literature: electric conductivity, high heat capacity, liquid crystal structures, and high electroelasticity [30, 33, 34]. Table 6.1 illustrates the comparison of some properties of ILs with organic solvents.

Table 6.1 Comparison of organic solvent properties with ILs.

Property	Organic solvent	Ionic liquids
Vapor pressure	Reasonably high	Negligible under normal condition
Combustibility	Commonly flammable	Commonly not flammable
Tunability	Narrow spectrum of solvents available	Almost limitless spectrum "designer solvent"
Viscosity (cP)	0.2–100	22–40,000
Density (g/cm^3)	0.6–1.7	0.8–3.3
Number of solvents	>1000	>1,000,000
Applicability	Single function	Multifunction

Over the last two decades, attributed to their ease in synthesis and unique physicochemical properties, a huge number of ILs with different anions and cations have been developed and exploited in a broad range of employments including electrochemistry [35], chromatography [36], catalysis [37], as well as biological [38] and pharmaceutical [39] sample preparation. In the recent years, owing to negligible vapor pressures and relatively nontoxicity, ILs have been gradually adopted to industrial-scale synthesis as green solvents. Many of the classical organic reactions, for example, Friedel-Crafts reactions have been accomplished using ILs as solvents [40]. Nucleoside-mediated antiviral medicines have been produced using ILs as solvents [41]. The ILs in these reactions were reported to be better than the conventional molecular solvents in terms of reaction rates and solubility. Very recently, there has been extensive development in the applications of IL-based

chemicals as chiral catalysts in organic synthesis. Thus, ILs possessing chirality have been explored as chiral catalysts for organic functionalization [42, 43]. ILs derived from, for example, proline have been used as chiral catalysts in asymmetric Mukaiyama aldol reactions [44–46]. However, investigations in the last decade reveal that some of the ILs may not be as eco-friendly as originally considered [47]. Therefore, construction of potent kind of ILs without adverse environmental impact is important for the effective employment of these chemicals for industrial-scale courses [48]. Furthermore, one of the main successes of ILs as reaction solvents has been in transition metal-catalyzed reactions. ILs are able to dissolve organometallic reagents and hence, offer a medium for transition metal catalysts. Based on the coordinating properties of the anion, the IL can be a cocatalyst or an inert solvent. One of the foremost properties of IL in catalysis and synthesis is that both the anionic and cationic components can be varied that are widely applicable to specific applications.

6.1.5 Green applications of ILs in medicinal chemistry

Over the last few decades, the pharmaceutical industry has been facing huge pressure and great challenges attributed to the environmental problems, long term and lengthening drug development method and customer expectation as a cost constrained on the health-care system. Regarding green chemistry principles, the generation of waste from the pharmaceutical manufacturing process is awful. In 2008, Sheldon proposed the *E*-factor (environmental) and defined it as kg waste/kg product. He further concluded that the pharmaceutical industry has the highest Sheldon *E*-factor (25–100), compared to the fine chemicals (5–50) and oil-refining (<0.1) industries [49]. Nowadays, clients are also demanding new therapies which are more economical and clinically better than the existing old therapies. Moreover, solubility and stability of drugs, extraction of bioactive drugs from natural products, pharmaceutical crystallization and purifications and biomedical analytics are also regarded as important issues [50, 51].

Investigations in the last two decade reveal that in order to resolve the aforementioned issues, the employment of ILs is one of the best solutions [30, 33, 34, 37, 48, 50, 51]. In literature of last two decade, ILs are extensively used for green synthesis of various bioactive compounds, as pharmaceutical ingredients, for biomedical analytics, in pharmaceutical crystallization and separations, and for extraction of medicinal natural ingredients. Interestingly, ILs are also reported to demonstrate potent biological activities. The main sections considered in this book chapter include application of ILs in synthesis and detection of bioactive compounds; usage of ILs as components of drugs; biological activity of ILs; and employment of ILs for extraction, crystallization, and separation of synthetic and natural bioactive compounds.

6.2 ILs in synthesis of drugs and drug precursors

ILs are utilized in many chemical courses including promising utility in the preparation of bioactive compounds and their precursors. ILs are used in the formation of heterocyclic compounds, for example, quinolines, thiazoles, oxazoles, furans,

imidazoles, and others, which are exploited in medicine and biology [52]. Due to their exclusive character, ILs can simultaneously play dual parts of catalysts and media; therefore, offering reduced quantities of volatile solvents and reduced amounts (or even elimination) of metal catalytic systems that may leach into the atmosphere. ILs can also effect the selectivity of enzymes employed in biotechnological approaches [53, 54].

Hydrogenation of 2-arylacrylic acids in the [BMIM][BF_4] **1** as reaction media was reported by Monteiro et al. in 1997. The authors used the method for creating the (*S*)-naproxen **2** (nonselective COX inhibitor) [55]. In 2000, the first high-yielding synthesis of a drug namely pravadoline **3** (antiinflammatory and analgesic agent) using [C_4MIM][PF_6] **4** as reaction media was reported by Earle et al. (Fig. 6.2) [56]. Thus, the age of ILs in the synthesis of drug has begun. In the past 15 years, many researchers have disclosed the application of ILs in several chemical processes, which are associated with the creation of pharmaceuticals, their intermediates or precursors, and other agents with appropriate biological potency [57–72]. In the majority of cases, ILs are employed as reaction media, which frequently also serves as catalyst, and the most useful and studied ILs in medicinal chemistry are imidazolium salts. The reason why imidazole-mediated ILs are among the most investigated ILs, is owing to their lower viscosity and to the stability of the imidazolium cation in reductive and oxidative conditions. Therefore, they have been utilized for numerous applications, such as catalysts and solvents in synthesis and as solubility enhancers in DDS. In terms of their employment as solubility promoters, their cytotoxicity may represent a shortcoming, mainly for those ILs with a long alkyl chain attached to the imidazolium cation and this should always be considered [73]. In this section, we will discuss some important examples, in which ILs have been used as solvent and/or catalyst in the synthesis of bioactive compounds and their precursors.

Deshmukh et al. reported an efficient and simple methodology for iodination of activated heteroaromatic and aromatic using reusable 1-butyl-3-methylpyridinium dichloroiodate (BMPDCI) **5** as an IL iodinating agent under organic solvent-free condition [57]. The foremost benefits are simple effective process, no need of any oxidizing agent or base/toxic transition metals, and high yields. The IL was regenerated and reused fivefold without important loss of efficacy. This protocol was employed for the formation of antiprotozoal agent iodoquinol **7** and antifungal agent clioquinol **6** (Fig. 6.2).

Candida rugosa lipase (CRL) is one of the enzymes most often employed in biotransformations. CRL-catalyzed Fischer esterification reaction of ibuprofen **8** (antiinflammatory painkilling drug) with propan-1-ol was accomplished by Hongwei et al. in the existence of [C_4MIM][PF_6] **4** [58]. In this reaction, the enantioselectivity observed ($E = 24.1$) was nearly double that of 2,2,4-trimethylpentane ($E = 13.0$) and, therefore, [C_4MIM][PF_6] **4** could be utilized to eliminate the harmful organic solvent (e.g., 2,2,4-trimethylpentane) in the Fischer esterification of **8**.

In another interesting approach, Kumar and Malhotra prepared nucleoside-mediated antiviral agents (stavudine **9**, brivudine **10**, and trifluridine **11**) using imidazolium-mediated ILs ([MoeMlm][Ms] **12**, [MoeMlm][TFA] **13** and [BMlm][TFA] **14**) as reaction medium (Fig. 6.2) [41]. In terms of solubility, ILs (**12**, **13**,

and **14**) demonstrated to be remarkable solvents as compared to conventionally solvents used for nucleosides. Synthesis in ILs (**12**, **13**, and **14**) completed at much higher rate and also requirements for the solvent are decreased by 10 times.

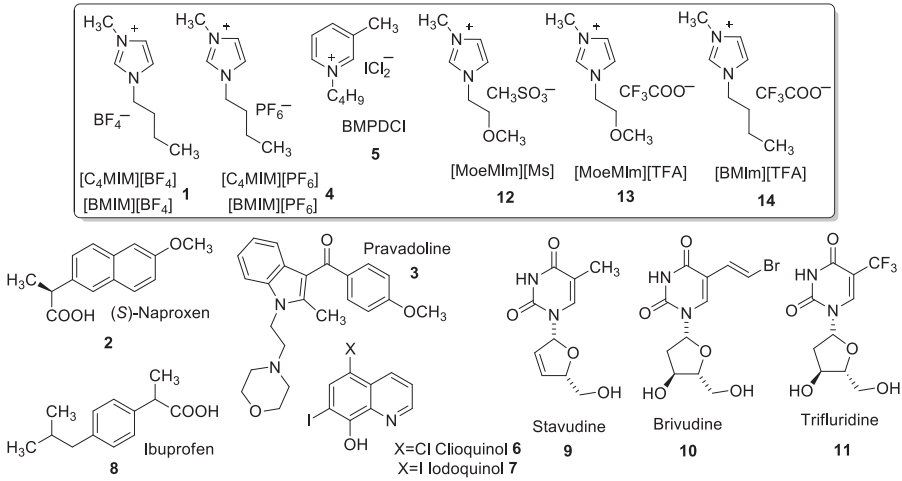

Fig. 6.2 Structure of [BMIM][BF_4], [BMIM][PF_6], BMPDCI, [MoeMIm][Ms], [MoeMIm][TFA], [BMIm][TFA], and bioactive drugs.

Hydrazinyl phthalazines **15** are very useful antimalarial agents. Subramanian et al. disclosed the synthesis of hydrazinyl phthalazines **15** using bronsted acidic IL, that is, 1,2,3-trimethylimidazolium methyl sulfate (BASF) **16** as a dehydrating agent [65]. The desired hydrazinyl phthalazines **15** were obtained in good yield and high purity. On the other hand, the application of bronsted acids (e.g., AcOH, PPA, HCl, H_2SO_4) as dehydrating agents lead toward the development of impure target compounds with inappropriate yield.

Modafinil **17** is a famous drug, which is used to medicate sleep disorders attributed to obstructive sleep apnea (OSA), shift work sleep disorder, or narcolepsy (Fig. 6.3). In a recent study, Guillen and coworkers performed the functionalization of [(diphenylmethyl)sulfanyl]acetic acid and its analogs in order to prepare modafinil **17** and its derivatives using [bmim][PF_6] **4** as a solvent [66]. The oxidation afforded higher yields and enantioselectivities. In the synthesis of isoxazoline derivatives **18**, which are important precursors of antimicrobial agents, improved yields and significant rate acceleration in [C_4MIM][BF_4] **1** have been observed by Chakraborty and Sharma [67].

(*R*)-Phenylacetylcarbinol (PAC) **19** is an important precursor of (1*S*,2*S*)-pseudoephedrine **20** and (1*R*,2*S*)-ephedrine **21**. Bioconversion of glucose and benzaldehyde by pyruvate decarboxylase (PDC) from baker's yeast yields PAC **19**. This bioconversion suffers from two major drawbacks. One is the formation of by-product (benzenemethanol) and other is the toxicity of the substrate. In the report by Kandar et al., IL [BMIM][PF_6] **4** in aqueous two-phase system (ATPS) was used to

improve the production of PAC **19** [68]. The results displayed excellent PAC **19** yield and productivity of nearly 1.5 times each in the two-phase bioconversion of phase volume ratio 0.05 relative to a single aqueous phase (traditional) bioconversion. Furthermore, the quantity of main by-product benzenemethanol was also 3.5 times lower in aqueous two-phase bioconversion (Fig. 6.3).

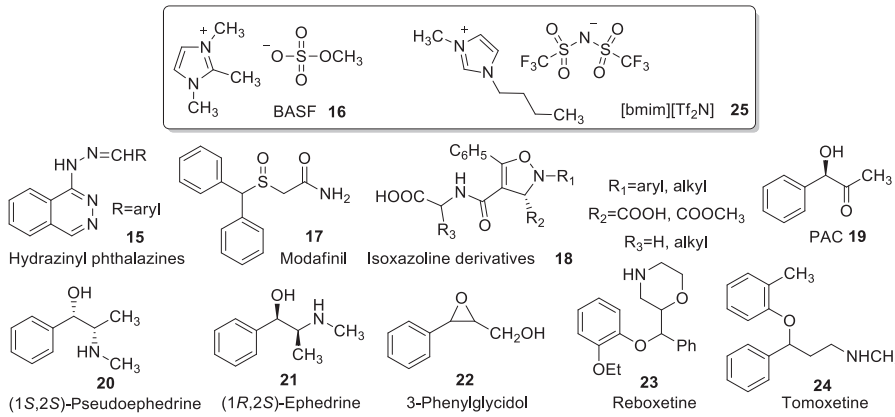

Fig. 6.3 Structure of BASF, [bmim][Tf_2N], and bioactive drugs.

Chirally pure (3-phenyloxiran-2-yl)methanol **22** is a main precursor in the production of a library of medicines, for example, reboxetine **23** and tomoxetine **24**. In order to disclose an efficient approach to deliver **22**, vanadium-catalyzed epoxidation reaction of 3-phenyl-2-propen-1-ol to (3-phenyloxiran-2-yl)methanol **22** in the presence of *t*-butyl hydroperoxide (TBHP) as the oxidant and imidazolium-based IL ([bmim][Tf_2N]) **25** as reaction media was investigated by Kazemi et al. An excellent yield and selectivity was observed [69].

(*R*,*S*)-1-Chloro-3-(3,4-difluorophenoxy)-2-propanol (rac-CDPP) **26** is a significant precursor for the development of the (*S*)-lubeluzole **27** (Prosynap). Direct transesterification reaction of rac-CDPP **26** with ethenyl butanoate by lipases from *Pseudomonas aeruginosa* was carried out by Singh et al. in hexane with IL [BMIM][PF_6] **4** as cosolvent [69]. The appropriate yield and enantiomeric excess was accomplished in 6 h at 30°C with [C_4MIM][PF_6] **4** as cosolvent in a biphasic system (Fig. 6.4). In a similar fashion, Zaidlewicz et al. synthesized the potential antitumor drug 4-borono-L-phenylalanine (L-BPA) **28** which is a clinically FDA-approved medicine. They reported on the employment of ILs such as [C_4MIM][BF_4] **1** and [BMIM][PF_6] **4** in the synthesis of L-BPA **28** [71, 72].

Fan and coworkers established an environment-friendly protocol for the formation of hybrid products mediated on pyrimidine nucleosides bonded with pyrano[4,3-*c*] pyranes and pyrimidine nucleosides bonded with pyrano[3,2-*c*]pyridines as potential antileishmanial and antiviral drugs, by using [BMIM][BF_4] **1** as a reaction medium [59]. This synthesis accomplished higher yields compared with other reported approaches was performed without any catalyst and offered recyclability of the

reaction media. In another interesting approach, Zhang et al. constructed pyrimidine nucleoside-4-thiazolinione hybrids **29** as potent antiparasitic agents, using [BMIM][PF_6] **4** as the reaction medium (Fig. 6.4) [60].

Kishimoto and coworkers reported a unique, effective biocatalytic process affording numerous phenethyl caffeate derivatives **30** with promising antiproliferative influence on tumor cells [61]. The authors used lipase B from *Candida antarctica* (CAL-B) in [bmim][Tf_2N] **25** as reaction medium and achieved an excellent yield of 92%, which is similar to that achieved when phenethyl caffeate derivatives **30** was prepared in 2,2,4-trimethylpentane. In an another report, Shaabani et al. investigated bioactive compounds mediated on acyclic nucleoside analogs, which have a potent antiviral potency and disclosed an effective and environment-friendly methodology for the construction of 3-amino-imidazo[1,2-α]pyridine derivatives **31** with novel antiviral affinity using the 3-butyl-1-methyl-1*H*-imidazol-3-ium bromide ([C_4mim][Br]) **32** IL (Fig. 6.4) [62, 63]. Replacing the frequently employed organic solvents by the commercially available imidazolium bromide advances the formation of the side chain-modified imidazo[1,2-α]pyridinics **31** in terms of yield, reaction rates, and solubility. In addition, the separation of [C_4mim][Br] **32** from the reaction mixture was possible by washing with H_2O and evaporating the solvent in vacuo.

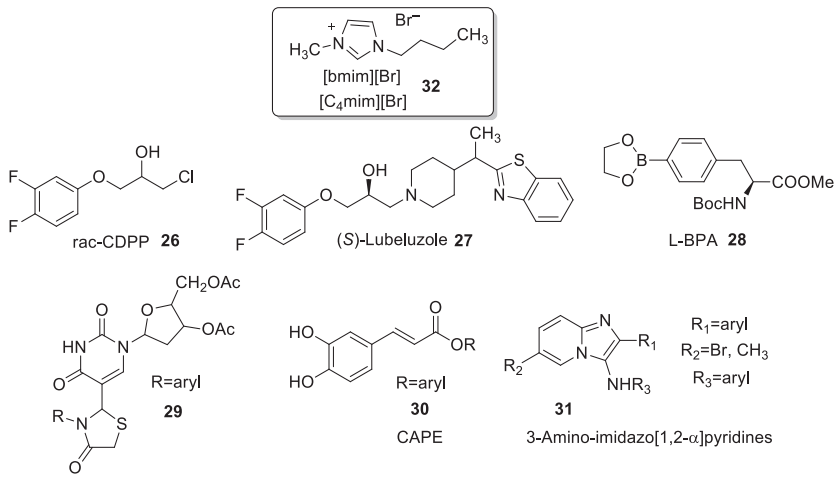

Fig. 6.4 Structure of [bmim][Br] and bioactive drugs.

ILs undoubtedly can be beneficially employed as alternative reaction media for the synthesis of diverse range of pharmaceutical agents. The replacement of the toxic organic solvents by ILs can frequently deliver improved reaction conditions, enhancing some more challenging reactions, as well as simplifying the isolation and purification of the required compound. From the pharmaceutical industrial perspective, ILs can be an promising choice as reaction media for synthesis of some specific drugs [64].

6.3 ILs for extraction of bioactive natural products from plants

IL-mediated extraction of natural ingredients from plants is now being examined as an alternative to traditional cloud point extraction, supercritical fluid extraction, and solvent extraction, where environmental, energy, cost impact may be enhanced [74]. For instance, in the recent years, Ribeiro and coworkers reported a significant investigation on potential of several cholinium- and imidazolium-mediated ILs in the extraction of polyphenols and saponins from mate and tea [75]. The investigation revealed that large quantity of saponins could be obtained using tripotassium phosphate hydrate (K_3PO_4) and (2-hydroxyethyl)trimethylammonium chloride following the recovery of saponins in H_2O. Therefore, the authors proposed that it is achievable to tune the IL potency for a specific solvent and significantly enhance the extraction yield of phenols and saponins. Currently, there are large number of examples in literature about the application of ILs in the extraction of bioactive ingredients from natural products using three main methods: (i) ultrasonic-assisted IL approach for the extraction of natural ingredients from plants; (ii) microwave-assisted IL approach for the extraction of natural ingredients from plants; and (iii) reactive dissolution of biomass in ILs to extract natural ingredients. In this section, each approach will be briefly discussed.

6.3.1 Extraction of bioactive natural products through ultrasonic-assisted ionic liquid approach

One of the most ordinary techniques for the extraction of bioactive natural products from plant sources is ultrasonic-assisted extraction (UAE) with the application of IL aqueous solutions as the extracting medium. For instance, Wang and coworkers described [C_4mim][BF_4] **1** for the extraction of four acetophenone derivatives, namely 2,4-dihydroxyacetophenone, baishouwubenzophenone, 2,5-dihydroxyacetophenone, and 4-hydroxyacetophenone from *Cynanchum bungei*, an important medicinal plant species in China (Fig. 6.2) [76]. Under optimized conditions, the efficiencies of extraction were much greater using ILs as compared to those obtained using traditional UAE and heat-reflux extraction in methanol.

Danshen (*Salvia miltiorrhiza Bunge*), *aka*. Chinese red sage, Chinese sage or tan shen, is a member of Lamiaceae class. It is valued in traditional Chinese medicine, mainly for the medication of cerebrovascular and cardiovascular diseases. Row and coworkers successfully extracted three bioactive ingredients of Danshen, *tanshinone II, tanshinone I*, and *cryptotanshinone* by using ultrasonic-assisted aqueous IL-based extraction approaches [77]. The extraction yields of this technique proved to be a few-fold greater as compared to using other solvent extraction systems. Furthermore, to isolate the extracted bioactive ingredients from the IL, the metathesis reaction to transform the IL from [C_8mim][Cl] **33** (1-octyl-3-methyl imidazolium chloride) to [C_8mim][PF_6] **34** (1-octyl-3-methylimidazolium hexafluorophosphate) was carried out in situ enabling phase separation and bioactive ingredients isolation from the IL (Fig. 6.5).

6.3.2 Extraction of bioactive natural products through microwave-assisted ionic liquid approach

ILs are promising microwave absorbers and this property has been utilized to assist the biomass dissolution in ILs, for instance, with the extraction or dissolution of chitin from crustacean shells [78] and cellulose from raw lignocellulosic biomass [25]. Therefore, microwave-assisted ionic liquid (MAIL) approaches have become famous among scientists developing natural ingredients extraction. Mostly, simple ILs are investigated, for example, [C_4mim][BF_4] **1**, [C_4mim][Br] **32**, [Amim][BF_4] **35**, [C_{10}mim][BF_4] **36** (1-decyl-3-methylimidazolium tetrafluoroborate), and these work quite well (Fig. 6.5) [79–81]. For instance, Wang and coworkers disclosed extraction of quercetin (natural flavonoid) from *Toona sinensis*, frequently known as Chinese Cedar or Chinese Mahogany, a deciduous tree found in woodland habitats [79]. Furthermore, Yuan et al. described extraction of extraction of rutin from *Flos Sophorae* and *Saururus chinensis* (Lour.) Bail. (*S. chinensis*) [81], and extraction of podophyllotoxin from *Diphylleia sinensis*, *Sinopodophyllum hexandrum*, and *Dysosma versipellis* [80]. As published by the authors, the main benefit of employing MAIL is the shorter time of the extraction course accompanied by the very large rates of recovery of the natural ingredients.

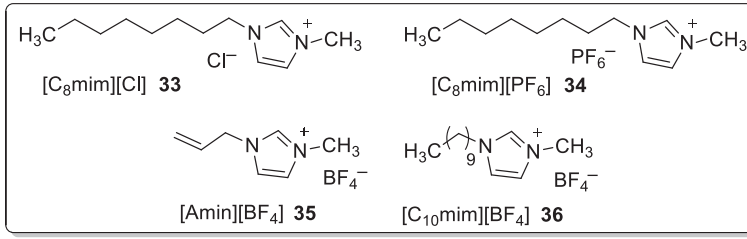

Fig. 6.5 Structure of [C_8mim][Cl], [C_8mim][PF_6], [Amim][BF_4], and [C_{10}mim][BF_4].

6.3.3 IL strategy for the reactive dissolution of biomass to extract natural ingredients

Recently, there has been growing attention in the employment of IL-mediated strategies for the environmentally benign and cost-effective reactive dissolution of biomass and extraction of valuable natural bioactive ingredients from biomass. The capability of ILs to dissolve or swell biomass can lead to a better access to the important natural ingredients from crude biomass. Bica and coworkers described the formation of an approach for the reactive dissolution of star anise seeds using Brønsted acidic ILs (**37**–**43**) (Fig. 6.6), where the IL serves as catalyst and solvent for the development of ethyl shikimate **44** and for the in situ development of ester ketal **45**. Both compounds (**44** and **45**) are important precursors in the formation of the antiviral agent Tamilut [82].

Ressmann et al. published the application of ILs such as [C_2mim][OAc] **46** (1-ethyl-3-methylimidazolium acetate) for extracting bioactive natural ingredient

botulin from birchbark with very high purity and extraction yield. Also, the recovery of the [C_2mim][OAc] **46** through azeotropic distillation of ethanol-water suggested that this extraction technique could be successfully employed at large scale (Fig. 6.6) [83]. Similarly, [C_4mim][Cl] **47** (1-Bbutyl-3-methyl-1*H*-imidazol-3-ium chloride) was utilized in microwave-assisted pretreatment of crude biomass in order to break cell walls of *Pycnostelma paniculatum* before extraction of phenol by using media such as ethanol, methanol, and water [84].

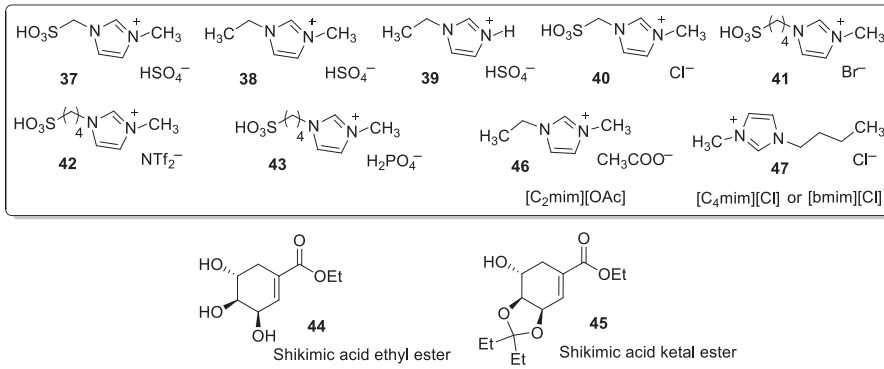

Fig. 6.6 Structure of Brønsted acidic ILs, [C_2mim][OAc], [C_4mim][Cl], and shikimic acid derivatives.

MacFarlane and coworkers reported the utility of the IL *N*-methylmethanamine dimethylcarbamate **48** (DIMCARB) for extracting tannins from plant materials, for example, myrobolan (*Terminalia chebula*) and catechu (*Acacia catechu*) [85]. Upon hydrolysis, these tannins are a rich natural source of a range of bioactive ingredients, for instance, catechin **49** and ellagic acid **50**. The DIMCARB **48** employed belongs to the protic family of ILs that is "distillable." This particular IL **48** is produced by combining dimethylamine and carbon dioxide in an approximately 2:1 ratio. As illustrated in Fig. 6.7, a two-step proton transfer occurs to develop the dimethylcarbamate cation and the dimethyl ammonium anion (DIMCARB).

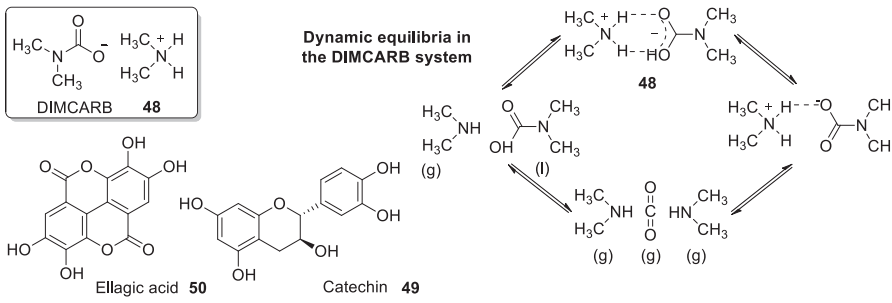

Fig. 6.7 Structure of DIMCARB and pharmaceutically active compounds.

6.4 ILs in the detection of pharmaceutically active compounds

On account of their flexible and unique properties, ILs find employment in diverse range of areas, along with those associated with chemical analysis. ILs are used in mass spectrometry (MS) [86–89], NMR [90–92], fluorescence, Raman, IR and ultraviolet (UV)-visible spectroscopy [85, 86], liquid and gas chromatography (LG and GC) [86, 87, 93, 94], extraction [87, 95, 96], electrophoresis [86, 87, 97], and numerous probe systems [98–100]. Recently, some excellent reviews have been documented on the subject [86, 87, 101]. Hence, in this part, we will highlight only important examples, which are related with utility of ILs in the analysis of pharmaceutical and natural compounds.

In one of the primary research efforts on the utility of ILs in analytical chemistry, imidazolium-based IL was pained onto the internal surface of a fused-silica capillary to afford imidazolium IL-coated capillary **51**. This IL-coated capillary **51** was employed for the analysis of sildenafil **52** in the blood serum of human via capillary zone electrophoresis (CZE) coupled to ion-trap (IT) MS (Fig. 6.8). The IL-coated capillary **51** offered precluded absorption of the compounds on the wall of fused-silica capillary and delivered enhanced resolution [97]. Application of imidazolium-mediated ILs (**1**, **4**, [EMIM][PF_6] **53** and [HMIM][BF_4] **54**) as additives of mobile phase in the reversed-phase high-performance liquid chromatography (RP-HPLC) improved isolation of common bioactive ingredients through resolving the problem of broad chromatographic bands, which appeared through interactions of the free silanol groups (–SiOH) of the reverse phase with positively charged drugs [102, 103]. In addition, the application of optically active ILs (**55** and **56**) as electrolyte additives during electrophoresis enabled isolating enantiomers of several bioactive compounds [104–106]. Likewise, in capillary electrophoresis (CE), an IL-bonded β-cyclodextrin **57** was effectively employed as chiral selector to separate many drugs [107]. A fluorescence method mediated on interactions of optically active IL **55** with enantiomers was disclosed for forming enantiomeric composition of biologically active compounds (Fig. 6.8) [108].

The IL-mediated microextraction coupled to CE was used for the analysis of analytes in biological fluids and delivered up to 1000 times sensitivity improvement [108]. Microextraction combined with MS and GC was disclosed for the detection of cancer biomarkers (CB) in samples of urea. This approach was fully automatic and permitted high-throughput detection [108]. In a similar fashion, for determination of the proportions of the drugs benznidazole **58** and nifurtimox **59** in the plasma, the IL-mediated microextraction coupled with LC was established. This technique required low quantities of sample and demonstrated very low limits of detection (LODs) (Fig. 6.9) [64].

Among other analytical techniques, MS and NMR are extremely needed [90–92]. Therefore, UV-light absorbing IL-mediated matrices (**60–63**) were successfully employed in matrix-assisted desorption/ionization MS (MALDI-MS) for sensing microbial toxins without preliminary purification and separation (Fig. 6.9) [109].

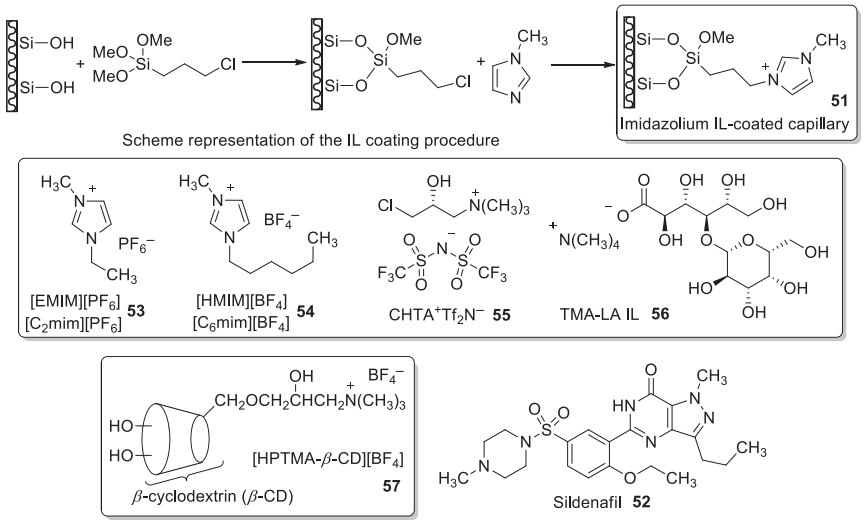

Fig. 6.8 Structure of imidazolium IL-coated capillary, imidazolium-based ILs, chiral ILs, IL-functionalized β-dextrin, and sildenafil.

As in several other industrial and scientific fields, the tunable nature of ILs has earned them a significant position in the area of electrochemical sensors. ILs are characterized by excellency electrochemical stability and broad electrochemical windows, which make them outstanding electrolytes [64]. Nonetheless, property of ionic conduction of ILs fully relies on their viscosity and chemical structure; therefore, imidazolium-based ILs show greater conductivity as compared to tetraalkylammonium or pyrrolidinium ones. Nevertheless, ILs are widely used in numerous electrochemical sensors, which are mediated on carbon paste, graphene, metal nanomaterial, carbon nanotubes (CNTs), and other materials [98, 100, 101].

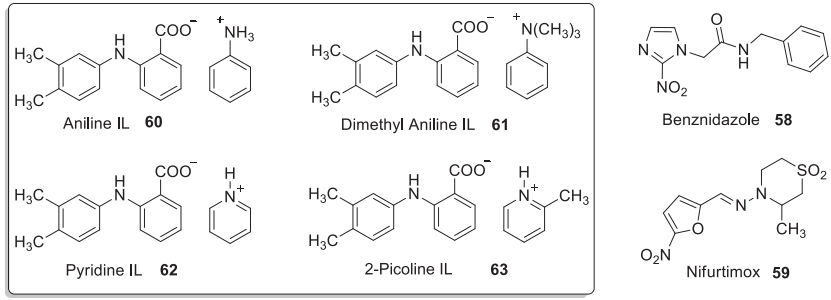

Fig. 6.9 Structure of IL-based matrices, benznidazole, and nifurtimox.

6.5 ILs for pharmaceutical crystallization

In the crystallization field, crystallization of active pharmaceutical ingredients (APIs) from traditional organic solvents can change its crystal habit and can produce crystals with poor physical properties which result into downstream processing problems. From the recent few research reports about the role of ILs in crystallization, it has been found that ILs provide promising results in the field of pharmaceutical crystallization. This section provides an overview of application of ILs in pharmaceutical crystallization.

In the recent years, investigations focusing on the utilization of ILs for designing polymorphs of the API, *bis*-POM PMEA **64**, in drowning-out crystallization have been disclosed [110, 111]. The IL 1-allyl-3-ethyl-1*H*-imidazol-3-ium tetrafluoroborate **65** ([aeim][BF_4]) was displayed to have the capability to separate new polymorphs of *bis*-POM PMEA **64** [111], which could not be separated through traditional organic solvents (Fig. 6.10). On account of the effect of [aeim][BF_4] **65** on the development of the intermolecular interactions of *bis*-POM PMEA **64** in solution, new hemihydrate and anhydrous crystals of **64** were formed when varying the crystallization temperature and proportion of IL. At a higher crystallization temperature (above 85°C) and a higher proportion of IL (above 50 vol%) in the mixture of water-[aeim][BF_4] **65**, a new anhydrous polymorph was crystallized. Whereas, at crystallization temperature of 80°C and above 50 vol% proportion of IL, a new hemihydrate crystal was crystallized. The conventional polymorph was produced at temperatures below 70°C in the same water-[aeim][BF_4] **65** mixture (50/50 vol%) [110].

In a similar fashion, purification of numerous APIs through cooling crystallization was reported using the nonviscous and thermally stable IL, 1-ethyl-3-methyl-1*H*-imidazolium bis(trifluoromethansulfonyl)imide **66** ([C_2mim][NTf_2]), consisting of relatively inert ions (Fig. 6.10) [112]. This IL was selected due to its low reactivity, thermal stability, miscibility with organic solvents of moderate polarity, and the capability to dissolve most APIs. When the IL **66** was evaluated for the purification of etomidate, naproxen, salicylic acids, acetylsalicylic, griseofulvin, itraconazole, fenofibrate, 4′-chloroacetanilide, 4-nitrophenol, 4-aminophenol, and acetaminophen, the results in all cases suggested that the purity of the crystallized products was equivalent to or even better than that of products achieved from other methods (such as antisolvent crystallization).

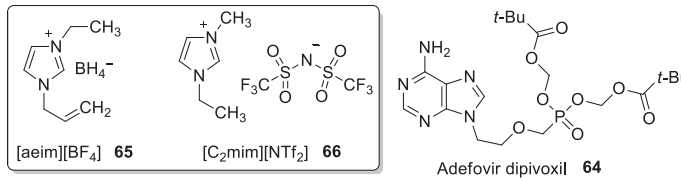

Fig. 6.10 Structure of [aeim][BF_4], [C_2mim][NTf_2], and adefovir dipivoxil.

6.6 ILs in pharmaceutical purification and separation

This section provides a detail description of the role of ILs in purification and separation of pharmaceutical substances.

6.6.1 Continuous pharmaceutical manufacturing using ILs

Currently, in order to improve efficiencies and reduce costs during manufacturing processes, pharmaceutical industries are considering continuous processing production. One of the key issues to address in a continuous process is the purification and separation of both water-insoluble and water-soluble reaction components. In order to achieve this target, ILs are appropriate chemicals because they have capability to dissolve numerous types of moieties (inorganic and organic, hydrophilic and hydrophobic, and nonpolar and polar), as well as have low toxicity, negligible volatility as compared to volatile organic compounds (VOCs) and high thermal stability [110].

In a recent publication, techniques mediated on successive two-phase systems made of ILs were disclosed for the isolation of required water-insoluble amide (precursor for aliskiren **67**) from the complex reaction mixtures obtained during the preparation (Fig. 6.11). These complex reaction mixtures involved not only the precursor imide itself but also the expensive reagents (e.g., water-soluble 2-ethylhexanoic acid and 3-amino-2,2-dimethylpropanamide and a water-insoluble lactone) [113]. Although the conventional methodology using the hydrophobic IL $[C_2mim][NTf_2]$ **66** coupled with chloroform and water enabled the partial separation of the entities, using the hydrophilic IL $[C_2mim][OAc]$ **46** enabled for the dissolution of all entities and then extremely effective stepwise isolation and purification. The additional benefit of a hydrophilic IL **46** was its easy recovery and recyclability by washing with distill H_2O, whereas in the case of hydrophobic IL, it was very challenging to fully recover the IL after the separation process [113].

Systems (e.g., **68** and **69**) bearing three or more than three ions can also be formed by "mixing" two or more than two ILs (Fig. 6.11). The ionic associations observed in the individual ILs are vanished and the "original" ILs can no longer be recognized when two ILs are mixed. However, in these systems, unexpected variations of solvating, spectroscopic, or physicochemical properties compared to the original ILs are frequently noticed and new separations can be accomplished mediated on new ion interactions [113]. Similar to crystalline double salts, these systems might be called new compounds instead of mixtures and, therefore, the concept "double salt ionic liquids" (DSILs) has been disclosed.

Mixings of two fully miscible ILs in a well-defined molar range permit the fine-tuning of properties of DSIL. For instance, it was possible to adjust the capability of the system to solubilize acidic vs basic pharmaceuticals with the adjustment of the hydrogen bond accepting capability (basicity) of the DSILs synthesized by combining $[C_2mim][OAc]$ **46** and $[C_2mim][NTf_2]$ **66**, namely $[C_2mim][OAc]_x[NTf_2]_{(1-x)}$ [26, 114]. DSILs bearing the $[P_{66614}]^+$ cation, $[C_2mim]_x[P_{66614}]_{(1-x)}[NTf_2]$, and $[C_4mim]_x[P_{66614}]_{(1-x)}[NTf_2]$ were utilized to tune the solubility of nonpolar, more

lipophilic solutes in the solution [115, 116]. DSIL systems were also employed in an aqueous system to enhance the solubility in H_2O of the bioactive agent albendazolum [117].

An enhancement in solubility of albendazolum was noticed in systems synthesized with H_2O/[C_4mim][PF_6] **4**/[C_6mim][Cl] **70**, H_2O/[C_4mim][PF_6] **4**/[C_6mim][BF_4] **54**, or H_2O/[C_4mim][PF_6] **4**/[C_4mim][BF_4] **1** at 1:1:1 M ratio, and the solubilities of the albendazolum were observed to be 7.95, 4.75, and 1.17 mmol/L, respectively, compared to its solubility in H_2O of 0.002 mmol/L (Fig. 6.11). Undoubtedly, there will be other separations and purifications where the application of the "DSIL approach" will be considered advantageous [110].

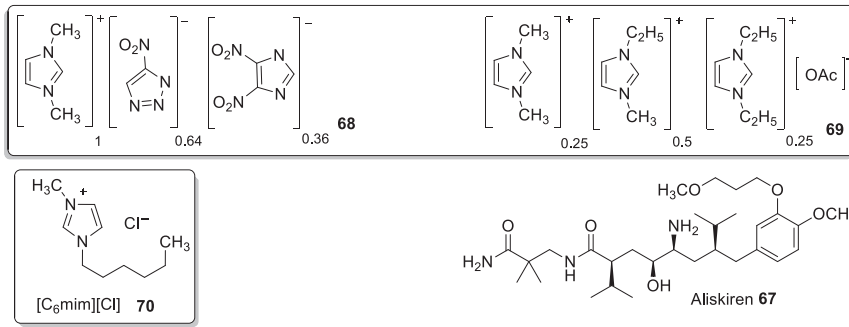

Fig. 6.11 Structure of double salt ionic liquids, [C_6mim][Cl] and aliskiren.

6.6.2 Chromatographic purifications using ILs

In analytical techniques, ILs have been employed as additives for mobile phase, where they serve as dissociated salts [118–121], as silanol blocking agents in RP LC [122–126], as stationary phases in GC [26], and as chiral selectors in micellar electrokinetic chromatography (MEKC) [127]. ILs have the promising property that both anion and cation are capable to interact with the stationary phase, which give them a dual character [127], meaning that both anion and cation can be adsorbed on the surface of stationary phase and result in the formation of promising interactions with the cationic basic drugs and anionic free silanols. This feature has received concentration for the employment of ILs for the separation of bioactive compounds.

The optical isomers of five profen agents—ketoprofen **71**, suprofen **72**, indoprofen **73**, fenoprofen **74**, and ibuprofen **75**—were separated simultaneously by MEKC, together with the use of heptakis(2,3,6-tri-*O*-methyl)-*β*-cyclodextrin **76** and the optically active cationic IL, L-UCLB **77**, which developed micelles in aqueous buffer solutions (Fig. 6.12) [127]. Enantio-separations of these bioactive compounds were enhanced by modifying the alkyl chain length and proportion of the IL surfactant by using a standard recipe bearing 5 mM sodium acetate and 35 mM TM-*β*-CD at pH 5. The batch-to-batch reproducibility of **77** was investigated and observed to have no important impact in terms of migration time, efficiency, and enantiomeric

resolution. This technique was also efficiently used for the quantitative analysis of ibuprofen **8** in pharmaceutical capsules.

A preparative high-speed countercurrent chromatography (HSCCC) for separation of mangiferin **78** and neomangiferin **79** from *Anemarrhena asphodeloides* Bge. was efficiently accomplished by using EtOAc-H_2O-[C_4mim][PF_6] **4** (25,25,1 *v*/v/v) as a biphasic solvent system [122]. From the crude extract of 150 mg, 70.6 mg of mangiferin **78** and 22.5 mg of neomangiferin **79** could be obtained (Fig. 6.12). The purity levels of mangiferin **78** and neomangiferin **79** were 98.1% and 97.2%, respectively, as evaluated through HPLC.

A technique for the detection of antidepressants in samples of urine was published using solid-phase microextraction (SPME) and high-performance liquid chromatography-ultraviolet (HPLC-UV) determination [123]. Homemade cartridges bearing 30 mg multiwalled carbon nanotubes (MWCNTs) were used for separation of the drugs from the samples, also enabling the preconcentration of the samples prior to the HPLC-UV determination. Chromatographic isolation and purification was accomplished in a C_8 RP analytical column using [C_4mim][BF_4] **1** as silanol affinity suppressor, which improved chromatographic resolution and peak symmetry. LODs were 90.1 ng/mL for fluoxetine **80** and 12.3 ng/mL for trazodone **81**. The repeatability of the disclosed technique varied between 5.0% (mianserine **82** and desipramine **83**) and 3.4% (fluoxetine **80**), indicating that this approach is appropriate for the therapeutic detecting of antidepressants in samples of urine (Fig. 6.12) [110].

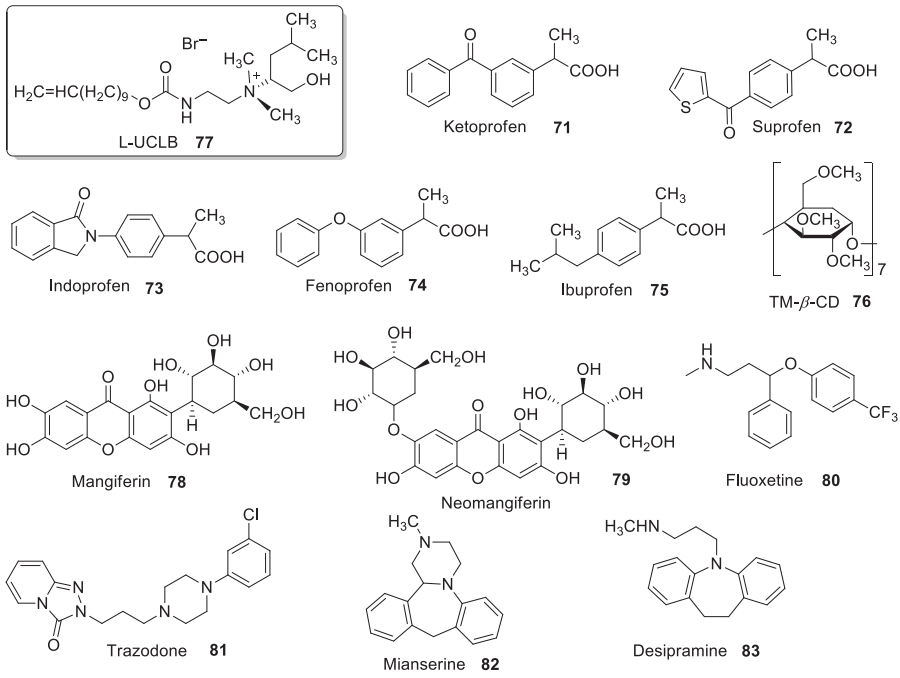

Fig. 6.12 Structure of L-UCLB and bioactive compounds.

For detection of the main opium alkaloids in pericarpium papaveris, a [C_4mim][Cl] **47**/salt aqueous biphasic approach, combined with HPLC, was documented as a effective, rapid, and simple pretreatment procedure [124]. To optimize the isolation conditions, the partitioning of papaverine **84** and codeine **85** was studied (Fig. 6.13). Several parameters were systematically taken into account, and the results suggested that both the salting-out capability of the salt and the pH value had a significant effect on phase separation. From aqueous samples of pericarpium papaveris, the recoveries of papaverine **84** and codeine **85** were 99.3%–102.0% and 90.0%–100.2%, respectively.

An effective, novel, and simple HPLC-based technique for isolation of ephedrine derivatives was accomplished by employing [C_4mim][BF_4] **1** as the mobile phase at pH 3 [118]. Again, the mechanism may be attributed to that the imidazolium ions can efficiently shield the silanol moieties of alkyl silica surface, thus reducing band tailing and enhancing the isolation efficiency.

Ionogenic (able of forming ion(s), particularly in aqueous solution) basic components belonging to the phenothiazine analogs were investigated in a RP HPLC, and the isolation yield was improved by the introduction of three ILs, [C_4mim][PF_6] **4**, [C_4mim][Cl] **47**, and [C_2mim][PF_6] **53** [119]. The influences of the amount and nature of IL on the analytes' efficiency, peak symmetry, and retention were also studied. The enhancement of system efficiency and rise of the analytes' retention factor followed the order: **4** > **53** > **47**.

An HPLC-mediated technique was reported for the separation and purification of five important medicines, by varying the proportion of the anions, pH, and IL [120]. Ketoprofen **86**, omeprazole **87**, propranolol **88**, bisoprolol **89**, and metoprolol **90** were efficiently separated and purified, using C_{18} HPLC column using a mixture of water and methanol (40:60 *v*/v), which contained 5 mmol/L IL as the eluent (Fig. 6.13). The application of IL reduces the retention time (RT) of acidic analytes and can, therefore, act as a promising mobile-phase additive in HPLC.

A detailed inquiry of the performance of four imidazolium-mediated ILs, [C_6mim][BF_4] **54**, [C_4mim][BF_4] **1**, [C_4mim][PF_6] **4**, and [C_2mim][PF_6] **53**, and their role as chromatographic modifiers for a group of β-adrenergic blocking agents was studied [102]. The ILs differed in the adsorption ability of the anion and cation on C_{18} HPLC columns. Eluent without additive and those bearing an anionic (sodium lauryl sulfate (SLS)) or cationic (triethylamine (TEA)) additive were employed as references for the evaluation of the system behavior. The association constants between additive in the mobile phase or modified stationary phase and solutes was investigated. Moreover, the silanol-suppressing potency of the additives was also examined. The investigations revealed that the IL [C_6mim][BF_4] **54** and SDS were the finest enhancers of chromatographic peak shape among those tested [110].

Residual solvents in pharmaceuticals are VOCs employed or created during the manufacture of pharmaceutical additives and drugs. Residual solvents in pharmaceuticals are usually known as organic volatile impurities (OVIs). In order to analyze the OVIs, ILs bring novel and valuable opportunities [39, 128]. The IL [C_4mim][PF_6] **4** was utilized as an alternative solvent to evaluate OVIs in pharmaceutical

additives and drugs by using headspace-gas chromatography–mass spectrometry (HS-GC-MS) analysis [128]. The technique was employed for the determination of dioxane, trichloromethane, and dichloromethane in finasteride **91** (Fig. 6.13). The LODs of dioxane, trichloromethane, and dichloromethane were 0.50, 0.02, and 0.2 ng, respectively, with RSDs lower than 4.6%. The results also demonstrated that the sensitivity of dichloromethane, trichloromethane, and dioxane achieved by $[C_4mim][PF_6]$ **4** HS-GC-MS technique is almost fivefold greater than achieved by the DMF-based HS-GC-MS method. The recoveries for dioxane, trichloromethane, and dichloromethane were in the range of 90.5%–112%.

In a another example, in order to study the OVIs in pharmaceutical synthesis with static HS-GC, Jiang and Liu employed ILs as matrix media [39]. For the preparation of *bis*-POM PMEA **64**, six solvents—DMF, *n*-butyl ether, toluene, *N*-methyl-2-pyrrolidone (NMP), dichloromethane, and acetonitrile—were dissolved in $[C_4mim][BF_4]$ **1**. The technique of external standard was utilized for quantitative analysis. The results revealed enhanced sensitivities for the six solvents with $[C_4mim][BF_4]$ **1** as the diluent in comparison to DMSO.

3-Butyl-1-methyl-1*H*-imidazol-3-ium dimethyl phosphate **92** ($[C_4mim][DMP]$) was recognized as the finest IL solvent for HS-GC detection of residual solvents (OVIs) with negligible vapor pressure such as sulfolane, *N*-methylpyrrolidone, ethylene glycol, DMSO, and 1,2,3,4-tetrahydronaphthalene in a realistic matrix of normally utilized excipients (corn starch, guar flour, magnesium stearate, and carboxymethyl cellulose) in pharmaceutical products [129]. LODs and limits of quantifications (LOQs) were extremely low (in μg/g range) and the determination of traces of tetramethylene sulfone in tablets of drug Vantin **93** indicated that this technique is practical and advantageous (Fig. 6.13).

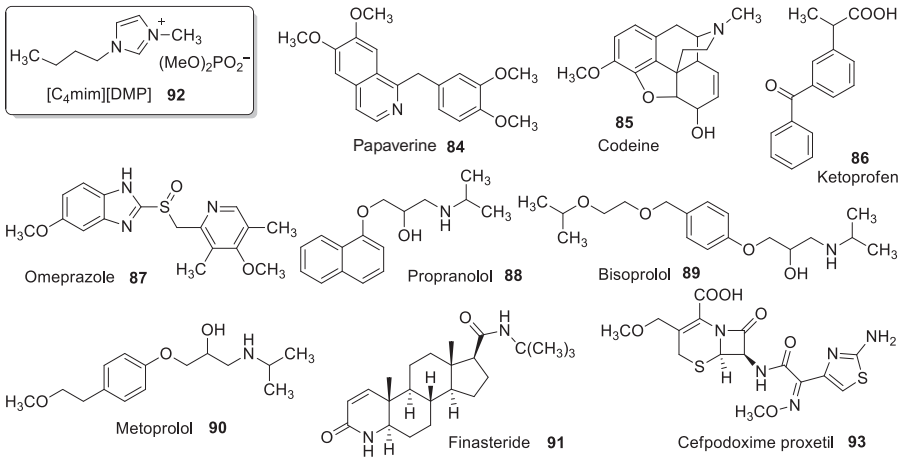

Fig. 6.13 Structure of $[C_4mim][DMP]$ and bioactive compounds.

6.7 Biological activities of ILs

In the recent years, the number of publications reporting biological activities of ILs are increasing, and this could be very interesting for the formation of new bioactive materials. In this section, we will review biological activities of ILs.

6.7.1 Antimicrobial activities of ILs

ILs contain tunable toxicity properties which may be valuable in the formation of antifouling, disinfectants, and antiseptics drugs. The antimicrobial potencies of five new series of choline-type substituted ammonium chloride ILs **94** were screened against a library of Gram-negative and Gram-positive bacteria. All the investigated ILs **94** exhibited reasonable antimicrobial affinity, and it was noticed that the lipophilicity was the chief parameter in evaluating antimicrobial affinity. Entities **94** with 12 carbon atoms alkyl chain on the cationic part of IL demonstrated the largest antimicrobial potency across all series of ILs screened, against a library of test microorganisms (Fig. 6.14) [130].

In another example, a library of 3-alkoxymethyl-1-methyl-1*H*-imidazol-3-ium ILs containing $[PF_6]^-$, $[BF_4]^-$, and $[Cl]^-$ anions **95** were screened against numerous fungi and bacterial species. The investigation showed that the smaller the length of alkyl chain on the cationic part of IL, the smaller the antimicrobial efficacy relative to the imidazolium entities **95** bearing 10, 11, and 12 carbon atoms alkyl chain in their alkoxy group. Further, the ILs **95** with alkoxy functionalities of 12 carbon atoms were the most potent against the fungi and bacteria investigated. The 1,3-(dialkloxymethyl)-functionalized imidazolium ILs **96** exhibited wide range of antimicrobial potency against several fungi, cocci, and bacterial [131]. In a similar fashion, pyridinium and imidazolium-cation ILs (**97** and **98**) with different carbon atoms alkyl chain functionalities on cation were also observed to contain appropriate antimicrobial biological profile against fungi, cocci, and rods. Similarly, it was observed that enhanced antimicrobial potency resulted from increasing the number of alkyl groups substituted as well as expanding the chain length of alkyl group on the cationic part of pyridinium and imidazolium-cation ILs (**97** and **98**) [132]. Changing the anionic part of IL did not effectively modify toxicity (Fig. 6.14). It has been noticed that the length of cationic alkyl chain substituent is responsible for antimicrobial capacity and the mechanism is via membrane disruption [133] as most of ILs have a framework comparable to cationic surfactants whose key operating principle is via disruption of protein-membrane binding. As demonstrated by the investigations of the inhibitory effects of pyridinium and imidazolium ILs (**99** and **100**), another proposed mechanism of toxicity and antimicrobial potency is the inhibition of the enzyme acetylcholinesterase, which were displayed to inhibit purified acetylcholinesterase with EC_{50} values <13 μM [134].

In a recent publication, Pernak et al. found that a library of trigeminal tricationic ILs based on pyridinium and imidazolium ring (**101** and **102**) have better antimicrobial activity as compared to the readily available benzalkonium chloride **103** [135].

Walkiewicz and coworkers have observed that the antimicrobial affinity of multifunctional long alkyl chain quaternary ammonium azolate-mediated ILs **104** demonstrated wide range promising antifungal and antibacterial efficacy, which was similar or greater to that of the original alkyldimethylbenzylammonium chloride **103** (Fig. 6.14) [136].

In another recent report, Yin and coworkers described the preparation and antimicrobial property of library of hydroxylammonium ILs **105** (Fig. 6.14). The antimicrobial potency was screened against Gram-negative and Gram-positive bacteria by using agar diffusion technique. The observed data of antimicrobial potency were compared against reference Garamycin (antibiotic). All the eight ILs **105** displayed antimicrobial affinity specifically against *Staphylococcus aureus* [137].

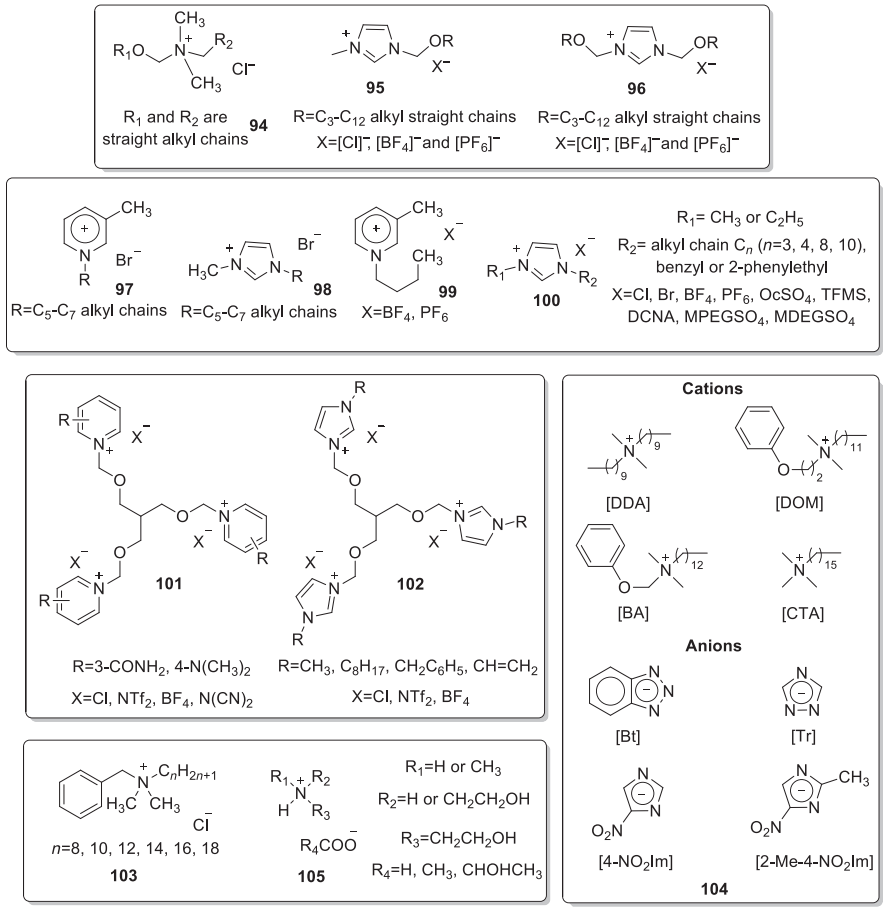

Fig. 6.14 Structure of ILs based on quaternary ammonium, pyridinium, imidazolium, and benzalkonium cations.

6.7.2 Antibiofilm activities of ILs

Gilmore and coworkers were the first to disclose the in vitro antibiofilm potency of a series of [$C_n$mim][Cl] ILs **106** against a range of clinically important bacterial and fungal pathogens (*Candida albicans*, *Chlorella regularis*, *Bacillus subtilis*, *S. aureus*, *Salmonella typhimurium,* and *Escherichia coli*) using the MBEC device [138]. The antibiofilm affinity of these ILs **106** was observed to be function of length of alkyl chain; as the length of alkyl chain was enhanced, the antibiofilm activity enhanced. ILs [$C_n$mim][Cl] **106** with $n \geq 10$ demonstrated novel, wide range antimicrobial efficacy. The compound with $n = 14$ showed greatest antibiofilm potency against all biofilms (Fig. 6.15). The result from this investigation revealed that Gram-negative bacterial biofilms were usually less susceptible to [$C_n$mim][Cl] ILs **106** relative to Gram-positive microbial, while *Candida tropicalis* biofilms displayed a comparable susceptibility data to these reagents as the representative Gram-positive organisms evaluated in this investigation [139].

Busetti et al. published the antibiofilm and antimicrobial potencies of a series of ($C_n$mquin) ILs **107** (Fig. 6.15). It was observed that ($C_n$mquin) ILs **107** have an excellent microbiological toxicity profile against both biofilm and planktonic cultures of a panel of fungi and bacteria frequently implicated in device associated and nosocomial infections [140].

These significant investigations outline the promising employments of ILs as antimicrobials in antiseptics, preservatives, disinfectants, and formation of antiinfective medical device surfaces for application in health care and as antibiofouling compounds for a host of industrial utilizations.

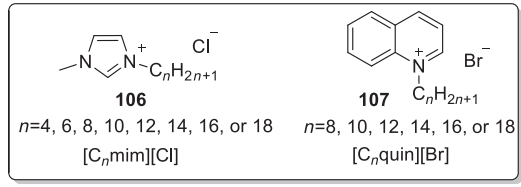

Fig. 6.15 Structure of [$C_n$mim][Cl] and [$C_n$quin][Br].

6.7.3 Antiproliferative profile of ILs

Owing to their toxicities and tunable properties, ILs could be utilized as promising antiviral, anticancer, and other therapeutic drugs. In national cancer institute, the anticancer affinity of three different kinds of ILs—ammonium **112**, phosphonium **111**, and imidazolium (**108**–**112**)—was examined among panels of human tumor cell lines (Fig. 6.16). It has been evaluated that the length of alkyl chain at N-3 location of imidazole moiety acts a vital part toward antitumor potency of ILs. The ILs (**108**–**112**) with 12 carbon atoms alkyl chain were observed to be most operative against all the 60 kinds of human tumor cell lines and described very minor cytotoxicity in nearly all cases. Further enhancement in length of alkyl chain resulted in increased growth

inhibition of human tumor cell lines. The phosphonium-mediated IL **111** were observed to be high cytotoxic relative to imidazolium (**108**–**112**) and ammonium **112** ILs [141].

In a recent study, Choi and colleagues investigated the antiproliferative potency of imidazolium and ammonium ILs (**113**–**116**) against T98G human brain cancer cells. It was noticed that the prepared ILs (**113**–**116**) were less toxic to human embryonic kidney (HEK) nonmalignant cells and more effective on T98G cancer cells. These ILs (**113**–**116**) may be served as lead compounds for a new family of cytotoxic drugs operative against T98G cells with appropriate drug delivery ability on account of their ability of chemosensitization and small size (Fig. 6.16). The IL [bmim][Cl] **115** exhibited important toxicity on T98G cells and the slightest toxicity on normal HEK cells and also inhibited the clonogenic growth of T98G cells in a concentration and time-dependent way [142].

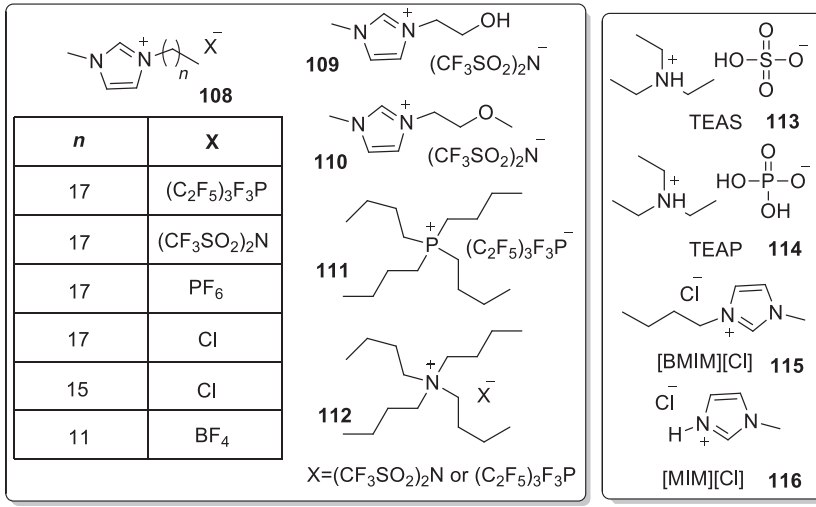

n	X
17	$(C_2F_5)_3F_3P$
17	$(CF_3SO_2)_2N$
17	PF_6
17	Cl
15	Cl
11	BF_4

Fig. 6.16 Structure of ammonium, imidazolium, and phosphonium-mediated ILs.

6.8 ILs as APIs

To date, the pharmaceutical industry's main focus is on solid dosage form such as powder form or tablets and, therefore, liquid forms are ignored on account of the cost, availability, and shelf life issue. The solid dosage form research is frequently struggling with their solubilization problems and this is the reason that drugs fail during the drug development phase. This is mostly owing to their noneffective release into the blood stream [143].

ILs with their outstanding physiochemical characteristics could bypass these delivery issues [144]. Worldwide most of the drugs are sold in salt states. Salts composed by ionic bonds which assist to keep the mixture liquid at room temperature could enhance stability, absorbability, and solubility [145]. Drug compounds transformed into salts by coupling acidic or basic drug compounds with counter ions may also address the physiochemical characteristics of the drug. The salt state of drugs may

display numerous advantages over original neutral formulations which relate to their pharmaceuticals characteristics, such as drug delivery, bioavailability and permeability, and in terms of physical characteristics, such as dissolution rate, hygroscopicity, crystallinity, and melting point. In the salt state, the counter ion plays an important part in influencing the pharmacokinetics of drug candidates. Regarding the counter ion tenability, the pharmacodynamics and toxicology profile can be modified or changed. Hence, the regulatory authorities consider the new salt form of drugs as new chemical entities which need to be registered.

From the above considerations, the physiochemical characteristics of ILs open new pathway in drug delivery and API-IL systems may have an exciting future. In the recent decade, there has been lots of research work going on in this area. This section provides an extensive summary about the role of ILs in the development of salt drugs.

In the first example, the salicylic acid **117** was transformed into a liquid salt by combining with procainium to afford procaine salicylate **118** (Scheme 6.2) [146]. The new formulation could provide the advantages of both compounds and opens new treatment options. Industry is looking for novel therapies which may are economically and clinically better than the old therapies [145].

In a another example, MacFarlane and coworkers [144] developed IL forms of the commonly used antimuscarinic agent propantheline bromide **119** in order to protect this drug from polymorphic transformation [147]. After an ion-exchange reaction to construct the acesulfamate analog, a new IL was achieved, propantheline acesulfamate **120** [148]. Similarly, in the recent years, Branco and coworkers published on the efficient formation and detection of ampicillin-mediated ILs **123** (Scheme 6.2), where the ampicillin anions **122** were coupled with several organic cations such as hexadecylpyridinium and cholinium [149, 150].

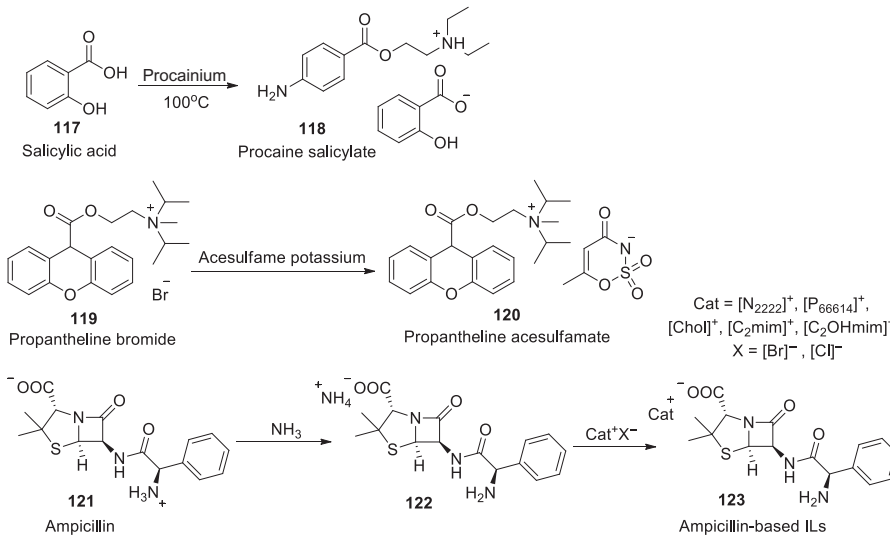

Scheme 6.2 Formation of procaine salicylate, propantheline acesulfamate, and ampicillin-based ILs.

The use of ILs in the pharmaceutical industry could offer access to painkillers that also contain antimicrobials or antibiotics [151, 152]. For instance, the painkiller aspirin (acetyl salicylate) which is usually utilized in tablet state or in solution has some issues, for example, bitter taste, poor solubility, and unpleasantly large tablets for desired dosages. A liquid salt form of aspirin could solve these problems and provide new delivery routes. Rogers and coworkers published the formation of dual functional IL types of acetyl salicylate by coupling bioactive cations [antibacterial (**124**–**128**), local anesthetics (**129**, **130**), antiarrhythmic **131**, and analgesic **132**] with anions of salicylic acid **133** and acetylsalicylic acid **134** (Fig. 6.17) [146]. The Rogers and coworkers also compared the physical characteristics of the synthetized salts with parent aspirin. With the exception of hexetidinium and tramadolium, all synthetized salicylates were observed to be of low melting. Comparison of the salicylate salts and the acetylsalicylate salts suggested an important decrease in phase transition temperatures for the acetylsalicylate salts; presumably, it is due to the absence of intra- or intermolecular hydrogen bonding in the acetylsalicylate anions.

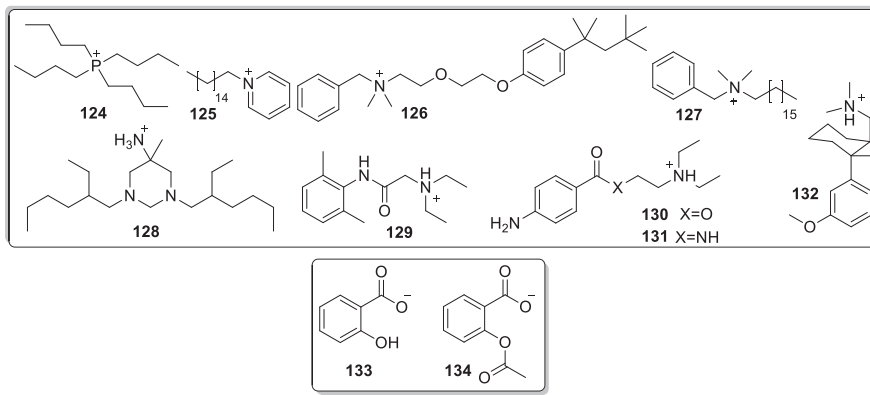

Fig. 6.17 Structure of pharmaceutically active cations and anion of salicylic acid and acetylsalicylic acid.

Recently, Restolho et al. exploited the tunability of ILs by using pharmaceutically active anions and cations, commonly designed on API. Didecyldimethylammonim ibuprofen **135** (DI), ranitidine docosate **136** (RD), and lidocaine docosate **137** (LD) were selected for their study (Fig. 6.18). They focused on the interfacial properties of **135**, **136**, and **137**, and determined the contact angles and the surface tension on both hydrophobic and hydrophilic surfaces within a wide temperature spectrum. Mediated on the wettability results, the polarity fractions were calculated. For the three IL-APIs (**135**, **136**, and **137**), liquid-liquid transition temperature occurred almost ambient temperature. Near this transition they showed abnormal behavior which was justified by the attendance of a mesophase between the vapor phase and the isotropic. The IL-APIs (**135**, **136**, and **137**) show low contact angles and low surface tension which was evaluated on both hydrophilic and hydrophobic surfaces. The

relatively low polarity fractions confirm the lesser influence of the coulomb interactions as compared to the dispersive interaction for ILs possessing larger ions [152].

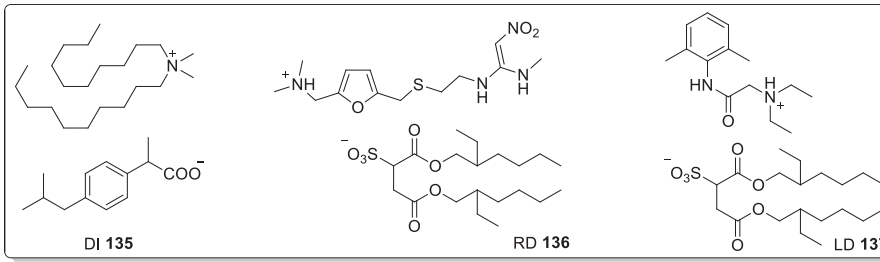

Fig. 6.18 Structure of DI, RD, and LD.

6.8.1 The oligomeric methodology: Stoichiometric to nonstoichiometric API-ILs with protic ion

Naturally, numerous bioactive ILs have been created from those protic APIs that are easily transformed into an anion or cation. Unlike aprotic ILs, protic ILs display Bronsted acidity attributed to the exchangeable protons, and therefore, their characteristics largely rely on hydrogen bonding and the extent of proton transfer ability from the acid to the base. Instances of studies on protic pharmaceutical ILs can be found in research work by MacFarlane et al., which reported the preparation of novel protic ILs, for example, 2-pyrrolidinoethanol, amantadine, and tuaminoheptane [153], and demonstrated the first membrane transport characteristics of prepared protonated ILs [154].

Noteworthy, the insertion of excess base or excess protic acid to a salt can result in the liquefaction of low melting salts via the development of oligomeric ions with complex hydrogen bonds (i.e., strong composites among ionized and unionized species) [155]. This "oligomeric methodology" was introduced by Rogers, Bica, and coworkers [156] as both a liquefaction approach (lowering melting points to room temperatures or below body) and a approach to enable the two bioactive ions to be dosed at different ratios. This is illustrated in Scheme 6.3 with salicylic acid **117** and lidocaine **138** [157].

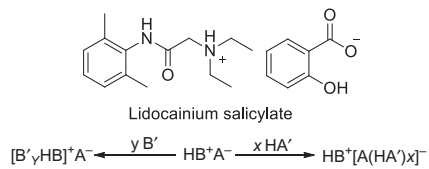

Scheme 6.3 Illustration of oligomeric methodology.

Noteworthy, when preparing protic ILs, that just because a liquid is formed when a base or acid is combined (even when both starting compounds are solid), does not

necessarily indicate that a salt has been developed. In the development of various compositions of lignocaine **138** with fatty acids, thermal and spectroscopic data confirmed the preparation of deep eutectic components which usually exist at the boundary level among partially ionized salts and simple mixtures. By varying the molar composition of the fatty acids or lignocaine **138**, single fraction mixtures of low melting point were achieved. For instance, the union of lignocaine **138** with oleic or decanoic acids (**140** and **130**) results in the formation of liquids which only demonstrated glass transition temperatures below 40°C (Fig. 6.19) [156]. The deep eutectic character was due to the formation of very powerful hydrogen bonding among acid and lignocaine **138**. These are comparable to the kinds of interaction forces being utilized to design cocrystals of APIs and, therefore, the terminology "liquid cocrystal" was utilized [156, 158, 159].

Another remarkable methodology to liquidity in API-ILs was introduced by Sesto and coworkers [160], where it was possible to achieve liquid forms by coupling zinc chloride with cationic pharmaceutical Lewis acids. The melting points of the parent pharmaceutical chloride salt could be depressed attributed to the oligomeric forms of $ZnCl_2$ anions. The group of Sesto synthesized a library of new API-ILs mediated on ranitidine **141**, ethambutol **142**, and homatropine **143** (Fig. 6.19). Furthermore, it was exposed that metal halide-mediated API-ILs frequently contain good shelf life.

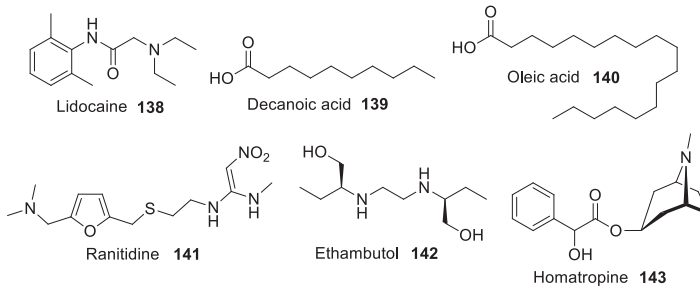

Fig. 6.19 Structure of lidocaine, decanoic acid, oleic acid, ranitidine, ethambutol, and homatropine.

6.8.2 Prodrug methodology

The API-IL methodology explained above desired that the API be ionizable, but numerous APIs are not readily ionizable. An efficient method to resolve this issue and to improve the bioavailability, permeability, and solubility of APIs is by combining them with prodrugs. Prodrug ILs offer additional benefits, for example, controlled discharge of the APIs in simulated fluids. This provides a significant scheme to enhance the characteristics of APIs. Cojocaru et al. confirmed this by preparation and utilization of API-ILs [161]. In the formation route of API-ILs, acetaminophen **144** (acetam) was initially converted to 4-(acetylamino)phenylchloroacetate **146** and subsequent treatment with a neutral amines to provide the chloride salts (**147**, **148**, **149**, and **150**). The chlorides (**147**, **148**, **149**, and **150**) were exchanged for the

docusate anions, lead toward the development of an API-ILs (**151**, **152**, **153**, and **154**). These salts (**151**, **152**, **153**, and **154**) could be readily hydrolyzed, resulting in **144** (Scheme 6.4).

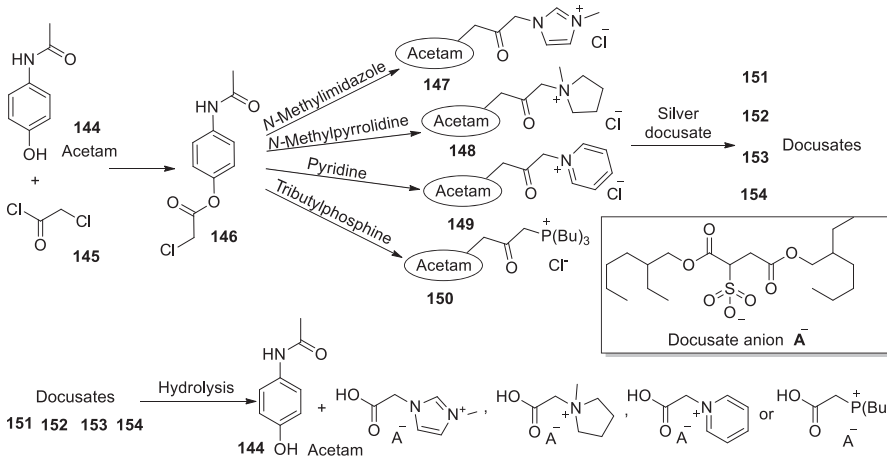

Scheme 6.4 Formation and hydrolysis of API-ILs.

6.9 Conclusion

Because of promising properties of ILs as well as the increasing ecological awareness and enormous anxieties of "green chemistry," use of ILs has received wide attention in multidisciplinary studies, especially in the field of pharmaceutics and medicine. From 1996 to 2019, research reports on the synthesis and utilization of ILs have grown at an astounding rate. To date, most literature of pharmaceutical ILs has focused on imidazolium-mediated ILs. The reason why imidazole-based ILs are among the most studied ILs is due to their lower viscosity and to the stability of the imidazolium cation in oxidative and reductive conditions. Hence, they have been used for several applications, such as solvents and catalysts in synthesis and as solubility enhancers in DDS. In terms of their use as solubility promoters, their cytotoxicity may represent a drawback, particularly for those ILs with a long alkyl chain attached to the imidazolium cations and this must always be considered. Summarily, ILs display control of ions development in solution and alteration of solvation characteristics in biological fluids and water to deliver a flexible method for alleviation of polymorphism, bioavailability, and solubility limitations of traditional drugs. Moreover, ILs have become "green alternates" of the VOS. Because of their unique properties, ILs have a great potential as reaction media in a broad spectrum of biocatalytic and conventional syntheses. The reaction yields with the use of ILs are mostly similar or higher than those achieved in traditional organic solvents. Hence, it is a cost-efficient and straightforward technique to produce highly tunable, diverse range of bioactive drugs with an almost limitless number of combinations of cations and anions. However, the current expenses of the

ILs are somewhat prohibitive in several feasible commercial applications. Hopefully, in the near future, the benefit/cost figures of the ILs will bring financial viability to their more common application. Naturally, further investigations must be performed in order to discover the full potential of their biomedical uses.

References

[1] P.T. Anastas, M.M. Kirchhoff, Origins, current status, and future challenges of green chemistry, Acc. Chem. Res. 35 (2002) 686–694.
[2] P.T. Anastas, J.C. Warner, Green Chemistry: Theory and Practice, Oxford University Press, Oxford, 2000.
[3] P.T. Anastas, T.C. Williamson, Green Chemistry: Frontiers in Benign Chemical Syntheses and Processes, Oxford University Press, New York, NY, 1998.
[4] P. Klumphu, Development of New Methodology in Organic Synthesis Enabled by Aqueous Micellar Catalysis, UC Santa Barbara, 2016. ProQuest ID: Klumphu_ucsb_0035D_13279. Merritt ID: ark:/13030/m5fc01sx. Retrieved from https://escholarship.org/uc/item/5480h1pm.
[5] F.M. Kerton, R. Marriott, Alternative Solvents for Green Chemistry, Royal Society of Chemistry, 2013.
[6] E. Buncel, R.A. Stairs, H. Wilson, The Role of the Solvent in Chemical Reactions, Oxford University Press, Oxford, 2003.
[7] J.M. DeSimone, Practical approaches to green solvents, Science 297 (2002) 799–803.
[8] J. Fraga-Dubreuil, G. Çomak, A.W. Taylor, M. Poliakoff, Rapid and clean synthesis of phthalimide derivatives in high-temperature, high-pressure H2O/EtOH mixtures, Green Chem. 9 (2007) 1067–1072.
[9] N.D. Gullickson, J.F. Scamehorn, J.H. Harwell, Liquid-coacervate extraction, in: Surfactant Based Separation Process, CRC Press, 1989, pp. 139–152.
[10] T. Welton, Room-temperature ionic liquids. Solvents for synthesis and catalysis, Chem. Rev. 99 (1999) 2071–2084.
[11] J.P. Hallett, T. Welton, Room-temperature ionic liquids: solvents for synthesis and catalysis. 2, Chem. Rev. 111 (2011) 3508–3576.
[12] N.V. Plechkova, K.R. Seddon, Applications of ionic liquids in the chemical industry, Chem. Soc. Rev. 37 (2008) 123–150.
[13] J. Flieger, E.B. Grushka, A. Czajkowska-Zelazko, Ionic liquids as solvents in separation processes, Austin J. Anal. Pharm. Chem. 1 (2014) 1–8.
[14] I. Rodríguez Palmeiro, Applications of Surface Active Ionic Liquids, Minerva, Repositorio institucional da USC, 2016.
[15] K.R. Seddon, Ionic liquids: designer solvents, in: The International George Papatheodorou Symposium: Proceedings. Institute of Chemical Engineering and High Temperature Chemical Processes …, 1999, pp. 131–135.
[16] P. Wasserscheid, T. Welton, Ionic Liquids in Synthesis, John Wiley & Sons, 2008.
[17] K.N. Marsh, J.A. Boxall, R. Lichtenthaler, Room temperature ionic liquids and their mixtures—a review, Fluid Phase Equilib. 219 (2004) 93–98.
[18] V.I. Pârvulescu, C. Hardacre, Catalysis in ionic liquids, Chem. Rev. 107 (2007) 2615–2665.
[19] T.L. Greaves, C.J. Drummond, Protic ionic liquids: properties and applications, Chem. Rev. 108 (2008) 206–237.

[20] C. Chiappe, D. Pieraccini, Ionic liquids: solvent properties and organic reactivity, J. Phys. Org. Chem. 18 (2005) 275–297.
[21] R. Sheldon, Catalytic reactions in ionic liquids, Chem. Commun. (2001) 2399–2407.
[22] C.M. Gordon, New developments in catalysis using ionic liquids, Appl. Catal. A Gen. 222 (2001) 101–117.
[23] M.J. Earle, K.R. Seddon, Ionic liquids. Green solvents for the future, Pure Appl. Chem. 72 (2000) 1391–1398.
[24] J. Dupont, G.S. Fonseca, A.P. Umpierre, et al., Transition-metal nanoparticles in imidazolium ionic liquids: recycable catalysts for biphasic hydrogenation reactions, J. Am. Chem. Soc. 124 (2002) 4228–4229.
[25] R.P. Swatloski, S.K. Spear, J.D. Holbrey, R.D. Rogers, Dissolution of cellose with ionic liquids, J. Am. Chem. Soc. 124 (2002) 4974–4975.
[26] D.W. Armstrong, L. He, Y.-S. Liu, Examination of ionic liquids and their interaction with molecules, when used as stationary phases in gas chromatography, Anal. Chem. 71 (1999) 3873–3876.
[27] C. DeCastro, E. Sauvage, M.H. Valkenberg, W.F. Hoelderich, Immobilised ionic liquids as Lewis acid catalysts for the alkylation of aromatic compounds with dodecene, J. Catal. 196 (2000) 86–94.
[28] K. Fukumoto, M. Yoshizawa, H. Ohno, Room temperature ionic liquids from 20 natural amino acids, J. Am. Chem. Soc. 127 (2005) 2398–2399.
[29] A.E. Visser, R.P. Swatloski, W.M. Reichert, et al., Task-specific ionic liquids for the extraction of metal ions from aqueous solutions, Chem. Commun. (2001) 135–136.
[30] O. Nacham, Synthesis of New Classes of Ionic Liquids and Their Utilization in Biological and Pharmaceutical Analysis, Graduate theses and dissertations, 2017, p. 15587. https://lib.dr.iastate.edu/etd/15587.
[31] C.E. Song, W.H. Shim, E.J. Roh, J.H. Choi, Scandium (III) triflate immobilised in ionic liquids: a novel and recyclable catalytic system for Friedel–crafts alkylation of aromatic compounds with alkenes, Chem. Commun. (2000) 1695–1696.
[32] N. Audic, H. Clavier, M. Mauduit, J.-C. Guillemin, An ionic liquid-supported ruthenium carbene complex: a robust and recyclable catalyst for ring-closing olefin metathesis in ionic liquids, J. Am. Chem. Soc. 125 (2003) 9248–9249.
[33] N. Wood, Toxicity of Ionic Liquids and Organic Solvents towards Escherichia coli and Pseudomonas putida, Doctoral dissertation, The University of Manchester, United Kingdom, 2011.
[34] A.L.G. Júlio, Ionic Liquids as Functional Ingredients in Drug Delivery Systems: Solubility, Permeation and Cytotoxicity Studies, Master's thesis, 2017.
[35] J.S. Wilkes, J.A. Levisky, R.A. Wilson, C.L. Hussey, Dialkylimidazolium chloroaluminate melts: a new class of room-temperature ionic liquids for electrochemistry, spectroscopy and synthesis, Inorg. Chem. 21 (1982) 1263–1264.
[36] X. Xiaohua, Z. Liang, L. Xia, J. Shengxiang, Ionic liquids as additives in high performance liquid chromatography: analysis of amines and the interaction mechanism of ionic liquids, Anal. Chim. Acta 519 (2004) 207–211.
[37] Q. Zhang, S. Zhang, Y. Deng, Recent advances in ionic liquid catalysis, Green Chem. 13 (2011) 2619–2637.
[38] R. Liu, J. Liu, Y. Yin, et al., Ionic liquids in sample preparation, Anal. Bioanal. Chem. 393 (2009) 871–883.
[39] F. Liu, Y. Jiang, Room temperature ionic liquid as matrix medium for the determination of residual solvents in pharmaceuticals by static headspace gas chromatography, J. Chromatogr. A 1167 (2007) 116–119.

[40] M. Earle, K. Seddon, C. Adams, Friedel–crafts reactions in room temperature ionic liquids, Chem. Commun. (1998) 2097–2098.
[41] V. Kumar, S.V. Malhotra, Synthesis of nucleoside-based antiviral drugs in ionic liquids, Bioorg. Med. Chem. Lett. 18 (2008) 5640–5642.
[42] M.L. Patil, H. Sasai, Recent developments on chiral ionic liquids: design, synthesis, and applications, Chem. Rec. 8 (2008) 98–108.
[43] M.Y. Machado, R. Dorta, Synthesis and characterization of chiral imidazolium salts, Synthesis (Stuttg) 2005 (2005) 2473–2475.
[44] H.-S. Gao, Z.-G. Hu, J.-J. Wang, et al., Synthesis and properties of novel chiral ionic liquids from L-proline, Aust. J. Chem. 61 (2008) 521–525.
[45] H. Liu, L. Peng, T. Zhang, Y. Li, L-Proline catalyzed asymmetric aldol reactions of protected hydroxyacetone, New J. Chem. 27 (2003) 1159–1160.
[46] N. RamakrishnaáReddy, S. ShameemáSultana, L-Proline catalyzed asymmetric transfer aldol reaction between diacetone alcohol and aldehydes, Chem. Commun. (2004) 2450–2451.
[47] T.P.T. Pham, C.-W. Cho, Y.-S. Yun, Environmental fate and toxicity of ionic liquids: a review, Water Res. 44 (2010) 352–372.
[48] N. Madria, Synthesis and Toxicity Studies of Imidazolium-Based Ionic Liquids, Masters theses, 2011, 5418. https://scholarsmine.mst.edu/masters_theses/5418.
[49] R.A. Sheldon, E factors, green chemistry and catalysis: an odyssey, Chem. Commun. (2008) 3352–3365.
[50] S. Platzer, Synthesis and Characterization of Novel Task-Specific Ionic Liquids for Heavy Metal Extraction, Doctoral dissertation, Universität Wien, 2016.
[51] R.V. Bansode, Functional Ionic Liquids in Crystal Engineering and Drug Delivery, Doctoral dissertation, University of Bradford, 2016.
[52] M.A.P. Martins, C.P. Frizzo, D.N. Moreira, et al., Ionic liquids in heterocyclic synthesis, Chem. Rev. 108 (2008) 2015–2050.
[53] T. Siódmiak, M. Piotr Marszall, A. Proszowska, Ionic liquids: a new strategy in pharmaceutical synthesis, Mini Rev. Org. Chem. 9 (2012) 203–208.
[54] I.M. Marrucho, L.C. Branco, L.P.N. Rebelo, Ionic liquids in pharmaceutical applications, Annu. Rev. Chem. Biomol. Eng. 5 (2014) 527–546.
[55] A.L. Monteiro, F.K. Zinn, R.F. de Souza, J. Dupont, Asymmetric hydrogenation of 2-arylacrylic acids catalyzed by immobilized Ru-BINAP complex in 1-n-butyl-3-methylimidazolium tetrafluoroborate molten salt, Tetrahedron Asymmetry 8 (1997) 177–179.
[56] M.J. Earle, P.B. McCormac, K.R. Seddon, The first high yield green route to a pharmaceutical in a room temperature ionic liquid, Green Chem. 2 (2000) 261–262.
[57] A. Deshmukh, B. Gore, H.V. Thulasiram, V.P. Swamy, Recyclable ionic liquid iodinating reagent for solvent free, regioselective iodination of activated aromatic and heteroaromatic amines, RSC Adv. 5 (2015) 88311–88315.
[58] Y. Hongwei, W. Jinchuan, C. Chi Bun, Kinetic resolution of ibuprofen catalyzed by Candida rugosa lipase in ionic liquids, Chirality 17 (2005) 16–21.
[59] X. Fan, D. Feng, Y. Qu, et al., Practical and efficient synthesis of pyrano [3, 2-c] pyridone, pyrano [4, 3-b] pyran and their hybrids with nucleoside as potential antiviral and antileishmanial agents, Bioorg. Med. Chem. Lett. 20 (2010) 809–813.
[60] X. Zhang, X. Li, D. Li, et al., Ionic liquid mediated and promoted eco-friendly preparation of thiazolidinone and pyrimidine nucleoside–thiazolidinone hybrids and their antiparasitic activities, Bioorg. Med. Chem. Lett. 19 (2009) 6280–6283.

[61] A. Kurata, Y. Kitamura, S. Irie, et al., Enzymatic synthesis of caffeic acid phenethyl ester analogues in ionic liquid, J. Biotechnol. 148 (2010) 133–138.
[62] A. Gueiffier, M. Lhassani, A. Elhakmaoui, et al., Synthesis of acyclo-C-nucleosides in the imidazo [1, 2-a] pyridine and pyrimidine series as antiviral agents, J. Med. Chem. 39 (1996) 2856–2859.
[63] A. Shaabani, E. Soleimani, A. Maleki, Ionic liquid promoted one-pot synthesis of 3-aminoimidazo [1, 2-a] pyridines, Tetrahedron Lett. 47 (2006) 3031–3034.
[64] K.S. Egorova, E.G. Gordeev, V.P. Ananikov, Biological activity of ionic liquids and their application in pharmaceutics and medicine, Chem. Rev. 117 (2017) 7132–7189.
[65] G. Subramanian, C.P.B. Rajeev, C.D. Mohan, et al., Synthesis and in vitro evaluation of hydrazinyl phthalazines against malaria parasite, plasmodium falciparum, Bioorg. Med. Chem. Lett. 26 (2016) 3300–3306.
[66] J. Ternois, F. Guillen, J.-C. Plaquevent, G. Coquerel, Asymmetric synthesis of modafinil and its derivatives by enantioselective oxidation of thioethers: comparison of various methods including synthesis in ionic liquids, Tetrahedron Asymmetry 18 (2007) 2959–2964.
[67] B. Chakraborty, C.D. Sharma, A new route to the synthesis of isoxazoline derivatives from dihydropyran via cycloaddition reaction in ionic liquid, Tetrahedron Lett. 54 (2013) 5532–5536.
[68] S. Kandar, A.K. Suresh, S.B. Noronha, (R)-PAC biosynthesis in [BMIM][PF 6]/aqueous biphasic system using Saccharomyces cerevisiae BY4741 cells, Appl. Biochem. Biotechnol. 175 (2015) 1771–1788.
[69] S. Kazemi, Á.B. Martín, D. Sordi, et al., Vanadium-catalyzed epoxidation reaction of cinnamyl alcohol in ionic liquids, Green Process. Synth. 1 (2012) 509–516.
[70] M. Singh, R.S. Singh, U.C. Banerjee, Stereoselective synthesis of (R)-1-chloro-3 (3, 4-difluorophenoxy)-2-propanol using lipases from pseudomonas aeruginosa in ionic liquid-containing system, J. Mol. Catal. B Enzym. 56 (2009) 294–299.
[71] M. Zaidlewicz, J. Cytarska, A. Dzielendziak, M. Ziegler-Borowska, Synthesis of boronated phenylalanine analogues with a quaternary center for boron neutron capture therapy, ARKIVOC 3 (2004) 11–21.
[72] J.S. Wilkes, M.J. Zaworotko, Air and water stable 1-ethyl-3-methylimidazolium based ionic liquids, J. Chem. Soc. Chem. Commun. (1992) 965–967.
[73] T. Santos de Almeida, A. Júlio, N. Saraiva, et al., Choline-versus imidazole-based ionic liquids as functional ingredients in topical delivery systems: cytotoxicity, solubility, and skin permeation studies, Drug Dev. Ind. Pharm. 43 (2017) 1858–1865.
[74] M. Smiglak, J.M. Pringle, X. Lu, et al., Ionic liquids for energy, materials, and medicine, Chem. Commun. 50 (2014) 9228–9250.
[75] B.D. Ribeiro, M.A.Z. Coelho, L.P.N. Rebelo, I.M. Marrucho, Ionic liquids as additives for extraction of saponins and polyphenols from mate (Ilex paraguariensis) and tea (Camellia sinensis), Ind. Eng. Chem. Res. 52 (2013) 12146–12153.
[76] Y. Sun, Z. Liu, J. Wang, et al., Aqueous ionic liquid based ultrasonic assisted extraction of four acetophenones from the Chinese medicinal plant Cynanchum bungei Decne, Ultrason. Sonochem. 20 (2013) 180–186.
[77] W. Bi, M. Tian, K.H. Row, Ultrasonication-assisted extraction and preconcentration of medicinal products from herb by ionic liquids, Talanta 85 (2011) 701–706.
[78] Y. Qin, X. Lu, N. Sun, R.D. Rogers, Dissolution or extraction of crustacean shells using ionic liquids to obtain high molecular weight purified chitin and direct production of chitin films and fibers, Green Chem. 12 (2010) 968–971.

[79] X. Liu, Y. Wang, J. Kong, et al., Application of ionic liquids in the microwave-assisted extraction of quercetin from Chinese herbal medicine, Anal. Methods 4 (2012) 1012–1018.
[80] Y. Yuan, Y. Wang, R. Xu, et al., Application of ionic liquids in the microwave-assisted extraction of podophyllotoxin from Chinese herbal medicine, Analyst 136 (2011) 2294–2305.
[81] H. Zeng, Y. Wang, J. Kong, et al., Ionic liquid-based microwave-assisted extraction of rutin from Chinese medicinal plants, Talanta 83 (2010) 582–590.
[82] A.K. Ressmann, P. Gaertner, K. Bica, From plant to drug: ionic liquids for the reactive dissolution of biomass, Green Chem. 13 (2011) 1442–1447.
[83] A.K. Ressmann, K. Strassl, P. Gaertner, et al., New aspects for biomass processing with ionic liquids: towards the isolation of pharmaceutically active betulin, Green Chem. 14 (2012) 940–944.
[84] R. Jin, L. Fan, X. An, Microwave assisted ionic liquid pretreatment of medicinal plants for fast solvent extraction of active ingredients, Sep. Purif. Technol. 83 (2011) 45–49.
[85] S.A. Chowdhury, R. Vijayaraghavan, D.R. MacFarlane, Distillable ionic liquid extraction of tannins from plant materials, Green Chem. 12 (2010) 1023–1028.
[86] M. Koel, Ionic liquids in chemical analysis, Crit. Rev. Anal. Chem. 35 (2005) 177–192.
[87] P. Sun, D.W. Armstrong, Ionic liquids in analytical chemistry, Anal. Chim. Acta 661 (2010) 1–16.
[88] L.L. Khemchyan, E.A. Khokhlova, M.M. Seitkalieva, V.P. Ananikov, Efficient sustainable tool for monitoring chemical reactions and structure determination in ionic liquids by ESI-MS, ChemistryOpen 2 (2013) 208–214.
[89] A. Tholey, E. Heinzle, Ionic (liquid) matrices for matrix-assisted laser desorption/ionization mass spectrometry—applications and perspectives, Anal. Bioanal. Chem. 386 (2006) 24–37.
[90] V.P. Ananikov, Characterization of molecular systems and monitoring of chemical reactions in ionic liquids by nuclear magnetic resonance spectroscopy, Chem. Rev. 111 (2010) 418–454.
[91] E.A. Khokhlova, V.V. Kachala, V.P. Ananikov, The first molecular level monitoring of carbohydrate conversion to 5-hydroxymethylfurfural in ionic liquids. B_2O_3—an efficient dual-function metal-free promoter for environmentally benign applications, ChemSusChem 5 (2012) 783–789.
[92] R. Giernoth, D. Bankmann, N. Schlörer, High performance NMR in ionic liquids, Green Chem. 7 (2005) 279–282.
[93] X. Shi, L. Qiao, G. Xu, Recent development of ionic liquid stationary phases for liquid chromatography, J. Chromatogr. A 1420 (2015) 1–15.
[94] A.A. Tietze, P. Heimer, A. Stark, D. Imhof, Ionic liquid applications in peptide chemistry: synthesis, purification and analytical characterization processes, Molecules 17 (2012) 4158–4185.
[95] C.F. Poole, S.K. Poole, Extraction of organic compounds with room temperature ionic liquids, J. Chromatogr. A 1217 (2010) 2268–2286.
[96] M.G. Freire, A.F.M. Claudio, J.M.M. Araujo, et al., Aqueous biphasic systems: a boost brought about by using ionic liquids, Chem. Soc. Rev. 41 (2012) 4966–4995.
[97] W. Qin, S.F.Y. Li, An ionic liquid coating for determination of sildenafil and UK-103,320 in human serum by capillary zone electrophoresis-ion trap mass spectrometry, Electrophoresis 23 (2002) 4110–4116.
[98] M. Opallo, A. Lesniewski, A review on electrodes modified with ionic liquids, J. Electroanal. Chem. 656 (2011) 2–16.

[99] K. Behera, S. Pandey, A. Kadyan, S. Pandey, Ionic liquid-based optical and electrochemical carbon dioxide sensors, Sensors 15 (2015) 30487–30503.
[100] A. Abo-Hamad, M.A. AlSaadi, M. Hayyan, et al., Ionic liquid-carbon nanomaterial hybrids for electrochemical sensor applications: a review, Electrochim. Acta 193 (2016) 321–343.
[101] M.J.A. Shiddiky, A.A.J. Torriero, Application of ionic liquids in electrochemical sensing systems, Biosens. Bioelectron. 26 (2011) 1775–1787.
[102] J.J. Fernández-Navarro, M.C. García-Álvarez-Coque, M.J. Ruiz-Angel, The role of the dual nature of ionic liquids in the reversed-phase liquid chromatographic separation of basic drugs, J. Chromatogr. A 1218 (2011) 398–407.
[103] J.J. Fernández-Navarro, J.R. Torres-Lapasió, M.J. Ruiz-Angel, M.C. García-Álvarez-Coque, 1-Hexyl-3-methyl imidazolium tetrafluoroborate: an efficient column enhancer for the separation of basic drugs by reversed-phase liquid chromatography, J. Chromatogr. A 1258 (2012) 168–174.
[104] M.C. Mavroudi, C.P. Kapnissi-Christodoulou, Combined use of l-alanine tert butyl ester lactate and trimethyl-β-cyclodextrin for the enantiomeric separations of 2-arylpropionic acids nonsteroidal anti-inflammatory drugs, Electrophoresis 36 (2015) 2442–2450.
[105] C.D. Tran, I. Mejac, Chiral ionic liquids for enantioseparation of pharmaceutical products by capillary electrophoresis, J. Chromatogr. A 1204 (2008) 204–209.
[106] Q. Zhang, Y. Du, S. Du, et al., Tetramethylammonium-lactobionate: a novel ionic liquid chiral selector based on saccharides in capillary electrophoresis, Electrophoresis 36 (2015) 1216–1223.
[107] J. Yu, L. Zuo, H. Liu, et al., Synthesis and application of a chiral ionic liquid functionalized β-cyclodextrin as a chiral selector in capillary electrophoresis, Biomed. Chromatogr. 27 (2013) 1027–1033.
[108] C.D. Tran, D. Oliveira, Fluorescence determination of enantiomeric composition of pharmaceuticals via use of ionic liquid that serves as both solvent and chiral selector, Anal. Biochem. 356 (2006) 51–58.
[109] H.N. Abdelhamid, M.S. Khan, H.-F. Wu, Design, characterization and applications of new ionic liquid matrices for multifunctional analysis of biomolecules: a novel strategy for pathogenic bacteria biosensing, Anal. Chim. Acta 823 (2014) 51–60.
[110] J.L. Shamshina, P. Berton, H. Wang, et al., Ionic liquids in pharmaceutical industry, in: Green Techniques for Organic Synthesis and Medicinal Chemistry, 2018, pp. 539–577.
[111] J.-H. An, J.-M. Kim, S.-M. Chang, W.-S. Kim, Application of ionic liquid to polymorphic design of pharmaceutical ingredients, Cryst. Growth Des. 10 (2010) 3044–3050.
[112] C.C. Weber, S.A. Kulkarni, A.J. Kunov-Kruse, et al., The use of cooling crystallization in an ionic liquid system for the purification of pharmaceuticals, Cryst. Growth Des. 15 (2015) 4946–4951.
[113] H. Wang, G. Gurau, S.P. Kelley, et al., Hydrophobic vs. hydrophilic ionic liquid separations strategies in support of continuous pharmaceutical manufacturing, RSC Adv. 3 (2013) 10019–10026.
[114] H. Wang, S.P. Kelley, J.W. Brantley, et al., Ionic fluids containing both strongly and weakly interacting ions of the same charge have unique ionic and chemical environments as a function of ion concentration, ChemPhysChem 16 (2015) 993–1002.
[115] H. Wang, P. Berton, A.S. Myerson, R.D. Rogers, Double salt ionic liquids containing the trihexyl (tetradecyl) phosphonium cation: the ability to tune the solubility of aromatics, ethers, and lipophilic compounds, ECS Trans. 75 (2016) 451–465.
[116] H. Wang, J. Pereira, A. Myerson, R.D. Rogers, Double salt ionic liquids prepared by mixing partially miscible ionic liquids: tuning the solubility of lipophilic molecules, ECS Trans. 64 (2014) 33–44.

[117] H. Mizuuchi, V. Jaitely, S. Murdan, A.T. Florence, Room temperature ionic liquids and their mixtures: potential pharmaceutical solvents, Eur. J. Pharm. Sci. 33 (2008) 326–331.
[118] L.J. He, W.Z. Zhang, B. Wen, et al., Separation of ephedrines using 1-butyl-3-methylimidazolium-tetrafluoroborate ionic liquids as eluent in high-performance liquid chromatography (HPLC), Chinese Chem. Lett. 14 (2003) 603–604.
[119] J. Flieger, Effect of ionic liquids as mobile-phase additives on chromatographic parameters of neuroleptic drugs in reversed-phase high-performance liquid chromatography, Anal. Lett. 42 (2009) 1632–1649.
[120] Z. Ma, P. Ji, Q. Wu, X. Guo, Separation of 5 drugs by ephedrine-based ionic liquid and its chromatographic behaviors, Cent. South Pharm. 9 (2009) 4.
[121] D. Han, Y. Wang, Y. Jin, K.H. Row, Analysis of some β-lactam antibiotics using ionic liquids as mobile phase additives by RP-HPLC, J. Chromatogr. Sci. 49 (2011) 63–66.
[122] L. Xu, A. Li, A. Sun, R. Liu, Preparative isolation of neomangiferin and mangiferin from rhizoma anemarrhenae by high-speed countercurrent chromatography using ionic liquids as a two-phase solvent system modifier, J. Sep. Sci. 33 (2010) 31–36.
[123] M. Cruz-Vera, R. Lucena, S. Cárdenas, M. Valcárcel, Combined use of carbon nanotubes and ionic liquid to improve the determination of antidepressants in urine samples by liquid chromatography, Anal. Bioanal. Chem. 391 (2008) 1139–1145.
[124] S. Li, C. He, H. Liu, et al., Ionic liquid-based aqueous two-phase system, a sample pretreatment procedure prior to high-performance liquid chromatography of opium alkaloids, J. Chromatogr. B 826 (2005) 58–62.
[125] F. Tang, L. Tao, X. Luo, et al., Determination of octopamine, synephrine and tyramine in citrus herbs by ionic liquid improved 'green' chromatography, J. Chromatogr. A 1125 (2006) 182–188.
[126] M.P. Marszałł, T. Baczek, R. Kaliszan, Evaluation of the silanol-suppressing potency of ionic liquids, J. Sep. Sci. 29 (2006) 1138–1145.
[127] B. Wang, J. He, V. Bianchi, S.A. Shamsi, Combined use of chiral ionic liquid and cyclodextrin for MEKC: Part I. simultaneous enantioseparation of anionic profens, Electrophoresis 30 (2009) 2812–2819.
[128] J. Hailiang, S. Haoyu, L. Zhanggao, Z. Saichun, Room temperature ionic liquid as a novel medium for the determination of solvent residuals in drug with headspace gas chromatography-mass spectrometry, Chinese J. Anal. Chem. 34 (2006) 1027–1029.
[129] G. Laus, M. Andre, G. Bentivoglio, H. Schottenberger, Ionic liquids as superior solvents for headspace gas chromatography of residual solvents with very low vapor pressure, relevant for pharmaceutical final dosage forms, J. Chromatogr. A 1216 (2009) 6020–6023.
[130] J. Pernak, P. Chwała, Synthesis and anti-microbial activities of choline-like quaternary ammonium chlorides, Eur. J. Med. Chem. 38 (2003) 1035–1042.
[131] J. Pernak, K. Sobaszkiewicz, J. Foksowicz-Flaczyk, Ionic liquids with symmetrical dialkoxymethyl-substituted imidazolium cations, Chem. Eur. J. 10 (2004) 3479–3485.
[132] K.M. Docherty, C.F. Kulpa Jr., Toxicity and antimicrobial activity of imidazolium and pyridinium ionic liquids, Green Chem. 7 (2005) 185–189.
[133] J. Pernak, J. Rogoża, I. Mirska, Synthesis and antimicrobial activities of new pyridinium and benzimidazolium chlorides, Eur. J. Med. Chem. 36 (2001) 313–320.
[134] F. Stock, J. Hoffmann, J. Ranke, et al., Effects of ionic liquids on the acetylcholinesterase–a structure–activity relationship consideration, Green Chem. 6 (2004) 286–290.
[135] J. Pernak, A. Skrzypczak, G. Lota, E. Frackowiak, Synthesis and properties of trigeminal tricationic ionic liquids, Chem. Eur. J. 13 (2007) 3106–3112.

[136] F. Walkiewicz, K. Materna, A. Kropacz, et al., Multifunctional long-alkyl-chain quaternary ammonium azolate based ionic liquids, New J. Chem. 34 (2010) 2281–2289.
[137] M.I. Hossain, M. El-Harbawi, Y.A. Noaman, et al., Synthesis and anti-microbial activity of hydroxylammonium ionic liquids, Chemosphere 84 (2011) 101–104.
[138] L. Carson, P.K.W. Chau, M.J. Earle, et al., Antibiofilm activities of 1-alkyl-3-methylimidazolium chloride ionic liquids, Green Chem. 11 (2009) 492–497.
[139] A.L. Smith, S.B. Fiel, N. Mayer-Hamblett, et al., Susceptibility testing of pseudomonas aeruginosa isolates and clinical response to parenteral antibiotic administration: lack of association in cystic fibrosis, Chest 123 (2003) 1495–1502.
[140] A. Busetti, D.E. Crawford, M.J. Earle, et al., Antimicrobial and antibiofilm activities of 1-alkylquinolinium bromide ionic liquids, Green Chem. 12 (2010) 420–425.
[141] V. Kumar, S.V. Malhotra, Antitumor Activity of Ionic Liquids on Human Tumor Cell Lines, ACS Symposium Series, Oxford University Press, 2010, pp. 91–102.
[142] N.K. Kaushik, P. Attri, N. Kaushik, E.H. Choi, Synthesis and antiproliferative activity of ammonium and imidazolium ionic liquids against T98G brain cancer cells, Molecules 17 (2012) 13727–13739.
[143] D.J. Hauss, Oral lipid-based formulations, Adv. Drug Deliv. Rev. 59 (2007) 667–676.
[144] J. Stoimenovski, D.R. MacFarlane, K. Bica, R.D. Rogers, Crystalline vs. ionic liquid salt forms of active pharmaceutical ingredients: a position paper, Pharm. Res. 27 (2010) 521–526.
[145] M. Shadid, G. Gurau, J.L. Shamshina, et al., Sulfasalazine in ionic liquid form with improved solubility and exposure, MedChemComm 6 (2015) 1837–1841.
[146] K. Bica, C. Rijksen, M. Nieuwenhuyzen, R.D. Rogers, In search of pure liquid salt forms of aspirin: ionic liquid approaches with acetylsalicylic acid and salicylic acid, Phys. Chem. Chem. Phys. 12 (2010) 2011–2017.
[147] L. Borka, J.K. Haleblian, Crystal polymorphism of pharmaceuticals, Acta Pharm. Jugosl. 40 (1990) 71–94.
[148] P.M. Dean, J. Turanjanin, M. Yoshizawa-Fujita, et al., Exploring an anti-crystal engineering approach to the preparation of pharmaceutically active ionic liquids, Cryst. Growth Des. 9 (2008) 1137–1145.
[149] R. Ferraz, L.C. Branco, I.M. Marrucho, et al., Development of novel ionic liquids based on ampicillin, MedChemComm 3 (2012) 494–497.
[150] C. Florindo, J.M.M. Araújo, F. Alves, et al., Evaluation of solubility and partition properties of ampicillin-based ionic liquids, Int. J. Pharm. 456 (2013) 553–559.
[151] W.L. Hough-Troutman, M. Smiglak, S. Griffin, et al., Ionic liquids with dual biological function: sweet and anti-microbial, hydrophobic quaternary ammonium-based salts, New J. Chem. 33 (2009) 26–33.
[152] J. Cybulski, A. Wiśniewska, A. Kulig-Adamiak, et al., Mandelate and prolinate ionic liquids: synthesis, characterization, catalytic and biological activity, Tetrahedron Lett. 52 (2011) 1325–1328.
[153] J. Stoimenovski, P.M. Dean, E.I. Izgorodina, D.R. MacFarlane, Protic pharmaceutical ionic liquids and solids: aspects of protonics, Faraday Discuss. 154 (2012) 335–352.
[154] J. Stoimenovski, D.R. MacFarlane, Enhanced membrane transport of pharmaceutically active protic ionic liquids, Chem. Commun. 47 (2011) 11429–11431.
[155] K.M. Johansson, E.I. Izgorodina, M. Forsyth, et al., Protic ionic liquids based on the dimeric and oligomeric anions: $[(AcO)_xH_{x-1}]^-$, Phys. Chem. Chem. Phys. 10 (2008) 2972–2978.
[156] K. Bica, J. Shamshina, W.L. Hough, et al., Liquid forms of pharmaceutical co-crystals: exploring the boundaries of salt formation, Chem. Commun. 47 (2011) 2267–2269.

[157] K. Bica, R.D. Rogers, Confused ionic liquid ions—a "liquification" and dosage strategy for pharmaceutically active salts, Chem. Commun. 46 (2010) 1215–1217.
[158] S.P. Kelley, A. Narita, J.D. Holbrey, et al., Understanding the effects of ionicity in salts, solvates, co-crystals, ionic co-crystals, and ionic liquids, rather than nomenclature, is critical to understanding their behavior, Cryst. Growth Des. 13 (2013) 965–975.
[159] S. Aitipamula, R. Banerjee, A.K. Bansal, et al., Polymorphs, salts, and cocrystals: what's in a name? Cryst. Growth Des. 12 (2012) 2147–2152.
[160] K.S. Lovejoy, C.A. Corley, E.K. Cope, et al., Utilization of metal halide species ambiguity to develop amorphous, stabilized pharmaceutical agents as ionic liquids, Cryst. Growth Des. 12 (2012) 5357–5364.
[161] O.A. Cojocaru, K. Bica, G. Gurau, et al., Prodrug ionic liquids: functionalizing neutral active pharmaceutical ingredients to take advantage of the ionic liquid form, MedChemComm 4 (2013) 559–563.

Synthesis of medicinally important heterocycles inside the nanoreactors built-in nonconventional reaction media

7

*Dripta De Joarder, Dilip K. Maiti**
Department of Chemistry, University of Calcutta, Kolkata, India
*Corresponding author. e-mail address: dkmchem@caluniv.ac.in

7.1 Introduction

In the emerging environmentally friendly era, the research professionals of academia and industries are devoting their efforts to discovering green strategies in science and technology. Various approaches such as replacement of conventional toxic organic solvents by an environmentally benign solvent, development of catalytic systems, and atom economic systems have been formulated to minimize the negative impact of environmental hazards [1]. The ultimate goal of a researcher is to develop efficient systems that mimic nature [2]. Extensive research is being dedicated to investigate the feasibility of water as a solvent for chemical transformation [3]. Water as the solvent has plenty of advantages such as it is inexpensive, nontoxic, nonflammable, resistant to greenhouse emissions, abundant in Nature, economical for isolation and purification, and have zero E factor value [4]. Moreover, it is not considered as a waste in chemical transformations, its large heat capacity and heat of evaporation allow easy control of exothermic reactions, and high polarity, the coexistence of hydrogen bond donor and acceptor binding sites often making catalysis feasible, rapid, and selective. In spite of a plethora of advantages, scientists of academia and industries have avoided water as solvent majorly because of the low solubility of a vast range of hydrophobic organic molecules possessing significantly low polar functionalities. Generally, heating is employed to improve the solubility of the hydrophobic molecules and making reactions feasible. However, heating conditions may decompose the labile organic substrates, reagents, and products, and also reduce the selectivity of the reactions. Initially, a number of phase transfer catalysts (PTC) [5] were designed for organic synthesis and developed to circumvent the problem of solubility under biphasic conditions. It has several limitations too such as extensive experimentation that might be required to determine the correct combination of substrate, catalyst, and surfactant. Moreover, separation and recovery of catalyst and surfactant might pose a serious problem.

Green Approaches in Medicinal Chemistry for Sustainable Drug Design. https://doi.org/10.1016/B978-0-12-817592-7.00007-1
© 2020 Elsevier Inc. All rights reserved.

7.2 Surfactant and nanodimensional micelle

The surfactant-assembled micelles are vessels for making hydrophobic reactant, reagent, and product soluble in water and remove the aforementioned obstacle to perform organic syntheses in water. Micelles are formed with assemblies of surfactants having hydrophobic hydrocarbon chain inside and hydrophilic cationic, anionic, or neutral head group in the outside of the vessels. Its dimension is in the range nanometer to micrometer and provides a hydrophobic pocket in aqueous media. The hydrophobic insides of the nanometer-micelles are the haven for all organic compounds to get the shelter eliminating the issues of the insolubility of substrates as well as bring them in the close vicinity to react faster. Surfactants are amphiphilic molecules containing one polar hydrophilic head group, and nonpolar hydrophobic tail group and have been used by human mankind for washing since 2500 BCE (Fig. 7.1). In an aqueous medium, the hydrophobic effect drives the formation of spontaneous micellar aggregates when the surfactant is present above the critical micelle concentration (cmc). The hydrophobic tails form the core of the micelles to avoid unfavorable interaction with the surrounded water molecules and hydrophilic head groups form the corona ensuring solubility through attractive interaction to water surroundings. The type of micelle formed depends on a number of factors such as (i) the chemical structure of the surfactant, (ii) the geometry of the molecule (iii) the ratio between hydrophilic and hydrophobic parts and (iv) the experimental conditions in which they are used such as temperature, pH, and ionic strength [6]. The effect of concentration is of prime importance to determine the structure of the micelles. Initially, typically spherical micelles are formed but as soon as the concentration increases ellipsoidal micelles, rods, hexagonal liquid crystal (LC) phase.

The hexagonal arrangement of long cylinders, lamellar LC phase and, eventually, reverse phases are possible. The unique feature of the micelle is that it provides hydrophobic, dry pockets in the water medium where water-insoluble organic moieties can take shelter (Fig. 7.2). Thus, micelles act as nanoreactors to bring the reactants together to provide a confined reaction environment [7]. Sorrenti [8] recently pointed out that micelle behaves as nanoreactors characterized by unique features. This concept of structuring is not only widely found in nature and many common applications but has also recently become of interest for the controlled design of more complex structures in the nanometer size range as well [9]. The benign and straightforward synthetic tool is efficiently used for synthesizing medicinally active compounds.

7.3 Properties and uses of the nanoreactors

All reactions performed in aqueous micellar media relies on one basic principle. The concept is that in water surfactant would form a nanoreactor having a hydrophobic core, through hydrophobic interactions and would host organic substrates inside. The proton (for Brønsted acid catalysis) or metal cations (for Lewis acid catalysis) would accumulate onto the surface of the droplets and enhance the rate to reach

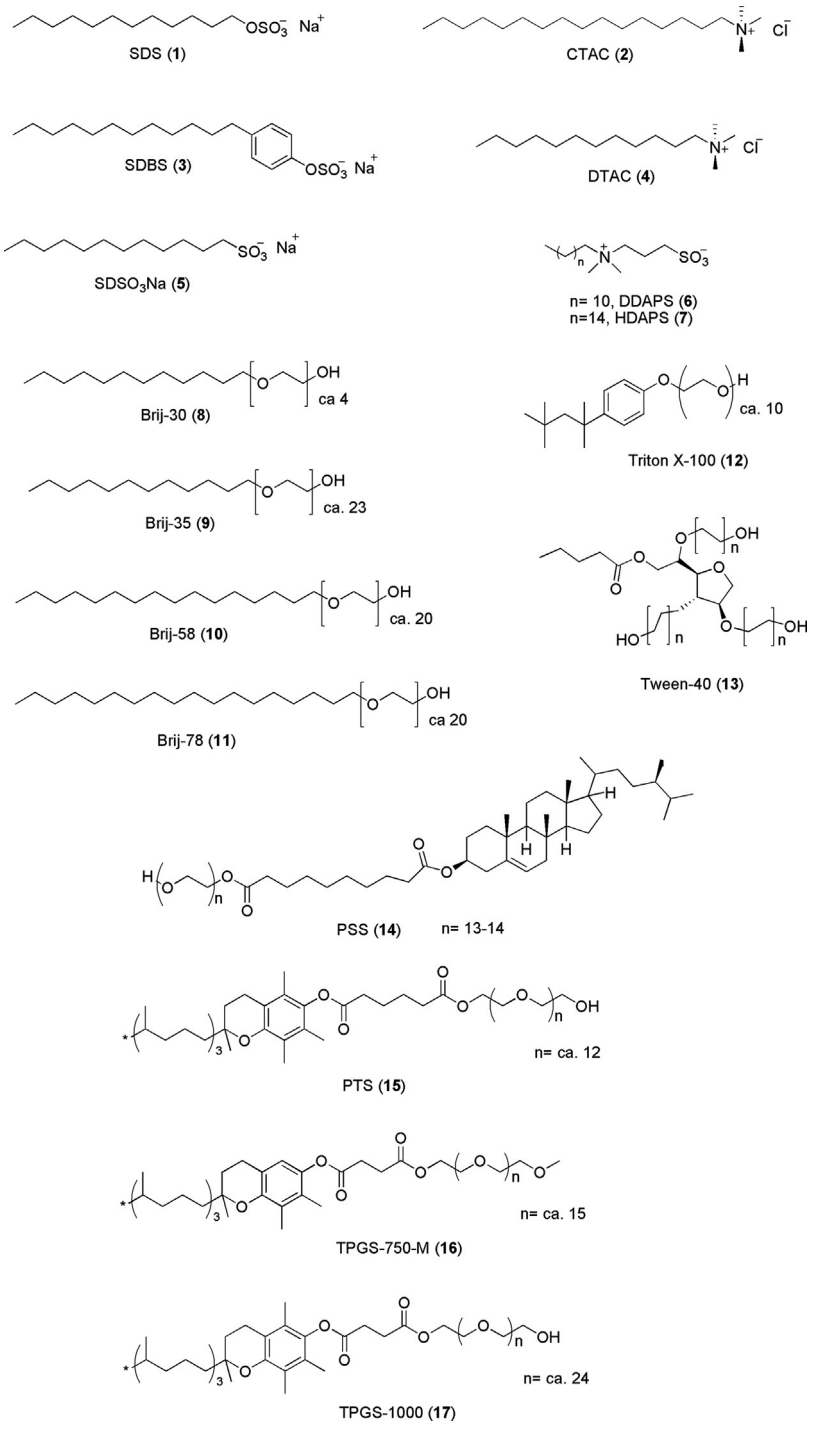

Fig. 7.1 Surfactants bearing cationic, anionic, and neutral head groups.

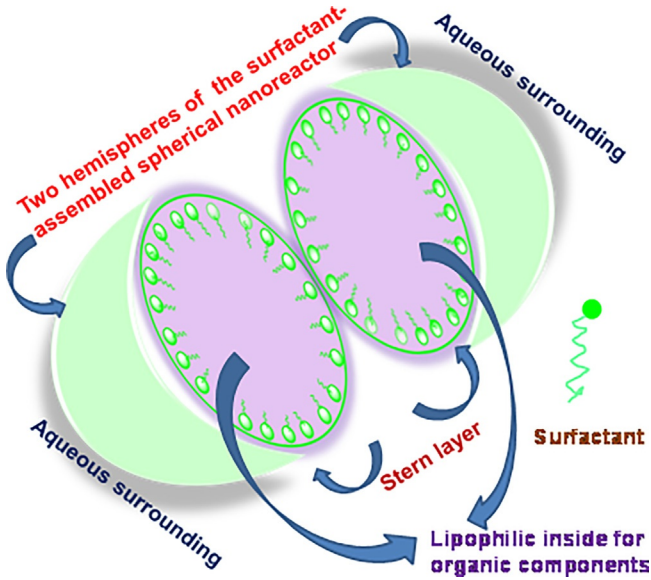

Fig. 7.2 Built-in surfactant-assembled nanoreactor in water.

equilibrium. Any polar molecules generated during the reaction would be removed from the interior of the nanoreactor due to its hydrophobic nature. Thus, micelles help to bring the reactants in close proximity to each other, often accelerate the reaction rate. The size of the nanoreactor could be measured using Dynamic Light Scattering instrument and the shape using optical microscopy (Fig. 7.3) [10]. Even though it sounds preposterous, it provides a dry and water-free microenvironment in water. This system imitates nature's way of performing reactions efficiently using enzymes. It opens up the opportunity to perform even a dehydration reaction in the water medium [11]. A myriad of reactions was reported mainly in the last decade using nanoreactors such as dehydration, cyclization, 1,3-dipolar cycloaddition, aziridination, multicomponent reactions, and even metal-catalyzed reactions which will be discussed in this chapter.

7.4 Dehydration reaction in water for syntheses of medicinally important esters, ethers, and thioethers

Esterification of carboxylic acids and alcohols is one of the most fundamental organic transformations with widespread application in fine chemicals, flavors, plasticizers, emulsifier, and biodiesel production and most important intermediates for drug formulations [12–15]. A number of drugs that are currently available in the market contain ether, thioether, and ester functional groups (**18**–**23**, Fig. 7.4). For example,

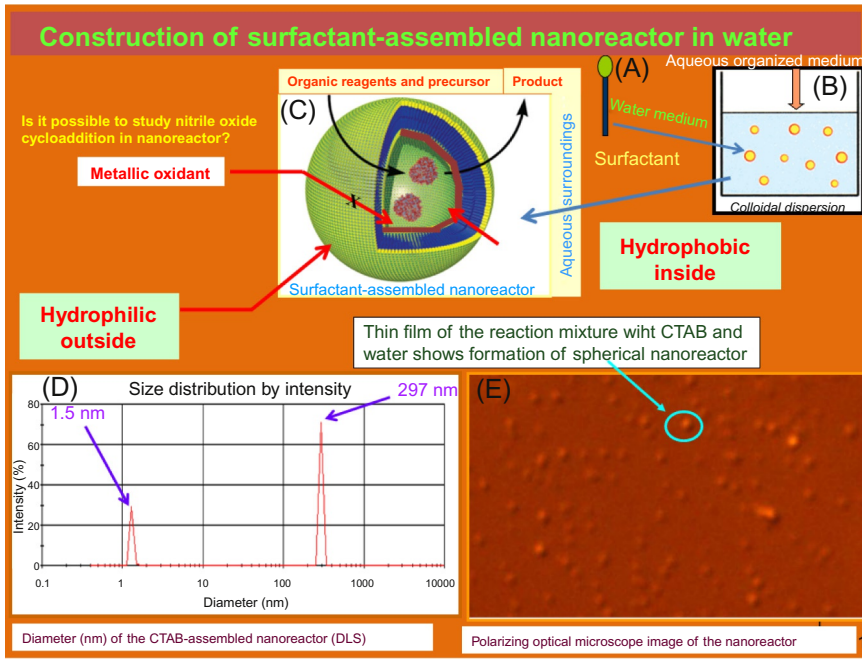

Fig. 7.3 Size, shape, and properties of nanoreactor built-in aqueous media. (A) Surfactant, (B) aqueous organized medium, (C) surfactant-assembled nanoreactor, (D) diameter (nm) of the CTAB-assembled nanoreactor (DLS), and (E) polarizing optical microscope image of the nanoreactor.

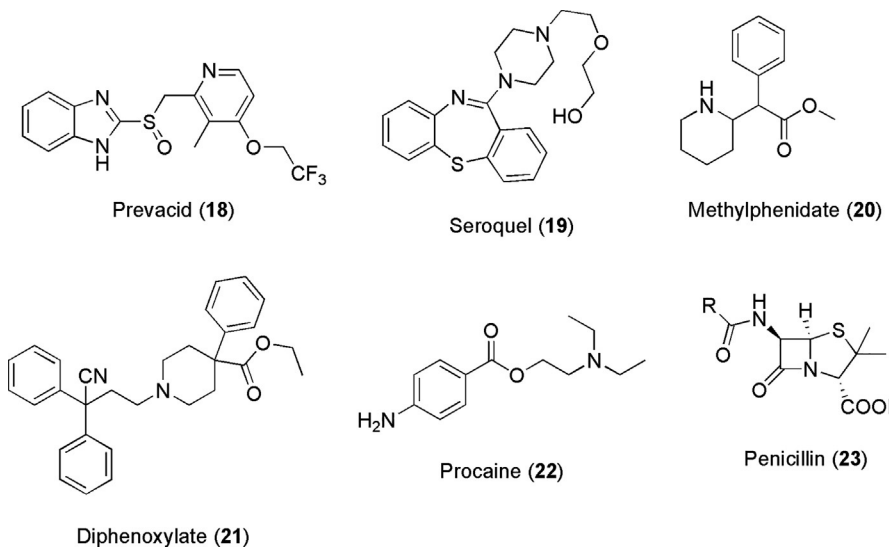

Fig. 7.4 Bioactive esters, ethers, and thioethers.

Prevacid (**18**) is a proton-pump inhibitor (PPI) that inhibits the stomach's production of gastric acids [15b]. Seroquel (**19**) is an atypical antipsychotic approved for the treatment of schizophrenia, bipolar disorder, and in the XR version along with a selective serotonin reuptake inhibitor (SSRI) to treat the major depressive disorder [15c]. Attention-deficit hyperactivity disorder drug methylphenidate (**20**) contains a methyl ester group. The antimotility drug co-phenotrope contains the ester diphenoxylate (**21**). Procaine (**22**) is used as a local anesthetic. The widely used antibiotic Penicillins (**23**) also features a thioether linkage.

As scientists discovered the advantages of using water as a solvent, reports started appearing in scientific journals describing various organic transformations in aqueous reaction media [11]. However, they were few in numbers. One of the most challenging classes of reactions to be carried out in water is the dehydrative organic transformations. In general, during dehydration water needs to be removed either azeotropically or by using dehydrating agents to drive the equilibrium forward. In 2002, Kobayashi and his team published a pathbreaking paper [16] reporting dehydration reactions in water in the presence of dodecylbenzene sulfonic acid (DBSA) (**26**) as a Brønsted acid-surfactant-combined catalyst (BASC). They also showed that the methodology could be applicable to various reactions including esterification, etherification, thioetherification, and dithioacetalization (Scheme 7.1). The general strategy

Scheme 7.1 Dehydration reaction investigated inside the lipophilic nanoreactor.

described the chemoselective dehydration protocol. They utilized the same concept described above, where organic substrates take shelter in the hydrophobic core of the nanoreactor, formed by the surfactant molecules. Water generated during reaction would be expelled from the hydrophobic interior to the hydrophilic exterior. For their study on dehydrative esterification reaction, they choose lauric acid and 3-phenyl-1-propanol as model substrates (eq. i, Scheme 7.2). Catalyst screening confirmed that DBSA was the catalyst of choice. The developed system worked for *trans*-esterification of methyl esters (eq. ii), etherification (eq. iii), thioetherification as well as for dithioacetalization reactions (eq. iv) in the water medium.

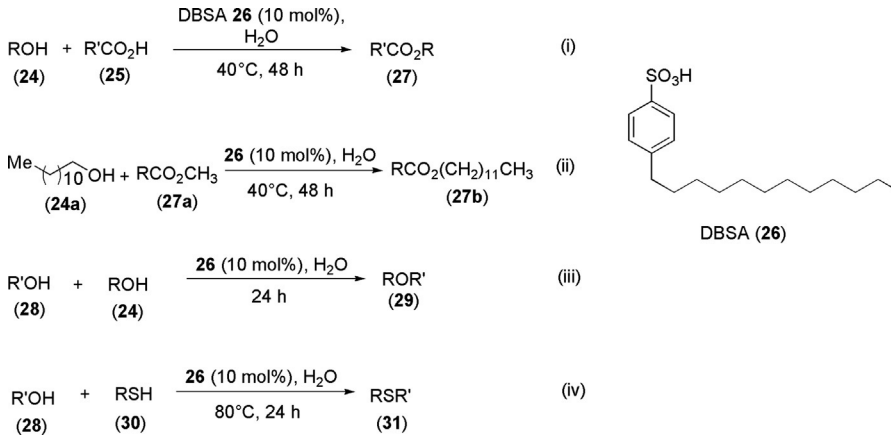

Scheme 7.2 Direct synthesis of esters, ethers, and thioethers in the water media.

The seminal paper by Kobayashi spurred interest among the scientific community. Developing novel surfactants became very important. Luque and his coworkers synthesized a novel glucose-derived nonionic, renewable-derived, biosurfactant (N-alkanoyl-*N*-methyl-1-glucamine polyol, C12MG, **34**) by reductive amination of glucose (**32**) followed by an amidation (eq. i, Scheme 7.3). This group also developed a catalytic system to carry out esterification of carboxylic acids with short-chain alcohols typically methanol or ethanol in aqueous media in the presence of C12MG (**34**). The reported protocol was applicable for various aliphatic and aromatic carboxylic acids under mild reaction conditions [17]. Water formed during the reaction gets thrown out from the hydrophobic core of the nanoreactor thus driving the equilibrium forward (eq. ii, Scheme 7.3).

7.5 Cyclization reaction developed inside the nanoreactor to achieve bioactive heterocycles

One of the most prominent classes of biologically active compounds is functionalized pyridine and its unsaturated analog, 1,4-dihydropyridine derivatives. 1,4-Dihydropyridines have been extensively used as calcium channel modulators [18] and were developed as cardiovascular, antihypertensive, and anticancer drugs, which include diludine (**35**), felodipine (**36**), isradipine (**37**), lacidipine (**38**), nitrendipine (**39**), nifedipine (**40**), and nemadipine B (**41**, Fig. 7.5) [19]. Their oxidized counterparts target a wide variety of biological receptors [20]. Due to the existence of pyridines in pharmaceuticals, agrochemicals, and natural products, their synthesis remains an area of intense current research

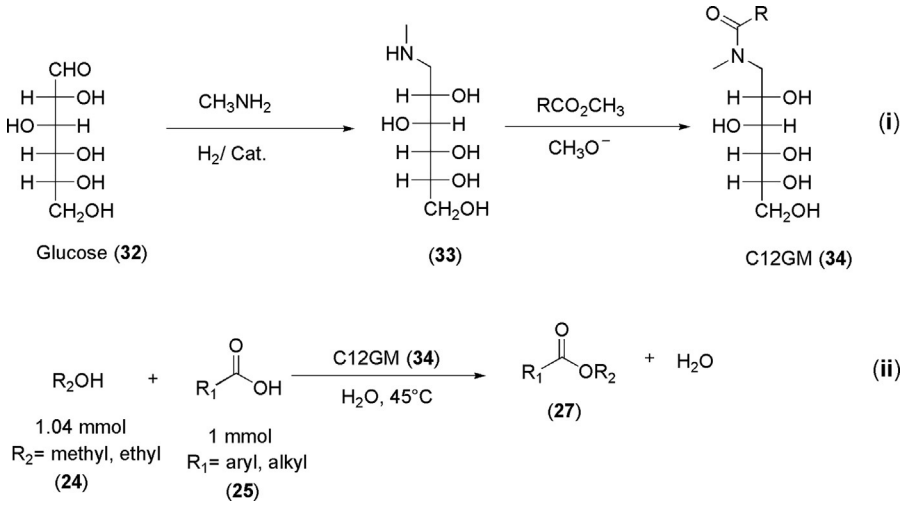

Scheme 7.3 Synthesis of C12MG (**34**) from glucose for esterification in water.

interest to the chemical community [21]. In 2013, Das et al. published a highly efficient one-pot, four-component Hantzsch reaction procedure for the preparation of 1,4-dihydropyridine derivatives (**45**, Scheme 7.4) using the nonionic surfactant Triton X-100 in aqueous media at room temperature [22]. For their optimization studies, they chose 3-nitrobenzaldehyde × (1 mmol), ethyl acetoacetate (2 mmol), and ammonium acetate (1.5 mmol) as model substrates. Screening of solvent, temperature, and surfactant revealed that 10 mol% Triton X-100 in water works best.

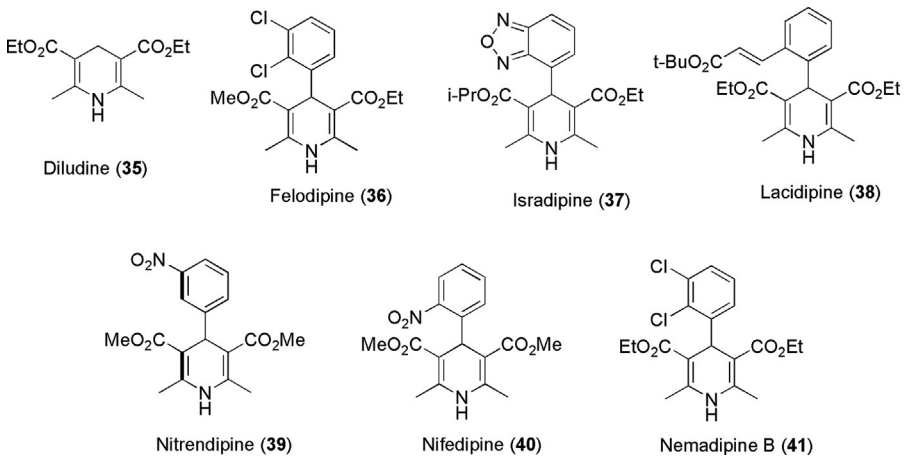

Fig. 7.5 Structures of some bioactive dihydropyridines.

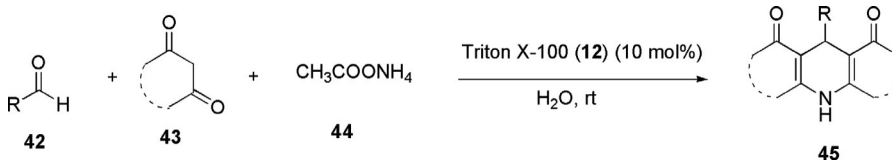

Scheme 7.4 Synthesis of medicinally important dihydropyridines in aqueous micellar media.

The reaction was applicable to a wide variety of aromatic and aliphatic aldehydes as well as active methylene compounds furnishing the desired products in more than 80% yield. The paper also described a new one-pot, potentially efficient, absolutely clean, versatile, environment friendly, light-induced, green procedure for the synthesis of pyridines (**46**) by efficient oxidation of Hantzsch 1,4-dihydropyridines (**45**) (Scheme 7.5) [23].

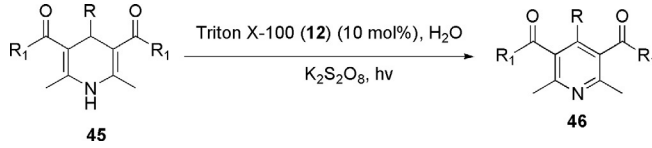

Scheme 7.5 Synthesis of substituted pyridines in water.

Another class of *N*-heterocycles which exhibit a broad spectrum of biological activities are quinoxaline-based compounds [24]. Over the years, a wide range of approaches were formulated for their synthesis [25–27]. However, the majority of these routes involve the use of toxic organic solvents, hazardous chemicals, expensive, moisture-sensitive reagents, high temperature, and complex workup procedures. In 2003, Prof. A. K. Chakraborti published a paper [28] detailing a simple, extremely efficient, and green protocol for the synthesis of quinoxalines (**49**) from 1,2-diketones (**48**) and 1,2-diamines (**47**) in the water at room temperature catalyzed by cheap, readily available and nontoxic surfactant Tween 40 (Scheme 7.6). Aromatic 1,2-diamino compounds containing electron-donating as well as electron-withdrawing groups,

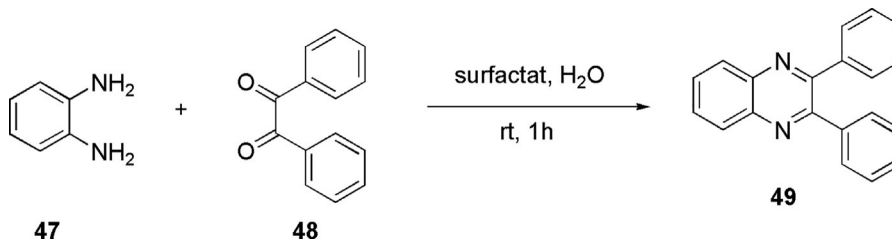

Scheme 7.6 Dehydrative cyclization to quinoxalines in water.

aliphatic 1,2-diamino compounds worked well with the diketo compounds furnishing the functionalized quinoxaline in high yield.

Scientists became curious about quinolone antibiotics due to their inhibitory effect on bacterial DNA gyrase [29]—an enzyme essential for DNA replication. After the discovery of nybomycin [30], a number of quinolone antibacterials have been developed which possess either 2-quinolone or 4-quinolone moieties in their core. Considerable interest has been noticed in developing 2-quinolones as anticancer, antiviral, and antihypertensive agents [31]. 4-Substituted 3-phenyl-2-quinolones exhibit high affinity in binding to the glycine site of *N*-methyl-D-aspartate receptor, and such antagonists hold promise for the treatment of several central nervous system disorders [32]. Amides of 3-hydroxy/alkyl-4-carboxylic acids of 2-quinolones also exhibit high affinity for the 5-HT3 serotonin receptor (Scheme 7.7) [32b].

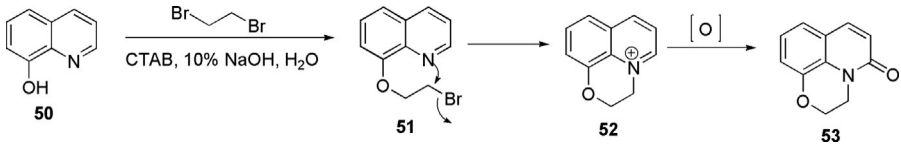

Scheme 7.7 Synthesis of fused tricyclic quinolones in the aqueous medium.

In 2010, a team of scientists led by Dr. Mondal published a simple, green methodology for the synthesis of fused tricyclic, tetracyclic, and pentacyclic quinolones (Scheme 7.8) in nanoreactor with excellent yields [33]. They used different derivatives of 8-hydroxyquinoline (**50**) and 1,ω-dihaloalkanes/xylenes/methyl-quinoxalines as alkylating agents to get the desired product (**53**) in high yields.

Benzimidazole and phthalimides are commonly occurring heterocyclic moiety in natural and synthetic compounds [34]. Recently, benzimidazole derivatives with substituents particularly at N-1 and/or C-2 positions have received considerable attention because of their broad range of biological functions and pharmacological applications. They are an integral part of various clinical medicines as well, for example, 2-substituted benzimidazole and Esomeprazole [35] are anti-ulcerative drugs. Albendazole [36] is used to treat parasitic diseases, whereas, 1,2-substituted benzimidazole, Astemizole is an antihistamine drug [37]. Although several synthetic pathways have been designed to construct these motifs; most of the routes involve toxic reagents/solvents. In 2013, Dr. A. Chatterjee and Dr. M. Banerjee chronicled a simple, environmentally benign methodology for the chemoselective synthesis of two-substituted benzimidazoles (**54**) in organized aqueous media in the presence of DBSA (**26**) surfactant and iodine as cocatalyst [38]. A green cascade cyclization process is reported by Prof. Maiti and co-researchers to access highly substituted phthalimides (**55**, eq. ii) [34].

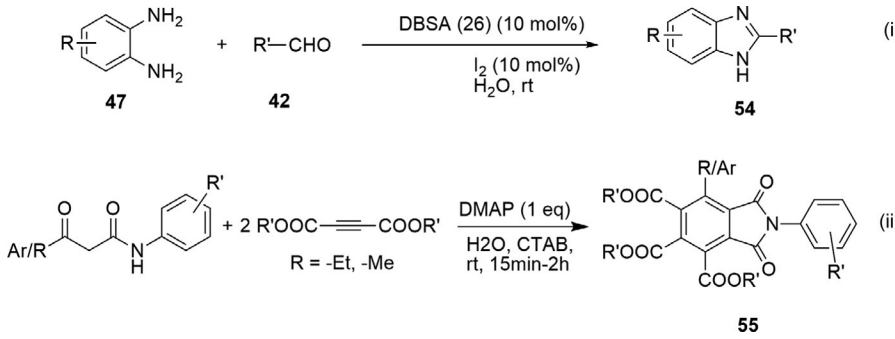

Scheme 7.8 Synthesis of functionalized benzimidazoles and phthalimides.

Compounds containing nitrone functional groups are desirable and found broad application as therapeutic agents [39]. For the first time in 2003, Prof. P. Bhattacharya and his team reported [40] synthesis of nitrones (**56**) in aqueous micellar medium followed by 1,3-dipolar cycloaddition with alkenes (Scheme 7.9). The technique worked well for aldehydes containing electron-donating as well as electron-withdrawing functional groups in the presence of cationic as well as anionic surfactants.

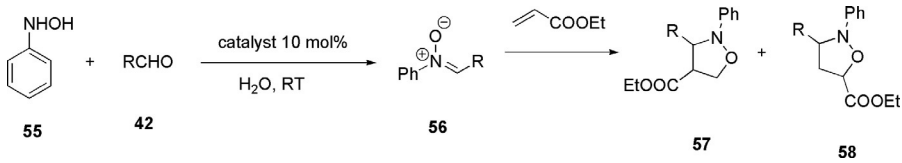

Scheme 7.9 Nitrone formation followed by cycloaddition.

In 2006, they extended the reaction scope [41] to include chiral sugar derivatives. The group was particularly interested in chiral sugar-based cyclic ether moieties as these are prevalent in naturally occurring biologically active compounds such as ciguatoxin [42], other marine toxins [43], zoapatanol [44], sepholenol [45], laurencin [46]. They chose 1,2:5,6-diisopropylidene-3-O-allyl furanoside (**59**) as the model substrate to carry out optimization studies. CTAB proved to be the surfactant of choice. The nitrones of 3-O-allyl glucofuranose and the corresponding allose derivatives, as well as crotyl derivatives, furnished bridged isoxazolidines, i.e., oxepanes (**60**) whereas nitrones of prenyl derivatives produced pyrans (**61**) (Scheme 7.10).

An array of nitrogen-containing five-membered heterocycles are known which are biologically and pharmaceutically important [47]. One of the most useful ways to fabricate such motifs is via 1,3-dipolar nitrone cycloaddition. In particular, intramolecular nitrone-olefin cycloadditions have been utilized to obtain structurally more complex bi- or tricyclic isoxazolidines of either biological significance or as useful

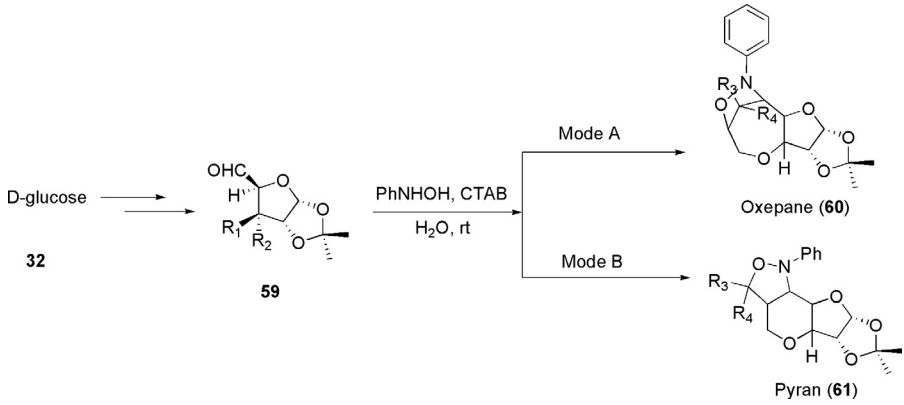

Scheme 7.10 Intramolecular nitrone cycloaddition of 3-O-allyl furanoside-5-aldehydes in water.

synthetic intermediates for target molecules [48]. Notably, certain fused isoxazoline/isoxazole with chromano moiety are known to possess antidepressant, antipsychotic, and antianxiolytic activities [49]. However, there are not many reported procedures for assembling chromano-isoxazoles [50a–c, 51]. Surfactant screening was carried out using O-allyl salicylaldehyde and phenylhydroxylamine. CTAB was found to be the best catalyst. A variety of substituted salicylaldehyde in the presence of N-substituted hydroxylamine furnished *cis*-fused 1-aryl-1,3*a*,4,9*b*-tetrahydro-3*H*-chromano[4,3-*c*]isoxazoles (**64**) in excellent yields (Scheme 7.11).

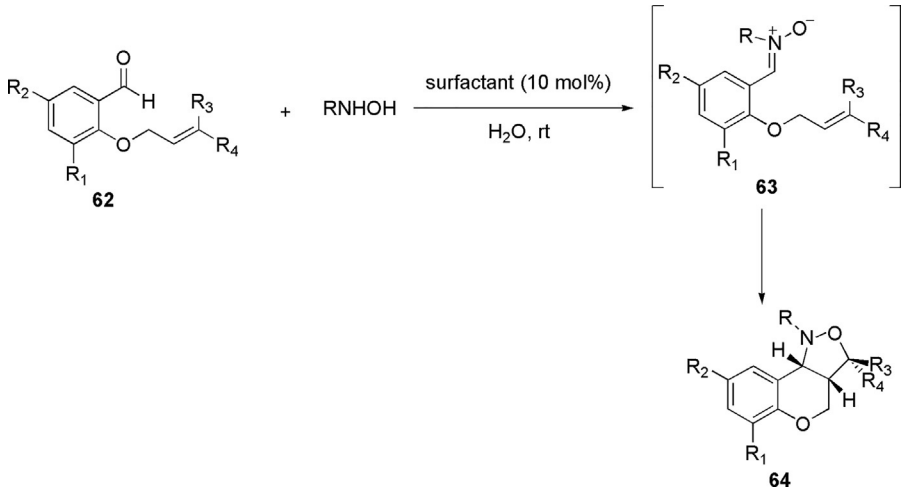

Scheme 7.11 Synthesis of *cis*-fused chromano[4.3.-*c*]isoxazoles inside a nanoreactor.

7.6 Oxidative cyclization

Aziridines are useful structural motifs that are abundant in pharmaceuticals [52]. Several methods have been reported for aziridination [53, 54], but most of the protocols suffers from limitations such as use of complex nitrogen-containing sources, multiple steps reactions and/or harsh reaction conditions. In 2008, Vos et al. [55] demonstrated a green, new method for synthesis of unprotected aziridines (**66**) from corresponding alkenes (**65**) by using ammonia as nitrogen source, under very mild and micellar conditions (Scheme 7.12).

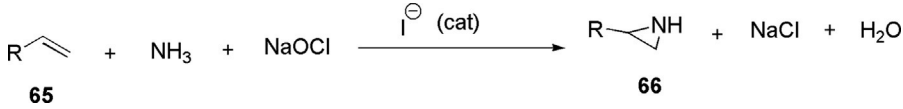

Scheme 7.12 Direct catalytic aziridination in water.

Optimization reactions were carried out with styrene. The catalytic use of iodide in combination with bleach as an oxidant gave the best yields. A variety of styrene derivatives underwent aziridination smoothly with excellent yields.

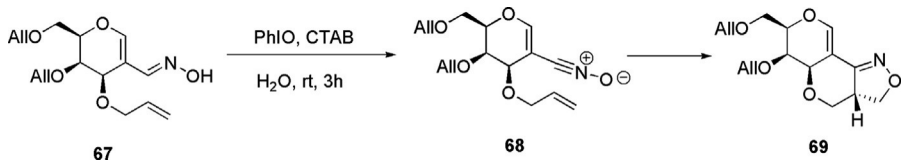

Scheme 7.13 Generation of glycal nitrile oxides in water and their 1,3-DC reaction.

1,3-DC reaction of nitrile oxides and alkenes are widely used by synthetic organic chemists to access Δ^2-isoxazolines [56]. These motifs are of particular interest as they can be easily converted into a variety of highly functionalized achiral and chiral compounds. In 2008, Maiti and his coworkers disclosed [57] the very first preparation of nitrile oxides in aqueous micellar media and utilized the developed methodology for the stereoselective synthesis of 3-(2′-C-3′,4′,6′-tri-O-benzyl glycal)-Δ^2-isoxazolines for the first time (**69**). The report also described the synthesis of an optically pure 1,4-pyranopyran motif found in bioactive natural products (Scheme 7.13).

7.7 Multicomponent reaction

Multicomponent reactions (MCRs) are extremely important tools in green chemistry as these are highly atom economical, uses readily available reactants, does not require isolation of any intermediates, several steps can be done in a single reaction flask, to

generate products of medicinal importance and other applications [58]. For instance, a number of drugs that are currently on the market contain indole nucleus [59] and can be synthesized in a greener way using MCR. Most of these compounds are belong to the 3-substituted indole family, which is an important intermediate for chemical synthesis and widely distributed in many important natural products [60]. Besides, this three-substituted indole is also an important class of pharmacophores having many biological activities, i.e., Sumatriptan (**70**), Frovatriptan (**71**), Zolmitriptan (**72**), and Rizatriptan (**73**) are used for migraine headaches [61], whereas azolylbenzyl indole (**74**) and bis-indole (**75**) are used as a breast cancer and HIV-1 integrase inhibitor, respectively (Fig. 7.6) [62, 63].

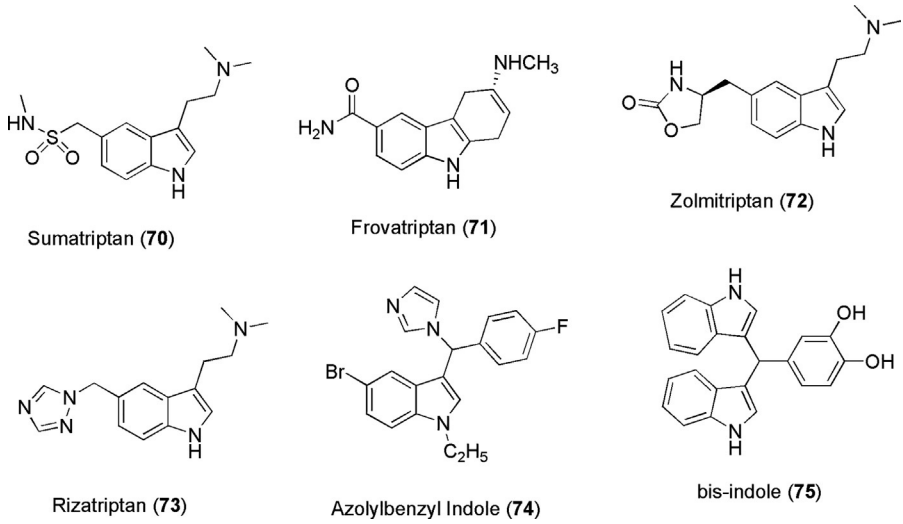

Fig. 7.6 Structure of some biologically active 3-substituted indoles.

A large number of natural products and pharmaceuticals including cytostatic alkaloids such as spirotryprostatins A, B, and strychnophylline contain spirooxindole ring as a core structure [64]. Among them, 4*H*-chromenes are of particular importance due to their wide range of useful biological properties, including spasmolitic-, diuretic-, anticoagulant-, anticancer-, and antianaphylactic activities [65]. There is also considerable interest in 5,6,7,8-tetrahydro-4H-chromene derivatives containing nitrile functionality, especially 2-amino-5-oxo-5,6,7,8-tetrahydro-4H-chromene-3-carbonitriles, as these could be potentially used in the treatment of human neurodegenerative disorders [66]. Wang and his group published a simple and efficient method [67] for the synthesis of spirooxindoles (**78**) with fused chromenes, through three-component one-pot reaction in aqueous micellar media, using sodium stearate as a Lewis base surfactant-combined catalyst. Model studies with isatin, dimedone, and malononitrile disclosed that reaction at 60°C with 10 mol% Sodium stearate gave the best yield. It is worth noting that neither the

use of traditional surfactants like SDS or SDBS, nor the use of weak bases such as acetate allowed achievement of the same yields of the desired products (Scheme 7.14).

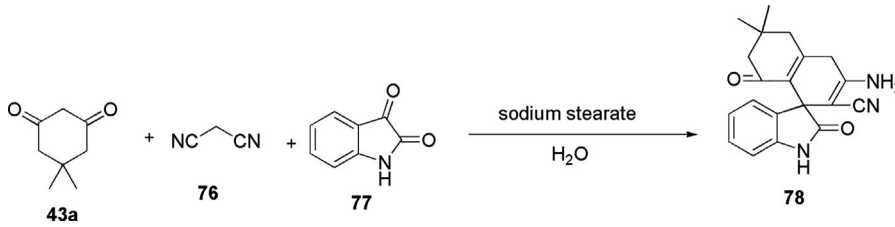

Scheme 7.14 Multicomponent reaction for the synthesis of spirooxindoles in micellar media.

In 2013, a group of scientists led by Dr. A. Kumar published a paper [68] describing the synthesis of 3-amino alkylated indoles (**80**) via a Mannich-type reaction of aromatic/heteroaromatic aldehydes, secondary amine/N-alkylanilines and indoles in water using SDS as the surfactant. Optimization reaction was performed using indole, piperidine, and benzaldehyde. Screening was performed using various acids, metal/nonmetal Lewis acids, ionic, and nonionic surfactants. After standardization, the methodology was applied to a variety of aldehydes both aromatic (containing electron-donating and electron-withdrawing substituent) and aliphatic with different diols. The beneficial aspects of this procedure are the high yield, operational simplicity, eco-friendliness, and very mild reaction conditions (Scheme 7.15).

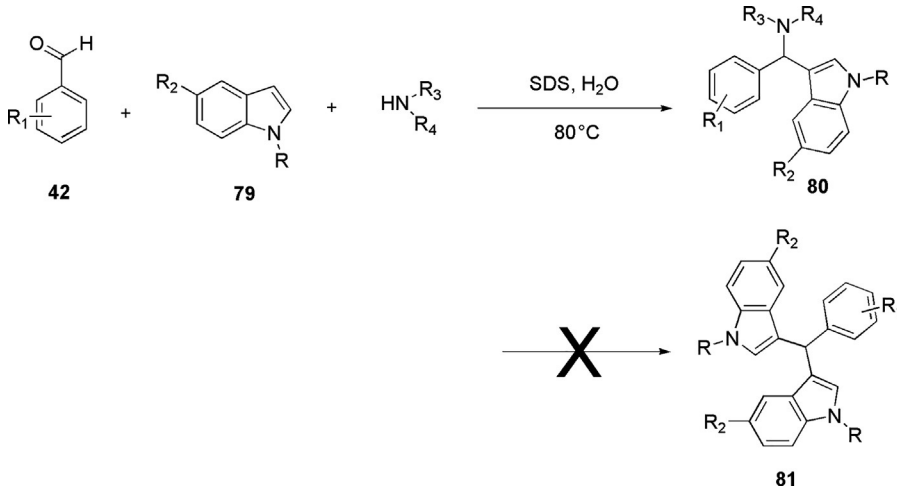

Scheme 7.15 Synthesis of 3-amino alkylated indoles via three-component Mannich-type reaction in aqueous micellar medium.

Thioesters are key intermediates in various biological systems [69], and are widely present in a number of biologically active and medicinal agents [70]. Conventional synthesis requires the use of difficult to handle, foul-smelling thiols or thiocarboxylates [71, 72]. In 2013, Prof. Cai and colleagues realized a green protocol [73] for the synthesis of thioesters (**85**) via one-pot, the three-component reaction of organic halides (**82**), thiourea (**83**), and benzoyl chlorides (**84**) (Scheme 7.16).

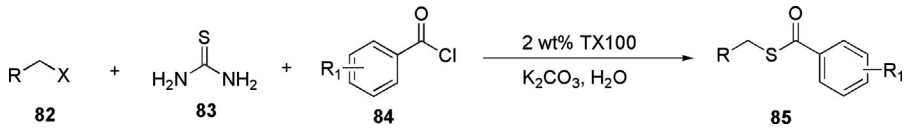

Scheme 7.16 Synthesis of thioesters in micellar media.

The newly developed procedure is free of organic solvents and foul-smelling thiols. These reactions and corresponding workups entail only an in-flask extraction with minimal amount of a single, recoverable organic solvent, making it more environmental friendly and suitable for large-scale operations. To showcase the usefulness of the developed protocol they performed the synthesis of a key intermediate (**86**) of compound **87** which displays potent anti-HIV properties in human macrophages (Scheme 7.17).

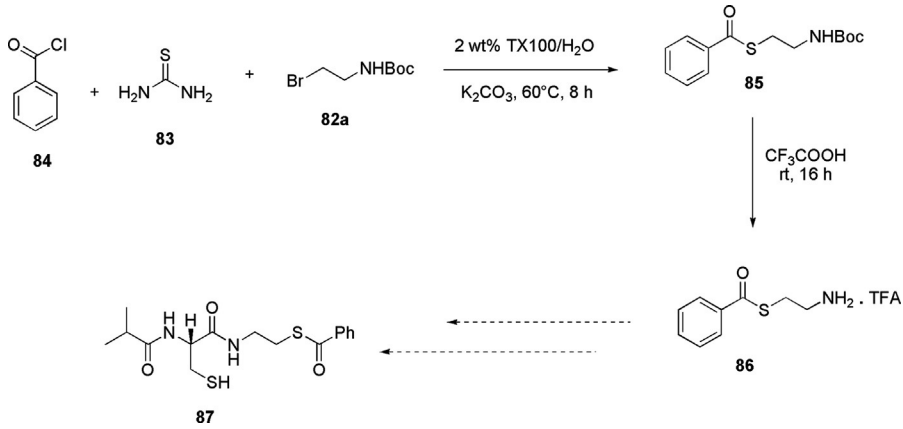

Scheme 7.17 A potential application of the protocol in organic synthesis.

7.8 C—C bond-forming reactions

Friedel Crafts acylation has been used extensively to functionalize aromatic compounds since its inception. This reaction normally requires a stoichiometric amount of Lewis acid as a catalyst. Even though Lewis acids are efficient catalysts [74], their use has a number of disadvantages such as prolonged reaction time, harsh reaction conditions (reflux temperature), use of metal triflates, mineral acids, and

stoichiometric amount of metal halides, which lead to the formation of intermediate complexes that upon hydrolysis produce hazardous corrosive waste-products such as acidic and salty wastewaters. Recently, scientists focused their attention toward selective acylation of 2-methoxynaphthalene as the reaction afforded useful intermediates for the synthesis of medicinally important drugs (Fig. 7.7) [75].

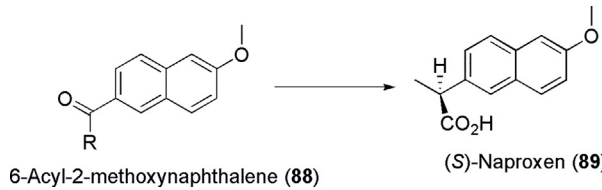

Fig. 7.7 Structure of anti-inflammatory drug (*S*)-naproxen and its intermediate.

In 2013, Prof. Rajanna and his team described a simple, practical, and environmentally responsible method for selective acylation of 1-halo-2-methoxynaphthalenes (**90**), 2-methoxynaphthalenes, anisole, 2-methoxypyridine, and 2-methoxypyrimidine in excellent yields in the presence of cationic micelles (CTAB and CTAC) under non-conventional reaction medium (Scheme 7.18) [76].

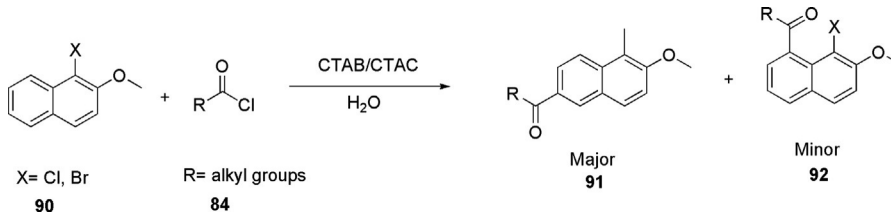

Scheme 7.18 Friedel-Crafts acylation of 1-halo-2-methoxynaphthalenes in aqueous media.

The Morita-Baylis-Hillman (MBH) reaction is a useful carbon-carbon sigma bond-forming synthetic tool which involves attachment between activated alkenes and carbon electrophiles in a tandem Michael-Aldol sequence [77]. The products of this reaction are of prime interest to the synthetic community as they provide quick access to intermediates for the synthesis of natural products [78], heterocycles [79], and drugs [80]. Traditional methodologies involve the use of organic bases such as DABCO [81], DMAP [82], imidazole [83], and DBU [84], use of strong Lewis acids ($TiCl_4$, Et_2Al) [85] or even physical methods such as high pressure [86] and microwave irradiation (Scheme 7.19) [87].

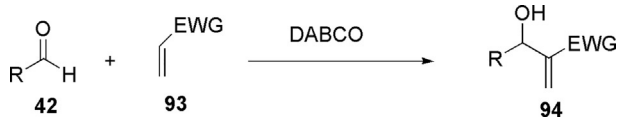

Scheme 7.19 Morita Baylis Hillman reaction of acyclic alkene with various aldehydes.

In 2013, Dr. Bhat and his team disclosed an efficient, environmentally responsible, and accelerated MBH protocol in an aqueous cationic micellar media for acyclic conjugated alkenes and cyclic enones using cationic surfactant CTAB (Scheme 7.20) [88]. The reaction worked well for an array of aromatic as well as aliphatic aldehydes.

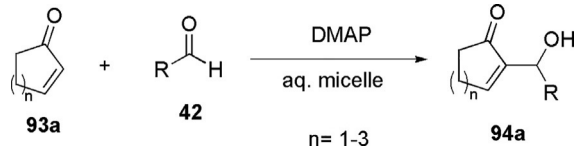

Scheme 7.20 MBH reaction of cyclic enones with various aldehydes.

7.9 Carbon-heteroatom bond-forming reactions

Keto functionality is widely present in drugs and other medicinally important compounds [89]. One of the best ways to access this functionality is by hydration of alkynes. However, traditional methods require use of Lewis or Brønsted acids, high temperatures [90], toxic metal salts, and often leads to low yields and unwanted polymers [91–93]. In 2013, Dr. Blum and co-researchers outlined [94] a green protocol for Markonikov addition of water to alkynes (**95**) in the presence of CTAB furnishing ketones (**96**) in excellent yields (90%) (Scheme 7.21).

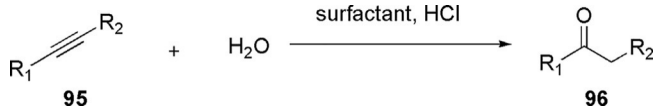

Scheme 7.21 Hydration of alkynes in aqueous micellar media.

The five- and six-membered heterocycles possessing N, O, and S play crucial roles in the pharmaceutical industry [95]. Routes targeting these moieties involve at least one nucleophilic aromatic substitution reaction (SN^{Ar}) [96]. Traditionally dipolar, aprotic solvents such as DMF, DMAc, NMP, and DMSO have been used for SN^2 and SN^{Ar} reactions and a recent survey revealed that for the past 14 years about 50% of these toxic organic solvents had been used either in SN^2 or SN^{Ar} reactions only [97]. To overcome this issue Lipshutz and his team published a report [98] in 2015 describing SN^{Ar} reactions studied under micellar catalysis conditions involving nonionic surfactants (Scheme 7.22).

Optimization reactions employing pyrimidine trichloride and pyrrolidine in equal amounts disclosed that best yield was obtained at room temperature in nanoreactors derived from TPGS-750-M in water using K_3PO_4 as a base.

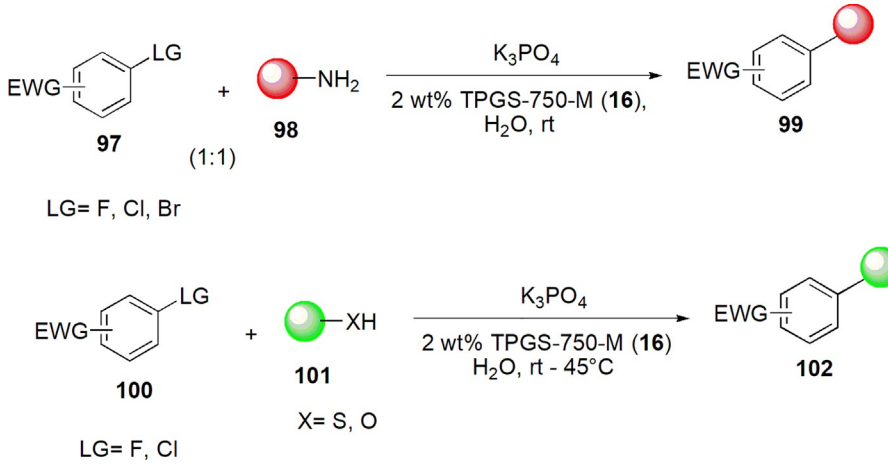

Scheme 7.22 SN^{Ar} reaction in aqueous micellar media.

7.10 Povarov reaction

One of the most important class of heterocyclic compounds in the pharmaceutical and agrochemical industries are Tetrahydroquinoline (THQ) derivatives. In particular, the 1,2,3,4-THQ ring is a prevalent structural motif and is found in several biologically active natural products and pharmacologically relevant therapeutic agents [99]. The easiest way to fabricate these compounds is by an inverse electron demand formal [4 + 2] cycloaddition reaction between *N*-arylimines and electron-rich dienophiles known as Povarov reaction. Generally, organic solvents are used for this reaction. In 2013, group of Dr. Kouznetsov delineated an elegant, general, and environmentally benign protocol [100] to obtain the privileged diastereospecific 2-methyl-THQs of highest biological interest in excellent yields via the domino type ABB′ imino DA reaction. This protocol is based on a well-established concept, activation of imines in water by acidic surfactants (Scheme 7.23).

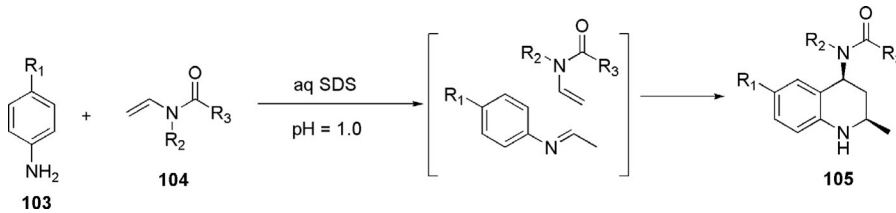

Scheme 7.23 Synthesis of 4-amido-N-yl-2-methyl-6-substituted THQs.

Structural motif Quinoline features in a number of biologically relevant molecules including antimalarial [101a], anti-asthmatic [101b], antihypertensive [101c], anti-inflammatory [101d], and several new generation antibacterial drugs [102]. Tetrahydroquinoline is also present in many naturally occurring alkaloids such as flindersine, oricine, and vesprine with psychotropic antiallergic and oestrogenic activities [103a–d]. Aryl tetrahydroquinolines are potential neuroprotective agents [103e] and act as anti-HIV agents in vitro [103f].

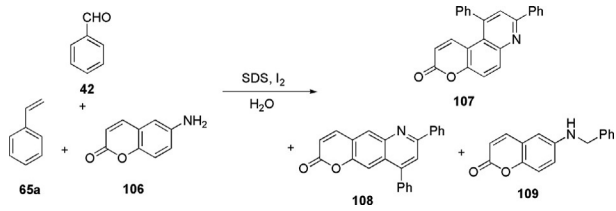

Scheme 7.24 Povarov-hydrogen transfer auto-tandem catalytic route with iodine in water.

In 2014, Dr. N. C. Ganguly and his team reported a green, direct route to synthesize pyrano[3.2-f]quinolin-3-ones and pyrano[2.3-g]quinolin-2-ones by three-component coupling of 6-aminocoumarin (**106**), aromatic aldehyde (**42**) and an excess of styrene (**65a**) by Povarov-hydrogen transfer auto-tandem catalytic route with iodine (5 mol%) in water in the presence of sodium dodecyl sulfate (Scheme 7.24) [104]. Model studies were carried out with 6-aminocoumarin, benzaldehyde, and styrene by varying surfactant, solvent, reaction time, and temperature. They applied the optimized reaction condition successfully to a diverse range of aromatic aldehydes substituted with electron-releasing and electron-withdrawing groups. The unusual linear fusion of the pyridine ring to the existing benzenoid ring of the coumarin and unprecedented autocatalytic role of iodine under essentially neutral micellar conditions are the key features of the protocol.

7.11 Hydrolysis

As previously indicated keto functionality is ubiquitous in drug and pharmaceutical industries. Synthetic strategies often require protection-deprotection of this group to attain target molecules. Traditionally oxime/imine deprotection is achieved by acidic reagents [105–109], oxidizing agents [110–113], metal salts [114–124] to name a few. In spite of the availability of a plethora of strategies, most of them involve the utilization of toxic chemicals, generation of waste, and hazardous handling. In 2005, Konwar et al. put forward [125] an efficient, green catalytic protocol for the deprotection of oximes and imines (**110**) to carbonyl compounds (**111**) in water under neutral conditions at 25–40°C. The protocol was applied to a variety of aliphatic as well as aromatic oximes/imines (Scheme 7.25).

Current interest in Green protocols made scientists focus on developing multicomponent reactions with nanocatalysis. One of the most widely studied multicomponent reaction (MCR) is the Ugi-4CR [126]. This type of reaction is of

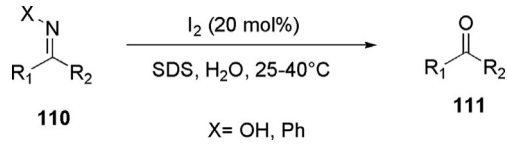

Scheme 7.25 Deprotection of imines and oximes in aqueous media.

particular interest to the synthetic community as these provide direct access to biologically active, Nitrogen-containing heterocyclic scaffolds such as Phenylacetimidamide [127], phenylacetamide [128], and α-amino acid [129]. A group of scientists led by Dr. A. Kumar published a paper [130] describing a highly efficient and environmental-friendly methodology for the synthesis of 2-arylamino-2-phenylacetimidamide derivatives (**114**) from an amine, aldehyde, and isocyanide by ZnO-nanoparticle catalyzed, Ugi-type three-component reaction in water.

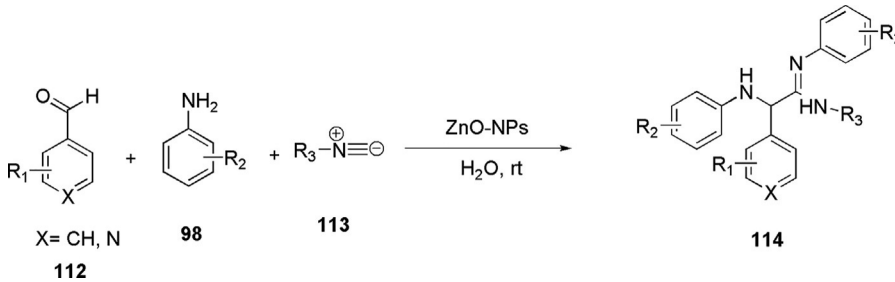

Scheme 7.26 ZnO-NP catalyzed Ugi three-component reaction in water.

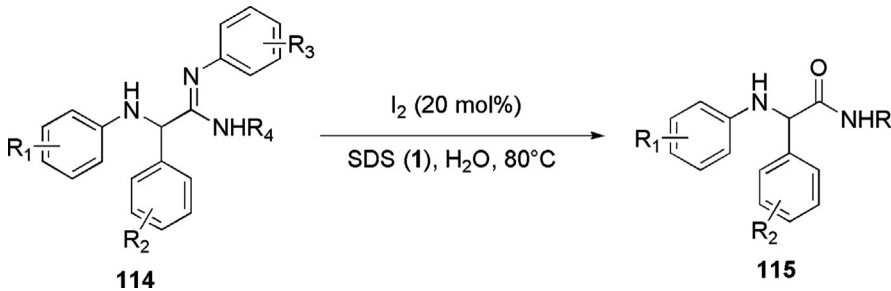

Scheme 7.27 Hydrolysis of phenylacetimidamide.

This reaction has been recently applied successfully for the transformation of 2-arylamino-2-phenylacetimidamide, obtained via the Ugi three-component reaction, into the corresponding 2-amino-2-phenylacetamide derivatives as attractive scaffolds for medicinal chemistry (Scheme 7.26). Neutral hydrolysis in the presence of I_2-SDS (sodium dodecyl sulfate)-water afforded (Scheme 7.27) the corresponding 2-amino-2-phenylacetamide derivatives (**114**).

7.12 Click reaction

Ribavirin (**116**) is a ribosyl-1,2,4-triazole (Fig. 7.8) that exhibits a broad-spectrum of antiviral activity against both DNA and RNA viruses [131]. Ribavirin has been used in combination therapy with interferon (Rebetrol). However, the main drawback is its toxicity. Researchers are focusing on developing analogs which are less toxic.

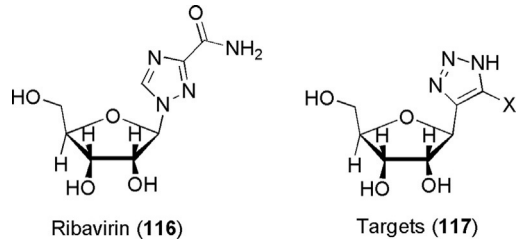

Fig. 7.8 Structure of Ribavirin and its analog.

A group of scientists from France undertook the challenge to synthesize C-ribosyl-1,2,3-triazoles using a C-alkynylation reaction of ribose and a 1,3-DCR. In 2009, they successfully carried out the regioselective synthesis of 1,2,3-triazoles of C-ribosides (**119**) via a Huisgen 1,3-dipolar cycloaddition reaction under a micellar catalysis (Scheme 7.28) [132].

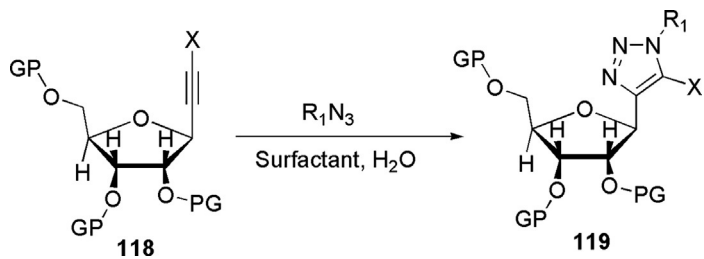

Scheme 7.28 Click reaction of C-alkynyl ribosides under micellar catalysis.

7.13 Reduction strategies in water

Optically active aliphatic hydroxy acids and derivatives are versatile chiral building blocks for many key structural elements in pharmaceuticals and natural products (Fig. 7.9) [133]. Chiral short-chain aliphatic hydroxyl acids and derivatives are key intermediates of many pharmaceuticals and natural products [134] describe the ATH of long-chain aliphatic ketoesters in neat water in the air using chiral surfactant-type metal catalyst with ligand L, providing excellent enantioselectivity for a broad range of substrates.

A green asymmetric reduction of methyl 2-oxodecanoate (**111**) was reported to explore ATH of α-ketoesters using chiral amphiphilic ligands (Scheme 7.29). Pre-catalyst was prepared by mixing the ligand with a metal precursor in the water at

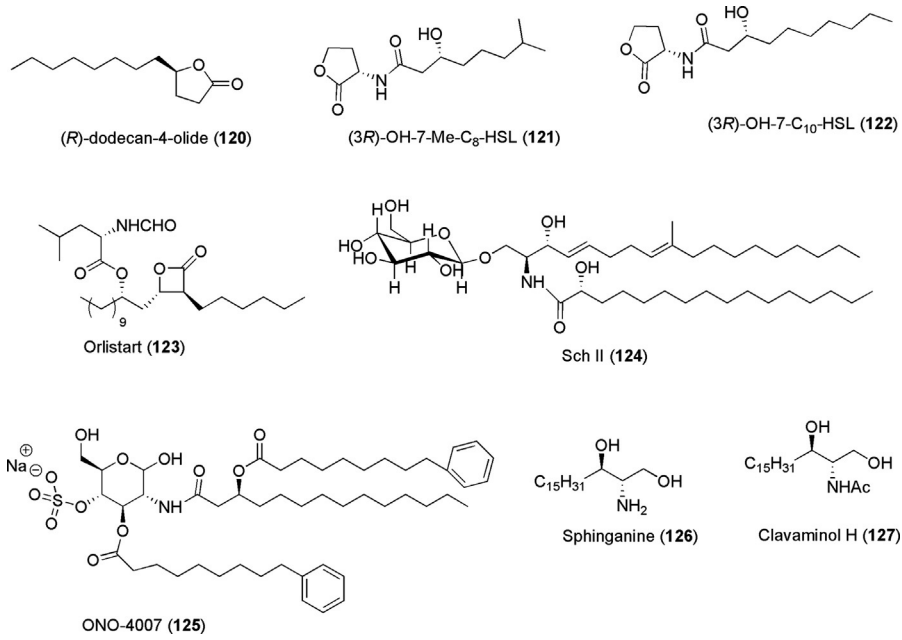

Fig. 7.9 Structures of some biologically active hydroxy acid derivatives.

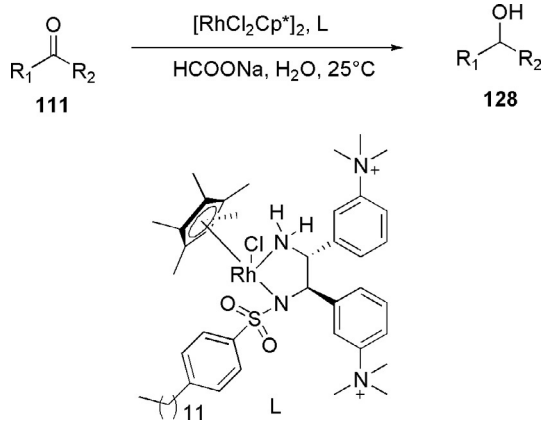

Scheme 7.29 Asymmetric transfer hydrogenation of ketoesters with surfactant type catalyst.

40°C for 2 h, and then it was subjected to catalyze ATH of **111** with HCO_2Na as a hydrogen source in neat water.

Aromatic and heteroaromatic amines feature in a number of pharmaceutically important molecules [135]. In 2016, Lipshutz and coresearchers developed a robust yet mild technology for chemoselective, and efficient reductions of nitrocompounds (**129**) in the water at ambient temperatures using Fe/ppm Pd-NPs in the presence of designer surfactant TPGS-750-M (Scheme 7.30) [136].

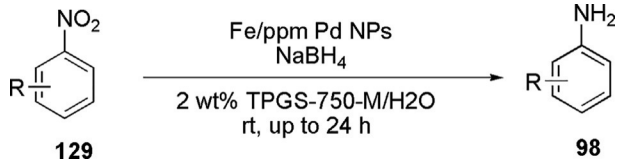

Scheme 7.30 Reduction of nitro-groups catalyzed by Fe/ppm Pd nanoparticles in water.

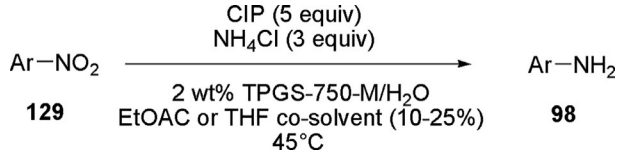

Scheme 7.31 CIP-mediated nitro-group reductions.

One of the direct routes to this class of compounds is by reducing the corresponding nitrocompounds. However, existing methods have several drawbacks such as high pressures and/or temperatures, pyrophoric materials, toxic or dangerous reagents, high-boiling or egregious dipolar, aprotic solvents, precious or toxic metals, long reaction times, expensive ligands, commercially unavailable materials, lack of selectivity, and highly variable yields. To overcome these issues Lipshutz and his group reported [137] a mild, safe, efficient, and environmentally benign reduction of aromatic and heteroaromatic nitro-group (**129**) using inexpensive highly active commercial grade carbonyl iron powder (CIP) in the presence of nanometer-micelles composed of TPGS-750-M in water (Scheme 7.31). Substrate scope revealed that the procedure is tolerant of several functional groups such as ester, halogen, cyano, and keto. The reaction could also be performed in gram-scale.

7.14 Halogenation

Our group also has long-standing interest in carrying out diverse organic transformations in aqueous micellar media. Vicinal difunctionalization is an important synthetic tool as it can lead to biologically important molecules [138]. However, traditional synthetic strategies to furnish halogenated synthons often involves harsh reaction conditions, and toxic reagents. In 2011, we communicated [139] a report delineating region- and stereoselective oxyhalogenation of alkenes and alkynes mediated by cationic surfactant and Lewis acid in water at room temperature. The protocol was applied to a wide variety of substrates including sugar derivatives (Scheme 7.32).

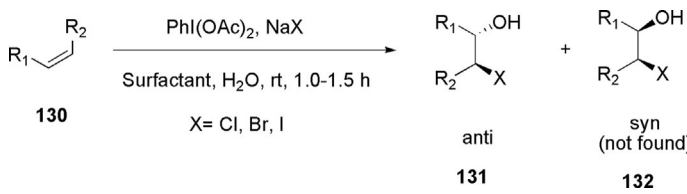

Scheme 7.32 Vicinal difunctionalization of olefin.

α,α-Dihaloketones are highly valuable structural motifs, especially due to their applications in the synthesis of medicinally important heterocycles [140], and pharmaceuticals [141]. Conventional routes targeting these structural motifs involve the use of either/or transition metal catalyst, expensive/toxic halogenating reagent, corrosive oxidant, or toxic organic solvents [142]. In 2018, the group of Dr. Handa reported a mild, general, sustainable, photo-assisted oxyhalogenation protocol that can be applied to synthesize α,α-dibromoketones (**135**) as well as α,α-dichloroketones (**136**) with the use of inexpensive and stable reagents NBS and NCS in water under very mild conditions (Scheme 7.33) [143].

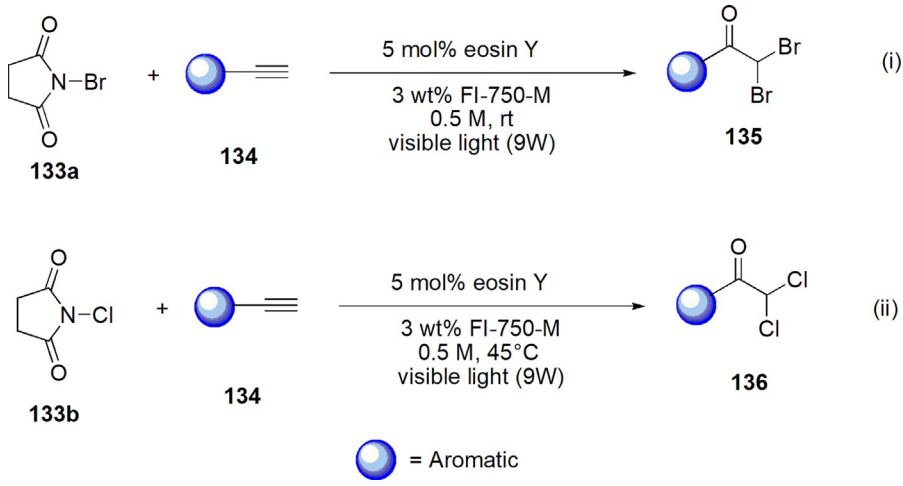

Scheme 7.33 Micellar oxyhaogenation reaction.

Optimization reactions were carried out using phenylacetylene and NBS as model substrates and by varying the surfactant. FI-750-M was found to be most effective in terms of yield and reaction kinetics. The methodology was then extended to micellar oxychlorination.

7.15 Metal-catalyzed C—C bond-forming reaction

Benzodiazepines [144a] are known to be anti-insectans [144b], antitumor agents [144c], muscarinic receptor ligands [144d], fibrinogenic receptor antagonist [144e] and human neurokinin NK1 receptors[144f]. Benzoxazepines are also known as interleukin-2 inhibitors [144g], apoptotic agents having therapeutic potential in both ex vivo chemotherapy-refractory patient samples and in vivo murine carcinoma models [144h], and antitumor agents [144i] many procedures have been developed toward the synthesis of these scaffolds [145]. However, the reactions often required the involvement of either more than a single step, drastic reaction conditions or the use of organic solvents. In 2014, a group of scientists led by Prof. Sen disclosed [146] a

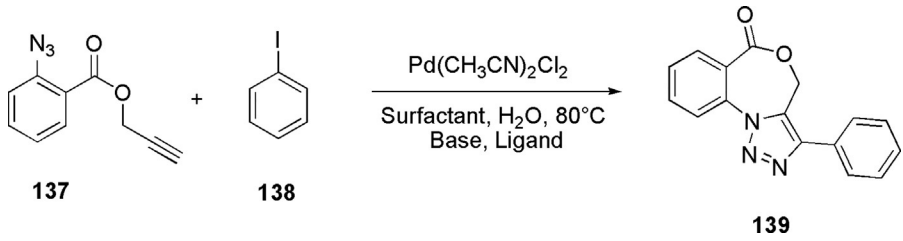

Scheme 7.34 Synthesis of 3-phenyl-[1,2,3]triazolo[1,5-a][4,1]benzoxazepines.

domino Sonogashira-azide alkyne cyclization reaction for the synthesis of triazole benzoxazepinesor benzodiazepines using $Pd(CH_3CN)_2Cl_2$ as a catalyst. They chose prop-2-ynyl 2-azidobenzoates (**137**) and phenyliodide (**138**) as model reactants for their optimization studies (Scheme 7.34). After screening several surfactants they concluded that CTAB worked best with 82% yield. An array of aryl and heteroaryl iodides took part in the reaction giving yields up to 90%.

Hydrocarboxylations of olefins and allenes are a significant synthetic tool for highly variable bioactive molecules [147]. In 2014, Lipshutz and his team members carried out asymmetric gold-catalyzed intramolecular cyclizations of β-allenic acids in aqueous micellar media which generated enantioenric lactones [148]. They screened a variety of chiral ligands such as BINAP, SEGPHOS, SYNPHOS, and BIPHEP to deduce that ligand depicted in Scheme 7.35 was the best. After optimizing reaction conditions with 5-cyclohexylidene-2,2-diphenylpent-4-enoic acid, the group proceeded to show that a variety of precursor allenic acids could be cyclized to afford high yields of product lactones with ee as high as 92%.

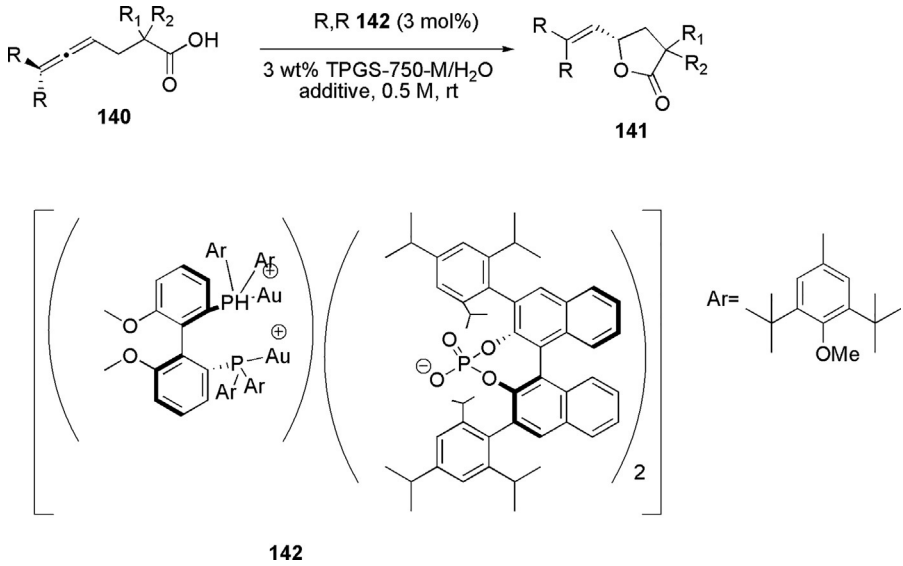

Scheme 7.35 Gold catalyzed lactonization in micellar media.

Since the Nobel Prize-winning Suzuki-Miyaura cross-coupling was put forward, it has been the most used strategy to access biaryl fragments [149]. Traditionally, palladium is the metal which has been used in this reaction. However, the limited availability of this precious platinoid made scientists look for other alternatives. Nickel seemed a logical alternative and has been extensively studied [150]. Most of the reported protocols suffer from drawbacks such as the use of toxic organic solvents, high temperature, and excess base. To address these issues, Lipshutz published [151] a study in 2015, describing nickel-catalyzed Suzuki-Miyaura cross coupling of various aryl and heteroaryl halides with boronic acid/esters in water medium (Scheme 7.36). Model study with 4-methoxybenzyl bromide with phenylboronic acid revealed that ligand 1,1′-bis(diisopropylphosphino)ferrocene(dippf) (**146c**) works best for aryl-aryl couplings while dippf gave best results for heteroaryl coupling partners. A wide variety of functional groups such as formyl, trifluoromethyl, carbamate, ester, acetal, and amide were tolerated during the reaction further proving the mild nature of the methodology.

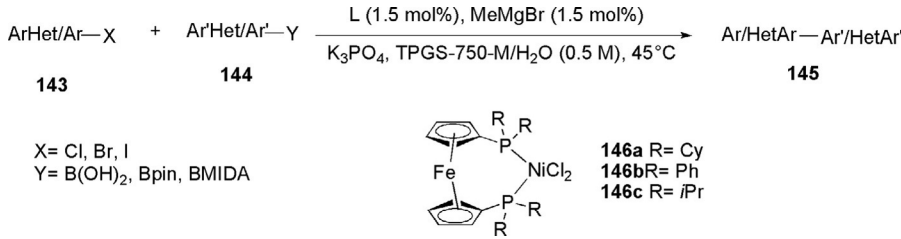

Scheme 7.36 Nanonickel-catalyzed Suzuki-Miyaura cross-couplings in water.

2-Pyridyl-substituted moieties are present in many biologically active natural products [152], pharmaceuticals [153], ligands [154], and fluorescent probes. [155] The best pathway to construct these motifs is by Suzuki-Miyaura cross-coupling reaction. But only few papers have been published on this topic due to the difficulties associated with transmetallation at the two-position of the pyridyl system due to the presence of Lewis basic and electronegative N atom [156–159]. Lipshutz et al. successfully coupled 2-pyridyl MIDA boronates with aryl halides under environmentally responsible micellar catalysis conditions [160]. The presence of F, Cl, or OPh group at the sixth position of 2-B(MIDA)-pyridyl systems assisted in the Suzuki-Miyaura cross-coupling reaction (Scheme 7.37).

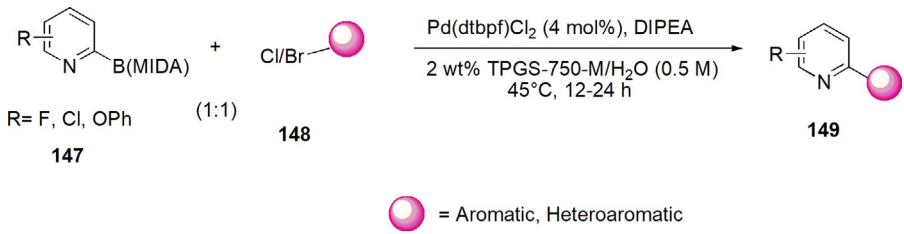

Scheme 7.37 Suzuki-Miyaura cross-couplings of 2-pyridyl MIDA boronates.

Heterobiaryl rings are versatile building blocks that are abundant in clinically used drugs, drug candidates, and structurally diverse natural products [161]. Traditionally these moieties are synthesized using various metal-catalyzed coupling reactions such as Hiyama, Negishi, Stille, and other often used reactions. Recently, Wang and his group reported Suzuki-Miyaura reaction in the presence of nonionic surfactant TPGS-750-M in water to carry out coupling of particularly challenging 2-pyridyl boronate esters [162]. This substrate is extremely difficult to handle as boronate esters placed next to basic nitrogen tend to undergo proto-deborylation under standard Suzuki coupling conditions [163]. Optimization study revealed that $PdCl_2$(dtbpf)/Et_3N/THF/2%TPGS-750-M water system at 40°C produced the best yield. Both electron-deficient pyridyl bromides and electron-rich phenyl bromides coupled with 6-chloro-2-pyridyl boronic ester to give good yields and good chemoselectivity. The reaction also worked pretty well for heteroaryl boronate esters giving up to 80% yield (Scheme 7.38).

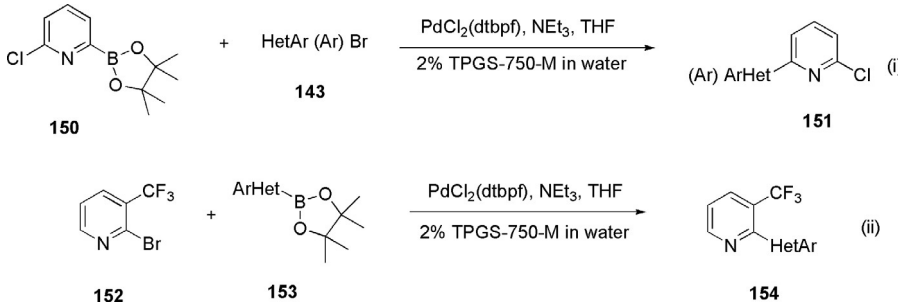

Scheme 7.38 Micellar Suzuki-Miyaura coupling.

7.16 Conclusion

Over the past decade, an array of reactions has been performed in aqueous micellar media and most of which are represented in this chapter. Hundreds of articles are being published on this active research area. It is needless to say that we are far from being as efficient as the performance of nature. Continuous and systematic effort in this regard is crucial for protecting nature and in turn mankind.

References

[1] (a) P.T. Anastas, J.C. Warner, Green Chemistry: Theory and Practice, Oxford University Press, New York, 1998. (b) P.T. Anastas, M.M. Kirchhoff, Origins, Current Status, and Future Challenges of Green Chemistry, Acc. Chem. Res. 35 (2002) 686–694. (c) C. Bolm, O. Beckmann, O.G.A. Dabard, Angew. Chem. Int. Ed. 37 (1999) 1198–1209.

[2] G. La Sorella, G. Strukul, A. Scarso, Recent advances in catalysis in micellar media, Green Chem. 17 (2015) 644–683.

[3] (a) U.M. Lindström, F. Andersson, Angew. Chem. Int. Ed., 45 (2006) 548–551. (b) D. Adams, P. Dyson, S. Tavener, Chemistry in Alternative Reaction Media, John Wiley & Sons, 2004. (c) C.J. Li, Organic reactions in aqueous media—with a focus on carbon-carbon bond formation, Chem. Rev. 93 (1993) 2023–2035. (d) C.J. Li, Organic reactions in aqueous media with a focus on carbon – carbon bond formations: a decade update, Chem. Rev. 105 (2005) 3095–3166.

[4] R.A. Sheldon, Green solvents for sustainable organic synthesis: state of the art, Green Chem. 7 (2005) 267–278.

[5] For reviews on phase-transfer catalysis, see: (a) Phase Transfer Catalysis, ed. E. V. Dehmlow and S. S. Dehmlow, VCH, Weinheim, 3rd ed., 1993. (b) C.M. Starks, C.L. Liotta, M. Halpern (Eds.), Phase-Transfer Catalysis, Chapman & Hall, New York, 1994. (c) Y. Sasson, R. Neumann (Eds.), Handbook of Phase-Transfer Catalysis, Blackie Academic & Professional, London, 1997. (d) M.E. Halpern (Ed.), Phase-Transfer Catalysis, American Chemical Society, Washington DC, 1997. ACS Symposium Series 659.

[6] J.N. Israelachvili, Intermolecular and Surface Forces, Academic Press, New York, 1985.

[7] (a) H.P. Lin, C.Y. Mou, S.B. Lin, Adv. Mater. 12 (2000) 103. (b) H.B.S. Chan, P.M. Budd, T.V. Naylor, Control of mesostructured silica particle morphology, J. Mater. Chem. 11 (2001) 951–957. (c) X. Gong, J. Liu, S. Baskaran, R.D. Voise, J.S. Young, Surfactant-assisted processing of carbon nanotube/polymer composites, Chem. Mater. 12 (2000) 1049–1052. (d) C.C. Chen, C.Y. Chao, Z.H. Lang, Simple solution-phase synthesis of soluble CdS and CdSe nanorods, Chem. Mater. 12 (2000) 1516–1518. (e) Y. Xiong, Y. Xie, J. Yang, R. Zhang, C.h. Wu, G.J. Du, In situ micelle–template–interface reaction route to CdS nanotubes and nanowires, Mater. Chem. 12 (2002) 3712–3716.

[8] A. Sorrenti, O. Illa, R.M. Ortuño, Amphiphiles in aqueous solution: well beyond a soap bubble, Chem. Soc. Rev. 42 (2013) 8200–8219.

[9] D.M. Vriezema, M.C. Aragonés, J.A.A.W. Elemans, J.J.L.M. Cornelissen, A.E. Rowan, R.J.M. Nolte, Self-assembled nanoreactors, Chem. Rev. 105 (2005) 1445–1490.

[10] P. Pandit, N. Chatterjee, S. Halder, S.K. Hota, A. Patra, D.K. Maiti, PhIO as a powerful cyclizing reagent: regiospecific [3+2]-tandem oxidative cyclization of imine toward cofacially self-aggregated low molecular mass organic materials, J. Org. Chem. 74 (2009) 2581–2584.

[11] (a) in: B. Cornils, W.A. Herrmann (Eds.), Aqueous-Phase Organometallic Catalysis. Concepts and Applications, Wiley-VCH, Weinheim, 1998. (b) J.B.F.N. Engberts, B.L. Feringa, E. Keller, S. Otto, Recl. TraV. Chim. Pays-Bas 115 (1996) 457. (c) F. Fringuelli, O. Piermatti, F. Pizzo, L. Vaccaro, Recent Advances in Lewis Acid Catalyzed Diels – Alder Reactions in Aqueous Media, Eur. J. Org. Chem. (2001) 439–455. (d) J.P. Genet, M. Savignac, Recent developments of palladium(0) catalyzed reactions in aqueous medium, J. Organomet. Chem. 576 (1999) 305–317. (e) S. Kobayashi, K. Manabe, in: M. Shibasaki, J.F. Stoddart, F. Vgtle (Eds.), Stimulating Concepts in Chemistry, Wiley-VCH, Weinheim, 2000. (f) S. Kobayashi, K. Manabe, Development of novel lewis acid catalysts for selective organic reactions in aqueous media, Acc. Chem. Res. 35 (2002) 209–217.

[12] (a) J. Otera, Esterification, Wiley-VCH, Weinheim, Germany, 2003. (b) J. Mulzer, in: B.M. Trost, L. Fleming (Eds.), Comprehensive Organic Synthesis, vol. 6, Pergamon Press, Oxford, 1991. p. 323.

[13] (a) Y. Liu, E. Ranucci, M.S. Lindblad, A.C. Albertsson, New biodegradable polymers from renewable sources: Polyester-carbonates based on 1,3-propylene-co-1,4-cyclohexanedimethylene succinate, J. Polym. Sci., Part A: Polym. Chem. 39 (2001) 2508–2519. (b) D. Shekhawat, K. Nagarajan, J.E. Jackson, D.J. Miller, Formation of

citraconic anhydride via condensation of dialkyl succinates and formaldehyde, Appl. Catal. A 223 (2002) 261–273.

[14] A. Orjuela, A.J. Yanez, A. Santhanakrishnan, C.T. Lira, D.J. Miller, Kinetics of mixed succinic acid/acetic acid esterification with Amberlyst 70 ion exchange resin as catalyst, Chem. Eng. J. 188 (2012) 98–107.

[15] (a) Diversified Natural Products Inc, http://www.dnpworld.com. (b) S.C. Piscitelli, T.F. Goss, J.H. Wilton, D.T. D'Andrea, H. Goldstein, J.J. Schentag, Effects of ranitidine and sucralfate on ketoconazole bioavailability, Antimicrob. Agents Chemother. 35 (1991) 1765–1771. (c) M.E. Thase, W. MacFadden, R.H. Weisler, W. Chang, B.R. Paulsson, A. Khan, J.R. Calabrese, G. Bolder, Efficacy of quetiapine monotherapy in bipolar I and II depression: a double-blind, placebo-controlled study (The BOLDER II Study), J. Clin. Psychopharmacol. 26 (2006) 600–609.

[16] K. Manabe, S. Iimura, X.-M. Sun, S. Kobayashi, Dehydration reactions in water. brønsted acid-surfactant-combined catalyst for ester, ether, thioether, and dithioacetal formation in water, J. Am. Chem. Soc. 124 (2002) 11971–11978.

[17] F. Rajabi, R. Luque, An efficient renewable-derived surfactant foraqueous esterification reactions, RSC Adv. 4 (2014) 5152–5155.

[18] (a) J.A. Joule, K. Mills, Heterocyclic Chemistry, fourth ed., Blackwell, Oxford, UK, 2000. (b) D.J. Triggle, 1,4-Dihydropyridines as calcium channel ligands and privileged structures, Cell. Mol. Neurobiol. 23 (2003) 293–303.

[19] (a) B. Love, M. Goodman, K. Snader, R. Tedeschi, E. Macko, Hantzsch-type dihydropyridine hypotensive agents, J. Med. Chem. 17 (1974) 956–965. (b) F. Bossert, H. Meyer, E. Wehinger, 4-Aryldihydropyridines, a new class of highly active calcium antagonists, Angew. Chem. Int. Ed. Engl. 20 (1981) 762–769. (c) S. Goldmann, J. Stoltefuss, 1,4-Dihydropyridines: effects of chirality and conformation on the calcium antagonist and calcium agonist activities, Angew. Chem. Int. Ed. Engl. 30 (1991) 1559–1578. (d) R.H. Fagard, Dihydropyridines and the treatment ofhyerptension, J. Clin. Basic Cardio. 2 (1999) 163–166. (e) V. Klusa, Drugs Future 20 (1995) 135–138. (f) I.O. Donkor, X. Zhou, J. Schmidt, K.C. Agrawal, V. Kishore, Synthesis and radioprotective effects of adamantyl substituted 1,4-dihydropyridine derivatives, Bioorg. Med. Chem. 6 (1998) 563–568. (g) T. Godfraid, R. Miller, M. Wibo, Calcium antagonism and calcium entry blockade, Pharmocol. Rev. 38 (1986) 321–416. (h) R.G. Bretzel, C.C. Bollen, E. Maeser, K.F. Federlin, Am. J. Kidney Dis. 21 (1993) 53. (i) R.G. Bretzel, C.C. Bollen, E. Maeser, K.F. Federlin, Drugs Future 17 (1992) 465. (j) R. Boer, V. Gekeler, Drugs Future 20 (1995) 499.

[20] G.D. Henry, De Novo Synthesis of Substituted Pyridines, Tetrahedron 60 (2004) 6043–6061.

[21] (a) D.A. Colby, R.G. Bergman, J.A. Ellman, Synthesis of dihydropyridines and pyridines from imines and alkynes via C-H Activation, J. Am. Chem. Soc. 130 (2008) 3645–3651. (b) J. Barluenga, M.A. Fernandez-Rodriguez, P. Garca, E. Aguilar, Gold-catalyzed intermolecular hetero-dehydro-diels – alder cycloaddition of captodative dienynes with nitriles: a new reaction and regioselective direct access to pyridines, J. Am. Chem. Soc. 130 (2008) 2764–2765. (c) K. Parthasarathy, M. Jeganmohan, C.H. Cheng, Rhodium-catalyzed one-pot synthesis of substituted pyridine derivatives from α, β-unsaturated ketoximes and alkynes, Org. Lett. 10 (2008) 325–328. (d) J. Dash, T. Lechel, H.U. Reissig, Scope of a novel three-component synthesis of highly functionalized pyridines(dagger), Org. Lett. 9 (2007) 5541–5544. (e) M. Movassaghi, M.D. Hill, O.K. Ahmad, Direct synthesis of pyridine derivatives, J. Am. Chem. Soc. 129 (2007) 10096–10097. (f) B.M. Trost, A.C. Gutierrez, Ruthenium-catalyzed

cycloisomerization – 6π-cyclization: a novel route to pyridines, Org. Lett. 9 (2007) 1473–1476. (g) M.D. Fletcher, T.E. Hurst, T.J. Miles, C.J. Moody, Synthesis of highly-functionalised pyridines via hetero-Diels–Alder methodology: reaction of 3-siloxy-1-aza-1,3-butadienes with electron deficient acetylenes, Tetrahedron 62 (2006) 5454–5463. (h) M. Movassaghi, M.D. Hill, Synthesis of substituted pyridine derivatives via the ruthenium-catalyzed cycloisomerization of 3-azadienynes, J. Am. Chem. Soc. 128 (2006) 4592–4593. (i) K. Tanaka, N. Suzuki, G. Nishida, Cationic rhodium(I)/modified-BINAP catalyzed [2+2+2] cycloaddition of alkynes with nitriles, Eur. J. Org. Chem. (2006) 3917–3922. (j) Y. Yamamoto, K. Kinpara, R. Ogawa, H. Nishiyama, K. Itoh, Ruthenium-catalyzed cycloaddition of 1,6-diynes and nitriles under mild conditions: role of the coordinating group of nitriles, Chem. A Eur. J. 12 (2006) 5618–5631. (k) M.M. McCormick, H.A. Duong, G. Zuo, J. Louie, A nickel-catalyzed route to pyridines, J. Am. Chem. Soc. 127 (2005) 5030–5031.

[22] P.P. Ghosh, P. Mukherjee, A.R. Das, Triton-X-100 catalyzed synthesis of 1,4-dihydropyridines and their aromatization to pyridinesand a new one pot synthesis of pyridines using visiblelight in aqueous media, RSC Adv. 3 (2013) 8220–8226.

[23] A. Dömling, I. Ugi, Multicomponent reactions with isocyanides, Angew. Chem. Int. Ed. 39 (2000) 3168–3210.

[24] (a) M.H. Fisher, A. Lusi, J.R. Egerton, Anthelmintic dihydroquinoxalino[2,3-b] quinoxalines, J. Pharm. Sci. 66 (1977) 1349–1352. (b) Antimicrobial:P. Sanna, A. Carta, M. Loriga, S. Zanetti, L. Sechi, Farmacoterapia 54 (1999) 169. (c) Antimycobacterial:L.E. Seitz, W.J. Suling, R.C. Reynolds, Synthesis and antimycobacterial activity of pyrazine and quinoxaline derivatives, J. Med. Chem. 45 (2002) 5604–5606. (d) Inhibitor of PDGF receptor tyrosine kinase:W. He, M.R. Myers, B. Hanney, A.P. Spada, G. Bilder, H. Galzcinski, D. Amin, S. Needle, K. Page, Z. Jayyosi, M.H. Perrone, Potent quinoxaline-Based inhibitors of PDGF receptor tyrosine kinase activity. Part 2: the synthesis and biological activities of RPR127963 an orally bioavailable inhibitor, Bioorg. Med. Chem. Lett. 13 (2003) 3097–3100. (e) Antiprotozoal:G. Aguirre, H. Cerecetto, R. DiMaio, M. Gonzales, M.E.M. Alfaro, A. Jaso, B. Zarranz, M.A. Ortega, I. Aldana, A. Monge-Vega, Quinoxaline N,N′-dioxide derivatives and related compounds as growth inhibitors of Trypanosoma cruzi. Structure–activity relationships, Bioorg. Med. Chem. Lett. 14 (2004) 3835–3839. (f) X. Hui, J. Desrivot, C. Bories, P.M. Loiseau, X. Franck, R. Hocquemiller, B. Figadere, Synthesis and antiprotozoal activity of some new synthetic substituted quinoxalines, Bioorg. Med. Chem. Lett. 16 (2006) 815–820. (g) Akt inhibitor: C.W. Lindsley, Z. Zhao, W.H. Leister, R.G. Robinson, S.F. Barnett, D. Defeo-Jones, R.E. Jones, G.D. Hartman, J.R. Huff, H.E. Huber, M.E. Duggan, Allosteric Akt (PKB) inhibitors: discovery and SAR of isozyme selective inhibitors, Bioorg. Med. Chem. Lett. 15 (2005) 761–764.

[25] (a) Z. Zhao, D.D. Wisnoski, S.E. Wolkenberg, W.H. Leister, Y. Wang, C.W. Lindsley, General microwave-assisted protocols for the expedient synthesis of quinoxalines and heterocyclic pyrazines, Tetrahedron Lett. 45 (2004) 4873–4876. (b) R.S. Bhosale, S.R. Sarda, S.S. Ardhapure, W.N. Jadhav, S.R. Bhusare, R.P. Pawar, An efficient protocol for the synthesis of quinoxaline derivatives at room temperature using molecular iodine as the catalyst, Tetrahedron Lett. 46 (2005) 7183–7186. (c) S. Ahmad, M. Ali, An efficient solid acid promoted synthesis of quinoxaline derivatives at room temperature, Chin. J. Chem. 25 (2007) 818–821. (d) J.-J. Cai, J.-P. Zou, X.-Q. Pan, W. Zhang, Gallium(III) triflate-catalyzed synthesis of quinoxaline derivatives, Tetrahedron Lett.

49 (2008) 7386–7390. (e) D.-Q. Shi, G.-L. Dou, S.-N. Ni, J.-W. Shi, X.-Y. Li, An efficient synthesis of quinoxaline derivatives mediated by stannous chloride, J. Heterocyclic Chem. 45 (2008) 1797–1801. (f) T.M. Potewar, S.A. Ingale, K.V. Srinivasan, Efficient synthesis of quinoxalines in the ionic liquid 1-n-butylimidazolium tetrafluoroborate ([Hbim]BF4) at ambient temperature, Synth. Commun. 38 (2008) 3601–3606. (g) J. Li, D.-N. Jiang, J.-X. Chen, M.-C. Liu, J.-C. Ding, H.-Y. Wua, Eco-friendly synthesis of quinoxaline derivatives by grinding under solvent-free conditions, J. Heterocyclic Chem. 48 (2011) 403–406. (h) R. Mahesh, A.K. Dhar, T.V.N.V. Tara Sasank, S. Thirunavukkarasu, T. Devadoss, Citric acid: an efficient and green catalyst for rapid one pot synthesis of quinoxaline derivatives at room temperature, Chin. Chem. Lett. 22 (2011) 389–392. (i) J.-P. Wan, S.-F. Gan, J.-M. Wu, Y. Pan, Water mediated chemoselective synthesis of 1,2-disubstituted benzimidazoles using o-phenylenediamine and the extended synthesis of quinoxalines, Green Chem. 11 (2009) 1633–1637. (j) S. Paul, B. Basu, Synthesis of libraries of quinoxalines through eco-friendly tandem oxidation–condensation or condensation reactions, Tetrahedron Lett. 52 (2011) 6597–6602.

[26] S. Antoniotti, E. Duñach, Direct and catalytic synthesis of quinoxaline derivatives from epoxides and ene-1,2-diamines, Tetrahedron Lett. 43 (2002) 3971–3973.

[27] (a) C. Mousset, O. Provot, A. Hamze, J. Bignon, J.-D. Brion, M. Alami, DMSO–PdI_2 as a powerful oxidizing couple of alkynes into benzils: one-pot synthesis of nitrogen-containing five- or six-membered heterocycles, Tetrahedron 64 (2008) 4287–4294. (b) S. Chandrasekhar, N.K. Reddy, V.P. Kumar, Oxidation of alkynes using PdCl2/CuCl2 in PEG as a recyclable catalytic system: one-pot synthesis of quinoxalines, Tetrahedron Lett. 51 (2010) 3623–3625. (c) M. Tingoli, M. Mazzella, B. Panunz, A. Tuzi, Elemental iodine or diphenyl diselenide in the [bis(trifluoroacetoxy)iodo]benzene-mediated conversion of alkynes into 1,2-diketones, Eur. J. Org. Chem. (2011) 399–404.

[28] D. Kumar, K. Seth, D.N. Kommi, S. Bhagat, A.K. Chakraborti, Surfactant micelles as microreactors for the synthesis of quinoxalines in water: scope and limitations of surfactant catalysis, RSC Adv. 3 (2013) 15157–15168.

[29] (a) T.D. Gootz, K.E. Brighty, Fluoroquinolone antibacterials: SAR mechanism of action, resistance, and clinical aspects, Med. Res. Rev. 16 (1996) 433–486. (b) B. Llorente, F. Leclerc, R. Cedergren, Using SAR and QSAR analysis to model the activity and structure of the quinolone—DNA complex, Bioorg. Med. Chem. 4 (1996) 61–71. (c) L. Ferrero, B. Cameron, B. Manse, D. Lagneaux, J. Crouzet, A. Famechon, F. Blanche, Cloning and primary structure of *Staphylococcus aureus* DNA topoisomerase IV: a primary target of fluoroquinolones, Mol. Microbiol. 13 (1994) 641–653. (d) M.P. Wentland, G.Y. Lesher, M. Reuman, M.D. Gruett, B. Singh, S.C. Aldous, P.H. Dorff, J.B. Rake, S.A. Coughlin, Mammalian topoisomerase II inhibitory activity of 1-cyclopropyl-6,8-difluoro-1,4-dihydro-7-(2,6-dimethyl-4-pyridinyl)-4-oxo-3-quinolinecarboxylic acid and related derivatives, J. Med. Chem. 36 (1993) 2801–2809. (e) S.H. Elsea, N. Osheroff, J.L. Nitiss, Cytotoxicity of quinolones toward eukaryotic cells. Identification of topoisomerase II as the primary cellular target for the quinolone CP-115, 953 in yeast, J. Biol. Chem. 267 (1992) 13150–13153. (f) P.G. Reddy, S. Baskaran, Microwave assisted amination of quinolone carboxylic acids: an expeditious synthesis of fluoroquinolone antibacterials, Tetrahedron Lett. 42 (2001) 6775–6777.

[30] (a) F. Strelitz, H. Flon, I.N. Asheshov, Proc. Natl. Acad. Sci. U. S. A. 41 (1955) 620. (b) T.E. Eble, G.A. Boyack, C.M. Large, W.H. DeVries, Antibiot. Chemother. 8 (1958) 627.

[31] (a) P. Ferrer, C. Aveñdano, M. Söllhuber, Liebigs Ann. (1995) 1895. (b) A. Afonso, J. Weinstein, M.J. Gentles, Schering Corp, PCT Int. Appl. (1992). WO9203327.

[32] (a) L.A. McQuaid, E.C.R. Smith, D. Lodge, E. Pralong, J.H. Wikel, D.O. Calligaro, P.J. O'Malley, 3-Phenyl-4-hydroxyquinolin-2(1H)-ones: potent and selective antagonists at the strychnine-insensitive glycine site on the N-methyl-D-aspartate receptor complex, J. Med. Chem. 35 (1992) 3423–3425. (b) R.W. Carling, P.D. Leeson, K.W. Moore, C.R. Moyes, M. Duncton, M.L. Hudson, R. Baker, A.C. Foster, S. Grimwood, J.A. Kemp, G.R. Marshall, M.D. Tricklebank, K.L. Saywell, 4-Substituted-3-phenylquinolin-2(1H)-ones: acidic and nonacidic glycine site N-methyl-d-aspartate antagonists with in vivo activity, J. Med. Chem. 40 (1997) 754–765. (c) H. Hayashi, Y. Miwa, I. Miki, S. Ichikawa, N. Yoda, A. Ishii, M. Kono, F. Suzuki, 5-HT3 receptor antagonists. 1. New quinoline derivatives, J. Med. Chem. 35 (1992) 4893–4902.

[33] S. Naskar, P. Saha, R. Paira, A. Hazra, P. Paira, S. Mondal, A. Maity, K.B. Sahu, S. Banerjee, N.B. Mondal, Synthesis of polycyclic fused 2-quinolones in aqueous micellar system, Tetrahedron Lett. 51 (2010) 1437–1440.

[34] (a) N. Singh, A. Pandurangan, K. Rana, P. Anand, A. Ahmad, A.K. Tiwari, Benzimidazole: a short review of their antimicrobial activities, Int. Curr. Pharm. J. 1 (2012) 119–127. (b) C. Mukhopadhyay, S. Ghosh, S. Sengupta, S. De, Synthesis of 2-alkyl substituted benzimidazoles under microwave irradiation: anti-proliferative effect of some representative compounds on human histiocytic lymphoma cell U937, RSC Adv. 1 (2011) 1033–1037. (c) S.Demirayak, I. Kayagil, L. Yurttas, Microwave supported synthesis of some novel 1,3-Diarylpyrazino[1,2-a]benzimidazole derivatives and investigation of their anticancer activities, Eur. J. Med. Chem. 46 (2011) 411–416. (d) J.E. Payne, C. Bonnefous, K.T. Symons, P.M. Nguyen, M. Sablad, N. Rozenkrants, Y. Zhang, L. Wang, N. Yazdani, A.K. Shiau, S.A. Noble, P. Rix, T.S. Rao, C.A. Hassig, N.D. Smith, Discovery of Dual Inducible/Neuronal Nitric Oxide Synthase (iNOS/nNOS) Inhibitor Development Candidate 4-((2-Cyclobutyl-1H-imidazo[4,5-b] pyrazin-1-yl)methyl)-7,8-difluoroquinolin-2(1H)-one (KD7332) Part 2: identification of a novel, potent, and selective series of benzimidazole-quinolinone iNOS/nNOS dimerization inhibitors that are orally active in pain models, J. Med. Chem. 53 (2010) 7739–7755. (e) R. Sevak, A. Paul, S. Goswami, D. Santani, Pharmacol. Res. 46 (2002) 351–356. (f) L.K. Labanauskas, A.B. Brukstus, P.G. Gaidelis, V.A. Bucinskaite, E.B. Udrenaite, V.K. Dauksas, Pharm. Chem. J. 34 (2000) 353–355. (g) B. Can-Eke, M.O. Puskullu, E. Buyukbingol, M. Iscan, A study on the antioxidant capacities of some benzimidazoles in rat tissues, Chem. Biol. Interact. 113 (1998) 65–77. and references cited there in. (h) S. Bhattacharya, P. Chaudhuri, Curr. Med. Chem. 15 (2008) 1762–1777. (i) M. Boiani, M. Gonz'alez, Imidazole and benzimidazole derivatives as chemotherapeutic agents, Mini-Rev. Med. Chem. 5 (2005) 409–424. (j) D.A. Horton, G.T. Bourne, M. L. Smythe, The combinatorial synthesis of bicyclic privileged structures or privileged substructures, Chem. Rev. 103 (2003) 893–930.

[35] L.J. Scott, C.J. Dunn, G. Mallarkey, M. Sharpe, Esomeprazole: a review of its use in the management of acid-related disorders, Drugs 62 (2002) 1503–1538.

[36] P.J. Venkatesan, Albendazole, J. Antimicrob. Chemother. 41 (1998) 145–147.

[37] H. Al Muhaimeed, A parallel-group comparison of astemizole and loratadine for the treatment of perennial allergic rhinitis, J. Int. Med. Res. 25 (1997) 175–181.

[38] V. Kumar, D.G. Khandare, A. Chatterjee, M. Banerjee, DBSA mediated chemoselective synthesis of 2-substituted benzimidazoles in aqueous media, Tetrahedron Lett. 54 (2013) 5505–5509.

[39] (a) R.A. Floyd, K. Hensley, M.J. Forster, J.A. Kelleher-Andersson, P.L. Wood, Mech. Ageing Dev. 123 (2002) 1021. (b) R.A. Floyd, Adv. Pharmarcol. 38 (1997) 361. (c) in: R.A. Floyd, K. Hensley, C.C. Chiuch (Eds.), Ann. N. Y. Acad. Sci. 899 (2000) 222. (d) Y. Kotake, Antioxid. Redox Signal. 1 (1999) 481. (e) K. Hensley, J.M. Carney, T. Tabatabaie, Q. Pye, R.A. Floyd, Int. Rev. Neurobiol. 40 (1999) 299. (f) G. Durand, A. Polidori, J.-P. Salles, B. Pucci, Synthesis of a new family of glycolipidic nitrones as potential antioxidant drugs for neurodegenerative disorders, Bioorg. Med. Chem. Lett. 13 (2003) 859–862.

[40] A. Chatterjee, D.K. Maiti, P.K. Bhattacharya, Water exclusion reaction in aqueous media: nitrone formation and cycloaddition in a single pot, Org. Lett. 5 (2003) 3967–3969.

[41] A. Chatterjee, P.K. Bhattacharya, Stereoselective synthesis of chiral oxepanes and pyrans through intramolecular nitrone cycloaddition in organized aqueous media, J. Org. Chem. 71 (2006) 345–348.

[42] P.J. Scheuer, W. Takahashi, J. Tsutsumi, T. Yoshida, Ciguatoxin: isolation and chemical nature, Science 155 (1967) 1267–1268.

[43] M. Murata, A.M. Legrand, T. Yasumoto, A probable partial structure of ciguatoxin isolated from the moray eel *Gymnothorax javanicus*, Tetrahedron Lett. 30 (1989) 3793–3796.

[44] (a) T. Yasumoto, M. Murata, Marine toxins, Chem. Rev. 93 (1993) 1897–1909. (b) S.D. Levine, R.E. Adams, R. Chem, M.L. Cotter, A.-F. Hirsch, V.V. Kane, R.M. Kanojia, C. Shaw, M.P. Wachter, E. Chin, R. Huettermann, P. Ostrowski, J.L. Mateos, L. Noriega, A. Guzmann, A. Mijazez, L. Tavor, Zoapatanol and montanol, novel oxepane diterpenoids, from the Mexican plant zoapatle (Montanoa tomentosa), J. Am. Chem. Soc. 101 (1979) 3404–3405.

[45] U. Shmueli, S. Carmely, A. Groweiss, Y. Kashman, Sipholenol and sipholenone, two new triterpenes from the marine sponge siphonochalina siphonella (levi), Tetrahedron Lett. 22 (1981) 709–712.

[46] T. Irie, M. Suzuki, T. Masamune, Laurencin, a constituent of Laurencia glandulifera Kützing, Tetrahedron 24 (1968) 4193–4205.

[47] (a) A. Padwa, W.H. Pearson, Synthetic Applications of 1,3-Dipolar Cycloaddition Chemistry Toward Heterocycles and Natural Products, Wiley, New York, 2003. Chapter 1. (b) J. Revuelta, S. Cicchi, A. Goti, A. Brandi, Enantiopure cyclic nitrones: a useful class of building blocks for asymmetric syntheses, Synthesis (2007) 485–504. (c) G. Broggini, Pyrrolizidine and indolizidine syntheses involving 1,3-dipolar cycloadditions, Synthesis (1999) 905–917. (d) M. Frederickson, Optically active isoxazolidines via asymmetric cycloaddition reactions of nitrones with alkenes: applications in organic synthesis, Tetrahedron 53 (1997) 403–425. (e) A. Piperno, S.V. Giofre, D. Iannazzo, R. Romeo, G. Romeo, U. Chiacchio, A. Rescifina, D.G. Piotrowska, Synthesis of C-4′Truncated Phosphonated Carbocyclic 2′-Oxa-3′-azanucleosides as antiviral agents, J. Org. Chem., 75 (2010) 2798–2805. (f) U. Chiacchio, E. Balestrieri, B. Macchi, D. Iannazzo, A. Piperno, A. Rescifina, R. Romeo, M. Saglimbeni, T. Sciortino, V. Vincenza, A. Mastino, G. Romeo, Synthesis of Phosphonated Carbocyclic 2′-Oxa-3′-aza-nucleosides: novel inhibitors of reverse transcriptase, J. Org. Chem. 48 (2005) 1389–1394. (g) A. Rescifina, M.A. Chiacchio, A. Corsaro, E.D. Clercq, D. Iannazzo, A. Mastino, A. Piperno, G. Romeo, R. Romeo, V. Valveri, Synthesis and biological activity of isoxazolidinyl polycyclic aromatic hydrocarbons: potential DNA intercalators, J. Med. Chem. 49 (2006) 709–715. (h) U. Chiacchio, D. Iannazzo, A. Piperno,

R. Romeo, G. Romeo, A. Rescifina, M. Saglimbeni, Synthesis and biological evaluation of phosphonated carbocyclic 2′-oxa-3′-aza-nucleosides, Bioorg. Med. Chem. 14 (2006) 955–959. (i) M.P. Sadashiva, H. Mallesha, N.A. Hitesh, K.S. Rangappa, Synthesis and microbial inhibition study of novel 5-imidazolyl substituted isoxazolidines, Bioorg. Med. Chem. 12 (2004) 6389–6395.

[48] (a) V. Nair, T.D. Suja, Intramolecular 1,3-dipolar cycloaddition reactions in targeted syntheses, Tetrahedron 63 (2007) 12247–12275. (b) J.H. Jeong, S.M. Weinreb, Formal Total Synthesis of the Cytotoxic Marine Ascidian Alkaloid Haouamine A, Org. Lett. 8 (2006) 2309–2312. (c) O. Tamura, N. Iyama, H. Ishibashi, Syntheses of (−)-funebrine and (−)-funebral, using sequential transesterification and intramolecular cycloaddition of a chiral nitrone, J. Org. Chem. 69 (2004) 1475–1480. (d) D.D. Dhavale, S.M. Jachak, N.P. Karche, C. Trombini, Synthesis of trihydroxy quinolizidine alkaloids: 1,3-addition reaction of allylmagnesium bromide to a sugar nitrone, Tetrahedron 60 (2004) 3009–3016. (e) J.D. White, J.D. Hansen, Asymmetric Synthesis of Epicylindrospermopsin via intramolecular nitrone cycloaddition. assignment of absolute configuration, J. Am. Chem. Soc. 124 (2002) 4950–4951. (f) G.W. Gribble, T.C. Barden, Stereocontrolled total syntheses of (−)-hobartine and (+)-aristoteline via an intramolecular nitrone-olefin cycloaddition, J. Org. Chem. 50 (1985) 5900–5902.

[49] (a) J. Ignacio Andrés, J. Alcázar, J.M. Alonso, R.M. Alvarez, M.H. Bakker, I. Biesmans, J.M. Cid, A.I. DeLucas, W. Drinkenburg, J. Fernández, L.M. Font, L. Iturrino, X. Langlois, I. Lenaerts, S. Martínez, A.A. Megens, J. Pastor, S. Pullan, T. Steckler, Tricyclic isoxazolines: identification of R226161 as a potential new antidepressant that combines potent serotonin reuptake inhibition and α2-adrenoceptor antagonism, Bioorg. Med. Chem. 15 (2007) 3649–3660. (b) J. Pastor, J. Alcázar, R.M. Alvarez, J.I. Andrés, J.M. Cid, A.I.D. Lucas, A. Díaz, J. Fernández, L.M. Font, L. Iturrino, C. Lafuente, S. Martínez, M.H. Bakker, I. Biesmans, L.I. Heylen, A.A. Megens, Synthesis of 3a,4-dihydro-3H-[1] benzopyrano [4, 3-c] isoxazoles, displaying combined 5-HT uptake inhibiting and α2-adrenoceptor antagonistic activities. Part 2: further exploration on the cinnamyl moiety, Bioorg. Med. Chem. Lett. 14 (2004) 2917–2922.

[50] (a) Q. Zhao, F. Han, D.L. Romero, A stereoselective intramolecular 1,3-dipolar nitrone cycloaddition for the synthesis of substituted chromanes, J. Org. Chem. 67 (2002) 3317–3322. (b) G. Broggini, L. Bruché, E. Cappelletti, G. Zecchi, J. Chem. Res. (1997) 36. (c) G. Broggini, F. Folcio, N. Sardone, M. Sonzogni, G. Zecchi, Synthesis of enantiopure 3-hydroxymethylchromanes via intramolecular nitrone cycloaddition, Tetrahedron: Asymm. 7 (1996) 797–806. (d) A.E. Kella-Bennani, M. Soufiaoui, A. Kerbal, S. Fkih-Tetouaniz, N. Bitit, Synthesis of a novel tetracyclic heterocycle: 1-carboxy-13-oxo-[1,2,3] triazolo [1′,5′,4,3,1,4] diazepino [6,7-c] chromane, using salicylaldehyde as a starting material, Tetrahedron 51 (1995) 10923–10928.

[51] (a) J.S. Yadav, B.V.S. Reddy, D. Narsimhaswamy, K. Narsimulub, A.C. Kunwarb, LiClO4- or LiOTf-accelerated 1,3-dipolar cycloaddition reactions: a facile synthesis of cis-fused chromano[4,3-c]isoxazoles, Tetrahedron Lett. 44 (2003) 3697–3700. (b) C. Baldoli, P. Del Buttero, E. Licandro, S. Maiorana, A. Papagni, Stereoselective intramolecular 1,3-dipolar cycloaddition of chiral chromium tricarbonyl complexed nitrone, Tetrahedron: Asymmetry 6 (1995) 1711–1717. (c) T. Aftab, R. Grigg, M. Ladlow, V. Sridharan, M. Thornton-Pett, Novel synthesis of fused isoxazolidines via a palladium catalysed allene insertion–intramolecular 1,3-dipolar cycloaddition cascade reaction, Chem. Commun. (2002) 1754–1755.

[52] (a) D. Tanner, Angew. Chem. Int. Ed. Engl. 33 (1994) 599–619. (b) J.B. Sweeney, Aziridines: epoxides' ugly cousins? Chem. Soc. Rev. 31 (2002) 247–258. (c) A.K. Yudin, Aziridines and Epoxidesin Organic Synthesis, Wiley-VCH, Weinheim, 2006.

[53] (a) Z. Li, R.W. Quan, E.N. Jacobsen, Mechanism of the (diimine)copper-catalyzed asymmetric aziridination of alkenes. nitrene transfer via ligand-accelerated catalysis, J. Am. Chem. Soc. 117 (1995) 5889–5890. (b) L. Simkhovich, Z. Gross, Iron (IV) corroles are potent catalysts for aziridination of olefins by Chloramine-T, Tetrahedron Lett. 42 (2001) 8089–8092. (c) B.M. Chanda, R. Vyas, A.V. Bedekar, Investigations in the transition metal catalyzed aziridination of olefins, amination, and other insertion reactions with Bromamine-T as the source of nitrene, J. Org. Chem. 66 (2001) 30–34. (d) J. Gullick, S. Taylor, P. McMorn, D. Bethell, P.C. Bulman Page, F.E. Hancock, F. King, G. Hutchings, Aziridination of styrene: comparison of [N-(p-tolylsulfonyl)imino] phenyliodinane and chloramine-T as nitrene donors, J. Mol. Catal. A 180 (2002) 85–89. (e) P. MMller, C. Fruit, Enantioselective catalytic aziridinations and asymmetric nitrene insertions into CH bonds, Chem. Rev. 103 (2003) 2905–2919. (f) Y. Cui, C. He, Efficient aziridination of olefins catalyzed by a unique disilver (I) compound, J. Am. Chem. Soc. 125 (2003) 16202–16203. (g) H. Kawabata, K. Omura, T. Katsuki, Asymmetric aziridination: a new entry to optically active non-N-protected aziridines, Tetrahedron Lett. 47 (2006) 1571–1574.

[54] (a) J.U. Jeong, B. Tao, I. Sagasser, H. Henniges, K.B. Sharpless, Bromine-catalyzed aziridination of olefins. A rare example of atom-transfer redox catalysis by a main group element, J. Am. Chem. Soc. 120 (1998) 6844–6845. (b) T. Ando, D. Kano, S. Minakata, I. Ryu, M. Komatsu, Tetrahedron 54 (1998) 13485–13494. (c) S.I. Ali, M.D. Nikalje, A. Sudalai, Pyridinium hydrobromide perbromide: a versatile catalyst for aziridination of olefins using chloramine-T, Org. Lett. 1 (1999) 705–707. (d) V.V. Thakur, A. Sudalai, N-Bromoamides as versatile catalysts for aziridination of olefins using chloramine-T, Tetrahedron Lett. 44 (2003) 989–992. (e) S. Minakata, D. Kano, Y. Oderaotoshi, M. Komatsu, Silica–water reaction media: its application to the formation and ring opening of aziridines, Angew. Chem. Int. Ed. 43 (2004) 79–81. (f) S. Minakata, Y. Morino, Y. Oderaotoshi, M. Komatsu, Novel aziridination of olefins: direct synthesis from sulfonamides using t-BuOI, Chem. Commun. (2006) 3337–3339.

[55] C. Varszegi, M. Ernst, F.V. Laar, B.F. Sels, E. Schwab, D.E. De Vos, A micellar iodide-catalyzed synthesis of unprotected aziridines from styrenes and ammonia, Angew. Chem. Int. Ed. 47 (2008) 1477–1480.

[56] (a) P. Caramella, P. Grünanger, in: A. Padwa (Ed.), 1,3-Dipolar Cycloaddition Chemistry, Vol. 1, John Wiley and Sons, New York, 1984. (b) K.B.G. Torssell, Nitrile Oxides, Nitrones and Nitronates in Organic Synthesis, VCH, New York, 1988. (c) D.P. Curran, Reduction of DELTA.2-isoxazolines. 3. Raney nickel catalyzed formation of. beta.-hydroxy ketones, J. Am. Chem. Soc. 105 (1983) 5826–5833. (d) A.P. Kozikowski, The isoxazoline route to the molecules of nature, Acc. Chem. Res. 17 (1984) 410–416. (e) J.W. Bode, E.M. Carreira, Stereoselective syntheses of epothilones A and B via directed nitrile oxide cycloaddition, J. Am. Chem. Soc. 123 (2001) 3611–3612. (f) S.-M. Paek, S.-Y. Seo, S.-H. Kim, J.-W. Jung, Y.-S. Lee, J.-K. Jung, Y.-G. Suh, Concise Syntheses of (+)-Macrosphelides A and B, Org. Lett. 7 (2005) 3159–3162. (g) J.Y. Lee, G. Schiffer, V. Jager, Synthesis of l-carbafuranomycin, an unnatural analogue of the antibiotic amino acid furanomycin, Org. Lett. 7 (2005) 2317–2320 and references therein.

[57] N. Chatterjee, P. Pandit, S. Halder, A. Patra, D.K. Maiti, Generation of nitrile oxides under nanometer micelles built in neutral aqueous media: synthesis of novel glycal-based

chiral synthonsand optically pure 2,8-dioxabicyclo [4.4.0] decene core, J. Org. Chem. 73 (2008) 7775–7778.

[58] For a monograph and reviews see: (a) J. Zhu, H. Bienayme (Eds.), Multicomponent Reactions, Wiley-VCH, Weinheim, 2005. (b) D. Bonne, Y. Coquerel, T. Constantieux, J. Rodriguez, Tetrahedron: Asymmetry 21 (2010) 1085–1109. (c) S. Dandapani, L.A. Marcaurelle, Current strategies for diversity-oriented synthesis, Curr. Opin. Chem. Biol. 14 (2010) 362–370. (d) B.B. Toure, D.G. Hall, Natural product synthesis using multicomponent reaction strategies, Chem. Rev. 109 (2009) 4439–4486. (e) S. Perreault, T. Rovis, Multi-component cycloaddition approaches in the catalytic asymmetric synthesis of alkaloid targets, Chem. Soc. Rev. 11 (2009) 3149–3159. (f) B. Ganem, Strategies for innovation in multicomponent reaction design, Acc. Chem. Res. 42 (2009) 463–472. (g) M. Gonzalez-Lopez, J.T. Shaw, Cyclic anhydrides in formal cycloadditions and multicomponent reactions, Chem. Rev. 109 (2009) 164–189. (h) D.M. D'Souza, T.J.J. Muller, Multi-component syntheses of heterocycles by transition-metal catalysis, Chem. Soc. Rev. 36 (2007) 1095–1108. (i) D. Tejedor, F. Garcia-Tellado, Chemo-differentiating ABB′ multicomponent reactions. Privileged building blocks, Chem. Soc. Rev. 36 (2007) 484–491. (j) A. Domling, Recent developments in isocyanide based multicomponent reactions in applied chemistry, Chem. Rev. 106 (2006) 17–89. (k) A. Dondoni, A. Massi, Design and synthesis of new classes of heterocyclic C-glycoconjugates and carbon-linked sugar and heterocyclic amino acids by asymmetric multicomponent reactions (AMCRs), Acc. Chem. Res. 39 (2006) 451–463. (l) D.J. Ramon, M. Yus, Asymmetric multicomponent reactions (AMCRs): the new frontier, Angew. Chem. Int. Ed. 44 (2005) 1602–1634. (m) M.D. Burke, S.L. Schreiber, A planning strategy for diversity-oriented synthesis, Angew. Chem. Int. Ed. 43 (2004) 46–58. (n) C. Simon, T. Constantieux, J. Rodriguez, Utilisation of 1,3-dicarbonyl derivatives in multicomponent reactions, Eur. J. Org. Chem. (2004) 4957–4980.

[59] (a) R.J. Sundberg, The Chemistry of Indoles, Academic Press, New York, 1996. (b) T.R. Garbe, M. Kobayashi, N. Shimizu, N. Takesue, M. Ozawa, H. Yukawa, Indolyl Carboxylic Acids by Condensation of Indoles with α-Keto Acids, J. Nat. Prod. 63 (2000) 596–598.

[60] For a recent review of indole containing natural products, see: (a) D. Faulkner, Marine natural products, Nat. Prod. Rep. 16 (1999) 155–198.

[61] (a) J.H. Wynne, W.M. Stalick, Synthesis of 3-[(1-Aryl)aminomethyl]indoles, J. Org. Chem. 67 (2002) 5850–5853. (b) A. Kumar, S. Sharma, R.A. Maurya, A novel multicomponent reaction of indole, formaldehyde, and tertiary aromatic amines, Tetrahedron Lett. 50 (2009) 5937–5940. (c) A.J. Kochanowska-Karamyan, M.T. Hamann, Marine indole alkaloids: potential new drug leads for the control of depression and anxiety, Chem. Rev. 110 (2010) 4489–4497.

[62] M.P. Lézé, M.L. Borgne, P. Marchand, D. Loquet, M. Kogler, G.L. Baut, A. Palusczak, R.W.J. Hartmann, 2- and 3-[(Aryl)(azolyl)methyl] indoles as potential non-steroidal aromatase inhibitors, J. Enzyme Inhib. Med. Chem. 19 (2004) 549–557.

[63] R. Contractor, I.J. Samudio, Z. Estrov, D. Harris, J.A. McCubrey, S.H. Safe, M. Andreeff, M. Konopleva, A novel ring-substituted diindolylmethane, 1,1-bis[3′-(5-methoxyindolyl)]-1-(p-t-butylphenyl) methane, inhibits extracellular signal-regulated kinase activation and induces apoptosis in acute myelogenous leukemia, Cancer Res. 65 (2005) 2890–2898.

[64] (a) R.M. Williams, R.J. Cox, Paraherquamides, brevianamides, and asperparalines: laboratory synthesis and biosynthesis: an interim report, Acc. Chem. Res. 36 (2003)

127–139. (b) J.F.M. da Silva, S.J. Garden, A.C. Pinto, J. Braz. Chem. Soc. (2001) 273–324.

[65] (a) J. Skommer, D. Wlodkowic, M. Mättö, M. Eray, J. Pelkonen, Leuk. Res. 30 (2006) 322–331. (b) N. Yu, J.M. Aramini, M.W. Germann, Z. Huang, Reactions of salicylaldehydes with alkyl cyanoacetates on the surface of solid catalysts: syntheses of 4H-chromene derivatives, Tetrahedron Lett. 41 (2000) 6993–6996. (c) L. Bonsignore, G. Loy, D. Secci, A. Calignano, Synthesis and Pharmacological Activaty of 2-Oxo-(2H)-1-benzopyran-3-carboxamide derivatives, Eur. J. Med. Chem. 28 (1993) 517–520. (d) E.C. Witte, P. Neubert, A. Roesch, Ger Offen.DE 3427985, 1986, Chem. Abstr. 104 (1986)224915. (e) L.L. Andreani, E. Lapi, Boll. Chim. Farm. 99 (1960) 583–587.

[66] C.S. Konkoy, D.B. Fick, S.X. Cai, N.C. Lan, J.F.W. Keana, PCT Int. Appl. WO0075123, Chem. Abstr. 2001 (134) (2000) 29313a.

[67] L.-M. Wang, N. Jiao, J. Qiu, J.-J. Yu, J.-Q. Liu, F.-L. Guo, Y. Liu, Sodium stearate-catalyzed multicomponent reactions for efficient synthesis of spirooxindoles in aqueous micellar media, Tetrahedron 66 (2010) 339–343.

[68] A. Kumar, M.K. Gupta, M. Mukesh Kumara, D. Deepti Saxenaa, Micelle promoted multicomponent synthesis of 3-amino alkylated indoles via a Mannich-type reaction in water, RSC Adv. 3 (2013) 1673–1678.

[69] (a) H. Spies, B. Noll, S. Noll, M. Findeisen, P. Brust, R. Syhre, R. Berger, Tc and Re chelates of 8α-amino-6-methyl-ergoline: synthesis and affinity to the dopamine D2 receptor, Bioorg. Med. Chem. 10 (2002) 3523–3528. (b) B. Horst, B.L. Feringa, A.J. Minnaard, Catalytic asymmetric synthesis of mycocerosic acid, Chem. Commun. (2007) 489–491. (c) M. Smietana, P. Clayette, P. Mialocq, J.-J. Vasseur, J. Oiry, Synthesis of new N-isobutyryl-l-cysteine/MEA conjugates: evaluation of their free radical-scavenging activities and anti-HIV properties in human macrophages, Bioorg. Chem. 36 (2008) 133–140. (d) J. Oiry, P. Mialocq, J.-Y. Puy, P. Fretier, N. Dereuddre-Bosquet, D. Dormont, J.-L. Imbach, P. Clayette, Synthesis and biological evaluation in human monocyte-derived macrophages of N-(N-Acetyl-l-cysteinyl)-S-acetylcysteamine analogues with potent antioxidant and anti-HIV activities, J. Med. Chem. 47 (2004) 1789–1795. (e) P. Blakskjær, B. Høj, D. Riber, T. Skrydstrup, SmI2 reduced thioesters as synthons of unstable acyl radicals: direct synthesis of potential protease inhibitors via intermolecular radical addition, J. Am. Chem. Soc. 125 (2003) 4030–4031.

[70] (a) G.S. Hamilton, Y.-Q. Wu, D.C. Limburg, D.E. Wilkinson, M.J. Vaal, J.-H. Li, C. Thomas, W. Huang, H. Sauer, D.T. Ross, R. Soni, Y. Chen, H. Guo, P. Howorth, H. Valentine, S. Liang, D. Spicer, M. Fuller, J.P. Steiner, Synthesis of N-glyoxyl prolyl and pipecolyl amides and thioesters and evaluation of their in vitro and in vivo nerve regenerative effects, J. Med. Chem. 45 (2002) 3549–3557. (b) P. Metzner, A. Thuillier, in: Sulfur Reagents in Organic Synthesis, Academic Press, New York, 1994. (c) A. Nudelman, in: The Chemistry of Optically Active Sulfur Compounds, Gordon and Breach, New York, 1984. (d) C. Chatgilialoglu, K. D. Asmus, in: Sulfur-Centered Reactive Intermediates in Chemistry and Biology, Springer, New York, 1991.

[71] (a) B.C. Ranu, R. Jana, Ionic liquid as catalyst and reaction medium: a simple, convenient and green procedure for the synthesis of thioethers, thioesters and dithianes using an inexpensive ionic liquid, [pm Im]Br, Adv. Synth. Catal. 347 (2005) 1811–1818. (b) S. Iimura, K. Manabe, S. Kobayashi, Chem. Commun. (2002) 94–95. (c) T. Uno, T. Inokuma, Y. Takemoto, Chem. Commun. 48 (2012) 1901–1903. (d) S. Magens, B. Plietker, Fe-Catalyzed thioesterification of carboxylic esters, Chem. A Eur. J. 17 (2011) 8807–8809. (e) N. Iranpoor, H. Firouzabadi, D. Khalili, S. Motevalli, Easily prepared

azopyridines as potent and recyclable reagents for facile esterification reactions. An efficient modified Mitsunobu reaction, J. Org. Chem. 73 (2008) 4882–4887. (f) Y. Kageyama, S. Murata, Oxidative formation of thiolesters in a model system of the pyruvate dehydrogenase complex, J. Org. Chem. 70 (2005) 3140–3147. (g) H. Cao, L. McNamee, H. Alper, Palladium-catalyzed thiocarbonylation of iodoarenes with thiols in phosphonium salt ionic liquids, J. Org. Chem. 73 (2008) 3530–3534. (h) E.A. Castro, Kinetics and mechanisms of reactions of thiol, thiono, and dithio analogues of carboxylic esters with nucleophiles, Chem. Rev. 99 (1999) 3505–3524.

[72] (a) E. Block, E.V. Dikarev, R.S. Glass, L.B. Jin, X. Li, S.-Z. Zhang, Synthesis, structure, and chemistry of new, mixed group 14 and 16 heterocycles: nucleophile-induced ring contraction of mesocyclic dications, J. Am. Chem. Soc. 128 (2006) 14949–14961. (b) M.A. Karimi Zarchi, M. Nejabat, J. Appl. Polym. Sci. 125 (2012) 1041–1048. (c) G. Petrillo, M. Novi, G. Garbarino, M. Filiberti, The reaction between arenediazonium tetrafluoroborates and alkaline thiocarboxylates in DMSO: a convenient access to aryl thiolesters and other aromatic sulfur derivatives, Tetrahedron 45 (1989) 7411–7420.

[73] G.-P. Lu, C. Cai, An odorless, one-pot synthesis of thioesters from organic halides, thiourea and benzoyl chlorides in water, Adv. Synth. Catal. 355 (2013) 1271–1276.

[74] (a) K. Smith, Z. Zhenhua, P.K.G. Hodgson, J. Mol. Catal. A: Chem. 134 (1998) 121. (b) M. Miura, H. Hashimoto, K. Itoh, M. Nomura, J. Chem. Soc., Perkin Trans 1 (1990) 2207. (c) K. Okuro, M. Furuune, M. Enna, M. Miura, M. Nomura, Synthesis of aryl- and vinylacetylene derivatives by copper-catalyzed reaction of aryl and vinyl iodides with terminal alkynes, J. Org. Chem. 58 (1993) 4716–4721.

[75] (a) M.E. Davis, Microporous Mesoporous Mater. 21 (1998) 173. (b) P.J. Harrington, E. Lodewijk, Org. Process Res. Dev. 1 (1997) 72. (c) D. Dowdy, P.H. Gore, D.N. Waters, J. Chem. Soc., Perkin Trans. 2 (1991) 1149. (d) S. Pivsa-Art, K. Okuro, M. Miura, S. Murata, M. Nomura, J. Chem. Soc., Perkin Trans. 1 (1994) 1703.

[76] K.R. Reddy, K.C. Rajanna, K. Uppalaiah, Environmentally benign contemporary Friedel–Crafts acylation of 1-halo-2-methoxynaphthalenes and its related compounds under conventional and nonconventional conditions, Tetrahedron Lett. 54 (2013) 3431–3436.

[77] For reviews, see: (a) V. Singh, S. Batra, Advances in the Baylis–Hillman reaction-assisted synthesis of cyclic frameworks, Tetrahedron 64 (2008) 4511–4574. (b) D. Basavaiah, A.J. Rao, T. Satyanarayana, Recent advances in the Baylis – Hillman reaction and applications, Chem. Rev. 103 (2003) 811–892. (c) P. Langer, New strategies for the development of an asymmetric version of the Baylis-Hillman reaction, Angew. Chem. Int. Ed. 39 (2000) 3049–3052. (d) E. Ciganek, Org. React. 51 (1997) 201. (e) D. Basavaiah, P.D. Rao, R.S. Hyma, The Baylis-Hillman reaction: a novel carbon-carbon bond forming reaction, Tetrahedron 52 (1996) 8001–8062.

[78] (a) Y.S. Reddy, P. Kadigachalam, R.K. Basak, A.P.J. Pal, Y.D. Vankar, Total synthesis of (+)-pericosine B and (+)-pericosine C and their enantiomers by using the Baylis–Hillman reaction and ring-closing metathesis as key steps, Tetrahedron Lett. 53 (2012) 132–136. (b) P.H.S. Paioti, F. Coelho, A Morita–Baylis–Hillman adduct allows the diastereoselective synthesis of styryl lactones, Tetrahedron Lett. 52 (2011) 6180–6184. (c) V. Kumar, P. Das, P. Ghosal, A.K. Shaw, Syntheses of (−)-gabosine A, (+)-4-epi-gabosine A, (−)-gabosine E, and (+)-4-epi-gabosine E, Tetrahedron 67 (2011) 4539–4546. (d) R.L. Reddy, P. Saravanan, E.J. Corey, A simple stereocontrolled synthesis of Salinosporamide A, J. Am. Chem. Soc. 126 (2004) 6230–6231. (e) Y. Iwabuchi, M. Furukawa, T. Esumi, S. Hatakeyama, An enantio- and stereocontrolled synthesis of (−)-mycestericin E via cinchona alkaloid-catalyzed

asymmetric Baylis–Hillman reaction, Chem. Commun. (2001) 2030–2031. (f) J.A. McCauley, K. Nagasawa, P.A. Lander, S.G. Mischke, M.A. Semones, Y. Kishi, Total synthesis of Pinnatoxin A, J. Am. Chem. Soc. 120 (1998) 7647–7648.

[79] (a) K.R. Luna-Freire, C.F. Tormena, F. Coelho, Heck reaction on Morita-Baylis-Hillman adducts: diastereoselective synthesis of pyrrolizidinones and pyrrolizidines, Synlett. (2011) 2059–2063. (b) A. Albrecht, L. Albrecht, T. Janecki, Eur. J. Org. Chem. 2746 (2011). (c) W. Zhong, Y. Liu, G. Wang, L. Hong, Y. Chen, X. Chen, Y. Zheng, W. Zhang, W. Ma, Y. Shen, Y. Yang, Org. Prep. Proced. Int. 43 (2011) 1. (d) S. Gowrisankar, H.S. Lee, S.H. Kim, Y.K.J. Lee, N. Kim, Recent advances in the Pd-catalyzed chemical transformations of Baylis–Hillman adducts, Tetrahedron (43) (2009) 8769–8780.

[80] (a) G.W. Amarante, M. Cavallaro, F. Coelho, Highly diastereoselective total synthesis of the anti-tumoral agent (±)-Spisulosine (ES285) from a Morita–Baylis–Hillman adduct, Tetrahedron Lett. 51 (2010) 2597–2599. (b) G.W. Amarante, P. Rezende, M. Cavallaro, F. Coelho, Acyloins from Morita–Baylis–Hillman adducts: an alternative approach to the racemic total synthesis of bupropion, Tetrahedron Lett. 49 (2008) 3744–3748. (c) L.K. Kohn, C.H. Pavam, D. Veronese, F. Coelho, J.E. Carvalho, W.P. Almeida, Antiproliferative effect of Baylis–Hillman adducts and a new phthalide derivative on human tumor cell lines, Eur. J. Med. Chem. 41 (2006) 738–744. (d) G.P.D. Silveira, F. Coelho, Enantioselective synthesis of 2-ethyl-2,3-dihydrobenzofuran carboxylic acid, direct precursor of (+)-efaroxan, from a Baylis–Hillman adduct, Tetrahedron Lett. 46 (2005) 6477–6481.

[81] (a) M. Shi, G.L. Zhao, Aza-Baylis–Hillman reactions of diisopropyl azodicarboxylate or diethyl azodicarboxylate with acrylates and acrylonitrile, Tetrahedron 60 (2004) 2083–2089. (b) D.J. Maher, S.J. Connon, Acceleration of the DABCO-promoted Baylis–Hillman reaction using a recoverable H-bonding organocatalyst, Tetrahedron Lett. 45 (2004) 1301–1305. (c) S. Chandrasekhar, C. Narsihmulu, B. Saritha, S.S. Sultana, Poly(ethyleneglycol) (PEG): a rapid and recyclable reaction medium for the DABCO-catalyzed Baylis–Hillman reaction, Tetrahedron Lett. 45 (2004) 5865–5867. (d) A. Patra, A.K. Roy, B.S. Joshi, R. Roy, S. Batra, A.P. Bhaduri, The Baylis–Hillman chemistry in aqueous media: elucidation of mechanism for synthesis of ether side-product leads to an efficient approach to C–O bond formation, Tetrahedron 59 (2003) 663–670.

[82] (a) Y. Sohtome, A. Tanatani, Y. Hashimoto, K. Nagasawa, Development of bis-thiourea-type organocatalyst for asymmetric Baylis–Hillman reaction, Tetrahedron Lett. 45 (2004) 5589–5592. (b) F. Rezgui, M.M. E1 Gaïed, DMAP-catalyzed hydroxymethylation of 2-cyclohexenones in aqueous medium through Baylis-Hillman reaction, Tetrahedron Lett. 39 (1998) 5965–5966.

[83] (a) S. Luo, B. Zhang, J. He, A. Janczuk, P.G. Wang, J. Cheng, Aqueous Baylis–Hillman reactions of cyclopent-2-enone using imidazole as catalyst, Tetrahedron Lett. 43 (2002) 7369–7371. (b) R. Gatri, M.M. El Gaïed, Imidazole-catalysed Baylis–Hillman reactions: a new route to allylic alcohols from aldehydes and cyclic enones, Tetrahedron Lett. 43 (2002) 7835–7836.

[84] (a) R. Ballini, L. Barboni, G. Bosica, D. Fiorini, E. Mignini, A. Palmieri, Fast diastereoselective Baylis–Hillman reaction by nitroalkenes: synthesis of di- and triene derivatives, Tetrahedron 60 (2004) 4995–4999. (b) V.K. Aggarwal, A. Mereu, Superior amine catalysts for the Baylis–Hillman reaction: the use of DBU and its implications, Chem. Commun. (1999) 2311–2312.

[85] (a) H. Kinoshita, S. Kinoshita, Y. Munechika, T. Iwamura, S. Watanabe, T. Kataoka, Chalcogeno Morita – Baylis – Hillman reaction of 2-(Methylchalcogeno)phenyl vinyl ketones with aldehydes, ketones, and α-dicarbonyl compounds, Eur. J. Org. Chem. (2003) 4852–4861. (b) H. Kinoshita, T. Osamura, S. Kinoshita, T. Iwamura, S. Watanabe, T. Kataoka, G. Tanabe, O. Muraoka, Chalcogeno – Morita – Baylis – Hillman reaction of enones with acetals: simple α-alkoxyalkylation of enones, J. Org. Chem. 68 (2003) 7532–7534. (c) W. Pei, H. Wei, G. Li, Lewis acid-promoted Baylis–Hillman-type reaction of α,β-unsaturated ethyl thioester with aldehydes without the use of a Lewis base, Chem. Commun. (2002) 1856–1857.

[86] Y. Hayashi, K. Okado, I. Ashimine, M. Shoji, The Baylis–Hillman reaction under high pressure induced by water-freezing, Tetrahedron Lett. 43 (2002) 8683–8686.

[87] M.K. Kundu, S.B. Mukherjee, N. Balu, R. Padmakumar, S.V. Bhat, Microwave mediated extensive rate enhancement of the Baylis-Hillman reaction, Synlett (1994) 444–445.

[88] B.A. Shairgojray, A.A. Ahmad Dar, B.A. Bhat, Micellar promiscuity: an expeditious approach to Morita–Baylis–Hillman reaction, Tetrahedron Lett. 54 (2013) 2391–2394.

[89] G.G. Zhanel, S. Fontaine, H. Adam, K. Schurek, M. Mayer, A.M. Noreddin, A.S. Gin, E. Rubinstein, D.J. Hoban, A review of new fluoroquinolones: focus on their use in respiratory tract infections, Treat. Respir. Med. 5 (2006) 437–465.

[90] N.A. Rebacz, P.E. Savage, Ind. Eng. Chem. Res. 49 (2010) 535–540. and references therein.

[91] (a) A. Desgrez, Ann. Chim. 8 (1894) 209. (b) R. Schaad, V.N. Ipatieff, Catalytic hydration of acetylene and of some alkylacetylenes, J. Am. Chem. Soc. 62 (1940) 178–180.

[92] J.M. Kremsner, C.O. Kappe, Microwave-assisted organic synthesis in near-critical water at 300°C—a proof-of-concept study, Eur. J. Org. Chem. (2005) 3672–3679.

[93] R.J. Thomas, K.N. Campbell, G.F. Hennion, Catalytic hydration of alkylacetylenes, J. Am. Chem. Soc. 60 (1938) 718–720 and references therein.

[94] Z. Nairoukh, D. Avnir, J. Blum, Acid-catalyzed hydration of alkynes in aqueous micro-emulsions, Chem. Sus. Chem. 6 (2013) 430–432.

[95] E. Vitaku, D.T. Smith, J.T. Njardarson, Analysis of the structural diversity, substitution patterns, and frequency of nitrogen heterocycles among U.S. FDA approved pharmaceuticals, J. Med. Chem. 57 (2014) 10257–10274.

[96] M. Baumann, I.R. Baxendale, An overview of the synthetic routes to the best selling drugs containing 6-membered heterocycles, Beilstein J. Org. Chem. 9 (2013) 2265–2319.

[97] C.P. Ashcroft, P.J. Dunn, J.D. Hayler, A.S. Wells, Survey of solvent usage in papers Published in Organic Process Research & Development 1997–2012, Org. Process Res. Dev. 19 (2015) 740–747.

[98] N.A. Isley, R.T.H. Linstadt, S.M. Kelly, F. Gallou, B.H. Lipshutz, Nucleophilic aromatic substitution reactions in water enabled by Micellar catalysis, Org. Lett. 17 (2015) 4734–4737.

[99] (a) V. Sridharan, P. Suryavanshi, J.C. Menéndez, Advances in the chemistry of tetrahydroquinolines, Chem. Rev. 111 (2011) 7157–7259. (b) A.R. Katritzky, S. Rachwal, B. Rachwal, Recent progress in the synthesis of 1,2,3,4,-tetrahydroquinolines, Tetrahedron 52 (1996) 15031–15070. (c) V. Kouznetsov, A. Palma, C. Ewert, A. Varlamov, Some aspects of reduced quinoline chemistry, J. Heterocyclic Chem. 35 (1998) 761–785.

[100] D.R. Merchán Arenas, C.A. Martínez Bonilla, V.V. Kouznetsov, Aqueous SDS micelle-promoted acid-catalyzed dominoABB' imino Diels–Alder reaction: a mild and efficientsynthesis of privileged 2-methyl-tetrahydroquinoline scaffolds, Org. Biomol. Chem. 11 (2013) 3655–3663.

[101] (a) P.J. Rosenthal, Antimalarial Chemotherapy: Mechanisms of Action, Resistance and New Directions in Drug Discovery, Humana, Totowa, NJ, 2001. (b) A. von Sprecher, M. Gerspacher, A. Beck, S. Kimmel, H. Wiestner, G.P. Anderson, U. Niederhauser, N. Subramanian, M.A. Bray, Synthesis and SAR of a novel, potent and structurally simple LTD4 antagonist of the quinoline class, Bioorg. Med. Chem. Lett. 8 (1998) 965–970. (c) P.L. Ferrarini, C. Mori, M. Badawneh, V. Calderone, R. Greco, C. Manera, A. Martinelli, P. Nieri, G. Saccomanni, Synthesis and β-blocking activity of (R,S)-(E)-oximeethers of 2,3-dihydro-1,8-naphthyridine and 2,3-dihydrothiopyrano [2,3-b]pyridine:potential antihypertensive agents—Part IX, Eur. J. Med. Chem. 35 (2000) 815–826. (d) G. Roma, M.D. Braccio, G. Grossi, F. Mattioli, M. Ghia, 1,8-Naphthyridines IV. 9-Substituted N,N-dialkyl-5-(alkylamino or cycloalkylamino) [1,2,4]triazolo[4,3-a][1,8]naphthyridine-6-carboxamides, new compounds with anti-aggressive and potent anti-inflammatory activities, Eur. J. Med. Chem. 35 (2000) 1021–1035.

[102] (a) A. Kleeman, J. Engel, Pharmaceutical Substances, fourth ed., Thieme, New York, NY, 2001, p. 482. (b) A. Kleeman, J. Engel, Pharmaceutical Substances, fourth ed., Thieme, New York, NY, 2001, p. 1479.

[103] (a) J.V. Johnson, S. Rauckman, P.D. Baccanari, B. Roth, J. Med. Chem. 1989 (1942) 32. (b) N. Yamada, S. Kadowaki, K. Takahashi, K. Umezu, Biochem. Pharmacol. 44 (1992) 1211. (c) M.J. Laughlin, R.P. Hsung, Total syntheses of pyranoquinoline alkaloids: simulenoline, huajiaosimuline, and (±)-7-demethoxyzanthodioline, J. Org. Chem. 66 (2001) 1049–1053. (d) J.P. Michael, Nat. Prod. Rep. 22 (2005) 627. (e) M. Gao, D. Kong, A. Clearfield, Q.-H. Zheng, Synthesis of carbon-11 and fluorine-18 labeled N-acetyl-1-aryl-6,7-dimethoxy-1,2,3,4-tetrahydroisoquinoline derivatives as new potential PET AMPA receptor ligands, Bioorg. Med. Chem. Lett. 16 (2006) 2229–2233. (f) P. Cheng, N. Huang, J.-Y. Jiang, Q. Zhang, Y.-T. Zheng, J.-J. Chen, X.-M. Zhang, Y.-B. Ma, 1-Aryl-tetrahydroisoquinoline analogs as active anti-HIV agents in vitro, Bioorg. Med. Chem. Lett. 18 (2008) 2475–2478.

[104] N.C. Ganguly, S. Chandra, One-pot access to pyridocoumarins via Povarov-hydrogen transfer cascade under auto-tandem catalysis of iodine in aqueous micelles, Tetrahedron Lett. 55 (2014) 1564–1568.

[105] G.H. Timms, E. Wildsmith, The reduction of oximes with tervalent titanium, a mild deoximation procedure and the partial synthesis of erythromycylamine, Tetrahedron Lett. (1971) 195–198.

[106] (a) M.P. Doyle, W. Wierenga, M.A. Zaleta, Reactions of the nitrosonium ion. IV. Nitrosative cleavage of the carbon-nitrogen double bond. Reaction of N-arylimines and ketimines with nitrosonium salts, J. Org. Chem. 37 (1972) 1597–1601. (b) M.P. Doyle, M.A. Zaleta, J.E. Deboer, W. Wierenga, Reactions of the nitrosonium ion. V. Nitrosative cleavage of the carbon-nitrogen double bond. Attempted exchange of oxygen for nitrogen, J. Org. Chem. 38 (1973) 1663–1667.

[107] E.J. Corey, P.B. Hopkins, S. Kim, S. Yoo, K.P. Nambiar, J.R. Falck, Total synthesis of erythromycins. 5. Total synthesis of erythronolide A, J. Am. Chem. Soc. 101 (1979) 7131–7134.

[108] C.H. Depuy, B.W. Ponder, Levulinic acid as a reagent for the hydrolysis of oximes and 2,4-dinitrophenylhydrazones, J. Am. Chem. Soc. 81 (1959) 4629–4631.

[109] E.B. Hershberg, Regeneration of steroid ketones from their semicarbazones with pyruvic acid, J. Org. Chem. 13 (1948) 542–546.

[110] S.B. Shim, K. Kim, Y.H. Kim, Direct conversion of oximes and hydrazones into their ketones with dinitrogen tetroxide, Tetrahedron Lett. 28 (1987) 645–648.

[111] R.E. Erickson, P.J. Andrulis Jr., J.C. Collins, M.L. Lungle, G.D. Mercer, Mechanism of ozonation reactions. IV. Carbon-nitrogen double bonds, J. Org. Chem. 34 (1969) 2961–2966.
[112] N.B. Barhate, A.S. Gajare, R.D. Wakharkar, A. Sudalai, Facile regeneration of carbonyl compounds from oximes and tosylhydrazones with TBHP, Tetrahedron Lett. 38 (1997) 653–656.
[113] G.H. Imanzadeh, A.R. Hajipour, S.E. Mallakpour, Solid state cleavage of oximes with potassium permanganate supported on alumina, Synth. Commun. 33 (2003) 735.
[114] E.C. Taylor, A. McKillop, J.D. Hunt, R.D. Naylor, Thallium in organic synthesis. XXVI. Direct conversion of oximes into aldehydes and ketones with thallium (III) nitrate (TTN), J. Am. Chem. Soc. 93 (1971) 4918–4919.
[115] E.J. Corey, J.E. Richman, Reaction of oxime O-acetates with chromous acetate. Method for the conversion of ketoximes to ketones under mild conditions, J. Am. Chem. Soc. 92 (1970) 5276–5277.
[116] C.G. Rao, A.S. Radhakrishna, B.B. Singh, S.P. Bhatnager, Oxidative cleavage of oximes with triethylammonium chlorochromate, Synthesis (1983) 808–809.
[117] J.M. Aizpurua, C. Palomo, Chlorotrimethylsilane/Chromium (VI) reagents as ndw and versatile oxidation systems, Tetrahedron Lett. 24 (1983) 4367–4370.
[118] J.R. Maloney, R.E. Lyle, J.E. Scaavedra, G.G. Lyle, Oxidative deoximation with pyridinium chlorochromate, Synthesis (1978) 212–213.
[119] J. Drabowicz, Rapid deoximation with pyridinium chlorochromate/hydrogen peroxide system, Synthesis (1980) 125–126.
[120] J.M. Aizpurua, M. Juaristi, B. Lecea, C. Palono, Reagents and synthetic methods—40: Halosilanes/chromium trioxide as efficient oxidizing reagents, Tetrahedron 41 (1985) 2903–2911.
[121] J.G. Lee, K.H. Kwak, J.P. Hwang, Regeneration of aldehydes and ketones from oximes using bis(trimethylsilyl)chromate, Synth. Commun. 22 (1992) 2425–2429.
[122] (a) S. Hamal, S.K. Mahto, G.L. Gujurel, Indian J. Chem., Sect. B 35 (1996) 1116. (b) M.B. Pravin, M.K. Bhushan, Microwave promoted regeneration of carbonyl compounds from oximes using silica supported chromium trioxide, Tetrahedron Lett. 39 (1998) 5867–5868.
[123] N. Narayanan, T.R.J. Balasubramaniam, Chem. Res., Synop. 4 (1992) 132.
[124] D.H.R. Barton, D.J. Lester, S.V. Ley, J. Chem. Soc. Chem. Commun. (1977) 445.
[125] P. Gogoi, P. Hazarika, D. Konwar, Surfactant/I_2/water: an efficient system for deprotection of oximes and imines to carbonyls under neutral conditions in water, J. Org. Chem. 70 (2005) 1934–1936.
[126] I. Ugi, The α-addition of immonium ions and anions to isonitriles accompanied by secondary reactions, Angew. Chem. Int. Ed. Engl. 1 (1962) 8–21.
[127] (a) J.B. Harborne, H. Baxter, G.P. Moss, Phytochemical Dictionary, Taylor & Francis, London, 1999. p. 9. (b) A.D. Patil, N.V. Kumar, W.C. Kokke, M.F. Bean, A.J. Freyer, C.D. Brosse, S. Mai, A. Truneh, D.J. Faulkner, B. Carte, A.L. Breen, R.P. Hertzberg, R.K. Johnson, J.W. Westley, B.C.M. Pottst, Novel alkaloids from the sponge Batzella sp.: inhibitors of HIV gp120-human CD4 binding, J. Org. Chem. 60 (1995) 1182–1188. (c) L. Heys, C.G. Moore, P.J. Murphy, The guanidine metabolites of Ptilocaulis spiculifer and related compounds; isolation and synthesis, Chem. Soc. Rev. 29 (2000) 57–67. (d) S. Patai, The Chemistry of Amidines and Imidates, vol. 2, John Wiley and Sons, New York, 1991.
[128] R. Ostazewski, J. Golab, G. Placha, D. Nowis, K. Wnkler, M. Mroczkiewich, Studies of the synthesis of all stereoisomers of MG-132 proteasome inhibitors in the tumor targeting approach, J. Med. Chem. 53 (2010) 1509–1518.

[129] C. Palomo, A.L. Palomo, F. Palomo, A. Mielgo, Soluble α-amino acid salts in acetonitrile: practical technology for the production of some dipeptides, Org. Lett. 4 (2002) 4005–4008.
[130] A. Kumar, D. Deepti Saxena, M.K. Gupta, Nanoparticle catalyzed reaction (NPCR): ZnO-NP catalyzed Ugi-reaction in aqueous medium, Green Chem. 15 (2013) 2699–2703.
[131] (a) R.G. Gish, Treating HCV with ribavirin analogues and ribavirin-like molecules, J. Antimicrob. Chemother. 57 (2006) 8–13. (b) J.Z. Wu, C.-C. Lin, Z. Hong, Ribavirin, viramidine and adenosine-deaminase-catalysed drug activation: implication for nucleoside prodrug design, J. Antimicrob. Chemother. 52 (2003) 543–546.
[132] R.A. Youcef, M.D. Dos Santos, S. Roussel, J.-P. Baltaze, N. Lubin-Germain, J. Uziel, Huisgen cycloaddition reaction of C-alkynyl ribosides under micellar catalysis: synthesis of ribavirin analogues, J. Org. Chem. 74 (11) (2009) 4318–4323.
[133] (a) A. Yajima, Recent progress in the chemistry and chemical biology of microbial signaling molecules: quorum-sensing pheromones and microbial hormones, Tetrahedron Lett. 55 (2014) 2773–2780. (b) P. Chalier, J. Crouzet, Enantiodifferentiation of four γ-lactones produced by Penicillium Roqueforti, Chirality 10 (1998) 786–790. (c) M. Mulzer, B.J. Tiegs, Y. Wang, G.W. Coates, G.A. O'Doherty, Total synthesis of tetrahydrolipstatin and stereoisomers via a highly regio- and diastereoselective carbonylation of epoxyhomoallylic alcohols, J. Am. Chem. Soc. 136 (2014) 10814–10820. (d) H.K. Grover, M.R. Emmett, M.A. Kerr, γ-Substituted butanolides from cyclopropane hemimalonates: an expedient synthesis of natural (R)-dodecan-4-olide, Org. Lett. 15 (2013) 4838–4841. (e) R. Ait-Youcef, X. Moreau, C. Greck, Asymmetric synthesis of sphinganine and clavaminol H, J. Org. Chem. 75 (2010) 5312–5315. (f) G. Ma, M. Zancanella, Y. Oyola, R.D. Richardson, J.W. Smith, D. Romo, Total synthesis and comparative analysis of orlistat, valilactone, and a transposed orlistat derivative: inhibitors of fatty acid synthase, Org. Lett. 8 (2006) 4497–4500. (g) A. Graul, A. Martel, J. Castaner, Drugs Future 22 (1997) 841–845.
[134] (a) A. Nicoletta, S. Silvia, B. Stefano, O. Ennio, A. Amjad, L.M. Manchu, WO2009/106470 A2, 2009. (b) K. Barral, S. Priet, J. Sire, J. Neyts, J. Balzarini, B. Canard, K. Alvarez, Synthesis, in vitro antiviral evaluation, and stability studies of novel α-borano-nucleotide analogues of 9-[2-(phosphonomethoxy)ethyl]adenine and (R)-9-[2-(phosphonomethoxy)propyl]adenine, J. Med. Chem. 49 (2006) 7799–7806. (c) L.A. Paquette, I. Collado, M. Purdie, Total synthesis of Spinosyn A. 2. Degradation studies involving the pure factor and its complete reconstitution, J. Am. Chem. Soc. 120 (1998) 2553–2562. (d) K.L. Yu, J.J. Bronson, H. Yang, A. Patick, M. Alam, V. Brankovan, R. Datema, M.J.M. Hitchcock, J.C. Martin, Synthesis and antiviral activity of methyl derivatives of 9-[2-(phosphonomethoxy)ethyl]guanine, J. Med. Chem. 35 (1992) 2958–2969.
[135] (a) R.S. Downing, P.J. Kunkeler, H. Bekkum, Catalytic syntheses of aromatic amines, Catal. Today 37 (1997) 121–136. (b) N. Ono, The Nitro Group in Organic Synthesis, Wiley-VCH, New York, 2001.
[136] J. Feng, S. Handa, F. Gallou, B.H. Lipshutz, Safe and selective nitro group reductions catalyzed by sustainable and recyclable Fe/ppm Pd nanoparticles in water at room temperature, Angew. Chem. Int. Ed. 55 (2016) 8979–8983.
[137] N.R. Lee, A.A. Bikovtseva, M. Cortes-Clerget, F. Gallou, B.H. Lipshutz, Carbonyl iron powder: a reagent for nitro group reductions under aqueous micellar catalysis conditions, Org. Lett. 19 (2017) 6518–6521.
[138] N. Shakya, N.C. Srivastav, N. Desroches, B. Agrawal, D.Y. Kunimoto, R. Kumar, 3′-Bromo analogues of pyrimidine nucleosides as a new class of potent inhibitors of *Mycobacterium tuberculosis*, J. Med. Chem. 53 (2010) 4130–4140.

[139] P. Pandit, K.S. Gayen, S. Khamarui, N. Chatterjee, D.K. Maiti, Addition of halide to p-bond directly from aqueous NaX solution: a general strategy for installation of two different functional groups, Chem. Commun. 47 (2011) 6933–6935.

[140] (a) G.A. Olah, Onium Ions, John Wiley & Sons, New York, 1998. (b) P.B.D. De la Mare, R. Bolton, Electrophilic Additions to Unsaturated Systems, vol. 9, Elsevier, Amsterdam, 2013. (c) P.B.D. De la Mare, Electrophilic Halogenation: Reaction Pathways Involving Attack by Electrophilic Halogens on Unsaturated Compounds, CUP Archive, 1976.

[141] T. Ostrowski, B. Golankiewicz, E. De Clercq, G. Andrei, R. Snoeck, Synthesis and anti-VZV activity of 6-heteroaryl derivatives of tricyclic acyclovir and 9-{[cis-1′,2′-bis (hydroxymethyl)cycloprop-1′-yl]methyl}guanine analogues, Eur. J. Med. Chem. 44 (2009) 3313–3317.

[142] (a) S. Madabhushi, R. Jillella, K.K.R. Mallu, K.R. Godala, V.S. Vangipuram, A new and efficient method for the synthesis of α,α-dihaloketones by oxyhalogenation of alkynes using oxone®–KX (X = Cl, Br, or I), Tetrahedron Lett. 54 (2013) 3993–3996. (b) J. Liu, W. Li, C. Wang, Y. Li, Z. Li, Selective 1,2-dihalogenation and oxy-1,1-dihalogenation of alkynes by N-halosuccinimides, Tetrahedron Lett. 52 (2011) 4320–4323. (c) W. He, L. Xie, Y. Xu, J. Xiang, L. Zhang, Electrophilicity of α-oxo gold carbene intermediates: halogen abstractions from halogenated solvents leading to the formation of chloro/bromomethyl ketones, Org. Biomol. Chem. 10 (2012) 3168–3171. (d) C. Wu, X. Xin, Z.-M. Fu, L.-Y. Xie, K.-J. Liu, Z. Wang, W. Li, Z.-H. Yuan, W.-M. He, Water-controlled selective preparation of α-mono or α,α′-dihalo ketones via catalytic cascade reaction of unactivated alkynes with 1,3-dihalo-5,5-dimethylhydantoin, Green Chem. 19 (2017) 1983–1989. (e) R. Mestres, J. Palenzuela, High atomic yield bromine-less benzylic bromination, Green Chem. 4 (2002) 314–316.

[143] L. Finck, J. Jeremy Brals, B. Bhavana Pavuluri, F. Fabrice Gallou, S. Handa, Micelle-enabled photoassisted selective oxyhalogenation of alkynes in water under mild conditions, J. Org. Chem. 83 (2018) 7366–7372.

[144] (a) A. Walser, R.I. Fryer, E.C. Taylor, A. Weissberger, Chemistry of Heterocyclic Compounds, Bicyclic Diazepines, Vol. 50, Wiley, Chichester, UK, 1991. p. 431. Chapters V–VIII. (b) W. Zhang, J.P. William, Y. Lu, T. Nagashima, Q. Chu, Fluorous synthesis of sclerotigenin-type benzodiazepine–quinazolinones, Tetrahedron Lett., 48 (2007) 563–565. (c) T. Kaneko, H. Wong, T.W. Doyle, W.C. Rose, W.T. Bradner, Bicyclic and tricyclic analogs of anthramycin, J. Med. Chem. 28 (1985) 388–392. (d) F. Novelli, A. Sparatore, B. Tass, F. Sparatore, Quinolizidinyl derivatives of 5,11-dihydro-6H-pyrido[2,3-b][1,4]benzodiazepin-6-one as ligands for muscarinic receptors, Bioorg. Med. Chem. Lett. 9 (1999) 3031–3034. (e) R.M. Keenam, J.F. Callaham, J.M. Samanen, W.E. Bondinell, R.R. Calvo, I. Chen, C. DeBrosse, D.S. Eggleston, R.C. Haltiwanger, S.M. Hwang, D.R. Jakes, T.W. Ku, W.H. Miller, K.A. Newlander, A. Nichols, M.F. Parker, L.S. Southhall, I. Uzinskas, J.A. Vasko-Moser, J.W. Venslavsky, A.S. Wong, W.F. Huffmann, Conformational preferences in a benzodiazepine series of potent nonpeptide fibrinogen receptor antagonists, J. Med. Chem. 42 (1999) 545–559. (f) T. Sugimori, T. Okawa, S. Eguchi, A. Kakehi, E. Yashima, Y. Okamoto, The first total synthesis of (−)-benzomalvin A and benzomalvin B via the intramolecular aza-Wittig reactions, Tetrahedron 54 (1998) 7997–8008. (g) S. Kalsoom, U. Rashid, A. Shaukat, O.M. Abdalla, K. Hussain, W. Khan, S. Nazir, M.A. Mesaik, M.A. Zaheer-ul-Haq, F.L. Ansari, Med. Chem. Res. 22 (2013) 5739. (h) L.M. Greene, D.P. Nolan, D. Regan-Komito, G. Campiani, D.C. Williams, D.M. Zisterer, Inhibition of late-stage autophagy synergistically enhances pyrrolo-1,5-benzoxazepine-6-induced apoptotic cell death in human colon cancer cells, Int. J. Oncol. 43 (2013) 927–935. (i) S.K.D. Dwivedi, K. Samanta, M. Yadav, A.K. Jana,

A.K. Singh, B. Chakravarti, S. Mondal, R. Konwar, A.K. Trivedi, N. Chattopadhyay, Amino acids derived benzoxazepines: design, synthesis and antitumor activity, Bioorg. Med. Chem. Lett. 23 (2013) 6816–6821.

[145] (a) L. Garanti, G. Molteni, G. Zecchi, Synthesis of [1,2,3]Triazolo[1,5-a][4,1] benzoxazepines via Intramolecular Azide Cycloaddition, Heterocycles 38 (1994) 291–296. (b) C. Chowdhury, A.K. Sasmal, B. Achari, An expedient and facile route for the general synthesis of 3-aryl substituted 1,2,3-triazolo[1,5-a][1,4]benzodiazepin-6-ones and 1,2,3-triazolo[1,5-a][1,5]benzodiazocin-7-ones, Org. Biomol. Chem. 8 (2010) 4971–4977.

[146] R. Pal, S. Sarkar, N. Chatterjee, A.K. Sen, A green-chemistry approach for the efficient synthesis of triazolobenzoxazepines or triazolo benzodiazepines in aqueous micellarsystem, Tetrahedron Lett. 55 (2014) 1452–1455.

[147] V. Andrushko, N. Andrushko, Stereoselective Synthesis of Drugs and Natural Products II, Wiley-VCH, Weinheim, 2013, pp. 1280–1836.

[148] S. Handa, D.J. Lippincott, D.H. Aue, B.H. Lipshutz, Asymmetric gold-catalyzed lactonizations in water at room temperature, Angew. Chem. Int. Ed. 53 (2014) 10658–10662.

[149] (a) C.C.C. Johansson Seechurn, M.O. Kitching, T.J. Colacot, V. Snieckus, Palladium-catalyzed cross-coupling: a historical contextual perspective to the 2010 Nobel Prize, Angew. Chem. Int. Ed. 51 (2012) 5062–5085. (b) N. Wang, Youji Huaxue 31 (2011) 1319. (c) B. Halford, Chem. Eng. News 88 (2010) 7. (d) B.H. Lipshutz, N.A. Isley, J.C. Fennewald, E.D. Slack, On the way towards Greener transition-metal-catalyzed processes as quantified by E factors, Angew. Chem. Int. Ed. 52 (2013) 10952–10958. (e) T.J.A. Colacot, Highly active palladium(I) dimer for pharmaceutical applications [Pd(μ-Br)(tBu3P)]2 as a practical cross-coupling catalyst, Platinum Met. Rev. 53 (2009) 183. (f)"New Trends in Cross-Couplings: Theory and Applications": T. Colacot, RCS Catalysis Series 2015, can be found under http://pubs.rsc.org/en/content/ebook/9781849738965#!divbookcontent. (g) J. Magano, S. Monfette, Development of an air-stable, broadly applicable nickel source for nickel-catalyzed cross-coupling, ACS Catal. 5 (2015) 3120–3123.

[150] (a) S. Saito, M. Sakai, N. Miyaura, A synthesis of biaryls via nickel(0)-catalyzed cross-coupling reaction of chloroarenes with phenylboronic acids, Tetrahedron Lett. 37 (1996) 2993–2996. (b) S. Saito, S. Oh-tani, N. Miyaura, Synthesis of Biaryls via a nickel(0)-catalyzed cross-coupling reaction of chloroarenes with arylboronic acids, J. Org. Chem. 62 (1997) 8024–8030. (c) F.-S. Han, Chem. Soc. Rev. 42 (2013) 5270.

[151] S. Handa, E.D. Slack, B.H. Lipshutz, Nanonickel-catalyzed Suzuki–Miyaura cross-couplings in water, Angew. Chem. Int. Ed. 54 (2015) 11994–11998.

[152] (a) W. Aida, T. Ohtsuki, X. Li, M. Ishibashi, Isolation of new carbamate- or pyridine-containing natural products, fuzanins A, B, C, and D from *Kitasatospora* sp. IFM10917, Tetrahedron 65 (2009) 369–373. (b) N.K. Kubota, E. Ohta, S. Ohta, F. Koizumi, M. Suzuki, M. Ichimura, S. Ikegami, Piericidins C5 and C6: new 4-pyridinol compounds produced by Streptomyces sp. and Nocardioides sp, Bioorg. Med. Chem. 11 (2003) 4569–4575. (c) M.C. Bagley, C. Glover, E.A. Merritt, Synlett (2007) 2459–2482. (d) P. Jakubec, A. Hawkins, W. Felzmann, D.J. Dixon, Total synthesis of Manzamine A and related alkaloids, J. Am. Chem. Soc. 134 (2012) 17482–17485.

[153] (a) D.A. DeGoey, D.J. Grampovnik, C.A. Flentge, W.J. Flosi, H.-J. Chen, C.M. Yeung, J.T. Randolph, L.L. Klein, T. Dekhtyar, L. Colletti, K.C. Marsh, V. Stoll, M. Mamo, D.C. Morfitt, B. Nguyen, J.M. Schmidt, S.J. Swanson, H. Mo, W.M. Kati, A. Molla, D.J. Kempf, J. Med. Chem. 52 (2009) 2571–2586. (b) R. Álvarez, L. Aramburu, P. Puebla, E. Caballero, M. González, A. Vicente, M. Medarde, R. Peláez, Curr. Med.

Chem. 23 (2016) 1100–1130. (c) A.A. Altaf, A. Shahzad, Z. Gul, N. Rasool, A. Badshah, B. Lal, E. Khan, J. Drug Des. Med. Chem. 1 (2015) 1–11. (d) MDL Drug Data Registry (MDDR), MDL Information Systems, Inc., San Leandro, CA.

[154] (a) C. Kaes, A. Katz, M.W. Hosseini, Bipyridine: the most widely used ligand. a review of molecules comprising at least two 2,2′-bipyridine units, Chem. Rev. 100 (2000) 3553–3590. (b) G. Chelucci, R.P. Thummel, Chiral 2,2′-bipyridines, 1,10-phenanthrolines, and 2,2′:6′,2′-terpyridines: syntheses and applications in asymmetric homogeneous catalysis, Chem. Rev. 102 (2002) 3129–3170. (c) C.K. Prier, D.A. Rankic, D.W.C. MacMillan, Visible Light Photoredox Catalysis with Transition Metal Complexes: Applications in Organic Synthesis, *Chem. Rev*. 113 (2013) 5322–5363. (d) H.-L. Kwong, H.-L. Yeung, C.-T. Yeung, W.-S. Lee, C.-S. Lee, W.-L. Wong, *Coord. Chem. Rev*. 251 (2007) 2188–2222. (e) M.N. Zafar, A.H. Atif, M.F. Nazar, S.H. Sumrra, Gul-E-Saba, R. Paracha, Russ. J. Coord. Chem. 42 (2016) 1–18.

[155] (a) B. Tang, F. Yu, P. Li, L. Tong, X. Duan, T. Xie, X. Wang, A near-infrared neutral pH fluorescent probe for monitoring minor pH changes: imaging in living HepG2 and HL-7702 cells, *J. Am. Chem. Soc*. 131 (2009) 3016–3023. (b) A. Wild, A. Winter, F. Schlutter, U.S. Schubert, Advances in the field of π-conjugated 2,2′:6′,2″-terpyridines, *Chem. Soc. Rev*. 40 (2011) 1459–1511.

[156] (a) J.R. Colombe, S. Bernhardt, C. Stathakis, S.L. Buchwald, P. Knochel, Synthesis of solid 2-pyridylzinc reagents and their application in Negishi reactions, *Org. Lett*. 15 (2013) 5754–5757. (b) M.R. Luzung, J.S. Patel, J. Yin, A mild Negishi cross-coupling of 2-heterocyclic organozinc reagents and aryl chlorides, *J. Org. Chem*. 75 (2010) 8330–8332. (c) S.M. Manolikakes, M. Ellwart, C.I. Stathakis, P. Knochel, Air-stable solid aryl and heteroaryl organozinc pivalates: syntheses and applications in organic synthesis, Chem. A Eur. J. 20 (2014) 12289–12297.

[157] (a) S. Gronowitz, P. Björk, J. Malm, A.-B.J. Hornfeldt, The effect of some additives on the Stille Pd0-catalyzed cross-coupling reaction, *J. Organomet. Chem*. 460 (1993) 127–129. (b) T.R. Bailey, Unsymmetrical heterobiaryl synthesis. A highly efficient palladium-catalyzed cross-coupling reaction of heteroaryl trialkylstannanes with aryl halides, *Tetrahedron Lett*. 27 (1986) 4407–4410.

[158] (a) P. Pierrat, P. Gros, Y. Fort, Hiyama cross-coupling of chloro-, fluoro-, and methoxypyridyltrimethylsilanes: room-temperature novel access to functional bi(het) aryl, *Org. Lett*. 7 (2005) 697–700. (b) D.C. Blakemore, L.A. Marples, Palladium(0)-catalysed cross-coupling of 2-trimethylsilylpyridine with aryl halides, *Tetrahedron Lett*. 52 (2011) 4192–4195.

[159] N-Phenyldiethanolamine 2-pyridylboronate: (a) B. Hodgson, F.H. Salingue, The preparation of a stable 2-pyridylboronate and its reactivity in the Suzuki–Miyaura cross-coupling reaction, Tetrahedron Lett. 45 (2004) 685–687. (b) N.A. Jones, J.W. Antoon, A.L. Bowie, J.B. Borak, E.P.J. Stevens, Synthesis of 2,2′-bipyridyl-type compounds via the suzuki-miyaura cross-coupling reaction, J. Heterocyclic Chem. 44 (2007) 363–367. B(MIDA): (c) G.R. Dick, E.M. Woerly, M.D. Burke, Angew. Chem. Int. Ed. 51 (2012) 2667–2672. (d) S. Sakashita, M. Takizawa, J. Sugai, H. Ito, Y. Yamamoto, Tetrabutylammonium 2-pyridyltriolborate salts for Suzuki–Miyaura cross-coupling reactions with aryl chlorides, Org. Lett. 15 (2013) 4308–4311. (e) J.Z. Deng, D.V. Paone, A.T. Ginnetti, H. Kurihara, S.D. Dreher, S.A. Weissman, S.R. Stauffer, C.S. Burgey, Copper-facilitated Suzuki reactions: application to 2-heterocyclic boronates, Org. Lett. 11 (2009) 345–347. (f) B.M. Crowley, C.M. Potteiger, J.Z. Deng, C.K. Prier, D.V. Paone, C.S. Burgey, Expanding the scope of the Cu assisted Suzuki–Miyaura reaction, Tetrahedron Lett. 52 (2011) 5055–5059.

(g) K. Chen, R. Peterson, S.K. Math, J.B. LaMunyon, C.A. Testa, D.R. Cefalo, Lithium trihydroxy/triisopropoxy-2-pyridylborate salts (LTBS): synthesis, isolation, and use in modified Suzuki–Miyaura cross-coupling reactions, Tetrahedron Lett. 53 (2012) 4873–4876. (h) W. Ren, J. Li, D. Zou, Y. Wu, Y. Wu, Palladium-catalyzed Suzuki–Miyaura cross-coupling reaction of potassium 2-pyridyl trifluoroborate with aryl (heteroaryl) halides, Tetrahedron 68 (2012) 1351–1358. (i) S. Laulhé, J.M. Blackburn, J.L. Roizen, Selective and serial Suzuki–Miyaura reactions of polychlorinated aromatics with alkyl pinacol boronic esters, Org. Lett. 18 (2016) 4440–4443.

[160] N.A. Isley, Y. Wang, F. Gallou, S. Handa, D.H. Aue, B.H. Lipshutz, A micellar catalysis strategy for Suzuki – Miyaura cross-couplings of 2-pyridyl mida boronates: no copper, in water, very mild conditions, ACS Catal. 7 (2017) 8331–8337.

[161] (a) J. Hassan, M. Sevignon, C. Gozzi, E. Schulz, M. Lemaire, Aryl – aryl bond formation one century after the discovery of the Ullmann reaction, Chem. Rev. 102 (2002) 1359–1470. (b) J.S. Carey, D. Laffan, C. Thomson, M.T. Williams, Analysis of the reactions used for the preparation of drug candidate molecules, Org. Biomol. Chem. 4 (2006) 2337–2347. (c) V. Bonnet, F. Mongin, F. Trecourt, G. Breton, F. Marsais, P. Knochel, G. Quequiner, Cross-coupling between 3-pyridylmagnesium chlorides and hetero-aromatic halides, Synlett. 6 (2002) 1008–1010. (d) S. Pestka, in: J.W. Corcoran, F.E. Hahn (Eds.), Antibiotics, vol. 3, Springer-Verlag, New York, 1975, p. 480. (e) R. Capdeville, E. Buchdunger, J. Zimmermann, A. Matter, Nat. Rev. Drug Discov. 1 (2002) 493. (f) A.M. Lewis, M. Ough, M.M. Hinkhouse, M.S. Tsao, L.W. Oberley, J. Cullen, J. Mol. Carcinog. 43 (2005) 215–224. (g) R.W. Friesen, C. Brideau, C.C. Chan, S. Charleson, D. Deschenes, D. Dube, D. Ethier, R. Fortin, J.Y. Gauthier, Y. Girard, R. Gordon, G.M. Greig, D. Riendeau, C. Savoie, Z. Wang, E. Wong, D. Visco, L.J. Xu, R.N. Young, 2-Pyridinyl-3-(4-methylsulfonyl)phenylpyridines: selective and orally active cyclooxygenase-2 inhibitors, Bioorg. Med. Chem. Lett. 8 (1998) 2777–2782. (h) W.R. Kem, R. Soti, D. Rittschof, Biomol. Eng. 20 (2003) 355.

[162] P. Guo, H. Zhang, J. Zhou, F. Gallou, M. Parmentier, H. Wang, Micelle-enabled Suzuki – Miyaura cross-coupling of heteroarylboronate esters, J. Org. Chem. 83 (2018) 7523–7527.

[163] (a) D.X. Yang, S.L. Colletti, K. Wu, M. Song, G.Y. Li, H.C. Shen, Palladium-catalyzed Suzuki – Miyaura coupling of pyridyl-2-boronic esters with aryl halides using highly active and air-stable phosphine chloride and oxide ligands, Org. Lett. 11 (2009) 381–384. (b) A. Bouillon, J.-C. Lancelot, J. Sopkova de Oliveira Santos, V. Collot, P.R. Bovy, S. Rault, Synthesis of novel halopyridinylboronic acids and esters. Part 4: halopyridin-2-yl-boronic acids and esters are stable, crystalline partners for classical Suzuki cross-coupling, Tetrahedron 59 (2003) 10043–10049. (c) S.D. Mandolesi, S.E. Vaillard, J.C. Podestá, R.A. Rossi, Synthesis of benzene- and pyridinediboronic acids via organotin compounds, Organometallics 21 (2002) 4886–4888. (d) K. Deshayes, R.D. Broene, I. Chao, C.B. Knobler, F. Diederich, Synthesis of the helicopodands: novel shapes for chiral clefts, J. Org. Chem. 56 (1991) 6787–6795. (e) A.A. Fuller, H.R. Hester, E.V. Salo, E.P. Stevens, In situ formation and reaction of 2-pyridylboronic esters, Tetrahedron Lett. 44 (2003) 2935–2938. (f) S. Lutzen, M. Hapke, Synthesis of 5-substituted 2,2′-bipyridines from substituted 2-chloropyridines by a modified Negishi cross-coupling reaction, Eur. J. Org. Chem. (2002) 2292–2297. (g) L.C. Campeau, K. Fagnou, Applications of and alternatives to π-electron-deficient azine organometallics in metal catalyzed cross-coupling reactions, Chem. Soc. Rev. 36 (2007) 1058–1068.

Further reading

[164] S. Samai, D. Ghosh, U.K. Das, S. Atta, S.K. Manna, D.K. Maiti, Water—the best solvent for DMAP-mediated dual cyclization towards metal-free first synthesis of fully substituted phthalimides, Green Chem. 18 (2016) 2961–2965.

Green synthesis of nanoparticles and nanocomposites: Medicinal aspects

8

Adya Jain[a,*], *Bimal Krishna Banik*[b,*]
[a]School of Studies in Chemistry, Jiwaji University, Gwalior, India, [b]Department of Mathematics and Natural Sciences, College of Sciences and Human Studies, Deanship of Research Development, Prince Mohammad Bin Fahd University, Al Khobar, Kingdom of Saudi Arabia
[*]Corresponding author. e-mail address: adyajain02@gmail.com; bimalbanik10@gmail.com; bbanik@pmu.edu.sa

8.1 Nanoparticles

Tetgure et al. [1] reported the synthesis of gold and silver nanoparticles using the latex of *Ficus racemosa*. The $HAuCl_4$ and $AgNO_3$ solutions were mixed with latex extract separately. The silver solution was kept in dark while the gold solution was kept in sunlight for 2 h. The change in color from colorless to black or brown in case of silver while light yellow to purple in case of gold solution indicated the formation of silver nanoparticles and gold nanoparticles, respectively. The formation was confirmed by UV-VIS spectroscopy and XRD studies. The morphology was determined by FESEM studies. The binding studies of nanoparticles with L-lysine, L-arginine, L-glutamine, and glycin was also described. Silver nanoparticles showed a good binding ability in acidic and neutral conditions whereas gold nanoparticles showed a good binding ability in acidic conditions regardless of the amino acids.

Kumar et al. [2] reported the synthesis of silver nanoparticles using aqueous stem bark extract (as reducing, stabilizing, and capping agent) of *Adansonia digitata* (L.) and aqueous solution (1 mM) of $AgNO_3$ at 60–80°C for 60 min. The change in color from light brown to thick brown indicated the formation of silver nanoparticles. The formation of silver nanoparticles was confirmed by FTIR and UV-VIS spectroscopy. The morphology was determined by XRD, SEM with EDAX, TEM, and AFM. Synthesized nanoparticles were screened for an antimicrobial activity against two Gram-positive bacteria (*Bacillus subtilis* and *Staphylococcus aureus*) and five Gram-negative bacteria (*Escherichia coli*, *Klebsiella pneumoniae*, *Proteus vulgaris*, *Pseudomonas aeruginosa*, and *Salmonella typhimurium*) whereas antifungal activity was screened against five fungal species (*Alternaria solani*, *Aspergillus niger*, *Aspergillus flavus*, *Penicillium chrysogenum*, and *Trichoderma harzianum*).

Sudhasree et al. [3] reported the synthesis of nickel nanoparticles by chemical and green approaches and compared their toxicity and biological activity. In a green synthesis, $NiCl_2$ solution and aqueous root extract of *Desmodium gangeticum* were mixed in three different

Green Approaches in Medicinal Chemistry for Sustainable Drug Design. https://doi.org/10.1016/B978-0-12-817592-7.00008-3
© 2020 Elsevier Inc. All rights reserved.

ratios. One part of $NiCl_2$ and different portion of aqueous root extracts were mixed. Then the mixtures were heated at 80°C with continuous stirring for 45 min. The change in color from brown to gray indicated the formation of nickel nanoparticles. It was reported that fine particles containing size of 0.5 nm is obtained from using two parts of aqueous extract phytoconstituents. In chemical synthesis $NiCl_2$ was added to N_2H_4 in four different concentrations. Then the solutions were mixed with different concentrations of NaOH and polyethylene glycol as a stabilizing agent. The mixtures were heated at 60°C for 15–20 min with periodic stirring. The change in color from bluish green to a blackish gray confirmed the formation of nanoparticles. The particle size 6.04 nm was reported when 1 M $NiCl_2$, 0.5 M NaOH, and 2% PEG were used. The formation of nanoparticles was confirmed by UV-Vis spectroscopy and FTIR while the morphology was determined by XRD, VSM, and zeta potential. It was reported that the nanoparticles synthesized by first method have better colloidal stability, magnetic property, antioxidant, and antimicrobial property than the chemically synthesized nanoparticles.

Synthesis of silver nanoparticles was reported by Sangeetha et al. [4] by mixing aqueous extract of *Excoecaria agallocha* and aqueous solution of $AgNO_3$ in different ratios and allowed to stand for 35 min. The appearance of brownish yellow color confirmed the synthesis of silver nanoparticles. The formation was confirmed by UV-Vis spectroscopy and XRD studies. The morphology was determined by TEM.

Synthesis of silver nanoparticles was studied by Dhiman et al. [5] by mixing seed extract of *Elettaria cardamom* (reducing agent) and silver nitrate aqueous solution. The mixture was kept in dark at room temperature for 24 h for the reduction of Ag^+ ions. Then the solution was centrifuged and ultrasonicated for 1 h. The change in color from pale yellow to yellowish brown indicated the formation of silver nanoparticles. The formation was confirmed by UV-Vis spectroscopy and XRD studies. The morphology was determined by SEM. The synthesized nanoparticles were also screened for an antibacterial activity against *Bacillus subtilis*.

Rajathi et al. [6] reported the synthesis of platinum nanoparticles using leaf extract of *Cerbera manghas* (as reducing agent) and aqueous solution of $H_2PtCl_6{\cdot}3H_2O$ at room temperature. The change in color from yellow to black indicated the formation of platinum nanoparticles. The formation was confirmed by UV-Vis and FTIR spectral analysis while morphology and size was determined by TEM and XRD. The synthesized nanoparticles were also tested for antibacterial activity against Gram-positive (*E. coli*) and Gram-negative bacteria (*S. aureus*).

SnO_2 nanoparticles were synthesized by Kamaraj et al. [7]. Leaf powder of *Cleistanthus collinus* and ethanol was heated at 60°C for 2 h. It was filtered and mixed with aqueous solution of tin oxide and heated at 80°C for 1 h. The change in color from greenish yellow to pale yellow indicated the formation of SnO_2 nanoparticles. The characterization was done by XRD, SEM, and EDAX. The average size of these nanoparticles was reported to 49.26 nm. Tin oxide nanoparticles exhibited strong antibacterial activity, antifungal activity, and antioxidant activity. Specifically, the synthesized nanoparticles were screened for antibacterial activity against *Escherichia coli* and *S. aureus*. It was reported that nanoparticles were found to be more active against *E. coli* as compared to *S. aureus*. Antifungal activity was screened against *Aspergillus niger* and *T. viridea*. Antioxidant activity was determined by DPPH free-radical scavenging assay method. These particles exhibited an excellent antioxidant property.

Divya et al. [8] synthesized zinc oxide nanoparticles by mixing the aqueous leaf extract of *Hibiscus rosa-sinensis* with $ZnSO_4 \cdot 7H_2O$, natural surfactant, and a solution of NaOH at room temperature. The appearance of white precipitate dictated the formation of ZnO nanoparticles. The identity was confirmed by UV-Vis spectroscopy. The morphology of nanoparticles was determined by SEM. The synthesized nanoparticles were screened for antibacterial activity against *Proteus vulgaris*, *Staphylococcus aureus*, *E. coli*, *Pseudomonas aeruginosa*, and *Klebsiella pneumonia*.

Mahdavi et al. [9] studied magnetic iron oxide (Fe_3O_4) nanoparticles using aqueous extract of *Sargassum muticum* (brown seaweeds) as reducing agent and $FeCl_3$ in 1:1 ratio. The mixture was stirred for 60 min and allowed to stand at room temperature for another 30 min. This colloidal suspension was centrifuged and washed with ethanol. Then, it was dried at 40°C. The structure was confirmed by FTIR, XRD, and UV-Vis spectroscopy. The morphology and size distribution were identified by TEM, FESEM, and VSM (vibrating sample magnetometry). The antimicrobial activity of nanoparticles synthesized by this method was higher than those synthesized by chemical method.

Subhankari et al. [10] reported the synthesis of copper nanoparticles by mixing 1:1 ratio of aqueous extract of *Syzygium aromaticum* (as reducing agent) and copper sulfate. The mixture was allowed to stand in an incubator for 1 h. The color change from dark brown to sea green confirmed the synthesis of copper nanoparticles. The formation was confirmed by UV-Vis spectroscopy and XRD studies. The morphology was determined by TEM and SEM.

Awwad et al. [11] reported the synthesis of silver nanoparticles by adding aqueous extract of *Ceratonia siliqua* (carob leaves) to an aqueous solution of $AgNO_3$. The quick change in color from yellow to black at room temperature confirmed the synthesis of silver nanoparticles. The characterization was done by FTIR, AAS, and UV-Vis while the morphology and size was determined by SEM and XRD. These synthesized nanoparticles were spherical with diameter of 5–40 nm. These silver nanoparticles exhibited strong antibacterial activity against *E. coli*.

Green synthesis of ZnO nanoparticles was reported by Vidya et al. [12]. An aqueous leaves extract of *Calotropis gigantea* (as a reducing agent) was heated to 60°C then zinc nitrate was added. The solution was boiled until a deep yellow colored paste was obtained. This paste was heated at 400°C for 2 h to obtain a light yellow colored powder which confirms the formation of ZnO nanoparticles. The particle size was in the range of 30–35 nm. The morphology and size of nanoparticles was confirmed by XRD and SEM.

Lalitha et al. [13] reported the synthesis of silver nanoparticles from leaves extract of *Azadirachta indica* and aqueous solution of silver nitrate. This mixture was kept in dark for 24 h. The appearance of brownish gray color indicated the formation of silver nanoparticles. The formation was confirmed by FTIR and UV-Vis spectral analysis. The synthesized particles were also screened for their antibacterial activity against Gram-positive (*Salmonella typhi)* and Gram-negative (*Klebsiella pneumoniae*) bacteria. The antioxidant activity of these particles was detected by DPPH and hydrogen peroxidase assay.

Das et al. [14] described the synthesis of gold nanoparticles using *Amaranthus spinosus* leaf extracts. Leaf powder was mixed with ethanol and the mixture was left in a shaking incubator operating at 200 rpm, 25°C for 24 h. The extracts were then

filtered and the filtrate was used for gold nanoparticles synthesis. Various concentrations (1%–5%, v/v) of the ethanolic leaf extracts were mixed with aqueous solution of $HAuCl_4$ (1 mM). The mixture solution was stirred at room temperature (25°C) and during this time a color change was observed. After 4 h, the color was changed from yellow to ruby red. It was found that 1 mM of $HAuCl_4{\cdot}4H_2O$ solution and 1% concentration of plant extracts is sufficient to obtain a correct size of gold nanoparticles (i.e., <50 nm). This was confirmed by SPR peaks. However, by increasing the concentration of plant extracts, the quantity of gold nanoparticles was increased. Nanoparticles obtained from 5% concentration of leaf extracts were mostly spherical with few triangular morphologies. The formation of nanoparticles was confirmed by FTIR and UV-Vis while the morphology and size was determined by TEM, XRD, and EDX. Cytotoxicity assay was screened against two cancer cells, i.e., HeLa and MCF-7 with different concentrations of gold nanoparticles (10–100 μM). These cancer cells exhibited an excellent viability up to 100 μM concentration which had an insignificant toxicity of gold nanoparticles. Thus, these nanoparticles can be used for biomedical applications, like drug delivery and molecular imaging.

Bansal et al. [15] reported the green synthesis of CdS nanoparticles using glucose as capping agent. Cadmium nitrate solution (0.1 M) was mixed with 0.1-M sodium sulfide with continuous stirring. After 15 h, the solution was divided into three parts and glucose solutions of different concentrations (0.01, 0.1, and 0.5 M) was separately added in each part. The obtained solutions were heated and incubated for 6 h at 100°C. The obtained precipitates were filtered and dried at 50°C for 4 h. The formation of nanoparticles was confirmed by UV-Vis spectroscopy. The size and morphology was determined by XRD. The characterization data revealed that the crystalline size was decreased from 43 to 13 nm as the concentration of glucose increased from 0.01 to 0.5 M.

Ahmad et al. [16] studied the biosynthesis of silver nanoparticles by mixing the aqueous fruit extracts of *Ananas comosus* with aqueous $AgNO_3$ in 1:10 ratio. Addition of the aqueous fruit extracts to aqueous $AgNO_3$ solution resulted in color change within minutes resulting in the formation of silver nanoparticles. The formation of nanoparticles was confirmed by UV-Vis spectroscopy and component elemental analysis was detected by EDAX. The morphology of synthesized nanoparticles was determined by HRTEM and SAED. The average size of silver nanoparticles was found 12 nm approximately.

Biosynthesis of CdO nanoparticles was reported by Andeani et al. [17] by mixing 25 mL of broth extract of flowers of *Achillea wilhelmsii* with 25 mL 10 mM aqueous cadmium chloride solution at room temperature. After few minutes, precipitate was formed at the bottom of the flask leaving colloidal supernatant at the top. This precipitate was purified by repeated centrifugation (14,000 rpm) for 5 min followed by redispersion of the pellet in deionized water. The formation of nanoparticle was confirmed by FTIR and UV-Vis spectral analysis and morphology was determined by FESEM.

Pandey et al. [18] synthesized gold nanoparticles by mixing fruit extracts of *Momordica charantia* (as nanofabricator) with solution of aurochlorate (50,000 ppm) salt at boiling temperature. The change in color from colorless to wine red indicated the formation of gold nanoparticles. They studied the impact of pH (4, 6, 8, and 10) at low (30°C) and high (100°C) temperature. The characterization was done by UV-Vis spectral analysis while morphology and size were determined by XRD and

HRTEM. Nitrate reductase assay and total protein estimation was performed to assay the possible role of nitrate reductase as reducing agent. The data indicated best results at pH 10 at 100°C. The impact of different temperatures (4, 28 ± 2°C, 60°C, 100°C) with 100 ppm aurochlorate concentration and different concentration of aurochlorate (50, 100, 150, 200, 250 ppm) with aqueous extracts of *Momordica charantia* at pH 10 were also studied.

Awwad et al. [19] reported green synthesis of magnetite nanoparticles (Fe_2O_3) using aqueous leaf extracts of *C. siliqua*. Iron salts, $FeCl_2{\cdot}4H_2O$ and $FeCl_3{\cdot}6H_2O$ were dissolved in water and heated at 80°C under mild stirring. After 10 min, aqueous leaf extracts were added which immediately changed yellowish color to reddish brown color. To it was added aqueous solution of NaOH with continuous magnetic stirring. The reddish brown mixture changed to black suspended particles. The mixture was allowed to cool at room temperature and magnetite nanoparticles were obtained by decantation. These nanoparticles were diluted with sterile distilled water, centrifuged to remove heavy biomaterials, and finally dried overnight at 80°C. The formation and stability of magnetite nanoparticles in aqueous colloidal solution was confirmed by UV-Vis and FT-IR analysis. The morphology and particle size was determined by XRD and SEM. Thermal stability of nanoparticles was determined by TG/DTA analysis. SEM study revealed that the average diameter of these nanoparticles was found 5–8 nm approximately.

Raj et al. [20] reported the synthesis of cobalt nanoparticles by mixing cobalt nitrate hexahydrate, dissolved in 95 wt% ethanol. Then vegetable oil was added to this mixture with continuous stirring at room temperature. Sucrose was added to this mixture at 90–100°C. A heating of the solution was continued until black gel is formed. It was filtered, washed with water to remove sucrose or ethanol from the sample. Cobalt nanoparticles were extracted with chloroform and thereafter precipitated by addition of ethanol and centrifuged. The morphology and size was confirmed by XRD and SEM. The XRD data revealed crystalline size 6.4 nm and FCC structure for cobalt nanoparticles. Thermal instability of nanoparticles was determined by TG/DTA analysis.

Nadagouda et al. [21] studied the green synthesis of silver and palladium nanoparticles using the aqueous extracts of coffee and tea. In the first method of silver nanoparticles synthesis, coffee extracts were mixed with $AgNO_3$ with constant stirring at room temperature. In the second method silver nanoparticles was prepared by the addition of tea extracts to 0.1-M $AgNO_3$ solution. Similarly, palladium nanoparticles were synthesized using $PdCl_2$ with coffee and tea extracts separately at room temperature. The formation of Ag and Pd nanoparticles was confirmed by UV-Vis spectral analysis and morphology was determined by TEM. TEM results indicated that silver and palladium nanoparticles were spherical with sizes ranging from as low as 5–100 nm depending on coffee and tea extracts used.

8.2 Nanocomposites

Synthesis of silver nanoparticles/attapulgite (APT) nanocomposite (Ag-NPs/APT) was reported by Wang et al. [22]. In a typical experiment ultrafine AgOAc powder was mixed with APT powder (mesh) in an agate mortar and then ground for

30 min. The ground mixture was calcined at 300°C for 2 h under argon atmosphere. On cooling at room temperature, a black powder was obtained. Similar experiment was done using AgOAc powder separately. The morphology of nanocomposite was determined by XRD and TEM analysis which showed spherical or quasi-spherical silver nanoparticles. Synthesized nanoparticles were also screened for catalytic activity. The nanocomposites showed excellent catalytic reducing properties for dye, which rapidly decolorized the Congo red (CR) solution within 2 min using a low dosage of catalyst. Therefore, the materials were suitable catalyst for the treatment of CR dye wastewater.

Patil et al. [23] reported the synthesis of polyaniline/nickel ferrite magnetic nanocomposite (PANI-$NiFe_2O_4$). In the first step, nickel ferrite nanoparticle ($NiFe_2O_4$) was synthesized by mixing aqueous solution of nickel chloride ($NiCl_2{\cdot}6H_2O$) and aqueous solution of ferric chloride ($FeCl_3{\cdot}6H_2O$). To this mixture, aqueous solution of ammonia was added and kept on vigorous stirring. The obtained nanoparticles were centrifuged. In the second step PANI-$NiFe_2O_4$ nanocomposite was synthesized by mixing aniline, $NiFe_2O_4$, and H_2SO_4 at room temperature. Ammonium persulfate was used as an oxidant. The precipitate was filtered and washed with water followed by methanol. The product was dried in oven at 70°C for 24 h to obtain black green powder of PANI-$NiFe_2O_4$ nanocomposite. The morphology was confirmed by EDS, SEM, and XRD. The magnetic properties were determined by vibrating sample magnetometer (VSM). PANI-$NiFe_2O_4$ nanocomposite can be used as an adsorbent for the removal of malachite green (MG) dye from aqueous solution.

Fu et al. [24] reported the synthesis of β-cyclodextrin-functionalized reduced graphene silver nanocomposites. Graphene oxide (GO) was dispersed into water by sonication. In this solution, polydiallyldimethylammonium chloride (PDDA) and β-cyclodextrin solution were successively added. The solution was vigorously stirred for 2 h. Ammonia and hydrazine hydrate were added to it. This mixture was heated at 90°C in a water bath for 4 h. Finally, black precipitate was collected by centrifugation followed by water washing cycle. After that β-CD/RGO dispersion (1 mg/mL) was mixed with water and $AgNO_3$ for half-hour stirring. Ammonia solution was then added into the mixture and kept stirring. Finally, the product was collected by centrifugation and washed with water. The formation of nanocomposite was confirmed by FT-IR and optical properties by UV-Vis analysis. Morphology and elemental composition were determined by SEM and EDS, respectively. Magnetic cyclic voltammetry measurements suggested that the synthesized nanocomposite exhibits an excellent electrochemical activity toward oxidation of nitrile due to the host-guest recognition. An increase capability of β-CD, as well as the outstanding electronic properties of RGO and Ag nanoparticles, was observed. Typical amperometric responses of the β-CD/RGO/Ag modified GCE to the addition of nitrile showed less responsive time which is due to high electronic conductivity and good catalytic activity.

Ocwelwang et al. [25] reported the synthesis of nitrogen and silver-doped TiO_2 nanoparticles using the sol-gel synthesis method. A solution of $TiCl_4$ was added to distilled water. The aqueous solution was heated at 100°C for complete hydrolysis and condensation. The pH was adjusted to 8.0 by adding NaOH. A white gel was formed which was separated by centrifugation. The obtained precipitate was washed

with deionized water. It was filtered and dried in oven at 150°C. The dried precipitate was crushed and pulverized into powder and calcinated at 600°C for 2 h. In the similar way nitrogen-doped TiO_2 nanoparticles was synthesized by the addition of urea as a nitrogen source. In the second step Cs-PVAE polymer blend of 80:20% (v/v) ratio was prepared and mixed with TiO_2, Ag/TiO_2, N/TiO_2 nanopowders to make respective composites and taken under high-voltage electrospinning. Thereafter, polymer solution was stretched out into fibers and then collected onto the grounded collector. Finally, it was dried in air overnight. The synthesized nanoparticles and electrospin nanocomposite fiber were characterized by FTIR. The size and morphology of nanoparticles was confirmed by XRD, SEM while EDS for elemental composition. Thermal stability of nanofiber composites was determined by TG/DTG analysis. The SEM results revealed average size of nanofibres in the range 234–270 nm and uniform.

Pandey et al. [26] reported the green synthesis of polysaccharide/gold nanoparticle nanocomposite using guar gum (GG) extract as reducing agent. An aqueous gold(III) chloride hydrate solution was mixed with GG solution followed by few drop of very dilute solution of sodium hydroxide (0.01 M) were added and stirred gently at 80°C for 160 min. The change in color from yellow to pink-red colored solution indicated the formation of GG/AuNPs nanocomposite. The formation and optical sensing properties of ammonia solution was confirmed by the means of UV-Vis spectra. The size and morphology was determined by XRD, SEM, and HRTEM. The HRTEM results revealed spherical shape and average particle size approximately 6.5 nm. The XRD results confirmed the FCC crystalline geometry of the synthesized nanoparticles. It was reported that GG/AuNPs nanocomposite can be used as optical ammonia sensor in clinical and medical diagnosis for detecting ultralow ammonia level in human. Colorimetric assays demonstrated high sensitivity, fast response time, and great reproducibility.

Synthesis of polyaniline-montmorillonite (PANI-MMT) nanocomposites was reported by Baldissera et al. [27] by adopting sonication method. MMT clay was dried at 80°C for 24 h to remove moisture and mixed to HCl solution. The solution was sonicated for 30 min by using an ultrasound probe. Then the monomer was added and the solution was sonicated for another 30 min. A solution of HCl containing the oxidizing agent $[(NH_4)_2S_2O_8]$ was added dropwise to this solution under constant stirring. The polymerization of aniline was carried out at −4 and 0°C for 6 h. The obtained PANI-MMT was filtered, washed and dried in oven at 60°C for 24 h. Formation of nanocomposites was confirmed by FT-IR. Crystalline phase and morphology was determined by XRD and TEM. Electrical conductivity was measured by four-point method. Thermal studies revealed that the synthesized nanocomposite was stable up to 200°C. The prepared nanocomposites have an excellent property of electrical conductivity.

Synthesis of unsaturated polyester resin (UPR)-silica nanocomposite was reported by Sudirman et al. [28]. Silica nanoparticles were prepared by using sodium silicate and caustic soda. Carbon dioxide was allowed to pass through the reaction system. The solution was filtered, washed with water, and collected as nano-silica. It was dried in oven at 70°C for 48 h. Silica NPs-UPR composite was prepared by mixing silica NPs

(as filler), UPR (as matrix), and methyl ethyl ketone peroxide in a mixer at room temperature for 30 min. The weight ratio of silica nanoparticles and UPR was varied at 0.5, 1.0, 1.5, 2.0, and 2.5 wt%. Then a composite film was prepared by casting the solution and dried. The structure and morphology of the synthesized nanocomposite were determined by FT-IR, electron microscopy, SEM, Young's modulus, and thermal analysis. Morphological studies revealed that silica nanoparticles were well dispersed in the matrix. Mechanical properties of composite were performed by Strograph VGS5E according to ASTM D-638 at room temperature and crosshead speed of 50 mm/min. Mechanical results indicated that tensile strength elongation and Young's modulus increase with the addition of silica nanoparticles up to 1.0 wt% and then decrease over 1.0 wt%.

Dong et al. [29] reported the synthesis of reduced grapheme-gold nanocomposite adopting microwave irradiation method. Graphene oxide was synthesized by mixing graphite to H_2SO_4. After sonication at room temperature, the solution was filtered to obtain pre-oxidized graphite powder. This powder and $KMnO_4$ were added into aqueous solution of H_2SO_4 with stirring in an ice-water bath at 10°C for 2 h. To this solution, H_2O_2 (30%) were added at room temperature. The suspending solution was precipitated for 12 h and the upper supernatant was collected and centrifuged. The obtained GO powder was washed with HCl and distilled water. Then GO was dispersed in distilled water to get a stable brown solution. Reduced graphene oxide-gold nanocomposite (rGO—Au) was synthesized by mixing hydrazine and sodium dodecyl sulfate (SDS) in aqueous solution of graphene oxide. The mixture solution was irradiated in microwave (900 W, 2.40 GHz) for 30 s and stable rGO dispersions were obtained. The reduced GO sheets were centrifuged and washed with distilled water and redissolved into aqueous SDS solution. Au nanoparticles were deposited on rGO sheets by using aqueous of $HAuCl_4$. The UV-Vis absorption, atomic force microscopy (AFM), SEM, TEM, and Raman spectroscopy were used to demonstrate the successful attachment of Au nanoparticles to graphene sheets. Morphology results indicated that Au nanoparticles were uniformly distributed and tightly attached to the surface of rGO sheets. FETs were used to investigate the effect of gold nanoparticles on the electrical property of rGO sheets. It was reported that rGO-Au sheets show higher hole mobility than pure rGO sheets. They also demonstrated that field-effect transistors (FET) based on rGO-Au nanocomposites are able to detect DNA hybridization. Based on above observation, it has been reported that rGO-Au nanocomposite can be used in nanoelectronics and bio-nanoelectronics.

Farghali et al. [30] reported the synthesis of graphene/magnetite nanocomposite (G/Fe_3O_4) using solvothermal method. Graphene oxide (GO) was prepared by mixing $NaNO_3$ and H_2SO_4, followed by stirring at 70°C for 30 min. Graphite powder was added to the mixture, followed by stirring at 70°C for 45 min. The mixture was kept in ice bath (below 5°C) and $KMnO_4$ was added into the mixture. Then the mixture was heated to 35°C and continuously stirred for 5 h until viscous reddish green paste was obtained. To this paste, deionized water was added followed by H_2O_2. Then the mixture was centrifuged and washed with 10% HCl solution and finally was dried at 60°C to obtain the brown GO sheets. The $G\text{-}Fe_3O_4$ nanocomposite was prepared by mixing sodium acetate and suspended solution of GO in ethylene glycol. Solid $FeCl_3$ was

added into the solution with stirring and the mixture was kept at 200°C for 10 h in autoclave. It was cooled, washed with ethanol/deionized water, and dried at 60°C. Similar procedure was used to synthesize six samples of G/Fe_3O_4 nanocomposites changing feeding weight ratios of Fe_3O_4: G (m Fe_3O_4: m G = 0.1:1, 0.2:1, 0.4:1, 0.6:1, 0.8:1, and 1:1). The prepared nanocomposites were analyzed by UV-Vis adsorption spectra. Morphology and crystalline structure was determined by XRD and HRTEM. Surface composition and elemental chemical oxidation states were determined by XPS. Magnetization was confirmed by VSM. The HRTEM results revealed a uniform sheet like shape of prepared graphene sheet and Fe_3O_4 nanoparticles. The VSM data revealed that the magnetization has increased sharply by increasing concentration of Fe_3O_4 nanoparticles. Adsorption of MB dye on different ratios of G/Fe_3O_4 nanocomposites was also studied and it is reported that on increasing Fe_3O_4 nanoparticles on the surface of G sheet the adsorption capacity decreased.

Agarwal et al. [31] reported the synthesis of zinc sulfide-poly methyl methacrylate nanocomposite (ZnS/PMMA). The PMMA was dissolved in tetrahydrofuran and ZnS nanoparticles with different (0, 2, 4, 6, and 8) wt% were dispersed. These solutions were agitated by ultrasonicator to obtain uniform distribution of ZnS nanoparticles. These solutions were poured in the petri dishes to obtain the ZnS/PMMA nanocomposite films. After 2 days, the nanocomposite films were taken out from the petri-dishes and dried in vacuum (10–2 Torr) for 6 h to remove the solvent. The thickness of prepared samples was approximately 0.12 mm. The morphology of synthesized ZnS/PMMA nanocomposite was determined by XRD and TEM. Transient plane source (TPS) technique was used to determine the effective thermal conductivity of nanocomposites over the temperature range from room (30°C) to 120°C. Thermal conductivity was increased up to 6 wt% and beyond this wt%, it was decreased. The TEM data revealed that the particles were well dispersed at lower wt% while agglomeration was enhanced as the wt% increased.

Tang et al. [32] studied the synthesis of polyacrylamide-calcium phosphate nanocomposites (PAM-CP) by two methods. In the first method (Sample A) in a basic medium, $CaCl_2{\cdot}2H_2O$, $(NH_4)_2S_2O_8$ and acrylamide were dissolved in deionized water under magnetic stirring. An aqueous solution of $(NH_4)_2HPO_4$ was added to the above solution. The pH value of the solution was maintained at 10 by using NH_4OH. The suspension was then heated to 80°C for 45 min by microwave heating. The obtained colloidal solution was added to ethanol to form a precipitate. The precipitate was filtered, washed with absolute ethanol, dried in air at 60°C and ground to powder. For the preparation of a typical sample in a weak acidic medium (sample B), the phosphate buffer solution was used. An aqueous solution containing $Ca(CH_3COO)_2{\cdot}H_2O$ was added to buffer solution (0.090 g $Na_2HPO_4{\cdot}12H_2O$ and 0.041 g $NaH_2PO_4{\cdot}2H_2O$, pH 5), then acrylamide and $(NH_4)_2S_2O_8$ were dissolved in the solution. The solution was heated to 80°C by microwave for 1 h. The formation of nanocomposite was confirmed by FT-IR and morphology was determined by XRD and TEM. TGA was used to determine its degradation. PAM-HAP (hydroxyapatite) nanocomposite were prepared in basic medium (Sample A) while PAM-ACP (amorphous calcium phosphate) nanocomposite were prepared in weak acidic medium (Sample B). TEM results showed that HAP phase consists of nanorods with diameter of 10–20 nm and lengths

of 25–40 nm while ACP phase consists of nanoparticles instead of nanorods with much smaller sizes (<10 nm). TGA analysis exhibited that the thermal stability of PAM is enhanced to some extent by the presence of small amount of ACP nanofiller. The similar result was also observed for the PAM-HAP nanocomposite.

Liu et al. [33] reported the synthesis of MoS_2/graphene nanocomposites. MoS_2/GS were prepared using ammonium tetrathiomolybdate (ATTM), functionalized graphene nanosheets (FGS), and deionized water at 70–80°C. The ATTM/FGS was dried in a vacuum oven at 60°C for 12 h. M-MoS_2/GS, T-MoS_2/GS and MoS_2/AC (activated carbon) were also prepared using microwave irradiation (at 800 W, 40 s) and conventional thermal annealing at 400°C for 1.5 h in flowing N_2/H_2 (1:1) and coconut shell activated carbon as support material, respectively. The characterization was determined by means of FT-IR and Raman spectroscopy. The morphology and size were determined by FESEM, TEM, and XRD. TEM results indicated particle sizes between 10 and 20 nm. Hydrodesulfurization (HDS) activity was studied by catalytic reduction of carbonyl sulfide (COS) and also from TEM which revealed catalytic activity of M-MoS_2/GS is superior to that of T-MoS_2/GS. MoS_2/AC displayed a lower catalytic activity for COS hydrogenation compared to M-MoS_2/GS. It had a higher specific surface area than M-MoS_2/GS hybrid.

Tavares et al. [34] studied the synthesis of polydimethylsiloxane (PDMS)/TiO_2 nanocomposite. TiO_2 nanoparticles were prepared by mixing titanium IV isopropoxide with ethanol under stirring for 5 min at room temperature. Then, acetic acid was added followed by the addition of sulfuric acid under constant stirring. Subsequently, the clear solution obtained was sonicated at 60°C for 1 h. Milky colloidal solution was obtained which was transferred to a Teflon-lined autoclave for hydrothermal treatment irradiated by microwave (2.45 GHz, 800 W) at 120°C for 2 h (at 25°C/min rate). After cooling, the precipitate was centrifuged, washed with distilled water and ethanol to decrease the solution acidity, and then dried at room temperature. PDMS/TiO_2 nanocomposite was prepared by adding polydimethylsiloxane (PDMS) with the polymerizing agent at a ratio of 10:1. Then the mixture was diluted with hexane in 1:2 ratio (PDMS: hexane) with subsequent dispersion of TiO_2 nanoparticles in three different proportions, i.e., 0%, 0.5%, and 1%. Then the mixture was sprayed on glass slides. Subsequently nanocomposites were placed in an oven with air circulation for 30 min at 60°C for polymerization. The formation of nanocomposite was confirmed by UV-Vis and FT-IR spectroscopy. The morphology and size was determined by XRD and FEG-SEM. FEG-SEM studies revealed that TiO_2 nanoparticles are spherical with different sizes from 70 to 300 nm. It was reported that spherical nanoparticles have large surface area and pore volume that increases the contact surface between particles. These nanoparticles can also be used as photocatalyst. Nanocomposite coating with 1% TiO_2 showed degradation rate of methylene blue dye slightly higher than 0.5% wt TiO_2.

Sedaghat et al. [35] reported the synthesis of polyaniline/MnO_2 nanocomposite (PANI/MnO_2). To HCl solution, MnO_2 and aniline were added simultaneously. Dark colored solution was obtained and kept for sonication in an ice bath for 30 min. The temperature of the solution decreased to 0°C until polymerization was stopped. It was filtered, washed, with deionized water followed by ethanol. The product was then

dried at 60°C in an oven for 1 h. the characterization was done by FT-IR while the morphology and size were determined by SEM. Polyaniline being intercalated between manganese oxide layers was revealed through FT-IR studies. SEM analysis showed that PANI/MnO_2 nanocomposite comprises plate-like particles of 50 nm thicknesses.

8.3 Conclusion

From this review, it can be concluded that biosynthetic method is a successful method for green synthesis of nanoparticles and nanocomposites. It has been found to be low cost, rapid eco-friendly approach for single-step synthesis of nonpathogenic nanoparticles and nanocomposites. UV-Vis and FTIR confirms the formation of NPs and NCs while the morphology has been determined by SEM and XRD. The synthesized NPs and NCs exhibit multiple green properties such as antibacterial, antifungal, and antioxidant property incorporated from green plant extract.

Acknowledgments

Bimal Krishna Banik is grateful to Prince Mohammad Bin Fahd University.

References

[1] S.R. Tetgure, A.U. Borse, B.R. Sankapal, V.J. Garole, D.J. Garole, Amino Acids 47 (4) (2015) 757.
[2] C.M.K. Kumar, P. Yugandhar, D. Suhrulatha, N. Savithramma, J. Pharm. Sci. Res. 7 (2) (2015) 76.
[3] S. Sudhasree, A.S. Banu, P. Brindha, G.A. Kurian, Toxicol. Environ. Chem. 96 (5) (2014) 743.
[4] A. Sangeetha, U. Saraswathi, G.J. Singaravelu, Int. J. Pharm. Sci. Inven. 3 (10) (2014) 54.
[5] J. Dhiman, V. Kundu, S. Kumar, R. Kumar, S.K. Chakarvarti, Am. J. Mater. Sci. Tech. 3 (1) (2014) 13.
[6] F.A.A. Rajathi, V.R.M.S. Nambaru, Int. J. Pharm. Bio. Sci 5 (1) (2014) 619.
[7] P. Kamaraj, R. Vennila, M. Arthanareeswari, S. Devikala, World J. Pharm. Pharm. Sci. 3 (9) (2014) 382.
[8] M.J. Divya, C. Sowmia, K. Joona, K.P. Dhanya, Res. J. Pharm., Biol. Chem. Sci. 4 (2) (2013) 1137.
[9] M. Mahdavi, F. Namvar, M.B. Ahmad, R. Mohamad, Molecules 18 (5) (2013) 5954.
[10] I. Subhankari, P.L. Nayak, World J. Nano Sci. Technol. 2 (1) (2013) 14.
[11] A.M. Awwad, N.M. Salem, A.O. Abdeen, Int. J. Ind. Chem. 4 (29) (2013) 1.
[12] C. Vidya, S. Hiremath, M.N. Chandraprabha, M.A.L. Antonyraj, I.V. Gopal, A. Jain, K. Bansal, Int. J. Curr. Eng. Tech. (2013) 118. Proceedings of National Conference on 'Women in Science & Engineering', Special Issue 1.
[13] A. Lalitha, R. Subbaiya, P. Ponmurugan, Int. J. Curr. Microbiol. App. Sci. 2 (6) (2013) 228.
[14] R.K. Das, N. Gogoi, P.J. Babu, P. Sharma, C. Mahanta, U. Bora, Adv. Mater. Phys. Chem. 2 (4) (2012) 275.
[15] P. Bansal, N. Jaggi, S.K. Rohilla, Res. J. Chem. Sci. 2 (8) (2012) 69.

[16] N. Ahmad, S. Sharma, Green Sustain. Chem. 2 (4) (2012) 141.
[17] J.K. Andeani, S. Mohsenzadeh, J. Chem. 2013 (2012) 1.
[18] S. Pandey, G. Oza, A. Mewada, M. Sharon, Arch, Appl. Sci. Res. 4 (2) (2012) 1135.
[19] A.M. Awwad, N.M. Salem, Nanosci. Nanotechnol. 2 (6) (2012) 208.
[20] K.J.A. Raj, B. Viswanathan, Bull. Cataly. Soc. Infias 9 (2011) 6.
[21] M.N. Nadagouda, R.S. Varma, Green Chem. 10 (2008) 859.
[22] W. Wang, Y. Kang, A. Wang, J. Nanopart. Res. 16 (2281) (2014) 1.
[23] M.R. Patil, V.S. Shrivastava, Appl. Nanosci. 5 (2015) 809.
[24] L. Fu, A. Yu, Preparation of β-Cyclodextrin functionalized reduced Graphene-Silver Nanocomposites: Application for sensing of nitrite, in: Proceedings of International Electronic Conference on Sensors and Applications, 1–16 June, 2014.
[25] A.R. Ocwelwang, L. Tichagwa, Int. J. Adv. Res. Chem. Sci. 1 (2) (2014) 28.
[26] S. Pandey, G.K. Goswami, K.K. Nanda, Carbohydr. Polym. 94 (2013) 229.
[27] A.F. Baldissera, J.F. Souza, C.A. Ferreira, Syn. Met. 183 (2013) 69.
[28] M. Sudirman, M. Anggaravidya, E. Budianto, I. Gunawan, Procedia Chem. 4 (2012) 107.
[29] X. Dong, W. Huang, P. Chen, Nanoscale Res. Lett. 6 (60) (2010) 1.
[30] M.A. Farghali, T.A.S. El-Di, A.M. Al-Enizi, R.M.E. Bahnasawy, Int. J. Electrochem. Sci. 10 (2015) 529.
[31] S. Agarwal, N.S. Saxena, V. Kumar, Appl. Nanosci. 5 (2015) 697.
[32] Q.L. Tang, K.W. Wang, Y.J. Zhu, F. Chen, Mater. Lett. 63 (2009) 1332.
[33] N. Liu, X. Wang, W. Xu, H. Hu, J. Liang, J. Qiu, Fuel 119 (2014) 163.
[34] M.T.S. Tavares, A.S.F. Santos, I.M.G. Santos, M.R.S. Silva, M.R.D. Bomio, E. Longo, C. A. Paskocimas, F.V. Motta, Surf. Coat. Tech. 239 (2014) 16.
[35] S. Sedaghat, F. Golbaz, J. Nanostructure Chem. 3 (65) (2013) 1.

Use of sustainable organic transformations in the construction of heterocyclic scaffolds

9

*Sarita Khandelwal, Yogesh Kumar Tailor, Esha Rushell, Mahendra Kumar**
Department of Chemistry, University of Rajasthan, Jaipur, India
*Corresponding author. e-mail address: mahendrapathak@gmail.com

9.1 Introduction

The green chemistry aims to design environmentally benign chemical processes and sustainable synthetic methodologies in order to eliminate or reduce the use of hazardous and toxic chemicals at any stage of production in the industry or laboratory [1]. According to the principles of green chemistry, the chemical reaction should be: (i) catalytic, (ii) atom-economical, (iii) environmentally friendly, (iv) with mild reaction conditions, and (v) operational simplicity and proceed without the need for protecting the atmosphere. The conventional organic solvents used extensively for dissolving reactants, extracting and washing the products and for separating the mixtures are generally volatile, flammable, explosive, and toxic for human beings, animals, and even plants. The conventional organic solvents are hazardous not only to the environment but also show acute and chronic toxicity, carcinogenicity, ecological toxicity, and nonbiodegradability. The precautions to minimize the effects of these solvents by improved recycling processes have limited success and cannot avoid some losses into the environment. Therefore, the replacement of these hazardous solvents with green and sustainable alternative solvents seems to be the only valid alternative for a sustainable use of solvents. The development of bio-renewable and biodegradable solvents that are not based on crude petroleum depends mainly on the substitution of petrochemically fabricated solvents with "bio-solvents" from renewable resources [2], and the substitution of hazardous solvents with ones that show better EHS (Environmental, Health, and Safety) properties [3]. Although the last couple of decades has seen a considerable sustainable development in chemical research with green technology in organic syntheses and catalysis with the use of a variety of unconventional solvents, such as water [4], ionic liquids (ILs) [5], fluorous media [6], supercritical fluids [7], and polyethylene glycol [8], but probably even a single system, in its own right, will ever be able to replace completely all conventional reagents and solvents as a truly environment friendly alternative because the use of these solvents is still subject to strict limitations, such as the instability and solubility of some reactive reagents or substrates in water, high prices and lack of data about the toxicity and

Green Approaches in Medicinal Chemistry for Sustainable Drug Design. https://doi.org/10.1016/B978-0-12-817592-7.00009-5
© 2020 Elsevier Inc. All rights reserved.

bio-compatibility for ILs, including the requirement of sophisticated equipment for supercritical fluids. It means that an ideal and universal "green" solvent for all situations does not exist because of the drawbacks associated with all of these systems, both from the point of view of applicability and sustainability. Therefore, the search for new reaction media is thus gaining prominence in organic synthesis.

In the last decade, ILs have attracted increasing interest in view of their uses in organic syntheses, catalysis, biocatalysis, and biomass pretreatment due to their unique chemical and physical properties such as biocompatibility, high viscosity, thermal and chemical stability, negligible volatility, high solubilization capacity for wide spectrum of solutes, high heat capacity, density, and conductivity [9]. ILs have been proposed as "fully green" alternative solvents because of their negligible vapor pressure and low flammability. The significance of ILs concerns not only to academia but also to the industry because their "green character" offers an interesting alternative solvents to toxic organic solvents in organic synthesis [10]. The exploration of ILs as alternative sustainable solvents can also be confirmed by the incredible amount of works in the literature [11]. However, several disadvantages such as limited solute solubility, high viscosity, poor biodegradability, environmental toxicity, and high cost are associated with the ILs. Many ILs, however, are dangerous environmental contaminants, with a toxicity similar to or even higher than that of organic solvents. Further, high purity is required for ILs, as even trace impurities affect the physical properties of ILs. Commonly used imidazolium and pyridinium-based ILs are not environmentally benign and show a wide range of toxicities toward microorganisms, vertebrates, and invertebrates because of their relatively high solubilities in water and their poor biodegradability [12]. Although, in view of the low vapor pressure of ILs, these may reduce the air pollution with respect to the typical volatile organic solvents, the release of ILs from industrial processes into aquatic environments may lead to water pollution because of their high solubility in water. Moreover, due to their high stability in water, the ILs could become as persistent pollutants in wastewaters and may have a toxic influence on the environment.

The development of alternative solvents from components that are inexpensive, nontoxic toward the environment, and are biodegradable or obtainable from biodegradable resources is therefore highly desirable to overcome these drawbacks. Deep eutectic solvents (DESs) have been regarded as one of the most promising environmentally benign and cost-effective alternatives to conventional ILs and volatile organic solvents. DESs not only retain the excellent merits of ILs but also overcome their shortcomings as these are constituted from natural and renewable nontoxic bio-resources. Thus DESs are emerging as a new generation of green and sustainable solvents.

DESs show similar physical and chemical properties to ILs, but they are much cheaper and safer for their use as solvents as compared to ILs in synthetic transformations. As compared to ILs, DESs have, however, notable advantages such as (i) their convenient synthesis with 100% atom economy, (ii) DESs can be prepared from readily accessible chemicals, and (iii) their low toxicity. The term "DESs" refers to low melting mixtures or low transition temperature mixtures (LTTMs) based on a combination of readily available, biodegradable, recyclable, and inexpensive components that are formed by mixing a quaternary ammonium or metal salt with a simple

hydrogen bond donor (HBD), such as acids, amides, amines and alcohols, and mostly exist as liquid at or below 100°C because the melting point is drastically reduced after mixing two components as compared to the melting points of the original two components. The charge delocalization occurring through hydrogen bond formation between the halide anion and the hydrogen donor moiety is responsible for the decrease in the freezing point of the mixture relative to the melting points of its individual components (Fig. 9.1). Moreover, DESs do not produce toxic metabolites and are biodegradable. Additionally, the synthesis of ILs is not environmentally friendly and generally requires a large amount of salts and solvents in order to completely exchange the anions. These drawbacks together with the high price of common ILs, unfortunately, restrict their industrial emergences such as metal electroplating, electrodeposition, and biocatalysts [13]. Like ILs, one of the most promising advantages of DES is their extremely low vapor pressure, i.e., low volatility, which is very attractive for their use in greener catalytic technologies [14].

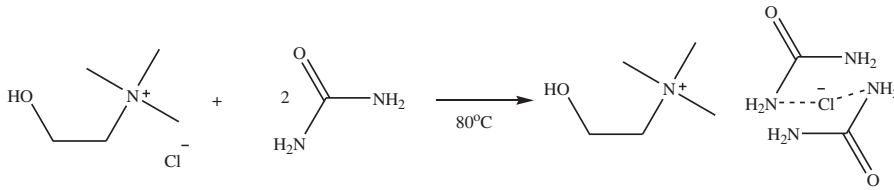

Fig. 9.1 Deep eutectic solvent with hydrogen bond interaction.

DES's can be used as sustainable, greener, and safer alternatives to many petroleum-based organic solvents in synthetic organic chemistry to increase the efficiency of organic transformations. Although DESs have attracted the attention of chemical research in many fields particularly, in the area of electroplating, the ability of deep eutectic mixtures to serve as solvents, however, has not been adequately explored in the field of synthetic organic chemistry. If a solvent displays slightly acidic or basic nature, it can also act as a catalyst for those reactions which are catalyzed in these conditions. The polar and protic DES may be acidic and basic depending on the nature of HBD. Besides this, the acidity/coordination properties of DESs can be tuned according to requirements of different reactions or processes by changing the combination of their cations and anions. So theoretically, large numbers of DES are possible with various combinations of cations and anions which provide great opportunity to design the most suitable catalytic condition with green approach. Moreover, like ILs, ionic characters of DES due to the presence of hydrogen bond interaction between cation and anion show improved catalytic activities over those conducted in conventional organic solvents. Therefore, DES is able to function not only as a modest inexpensive and environmentally benign solvents but also recyclable and reusable organocatalysts and can play a dual role in organic transformations. In the present article, the recent advances in the synthesis of heterocyclic scaffolds with the use of sustainable organic transformations involving the dual role of DESs as environmentally benign sustainable solvents and catalysts along with the recent literature have been presented.

9.2 Organic transformations in deep eutectic solvents

9.2.1 Synthesis of heterocyclic scaffolds

9.2.1.1 Synthesis of pyrroles

Pyrrole nucleus is one of the most relevant simple heterocycles present in the core structures of many biologically active products such as alkaloids, vitamins, anticancer agents, and antibiotics [15]. The syntheses and further functionalization of pyrroles have received considerable interest and a number of synthetic methods including Hantzsch synthesis [16], Paal-Knorr synthesis [17], Clauson-Kaas synthesis [18], Buchwald-Hartwig coupling [19], and Barton-Zard synthesis [20] have been reported. The Paal-Knorr synthesis of pyrroles is a versatile method with the use of different reaction conditions, including Lewis acid catalysis [21], heterogeneous catalysis [22], microwaves [23], different solvent variations (RTIL and solvent-free) [24], and ultrasound (US) or microflow conditions [25]. In recent years, DESs have emerged as a promising green reaction media for organic transformations [14b, 26] and used as effective solvents/catalysts for Paal-Knorr reactions to synthesize pyrroles. Handy et al. synthesized pyrroles via the Paal-Knorr synthesis by stirring the equimolar mixture of dione and amine as a 1 M solution in choline chloride/urea at 80°C (Schemes 9.1 and 9.2). The synthetic strategy was also extended successfully with less nucleophilic anilines, but required longer reaction times and the products were obtained in nearly quantitative yields. These reaction conditions are simple and highly environmentally friendly in view of nontoxic, and recyclable nature of the DES [27].

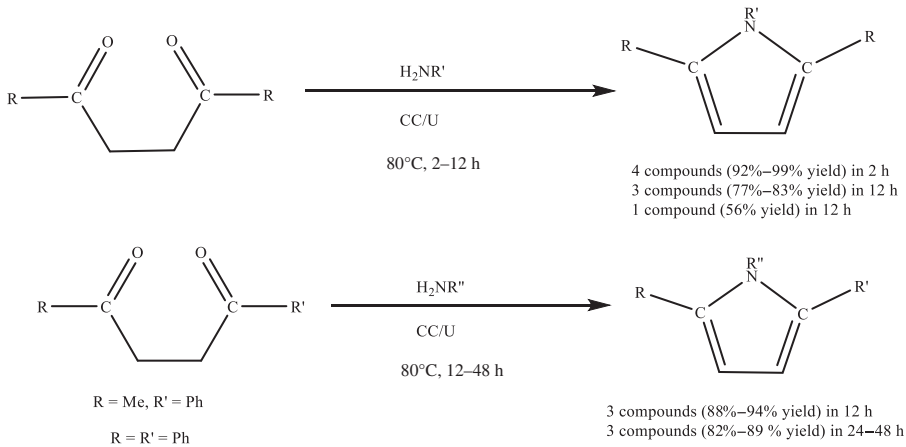

Scheme 9.1 Paal-Knorr pyrrole synthesis.

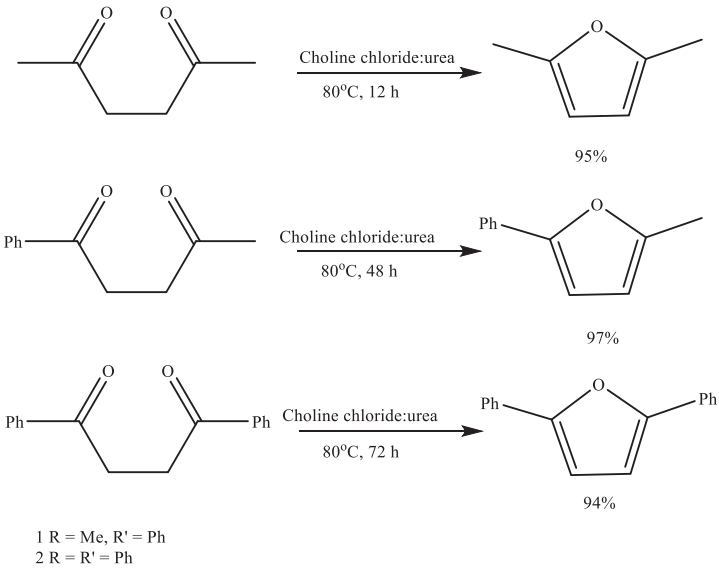

Scheme 9.2 Paal-Knorr furan synthesis.

Zhang et al. reported the synthesis of *N*-protected functionalized pyrroles by one-pot, four-component reaction of amines, aldehydes, 1,3-dicarbonyl compounds and nitromethane in the presence of DES as catalyst and solvent [28] (Scheme 9.3).

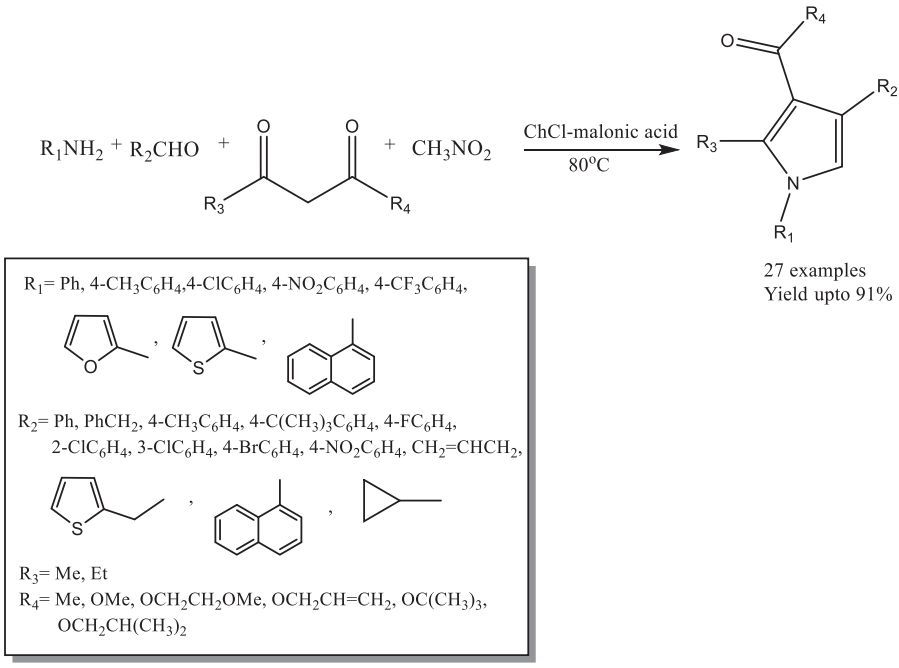

Scheme 9.3 Synthesis of functionalized pyrroles.

The reaction was performed with the use of ChCl-based DESs such as ChCl + oxalic acid (OA)/tartaric acid (TA)/citric acid/itaconic acid/fumaric acid/malic acid/succinic acid/malonic acid $FeCl_3$ and $ZnBr_2$ to optimize the reaction conditions ChCl-malonic acid was found to be more efficient medium and provided desired product in remarkably high yield. The proposed reaction mechanism is presented in Scheme 9.4.

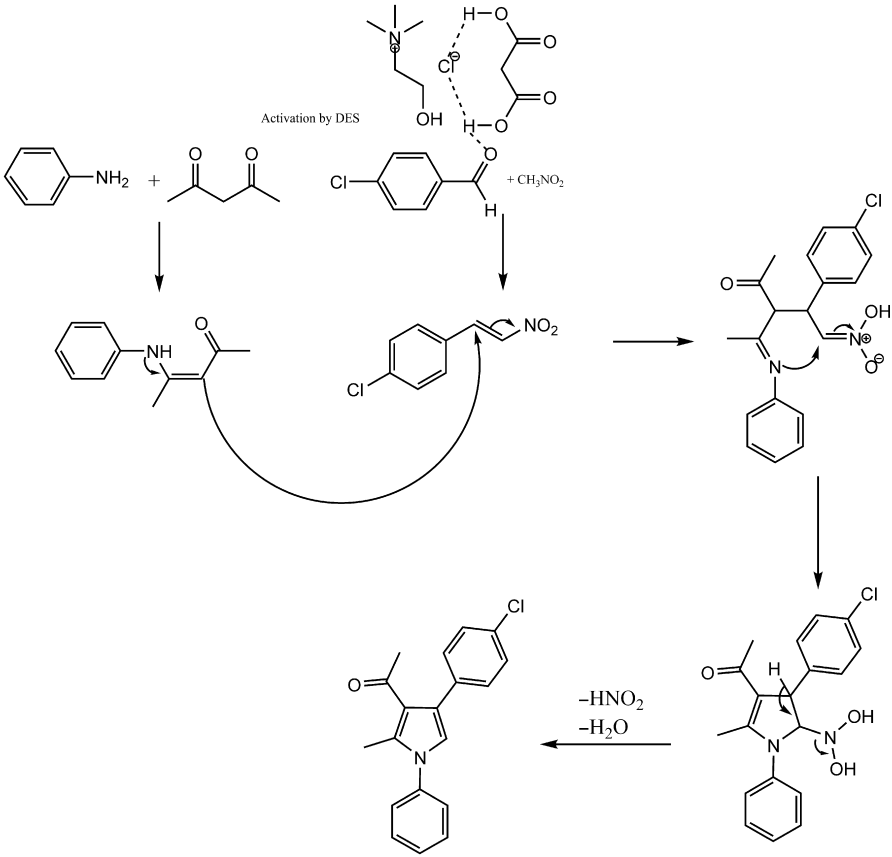

Scheme 9.4 Plausible mechanism for the synthesis of pyrrole.

2,3,4-Trisubstituted 1*H*-pyrroles are the privileged scaffolds and are structural constituents of bioactive natural products, pharmaceuticals, and agrochemicals [15a, b, 29]; porphobilinogen [30], and marine natural products lamellarin O [31] and lukianol A [32] (Fig. 9.2).

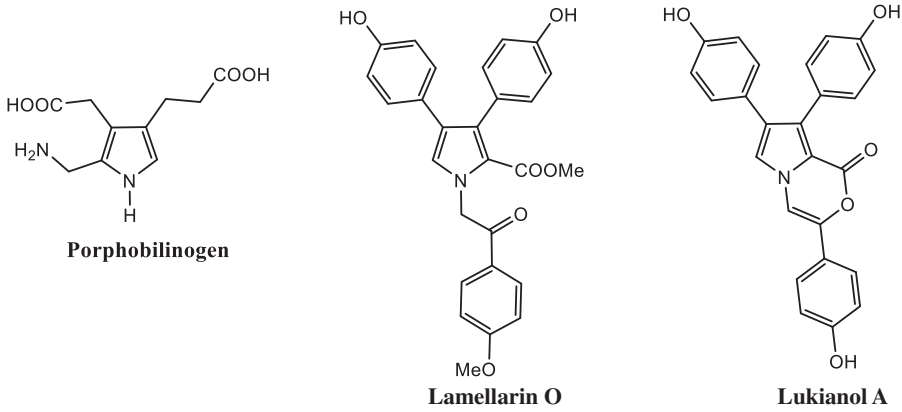

Fig. 9.2 Bioactive pyrroles.

Chaskar et al. used choline hydroxide as an efficient basic catalyst as well as reaction media for the regioselective synthesis of 2,3,4-trisubstituted 1*H*-pyrroles [33] (Scheme 9.5).

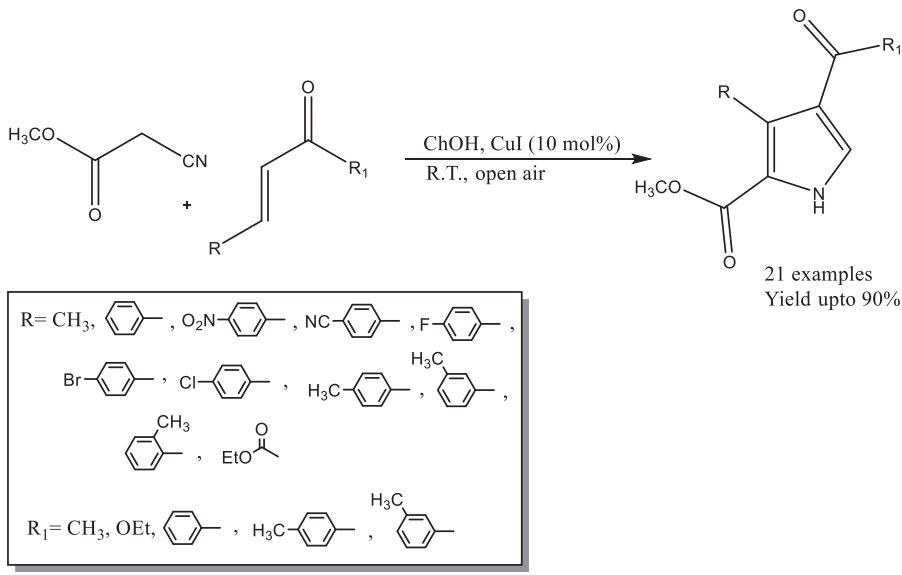

Scheme 9.5 Synthesis of 2,3,4-trisubstituted 1*H*-pyrroles.

The reaction was performed in acidic (such as ChCl:PTSA), neutral and basic DESs (mixture of choline chloride:urea). Various copper salts were also tested under this condition for their catalytic activity. The use of choline hydroxide as a base and reaction media and CuI as a catalyst in the reaction provided the best results. The reaction was considered to proceed through the 1,4-conjugate addition of methyl 2-isocyanoacetate with α,β-unsaturated ketones followed by intramolecular cyclization-oxidation reaction to provide the final product as presented in Scheme 9.6.

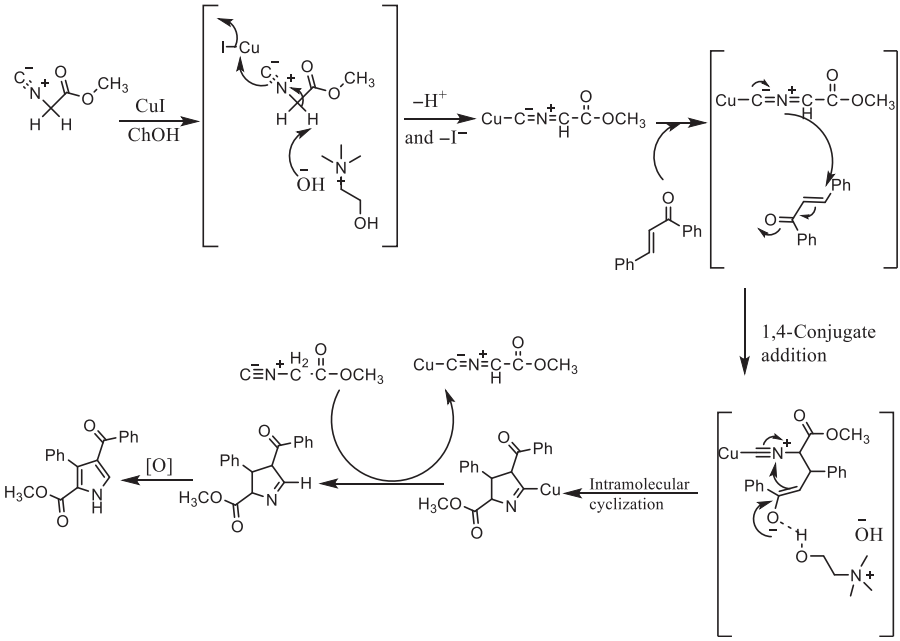

Scheme 9.6 Proposed reaction mechanism.

9.2.1.2 Synthesis of furans (naphthofurans)

2-Aminonaphtho [2,3-*b*]furan-4,9-diones [34] are promising cytotoxic agents operating through oxidative damage of DNA and alkylation of bioorganic molecules in tumor cells [35]. Rad-Moghadam et al. synthesized 2-aminonaphtho[2,3-*b*] furan-4,9-diones via the domino reaction among 2-hydroxy-1,4-naphthoquinone, β-nitrostyrenes, and ammonium acetate in the presence of DES consisting of sorbitol and metformin.HCl [36] (Scheme 9.7). The method offers operation simplicity and mild reaction conditions with the use of the biocompatible and easily recyclable eutectic mixture.

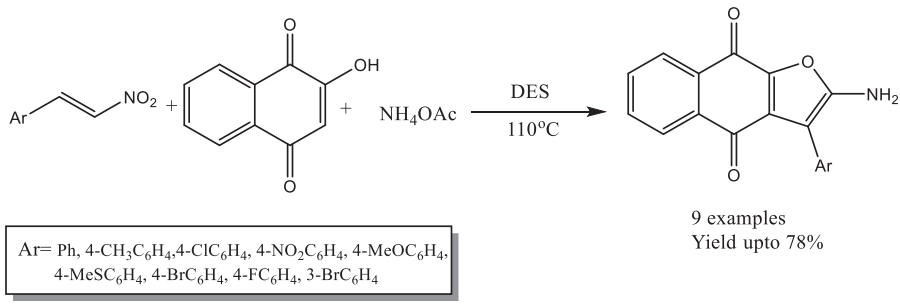

Scheme 9.7 Synthesis of 2-amino-3-phenylnaphtho[2,3-*b*]furan-4,9-diones.

In the reaction, the efficiency of the eutectic melt that brings the two reacting components in close vicinity to each other is partially due to multiple hydrogen-bonding of MetHCl with β-nitrostyrenes and 2-hydroxy-1,4-naphthoquinone. According to plausible mechanism [37], these zwitterionic intermediates undergo a dipolar dimerization reaction to yield the intermediate 1,4,2,5-dioxadiazines followed by a chain of thermal reactions involving electrocyclic scission of the dioxadiazine ring and conversion of the resulting two fragments into naphtho[2,3-*b*]furan-4,9-diones. Upon heating, the fragmented intermediate is presumed to undergo a direct cyclization, while its twin undergoes cyclocondensation with ammonia to provide the product (Scheme 9.8).

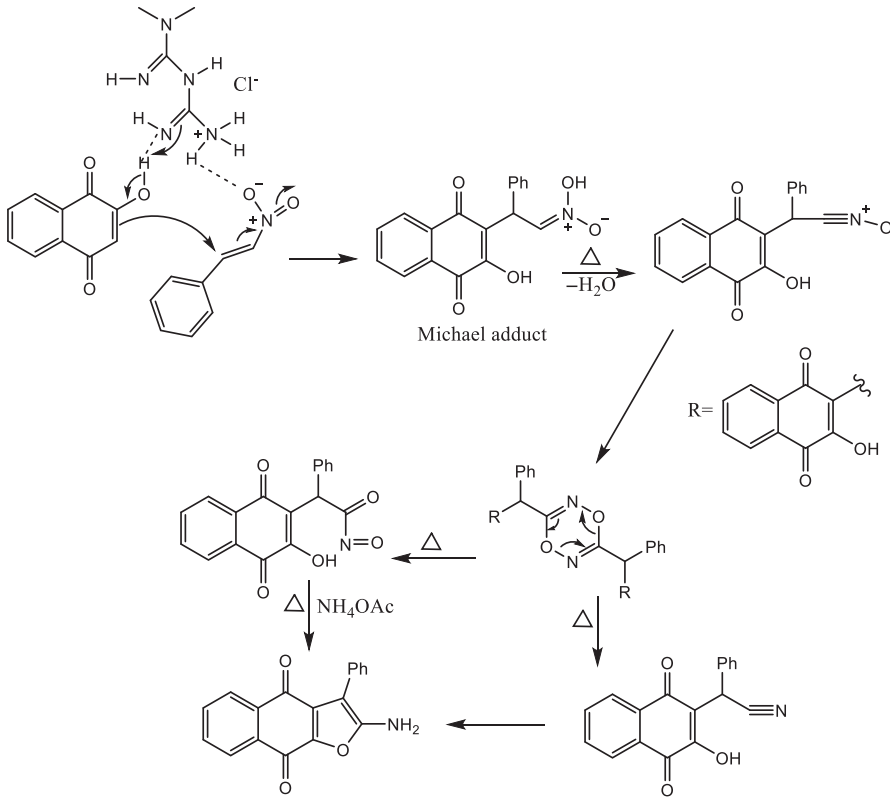

Scheme 9.8 A plausible mechanism for synthesis of 2-amino-3-phenylnaphtho[2,3-*b*]furan-4,9-diones.

9.2.1.3 Synthesis of thiophenes

The Gewald reaction is the most versatile reaction and involves one-pot cyclocondensation of ketones or aldehydes with activated nitrile derivatives and elemental sulfur to provide 2-aminothiophenes [38]. Gewald three-component reaction has been valuable for the pharmaceutical industry [39], for example, olanzapine (I) is

an antipsychotic drug used in the treatment of schizophrenia [40] and tinoridine (II) is a nonsteroidal basic antiinflammatory drug with a potent antiperoxidative property (Fig. 9.3).

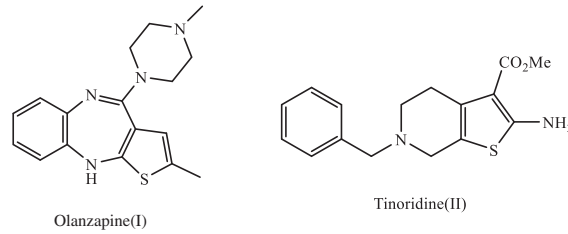

Fig. 9.3 Pharmaceutical agents-containing 2-aminothiophene ring.

The synergic effect of choline chloride/urea as a DES was investigated by Shaabani et al. in the synthesis of 2-aminothiophene derivatives via a three-component cyclocondensation of a ketone or an aldehyde with activated nitriles and elemental sulfur catalyzed by NaOH as base [41]. The reaction conditions were optimized using various choline chloride-based DESs (hydrogen-bond donors: urea, citric acid, ethylene glycol (EG), imidazole, resorcinol, and metal salts such as $ZnCl_2$ and $FeCl_3$) in the presence of different organic and inorganic bases. The results showed that the choline chloride/urea in NaOH (0.1 cm^3 of a 4 mol dm^{-3} aqueous solution) at 60°C provided excellent yield in shorter reaction time (Scheme 9.9).

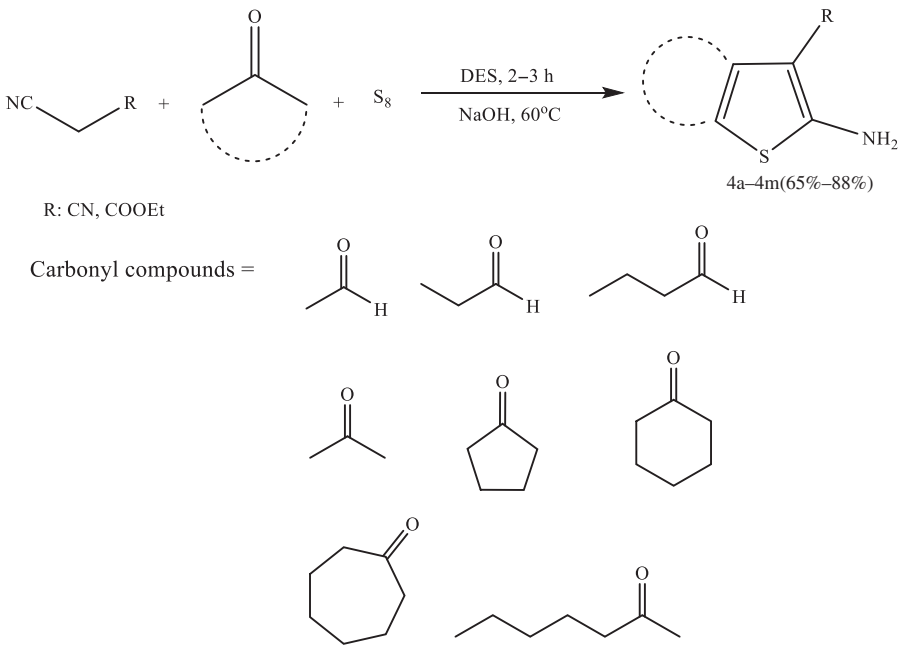

Scheme 9.9 Synthesis of 2-aminothiophene derivatives.

The reaction proceeds with the initial formation of conjugated electron-deficient heterodyne by Knoevenagel condensation of malononitrile and carbonyl compounds to produce an acrylonitrile [A], followed by a base catalyzed thiolation at the methylene group with elemental sulfur. The sulfurated compound [B] undergoes ring closure via nucleophilic mercaptide attack at the cyano carbon to provide intermediate [C] which on prototropic rearrangement affords 2-aminothiophenes (Scheme 9.10).

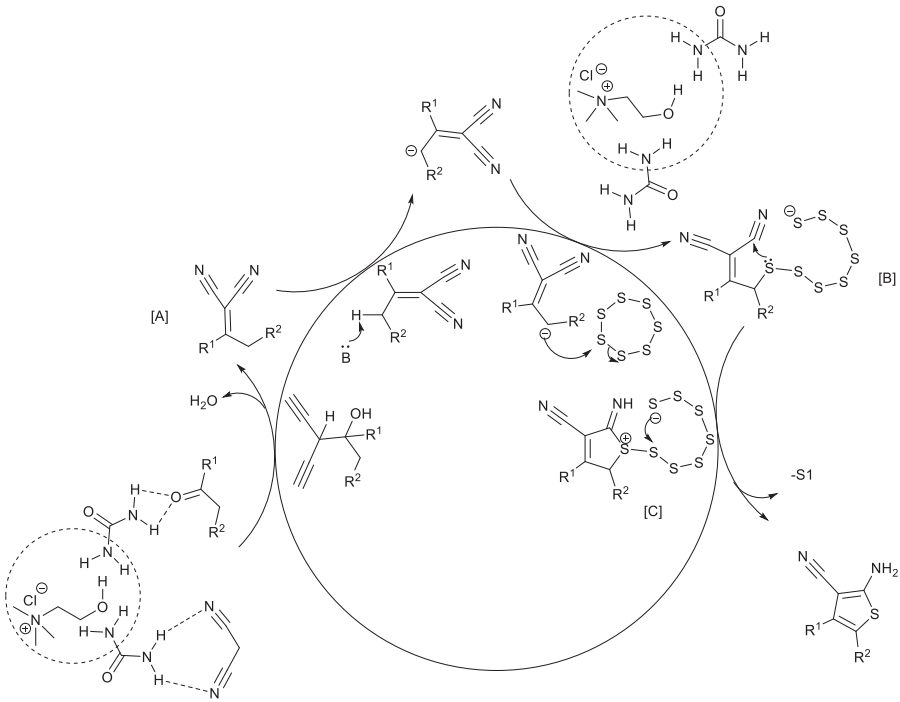

Scheme 9.10 Plausible mechanism for the synthesis of 2-aminothiophenes.

9.2.1.4 Synthesis of pyrazoles

Pyrazole derivatives have been reported to exhibit a wide range of applications in medicinal chemistry and pharmacology. A large number of drugs incorporating pyrazole structure have been utilized as partial agonists for nicotinic acid receptors [42], CDK inhibitors [43], p38 kinase inhibitors [44], antidepressants [45], antimicrobial agents [46], antiviral agents [47], and antifungal agents [48] solely or along with the combination of other structural motifs. The application of pyrazole derivatives in the development of anticancer agents has been thoroughly investigated and verified [49]. Moreover, the medicinal features of a number of natural products incorporating pyrazole moiety such as pyrazofurin, pyrazofurin B, pyrazole-3(5)-carboxylic acid and 4-methylpyrazole-3(5)-carboxylic acid have been reported [50] (Fig. 9.4).

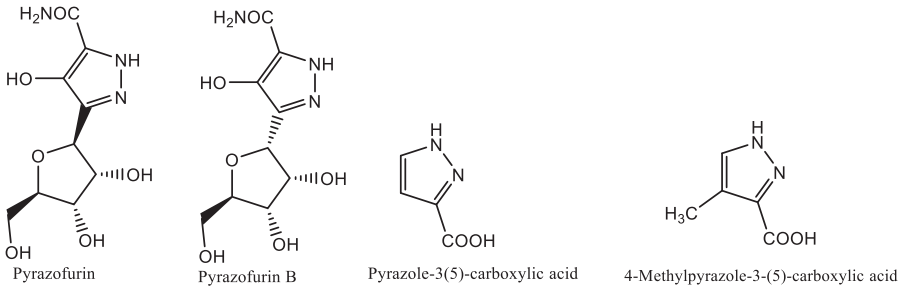

Fig. 9.4 Natural products incorporating pyrazole ring.

Pyrazole heterocycles have a great potential from the medicinal chemistry viewpoints to be considered as the target for diversity-oriented organic synthesis (DOS) involving high regioselectivity, diversity, and least number of synthetic steps [51]. Among pyrazoles, 4,4-(arylmethylene)-bis-(3-methyl-1-phenyl-1*H*-pyrazol-5-ols) have gained much importance because of their uses as antiinflammatory [52], antipyretic [53], antioxidant [54], antidepressant [55], and antibacterial agents [56]. Kamble et al. synthesized 4,4′-(arylmethylene)-bis-(3-methyl-1-phenyl-1*H*-pyrazol-5-ols) by tandem Knoevenagel-Michael addition reactions of aldehyde, phenyl hydrazine, and ethyl acetoacetate using a combination of DES (ChCl:TA) and US in water (Scheme 9.11). A plausible mechanism is presented in Scheme 9.12. Moreover, the DES was recycled five times without considerable loss of activity. The reaction conditions were optimized with various DES under different conditions and observed that the amalgamation of DES with US facilitated the reaction at benign conditions [57].

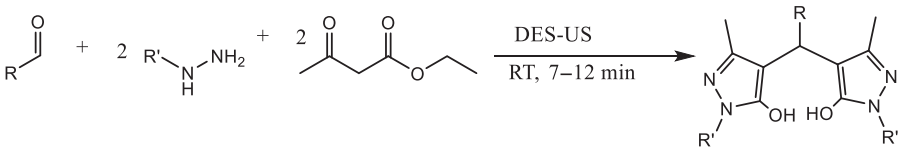

Scheme 9.11 Synthesis of 4,4-(arylmethylene)-bis-(3-methyl-1-phenyl-1*H*-pyrazol-5-ols).

Aryan et al. synthesized highly substituted pyrazole-4-carbonitrile derivatives using biocompatible glucose-based DES under catalyst-free condition involving the reaction of malononitrile, aromatic aldehydes and various hydrazine derivatives as

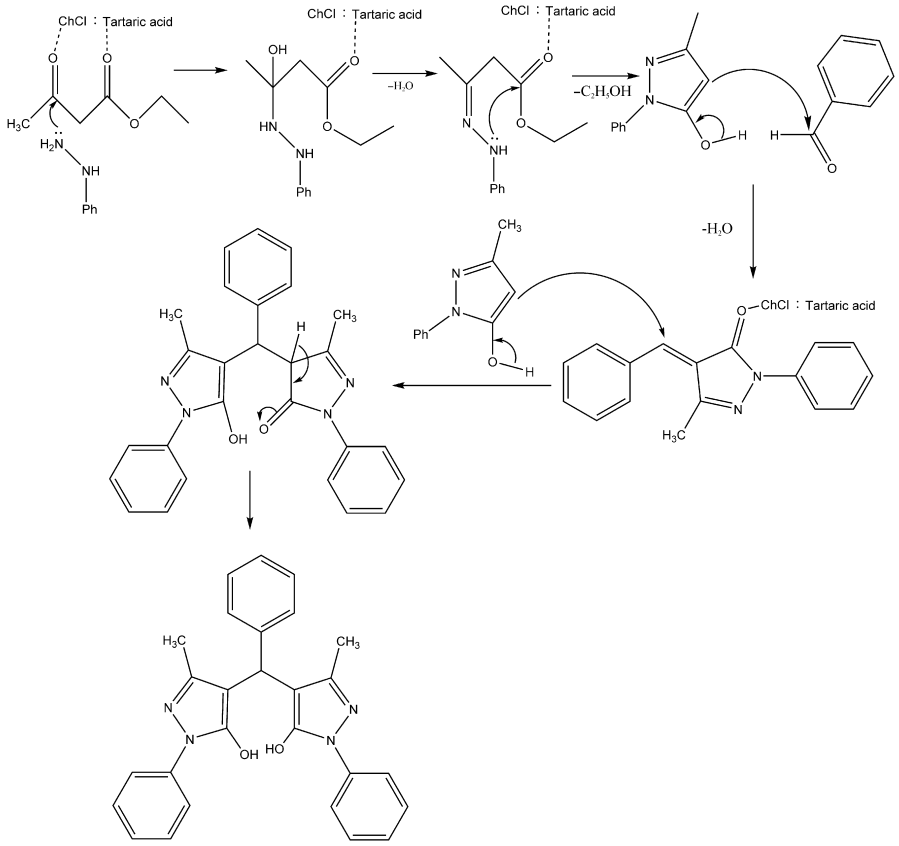

Scheme 9.12 Plausible reaction mechanism.

nitrogen source at room temperature [58] (Scheme 9.13). The DES was also recycled and reused at least four times with a slight loss in catalytic efficiency. A plausible mechanism was proposed in which DES facilitated the reaction through hydrogen bonding as presented in Scheme 9.14.

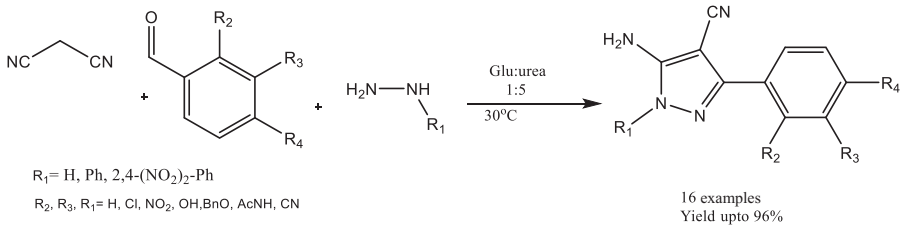

Scheme 9.13 Synthesis of highly substituted pyrazole-4-carbonitrile derivatives.

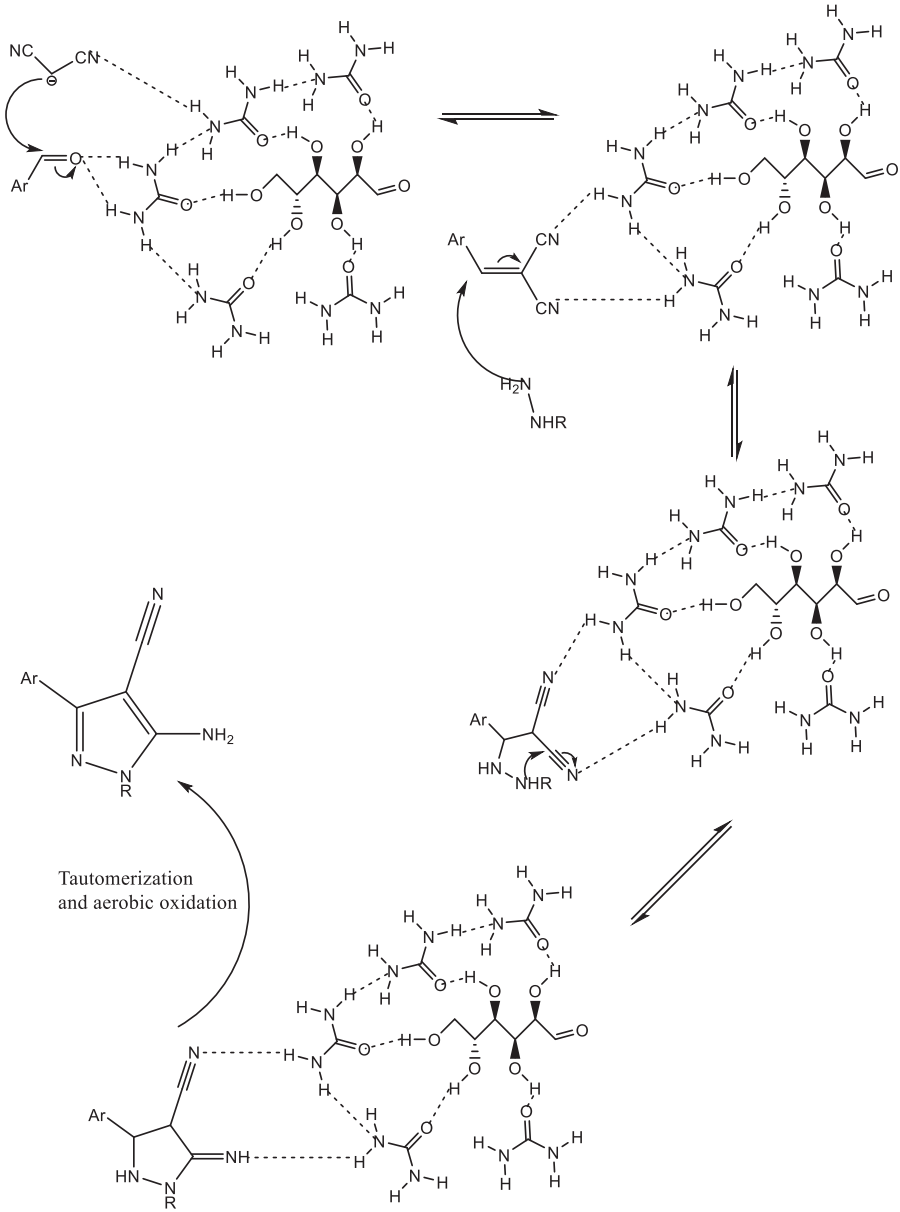

Scheme 9.14 Proposed reaction mechanism for the synthesis of pyrazole-4-carbonitriles.

Annes et al. synthesized 1,3,5-trisubstituted pyrazolines involving regioselective tandem one-pot intermolecular electrocyclization reaction of aldehyde, hydrazines, and alkenes under metal-free DES mediated conditions [51] (Scheme 9.15). The

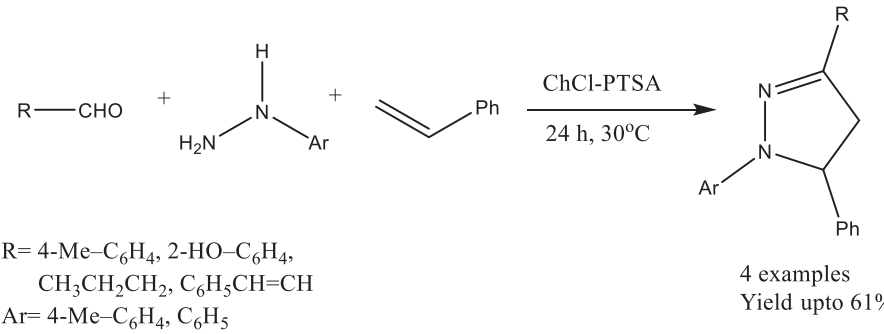

Scheme 9.15 Synthesis of various pyrazolines.

synthetic methodology was also used in the synthesis of a natural product alkaloid obtained from aerial parts of *Euphorbia guyoniana* [59].

The authors screened various deep eutectic mixtures as media for this transformation in which ChCl:PTSA was reported to be more effective as compared to other catalysts. The reaction mechanism is considered to involve the more stabilized benzylic carbocation and directs the reaction pathway toward the formation of 5-phenyl substituted product regioselectively as presented in Scheme 9.16.

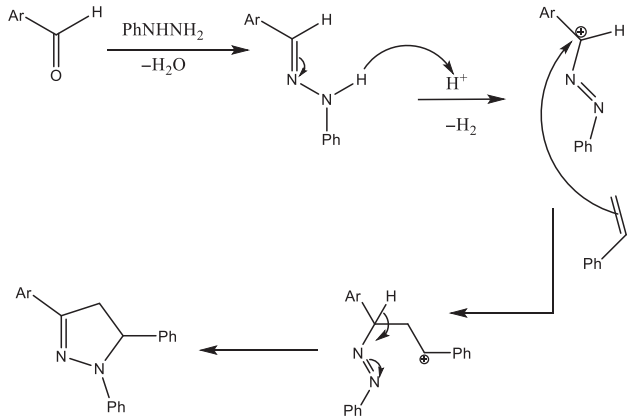

Scheme 9.16 Regioselectivity in the formation of pyrazolines.

9.2.1.5 Synthesis of pyranopyrazoles

Pyranopyrazoles have occupied an important position in medicinal chemistry because of their pharmacological [60] and biological activities [61] such as antibacterial activity comparable with cefazolin and ciprofloxacin [62], antimicrobial [63], antifungal [64], antitumor, anticancer [65], analgesic and antiinflammatory [66], anti-Alzheimer's disease [67], antioxidant [68], and also as potential inhibitors of human Chk1 kinase [69].

Dehbalaei et al. synthesized 6-amino-4-aryl-2,4-dihydro-3-phenyl pyrano[2,3-*c*] pyrazole-5-carbonitriles involving one-pot, four-component reaction of aryl aldehydes, hydrazine hydrate, ethyl benzoylacetate and malononitrile under ultrasonic irradiation conditions [70] (Scheme 9.17). The reaction conditions were optimized with the catalysts such as alumina, DABCO, L-proline, benzyl triphenyl phosphonium chloride (BTPPC) and choline chloride:thiourea and choline chloride:urea (DES).

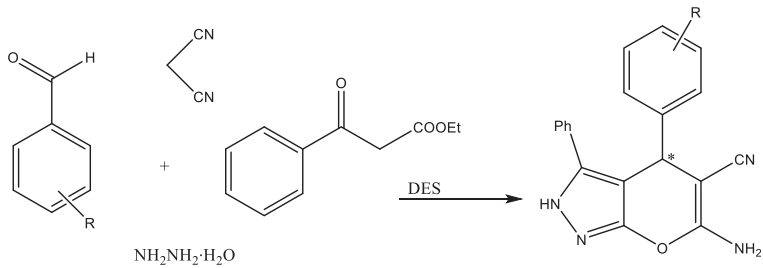

R= 4-Me, 3-NO_2, 3-OH, 2-Me, 4-OH, 2-NO_2, 4-OMe, 4-Cl, 4-Br, 4-$N(Me)_2$,4-$N(Me)_2$, 4-$CH(Me)_2$, 4-$CH(Me)_2$, 4-NO_2, 2-Cl, 3-Br

Scheme 9.17 Synthesis of pyranopyrazoles.

The reaction is considered to proceed with Knoevenagel condensation between aryl aldehyde and malononitrile to form an intermediate which undergoes Michael addition with pyrazolone (formed in situ from hydrazine hydrate and ethylbenzoylacetate) and subsequently intramolecular cyclization to provide polyfunctionalized pyrano[2,3-*c*]pyrazoles (Scheme 9.18).

Dihydropyrano[2,3-*c*]pyrazole also represents a fascinating template in the pharmaceutical field [71] and is responsible for a wide spectrum of biological activities such as antimicrobial [72], anticancer [73], antiinflammatory [74], and inhibition of human Chk1 kinase [69] activities. Bhosle et al. synthesized 6-amino-2*H*, 4*H*-pyrano[2,3-*c*]pyrazole-5-carbonitriles involving one-pot four-component cyclocondensation of aromatic aldehydes, malononitrile, ethyl acetoacetate, and hydrazine hydrate in the presence of DES [75] (choline chloride:urea) (Scheme 9.19).

The reaction was also performed in various green solvents like PEG-400, ILs and DES. But the reaction carried out in DES, derived from a mixture of choline chloride: urea, provided the best results in terms of yields and reaction times. A plausible mechanism, supporting the role of the DES in rate enhancement is presented in Scheme 9.20.

Sanam et al. used morpholinium and piperidinium based DES with different HBDs (urea, diethylene glycol (DEG), carboxylic acid, thiourea, ethanol, and methanol) to synthesize pyranopyrazole-5-carbonitriles [76] (Scheme 9.21). Moreover, it was experimentally observed that the DES melts with strong hydrogen bonds were considered suitable as compared to DES with weak hydrogen bonds.

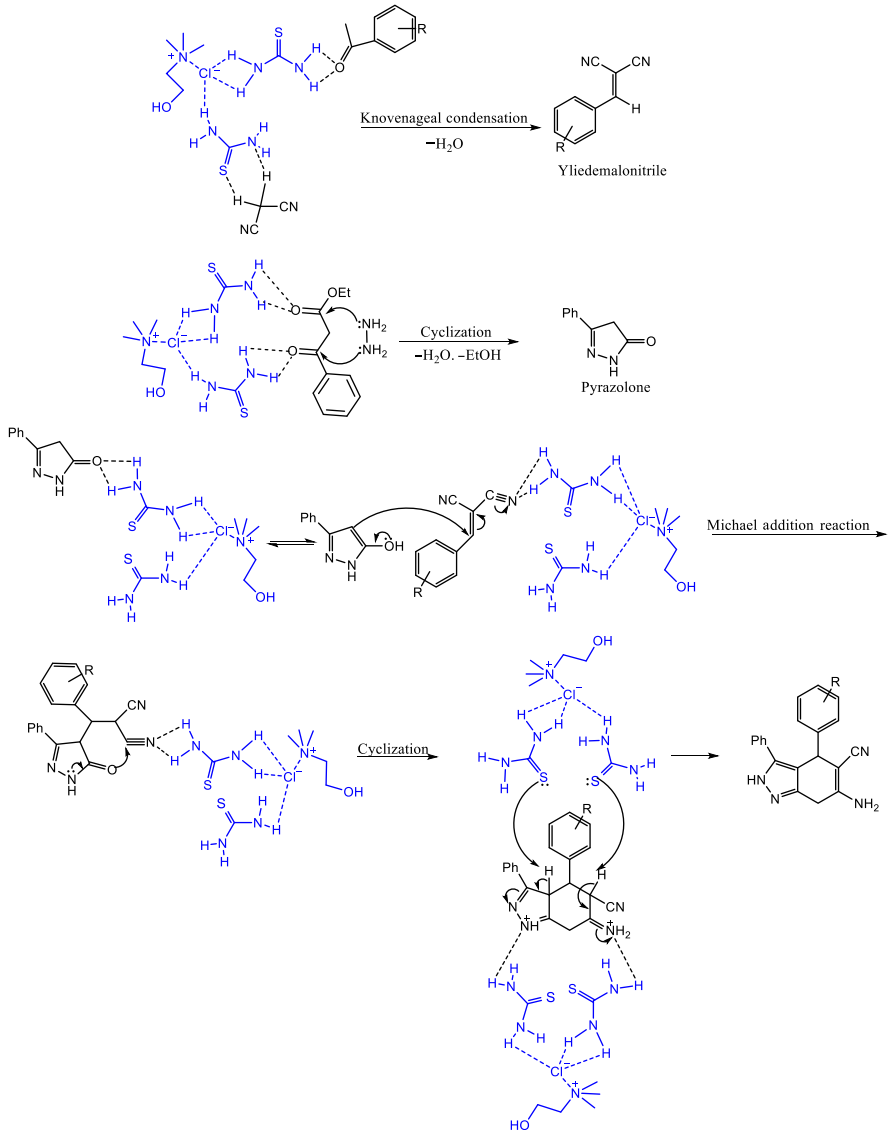

Scheme 9.18 Plausible mechanism for the synthesis of substituted pyrano[2,3-*c*]pyrazoles.

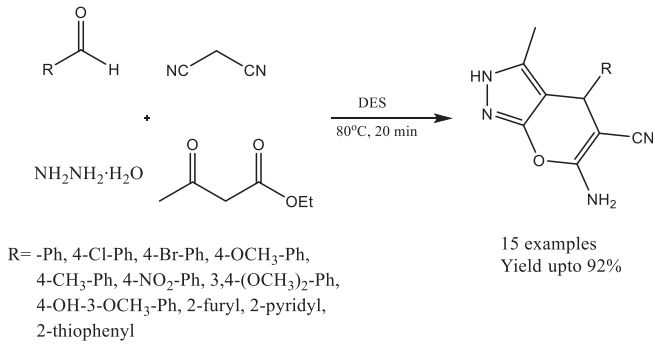

Scheme 9.19 6-Amino-4-(4-substituted phenyl)-3-methyl-1,4-dihydropyrano[2,3-*c*]pyrazole-5-carbonitriles.

9.2.1.6 Synthesis of imidazoles

Naturally occurring as well as synthetic derivatives of imidazoles play an important role in chemical and biological systems. Many of the substituted imidazoles are known as plant growth regulators and attractive targets in medicinal chemistry as the antiulcerative agent cimetidine, the proton pump inhibitor omeprazole, the fungicide ketoconazole, the benzodiazepine antagonist flumazenil and anticancer agents [77] (Fig. 9.5).

Tetrasubstituted imidazoles were synthesized by Aziizi et al. involving the four-component reaction of aldehydes, amines, ammonium acetate, and 1,2-diphenylethane-1,2-dione. The reaction progressed smoothly in the presence of deep eutectic mixture stabilized iron oxide nanoparticles at 60°C to give a range of imidazole derivatives in moderate to good yields. Initially, solvent-free conditions and a wide variety of solvents were also explored but yield of the desired product in these systems was not satisfactory. Furthermore, it was also observed that when the reaction was carried out in DES without ferrofluids, yield of the desired product reduced to 25%. In this synthetic protocol, DES played a triple role: as ionic reaction media, as hydrogen bond catalyst, and as a stabilizer of Fe_3O_4 nanoparticles [78] (Scheme 9.22).

Wang et al. used a Brønsted acidic DES based on choline chloride and *p*-toluenesulfonic acid for the one-pot synthesis of 2,4,5-trisubstituted and 1,2,4,5-tetrasubstituted imidazoles with high yields [79].

Amiri et al. also synthesized 2,4,5-trisubstituted- and 1,2,4,5-tetrasubstituted imidazoles by the condensation reaction of benzil, aldehydes, and ammonium acetate/aniline in the presence of DESs as eco-friendly IL catalysts under solvent-free conditions at 100°C. The reaction conditions were optimized with the model reaction of benzil (1 mmol), benzaldehyde (1 mmol), and ammonium acetate (3 mmol) in the presence of five ILs and observed that $ChCl{\cdot}2ZnCl_2$ IL showed superiority over other ILs as a catalyst to produce 2,4,5-triphenylimidazole. The one-pot four-component reaction of benzil (1 mmol), benzaldehyde (1 mmol), ammonium acetate (1.5 mmol), and aniline

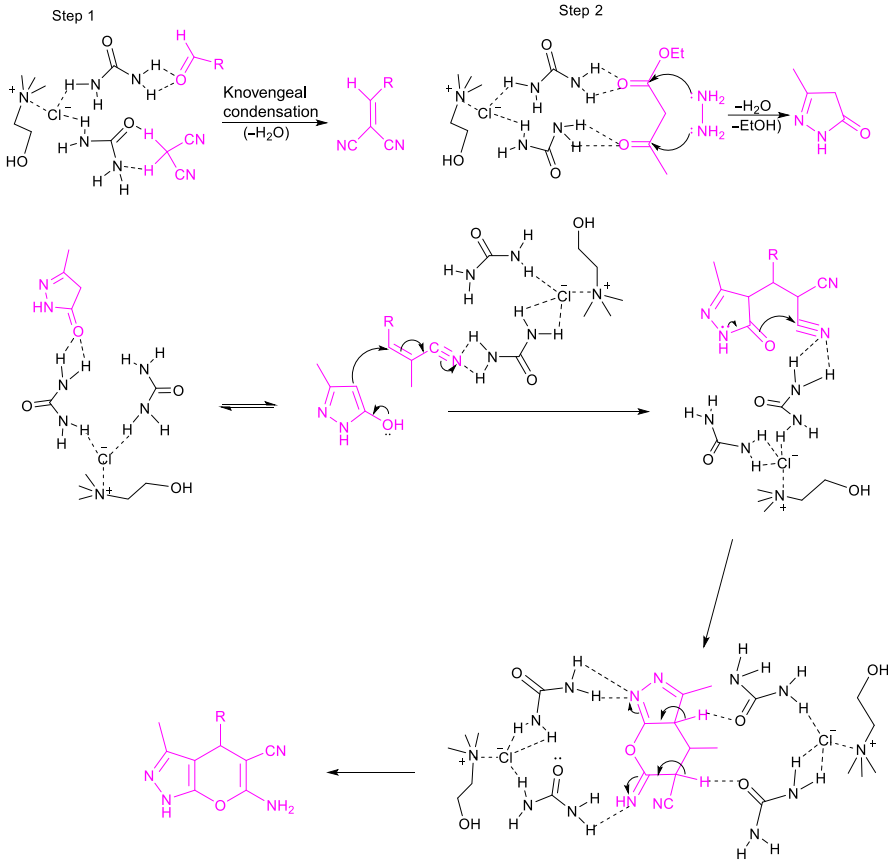

Scheme 9.20 Plausible mechanism for the synthesis of pyranopyrazoles.

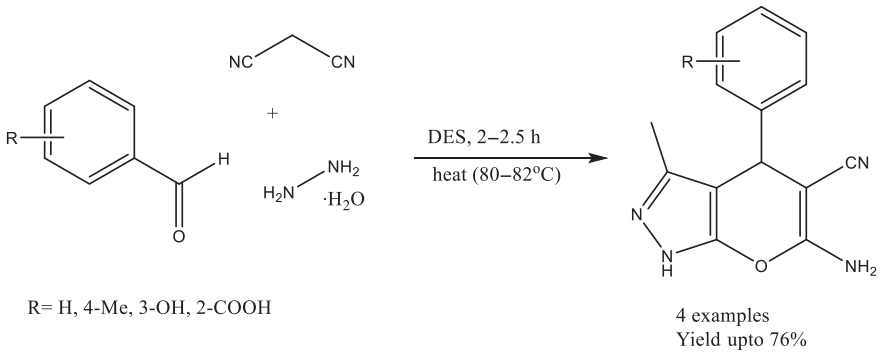

Scheme 9.21 Synthesis of pyrazole-5-carbonitriles in morpholinium-based deep eutectic solvent.

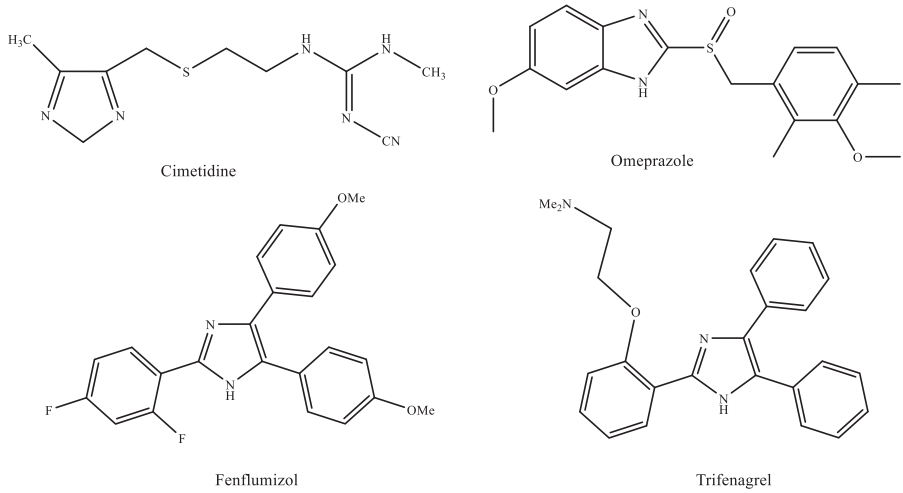

Fig. 9.5 Examples of bioactive 2,5-diarylimidazoles.

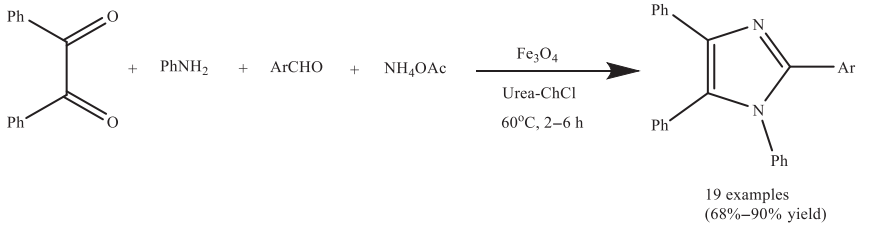

Scheme 9.22 Synthesis of 1,2,4,5-tetrasubstituted imidazoles.

(1 mmol) was also examined and showed the superiority of $ChCl{\cdot}2ZnCl_2$ IL over other catalysts. The reaction was successfully extended under optimized reaction conditions with different aldehydes (Scheme 9.23) [80].

In the proposed mechanism, $ChCl{\cdot}2ZnCl_2$ catalyst activated the carbonyl groups of benzaldehyde and benzil, and then nucleophilic attack of the nitrogen of ammonia (obtained from ammonium acetate) and aniline to the activated carbonyl group of benzaldehyde produced diamine intermediate 1. In the presence of $ChCl{\cdot}2ZnCl_2$, benzil is condensed with diamine intermediate 1 to form diamine intermediate 2, which is rearranged with the elimination of water to provide the corresponding imidazole. Similarly, in the case of ChCl·2urea catalyst, the hydrogen of urea can activate the carbonyl group of benzaldehyde and benzil via the formation of hydrogen bonding (Scheme 9.24).

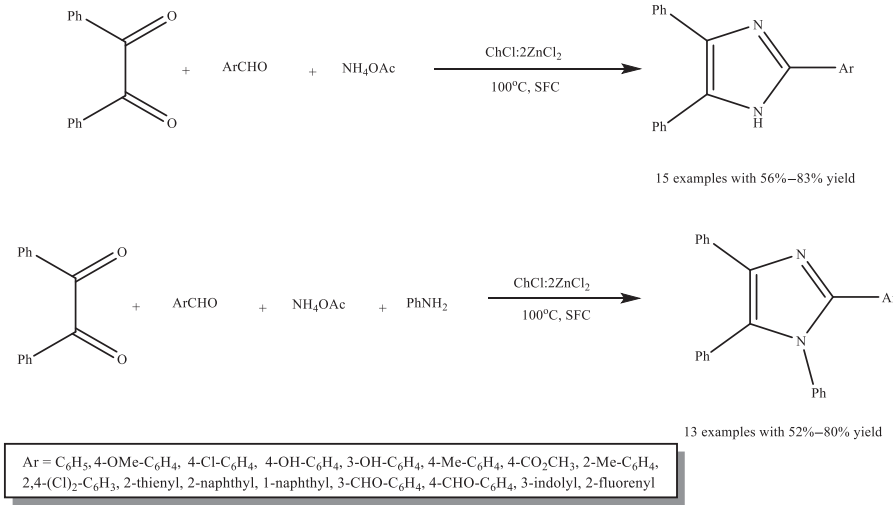

Scheme 9.23 Synthesis of 2,4,5-trisubstituted and 1,2,4,5-tetrasubstituted imidazoles.

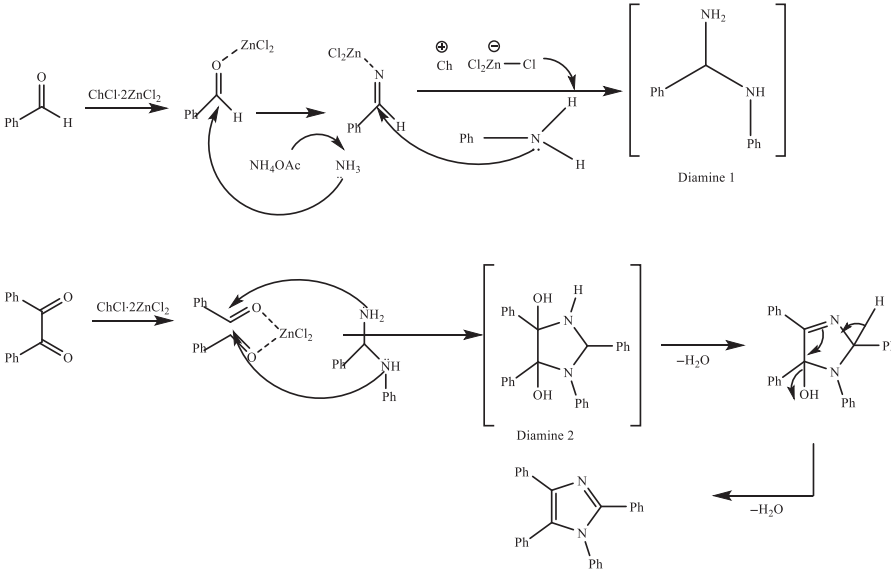

Scheme 9.24 Proposed reaction mechanism for the synthesis of 1,2,4,5-tetrasubstituted imidazoles.

9.2.1.7 Synthesis of substituted hydantoins

The hydantoin moiety is an important structural scaffold present in a number of biologically active compounds [81]. Many hydantoin derivatives have been identified as anticonvulsant, antiulcer, antiarrhythmic, antimuscarinic, antiviral, and antidiabetic agents [82]. Some hydantoin derivatives have also been used as antidepressants as well as platelet aggregation inhibitors [83] (Fig. 9.6).

A number of synthetic methods have been reported in the literature for the preparation of hydantoin derivatives from diverse starting materials [84]. The classic methods for the synthesis of hydantoin include the Bucherer-Bergs synthesis and the reaction of urea with carbonyl compounds [85]. In particular, the synthesis of highly substituted hydantoins is accomplished by reacting *N*-substituted α-amino acids or their esters with isocyanates [86]. Alternative strategies for the synthesis of substituted hydantoins used transition metal-catalyzed reactions [87], Ugi reaction [88], the reaction of α,β-unsaturated carboxylic acids with carbodiimide [89], and the reaction of α-amino amides with phosgene [90]. König et al. reported mild and environmentally benign domino synthesis of 1,3,5-trisubstituted hydantoin involving the exposure of β,γ-unsaturated ketoacid to the low melting mixture of L-(+)-TA-dimethylurea (DMU). The melt medium serves simultaneously as a solvent, a catalyst, and a reactant in the reaction. The reaction was extended with various β,γ-unsaturated ketoacids derived from electron-rich as well as electron deficient aldehydes under the melt conditions and synthesized the corresponding substituted hydantoin derivatives in good to excellent yields (84%–92%) [91] (Scheme 9.25).

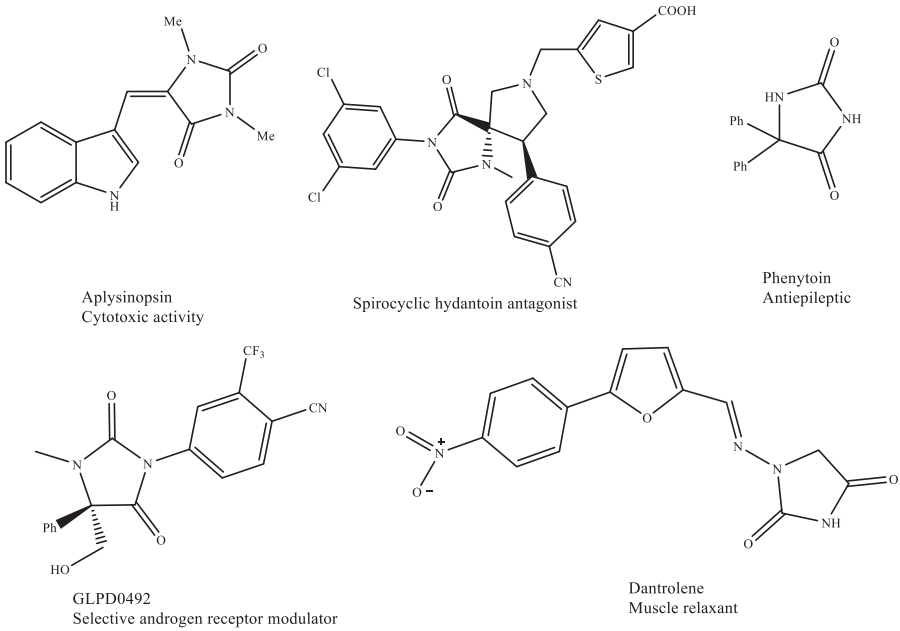

Fig. 9.6 Biologically active hydantoins.

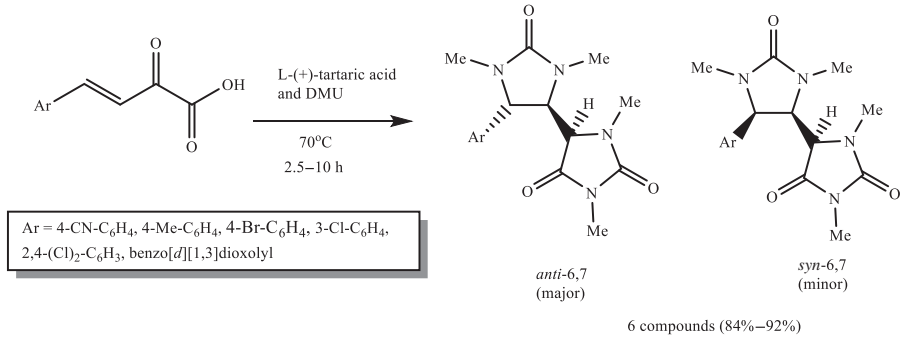

Scheme 9.25 Synthesis of 1,3,5-trisubstituted hydantoin derivatives.

9.2.1.8 Synthesis of isoxazoles

Isoxazoles and related 4,5-dihydroisoxazoles constitute a class of heterocyclic compounds and find their applications in pharmaceutical chemistry and in agriculture [92]. The synthetic methods reported for the construction of isoxazole and 4,5-dihydroisoxazole framework involve regioselective cycloaddition reaction using metallic derivatives, but the use of toxic transition metals is undesirable and therefore the metal-free protocols are necessarily required.

Ramón et al. synthesized 3,5-disubstituted isoxazoles and related isoxazolines from aldehydes and alkynes or alkenes in a one-pot three-step reaction using choline chloride: urea as DES [93]. In this method, hydroxylammonium chloride and solid NaOH were added to form the corresponding oxime. The addition of *N*-chlorosuccinimide to the basic reaction mixture results in the formation of hydroxyiminoyl chloride which on reaction with present phenylacetylene provides the corresponding isoxazole. The use of highly nucleophilic functionalized DES did not affect the process where highly electrophilic reagents or intermediates are involved.

Various DESs such as ChCl:glycerol, ChCl:trifluoroacetamide, ChCl:EG, $Ph_3P^+MeBr^-$:glycerol, AcChCl:urea were also examined in the reaction, but DES ChCl:urea proved its superiority in terms of yield and reaction time (73%, 4 h) (Schemes 9.26 and 9.27).

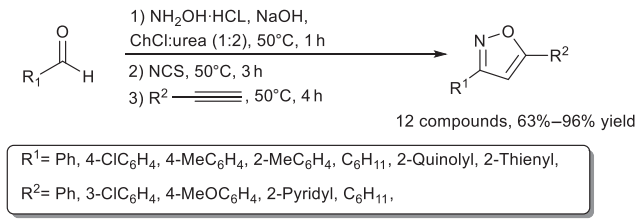

Scheme 9.26 Preparation of isoxazoles.

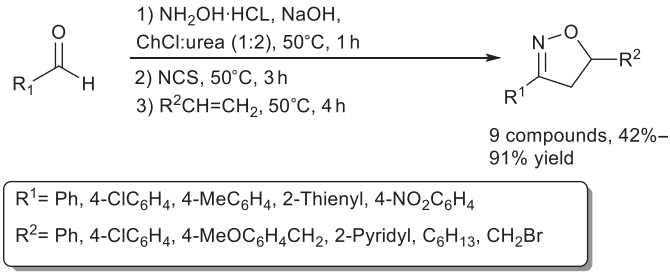

Scheme 9.27 Synthesis of isoxazolines.

Isoxazoline derivatives were synthesized also by the reaction of chalcones and hydroxylamine hydrochloride using ultrasonic radiations. The chalcones were synthesized by Claisen-Schmidt condensation using 2-bromo-4-chloroacetophenone with substituted aldehydes through the solvent-less mechano-chemical grinding method in the presence of solid NaOH. DESs consisting of benzalkonium chloride and urea in a 1:2 M ratio were used in combination with US for the synthesis of selective isoxazoline derivatives The reactions were also performed by nonultrasonic (NUS)/thermal method using the conventional solvent system. The results showed advantages in terms of reaction time and energy consumption when DES and US combination was used for the synthesis of isoxazolines (Scheme 9.28).

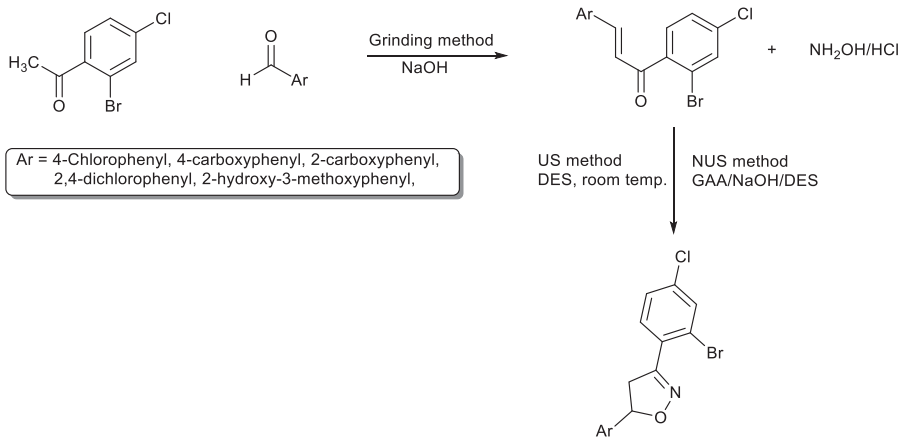

Scheme 9.28 Thermal and ultrasonic mediated synthesis of isoxazolines.

9.2.1.9 Synthesis of oxazoles

Oxazole derivatives have attracted the considerable interest in pharmaceutical research and organic synthesis in view of their biological activity such as antibacterial, antifungal, antitubercular, antiinflammatory [94], etc. and their utility as valuable

precursors in many useful synthetic transformations [95]. Oxazoles have shown their importance also in colorant chemistry especially as scintillating compounds and as fluorescent whitening agents for textiles [96] (Fig. 9.7).

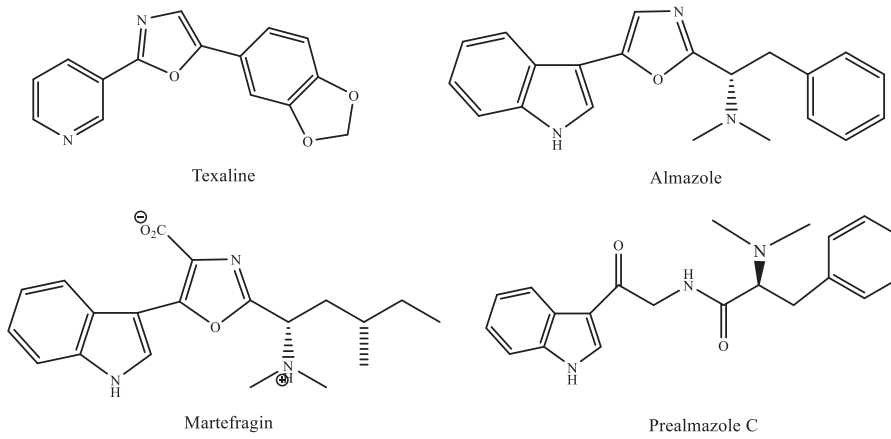

Fig. 9.7 Oxazole-containing bioactive natural products.

Recently, Shankarling et al. reported the synthesis of oxazole derivatives by the reaction of 4′-substituted phenacyl bromide and amide derivatives in DES. In their work, the organic synthesis was performed using an effective combination of DESs and US technique. The reaction was also conducted by thermal method (NUS) and observed that applying US not only improved yields and reduced reaction times but also saved more than 85% energy consumption. The advantages of using DES as a reaction medium was highlighted from the fact that it is biodegradable, non-toxic, recyclable, and can be easily prepared using inexpensive raw materials [57] (Scheme 9.29).

In this reaction, the urea component in DES (choline chloride:urea) facilitated the reaction via hydrogen bond catalysis. Urea component in DES might stabilize the oxygen atom of carbonyl group via hydrogen bonding that facilitated the attack of amide on phenacyl bromide derivative resulting in cyclization with the formation of oxazole (Scheme 9.30).

The present synthetic protocol with the combined use of DES and US radiation was extended for the synthesis of 2-aminooxazoles involving the reaction of phenacyl bromide derivative with urea in DES. It was observed that US-assisted method gave 90% yield in just 8 min as against 3.5 h required to obtain 69% yield by the conventional method. It was observed that the use of US radiation not only increased the rate of reaction but also improved the quality of the product obtained in terms of crystallinity. In addition, US-assisted synthesis also saved more than 70% energy. Moreover, the use of DES in sonochemical organic synthesis is quite suitable in view of their negligible vapor pressure [97] (Scheme 9.31).

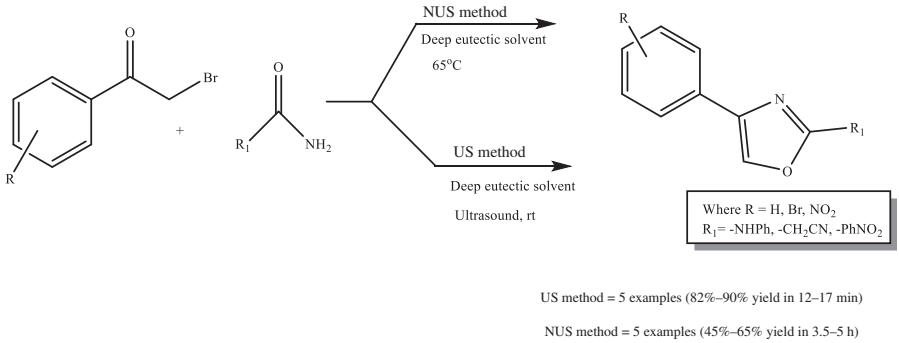

Scheme 9.29 Synthesis of oxazole derivatives.

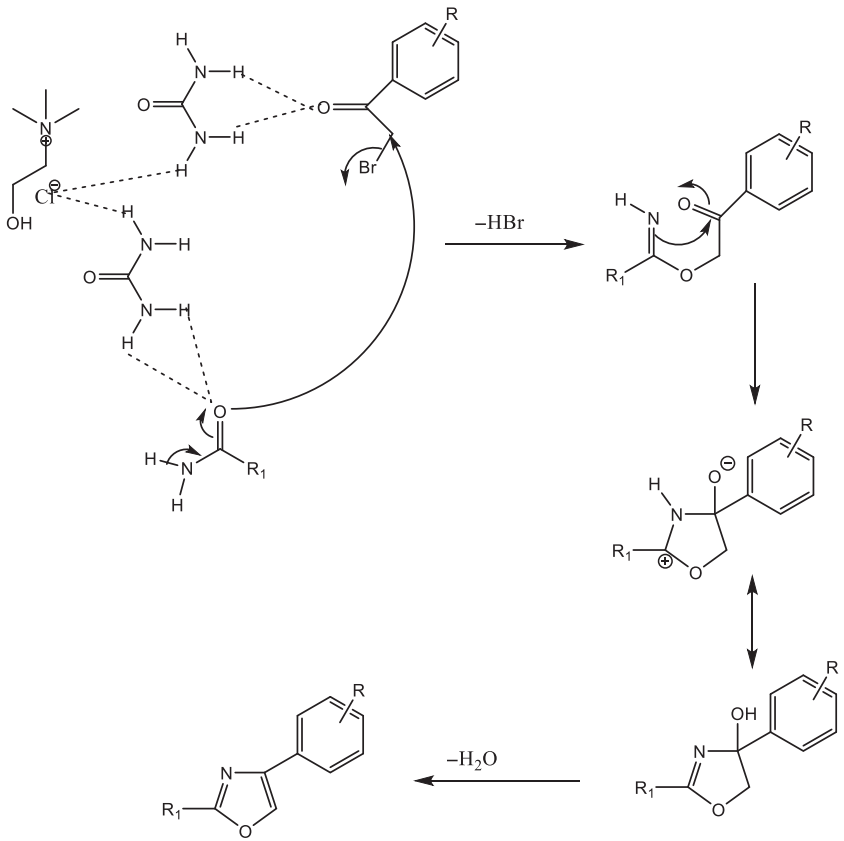

Scheme 9.30 Proposed reaction mechanism.

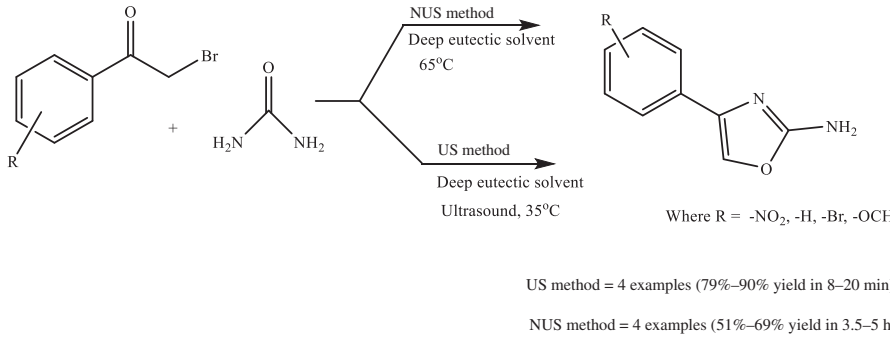

Scheme 9.31 Synthesis of 2-aminooxazole derivatives.

9.2.1.10 Synthesis of thiazoles

Thiazole derivatives have been reported to be associated with several biological activities which have made them extremely useful in the treatment of hypertension, schizophrenia, inflammation, and HIV infections [98]. Its derivatives like aminothiazoles are known to be ligands of estrogen receptors and also adenosine receptor antagonists [99] (Fig. 9.8).

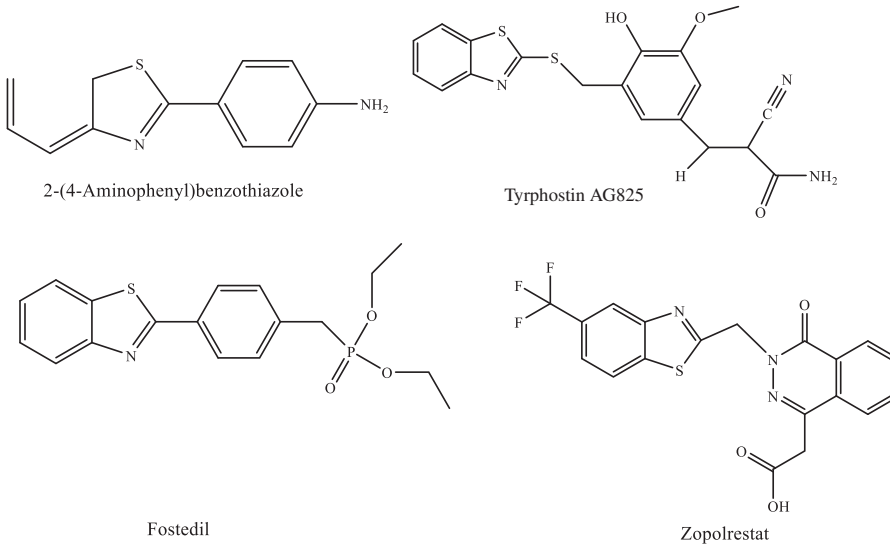

Fig. 9.8 Synthetic drugs-containing thiazole moiety.

In view of their extensive biological properties, many improved methods have been reported for the synthesis of thiazoles using various catalysts [100]. Although these methods are efficient in terms of yields and some even use greener methods, however,

most of these methods suffer from some limitations. Synthesis of thiazoles has also been performed in ILs, however, the ILs based on imidazole and fluorinated anions suffer from the demerits of being toxic and commercially expensive [101]. Shankarling et al. used ammonium-based deep eutectic mixture (choline chloride-urea) as an efficient catalyst for aqueous-phase synthesis of methylthiazole and aminothiazole derivatives involving the reaction of phenacyl bromide and thioamide derivatives. The deep eutectic catalyst, easily synthesized from choline chloride and urea, is inexpensive, recyclable and biodegradable, thus making it suitable for industrial applications [102] (Scheme 9.32).

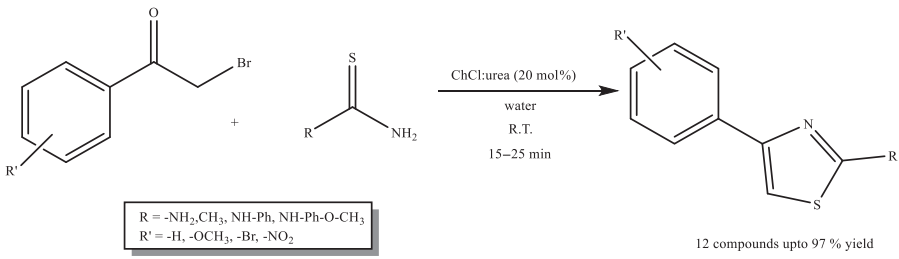

Scheme 9.32 Synthesis of thiazoles.

9.2.1.11 *Synthesis of thiazolidin-4-ones*

Thiazolidin-4-one derivatives constitute an important class of heterocyclic compounds and find their uses in organic syntheses to prepare heterocyclic compounds with diverse biological and pharmaceutical activities [103]. The functionalized thiazolidinones have been used as antimicrobial [104], antitubercular [105], antiinflammatory [106], HIV Inhibitor [107], antihypertensive [108], anticonvulsant [109], antihepatitis [110], antihyperglycemic [111], antioxidant [112], antifungal [113], and antiproliferative agents [114].

Thiazolidinones were earlier prepared by two- or three-step procedures [115]. But Amiri et al. proposed a one-step synthetic strategy involving the reaction of thioureas with chloroacetyl chloride and an aldehyde in natural DES (urea/choline chloride) to synthesize thiazolidin-4-ones. The methodology is mild and rapid for green synthesis of various 4-thiazolidinones in good to excellent yields in natural DES as a catalyst and reaction media [116] (Scheme 9.33).

Mane et al. proposed an alternative synthetic route for an antidiabetic drug, rosiglitazone, incorporating thiazolidine-2,4-dione nucleus. The reaction involves four steps. The first step involves Knoevenagel condensation of 4-fluorobenzaldehyde and 2,4-thiazolidinedione providing 5-(4-fluorobenzylidene) thiazolidine-2,4-dione. The condensation was carried out using a safer nonvolatile solvent. The reaction conditions were optimized for the condensation of 4-fluorobenzaldehyde and 2,4-thiazolidinedione to synthesize 5-(4-fluorobenzylidene) thiazolidine-2,4-dione by using various reaction media and organic/inorganic bases. It was observed that freshly prepared DES worked

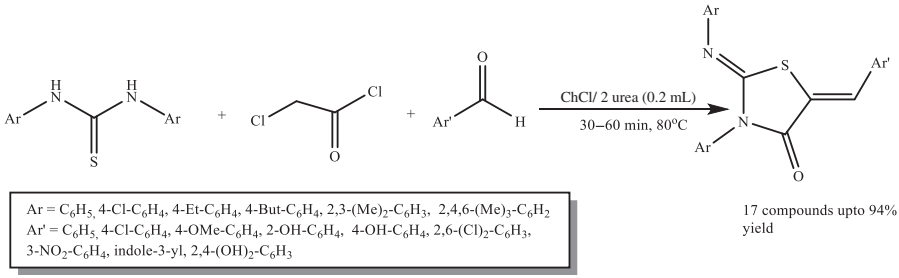

Scheme 9.33 Synthesis of thiazolidin-4-one derivatives.

as a better medium and catalyst. It was also noted that maximum conversion was obtained at 80°C and DES could be recovered and recycled for another batch of reaction [117] (Scheme 9.34).

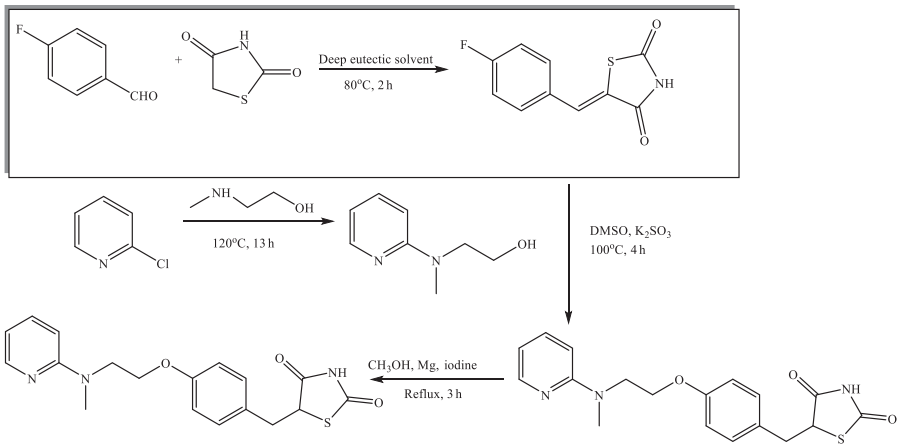

Scheme 9.34 Synthesis of rosiglitazone drug.

Yedage et al. reported the synthesis of biologically active 1,3-thiazolidin-4-ones involving the multicomponent reaction of substituted anilines, aromatic aldehydes and thioglycolic acid in the presence of DES, as a catalyst and reaction media. The reaction conditions were optimized with several choline chloride-based DESs as a reaction media at 85°C. Choline chloride:glycerol (1:2) DES was found to be an efficient catalyst that provided an excellent yield of 1,3-thiazolidin-4-one derivatives (Scheme 9.35) [118].

The plausible DES catalyzed mechanism involved in the synthesis of 1,3-thazolidin-4-ones is presented in Scheme 9.36. In the first step, DES interacts with the oxygen atom of the carbonyl group of the aldehyde and increases the electrophilicity of the carbonyl group of the aldehyde to facilitate the formation of imine intermediate (I). Sulfur atom of thioglycolic acid attacks the activated imine intermediate

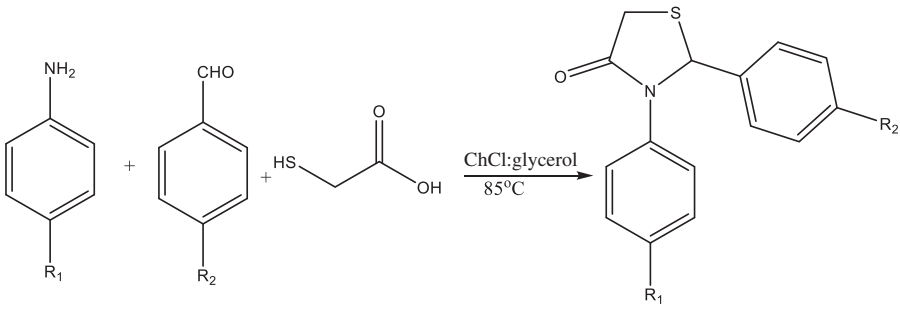

Aniline= $PhNH_2$, 4-$MeC_6H_4NH_2$, 4-$ClC_6H_4NH_2$, 4-$OMeC_6H_4NH_2$, 4-$FC_6H_4NH_2$
Aldehyde= PhCHO, 4-ClC_6H_4CHO, 4-MeC_6H_4CHO, 4-$OMeC_6H_4CHO$, 4-FC_6H_4CHO, 4-BrC_6H_4CHO, 4-$NO_2C_6H_4CHO$

17 examples
Yield upto 97%

Scheme 9.35 DES catalyzed synthesis of 1,3-thiazolidin-4-ones.

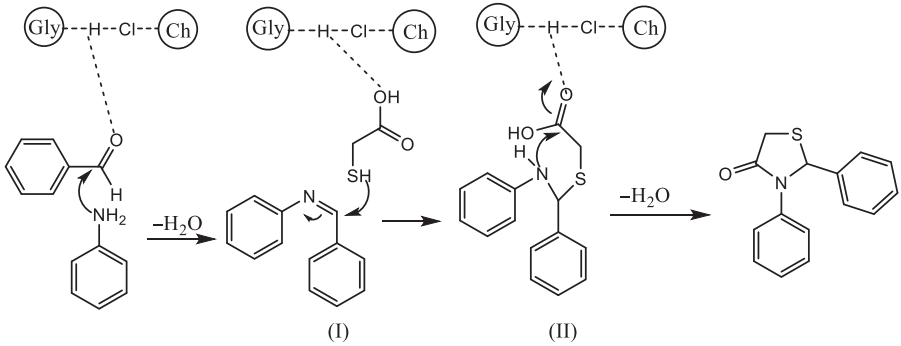

Scheme 9.36 Plausible mechanism for the synthesis of 1,3-thiazolidin-4-ones.

(I) and thereby, facilitates the formation of intermediate (II). Further, the DES activates intermediate (II) to undergo subsequently intramolecular cyclization to provide the desired product.

9.2.1.12 Synthesis of triazole derivatives

Triazole is a medicinally privileged heterocyclic system and incorporated in synthetic pharmaceuticals and bioactive natural products. Triazoles have shown bactericidal [119] and antihistamine activity [120], in addition to their uses as potassium channel activators [121] and tuberculosis and protein inhibitors [122]. The heterocycles with triazole skeleton are important pharmacophores for the development of drugs, mainly because they are stable compounds that can mimic peptide bonds [123].

The reaction of alkynes and azides is the most common 1,3-dipolar cycloaddition and is considered as the most used synthetic route for 1,2,3-triazoles. The importance of this synthetic route increased when Sharpless and Meldal introduced copper as the catalyst in this reaction, which made it possible to obtain 1,4-disubstituted 1,2,3-triazoles with high regioselectivity. Martins et al. synthesized 4-acyl-1-substituted-1,2,3-triazoles by the reaction of β-enaminones with an azide using DES-containing ChCl and EG (1:2 ratio) as the reaction medium [124] (Scheme 9.37).

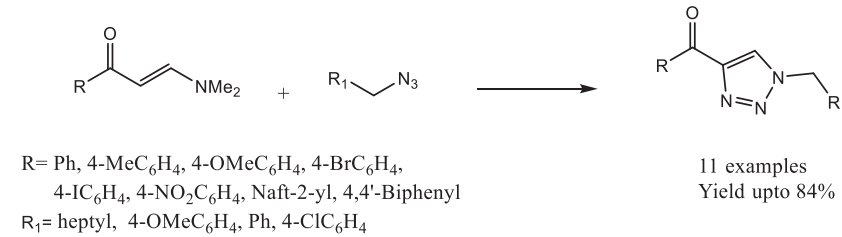

Scheme 9.37 Synthesis of 4-acyl-1-substituted-1,2,3-triazoles.

In the proposed mechanism, one equivalent of EG interacts with the azide, and other equivalent interacts with the carbonyl of β-enaminone via hydrogen bonds. Additionally, the choline hydroxyl group can form a complex with the double bond of β-enaminone. These interactions probably facilitate the reaction (Scheme 9.38).

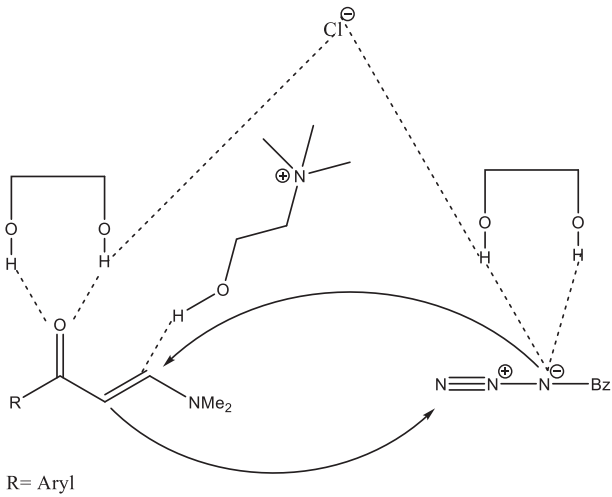

Scheme 9.38 Proposed mechanism for 4-acyl-1-substituted-1,2,3-triazoles.

9.2.1.13 Synthesis of pyridines

Pyridines constitute an important class of heterocyclic compounds including bioactive natural products and synthetic pharmaceuticals with a wide spectrum of biological activities [125] and photophysical properties. Among numerous pyridine derivatives,

2,4,6-triarylpyridine derivatives, specifically, are widely practiced as anticancer drugs [126]. Kamble et al. synthesized 2,4,6-triarylpyridines involving one-pot multicomponent reaction of aldehydes, acetophenone, and ammonium acetate in the presence of DESs using concentrated solar radiations (CSRs) [127] (Scheme 9.39). The reaction was performed in the presence of choline hydroxide (ChOH), and also in different acidic DES, such as ChCl:oxalic acid (ChCl:OA), ChCl:malonic acid (ChCl:MA), ChCl:tartaric acid (ChCl:TA), and ChCl:$ZnCl_2$. The authors reported excellent results with DES-containing ChCl:malonic acid and DES served as catalyst and solvent in the reaction.

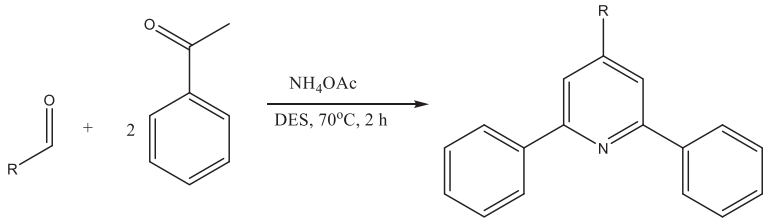

R= Ph-, 2,6-Di Cl-phenyl-, 2-MeO-Ph, 2-Thenyl-,
4-Me-Ph, 3-Cl-Ph-, 3-PhO-

Scheme 9.39 Synthesis of 2,4,6-triphenylpyridines.

The 2-amino-3,5-dicarbonitrile-6-arylthiopyridine scaffold is of significant medicinal relevance and various compounds with this structural motif exhibit diverse biological activities [128] (Fig. 9.9).

Therapeutic agents incorporating 6-arylthiopyridine molecular framework have been reported as antiviral, antitumor, antibacterial, analgesic, antiinflammatory, and anticancer agents [129] in addition to their uses in the treatment of asthma, nephropathy, cancer, and Parkinson's disease [130]. Azizi et al. synthesized highly substituted 6-arylthiopyridines involving the multicomponent reaction of aromatic aldehyde, malononitrile, and thiophenol using DES in dual role as a catalyst and as solvent (Scheme 9.40) [131].

A plausible mechanism for the synthesis of pyridines in DES is presented in Scheme 9.41. In the proposed mechanism DES has two functions: (i) to activate carbonyl and nitrile groups through hydrogen bonding to enable the nucleophilic addition of malononitrile; (ii) to simultaneously, act as a base for capturing a proton of malononitrile and thiophenol to form the corresponding anions. Activation of aldehyde by hydrogen bonding increases the electrophilicity of the aldehyde and assists the Knoevenagel condensation with malononitrile. Then, the second molecule of malononitrile undergoes Michael addition followed by simultaneous thiolate addition to the activated CN of the adduct. The cyclization leading to dihydropyridine is followed by oxidative aromatization to provide the highly substituted pyridine.

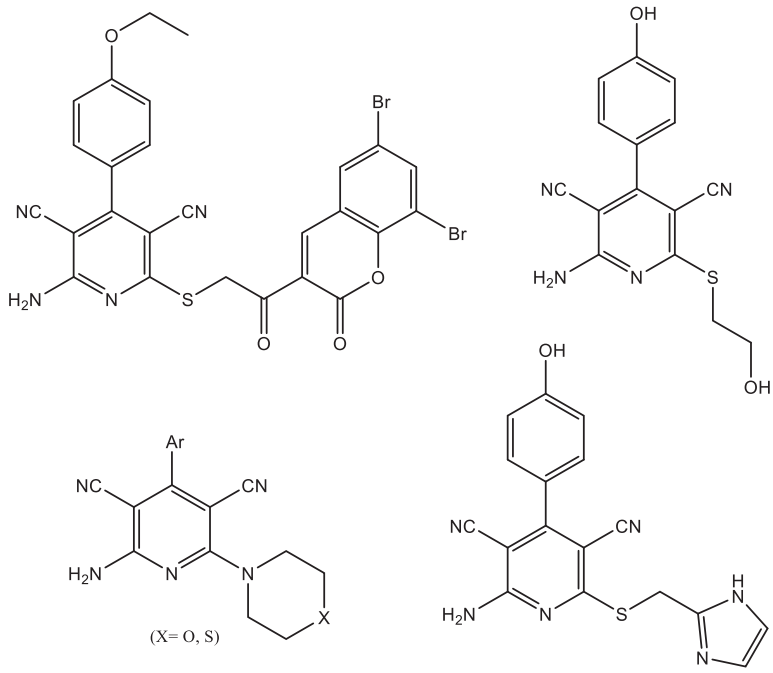

Fig. 9.9 Biologically active 2-amino-3,5-dicarbonitrile-6-arylthiopyridine scaffold.

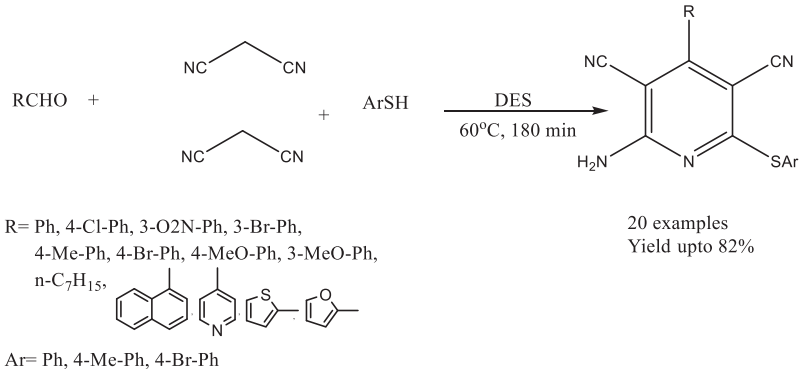

Scheme 9.40 Synthesis of 6-arylthiopyridines.

9.2.1.14 Synthesis of 1,4-dihydropyridines

1,4-Dihydropyridines (1,4-DHPs) constitute an important class of bioactive molecules. 1,4-Dihydropyridines are well known for their role as calcium channel modulators and used extensively for the treatment of hypertension [132]. The derivatives of

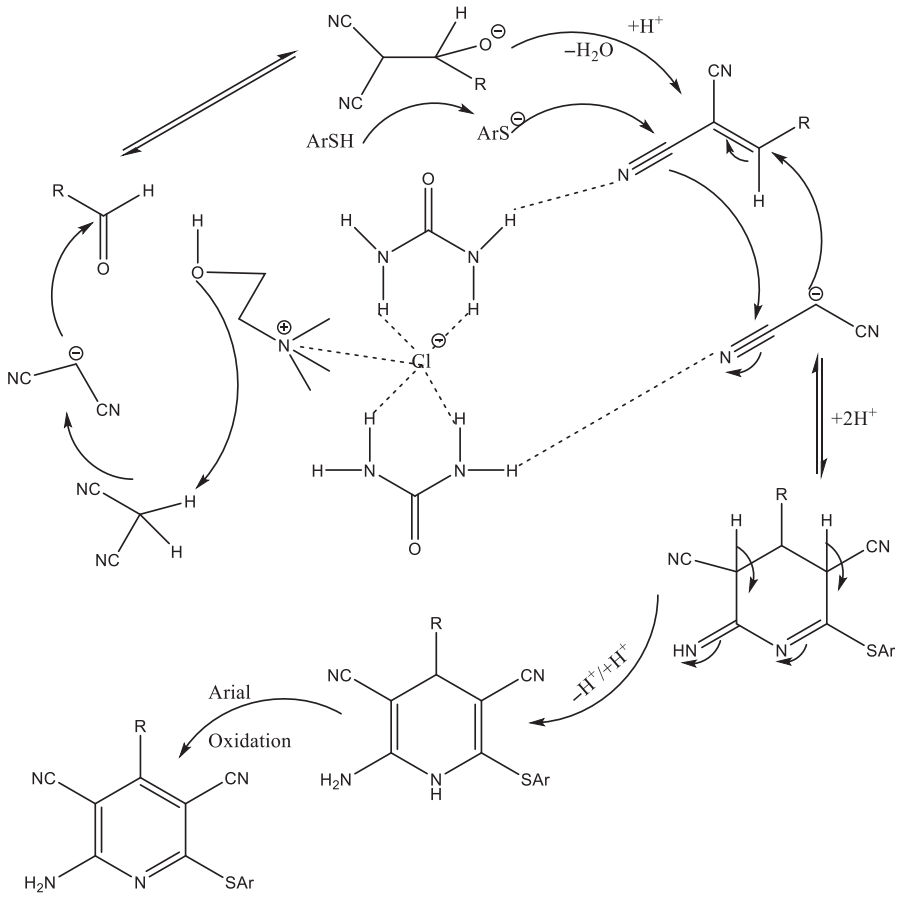

Scheme 9.41 The proposed mechanism for the synthesis of 6-arylthiopyridines.

1,4-DHPs have shown their uses as vasodilators, bronchodilators, and antitumors, including their hepatoprotective and geroprotective activity [133]. Commercial drugs incorporating 1,4-DHP structure has been used extensively in both antianginal and antihypertensive treatment [134] (Fig. 9.10).

Pednekar et al. reported the one-pot multicomponent synthesis of 1,4-dhydropyridines by the reaction of aldehydes, dimedone, ethyl acetoacetate, and ammonium acetate in the presence of biocompatible DES. Initially, the reaction conditions were optimized with water, various DES and some polar and nonpolar conventional organic solvents. But results clearly indicated that DES has more potential than conventional organic solvent for the synthesis of 1,4-DHPs. The synthetic protocol provided excellent yields with the recyclability of DESs without any appreciable loss in activity up to five recycles [135] (Scheme 9.42).

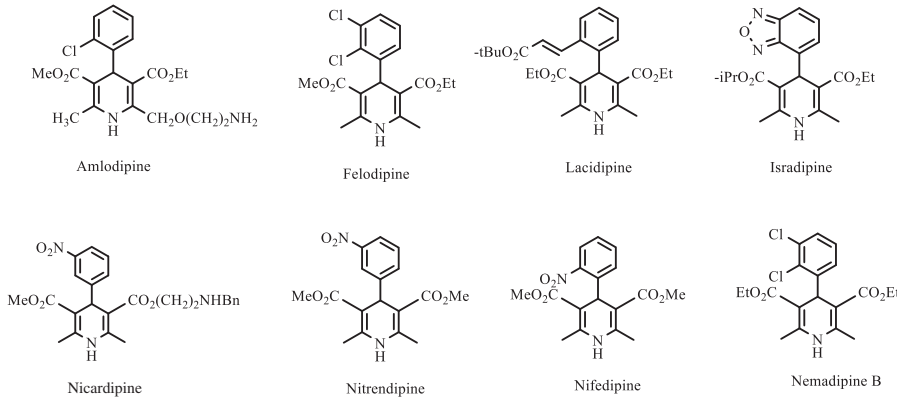

Fig. 9.10 Clinically used dihydropyridyl cardiovascular drugs.

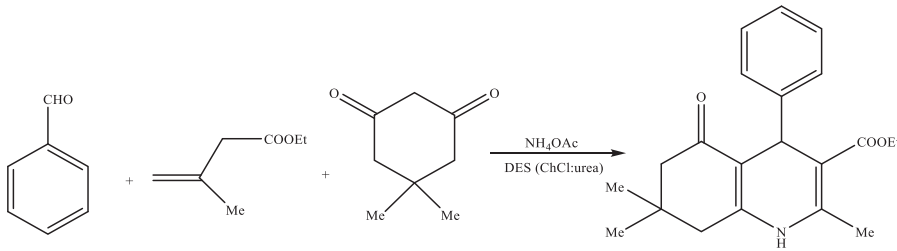

Scheme 9.42 Synthesis of 1,4-dhydropyridines.

9.2.1.15 *Synthesis of imidazo[1,2-a]pyridines*

Functionalized heterocyclic scaffolds derived from imidazo[1,2-*a*]pyridines have been reported to exhibit antimicrobial [136], antiviral [137], antituberculosis [138], antitubercular [139], antimicrobial [140], VEGFR2 kinase inhibitor [141], IGF-1R tyrosine kinase inhibitor [142], ASK1 inhibitor [143], and antiepileptic activities [144]. The imidazo[1,2-*a*]pyridine nucleus appears in bioactive natural products and synthetic pharmaceuticals. The representative examples include alpidem, zolpidem, necopidem, zolimidine, and miroprofen (Fig. 9.11).

Lu et al. synthesized imidazo[1,2-*a*]pyridines involving one-pot, three-component reaction of 2-aminopyridines, aldehydes, and alkynes using $CuFeO_2$ as a catalyst in citric acid-dimethylurea (DMU) melt as solvent (Scheme 9.43) [145].

The influence of different solvents on the reaction was investigated and observed that the reaction was not successful in methanol, ethanol, water, toluene, acetonitrile, *N*,*N*-dimethylformamide, poly(ethyleneglycol), D-(−)-fructose-DMU, mannose-DMU-NH_4Cl, lactose-DMU-NH_4Cl, and L-(+)-tartaric acid-choline chloride at their minimal melting temperatures but the yield increased to as high as 95% when citric

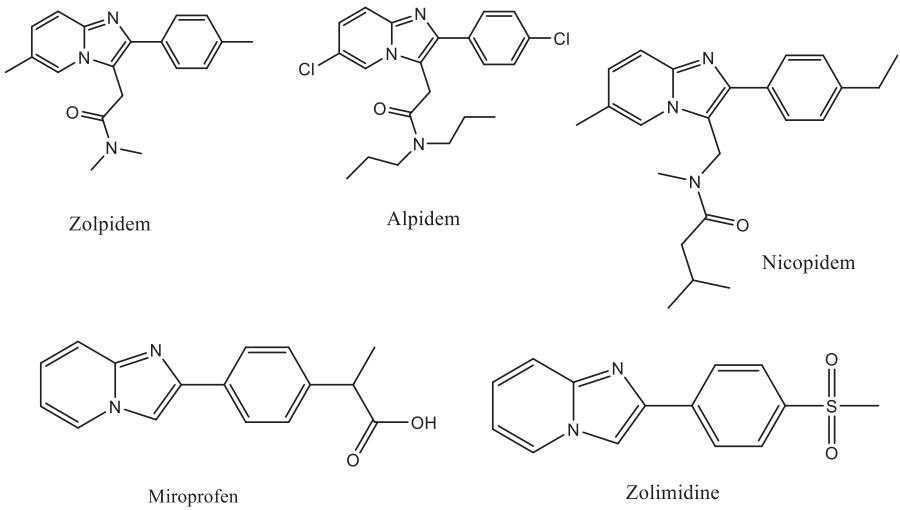

Fig. 9.11 Imidazo[1,2-*a*]pyridine nucleus-containing drugs.

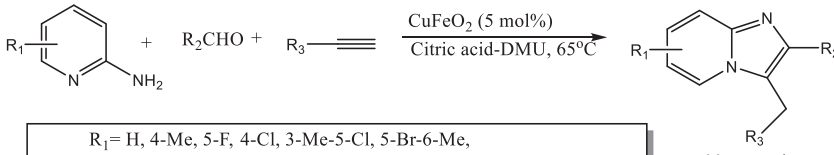

R_1= H, 4-Me, 5-F, 4-Cl, 3-Me-5-Cl, 5-Br-6-Me,
4-Me-5-Br, 4-MeO_2C, 3-Br, 3,5-Cl_2
Aldehyde= PhCHO, 3-$MeOC_6H_4CHO$, 3-$PhOC_6H_4CHO$,
4-$CH_3(CH_2)_2OC_6H_4CHO$, 4-$CH_3(CH_2)_4OC_6H_4CHO$,
4-$CH_3C_6H_4CHO$, 4-$CMe_3C_6H_4CHO$, 4-$SCH_3C_6H_4CHO$.
4-FC_6H_4CHO, 2-ClC_6H_4CHO, 3-ClC_6H_4CHO, 4-ClC_6H_4CHO,
4-BrC_6H_4CHO, 3-$CF_3C_6H_4CHO$,4-$CF_3C_6H_4CHO$,
furan-2-carbaldehyde, thiophene-2-carbaldehyde, 4-Me PhCHO
R_3= Ph,4-$CH_3C_6H_4$, 4-$CH_3(CH_2)_3C_6H_4$, 4-FC_6H_4

Scheme 9.43 Synthesis of imidazo[1,2-*a*]pyridines.

acid-DMU was used as solvent. It was also observed that 2-aminopyridines with either electron-donating or electron-withdrawing substituents provided the desired products in good to excellent yields.

Imidazo[1,2-*a*]pyridines were synthesized also by Groebke multicomponent reaction of 2-aminopyridine, aromatic aldehydes and cyclohexyl isocyanide using choline chloride-based DES (Scheme 9.44). The reaction conditions were optimized with six different choline chloride-based DESs and reported urea-choline chloride as an efficient solvent for this isocyanide-based multicomponent reaction [146].

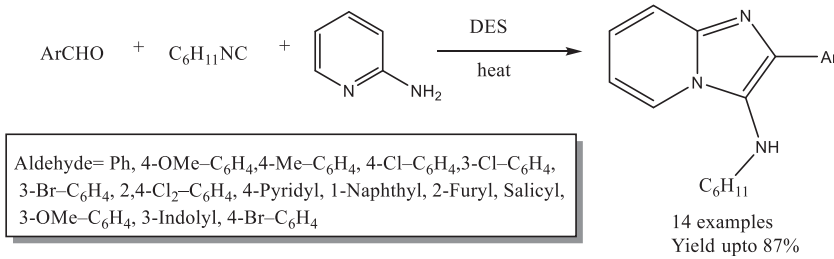

Scheme 9.44 Synthesis of imidazo[1,2-*a*]pyridines.

DES catalyzed mechanism of the reaction is presented in Scheme 9.45. DES facilitates imine intermediate (A) formation through the nucleophilic addition of an amine to activated aldehyde. DES can activate imine for isocyanide nucleophilic attack. Cycloaddition reaction of intermediate (A) with cyclohexyl isocyanide produces bicyclic adduct (B) which on internal rearrangement via 1,3-H shift provides the target product as presented in Scheme 9.45.

*9.2.1.16 Synthesis of pyrazolo[3,4-*b*]pyridines*

Pyrazolo[3,4-*b*]pyridines constitute a promising class of nitrogen-containing heterocyclic compounds present in many active biological products, natural products, and functional materials with applications in diverse areas, such as pharmaceuticals [147], dyes [148], and luminescence materials [149]. Pyrazolo[3,4-*b*]pyridines have also been reported to possess diverse biological activities, such as antimicrobial [150], antibiofilm [151], antimicrobial [152], and antioxidant [153], antiplatelet [154], antifungal [155], anticancer [156], antimicrobial, and antiproliferative [150]. Moreover, they have also been reported to behave as potent dual orexin receptor antagonists [157], c-Met [158], selective FGFR kinase inhibitors [159], and also as corrosion inhibitors for metals and alloys in acid medium.

Zhang et al. synthesized 3,6-di(pyridin-3-yl)-1*H*-pyrazolo[3,4-*b*]pyridine-5-carbonitriles via one pot, three-component reaction of 1-phenyl-3-(pyridin-3-yl)-1*H*-pyrazol-5-amine with 3-oxo-3-(pyridin-3-yl)propanenitrile and aldehydes in the presence of choline chloride/glycerol (DES) under microwave irradiation using magnetically separable graphene oxide anchored sulfonic acid catalyst (Scheme 9.46) [160].

The reaction conditions were optimized under various solvents and obtained the best results with the use of DES ChCl/glycerol. It was also observed that the product yield increased with the increasing proportion of glycerol in the DES. A number of aromatic aldehydes substituted with electron-rich or electron-poor groups on aromatic ring provided the desired products in high yields.

A plausible mechanism for the formation of 3,6-di(pyridin-3-yl)-1*H*-pyrazolo[3,4-*b*]pyridine-5-carbonitriles in the presence of $CoFe_2O_4$-GO-SO_3H is presented in

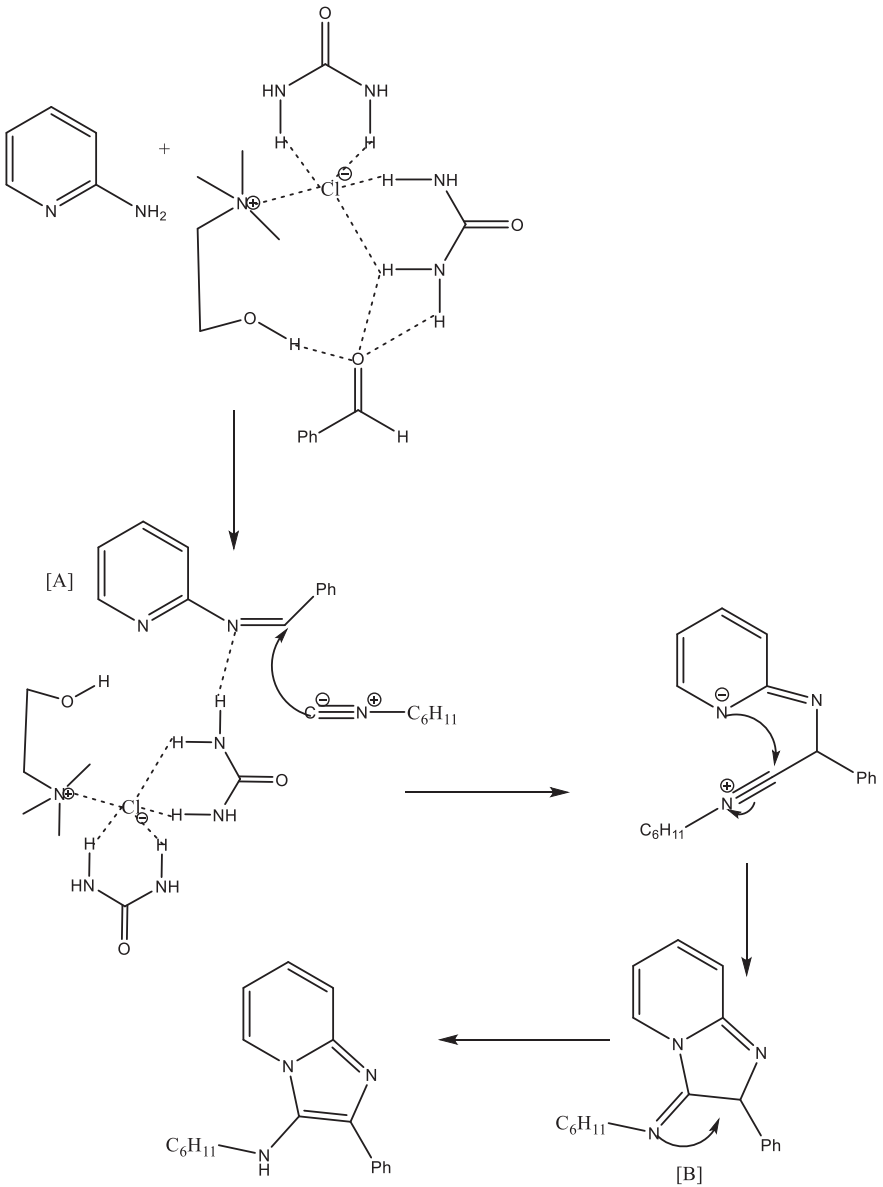

Scheme 9.45 DES catalyzed mechanism for the synthesis of imidazo[1,2-*a*]pyridines.

Scheme 9.47. The reaction proceeds with the initial Knoevenagel condensation of aldehyde and 3-oxo-3-(pyridin-3-yl)propanenitrile to afford the intermediate (**I**). The $CoFe_2O_4$-GO-SO_3H-activated intermediate (**I**), subsequently undergoes Michael addition with 1-phenyl-3-(pyridin-3-yl)-1*H*-pyrazol-5-amine (**1**) via attack of the

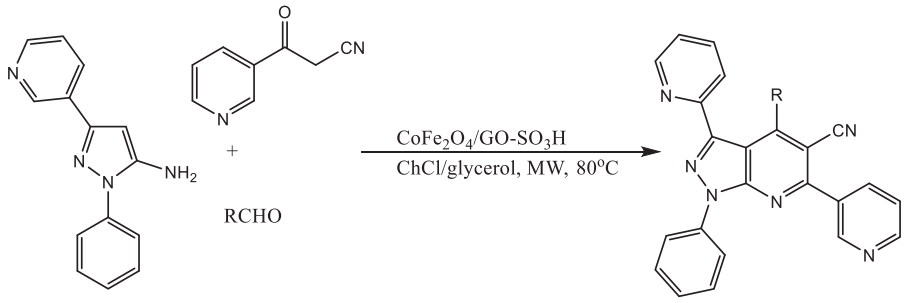

R= PhCHO, 2-MeOC$_6$H$_4$CHO, 3-MeOC$_6$H$_4$CHO,
4-MeOC$_6$H$_4$CHO, 4-MeC$_6$H$_4$CHO, 3-ClC$_6$H$_4$CHO,
4-ClC$_6$H$_4$CHO,3-BrC$_6$H$_4$CHO, 4-BrC$_6$H$_4$CHO,
2-NO$_2$C$_6$H$_4$CHO, 3-NO$_2$C$_6$H$_4$CHO, 4-NO$_2$C$_6$H$_4$CHO,

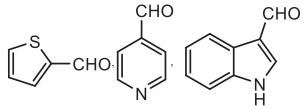

15 examples
Yield upto 95%

Scheme 9.46 Synthesis of 3,6-di(pyridin-3-yl)-1*H*-pyrazolo[3,4-*b*]pyridine-5-carbonitriles.

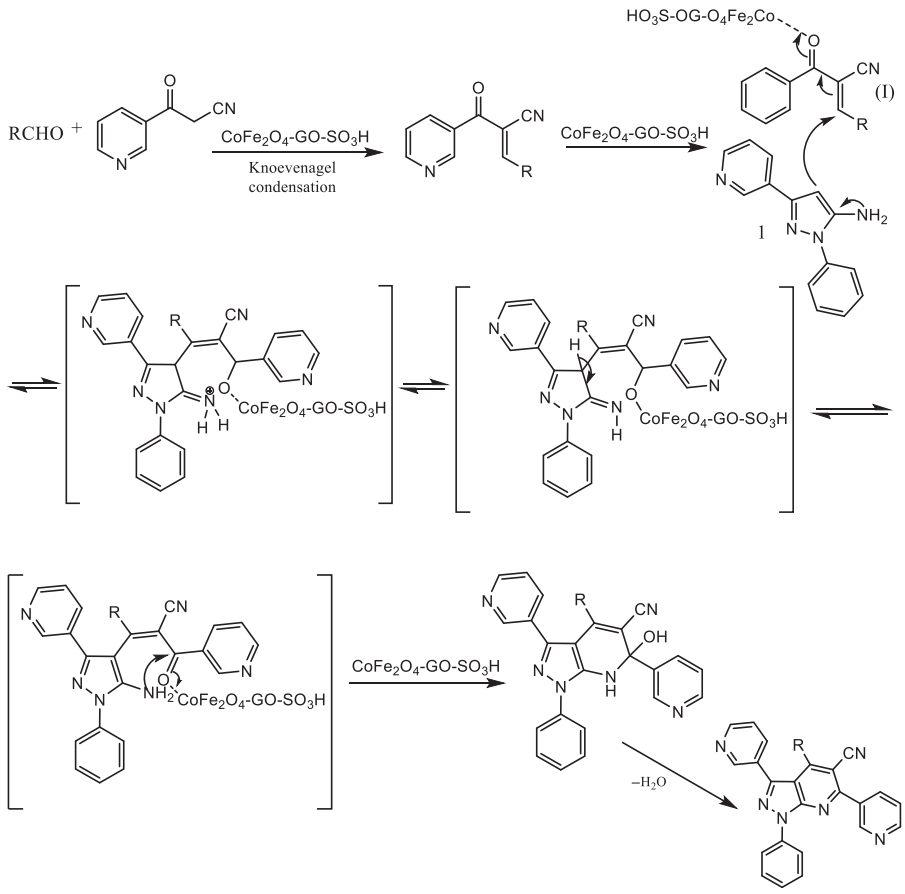

Scheme 9.47 Plausible mechanism for synthesis of 3,6-di(pyridin-3-yl)-1*H*-pyrazolo[3,4-*b*] pyridine-5-carbonitriles.

nucleophilic C-4 of the pyrazolamine, followed by intramolecular cyclization with loss of H_2O to afford the desired product.

9.2.1.17 Synthesis of pyrimidines

Pyrimidine is a medicinally privileged scaffold and is incorporated in synthetic pharmaceuticals and bioactive natural products with wide-ranging activities including antitumor, analgesic, antiarrhythmic, antibacterial, antifungal, antimalarial, anticonvulsant, etc. [161]. Pyrimidine is also a key constituent of some important drugs used for the treatment of hyperthyroidism, acute leukemia in children and adult granulocytic leukemia [162]. Pyrimidines also find their applications in polymer and supramolecular chemistry [163]. In addition, the compounds incorporating pyrimidine nucleus with extended conjugation are potential candidates for light-emitting devices [164] and molecular wires [165].

Vadagaonkar et al. reported the synthesis of substituted pyrimidines from α,β-unsaturated ketones and benzamidine hydrochloride using choline hydroxide (ChOH) in a dual role, as a catalyst and reaction medium (Scheme 9.48) [166].

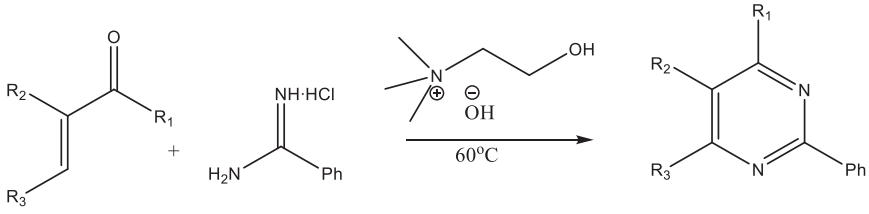

R_1=PhCHO, 4-Me-C_6H_4CHO, 3-Cl-C_6H_4CHO, Me
R_2= H
R_3= Ph, 4-F-C_6H_4CHO, 2-Cl-C_6H_4CHO, 4-Cl-C_6H_4CHO, 4-Br-C_6H_4CHO,

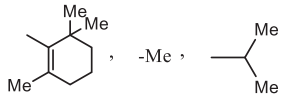

Scheme 9.48 Synthesis of substituted pyrimidines.

The reaction was screened in different solvents, including ChOH under reflux conditions, but obtained excellent results with ChOH. The reaction proceeds with the DES catalyzed facilitation involving conjugate addition of benzamidine to the α,β-unsaturated ketone to provide an intermediate (enolate), which is stabilized through hydrogen bonding. This intermediate after tautomerization undergoes intramolecular cycloaddition and subsequent dehydration to produce dihydropyrimidine (DHPM) which is aromatized in the presence of molecular oxygen to provide substituted pyrimidine as presented in Scheme 9.49.

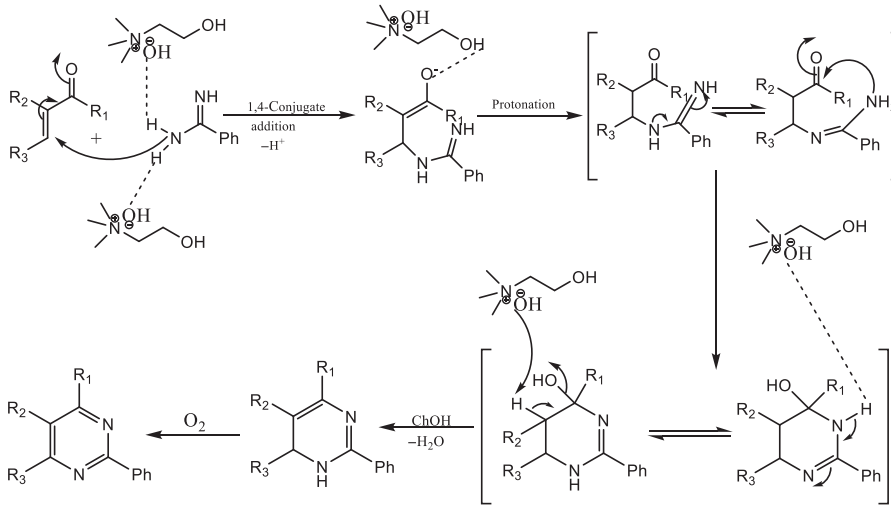

Scheme 9.49 Plausible reaction mechanism for the synthesis of substituted pyrimidines using DES as catalyst.

9.2.1.18 Synthesis of dihydropyrimidines

DHPM-5-carboxamides constitute an important class of *N*-heterocycles and exhibit a wide spectrum of biological and pharmacological activities including antitubercular [167], antihypertensive [168], antiinflammatory [169], anticancer [170], antimicrobial [171], anti-HIV-1 [172], and antimycobacterial activities [173]. DHPM-5-carboxamides are active specifically against dormant TB bacilli [174] and herpes simplex virus [175]. In addition, DHPM-5-carboxamide analogs have also been reported to be excellent templates for selective α1a receptor subtype antagonists to warrant further consideration for the treatment of benign prostatic hyperplasia (BPH) [176].

Liu et al. reported the synthesis of DHPM-5-carboxamides involving one-pot reaction of *N*-acetoacetanilide with various aldehydes using a low melting mixture of betaine hydrochloride/urea (DES) which plays a triple role: as a catalyst, solvent, and reactant (Scheme 9.50) [177].

Subsequently, the reaction was investigated in various low melting mixtures (such as $ZnCl_2$/urea or tartaric acid/mannitol/urea) and observed excellent yield (92%–93%) with betaine hydrochloride/urea-based DES. It was also observed that the yield of the product decreased with the use of aliphatic aldehyde as a substrate, but the presence of electron-rich/electron-poor groups on the phenyl ring of *N*-acetoacetanilides provided comparatively better yields of the corresponding DHPM-5-carboxamides.

In the proposed mechanism, the first step involves acid-catalyzed reaction of an aldehyde with urea to form intermediate **A**, which on dehydration gives acylimine

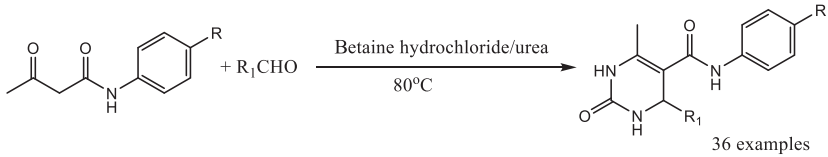

R= H, Cl, Me
Aldehyde= PhCHO, 2-MeO-C_6H_4CHO, 3-MeO-C_6H_4CHO, 4-MeO-C_6H_4CHO, 3,4-(MeO)2-C_6H_3CHO, 3-OH-C_6H_4CHO, 4-OH-C_6H_4CHO, 3-OPh-C_6H_4CHO, 4-Me-C_6H_4CHO, 4-t-Bu-C_6H_4CHO, 2-F-C_6H_4CHO, 2-Cl-C_6H_4CHO, 3-Cl-C_6H_4CHO, 4-Cl-C_6H_4CHO, 2-Br-C_6H_4CHO, 3-Br-C_6H_4CHO, 4-Br-C_6H_4CHO, 3-NO_2-C_6H_4CHO, 4-NO_2-C_6H_4CHO, 4-CN-C_6H_4CHO, 1-Naphthaldehyde, 2-Thiophene-carbaldehyde, Terephthalaldehyde, CH3CH2CHO

Scheme 9.50 Synthesis of dihydropyrimidine-5-carboxamides.

intermediate **B**. Subsequently, the addition of enol tautomer of *N*-acetoacetanilide to the electron-deficient acylimine intermediate **B** produces an open-chain ureide intermediate **C**, which subsequently on cyclization and dehydration provides DHPM-5-carboxamide (Scheme 9.51).

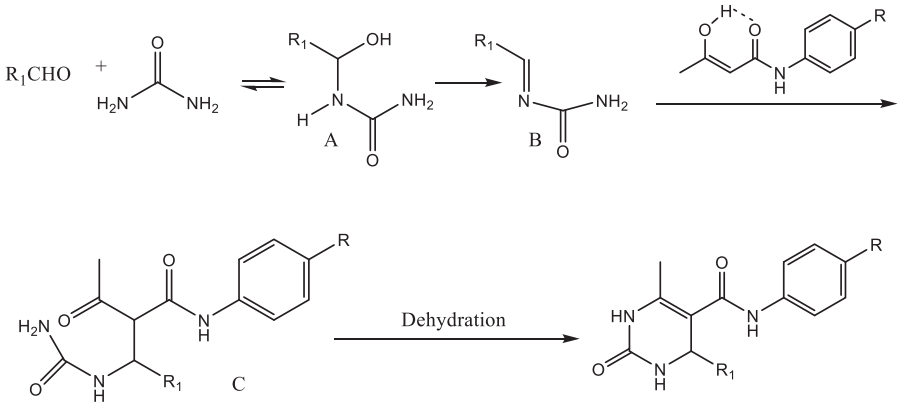

Scheme 9.51 Proposed mechanism for the synthesis of dihydropyrimidine-5-carboxamides.

9.2.1.19 *Synthesis of dihydropyrimidinones*

Dihydropyrimidinones occupy an important place in the realm of natural and synthetic organic chemistry (Fig. 9.12) [178]. In addition to their wide-ranging pharmacological activities, dihydropyrimidinones have emerged as potent calcium channel blockers [179]. Numerous marine alkaloids containing the dihydropyrimidinone skeleton have shown interesting biological properties [180].

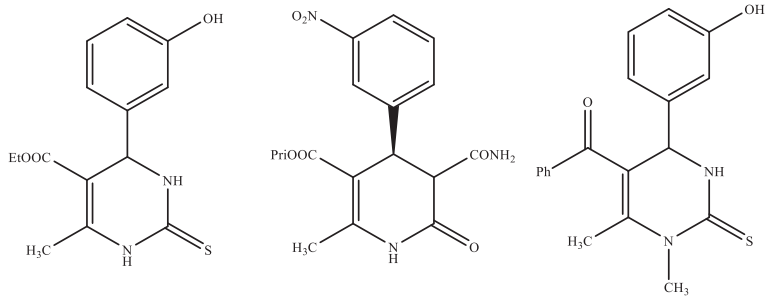

Fig. 9.12 Pharmacologically active DHPMs.

Azizi et al. reported synthesis of 3,4-dihydropyrimidin 2(1*H*)-ones via Biginelli reaction involving the reaction of aromatic and aliphatic aldehydes, 1,3-dicarbonyl compounds, and urea using simple DES based on tin (II) chloride as a catalyst and environmentally benign reaction medium. The reaction conditions were optimized with the screening of five choline-based DESs and ChCl:$SnCl_2$ DES reported to be the most appropriate with excellent yields of the products. Under optimized reaction conditions, the reaction was extended with structurally diverse 1,3-dicarbonyl compounds, aromatic and aliphatic aldehydes, and urea using choline chloride and tin chloride as a solvent to produce the corresponding dihydropyrimidinones (Scheme 9.52) [181].

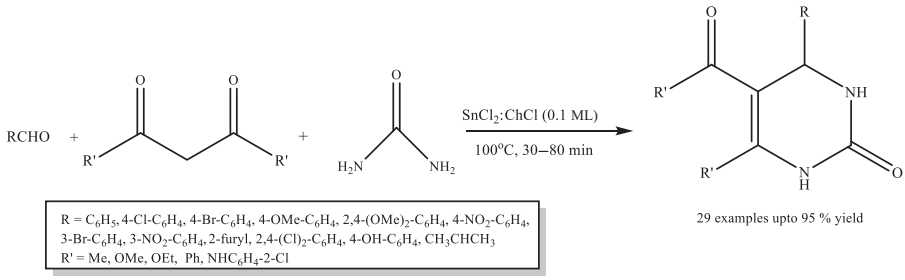

Scheme 9.52 Synthesis of dihydropyrimidinones.

Koenig et al. reported that these heterocycles can also be synthesized by one-pot multicomponent reaction of benzaldehyde, ethylacetoacetate under mild reaction condition by using low melting mixtures of L-(+)-tartaric acid and urea derivatives as a reaction medium. The melt played a triple role: as a solvent, as a catalyst, and as a reactant, providing highly functionalized dihydropyrimidinones in good to excellent yields. Initially, five melt systems were screened for optimization of the reaction conditions with the model reaction of 4-nitrobenzaldehyde, ethylacetoacetate, and

dimethylurea, as one of the melt components at different temperatures. It was observed that the reaction progressed fastest in L-(+)-tartaric acid-DMU melt and the corresponding DHPM was isolated in excellent yield (96%). The multicomponent reaction was extended with different aldehydes and β-ketoesters to provide the library of highly functionalized DHPMs (Scheme 9.53) [182].

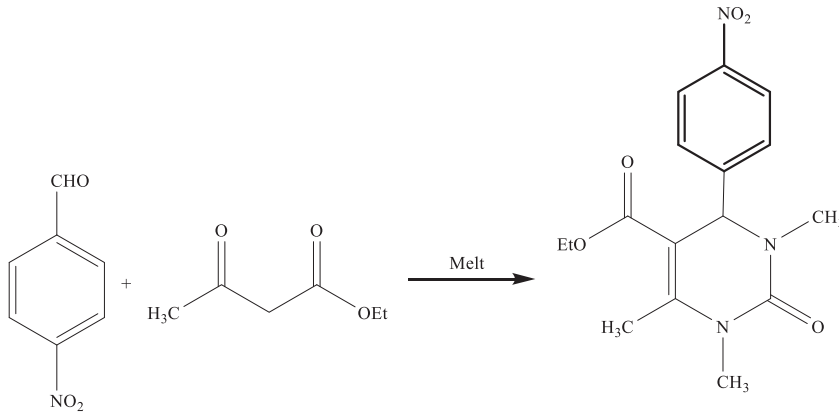

Melt: Citric acid-DMU, L-(+)-Tartaric acid-DMU, D-(−)-Fructose-DMU, Sorbitol-DMU-NH_4Cl, D-(+) Mannose-DMU

Scheme 9.53 Synthesis of dihydropyrimidinones.

Dihydropyrimidin-2(1*H*)-ones were also synthesized via one-pot three-component reaction of active methylene group containing compounds, urea/thiourea, and aldehyde using *Rhizopus oryzae* lipase biocatalyst in DES by Shukla et al. To check the feasibility of reaction and to optimize the reaction conditions, various conventional catalysts such as K_2CO_3 and t-BuOK and biocatalyst such as proline, L-histidine, and lipase were used to afford the product, but the catalytic activity of the lipase biocatalyst was found to be more effective than the other biocatalysts and conventional catalysts used in the reaction. Different organic solvents were also screened with lipase to observe their efficiency in the reaction. It was observed that the reaction progressed smoothly and in a better way in DES solvents than progressed in water, methanol, dioxane, and DMF in terms of yield of desired product and reaction time. The quantity of the lipase was also optimized and 5% w/w of lipase was found to be optimal. Under the optimized conditions, various substituted aromatic aldehydes were reacted to obtain the corresponding products. The reported synthetic protocol was characterized by high efficiency and selectivity with short reaction time and environmentally friendly reaction conditions. The yields were found to be significantly higher and the reuse of both lipase and DES was possible up to four consecutive cycles. The products were found to exhibit appreciable in vitro antibacterial activity against *Escherichia coli*, *Pseudomonas neumoniae*, and in vitro antifungal activity against *Aspergillus niger* and *Candida albicans* (Scheme 9.54) [183].

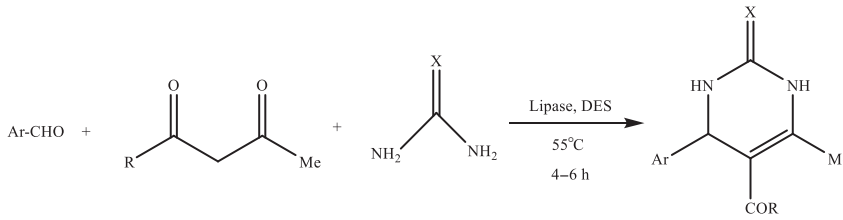

R = Me, OEt
X = O & S
ArCHO = 6-methoxy-2-naphthaldehyde, 9-ethyl-9*H*-fluorene-3-carbaldehyde, 4,4'-(phenylazanediyl)dibenzaldehyde 4,4'-((6l^3-hexyl)azanediyl)dibenzaldehyde

Scheme 9.54 Synthesis of DHPMs.

9.2.1.20 Synthesis of triazolopyrimidines

Martins et al. reported the synthesis of a methylthiotriazolo[1,5-*a*]pyrimidines involving the reaction between 4-dimethylamino-1-phenyl-3-buten-2-one and 3-amino-5-methylthio-1*H*-1,2,4-triazole in the presence of choline chloride-based DES (Scheme 9.55) [184]. The reaction conditions were optimized and the best results were reported with ChCl:TsOH (1:2 ratio).

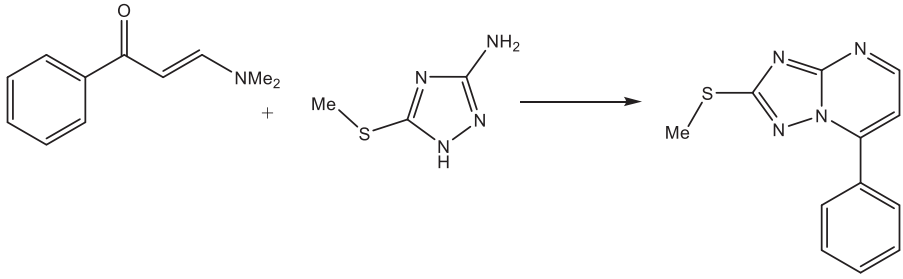

Scheme 9.55 Synthesis of a methylthiotriazolo[1,5-*a*]pyrimidines.

9.2.1.21 Synthesis of pyridopyrimidines

Pyrido[2,3-*d*]pyrimidines are the privileged motifs present in the medicinally significant compounds with diverse bioactivity effects [185]. Palbociclib [186] with pyridopyrimidine skeleton plays a key role in regulating the G1- to S-cell-cycle transition phase via regulation of phosphorylation of the retinoblastoma (Rb) protein (Fig. 9.13A). Also, voxtalisib [187] has been used extensively in clinical trials in order to treat cancer, melanoma, lymphoma, glioblastoma, and breast cancer (Fig. 9.13B). Partially saturated pyrido[2,3-*d*]pyrimidine derivatives (Fig. 9.13C) have

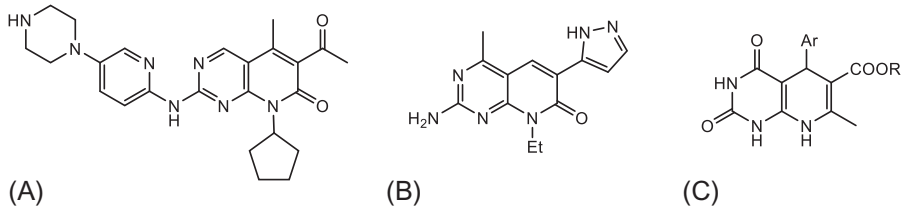

Fig. 9.13 Medicinally important pyrido[2,3-*d*]pyrimidines. (A) Palbociclib, (B) Voxtalisib, (C) Pyrido[2,3-d]pyrimidines.

been reported for calcium channel blocking effects [188]. Pyridopyrimidines have also been reported recently to exhibit anticancer activity [189], HCV NS5A inhibition [190], highly selective inhibition of protein tyrosine phosphatase 1B [191], antiproliferative inhibition of CDK2 [192], and mTOR kinase inhibition [193].

Aryan et al. reported the synthesis of highly substituted pyrido[2,3-*d*]pyrimidines involving the reaction of 4-chlorobenzaldehyde, malononitrile, and 4(6)-aminouracil in the presence of DESs as reaction media and promoters [194] (Scheme 9.56).

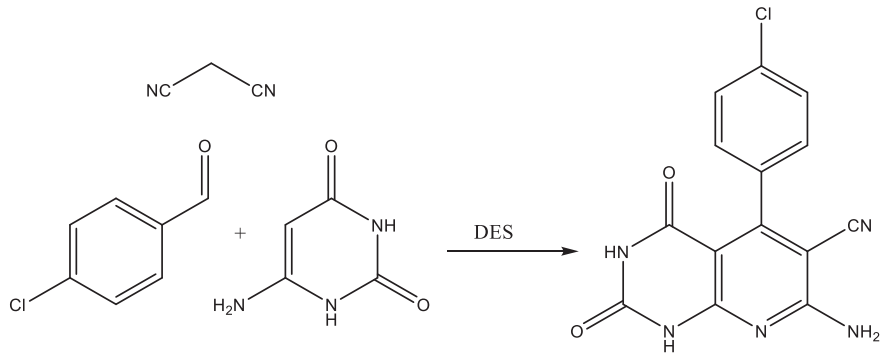

Scheme 9.56 DES catalyzed synthesis of pyrido[2,3-*d*]pyrimidines.

The authors reported choline chloride/urea (1:2) mixture as the best DES in terms of product yields and reaction times without using any extra oxidant and/or catalyst.

9.2.1.22 Synthesis of pyrimidopyrimidinediones

Fused pyrimidine systems, particularly, pyrimidopyrimidine (Fig. 9.14), have attracted the increasing interest of synthetic and medicinal research and reported to exhibit wide-ranging potential biological activities and inhibitory action regarding the tyrosine kinase domain of epidermal growth factor receptor [195], 5-phosphoribosyl-1-pyrophosphate synthetase [196], and dihydrofolate-reductase [197].

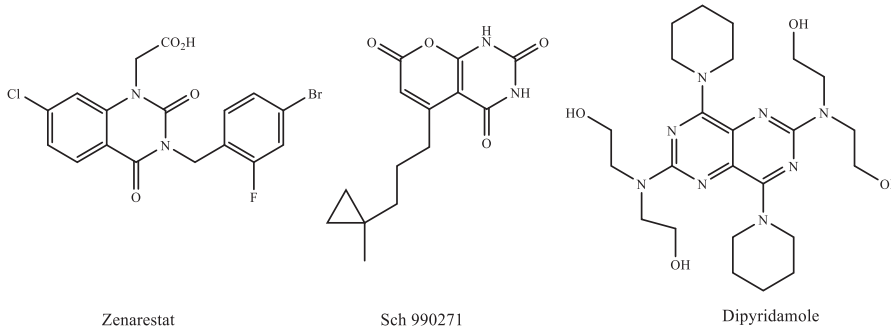

Fig. 9.14 Bioactive fused pyrimidine derivative.

Koenig et al. synthesized pyrimidopyrimidinediones, six-membered analogs of glycoluril, by the reaction of acetophenone derivatives and paraformaldehyde using low melting L-(+)-tartaric acid-dimethyl urea mixture as reaction medium. In the reaction, the melt acted not only as the solvent but at the same time acted also as a catalyst and reactant. In order to improve the efficiency of the synthesis, initially, the reaction was carried out under various melt conditions. It was observed that in the case of L-(+)-tartaric acid-DMU melt (tartaric acid: pKa = 2.95), the reaction provided the corresponding pyrimidopyrimidinedione in excellent yield (90°C, 7 h, 95%) and indicated the catalytic role of an acidic component in DES. The reaction with optimal conditions was extended with different aryl ketones and obtained the products in good to excellent yields (79%–96%) (Scheme 9.57) [198].

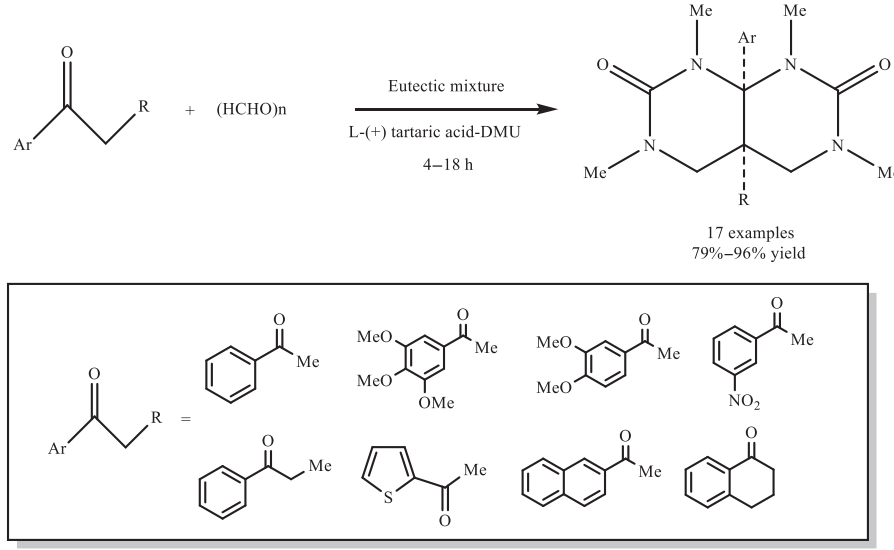

Scheme 9.57 Synthesis of pyrimidopyrimidinediones.

9.2.1.23 Synthesis of chromenothiazolopyrimidinones

Chromene fused derivatives constitute an important class of heterocyclic compounds because of their incorporation in pharmaceuticals and agrochemicals [199]. Chromene scaffolds with thiazolopyrimidine moiety have also been reported to exhibit wide spectrum of activity [200] including anticancer [201], antituberculotic [202], antimicrobial [203], antiinflammatory [204], and analgesic [205], insecticidal [206], herbicidal [207], antioxidant [208], acetylcholinesterase inhibitors [209], antimalarial [210], anti-HIV [211], etc.

Reddy et al. reported the synthesis of chromeno fused thiazolopyrimidines [212], but these methods suffered from some limitations such as the use of expensive reagents and solvents, longer reaction time, and lower selectivity of catalyst, environmental hazards, and the problem relating to catalyst reusability. In view of significance of DES as eco-friendly and bio-renewable solvents, DES consisting of glycerol and proline with proportion (1:1) was prepared and used as a reaction promoting medium for the synthesis of chromeno[4,3-*d*]thiazolo[3,2-*a*]pyrimidinones involving the reaction of 4-hydroxycoumarin, 4-chlorobenzaldehyde, and 2-amino-5-methylthiazole using different reaction conditions. The reaction conditions were optimized with the use of a variety of polar and nonpolar solvents including DES and observed that glycerol:proline (1:1) provided the better yield of the product (Scheme 9.58) [213].

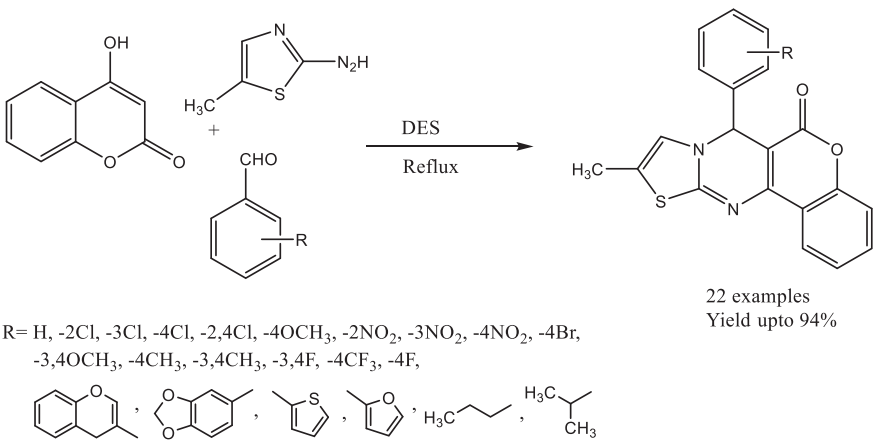

Scheme 9.58 DES mediated synthesis of chromeno[4,3-*d*]thiazolo[3,2-*a*]pyrimidines.

The proposed mechanism for the synthesis of 7-(aryl)-10-methyl-6*H*,7*H*-chromeno[4,3-*d*]thiazolo[3,2-*a*]pyrimidin-6-ones is presented in Scheme 9.59. The reaction is considered to proceed through a sequence of reactions involving Knoevenagel condensation-aza Michael addition-intramolecular cyclization-dehydration to provide the desired product. The catalyst increases the electrophilicity of the carbonyl groups in the reaction and the recycled DES was successively reused for the next reactions without any appreciable loss in catalytic efficiency.

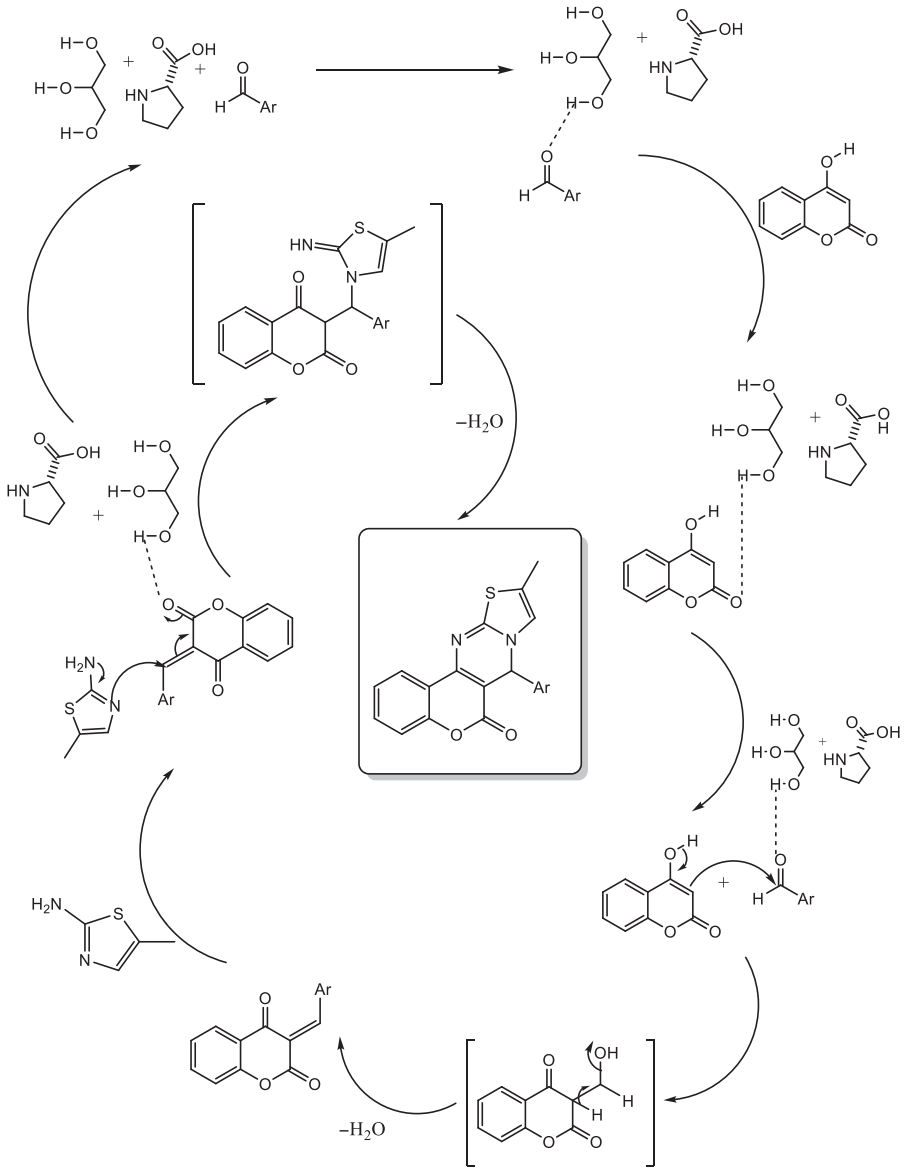

Scheme 9.59 Mechanistic pathway of 7-(aryl)-10-methyl-6*H*,7*H*-chromeno[4,3-*d*]thiazolo [3,2-*a*]pyrimidin-6-ones.

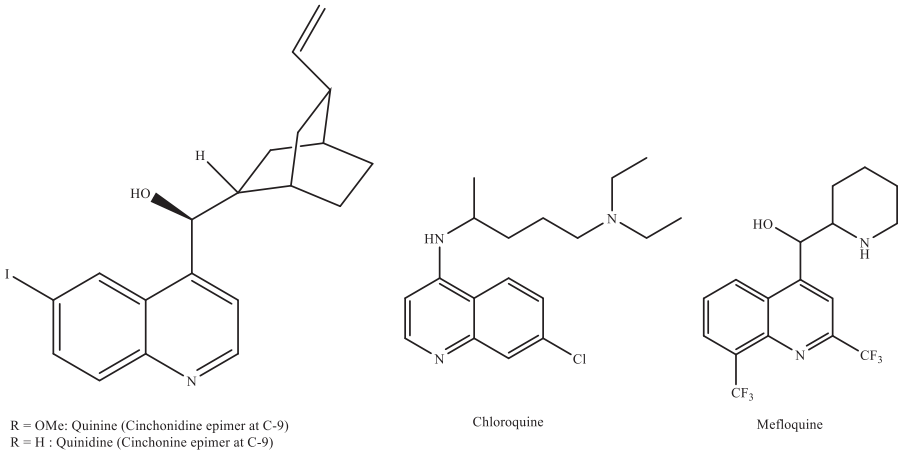

Fig. 9.15 Natural products incorporating quinoline moiety.

9.2.1.24 *Synthesis of quinoline derivatives*

The quinoline ring system is present in many naturally occurring alkaloids, therapeutics, and synthetic analogs with interesting biological activities [214] (Fig. 9.15). Quinoline derivatives have received much attention in view of their broad range of bioactivities such as antiviral [215], antimalarial [216], antibacterial [217], anticancer [218], antifungals [219], antiinflammatory [220], and antihypertensive [221] activities. Quinolines find their applications in the formation of conjugated molecules and polymers [222]. These materials combined enhanced electronic, optoelectronic, or nonlinear optical properties with excellent mechanical properties [223]. Quinoline derivatives have also been used in the synthesis of fungicides, biocides, and flavoring agents [224]. Furthermore, these compounds are useful in the chemistry of transition metal catalysts, uniform polymerization, and luminescence chemistry [225], in addition to their applications as antifoaming agents in refineries [226].

Biologically important quinoline derivatives were synthesized by Zhang et al. via the Friedländer heteroannulation reaction of 2-aminoaryl ketones and α-methylene ketones using low melting mixtures of L-(+)-tartaric acid and urea derivatives as an inexpensive, nontoxic, easily biodegradable reaction medium. The melt acts as both the reaction medium and catalyst, providing quinolines in high to excellent yields (Scheme 9.60) [227].

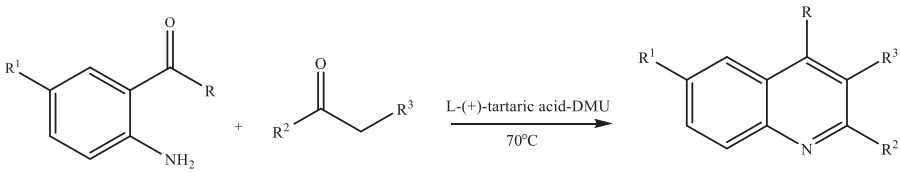

Scheme 9.60 Synthesis of quinoline derivatives.

Tavakol and Shahabi synthesized quinolines involving one-pot, three-component reaction of anilines, aromatic aldehydes and enolizable aldehydes using choline chloride/tin(II)

chloride ($ChCl{\cdot}2SnCl_2$) DES. In the reaction, DES plays both roles of solvent and catalyst as presented in the proposed mechanism (Schemes 9.61 and 9.62) [228].

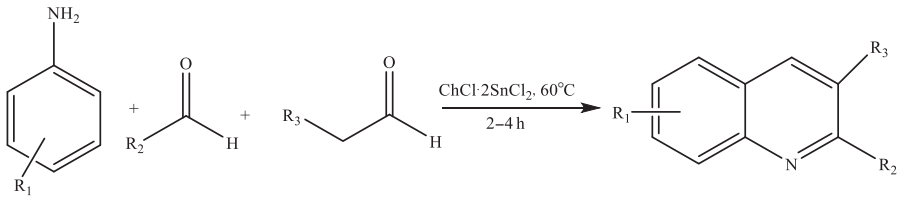

Scheme 9.61 Synthesis of quinoline derivatives.

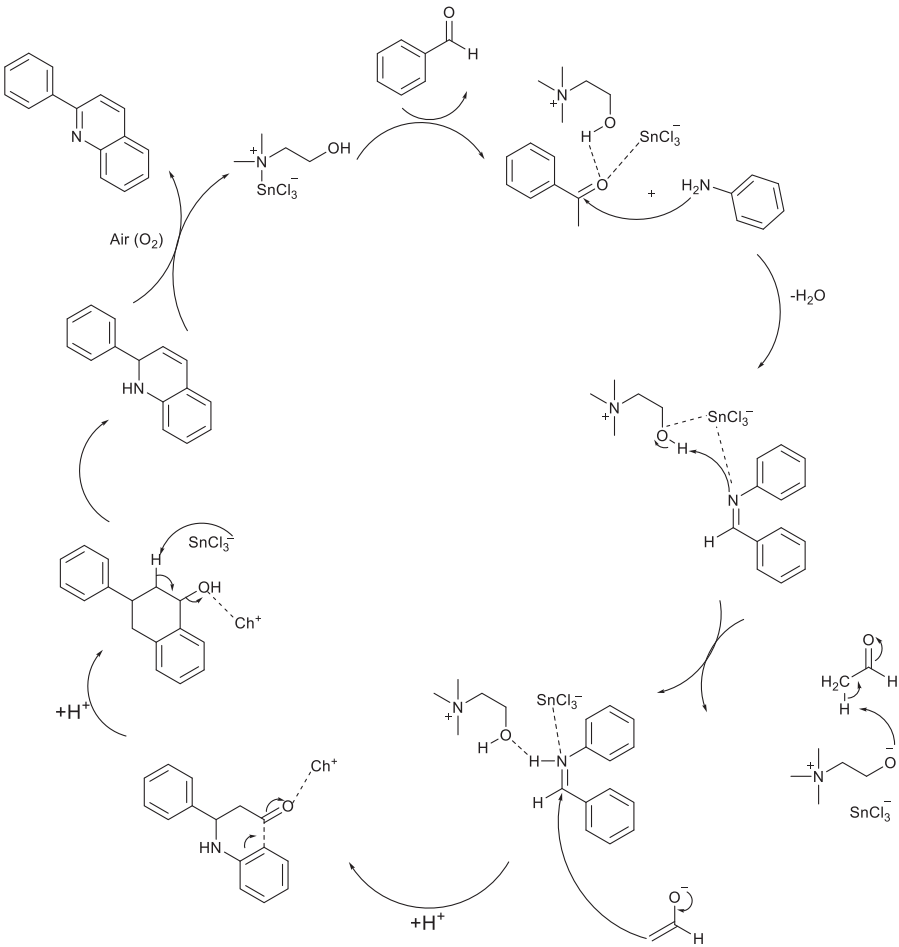

Scheme 9.62 Proposed mechanism of quinoline derivatives.

9.2.1.25 Synthesis of quinazolines

Quinazoline is one of the privileged nitrogen heterocycles commonly found in a wide variety of natural products, pharmaceutical molecules, and functional materials [229]. Quinazoline derivatives have been reported to possess diverse biological and therapeutic properties such as antibacterial, antiinflammatory, antiplasmodial, antitumor, antimicrobial, and antioxidant [230]. In addition, they have also been used as photochemotherapeutic agents, DNA-gyrase, JAK2, PDE5, and EGFR tyrosine kinase inhibitors, as well as CB2 receptor agonists [231].

Certain quinazolinones marketed as drugs, like methaqualone (quaalude), mebroqualone, mecloqulaone (Casfen) possess sedative, hypnotic, and anxiolytic properties and are used for the treatment of insomnia. In 2011, Wang and Che group isolated two alkaloids, penipanoid C, and 2-(4-hydroxybenzyl)quinazolin-4(3*H*)-one from the marine sediment-derived fungus *Penicillium paneum* SD-44 that exhibits cytotoxicity against the human lung carcinoma cell line A549 and BEL-7402 cell lines with IC50 values of 17.5 and 19.8 μM, respectively [232]. Due to this undeniable impression of quinazolinone alkaloids over pharmacological industry, there is a continuous interest among the researchers to develop new methods for synthesis of quinazolinone core.

In recent years, low melting mixtures consisting of carbohydrates, urea, and inorganic salts have been introduced as new alternative sustainable solvents for organic transformations. Zhang et al. employed a low melting mixture of maltose-dimethylurea (DMU)-NH_4Cl as an inexpensive, nontoxic, easily biodegradable and effective reaction medium in the catalyst-free synthesis of quinazoline derivatives. The screening of solvent was performed on model reaction of 2-aminobenzophenone with 4-nitrobenzaldehyde and ammonium acetate in different solvents under aerobic oxidation conditions. Only a trace amount of product was detected when the reactions were carried out in EtOH or H_2O. Poor to low yields were observed when the reactions proceeded in CH_3CN, DMF, DMSO, toluene, or in neat conditions. The reaction conditions were optimized with the screening of the various DESs such as citric acid-DMU, D-(−)-fructose-DMU, L-(+)-tartaric acid-DMU, L-(+)-tartaric acid-choline chloride, mannose-DMU-NH_4Cl, lactose-DMU-NH_4Cl, and maltose-DMU-NH_4Cl at their minimal melting temperature. The reaction progressed smoothly in these melt mixtures, and the corresponding product was obtained in 75%–92% yields. Further investigation of this reaction was achieved by using these melt mixtures at 90°C. At this temperature, Maltose-DMU-NH_4Cl was found to be superior to other melts and provided 93% yield of the product.

The optimized synthetic protocol was extended with a wide range of 2-aminoaryl ketones and aldehydes under aerobic oxidation conditions and products were obtained in good to excellent yields with operational simplicity and mild reaction conditions (Scheme 9.63) [233].

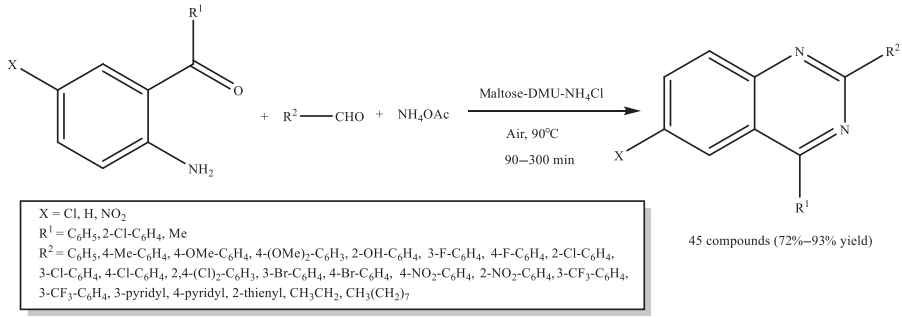

Scheme 9.63 Synthesis of quinazolines.

2,3-Dihydroquinazolinones possess a wide range of biological and pharmaceutical activities [234]. Some examples of very significant quinazolinone molecules include medicinally approved drugs like metolazone, quinethazone, raltitrexed, fenquizone as well as bioactive natural products such as febrifugine and isofebrifugine (Fig. 9.16) [235].

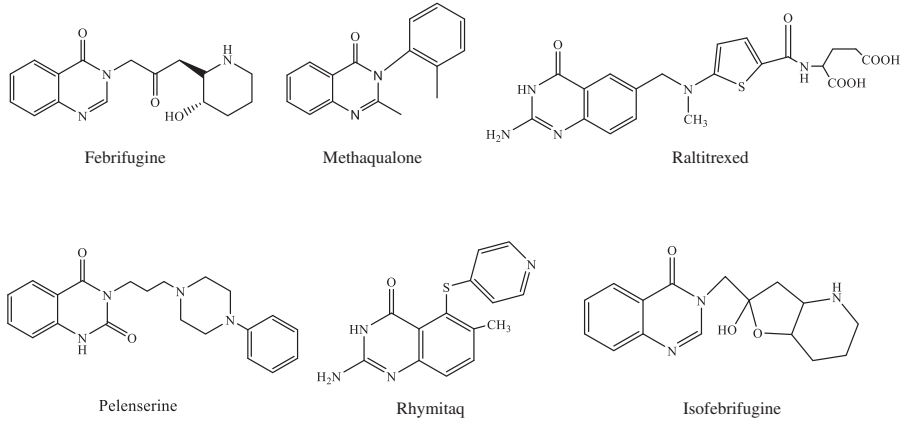

Fig. 9.16 Bioactive dihydroquinazolinone derivatives.

2,3-Dihydroquinazolin-4(1*H*)-ones were synthesized via one-pot multicomponent reaction of isatoic anhydride, aldehyde, and aromatic amines by Shankarling et al. using DES (choline chloride:malonic acid) in methanol. Initially, various deep eutectic mixtures were screened as catalysts in methanolic media to derive the best outcome. The DESs generated from glycerol or urea provided very poor yields due to their lower acidity than DES consisting of acidic components. However, the eutectic mixture of choline chloride: malonic acid provided the best results among all other eutectic mixtures and 20% (v/v) of DES catalyst in methanol was suggested the optimum quantity for effective results. Moreover, such eutectic mixtures are

cost-effective, recyclable, nontoxic, and biodegradable. The reaction was extended with a variety of aromatic as well as heteroaromatic aldehydes and amines to provide 2,3-dihydroquinazolin-4(1*H*)-one derivatives (Scheme 9.64) [236].

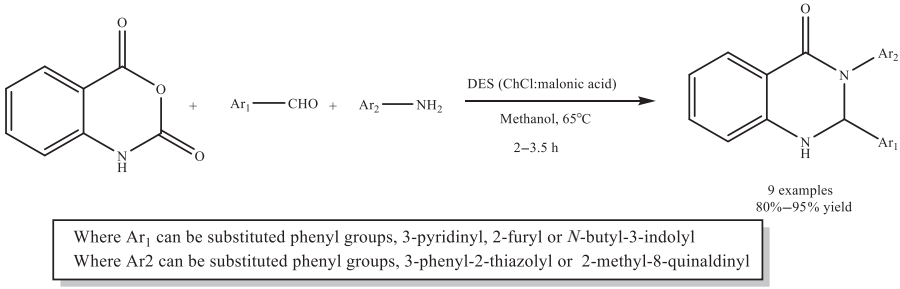

Scheme 9.64 Synthesis of quinazolinones.

Nagarajan and Ghosh synthesized substituted quinazolinones and dihydroquinazolinones involving DES mediated cyclization with a series of aliphatic, aromatic, heteroaromatic aldehydes. Initially, few of the DESs mixture like, citric acid-*N*,-*N*′-Dimethylurea (DMU), D-(−)-fructose DMU, L-(+)-tartaric acid-DMU, and mannose-DMU-NH_4Cl were screened for the synthesis of 2-(*o*-tolyl)quinazolin-4 (3*H*)-one with model substrates anthranilamide (1.0 equiv.) and *o*-tolualdehyde (1.2 equiv). Among them, L-(+)-tartaric acid-DMU (3:7) mixture melt at 90°C was found to be the most effective to give the maximum yield of the desired compound. The reaction was carried out in an open-air atmosphere to aromatize the initially formed dihydroquinazolinone to quinazolinone product via aerobic oxidation. A variety of aldehydes (aromatic, aliphatic, and heterocyclic) were exposed to these conditions with substituted/unsubstituted anthranilamides and corresponding dihydroquinazolinones/quinazolinones were obtained depending on the time of the reaction (Scheme 9.65) [237].

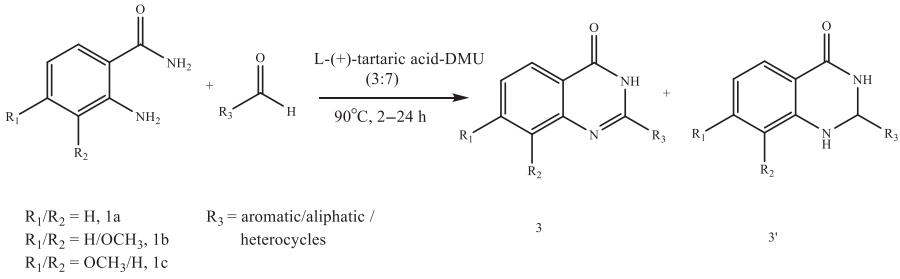

Scheme 9.65 Synthesis of quinazolinones and dihydroquinazolinones.

Effects of electron-donating and electron-withdrawing substituents were also observed on the yield of the products. Further, the present DES-mediated protocol was also applied for synthesizing indoloquinazoline alkaloids such as bouchardatine and schizocommunin (Scheme 9.66).

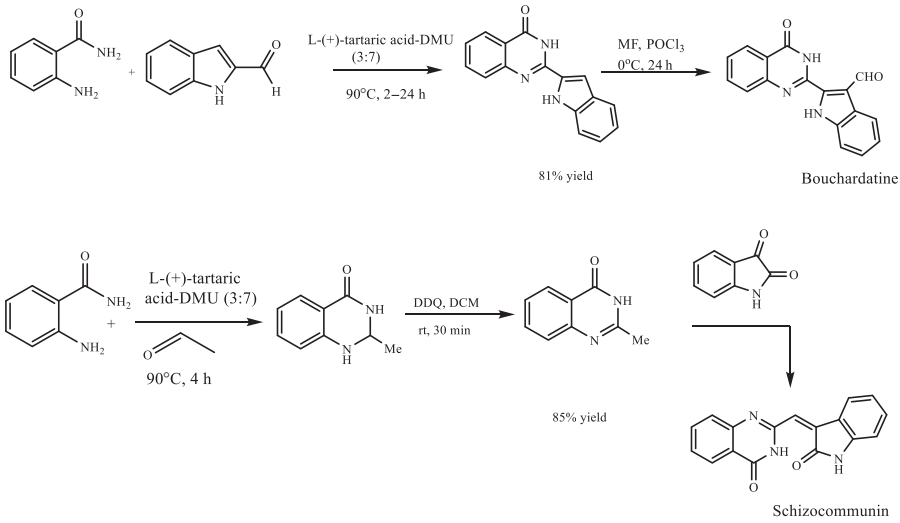

Scheme 9.66 Synthesis of bouchardatine and schizocommunin, indoloquinazoline alkaloids.

2,2-Disubstitued quinazolinones with wide spectrum of pharmacological activities were also synthesized by the reaction of ketones (aliphatic-aliphatic, aliphatic-aromatic, aromatic-aromatic, cyclic ketones, and isatin) with anthranilamide at 90°C in the presence DES (Scheme 9.67).

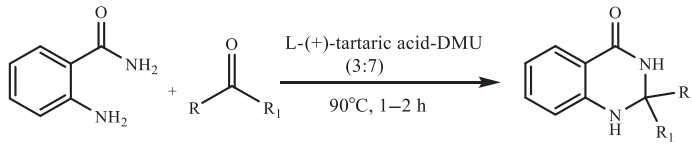

Scheme 9.67 Synthesis of 2,2′-disubstitued quinazolinone derivatives.

This protocol was also successfully applied for the synthesis of 2,3-disubstitued quinazolinones which have numerous pharmacological properties. Penipanoid C, a quinazoline alkaloid shows moderate inhibitory activity against tobacco mosaic virus (TMV) and human gastric cancer cell SGC-7901. Similarly, 2-(4-hydroxybenzyl) quinazolin-4(3*H*)-one alkaloid, reported for its significant cytotoxic activity against the A-549 and BEL-7402 cell lines cell with IC50 values of 17.5 and 19.8 μM, also

exhibits strong inhibitory activity on the replication of TMV. Hence, synthesis of these natural quinazoline alkaloids is very fascinating due to their low abundance and wide biological spectrum.

Nagarajan and Ghosh also reported synthesis of penipanoid C, 2-(4-hydroxybenzyl)quinazolin-4(3*H*)-one and NU1025 drug by using DES mixture. Initially, 2-(4-(benzyloxy)phenyl)acetaldehyde was reacted with anthranilamide in the presence of L-(+)-tartaric acid-DMU mixture (3:7) at 90°C and corresponding dihydroquinazolinone was obtained in 80% yield. Further, aromatization of dihydroquinazolinone was carried out in DDQ/DCM and corresponding aromatized product 2-(4-(benzyloxy)benzyl)quinazolin-4(3*H*)-one was obtained in 82% yield. The benzylic oxidation was achieved with KBr/Oxone in DCM-$MeNO_2$ solvent. Next, the deprotection of the benzyl group with H_2 on Pd/C and again reoxidation of hydroxyl group in presence of pyridinium chlorochromate (PCC) in DCM provided penipanoid C in 85% yield (Schemes 9.68 and 9.69) [238].

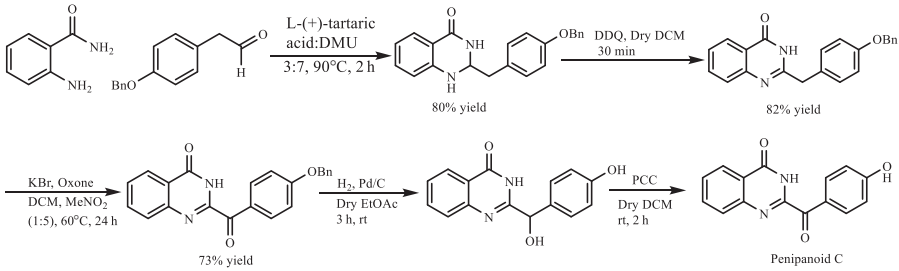

Scheme 9.68 Synthesis of penipanoid C.

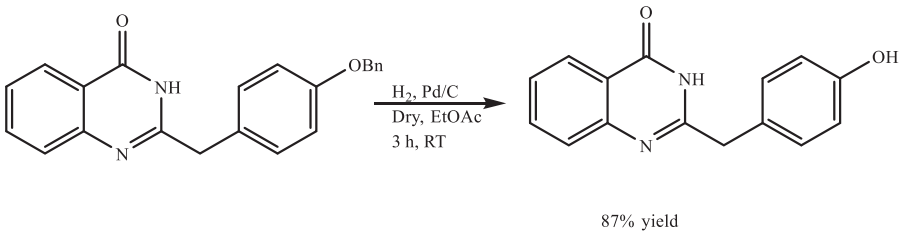

Scheme 9.69 Synthesis of 2-(4-hydroxybenzyl)quinazolin-4(3*H*)-one.

Similarly, for the synthesis of NU1025 2-(4-hydroxybenzyl)quinazolin-4(3*H*)-one, initially, 2-amino-3-methoxybenzamide was synthesized from 3-methoxy-2-aminobenzoic acid via two-step process which on treatment with acetaldehyde solution in low melting mixtures at 90°C provided 8-methoxy-2-methyl-2,-3-dihydroquinazolin-4(1*H*)-one which further aromatized to quinazolinone with 10% Pd/C at rt. Deprotection of the methoxy group by BBr_3 in dry DCM provided NU1025 in 73% yield (Scheme 9.70).

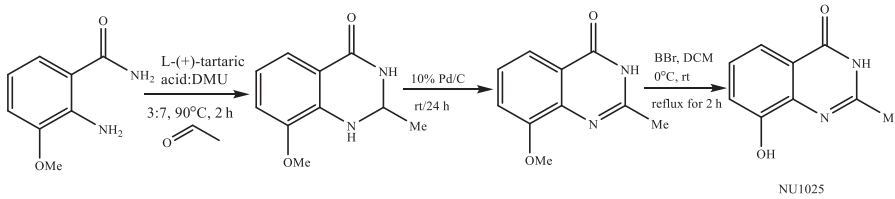

Scheme 9.70 Synthesis of NU1025.

9.2.1.26 Synthesis of acridines

Acridines constitute an important class of bioactive heterocycles and present in bioactive natural products and synthetic dye-stuffs [239] with their applications as pharmaceuticals, optical materials, and sensors [240]. Furthermore, acridines have been reported to exhibit antibacterial [241], antimalarial [242], antifungal [243], antitumor [244], anticancer [245], cytotoxic [246], and antimultidrug-resistant properties (Fig. 9.17) [247].

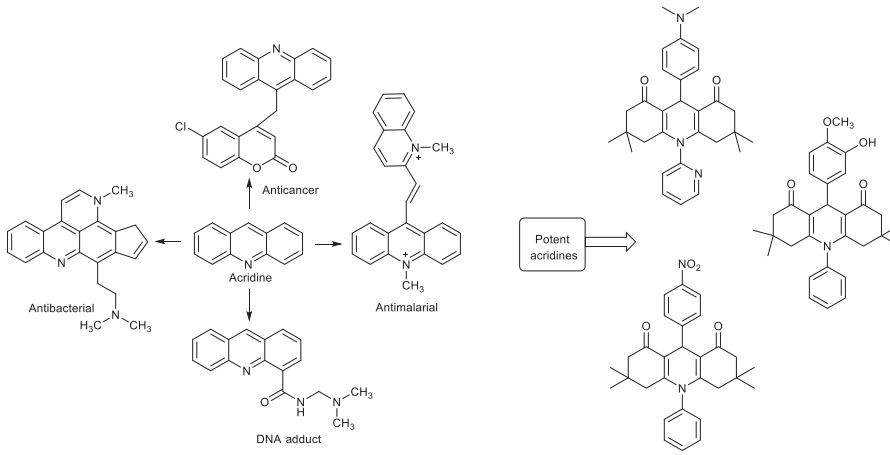

Fig. 9.17 Bioactive acridines.

There are various reports in the literature for three-component Hantzsch-type synthesis of acridines involving condensation of aromatic aldehydes, anilines, and dimedone via the conventional methods [248], under MW irradiation [249], and using catalysts, for example, *p*-toluenesulfonic acid [250], *p*-dodecylbenzenesulfonic acid [251], ceric ammonium nitrate [252] (CAN), $InCl_3$-IL [253], montmorillonite [254], Fe_3O_4@SiO_2-MoO_3H nanoparticles [255], silica-bonded *N*-propyl sulfamic

acid (SBNPSA) [256], amberlyst-15 [257], benzyltriethylammonium chloride (TEBAC) [258], etc. However, many of these methods suffered some limitations.

Bhosle et al. synthesized *N*-substituted decahydroacridine-1,8-diones involving three-component reaction between aromatic aldehydes, dimedone, and aromatic amines in the presence of ChCl:urea DES as a recyclable organocatalyst and reaction medium (Scheme 9.71) [259].

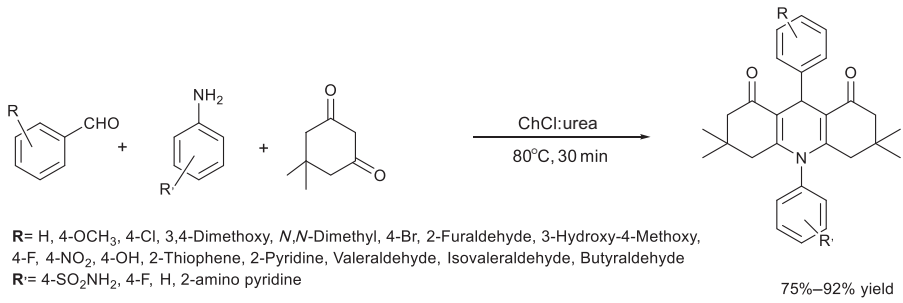

Scheme 9.71 Synthesis of acridinones.

This reaction was examined in different catalysts such as CAN, p-TSA, acetic acid, *N*-methyl pyridinium tosylate, DIPEAc, dicationinic IL, ChCl:2glycerol and ChCl:urea but best results were obtained with ChCl:urea. Probably, hydrogen bonding and the Brønsted basicity of urea are the main factors that influence the reactivity and selectivity of the process. Moreover, it was also observed that aromatic and heteroaromatic aldehydes-containing electron-donating, electron-withdrawing, and halogen substituents provided excellent yields of acridinones.

The proposed mechanism of ChCl:urea catalyzed reaction is presented in Scheme 9.72. The reaction is considered to proceed with Knoevenagel condensation—Micheal-type addition and dehydrative cyclization to produce *N*-substituted decahydroacridine-1,8-dione derivatives.

9.2.1.27 Synthesis of naphthyridines

Functionalized naphthyridines and their benzo/heterofused analogs are present in numerous marine products and reported to possess wide-ranging activities such as antiproliferative [260], antiaggressive [261], and HIV-1 integrase inhibition [262] in addition to their use as anti-HCV agents [263] (Fig. 9.18).

Shaabani et al. synthesized naphthyridines involving domino four-component reaction of diamine, 1,1-bis(methylthio)-2-nitroethylene, 2-aminoprop-1-ene-1,1,3-tricarbonitrile, and carbonyl compounds using DES, choline chloride/urea (Scheme 9.73). The reaction conditions were optimized with different bases in ethanol including DES (choline chloride/urea) solvents on model reaction and observed that the use of choline chloride/urea as DES provided excellent results [264].

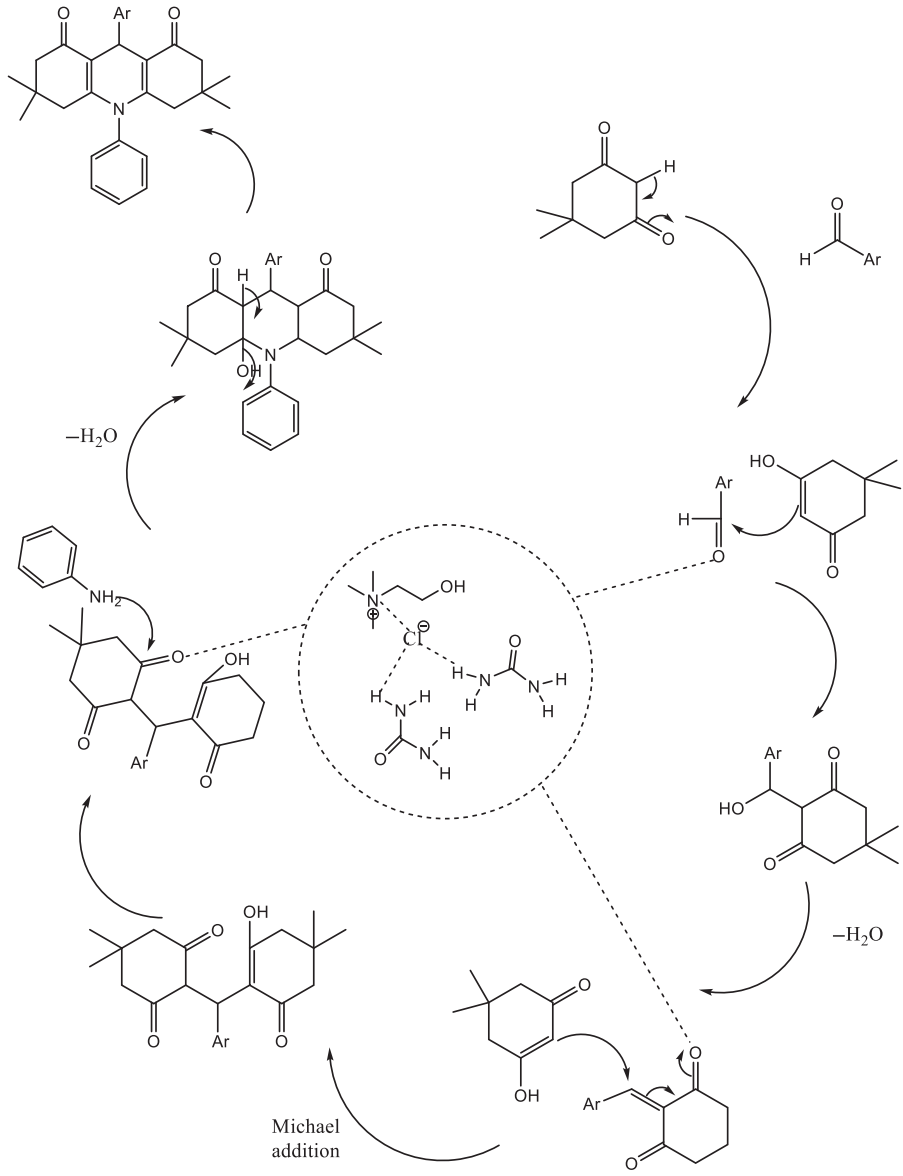

Scheme 9.72 Plausible mechanism for the synthesis of *N*-substituted-1,8-dioxo-decahydroacridines.

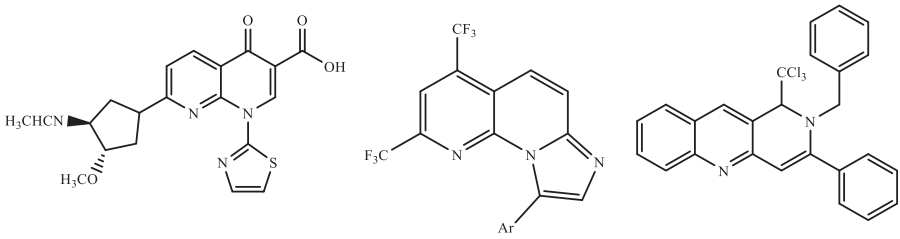

Fig. 9.18 Biologically active compounds with naphthyridine scaffold.

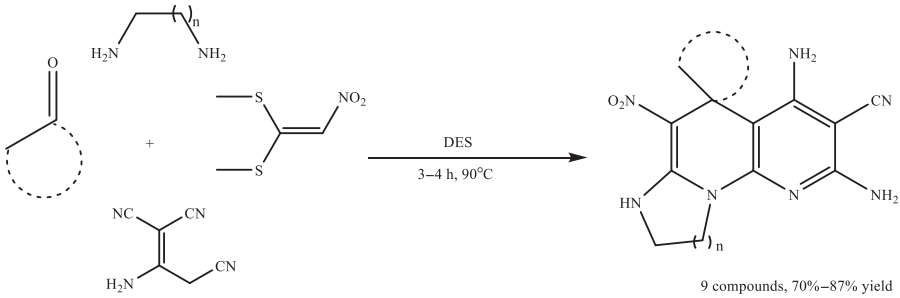

Scheme 9.73 Synthesis of 1,8-naphthyridines derivatives via a domino four-component reaction in ChCl/urea.

The proposed mechanism of the reaction is presented in Scheme 9.74.

The reaction was extended with various diamines and carbonyl compounds which included various benzaldehyde derivatives, isatins, ninhydrin, and naphthyl-2-carbaldehyde to synthesize naphthyridines.

9.2.1.28 Synthesis of pyran derivatives

The pyran is an important pharmacophore and incorporated in the bioactive compounds with antitumor, antibiotic, antibacterial, antiallergic, hypolipidemic, and immunomodulating activities [265]. Furthermore, the substitution of the hydrogen atom of pyran with an amino or cyano group makes these compounds as synthons for natural products [266] (Fig. 9.19).

Azizi et al. presented an eco-friendly one-pot multicomponent synthetic protocol involving the reaction of 1,3-dicarbonyl compounds, aldehydes, and malononitrile in DES based on choline chloride, to synthesize highly functionalized benzopyran and pyran derivatives under catalyst-free conditions. To check the feasibility of reaction and to optimize the reaction conditions, various conventional solvents and ChCl-based DESs were screened on the model reaction of benzaldehyde, malononitrile, and dimedone. The effect of temperature was also screened on the efficiency of ChCl:urea DES. After screening different solvents with reaction conditions, the

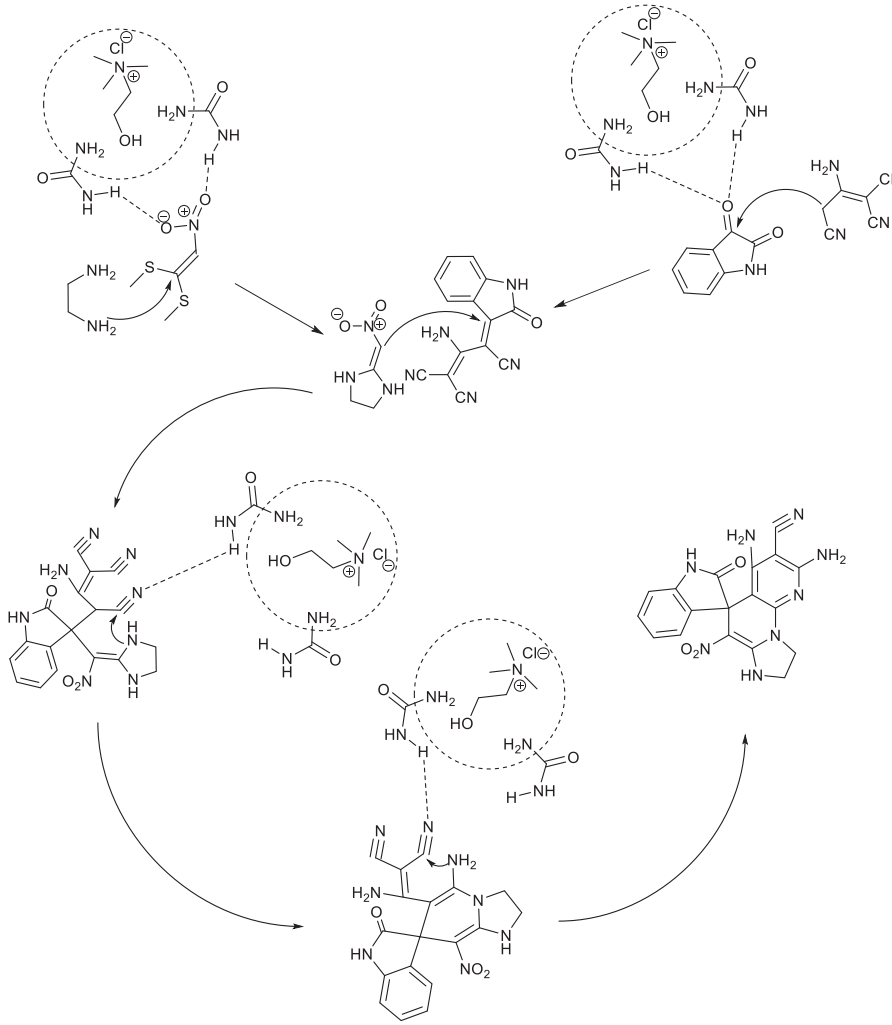

Scheme 9.74 Proposed reaction mechanism for the synthesis of 1,8-naphthyridines.

DES, ChCl:urea, at 80°C showed superiority over other solvent systems as the desired product was obtained within 60 min with excellent yield (95%). The DES, urea:choline chloride, was considered the best solvent and applied successfully to a wide range of aldehydes and active methylene compounds. The products were obtained with high yields (75%–95%) in short reaction times (1–4 h). The present method offers the advantages of catalyst-free reaction, easy purification, short reaction time, and high yield (Scheme 9.75) [267].

The proposed mechanism involves the catalytic role of DES in the synthesis of pyran derivatives. The reversible hydrogen bonding between urea and carbonyl

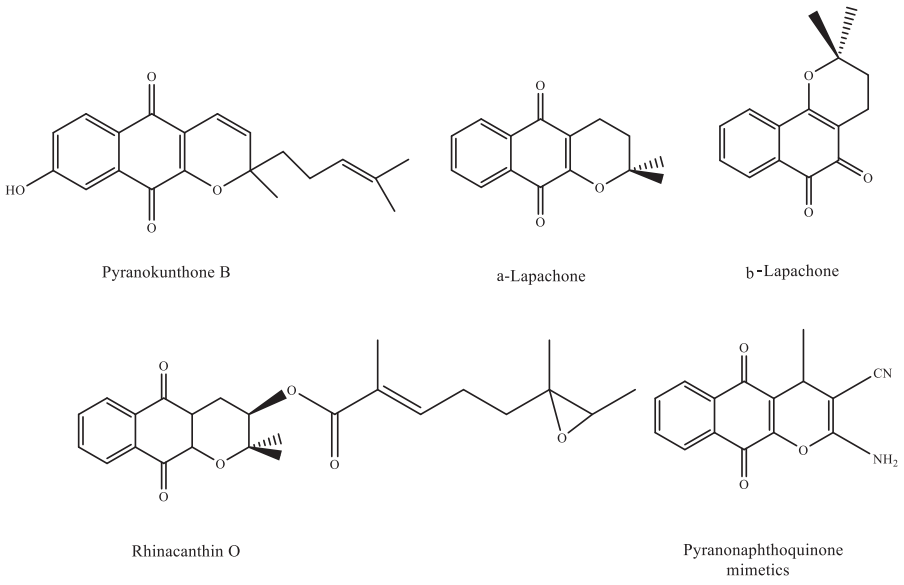

Fig. 9.19 Biologically active pyran derivatives.

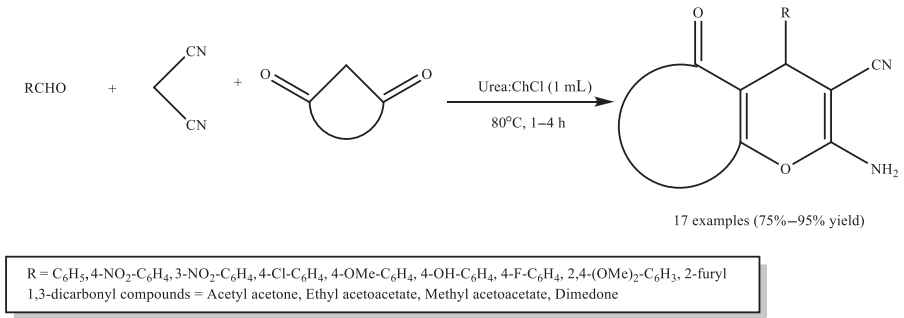

Scheme 9.75 Synthesis of pyran and benzopyran derivatives.

groups giving substrate-solvent complex-activated aldehydes. The initial condensation of carbonyl groups with activated malononitrile with urea in the DES leads to the formation of arylidene malononitrile with the loss of a water molecule. The nucleophilic addition of the enolizable ketone to arylidene malononitrile followed by intramolecular cyclization provided 4*H*-pyran derivatives (Scheme 9.76).

*9.2.1.29 Synthesis of 4*H*-chromenes*

Chromenes or benzopyrans constitute an important class of heterocycles with their pharmaceutical activities such as spasmolytic, diuretic, antiviral, antitumoral, and antianaphylactic, among others [268]. Furthermore, the chromene skeleton is present

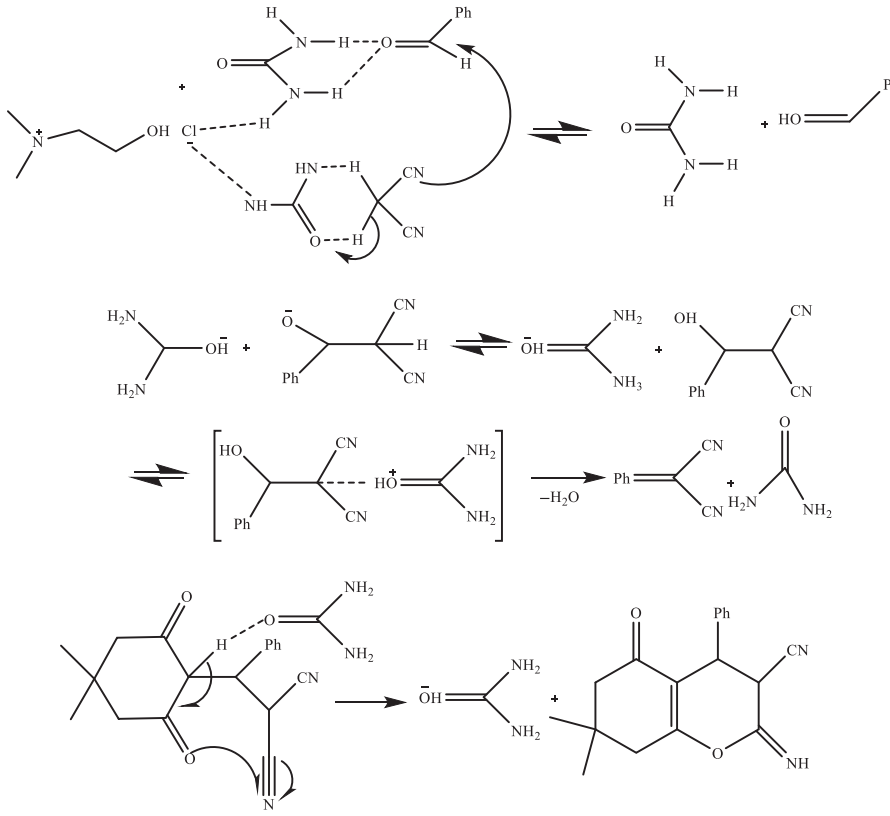

Scheme 9.76 Proposed reaction mechanism.

in numerous natural products used as pigments, photoactive compounds, and biodegradable agrochemicals [269] (Fig. 9.20).

In view of wide-ranging properties of chromenes, considerable efforts have been diverted to develop synthetic methods of chromenes. Azizi et al. presented a facile, atom-economic, and environmentally benign one-pot synthetic protocol involving the reaction of salicylaldehyde and malononitrile with various nucleophiles, including indoles, thiols, secondary amines, cyanide, and azide in choline chloride-based DES. In this protocol, the formation of the products depend on the nature of the nucleophile used in the reaction. The reaction of salicylaldehyde derivatives and malononitrile with thiols, indoles, and cyanide gave 2-amino-3-cyano-4*H*-chromene derivatives. But the use of secondary amines in the reaction provided benzopyrano[2,3-*d*]pyrimidines due to further reaction of salicylaldehyde with 4*H*-chromene under the reaction conditions. The DES was recycled and reused without any appreciable reduction in activity or yield [270] (Scheme 9.77).

2-Aminochromenes are present as the main components of many naturally occurring products employed as cosmetics and pigments [271] and utilized as potential

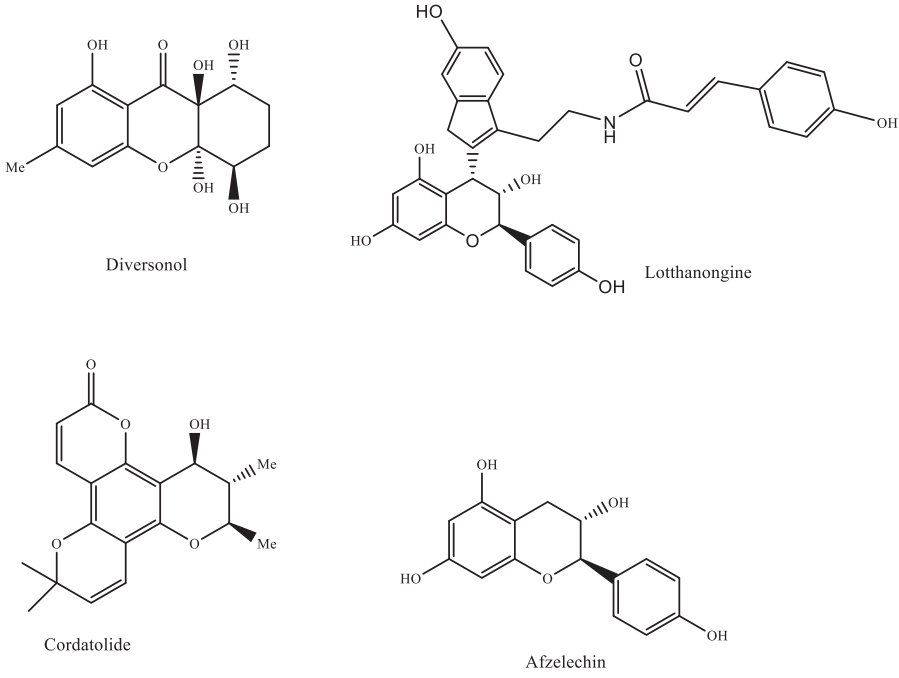

Fig. 9.20 Natural products with chromene skeleton.

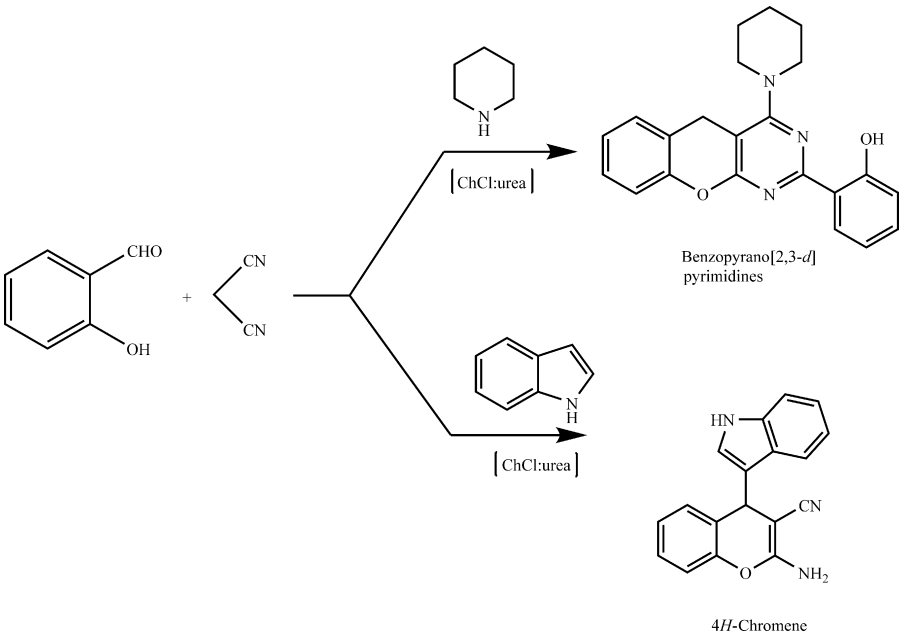

Scheme 9.77 Synthesis of 4*H*-chromenes and benzopyrano[2,3-*d*]pyrimidines.

biodegradable agrochemicals [272]. Multifunctional 2-aminochromenes were synthesized by Chaskar et al. in aqueous medium at room temperature using a deep eutectic mixture of choline chloride: urea. In the reaction benzylidenemalononitrile formed by Knoevenagel condensation of aldehyde and malononitrile eventually underwent Michael-type addition-cyclization with dimedone and provided the chromenes in good to excellent yields (Scheme 9.78) [273].

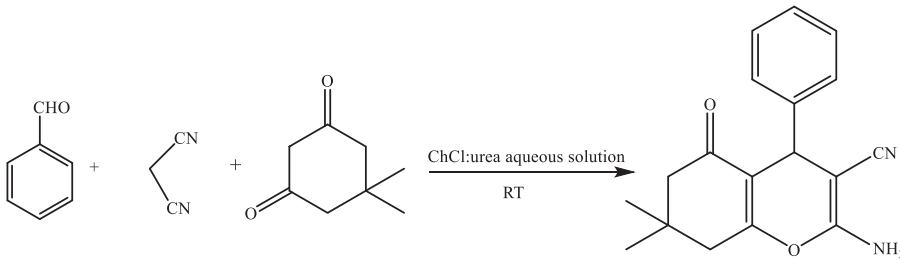

Scheme 9.78 Synthesis of 2-aminochromenes.

9.2.1.30 Synthesis of xanthenes and tetraketones

Xanthene derivatives also constitute an important class of heterocyclic compounds present in bioactive natural products and pharmaceuticals exhibiting wide-ranging pharmaceutical and biological activities, such as antimicrobial [274], antiproliferative [275], antibacterial [276], antiviral and antinociceptive activities [277], and antioxidant activity [278]. Xanthenes can also be used in the preparation of stable laser dyes [279], fluorescent sensor [280] and protein labeling fluorophores [281] used in laser technology [282], functional materials for visualization of biomolecular assemblies [283], photodynamic therapy [284], and as antagonists [285].

Tetraketones are important structural units in heterocycles with three-ring systems, such as xanthenedione and acridinedione. Meanwhile, tetraketones are also interesting because their properties are similar to those of 1,4-dihydropyridines, and their structures are similar to those of biologically important compounds, such as NADH and NADPH [286].

The tandem Knoevenagel condensations and Michael addition of aldehydes with active methylene compounds in the presence of acid or alkaline catalysts are widely used as important versatile methods for the synthesis of tetraketones [287]. Because of their practical importance, several methods have been proposed, employing different catalysts and promoters, such as NaOH [288], KOH [289], piperidine [290], and proline [290]. Furthermore, catalyst-free reactions in pure water [287], in the solid state, and in melts have been reported. Similarly, the numerous methods involving the condensation of aldehydes with active methylene compounds in the presence of an acidic catalyst or a promoter have been reported for the synthesis of xanthene in the literature [291]. Some of these methods suffer from prolonged reaction times, high cost, or the catalysts' sensitivity to moisture.

Azizi et al. proposed three-component tandem synthesis of xanthenes and tetraketones from aldehydes and active methylene compounds in choline chloride-based DESs. In the optimization experiment on the model reaction of benzaldehyde and dimedone, it was observed that the DES-based choline chloride-urea and choline chloride-$SnCl_2$ provided tetraketones in higher yields and shorter reaction times than methods using other DESs. On the other hand, in choline chloride-$ZnCl_2$ and choline chloride-malonic acid mixtures, the reaction proceeded selectively to generate xanthene derivatives. The synthetic protocol was extended with a range of functionalized aromatic aldehydes and dimedone to examine the substrate scope of the reaction in choline chloride-urea for tetraketones and choline chloride-$ZnCl_2$ for xanthene derivatives. The reaction can be extended with a wide range of structurally varied aldehydes, and the electronic variation on the aryl aldehydes caused no appreciable changes in the efficiency of the condensations. Electron-rich, electron-poor, aromatic, heterocyclic, and sterically encumbered aldehydes were all well tolerated in these reaction conditions. The procedure has been reported to be simple with mild reaction conditions and operational simplicity as compared to the other reported methods (Scheme 9.79) [292].

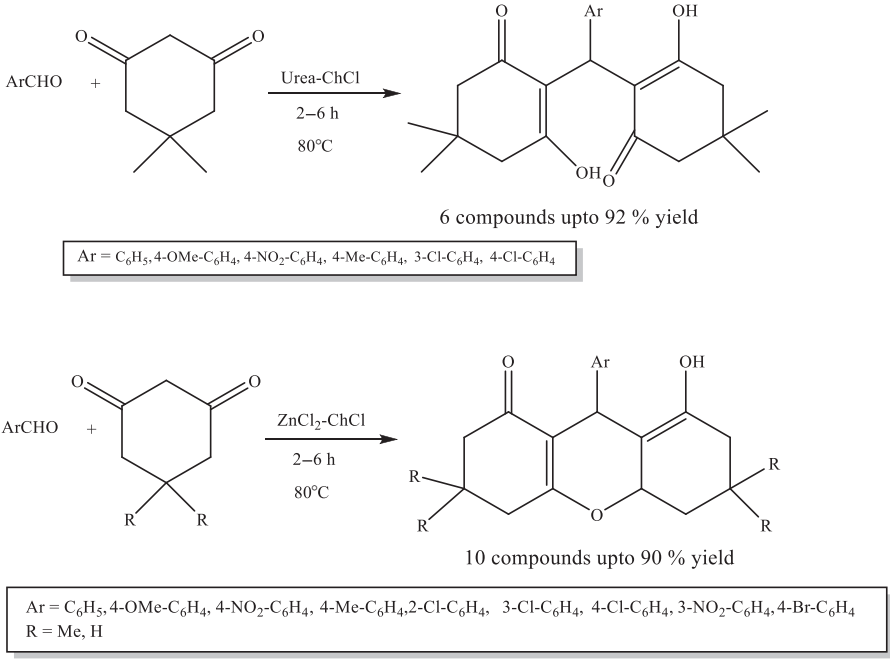

Scheme 9.79 Synthesis of xanthenes and tetraketones.

Liu et al. reported the synthesis of 13-aryl-5*H*-dibenzo[*b*,*i*]xanthene-5,7,12,14 (13*H*)-tetraones by the reaction of 2-hydroxynaphthalene-1,4-dione with various

aldehydes using choline chloride and itaconic acid-based DES as an effective catalyst and reaction medium (Scheme 9.80) [293].

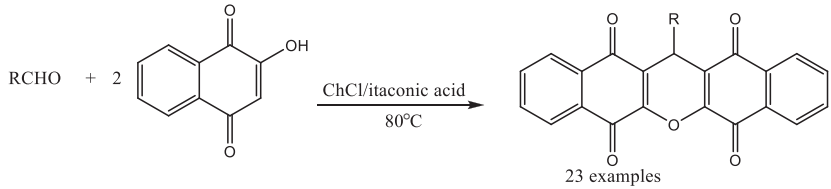

Aldehyde= PhCHO, 4-MeC_6H_4CHO, 2-HOC_6H_4CHO, 2-$MeOC_6H_4CHO$, 4-$MeOC_6H_4CHO$, 3-MeO-4-HOC_6H_3CHO, 3,4-$(MeO)_2C_6H_3CHO$, 3-$C_6H_4OC_6H_4CHO$, 4-$(CH_3)_3CC_6H_4CHO$, 2-FC_6H_4CHO, 4-FC_6H_4CHO, 2-BrC_6H_4CHO, 4-BrC_6H_4CHO, 2-ClC_6H_4CHO, 3-ClC_6H_4CHO, 4-ClC_6H_4CHO, 2-$NO_2C_6H_4CHO$, 3-$NO_2C_6H_4CHO$, 4-$NO_2C_6H_4CHO$, 3-Br-5-Cl-2-HOC_6H_2CHO, 2-Thiophenecarbaldehyde, 1-Naphthaldehyde, Terephthalaldehyde

Scheme 9.80 Synthesis of 13-aryl-5*H*-dibenzo[*b*,*i*]xanthene-5,7,12,14(13*H*)-tetraones.

But the reaction of 2-hydroxynaphthalene-1,4-dione with *p*-phthalaldehyde in the presence of DES (choline chloride and itaconic acid) provided (1,4-phenylene)bis (5*H*-dibenzo[*b*,*i*]xanthene-5,7,12,14(13*H*)-tetraone) (Scheme 9.81).

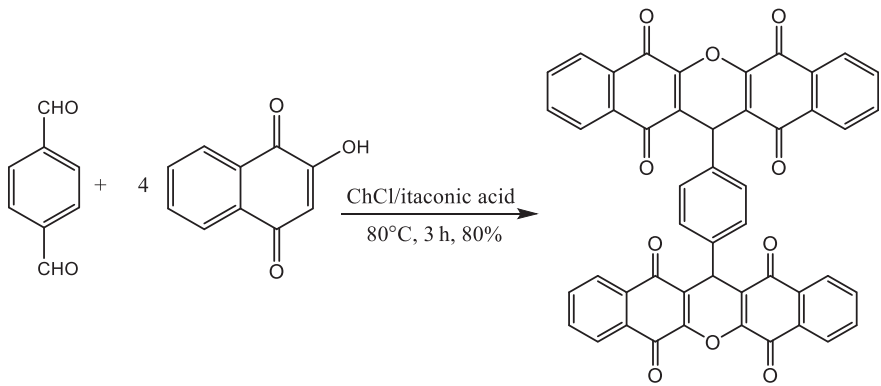

Scheme 9.81 Synthesis of (1,4-phenylene)bis(5*H*-dibenzo[*b*,*i*]xanthene-5,7,12,14(13*H*)-tetraone).

The reaction was extended for the synthesis of 14-phenyl-14*H*-dibenzo[*a*,*j*] xanthene and 3,3,6,6-tetramethyl-9-phenyl-3,4,5,6,7,9-hexahydro-1*H*-xanthene-1,8 (2*H*)-dione using the reaction of benzaldehyde with β-naphthol or dimedone as presented (Scheme 9.82).

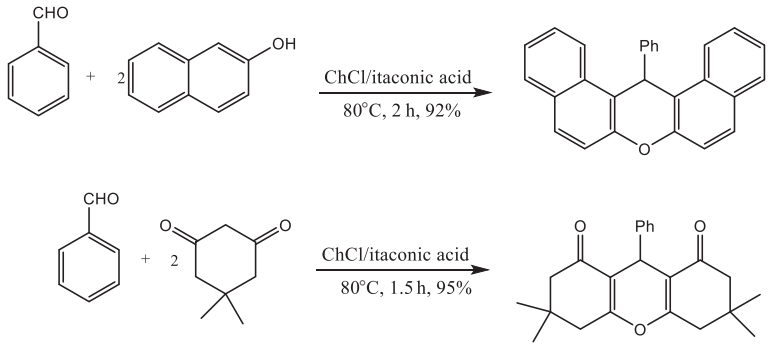

Scheme 9.82 Synthesis of 14-phenyl-14*H*-dibenzo[*a*,*j*]xanthene and 3,3,6,6-tetramethyl-9-phenyl-3,4,5,6,7,9-hexahydro-1*H*-xanthene-1,8(2*H*)-dione.

Shahabi et al. also reported synthesis of xanthene derivatives by the reaction of 2-naphthol derivatives with aromatic or aliphatic aldehydes using choline chloride/tin(II) chloride ($ChCl{\cdot}2SnCl_2$) DES, alone, or in the presence of Fe_3O_4/γ-carrageenan/Zn(II) magnetic bionanocatalyst (Scheme 9.83) [294].

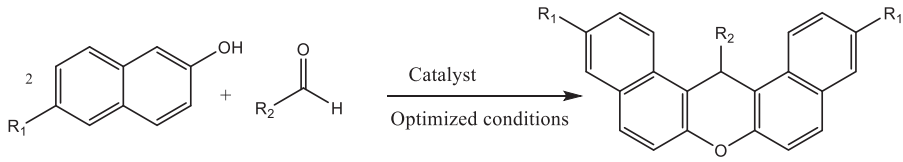

R_1= H, Br

R_2= Ph, 4-MeC_6H_4, 4-$MeOC_6H_4$, 2-ClC_6H_4CHO, 3-ClC_6H_4CHO, 4-ClC_6H_4CHO, 3-$NO_2C_6H_4CHO$, 4-$NO_2C_6H_4CHO$, C_4H_9, C_5H_{11}

Scheme 9.83 Synthesis of xanthene derivatives.

The proposed mechanism involving the role of the catalyst (DES or DES and nanomagnetic) is presented in Scheme 9.84.

Navarro et al. used sodium acetate trihydrate-urea DES as a reaction media for the Biginelli reaction to synthesize polyhydroquinoxaline derivatives but obtained unexpected products: methylenebis(3-hydroxy-5,5-dimethylcyclohex-2-enones), hexahydroxanthene-1,8-diones and hexahydroacridine-1,8-diones [295].

Initially, when the reaction was carried out between dimedone, 4-chlorobenzaldehyde, and urea in DES at 90°C for 6 h, the expected polyhydroquinoxaline was not synthesized, and instead, under the reaction conditions the hexahydroxacridine-1,8-dione was obtained (Scheme 9.85).

Furthermore, when the same reaction was performed at 60°C and after 2 h a white solid of bis-hydroxy derivative was obtained (Scheme 9.86).

The reaction was further applied using different aldehydes where the same type of bis-hydroxy derivatives were obtained in moderate to good yields (Scheme 9.87).

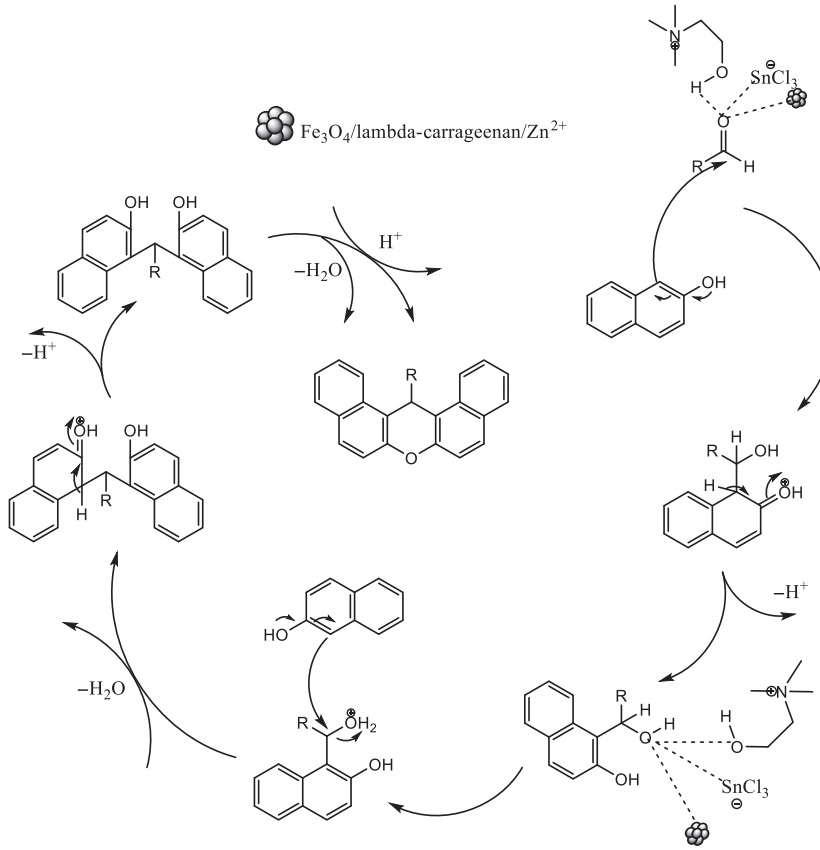

Scheme 9.84 Proposed mechanism for the synthesis of xanthenes catalyzed by $ChCl{\cdot}2SnCl_2$/Fe_3O_4/γ-carrageenan/Zn(II).

9.2.1.31 Synthesis of spirooxindoles

The heterocyclic spirooxindoles are very promising and attractive targets in organic and medicinal chemistry research because the spirooxindoles are encountered in the core structure of many pharmaceuticals and bioactive natural products (Fig. 9.21) [296]. Spirooxindoles are considered as privileged scaffolds for the drug development [297].

An efficient and environmentally benign one-pot four-component domino protocol has been reported by Kumar et al. for the synthesis of structurally diverse spirooxindoles. Four series of spirooxindoles spiroannulated with pyrazolopyrimidophthalazines, indenopyrazolophthalazines, chromenopyrazolophthalazines, and indazolophthalazines have been synthesized in DES (choline chloride:urea: 1:2) by the reaction of phthalic anhydride, hydrazine hydrate, isatins, and cyclic diketones/diamides. The reaction conditions were optimized with the screening of DES and two other solvent systems, but DES

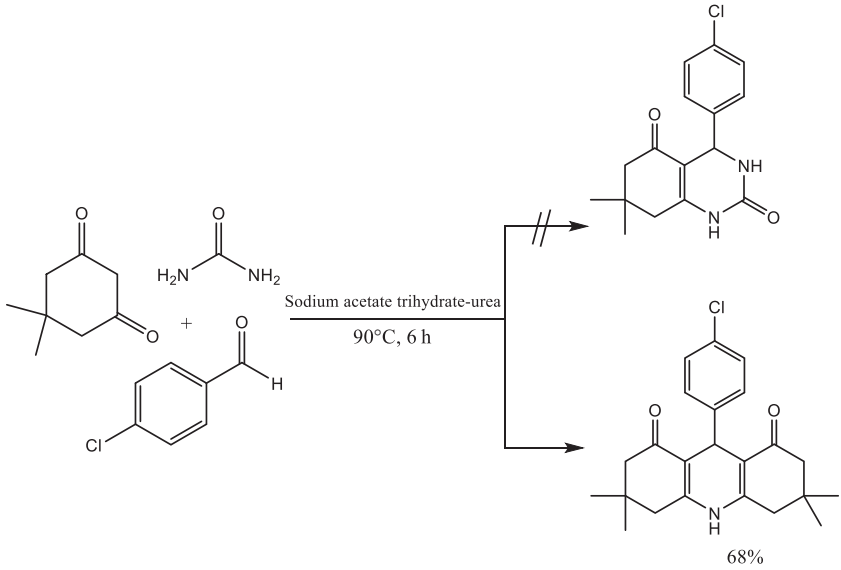

Scheme 9.85 Unexpected one-pot multicomponent synthesis of the hexahydroxacridine-1,8-dione.

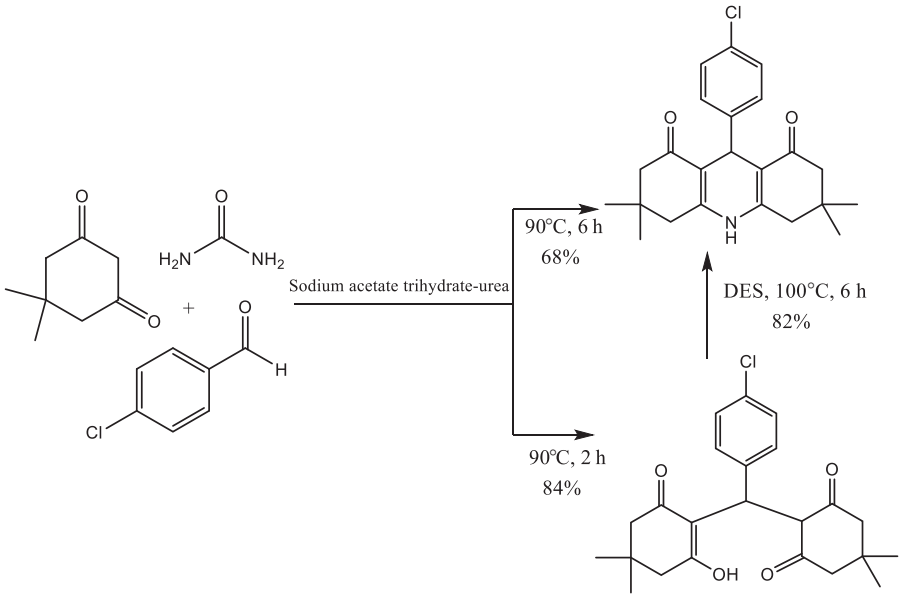

Scheme 9.86 Synthesis of the bis-hydroxy derivative and the hexahydroxacridine-1,8-dione in sodium acetate trihydrate urea DES under different conditions.

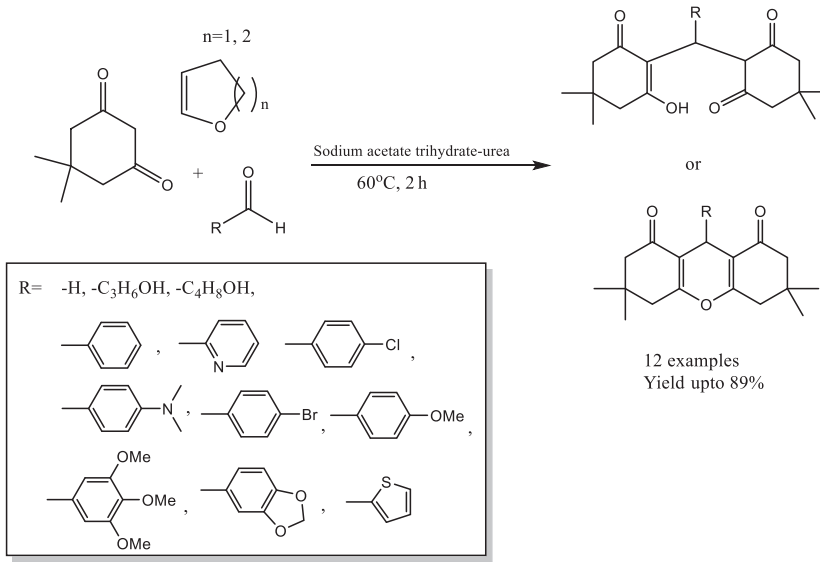

Scheme 9.87 Synthesis of bis-hydroxy derivatives and hexahydroxanthene-1,8-diones.

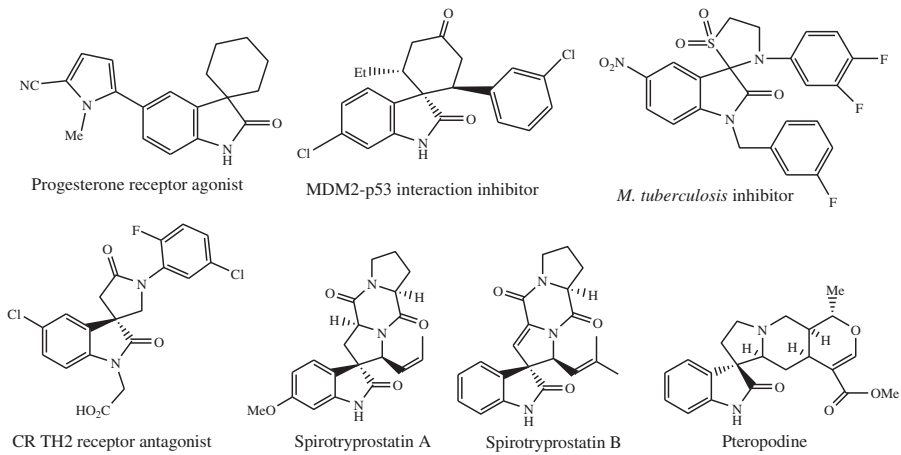

Fig. 9.21 Spirooxindole-containing synthetic drugs and natural products.

showed superiority over the other solvent system with its dual role as catalyst and solvent and the desired products were obtained in excellent yields in shorter reaction time. Moreover, the DES used as a catalytic solvent system in the reaction was recycled up to four times without an appreciable loss in catalytic activity (Scheme 9.88) [298].

The reaction proceeds to involve the following reaction mechanism (Scheme 9.89).

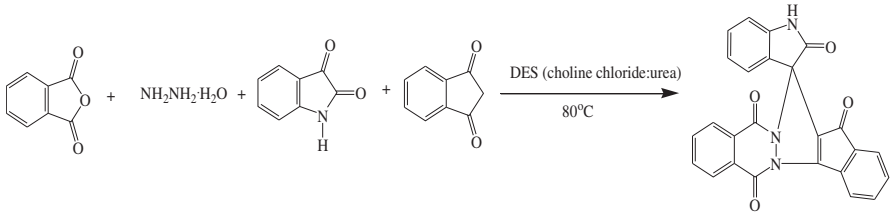

Scheme 9.88 Synthesis of spirooxindoles.

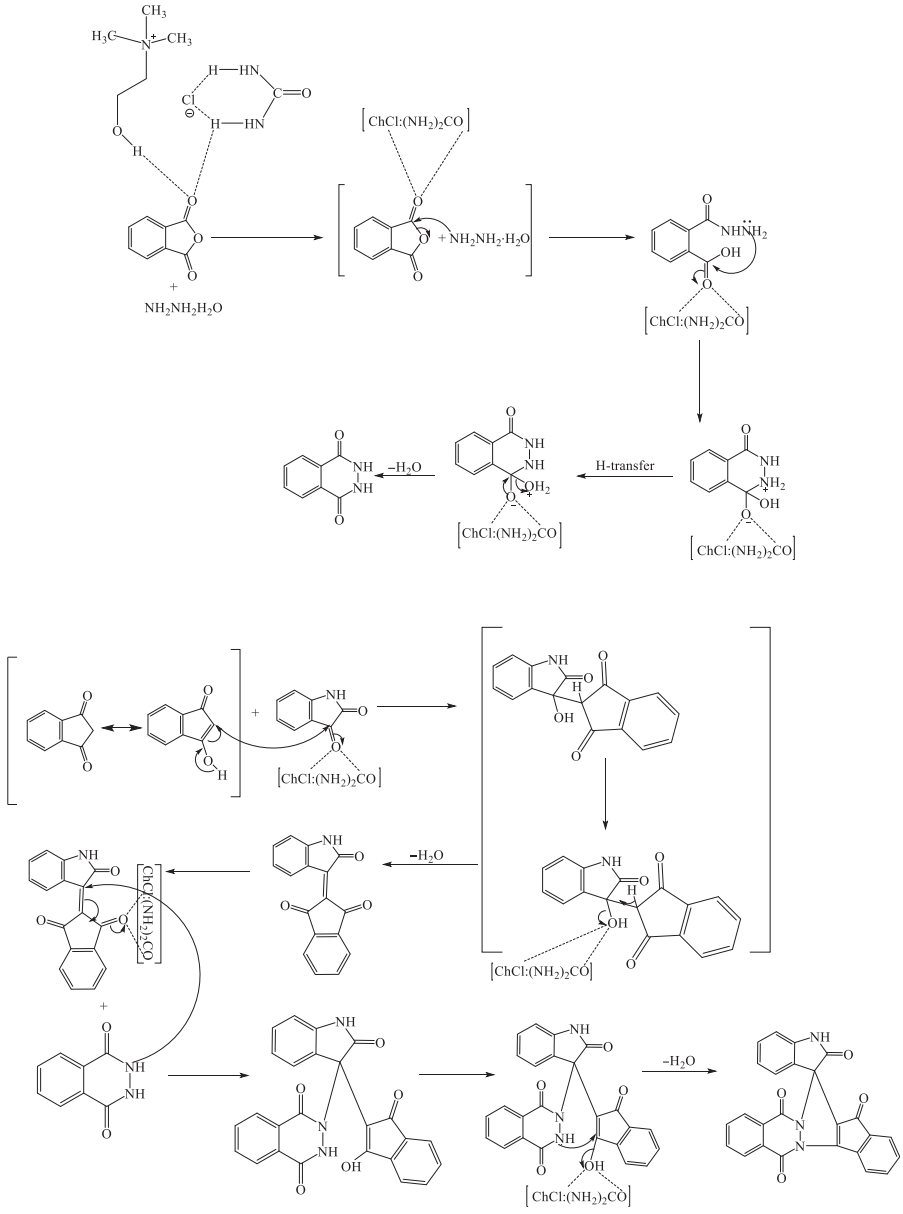

Scheme 9.89 Plausible reaction mechanism of spirooxindoles.

Structurally diverse spirooxindoles spiroannulated with pyranopyridopyrimidines, indenopyridopyrimidines, and chromenopyridopyrimidines were also synthesized by Kumar et al. by an efficient and environmentally benign domino protocol involving three-component reaction of aminouracils, isatins, and cyclic carbonyl compounds in DES (choline chloride-oxalic acid: 1:1) which acts as an efficient catalyst and environmentally benign reaction medium. Initially, four DESs were screened to check the feasibility of the reaction and to optimize the reaction conditions. But it was observed that when the reaction was performed in DES (ChCl:OA), the excellent yield of the desired product was obtained in shorter reaction time than that obtained with the use of other DESs. Thus, the results clearly indicate that DES (ChCl:OA) shown superiority over the other systems as solvents and catalyzed the reaction efficiently to facilitate the synthesis of spiroheterocycles in excellent yields. The DES (ChCl:OA) catalyzed synthetic protocol was extended with 6-aminouracil using different isatins and carbonyl compounds to synthesize structurally diverse spirooxindoles in excellent yields. The present protocol offers several advantages such as operational simplicity with easy workup, shorter reaction times excellent yields with superior atom economy and environmentally benign reaction conditions with the use of cost effective, recyclable, nontoxic, and biodegradable DES as catalyst/solvent (Scheme 9.90) [299].

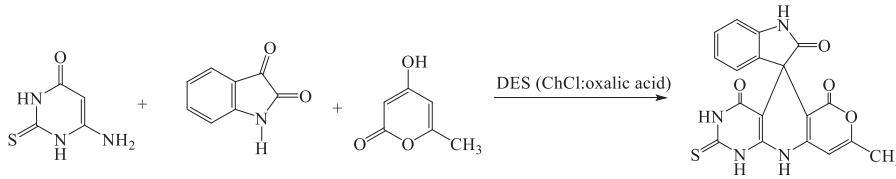

Scheme 9.90 Synthesis of spirooxindoles.

The reaction mechanism proposed for the synthesized structurally diverse heterocycles is presented in Scheme 9.91.

Azizi et al. also synthesized spirooxindole derivatives via multicomponent reaction of isatin or acenaphthoquinone and malononitrile or cyanoacetic ester with 1,3-dicarbonyl compounds, naphthol and 4-hydroxycumarin in biodegradable choline chloride-based DES. The reaction conditions were optimized with the screening of the various ChCl-based DES applied on model reaction to check their catalytic efficiency. It was observed that urea-choline chloride provided excellent results (95%) and proved to be the most effective reaction media and catalyst. The optimized synthetic protocol was further extended with a variety of 1,3-dicarbonyl compounds, malononitrile or cyanoacetic ester and isatin. The results clearly demonstrated that DES is an excellent catalyst and reaction media in terms of yields and times (Scheme 9.92) [300].

Spiropyrazolo[3,4-*b*]pyridines also represent an important class of heterocyclic compounds. Incorporation of pyrazolo[3,4-*b*]pyridine backbones and spirooxindole motif into one molecular structure results in a series of structural and biologically interesting compounds with enhanced pharmacological activity. Zhang et al.

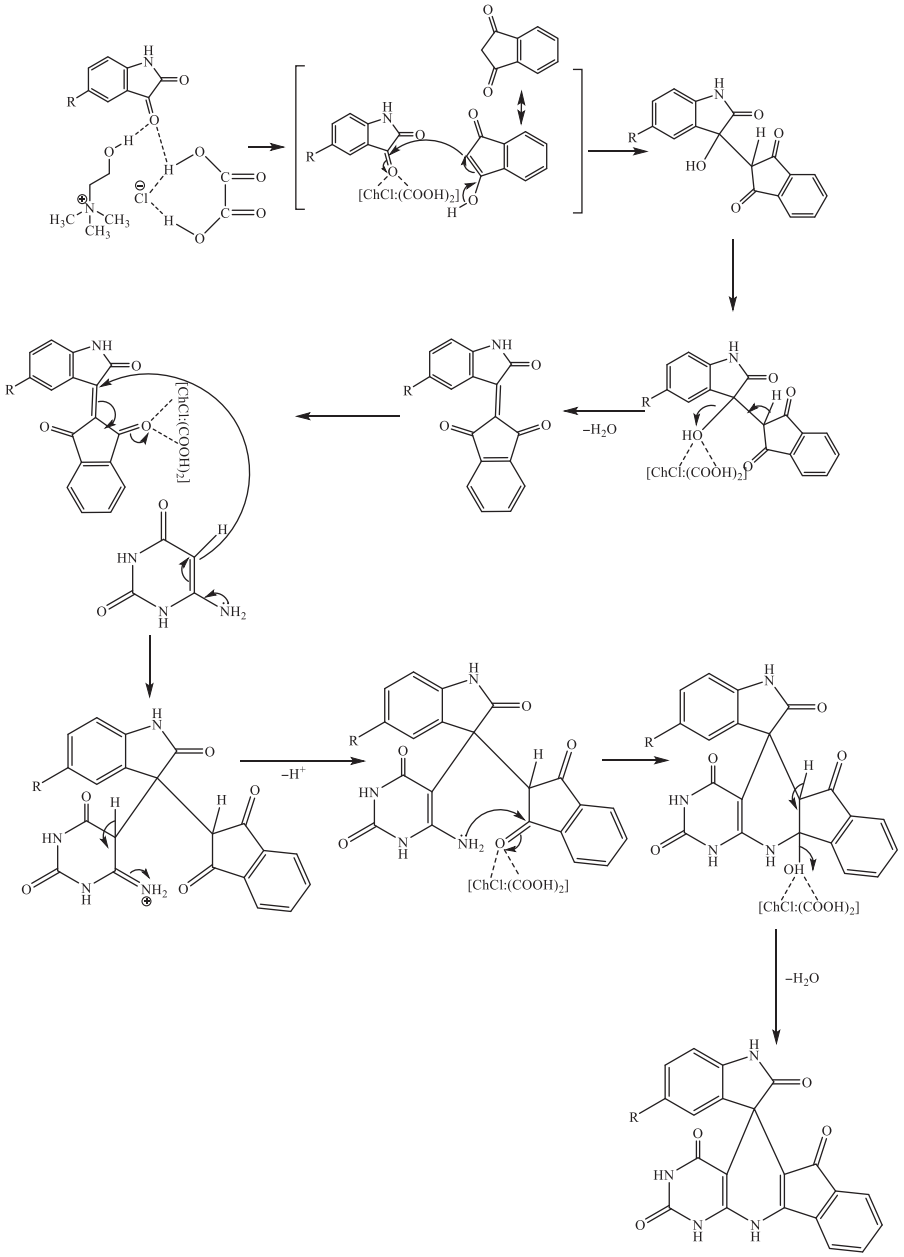

Scheme 9.91 Plausible reaction mechanism for the synthesis of spirooxindoles.

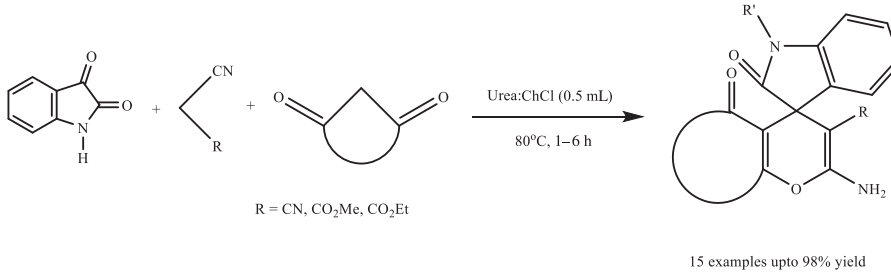

Scheme 9.92 Synthesis of spirooxindole derivatives.

synthesized spiro[indoline-3,4′-pyrazolo[3,4-*b*]pyridines] and other similar spiroheterocycles via three-component one-pot reaction of 1*H*-pyrazol-5-amin, isatin and enolizable ketone (C—H activated compound) by combining the microwave-assisted organic synthesis (MAOS) with natural DES (Scheme 9.93) [301].

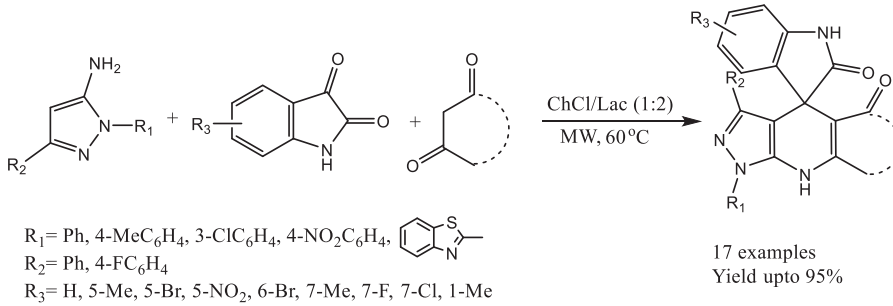

Scheme 9.93 Synthesis of pyrazolo[3,4-*b*]quinoline spirooxindoles in ChCl/Lac.

The reaction conditions were optimized with the use of various DES such as ChCl/$ZnCl_2$, ChCl/$ZnBr_2$, ChCl/glycerol (G), ChCl/proline (Pro), ChCl/malonic acid (MA), ChCl/EG, ChCl/1,3-dimethylurea (DU), ChCl/TA, and ChCl/Lac and observed high yield in ChCl/Lac (1:2). The presence of substituents, electron-rich or electron-poor groups, in various positions does not affect the yield of the product.

The proposed mechanism is presented in Scheme 9.94. The first step involved Knoevenagel condensation of isatin and 5,5-dimethylcyclohexane-1,3-dione to give intermediate **I** in the presence of a NDDES. Michel-type addition of 1,3-diphenyl-1*H*-pyrazol-5-amine to the C═C bond of intermediate **I** occurred with the formation of the adduct **II**. Subsequently, intramolecular cyclic condensation between the amino and the carbonyl groups of the Michael adduct **II** produces intermediate **III**, which upon elimination of water provides the expected product. In the reaction, DES acts as a solvent and also participates as a hydrogen-bonding catalyst and is responsible for the formation of Knoevenagel condensation product as well as enhanced electrophilic character of carbonyl carbons in both intermediates **I** and **II**.

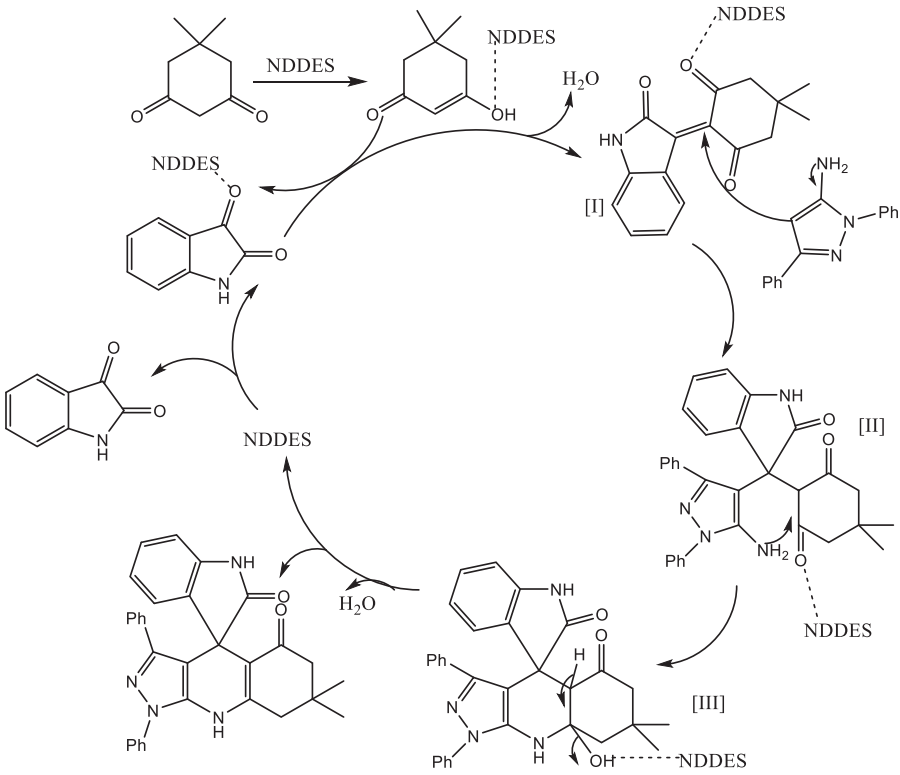

Scheme 9.94 A plausible mechanism for the formation of pyrazolo[3,4-*b*]quinoline spirooxindoles.

Spiropyrrolidine is a privileged core structure present in many naturally occurring compounds exhibiting numerous biological activities, e.g., coerulescine, the simplest spirooxindole-pyrrolidine hybrid exhibits local anesthetic effect, pteropodine modulates the function of muscarinic serotonin receptors [302]. The spirotryprostatins A has been identified as a novel inhibitor of microtubular assembly [303], and the recently discovered small-molecule MDM2 inhibitor MI-219 and its analogs are in advanced preclinical development for cancer therapeutics [304] (Fig. 9.22). In addition, spiro[5.5]undecane and heterospiro[5.5]undecane motifs with their unique structural properties [305] are present in several naturally occurring products such as elatol, isoobtusol, and (−) sibirine [306] (Fig. 9.22).

Singh et al. reported a regio- and diastereoselective synthesis of trispiro hybrid heterocycles comprising spiropyrrolidine/pyrrolothiazole and spiro[5.5]undecane by the 1,3-dipolar cycloaddition reaction of azomethine ylides (generated "in situ" in the reaction) from dipolarophile 8,10-bis[(*E*)arylidene]-3,3-dimethyl-1,5-dioxaspiro [5.5]undecan-9-one, sarcosine and isatin/acenaphthenequinone using choline chloride and urea-based DES (Scheme 9.95) [307].

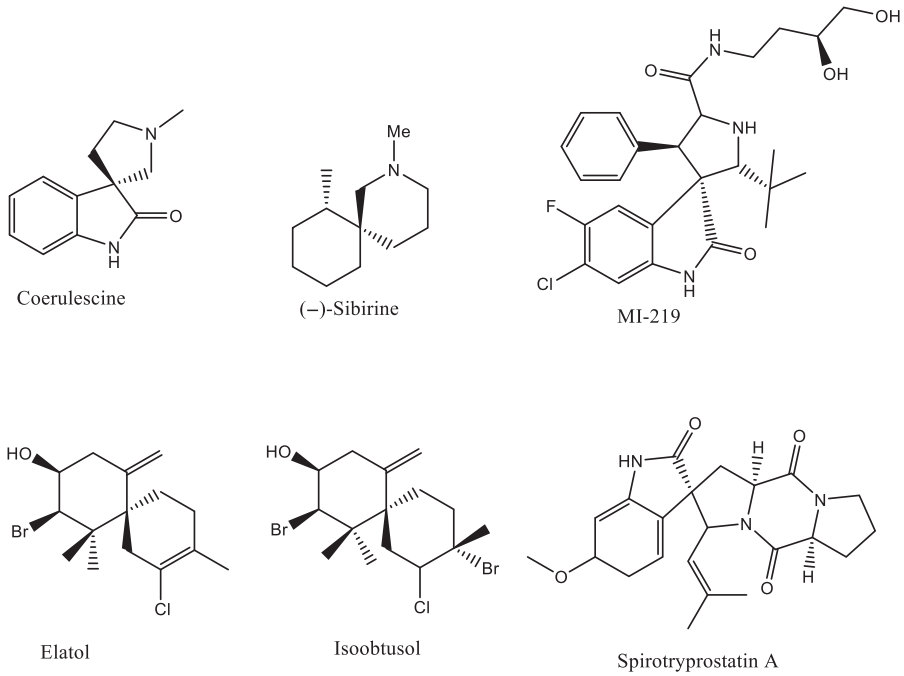

Fig. 9.22 Some naturally occurring products with spiropyrrolidinyl oxindole and spiro[5.5] undecane.

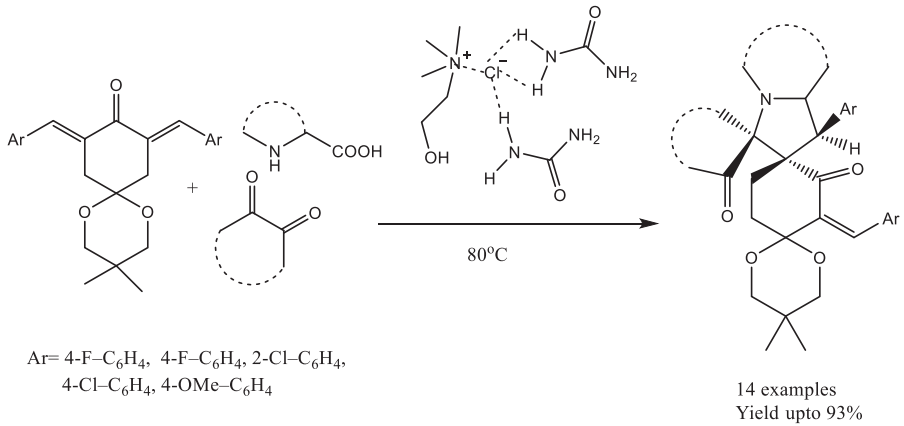

Scheme 9.95 Synthesis of trispiropyrrolidine derivatives.

For optimization of three-component reaction of bis-arylidene-1,5-dioxaspiro[5] decane, sarcosine and isatin, different choline chloride-based DES were screened and observed that the urea-choline chloride DES (mixture of 1:2 composition) provided an excellent yield of the desired product. The stronger hydrogen bonding

capabilities of DES activated the electrophilic character of carbonyl carbons of the isatin as well as dipolarophile and catalyzed the reaction as presented in Scheme 9.96.

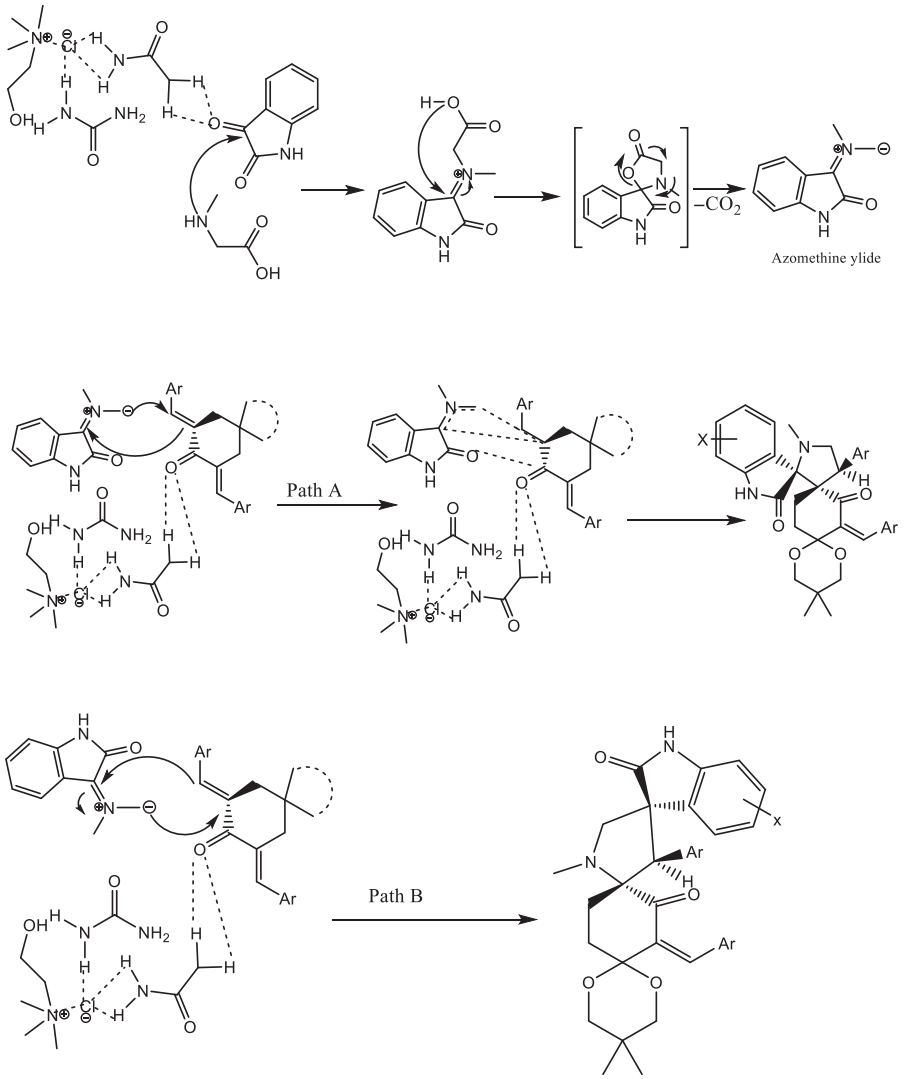

Scheme 9.96 Plausible mechanism for the formation of the trispiro adducts.

The pyrroloisoquinoline structural framework is present in a number of alkaloids including the ecteinascidin family, and cactus and Hippeastrum genus alkaloids (Fig. 9.23), and reported to exhibit not only remarkable activities in the central nervous system (CNS) [308] but also antitubercular [309], antihypertensive [310], anti-HIV-1 [311], antileukemic [312], and anticancer activities [313]. The analogs of

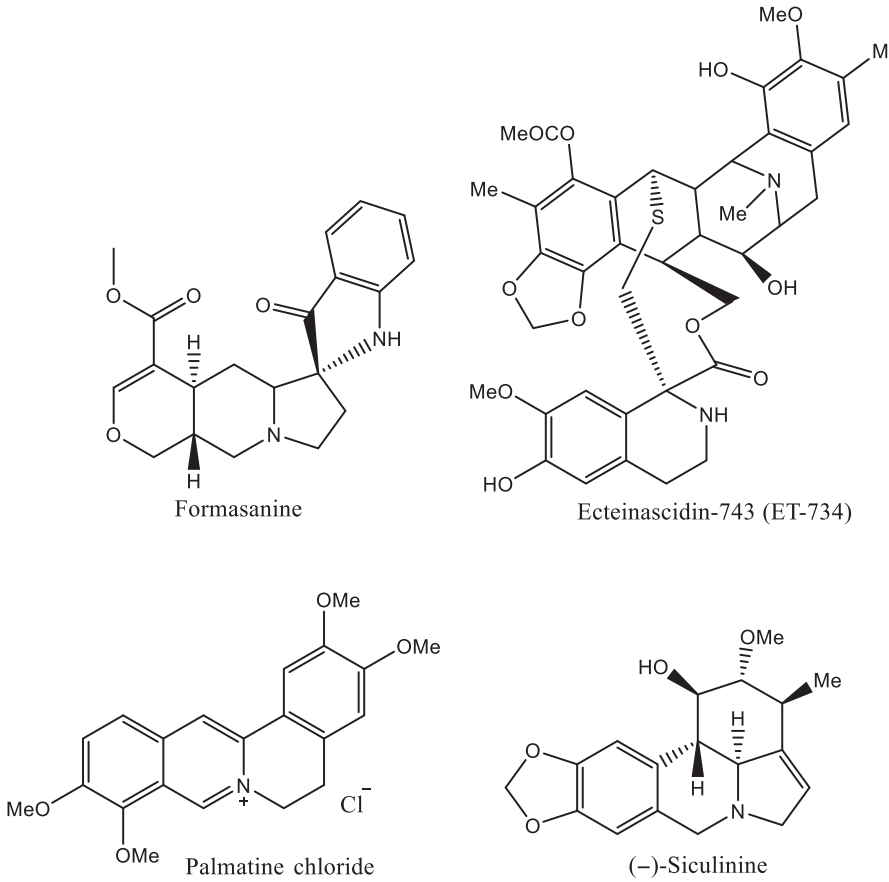

Fig. 9.23 Pyrrolo[1,2-*b*]isoquinoline core and spirocenter natural products.

pyrroloisoquinolines can be used as radiotracers in positron emission tomography (PET) for imaging serotonin uptake sites [314].

Periyasami et al. reported synthesis of multifunctionalized linear tricyclic spiropyrrolo[1,2-*b*]isoquinolines in good to excellent yields (85%–92%) involving 1,3-dipolar cycloaddition reactions of azomethine ylides generated in situ from an equimolar amount of a cyclic amino acid, a diketone and various substituted dipolarophiles in an eco-friendly acetylcholine iodide (ACI)-EG deep eutectic mixture (Scheme 9.97) [315].

Spiropyrroloisoquinoline with a chalcone group is an excellent candidate in medicinal chemistry particularly in Alzheimer's disease treatment [316], and it is also capable of inducing apoptosis [317] and uncoupling mitochondrial respiration [318]. In general, chalcone compounds did not show genotoxic effects and they may be devoid of this significant side effect [319]. It was observed that the chalcone group was retained in the spiro adduct during the synthesis, which may be due to the stability of the monoadduct and to avoid the formation of the sterically hindered bis cycloadduct.

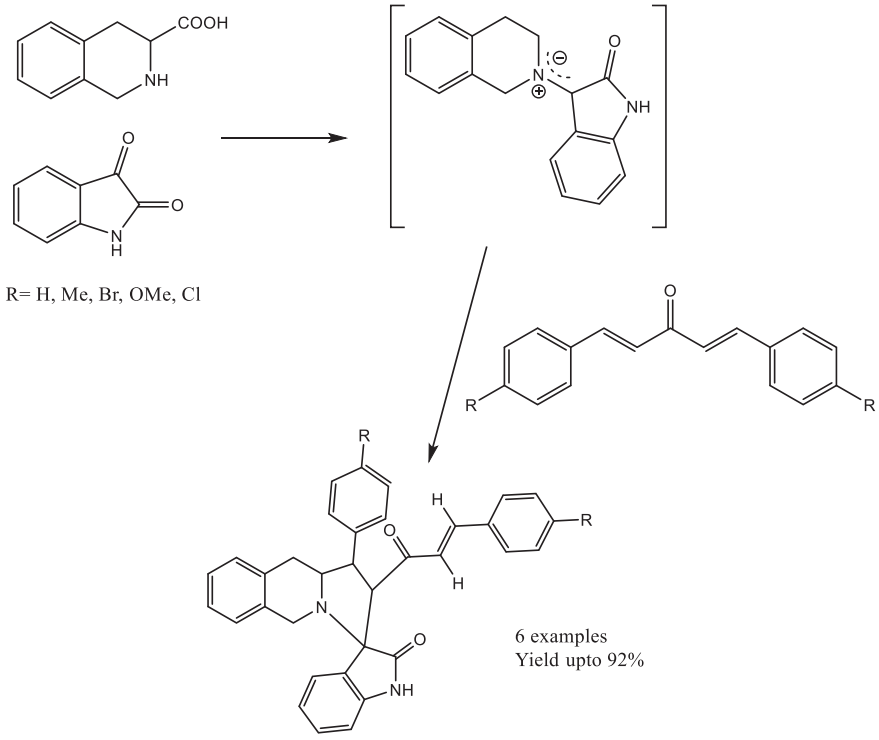

Scheme 9.97 Synthesis of spiropyrrolo[1,2-*b*]isoquinolines.

9.2.1.32 *Synthesis of seven-membered heterocycles*

Seven-membered heterocycles constitute an integral part of natural alkaloids, antibiotics, and synthetic drugs [320]. Benzo-fused seven-membered heterocycles, 1,4-benzodiazepine, and 1,4-benzoxazepine derivatives find their applications in medicinal chemistry due to their wide spectrum of biological activities (Fig. 9.24) [321]. 1,4-Benzodiazepines have demonstrated considerable utility in CNS-drug design, and as key intermediates for the preparation of fused ring compounds [322]. 1,4-Benzodiazepines; diazepam; and chlordiazepoxide act as antianxiety drugs and 1,4-benzoxazepines are used as nonnucleoside HIV-1 reverse transcriptase inhibitor [323], a histamine receptor agonist [321d], and calcium antagonists [324], as well as antidepressants and analgesics [325].

Shaabani et al. synthesized benzo-fused seven-membered heterocycles, 1,4-benzodiazepines, and 1,4-benzoxazepines, via one-pot, three-component reaction of *o*-phenylenediamine or 2-aminophenol, dimedone, and various aromatic aldehydes at 80°C in the presence of choline chloride and urea as a DES [326].

The scope and limitations of this reaction were explored by utilizing various *o*-phenylenediamines or 2-aminophenols, dimedone, and various benzaldehyde derivatives. It was observed that the benzodiazepines were obtained in higher yields

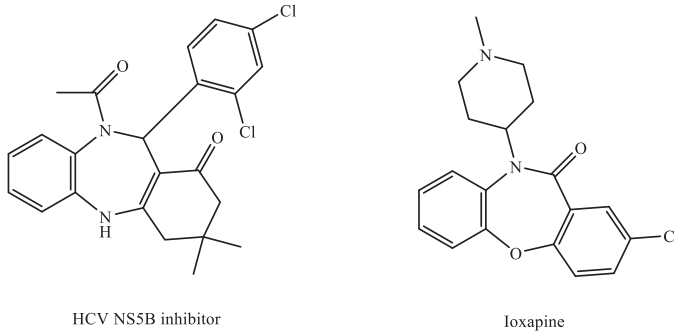

Fig. 9.24 Benzo-fused seven-membered heterocyclic scaffolds.

(80%–94%) with shorter reaction times (20–30 min) relative to the benzoxazepines (68%–88%, 30–40 min). The presence of electron-withdrawing groups on benzaldehyde showed increased yields in comparison to electron-donating groups (Scheme 9.98).

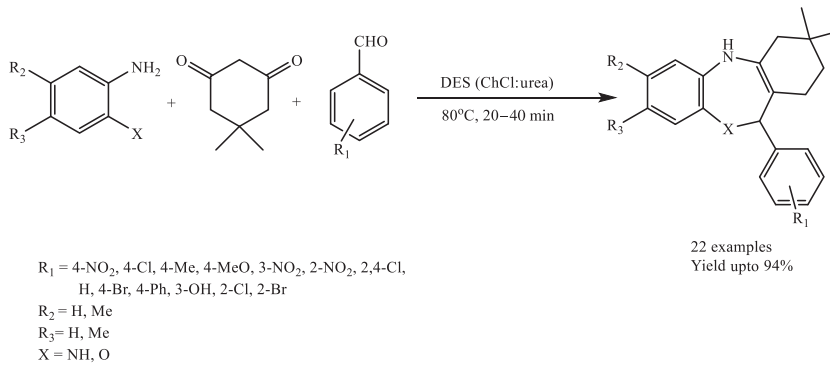

Scheme 9.98 Synthesis of benzo-fused seven-membered heterocycles via a three-component reaction in DES.

In the proposed mechanism, DES facilitates the reaction with the activation of the carbonyl group of dimedone and then undergoes condensation with *o*-phenylenediamine to form an intermediate imine [A]. The nucleophilic addition of NH_2 group of [A] with the DES activated carbonyl group of benzaldehyde derivatives and then subsequent intramolecular cyclization provides the products. Benzoxazepine derivatives may undergo an analogous mechanism in which intermediate [B] is replaced by the corresponding oxonium intermediate. DES can play a dual role in this reaction: (i) as a solvent and (ii) as a catalyst which activates the carbonyl and imine functional groups via hydrogen bonding. The proposed mechanism is presented in Scheme 9.99.

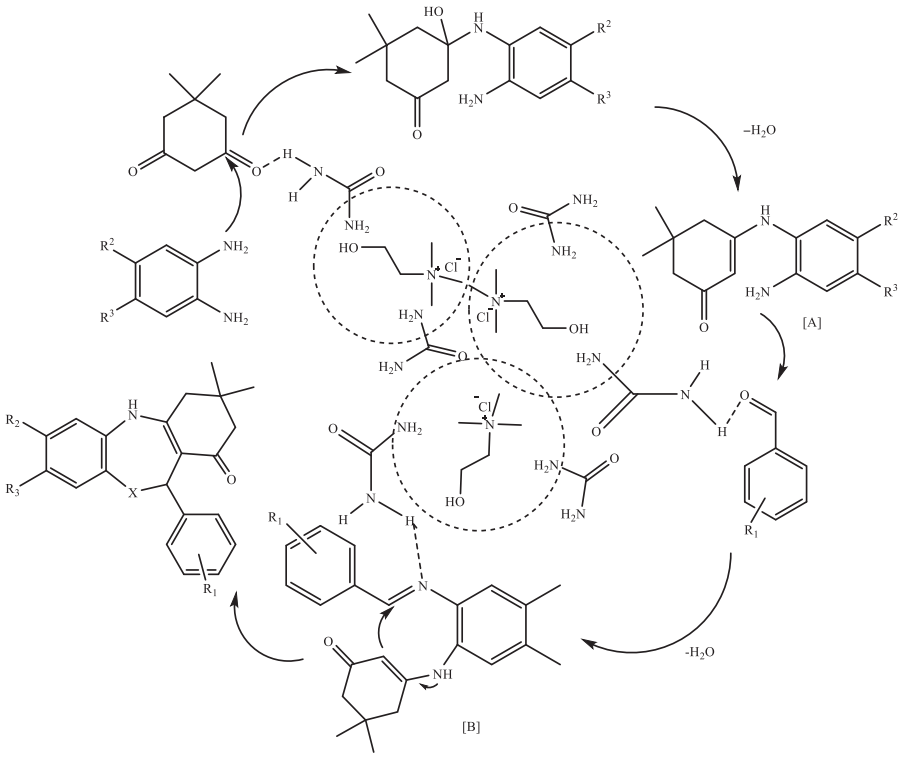

Scheme 9.99 Proposed mechanism for the synthesis of benzo-fused seven-membered heterocycles in choline chloride/urea.

9.3 Conclusion

The present chapter includes the recent advances in the synthesis of heterocyclic scaffolds with the use of sustainable organic transformations involving the use of DESs as green and sustainable solvents and catalysts. DESs have been regarded as one of the most promising environmentally benign and cost-effective alternatives to conventional ILs and volatile organic solvents. DESs not only retain the excellent merits of ILs but also overcome their shortcomings as these are constituted from natural and renewable nontoxic bio-resources. Thus DESs are emerging as a new generation of green and sustainable solvents. Although DESs have attracted the attention of chemical research in many fields, the ability of deep eutectic mixtures to serve as solvents, however, has not been adequately explored in the field of synthetic organic chemistry field The heterocyclic scaffolds with structural diversity and molecular complexity will contribute not only to chemical research but also significantly to medicinal and pharmaceutical chemistry research. It will be an important contribution to drug discovery research in view of the synthesis of hybrid molecules using multicomponent reactions. Academically, it will be a significant contribution for the advanced graduates pursuing research in green and sustainable organic transformations.

References

[1] (a) Green Chemistry: Designing Chemistry for the Environment Edited by Paul T. Anastas and Tracy C. Williamson (U.S. Environmental Protection Agency). ACS: Washington, DC. 1996. xii + 251 pp. $89.95. ISBN 0-8412-3399-3, J. Am. Chem. Soc., 118 (44) (1996) 10945; (b) P.T. Anastas, J.C. Warner, Green Chemistry: Theory and Practice, Oxford University Press, Oxford [England]; New York, 1998; (c) N.N. Sauer, Green Chemistry: Frontiers in Benign Chemical Syntheses and Processes Edited by Paul T. Anastas and Tracy C. Williamson (U. S. Environmental Protection Agency). Oxford University Press: New York, NY. 1999. 360 pp. $115.00. ISBN 0-19-850170-6, J. Am. Chem. Soc. 122 (22) (2000) 5419–5420; (d) P.J. Dunn, The importance of green chemistry in process research and development, Chem. Soc. Rev. 41 (4) (2012) 1452–1461; (e) P.T. Anastas, J.B. Zimmerman, Peer reviewed: design through the 12 principles of green engineering, Environ. Sci. Technol. 37 (5) (2003) 94A–101A.

[2] Y. Gu, F. Jérôme, Bio-based solvents: an emerging generation of fluids for the design of eco-efficient processes in catalysis and organic chemistry, Chem. Soc. Rev. 42 (24) (2013) 9550–9570.

[3] B.C. Ranu, A. Saha, R. Dey, Using more environmentally friendly solvents and benign catalysts in performing conventional organic reactions, Curr. Opin. Drug Discov. Dev. 13 (6) (2010) 658–668.

[4] E. Feng, Y. Zhou, F. Zhao, X. Chen, L. Zhang, H. Jiang, H. Liu, Gold-catalyzed tandem reaction in water: an efficient and convenient synthesis of fused polycyclic indoles, Green Chem. 14 (7) (2012) 1888–1895.

[5] M. Petkovic, K.R. Seddon, L.P.N. Rebelo, C. Silva Pereira, Ionic liquids: a pathway to environmental acceptability, Chem. Soc. Rev. 40 (3) (2011) 1383–1403.

[6] M. Hong, C. Cai, W.-B. Yi, Hafnium (IV) bis(perfluorooctanesulfonyl)imide complex catalyzed synthesis of polyhydroquinoline derivatives via unsymmetrical Hantzsch reaction in fluorous medium, J. Fluor. Chem. 131 (1) (2010) 111–114.

[7] P.G. Jessop, Homogeneous catalysis using supercritical fluids: recent trends and systems studied, J. Supercrit. Fluids 38 (2) (2006) 211–231.

[8] M. Veeranarayana Reddy, J.S. Kim, K.T. Lim, Y. Tae Jeong, Polyethylene glycol (PEG-400): an efficient green reaction medium for the synthesis of benzo[4,5]imidazo[1,2-a]-pyrimido[4,5-d]pyrimidin-4(1H)-ones under catalyst-free conditions, Tetrahedron Lett. 55 (47) (2014) 6459–6462.

[9] (a) J.P. Hallett, T. Welton, Room-temperature ionic liquids: solvents for synthesis and catalysis. 2, Chem. Rev. 111 (5) (2011) 3508–3576; (b) N. Isambert, M.d.M. S. Duque, J.-C. Plaquevent, Y. Génisson, J. Rodriguez, T. Constantieux, Multicomponent reactions and ionic liquids: a perfect synergy for eco-compatible heterocyclic synthesis, Chem. Soc. Rev. 40 (3) (2011) 1347–1357.

[10] Q. Zhang, S. Zhang, Y. Deng, Recent advances in ionic liquid catalysis, Green Chem. 13 (10) (2011) 2619–2637.

[11] (a) Z. Chen, R. Fu, W. Chai, H. Zheng, L. Sun, Q. Lu, R. Yuan, An eco-benign and highly efficient procedure for N-acylation catalyzed by heteropolyanion-based ionic liquids using carboxylic acid under solvent-free conditions, Tetrahedron 70 (13) (2014) 2237–2245; (b) D. Gavaskar, A.R. Suresh Babu, R. Raghunathan, M. Dharani, S. Balasubramanian, Ionic liquid accelerated multicomponent sequential assembly of ferrocene grafted spiro-heterocycles, J. Organomet. Chem. 768 (2014) 128–135; (c)

H. Singh, S. Kumari, J.M. Khurana, A new green approach for the synthesis of 12-aryl-8,9,10,12-tetrahydrobenzo[a]xanthene-11-one derivatives using task specific acidic ionic liquid [NMP]H2PO4, Chin. Chem. Lett. 25 (10) (2014) 1336–1340; (d) M. Rahman, A. Sarkar, M. Ghosh, A. Majee, A. Hajra, Catalytic application of task specific ionic liquid on the synthesis of benzoquinazolinone derivatives by a multicomponent reaction, Tetrahedron Lett. 55 (1) (2014) 235–239.

[12] (a) A. Romero, A. Santos, J. Tojo, A. Rodríguez, Toxicity and biodegradability of imidazolium ionic liquids, J. Hazard. Mater. 151 (1) (2008) 268–273; (b) E. Durand, J. Lecomte, P. Villeneuve, Deep eutectic solvents: synthesis, application, and focus on lipase-catalyzed reactions, Eur. J. Lipid Sci. Technol. 115 (4) (2013) 379–385; (c) D. Zhao, Y. Liao, Z. Zhang, Toxicity of ionic liquids, CLEAN Soil Air Water 35 (1) (2007) 42–48; (d) M. El-Harbawi, Toxicity measurement of imidazolium ionic liquids using acute toxicity test, Procedia Chem. 9 (2014) 40–52.

[13] (a) E.L. Smith, A.P. Abbott, K.S. Ryder, Deep eutectic solvents (DESs) and their applications, Chem. Rev. 114 (21) (2014) 11060–11082; (b) N.V. Plechkova, K.R. Seddon, Applications of ionic liquids in the chemical industry, Chem. Soc. Rev. 37 (1) (2008) 123–150; (c) T.P.T. Pham, C.-W. Cho, Y.-S. Yun, Environmental fate and toxicity of ionic liquids: a review, Water Res. 44 (2) (2010) 352–372; (d) C. Austen Angell, Y. Ansari, Z. Zhao, Ionic Liquids: past, present and future, Faraday Discuss. 154 (2012) 9–27.

[14] (a) Q. Zhang, K. De Oliveira Vigier, S. Royer, F. Jérôme, Deep eutectic solvents: syntheses, properties and applications, Chem. Soc. Rev. 41 (21) (2012) 7108–7146; (b) A.P. Abbott, R.C. Harris, K.S. Ryder, C. D'Agostino, L.F. Gladden, M.D. Mantle, Glycerol eutectics as sustainable solvent systems, Green Chem. 13 (1) (2011) 82–90; (c) C. Ruß, B. König, Low melting mixtures in organic synthesis—an alternative to ionic liquids? Green Chem. 14 (11) (2012) 2969–2982; (d) Z. Maugeri, P. Domínguez de María, Novel choline-chloride-based deep-eutectic-solvents with renewable hydrogen bond donors: levulinic acid and sugar-based polyols, RSC Adv. 2 (2) (2012) 421–425; (e) A.P. Abbott, G. Capper, D.L. Davies, R.K. Rasheed, V. Tambyrajah, Novel solvent properties of choline chloride/urea mixtures, Chem. Commun. 1 (2003) 70–71.

[15] (a) J.M. Gottesfeld, L. Neely, J.W. Trauger, E.E. Baird, P.B. Dervan, Regulation of gene expression by small molecules, Nature 387 (6629) (1997) 202–205; (b) T. Lindel, M. Hochgürtel, M. Assmann, M. Köck, Synthesis of the marine natural product Nα-(4-bromopyrrolyl-2-carbonyl)-l-homoarginine, a putative biogenetic precursor of the pyrrole – imidazole alkaloids, J. Nat. Prod. 63 (11) (2000) 1566–1569; (c) S.M. Rokade, A.M. Garande, N.A.A. Ahmad, P.M. Bhate, Acid- and metal-free synthesis of annulated pyrroles in a deep eutectic solvent, RSC Adv. 5 (3) (2015) 2281–2284; (d) H. Fan, J. Peng, M.T. Hamann, J.-F. Hu, Lamellarins and related pyrrole-derived alkaloids from marine organisms, Chem. Rev. 108 (1) (2008) 264–287; (e) B.T. Parr, C. Economou, S.B. Herzon, A concise synthesis of (+)-batzelladine B from simple pyrrole-based starting materials, Nature 525 (2015) 507; (f) M.T. Wilson, B.J. Reeder, Oxygen-binding haem proteins, Exp. Physiol. 93 (1) (2008) 128–132; (g) S. Michlik, R. Kempe, A sustainable catalytic pyrrole synthesis, Nat. Chem. 5 (2013) 140; (h) X.-B. Ding, M.A. Brimble, D.P. Furkert, Nitropyrrole natural products: isolation, biosynthesis and total synthesis, Org. Biomol. Chem. 14 (24) (2016) 5390–5401; (i) B. Xu, G. Li, J. Li, Y. Shi, Total synthesis of the proposed structure of marineosin A, Org. Lett. 18 (9) (2016) 2028–2031.

[16] V. Estévez, M. Villacampa, J.C. Menéndez, Three-component access to pyrroles promoted by the CAN–silver nitrate system under high-speed vibration milling conditions:

a generalization of the Hantzsch pyrrole synthesis, Chem. Commun. 49 (6) (2013) 591–593.

[17] Z.-H. Zhang, J.-J. Li, T.-S. Li, Ultrasound-assisted synthesis of pyrroles catalyzed by zirconium chloride under solvent-free conditions, Ultrason. Sonochem. 15 (5) (2008) 673–676.

[18] F.-P. Ma, P.-H. Li, B.-L. Li, L.-P. Mo, N. Liu, H.-J. Kang, Y.-N. Liu, Z.-H. Zhang, A recyclable magnetic nanoparticles supported antimony catalyst for the synthesis of N-substituted pyrroles in water, Appl. Catal. A Gen. 457 (2013) 34–41.

[19] (a) R. Martín, M. Rodríguez Rivero, S.L. Buchwald, Domino Cu-catalyzed C–N coupling/hydroamidation: a highly efficient synthesis of nitrogen heterocycles, Angew. Chem. Int. Ed. 45 (42) (2006) 7079–7082; (b) X. Yuan, X. Xu, X. Zhou, J. Yuan, L. Mai, Y. Li, Copper-catalyzed double N-alkenylation of amides: an efficient synthesis of di- or trisubstituted N-acylpyrroles, J. Org. Chem. 72 (4) (2007) 1510–1513; (c) M.R. Rivero, S.L. Buchwald, Copper-catalyzed vinylation of hydrazides. A regioselective entry to highly substituted pyrroles, Org. Lett. 9 (6) (2007) 973–976.

[20] (a) A. Bhattacharya, S. Cherukuri, R.E. Plata, N. Patel, V. Tamez, J.A. Grosso, M. Peddicord, V.A. Palaniswamy, Remarkable solvent effect in Barton–Zard pyrrole synthesis: application in an efficient one-step synthesis of pyrrole derivatives, Tetrahedron Lett. 47 (31) (2006) 5481–5484; (b) J.G. Greger, S.J.P. Yoon-Miller, N.R. Bechtold, S.A. Flewelling, J.P. MacDonald, C.R. Downey, E.A. Cohen, E.T. Pelkey, Synthesis of unsymmetrical 3,4-diaryl-3-pyrrolin-2-ones utilizing pyrrole Weinreb amides, J. Org. Chem. 76 (20) (2011) 8203–8214; (c) A.R. Coffin, M.A. Roussell, E. Tserlin, E. T. Pelkey, Regiocontrolled synthesis of pyrrole-2-carboxaldehydes and 3-pyrrolin-2-ones from pyrrole Weinreb amides, J. Org. Chem. 71 (17) (2006) 6678–6681.

[21] (a) N. Azizi, A. Khajeh-Amiri, H. Ghafuri, M. Bolourtchian, M.R. Saidi, Iron-catalyzed inexpensive and practical synthesis of N-substituted pyrroles in water, Synlett 2009 (14) (2009) 2245–2248; (b) A. Rahmatpour, ZrOCl2·8H2O as a highly efficient, eco-friendly and recyclable Lewis acid catalyst for one-pot synthesis of N-substituted pyrroles under solvent-free conditions at room temperature, Appl. Organomet. Chem. 25 (8) (2011) 585–590; (c) K. Aghapoor, L. Ebadi-Nia, F. Mohsenzadeh, M. Mohebi Morad, Y. Balavar, H.R. Darabi, Silica-supported bismuth(III) chloride as a new recyclable heterogeneous catalyst for the Paal–Knorr pyrrole synthesis, J. Organomet. Chem. 708–709 (2012) 25–30.

[22] (a) A. Devi, Shallu, M.L. Sharma, J. Singh, Paal–Knorr pyrrole synthesis using recyclable amberlite IR 120 acidic resin: a green approach, Synth. Commun. 42 (10) (2012) 1480–1488; (b) A. Ali Jafari, S. Amini, F. Tamaddon, A green, chemoselective, and efficient protocol for Paal–Knorr pyrrole and bispyrrole synthesis using biodegradable polymeric catalyst PEG-SO3H in water, J. Appl. Polym. Sci. 125 (2) (2012) 1339–1345.

[23] M.A. Wilson, G. Filzen, G.S. Welmaker, A microwave-assisted, green procedure for the synthesis of N-aryl sulfonyl and N-aryl pyrroles, Tetrahedron Lett. 50 (34) (2009) 4807–4809.

[24] G. Wang, Z. Guan, R. Tang, Y. He, Ionic liquid as catalyst and reaction medium: a simple and efficient procedure for Paal–Knorr furan synthesis, Synth. Commun. 40 (3) (2010) 370–377.

[25] (a) P.J. Nieuwland, R. Segers, K. Koch, J.C.M. van Hest, F.P.J.T. Rutjes, Fast scale-up using microreactors: pyrrole synthesis from micro to production scale, Org. Process Res. Dev. 15 (4) (2011) 783–787; (b) V.S.V. Satyanarayana, A. Sivakumar, Ultrasound-assisted synthesis of 2,5-dimethyl-N-substituted pyrroles catalyzed by uranyl nitrate hexahydrate, Ultrason. Sonochem. 18 (5) (2011) 917–922.

[26] (a) M. Francisco, A. van den Bruinhorst, M.C. Kroon, Low-transition-temperature mixtures (LTTMs): a new generation of designer solvents, Angew. Chem. Int. Ed. 52 (11) (2013) 3074–3085; (b) J. García-Álvarez, Deep eutectic mixtures: promising sustainable solvents for metal-catalysed and metal-mediated organic reactions, Eur. J. Inorg. Chem. 2015 (31) (2015) 5147–5157.
[27] S. Handy, K. Lavender, Organic synthesis in deep eutectic solvents: Paal–Knorr reactions, Tetrahedron Lett. 54 (33) (2013) 4377–4379.
[28] H.-C. Hu, Y.-H. Liu, B.-L. Li, Z.-S. Cui, Z.-H. Zhang, Deep eutectic solvent based on choline chloride and malonic acid as an efficient and reusable catalytic system for one-pot synthesis of functionalized pyrroles, RSC Adv. 5 (10) (2015) 7720–7728.
[29] (a) D.E.N. Jacquot, M. Zöllinger, T. Lindel, Totalsynthese des marinen Naturstoffs rac-Dibromphakellstatin, Angew. Chem. 117 (15) (2005) 2336–2338; (b) B.D. Roth, C.J. Blankley, A.W. Chucholowski, E. Ferguson, M.L. Hoefle, D.F. Ortwine, R.S. Newton, C.S. Sekerke, D.R. Sliskovic, M. Wilson, Inhibitors of cholesterol biosynthesis. 3. Tetrahydro-4-hydroxy-6-[2-(1H-pyrrol-1-yl)ethyl]-2H-pyran 2-one inhibitors of HMG-CoA reductase. 2. Effects of introducing substituents at positions three and four of the pyrrole nucleus, J. Med. Chem. 34 (1) (1991) 357–366.
[30] D.K. Lavallee, A Review of: "Porphyrins and Metalloporphyrins, K.M. Smith, Ed., Elsevier Scientific Publishing Company, New York, N.Y., 1975, 910 pp, $112.20 (hardcover), $36.50 (paperback).", Synth. React. Inorg. Met. Org. Chem. 8 (1) (1978) 97–98.
[31] S. Urban, M. Butler, R. Capon, Lamellarins O and P: new aromatic metabolites from the Australian marine sponge *Dendrilla cactos*, Aust. J. Chem. 47 (10) (1994) 1919–1924.
[32] W.Y. Yoshida, K.K. Lee, A.R. Carroll, P.J. Scheuer, A complex pyrrolo-oxazinone and its iodo derivative isolated from a tunicate, Helv. Chim. Acta 75 (5) (1992) 1721–1725.
[33] H.P. Kalmode, K.S. Vadagaonkar, K. Murugan, S. Prakash, A.C. Chaskar, Deep eutectic solvent: a simple, environmentally benign reaction media for regioselective synthesis of 2,3,4-trisubstituted 1H-pyrroles, RSC Adv. 5 (44) (2015) 35166–35174.
[34] X. Zhu, X.-P. Xu, C. Sun, T. Chen, Z.-L. Shen, S.-J. Ji, I-MCR-Ullmann cascade toward furo[2,3-b]indole scaffold, Tetrahedron 67 (34) (2011) 6375–6381.
[35] S. Jiménez-Alonso, J. Guasch, A. Estévez-Braun, I. Ratera, J. Veciana, A.G. Ravelo, Electronic and cytotoxic properties of 2-amino-naphtho[2,3-b]furan-4,9-diones, J. Org. Chem. 76 (6) (2011) 1634–1643.
[36] K. Rad-Moghadam, S.A.R. Mousazadeh Hassani, S. Toorchi Roudsari, The deep eutectic melt of sorbitol and metformin hydrochloride: synthesis of 3-substituted 2-aminonaphtho [2,3-b]furan-4,9-diones and their photophysical properties, RSC Adv. 6 (16) (2016) 13152–13159.
[37] M.R. Zanwar, V. Kavala, S.D. Gawande, C.-W. Kuo, T.-S. Kuo, M.-L. Chen, C.-H. He, C.-F. Yao, Synthesis of 3-substituted 2-aminonaphtho[2,3-b]furan-4,9-diones from 2-hydroxy-1,4-naphthoquinone and nitroalkenes, Eur. J. Org. Chem. 2013 (36) (2013) 8288–8298.
[38] K. Gewald, Zur Reaktion von α-Oxo-mercaptanen mit Nitrilen, Angew. Chem. 73 (3) (1961) 114.
[39] Y. Huang, A. Dömling, The Gewald multicomponent reaction, Mol. Divers. 15 (1) (2011) 3–33.
[40] H.Y. Meltzer, H.C. Fibiger, Olanzapine: a new atypical antipsychotic drug, Neuropsychopharmacology 14 (2) (1996) 83–85.
[41] A. Shaabani, S.E. Hooshmand, H. Afaridoun, A green chemical approach: a straightforward one-pot synthesis of 2-aminothiophene derivatives via Gewald reaction in deep eutectic solvents, Monatsh. Chem. Chem. Mon. 148 (4) (2017) 711–716.

[42] T. van Herk, J. Brussee, A.M.C.H. van den Nieuwendijk, P.A.M. van der Klein, A.P. Ijzerman, C. Stannek, A. Burmeister, A. Lorenzen, Pyrazole derivatives as partial agonists for the nicotinic acid receptor, J. Med. Chem. 46 (18) (2003) 3945–3951.
[43] V. Kryštof, P. Cankař, I. Fryšová, J. Slouka, G. Kontopidis, P. Džubák, M. Hajdúch, J. Srovnal, W.F. de Azevedo, M. Orság, M. Paprskářová, J. Rolčík, A. Látr, P.M. Fischer, M. Strnad, 4-Arylazo-3,5-diamino-1H-pyrazole CDK inhibitors: SAR study, crystal structure in complex with CDK2, selectivity, and cellular effects, J. Med. Chem. 49 (22) (2006) 6500–6509.
[44] M.J. Graneto, R.G. Kurumbail, M.L. Vazquez, H.-S. Shieh, J.L. Pawlitz, J.M. Williams, W.C. Stallings, L. Geng, A.S. Naraian, F.J. Koszyk, M.A. Stealey, X.D. Xu, R.M. Weier, G.J. Hanson, R.J. Mourey, R.P. Compton, S.J. Mnich, G.D. Anderson, J.B. Monahan, R. Devraj, Synthesis, crystal structure, and activity of pyrazole-based inhibitors of p38 kinase, J. Med. Chem. 50 (23) (2007) 5712–5719.
[45] M. Abdel-Aziz, G.E.-D.A. Abuo-Rahma, A.A. Hassan, Synthesis of novel pyrazole derivatives and evaluation of their antidepressant and anticonvulsant activities, Eur. J. Med. Chem. 44 (9) (2009) 3480–3487.
[46] M.A. Gouda, M.A. Berghot, A.I. Shoeib, A.M. Khalil, Synthesis and antimicrobial of new anthraquinone derivatives incorporating pyrazole moiety, Eur. J. Med. Chem. 45 (5) (2010) 1843–1848.
[47] O.I. El-Sabbagh, M.M. Baraka, S.M. Ibrahim, C. Pannecouque, G. Andrei, R. Snoeck, J. Balzarini, A.A. Rashad, Synthesis and antiviral activity of new pyrazole and thiazole derivatives, Eur. J. Med. Chem. 44 (9) (2009) 3746–3753.
[48] H. Bendaha, L. Yu, R. Touzani, R. Souane, G. Giaever, C. Nislow, C. Boone, S. El Kadiri, G.W. Brown, M. Bellaoui, New azole antifungal agents with novel modes of action: synthesis and biological studies of new tridentate ligands based on pyrazole and triazole, Eur. J. Med. Chem. 46 (9) (2011) 4117–4124.
[49] (a) T.S. Reddy, H. Kulhari, V.G. Reddy, V. Bansal, A. Kamal, R. Shukla, Design, synthesis and biological evaluation of 1,3-diphenyl-1H-pyrazole derivatives containing benzimidazole skeleton as potential anticancer and apoptosis inducing agents, Eur. J. Med. Chem. 101 (2015) 790–805; (b) H. Kumar, D. Saini, S. Jain, N. Jain, Pyrazole scaffold: a remarkable tool in the development of anticancer agents, Eur. J. Med. Chem. 70 (2013) 248–258.
[50] V. Kumar, K. Kaur, G.K. Gupta, A.K. Sharma, Pyrazole containing natural products: synthetic preview and biological significance, Eur. J. Med. Chem. 69 (2013) 735–753.
[51] S.B. Annes, P. Vairaprakash, S. Ramesh, TfOH mediated intermolecular electrocyclization for the synthesis of pyrazolines and its application in alkaloid synthesis, RSC Adv. 8 (53) (2018) 30071–30075.
[52] S. Sugiura, S. Ohno, O. Ohtani, K. Izumi, T. Kitamikado, H. Asai, K. Kato, M. Hori, H. Fujimura, Syntheses and antiinflammatory and hypnotic activity of 5-alkoxy-3-(N-substituted carbamoyl)-1-phenylpyrazoles. 4, J. Med. Chem. 20 (1) (1977) 80–85.
[53] K. Sujatha, G. Shanthi, N.P. Selvam, S. Manoharan, P.T. Perumal, M. Rajendran, Synthesis and antiviral activity of 4,4′-(arylmethylene)bis(1H-pyrazol-5-ols) against peste des petits ruminant virus (PPRV), Bioorg. Med. Chem. Lett. 19 (15) (2009) 4501–4503.
[54] X. Yang, P. Zhang, Y. Zhou, J. Wang, H. Liu, Synthesis and antioxidant activities of novel 4,4′-arylmethylene-bis(1H-pyrazole-5-ol)s from lignin, Chin. J. Chem. 30 (3) (2012) 670–674.
[55] D.M. Bailey, P.E. Hansen, A.G. Hlavac, E.R. Baizman, J. Pearl, A.F. DeFelice, M.E. Feigenson, 3,4-Diphenyl-1H-pyrazole-1-propanamine antidepressants, J. Med. Chem. 28 (2) (1985) 256–260.

[56] D.H. Jani, H.S. Patel, H. Keharia, C.K. Modi, Novel drug-based Fe(III) heterochelates: synthetic, spectroscopic, thermal and in-vitro antibacterial significance, Appl. Organomet. Chem. 24 (2) (2010) 99–111.
[57] B.S. Singh, H.R. Lobo, D.V. Pinjari, K.J. Jarag, A.B. Pandit, G.S. Shankarling, Ultrasound and deep eutectic solvent (DES): a novel blend of techniques for rapid and energy efficient synthesis of oxazoles, Ultrason. Sonochem. 20 (1) (2013) 287–293.
[58] R. Aryan, H. Beyzaei, M. Nojavan, M. Rezaei, Novel biocompatible glucose-based deep eutectic solvent as recyclable medium and promoter for expedient multicomponent green synthesis of diverse three and four substituted pyrazole-4-carbonitrile derivatives, Res. Chem. Intermed. 43 (8) (2017) 4731–4744.
[59] T.D. Penning, J.J. Talley, S.R. Bertenshaw, J.S. Carter, P.W. Collins, S. Docter, M.J. Graneto, L.F. Lee, J.W. Malecha, J.M. Miyashiro, R.S. Rogers, D.J. Rogier, S.S. Yu, G.D. Anderson, E.G. Burton, J.N. Cogburn, S.A. Gregory, C.M. Koboldt, W.E. Perkins, K. Seibert, A.W. Veenhuizen, Y.Y. Zhang, P.C. Isakson, Synthesis and biological evaluation of the 1,5-diarylpyrazole class of cyclooxygenase-2 inhibitors: identification of 4-[5-(4-methylphenyl)-3- (trifluoromethyl)-1H-pyrazol-1-yl] benzenesulfonamide (SC-58635, celecoxib), J. Med. Chem. 40 (9) (1997) 1347–1365.
[60] N.J. Parmar, B.R. Pansuriya, B.D. Parmar, H.A. Barad, Solvent-free, one-pot synthesis and biological evaluation of some new dipyrazolo [3,4-b:4′,3′-e]pyranylquinolones and their precursors, Med. Chem. Res. 23 (1) (2014) 42–56.
[61] A. Mobinikhaledi, N. Foroughifar, T. Mosleh, A. Hamta, Synthesis of some novel chromenopyrimidine derivatives and evaluation of their biological activities, Iran. J. Pharm. Res. 13 (3) (2014) 873–879.
[62] S.R. Mandha, S. Siliveri, M. Alla, V.R. Bommena, M.R. Bommineni, S. Balasubramanian, Eco-friendly synthesis and biological evaluation of substituted pyrano[2,3-c]pyrazoles, Bioorg. Med. Chem. Lett. 22 (16) (2012) 5272–5278.
[63] H. Junek, H. Aigner, Synthesen mit Nitrilen, XXXV. Reaktionen von Tetracyanäthylen mit Heterocyclen, Chem. Ber. 106 (3) (1973) 914–921.
[64] A.H. Abdel-Rahman, E.M. Keshk, M.A. Hanna, S.M. El-Bady, Synthesis and evaluation of some new spiro indoline-based heterocycles as potentially active antimicrobial agents, Bioorg. Med. Chem. 12 (9) (2004) 2483–2488.
[65] S.M. Bensaber, H.A. Allafe, N.B. Ermeli, S.B. Mohamed, A.A. Zetrini, S.G. Alsabri, M. Erhuma, A. Hermann, M.I. Jaeda, A.M. Gbaj, Chemical synthesis, molecular modelling, and evaluation of anticancer activity of some pyrazol-3-one Schiff base derivatives, Med. Chem. Res. 23 (12) (2014) 5120–5134.
[66] D. Kaushik, R. Kumar, S.A. Khan, G. Chawla, Pharmacological screening for anti-inflammatory, analgesic activity of pyrazolyl derivatives along with molecular docking studies, Med. Chem. Res. 21 (11) (2012) 3646–3655.
[67] K. Yamamoto, M. Fujita, K. Tabashi, Y. Kawashima, E. Kato, M. Oya, T. Iso, J. Iwao, Novel calcium antagonists. Synthesis and structure-activity relationship studies of benzothiazoline derivatives, J. Med. Chem. 31 (5) (1988) 919–930.
[68] A. Dandia, D. Saini, S. Bhaskaran, D.K. Saini, Ultrasound promoted green synthesis of spiro[pyrano[2,3-c]pyrazoles] as antioxidant agents, Med. Chem. Res. 23 (2) (2014) 725–734.
[69] N. Foloppe, L.M. Fisher, R. Howes, A. Potter, A.G.S. Robertson, A.E. Surgenor, Identification of chemically diverse Chk1 inhibitors by receptor-based virtual screening, Bioorg. Med. Chem. 14 (14) (2006) 4792–4802.
[70] M.G. Dehbalaei, N. Foroughifar, H. Pasdar, A. Khajeh-Amiri, N. Foroughifar, M. Alikarami, Choline chloride based thiourea catalyzed highly efficient, eco-friendly

synthesis and anti-bacterial evaluation of some new 6-amino-4-aryl-2,4-dihydro-3-phenyl pyrano [2,3-c] pyrazole-5-carbonitrile derivatives, Res. Chem. Intermed. 43 (5) (2017) 3035–3051.

[71] A.V. Stachulski, N.G. Berry, A.C. Lilian Low, S.L. Moores, E. Row, D.C. Warhurst, I.S. Adagu, J.-F. Rossignol, Identification of isoflavone derivatives as effective anti-cryptosporidial agents in vitro and in vivo, J. Med. Chem. 49 (4) (2006) 1450–1454.

[72] P.W. Smith, S.L. Sollis, P.D. Howes, P.C. Cherry, I.D. Starkey, K.N. Cobley, H. Weston, J. Scicinski, A. Merritt, A. Whittington, P. Wyatt, N. Taylor, D. Green, R. Bethell, S. Madar, R.J. Fenton, P.J. Morley, T. Pateman, A. Beresford, Dihydropyran-carboxamides related to zanamivir: a new series of inhibitors of influenza virus sialidases. 1. Discovery, synthesis, biological activity, and structure – activity relationships of 4-guanidino- and 4-amino-4H-pyran-6-carboxamides, J. Med. Chem. 41 (6) (1998) 787–797.

[73] J.L. Wang, D. Liu, Z.J. Zhang, S. Shan, X. Han, S.M. Srinivasula, C.M. Croce, E.S. Alnemri, Z. Huang, Structure-based discovery of an organic compound that binds Bcl-2 protein and induces apoptosis of tumor cells, Proc. Natl. Acad. Sci. U. S. A. 97 (13) (2000) 7124–7129.

[74] S.C. Kuo, L.J. Huang, H. Nakamura, Studies on heterocyclic compounds. 6. Synthesis and analgesic and antiinflammatory activities of 3,4-dimethylpyrano[2,3-c] pyrazol-6-one derivatives, J. Med. Chem. 27 (4) (1984) 539–544.

[75] M.R. Bhosle, L.D. Khillare, S.T. Dhumal, R.A. Mane, A facile synthesis of 6-amino-2H, 4H-pyrano[2,3-c]pyrazole-5-carbonitriles in deep eutectic solvent, Chin. Chem. Lett. 27 (3) (2016) 370–374.

[76] Sanam, K. Bux, M. al-Rashida, R.D. Alharthy, S.T. Moin, A. Hameed, Morpholinium and piperidinium based deep eutectic solvents for synthesis of pyrazole-5-carbonitriles, indoles and tetrazoles: bulk properties via molecular dynamics simulations, ChemistrySelect 3 (45) (2018) 12907–12917.

[77] (a) F.T. Greenaway, L.M. Brown, J.C. Dabrowiak, M.R. Thompson, V.W. Day, Copper (II) complexes of the antiulcer drug cimetidine, J. Am. Chem. Soc. 102 (26) (1980) 7782–7784; (b) C. Wagner, V.C. Barth, S.D. de Oliveira, M.M. Campos, Effectiveness of the proton pump inhibitor omeprazole associated with calcium hydroxide as intracanal medication: an in vivo study, J. Endod. 37 (9) (2011) 1253–1257; (c) X.-Q. Wang, L.-X. Liu, Y. Li, C.-J. Sun, W. Chen, L. Li, H.-B. Zhang, X.-D. Yang, Design, synthesis and biological evaluation of novel hybrid compounds of imidazole scaffold-based 2-benzylbenzofuran as potent anticancer agents, Eur. J. Med. Chem. 62 (2013) 111–121.

[78] N. Aziizi, Z. Manochehri, A. Nahayi, S. Torkashvand, A facile one-pot synthesis of tetrasubstituted imidazoles catalyzed by eutectic mixture stabilized ferrofluid, J. Mol. Liq. 196 (2014) 153–158.

[79] L. Wang, X. Zhong, M. Zhou, W.-y. Zhou, Q. Chen, M.-Y. He, One-pot synthesis of polysubstituted imidazoles in a Brønsted acidic deep eutectic solvent, J. Chem. Res. 37 (4) (2013) 236–238.

[80] A. Mobinikhaledi, A.K. Amiri, One-pot synthesis of tri- and tetrasubstituted imidazoles using eutectic salts as ionic liquid catalyst, Res. Chem. Intermed. 41 (4) (2015) 2063–2070.

[81] M. Meusel, M. Gütschow, Recent developments in hydantoin chemistry. A review, Org. Prep. Proced. Int. 36 (5) (2004) 391–443.

[82] (a) J.C. Thenmozhiyal, P.T.-H. Wong, W.-K. Chui, Anticonvulsant activity of phenylmethylenehydantoins: a structure – activity relationship study, J. Med. Chem. 47 (6) (2004) 1527–1535; (b) M.A. Khanfar, K.A. El Sayed, Phenylmethylene

hydantoins as prostate cancer invasion and migration inhibitors. CoMFA approach and QSAR analysis, Eur. J. Med. Chem. 45 (11) (2010) 5397–5405.

[83] (a) F.L. Wessels, T.J. Schwan, S.F. Pong, Synthesis and antidepressant activity of 5- (4-dimethylaminobenzyl)imidazolidine-2,4-dione, J. Pharm. Sci. 69 (9) (1980) 1102–1104; (b) A.G. Caldwell, C.J. Harris, R. Stepney, N. Whittaker, Heterocyclic prostaglandin analogues. Part 2. Hydantoins and other imidazole analogues, J. Chem. Soc., Perkin Trans. 1 (1980) 495–505.

[84] (a) H. Rmedi, A. Baklouti, A new approach for the synthesis of N-sulfonyl hydantoins, Tetrahedron Lett. 55 (26) (2014) 3585–3587; (b) V. Mehra, V. Kumar, Facile diastereoselective synthesis of functionally enriched hydantoins via base-promoted intramolecular amidolysis of C-3 functionalized azetidin-2-ones, Tetrahedron Lett. 54 (45) (2013) 6041–6044; (c) J. Charton, S. Delarue, S. Vendeville, M.-A. Debreu-Fontaine, S. Girault-Mizzi, C. Sergheraert, Convenient synthesis of tetrahydroisoquinoline-hydantoins, Tetrahedron Lett. 42 (43) (2001) 7559–7561.

[85] M. Beller, M. Eckert, W.A. Moradi, H. Neumann, Palladium-catalyzed synthesis of substituted hydantoins—a new carbonylation reaction for the synthesis of amino acid derivatives, Angew. Chem. Int. Ed. 38 (10) (1999) 1454–1457.

[86] J. Matthews, R.A. Rivero, Base-promoted solid-phase synthesis of substituted hydantoins and thiohydantoins, J. Org. Chem. 62 (17) (1997) 6090–6092.

[87] T. Miura, Y. Mikano, M. Murakami, Nickel-catalyzed synthesis of 1,3,5-trisubstituted hydantoins from acrylates and isocyanates, Org. Lett. 13 (14) (2011) 3560–3563.

[88] J.M. Ignacio, S. Macho, S. Marcaccini, R. Pepino, T. Torroba, A facile synthesis of 1,3,5-trisubstituted hydantoins via Ugi four-component condensation, Synlett 2005 (20) (2005) 3051–3054.

[89] A. Volonterio, C. Ramirez de Arellano, M. Zanda, Synthesis of 1,3,5-trisubstituted hydantoins by regiospecific domino condensation/aza-Michael/O→N acyl migration of carbodiimides with activated α,β-unsaturated carboxylic acids, J. Org. Chem. 70 (6) (2005) 2161–2170.

[90] D. Zhang, X. Xing, G.D. Cuny, Synthesis of hydantoins from enantiomerically pure α-amino amides without epimerization, J. Org. Chem. 71 (4) (2006) 1750–1753.

[91] S. Gore, K. Chinthapally, S. Baskaran, B. König, Synthesis of substituted hydantoins in low melting mixtures, Chem. Commun. 49 (44) (2013) 5052–5054.

[92] (a) G. Lopopolo, F. Fiorella, M. de Candia, O. Nicolotti, S. Martel, P.-A. Carrupt, C. Altomare, Biarylmethoxy isonipecotanilides as potent and selective inhibitors of blood coagulation factor Xa, Eur. J. Pharm. Sci. 42 (3) (2011) 180–191; (b) S. Castellano, D. Kuck, M. Viviano, J. Yoo, F. López-Vallejo, P. Conti, L. Tamborini, A. Pinto, J.L. Medina-Franco, G. Sbardella, Synthesis and biochemical evaluation of Δ2-isoxazoline derivatives as DNA methyltransferase 1 inhibitors, J. Med. Chem. 54 (21) (2011) 7663–7677; (c) S.S. Panda, P.V.R. Chowdary, B.S. Jayashree, Synthesis, antiinflammatory and antibacterial activity of novel indolyl-isoxazoles, Indian J. Pharm. Sci. 71 (6) (2009) 684–687; (d) K.-Y. Dong, H.-T. Qin, X.-X. Bao, F. Liu, C. Zhu, Oxime-mediated facile access to 5-methylisoxazoles and applications in the synthesis of valdecoxib and oxacillin, Org. Lett. 16 (20) (2014) 5266–5268.

[93] J.M. Pérez, D.J. Ramón, Synthesis of 3,5-disubstituted isoxazoles and isoxazolines in deep eutectic solvents, ACS Sustain. Chem. Eng. 3 (9) (2015) 2343–2349.

[94] A.C. Giddens, H.I.M. Boshoff, S.G. Franzblau, C.E. Barry, B.R. Copp, Antimycobacterial natural products: synthesis and preliminary biological evaluation of the oxazole-containing alkaloid texaline, Tetrahedron Lett. 46 (43) (2005) 7355–7357.

[95] H.H. Wasserman, R.J. Gambale, Synthesis of (+)-antimycin A3. Use of the oxazole ring in protecting and activating functions, J. Am. Chem. Soc. 107 (5) (1985) 1423–1424.
[96] I.H. Leaver, B. Milligan, Fluorescent whitening agents—a survey (1974-82), Dyes Pigments 5 (2) (1984) 109–144.
[97] B.S. Singh, H.R. Lobo, D.V. Pinjari, K.J. Jarag, A.B. Pandit, G.S. Shankarling, Comparative material study and synthesis of 4-(4-nitrophenyl)oxazol-2-amine via sonochemical and thermal method, Ultrason. Sonochem. 20 (2) (2013) 633–639.
[98] (a) W.C. Patt, H.W. Hamilton, M.D. Taylor, M.J. Ryan, D.G. Taylor, C.J.C. Connolly, A.M. Doherty, S.R. Klutchko, I. Sircar, Structure-activity relationships of a series of 2-amino-4-thiazole-containing renin inhibitors, J. Med. Chem. 35 (14) (1992) 2562–2572; (b) J.C. Jaen, L.D. Wise, B.W. Caprathe, H. Tecle, S. Bergmeier, C.C. Humblet, T.G. Heffner, L.T. Meltzer, T.A. Pugsley, 4-(1,2,5,6-Tetrahydro-1-alkyl-3-pyridinyl)-2-thiazolamines: a novel class of compounds with central dopamine agonist properties, J. Med. Chem. 33 (1) (1990) 311–317; (c) F.W. Bell, A. S. Cantrell, M. Hoegberg, S.R. Jaskunas, N.G. Johansson, C.L. Jordan, M.D. Kinnick, P. Lind, J.M. Morin, Phenethylthiazolethiourea (PETT) compounds, a new class of HIV-1 reverse transcriptase inhibitors. 1. Synthesis and basic structure-activity relationship studies of PETT analogs, J. Med. Chem. 38 (25) (1995) 4929–4936.
[99] (a) B.E. Fink, D.S. Mortensen, S.R. Stauffer, Z.D. Aron, J.A. Katzenellenbogen, Novel structural templates for estrogen-receptor ligands and prospects for combinatorial synthesis of estrogens, Chem. Biol. 6 (4) (1999) 205–219; (b) J.E. van Muijlwijk-Koezen, H. Timmerman, R.C. Vollinga, J. Frijtag von Drabbe Künzel, M. de Groote, S. Visser, A.P. Ijzerman, Thiazole and thiadiazole analogues as a novel class of adenosine receptor antagonists, J. Med. Chem. 44 (5) (2001) 749–762.
[100] (a) B. Das, V. Saidi Reddy, R. Ramu, A rapid and high-yielding synthesis of thiazoles and aminothiazoles using ammonium-12-molybdophosphate, J. Mol. Catal. A Chem. 252 (1) (2006) 235–237; (b) M. Narender, M.S. Reddy, R. Sridhar, Y.V.D. Nageswar, K.R. Rao, Aqueous phase synthesis of thiazoles and aminothiazoles in the presence of β-cyclodextrin, Tetrahedron Lett. 46 (35) (2005) 5953–5955.
[101] T.M. Potewar, S.A. Ingale, K.V. Srinivasan, Efficient synthesis of 2,4-disubstituted thiazoles using ionic liquid under ambient conditions: a practical approach towards the synthesis of Fanetizole, Tetrahedron 63 (45) (2007) 11066–11069.
[102] H.R. Lobo, B.S. Singh, G.S. Shankarling, Lipase and deep eutectic mixture catalyzed efficient synthesis of thiazoles in water at room temperature, Catal. Lett. 142 (11) (2012) 1369–1375.
[103] (a) M. D'Hooghe, N. De Kimpe, Synthetic approaches towards 2-iminothiazolidines: an overview, Tetrahedron 62 (4) (2006) 513–535; (b) D.R. St. Laurent, Q. Gao, D. Wu, M.H. Serrano-Wu, Regioselective synthesis of 3-(heteroaryl)-iminothiazolidin-4-ones, Tetrahedron Lett. 45 (9) (2004) 1907–1910.
[104] D.N. Pansare, N.A. Mulla, C.D. Pawar, V.R. Shende, D.B. Shinde, One pot three components microwave assisted and conventional synthesis of new 3-(4-chloro-2-hydroxyphenyl)-2-(substituted) thiazolidin-4-one as antimicrobial agents, Bioorg. Med. Chem. Lett. 24 (15) (2014) 3569–3573.
[105] S.A. El Bialy, M.M. Nagy, H.M. Abdel-Rahman, Efficient regioselective three-component domino synthesis of 3-(1,2,4-triazol-5-yl)-1,3-thiazolidin-4-ones as potent antifungal and antituberculosis agents, Arch. Pharm. 344 (12) (2011) 821–829.
[106] L.D. Khillare, M.R. Bhosle, A.R. Deshmukh, R.A. Mane, Synthesis and anti-inflammatory evaluation of new pyrazoles bearing biodynamic thiazole and thiazolidinone scaffolds, Med. Chem. Res. 24 (4) (2015) 1380–1386.

[107] V. Murugesan, V.S. Tiwari, R. Saxena, R. Tripathi, R. Paranjape, S. Kulkarni, N. Makwana, R. Suryawanshi, S.B. Katti, Lead optimization at C-2 and N-3 positions of thiazolidin-4-ones as HIV-1 non-nucleoside reverse transcriptase inhibitors, Bioorg. Med. Chem. 19 (22) (2011) 6919–6926.
[108] C.M. Bhalgat, P.V. Darda, K.G. Bothara, S.V. Bhandari, J. Gandhi, B. Ramesh, Synthesis and pharmacological screening of some novel anti-hypertensive agents possessing 5-benzylidene-2-(phenylimino)-thiazolidin-4-one ring, Eur. J. Med. Chem. 76 (2014) 580–588.
[109] R.V. Shingalapur, K.M. Hosamani, R.S. Keri, M.H. Hugar, Derivatives of benzimidazole pharmacophore: synthesis, anticonvulsant, antidiabetic and DNA cleavage studies, Eur. J. Med. Chem. 45 (5) (2010) 1753–1759.
[110] G. Çakır, İ. Küçükgüzel, R. Guhamazumder, E. Tatar, D. Manvar, A. Basu, B.A. Patel, J. Zia, T.T. Talele, N. Kaushik-Basu, Novel 4-thiazolidinones as non-nucleoside inhibitors of hepatitis C virus NS5B RNA-dependent RNA polymerase, Arch. Pharm. 348 (1) (2015) 10–22.
[111] S. Raza, S.P. Srivastava, D.S. Srivastava, A.K. Srivastava, W. Haq, S.B. Katti, Thiazolidin-4-one and thiazinan-4-one derivatives analogous to rosiglitazone as potential antihyperglycemic and antidyslipidemic agents, Eur. J. Med. Chem. 63 (2013) 611–620.
[112] A.M. Isloor, D. Sunil, P. Shetty, S. Malladi, K.S.R. Pai, N. Maliyakkl, Synthesis, characterization, anticancer, and antioxidant activity of some new thiazolidin-4-ones in MCF-7 cells, Med. Chem. Res. 22 (2) (2013) 758–767.
[113] A. Kunzler, P.D. Neuenfeldt, A.M. das Neves, C.M.P. Pereira, G.H. Marques, P.S. Nascente, M.H.V. Fernandes, S.O. Hübner, W. Cunico, Synthesis, antifungal and cytotoxic activities of 2-aryl-3-((piperidin-1-yl)ethyl)thiazolidinones, Eur. J. Med. Chem. 64 (2013) 74–80.
[114] K.S. Sharath Kumar, A. Hanumappa, M. Hegde, K.H. Narasimhamurthy, S.C. Raghavan, K.S. Rangappa, Synthesis and antiproliferative effect of novel 4-thiazolidinone-, pyridine- and piperazine-based conjugates on human leukemic cells, Eur. J. Med. Chem. 81 (2014) 341–349.
[115] J. Blanchet, J. Zhu, Reeve's synthesis of 2-imino-4-thiazolidinone from alkyl (aryl) trichloromethylcarbinol revisited, a three-component process from aldehyde, chloroform and thiourea, Tetrahedron Lett. 45 (23) (2004) 4449–4452.
[116] A. Mobinikhaledi, A.K. Amiri, Natural eutectic salts catalyzed one-pot synthesis of 5-arylidene-2-imino-4-thiazolidinones, Res. Chem. Intermed. 39 (3) (2013) 1491–1498.
[117] D.V. Jawale, U.R. Pratap, R.A. Mane, An alternative synthetic route for an antidiabetic drug, rosiglitazone, Bioorg. Med. Chem. Lett. 22 (2) (2012) 924–928.
[118] D.B. Yedage, D.V. Patil, Environmentally benign deep eutectic solvent for synthesis of 1,3-thiazolidin-4-ones, ChemistrySelect 3 (13) (2018) 3611–3614.
[119] M.J. Genin, D.A. Allwine, D.J. Anderson, M.R. Barbachyn, D.E. Emmert, S.A. Garmon, D.R. Graber, K.C. Grega, J.B. Hester, D.K. Hutchinson, J. Morris, R.J. Reischer, C.W. Ford, G.E. Zurenko, J.C. Hamel, R.D. Schaadt, D. Stapert, B.H. Yagi, Substituent effects on the antibacterial activity of nitrogen−carbon-linked (azolylphenyl) oxazolidinones with expanded activity against the fastidious gram-negative organisms *Haemophilus influenzae* and *Moraxella catarrhalis*, J. Med. Chem. 43 (5) (2000) 953–970.
[120] D.R. Buckle, D.J. Outred, C.J.M. Rockell, H. Smith, B.A. Spicer, Studies on v-triazoles. 7. Antiallergic 9-oxo-1H,9H-benzopyrano[2,3-d]-v-triazoles, J. Med. Chem. 26 (2) (1983) 251–254.

[121] V. Calderone, I. Giorgi, O. Livi, E. Martinotti, E. Mantuano, A. Martelli, A. Nardi, Benzoyl and/or benzyl substituted 1,2,3-triazoles as potassium channel activators. VIII, Eur. J. Med. Chem. 40 (6) (2005) 521–528.

[122] (a) K. Dabak, Ö. Sezer, A. Akar, O. Anaç, Synthesis and investigation of tuberculosis inhibition activities of some 1,2,3-triazole derivatives, Eur. J. Med. Chem. 38 (2) (2003) 215–218; (b) J. Xie, C.T. Seto, A two stage click-based library of protein tyrosine phosphatase inhibitors, Bioorg. Med. Chem. 15 (1) (2007) 458–473.

[123] S.B. Coffey, G. Aspnes, A.T. Londregan, Expedient synthesis of N1-substituted triazole peptidomimetics, ACS Comb. Sci. 17 (12) (2015) 706–709.

[124] M.A.P. Martins, G.C. Paveglio, L.V. Rodrigues, C.P. Frizzo, N. Zanatta, H.G. Bonacorso, Promotion of 1,3-dipolar cycloaddition between azides and β-enaminones by deep eutectic solvents, New J. Chem. 40 (7) (2016) 5989–5992.

[125] A. Altaf, A. Shahzad, Z. Gul, N. Rasool, A. Badshah, D.B. Lal Bhatia, E. Khan, A review on the medicinal importance of pyridine derivatives, J. Drug Des. Med. Chem. 1 (2015) 1–11.

[126] P. Thapa, R. Karki, M. Yun, T.M. Kadayat, E. Lee, H.B. Kwon, Y. Na, W.-J. Cho, N. D. Kim, B.-S. Jeong, Y. Kwon, E.-S. Lee, Design, synthesis, and antitumor evaluation of 2,4,6-triaryl pyridines containing chlorophenyl and phenolic moiety, Eur. J. Med. Chem. 52 (2012) 123–136.

[127] S. S. Kamble, G. S. Shankarling, Amalgamation of CSR and DES: an energy efficient protocol for the one-pot synthesis of 2,4,6-triaryl pyridine derivatives, ChemistrySelect 3 (37) (2018) 10464–10467.

[128] T.R.K. Reddy, R. Mutter, W. Heal, K. Guo, V.J. Gillet, S. Pratt, B. Chen, Library design, synthesis, and screening: pyridine dicarbonitriles as potential prion disease therapeutics, J. Med. Chem. 49 (2) (2006) 607–615.

[129] B.C.H. May, J.A. Zorn, J. Witkop, J. Sherrill, A.C. Wallace, G. Legname, S.B. Prusiner, F.E. Cohen, Structure – activity relationship study of prion inhibition by 2-aminopyridine-3,5-dicarbonitrile-based compounds: parallel synthesis, bioactivity, and in vitro pharmacokinetics, J. Med. Chem. 50 (1) (2007) 65–73.

[130] (a) Y. Gu, Multicomponent reactions in unconventional solvents: state of the art, Green Chem. 14 (8) (2012) 2091–2128; (b) N.M. Evdokimov, A.S. Kireev, A. A. Yakovenko, M.Y. Antipin, I.V. Magedov, A. Kornienko, One-step synthesis of heterocyclic privileged medicinal scaffolds by a multicomponent reaction of malononitrile with aldehydes and thiols, J. Org. Chem. 72 (9) (2007) 3443–3453; (c) B.C. Ranu, R. Jana, S. Sowmiah, An improved procedure for the three-component synthesis of highly substituted pyridines using ionic liquid, J. Org. Chem. 72 (8) (2007) 3152–3154.

[131] N. Azizi, M.S. Haghayegh, Greener and additive-free reactions in deep eutectic solvent: one-pot, three-component synthesis of highly substituted pyridines, ChemistrySelect 2 (28) (2017) 8870–8873.

[132] S. Cihat, S. Rahime, Fused 1,4-dihydropyridines as potential calcium modulatory compounds, Mini-Rev. Med. Chem. 6 (7) (2006) 747–755.

[133] (a) A. Hilgeroth, H. Lilie, Structure-activity relationships of first bishydroxymethyl-substituted cage dimeric 4-aryl-1,4-dihydropyridines as HIV-1 protease inhibitors, Eur. J. Med. Chem. 38 (5) (2003) 495–499; (b) M. Kawase, A. Shah, H. Gaveriya, N. Motohashi, H. Sakagami, A. Varga, J. Molnár, 3,5-Dibenzoyl-1,4-dihydropyridines: synthesis and MDR reversal in tumor cells, Bioorg. Med. Chem. 10 (4) (2002) 1051–1055; (c) N. Edraki, A.R. Mehdipour, M. Khoshneviszadeh, R. Miri, Dihydropyridines: evaluation of their current and future pharmacological applications,

Drug Discov. Today 14 (21) (2009) 1058–1066; (d) F. Cateni, M. Zacchigna, N. Pedemonte, L.J.V. Galietta, M.T. Mazzei, P. Fossa, M. Giampieri, M. Mazzei, Synthesis of 4-thiophen-2′-yl-1,4-dihydropyridines as potentiators of the CFTR chloride channel, Bioorg. Med. Chem. 17 (23) (2009) 7894–7903.

[134] B. Loev, M.M. Goodman, K.M. Snader, R. Tedeschi, E. Macko, Hantzsch-type dihydropyridine hypotensive agents, J. Med. Chem. 17 (9) (1974) 956–965.

[135] S. Pednekar, R. Bhalerao, N. Ghadge, One-pot multi-component synthesis of 1,4-dihydropyridine derivatives in biocompatible deep eutectic solvents, J. Chem. Sci. 125 (3) (2013) 615–621.

[136] T.H. Al-Tel, R.A. Al-Qawasmeh, R. Zaarour, Design, synthesis and in vitro antimicrobial evaluation of novel imidazo[1,2-a]pyridine and imidazo[2,1-b][1,3]benzothiazole motifs, Eur. J. Med. Chem. 46 (5) (2011) 1874–1881.

[137] J.-M. Chezal, J. Paeshuyse, V. Gaumet, D. Canitrot, A. Maisonial, C. Lartigue, A. Gueiffier, E. Moreau, J.-C. Teulade, O. Chavignon, J. Neyts, Synthesis and antiviral activity of an imidazo[1,2-a]pyrrolo[2,3-c]pyridine series against the bovine viral diarrhea virus, Eur. J. Med. Chem. 45 (5) (2010) 2044–2047.

[138] G.C. Moraski, L.D. Markley, P.A. Hipskind, H. Boshoff, S. Cho, S.G. Franzblau, M.J. Miller, Advent of imidazo[1,2-a]pyridine-3-carboxamides with potent multi- and extended drug resistant antituberculosis activity, ACS Med. Chem. Lett. 2 (6) (2011) 466–470.

[139] G.C. Moraski, L.D. Markley, M. Chang, S. Cho, S.G. Franzblau, C.H. Hwang, H. Boshoff, M.J. Miller, Generation and exploration of new classes of antitubercular agents: the optimization of oxazolines, oxazoles, thiazolines, thiazoles to imidazo [1,2-a]pyridines and isomeric 5,6-fused scaffolds, Bioorg. Med. Chem. 20 (7) (2012) 2214–2220.

[140] T.H. Al-Tel, R.A. Al-Qawasmeh, Post Groebke–Blackburn multicomponent protocol: synthesis of new polyfunctional imidazo[1,2-a]pyridine and imidazo[1,2-a]pyrimidine derivatives as potential antimicrobial agents, Eur. J. Med. Chem. 45 (12) (2010) 5848–5855.

[141] S. Matsumoto, N. Miyamoto, T. Hirayama, H. Oki, K. Okada, M. Tawada, H. Iwata, K. Nakamura, S. Yamasaki, H. Miki, A. Hori, S. Imamura, Structure-based design, synthesis, and evaluation of imidazo[1,2-b]pyridazine and imidazo[1,2-a]pyridine derivatives as novel dual c-Met and VEGFR2 kinase inhibitors, Bioorg. Med. Chem. 21 (24) (2013) 7686–7698.

[142] R. Ducray, C.D. Jones, F.H. Jung, I. Simpson, J. Curwen, M. Pass, Novel imidazo[1,2-a] pyridine based inhibitors of the IGF-1 receptor tyrosine kinase: optimization of the aniline, Bioorg. Med. Chem. Lett. 21 (16) (2011) 4702–4704.

[143] Y. Terao, H. Suzuki, M. Yoshikawa, H. Yashiro, S. Takekawa, Y. Fujitani, K. Okada, Y. Inoue, Y. Yamamoto, H. Nakagawa, S. Yao, T. Kawamoto, O. Uchikawa, Design and biological evaluation of imidazo[1,2-a]pyridines as novel and potent ASK1 inhibitors, Bioorg. Med. Chem. Lett. 22 (24) (2012) 7326–7329.

[144] S. Ulloora, R. Shabaraya, A.V. Adhikari, Facile synthesis of new imidazo[1,2-a] pyridines carrying 1,2,3-triazoles via click chemistry and their antiepileptic studies, Bioorg. Med. Chem. Lett. 23 (11) (2013) 3368–3372.

[145] J. Lu, X.-T. Li, E.-Q. Ma, L.-P. Mo, Z.-H. Zhang, Superparamagnetic CuFeO2 nanoparticles in deep eutectic solvent: an efficient and recyclable catalytic system for the synthesis of imidazo[1,2-a]pyridines, ChemCatChem 6 (10) (2014) 2854–2859.

[146] N. Azizi, S. Dezfooli, Catalyst-free synthesis of imidazo [1,2-a] pyridines via Groebke multicomponent reaction, Environ. Chem. Lett. 14 (2) (2016) 201–206.

[147] A. Ghaedi, G.R. Bardajee, A. Mirshokrayi, M. Mahdavi, A. Shafiee, T. Akbarzadeh, Facile, novel and efficient synthesis of new pyrazolo[3,4-b]pyridine products from condensation of pyrazole-5-amine derivatives and activated carbonyl groups, RSC Adv. 5 (109) (2015) 89652–89658.
[148] J. Chen, W. Liu, J. Ma, H. Xu, J. Wu, X. Tang, Z. Fan, P. Wang, Synthesis and properties of fluorescence dyes: tetracyclic pyrazolo[3,4-b]pyridine-based coumarin chromophores with intramolecular charge transfer character, J. Org. Chem. 77 (7) (2012) 3475–3482.
[149] S. P Patil, D. P Shelar, R. Toche, Synthesis of pyrazolopyridine annulated heterocycles and study the effect of substituents on photophysical properties, J. Fluoresc. 22 (2011) 31–41.
[150] M.S. Salem, M.A. Ali, Novel pyrazolo[3,4-b]pyridine derivatives: synthesis, characterization, antimicrobial and antiproliferative profile, Biol. Pharm. Bull. 39 (4) (2016) 473–483.
[151] P. Nagender, G. Malla Reddy, R. Naresh Kumar, Y. Poornachandra, C. Ganesh Kumar, B. Narsaiah, Synthesis, cytotoxicity, antimicrobial and anti-biofilm activities of novel pyrazolo[3,4-b]pyridine and pyrimidine functionalized 1,2,3-triazole derivatives, Bioorg. Med. Chem. Lett. 24 (13) (2014) 2905–2908.
[152] M.A. El-borai, H.F. Rizk, M.F. Abd-Aal, I.Y. El-Deeb, Synthesis of pyrazolo[3,4-b] pyridines under microwave irradiation in multi-component reactions and their antitumor and antimicrobial activities—Part 1, Eur. J. Med. Chem. 48 (2012) 92–96.
[153] M.A. El-Borai, H.F. Rizk, D.M. Beltagy, I.Y. El-Deeb, Microwave-assisted synthesis of some new pyrazolopyridines and their antioxidant, antitumor and antimicrobial activities, Eur. J. Med. Chem. 66 (2013) 415–422.
[154] A. Ramzan, S. Siddiqui, A. Irfan, A.G. Al-Sehemi, A. Ahmad, F. Verpoort, A.H. Chughtai, M.A. Khan, M.A. Munawar, M.A.R. Basra, Antiplatelet activity, molecular docking and QSAR study of novel N′-arylmethylidene-3-methyl-1-phenyl-6-p-chlorophenyl-1H-pyrazolo[3,4-b] pyridine-4-carbohydrazides, Med. Chem. Res. 27 (2) (2018) 388–405.
[155] J. Quiroga, Y. Villarreal, J. Galvez, A. Ortiz, B. Insuasty, R. Abonia, M. Raimondi, S. Zacchino, Synthesis and antifungal in vitro evaluation of pyrazolo[3,4-b]pyridines derivatives obtained by Aza-Diels-Alder reaction and microwave irradiation, Chem. Pharm. Bull. (Tokyo) 65 (2) (2017) 143–150.
[156] P. Nagender, R. Naresh Kumar, G. Malla Reddy, D. Krishna Swaroop, Y. Poornachandra, C. Ganesh Kumar, B. Narsaiah, Synthesis of novel hydrazone and azole functionalized pyrazolo[3,4-b]pyridine derivatives as promising anticancer agents, Bioorg. Med. Chem. Lett. 26 (18) (2016) 4427–4432.
[157] D. Behnke, S. Cotesta, S. Hintermann, M. Fendt, C.E. Gee, L.H. Jacobson, G. Laue, A. Meyer, T. Wagner, S. Badiger, V. Chaudhari, M. Chebrolu, C. Pandit, D. Hoyer, C. Betschart, Discovery of 1H-pyrazolo[3,4-b]pyridines as potent dual orexin receptor antagonists (DORAs), Bioorg. Med. Chem. Lett. 25 (23) (2015) 5555–5560.
[158] N. Liu, Y. Wang, G. Huang, C. Ji, W. Fan, H. Li, Y. Cheng, H. Tian, Design, synthesis and biological evaluation of 1H-pyrrolo[2,3-b]pyridine and 1H-pyrazolo[3,4-b]pyridine derivatives as c-Met inhibitors, Bioorg. Chem. 65 (2016) 146–158.
[159] B. Zhao, Y. Li, P. Xu, Y. Dai, C. Luo, Y. Sun, J. Ai, M. Geng, W. Duan, Discovery of substituted 1H-pyrazolo[3,4-b]pyridine derivatives as potent and selective FGFR kinase inhibitors, ACS Med. Chem. Lett. 7 (6) (2016) 629–634.
[160] M. Zhang, P. Liu, Y.-H. Liu, Z.-R. Shang, H.-C. Hu, Z.-H. Zhang, Magnetically separable graphene oxide anchored sulfonic acid: a novel, highly efficient and recyclable

catalyst for one-pot synthesis of 3,6-di(pyridin-3-yl)-1H-pyrazolo[3,4-b] pyridine-5-carbonitriles in deep eutectic solvent under microwave irradiation, RSC Adv. 6 (108) (2016) 106160–106170.

[161] (a) M. Johar, T. Manning, D.Y. Kunimoto, R. Kumar, Synthesis and in vitro antimycobacterial activity of 5-substituted pyrimidine nucleosides, Bioorg. Med. Chem. 13 (24) (2005) 6663–6671; (b) N. Azas, P. Rathelot, S. Djekou, F. Delmas, A. Gellis, C. Di Giorgio, P. Vanelle, P. Timon-David, Antiparasitic activity of highly conjugated pyrimidine-2,4-dione derivatives, Il Farmaco 58 (12) (2003) 1263–1270; (c) A. Agarwal, K. Srivastava, S.K. Puri, P.M.S. Chauhan, Synthesis of 2,4,6-trisubstituted pyrimidines as antimalarial agents, Bioorg. Med. Chem. 13 (15) (2005) 4645–4650.

[162] N.A. Abdel-Latif, N.M. Sabry, A.M. Mohamed, M.M. Abdulla, Synthesis, analgesic, and antiparkinsonian profiles of some pyridine, pyrazoline, and thiopyrimidine derivatives, Monatsh. Chem. Chem. Mon. 138 (7) (2007) 715–724.

[163] (a) R. Gompper, H.-J. Mair, K. Polborn, Synthesis of oligo(diazaphenyls). Tailor-made fluorescent heteroaromatics and pathways to nanostructures, Synthesis 1997 (06) (1997) 696–718; (b) K. Takaki, K. Takashi, S. Nobuo, K. Isao, K. Kenji, Y. Takakazu, Preparation and properties of highly electron-accepting poly(pyrimidine-2,5-diyl), Chem. Lett. 21 (4) (1992) 583–586.

[164] K.-T. Wong, T.S. Hung, Y. Lin, C.-C. Wu, G.-H. Lee, S.-M. Peng, C.H. Chou, Y.O. Su, Suzuki coupling approach for the synthesis of phenylene – pyrimidine alternating oligomers for blue light-emitting material, Org. Lett. 4 (4) (2002) 513–516.

[165] A. Harriman, R. Ziessel, Making photoactive molecular-scale wires, Chem. Commun. (15) (1996) 1707–1716.

[166] K.S. Vadagaonkar, H.P. Kalmode, S. Prakash, A.C. Chaskar, Greener [3+3] tandem annulation–oxidation approach towards the synthesis of substituted pyrimidines, New J. Chem. 39 (5) (2015) 3639–3645.

[167] V. Virsodia, R.R.S. Pissurlenkar, D. Manvar, C. Dholakia, P. Adlakha, A. Shah, E.C. Coutinho, Synthesis, screening for antitubercular activity and 3D-QSAR studies of substituted N-phenyl-6-methyl-2-oxo-4-phenyl-1,2,3,4-tetrahydro-pyrimidine-5-carboxamides, Eur. J. Med. Chem. 43 (10) (2008) 2103–2115.

[168] O. Alam, S.A. Khan, N. Siddiqui, W. Ahsan, S.P. Verma, S.J. Gilani, Antihypertensive activity of newer 1,4-dihydro-5-pyrimidine carboxamides: synthesis and pharmacological evaluation, Eur. J. Med. Chem. 45 (11) (2010) 5113–5119.

[169] M.M. Alam, M. Akhter, A. Husain, A. Marella, O.P. Tanwar, R. Ali, S.M. Hasan, H. Kumar, R. Haider, M. Shaquiquzzaman, Anti-inflammatory and antimicrobial activity of 4,5-dihydropyrimidine-5-carbonitrile derivatives: their synthesis and spectral elucidation, Acta Pol. Pharm. 69 (6) (2012) 1077–1085.

[170] V. Denish, M. Sheefa, S. Faraz, K. Rajesh, R. Anand, J. Nayan, R. Rakesh, S. Anamik, Design and synthesis of 1,4-dihydropyridine derivatives as anti-cancer agent, Anti Cancer Agents Med. Chem. 17 (7) (2017) 1003–1013.

[171] B. Sedaghati, A. Fassihi, S. Arbabi, M. Ranjbar, H.R. Memarian, L. Saghaie, A. Omidi, A. Sardari, M. Jalali, D. Abedi, Synthesis and antimicrobial activity of novel derivatives of Biginelli pyrimidines, Med. Chem. Res. 21 (12) (2012) 3973–3983.

[172] O. Sari, V. Roy, M. Metifiot, C. Marchand, Y. Pommier, S. Bourg, P. Bonnet, R.F. Schinazi, L.A. Agrofoglio, Synthesis of dihydropyrimidine alpha,gamma-diketobutanoic acid derivatives targeting HIV integrase, Eur. J. Med. Chem. 104 (2015) 127–138.

[173] P. Zalavadiya, S. Tala, J. Akbari, H. Joshi, Multi-component synthesis of dihydropyrimidines by iodine catalyst at ambient temperature and in-vitro antimycobacterial activity, Arch. Pharm. 342 (8) (2009) 469–475.

[174] R.R. Joshi, A. Barchha, V.M. Khedkar, R.R.S. Pissurlenkar, S. Sarkar, D. Sarkar, R.R. Joshi, R.A. Joshi, A.K. Shah, E.C. Coutinho, Targeting dormant tuberculosis bacilli: results for molecules with a novel pyrimidone scaffold, Chem. Biol. Drug Des. 85 (2) (2015) 201–207.
[175] H. Zhu, Y. Yang, T. Lian, Multiexciton annihilation and dissociation in quantum confined semiconductor nanocrystals, Acc. Chem. Res. 46 (6) (2013) 1270–1279.
[176] J.C. Barrow, P.G. Nantermet, H.G. Selnick, K.L. Glass, K.E. Rittle, K.F. Gilbert, T.G. Steele, C.F. Homnick, R.M. Freidinger, R.W. Ransom, P. Kling, D. Reiss, T.P. Broten, T.W. Schorn, R.S.L. Chang, S.S. O'Malley, T.V. Olah, J.D. Ellis, A. Barrish, K. Kassahun, P. Leppert, D. Nagarathnam, C. Forray, In vitro and in vivo evaluation of dihydropyrimidinone C-5 amides as potent and selective α1A receptor antagonists for the treatment of benign prostatic hyperplasia, J. Med. Chem. 43 (14) (2000) 2703–2718.
[177] P. Liu, J. Hao, Z.-H. Zhang, A general, effcient and green procedure for synthesis of dihydropyrimidine-5-carboxamides in low melting betaine hydrochloride/urea mixture, Chin. J. Chem. 34 (2016) 637–645.
[178] C.O. Kappe, Biologically active dihydropyrimidones of the Biginelli-type—a literature survey, Eur. J. Med. Chem. 35 (12) (2000) 1043–1052.
[179] K.S. Atwal, S. Moreland, Dihydropyrimidine calcium channel blockers 51: bicyclic dihydropyrimidines as potent mimics of dihydropyridines, Bioorg. Med. Chem. Lett. 1 (6) (1991) 291–294.
[180] B.B. Snider, Z. Shi, Biomimetic synthesis of (.+-.)-crambines A, B, C1, and C2. Revision of the structure of crambines B and C1, J. Org. Chem. 58 (15) (1993) 3828–3839.
[181] N. Azizi, S. Dezfuli, M.M. Hahsemi, Eutectic salt catalyzed environmentally benign and highly efficient Biginelli reaction, Sci. World J. 2012 (2012) 6.
[182] S. Gore, S. Baskaran, B. Koenig, Efficient synthesis of 3,4-dihydropyrimidin-2-ones in low melting tartaric acid–urea mixtures, Green Chem. 13 (4) (2011) 1009–1013.
[183] B. N Borse, V. S Borude, S. Shukla, Synthesis of novel dihydropyrimidin-2(1H)-ones derivatives using lipase and their antimicrobial activity, Curr. Chem. Lett. 1 (2012) 59–68.
[184] M.A.P. Martins, G.C. Paveglio, T.S. Munchen, A.R. Meyer, D.N. Moreira, L.V. Rodrigues, C.P. Frizzo, N. Zanatta, H.G. Bonacorso, P.A. Melo, S.R. Krzyzaniak, Deep eutectic solvent mediated synthesis of thiomethyltriazolo[1,5-a]pyrimidines, J. Mol. Liq. 223 (2016) 934–938.
[185] P. Supaluk, P. Ratchanok, W. Apilak, S. Nujarin, P. Veda, R. Somsak, P. Virapong, Roles of pyridine and pyrimidine derivatives as privileged scaffolds in anticancer agents, Mini-Rev. Med. Chem. 17 (10) (2017) 869–901.
[186] K.A. Cadoo, A. Gucalp, T.A. Traina, Palbociclib: an evidence-based review of its potential in the treatment of breast cancer, Breast Cancer 6 (2014) 123–133 (Dove Medical Press).
[187] P. Yu, A.D. Laird, X. Du, J. Wu, K.-A. Won, K. Yamaguchi, P.P. Hsu, F. Qian, C.T. Jaeger, W. Zhang, C.A. Buhr, P. Shen, W. Abulafia, J. Chen, J. Young, A. Plonowski, F.M. Yakes, F. Chu, M. Lee, F. Bentzien, S.T. Lam, S. Dale, D.J. Matthews, P. Lamb, P. Foster, Characterization of the activity of the PI3K/mTOR inhibitor XL765 (SAR245409) in tumor models with diverse genetic alterations affecting the PI3K pathway, Mol. Cancer Ther. 13 (5) (2014) 1078.
[188] A. Pastor, R. Alajarin, J. J. Vaquero, J. Alvarez-Builla, M. Fau de Casa-Juana, C. Sunkel, J. G. Priego, I. Fonseca, J. Sanz-Aparicio, Synthesis and structure of new pyrido[2,3-d] pyrimidine derivatives with calcium channel antagonist activity, Tetrahedron 50 (27) (1994) 8085–8098.

[189] H.-J. Zhang, S.-B. Wang, X. Wen, J.-Z. Li, Z.-S. Quan, Design, synthesis, and evaluation of the anticonvulsant and antidepressant activities of pyrido[2,3-d]pyrimidine derivatives, Med. Chem. Res. 25 (7) (2016) 1287–1298.
[190] D.A. DeGoey, D.A. Betebenner, D.J. Grampovnik, D. Liu, J.K. Pratt, M.D. Tufano, W. He, P. Krishnan, T.J. Pilot-Matias, K.C. Marsh, A. Molla, D.J. Kempf, C.J. Maring, Discovery of pyrido[2,3-d]pyrimidine-based inhibitors of HCV NS5A, Bioorg. Med. Chem. Lett. 23 (12) (2013) 3627–3630.
[191] A.W.-H. Cheung, B. Banner, J. Bose, K. Kim, S. Li, N. Marcopulos, L. Orzechowski, J.A. Sergi, K.C. Thakkar, B.-B. Wang, W. Yun, C. Zwingelstein, S. Berthel, A.R. Olivier, 7-Phenyl-pyrido[2,3-d]pyrimidine-2,4-diamines: novel and highly selective protein tyrosine phosphatase 1B inhibitors, Bioorg. Med. Chem. Lett. 22 (24) (2012) 7518–7522.
[192] D.A. Ibrahim, N.S.M. Ismail, Design, synthesis and biological study of novel pyrido [2,3-d]pyrimidine as anti-proliferative CDK2 inhibitors, Eur. J. Med. Chem. 46 (12) (2011) 5825–5832.
[193] K. Malagu, H. Duggan, K. Menear, M. Hummersone, S. Gomez, C. Bailey, P. Edwards, J. Drzewiecki, F. Leroux, M.J. Quesada, G. Hermann, S. Maine, C.-A. Molyneaux, A. Le Gall, J. Pullen, I. Hickson, L. Smith, S. Maguire, N. Martin, G. Smith, M. Pass, The discovery and optimisation of pyrido[2,3-d]pyrimidine-2,4-diamines as potent and selective inhibitors of mTOR kinase, Bioorg. Med. Chem. Lett. 19 (20) (2009) 5950–5953.
[194] R. Aryan, H. Beyzaei, M. Nojavan, F. Pirani, H. Samareh Delarami, M. Sanchooli, Expedient multicomponent synthesis of a small library of some novel highly substituted pyrido[2,3-d]pyrimidine derivatives mediated and promoted by deep eutectic solvent and in vitro and quantum mechanical study of their antibacterial and antifungal activities, Mol. Divers. 23 (1) (2019) 93–105.
[195] G.W. Rewcastle, A.J. Bridges, D.W. Fry, J.R. Rubin, W.A. Denny, Tyrosine kinase inhibitors. 12. Synthesis and structure − activity relationships for 6-substituted 4-(phenylamino)pyrimido[5,4-d]pyrimidines designed as inhibitors of the epidermal growth factor receptor, J. Med. Chem. 40 (12) (1997) 1820–1826.
[196] H. Alonso, A.A. Bliznyuk, J.E. Gready, Combining docking and molecular dynamic simulations in drug design, Med. Res. Rev. 26 (5) (2006) 531–568.
[197] W.S. Hamama, M.A. Ismail, H.A. Al-Saman, H.H. Zoorob, Facile construction of substituted pyrimido[4,5-d]pyrimidones by transformation of enaminouracil, J. Adv. Res. 4 (2) (2013) 115–121.
[198] S. Gore, S. Baskaran, B. Koenig, Synthesis of pyrimidopyrimidinediones in a deep eutectic reaction mixture, Adv. Synth. Catal. 354 (13) (2012) 2368–2372.
[199] S. Khaksar, A. Rouhollahpour, S.M. Talesh, A facile and efficient synthesis of 2-amino-3-cyano-4H-chromenes and tetrahydrobenzo[b]pyrans using 2,2,2-trifluoroethanol as a metal-free and reusable medium, J. Fluor. Chem. 141 (2012) 11–15.
[200] V.S. Dinakaran, B. Bomma, K.K. Srinivasan, Fused pyrimidines: the heterocycle of diverse biological and pharmacological, Significance 4 (2012) 255–265.
[201] M.M. Kandeel, A.M. Kamal, E.K.A. Abdelall, H.A.H. Elshemy, Synthesis of novel chromene derivatives of expected antitumor activity, Eur. J. Med. Chem. 59 (2013) 183–193.
[202] T. Ram Reddy, L. Srinivasula Reddy, G. Rajeshwar Reddy, V.S. Nuthalapati, Y. Lingappa, S. Sandra, R. Kapavarapu, P. Misra, M. Pal, A Pd-mediated new strategy to functionalized 2-aminochromenes: their in vitro evaluation as potential anti tuberculosis agents, Bioorg. Med. Chem. Lett. 21 (21) (2011) 6433–6439.

[203] O. A. El-Gammal, G. Abu El-Reash, S. Ahmed, Structural, spectral, thermal and biological studies on 2-oxo-N′-((4-oxo-4H-chromen-3-yl)methylene)-2-(phenylamino)acetohydrazide (H2L) and its metal complexes, J. Mol. Struct. 1007 (2012) 1–10.
[204] A.A. Bekhit, H.T.Y. Fahmy, S.A.F. Rostom, A.M. Baraka, Design and synthesis of some substituted 1H-pyrazolyl-thiazolo[4,5-d]pyrimidines as anti-inflammatory–antimicrobial agents, Eur. J. Med. Chem. 38 (1) (2003) 27–36.
[205] E. Rajanarendar, M. Nagi Reddy, S. Rama Krishna, K. Rama Murthy, Y.N. Reddy, M.V. Rajam, Design, synthesis, antimicrobial, anti-inflammatory and analgesic activity of novel isoxazolyl pyrimido[4,5-b]quinolines and isoxazolyl chromeno[2,3-d] pyrimidin-4-ones, Eur. J. Med. Chem. 55 (2012) 273–283.
[206] S.M. Sherif, M.M. Youssef, K.M. Mobarak, A.-S.M. Abdel-Fattah, A convenient synthesis of thiazolopyrimidines, thiazolodipyrimidines and heterocyclothiazolopyrimidines, Tetrahedron 49 (42) (1993) 9561–9572.
[207] A.A. Abu-Hashem, M.M. Youssef, H.A.R. Hussein, Synthesis, antioxidant, antituomer activities of some new thiazolopyrimidines, pyrrolothiazolopyrimidines and triazolopyrrolothiazolopyrimidines derivatives, J. Chin. Chem. Soc. 58 (1) (2011) 41–48.
[208] S. Jabeen, O.A. Chat, G.M. Rather, A.A. Dar, Investigation of antioxidant activity of quercetin (2-(3, 4-dihydroxyphenyl)-3,5,7-trihydroxy-4H-chromen-4-one) in aqueous micellar media, Food Res. Int. 51 (1) (2013) 294–302.
[209] H. Zhi, L.-M. Chen, L.-L. Zhang, S.-J. Liu, D. Wan, C. Wan, H. Lin, C. Hu, Design, synthesis, and biological evaluation of 5H-thiazolo[3,2-a]pyrimidine derivatives as a new type of acetylcholinesterase inhibitors, Arkivoc 13 (2008) 266–277.
[210] S. Fatima, A. Sharma, R. Saxena, R. Tripathi, S.K. Shukla, S.K. Pandey, R. Tripathi, R.P. Tripathi, One pot efficient diversity oriented synthesis of polyfunctional styryl thiazolopyrimidines and their bio-evaluation as antimalarial and anti-HIV agents, Eur. J. Med. Chem. 55 (2012) 195–204.
[211] K. Danel, E.B. Pedersen, C. Nielsen, Synthesis and anti-HIV-1 activity of novel 2,3-dihydro-7H-thiazolo[3,2-a]pyrimidin-7-ones, J. Med. Chem. 41 (2) (1998) 191–198.
[212] A.V.S. Reddy, Y.T. Jeong, Highly efficient and facile synthesis of densely functionalized thiazolo[3,2-a]chromeno[4,3-d]pyrimidin-6(7H)-ones using [Bmim]BF4 as a reusable catalyst under solvent-free conditions, Tetrahedron 72 (1) (2016) 116–122.
[213] P.P. Mohire, D.R. Chandam, R.B. Patil, A.A. Patravale, J.S. Ghosh, M.B. Deshmukh, Low melting mixture glycerol:proline as an innovative designer solvent for the synthesis of novel chromeno fused thiazolopyrimidinone derivatives: an excellent correlation with green chemistry metrics, J. Mol. Liq. 283 (2019) 69–80.
[214] (a) O. Afzal, S. Kumar, M.R. Haider, M.R. Ali, R. Kumar, M. Jaggi, S. Bawa, A review on anticancer potential of bioactive heterocycle quinoline, Eur. J. Med. Chem. 97 (2015) 871–910; (b) J.P. Michael, Quinoline, quinazoline and acridone alkaloids, Nat. Prod. Rep. 25 (1) (2008) 166–187.
[215] C. de la Guardia, D.E. Stephens, H.T. Dang, M. Quijada, O.V. Larionov, R. Lleonart, Antiviral activity of novel quinoline derivatives against dengue virus serotype 2, Molecules (Basel, Switzerland) 23 (3) (2018) 672.
[216] H.C. Hoppe, D.A. van Schalkwyk, U.I. Wiehart, S.A. Meredith, J. Egan, B.W. Weber, Antimalarial quinolines and artemisinin inhibit endocytosis in *Plasmodium falciparum*, Antimicrob. Agents Chemother. 48 (7) (2004) 2370–2378.
[217] C. Gómez, V. Kouznetsov, Recent developments on antimicrobial quinoline Chemistry, in: Microbial Pathogens and Strategies for Combating Them: Science, Technology and Education, Formatex Research Center, Badajoz, 2013.

[218] V. Sharma, D.K. Mehta, R. Das, Synthetic methods of quinoline derivatives as potent anticancer agents, Mini Rev. Med. Chem. 17 (16) (2017) 1557–1572.
[219] R. Musiol, J. Jampilek, V. Buchta, L. Silva, H. Niedbala, B. Podeszwa, A. Palka, K. Majerz-Maniecka, B. Oleksyn, J. Polanski, Antifungal properties of new series of quinoline derivatives, Bioorg. Med. Chem. 14 (10) (2006) 3592–3598.
[220] S. Mukherjee, M. Pal, Medicinal chemistry of quinolines as emerging anti-inflammatory agents: an overview, Curr. Med. Chem. 20 (35) (2013) 4386–4410.
[221] N. Muruganantham, R. Sivakumar, N. Anbalagan, V. Gunasekaran, J.T. Leonard, Synthesis, anticonvulsant and antihypertensive activities of 8-substituted quinoline derivatives, Biol. Pharm. Bull. 27 (10) (2004) 1683–1687.
[222] G.E. Tumambac, C.M. Rosencrance, C. Wolf, Selective metal ion recognition using a fluorescent 1,8-diquinolylnaphthalene-derived sensor in aqueous solution, Tetrahedron 60 (49) (2004) 11293–11297.
[223] (a) S.A. Jenekhe, L. Lu, M.M. Alam, New conjugated polymers with donor−acceptor architectures: synthesis and photophysics of carbazole−quinoline and phenothiazine −quinoline copolymers and oligomers exhibiting large intramolecular charge transfer, Macromolecules 34 (21) (2001) 7315–7324; (b) G. Jégou, S.A. Jenekhe, Highly fluorescent poly(arylene ethynylene)s containing quinoline and 3-alkylthiophene, Macromolecules 34 (23) (2001) 7926–7928.
[224] B.S. Holla, M. Mahalinga, M.S. Karthikeyan, P.M. Akberali, N.S. Shetty, Synthesis of some novel pyrazolo[3,4-d]pyrimidine derivatives as potential antimicrobial agents, Bioorg. Med. Chem. 14 (6) (2006) 2040–2047.
[225] (a) S. Całus, E. Gondek, A. Danel, B. Jarosz, M. Pokładko, A.V. Kityk, Electroluminescence of 6-R-1,3-diphenyl-1H-pyrazolo[3,4-b]quinoline-based organic light-emitting diodes (R=F, Br, Cl, CH3, C2H3 and N(C6H5)2), Mater. Lett. 61 (14) (2007) 3292–3295; (b) G. Caeiro, J.M. Lopes, P. Magnoux, P. Ayrault, F. Ramôa Ribeiro, A FT-IR study of deactivation phenomena during methylcyclohexane transformation on H-USY zeolites: nitrogen poisoning, coke formation, and acidity–activity correlations, J. Catal. 249 (2) (2007) 234–243.
[226] G. Caeiro, P. Magnoux, J.M. Lopes, F. Lemos, F.R. Ribeiro, Kinetic modeling of the methylcyclohexane transformation over H-USY: deactivating effect of coke and nitrogen basic compounds, J. Mol. Catal. A Chem. 249 (1) (2006) 149–157.
[227] F.-P. Ma, G.-T. Cheng, Z.-G. He, Z.-H. Zhang, A new and efficient procedure for Friedländer synthesis of quinolines in low melting tartaric acid-urea mixtures, Aust. J. Chem. 65 (4) (2012) 409–416.
[228] D. Shahabi, H. Tavakol, One-pot synthesis of quinoline derivatives using choline chloride/tin (II) chloride deep eutectic solvent as a green catalyst, J. Mol. Liq. 220 (2016) 324–328.
[229] (a) V.G. Ugale, S.B. Bari, Quinazolines: new horizons in anticonvulsant therapy, Eur. J. Med. Chem. 80 (2014) 447–501; (b) A.M. Alanazi, A.A.M. Abdel-Aziz, I.A. Al-Suwaidan, S.G. Abdel-Hamide, T.Z. Shawer, A.S. El-Azab, Design, synthesis and biological evaluation of some novel substituted quinazolines as antitumor agents, Eur. J. Med. Chem. 79 (2014) 446–454.
[230] (a) C. Balakumar, P. Lamba, D. Pran Kishore, B. Lakshmi Narayana, K. Venkat Rao, K. Rajwinder, A. Raghuram Rao, B. Shireesha, B. Narsaiah, Synthesis, anti-inflammatory evaluation and docking studies of some new fluorinated fused quinazolines, Eur. J. Med. Chem. 45 (11) (2010) 4904–4913; (b) A.M. Alafeefy, A. A. Kadi, O.A. Al-Deeb, K.E.H. El-Tahir, N.A. Al-jaber, Synthesis, analgesic and anti-inflammatory evaluation of some novel quinazoline derivatives, Eur. J. Med. Chem.

45 (11) (2010) 4947–4952; (c) Y. Kabri, N. Azas, A. Dumètre, S. Hutter, M. Laget, P. Verhaeghe, A. Gellis, P. Vanelle, Original quinazoline derivatives displaying antiplasmodial properties, Eur. J. Med. Chem. 45 (2) (2010) 616–622; (d) M.N. Noolvi, H.M. Patel, V. Bhardwaj, A. Chauhan, Synthesis and in vitro antitumor activity of substituted quinazoline and quinoxaline derivatives: search for anticancer agent, Eur. J. Med. Chem. 46 (6) (2011) 2327–2346.

[231] (a) P. Barraja, L. Caracausi, P. Diana, A. Montalbano, A. Carbone, A. Salvador, P. Brun, I. Castagliuolo, S. Tisi, F. Dall'Acqua, D. Vedaldi, G. Cirrincione, Pyrrolo[3,2-h] quinazolines as photochemotherapeutic agents, ChemMedChem 6 (7) (2011) 1238–1248; (b) S. Boyapati, U. Kulandaivelu, S. Sangu, M.R. Vanga, Synthesis, antimicrobial evaluation, and docking studies of novel 4-substituted quinazoline derivatives as DNA-gyrase inhibitors, Arch. Pharm. 343 (10) (2010) 570–576; (c) S.H. Yang, D.B. Khadka, S.H. Cho, H.-K. Ju, K.Y. Lee, H.J. Han, K.-T. Lee, W.-J. Cho, Virtual screening and synthesis of quinazolines as novel JAK2 inhibitors, Bioorg. Med. Chem. 19 (2) (2011) 968–977; (d) Y.H. Kim, H. Choi, J. Lee, I.-C. Hwang, S.K. Moon, S.J. Kim, H.W. Lee, D.S. Im, S.S. Lee, S.K. Ahn, S.W. Kim, C.K. Han, J.H. Yoon, K.J. Lee, N.S. Choi, Quinazolines as potent and highly selective PDE5 inhibitors as potential therapeutics for male erectile dysfunction, Bioorg. Med. Chem. Lett. 18 (23) (2008) 6279–6282.

[232] C. Ma, Y. Li, S. Niu, H. Zhang, X. Liu, Y. Che, N-Hydroxypyridones, phenylhydrazones, and a quinazolinone from *Isaria farinosa*, J. Nat. Prod. 74 (1) (2011) 32–37.

[233] Z.-H. Zhang, X.-N. Zhang, L.-P. Mo, Y.-X. Li, F.-P. Ma, Catalyst-free synthesis of quinazoline derivatives using low melting sugar–urea–salt mixture as a solvent, Green Chem. 14 (5) (2012) 1502–1506.

[234] M. Narasimhulu, Y.R. Lee, Ethylenediamine diacetate-catalyzed three-component reaction for the synthesis of 2,3-dihydroquinazolin-4(1H)-ones and their spirooxindole derivatives, Tetrahedron 67 (49) (2011) 9627–9634.

[235] S.B. Mhaske, N.P. Argade, The chemistry of recently isolated naturally occurring quinazolinone alkaloids, Tetrahedron 62 (42) (2006) 9787–9826.

[236] H.R. Lobo, B.S. Singh, G.S. Shankarling, Bio-compatible eutectic mixture for multicomponent synthesis: a valuable acidic catalyst for synthesis of novel 2,3-dihydroquinazolin-4(1H)-one derivatives, Catal. Commun. 27 (2012) 179–183.

[237] S.K. Ghosh, R. Nagarajan, Deep eutectic solvent mediated synthesis of quinazolinones and dihydroquinazolinones: synthesis of natural products and drugs, RSC Adv. 6 (33) (2016) 27378–27387.

[238] S.K. Ghosh, R. Nagarajan, Total synthesis of penipanoid C, 2-(4-hydroxybenzyl)-quinazolin-4(3H)-one and NU1025, Tetrahedron Lett. 57 (38) (2016) 4277–4279.

[239] (a) K. Niknam, M. Damya, 1-Butyl-3-methylimidazolium hydrogen sulfate [Bmim] HSO4: an efficient reusable acidic ionic liquid for the synthesis of 1,8-dioxo-octahydroxanthenes, J. Chin. Chem. Soc. 56 (3) (2009) 659–665; (b) A. Islam, P. Murugan, K.C. Hwang, C.-H. Cheng, Blue light-emitting devices based on 1,8-acridinedione derivatives, Synth. Met. 139 (2) (2003) 347–353; (c) G. Cholewinski, K. Dzierzbicka, A.M. Kolodziejczyk, Natural and synthetic acridines/acridones as antitumor agents: their biological activities and methods of synthesis, Pharmacol. Rep. 63 (2) (2011) 305–336; (d) M. Gensicka-Kowalewska, G. Cholewiński, K. Dzierzbicka, Recent developments in the synthesis and biological activity of acridine/acridone analogues, RSC Adv. 7 (26) (2017) 15776–15804.

[240] (a) W. Jaber, A. Al-Zahra, L. Hassan Aboud, Z. Bawi, Linear and nonlinear optical properties of acridine dye doped PMMA, Polymer 6 (2015) 1–8; (b) W.R. Tompkin,

R.W. Boyd, D.W. Hall, P.A. Tick, Nonlinear-optical properties of lead–tin fluorophosphate glass containing acridine dyes, J. Opt. Soc. Am. B 4 (6) (1987) 1030–1034; (c) D. Zhang, X. Jiang, H. Yang, A. Martinez, M. Feng, Z. Dong, G. Gao, Acridine-based macrocyclic fluorescent sensors: self-assembly behavior characterized by crystal structures and a tunable bathochromic-shift in emission induced by H2PO4(-)via adjusting the ring size and rigidity, Org. Biomol. Chem. 11 (20) (2013) 3375–3381.

[241] P. Mitra, P.K. Chakraborty, P. Saha, P. Ray, S. Basu, Antibacterial efficacy of acridine derivatives conjugated with gold nanoparticles, Int. J. Pharm. 473 (1) (2014) 636–643.

[242] A.F.-C. Valdés, Acridine and acridinones: old and new structures with antimalarial activity, Open Med. Chem. J. 5 (2011) 11–20.

[243] S.M. Viscia, D.C. Brodie, The in vitro antifungal activity of a series of acridine salts*, J. Am. Pharm. Assoc. (Scientific Ed.) 43 (1) (1954) 52–54.

[244] P. Belmont, J. Bosson, T. Godet, M. Tiano, Acridine and acridone derivatives, anticancer properties and synthetic methods: where are we now? Anti Cancer Agents Med. Chem. 7 (2) (2007) 139–169.

[245] S.A. Gamage, J.A. Spicer, G.J. Atwell, G.J. Finlay, B.C. Baguley, W.A. Denny, Structure – activity relationships for substituted bis(acridine-4-carboxamides): a new class of anticancer agents, J. Med. Chem. 42 (13) (1999) 2383–2393.

[246] I. Antonini, P. Polucci, L.R. Kelland, E. Menta, N. Pescalli, S. Martelli, 2,3-Dihydro-1H,7H-pyrimido[5,6,1-de]acridine-1,3,7-trione derivatives, a class of cytotoxic agents active on multidrug-resistant cell lines: synthesis, biological evaluation, and structure – activity relationships, J. Med. Chem. 42 (14) (1999) 2535–2541.

[247] S. Gallo, S. Atifi, A. Mahamoud, C. Santelli-Rouvier, K. Wolfárt, J. Molnar, J. Barbe, Synthesis of aza mono, bi and tricyclic compounds. Evaluation of their anti MDR activity, Eur. J. Med. Chem. 38 (1) (2003) 19–26.

[248] N. Martín, M. Quinteiro, C. Seoane, J.L. Soto, A. Mora, M. Suárez, E. Ochoa, A. Morales, J.R.D. Bosque, Synthesis and conformational study of acridine derivatives related to 1,4-dihydropyridines, J. Heterocyclic Chem. 32 (1) (1995) 235–238.

[249] S.-J. Tu, C.-B. Miao, Y. Gao, Y.-J. Feng, J.-C. Feng, Microwave-prompted reaction of cinnamonitrile derivatives with 5,5-dimethyl-1,3-cyclohexanedione, Chin. J. Chem. 20 (7) (2002) 703–706.

[250] R. Ramesh, One-pot synthesis of symmetrical and unsymmetrical acridine sulfonamide derivatives catalyzed by p-TSA, Res. Chem. Intermed. 43 (7) (2017) 4165–4173.

[251] T.-S. Jin, J.-S. Zhang, T.-T. Guo, A.-Q. Wang, T.-S. Li, One-pot clean synthesis of 1,8-dioxo-decahydroacridines catalyzed by p-dodecylbenezenesulfonic acid in aqueous media, ChemInform 36 (2004) 2001–2005.

[252] M. Kidwai, D. Bhatnagar, Ceric ammonium nitrate (CAN) catalyzed synthesis of N-substituted decahydroacridine-1,8-diones in PEG, Tetrahedron Lett. 51 (20) (2010) 2700–2703.

[253] X. Fan, X. Hu, X. Zhang, J. Wang, InCl3·4H2O-promoted green preparation of xanthenedione derivatives in ionic liquids, Can. J. Chem. 83 (1) (2005) 16–20.

[254] G. Song, B. Wang, H. Luo, L. Yang, Fe3+-montmorillonite as a cost-effective and recyclable solid acidic catalyst for the synthesis of xanthenediones, Catal. Commun. 8 (4) (2007) 673–676.

[255] M. Kiani, M. Mohammadipour, Fe 3 O 4 @SiO 2 –MoO 3 H nanoparticles: a magnetically recyclable nanocatalyst system for the synthesis of 1,8-dioxo-decahydroacridine derivatives, RSC Adv. 7 (2017) 997–1007.

[256] F. Rashedian, D. Saberi, K. Niknam, Silica-bonded N-propyl sulfamic acid: a recyclable catalyst for the synthesis of 1,8-dioxo-decahydroacridines, 1,8-dioxo-octahydroxanthenes and quinoxalines, J. Chin. Chem. Soc. 57 (5A) (2010) 998–1006.
[257] B. Das, P. Thirupathi, I. Mahender, V.S. Reddy, Y.K. Rao, Amberlyst-15: an efficient reusable heterogeneous catalyst for the synthesis of 1,8-dioxo-octahydroxanthenes and 1,8-dioxo-decahydroacridines, J. Mol. Catal. A Chem. 247 (1) (2006) 233–239.
[258] X.S. Wang, D. Shi, Y.F. Zhang, S.H. Wang, S.J. Tu, Synthesis of 9-arylpolyhydroacridine in water catalyzed by triethylbenzylammonium chloride (TEBA), Chin. J. Org. Chem. 24 (2004) 430–432.
[259] M.R. Bhosle, D. Nipte, J. Gaikwad, M.A. Shaikh, G.M. Bondle, J.N. Sangshetti, A rapid and green method for expedient multicomponent synthesis of N-substituted decahydroacridine-1,8-diones as potential antimicrobial agents, Res. Chem. Intermed. 44 (11) (2018) 7047–7064.
[260] S. Rudys, C. Ríos-Luci, E. Pérez-Roth, I. Cikotiene, J.M. Padrón, Antiproliferative activity of novel benzo[b][1,6]naphthyridines in human solid tumor cell lines, Bioorg. Med. Chem. Lett. 20 (5) (2010) 1504–1506.
[261] S. Huang, J. Qing, S. Wang, H. Wang, L. Zhang, Y. Tang, Design and synthesis of imidazo[1,2-α][1,8]naphthyridine derivatives as anti-HCV agents via direct C–H arylation, Org. Biomol. Chem. 12 (15) (2014) 2344–2348.
[262] M. Di Braccio, G. Roma, M. Ghia, F. Mattioli, 1,8-Naphthyridines II. 2,4-disubstituted N,N-dialkyl-1,8-naphthyridine-3-carboxamides with anti-inflammatory and/or antiaggressive activities, Farmaco 49 (1) (1994) 25–32.
[263] B.A. Johns, J.G. Weatherhead, S.H. Allen, J.B. Thompson, E.P. Garvey, S.A. Foster, J.L. Jeffrey, W.H. Miller, 1,3,4-Oxadiazole substituted naphthyridines as HIV-1 integrase inhibitors. Part 2: SAR of the C5 position, Bioorg. Med. Chem. Lett. 19 (6) (2009) 1807–1810.
[264] A. Shaabani, S.E. Hooshmand, A.T. Tabatabaei, Synthesis of fully substituted naphthyridines: a novel domino four-component reaction in a deep eutectic solvent system based on choline chloride/urea, Tetrahedron Lett. 57 (3) (2016) 351–353.
[265] D. Kumar, V.B. Reddy, S. Sharad, U. Dube, S. Kapur, A facile one-pot green synthesis and antibacterial activity of 2-amino-4H-pyrans and 2-amino-5-oxo-5,6,7,8-tetrahydro-4H-chromenes, Eur. J. Med. Chem. 44 (9) (2009) 3805–3809.
[266] (a) Y. Peng, G. Song, Amino-functionalized ionic liquid as catalytically active solvent for microwave-assisted synthesis of 4H-pyrans, Catal. Commun. 8 (2) (2007) 111–114; (b) S. Tu, B. Jiang, J. Zhang, Y. Zhang, R. Jia, C. Li, D. Zhou, L. Cao, Q. Shao, A facile and efficient synthesis of new polysubstituted indeno[1,2- b]pyri-dines via one-pot, three-component microwave-assisted reaction, Synlett 2007 (2007) 0480–0484.
[267] N. Azizi, S. Dezfooli, M. Khajeh, M.M. Hashemi, Efficient deep eutectic solvents catalyzed synthesis of pyran and benzopyran derivatives, J. Mol. Liq. 186 (2013) 76–80.
[268] (a) N. Thomas, S.M. Zachariah, Pharmacological activities of chromene derivatives: an overview, Asian J. Pharm. Clin. Res., 6 (2013) 11–15; (b) P. Proksch, E. Rodriguez, Chromenes and benzofurans of the asteraceae, their chemistry and biological significance, Phytochemistry, 22 (11) (1983) 2335–2348; (c) J.D. Hepworth, C.D. Gabbutt, B.M. Heron, 5.08—Pyrans and their benzo derivatives: synthesis, in: A. R. Katritzky, C.W. Rees, E.F.V. Scriven (Eds.), Comprehensive Heterocyclic Chemistry II, Pergamon, Oxford, 1996, pp. 351–468; (d) C. Hardouin, L. Burgaud, A. Valleix, E. Doris, Enantioselective synthesis of chromenes, Tetrahedron Lett., 44 (3) (2003) 435–437; (e) R.S. Kenny, U.C. Mashelkar, D.M. Rane, D.K. Bezawada, Intramolecular

electrophilic hydroarylation via Claisen rearrangement: synthesis of chromenes, heterothiochromenes and heterodihydrothiochromenes, Tetrahedron, 62 (39) (2006) 9280–9288.

[269] (a) Y.-L. Shi, M. Shi, The synthesis of chromenes, chromanes, coumarins and related heterocycles via tandem reactions of salicylic aldehydes or salicylic imines with α,β-unsaturated compounds, Org. Biomol. Chem. 5 (10) (2007) 1499–1504; (b) T. Kanchanapoom, R. Kasai, P. Chumsri, K. Kraisintu, K. Yamasaki, Lotthanongine, an unprecedented flavonoidal indole alkaloid from the roots of Thai medicinal plant, *Trigonostemon reidioides*, Tetrahedron Lett. 43 (16) (2002) 2941–2943.

[270] N. Azizi, M. Mariami, M. Edrisi, Greener construction of 4H-chromenes based dyes in deep eutectic solvent, Dyes Pigments 100 (2014) 215–221.

[271] (a) E. Adbel Aziz Hafez, E. Hafez, M. Elnagdi, A. Ghani Ali Elagamey, F. Mohamed Abdel Aziz El-Taweel, Nitriles in heterocyclic synthesis: novel synthesis of benzo[c] coumarin and of benzo[c]pyrano[3,2-c]quinoline derivatives, Heterocycles 26 (1987); (b) M. Elinson, A.S. Dorofeev, F. Miloserdov, A.I. Ilovaisky, S.K. Feducovich, P.A. Belyakov, G.I. Nikishin, Catalysis of salicylaldehydes and two different C–H acids with electricity: first example of an efficient multicomponent approach to the design of functionalized medicinally privileged 2-amino-4 H-chromene scaffold, Adv. Synth. Catal. 350 (2008) 591–601.

[272] R. Pratap, V.J. Ram, Natural and synthetic chromenes, fused chromenes, and versatility of dihydrobenzo[h]chromenes in organic synthesis, Chem. Rev. 114 (20) (2014) 10476–10526.

[273] C. Atul, Catalyst free one-pot three-component synthesis of 2-amino-4Hchromene derivatives in aqueous deep eutectic mixture at room temperature, Lett. Org. Chem. 11 (7) (2014) 480–486.

[274] H. Singh, B. Nand, J. Sindhu, J.M. Khurana, C. Sharma, K.R. Aneja, Efficient one pot synthesis of xanthene-triazole-quinoline/phenyl conjugates and evaluation of their antimicrobial activity, J. Braz. Chem. Soc. 25 (2014) 1178–1193.

[275] C. Spatafora, V. Barresi, V.M. Bhusainahalli, S. Di Micco, N. Musso, R. Riccio, G. Bifulco, D. Condorelli, C. Tringali, Bio-inspired benzo[k,l]xanthene lignans: synthesis, DNA-interaction and antiproliferative properties, Org. Biomol. Chem. 12 (17) (2014) 2686–2701.

[276] S. Naseem, M. Khalid, M.N. Tahir, M.A. Halim, A.A.C. Braga, M.M. Naseer, Z. Shafiq, Synthesis, structural, DFT studies, docking and antibacterial activity of a xanthene based hydrazone ligand, J. Mol. Struct. 1143 (2017) 235–244.

[277] E.F. Llama, C. del Campo, M. Capo, M. Anadon, Synthesis and antinociceptive activity of 9-phenyl-oxy or 9-acyl-oxy derivatives of xanthene, thioxanthene and acridine, Eur. J. Med. Chem. 24 (4) (1989) 391–396.

[278] T. Nishiyama, T. Ishida, K. Nakatani, T. Ishimaru, T. Yamamura, Antioxidant activity of the fused heterocyclic compounds, 9H-xanthene-2, 7-diols, J. Jpn. Oil Chem. Soc. 44 (1995) 960–965.

[279] M. Ahmad, T. A King, D.-K. Ko, B. Heon Cha, J. Lee, Performance and photostability of xanthene and pyrromethene laser dyes in sol-gel phases, J. Phys. D. Appl. Phys. 35 (2002) 1473.

[280] F. Muñoz Muñiz, L. Simón, S. Sáez, C. Raposo, V. Alcázar, J. R Morán, A fluorescent sensor for dinitrobenzoic acid based on a cyanuric acid and xanthene skeleton, Sensors 8 (2008) 1637.

[281] V.I. Martynov, A.A. Pakhomov, N.V. Popova, I.E. Deyev, A.G. Petrenko, Synthetic fluorophores for visualizing biomolecules in living systems, Acta Nat. 8 (4) (2016) 33–46.

[282] S. De, S. Das, A. Girigoswami, Environmental effects on the aggregation of some xanthene dyes used in lasers, Spectrochim. Acta, Part A 61 (2005) 1821–1833.
[283] A. Bekaert, J. Andrieux, M. Plat, New total synthesis of bikaverin, Tetrahedron Lett. 33 (20) (1992) 2805–2806.
[284] S. T. G. Buck, F. Bettanin, E. Orestes, P. Homem-de-Mello, H. Imasato, R. Viana, J. R. Perussi, A. B. F. da Silva, Photodynamic efficiency of xanthene dyes and their phototoxicity against a carcinoma cell line: a computational and experimental study, J. Chem. 2017 (2017) 1–9.
[285] A. Naya, M. Ishikawa, K. Matsuda, K. Ohwaki, T. Saeki, K. Noguchi, N. Ohtake, Structure-activity relationships of xanthene carboxamides, novel CCR1 receptor antagonists, Bioorg. Med. Chem. 11 (6) (2003) 875–884.
[286] F.T. McNamara, J.W. Nieft, J.F. Ambrose, E.S. Huyser, Structure and rearrangement of the reduction dimers of N-alkyl pyridinium cations, J. Org. Chem. 42 (6) (1977) 988–993.
[287] J.-J. Yu, L.-M. Wang, J.-Q. Liu, F.-L. Guo, Y. Liu, N. Jiao, Synthesis of tetraketones in water and under catalyst-free conditions, Green Chem. 12 (2) (2010) 216–219.
[288] G. Cravotto, A. Demetri, G.M. Nano, G. Palmisano, A. Penoni, S. Tagliapietra, The aldol reaction under high-intensity ultrasound: a novel approach to an old reaction, Eur. J. Org. Chem. 2003 (22) (2003) 4438–4444.
[289] M. Brito-Arias, M. Tapia-Albarrán, I. Padilla-Martínez, F. Martínez-Martínez, G. Espinosa, E. Molins, E. Espinosa, 9-(2-Methylphenyl)-3,4,5,6,9,10-hexahydroxanthene-1,8(2H,7H)-dione, J. Chem. Crystallogr. 29 (7) (1999) 759–763.
[290] F.E. King, D.G.I. Felton, 276. cycloHexa-1 : 3-dione: a reagent for the characterisation of aldehydes, J. Chem. Soc. (1948) 1371–1372 (Resumed).
[291] (a) Z. Ren, W. Cao, W. Tong, X. Jing, Knoevenagel condensation of aldehydes with cyclic active methylene compounds in water, Synth. Commun. 32 (13) (2002) 1947–1952; (b) B. Das, J. Kashanna, R.A. Kumar, P. Jangili, Efficient organocatalytic synthesis of 1,8-dioxo-octahydroxanthenes, Synth. Commun. 42 (19) (2012) 2876–2884.
[292] N. Azizi, S. Dezfooli, M.M. Hashemi, Chemoselective synthesis of xanthenes and tetraketones in a choline chloride-based deep eutectic solvent, C. R. Chim. 16 (11) (2013) 997–1001.
[293] P. Liu, J.-W. Hao, S.-J. Liang, G.-L. Liang, J.-Y. Wang, Z.-H. Zhang, Choline chloride and itaconic acid-based deep eutectic solvent as an efficient and reusable medium for the preparation of 13-aryl-5H-dibenzo[b,i]xanthene-5,7,12,14(13H)-tetraones, Monatsh. Chem. 147 (2015) 801–808.
[294] D. Shahabi, H. Tavakol, Synthesis of 14H-dibenzo xanthene derivatives using choline chloride/tin(II) chloride deep eutectic solvent and Fe3O4/ƛ-carrageenan/Zn(II), J. Iran. Chem. Soc. 14 (2016) 135–142.
[295] C.A. Navarro, C.A. Sierra, C. Ochoa-Puentes, Evaluation of sodium acetate trihydrate–urea DES as a benign reaction media for the Biginelli reaction. Unexpected synthesis of methylenebis(3-hydroxy-5,5-dimethylcyclohex-2-enones), hexahydroxanthene-1,-8-diones and hexahydroacridine-1,8-diones, RSC Adv. 6 (70) (2016) 65355–65365.
[296] M.M.M. Santos, Recent advances in the synthesis of biologically active spirooxindoles, Tetrahedron 70 (52) (2014) 9735–9757.
[297] (a) B. Yu, Y.C. Zheng, X.J. Shi, P.P. Qi, H.M. Liu, Natural product-derived spirooxindole fragments serve as privileged substructures for discovery of new anticancer agents, Anti Cancer Agents Med. Chem. 16 (10) (2016) 1315–1324; (b) B. Yu, Z. Yu, P.P. Qi, D.Q. Yu, H.M. Liu, Drug discovery using spirooxindole cores: success and challenges [corrected], Eur. J. Med. Chem. 95 (2015) 35–40; (c) Y. Zheng, C.M. Tice, S.B. Singh, The use of spirocyclic scaffolds in drug discovery, Bioorg. Med. Chem. Lett. 24 (16) (2014) 3673–3682.

[298] A. Rajawat, S. Khandelwal, M. Kumar, Deep eutectic solvent promoted efficient and environmentally benign four-component domino protocol for synthesis of spirooxindoles, RSC Adv. 4 (10) (2014) 5105–5112.
[299] K. Sarita, R. Anshu, T. Yogesh Kumar, K. Mahendra, A simple, efficient and environmentally benign synthetic protocol for the synthesis of spirooxindoles using choline chloride-oxalic acid eutectic mixture as catalyst/solvent system, Comb. Chem. High Throughput Screen. 17 (9) (2014) 763–769.
[300] N. Azizi, S. Dezfooli, M. Mahmoudi Hashemi, Greener synthesis of spirooxindole in deep eutectic solvent, J. Mol. Liq. 194 (2014) 62–67.
[301] W.-H. Zhang, M.-N. Chen, Y. Hao, X. Jiang, X.-L. Zhou, Z.-H. Zhang, Choline chloride and lactic acid: a natural deep eutectic solvent for one-pot rapid construction of spiro [indoline-3,4′-pyrazolo[3,4-b]pyridines], J. Mol. Liq. 278 (2019) 124–129.
[302] T.H. Kang, K. Matsumoto, M. Tohda, Y. Murakami, H. Takayama, M. Kitajima, N. Aimi, H. Watanabe, Pteropodine and isopteropodine positively modulate the function of rat muscarinic M(1) and 5-HT(2) receptors expressed in Xenopus oocyte, Eur. J. Pharmacol. 444 (1–2) (2002) 39–45.
[303] A. Bertamino, C. Aquino, M. Sala, N.d. Simone, C.A. Mattia, L. Erra, S. Musella, P. Iannelli, A. Carotenuto, P. Grieco, E. Novellino, P. Campiglia, I. Gomez-Monterrey, Design and synthesis of spirotryprostatin-inspired diketopiperazine systems from prolyl spirooxoindolethiazolidine derivatives, Bioorg. Med. Chem. 18 (12) (2010) 4328–4337.
[304] (a) K. Ding, Y. Lu, Z. Nikolovska-Coleska, S. Qiu, Y. Ding, W. Gao, J. Stuckey, K. Krajewski, P.P. Roller, Y. Tomita, D.A. Parrish, J.R. Deschamps, S. Wang, Structure-based design of potent non-peptide MDM2 inhibitors, J. Am. Chem. Soc. 127 (29) (2005) 10130–10131; (b) K. Ding, Y. Lu, Z. Nikolovska-Coleska, G. Wang, S. Qiu, S. Shangary, W. Gao, D. Qin, J. Stuckey, K. Krajewski, P.P. Roller, S. Wang, Structure-based design of spiro-oxindoles as potent, specific small-molecule inhibitors of the MDM2 – p53 interaction, J. Med. Chem. 49 (12) (2006) 3432–3435.
[305] (a) P. Deslongchamps, D.D. Rowan, N. Pothier, G. Sauvé, J.K. Saunders, 1,7-Dioxaspiro [5.5]undecanes. An excellent system for the study of stereoelectronic effects (anomeric and exo-anomeric effects) in acetals, Can. J. Chem. 59 (7) (1981) 1105–1121; (b) D. Nori-Shargh, H. Yahyaei, S.N. Mousavi, M. Kianpour, Conformational behaviors of 1,7-dioxa-spiro[5,5]undecane and its dithia and diselena analogs in relation to the anomeric effect: a hybrid-DFT, ab initio MO study and NBO interpretation, Comput. Theor. Chem. 974 (1) (2011) 79–85.
[306] (a) D.J. Newman, G.M. Cragg, Natural products as sources of new drugs over the 30 years from 1981 to 2010, J. Nat. Prod. 75 (3) (2012) 311–335; (b) A.R. Díaz-Marrero, I. Brito, J.M. de la Rosa, L. D'Croz, O. Fabelo, C. Ruiz-Pérez, J. Darias, M. Cueto, Novel lactone Chamigrene-derived metabolites from *Laurencia majuscula*, Eur. J. Org. Chem. 2009 (9) (2009) 1407–1411; (c) E. Dorta, A.R. Dı´az-Marrero, M. Cueto, L. D'Croz, J.L. Maté, J. Darias, Chamigrenelactone, a polyoxygenated sesquiterpene with a novel structural type and devoid of halogen from *Laurencia obtusa*, Tetrahedron Lett. 45 (38) (2004) 7065–7068.
[307] R. Singh, A. Singh, Regio- and stereoselective synthesis of novel trispiropyrrolidine/thiapyrrolizidines using deep eutectic solvent as an efficient reaction media, J. Iran. Chem. Soc. 14 (2017) 1119–1129.
[308] C.A. Demerson, A.H. Philipp, L.G. Humber, M.J. Kraml, M.P. Charest, H. Tom, I. Vavra, Pyrrolo[4,3,2-de]isoquinolines with central nervous system and antihypertensive activities, J. Med. Chem. 17 (11) (1974) 1140–1145.

[309] R. Ranjith Kumar, S. Perumal, S.C. Manju, P. Bhatt, P. Yogeeswari, D. Sriram, An atom economic synthesis and antitubercular evaluation of novel spiro-cyclohexanones, Bioorg. Med. Chem. Lett. 19 (13) (2009) 3461–3465.
[310] J.-M. Ferland, C.A. Demerson, L.G. Humber, Synthesis of derivatives of isoindole and of pyrazino[2,1-a]isoindole, Can. J. Chem. 63 (2) (1985) 361–365.
[311] X.Z. Zhao, K. Maddali, C. Marchand, Y. Pommier, T.R. Burke, Diketoacid-genre HIV-1 integrase inhibitors containing enantiomeric arylamide functionality, Bioorg. Med. Chem. 17 (14) (2009) 5318–5324.
[312] E.C. Taylor, P. Zhou, L.D. Jennings, Z. Mao, B. Hu, J.-G. Jun, Novel synthesis of a conformationally-constrained analog of DDATHF, Tetrahedron Lett. 38 (4) (1997) 521–524.
[313] K.R. Senwar, P. Sharma, T.S. Reddy, M.K. Jeengar, V.L. Nayak, V.G.M. Naidu, A. Kamal, N. Shankaraiah, Spirooxindole-derived morpholine-fused-1,2,3-triazoles: design, synthesis, cytotoxicity and apoptosis inducing studies, Eur. J. Med. Chem. 102 (2015) 413–424.
[314] M. Suehiro, U. Scheffel, R.F. Dannals, H.T. Ravert, G.A. Ricaurte, H.N. Wagner Jr., A PET radiotracer for studying serotonin uptake sites: carbon-11-McN-5652Z, J. Nucl. Med. 34 (1) (1993) 120–127.
[315] G. Periyasami, N. Arumugam, M. Rahaman, R.S. Kumar, M. Manikandan, M.A. Alfayez, D. Premnath, A. Aldalbahi, ACI/EG eutectic mixture mediated synthesis, characterization and in vitro osteoblast differentiation assessment of spiropyrrolo[1,2-b] isoquinoline analogues, RSC Adv. 8 (29) (2018) 16303–16313.
[316] (a) B. Zhou, C. Xing, Diverse molecular targets for chalcones with varied bioactivities, Med. Chem. (Los Angeles) 5 (8) (2015) 388–404; (b) K.V. Sashidhara, R.K. Modukuri, P. Jadiya, R.P. Dodda, M. Kumar, B. Sridhar, V. Kumar, R. Haque, M.I. Siddiqi, A. Nazir, Benzofuran–chalcone hybrids as potential multifunctional agents against Alzheimer's disease: synthesis and in vivo studies with transgenic *Caenorhabditis elegans*, ChemMedChem 9 (12) (2014) 2671–2684.
[317] T. Sakai, R.N. Eskander, Y. Guo, K.J. Kim, J. Mefford, J. Hopkins, N.N. Bhatia, X. Zi, B.H. Hoang, Flavokawain B, a kava chalcone, induces apoptosis in synovial sarcoma cell lines, J. Orthop. Res. 30 (7) (2012) 1045–1050.
[318] D. Chakraborty, A. Maity, C.K. Jain, A. Hazra, Y.P. Bharitkar, T. Jha, H.K. Majumder, S. Roychoudhury, N.B. Mondal, Cytotoxic potential of dispirooxindolo/acenaphthoquino andrographolide derivatives against MCF-7 cell line, MedChemComm 6 (4) (2015) 702–707.
[319] H.-J. Zhang, Y. Qian, D.-D. Zhu, X.-G. Yang, H.-L. Zhu, Synthesis, molecular modeling and biological evaluation of chalcone thiosemicarbazide derivatives as novel anticancer agents, Eur. J. Med. Chem. 46 (9) (2011) 4702–4708.
[320] L.H. Sternbach, The benzodiazepine story, J. Med. Chem. 22 (1) (1979) 1–7.
[321] (a) J. Bremner, S. Samosorn, Azepines and their fused-ring derivatives, in: Comprehensive Heterocyclic Chemistry III, vol. 13, Elsevier, 2008, pp. 1–43; (b) I. Cepanec, M. Litvić, I. Pogorelić, Efficient synthesis of 3-hydroxy-1,4-benzodiazepines oxazepam and lorazepam by new acetoxylation reaction of 3-position of 1,4-benzodiazepine ring, Org. Process Res. Dev., 10 (6) (2006) 1192–1198; (c) T. Miki, M. Kori, H. Mabuchi, R.-i. Tozawa, T. Nishimoto, Y. Sugiyama, K. Teshima, H. Yukimasa, Synthesis of novel 4,1-benzoxazepine derivatives as squalene synthase inhibitors and their inhibition of cholesterol synthesis, J. Med. Chem., 45 (20) (2002) 4571–4580; (d) R.A. Smits, H.D. Lim, B. Stegink, R.A. Bakker, I.J.P. de Esch, R. Leurs, Characterization of the histamine H4 receptor binding site. Part 1. Synthesis

and pharmacological evaluation of dibenzodiazepine derivatives, J. Med. Chem., 49 (15) (2006) 4512–4516; (e) A. Ursini, A.M. Capelli, R.A.E. Carr, P. Cassarà, M. Corsi, O. Curcuruto, G. Curotto, M. Dal Cin, S. Davalli, D. Donati, A. Feriani, H. Finch, G. Finizia, G. Gaviraghi, M. Marien, G. Pentassuglia, S. Polinelli, E. Ratti, A. Reggiani, G. Tarzia, G. Tedesco, M.E. Tranquillini, D.G. Trist, F.T.M. Van Amsterdam, Synthesis and SAR of new 5-phenyl-3-ureido-1,5-benzodiazepines as cholecystokinin-B receptor antagonists, J. Med. Chem., 43 (20) (2000) 3596–3613.

[322] M. Essaber, A. Baouid, A. Hasnaoui, A. Benharref, J.P. Lavergne, Synthesis of new tri- and tetraheterocyclic systems: 1,3-dipolar cycloaddition of nitrilimines on 2,7-dimethyl-4-phenyl-3H-1,5-benzodiazepine, Synth. Commun. 28 (22) (1998) 4097–4104.

[323] J.M. Klunder, K.D. Hargrave, M. West, E. Cullen, K. Pal, M.L. Behnke, S.R. Kapadia, D.W. McNeil, J.C. Wu, G.C. Chow, J. Adams, Novel non-nucleoside inhibitors of HIV-1 reverse transcriptase. 2. Tricyclic pyridobenzoxazepinones and dibenzoxazepinones, J. Med. Chem. 35 (10) (1992) 1887–1897.

[324] R.-K. Li, D.A.G. Mickle, R.D. Weisel, M.K. Mohabeer, J. Zhang, Cardiac cell transplantation, in: P.K. Singal, I.M.C. Dixon, R.E. Beamish, N.S. Dhalla (Eds.), Mechanisms of Heart Failure, Springer US, Boston, MA, 1995, pp. 337–347.

[325] K. Nagarajan, J. David, Y.S. Kulkarni, Piperazinylbenzonaphthoxazepines with CNS depressant properties, Eur. J. Med. Chem. 21 (1986) 21–26.

[326] A. Shaabani, S.E. Hooshmand, M.T. Nazeri, R. Afshari, S. Ghasemi, Deep eutectic solvent as a highly efficient reaction media for the one-pot synthesis of benzo-fused seven-membered heterocycles, Tetrahedron Lett. 57 (33) (2016) 3727–3730.

One-pot strategy: A highly economical tool in organic synthesis and medicinal chemistry

10

Ram Naresh Yadav[a], *Ashok Kumar Srivastava*[a], *Bimal Krishna Banik*[b,*]
[a]Department of Chemistry, Faculty of Engineering & Technology, Veer Bahadur Singh Purvanchal University, Jaunpur, India, [b]Department of Mathematics and Natural Sciences, College of Sciences and Human Studies, Deanship of Research Development, Prince Mohammad Bin Fahd University, Al Khobar, Kingdom of Saudi Arabia
[*]Corresponding author. e-mail address: bimalbanik10@gmail.com; bbanik@pmu.edu.sa

10.1 Introduction

Improving the efficiency and environmental compatibility of a chemical reaction is perhaps one of the most challenging areas in contemporary organic and medicinal chemistry. A convergent organic synthetic protocol needs to address these issues effectively. Synthesis of valuable target molecules on diverse interests is highly demanding. In the past few decades, one-pot synthetic strategy has gained tremendous attention from the scientific community across the globe. It offers multiple synthetic transformations and bond formations simultaneously in a single-pot reaction in a highly effective manner. In addition, it also circumvents several tedious purifications and reduction time that are required.

In fact, many years ago, one-pot synthetic approach was employed in chemistry. For instance, Robinson in 1917 reported the total synthesis of tropinone alkaloids using one-pot procedure (Scheme 10.1) [1].

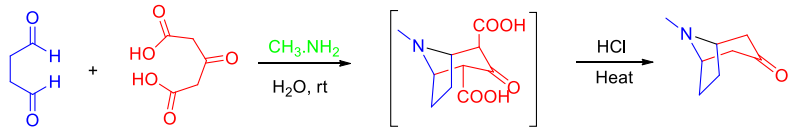

Scheme 10.1 Robinson double Mannich reaction one-pot synthesis of tropinone (1917).

Green Approaches in Medicinal Chemistry for Sustainable Drug Design. https://doi.org/10.1016/B978-0-12-817592-7.00010-1
© 2020 Elsevier Inc. All rights reserved.

Many other classical efforts were also made in the synthesis of numerous natural products. The most notable examples were biomimetic approaches for one-pot total synthesis of progesterone [2], endiandric acid [3–6], and proto-daphniphylline [7].

The multicatalytic system is one of the fast-growing diverse organic transformations using organo-catalyzed [8–11] and metal-catalyzed transformations in a one-pot reaction protocol [12–15]. Herein, we report some novel synthesis based on one-pot multicomponent strategies in diverse field of organic chemistry.

10.2 One-pot synthesis in carbohydrate chemistry

Synthetic carbohydrate chemistry is one of the fast-growing areas in organic chemistry. The structural complexity and multifaceted significance of carbohydrates in diverse disciplines of synthetic organic chemistry, biochemistry, medicinal chemistry, microbiology, and many other branches of science occupy the central importance. Carbohydrates serve as one of the most fundamental units in stereoselective synthesis of biologically relevant molecules. Carbohydrate motifs are frequently encountered in blood groups [16] and surface materials [17]. The carbohydrate conjugates in the form of glycolipids and glycoprotein are important in cell interaction process in nature. Traditionally, carbohydrates are widely distributed as energy storage materials, structural materials, and metabolites and as building blocks (BBLs) of living systems. The structural diversity of these molecules in living systems poses a challenge to structure elucidation, configurational and conformational analysis, and development of new synthetic methodology. The most notable reaction in carbohydrate is glycosylation for the synthesis of biological relevant glycosides [18–21].

10.3 One-pot glycosylation strategy in synthesis of medicinally privileged glycosides

Glycosides are the main structural motif in a large number of naturally occurring compounds. A considerable effort has been made in the stereoselective synthesis of glycosides. One-pot glycosylation (OPG) strategy was first reported by Kanhe and Raghavan in 1993 in sulfoxide-based stereoselective synthesis of naturally occurring ciclamycin-*O*-trisaccharide. This strategy offered the direct synthesis of trisaccharide unit of ciclamycin O in a single-pot operation with 25% yield (Scheme 10.2) [22]. The most notable point of this study was sequential glycosylation of glycosyl sulfoxide donor **5–7** in the presence of triflic acid as glycosyl activator at −78 to 70°C. Mechanistically, this approach describes the triflation of glycosyl sulfoxide at the rate-determining step. The rate of sequencing reaction was greatly influenced by the substitution pattern of the aromatic ring at *para*-position on the glycosyl donor.

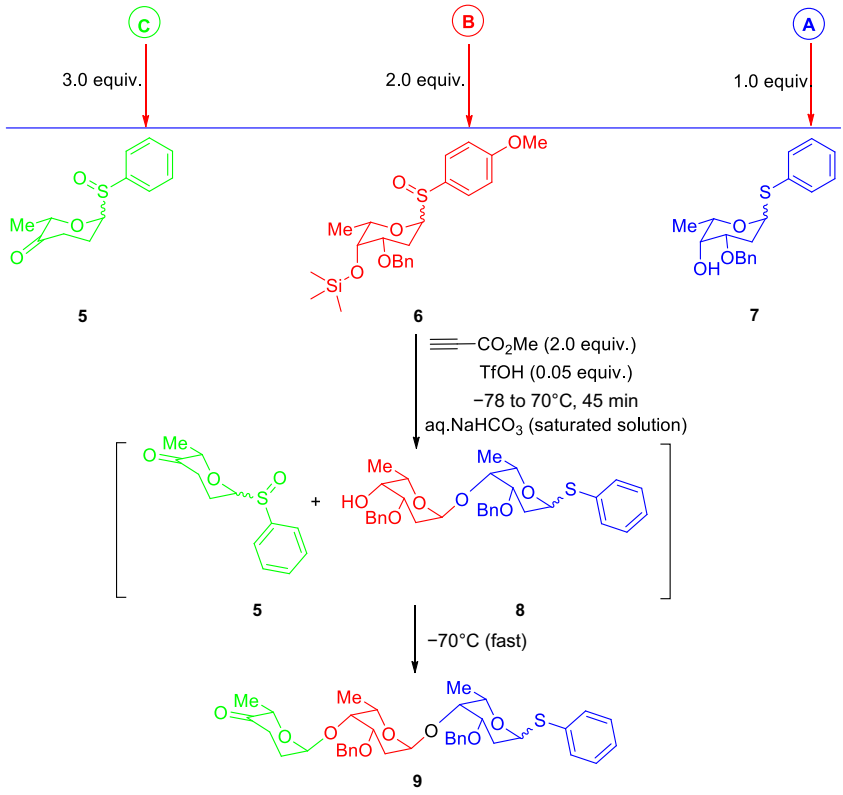

Scheme 10.2 One-pot sequential glycosylation for the synthesis of trisaccharides.

It was noted that the electronically rich aromatic ring makes the glycosyl donor more reactive than electron-deficient congener. The reactivity order was OMe > H > NO_2. The major product trisaccharide **9** was isolated in 25% yield. Other trisaccharides were isolated during this investigation. This protocol suffered from low yield and it was due to the instability of the glycosyl donor **5**. It decomposed substantially at room temperature even in the presence of glycosyl activator.

This methodology was further extended in the stereoselective synthesis of an important class of anthracycline antibiotic ciclamycin O. To complete the synthesis of ciclamycin O (**12**), the trisaccharide **10** was simply hooked up with aglycone pyrromycinone **11** in the presence of triflic anhydride under controlled condition at low temperature (Scheme 10.3) [23].

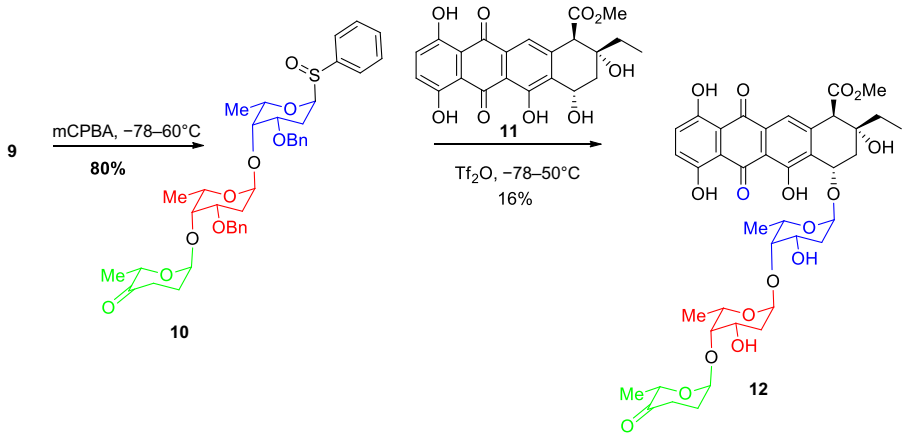

Scheme 10.3 Synthesis of ciclamycin O.

Over the last two decades, significant development has been made in OPG in synthesis of numerous compounds of multifaceted importance. This strategy has several significant advantages over conventional methods in glycosylation chemistry. This advantage includes circumventing of the separation, extraction, and exhaustive purification of the products. Recently, OPG approach has received tremendous attention across the globe. This synthetic method realizes on three broad categories: (**I**) chemoselective (arm-disarm thioglycosides), (**II**) orthogonal donors and activators condition, and (**III**) preactivation of donors.

The protecting groups played a pivotal role in chemoselective glycosylation. The one-pot chemoselective glycosylation was introduced by Fraiser-Reid and coworkers based on the concept of armed/disarmed glycosyl donors (Fig. 10.1) [24, 25].

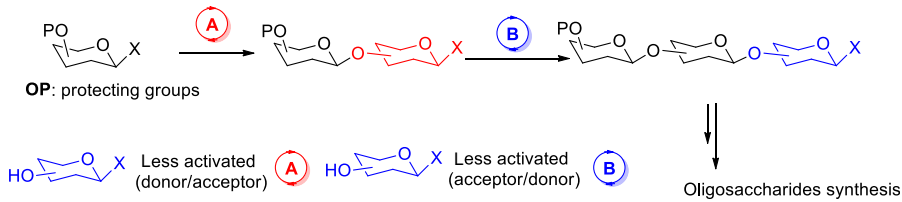

Fig. 10.1 Chemoselective one-pot glycosylation (OPG) method.

The activated donor reacted preferentially with the promotor followed by glycosylation with less activated donor/acceptor. The stereoselectivity of glycosylation reaction greatly depended on the nature of the protecting groups at the C-2 position of glycosyl donor [26]. Moreover, the refinement of the strategy of glycosylation was dependent on the nature of the protecting groups, conformation, solvent, and temperature of the reaction conditions [27–29]. These conditions were maintained

carefully to create a newly desired glycosidic bond in regio- and stereoselective manner.

The recognition of carbohydrates as therapeutically relevant biomolecules inspired scientists for further development in this area. A significant development was made in using synthetic carbohydrate as a drug candidate for the treatment of various diseases. The most important carbohydrate-based chemotherapeutic agents include cancer vaccine [30–34], sialidase inhibitors for the treatment of influenza virus [35–37], and small molecule selectin inhibitors [38]. The primary stage of the microbial infections recognized glycoconjugates in the host cell by the assailant microorganism [39]. The biological activity merely depended on the glycoconjugate structure not on the monosaccharide unit. Due to its complex structure and multiple stereogenic centers, synthesis of oligosaccharides and their conjugates was extremely difficult. The development of a program for the synthesis of oligosaccharides was immensely demanding. The traditional synthesis of this class of molecule was based on sequential protection/deprotection strategy with complete stereocontrol [40]. However, further advancement in automated synthesis of the polysaccharides was also achieved [41–46].

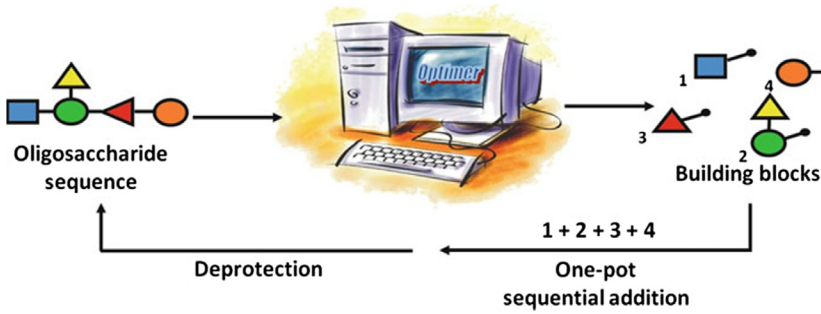

Fig. 10.2 Programmable one-pot synthesis of oligosaccharides.

A new synthetic strategy based on the merger of chemical and enzymatic method was introduced by Wong *et al.* in 1999 (Fig. 10.2) [26, 47]. The programmable one-pot synthesis of oligosaccharides provided complete structure and reactivity correlation in designing the synthesis of complex oligosaccharides of diverse interests. It offered an elegant information of the complex structure of the carbohydrates. The relative reactivity value (RRV) of the starting compound was calculated. This value greatly helped in designing the program for performing one-pot sequential glycosylation. The authors reported the synthesis of various oligosaccharides, building block of medicinally crucial molecules. A representative example reported by Wong *et al.* in synthesis of tetrasaccharides programmable one-pot approaches is delineated (Scheme 10.4). Theoretical calculation of RRV helped in predicting the reactivity of the glycosyl donor. A higher value of RRV indicated greater reactivity of glycosyl donor molecules. The RRV database offered the information for the possible combination of glycosyl BBLs in practical synthesis of oligosaccharides. In this investigation, authors used the reactivity difference for the synthesis of **13–14** and for **15–16** for the two glycosylation steps. This difference was fairly suitable for the synthesis of target tetra saccharides **(17)**.

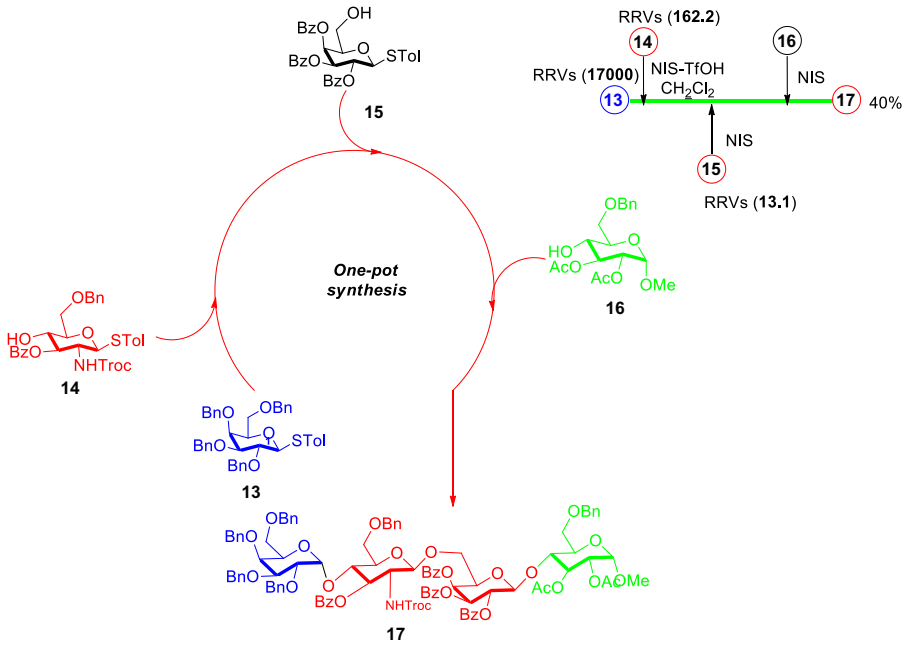

Scheme 10.4 One-pot synthesis of programmable tetrasaccharides.

The noticeable point for this investigation was the low efficiency of this protocol than predicted by OptiMer analysis (82% as predicted). This was explained due to the fact that OptiMer program does not recognize any decomposition, deactivation after the new glycosidic bond formation and any other side reaction during the process of the reaction. The theoretical yield predicted by OptiMer program is actually 100% of any normal reaction.

The major sequencing in OPG toward complex oligosaccharides was as follows:

[I] [1+2+2] one-pot strategy in heparin pentasaccharides
[II] [1+3+2] one-pot hexasaccharides synthesis
[III] [2+1+3] one-pot synthesis of sialic acid saccharides

In connection of programmable one-pot synthesis of structurally complex saccharides, Wong and his groups developed a pioneer work in this area using a diverse possible combination of monosaccharides units *viz*. [1+2+2], [1+3+2], and [2+1+3] pattern in synthesizing a number of chemotherapeutic oligosaccharides. This group published an elegant method for the synthesis of heparin pentasaccharides based on programmable and experimental OPG toward this endeavor. The heparin pentasaccharides with stereodefined pattern of sulphite group exhibited excellent anticoagulant properties [48]. Heparin and heparinsulfates are important class of compounds that belong to glycosaminoglycans (GAGs) family. The chemical synthesis of this complex molecule initially involved the coupling of azio glucosyl thio donor **18** (RRV 57.3) with disaccharide

acceptor **19** (RRV 18.2) in the presence of *N*-iodosuccinimide and triflic acid as promoter at −45°C to room temperature followed by the addition of methyl disaccharides acceptor **20** (RRV 0). Under this stated condition the fully protected heparin pentasaccharide **21** was obtained in 20% yield. The oligosaccharide **21** was transformed into polyanionic sulfated heparin derivative **22** by base-assisted hydrolysis, hydrogenolysis, and chemoselective sulfonation (Scheme 10.5).

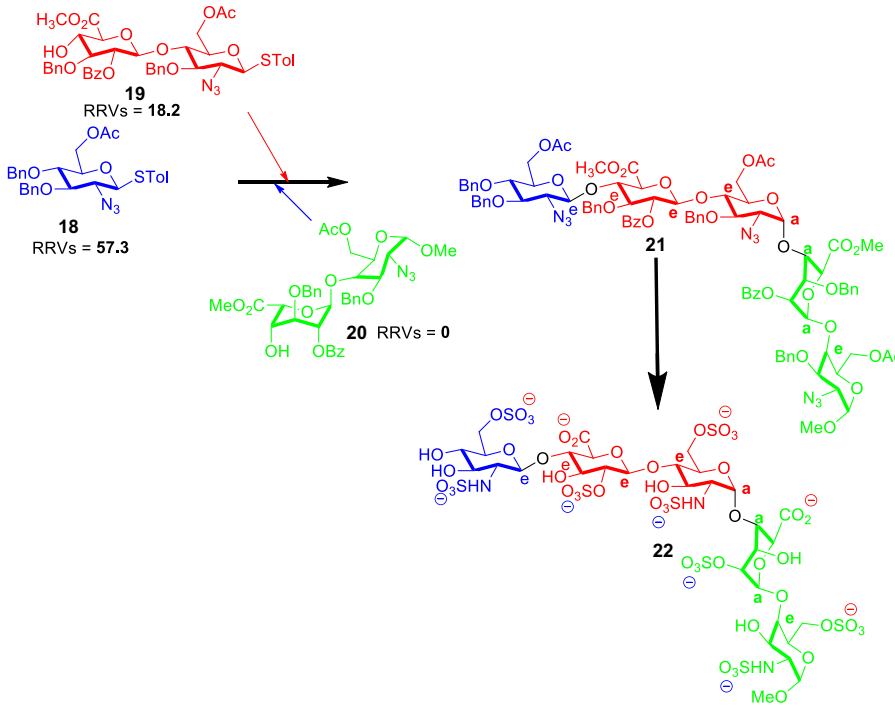

Scheme 10.5 One-pot synthesis of heparin pentasaccharides based on [1+2+2] sequence. *Reagent and conditions*: (**a**) (i) NIS, TfOH, CH_2Cl_2, −45 → 25°C; (ii) NIS, TfOH, CH_2Cl_2, −45 → 25°C, 20%; (**b**) (i) LiOH, THF; (ii) $Et_3N{\cdot}SO_3$, DMF; (iii) H_2, Pd/C; (iv) $Pyr{\cdot}SO_3$, 33%.

The authors recently modified the protocol by manipulating the protecting groups in glycosyl donor and acceptor in order to get a better yield. The modified synthetic route for one-pot synthesis of heparin pentasaccharides was based on the coupling of azido-thioglucosyl donor **23** (RRV 132) with disaccharides **24a–b** (RRV 18.2, 34.2) followed by the addition of reducing disaccharides **25a–d** in the presence of NIS/TfOH as activator/catalyst to furnish the title saccharides **26a–d** in moderate to good yield (Table 10.1, Scheme 10.6) [49, 50].

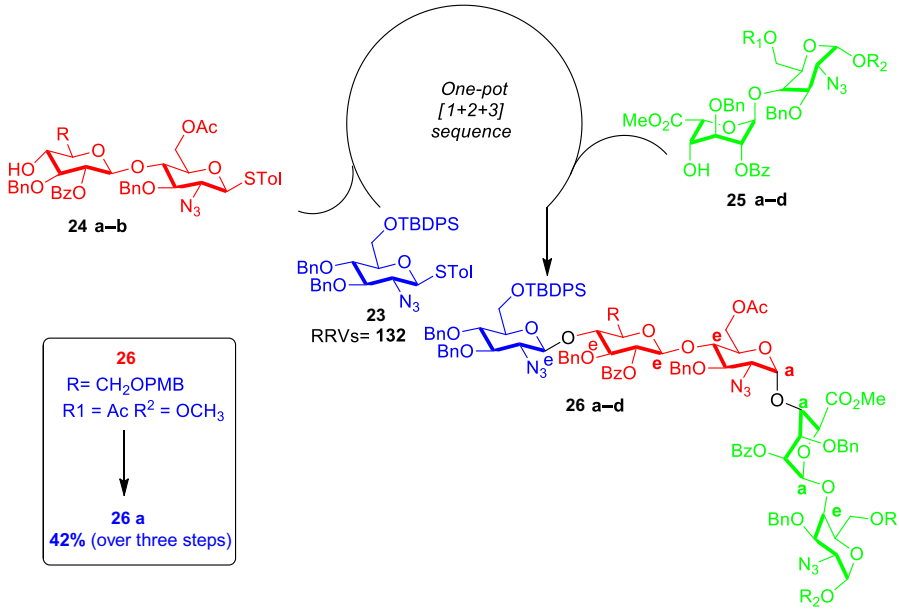

Scheme 10.6 Improved synthesis of heparin pentasaccharides in one-pot procedure. *Reagent and Conditions*: (**a**) NIS, TfOH, CH_2Cl_2, AW 300 MS, −40 → −25°C (**b**) (i) DDQ, CH_2Cl_2:H_2O (10:1), rt, 1 h; (ii) BAIB, TEMPO, CH_2Cl_2:H_2O (2:1), rt, 2 h; (iii) CH_3I, $KHCO_3$, DMF, 0°C to rt, 4 h.

Table 10.1 One-pot synthesis of heparin-pentasaccharides at −40 → −25°C.

Entry	24(a–b)		25(a–d)			26(a–d)			Yield (%)
	R	RRVs	R^1	R^2	RRVs	R	R^1	R^2	
01	CO_2Me	18.2	Ac	OCH_3	0	CO_2Me	Ac	OCH_3	54
02	CO_2Me	18.2	Lev	OCH_3	0	CO_2Me	Lev	OCH_3	48
03	CO_2Me	18.2	Ac	$(CH_2)_5NCbzBn$	0	CO_2Me	Ac	$(CH_2)_5NCbzBn$	50
04	CO_2Me	18.2	Lev	$(CH_2)_5NCbzBn$	0	CO_2Me	Lev	$(CH_2)_5NCbzBn$	42
05	CH_2OPMB	38.2	Ac	OCH_3	0	CO_2Me	Lev	$(CH_2)_5NCbzBn$	–

The stereochemistry at the anomeric position was established by the coupling constant of the C—H bond which is easily measured by C^{13} coupled HMQC experiment. The $^1J_{C-H}$ coupling values for **26b** were found $^1J_{C-H} = 178.15$ Hz (α), 176.06 Hz (α), 177.65 Hz (α), 172.56 Hz (α), and 163.3 Hz (β), signifying the existence of four α-glycosidic bonds and one β-glycosidic bond in pentasaccharides.

The [2+1+3] one-pot strategy was employed in the synthesis of onco-glycosides SSEA-4 for embryonic malignant tumor cell markers [51, 52]. This saccharide consisted of [*a*-2,3]-sialic acid as the main structural components which serves as a

nonreducing unit in SSEA-4. Because of low reactivity, sialic acid failed to act as a glycosyl donor BBL for this reaction.

A programmable one-pot synthetic protocol was designed for the synthesis of complex hexasaccharide **30**. This synthetic route comprised a series of reactions. For example, sialic acid disaccharide **27** was coupled with thioaminoglycosides **28** as glycosyl acceptor followed by the addition of trisaccharide **29** which eventually led the title compound **30** with **43%** yield. The relative rate velocity of each BBL was determined computationally to establish the reactivity order of each donor and acceptor (Scheme 10.7) [49].

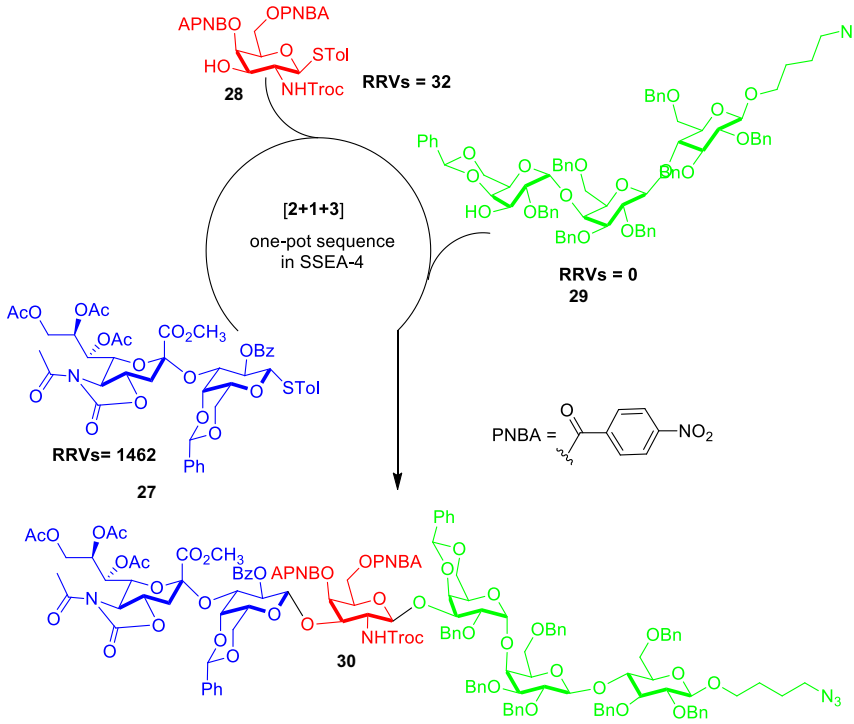

Scheme 10.7 Synthesis of SSEA-4 hexasaccharides in one-pot procedure. *Reagent and Condition*: (**a**) (i) TfOH, NIS, CH_2Cl_2, −40°C, 3 h; (ii) TfOH, NIS, CH_2Cl_2, −20°C.

Fucose GM1 (**31**) is a sialic acid containing important class gangliosides having hexasaccharides motif with reducing terminal ceramide group (Fig. 10.3). This tetrasaccharide was first isolated from thyroid gland tissue of bovine in 1979 [53]. This was usually traced in tumor tissue of small cell lung-cancer of animal and comprised 20% of lung cancer in bovine in United States. Among other cancer antigen, Fuc-GM1 had very restricted spread in normal tissue. Due to this activity, this antigen became a good target for active immunization. Among the discoveries in the area of

cancer vaccine immunization program based on oligosaccharides structure, it was developed to use for diverse cancers [31, 54–56]. The first cancer vaccine based on carbohydrate-based Fuc-GM1 glycoside was developed by Danishefsky and coworkers [57]. In this context, Wong and coworkers developed a programmable one-pot strategy for the total synthesis of anti-Fuc-GM1 vaccine based on glycosylation reaction [58].

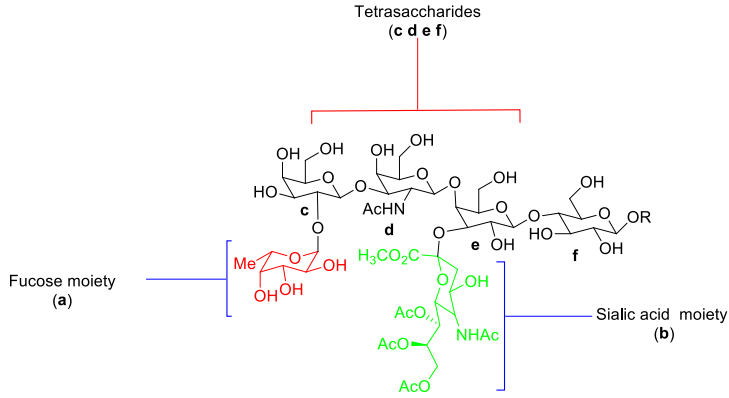

Fig. 10.3 Structure of Fuc-GM1 (**31**) anticancer vaccine.

Based on retrosynthetic analysis, the glycosides **33**, **34**, and **35** were found to be the main BBLs for this target molecule. The author stated that the per benzylated fucosyl thioglycosides **33** were synthesized by known literature method (Fig. 10.4). The disaccharides BBL **34** was assembled by the glycosylation between glactosyl donor and glactosaminyl acceptor. The sialylated trisaccharide BBL **35** was synthesized by glycosylation of sialylphosphite and lactoside acceptor in 53% isolated yield.

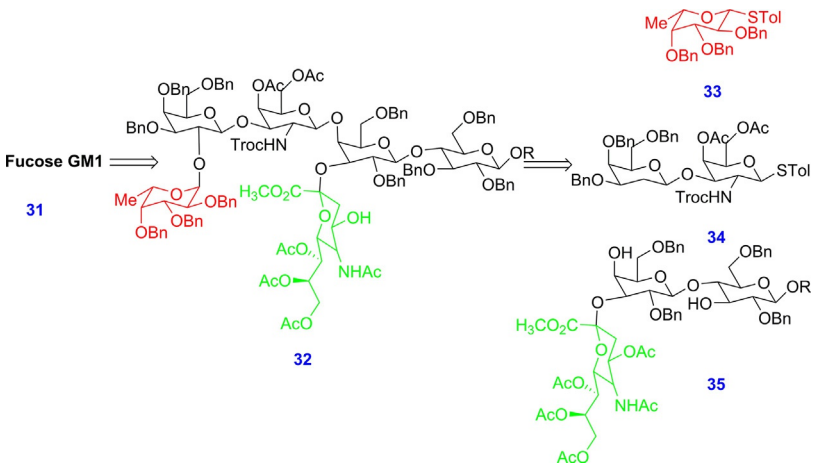

Fig. 10.4 Retrosynthetic analysis of fucose GM1 (**31**).

The final target molecule was synthesized by NIS/TfOH-promoted glycosylation in 36% yield of Fuc-GM1 **31**. In order to improve the yield, the strategy was modified to include a better promoter. Using1-benzenesulfinyl/triflicanhydride (BSP/Tf_2O)-promoted OPG reaction originally developed by Crich and Smith [59] gave a promising yield of 47% (Scheme 10.8).

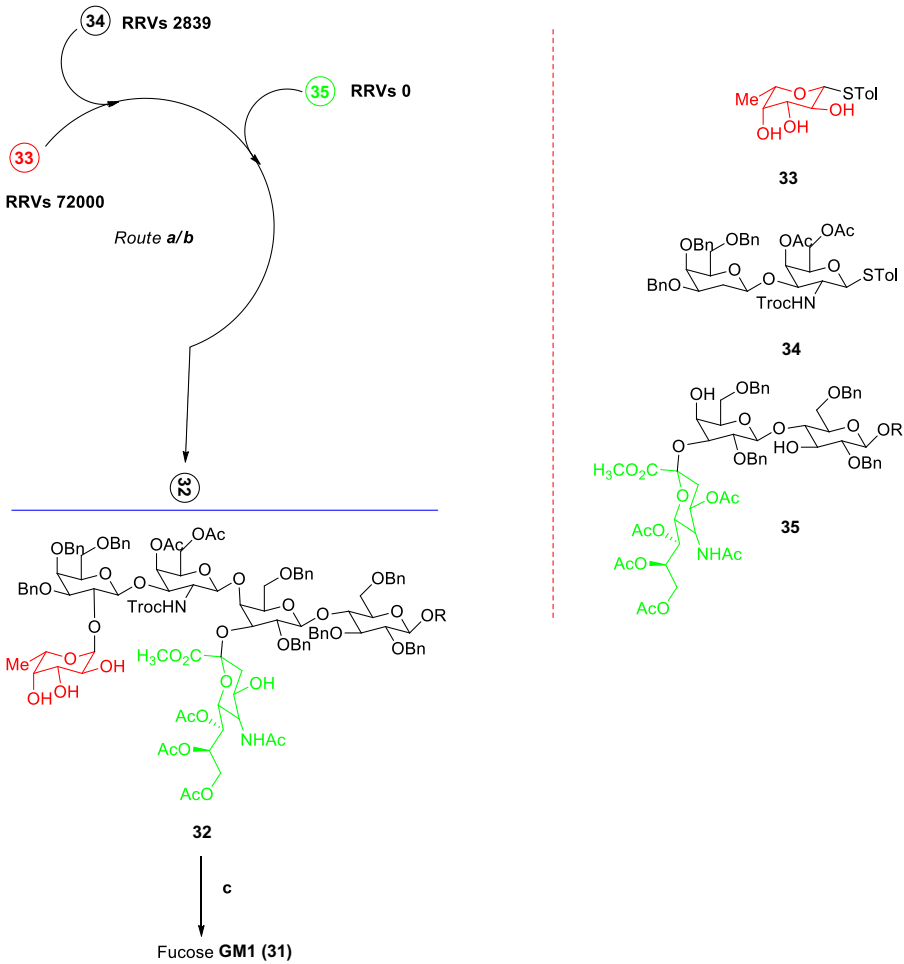

Scheme 10.8 One-pot programmable total synthesis of Fuc-GM1 carbohydrate epitope. *Reagent and Condition*: Route (**a**) (i) NIS, TfOH, CH_2Cl_2, 70°C, 36%; (ii) DMTST, 0°C, 36%. Route (**b**) (i) BSP, Tf_2O, CH_2Cl_2, 70–10°C, 47%; (ii) BSP, Tf_2O, CH_2Cl_2, 70–0°C, 47%. Route (**c**) (i) Zn dust, acetic anhydride/CH_2Cl_2, 4-(dimethylamino) pyridine; (ii) NaOMe, CH_2Cl_2/MeOH; (ii) NaOH, THF/MeOH/H_2O; (iii) Pd-black, MeOH with 10% (vol/vol) formic acid, H_2 (1 atm), 44% over four steps.

Polyphenolic naturally occurring glycoside has a wide spectrum of biological activity like antitumor and antiviral and these are because of specific polyphenol-protein interactions [60, 61]. In this area, ellagitannins, naturally occurring polyhydroxy bisphenolic glycosides can be mentioned (Fig. 10.5).

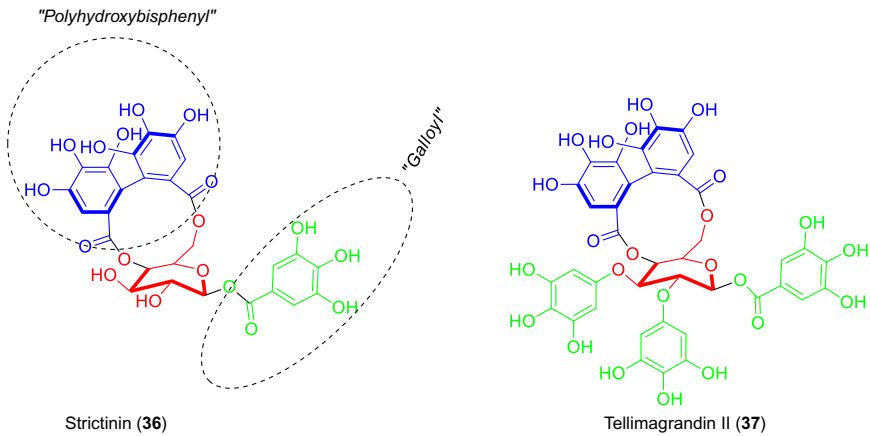

Fig. 10.5 Naturally occurring polyhydroxy bis-phenolic glycosides "ellagitannins."

Ellagitannins have been known for long time in literature, owing to its complex structure. The potential bioactivity of these compounds attracted the attention of scientific community for their chemical synthesis. Strictinin **36** and tellimagrandin II **37** are important compounds in this class. These compounds specially show anti-HSV [62], antitumor [63], antiinfluenza virus [64], and antiallergic activity [65]. Kawabata *et al.* developed a program for the synthesis of strictinin **36** based on one-pot stereoselective glycosylation as the key reaction. The rational retrosynthetic analysis for the synthesis of this molecule is given here (Fig. 10.6).

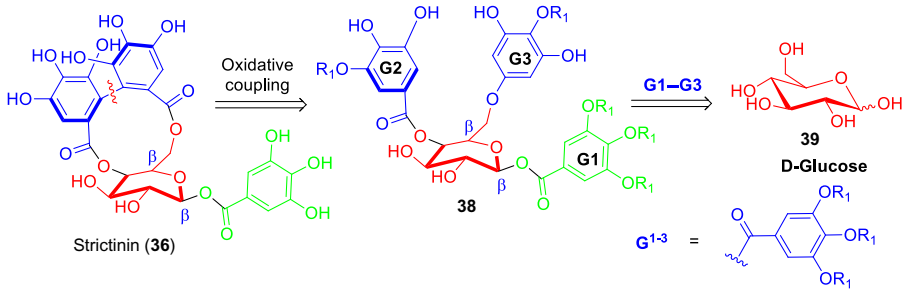

Fig. 10.6 Rational retrosynthetic analysis.

The synthetic procedure of this target molecule was based on highly stereoselective direct glycosylation of unprotected D-glucose as glycosyl donor **39** with MOM-ether of gallic acid as glycosyl acceptor **40** under Mitsunobu condition. The reaction involved in the treatment of D-glucose suspension in 1,4-dioxane with diisopropyl azodicarboxylate (DIAD) followed by the addition of triphenylphosphine (PPh_3) at room temperature over 30 min to produce the target compound **41** in 78% yield with excellent anomeric selectivity (1:99) (Scheme 10.9) [66].

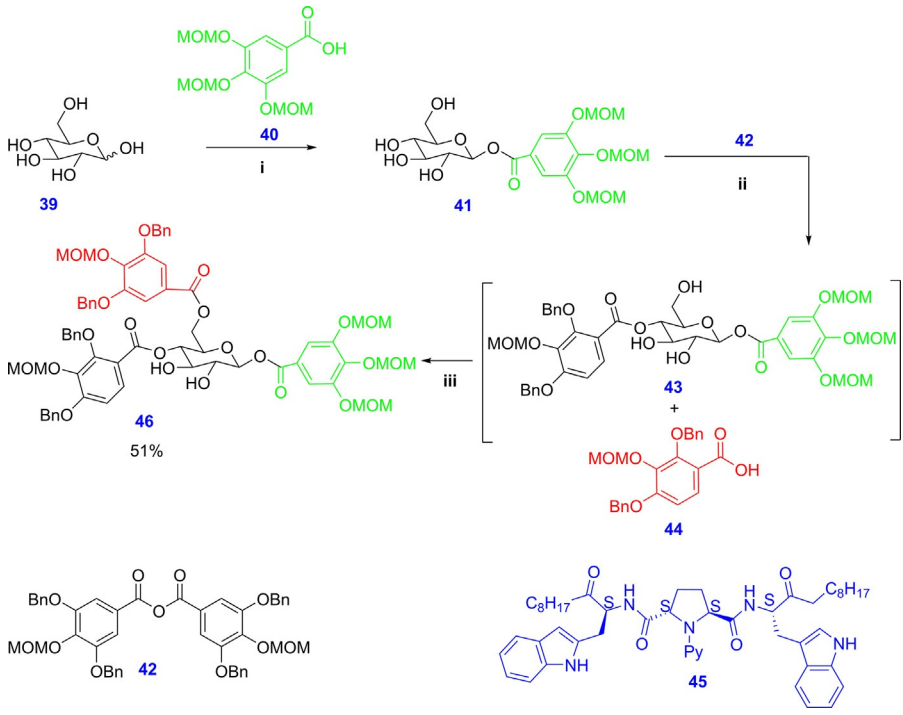

Scheme 10.9 Direct glycosylation and regioselective organo-catalyzed substrate controlled acylation. *Reagent and Condition*: **(i) 40** (1.0 equiv.); DIAD (2.0 equiv.); PPh_3 (2.0 equiv.); 1,4-dioxane; 30 min; (78% β/α ratio: 99:1); **(ii)** Cat. **45** (10 mol%); **44** (1.06 equiv.); −40°C, 72 h; **(iii)** DMC/DMAP; Py; 5°C 8h (51%); one-pot.

The β-glycoside was employed for the one-pot regioselective organocatalyzed O-galloylation at C-4 position followed by C-6 O-galloylation to the target compound **46** in a single-pot operation. This protocol had an excellent scalability and reproducibility.

The β-glycoside **46** was employed in the total synthesis of strictinin **36** and tellomagrandin **37** based on global protection and deprotection of the hydroxy function in glucose and aromatic group in compound **46** followed by the

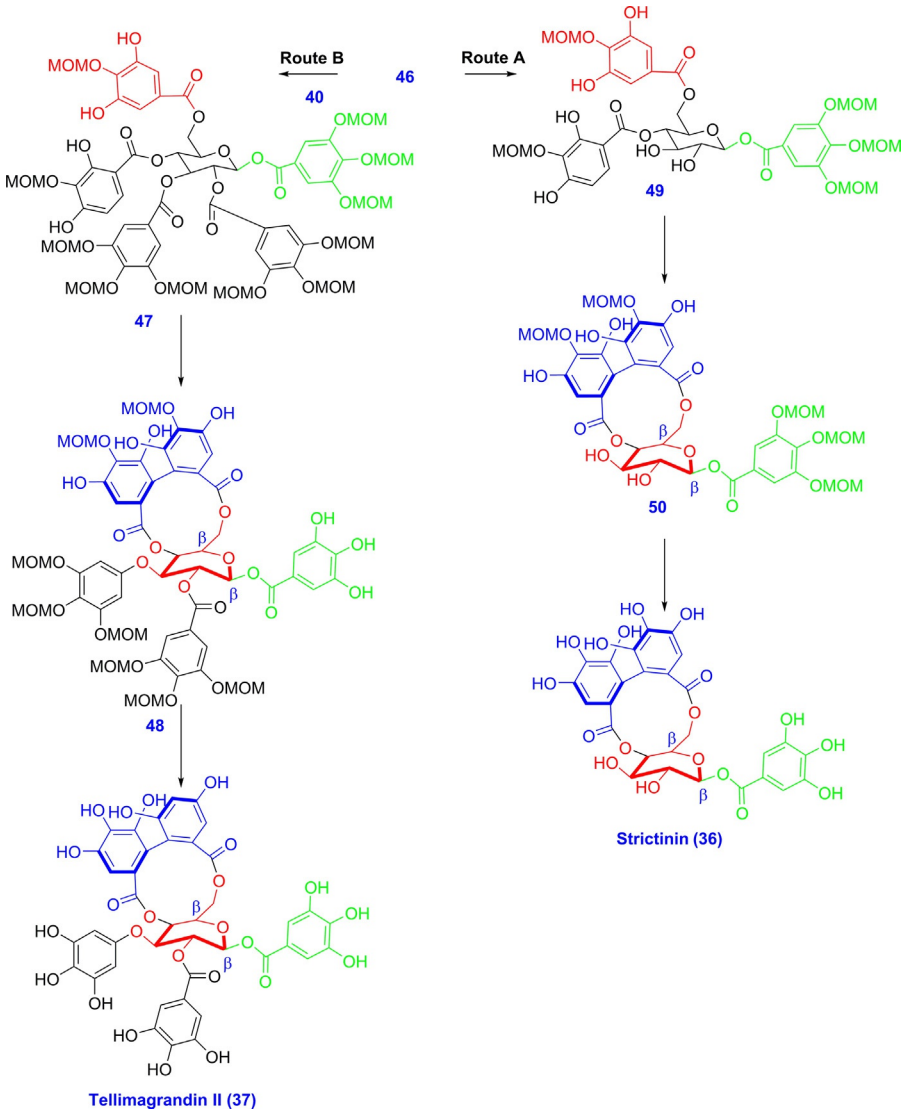

Scheme 10.10 Total synthesis of strictinin **36** and tellomagrandin **37**. *Reagent and Condition*: **Route A** (i) H_2; $Pd(OH)_2$/C; THF; rt; (ii) CuCl; MeOH/$CHCl_3$ (1:1), rt; (iii) conc. HCl/^{i}PrOH/THF (1:50:50); rt; 21%; overall yield (**36**); **Route B** (i) **40;** EDCI·HCl, DMAP, CH_2Cl_2, rt; and then H_2, $Pd(OH)_2$/C, THF, rt; same as (ii) and (iii) 18%; overall yield (**37**).

copper-catalyzed oxidative coupling to generate 11-membered rings on the sugar moiety (Scheme 10.10) [66].

A phosphorylated trisaccharide was found in the cell wall of *Providencia alcalifaciens* O22, a genus of Gram-negative bacteria of Enterobacteriaceae family.

This phosphorylated trisaccharides structurally constitute units of *O*-polysaccharides having two BBLs of 2-acetamido-4-amino-2,4,6-trideoxy-D-galactose (D-FucNAc4N) and D-glyceramide-2-phosphate (GroAN-2-P). The complete structure was established to be -4)-(D-GroAN-2-P-3-)-β-D-GalNAc-(1–4)-β-D-Gal-(1–3)-β-D-Fuc-NAc4N-(1-) (Fig. 10.7) [67].

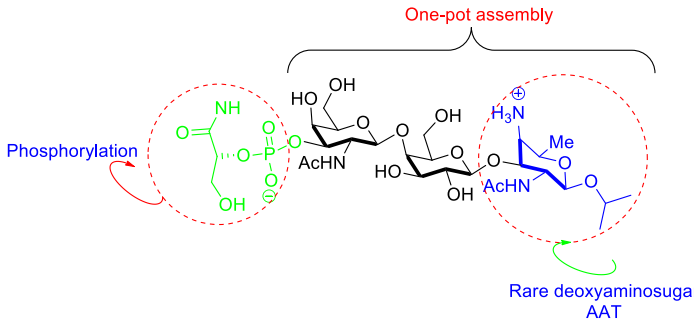

Fig. 10.7 Repeating unit of *O*-polysaccharides (**51**).

These bacteria were isolated and identified from a wide variety of organisms including fruit flies, marine animal, and human [68] and known to be as opportunistic pathogens. Some of the species such as *P. alcalifaciens*, *Providencia rustigianii*, *Providencia rettgeri*, and *Providencia stuartii* were the main causative agents especially for urinary tract infection, and enteric diseases [69]. This pathogen caused the erratic meningitis [70] and ocular infection [71]. It was proved that such carbohydrate-based phosphorylated zwitterionic saccharides activate the T-cell receptors in conjugation with carrier protein which provoked greater immunological response [67].

Kulkarni *et al*. in 2017 developed a one-pot synthetic protocol for the total synthesis of the trisaccharides which is an integral part of *O*-polysaccharides found in *P. alcalifaciens* O22. The biggest challenge was to find the orthogonally protected rare sugar AAT and subsequent phosphorylation of secondary alcohol functionality in D-glyceramide unit next to the amide linkage. To combat this challenge author proposed the plausible retrosynthetic analysis for this target (Fig. 10.8). The main BBL of the trisaccharide was **56**–**58** which is effectively designed to access **53**. A highly regioselective NIS/TfOH-promoted glycosylation was performed by thioglycosyl donor **57** and glycosyl acceptor **58** for 1 h. The generated disaccharide reacted with glycosyl donor **56** in the same pot. The excess acidic promotor quenched with triethylamine and deprotection of Fmoc group gave 3-OH free trisaccharides in 72% yield in overall three steps in a single-pot reaction. The complete structure was established by ^{1}H NMR, ^{13}C NMR, ^{1}H-^{13}C HSQC, and ^{1}H-^{1}H COSY analysis (Scheme 10.11) [72].

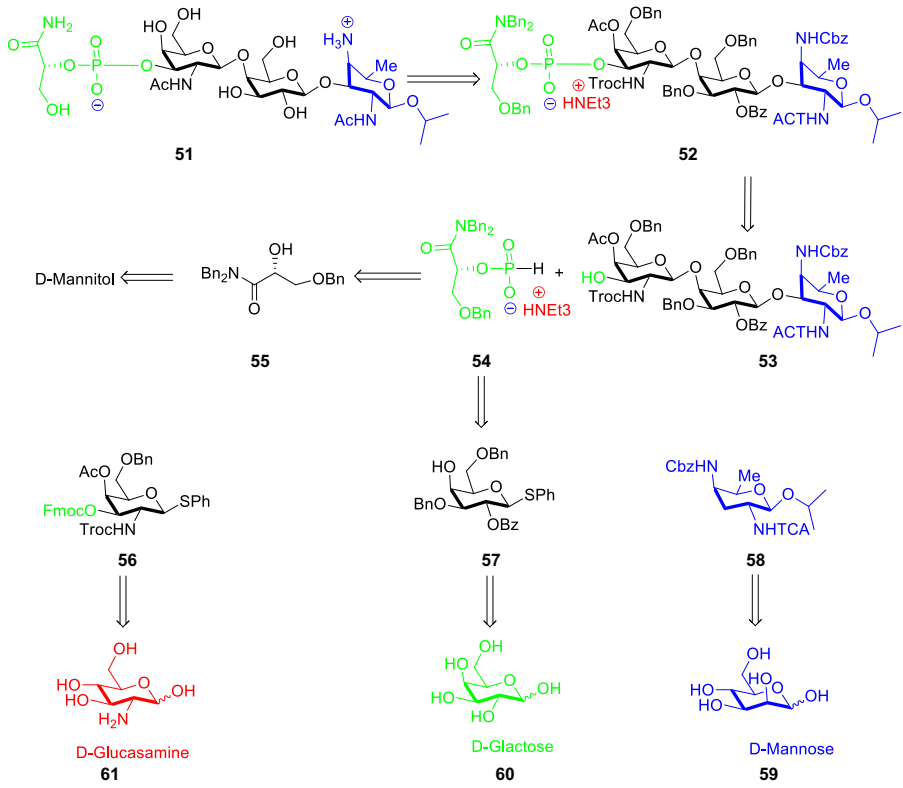

Fig. 10.8 Retrosynthetic analysis.

The corresponding disaccharides and trisaccharide intermediates (IMs) were also established by NMR analysis and TLC development prior to performing OPG of the target molecule. The D-glyceramide BBL was easily accessible from dicyclohexylidene D-mannitol. The synthesis of the final target molecule was completed by phosphorylation of 3OH group and followed by the global deprotection of the diverse functionality in **51**. The first total synthesis of immunologically potent zwitterionic phosphorylated trisaccharide was reported in 64% isolated yield. The key feature of this protocol was highly stereoselective glycosylation and synthesis of appropriately protected rare sugar AAT BBL. The final compound **51** was characterized by conducting extensive ^{1}H, ^{13}C, ^{31}P NMR, and HRMS analyses.

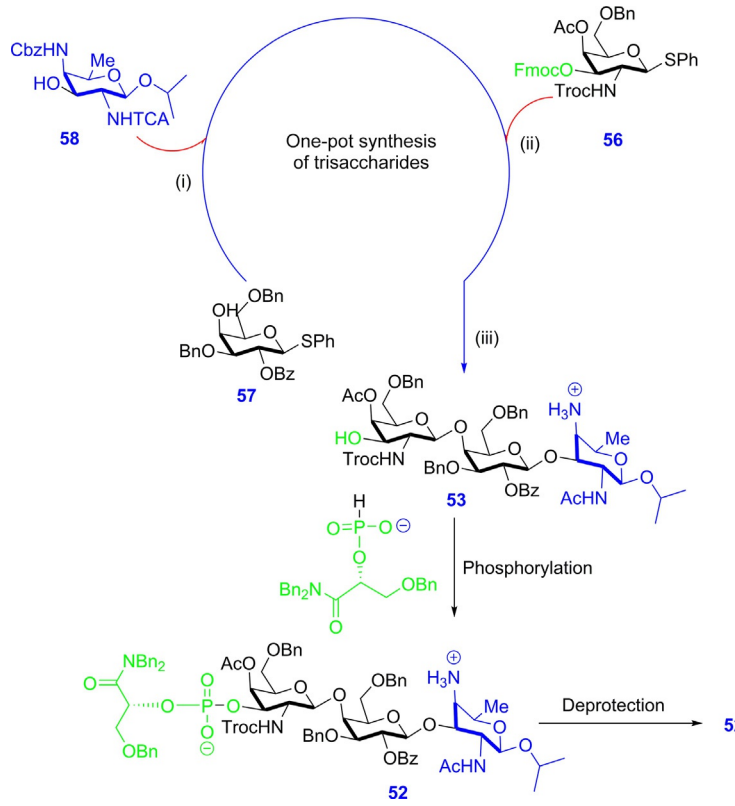

Scheme 10.11 One-pot synthesis of trisaccharides **53**. *Reagent and Conditions*: (i) NIS (2.0 equiv.); TMSOTf (1.0 equiv.); CH_2Cl_2; 1 h; (ii) NIS (2.0 equiv.); TMSOTf (1.0 equiv.); 1 h; (iii) TEA (64%).

10.4 One-pot synthesis of iminosugar

Iminosugars are important class of naturally occurring N-analogs of carbohydrates in which the ring oxygen is replaced by nitrogen atom. Therefore, iminosugars are considered as polyhydroxylated secondary and tertiary amine with close resemblance with monosaccharides in which endocyclic nitrogen atom is located instead of oxygen (Fig. 10.9). This alteration and close stereochemical similarities make iminosugars as

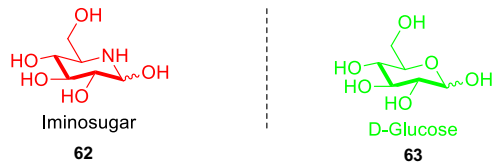

Fig. 10.9 Basic structure of iminosugars.

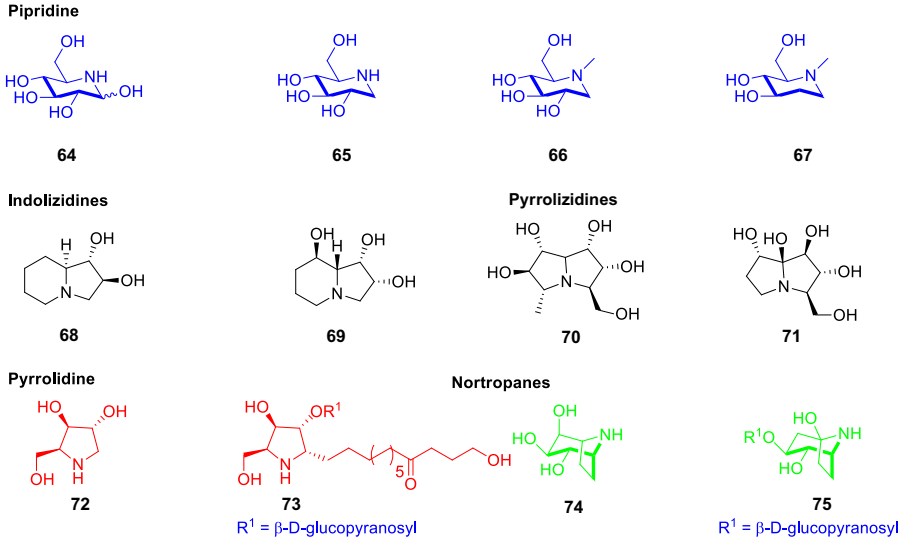

Fig. 10.10 Nojirimycin **64**; 1-Deoxynojirimycin **65**; *N*-methyl-deoxynojirimycin **66**; Fagomine **67**; Lentiginosine **68**; Swainsonine **69**; Hyacinthacine C_1 **70**; Australine **71**; 1,4-Dideoxy-1,4-imino-D-arabinitol **72**; Broussonetin B **73**; Calystegine B4 **74**; Calystegine B1-3-*O*-β-D-glucopyranoside **75**.

glycosidase inhibitors [73] and glycotransferase [74]. These compounds are also known as azasugar, glycosidase inhibitors, and sugar analogous. Like the carbohydrates, iminosugars are frequently encountered in nature with piperidine and pyrrolidine ring systems. Other bicyclic iminosugars are analogs to disaccharides that include pyrrolizidines, indolizines, and notropanes (Fig. 10.10). These class of compounds believe to exhibit glycosidase inhibitor properties and these characteristics are supported by isolation and synthesis [75]. However, it is clear from several studies that these compounds do not act as glycosidase inhibitors for displaying their pharmacological bioactivity rather acts as immunological modulator and chaperones off misfolded protein without inhibiting glycosidases [76, 77].

These classes of molecules have numerous chemotherapeutic applications. Many N-alkylated iminosugar Miglitol was used as drug candidates for combating the diabetes mellitus type 2 [78]. In the past few decades, a wide range of iminosugar was isolated from different parts of the mulberry tree (Morus spp.). The most notable were 1-deoxynojirimycin **65**, fagomine **67**, *N*-methyl-deoxynojirimycin **66**, and 1,4-dideoxy-1,4-imino-D-arabinitol **72** [79–81].

Due to the excellent drug profile and diverse stereogenic centers, these molecules attracted the attention of the scientists to develop a synthetic strategy for their preparation and biological activity evaluation.

In 2008, Zhang *et al*. reported an expeditious highly diastereoselective synthesis of 1,6-dideoxy N-alkylated iminosugar and analog of nojirimycin in single-pot operation using double reductive amination by $NaCNBH_3$ of the IM **78**. Authors used methyl α-D-glucopyranoside **76** as key starting material for the synthesis of diverse

iminosugar derivatives. The unsaturated glycoside **76** was treated with catalytic amount of triflic acid to allow the facile hydration of the exocyclic double to give the compound **77** which underwent concomitant loss of methoxy group followed by rearrangement to 1,5-dicarbonyl IM **78**. The IM allowed to react with diverse amines in the presence of sodium cyanoborohydride ($NaCNBH_3$) to afford the iminosugar **79a–e** in good to excellent yield. In this present study the noteworthy point was stereoselective amination that produces a single stereoisomer in all cases. The catalytic hydrogenolysis of the compounds **79a–e** over Pd/C in $THF/H_2O/CH_3COOH$ gave free hydroxy derivative of iminosugar **80a–e** in excellent yield. It was found that the synthetic N-alkylated iminosugars show inhibitory effects on the release of the cytokines IFN-γ and IL-4 from the mouse splenocytes (Scheme 10.12) [82].

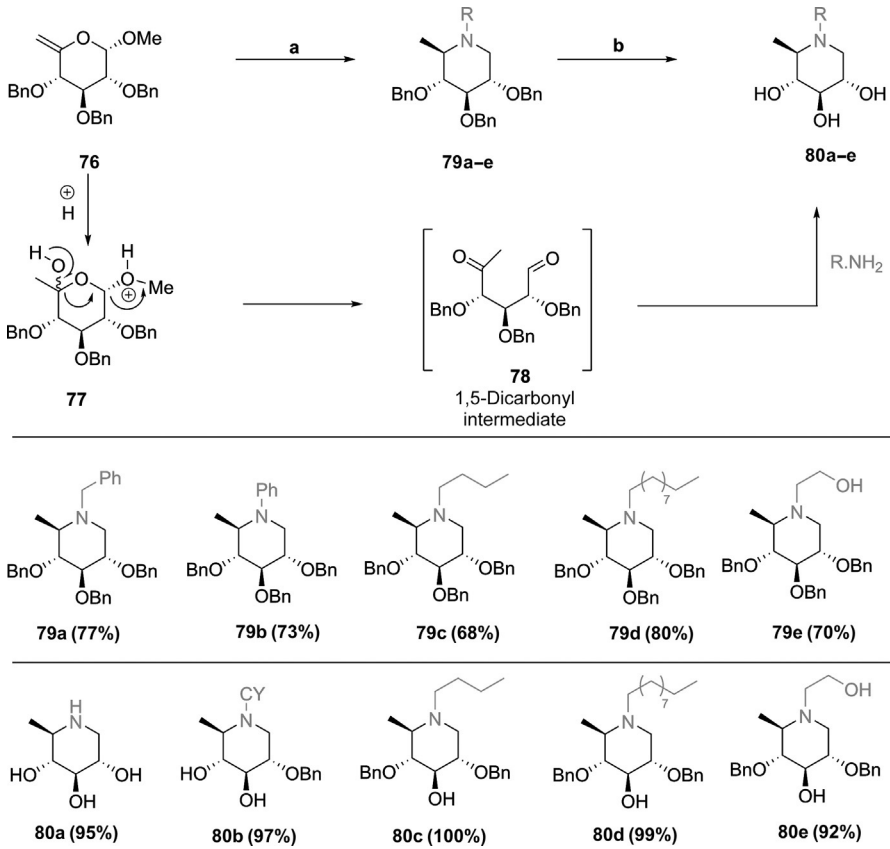

Scheme 10.12 One-pot synthesis of 1,6-dideoxy-N-alkylated nojirimycin analogs. *Reagents and Conditions*: (a) CF_3COOH; MeOH then RNH_2; $NaCNBH_3$; CH_3COOH; (b) Pd–C H_2.

Barbas III *et al*. reported a simple and powerful methodology to prepare pyranoside analog of iminosugar having *talo*- and *manno*-cofiguration based on organocatalytic intermolecular Michael-Henry reaction in a single one-pot operation starting from

achiral noncarbohydrate as the key starting material. The Michael reaction of silylated aldehyde **82** with nitrostyrene **81**(**a–e**) in the presence of 20 mol% of thiourea-based primary amine as organocatalyst afforded high *anti*-selective Michael adduct **84** (anti/syn, 98/2) in excellent stereochemical control [83]. The anti-Michael adduct without purification was allowed to react with *p*-toluene sulfonyl imine **85** in the presence of a variety of bases at room temperature. This reaction afforded the compounds **86** and **87**(**a–e**) in moderate to good yield. A wide range of bases was screened to obtain a better yield. The base, *N*,*N*,*N*,*N*-tetramethylguanidine in combination with acetic acid was found to be an excellent choice. Under this optimized condition, this group performed the reaction of diverse β-nitro styrenes with both electron donating and withdrawing groups and produced iminosugar derivatives in good yield with excellent enantiomeric selectivity (Scheme 10.13, Table 10.2) [84].

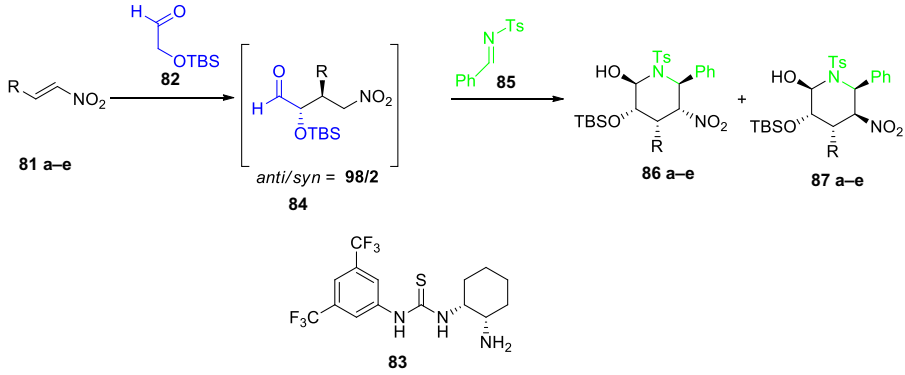

Scheme 10.13 Organo-catalyzed one-pot enantioselective synthesis of iminosugar derivative based *on anti*-Michael-*anti*-aza Henry reaction. *Reagent and Conditions*: (i) **83** (20 mol%); CH_2Cl_2; rt; 4 h; (b) *N*,*N*,*N*,*N*-tetramethylguanidine (1.5 equiv.); AcOH (0.5 equiv.); 0°C; 0.5 h.

Table 10.2 Optimized conditions and substrate scope of the one-pot anti-Michael-aza-Henry reaction in synthesis of iminosugars.

	β-Nitrostyrene (R)		Time	Yield (%)	dr[a] (%)	
	81(a–e)					
Entry	81	R	h	86 + 87	86:87	ee[b] (%)
1	**81a**	Phenyl	4	68	7:1	99
2	**81b**	4-Methoxy phenyl	8	64	10:1	99
3	**81c**	4-Bromophenyl	4	69	4:1	99
4	**81d**	3-Bromophenyl	4	59	4:1	99
5	**81e**	2-Trifluromethy phenyl	24	65	0:1	99

[a] Determined by ^{1}H NMR analysis of the crude mixture of **86** and **87**.
[b] Determined by chiral-phase HPLC analysis of the major diastereoisomers.

The noteworthy point indeed of this study was the induction of chirality in aza-Henry reaction. The two contiguous stereocenter was fixed and the stereochemical outcome was controlled in the later stage in the synthesis of pyranoid iminosugar derivatives [84].

The polyhydroxylated indolizidines and quinolizidines are vital scaffolds frequently encountered in castanospermine, swainsonine, and lentiginosine bicyclic iminosugar. These classes of iminosugars have received considerable attention due its diverse therapeutic applications in medical field.

Many strategies have been developed to access the bicyclic iminosugar based on chiral pool or enantio and diastereoselective approach as the key reaction [75, 85–90]. In this connection, a remarkable one-pot asymmetric synthesis was reported by Stecko *et al*. A one-pot reduction, Mannich and Michael sequence of reactions of sugar-derived imine in situ from corresponding lactam was investigated (Scheme 10.14, Table 10.3) [91].

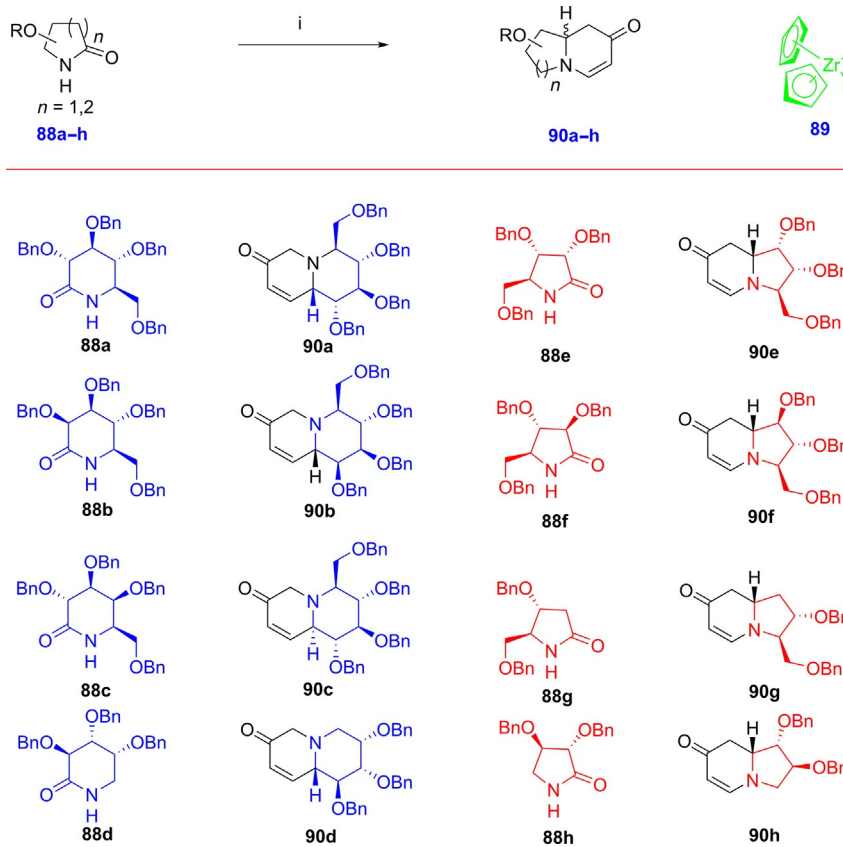

Scheme 10.14 One-pot strategy for the synthesis of indolizidines and quinolizidines *via* reduction/Mannich/Michael domino reaction of sugar-derived lactam(s).

Table 10.3 One-pot reduction/aza_Mannich/Michael domino reaction for indolizidines and quinolizidines.

Entry	Lactam(s) 88(a–d)	Product(s) 90(a–d)	Yield[a] (%)	dr[b]	Entry	Lactam(s) 88(e–h)	Product(s) 90(e–h)	Yield[a] (%)	dr[b]
1	**88a**	**90a**	80	98:2	5	**88e**	**90e**	61	87:13
2	**88b**	**90b**	73	94:6	6	**88f**	**90f**	55	90:10
3	**88c**	**90c**	81	90:10	7	**88g**	**90g**	63	86:14
4	**88d**	**90d**	67	88:12	8	**88h**	**90h**	63	80:20

[a] Isolated yield.
[b] Determined by ^{1}H NMR or performing analysis of HPLC of the crude reaction mixture.

The sugar-derived imines was easily accessible by the reduction of sugar lactams with Zirconocene hydrochloride (Schwartz's reagent) [92–97]. The diverse sugars-derived lactams, pyrano, and furano **88a–h** were successfully reduced to corresponding imines with Swartz's reagent **89** (1.6 equiv.) in THF. The in situ generated corresponding imines was employed for the one-pot reduction, aza-Mannich, and Michael reaction in the presence of $Yb(OTf)_3$ (10 mol%) with Danishefsky's diene (2.0 equiv.) at −25°C to room temperature. This strategy offered diverse bicyclic enaminones **90a–h** in good yield with excellent diastereoselectivity (dr 94:6) (Table 10.3). The absolute stereochemistry at bridgehead position was determined by ^{1}H NMR coupling constant and NOE corelation experiment. An effort was made to modify the reaction strategy by changing the protecting groups in diene. The derivatization of the resulting products with various other protecting groups such as silyl, benzoyl (Bz), *p*-methoxy benzyl ether, and tetrahydropyran was also attempted.

Furman and coworkers devolved an efficient one-pot synthetic route to access the densely functionalized polyhydroxylated pyrrolidine and piperidine scaffold present in iminosugar. This strategy was based on reduction of lactams to sugar imine which on direct functionalization with diverse nucleophiles produced the target scaffold in good yield with high degree of stereoselectivity. The present one-pot lactam reduction/addition of nucleophile offered the shortest route for the synthesis of the central core structure of the medicinally relevant carbohydrates mimetics-azasugar. The authors extended the scope of this methodology for the synthesis of potential β-mannosidase and α-glucosidase inhibitor as pyrrolidine derivatives of 6-deoxy-DMP and radicamine B (Scheme 10.15, Table 10.4) [94].

Baskaran and coworkers developed an efficient and operationally simple versatile strategy for the stereoselective synthesis of β-nitromethyl *C*-glycoside of medicinally privileged iminosugar scaffold frequently encountered in diverse naturally occurring iminosugar alkaloids. The synthetic approach involved in the amination of tosylate of D-ribose/D-xylose with allylamine at room to elevated temperature followed by the alkylation of in situ generated iminium ion with nitromethane. This method offered

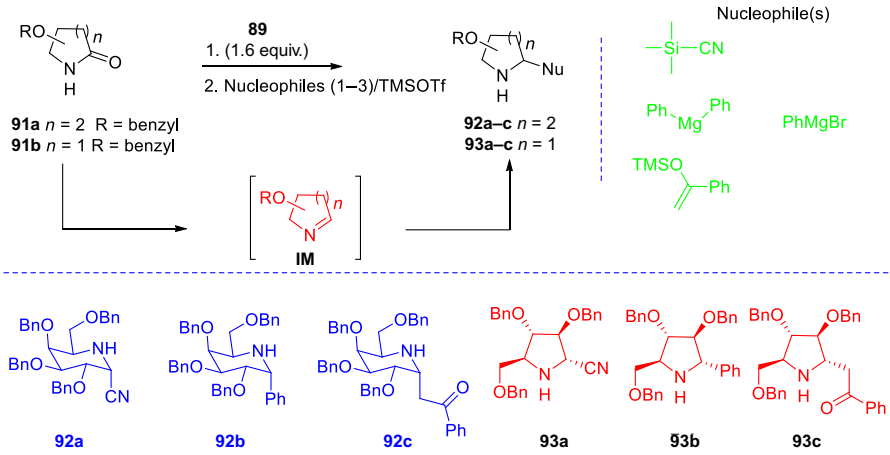

Scheme 10.15 One-pot reduction/addition to sugar-derived lactam **91a–b** and direct functionalization to iminosugar analogs.

Table 10.4 Direct functionalization of in situ generated sugar imines.

Entry	Lactams	Nucleophiles (equiv.)	Lewis acid[a]	Major products	Yield[b] (%)	dr[c]
1	**91a** ($n = 2$)	1 (2.0)	TMSOTf	**92a**	65	>95:5
2		2 (6.0)	–	**92b**	72	2.3:1
3		3 (2.0)	TMSOTf	**92c**	94	>95:5
4	**91b** ($n = 1$)	1 (2.0)	TMSOTf	**93a**	88	60:40
5		4 (6.0)	–	**93b**	65	>95:5
6		3 (2.0)	TMSOTf	**93c**	65	60:40

[a] Lewis acid 1.0 equiv.
[b] Isolated yield of the pure compounds.
[c] Determined by ^{1}H NMR of the crude reaction mixture.

the β-*C*/α-*C*-nitromethyl pyridine-based iminosugar glycosides in good to excellent yield with a high degree of diastereoselectivity in a single-pot reaction.

This methodology was further extended to access the pyrrolidine-based iminosugar glycosides from L-rhamnose mesylate. The structure of the newly synthesized iminosugar glycosides was firmly established by single-crystal analysis. The scope of this synthetic methodology was established with diverse primary amines and the result was summarized (Scheme 10.16, Table 10.5) [98].

The nitromethyl functionality in α/β iminosugar *C*-glycosides served as a potential precursor for accessing a wide range of densely functionalized bicyclic iminosugar derivatives. It was worthy to note that the authors reported unusual nitro-olefin dipolar cycloaddition without using any promoters en route to bicyclic polyhydroxylated indolizidine derivatives of (Z/E) mixture of inseparable oxime at room temperature or refluxing toluene.

Mechanistically, the formation of bicyclic *C*-glycosides was possible *via* oxidative SET (single-electron transfer) pathway. The *N*-allyl or propargyl piperidine and pyrrolidine (**97b** and **97c**) underwent facile 5-*exo-trig* cyclization smoothly to afford the title compounds in excellent yield. Silver (I) oxide and DBU mediated condition were used and it was established by Kamimura *et al*. [99, 100].

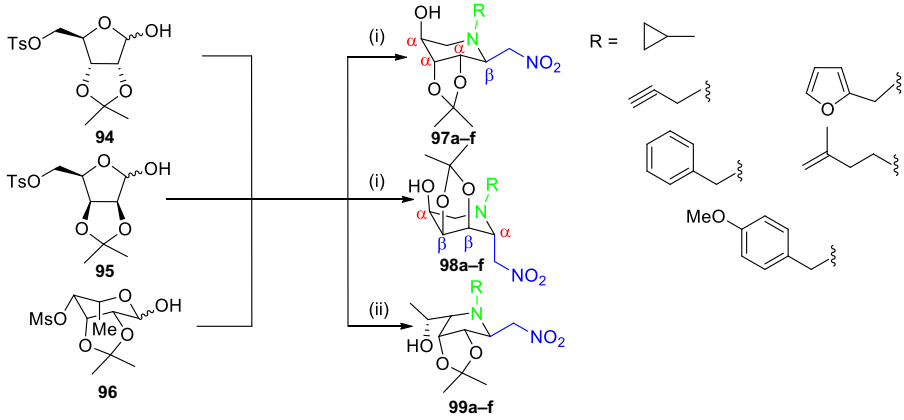

Scheme 10.16 One-pot synthesis of α/β-*C* glycoside iminosugar.

Table 10.5 Synthesis of iminosugar α/β-*C*-nitromethyl glycosides derived from D-ribose/xylose tosylate and L-rhamnose mesylate.[a]

Entry	Product Major	Time (h)	Yield (%)[b]	dr	Entry	Product Major	Time (h)	Yield (%)[b]	dr
1	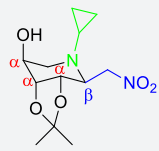 97a	20	77	1:0	6	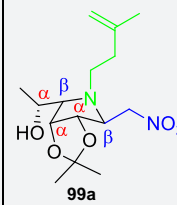 99a	24	75	n.d
2	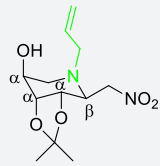 97b	12	83	1:0	7	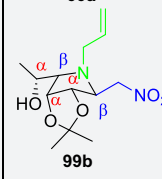 99b	18	75	n.d
3	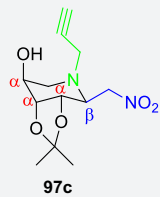 97c	24	71	1:0	8	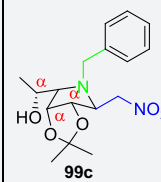 99c	16	84	n.d

Table 10.5 Continued

Entry	Product Major	Time (h)	Yield (%)	dr	Entry	Product Major	Time (h)	Yield (%)	dr
4	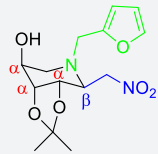 **97d**	12	78	9:1	9	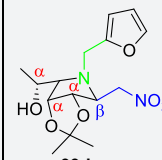 **99d**	20	75	n.d
5	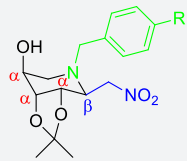 **97e**, R = H **97f**, R = OMe	14 16	92 75	9:1 9:1	10	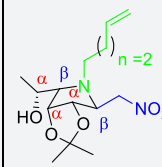 **99e**	24	72	n.d
6	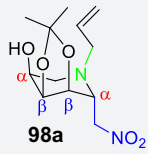 **98a**	20	81	3:1	11	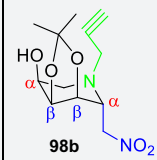 **98b**	24	70	9:1

[a] *Reagents and conditions*: (i) R·NH_2 (2.0 equiv.); anhy·CH_2Cl_2; Et_3N (1.0 equiv.); CH_3NO_2 (5.0 equiv.); rt, 12–24 h; (ii) R·NH_2 (2.0 equiv.); anhy·DMF; Et_3N (1.0 equiv.); CH_3NO_2 (5.0 equiv.); rt, 16–24 h.
[b] Isolated yield after column chromatography.

Molecular iodine produced cyclopropyl ring embedded indolizidines in good yield with high stereoselectivity (Scheme 10.17).

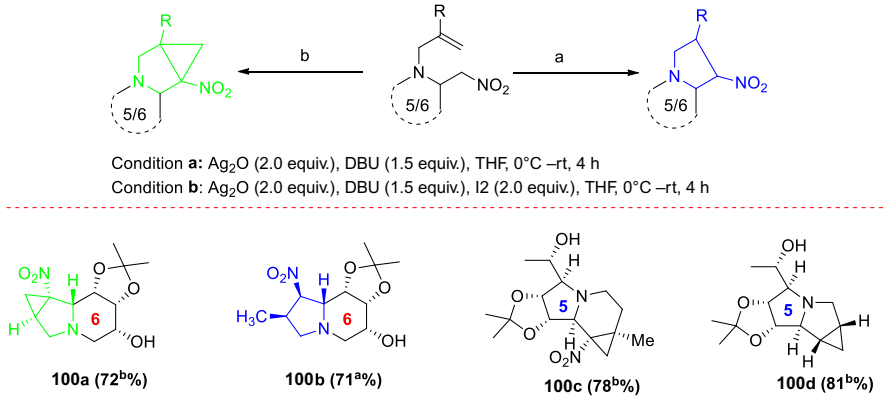

Scheme 10.17 *exo-trig* radicle cyclization to indolizidines and its cyclopropane derivatives.

The scope of this novel intramolecular radical cascade cyclization was further exploited in the stereoselective synthesis of the analog of natural products such as epiquinamide, indolizidines, and benzoquinolizidines.

10.5 One-pot synthesis of bioactive heterocycles

Heterocycles are an important class of molecules, widely spread in nature of numerous significances. Due to their intriguing structures and wide range of pharmacological properties, research on heterocycles becomes highly significant. This property of heterocyclic compounds makes them as one of the prime interests in pharmaceutical industries. The heterocyclic compounds play an important role in regulating the biochemical process in living system. The compounds may be genetic material, hormones, and enzymes. The common heterocyclic compounds that serve as potential leading drug candidates include amino acid, vitamins, and coenzymes. The piperidine, pyrimidines, pyrroles, oxadiazoles, and their derivatives are important heterocyclic compound and they play a vital role in determining the chemotherapeutical applications as antibacterial, anticancer, hypnotics, antiplasmodial, antidiarrheal, cardiovascular activities, and antidiabatic agents. The heterocycles are not only used as a regular clinical compound but they also play a crucial role in material science research.

10.6 Nitrogen-based bioactive heterocycles

N-Heterocycles are the ubiquitous motif of various bioactive compounds which serve as privileged structures in drug discovery. The unique feature of N-heterocyclic moiety present in medicinally active molecules improves the oral solubility and biocompatibility significantly in living systems. Piperidine and its derivative are one of the important precursors for the synthesis of novel chemotherapeutics of diverse applications. Piperidine is nonfused six-membered saturated nitrogen-containing ring and this system is present in many life-saving agents (Fig. 10.11).

Piperidine structural motifs are also frequently encountered in numerous alkaloids having various pharmacological activities. The most significant alkaloids containing piperidine from a pharmacological point of view derived from deferent natural sources with remarkable bioactivities are shown here (Fig. 10.12).

It is worth to develop a synthetic route to access this unique molecule. A significant achievement was made for the chemical synthesis of piperidine motif for the past many years. There were several methodologies known for this endeavor. However, most of the methods were either lengthy or involved several steps. One-pot multicomponent reaction strategies for this synthesis of piperidine motif were developed.

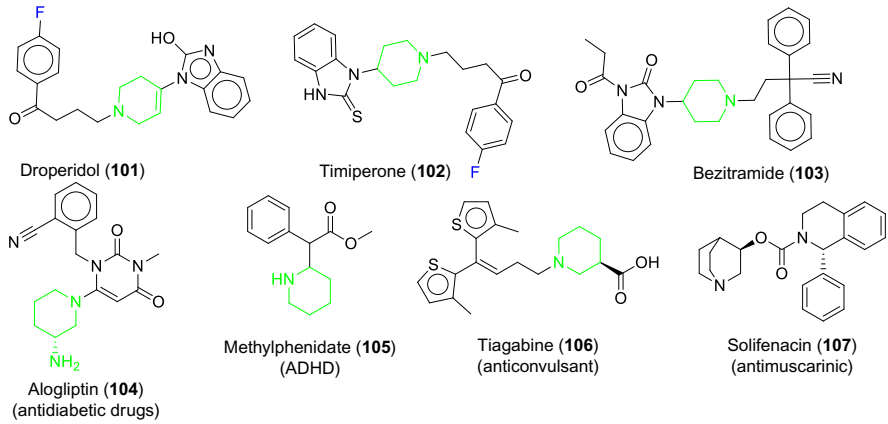

Fig. 10.11 Piperidine ring containing chemotherapeutic agent of diverse bioactivity.

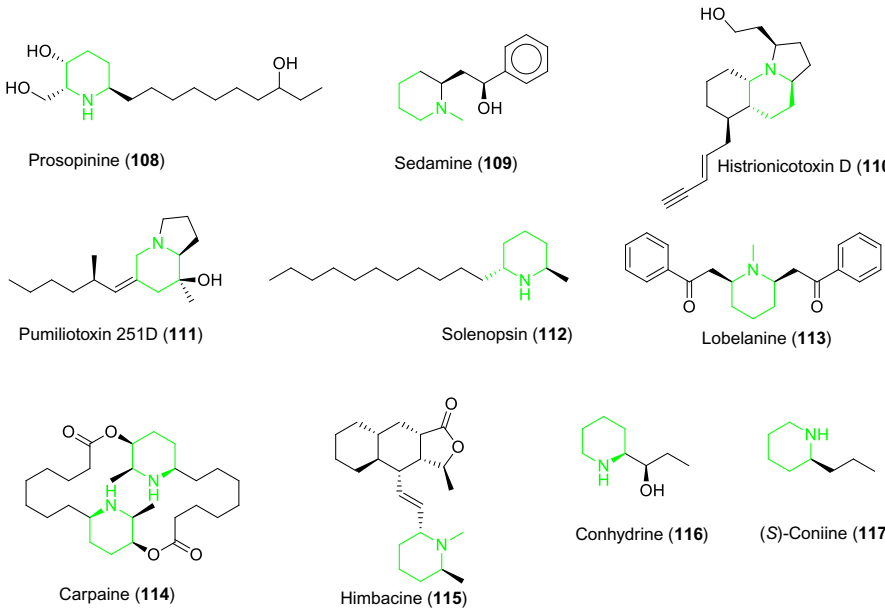

Fig. 10.12 Piperidine ring containing natural products.

10.7 Regioselective ring opening/ring expansion of chiral aziridine

In connection with this endeavor elegant one-pot multicomponent reaction strategy for the stereocontrolled synthesis of enantiopure 2,6-*cis*-disubstituted piperidine alkaloids starting from chiral aziridine was developed [101].

The main crucial points of this synthetic method included a facile aziridine ring opening (ARO), hydrogenolysis of N-benzyl protecting group followed by intramolecular reductive amination of the 2-amino-6-alkanone generated in situ. The plausible retrosynthetic route for the synthesis of numerous piperidine alkaloids was proposed (Fig. 10.13).

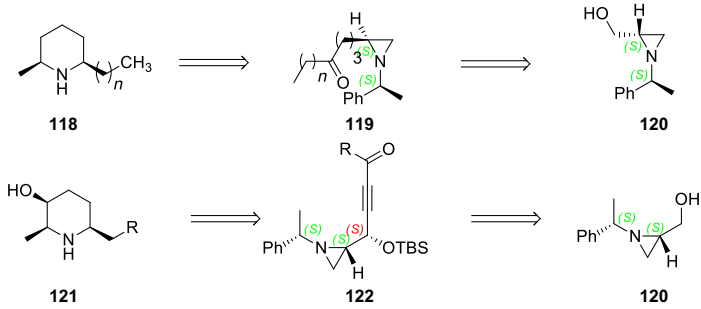

Fig. 10.13 Retrosynthetic analysis.

The synthesis of advanced precursors **119** and **122** of piperidine derivatives **118** and **121** was easily accessible from commercially available (*S*)-1-((*S*)-1-phenylethyl) (aziridin-2-yl) methanol **120** by chemical manipulation [102, 103].

The advanced synthons **119** and **122** were employed under hydrogen atmosphere with 20% $Pd^{II}(OH)_2$ as a catalyst. Four consecutive sequential reactions including reduction of alkyne, regioselective ARO, debenzylation followed by ring closure to afford the piperidine nucleus of various chemotherapeutically active alkaloids was achieved in excellent yield (Schemes 10.18 and 10.19).

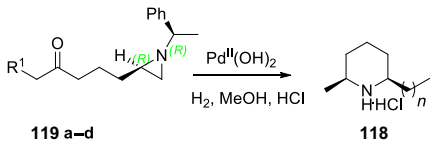

Sr. No	R^1	*n*	118a–d
1	Et	2	(−)-Dihydropinidine (**118a**), 88%
2	Octyl	8	(2*S*,6*R*)-Isosolenopsin (**118b**), 94%
3	Decyl	10	(2*S*,6*R*)-Isosolenopsin **A** (**118b**), 92%
4	Dodecyl	14	(2*S*,6*R*)-Isosolenopsin **C** (**118c**), 89%

Scheme 10.18 Synthesis of dihydropyrimidine and solenopsin derivatives.

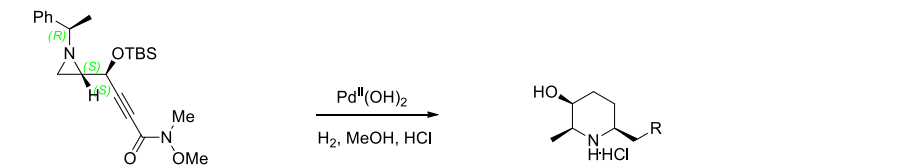

122 a R = $C_{12}H_{25}$
122 b R = $C_{12}H_{20}C(OCH_2)_2CH_3$

121 a R = $C_{11}H_{23}$, (+)-Deoxocassine, 96%
121 b R = $C_{11}H_{23}COCH_3$, (+)-Spectaline, 92%

Scheme 10.19 Synthesis of (+)-deoxocassine and (+)-spectaline.

A plausible reaction pathway was described. A facile regioselective ARO ring from the less hindered site (a-face) was the first step during catalytic hydrogenolysis step. The diastereoselectivity presumably depends on the steric hindrance caused by the axial methyl group which allows the approach of hydrogen from the less hindered phase of the C═N bond. The driving force for easy opening of the aziridine ring may also be attributed to the cooperating attraction of the aziridine ring and the appended carbonyl group of the side chain (Fig. 10.14).

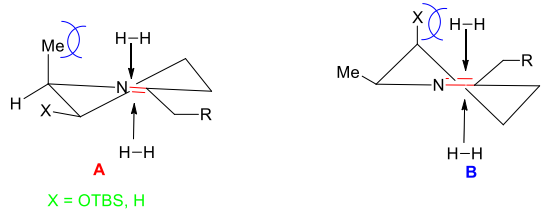

Fig. 10.14 Plausible reaction course for the hydrogenolysis steps.

Coldham *et al*. developed a powerful method for the stereoselective synthesis of piperidine motif following ring expansion/rearrangement of keto-aziridines using aza-Wittig reaction as the key steps. In an initial attempt the keto-aziridine **123a**→**c** was transformed into the corresponding vinyl aziridine by Wittig olefination. It was worthy to note that the bulkier groups such as *n*-butyl and isopropyl in vinyl-aziridine ring makes the ring unstable significantly (**123b**→**c**). For example, N-alkylation with butlybromoacetate produced product with low yield. The low yield was attributed to the ARO. The vinyl-aziridine was very unstable and they underwent simultaneous 1,5 hydrogen shift at room temperature.

Aziridines on reaction with LDA or Lewis acid-mediated reaction failed to give piperidines. Rather decomposition of the starting materials was noted. However, the aziridine R→Me gave the rearranged product as single diastereomer (cis-isomer) upon treatment with lithium isopropylamide (LDA) at −78°C.

A significant fall in the yield of piperidine gets noticed if the starting material aziridine is not utilized for rearrangement reaction immediately. To overcome this drawback and in search of robust methods for the rearrangement en route to piperidine synthesis single-pot strategy involving Wittig olefination followed by rearrangement was investigated. N-protected keto-aziridine **123a**→**c** was treated with two equivalents of phosphonium ylide with n-BuLi in dimethoxyethane (DME) at room temperature. Under this condition, a concomitant olefination followed by [2,3]-Wittig rearrangement was observed to afford exclusively *cis* diastereomer of piperidine in good to excellent yield. A high degree of diastereoselectivity was achieved during this investigation (Scheme 10.20) [104, 105].

The viability of the rearrangement reaction was likely to depend on the orientation of the vinyl group with respect to the butyl ester group. A *cis* orientation facilitated the reaction. However, it was necessary to keep the ester group in *endo* form in a five-membered transition state (Fig. 10.15).

Densely functionalized azepanes are valuable aza-heterocyclic compounds. They represent a ubiquitous structural motif in a variety of interesting naturally occurring

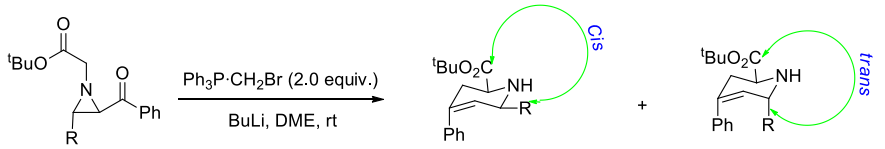

123	R
a	Me
b	^{n}Bu
c	Pr^{i}

124 **a–c (*cis*)** **125** **a–c (*trans*)**

124	R	*dr*	Yield
124a	Me	**124a**:**125a** (100:0)	57%
124b	Bu^{i}	**124b**:**125b** (100:0)	55%
124c	Pr^{i}	**124c**:**125c** (100:0)	66%

Scheme 10.20 Synthesis of 2,4,6-trisubstituted piperidines *via* ring expansion of aziridines through aza-Wittig reaction.

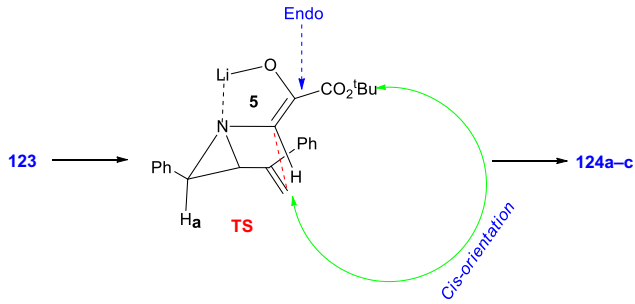

Fig. 10.15 Possible transition state for [2,3]-Wittig rearrangement.

bioactive molecules such as cephalotaxine, tubrostemonine, and balanol [106–110]. The biological activity is attributed to the stretchy and conformational diversity in their structures (Fig. 10.16).

Due to the wide spectrum of chemotherapeutically relevant target, huge global efforts have been paid for the synthesis of these classes of molecules.

Yeung *et al*. reported a novel stereoselective synthesis of highly functionalized azepane ring using bromo-amino cyclization of enantiomerically pure olefinic aziridine **132a**→**g**. The starting compound was synthesized from L-glutamic acid and allowed to react with *N*-bromosuccinimide as electrophilic reagent and $NsNH_2$ (nosyl amine) as the nucleophile. This process produced azepane **133a–g** in good to excellent yield (Scheme 10.21) [111]. It was found that at −30°C, ethyl acetate solvent was the best choice for this investigation.

The plausible mechanistic pathway for this cyclization involved $NsNH_2$-activated electrophilic addition of bromine to olefinic double bond to give cyclic bromonium ion (IA) which was opened by a nucleophilic attack of the aziridine ring to give cyclopropylpiperidinium ion IM (IIA). Furthermore, the $NsNH_2$ opened the ring in SN^2 fashion to give azepane **133** exclusively (Scheme 10.22).

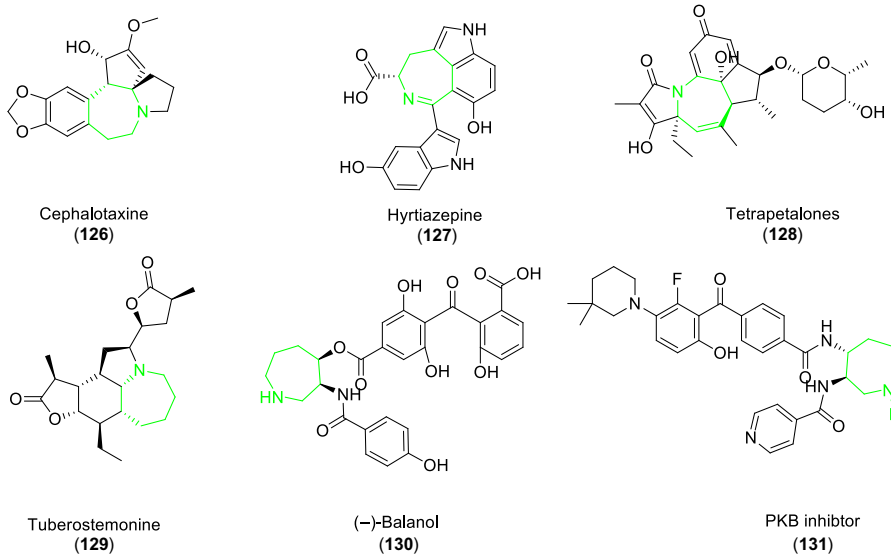

Fig. 10.16 Bioactive azepane natural products.

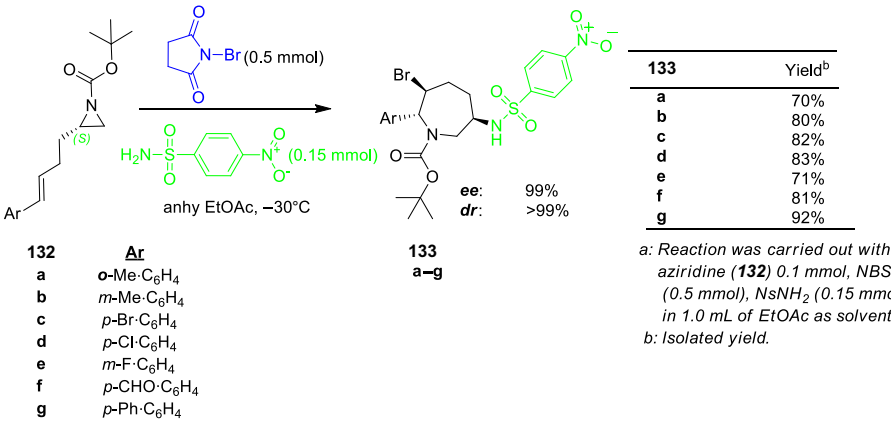

132	Ar
a	*o*-Me·C_6H_4
b	*m*-Me·C_6H_4
c	*p*-Br·C_6H_4
d	*p*-Cl·C_6H_4
e	*m*-F·C_6H_4
f	*p*-CHO·C_6H_4
g	*p*-Ph·C_6H_4

133 a–g

133	Yield[b]
a	70%
b	80%
c	82%
d	83%
e	71%
f	81%
g	92%

*a: Reaction was carried out with aziridine (**132**) 0.1 mmol, NBS (0.5 mmol), $NsNH_2$ (0.15 mmol) in 1.0 mL of EtOAc as solvent.*
b: Isolated yield.

Scheme 10.21 *N*-Bromosuccinimide induced aziridine ring expansion in synthesis of azipine.[a]

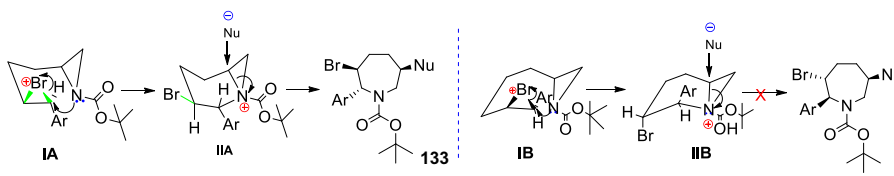

Scheme 10.22 Mechanistic pathway of cyclization.

However, the reaction pathway IB → IIB was not helpful to cyclization due to the steric repulsion of the aromatic group in pseudo six-membered transition state (IB).

An elegant protocol was established for the facile synthesis of diverse structurally complex 1,4-benzo-oxazepinones based on one-pot ring opening/carboxamidation of a wide range of *N*-tosylaziridine of 2-halophenol as the key steps mediated by phase transfer catalysis [112]. The cyclic/acyclic *N*-tosylaziridine allowed to react with a series of *o*-halophenol under 200–400 psi of carbon monoxide pressure at high temperature using high boiling solvent, like DMF. This facile ARO ring/carboxymidation domino reaction was achieved in the presence of $PdCl_2(PPh_3)_2$ (1.5 mmol%), triphenylphosphine (1.5 mmol%), 10 mmol% of base and benzyltriethylammonium chloride (TEBA) as a phase transfer catalyst in good to excellent yield (Scheme 10.23).

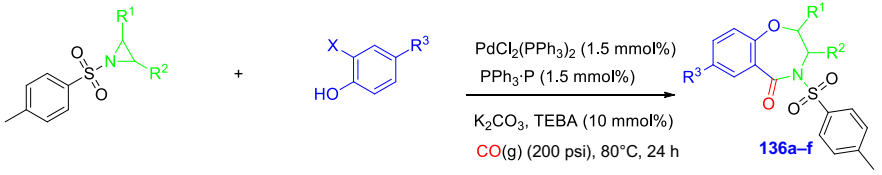

134	R1	R2
a	$C_6H_5{\cdot}CH_2$	H
b	$4(OMe){\cdot}C_6H_4{\cdot}CH_2$	H
c	$3,4(OMe)_2C_6H_3{\cdot}CH_2$	H

135	R^3
a	H
b	Bu^t
c	CO_2Me
d	Cl
e	Ph

136	R1	R2	R3	Yield
a	$C_6H_5{\cdot}CH_2$	H	H	74%
b	$C_6H_5{\cdot}CH_2$	H	Bu^t	64%
c	$C_6H_5{\cdot}CH_2$	H	CO_2Me	92%
d	$4(OMe){\cdot}C_6H_4{\cdot}CH_2$	H	Cl	72%
e	$4(OMe){\cdot}C_6H_5{\cdot}CH_2$	H	Ph	88%
f	$3,4(OMe){\cdot}C_6H_4{\cdot}CH_2$	H	Ph	91%

Scheme 10.23 Domino one-pot sequential ring opening/carboxymidation of aziridine en route to synthesis of 1,4-azapinone. *Reagent and conditions*: **134a → c** (1.0 mmol); **135a → e** (1.1 mmol); $Pd^{II}Cl_2(PPh_3)_2$ (3.0 mmol); K_2CO_3 (3.0 equiv.); TEBA (10 mmol%); DMF (5.0 mL); 130°C; 48 h. Reaction was carried out at 200 → 400 psi CO(g) pressure in DMF.

This protocol was also equally applicable to the synthesis of pyrido-1,-4-oxazepinones from *o*-hydroxy halogenated pyridines. The mechanistic pathway was established for this investigation. Initially, the reaction proceeded with nucleophilic ARO with halophenol under base-assisted phase transfer catalytic system to afford the amine chain tethered aromatic ether **137a**. Then oxidative insertion took place in the presence of Pd^0 complex to **137b**. Subsequently, carbonyl insertion took place through aryl-palladium bond cleavage to generate another IM **137c** in the catalytic cycle. Ultimately, a nucleophilic attack of *N*-tosyl amine to aryl palladium complex generated IM **137d** which underwent reductive elimination to afford the aryl-1,4-oxazepinones **136a–f**. The entire process made Pd^0 free and thus completed the catalytic cycle (Fig. 10.17).

Vinyl aziridines are well-known important strained (27 kcal mol^{-1}) heterocyclic molecules and these serve as electrophilic partners in organic chemistry. Because

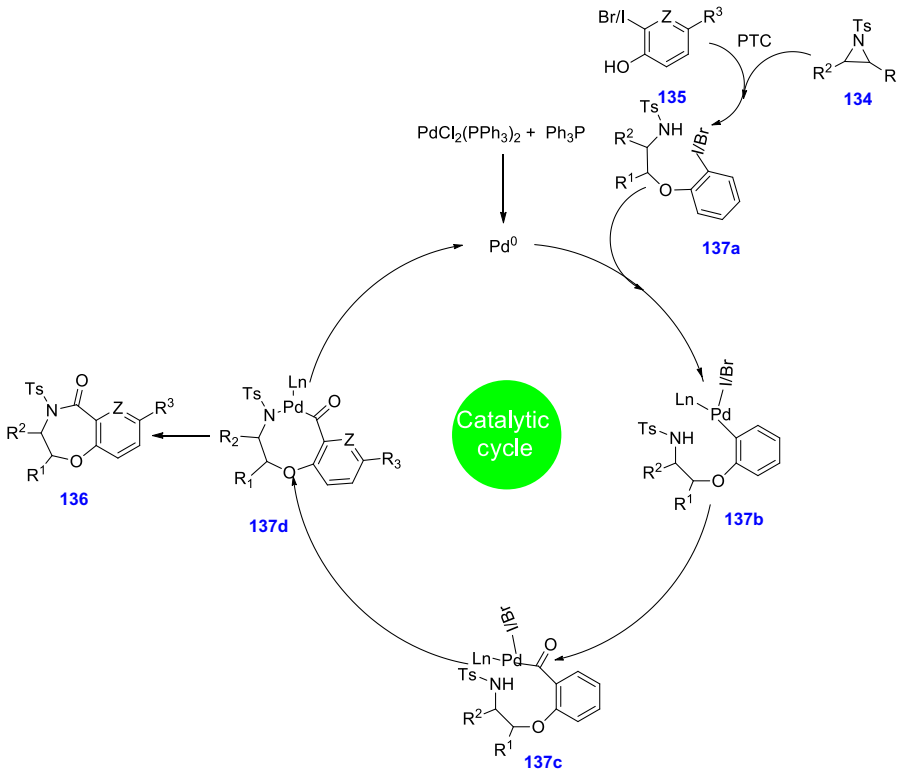

Fig. 10.17 Plausible mechanistic pathway of Pd^{II} catalyzed annelation.

of their energy, these rings are highly reactive and versatile starting materials in the synthesis of natural products and pharmaceuticals with diverse biological and medicinal properties. Vinyl aziridine chemistry is studied and well explored in the synthesis of complex heterocyclic molecules.

Zhang *et al*. developed a catalytic method for the enantio-specific synthesis of fused 2,5-dihydroazepines starting from chiral vinyl aziridine *via* intramolecular hetero [5+2] cycloaddition strategy with inactivated alkyne. In this investigation, a variety of Rh(I) catalysts was screened toward the synthesis of novel enantiopure fused 2,5-dihydroazepines. Initially, the compound **138a** was chosen as the starting material and allowed to react with di-μ-chlorotetracarbonyldirhodium(I) catalyst at 80°C. But this reaction failed to produce the desired product. Then, 5 mol% of [Rh (BND)$_2$]. BF_4 in combination with dichloroethane at ambient temperature was found the choice for this investigation.

To explore the versatility and scope of the method, a diverse enantiomerically pure olefinic aziridine **138a–f** was synthesized from commercially available amino acid methyl ester hydrochloride of D-serine in excellent yield with high degree of enantiomeric excess (99%) (Scheme 10.24, Table 10.6) [113].

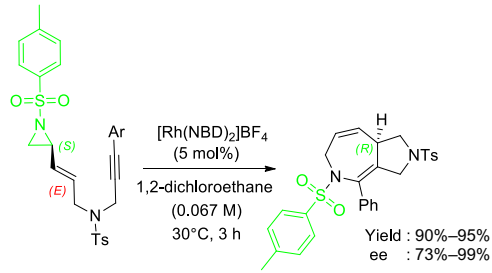

138	Ar
a	C_6H_5
b	4-OMe·C_6H_4
c	4-Cl·C_6H_5
d	2-benzofuryl
e	Me
f	$^nC_4H_9$

139a–f

Scheme 10.24 [5+2] Cycloaddition reaction synthesis of 2,5-dihydroazepines **139a–f**.[a]

Table 10.6 A summary for the synthesis of 2,5-dihydroazepines catalyzed by Rh(I) catalyst *via* intramolecular [5+2] cycloaddition reaction.

Entry	138	ee (%)	139	Yield[a] (%)	ee[b] (%)
1	(*S*)**138a**	90	(*S*)**138a** →(*R*)**139a**	90	90
	(*R*)**138a**	99	(*R*)**138a** →(*S*)**139a**		99
2	(*S*)**138b**	87	(*S*)**138b** →(*R*)**139b**	94	90
	(*R*)**138b**	98	(*R*)**138b** →(*S*)**139b**		95
3	(*S*)**138c**	90	(*S*)**138c** →(*R*)**139c**	93	90
	(*R*)**138c**	99	(*R*)**138c** →(*S*)**139c**		99
4	(*S*)**138d**	99	(*S*)**138d** →(*R*)**139d**	91	97
	(*R*)**138d**	99	(*R*)**138d** →(*S*)**139d**		99
5	(*S*)**138e**	84	(*S*)**138e** →(*R*)**139e**	95	85
	(*R*)**138e**	73	(*R*)**138e** →(*S*)**139e**		73
6	(*S*)**138f**	88	(*S*)**138f** →(*R*)**139f**	93	90
	(*R*)**138f**	93	(*R*)**138f** →(*S*)**139f**		92

[a] Average isolated yield of the product formed from (*S*)-**138** and its enantiomers.
[b] Determined by HPLC analysis using chiral stationary phase.

A diverse stereodefined aryl, alkyl, and heteroaryl substituted 2,5-dihydroazepines were synthesized with excellent enantiomeric excess. Noteworthy, the condition was well compatible with terminal and internal alkynes.

The stereochemistry of the products at the junction of the ring depended on the conformation of the olefinic bond in aziridine chain. It was important to observe that the (*S*)-*E* configuration delivers the *R*-azepines while (*R*)-*Z* gives corresponding opposite stereoisomeric (*S*)-azepines (Scheme 10.25).

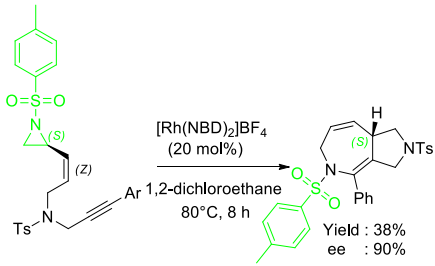

Scheme 10.25 [5+2] Cycloaddition reaction synthesis of 2,5-dihydroazepines **141**.

In continuation, a seminal study was carried out by the same group in the divergent synthesis of azepines and related azaheterocycles based on Rh(I) catalyzed intermolecular [5+2] cycloaddition strategy using chiral vinyl aziridines as starting materials. The most notable feature of this study was the synthesis of different classes of compounds from identical starting materials by controlling or altering the catalyst which changes the mode of cycloaddition and led the formation of enantiomerically pure 2,3-dihyropyrroles *via* [3+2] cycloaddition (Schemes 10.26 and 10.27).

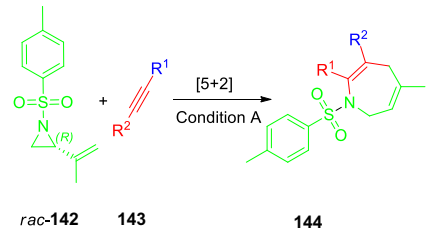

Scheme 10.26 Intermolecular [5+2] cycloaddition approach for the synthesis 2,5-dihydroazepines (**144**) *via* aziridine ring expansion.

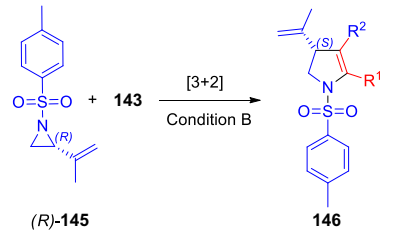

Scheme 10.27 Intermolecular [3+2] cycloaddition approach for the synthesis 2,3-dihydrophrole (**146**) *via* aziridine ring expansion.

The chiral aziridine (*R*)-**145** and *rac*-**142** were easily obtained from commercially available methyl hydrochloride ester of (*L*)-serine [114–116]. The *racemic N*-tosyl vinyl aziridine was employed under the optimized condition **A** with diverse terminal

alkyne **143a→h** with 5 mol% of the catalyst [Rh (η^6-$C_{10}H_8$) (COD)] SbF_6 in 1,2-dichloroethane as a solvent at 0°C to rt. By extending this concept, synthesis of 2,5-dihydroazepines derivatives **144a→h** was achieved with high to excellent yield *via* [5+2] cycloaddition reaction (Table 10.7). It was important to note that this method has limitation and did not proceed with internal alkynes.

Table 10.7 2,5-Dihydroazepines (**144**) *via* [5+2] cycloaddition.[a]

Entry	R^1	R^2	Yield[b] (%)
	143(a → h) [R^1→R^2]		
1	Ph	H	90 (**144a**)
2	*p*-$EtOC_6H_4$	H	94 (**144b**)
3	*p*-$tBuC_6H_4$	H	93 (**144c**)
4	*p*-MeC_6H_4	H	90 (**144d**)
5	*p*-FC_6H_4	H	91 (**144e**)
6	*p*-ClC_6H_4	H	75 (**144f**)
7	*p*-BrC_6H_4	H	60 (**144g**)
8	*p*-AcC_6H_4	H	17 (**144h**)

[a] *rac*-**142** (0.25 mmol); **143a→h** (1.5 equiv.); 5 mol% [Rh (η^6-$C_{10}H_8$) (COD)] SbF_6; 1,2-dichloroethane (2.5 mL); 0°C, 30 min (0°C) → 15 min (rt).
[b] Isolated yield.

Interestingly, switching the catalyst, alkyne **143a→h** and internal alkyne underwent different mode of cycloaddition *via* [3+2] procedure (condition B). This method afforded an enantiomerically pure densely functionalized 2,3-dihydropyrroles **146a→h** with promising yield. It was worthy to note that the chirality of aziridine ((*R*)-**145**) was completely transferred in the products with 90%–99% ee (Table 10.8). There were a number of other methods based on one-pot transition

Table 10.8 Optically active 2,3-dihydropyrroles (**146**) *via* [3+2] cycloaddition.[a]

Entry	R^1	R^2	ee (%)	Yield[b] (%)
	143 (a → h) [R^1→R^2]			
1	Ph	H	80	97 (**146a**)
2	*p*-$EtOC_6H_4$	H	70	98 (**146b**)
3	*p*-$^tBuC_6H_4$	H	93	96 (**146c**)
4	*p*-MeC_6H_4	H	72	97 (**146d**)
5	*p*-FC_6H_4	H	91	98 (**146e**)
6	*p*-ClC_6H_4	H	82	96 (**146f**)
7	*p*-BrC_6H_4	H	86	94 (**146g**)
8	*p*-AcC_6H_4	H	70	97 (**146h**)

[a] (*R*)-128 (0.25 mmol); **143a→h** (1.2 equiv.); $[Rh(NBD)_2]BF_4$ (5 mol%); 1,2-dichloroethane (2.5 mL); rt; 15 min;
[b] Isolated yield.

metal-catalyzed synthesis of diverse pyrrolidine derivatives. Vinyl aziridine was used as the starting material *via* [3+2] cycloaddition reaction extensively [117–121].

10.8 N, O, and S-based bioactive heterocycles

Morpholine and piperazine ring are essential motifs in diverse marked drugs and natural products. (*R*,*R*)-Reboxetine **147** is a well-known antidepressant drug that acts as a selective noradrenaline reuptake inhibitor (NaRI) [122]. Levofloxacin **149**, a morpholine-based broad spectrum antibiotic demonstrated a wide range of antibacterial efficacy against the treatment of variety of infectious diseases and complicated urinary tract infections [123]. Also, the gefitinib **151** is an anilinoquinazoline class of molecule having a morpholine motif serves as a potential anticancer drug in treatment of lung cancer [124]. Aprepitant **152** is a potential neurokinin-1(NK1) receptor antagonist that has effective clinical application in the prevention of acute and delayed chemotherapy-induced nausea and vomiting associated with single or multiple cycles of highly emetogenic chemotherapy (HEG). It is also very effective against postoperative nausea and vomiting (PNV) [125].

Gatifloxacin is a novel broad-spectrum antibiotic with a fluoroquinolone nucleus and piperazine motif **154** demonstrated excellent antibacterial activities and effective against pneumonia, chronic bronchitis, tuberculosis, and gonococcal infection [126]. Buclizine (BCZ) **155** is another important drug of piperazine derivative which has an excellent pharmacological profile, antihistaminic, antiemetic, antimuscarinic, and moderate sedative properties. It demonstrated powerful curative properties against the motion sickness, nausea, and vomiting caused by prolonged medication of analgesic drugs. It is also used for the treatment of migraine and appetite stimulant owing to its orexigenic effect. BCZ hydrochloride salt was also effective against the treatment of vertigo-related disorder of the vestibular system (Fig. 10.18) [127].

Owing to the excellent pharmacological profiles and medicinal properties, these molecules have driven the recent attention of the scientific community in developing a powerful and general strategy for the synthesis and constructing the skeleton of this class of bioactive natural products.

10.9 Regioselective oxirane ring opening/expansion

Oxiranes are three-membered strained heterocyclic molecules. Some of the architecturally complex natural products can be synthesized by the regioselective ring opening of oxiranes. The synthesis of brevotoxin, yessotoxin, ciguatoxin, and related polyether was achieved by sequential reaction or "cascade" of epoxide ring opening through catalytic system or in aqueous medium [128–131]. The ring strain makes the epoxide vulnerable with various reagents like acid/base, electrophiles, and nucleophiles to afford the diverse scaffolds for molecules synthesis. Toward the synthesis of morpholine-derived compound, phenmetrazine (preludin) **150**, Yeung and coworkers developed a facile and efficient one-pot metal-free novel electrophilic MCRs amino alkylation of an alkene (Scheme 10.28) [132]. Initially, the mixtures of alkene **156**,

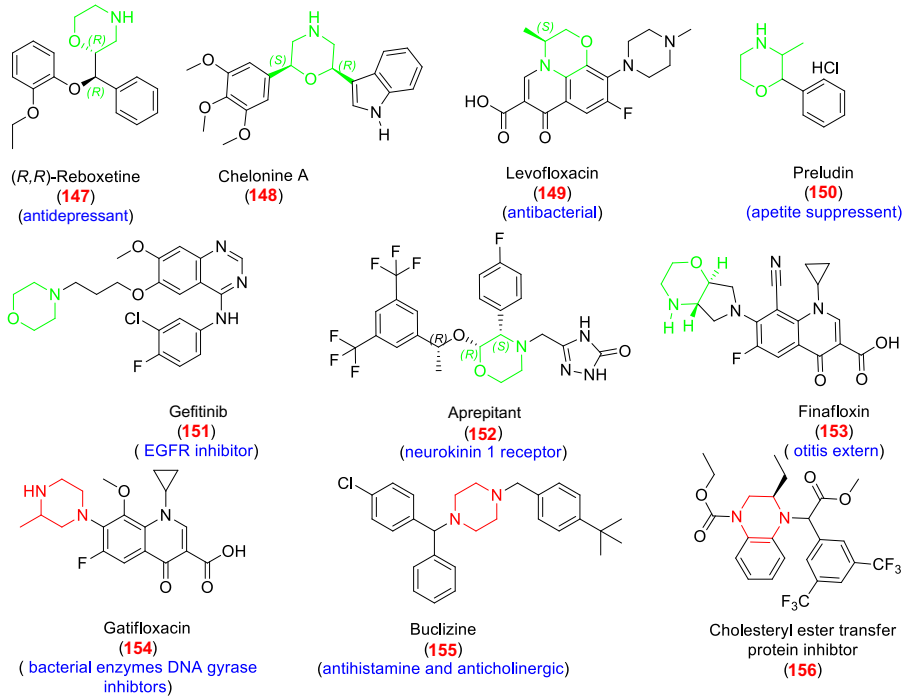

Fig. 10.18 Representative examples of biologically active molecules having morpholine and piperazine motif as central core structure.

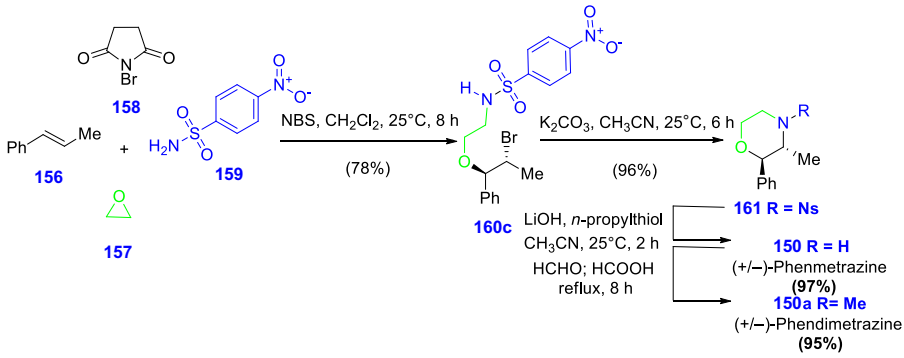

Scheme 10.28 Metal-free electrophilic aminoalkylation of an epoxide in synthesis of an morpholine derivatives.

epoxide **157**, *N*-bromosuccinimide **158**, and nosylamine **159** in anhydrous dichloromethane at room temperature for 8 h produced **160c** in 74% yield which was then transformed into morpholine derivative **161** by the reaction of K_2CO_3 in acetonitrile in

96% yield. The *N*-nosyl group was then deprotected and subsequent *N*-methylation to obtain the norepinephrine-dopamine–releasing agents (**150** and **150a**).

Based on electrophilic cascade, the author envisioned that the epoxide acts as the nucleophile and opens the cyclic bromonium IM (A) which is formed by the NBS-mediated electrophilic addition of bromonium ion to π-bond of an olefin (I) to generate the other IM oxonium ion B. The reaction of B with amine (IV) produced the amino ether derivative C. The amino ether was successfully transformed into diverse morpholine scaffolds under based-assisted annellation (Fig. 10.19).

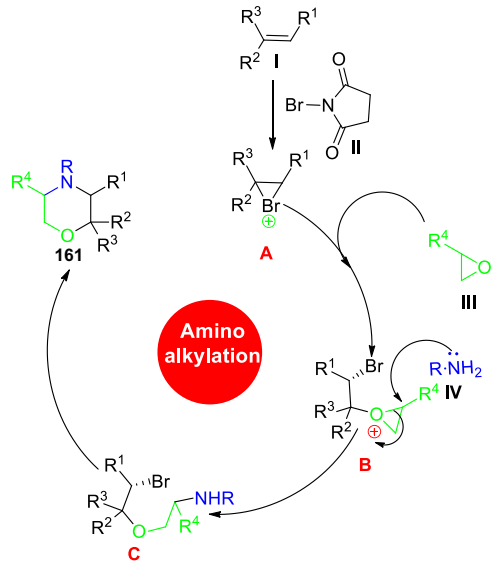

Fig. 10.19 Mechanism of one-pot MCRs to functionalized morpholine scaffolds.

Cossy *et al*. developed an elegant method for the diastereoselective synthesis of densely functionalized morpholine scaffold starting from readily available vinyl oxirane and amino alcohol under one-pot sequential Pd^0 and Fe (III)-catalyzed hetero-annulation strategy. This method offered an easy accesses of diversely substituted morpholines with high diastereoselectivity at ambient temperature through the formation of ω-hydroxy allylic alcohol IM in situ (**IMa** → e, Scheme 10.29) [133]. It was worthy to note that the diastereoselectivity of the product formation is independent on the configuration of the olefinic bond in vinyl aziridine. In contrast, diastereoselectivity of other methods was dependent on the configuration of the olefinic bond and was most likely favorable with *Z*-configuration [134, 135].

The iron-catalyzed cyclodehydration reaction of ω-hydroxy allylic alcohol IM was deactivated and it was noticed with THF solvent and high Pd^0 catalyst loading. This was attributed to the complexing nature of Fe (III) with either Pd^0 or solvent which

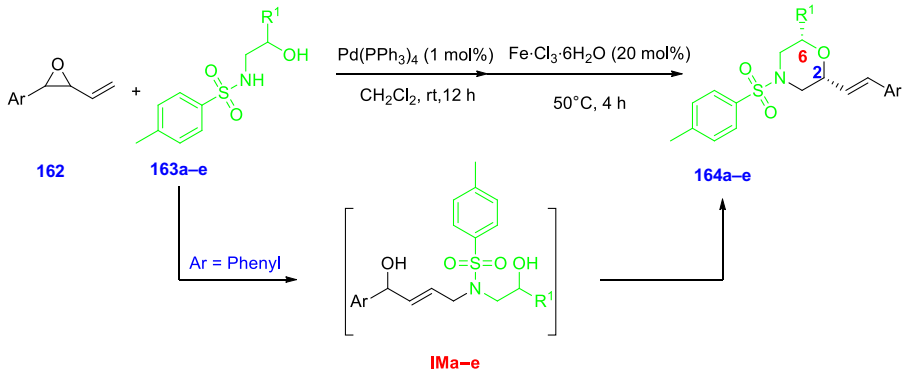

Scheme 10.29 Diastereoselective one-pot synthesis of 2,6-*cis*-disubstituted morpholine (**164**).

further decreases the yield of the reaction. A switch to a noncoordinating solvent like dichloromethane and reducing the amount of Pd^0 catalyst improved the conversion rate of the reaction.

To prove generality and the scope of the methodology, diversely substituted amino-alcohols **163a–e** were reacted with 1 mol% $Pd(PPh_3)_4$ and 20 mol% of $FeCl_3{\cdot}6H_2O$ in anhydrous dichloromethane at 50°C for 4 h. A very clean reaction was observed with good to excellent yield of *cis*-2,6-disubstituted morpholine **164a → e** along with excellent diastereoselectivity (Scheme 10.29). During this investigation, it was noticed that the reaction is also feasible even at room temperature with poor diastereoselectivity with 10 mol% of Fe (III) catalyst. At elevated temperature with high amount of $FeCl_3{\cdot}6H_2O$ catalyst, diastereomeric ratio (*dr*) of the products was increased significantly. It appeared that Fe-catalyzed reaction underwent a *cis-trans* isomerization toward the most stable isomer [136, 137].

This methodology was further extended for the synthesis of polysubstituted, *cis*-2,3 and 2,5-disubstituted morpholine successfully. A diverse alkyl, aryl, and heteroaryl *cis*-2,5-disubstituted morpholines **169a → e** were synthesized with good yield and diastereoselectivity (Scheme 10.30).

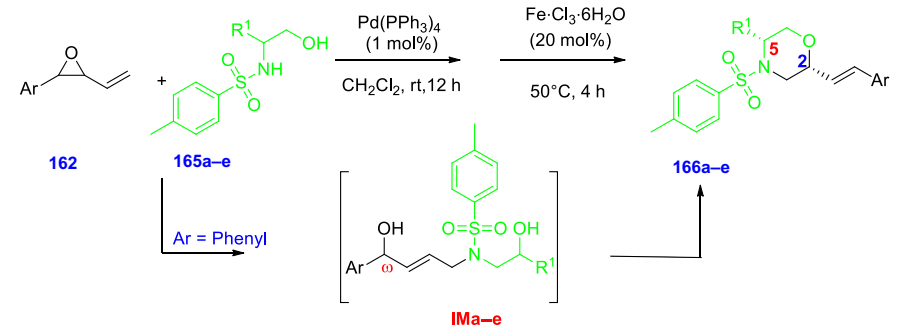

Scheme 10.30 Diastereoselective one-pot synthesis of 2,5-*cis*-disubstituted morpholine (**166**).

The yield of *cis*-2,5-substituted morpholine was comparatively lower than 2,6-disubstituted products. This was probably due to the substituent R^1 which causes steric hindrance. Owing to the flexible structure, morpholine ring preferred to adopt a chair conformation and the *N*-tosyl group oriented in an equatorial position. In the 2,6-*cis*-morpholine the favored conformation was (II) over (I). The conformation (**I**) corresponding to the *trans* diastereoisomer suffered greater 1,3-diaxial interactions. The 2,5-*cis* morpholine was formed through the most favorable conformation (**III**) with low steric hindrance (Fig. 10.20, Tables 10.9 and 10.10).

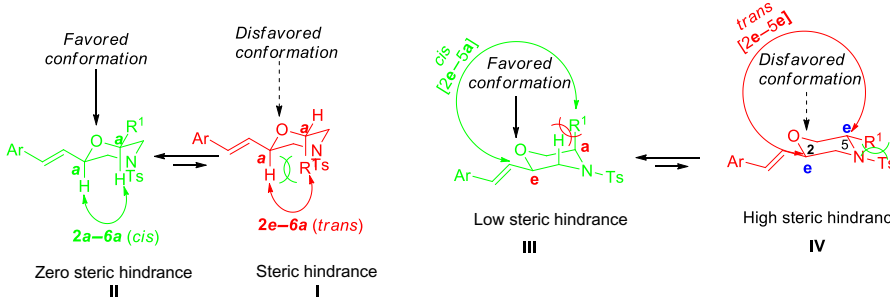

Fig. 10.20 Diastereoselectivity in 2,6 and 2,5-disubstituted morpholine derivative.

Table 10.9 *Cis*-2,6 disubstituted morpholine derivatives (**164**).

164	**R^1**	***Cis*/*Trans***	**Yield (%)**
a	Phenyl	95:5	89
b	Vinyl	93:7	71
c	Cyclopropyl	92:8	87
d	*n*-Pentyl	92:8	83
e	Cyclohexyl	–	93

Table 10.10 *Cis*-2,5 disubstituted morpholine derivatives (**166**).

166	**R^1**	***Cis*/*Trans***	**Yield (%)**
a	Phenyl	85:15	72
b	Isopropyl	95:5	60
c	Ethyl	95:5	60
d	(MM)Ph[a]	90:10	62
e	2-(M)TP[b]	94:6	50

[a] (MM)Ph: (Methoxymethyl)phenyl.
[b] 2-(M) TP: 2-(Methyl)thiophenyl.

The 2-hydroxymethyl-substituted morpholine scaffolds are imperative synthetic precursors in the synthesis of advanced heterocyclic compounds.

Breuning *et al*. developed an expeditious one-pot stereoselective approach for the synthesis of enantiomerically rich 2-hydroxymethyl morpholine with densely functionalized structure. The key step of this methodology was involved in high regioselective Lewis acid-mediated nucleophilic ring opening of enantiomerically pure (*R*/*S*) epichlorohydrin with various substituted β-amino alcohols followed by base-assisted 6-*exo*-*tet* intramolecular annellation.

In one-pot procedure the protocol was demonstrated for the synthesis of diverse chiral morpholines in good to excellent yield with outstanding chirality transfer. Primarily, a diverse substituted chiral β-amino alcohols **167a**→**e** was reacted with commercially available (*S*)-epichlorohydrin (97% ee) **168** in the presence of $LiClO_4$ in toluene at 20–50°C for 14–18 h to enhance a complete transformation of IM(III) (Fig. 10.21). Addition of the base (NaOMe) in MeOH to the same reaction flask and continued stirring for additional 14–72 h at the same temperature furnished the compounds **169a**→**e** in good to excellent yield (Scheme 10.31) [138].

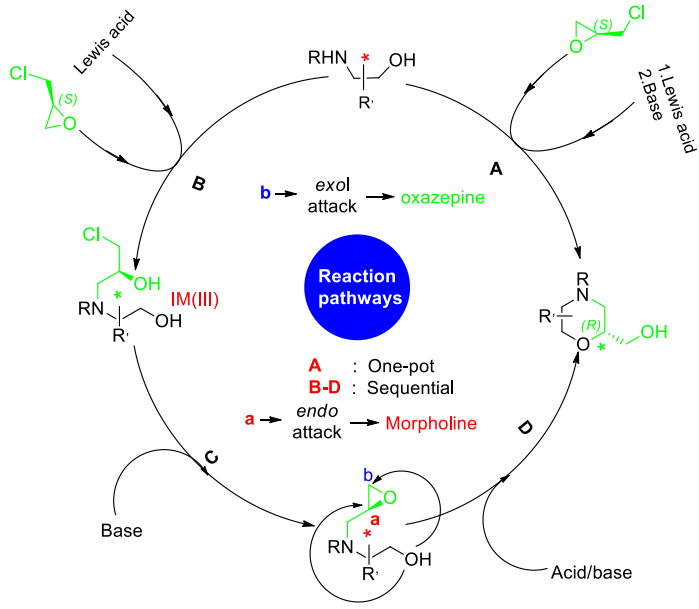

Fig. 10.21 Sequential and one-pot reaction pathway.

The structure of newly synthesized morpholines derivatives was explicitly established by extensive 2-D NMR analysis.

The reaction followed a highly selective ring opening of epoxide by nucleophilic attack of amino alcohols through the formation of various IMs following the path **B**→**C** in stepwise and this process forms morpholine **B**→**C**→**D** (Fig. 10.21). The

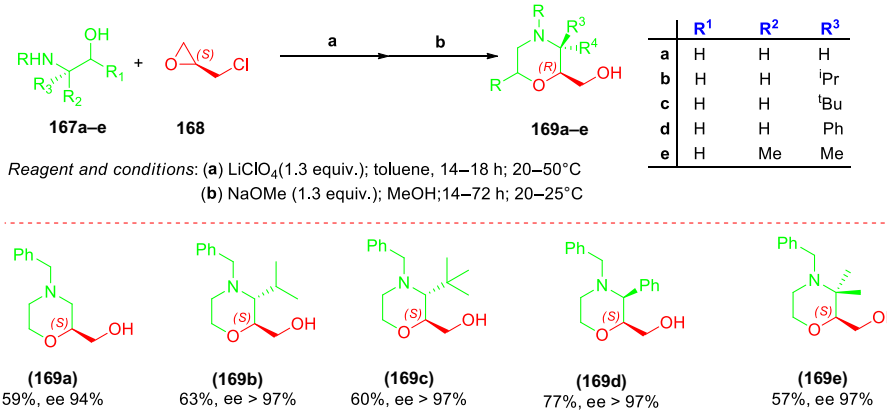

	R^1	R^2	R^3
a	H	H	H
b	H	H	^{i}Pr
c	H	H	^{t}Bu
d	H	H	Ph
e	H	Me	Me

Scheme 10.31 Stereoselective one-pot synthesis of 2-(hydroxymethyl)-morpholine(*S*)-epichlorohydrin (**169**) under Lewis acid catalyst.

reaction probably took a concerted route in a one-pot reaction delivering the targeted compound adopting the pathway **A** (Fig. 10.21). It was important to note that *endo-trig* cyclization eventually took place to circumvent the *exo-trig* cyclization which leads to the formation of 1,4-oxazepines.

Panda *et al*. discovered a general method to access the diverse *cis*-3,6-disubstituted morpholines and 3,6-disubstituted 1,4-oxazepanes derivatives, derived from the base-catalyzed tandem one-pot regioselective aziridine/epoxide ring opening as the key reactions [139].

Initially, (*S*)-2-isopropyl-1-tosylaziridine **170a** was chosen as the model substrate to investigate the reaction with (*R*)-glycidol **171** in the synthesis of morpholine and 1,4-oxazepane derivatives through regioselective nucleophilic ARO by NaH-mediated reaction. It was important to note that a very clean reaction proceeded at room temperature and an inseparable mixture of compounds **172a** and **173a** were formed in 2.1:1 ratio which was confirmed by NMR analysis (Scheme 10.32).

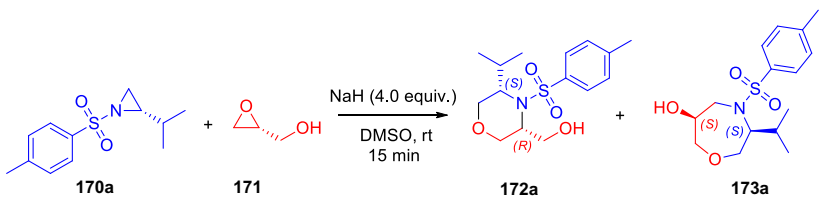

Scheme 10.32 Investigation on the synthesis of *cis*-2,6 and 3,6-disubstituted morpholine and 1,4-oxazepanes.

It was worthy to note the reaction proceeds through the facile tandem aziridine-epoxide ring opening sequence. It was found that ^{t}BuOK (1.2 equiv.) in DMSO is the best reagent for this investigation, but it failed to improve the diastereomer ratios of the products distribution. The scope of the methodology was examined with diverse substituted chiral aziridines **170b–f** with (*R*)-glycidol in the synthesis of a wide range of stereodefined *cis*-3,5 and 3,6-disubstituted morpholines and 1,4-oxazepanes (Scheme 10.33).

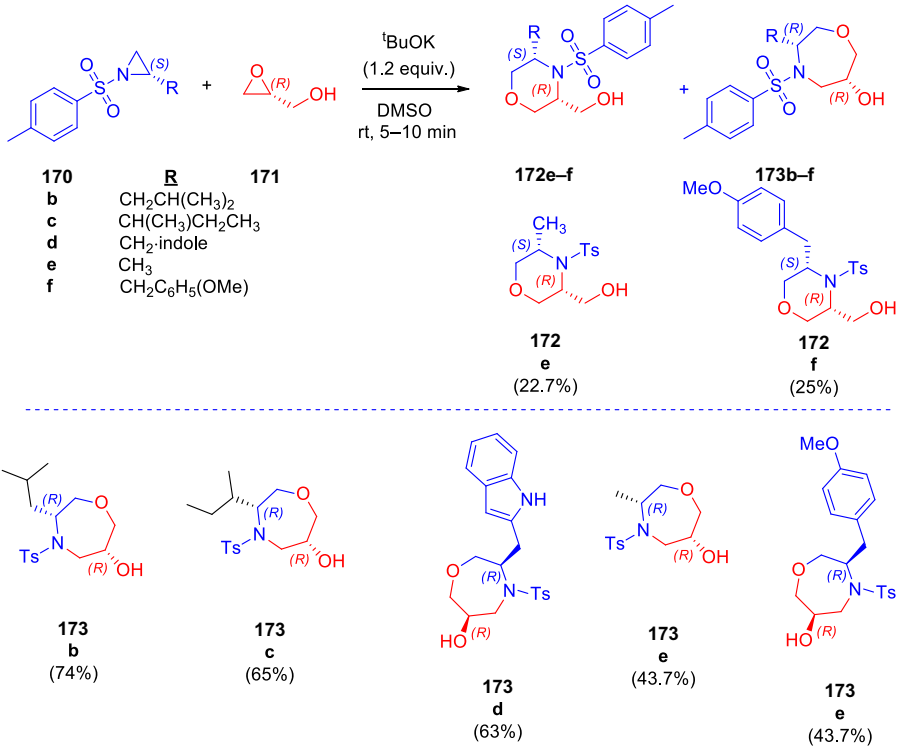

Scheme 10.33 One-pot synthesis of 3,5 and 3,6-disubstituted morpholine and 1,4-oxazepanes by tandem ring opening of chiral aziridine and (*R*)-glycidol at room temperature.

It was found that high steric appealing group present in aziridine ring (sec-butyl, isobutyl, and indole-substituted) fail to give the morpholine derivatives. It produced azepanes which are further supported by an extensive NMR and chemical analysis of the products. This was attributed to *exo-trig* ring opening of the epoxide and follows the reaction path **B** to furnish the corresponding azepane derivatives exclusively (Fig. 10.22).

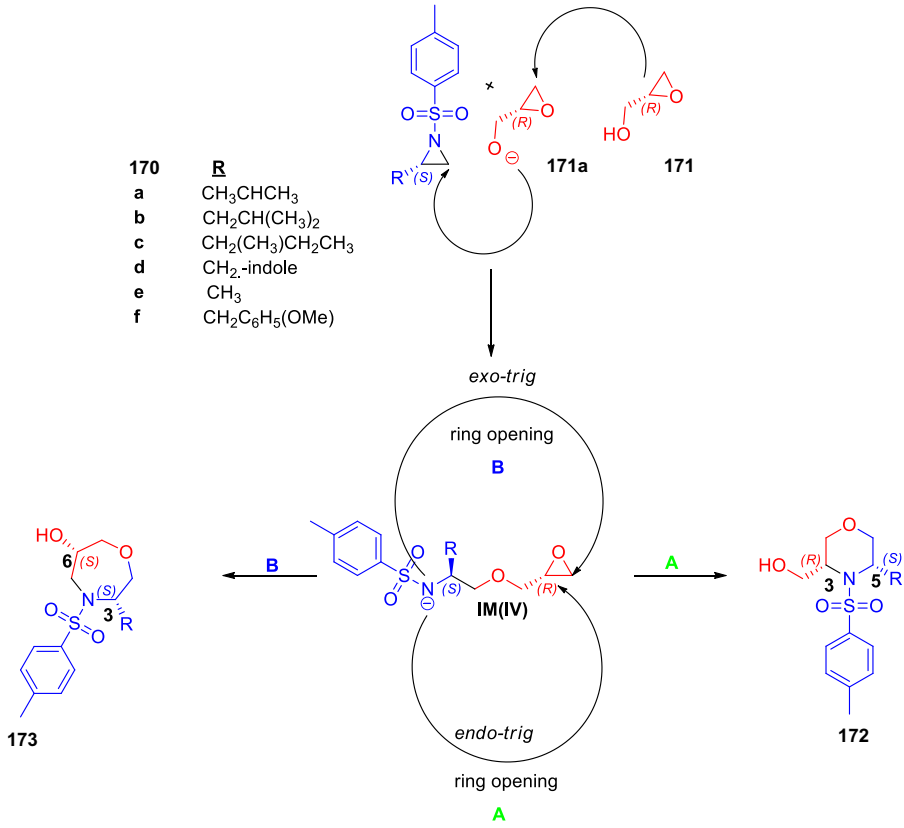

Fig. 10.22 Regioselectivity of epoxide ring opening in synthesis of *cis*-3,5 and 3,6-disubstituted morpholine and 1,4-oxazepanes.

10.10 Regioselective ring opening/expansion of oxetanes

Oxetanes are an important four-membered cyclic ether principally occupied as an attractive structural motif in diverse medicinally and bioactive molecules. Apart from this, oxetane serves as a powerful IM in advanced synthesis of a wide range of pharmacologically active molecules. The inherent ring strain (106 kcal mol^{-1}) associated with oxetane enhanced the efficacy of its synthetic utility in organic and medicinal chemistry. The ring opening reaction of an oxetane ring depended on the nature of the nucleophiles and the substitution pattern of the ring system. An extensive research was performed in the field of oxetane and its synthetic application [140–144].

The synthesis of multifaceted heterocycles through oxetane ring opening/ring expansion strategy in a one-pot operation is discussed here.

The opening of oxetane was used for an expeditious route in the synthesis of densely functionalized heterocyclic molecules.

10.11 Synthesis of morpholine/piperazine/thiazine

Carreira and coworkers devolved a powerful strategy for the rapid access of diverse heterocycles corresponding to morpholine, piperazine, thiomorpholine, and spirocyclic congers efficiently. These were based on Lewis acid-mediated intramolecular ring expansion of masked spirocyclic oxazolidines which were derived from commercially available oxetan-3-one and substituted β-amino-alcohols [145].

The oxazolidine **174a** was treated with 2 mol% of $In(OTf)_3$ in the presence of trimethylcynide (TMSCN) (1.5 equiv.) which leads to the morpholine derivative **175a** in 92% yield with excellent diastereoselectivity (>20:1). A nucleophilic attack by TMSCN produced the oxetane amino acid nitrile derivative **174a$_1$** under Strecker condition followed by the oxyphilic ring expansion of the activated oxetane ring through the TS1 (intramolecular *exo-trig* cyclization) eventually generated the morpholine **175a** (Scheme 10.34).

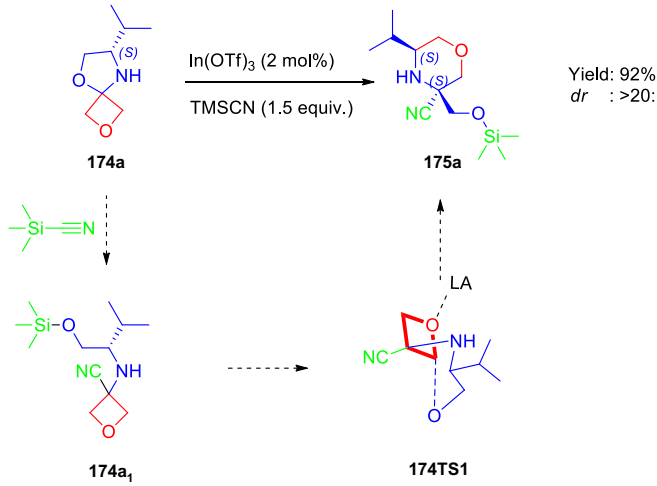

Scheme 10.34 Synthesis of morpholine derivatives from ring expansion of oxetane hemiaminal ether under Lewis acid catalysis.

The X-rays analysis supported the **TS1** in which the CN group prefers to occupy the axial position while the bulkier group adopts the equatorial position.

With this existing result in hand, this group next focused to develop the synthesis of substituted morpholine (**X = O**), piperazine (**X = N**), and thiomorpholine (**X = S**) derivatives in good to excellent yield in a highly stereocontrolled fashion (Scheme 10.35).

The use of diethyl trimethylsilyl phosphite was proven to be an excellent nucleophilic regent for this type of study and lead the formation of phosphonates **176** and **177** derivatives in excellent yield with consistent diastereoselectivity (Scheme 10.36). The nitrile functionality was directly converted to several other groups under different reaction

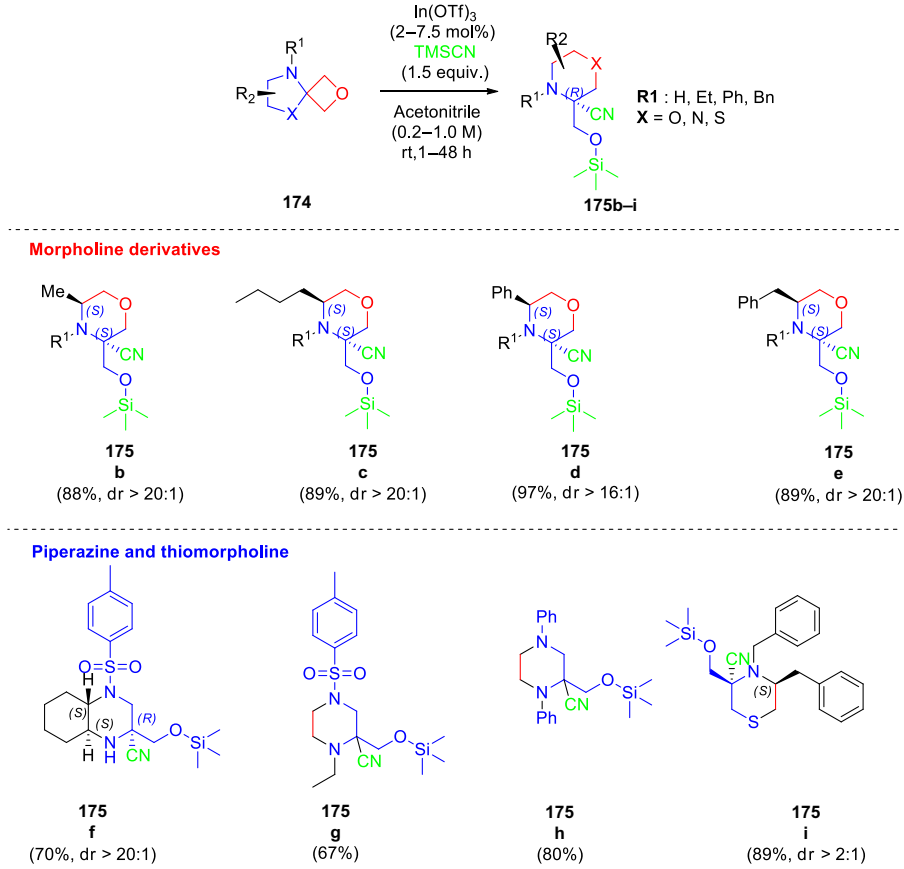

Scheme 10.35 Substrate scope and diversity in product formation.

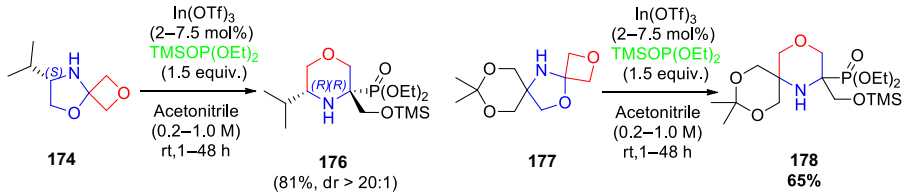

Scheme 10.36 Synthesis of phosphonate morpholine using diethyl trimethylsilyl phosphite.

conditions. It was worthy to note that important BBLs are created that are useful for the preparation of azetidine, triazole, and lactams fused with morpholine ring.

Very recently, the same group reported boron trifluoride etherate-catalyzed nucleophilic ring opening of N,Oacetal of spirocyclic oxetane **179** with potassium trifluoroborate to **181a–f**. This was a viable route for the synthesis of benzo morpholine derivatives (Scheme 10.37) [146].

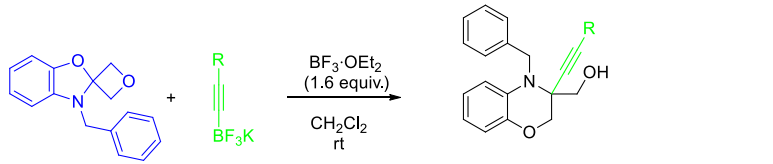

179

180	R	181	R	Yield (%)
a	*p*-Cl·C_6H_4	a	*p*-Cl·C_6H_4	85
b	Ph	b	Ph	69
c	H	c	H	81
d	TMS	d	TMS	75
e	Cy	e	Cy	64
f	(CH_2)Cl	f	(CH_2)Cl	82

Scheme 10.37 Synthesis of benzo[1,4]-oxazin derivatives *via* spirocyclic oxetane ring expansion.

10.12 Synthesis of functionalized isoxazoles

Isoxazoles are five-membered heterocyclic compounds having nitrogen and oxygen in the ring. Owing to their excellent chemotherapeutic profile, isoxazole occupied a dominant position in the industry and medicinal chemistry research. A wide range of isoxazoles was used to fight against infectious diseases. For instance, flucloxacillin **182**, a new isoxazole penicillin antibiotic including its analog cloxacillin **183**, and oxacillin **184** are well-established antibiotics with wide spectrum of clinical application. This class of antibiotics have antimicrobial activities and are active against penicillinase-producing strain of *Staphylococcus aureus*. Isoxazoles were also found in valdecoxib **185**, a nonsteroidal antiinflammatory drug (NSAID) and a COX-inhibitors used in the treatment of the pain associated with osteoarthritis, rheumatoid arthritis, and menstrual complication. It is also very effective against the pain associated with postsurgical analgesia [147–149].

Leflunomide **186** is an immunomodulator antirheumatic cytotoxic drug that inhibits cell proliferation of lymphocytes in a patient suffering from acute rheumatoid arthritis [150].

The development of general and versatile synthetic methodology for the isoxazole synthesis is of great interest for the chemists and a significant development has also been made toward the synthesis and chemotherapeutic evaluation of this unique class of molecules (Fig. 10.23).

Gold (I)-catalyzed cycloisomerization of α,β-unsaturated acetylenic oxime [151], iodine (III)-mediated [3+2] cyclization for synthesis of benzo-fused isoxazole [152], epoxide ring opening reaction [153], Fe (III)-catalyzed reaction of alkyne [154], Cu-catalyzed reaction of amine and alkyne [155], β-enaminodiketone [156], cesium carbonate-mediated reaction [157], and ruthenium-catalyzed cycloaddition of nitrile oxide to alkyne [158] are few of the notable synthesis of isoxazoles.

Carreira and co-workers [159] developed a cascade one-pot approach for the synthesis of 3-substituted isoxazole-4-cabaldehyde in a one-pot operation. This synthesis was realized through three-step sequence of reactions by the base-catalyzed Henry addition reaction of nitroalkane **190** with oxeta-3-none **189**, an elimination followed by rearrangement to isoxazole derivatives **191** (Scheme 10.38).

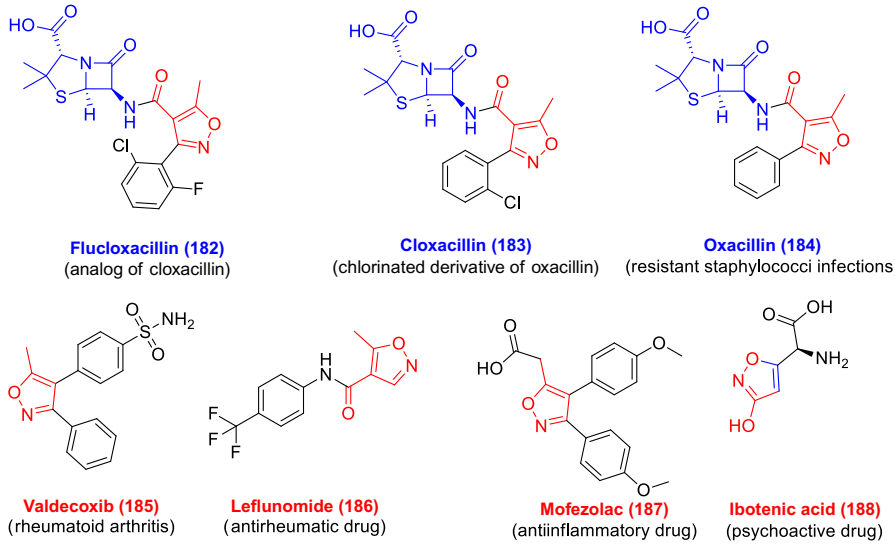

Fig. 10.23 Representative isoxazole drugs candidates in chemotherapy.

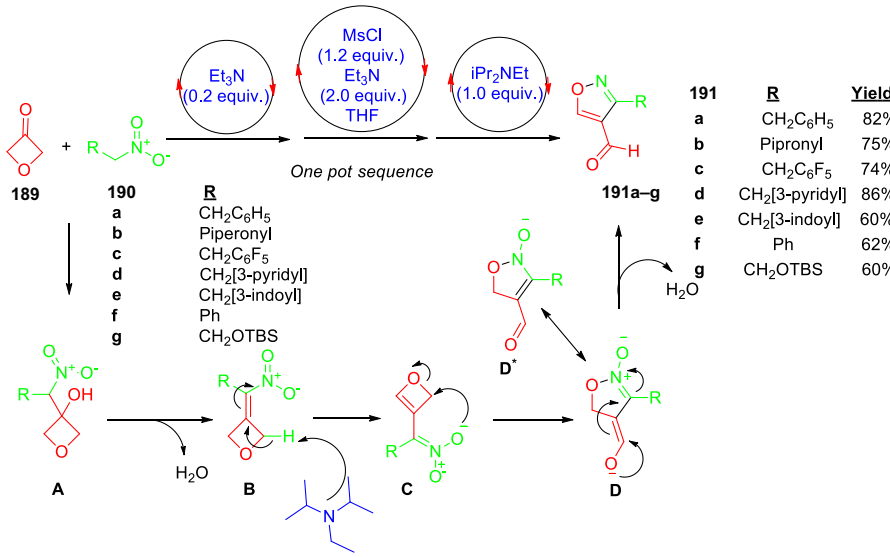

Scheme 10.38 A cascade one-pot approach to isoxazole from oxetane rearrangement. *Reagent and conditions*: nitroalkane (0.75 mmol, 1.0 equiv.); oxetan-3-one (0.98 mmol, 1.3 equiv.), THF (0.1 M); [a] yield reported is isolated yield (%) after column chromatography.

The nitroalkane **190** and oxeta-3-one **189** was taken together in the presence of catalytic amount of triethylamine (0.2 equiv.) at room temperature and then the reaction mixture was diluted with THF and allowed to cool at −78°C followed by the addition of Et_3N and methane sulfonyl chloride. After the addition of $^{i}Pr_2Net$ (*N*,*N*-di-isopropyl

N-ethyl amine) and keeping the reaction at room temperature produced the isoxazole in good yield.

Mechanistically, this cascade reaction to isoxazole followed the deprotonation of *exocyclic* oxetane nitrone **B** by $^{i}Pr_2NEt$ in a rate-limiting steps to form.

Oxetane IM **C** which then undergoes ring expansion to give another IM **D**→**D***. This IM on dehydration furnished the targeted isoxazole **191a**→**g** in good to excellent yield. All newly synthesized 3-substituted isoxazole-3-carbaldehyde has a great scope for synthetic application and these can serve as advanced BBLs in drug discovery.

10.13 Synthesis of polycyclic azaheterocycles

The Diels-Alder reaction is one of the most popular reactions that creates high level of molecular complexity in concerted fashion. In 2013, Sun and coworkers [160] reported very powerful methods to access the complex bio-active indole alkaloids. This methodology realized a stereoselective organo-catalyzed multicomponent reaction based on an intermolecular aza [3+2] cycloaddition strategy in a single-pot operation.

This synthesis required the presence of an oxetane ring in close proximity of an aldehyde group to influence on the reaction. It minimized the energy required to reach the transition state of the reaction and thus the reaction proceeds at room temperature. It is worthy to note that four consecutive C—C and C—N bonds and formation of four contiguous centers was achieved successfully in a single-pot operation with excellent yield along with high degree of enantioselectivity (Scheme 10.39, Table 10.11).

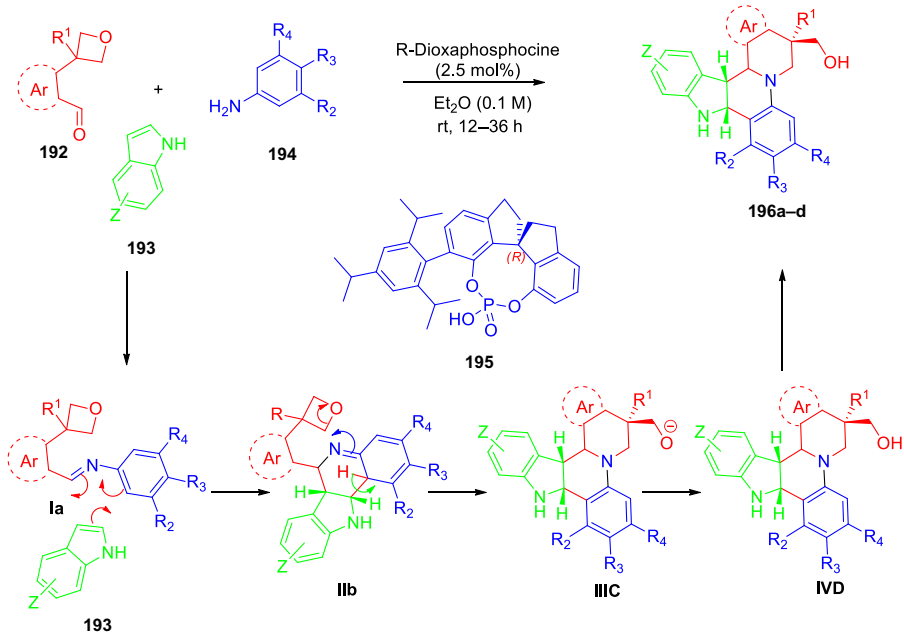

Scheme 10.39 One-pot multicomponent aza-[3+2] cycloaddition reaction in synthesis of polycyclic heterocycles.

Table 10.11 Aza-[3+2] cycloaddition reaction result and substituents.

196	Ar	Z	R^1	R^2	R^3	R^4	Yield (%)	ee (%)	dr
a	2,3-Phenyl	H	H	OMe	OMe	OMe	45	66	>95:5
b	2,3-Phenyl	H	OAc	OMe	H	OMe	67	63	>90:10
c	4-(F)-2,3-Phenyl	Br	H	OMe	H	OMe	67	88	>95:5
d	3,4-Perinyl	Br	H	OMe	H	OMe	93	78	>95:5

The resulting molecules have a close structural resemblance to the naturally occurring indole alkaloids, (+)-melonine, and MCH-I receptor antagonist [161]. These molecules demonstrated promising anticancer activity against human lung carcinoma (A549) and human cervical carcinoma (HeLa cell) when tested through MTT assay.

10.14 Synthesis of pyrone derivatives

Pyrone derivatives are six-membered oxa-heterocycles and extremely prevalent structural motif in diverse naturally and synthetically occurring bioactive molecules having a broad array of chemotherapeutic potentials. The macrolide antibiotic with dihydropyran ring (DHP) as principle structural motif is (+)-sorangicin. This exhibited potential antibiotic activity against both Gram-positive and Gram-negative rifampicin-resistant bacteria [162, 163]. Some examples of this group included Psymberin (inhibitory action of cancer cell proliferation) [164], Aspergillide B (cytotoxic activity against lymphocytic leukemia cell in mouse) [165], and Diospongin B (antiosteoporotic activity) [166].

Owing to their excellent biological activity and complex structural features they received much attention toward their synthesis and evaluation as drug candidates. The notable methods in literature for their synthesis were Oxa-Michael reaction [167], Maitland-Japp reaction [168], Prince cyclization [169, 170], and [4+2] cycloaddition [171].

Njardarson and coworkers developed a facile one-pot asymmetric synthesis of diverse substituted dihydropyrans *via* catalytic ring expansion of vinyl oxetane (Scheme 10.40) [172].

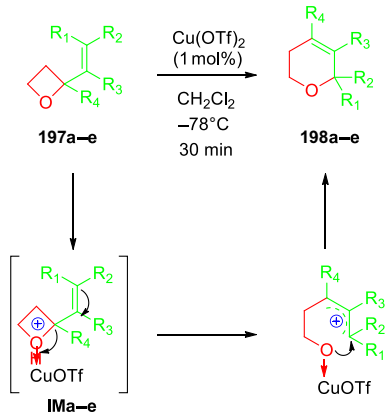

Scheme 10.40 Ring expansion of vinyloxetane in synthesis of dihydropyrons (DHPs).

The reported method equally worked with Brønsted acid (1 mol%, TfOH) at low temperature and Lewis acid (1 mol%, $Cu(OTf)_2$). The vinyl derivative of oxetane **197a**→**e** was treated with either 1 mol% of either $Cu(OTf)_2$ or 1 mol% of TfOH in anhydrous dichloromethane at −78°C. A facile ring expansion was reported with excellent yield of the products **198a**→**b** (Table 10.12). This method had a wide scope with diverse substrates. The ring expansion proceeded through the formation of allyl cationic IM(I) which then undergoes *endo* cyclization through oxygen atom to give DHPs. Notably, there was no detrimental effect of cationic stabilizing group present on the allylic cationic IM.

Table 10.12 $Cu(OTf)_2$ catalyzed ring expansion of vinyl oxetane.

198	R^4	R^3	R^2	R^1	Yield (%)[a]
a	Ph	H	H	H	95
b	Ph	H	H	Me	91
c	Ph	Me	H	Me	89
d	Ph	Me	H	H	93
e	C_6H_{13}	H	H	H	78

[a] Isolated yield after column chromatography.

The authors also employed chiral catalyst for the desymmetrization of divinyl oxetane successfully with a high level of enantioselectivity. It was observed that using copper catalyst **200**, the ring expansion proceeds smoothly with poor enantioselectivity while the use of chiral phosphoric acid derivative catalyst **201** gives promising result in moderate yield with high enantioselectivity (Scheme 10.41, Tables 10.1 and 10.2). The best enantioselectivity was observed with phosphoric acid (X→NHTs, Ar→9-anthracene) at 10°C (Table 10.13, entry f, Table 10.14)

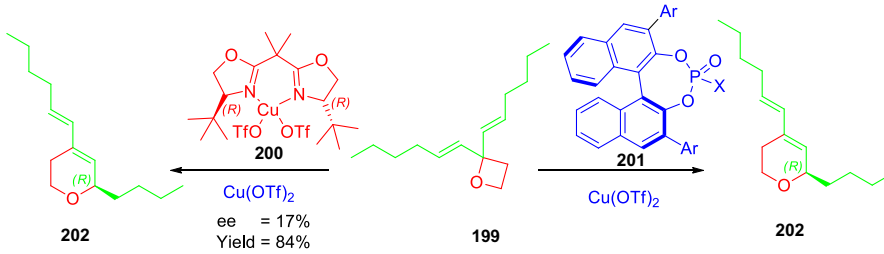

Scheme 10.41 Catalytic desymmetrization of divinyl oxetane in synthesis of DHPs. **Condition A**: 5 mol% of Cu(OTf)$_2$ and **200**, CH_2Cl_2, −78°C, 30 min.

Table 10.13 **[Ar]**→9-anthracene.

201	X	ee (%)	Yield (%)
d	OH	71	51
e	NHTf	73	38
f	NHTs	90	41

Condition B: 10 mol% of **201**(**d**–**f**), toluene, RT, 100 h.

Table 10.14 **[Ar]**→2,4,6-(^{i}Pr)$_3$C$_6$H$_2$.

201	X	ee (%)	Yield (%)
a	OH	19	55
b	NHTf	23	42
c	NHTs	59	47

Condition B: 10 mol% of **201**(**a**–**c**), toluene, RT, 100 h.

10.15 Cyclopropane ring expansion

Cyclopropane is a highly strained three-membered carbocyclic ring (27 kcal mol^{-1}) that shows high reactivity with nucleophilic reagent. The ring opening of cyclopropane under thermal or photochemical condition was studied in organic synthesis. The strain associated with ring was the main driving force for the catalytic cleavage of the C—C bond. The electron-withdrawing group in cyclopropane ring was used to further activate the C—C bond cleavage with nucleophilic reagents in the synthesis of diverse heterocyclic scaffold of medicinally privileged molecules. In the past decades, several reviews were published on the ring opening reaction of cyclopropane [173–177].

Therefore, the synthetic method based on cyclopropane ring expansion or rearrangement was a pivotal step in a crucial synthetic strategy.

A few synthetic strategies based on cyclopropane ring expansion in a one-pot reaction is described here.

10.16 Synthesis of aza-heterocycles in one-pot ring opening

Piperidine is ubiquitous structural motif widely occurred in diverse synthetically and naturally occurring bioactive molecules. The most notable natural products of this class include Lofentanil, (−)-Arbaricine, (+)-Pergolide, and (+)-Lepadin. Kerr *et al.* [178] developed a versatile synthesis of densely functionalized piperidine scaffold based on a catalytic one-pot ring opening of cyclopropane followed by conia-ene cyclization. This synthesis depended on the nucleophilic ring expansion of *gem*-cyclopropanediester with *N*-benzyl protected propargyl amine as the nucleophile. This produced the substrate for the conia-ene cyclization step in the presence of Lewis acid catalyst. It was discovered that $Zn(NTf_2)_2$ is the best catalyst for carrying out the two-steps reaction of ring opening and subsequent cyclization in a single-pot operation (Scheme 10.42).

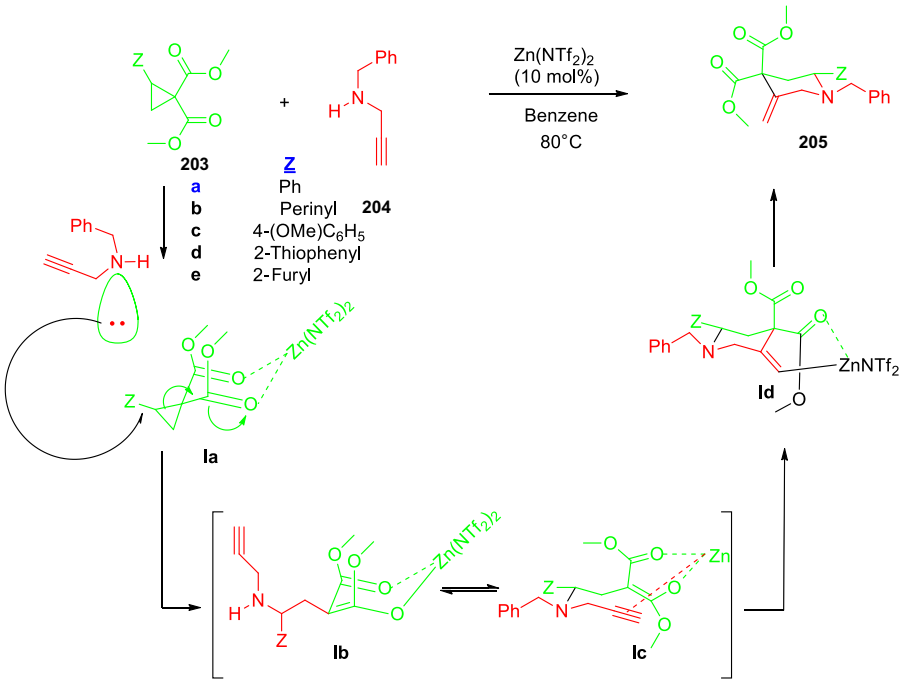

205	Z	Yield (%)[a]
a	Ph	96
b	Perinyl	95
c	4-(OMe)C_6H_5	95
d	2-Thiophenyl	92
e	2-Furyl	84

Scheme 10.42 One-pot synthesis of piperidine *via* tandem cyclopropane ring opening/conia-ene cyclization.

It was realized that 5 mol% of the $Zn(NTf_2)_2$ facilitated the reaction but took longer reaction time to complete while 10 mol% of the catalyst was very effective. The methodology has a diverse scope with aryl rings that have activating/deactivating groups. Heteroaryl-substituted cyclopropyl ring was opened regioselectively with *N*-propargyl amine with excellent yield.

Pyrrolidine rings are interesting scaffold and are often found in many natural products. The typical pyrrolidine alkaloids are kainic acid, condonopsinine, isodomoic acid C, and nicotine. Some novel synthetic methodologies based on one-pot ring expansion of cyclopropane ring toward pyrrolidine scaffolds are described below.

In this connection Lautens *et al*. [179] reported an efficient diastereoselective magnesium iodide-mediated (MgI_2) ring expansion of methylenecyclopropane ring **207** with chiral *N*-sulfinimines **206**. This methodology was employed for the preparation of substituted *N*-sulfinimines **206a–e** which were used in the synthesis of pyrrolidine derivatives **208a–e** successfully (Scheme 10.43). The substitution pattern in aromatic ring had no effects on the diastereochemical outcome of the products (Table 10.15).

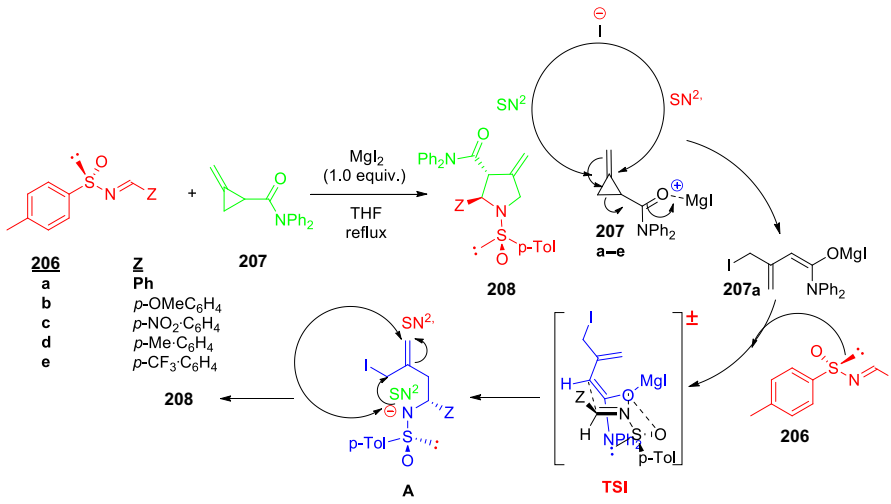

Scheme 10.43 Diastereoselective ring expansion of methylenecyclopropane in synthesis of pyrrolidine.

Table 10.15 Substrate scope and dr ratio.

208	Z	Yield (%)[a]	dr (%)[b]
a	Ph	90	>20:1
b	*p*-$OMeC_6H_4$	76	>20:1
c	*p*-$NO_2{\cdot}C_6H_4$	72	>20:1
d	*p*-$Me{\cdot}C_6H_4$	85	>20:1
e	*p*-$CF_3{\cdot}C_6H_4$	94	>20:1

[a] Isolated yield.
[b] Determined from crude ^1H NMR.

However, the yield of pyrrolidine depended on the substitution pattern of the aromatic rings present in the *N*-sulfinimines.

A highly efficient method based on rare earth metal-catalyzed diastereoselective synthesis of 2,5-*cis* pyrrolidine scaffold of medicinally privileged molecules was achieved by Kerr and coworker [180].

This synthesis realized the [3+2]-cycloaddition of imine **A** derived from the condensation of amine **210** and aldehyde **209** in situ with *gem*-cyclopropanediester **211** in the presence of $Yb(OTf)_3$ as a catalyst. The presence of a high electron-withdrawing group (i.e., NO_2) in aldehyde failed to deliver the expected product. The disposition of the substituents in the aromatic of imines greatly influenced the diastereoselectivity of the products formation. It was observed that the aldimine derived from to 2-furyl (entry b, Table 10.16) and 2-thiophenyl (entry e, Table 10.16) gave a poor diastereoselectivity as a comparison to the aldimine derived from phenyl group.

Table 10.16 Synthesis of 2,5-*cis* pyrrolidine (**212**).

212	R^1	R^2	R^3	Yield (%)	Syn/anti
a	Bn	Ph	Ph	96	93:7
b	Bn	2-Furyl	Ph	93	55:45
c	Bn	*p*-$OMeC_6H_4$	Ph	95	>99:1
d	^nBu	Ph	Ph	82	96:4
e	Bn	2-Thiphenyl	Ph	96	85:15

A model to explain the formation of pyrrolidine was proposed (Fig. 10.24). The formation of the major *syn* products was favored *via* the conformation B in which the bulkier R^2 are present in an equatorial position causing less steric hindrance

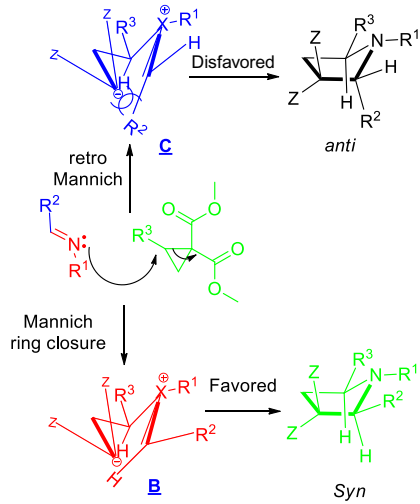

Fig. 10.24 Proposed model for the products formation.

and leads the formation of 2,5-*cis* derivatives of pyrrolidine **212a–e** as the major products (Scheme 10.44, Table 10.16). The E/Z configuration of imine played a crucial role in dictating the products formation.

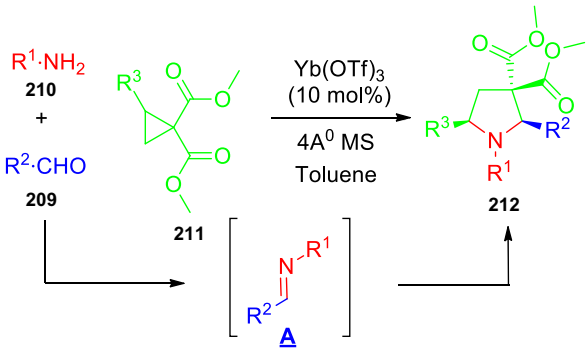

Scheme 10.44 Multicomponent reaction (MCRs) for the synthesis pyrrolidine *via* cyclopropane ring expansion.

The same group developed a highly diastereoselective intramolecular method to access the *cis* and *trans* pyrrolo-isoxazolidines as the precursor for pyrrolidine starting from (*Z*) and (*E*) isomer of oxime ether tethered with activated cyclopropane ring [181]. The oxime ethers **213** and **214** corresponding to diverse aryl, hetroaryl, and alky groups were annulated to pyrrolo-isoxazolidines **215** and **216a–e** derivatives with 5 mol% of $Yb(OTf)_3$ in excellent yield (Scheme 10.45, Table 10.17). The diastereoselectivity greatly depended on the configuration of the oxime ethers. It was found that (*E*)-oxime ether gives 2,5-*trans* products while (*Z*)-isomer gives corresponding 2,5-*cis*-pyrrolo-isoxazolidine derivatives exclusively. This method

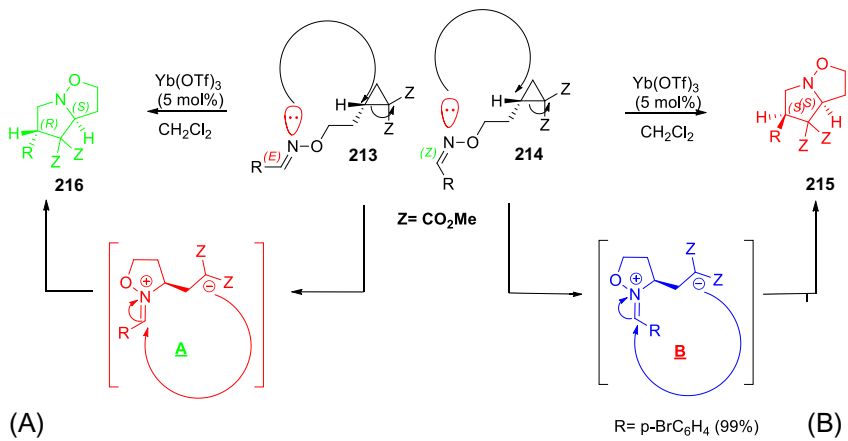

Scheme 10.45 (A) Synthesis of 2,5-*trans*-pyrrolo-isoxazolidines from (*E*)-isomer of oxime ether. (B) Synthesis of 2,5-*cis*-pyrrolo-isoxazolidines from (*Z*)-isomer of oxime ether.

Table 10.17 Synthesis of *trans*-pyrrolo-isoxazolidines.

216	R	Yield (%)
a	Ph	98
b	*p*-BrC_6H_4	99
c	*p*-OMeC_6H_4	99
d	*p*-$NO_2C_6H_4$	99
e	2-Pyridyl	97

offered the stereospecific annulation to access the *cis* and *trans* products from the same starting materials. A cleavage of the N—O bond of the isoxazolidines provided the access of highly substituted complex pyrrolidine in very high yield.

Tang *et al*. developed a highly stereoselective synthesis of tetra-substituted pyrrolidines by the direct nucleophilic ring of activated 1,1-cyclopropanediesters under Sc(OTf)$_3$-catalyzed reaction. The annulation of 1,1-cyclopropanediester **218** with varied substituent to highly substituted pyrrolidines **219a–e** was achieved with the reaction of imine **217** in the presence of 5 mol% of Sc(OTf)$_3$ as a catalyst in dichloromethane as the solvent. The protocol was successfully employed in the synthesis of a wide range of pyrrolidine derivatives with varied substitution patterns proving the generality and scope of the methodology [182] (Scheme 10.46, Table 10.18). The cycloaddition reaction worked equally with electron-rich and deficient imines.

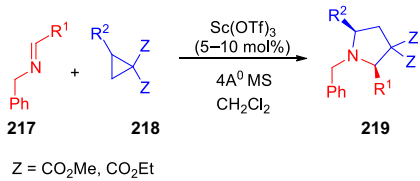

Scheme 10.46 Sc(OTf)$_3$ catalyzed cycloaddition of imine to *gem*-cyclopropanediesters.

Table 10.18 Reaction of *gem*-cyclopropanediester with imines.[a]

219	R^1	R^2	Z	dr[b]	Yield (%)[c]
a	Ph	Styryl	CO_2Me	9:1	91
b	4-FC_6H_4	Styryl	CO_2Me	10:1	94
c	4-MeOC_6H_4	Styryl	CO_2Me	9:1	86
d	4-ClC_6H_4	Vinyl	CO_2Me	6:1	92
e	4-ClC_6H_4	Ph	CO_2Et	24:1	85

[a] 0.25 mmol scale of reaction.
[b] dr determined by ^{1}H NMR.
[c] Isolated yield.

Mechanistically, the cycloaddition pathway was assisted by the direct nucleophilic attack of imine to the cyclopropylcarboxy ester to give dipolar IM B and C. The 1,3-*cis* conformation **C** was energetically and sterically favored and undergoes facile annulation to afford *cis*-pyrrolidine derivatives as the major products (Fig. 10.25).

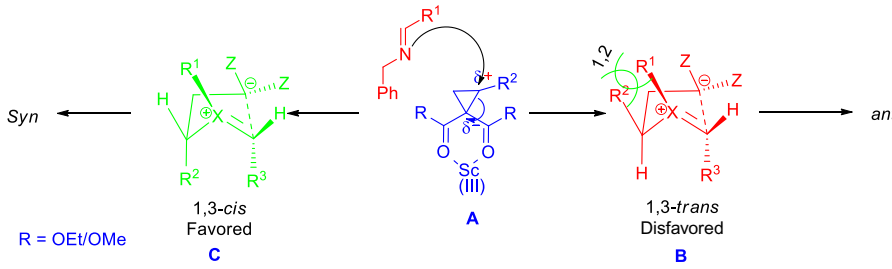

Fig. 10.25 Proposed conformation for the product formation.

10.17 Synthesis of oxacyclic heterocycles in one-pot

Tetrahydropyrans and furans principally constitute as a central motif in diverse medicinally privileged molecules [183]. The most notable anticancer agent, bryostatin, and eribulin are marine macrolides having intriguing tetrahydropyran and furan motif [184, 185]. There is large number of marine macrolide natural products that contain tetrahydropyran and tetrahydrofuran ring together. For instance, goniodomin **A** (actin targeting polyether), prorocentrolide (toxin halistatins), and percentotoxine [186].

Due to their promising biological activity it attracts the attention of the scientific community for their synthesis and structural elucidation. The synthetic strategy for the synthesis of tetrahydrofuran scaffolds based on one-pot ring expansion of cyclopropane ring was developed. The activated cyclopropane is valuable synthetic precursor in organic synthesis. The dual behavior (donor-acceptor) of cyclopropane is a good choice for performing cascade reaction with high degree of molecular complexity.

Johnson and group developed a powerful synthetic approach for the enantioselective synthesis of 2,5-substituted *cis*-tetrahydrofuran based on Lewis acid-mediated [3+2] cycloaddition of enantiomerically rich donor-acceptor *S*-cyclopropanediester with various aldehydes [187]. The synthesis was accomplished by the reaction of (*S*)-dimethyl 2-phenylcyclopropane-1,1-dicarboxylate (**220**, 1.0 equiv.), benzaldehyde (R → Ph, 3.0 equiv.) in the presence of $Sn(OTf)_2$ (5 mol%) to form tetrahydrofuran (**222**) in quantitative yield with 96% of enantioselectivity at room temperature (Scheme 10.47). A chirality transfer from cyclopropane to products was achieved. To establish the scope and the generality, various aldehydes (electron-rich/deficient) were tested and successful results were realized (Table 10.19). An electron-deficient aldehyde needed longer reaction time with high

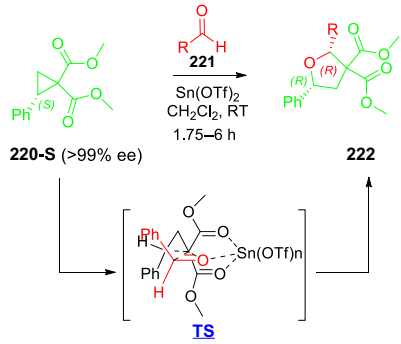

Scheme 10.47 [3+2]-Cycloaddition for synthesis of 2,5-substituted tetrahydrofuran (THF).

Table 10.19 Scope of [3+2] cycloaddition reaction of aldehyde and cyclopropane (donor-acceptor).[a]

222	R	dr	ee (%)	Yield (%)[b]
a	C_6H_5	>100:1	96	100
b	*p*-Cl-C_6H_4	>83:1	96	97
c	*p*-OMe-C_6H_4	>84:1	99	99
d	2-Furyl	24:1	99	83
e	2-Thienyl	>92:1	98	98

[a] Cyclopropane (1.0 equiv.), aldehyde (3.0 equiv.), $Sn(OTf)_2$ (5 mol%), 23–29°C.
[b] Isolated yield.

catalyst loading, furnishing the product with enantioselectivity (ee < 96%). This method was not effective with aliphatic aldehydes. The use of $SnCl_4$ greatly improved the synthesis of title compound with excellent diastereoselectivity and enantioselectivity. All newly synthesized tetrahydrofuran scaffolds were transformed into other valuable medicinally privileged molecules by chemical manipulation.

It was believed that the mechanism followed a concerted SN^2 pathway for the major product. The HOMO of the cyclopropane has a strong interaction with LUMO of the aldehyde regardless of the nature of the aldehyde.

The same group developed a synthetic protocol based on cyclopropane-aldehyde [3+2]-cycloaddition at the quaternary donor site of cyclopropane ring in stereoselective synthesis of highly substituted tetrahydrofuran motif under Lewis acid-catalyzed condition [188]. The cyclopropane was exploited in the synthesis of biologically relevance tetrahydrofuran scaffolds principally constituted in a wide range of natural products. The quaternary center in D-A cyclopropanediester **223ac**–were involved in C—O bond formation by the nucleophilic attack of aldehyde **224a–i** with complete stereochemical inversion at the donor site (Scheme 10.48, Table 10.20).

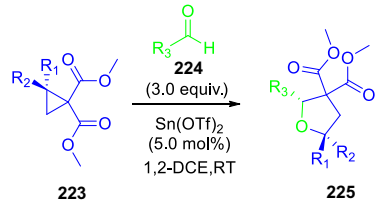

Scheme 10.48 [3+2]-Cycloaddition for synthesis of 2,2,5-substituted tetrahydrofuran (THF) motifs.

Table 10.20 Scope of [3+2] cycloaddition reaction and selectivity.[a]

Entry	D-A cyclopropane (223a→c)			225(a→i)	Yield[b] (%)	dr[c]
	R^1	R^2	R^3			
1	Isopropenyl	Me	Ph	**225a**	90	96:4
			p-Cl·C_6H_4	**225b**	90	99:1
			Et	**225c**	55	99:1
2	*p*-CNC_6H_4	Me	Ph	**225d**	90	95:5
			p-Cl·C_6H_4	**225e**	90	95:5
			Et	**225f**	59	96:4
3	*p*-$MeOC_6H_4$	Me	Ph	**225g**	91	96:4
			p-Cl·C_6H_4	**225h**	87	97:3
			Et	**225i**	74	90:10

[a] Reaction was performed with 1.0 equiv. of **223(a→c)**; 3.0 equiv. of aldehyde **224** followed with 5.0 mol% of $Sn(OTf)_2$ in a sealed Teflon vessel.
[b] Isolated yield.
[c] Determined by H^1NMR analysis.

10.18 Conclusions

It can be seen that a number of one-pot methods are discovered for the green synthesis of numerous medicinally active compounds. The reactivity differences of the starting compounds and catalysts are the key factors to realize the successful one-pot strategy. Many of these structures are highly complex and functionalized. It is very crucial to prepare many of these molecules in optically active forms. Interestingly, synthesis of many of these compounds may not prove to be effective if these are attempted to prepare through a stepwise process. However, designing one-pot synthesis remains a great challenge for the chemists.

Acknowledgments

Bimal Krishna Banik is grateful to Prince Mohammad Bin Fahd University. R.N.Y. and A.K.S. are thankful to VBS Purvanchal University for providing necessary facilities to complete the manuscript.

References

[1] R. Robinson, LXIII.—A synthesis of tropinone, J. Chem. Soc. Trans. 111 (1917) 762–768, https://doi.org/10.1039/CT9171100762.

[2] W.S. Johnson, M.B. Gravestock, B.E. McCarry, Acetylenic bond participation in biogenetic-like olefinic cyclizations. II. Synthesis of dl-progesterone, J. Am. Chem. Soc. 93 (1971) 4332–4334, https://doi.org/10.1021/ja00746a062.

[3] K.C. Nicolaou, N.A. Petasis, R.E. Zipkin, J. Uenishi, The endiandric acid cascade. Electrocyclizations in organic synthesis. 1. Stepwise, stereocontrolled total synthesis of endiandric acids A and B, J. Am. Chem. Soc. 104 (1982) 5555–5557, https://doi.org/10.1021/ja00384a077.

[4] K.C. Nicolaou, N.A. Petasis, J. Uenishi, R.E. Zipkin, The endiandric acid cascade. Electrocyclizations in organic synthesis. 2. Stepwise, stereocontrolled total synthesis of endiandric acids C-G, J. Am. Chem. Soc. 104 (1982) 5557–5558, https://doi.org/10.1021/ja00384a078.

[5] K.C. Nicolaou, R.E. Zipkin, N.A. Petasis, The endiandric acid cascade. electrocyclizations in organic synthesis. 3. "Biomimetic" approach to endiandric acids A-G. Synthesis of precursors, J. Am. Chem. Soc. 104 (1982) 5558–5560, https://doi.org/10.1021/ja00384a079.

[6] K.C. Nicolaou, N.A. Petasis, R.E. Zipkin, The endiandric acid cascade. electrocyclizations in organic synthesis. 4. "Biomimetic" approach to endiandric acids A-G. Total synthesis and thermal studies, J. Am. Chem. Soc. 104 (1982) 5560–5562, https://doi.org/10.1021/ja00384a080.

[7] S. Piettre, C.H. Heathcock, Biomimetic total synthesis of proto-daphniphylline, Science (80-.) 248 (1990) 1532–1534, https://doi.org/10.1126/science.248.4962.1532.

[8] M.L. Ji, Y. Na, H. Han, S. Chang, Cooperative multi-catalyst systems for one-pot organic transformations, Chem. Soc. Rev. 33 (2004) 302–312, https://doi.org/10.1039/b309033g.

[9] L. Albrecht, H. Jiang, K.A. Jørgensen, A simple recipe for sophisticated cocktails: organocatalytic one-pot reactions-concept, nomenclature, and future perspectives, Angew. Chem. Int. Ed. 50 (2011) 8492–8509, https://doi.org/10.1002/anie.201102522.

[10] M. Misra, S.K. Pandey, V.P. Pandey, J. Pandey, R. Tripathi, R.P. Tripathi, Organocatalyzed highly atom economic one pot synthesis of tetrahydropyridines as antimalarials, Bioorg. Med. Chem. 17 (2009) 625–633, https://doi.org/10.1016/j.bmc.2008.11.062.

[11] H. Jiang, P. Eisner, K.L. Jensen, A. Falcicchio, V. Marcos, K.A. Jørgensen, Achieving molecular complexity by organocatalytic one-pot strategies—a fast entry for synthesis of sphingoids, amino sugars, and polyhydroxylated a-amino acids, Angew. Chem. Int. Ed. 48 (2009) 6844–6848, https://doi.org/10.1002/anie.200901446.

[12] M. Gruber, S. Chouzier, K. Koehler, L. Djakovitch, Palladium on activated carbon: a valuable heterogeneous catalyst for one-pot multi-step synthesis, Appl. Catal. A Gen. 265 (2004) 161–169, https://doi.org/10.1016/j.apcata.2004.01.012.

[13] M.J. Climent, A. Corma, S. Iborra, Heterogeneous catalysts for the one-pot synthesis of chemicals and fine chemicals, Chem. Rev. 111 (2011) 1072–1133, https://doi.org/10.1021/cr1002084.

[14] J. Moon, M. Jeong, H. Nam, J. Ju, J.H. Moon, H.M. Jung, S. Lee, One-pot synthesis of diarylalkynes using palladium-catalyzed sonogashira reaction and decarboxylative coupling of sp carbon and sp2 carbon, Org. Lett. 10 (2008) 945–948, https://doi.org/10.1021/ol703130y.

[15] N. Chernyak, V. Gevorgyan, General and efficient copper-catalyzed three-component coupling reaction towards imidazoheterocycles: one-pot synthesis of alpidem and zolpidem, Angew. Chem. Int. Ed. 49 (2010) 2743–2746, https://doi.org/10.1002/anie.200907291.
[16] D. Aminoff, W.T.J. Morgan, Hexosamine components of the human blood group substances, Nature 162 (1948) 579, https://doi.org/10.1038/162579a0.
[17] O.T. Avery, M. Heidelberger, Immunological relationships of cell constituents of pneumococcus, Exp. Biol. Med. 38 (2013) 81, https://doi.org/10.3181/00379727-20-217.
[18] J. Popiołkiewicz, K. Polkowski, J.S. Skierski, A.P. Mazurek, In vitro toxicity evaluation in the development of new anticancer drugs—genistein glycosides, Cancer Lett. 229 (2005) 67–75, https://doi.org/10.1016/j.canlet.2005.01.014.
[19] X. Tian, X. Zhang, H. Tang, H. Lin, S. Wang, G. Cheng, Saponins: the potential chemotherapeutic agents in pursuing new anti-glioblastoma drugs, Mini Rev. Med. Chem. 13 (2013) 1709–1724, https://doi.org/10.2174/13895575113136660083.
[20] L. Menger, E. Vacchelli, S. Adjemian, I. Martins, Y. Ma, S. Shen, T. Yamazaki, A. Q. Sukkurwala, M. Michaud, G. Mignot, F. Schlemmer, E. Sulpice, C. Locher, X. Gidrol, F. Ghiringhelli, N. Modjtahedi, L. Galluzzi, F. André, L. Zitvogel, O. Kepp, G. Kroemer, Cardiac glycosides exert anticancer effects by inducing immunogenic cell death, Sci. Transl. Med. 4 (2012) 143ra99, https://doi.org/10.1126/scitranslmed.3003807.
[21] H.X. Sun, Y. Xie, Y.P. Ye, Advances in saponin-based adjuvants, Vaccine 27 (2009) 1787–1796, https://doi.org/10.1016/j.vaccine.2009.01.091.
[22] S. Raghavan, D. Kabne, A one-step synthesis of the ciclamycin trisaccharide, J. Am. Chem. Soc. 115 (1993) 1580–1581, https://doi.org/10.1021/ja00057a056.
[23] J. Gildersleeve, A. Smith, K. Sakurai, S. Raghavan, D. Kahne, Scavenging byproducts in the sulfoxide glycosylation reaction: application to the synthesis of ciclamycin 0, J. Am. Chem. Soc. 121 (1999) 6176–6182, https://doi.org/10.1021/ja990690a.
[24] B. Fraser-Reid, Z. Wu, U.E. Udodong, H. Ottosson, Armed/disarmed effects in glycosyl donors: rationalization and sidetracking, J. Org. Chem. 55 (1990) 6068–6070, https://doi.org/10.1021/jo00312a004.
[25] D.R. Mootoo, P. Konradsson, U. Udodong, B. Fraser-Reid, "Armed" and "disarmed" n-pentenyl glycosides in saccharide couplings leading to oligosaccharides, J. Am. Chem. Soc. 110 (1988) 5583–5584, https://doi.org/10.1021/ja00224a060.
[26] Z. Zhang, I.R. Ollmann, X.S. Ye, R. Wischnat, T. Baasov, C.H. Wong, Programmable one-pot oligosaccharide synthesis, J. Am. Chem. Soc. 121 (1999) 734–753, https://doi.org/10.1021/ja982232s.
[27] D. Crich, M. Smith, Solid-phase synthesis of β-mannosides, J. Am. Chem. Soc. 124 (2002) 8867–8869, https://doi.org/10.1021/ja011406u.
[28] D. Crich, S. Sun, Direct formation of β-mannopyranoside and other hindered glycosides from thioglycosides, J. Am. Chem. Soc. 120 (1998) 435–436, https://doi.org/10.1021/ja9734814.
[29] T. Angles d'Ortoli, C. Hamark, G. Widmalm, Structure-reactivity relationships of conformationally armed disaccharide donors and their use in the synthesis of a hexasaccharide related to the capsular polysaccharide from *Streptococcus pneumoniae* type 37, J. Org. Chem. 82 (2017) 8123–8140, https://doi.org/10.1021/acs.joc.7b01264.
[30] S.J. Danishefsky, From the laboratory to the clinic: a retrospective on fully synthetic carbohydrate-based anticancer vaccines, Angew. Chem. Int. Ed. 39 (2000) 836–863.
[31] T. Buskas, P. Thompson, G.J. Boons, Immunotherapy for cancer: synthetic carbohydrate-based vaccines, Chem. Commun. 36 (2009) 5335–5349, https://doi.org/10.1039/b908664c.

[32] Z. Guo, Q. Wang, Recent development in carbohydrate-based cancer vaccines, Curr. Opin. Chem. Biol. 13 (2009) 608–617, https://doi.org/10.1016/j.cbpa.2009.08.010.
[33] J. Zhu, J.D. Warren, S.J. Danishefsky, Synthetic carbohydrate-based anticancer vaccines: the Memorial Sloan-Kettering experience, Expert Rev. Vaccines 8 (2009) 1399–1413, https://doi.org/10.1586/erv.09.95.
[34] R.D. Astronomo, D.R. Burton, Carbohydrate vaccines: developing sweet solutions to sticky situations? Nat. Rev. Drug Discov. 9 (2010) 308–324, https://doi.org/10.1038/nrd3012.
[35] M. Von Itzstein, W.Y. Wu, G.B. Kok, M.S. Pegg, J.C. Dyason, B. Jin, T. Van Phan, M. L. Smythe, H.F. White, S.W. Oliver, P.M. Colman, J.N. Varghese, D.M. Ryan, J. M. Woods, R.C. Bethell, V.J. Hotham, J.M. Cameron, C.R. Penn, Rational design of potent sialidase-based inhibitors of influenza virus replication, Nature 363 (1993) 418–423, https://doi.org/10.1038/363418a0.
[36] C.U. Kim, W. Lew, M.A. Williams, H. Liu, L. Zhang, S. Swaminathan, N. Bischofberger, M.S. Chen, D.B. Mendel, C.Y. Tai, W.G. Laver, R.C. Stevens, Influenza neuraminidase inhibitors possessing a novel hydrophobic interaction in the enzyme active site: design, synthesis, and structural analysis of carbocyclic sialic acid analogues with potent anti-influenza activity, J. Am. Chem. Soc. 119 (1997) 681–690, https://doi.org/10.1021/ja963036t.
[37] J. Magano, Synthetic approaches to the neuraminidase inhibitors zanamivir (Relenza) and oseltamivir phosphate (Tamiflu) for the treatment of influenza, Chem. Rev. 109 (2009) 4398–4438, https://doi.org/10.1021/cr800449m.
[38] E.E. Simanek, G.J. McGarvey, J.A. Jablonowski, C.H. Wong, Selectin-carbohydrate interactions: from natural ligands to designed mimics, Chem. Rev. 98 (1998) 833–862, https://doi.org/10.1021/cr940226i.
[39] K.A. Karlsson, Microbial recognition of target-cell glycoconjugates, Curr. Opin. Struct. Biol. 5 (1995) 622–635, https://doi.org/10.1016/0959-440X(95)80054-9.
[40] K.C. Nicolaou, H.J. Mitchell, ChemInform Abstract: Adventures in carbohydrate chemistry: new synthetic technologies, chemical synthesis, molecular design, and chemical biology, Angew. Chem. Int. Ed. 40 (2001) 1576–1624, https://doi.org/10.1002/chin.200132256.
[41] O.J. Plante, E.R. Palmacci, P.H. Seeberger, Automated solid-phase synthesis of oligosaccharides, Science (80-.) 291 (2001) 1523–1527, https://doi.org/10.1126/science.1057324.
[42] M.T.C. Walvoort, A.G. Volbeda, N.R.M. Reintjens, H. Van Den Elst, O.J. Plante, H. S. Overkleeft, G.A. Van Der Marel, J.D.C. Codée, Automated solid-phase synthesis of hyaluronan oligosaccharides, Org. Lett. 14 (2012) 3776–3779, https://doi.org/10.1021/ol301666n.
[43] P.H. Seeberger, D.B. Werz, Automated synthesis of oligosaccharides as a basis for drug discovery, Nat. Rev. Drug Discov. 4 (2005) 751–763, https://doi.org/10.1038/nrd1823.
[44] P.H. Seeberger, Automated oligosaccharide synthesis, Chem. Soc. Rev. 37 (2008) 19–28, https://doi.org/10.1039/b511197h.
[45] C.H. Hsu, S.C. Hung, C.Y. Wu, C.H. Wong, Toward automated oligosaccharide synthesis, Angew. Chem. Int. Ed. 50 (2011) 11872–11923, https://doi.org/10.1002/anie.201100125.
[46] M.C. Hewitt, D.A. Snyder, P.H. Seeberger, Rapid synthesis of a glycosylphosphatidylinositol-based malaria vaccine using automated solid-phase oligosaccharide synthesis, J. Am. Chem. Soc. 124 (2002) 13434–13436, https://doi.org/10.1021/ja027538k.
[47] C.Y. Wu, C.H. Wong, Programmable one-pot glycosylation, Top. Curr. Chem. 301 (2011) 223–252, https://doi.org/10.1007/128_2010_109.

[48] T. Polat, C.H. Wong, Anomeric reactivity-based one-pot synthesis of heparin-like oligosaccharides, J. Am. Chem. Soc. 129 (2007) 12795–12800, https://doi.org/10.1021/ja073098r.
[49] C.W. Cheng, Y. Zhou, W.H. Pan, S. Dey, C.Y. Wu, W.L. Hsu, C.H. Wong, Hierarchical and programmable one-pot synthesis of oligosaccharides, Nat. Commun. 9 (2018) 5202, https://doi.org/10.1038/s41467-018-07618-8.
[50] S. Dey, C.H. Wong, Programmable one-pot synthesis of heparin pentasaccharides enabling access to regiodefined sulfate derivatives, Chem. Sci. 9 (2018) 6685–6691, https://doi.org/10.1039/c8sc01743c.
[51] Y.-L. Huang, J.-T. Hung, S.K.C. Cheung, H.-Y. Lee, K.-C. Chu, S.-T. Li, Y.-C. Lin, C.-T. Ren, T.-J.R. Cheng, T.-L. Hsu, A.L. Yu, C.-Y. Wu, C.-H. Wong, Carbohydrate-based vaccines with a glycolipid adjuvant for breast cancer, Proc. Natl. Acad. Sci. 110 (2013) 2517–2522, https://doi.org/10.1073/pnas.1222649110.
[52] Y.-W. Lou, P.-Y. Wang, S.-C. Yeh, P.-K. Chuang, S.-T. Li, C.-Y. Wu, K.-H. Khoo, M. Hsiao, T.-L. Hsu, C.-H. Wong, Stage-specific embryonic antigen-4 as a potential therapeutic target in glioblastoma multiforme and other cancers, Proc. Natl. Acad. Sci. U. S. A. 111 (2014) 2482–2487, https://doi.org/10.1073/pnas.1400283111.
[53] B.A. Macher, T. Pacuszka, B.R. Mullin, C.C. Sweeley, R.O. Brady, P.H. Fishman, Isolation and identification of a fucose-containing ganglioside from bovine thyroid gland, Biochim. Biophys. Acta Gen. Subj. 588 (1979) 35–43, https://doi.org/10.1016/0304-4165(79)90368-4.
[54] J. Zhu, Q. Wan, G. Ragupathi, C.M. George, P.O. Livingston, S.J. Danishefsky, Biologics through chemistry: total synthesis of a proposed dual-acting vaccine targeting ovarian cancer by orchestration of oligosaccharide and polypeptide domains, J. Am. Chem. Soc. 131 (2009) 4151–4158, https://doi.org/10.1021/ja810147j.
[55] D.P. Galonić, D.Y. Gin, Chemical glycosylation in the synthesis of glycoconjugate antitumour vaccines, Nature 446 (2007) 1000–1007, https://doi.org/10.1038/nature05813.
[56] S.F. Slovin, S.J. Keding, G. Ragupathi, Carbohydrate vaccines as immunotherapy for cancer, Immunol. Cell Biol. 83 (2005) 418–428, https://doi.org/10.1111/j.1440-1711.2005.01350.x.
[57] J.R. Allen, S.J. Danishefsky, New applications of the n-pentenyl glycoside method in the synthesis and immunoconjugation of fucosyl GM1: a highly tumor-specific antigen associated with small cell lung carcinoma, J. Am. Chem. Soc. 121 (1999) 10875–10882, https://doi.org/10.1021/ja992594f.
[58] T.K.-K. Mong, H.-K. Lee, S.G. Duron, C.-H. Wong, Reactivity-based one-pot total synthesis of fucose GM1 oligosaccharide: a sialylated antigenic epitope of small-cell lung cancer, Proc. Natl. Acad. Sci. 100 (2003) 797–802, https://doi.org/10.1073/pnas.0337590100.
[59] D. Crich, M. Smith, 1-Benzenesulfinyl piperidine/trifluoromethanesulfonic anhydride: a potent combination of shelf-stable reagents for the low-temperature conversion of thioglycosides to glycosyl triflates and for the formation of diverse glycosidic linkages, J. Am. Chem. Soc. 123 (2001) 9015–9020, https://doi.org/10.1021/ja0111481.
[60] S. Quideau, K.S. Feldman, Ellagitannin chemistry, Chem. Rev. 96 (1999) 475–504, https://doi.org/10.1021/cr940716a.
[61] S. Quideau, D. Deffieux, C. Douat-Casassus, L. Pouységu, Plant polyphenols: chemical properties, biological activities, and synthesis, Angew. Chem. Int. Ed. 50 (2011) 586–621, https://doi.org/10.1002/anie.201000044.
[62] M. Kurokawa, T. Hozumi, M. Tsurita, S. Kadota, T. Namba, K. Shiraki, Biological characterization of eugeniin as an anti-herpes simplex virus type 1 compound in vitro and in vivo, J. Pharmacol. Exp. Ther. 297 (2001) 372–379.

[63] Y. Kashiwada, G.-.I. Nonaka, I. Nishioka, K.J. Lee, I. Bori, Y. Fukushima, K.F. Bastow, K.-.H. Lee, Tannins as potent inhibitors of DNA topoisomerase II in vitro, J. Pharm. Sci. 82 (1993) 487–492, https://doi.org/10.1002/jps.2600820511.

[64] R.K. Saha, T. Takahashi, Y. Kurebayashi, K. Fukushima, A. Minami, N. Kinbara, M. Ichitani, Y.M. Sagesaka, T. Suzuki, Antiviral effect of strictinin on influenza virus replication, Antivir. Res. 88 (2010) 10–18, https://doi.org/10.1016/j.antiviral.2010.06.008.

[65] H. Tachibana, T. Kubo, T. Miyase, S. Tanino, M. Yoshimoto, M. Sano, M. Yamamoto-Maeda, K. Yamada, Identification of an inhibitor for interleukin 4-induced ε germline transcription and antigen-specific IgE production in vivo, Biochem. Biophys. Res. Commun. 280 (2001) 53–60, https://doi.org/10.1006/bbrc.2000.4069.

[66] H. Takeuchi, K. Mishiro, Y. Ueda, Y. Fujimori, T. Furuta, T. Kawabata, Total synthesis of ellagitannins through regioselective sequential functionalization of unprotected glucose, Angew. Chem. Int. Ed. 54 (2015) 6177–6180, https://doi.org/10.1002/anie.201500700.

[67] O.G. Ovchinnikova, N.A. Kocharova, M. Bialczak-Kokot, A.S. Shashkov, A. Rozalski, Y.A. Knirel, Structure of the o-polysaccharide of *Providencia alcalifaciens* o22 containing d-glyceramide 2-phosphate, Eur. J. Org. Chem. 2012 (2012) 3500–3506, https://doi.org/10.1002/ejoc.201200318.

[68] M.R. Galac, B.P. Lazzaro, Comparative pathology of bacteria in the genus Providencia to a natural host, *Drosophila melanogaster*, Microbes Infect. 13 (2011) 673–683, https://doi.org/10.1016/j.micinf.2011.02.005.

[69] M. Yoh, J. Matsuyama, M. Ohnishi, K. Takagi, H. Miyagi, K. Mori, K.S. Park, T. Ono, T. Honda, Importance of Providencia species as a major cause of travellers' diarrhoea, J. Med. Microbiol. 54 (2005) 1077–1082, https://doi.org/10.1099/jmm.0.45846-0.

[70] O.R. Sipahi, S. Bardak-Ozcem, E. Ozgiray, S. Aydemir, T. Yurtseven, T. Yamazhan, M. Tasbakan, S. Ulusoy, Meningitis due to *Providencia stuartii*, J. Clin. Microbiol. (2010), https://doi.org/10.1128/JCM.01349-10.

[71] A.F. Koreishi, B.A. Schechter, C.L. Karp, Ocular infections caused by *Providencia rettgeri*, Ophthalmology 113 (2006) 1463–1466, https://doi.org/10.1016/j.ophtha.2006.03.047.

[72] A.R. Podilapu, S.S. Kulkarni, Total synthesis of repeating unit of O-polysaccharide of *Providencia alcalifaciens* O22 via one-pot glycosylation, Org. Lett. 19 (2017) 5466–5469, https://doi.org/10.1021/acs.orglett.7b02791.

[73] N. Asano, R.J. Nash, R.J. Molyneux, G.W.J. Fleet, Sugar-mimic glycosidase inhibitors: natural occurrence, biological activity and prospects for therapeutic application, Tetrahedron Asymmetry 11 (2000) 1645–1680, https://doi.org/10.1016/S0957-4166(00)00113-0.

[74] P. Compain, O.R. Martin, Carbohydrate mimetics-based glycosyltransferase inhibitors, Bioorg. Med. Chem. 9 (2001) 3077–3092, https://doi.org/10.1016/S0968-0896(01)00176-6.

[75] P. Compain, O.R. Martin, Iminosugars: From Synthesis to Therapeutic Applications, 2008. https://doi.org/10.1002/9780470517437.

[76] G. Horne, F.X. Wilson, J. Tinsley, D.H. Williams, R. Storer, Iminosugars past, present and future: medicines for tomorrow, Drug Discov. Today 16 (2011) 107–118, https://doi.org/10.1016/j.drudis.2010.08.017.

[77] G. Horne, F.X. Wilson, Therapeutic applications of iminosugars: current perspectives and future opportunities, Prog. Med. Chem. 50 (2011) 135–176, https://doi.org/10.1016/B978-0-12-381290-2.00004-5.

[78] L.J. Scott, C.M. Spencer, Miglitol: a review of its therapeutic potential in type 2 diabetes mellitus, Drugs 59 (2000) 521–549, https://doi.org/10.2165/00003495-200059030-00012.
[79] N. Asano, T. Yamashita, K. Yasuda, K. Ikeda, H. Kizu, Y. Kameda, A. Kato, R.J. Nash, H.S. Lee, K.S. Ryu, Polyhydroxylated alkaloids isolated from mulberry trees (*Morus alba* L.) and silkworms (*Bombyx mori* L.), J. Agric. Food Chem. 49 (2001) 4208–4213, https://doi.org/10.1021/jf010567e.
[80] N. Asano, E. Tomioka, H. Kizu, K. Matsui, Sugars with nitrogen in the ring isolated from the leaves of *Morus bombycis*, Carbohydr. Res. 253 (1994) 235–245, https://doi.org/10.1016/0008-6215(94)80068-5.
[81] N. Asano, K. Oseki, E. Tomioka, H. Kizu, K. Matsui, N-containing sugars from *Morus alba* and their glycosidase inhibitory activities, Carbohydr. Res. 259 (1994) 243–255, https://doi.org/10.1016/0008-6215(94)84060-1.
[82] J. Zhou, Y. Zhang, X. Zhou, J. Zhou, L.H. Zhang, X.S. Ye, X.L. Zhang, An expeditious one-pot synthesis of 1,6-dideoxy-N-alkylated nojirimycin derivatives and their inhibitory effects on the secretion of IFN-γ and IL-4, Bioorg. Med. Chem. 16 (2008) 1605–1612, https://doi.org/10.1016/j.bmc.2007.11.036.
[83] H. Uehara, C.F. Barbas, Anti-selective asymmetric Michael reactions of aldehydes and nitroolefins catalyzed by a primary amine/thiourea, Angew. Chem. Int. Ed. 48 (2009) 9848–9852, https://doi.org/10.1002/anie.200905313.
[84] R. Imashiro, H. Uehara, C.F. Barbas, One-pot enantioselective syntheses of iminosugar derivatives using organocatalytic anti-Michael- anti-aza-henry reactions, Org. Lett. 12 (2010) 5250–5253, https://doi.org/10.1021/ol102292a.
[85] A. Brandi, F. Cardona, S. Cicchi, F.M. Cordero, A. Goti, Stereocontrolled cyclic nitrone cycloaddition strategy for the synthesis of pyrrolizidine and indolizidine alkaloids, Chem. Eur. J. 15 (2009) 7808–7821, https://doi.org/10.1002/chem.200900707.
[86] A. Pepe, M. Pamment, G.I. Georg, S.V. Malhotra, Synthesis of fused bicyclic systems with nitrogen atom at the bridgehead, including indolizidines and quinolizidines, J. Org. Chem. 76 (2011) 3527–3530, https://doi.org/10.1021/jo102558u.
[87] N.B. Kalamkar, D.D. Dhavale, Chiron approach strategy to the bicyclic oxazolidinylpiperidine: a building block for preparing mono-and bi-cyclic iminosugars, Tetrahedron Lett. 52 (2011) 6363–6365, https://doi.org/10.1016/j.tetlet.2011.09.039.
[88] I. Dragutan, V. Dragutan, A. Demonceau, H. Vosloo, Synthesis of castanospermine and epimers by metathesis routes, Curr. Org. Chem. 17 (2013) 2721–2739, https://doi.org/10.2174/13852728113179990114.
[89] M. Malinowski, T. Rowicki, P. Guzik, M. Gryszel, S. Łapczyński, M. Wielechowska, K. Czerwińska, I. Madura, W. Sas, [1,4]-Sigmatropic rearrangement of chiral nitrones and their utilization in the synthesis of new iminosugars, Org. Biomol. Chem. 14 (2016) 470–482, https://doi.org/10.1039/c5ob01432h.
[90] X.P. Jiang, Y. Cheng, G.F. Shi, Z.M. Kang, A versatile strategy for divergent and diastereoselective synthesis of natural product-like polyhydroxylated indolizidines, J. Org. Chem. 72 (2007) 2212–2215, https://doi.org/10.1021/jo0624290.
[91] P. Szczešniak, S. Stecko, E. Maziarz, O. Staszewska-Krajewska, B. Furman, Synthesis of polyhydroxylated quinolizidine and indolizidine scaffolds from sugar-derived lactams via a one-pot reduction/Mannich/Michael sequence, J. Org. Chem. 79 (2014) 10487–10503, https://doi.org/10.1021/jo502146z.
[92] D.J.A. Schedler, A.G. Godfrey, B. Ganem, Reductive deoxygenation by Cp2ZrHCl: selective formation of imines via zirconation/hydrozirconation of amides, Tetrahedron Lett. 34 (1993) 5035–5038, https://doi.org/10.1016/S0040-4039(00)60669-X.

[93] D.J.A. Schedler, J. Li, B. Ganem, Reduction of secondary carboxamides to imines, J. Org. Chem. 61 (1996) 4115–4119, https://doi.org/10.1021/jo960286j.
[94] P. Szcześniak, S. Stecko, O. Staszewska-Krajewska, B. Furman, Sugar-derived cyclic imines: one-pot synthesis and direct functionalization, Tetrahedron 70 (2014) 1880–1888, https://doi.org/10.1016/j.tet.2014.01.039.
[95] A. Chardon, E. Morisset, J. Rouden, J. Blanchet, Recent advances in amide reductions, Synthesis 50 (2018) 984–997, https://doi.org/10.1055/s-0036-1589144.
[96] D.L.J. Pinheiro, E.P. Ávila, G.M.F. Batista, G.W. Amarante, Chemoselective reduction of azlactones using Schwartz's reagent, J. Org. Chem. 82 (2017) 5981–5985, https://doi.org/10.1021/acs.joc.7b00820.
[97] Zhao, Y., Snieckus, V.A., 2012. Schwartz reagents: Methods of in situ generation and use (U.S. Patent).
[98] S.S. Prasad, S. Senthilkumar, A. Srivastava, S. Baskaran, Iminosugar C-nitromethyl glycosides and divergent synthesis of bicyclic iminosugars, Org. Lett. 19 (2017) 4403–4406, https://doi.org/10.1021/acs.orglett.7b02175.
[99] A. Kamimura, A. Kadowaki, T. Yoshida, R. Takeuchi, H. Uno, Stereoselective synthesis of bicyclic nitrocyclopropanes by a radical-anion domino reaction, Chem. Eur. J. 15 (2009) 10330–10334, https://doi.org/10.1002/chem.200901920.
[100] A. Kamimura, T. Moriyama, Y. Ito, T. Kawamoto, H. Uno, Asymmetric synthesis of bicyclic nitrocyclopropanes from primary nitro compounds and stereoselective formation of tetrahydro-2H-cyclopenta[b]furans via ring expansion/cyclization reaction, J. Org. Chem. 81 (2016) 4664–4681, https://doi.org/10.1021/acs.joc.6b00566.
[101] N.N. Yadav, J. Choi, H.J. Ha, One-pot multiple reactions: asymmetric synthesis of 2,6-Cis-disubstituted piperidine alkaloids from chiral aziridine, Org. Biomol. Chem. 14 (2016) 6426–6434, https://doi.org/10.1039/c6ob00806b.
[102] W.K. Lee, H.J. Ha, Highlights of the chemistry of enantiomerically pure aziridine-2-carboxylates, Aldrichimica Acta 36 (2003) 57–63.
[103] B.K. Lee, B.J. Sung, W.K. Lee, D.H. Yoon, H.J. Ha, Selective reduction of C-C double bonds of 2-vinylaziridnes: preparation of enationmerically pure 2-alkylaziridines, Bull. Kor. Chem. Soc. 30 (2009) 3123–3126, https://doi.org/10.5012/bkcs.2009.30.12.3123.
[104] I. Coldham, A.J. Collis, R.J. Mould, R.E. Rathmell, Ring expansion of aziridines to piperidines using the aza-wittig rearrangement, Tetrahedron Lett. 36 (1995) 3557–3560, https://doi.org/10.1016/0040-4039(95)00557-S.
[105] I. Coldham, A.J. Collis, R.J. Mould, R.E. Rathmell, Synthesis of 4-phenylpiperidines by tandem Wittig olefination–aza-Wittig rearrangement of 2-benzoylaziridines, J. Chem. Soc. Perkin Trans. 1 1 (1995) 2739–2745, https://doi.org/10.1039/p19950002739.
[106] A.R. Patel, G. Ball, L. Hunter, F. Liu, Conformational regulation of substituted azepanes through selective monofluorination, Org. Biomol. Chem. 11 (2013) 3781–3785, https://doi.org/10.1039/c3ob40391b.
[107] F. Marcelo, Y. He, S.A. Yuzwa, L. Nieto, J. Jimenez-Barbero, M. Sollogoub, D.J. Vocadlo, G.D. Davies, Y. Blériot, Molecular basis for inhibition of GH84 glycoside hydrolases by substituted azepanes: conformational flexibility enables probing of substrate distortion, J. Am. Chem. Soc. 131 (2009) 5390–5392, https://doi.org/10.1021/ja809776r.
[108] C.B. Breitenlechner, T. Wegge, L. Berillon, K. Graul, K. Marzenell, W.G. Friebe, U. Thomas, R. Schumacher, R. Huber, R.A. Engh, B. Masjost, Structure-based optimization of novel azepane derivatives as PKB inhibitors, J. Med. Chem. 47 (2004) 1375–1390, https://doi.org/10.1021/jm0310479.
[109] S. Barluenga, K.B. Simonsen, E.S. Littlefield, B.K. Ayida, D. Vourloumis, G.C. Winters, M. Takahashi, S. Shandrick, Q. Zhao, Q. Han, T. Hermann, Rational design of azepane-

glycoside antibiotics targeting the bacterial ribosome, Bioorg. Med. Chem. Lett. 14 (2004) 713–718, https://doi.org/10.1016/j.bmcl.2003.11.028.
[110] E. Cini, G. Bifulco, G. Menchi, M. Rodriquez, M. Taddei, Synthesis of enantiopure 7-substituted azepane-2-carboxylic acids as templates for conformationally constrained peptidomimetics, Eur. J. Org. Chem. 2012 (2012) 2133–2141, https://doi.org/10.1002/ejoc.201101387.
[111] J. Zhou, Y.Y. Yeung, N-bromosuccinimide-induced aminocyclization-aziridine ring-expansion cascade: an asymmetric and highly stereoselective approach toward the synthesis of azepane, Org. Lett. 16 (2014) 2134–2137, https://doi.org/10.1021/ol5005609.
[112] G. Chouhan, H. Alper, Domino ring-opening/carboxamidation reactions of N-tosyl aziridines and 2-halophenols/pyridinol: efficient synthesis of 1,4-benzo- and pyrido-oxazepinones, Org. Lett. 12 (2010) 192–195, https://doi.org/10.1021/ol902598d.
[113] J.J. Feng, T.Y. Lin, H.H. Wu, J. Zhang, Transfer of chirality in the rhodium-catalyzed intramolecular formal hetero-[5 + 2] cycloaddition of vinyl aziridines and alkynes: stereoselective synthesis of fused azepine derivatives, J. Am. Chem. Soc. 137 (2015) 3787–3790, https://doi.org/10.1021/jacs.5b01305.
[114] A.K. Yudin, Aziridines and Epoxides in Organic Synthesis, John Wiley & Sons, 2006https://doi.org/10.1002/3527607862.
[115] D.J. MacK, J.T. Njardarson, Recent advances in the metal-catalyzed ring expansions of three- and four-membered rings, ACS Catal. 3 (2013) 272–286, https://doi.org/10.1021/cs300771d.
[116] H. Ohno, Synthesis and applications of vinylaziridines and ethynylaziridines, Chem. Rev. 114 (2014) 7784–7814, https://doi.org/10.1021/cr400543u.
[117] N.T. Patil, Y. Yamamoto, Palladium catalyzed cascade reactions involving π-allyl palladium chemistry, in: Topics in Organometallic Chemistry, Springer, Berlin, Heidelberg, 2006, pp. 91–113, https://doi.org/10.1007/3418_014.
[118] K. Aoyagi, H. Nakamura, Y. Yamamoto, Palladium-catalyzed aminoallylation of activated olefins with allylic halides and phthalimide, J. Org. Chem. 67 (2002) 5977–5980, https://doi.org/10.1021/jo025747h.
[119] M.A. Lowe, M. Ostovar, S. Ferrini, C.C. Chen, P.G. Lawrence, F. Fontana, A. A. Calabrese, V.K. Aggarwal, Palladium-mediated annulation of vinyl aziridines with Michael acceptors: stereocontrolled synthesis of substituted pyrrolidines and its application in a formal synthesis of (-)-α-kainic acid, Angew. Chem. Int. Ed. 50 (2011) 6370–6374, https://doi.org/10.1002/anie.201101389.
[120] G. Arena, C.C. Chen, D. Leonori, V.K. Aggarwal, Concise synthesis of (+)-allo-kainic acid via MgI2-mediated tandem aziridine ring opening-formal [3 + 2] cycloaddition, Org. Lett. 15 (2013) 4250–4253, https://doi.org/10.1021/ol4020333.
[121] C.F. Xu, B.H. Zheng, J.J. Suo, C.H. Ding, X.L. Hou, Highly diastereo- and enantioselective palladium-catalyzed[3+2] cycloaddition of vinyl aziridines and α,β-unsaturated ketones, Angew. Chem. Int. Ed. 54 (2015) 1604–1607, https://doi.org/10.1002/anie.201409467.
[122] J.M. Kent, SNaRIs, NaSSAs, and NaRIs: new agents for the treatment of depression, Lancet 355 (2000) 911–918, https://doi.org/10.1016/S0140-6736(99)11381-3.
[123] R. Davis, H.M. Bryson, Levofloxacin: a review of its antibacterial activity, pharmacokinetics and therapeutic efficacy, Drugs 47 (1994) 677–700, https://doi.org/10.2165/00003495-199447040-00008.
[124] M.H. Cohen, FDA drug approval summary: gefitinib (ZD1839) (Iressa(R)) tablets, Oncologist 8 (2004) 303–306, https://doi.org/10.1634/theoncologist.8-4-303.

[125] M. Aapro, A. Carides, B.L. Rapoport, H.-J. Schmoll, L. Zhang, D. Warr, Aprepitant and fosaprepitant: a 10-year review of efficacy and safety, Oncologist 20 (2015) 450–458, https://doi.org/10.1634/theoncologist.2014-0229.
[126] D.M. Grasela, Clinical pharmacology of gatifloxacin, a new fluoroquinolone, Clin. Infect. Dis. 31 (2002) S51–S58, https://doi.org/10.1086/314061.
[127] G. Kuminek, H.K. Stulzer, M.P. Tagliari, P.R. Oliveira, L.S. Bernardi, G. Rauber, S. G. Cardoso, Development and validation of a stability-indicating HPLC method for the determination of buclizine hydrochloride in tablets and oral suspension and its application to dissolution studies, Quim Nova 35 (2012) 207–212, https://doi.org/10.1590/S0100-40422012000100036.
[128] I. Vilotijevic, T.F. Jamison, Epoxide-opening cascades promoted by water, Science (80-.) 317 (2007) 1189–1192, https://doi.org/10.1126/science.1146421.
[129] C.J. Morten, J.A. Byers, A.R. Van Dyke, I. Vilotijevic, T.F. Jamison, The development of endo-selective epoxide-opening cascades in water, Chem. Soc. Rev. 38 (2009) 3175–3192, https://doi.org/10.1039/b816697h.
[130] G.L. Simpson, T.P. Heffron, E. Merino, T.F. Jamison, Ladder polyether synthesis via epoxide-opening cascades using a disappearing directing group, J. Am. Chem. Soc. 128 (2006) 1056–1057, https://doi.org/10.1021/ja057973p.
[131] K.W. Armbrust, M.G. Beaver, T.F. Jamison, Rhodium-catalyzed endo-selective epoxide-opening cascades: formal synthesis of (-)-brevisin, J. Am. Chem. Soc. 137 (2015) 6941–6946, https://doi.org/10.1021/jacs.5b03570.
[132] L. Zhou, C.K. Tan, J. Zhou, Y.Y. Yeung, Facile, efficient, and catalyst-free electrophilic aminoalkoxylation of olefins: scope and application, J. Am. Chem. Soc. 132 (2010) 10245–10247, https://doi.org/10.1021/ja104168q.
[133] T. Aubineau, J. Cossy, A one-pot reaction toward the diastereoselective synthesis of substituted morpholines, Org. Lett. 20 (2018) 7419–7423, https://doi.org/10.1021/acs.orglett.8b03141.
[134] M. Borah, U. Borthakur, A.K. Saikia, Diastereoselective synthesis of substituted morpholines from N-tethered alkenols: total synthesis of (±)-chelonin A, J. Org. Chem. 82 (2017) 1330–1339, https://doi.org/10.1021/acs.joc.6b02260.
[135] M. Bandini, M. Monari, A. Romaniello, M. Tragni, Gold-catalyzed direct activation of allylic alcohols in the stereoselective synthesis of functionalized 2-vinyl-morpholines, Chem. Eur. J. 16 (2010) 14272–14277, https://doi.org/10.1002/chem.201002606.
[136] J. Cornil, L. Gonnard, C. Bensoussan, A. Serra-Muns, C. Gnamm, C. Commandeur, M. Commandeur, S. Reymond, A. Guérinot, J. Cossy, Iron- and indium-catalyzed reactions toward nitrogen- and oxygen-containing saturated heterocycles, Acc. Chem. Res. 48 (2015) 761–773, https://doi.org/10.1021/ar5004412.
[137] B.M. Trost, D.L. Van Vranken, Asymmetric transition metal-catalyzed allylic alkylations, Chem. Rev. 96 (1996) 395–422, https://doi.org/10.1021/cr9409804.
[138] M. Breuning, M. Winnacker, M. Steiner, Efficient one-pot synthesis of enantiomerically pure 2-(hydroxymethyl)-morpholines, Eur. J. Org. Chem. 2007 (2007) 2100–2106, https://doi.org/10.1002/ejoc.200601006.
[139] K. Samanta, G. Panda, One pot synthesis of amino acid derived chiral disubstituted morpholines and 1,4-oxazepanes via tandem aziridine/epoxide ring opening sequences, Org. Biomol. Chem. 9 (2011) 7365–7371, https://doi.org/10.1039/c1ob05462g.
[140] J.A. Bull, R.A. Croft, O.A. Davis, R. Doran, K.F. Morgan, Oxetanes: recent advances in synthesis, reactivity, and medicinal chemistry, Chem. Rev. 116 (2016) 12150–12233, https://doi.org/10.1021/acs.chemrev.6b00274.

[141] J.A. Burkhard, G. Wuitschik, M. Rogers-Evans, K. Müller, E.M. Carreira, Oxetanes as versatile elements in drug discovery and synthesis, Angew. Chem. Int. Ed. 49 (2010) 9052–9067, https://doi.org/10.1002/anie.200907155.
[142] C.A. Malapit, A.R. Howell, Recent applications of oxetanes in the synthesis of heterocyclic compounds, J. Org. Chem. 80 (2015) 8489–8495, https://doi.org/10.1021/acs.joc.5b01255.
[143] J.T. Njardarson, Catalytic ring expansion adventures, Synlett 24 (2013) 787–803, https://doi.org/10.1055/s-0032-1318326.
[144] Z. Wang, Z. Chen, J. Sun, Catalytic asymmetric nucleophilic openings of 3-substituted oxetanes, Org. Biomol. Chem. 12 (2014) 6028–6032, https://doi.org/10.1039/c4ob00920g.
[145] S.A. Ruider, S. Müller, E.M. Carreira, Ring expansion of 3-oxetanone-derived spirocycles: facile synthesis of saturated nitrogen heterocycles, Angew. Chem. Int. Ed. 52 (2013) 11908–11911, https://doi.org/10.1002/anie.201306563.
[146] P.B. Brady, E.M. Carreira, Addition of trifluoroborates to oxetanyl N,O-acetals: entry into spiro and fused saturated heterocycles, Org. Lett. 17 (2015) 3350–3353, https://doi.org/10.1021/acs.orglett.5b01607.
[147] S.J. Enna, D.B. Bylund, Valdecoxib, XPharm Compr. Pharmacol. Ref. 62 (2011) 2059–2071, https://doi.org/10.1016/B978-008055232-3.63313-6.
[148] J.J. Talley, D.L. Brown, J.S. Carter, M.J. Graneto, C.M. Koboldt, J.L. Masferrer, W. E. Perkins, R.S. Rogers, A.F. Shaffer, Y.Y. Zhang, B.S. Zweifel, K. Seibert, 4-[5-Methyl-3-phenylisoxazol-4-yl]-benzenesulfonamide, valdecoxib: a potent and selective inhibitor of COX-2 [4], J. Med. Chem. 43 (2000) 775–777, https://doi.org/10.1021/jm990577v.
[149] N.A. Nussmeier, A.A. Whelton, M.T. Brown, R.M. Langford, A. Hoeft, J.L. Parlow, S. W. Boyce, K.M. Verburg, Complications of the COX-2 inhibitors parecoxib and valdecoxib after cardiac surgery, N. Engl. J. Med. 352 (2005) 1081–1091, https://doi.org/10.1056/nejmoa050330.
[150] R.P. Baughman, E.E. Lower, Leflunomide for chronic sarcoidosis, Sarcoidosis Vasc. Diffuse Lung Dis. 21 (2004) 43–48.
[151] C. Praveen, A. Kalyanasundaram, P.T. Perumal, Gold(III)-catalyzed synthesis of isoxazoles by cycloisomerization of α,β-acetylenic oximes, Synlett 2010 (2010) 777–781, https://doi.org/10.1055/s-0029-1219342.
[152] Y. Hou, S. Lu, G. Liu, Iodine(III)-mediated [3 + 2] cyclization for one-pot synthesis of benzo[d]isoxazole-4,7-diols in aqueous medium, J. Org. Chem. 78 (2013) 8386–8395, https://doi.org/10.1021/jo401077q.
[153] X. Hou, H. Zhang, B.C. Chen, Z. Guo, A. Singh, A. Goswami, J.L. Gilmore, J. E. Sheppeck, A.J. Dyckman, P.H. Carter, A. Mathur, Regioselective epoxide ring opening for the stereospecific scale-up synthesis of BMS-960, a potent and selective isoxazole-containing S1P 1 receptor agonist, Org. Process. Res. Dev. 21 (2017) 200–207, https://doi.org/10.1021/acs.oprd.6b00366.
[154] Z. Lai, Z. Li, Y. Liu, P. Yang, X. Fang, W. Zhang, B. Liu, H. Chang, H. Xu, Y. Xu, Iron-mediated synthesis of isoxazoles from alkynes: using iron(III) nitrate as a nitration and cyclization reagent, J. Org. Chem. 83 (2018) 145–153, https://doi.org/10.1021/acs.joc.7b02483.
[155] X.W. Zhang, W.L. Hu, S. Chen, X.G. Hu, Cu-catalyzed synthesis of fluoroalkylated Isoxazoles from commercially available amines and alkynes, Org. Lett. 20 (2018) 860–863, https://doi.org/10.1021/acs.orglett.7b04028.
[156] R.G.M. Silva, M.J.V. Da Silva, A.P. Jacomini, S. Moura, D.F. Back, E.A. Basso, F. A. Rosa, Development of methodologies for the regioselective synthesis of four series

of regioisomer isoxazoles from b-enamino diketones†, RSC Adv. 8 (2018) 4773–4778, https://doi.org/10.1039/c7ra13343j.

[157] D. Chenlu, L. Naili, W. Shan, W. Cunde, Cesium-carbonate-mediated benzalation of substituted 2-aryl-3-nitro-2H-chromenes with substituted 4-benzylidene-2-phenyloxazol-5 (4H)-ones, Org. Lett. 21 (2019) 2828–2832, https://doi.org/10.1021/acs.orglett.9b00776.

[158] S. Grecian, V.V. Fokin, Ruthenium-catalyzed cycloaddition of nitrile oxides and alkynes: practical synthesis of isoxazoles, Angew. Chem. Int. Ed. 47 (2008) 8285–8287, https://doi.org/10.1002/anie.200801920.

[159] J.A. Burkhard, B.H. Tchitchanov, E.M. Carreira, Cascade formation of isoxazoles: facile base-mediated rearrangement of substituted oxetanes, Angew. Chem. Int. Ed. 50 (2011) 5379–5382, https://doi.org/10.1002/anie.201100260.

[160] Z. Chen, B. Wang, Z. Wang, G. Zhu, J. Sun, Complex bioactive alkaloid-type polycycles through efficient catalytic asymmetric multicomponent aza-diels-alder reaction of indoles with oxetane as directing group, Angew. Chem. Int. Ed. 52 (2013) 2027–2031, https://doi.org/10.1002/anie.201206481.

[161] S. Baassou, H.M. Mehri, A. Rabaron, M. Plat, (+) Melonine and NB-oxy melonine, a new indoline skeleton, Tetrahedron Lett. 24 (1983) 761–762, https://doi.org/10.1016/S0040-4039(00)81519-1.

[162] R. Jansen, V. Wray, H. Irschik, H. Reichenbach, G. Höfle, Isolation and spectroscopic structure elucidation of sorangicin a, a new type of macrolide-polyether antibiotic from gliding bacteria - XXX, Tetrahedron Lett. 26 (1985) 6031–6034, https://doi.org/10.1016/S0040-4039(00)95117-7.

[163] E.A. Campbell, O. Pavlova, N. Zenkin, F. Leon, H. Irschik, R. Jansen, K. Severinov, S. A. Darst, Structural, functional, and genetic analysis of sorangicin inhibition of bacterial RNA polymerase, EMBO J. 24 (2005) 674–682, https://doi.org/10.1038/sj.emboj.7600499.

[164] G.R. Pettit, J.P. Xu, J.C. Chapuis, R.K. Pettit, L.P. Tackett, D.L. Doubek, J.N.A. Hooper, J.M. Schmidt, Antineoplastic Agents. 520. Isolation and structure of irciniastatins A and B from the Indo-Pacific marine sponge *Ircinia ramosa*, J. Med. Chem. 47 (2004) 1149–1152, https://doi.org/10.1021/jm030207d.

[165] K. Kito, R. Ookura, S. Yoshida, M. Namikoshi, T. Ooi, T. Kusumi, New cytotoxic 14-membered macrolides from marine-derived fungus *Aspergillus ostianus*, Org. Lett. 10 (2008) 225–228, https://doi.org/10.1021/ol702598q.

[166] J. Yin, K. Kouda, Y. Tezuka, Q. Le Tran, T. Miyahara, Y. Chen, S. Kadota, New diarylheptanoids from the rhizomes of *Dioscorea spongiosa* and their antiosteoporotic activity, Planta Med. 70 (2004) 54–58, https://doi.org/10.1055/s-2004-815456.

[167] C.F. Nising, S. Bräse, Recent developments in the field of oxa-Michael reactions, Chem. Soc. Rev. 41 (2012) 988–999, https://doi.org/10.1039/c1cs15167c.

[168] P.A. Clarke, P.B. Sellars, N.M. Nasir, A Maitland-Japp inspired synthesis of dihydropyran-4-ones and their stereoselective conversion to functionalised tetrahydropyran-4-ones, Org. Biomol. Chem. 13 (2015) 4743–4750, https://doi.org/10.1039/c5ob00292c.

[169] R.J. Beattie, T.W. Hornsby, G. Craig, M.C. Galan, C.L. Willis, Stereoselective synthesis of protected l- and d-dideoxysugars and analogues via Prins cyclisations, Chem. Sci. 7 (2016) 2743–2747, https://doi.org/10.1039/c5sc04144a.

[170] C. Olier, M. Kaafarani, S. Gastaldi, M.P. Bertrand, Synthesis of tetrahydropyrans and related heterocycles via prins cyclization; extension to aza-prins cyclization, Tetrahedron 66 (2010) 413–445, https://doi.org/10.1016/j.tet.2009.10.069.

[171] K. Gademann, D.E. Chavez, E.N. Jacobsen, Highly enantioselective inverse-electron-demand hetero-Diels-Alder reactions of α,β-unsaturated aldehydes, Angew. Chem. Int. Ed. 41 (2002) 3059–3061, https://doi.org/10.1002/1521-3773(20020816)41:16<3059::AID-ANIE3059>3.0.CO;2-I.

[172] B. Guo, G. Schwarzwalder, J.T. Njardarson, Catalytic ring expansion of vinyl oxetanes: asymmetric synthesis of dihydropyrans using chiral counterion catalysis, Angew. Chem. Int. Ed. 51 (2012) 5675–5678, https://doi.org/10.1002/anie.201201367.
[173] G. Fumagalli, S. Stanton, J.F. Bower, Recent methodologies that exploit C-C single-bond cleavage of strained ring systems by transition metal complexes, Chem. Rev. 117 (2017) 9404–9432, https://doi.org/10.1021/acs.chemrev.6b00599.
[174] P. Tang, Y. Qin, Recent applications of cyclopropane-based strategies to natural product synthesis, Synthesis (Stuttg.) 44 (2012) 2969–2984, https://doi.org/10.1055/s-0032-1317011.
[175] C.A. Carson, M.A. Kerr, Heterocycles from cyclopropanes: applications in natural product synthesis, Chem. Soc. Rev. 38 (2009) 3051–3060, https://doi.org/10.1039/b901245c.
[176] H.-U. Reissig, R. Zimmer, Donor – acceptor-substituted cyclopropane derivatives and their application in organic synthesis †, Chem. Rev. 103 (2003) 1151–1196, https://doi.org/10.1021/cr010016n.
[177] M.A. Cavitt, L.H. Phun, S. France, Intramolecular donor-acceptor cyclopropane ring-opening cyclizations, Chem. Soc. Rev. 43 (2014) 804–818, https://doi.org/10.1039/c3cs60238a.
[178] T.P. Lebold, A.B. Leduc, M.A. Kerr, Zn(II)-catalyzed synthesis of piperidines from propargyl amines and cyclopropanes, Org. Lett. 11 (2009) 3770–3772, https://doi.org/10.1021/ol901435k.
[179] M.E. Scott, W. Han, M. Lautens, A highly diastereoselective Mgl2-mediated ring expansion of methylenecyclopropanes, Org. Lett. 6 (2004) 3309–3312, https://doi.org/10.1021/ol048769u.
[180] C.A. Carson, M.A. Kerr, Diastereoselective synthesis of pyrrolidines via the Yb(OTf)3 catalyzed three-component reaction of aldehydes, amines, and 1,1-cyclopropanediesters, J. Org. Chem. 70 (2005) 8242–8244, https://doi.org/10.1021/jo0512251.
[181] S.K. Jackson, A. Karadeolian, A.B. Driega, M.A. Kerr, Stereodivergent methodology for the synthesis of complex pyrrolidines, J. Am. Chem. Soc. 130 (2008) 4196–4201, https://doi.org/10.1021/ja710289k.
[182] Y.B. Kang, Y. Tang, X.L. Sun, Scandium triflate catalyzed cycloaddition of imines with 1,1-cyclopropanediesters: efficient and diastereoselective synthesis of multisubstituted pyrrolidines, Org. Biomol. Chem. 4 (2006) 299–301, https://doi.org/10.1039/b512195g.
[183] Y.S. Lin, J.H. Lin, C.C. Chang, S.S. Lee, Tetrahydropyran- and tetrahydrofuran-containing diarylheptanoids from *Hedychium coronarium* rhizomes, J. Nat. Prod. 78 (2015) 181–187, https://doi.org/10.1021/np500441r.
[184] K.L. Jackson, J.A. Henderson, A.J. Phillips, The halichondrins and E7389, Chem. Rev. 109 (2009) 3044–3079, https://doi.org/10.1021/cr900016w.
[185] H. Ledford, Complex synthesis yields breast-cancer therapy, Nature 468 (2010) 608–609, https://doi.org/10.1038/468608a.
[186] A. Lorente, J. Lamariano-Merketegi, F. Albericio, M. Álvarez, Tetrahydrofuran-containing macrolides: a fascinating gift from the deep sea, Chem. Rev. 113 (2013) 4567–4610, https://doi.org/10.1021/cr3004778.
[187] P.D. Pohlhaus, J.S. Johnson, Enantiospecific Sn(II)- and Sn(IV)-catalyzed cycloadditions of aldehydes and donor-acceptor cyclopropanes, J. Am. Chem. Soc. 127 (2005) 16014–16015, https://doi.org/10.1021/ja055777c.
[188] A.G. Smith, M.C. Slade, J.S. Johnson, Cyclopropane-aldehyde annulations at quaternary donor sites: stereoselective access to highly substituted tetrahydrofurans, Org. Lett. 13 (2011) 1996–1999, https://doi.org/10.1021/ol200395e.

Organocatalytic cycloaddition reaction: A gateway for molecular complexity

11

Ram Naresh Yadav[a], *Gildardo Rivera*[b], *Ashok Kumar Srivastava*[a], *Bimal Krishna Banik*[c,*]

[a]Department of Chemistry, Faculty of Engineering & Technology, Veer Bahadur Singh Purvanchal University, Jaunpur, India, [b]Laboratory of Pharmaceutical Biotechnology, Center for Genomic Biotechnology, National Polytechnic Institute, Reynosa, Mexico, [c]Department of Mathematics and Natural Sciences, College of Sciences and Human Studies, Deanship of Research Development, Prince Mohammad Bin Fahd University, Al Khobar, Kingdom of Saudi Arabia

[*]Corresponding author. e-mail address: bimalbanik10@gmail.com; bbanik@pmu.edu.sa

11.1 Introduction

In chemistry, a catalyst is any substance that can be added to a reaction to accelerate the reaction without getting consumed in the process. Catalyst typically speedup the reaction by lowering the activation energy or alter the mechanistic pathways of the reaction and achieving the goal under milder reaction condition. Based on their chemical composition, catalyst may be homogeneous or heterogenous in nature [1–3]. Transition metal and organometallic catalysis emerge as a powerful tool for organic synthesis for many years [4–8]. However, the use of biocatalysts for organic transformations also plays a key role in this area [9–14]. In contrast, the use of metal-based catalysts imposes a great environmental concern mostly owing to their toxicity and waste created by this process [15].

In this context, identifying a greener catalytic system for sustainable development of the reaction system in synthesis is worth for the scientists. Toward this goal, organocatalysis plays a pivotal role in the design and synthesis of a vast number of challenging molecules of diverse interests in an efficient manner. In past few decades, organocatalysis has become a promising tool in the development of challenging asymmetric synthesis. The most challenging areas include asymmetric biomimetic synthesis [16], Mannich reaction [17], Michael reaction [18], Cascade reaction [19], Friedel-Crafts reaction [20–23], glycosylation reaction in carbohydrates [24, 25], aldol reaction [26], Morita-Baylis-Hillman reaction [27, 28], Streker reaction [29], and flurocyclization [30]. The focal point of this chapter is to consider cycloaddition reaction catalyzed by using small organic molecules. Cycloaddition reactions are fascinating tool for chemists to creating high level of molecular complexity and stereoselectivity in concerted pathways under thermal and photochemical conditions [31, 32].

Green Approaches in Medicinal Chemistry for Sustainable Drug Design. https://doi.org/10.1016/B978-0-12-817592-7.00011-3
© 2020 Elsevier Inc. All rights reserved.

11.2 [4 + 2] Cycloaddition reaction

The Diels-Alder reaction is incredibly a valuable classical reaction that offers an elegant method for the synthesis of six-membered cyclic compounds in high regio- and stereoselective manner. This method basically involves the reaction of a diene (4-π electron) and a dienophile (2-π electron) under thermal condition. The main driving force of this reaction is the formation of new σ bond which is energetically more stable than the π bonds. In general, this reaction follows molecular orbital rule developed by Woodward and Hoffmann rules for pericyclic reactions. An overlap of the highest occupied molecular orbital (HOMO) of the diene and lowest occupied molecular orbital (LUMO) of the dienophile takes place in this process. The reaction is accelerated by the electronically rich dienes and deficient dienophiles.

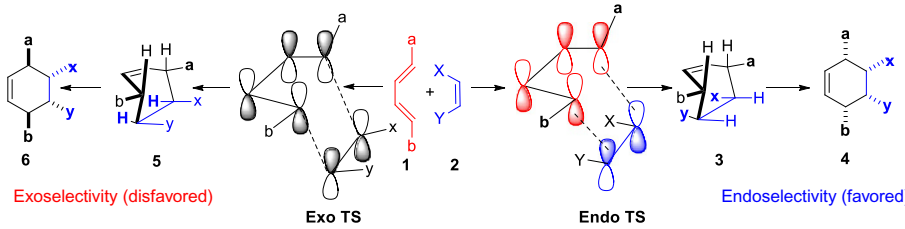

Scheme 11.1 Regioselectivity in Diels-Alder reaction.

The regioselectivity is greatly controlled by the relative size of the orbital coefficient of the HOMO and LUMO involved in the reaction [33].

As shown in Scheme 11.1, endo transition is sterically highly congested and thermodynamically less favored but the endo adduct is the predominant product due to the secondary orbital overlap of diene HOMO.

With its diverse synthetic application and simple operation, the Diels-Alder reaction has become the most powerful synthetic method for the synthesis of unsaturated six-membered rings. This reaction has been exploited extensively by the scientific community. It is a highly atom economical method and generally does not require any catalysts under thermal conditions. However, sometimes it may require a high temperature for completing the reaction. Over a few decades an extensive study has been made in this area and lots of modifications have been made to perform this reaction at ambient temperature with excellent stereoselectivity. In this context, Lewis acid-catalyzed [34, 35], chiral auxiliary-controlled [36–38], and catalytic asymmetric Diels-Alder reaction [39–41] are the major achievements. This methodology has also been further exploited toward the total synthesis of bioactive complex natural products [42–49].

Despite several spectacular extensive studies, challenging efforts have been applied in the seminal areas for utilizing small organic molecules as catalyst in Diel-Alder reaction. This catalyst has received an incredible attention by the scientific community due to its widespread availability in enantiomeric pure forms. Some of the excellent methods are described here.

11.3 [4 + 2] Cycloaddition via iminium ion activation

In 2000, MacMillan and his coworkers developed an elegant strategy based on organocatalytic enantioselective Diels-Alder reaction. The authors hypothesized a reversible condensation of aldehydic function with chiral amines to produce iminium ion which lowers the LUMO energy of the dienophile and facilitates the reaction. Keeping this hypothesis in mind a reaction of diverse α,β-unsaturated aldehyde with cyclic diene in the presence of 10 mol% of chiral amines were performed in high yield (up to 99%) and good to excellent *endo:exo* selectivity (2.7:1–1.3:1) at ambient temperature using methanol and water as the solvent (Scheme 11.2) [50].

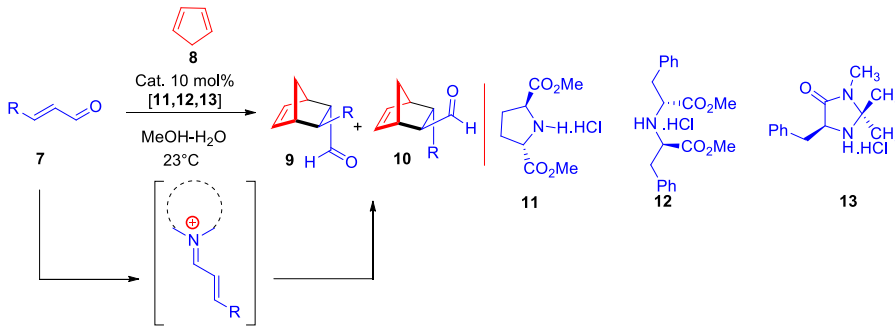

Scheme 11.2 Enantioselective organocatalyzed Diels-Alder reaction in MeOH/H_2O.

This methodology was further exploited with a series of chiral secondary amine hydrochloric acid salt (**11 – 13**). This catalytic system lowered the LUMO energy with catalytic amount of chiral amines (S-proline methyl ester (**11**) and S-arbine methyl ester) and produced cycloadduct in excellent yield. The use of sterically constrained imine (**13**) demonstrated the greatest enantioselectivity (>99% ee) and proved the optimal catalyst for further exploration of this methodology.

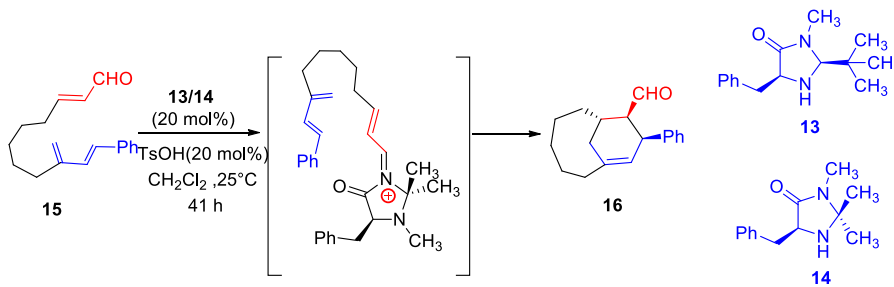

Scheme 11.3 IMDA approach for central core of Solanapyrone D.

This group extended the methodology for the total synthesis of marine metabolite Solanapyrone D through intramolecular Diels-Alder reaction (IMDA) through

iminium ion activation of α,β-unsaturated aldehyde as dienophiles as a key reaction (Scheme 11.3) [51]. For these transformations the catalyst **13**/**14** worked equally well, affording bicycloadduct in excellent yield and demonstrated excellent enatio- and diastereoselectivity as well.

In this context a long-standing challenge associated with [4 + 2] cycloaddition reaction, the MacMillan group in 2001 demonstrated a remarkable study on catalytic enantioselective Diels-Alder reaction of a series of simple α,β-unsaturated enones (cyclic/acyclic) with cyclic/acyclic diene via imidazolidinone-derived iminium ion as an activator.

A computational model was established to explain the asymmetric induction in cycloadduct through the formation of isomeric *cis* and *trans* iminium ion reactive intermediate (**17a**/**17b**) which could eventually form during the course of reaction. The delineated model showed that when R group in dienophile is methyl or bulky group, Re face of the dienophiles is blocked and therefore, not accessible for the diene. The suitable formation of the transition state allowed when the R group is hydrogen. *trans*-Iminium intermediates were energetically disfavored and authors envisioned that it is due to a nonbonding interaction between the R group and benzyl group of the catalyst. Importantly the reaction went through the si-face of the iminium *cis*-isomer which are accessible for diene in the transition state affording the cycloadduct in excellent enantiomeric selectivity (Scheme 11.4) [41].

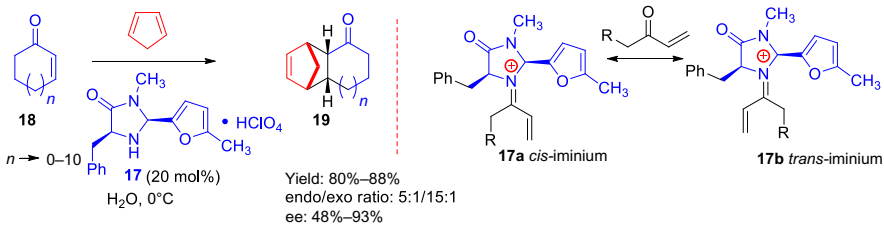

Scheme 11.4 Organocatalytic enantioselective Diel-Alder reaction of α,β-unsaturated enones.

11.4 [4 + 2] Cycloaddition via enamine activation

HOMO activation, inverse electron demand strategy of Diels-Alder reaction of dienophiles through dienamines formation from the reaction between amine and unsaturated carbonyl compounds are well documented in Diels and hetero-Diels-Alder reaction [52, 53]. In this context a pioneer work was reported by Meyers and Jorgenson et al. [54–56] independently in the stereoselective synthesis of tetrahydropyranone with contiguous stereocenters based on inverse electron demand silica gel-assisted hetero Diels-Alder protocol in good to excellent yield. In this reaction the proline-based catalyst (**21**) initially reacted with the aldehyde (**20**) generating the reactive enamine as an intermediate which serves as dienophile and approaches electron-deficient 4π electron system of α,β-unsaturated esters which acts as a hetero diene. The main driving force for this reaction was due to a lowering of the energy of the HOMO of dienophiles.

This methodology was further extended for the synthesis of densely functionalized core structures of tetrahydroquinoxaline, piperidines, and cyclohexanes of diverse interests. (Scheme 11.5) [57–59].

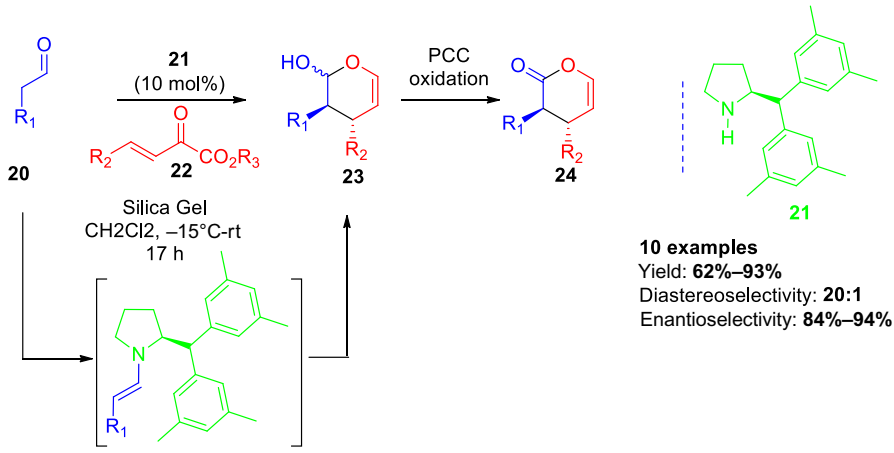

Scheme 11.5 Enamine mediated inverse electron demand Hetero Diels-Alder reaction.

In 2008, a pioneer study was carried out by Christmann and his coworker for the synthesis of cyclic system mediated through dienamine activation of α,β-unsaturated aldehydes using Jørgensen-Hayashicatalyst (**25**). This protocol was possible because of an intramolecular [4 + 2] cycloaddition reaction of in situ generated dienamine intermediates. In this catalysis combination, benzoic acid was required as an additive. This author achieved good to excellent yield of bicycloadduct with high *enantio*selectivity (Scheme 11.6) [60].

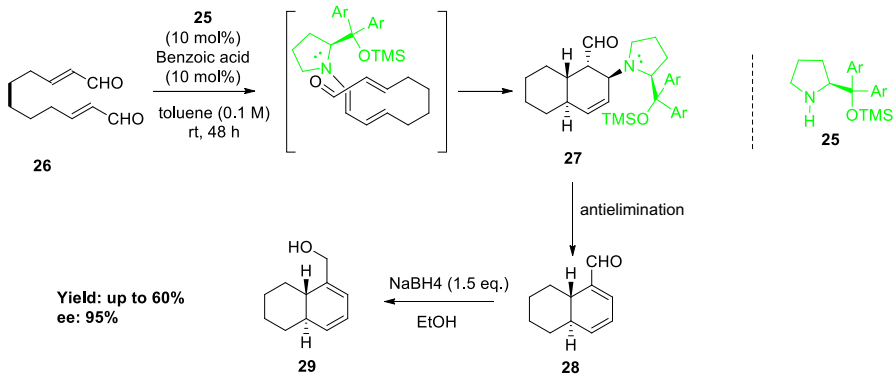

Scheme 11.6 Intramolecular [4 + 2] cycloaddition reaction via dienamine activation.

This work was undertaken by Gil Santo and his group to perform a computational study of density functional theory (DFT) calculation to establish the enantio and diastereoselectivity of the product formation. This study also explored to identify the role of the additive for this reaction [61]. It was interesting to note that benzoic acid is required for the dienamine formation and help in the elimination process toward the formation of the conjugated system.

In 2013, Yang and his coworkers proposed the synthesis of dihydrodibenzofurans scaffold through dienamine-mediated intramolecular [4 + 2] cycloaddition reaction using sterically hindered organocatalyst (**30**) with moderate enantioselectivity. The low enantioselectivity was due to highly strained *Z*-dienamine intermediate (Scheme 11.7) [62]. Dihydrodibenzofurans are an important scaffold found in many naturally occurring molecules.

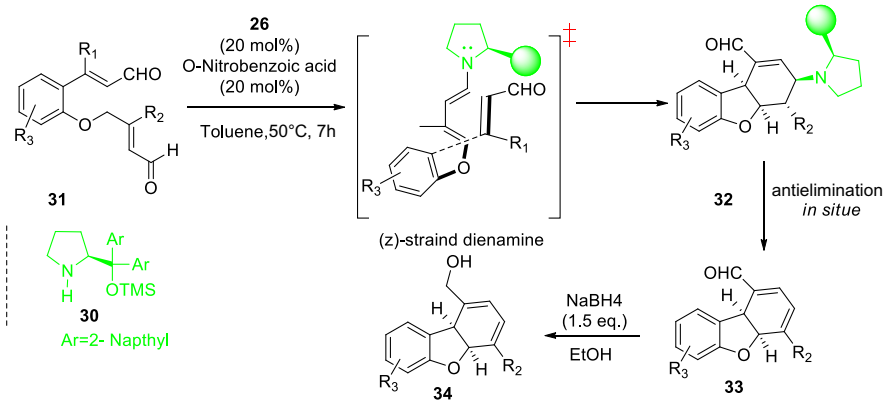

Scheme 11.7 Intramolecular [**4 + 2**] cycloaddition reaction via dienamine activation in the synthesis of dihydrobenzofuran.

This strategy worked with a wide range of substrates and provided a facile route for the synthesis of *cis*-diastereoisomers of dihydrodibenzofurans in high yield with excellent enantioselectivity. Based on the enantioselectivity, authors proposed concerted *exo*-transition state for product formation.

In 2009, Xu and his coworkers [63] demonstrated efficient organocatalytic enantioselective Diels-Alder protocol for cyclic enones with aromatic nitro olefins via enamine activation in the synthesis of densely functionalized bicyclic scaffolds under aqueous solution of salt. It was known that Diels-Alder reaction under aqueous medium may proceed with acceleration in reaction rate and produced products with selectivity. Initially, the reaction of cyclohexanone and β-nitrostyrene was carried out in tetrahydrofuran (THF) as solvent using amine as catalyst at room temperature. The very low conversion with poor enantioselectivity was recorded. On the other hand, this reaction in aqueous medium had a dramatic acceleration in conversion rate with good enantioselectivity in comparison to the THF medium. The Diels-Alder reaction was further improved by using water and saturated brine solution or seawater as the solvent for this study. The author achieved the best results when the reaction was carried out in fresh seawater. This investigation suggested that the salt has important role in the

reaction profile. The concentration of aqueous salt solution deeply affected the course of reaction in terms of the conversion rate, high diastereo- and enantioselectivity. For example, 100% conversion rate and excellent diastereoselectivity were achieved with 7.5% of aqueous brine solution.

A variety of organocatalyst was tested for this reaction in combination with additives. It was found that the combination of p-(trifluromethyl)-benzoic acid **39** and hydroxyl methyl proline-derived catalyst **38** is the ideal asymmetric catalytic system for investigating this Diels-Alder reaction in the aqueous salt solution. In general, it took 12–20 h for complete conversion with 94%–96% enantioselectivity.

A diverse cyclohexan-2-enones and substituted β-styrene were treated with 7.5% aqueous NaCl solution in the presence of catalyst **38** (20 mol%) and acid additive **39** (20 mol%) at room temperature (Scheme 11.8). A smooth reaction was observed. Interestingly, the substitution pattern of the aromatic ring in nitro-olefins **36** had no detrimental effect on diastereo- and enantioselectivity of the reaction. However, it appeared the *p*-substituted aryl ring formed in greater yield comparatively **37a**→**c**

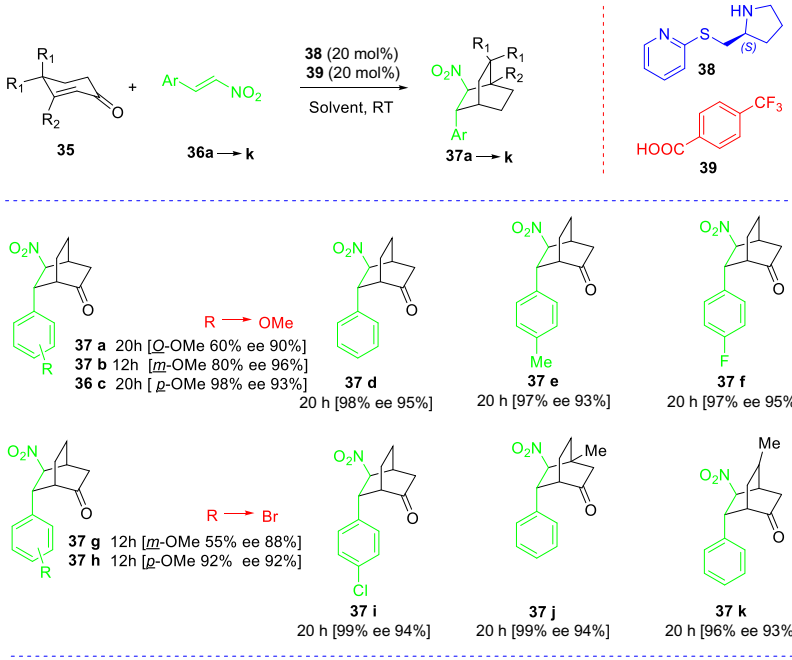

Scheme 11.8 Enamine mediated organocatalyzed [4 + 2] cycloaddition reaction in the synthesis of substituted bicyclo-[2,2,2]-cyclooctane derivatives. (All reaction(s) was carried out either in seawater or 7.5% of sodium chloride solution (1.0 mL) using 20 mol% of catalyst **38** and acid additive **39**, cyclohe-2-enone **35** (1.0 mmol) and nitro-olefine **36** (0.75) at room temperature with consistent stirring.)

(*o*, *m,* and *p*). The stereochemical assignment of the cycloadduct was established on the basis of single-crystal X-ray data.

The scope of the present methodology was extended to diversely substituted nitro-olefins. It was worthy to note that heterocyclic nitro-olefins react smoothly under the

delineated condition to give desired bicyclic compounds with excellent enantioselectivities and good yield (96%, 92%–94% ee).

Furthermore, the 3- and 4-substituted cyclohexanones surprisingly underwent facile Diels-Alder reaction to give corresponding cycloadducts 37j→k with excellent yield and high level of enantioselectivity. The diverse functional groups present in diene and dienophile were well tolerated under this condition.

It was important to note that the seawater and the brine solution both give excellent results with a high level of enantioselectivity.

The author, proposed a mechanistic pathway for this Diels-Alder reaction. At the beginning the catalyst **38** was condensed with cyclohexanone **35** that leads the equivalent chiral enamine intermediate analogsof diene **A** which then forms a complex **B**

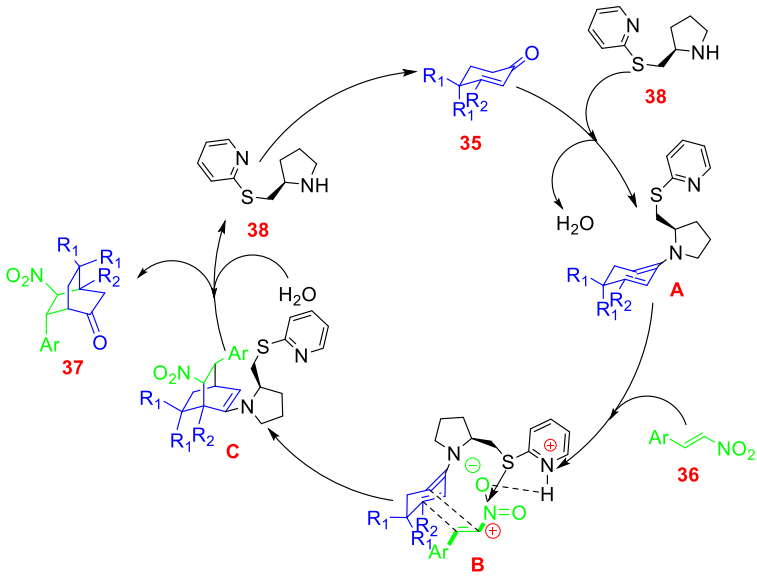

Fig. 11.1 Catalytic cycle and T.S for enamine-mediated cycloaddition reaction.

with nitro-olefins **36**. A [4 + 2] cycloaddition took place between the activated nitro-olefins and diene-enamines through the complex transition state **B** which was further transformed to the other enamine intermediate **C**. The intermediate **C** was eventually hydrolyzed to equivalent cycloadduct **37a→k** and finally released the active catalyst which further sustained the catalytic cycle (Fig. 11.1). It was worthy to note that the existence of reactive intermediates **A** and **C** was established through conducting electrospray ionization-mass spectrometry (ESI-MS) experiment. The peak corresponding 273.1 for A and 422.2 for C supported the proposed catalytic cycle. It was also evident that the salt solution plays a crucial role in stabilizing the transition state **B** via formation of hydrogen bond with acid additive. In this study, the authors concluded that no Michael adduct was formed during this investigation, rather the reaction proceeded through the concerted cycloaddition pathways.

Chen and his coworkers [64] described a versatile asymmetric synthetic [4 + 2] cycloaddition strategy in the synthesis of bicyclic scaffold via amine-catalyzed

regioselective cycloaddition of α,β-unsaturated cyclic enones. In this study, the authors expanded the application of dienamine derived from cyclic enones as the diene equivalent, with extended conjugated malononitrile as dienophiles in a regioselective [4 + 2] cycloaddition reaction. This reaction was catalyzed through hydrogen bond-assisted chiral primary amine as organocatalyst.

In this study, the authors screened a variety of organocatalysts derived from naturally occurring cinchona alkaloids and noticed successful reaction with excellent selectivity. However, the catalyst 46 and 47 (20 mol%) in the presence of salicylic acid 45 (40 mol%) as additive was found to be an ideal catalytic system for this reaction in all respects to its enantioselectivity and diastereoselectivity.

Under this optimized condition a wide range of cyclohexanone 40 and conjugated malononitriles 41a → d and 43a → d in the presence of catalyst 46/47 and acid additive 45 were allowed to react at elevated temperature using toluene as solvent.

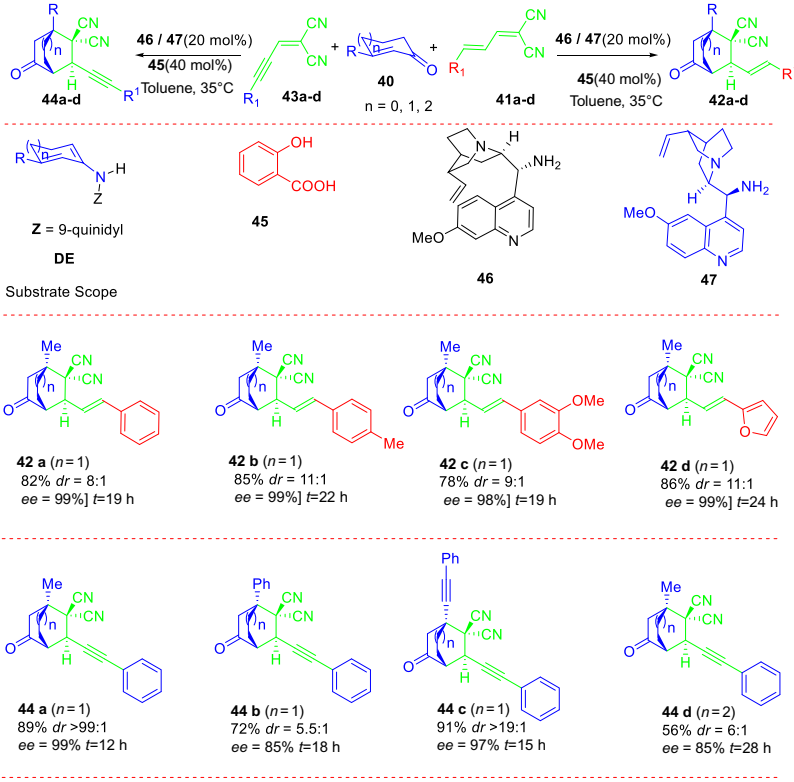

Scheme 11.9 Highly *endo*-selective [4 + 2] cycloaddition reaction of cyclic enone with allylidenemalononitriles and alkynylidenemalononitriles via dienamine activation.

It was worthy to note that a diversely substituted dienophiles with electron withdrawing or electron donating groups are well tolerated to proceed smoothly and gives corresponding cycloadducts **42a → d** and **44a → d** in good to excellent diastereo- and enantioselectivity along with excellent yield (Scheme 11.9). The heterocyclic-derived

conjugated malononitrile gave comparable results **42d** (Scheme 11.9). This protocol worked well in the synthesis of a wide range of densely functionalized bicyclo [2.2.2]-octanes.

The mechanistic insights were also investigated. Usually an amine-catalyzed reaction of this type proceeded through the initial formation of 2-amino-1,3-butadiene in situ followed by the concerted [4 + 2] cycloaddition reaction. Herein, the author proposed a stepwise mechanism for dienamine amino catalysis for [4 + 2] reaction involving double Michael addition pathway that has direct experimental evidences [65]. An excellent stereodivergent product formation was achieved due to hydrogen-bond interaction with the substrate.

Trienamine catalysis served as a powerful tool in the synthesis of architecturally complex bioactive molecules which was first documented by the Jørgensen and his group in asymmetric organocatalyzed [4 + 2] cycloaddition reaction [66].

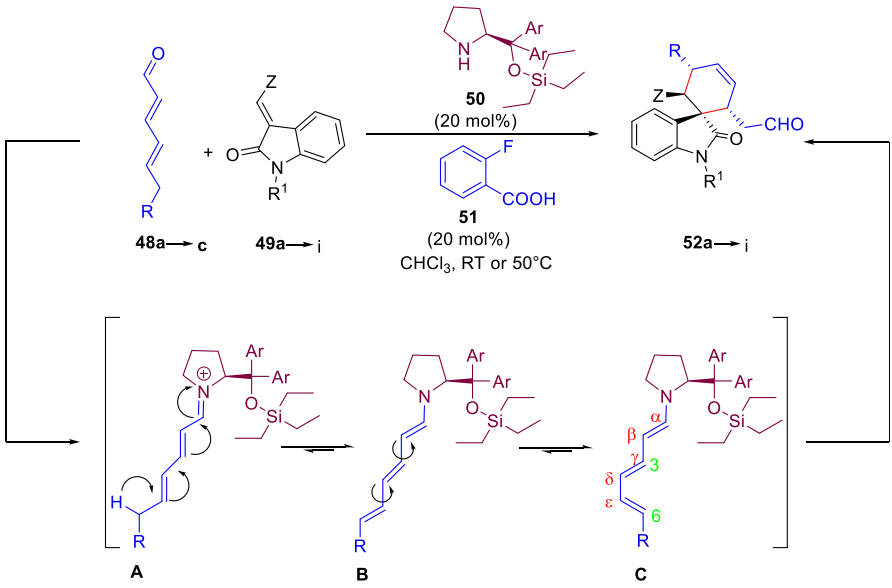

Scheme 11.10 Trienamine mediated activation of [4 + 2] cycloaddition reaction of 3-olefinic.

11.5 Ox-indoles in the synthesis of spirocyclic indoles

Chen and Jorgensen and his coworkers [66] explored the elegant methodology for the synthesis of complex spirocyclic indoles via asymmetric organocatalytic [4 + 2] cycloaddition reaction through the formation of trienamine catalytic activation. In support of this strategy, the authors performed DFT-calculation. The promising results encouraged to perform the reaction of 3-olefinicoxindoles 49a→I as dienophiles and 2,4-hexadienal 48a→c as diene in the presence of diphenylprolinolsilylether 50 and *O*-flurobenzoic acid. The reaction worked very well in the presence of chlorinated

Table 11.1 Substrate scope of [4 + 2] cycloaddition reaction of 3-olefinic-oxindoles.

Entry	48	49	52	Yield[a] [%]	dr [%]	ee[b] [%]
1	**48a** R → H	**49a** R^1 → Boc Z → CO_2Et	**52a**	92	Single	98
2	**48b** R → H	**49b** R^1 → Me Z → COMe	**52b**	99	Single	97
3	**48c** R → H	**49c** R^1 → Boc Z → COPh	**52c**	97	Single	98
4	**48d** R → H	**49d** R^1 → Boc Z → CN	**52d**	90	93:7	98
5	**48e** R → H	**49e** R^1 → Boc Z → Ph	**52e**	67	92:8	97
6	**48f** R → H	**49f** R^1 → Boc Z → *p*-Me.C_6H_4	**52f**	58	92:8	98
7	**48g** R → H	**49g** R^1 → Boc Z → *p*-Cl.C_6H_4	**52g**	82	88:12	99
8	**48h** R → Me	**49g** R^1 → Boc Z → COPh	**52h**	94	79:21	94
9	**48i** R → n-C_4H_9	**49i** R^1 → Boc Z → COPh	**52i**	90	91:9	96

[a]Isolated yield.
[b]Determined by chiral-phase HPLC analysis.

solvent (i.e., chloroform) at room temperature to 50°C to afford the spirocyclicoxindoles 52a → i in good yield along with excellent enantioselectivity. The proposed methodology worked with a wide range of substrates with excellent yield (Scheme 11.10, Table 11.1).

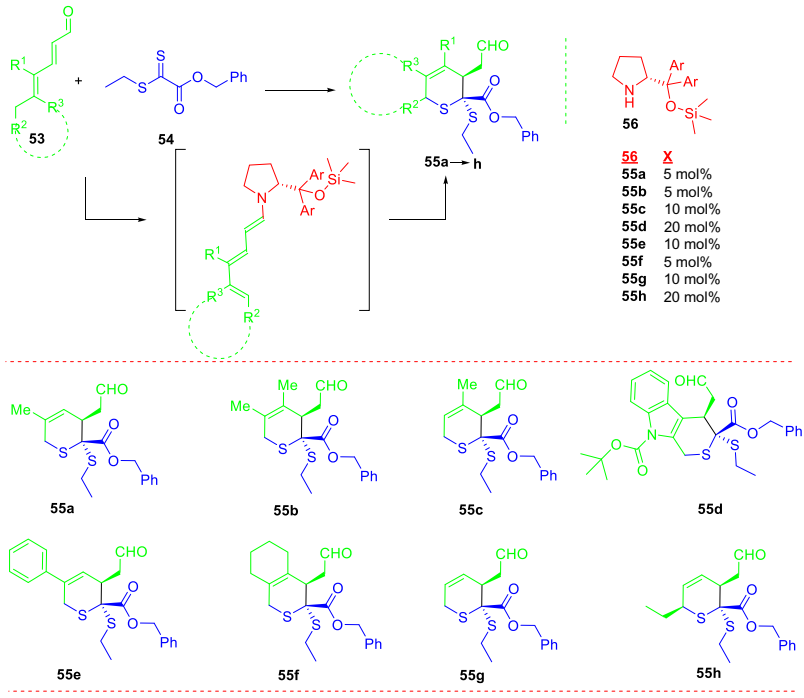

Scheme 11.11 Trienamine mediated [4 + 2] thio-cycloaddition reaction in the synthesis of thio-cyclohexene derivatives.

This group also reported the thio-Diels-Alder reaction via trienamine activation [67]. This method offered the synthesis of sulfur-based enantioenriched heterocycles and their transformation to the advanced medicinally privileged molecules. It was worthy to note that the thio-dienophiles have different reactivity pattern than the conventional dienophiles used in the Diels-Alder reaction. The character of sulfur dienophiles was different since it has high reactivity and poor coordinating ability to the chiral catalyst. This challenge was met by employing different catalytic systems in the synthesis of chiral thio-dihydropyrans using [4 + 2] cycloaddition with remarkable stereoselectivity.

To validate the synthetic design, the author had chosen the diversely substituted dienal 53 as diene and thiocarbonyl **54** as a diene in the presence of 5–20 mol% of catalyst 56 and benzoic acid in the presence of halogenated solvent. Under this condition a smooth and facile reaction to diverse substituted thio-dihydropyrone 55a→h was achieved successfully (Scheme 11.11).

This synthetic methodology was tested with a wide range of aldehydes as diene precursor in the development of organocatalyzed trienamine mode activation in the synthesis of sulfur heterocycles (Table 11.2). This method offered the synthetic useful

Table 11.2 Substrate scope for amino-catalytic thio-[4 + 2]cycloaddition reaction.

Entry	55		T [°C]	Time [h]	Yield[a] [%]	dr [%]	ee[b] [%]
1	**55a**	$R^1 \rightarrow H$ $R^2 \rightarrow H$ $R^3 \rightarrow Me$	4.0	72	87	94:6	92
2	**55b**	$R^1 \rightarrow Me$ $R^2 \rightarrow H$ $R^3 \rightarrow Me$	rt	48	95	91:1	93
3	**55c**	$R^1 \rightarrow Me$ $R^2 \rightarrow H$ $R^3 \rightarrow H$	rt	48	82	90:10	93
4	**55d**	R^1 $R^3 \rightarrow$ Indoyl $R^2 \rightarrow H$	40	48	84	80:20	92
5	**55e**	$R^1 \rightarrow H$ $R^2 \rightarrow H$ $R^3 \rightarrow Ph$	rt	48	78	>95:5	85
6	**55f**	R^1 $R^3 \rightarrow$ Cyclohexyl $R^2 \rightarrow H$	40	48	84	86:14	90
7	**55e**	$R^1 \rightarrow H$ $R^2 \rightarrow H$ $R^3 \rightarrow H$	40	48	82	90:10	91
8	**55h**	$R^1 \rightarrow H$ $R^2 \rightarrow$ Ethyl $R^3 \rightarrow H$	40	48	62	85:8:7	85

[a]Isolated yields.
[b]Determined by chiral-phase HPLC analysis.

precursor of diverse interests. To explore the mechanistic pathway, DFT calculation was performed. It was envisioned that reaction adopts the stepwise mechanism via the formation of zwitterionic intermediates.

Chen et al. reported the aza-Diels-Alder reaction of 2-aryl-3H-indol-3-ones and 2,4-dienals via trienamine catalysis and proline-based chiral catalyst [68].

To validate the design of synthetic protocol, this group selected densely substituted 2-phenyl-3H-indol-3-one 58 and 2,4-dienal 57 in the presence of catalyst 61 and benzoic acid 62 in xylene at 10°C to afford the cycloadduct 60 after $NaBH(OAc)_3$ with excellent diastereoselectivity (*exo*/*endo* > 19:1) (Scheme 11.12).

It was found that the enantioselectivity was further reduced under THF and acetonitrile solvent system. The similar observation was made under halogenated solvents. Xylene gave excellent enantioselectivity. For this study a variety of acid activators was screened. The better result was obtained using salicylic acid.

Under the optimized reaction conditions, a wide range of tricyclic indanes 60a→j was synthesized using 20 mol% of amine catalyst 61 and 20 mol% of OHBA 62 (*O*-hydroxybenzoic acid) followed by the reduction of cycloadduct with $NaBH(OAc)_3$ to the corresponding alcohols. The results were summarized in Table 11.3. The reaction proceeded through the formation of trienamine intermediate A.

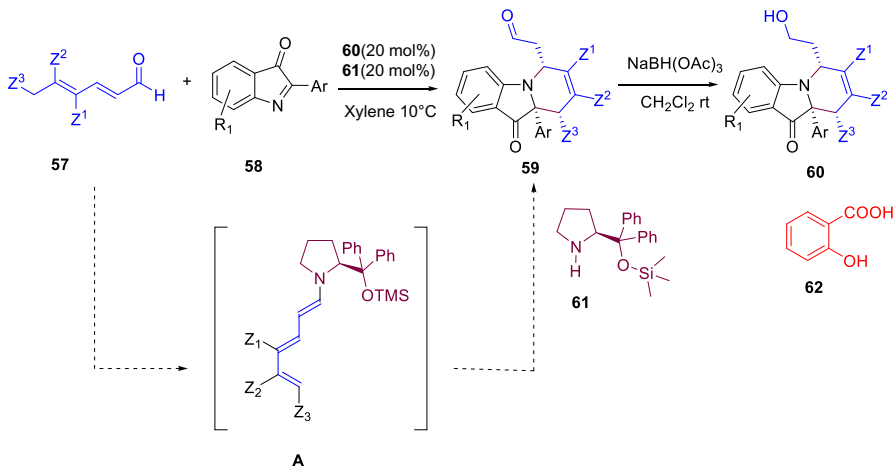

Scheme 11.12 Trienamine mediated [4 + 2]-azacycloaddition reaction in the synthesis of tricylces.

The presence of either electron withdrawing groups or electron donating groups in phenyl ring of dienophiles had no effects on the reaction course and the reaction proceeded smoothly with a high degree of enantioselectivity regardless of the groups present in the systems. This method offered a synthetically useful tricyclic polyhydropyrido[1,2-*a*]indole scaffolds having quaternary center with high degree of molecular complexity.

Table 11.3 Substrate scope of trienamine catalyzed [4 + 2]-*aza*-Diels-Alder reaction.

Entry	60 [a→j]		Time [h]	Yield[a] [%]	ee[b] [%]
1	**60a**	$R^1 \rightarrow H$ $Z^1 \rightarrow Ph$ $Z^2 \rightarrow H$ $Z^3 \rightarrow H$ $Ar \rightarrow Ph$	12	95	91
2	**60b**	$R^1 \rightarrow 4\text{-Me}$ $Z^1 \rightarrow Ph$ $Z^2 \rightarrow H$ $Z^3 \rightarrow H$ $Ar \rightarrow Ph$	12	77	83
3	**60c**	$R^1 \rightarrow 5\text{-OMe}$ $Z^1 \rightarrow Ph$ $Z^2 \rightarrow H$ $Z^3 \rightarrow H$ $Ar \rightarrow Ph$	4	97	90
4	**60d**	$R^1 \rightarrow 5\text{-Cl}$ $Z^1 \rightarrow Ph$ $Z^2 \rightarrow H$ $Z^3 \rightarrow H$ $Ar \rightarrow Ph$	8	74	85
5	**60e**	$R^1 \rightarrow 6\text{-Cl}$ $Z^1 \rightarrow Ph$ $Z^2 \rightarrow H$ $Z^3 \rightarrow H$ $Ar \rightarrow Ph$	8	76	84
6	**60f**	$R^1 \rightarrow 5\text{-Br}$ $Z^1 \rightarrow Ph$ $Z^2 \rightarrow H$ $Z^3 \rightarrow H$ $Ar \rightarrow Ph$	8	82	85
7	**60g**	$R^1 \rightarrow H$ $Z^1 \rightarrow Ph$ $Z^2 \rightarrow H$ $Z^3 \rightarrow H$ $Ar \rightarrow p\text{-Me-}C_6H_4$	8	69	89
8	**60h**	$R^1 \rightarrow H$ $Z^1 \rightarrow Ph$ $Z^2 \rightarrow H$ $Z^3 \rightarrow H$ $Ar \rightarrow m\text{-Me-}C_6H_4$	10	72	87
9	**60i**	$R^1 \rightarrow H$ $Z^1 \rightarrow Ph$ $Z^2 \rightarrow H$ $Z^3 \rightarrow H$ $Ar \rightarrow p\text{-MeO-}C_6H_4$	6	84	91
10	**60j**	$R^1 \rightarrow H$ $Z^1 \rightarrow Ph$ $Z^2 \rightarrow H$ $Z^3 \rightarrow H$ $Ar \rightarrow p\text{-Cl-}C_6H_4$	12	84	82

[a]Isolated yield(s).
[b]Determined from chiral HPLC analysis.

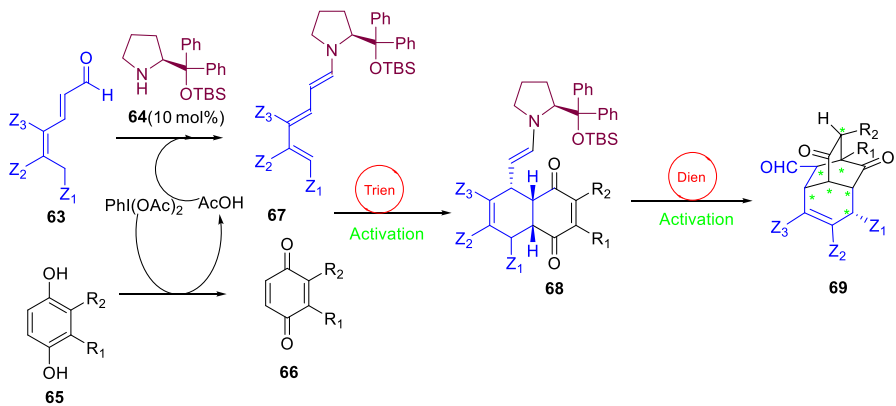

Scheme 11.13 Oxidative-dearomatization strategy in tandem trienamine/dienamine catalyzed Diels-Alder/Michael addition in tricyclic architectures.

Table 11.4 Substrate scope of tricyclic architecture through Diels-Alder/Michael addition reaction.

Entry	69		Time [h]	Yield[a] [%]	ee[b] [%]
1	**69a**	R^1& R^2 → H Z1 → H Z2 → H Z3 → Me	16	53	97
2	**69b**	R^1& R^2 → H Z1 → Me Z2 → H Z3 → Me	16	43	94
3	**69c**	R^1& R^2 → H Z1 → H Z2 → Me Z3 → H	72	30	90
4	**69d**	R^1& R^2 → H Z1 → H Z2 → H Z3 → Ph	16	48	98
5	**69e**	R^1& R^2 → H Z1 → ^{i}Pr Z2 → H Z3 → Ph	65	43	94
6	**69f**	R^1& R^2 → H Z1 → H Z2 &Z3 → N-Boc-2,3-Indoyl	40	40	92
7	**69g**	R^1& R^2 → H Z1 → H Z2 → *p*-$MeOC_6H_4$ Z3 → H	16	25	n.d.

[a]Isolated yield.
[b]Determined by chiral HPLC analysis.

Greck et al. developed a synthetic strategy based on an oxidative de-aromatization and trienamine/enamine tandem catalysis in enantioselective synthesis of enantio-enriched tricyclic scaffold having contiguous stereocenters in a single-pot operation [69].

This single-pot operation proceeded through the formation of hydroquinone derivative 66 by $PhI(OAc)_2$-mediated oxidative dearomatization of benzene-1,4-diol 65. The generated acetic acid of this reaction acted as a cocatalyst to trigger the transformation of trienamine/enamine intermediates 67 and 68 toward the formation of 69 via [4 + 2] cycloaddition followed by intramolecular Michael addition reaction (Scheme 11.13).

Under the optimized reaction condition this protocol was tested with a wide range of hydroquinone's derivatives in the presence of 10 mol% of catalyst 64 and 1.4 equiv. of $PhI(OAc)_2$ in chloroform at 55°C. Excellent level of enantioselectivity was achieved irrespective of the electronic and stearic factor of diene substituents (Table 11.4).

Jørgensen et al. established an organocatalyzed tandem reaction in diversity-oriented synthesis (DOS) of highly functionalized hydroisoquinoline scaffolds via trienamine-mediated enantioselective [4 + 2] cycloaddition of cyno-acrylamide as dienophile with conjugated dienal followed by nucleophilic ring closer reaction [70]. This method was based on trienamine activation organocatalytic Diel-Alder/nucleophilic ring-closer cascade reactions through DOS.

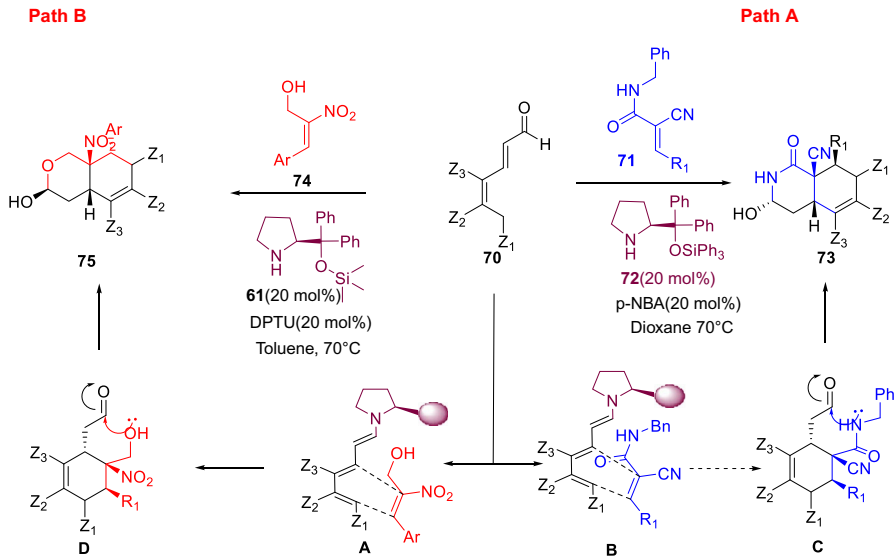

Scheme 11.14 Trienamine catalyzed [4 + 2] cycloaddition cascade in the synthesis of hydroisoquinoline and hydroisochromenes.

A wide range of hexa-2,4-dienal 70 and N-benzylcynoacrylamide 71 was treated in the presence of 20 mol% of silylated proline catalyst 72 and *p*-nitrobenzoic acid in 1,4-dioxane as the solvent at 70°C. This method produced densely functionalized hydroisoquinoline derivatives 73a→g (Scheme 11.14, Path A, Table 11.5). All the reactions proceeded very well with excellent stereoselectivity. The stereoselectivity greatly depended on the stearic bulkiness of the substituents of the silyl protecting groups. The catalyst having the Ph_3Si-protecting group offered an excellent stereoselectivity in product formation. After the cycloaddition, a nucleophilic addition reaction had occurred between the nitrogen atom of the acrylamide and the aldehyde group of dienal to get the corresponding hydroisoquinolinein excellent yield with a high degree of enantioselectivity and diastereoselectivity.

The hydroisochromene was synthesized by the same group following enamine cascade strategy under organocatalytic condition. The [4 + 2] cycloaddition/nucleophilic ring closure strategy was followed toward the synthesis of stereodefined hydroisochromene scaffolds 75a→g. The substitution pattern in dienal had no effects on the reaction course. The electron withdrawing and donating groups present in the substituents maintained a high conversion rate and excellent stereoselectivity [71].

Under this condition a variety of dienal 70 and (*E*)-nitroalcohols 74 was allowed to react in the presence of 20 mol% of catalyst 61 and 20 mol% of DPTU (*N*,*N*′-diphenylthiourea) in toluene at 70°C (Scheme 11.14 Path B, Table 11.5).

This method offered a synthetically useful method for the synthesis of hydroisochromene with contiguous stereo centers. The functionalized hydroisochromenes was further transformed into other useful synthetic intermediates of the diverse interests.

Table 11.5 Substrate scope of cascade Diels-Alder reaction in the synthesis of Hydroisoquinoline (**73a→g**) and Hydroisochromine (**75a→g**).

Entry	73a→g		Yield [%]	dr [%]	ee [%]	75a→g		Yield [%]	dr [%]	ee [%]
1	**73a**	R1→Ph Z1 → H Z2 → Me Z3 → H	80	90:10	95	**75a**	Ar→Ph Z1 → H Z2 → Me Z3 → H	70	80:20	96
2	**73b**	R1→*p*-BrC_6H_4 Z1 → H Z2 → Me Z3 → H	69	85:15		**75b**	Ar→*p*-BrC_6H_4 Z1 → H Z2 → Me Z3 → H	44	78:22	92
3	**73c**	R1→*p*-ClC_6H_4 Z1 → H Z2 → Me Z3 → H	79	84:16	94	**75c**	Ar→*p*-NO_2.C_6H_4 Z1 → H Z2 → Me Z3 → H	38	72:28	92
4	**73d**	R1→*p*-ClC_6H_4 Z1 → H Z2 → Me Z3 → H	64	81:19	91	**75d**	Ar→*p*-MeO.C_6H_4 Z1 → H Z2 → Me Z3 → H	70	77:23	92
5	**73e**	R1→*p*-MeOC_6H_4 Z1 → H Z2 → Me Z3 → H	80	81:19	96	**75e**	Ar→*p*-Me.C_6H_4 Z1 → H Z2 → Me Z3 → H	37	70:30	89
6	**73f**	R1→2-Furyl Z1 → H Z2 → Me Z3 → H	60	85:15	96	**75f**	Ar→2-furyl Z1 → H Z2 → Me Z3 → H	85	74:26	96
7	**73g**	R1→2thiophenyl Z1 → H Z2 → Me Z3 → H	74	90:10	95	**75g**	Ar → Ph Z1 → H Z2 → Ph Z3 → H	85	65	92

11.6 Conclusions

The important organocatalyzed reactions toward cycloaddition are demonstrated. The methods are extremely attractive, but complex to understand. The ideas of using these types of catalysts and producing these complex organic molecules deserve significant challenges. Clearly, this research will help to create additional methods which are unprecedented and therefore, synthesis of many molecules with complete stereochemical control can be performed.

Acknowledgments

BKB is thankful to Prince Mohammad Bin Fahd University, Kingdom of Saudi Arabia for providing academic support and encouragement. RNY thanks VBS Purvanchal University for providing the necessary facility for the preparation of the manuscript.

References

[1] S.J. Teh, T.L. Tan, C.W. Lai, K.M. Lee, Catalysis, Carbon Nanost. (2018) 107–125, https://doi.org/10.1007/978-3-319-95603-9_5.
[2] R. Schlögl, Heterogeneous catalysis, Angew. Chem. Int. Ed. 54 (2015) 3465–3520, https://doi.org/10.1002/anie.201410738.
[3] L. Lloyd, Industrial catalysts, in: Handbook of Industrial Catalysts, Springer, Boston, MA, 2011, pp. 1–22.
[4] D. Astruc, Organometallic Chemistry and Catalysis, (2007), https://doi.org/10.1007/978-3-540-46129-6.
[5] D. Bulfield, S.M. Huber, Halogen bonding in organic synthesis and organocatalysis, Chem. Eur. J. 22 (2016) 14434–14450, https://doi.org/10.1002/chem.201601844.
[6] W.A. Herrmann, N-heterocyclic carbenes: a new concept in organometallic catalysis, Angew. Chem. Int. Ed. (2002), https://doi.org/10.1002/1521-3773(20020415)41:8<1290::AID-ANIE1290>3.0.CO;2-Y.
[7] K. Fagnou, M. Lautens, Rhodium-catalyzed carbon – carbon bond forming reactions of organometallic compounds, Chem. Rev. (2003), https://doi.org/10.1021/cr020007u.
[8] A.L. Noffke, A. Habtemariam, A.M. Pizarro, P.J. Sadler, Designing organometallic compounds for catalysis and therapy, Chem. Commun. 48 (2012) 5219–5246, https://doi.org/10.1039/c2cc30678f.
[9] L.M. Pera, M.D. Baigori, A. Pandey, G.R. Castro, Industrial Biorefineries & White Biotechnology, 2015, pp. 391–408, https://doi.org/10.1016/B978-0-444-63453-5.00012-4.
[10] A. Schmid, J.S. Dordick, B. Hauer, A. Kiener, M. Wubbolts, B. Witholt, Industrial biocatalysis today and tomorrow, Nature 409 (2001) 258–268, https://doi.org/10.1038/35051736.
[11] D.C. Harrowven, Handbook of organopalladium chemistry for organic synthesis, Synthesis (Stuttgart) (2003), https://doi.org/10.1055/s-2003-37640.
[12] B.M. Nestl, S.C. Hammer, B.A. Nebel, B. Hauer, New generation of biocatalysts for organic synthesis, Angew. Chem. Int. Ed. (2014), https://doi.org/10.1002/anie.201302195.
[13] A. Zaks, Industrial biocatalysis, Curr. Opin. Chem. Biol. (2001), https://doi.org/10.1016/S1367-5931(00)00181-2.
[14] R.A. Sheldon, Selective catalytic synthesis of fine chemicals: opportunities and trends, J. Mol. Catal. A Chem. (1996), https://doi.org/10.1016/1381-1169(95)00229-4.

[15] P.C. Nagajyoti, K.D. Lee, T.V.M. Sreekanth, Heavy metals, occurrence and toxicity for plants: a review, Environ. Chem. Lett. 8 (2010) 199–216, https://doi.org/10.1007/s10311-010-0297-8.
[16] A. Berkessel, H. Gröger, Asymmetric Organocatalysis: From Biomimetic Concepts to Applications in Asymmetric Synthesis, (2005), https://doi.org/10.1002/3527604677.
[17] J.M.M. Verkade, L.J.C. Van Hemert, P.J.L.M. Quaedflieg, F.P.J.T. Rutjes, Organocatalysed asymmetric Mannich reactions, Chem. Soc. Rev. (2008), https://doi.org/10.1039/b713885g.
[18] S. Mossé, A. Alexakis, First organocatalyzed asymmetric Michael addition of aldehydes to vinyl sulfones, Org. Lett. (2005), https://doi.org/10.1021/ol051488h.
[19] X. Yu, W. Wang, Organocatalysis: asymmetric cascade reactions catalysed by chiral secondary amines, Org. Biomol. Chem. (2008), https://doi.org/10.1039/b800245m.
[20] V. Terrasson, R.M. De Figueiredo, J.M. Campagne, Organocatalyzed asymmetric friedel-crafts reactions, Eur. J. Org. Chem. (2010) 2635–2655, https://doi.org/10.1002/ejoc.200901492.
[21] S.L. You, Q. Cai, M. Zeng, Chiral Brønsted acid catalyzed Friedel-Crafts alkylation reactions, Chem. Soc. Rev. (2009), https://doi.org/10.1039/b817310a.
[22] T.B. Poulsen, K.A. Jørgensen, Catalytic asymmetric Friedel – Crafts Alkylation reactions–copper showed the way, Chem. Rev. (2008), https://doi.org/10.1021/cr078372e.
[23] A.J. Boersma, B.L. Feringa, G. Roelfes, Enantioselective Friedel-Crafts reactions in water using a DNA-based catalyst, Angew. Chem. Int. Ed. (2009), https://doi.org/10.1002/anie.200900371.
[24] E.I. Balmond, M.C. Galan, E.M. McGarrigle, Recent developments in the application of organocatalysis to glycosylations, Synlett (2013), https://doi.org/10.1055/s-0033-1338970.
[25] R. Williams, M.C. Galan, Recent advances in organocatalytic glycosylations, Eur. J. Org. Chem. (42) (2017) 6247–6264, https://doi.org/10.1002/ejoc.201700785.
[26] F.R. Clemente, K.N. Houk, C. Allemann, R. Gordillo, C. PH-Y, Theory of asymmetric organocatalysis of aldol and related reactions: rationalizations and predictions, Acc. Chem. Res. (2004), https://doi.org/10.1021/ar0300524.
[27] N.T. McDougal, S.E. Schaus, Asymmetric Morita-Baylis-Hillman reactions catalyzed by chiral Brønsted acids, J. Am. Chem. Soc. (2003), https://doi.org/10.1021/ja037705w.
[28] Y. Takemoto, Development of chiral thiourea catalysts and its application to asymmetric catalytic Reactions, Chem. Pharm. Bull.(Tokyo) (2010), https://doi.org/10.1248/cpb.58.593.
[29] P. Merino, E. Marqués-López, T. Tejero, R.P. Herrera, Organocatalyzed Strecker reactions, Tetrahedron (2009), https://doi.org/10.1016/j.tet.2008.11.020.
[30] O. Lozano, G. Blessley, T. Martinez Del Campo, A.L. Thompson, G.T. Giuffredi, M. Bettati, et al., Organocatalyzed enantioselective fluorocyclizations, Angew. Chem. Int. Ed. (2011), https://doi.org/10.1002/anie.201103151.
[31] M. East, Pericyclic Reactions, in: Handbook of Chiral Chemicals, Second ed., 2010, https://doi.org/10.1201/9781420027303.ch26.
[32] N. Dennis, Addition reactions: cycloaddition, in: Organic Reaction Mechanisms 2014: An Annual Survey Covering the Literature Dated January to December 2014, 2017, https://doi.org/10.1002/9781118941829.ch11.
[33] A.C. Aragonès, N.L. Haworth, N. Darwish, S. Ciampi, N.J. Bloomfield, G.G. Wallace, et al., Electrostatic catalysis of a Diels-Alder reaction, Nature (2016), https://doi.org/10.1038/nature16989.
[34] K.N. Houk, R.W. Strozier, On Lewis acid catalysis of Diels-Alder reactions, J. Am. Chem. Soc. (1973), https://doi.org/10.1021/ja00793a070.

[35] S. Otto, F. Bertoncin, J.B.F.N. Engberts, Lewis acid catalysis of a Diels-Alder reaction in water, J. Am. Chem. Soc. (1996), https://doi.org/10.1021/ja960318k.
[36] D.A. Evans, G. Helmchen, M. Rüping, Chiral auxiliaries in asymmetric synthesis, in: Asymmetric Synthesis—The Essentials, Wiley, 2007, pp. 3–9.
[37] J.R. Henderson, M. Parvez, B.A. Keay, Diastereoselective Diels-Alder reactions of a novel cyclopropenyl-containing chiral auxiliary, Org. Lett. (2007), https://doi.org/10.1021/ol702280q.
[38] H.B. Kagan, O. Riant, Catalytic asymmetric Diels-Alder reactions, Chem. Rev. (1992), https://doi.org/10.1021/cr00013a013.
[39] L. Deloux, M. Srebnik, Asymmetric boron-catalyzed reactions, Chem. Rev. (1993), https://doi.org/10.1021/cr00018a007.
[40] E.J. Corey, Catalytic enantioselective Diels-Alder reactions: methods, mechanistic fundamentals, pathways, and applications, Angew. Chem. Int. Ed. (2002), https://doi.org/10.1002/1521-3773(20020517)41:10<1650::AID-ANIE1650>3.0.CO;2-B.
[41] A.B. Northrup, D.W.C. MacMillan, The first general enantioselective catalytic Diels-Alder reaction with simple α,β-unsaturated ketones, J. Am. Chem. Soc. (2002), https://doi.org/10.1021/ja017641u.
[42] K.C. Nicolaou, S.A. Snyder, T. Montagnon, G. Vassilikogiannakis, The Diels-Alder reaction in total synthesis, Angew. Chem. Int. Ed. (2002), https://doi.org/10.1002/1521-3773(20020517)41:10<1668::AID-ANIE1668>3.0.CO;2-Z.
[43] Y. Nishiyama, Y. Han-Ya, S. Yokoshima, T. Fukuyama, Total synthesis of (−)-Lepenine, J. Am. Chem. Soc. (2014), https://doi.org/10.1021/ja503023h.
[44] T. Yamamoto, T. Shinmyozu, T. Takeda, P. Merino, F. Aldabbagh, E. Zysman-Colman, et al., Total synthesis, in: Monocyclic Arenes, Quasiarenes, Annulenes, 2013, https://doi.org/10.1055/sos-sd-045-01225.
[45] F.-E. Chen, J. Huang, Reserpine: a challenge for total synthesis of natural products, Chem. Rev. (2005) https://doi.org/10.1021/cr050521a.
[46] A. Shvartsbart, A.B. Smith, Total synthesis of (-)-calyciphylline N, J. Am. Chem. Soc. (2014), https://doi.org/10.1021/ja411539w.
[47] M.J. Goldstein, The Diels-Alder reaction, Science (80-) (1984), https://doi.org/10.1126/science.224.4646.239-b.
[48] K.C. Nicolaou, Y. Tang, J. Wang, Total synthesis of sporolide B, Angew. Chem. Int. Ed. (2009), https://doi.org/10.1002/anie.200900264.
[49] W. Carruthers, Cycloaddition Reactions in Organic Synthesis, (1990), https://doi.org/10.1002/3527600256.
[50] K.A. Ahrendt, C.J. Borths, D.W.C. MacMillan, New strategies for organic catalysis: the first highly enantioselective organocatalytic diels—Alder reaction, J. Am. Chem. Soc. (2000), https://doi.org/10.1021/ja000092s.
[51] R.M. Wilson, W.S. Jen, D.W.C. MacMillan, Enantioselective organocatalytic intramolecular Diels-Alder reactions. The asymmetric synthesis of solanapyrone D, J. Am. Chem. Soc. (2005), https://doi.org/10.1021/ja054008q.
[52] J.L. Li, T.Y. Liu, Y.C. Chen, Aminocatalytic asymmetric Diels-Alder reactions via HOMO activation, Acc. Chem. Res. (2012), https://doi.org/10.1021/ar3000822.
[53] E. Arceo, P. Melchiorre, Extending the aminocatalytic HOMO-raising activation strategy: where is the limit? Angew. Chem. Int. Ed. 51 (2012) 5290–5292, https://doi.org/10.1002/anie.201201347.
[54] S.L. Schreiber, H.V. Meyers, Synthetic studies in the brefeldin series: asymmetric enamine-enal cycloaddition and intramolecular Nozaki reactions, J. Am. Chem. Soc. (1988), https://doi.org/10.1021/ja00223a053.

[55] K. Juhl, K.A. Jørgensen, The first organocatalytic enantioselective inverse-electron-demand hetero-Diels-Alder reaction, Angew. Chem. Int. Ed. (2003), https://doi.org/10.1002/anie.200250652.
[56] X. Jiang, X. Shi, S. Wang, T. Sun, Y. Cao, R. Wang, Bifunctional organocatalytic strategy for inverse-electron-demand diels-alder reactions: highly efficient in-situ substrate generation and activation to construct azaspirocyclic skeletons, Angew. Chem. Int. Ed. (2012), https://doi.org/10.1002/anie.201107716.
[57] B. Han, J.L. Li, C. Ma, S.J. Zhang, Y.C. Chen, Organocatalytic asymmetric inverse-electron-demand aza-Diels-Alder reaction of N-sulfonyl-1-aza-1,3-butadienes and aldehydes, Angew. Chem. Int. Ed. (2008), https://doi.org/10.1002/anie.200804183.
[58] J.L. Li, B. Han, K. Jiang, W. Du, Y.C. Chen, Organocatalytic enantioselective hetero-Diels-Alder reaction of aldehydes and o-benzoquinone diimide: synthesis of optically active hydroquinoxalines, Bioorg. Med. Chem. Lett. (2009), https://doi.org/10.1016/j.bmcl.2009.03.013.
[59] X. Jiang, D. Fu, X. Shi, S. Wang, R. Wang, PPh3-catalyzed synthesis of dicyano-2-methylenebut-3-enoates as efficient dienes in catalytic asymmetric inverse-electron-demand Diels-Alder reaction, Chem. Commun. (2011), https://doi.org/10.1039/c1cc12834e.
[60] R.M. De Figueiredo, R. Fröhlich, M. Christmann, Amine-catalyzed cyclizations of tethered α,β-unsaturated carbonyl compounds, Angew. Chem. Int. Ed. 47 (2008) 1450–1453, https://doi.org/10.1002/anie.200704688.
[61] F.J.S. Duarte, A.G. Santos, Enantioselective organocatalytic intramolecular Diels-Alder reactions: a computational study, J. Org. Chem. 77 (2012) 3252–3261, https://doi.org/10.1021/jo300005e.
[62] Z.Y. Wang, W.T. Wong, D. Yang, Organocatalyzed asymmetric synthesis of dihydrodibenzofurans based on a dienamine process, Org. Lett. 15 (2013) 4980–4983, https://doi.org/10.1021/ol402288y.
[63] D.Q. Xu, A.B. Xia, S.P. Luo, J. Tang, S. Zhang, J.R. Jiang, et al., In situ enamine activation in aqueous salt solutions: highly efficient asymmetric organocatalytic Diels-Alder reaction of cyclohexenones with nitroolefins, Angew. Chem. Int. Ed. 48 (2009) 3821–3824, https://doi.org/10.1002/anie.200900269.
[64] X. Feng, Z. Zhou, R. Zhou, Q.Q. Zhou, L. Dong, Y.C. Chen, Stereodivergence in amine-catalyzed regioselective [4 + 2] cycloadditions of β-substituted cyclic enones and polyconjugated malononitriles, J. Am. Chem. Soc. 134 (2012) 19942–19947, https://doi.org/10.1021/ja3106219.
[65] A.B. Xia, D.Q. Xu, C. Wu, L. Zhao, Z.Y. Xu, Organocatalytic Diels-Alder reactions catalysed by supramolecular self-assemblies formed from chiral amines and poly(alkene glycol)s, Chem. Eur. J. 18 (2012) 1055–1059, https://doi.org/10.1002/chem.201102766.
[66] Z.J. Jia, H. Jiang, J.L. Li, B. Gschwend, Q.Z. Li, X. Yin, et al., Trienamines in asymmetric organocatalysis: Diels-Alder and tandem reactions, J. Am. Chem. Soc. 133 (2011) 5053–5061, https://doi.org/10.1021/ja1112194.
[67] H. Jiang, D.C. Cruz, Y. Li, V.H. Lauridsen, K.A. Jørgensen, Asymmetric organocatalytic thio-diels-alder reactions via trienamine catalysis, J. Am. Chem. Soc. 135 (2013) 5200–5207, https://doi.org/10.1021/ja4007244.
[68] J.X. Liu, Q.Q. Zhou, J.G. Deng, Y.C. Chen, An asymmetric normal-electron-demand aza-Diels-Alder reaction via trienamine catalysis, Org. Biomol. Chem. 11 (2013) 8175–8178, https://doi.org/10.1039/c3ob41698d.
[69] F. Portalier, F. Bourdreux, J. Marrot, X. Moreau, V. Coeffard, C. Greck, Merging oxidative dearomatization and aminocatalysis: one-pot enantioselective synthesis of tricyclic architectures, Org. Lett. 15 (2013) 5642–5645, https://doi.org/10.1021/ol402546h.

[70] C.V. Gómez, D.C. Cruz, R. Mose, K.A. Jørgensen, Organocatalytic cascade reactions: diversity-oriented synthesis for the construction of hydroisoquinoline scaffolds, Chem. Commun. 50 (2014) 6035–6038, https://doi.org/10.1039/c4cc01231c.

[71] D. Cruz Cruz, R. Mose, C. Villegas Gõmez, S.V. Torbensen, M.S. Larsen, K.A. Jørgensen, Organocatalytic cascade reactions: towards the diversification of hydroisochromenes and chromenes through two different activation modes, Chem. Eur. J. 20 (2014) 11331–11335, https://doi.org/10.1002/chem.201403505.

Diverse synthesis of medicinally active steroids

12

Preetismita Borah[a], *Bimal Krishna Banik*[b,*]
[a]CSIR-Central Scientific Instruments Organization, Chandigarh, India, [b]Department of Mathematics and Natural Sciences, College of Sciences and Human Studies, Deanship of Research Development, Prince Mohammad Bin Fahd University, Al Khobar, Kingdom of Saudi Arabia
[*]Corresponding author. e-mail address: bimalbanik10@gmail.com; bbanik@pmu.edu.sa

12.1 Background on steroid

Steroids are extremely important medicinally active organic compounds with four rings constructed in a highly specific perhydrocyclopentano[α]phenanthrene (Fig. 12.1) orientation. Many steroids are the constituents of plants, animals, and living organisms [1]. In general, the steroid core structure has 17 carbon atoms connected with 4 fused rings in a specific way. Three of these are cyclohexanes (A, B, and C) and one is cyclopentane system (D ring). Sterols are obtained from steroids with an alcoholic group at C-3 with a cholestane type of compound [2].

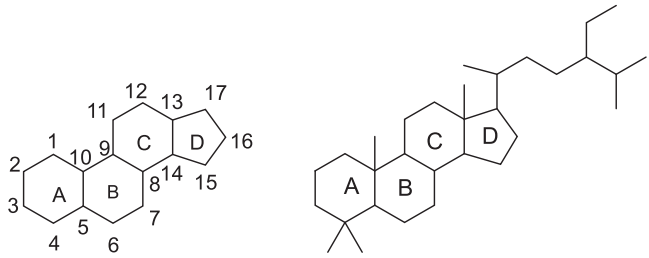

Fig. 12.1 Steroid backbones.

The structures of steroids are altered by a number of ways to make other types of steroids. For example, a cleavage of one of the rings in steroid produces secosteroidal compounds. Importantly, steroid hormones control endocrine systems and regulate metabolic pathways. These hormones influence endocrine functions such as sexual differentiation and reproductive life. They also maintain salt and sugar metabolism in the human body. Several glucocorticoids, vitamin D, bile acids, progestin, and sterols are also distributed in cells (Fig. 12.2).

Green Approaches in Medicinal Chemistry for Sustainable Drug Design. https://doi.org/10.1016/B978-0-12-817592-7.00012-5
© 2020 Elsevier Inc. All rights reserved.

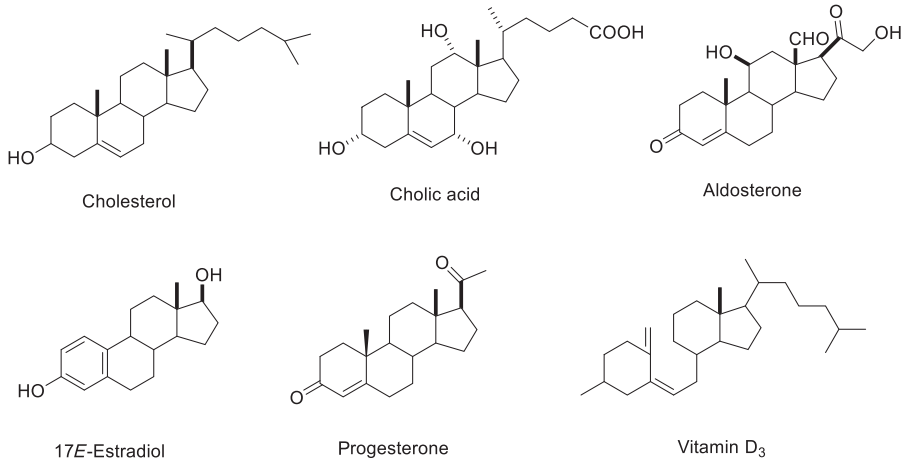

Fig. 12.2 Examples of naturally occurring steroids [2a].

The chemical modifications of steroids have emerged as a great synthetic tool for chemists. Cholesterol, stigmasterol, and lanosterol and the products obtained from them are crucial molecules in the treatment of diverse cancers. Estrogen derivatives are used in the treatment of breast cancer. Cortisones are useful against rheumatoid arthritis. Testosterone derivatives serve as antilymphocytic leukemia. Glucocorticoids are important antiinflammatory agents [3]. Numerous steroidal molecules isolated from marine sources demonstrate cytotoxic properties [4]. Most importantly, many steroids are accepted as clinical active medicines. Often, they serve as drug or enzyme templates due to their ability to penetrate cells, strong lipophilic characters, and above all conformational rigidities [5]. Although many of these steroids can be isolated naturally or through synthetic methods, however, an easy access of medicinally active steroids is essential and highly demanding topic.

12.2 Isolation of steroids molecules

Structurally steroids are not triterpenes because it has C19–C29 skeletons. In contrast, a C30 skeleton is observed in the triterpene system. Steroids are obtained from the 30 carbon-containing molecule, the squalene (**1**). The squalene (**1**) is made by the combination of two *trans*-farnesyl systems connected through head to head [6]. It was obtained from shark liver oil and found it was in almost all living organisms [7]. The squalene (**1**) to steroid preparatory route was demonstrated by Bucourt et al. [8]. The chemical sequence of squalene to steroid proceeded through acid-mediated reaction of epoxide and subsequent formation of cationic unstable species [6].

Squalene was converted to lanosterol in animal (**2**) and this sequence then formed cholesterol. Hormones were prepared from cholesterol following numerous pathways. In plants, squalene (**1**) produced cycloartenol (**3**) which generates diverse phytosterols. Squalene (**1**) was also transformed into lanosterol (**4**) in lower organisms through biochemical pathways. Lanosterol produced ergosterol (**5**) [9] (Scheme 12.1).

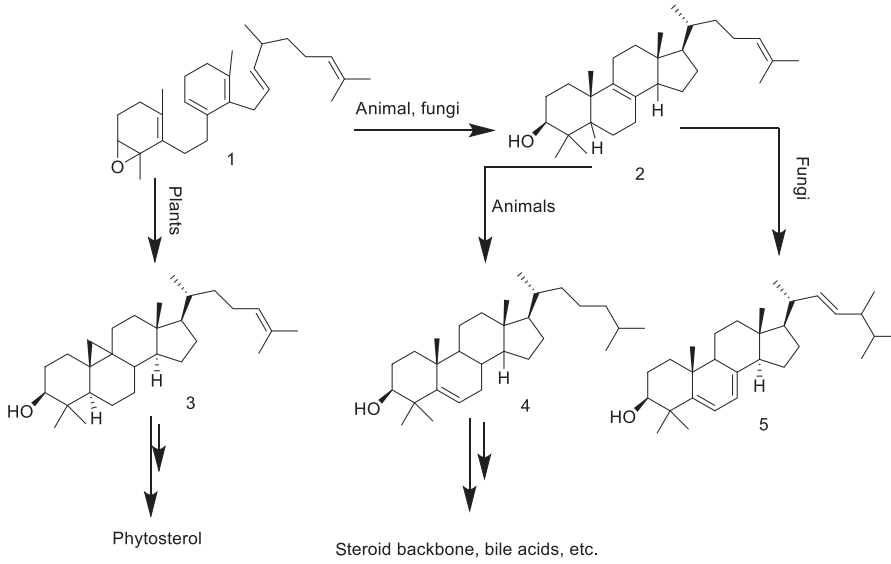

Scheme 12.1 Steroidal biosynthesis.

12.2.1 Bachmann's synthesis of equilenin

In 1940, Bachmann et al. described the use of AB → ABC → ABCD approach for the preparation of equilenin 7. 1-Naphthylamine-2-sulfonic acid **6** was selected as the starting material that has the AB ring of this steroid. Ring C was constructed on AB ring and then the D ring was prepared following a cyclization pathway (Scheme 12.2) [10].

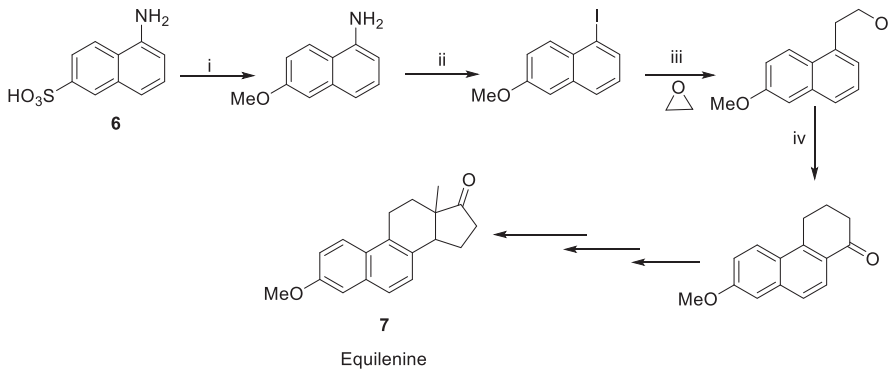

Scheme 12.2 *Reagent and conditions:* (i) KOH, heat, Me_2SO_4, NaOH, H^+; (ii) $NaNO_2$, H_2SO_4, KI; (iii) Mg; and (iv) PBr_3, malonic ester synthesis, $SOCl_2$, and $SnCl_2$.

12.2.2 Woodward's synthesis of cholesterol

The synthesis of cholesterol by Woodward was complicated since it is difficult to explain the ring construction strategy (Scheme 12.3) [11]. One pair of diastereomer was prepared out of 256 optical isomers. However, this synthesis was stereospecific. The D ring present in it served for further elaboration by variations in the chain. The alkene bond in the C ring was helpful for the preparation of cortisone **9**.

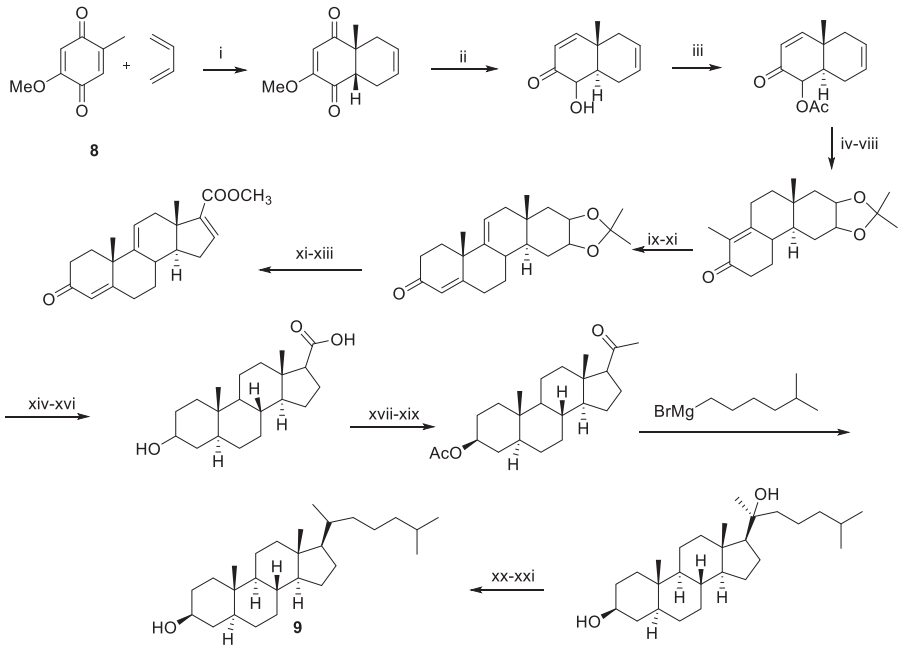

Scheme 12.3 *Reagent and conditions:* (i) PhH, 100°C; (ii) KOH, dioxane, CAH, 2N H_2SO_4; (iii) Ac_2O, Py (iv) Zn/Ac_2O; (v) HOOEt, EtOH, PhH; (vi) aq KOH, dioxane; (vii) OsO_4, Et_2O, acetone, $CuSO_4$; (viii) H_2, Pd-$SrCO_3$, PhH, rt.; (ix) Triton B, aq KOH; (x) NaOAc/HOAc; (xi) MeMgI, −19°C; (xii) dil HCl, dioxane, rt.; (xiii) Na_2CrO_7, HOAc, rt., CH_2N_2; (xiv) Adam's catalyst, hydration; (xv) CrO_3; (xvi) $NaBH_4$; (xvii) H^+/H_2O; (xviii) $SOCl_2$, CH_3Cd; (xix) CH_3COOH; (xx) Pd/C; and (xxi) H^+/H_2O.

12.2.3 Synthesis of estrone

Because of the medicinal activities of estrone, **11** many synthetic chemists had focused to synthesize this complex molecule. An important method for the construction of the D ring, following a cyclization of the C ring was developed by Chein (Scheme 12.4) [12]. Certainly, this method was very attractive and modifications of this method to introduce different other functionalities were feasible.

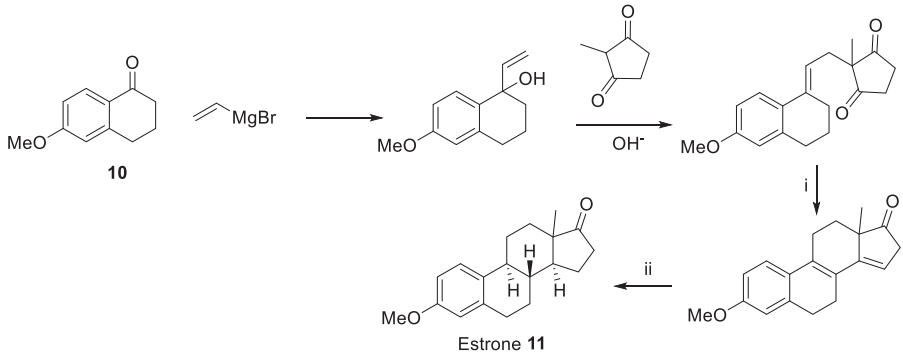

Scheme 12.4 *Reagent and conditions:* (i) TsOH and (ii) HI/H_2, K/NH_2, CrO_3, Py. HCl.

Weimar et al. reported the formation of CD ring using Dane's diene as AB- and a D-ring as dienophile (Scheme 12.5) [13].

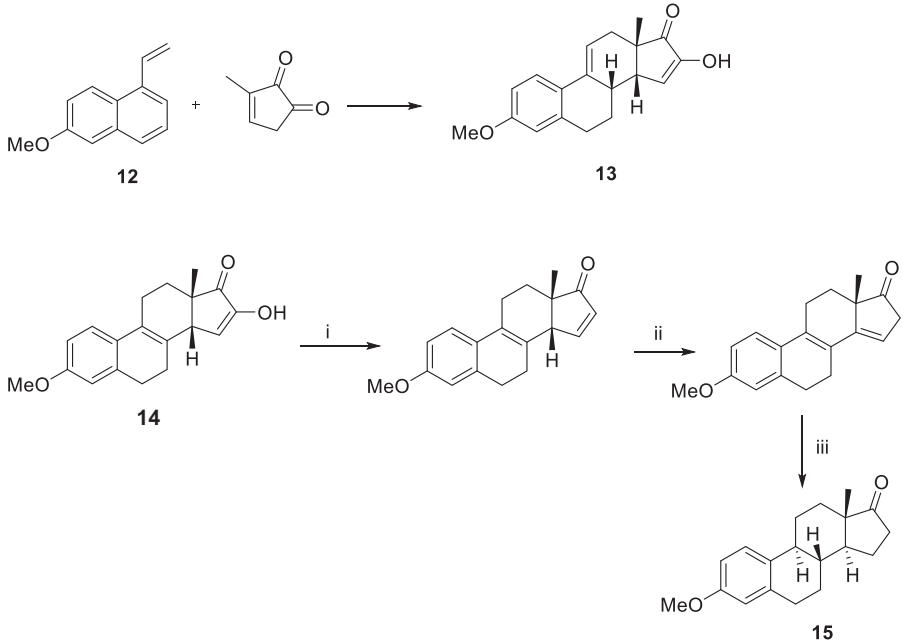

Scheme 12.5 *Reagent and conditions:* (i) Tf_3O, 2,6-lutidine, EtSiH, $PdCl_2$, DMF, 60°C; (ii) LiHMDS, THF, −78°C, AcOH; and (iii) H_2/Pd-C, PhH, 0°C, TFA, Et_2SiH, rt.

12.2.4 Synthesis of cortisone

Research on cortisone was challenging since it has a complicated structure with useful medicinal activities. Sarrett used an ABC-ABCD approach that has all the components present at the A, B, and C rings of cortisone **17**. The D-ring was constructed using the C11-OH group and ketone. Stereoelectronic restriction of anions reactions on a rigid six-membered carbon-frame was used to construct the C/D *trans* system (Scheme 12.6) [14].

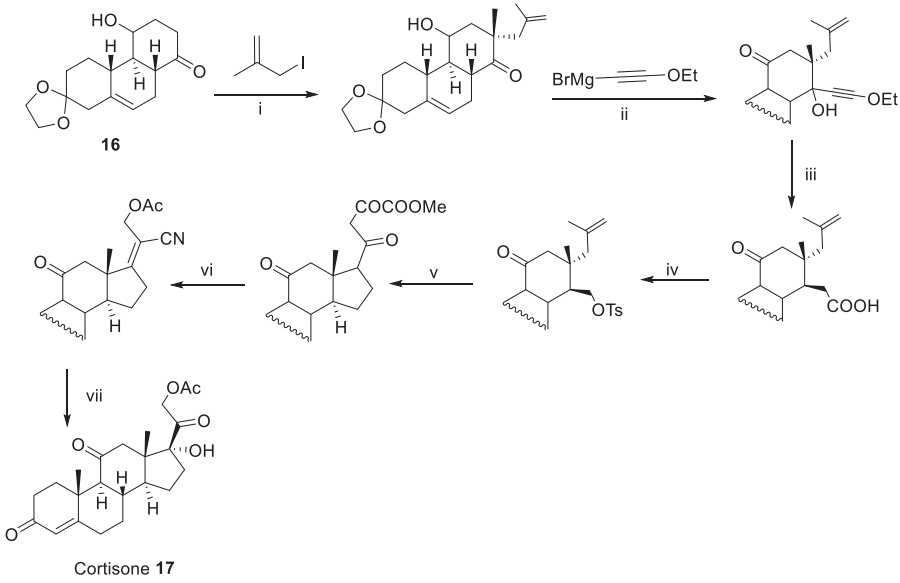

Scheme 12.6 *Reagent and conditions:* (i) t-BuOK, MeI; (ii) CrO_3, py; (iii) aq. H_2SO_4, $NaBH_4$, $K/NH_3/PrOH$; (iv) LAH, TsCl, CrO_3, Py; (v) OsO_4, HIO_4 NaOEt, COOMe, NaOMe; (vi) H_3O, iodination, acetolysis KCN, $POCl_3$, py, and (vii) $KMnO_4$, piperidine.

12.3 Structural classifications, use, and importance

Steroids are classified based on their chemical structures (e.g., a side chain attached to the D-ring), locations of production (e.g., ovarian or adrenal), biological actions (e.g., brain or sex organs), and molecular mechanism of actions [e.g., an estrogen receptor (ER) agonist] and also their biochemical effects [15, 16].

Moreover, steroids were divided into three categories based on the type of organisms in which they are found. For example, steroids were grouped as follows:

1. Insect steroids;
2. Vertebrate steroids; and
3. Plant steroids.

12.3.1 Insect steroids or ecdysteroids

Ecdysteroids or the insect steroids are composed of polyhydroxy derivatives with a *cis*-AB-ring stereochemistry. These types of steroids produced by specific plants (e.g., *Cyanotis vaga*) were accepted by insects as food. 20-Hydroxyecdysone is a natural ecdysteroid hormone. Ecdysteroids were active in cell proliferation, growth, and apoptosis. They controlled gene expressions that are involved in ecdysis and metamorphosis process in insects. Ecdysone is a molting hormone in insects, crabs, and some worms. This hormone interfered with their molting and reproduction [17].

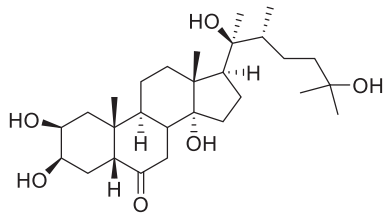

18

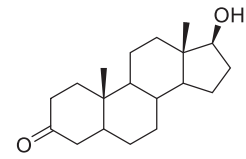

19

These were used in helping muscle growth and losing fat. They lowered side effects that are associated with anabolic steroids [18]. Interestingly, this increased the production of testosterone and dihydrotestosterone (DHT) in males. Some androgenic alterations in females were also observed. These included the growth of facial and body hair and the change of the voice [19]. They also used as immunomodulators [20].

12.3.2 Vertebrate steroids

Vertebrate steroids are hormones, cholesterol, and neurosteroids.

Steroid hormones: The hormones are the chemical entities that manage a variety of medical functions. Steroid hormones are grouped into sex steroids, corticosteroids, anabolic steroids, and vitamin D. They control a number of biological processes. For example, they regulate metabolism of carbohydrates, proteins, and fats; homeostasis; immune system; blood amount; and renal excretion of electrolytes. Due to their *anti*inflammatory nature (e.g., C60 glucocorticoid) [21], some of these are used against arthritis and dermatitis. They are also active against autoimmune diseases. They act as posttransplantory immunosuppressants medicine [22], against cancer [23], and heart disease (e.g., digitoxigenin 15) [24].

The gonadal hormones (estrogens, androgens, and progesterones) involve in interaction with vertebrate androgen or ERs, induce the shape of the body, and help to make primary and secondary sex characteristics [25].

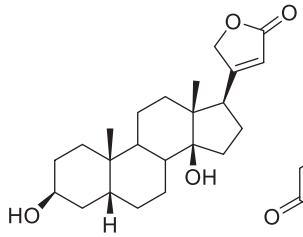

Digitoxgenin
20

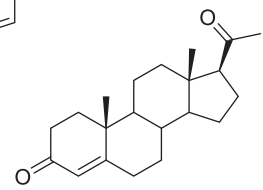

Progestrones
21

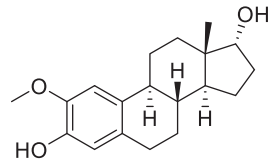

2-Methoxyestradiol
22

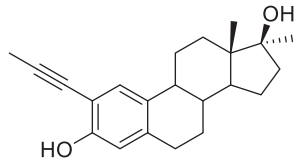

Estramustane
23

The medicinal effects of these sex hormones were not for reproductive functions only. It was found that citrate salt of androgenic steroid [26] and estrogen derivative (2-methoxyestradiol 17) have anticancer activities. The 2-methoxyestradiol derivatives, for example, [27, 28] estramustine **24** and furanosteroidal antibiotic viridian **25** [29], had effects on cell proliferation and cytotoxicity in human cancer cell lines. Moreover, estrogen derivatives with substituents at C^{16} and lactones at C^{16}, for example, estrone **26** were effective as estrogenic inhibitors of the 17β-hydroxysteroid dehydrogenase [30].

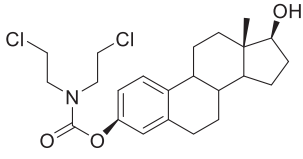

Estramustane
24

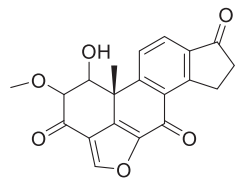

Viridin
25

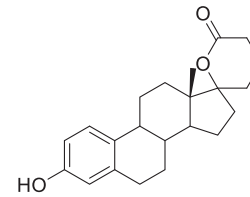

Estrogen
26

12.4 Classification based on medicinal properties

Steroids involved in an increased medicinal activities. Steroids demonstrate an increased biological activity through chelation compared with the free ligand. Therefore, a number of studies are performed to carry out the preparation of steroidal metal complexes for their biological evaluation. Following a similar concept, metal

complexes of estrogens are synthesized to explore the cellular delivery of metal to ERs [31]. In continuation of research on steroidal metal complex, tin containing derivatives (triphenyltin cholesteryl ether) **27** was prepared and evaluated as insecticide, bactericide, and fungicide [32]. Hormones labeled with titanium were prepared and their aromatase activity was examined. High level of aromatase in endometrium cancer patients was not a good indication [33]. The organometallic complexes of male sex hormones (testosterone and DHT) were synthesized and their use as tracers in nonisotopic carbonyl-metal immunoassay (CMIA) was examined [34]. The $CpRe(CO)_3$-substituted steroids **28** obtained from fulvenes were tested as active radiopharmaceuticals [35]. Testosterone acetate thiosemicarbazone (TATSC) was converted to complex of the type $[M(TATSC)CI_2]$ (M = Cu/Pt). This was tested against human breast cancer cell lines [36].

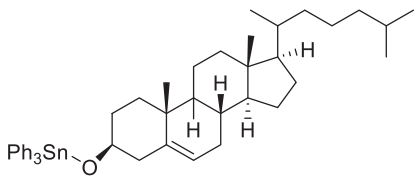

27

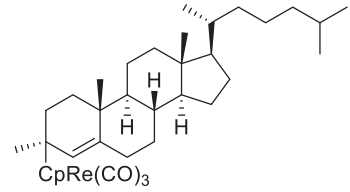

28

12.4.1 Corticosteroids

These are involved in controlling various physiological disorders, such as body stress, immune system, regulation of inflammation, food metabolism, protein catabolism, mental function, and blood fluid and kidney function. The most important examples of corticosteroids are cortisol and aldosterone. Synthetic corticosteroids are highly medicinally active molecules widely used in the treatment of brain tumors and skin disease. Medical applications of these types of molecules include bronchopulmonary dysplasia (BPD) in infants [37], arthritis, dermatitis, allergy, asthma, hepatitis, systemic lupus erythematosus, inflammatory bowel disease, sarcoidosis, and eye infections [38]. A few synthetic corticosteroid compounds are hydrocortisone (cortisol), fludrocortisone, and dexamethasone.

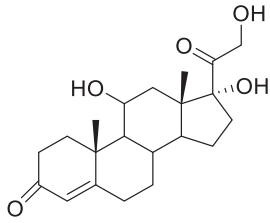

29

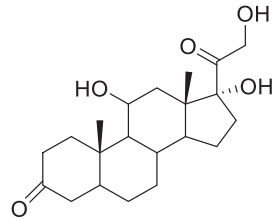

30

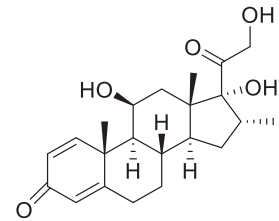

31

Immunosuppressive drugs are prescribed against autoimmune chronic active hepatitis. The combination of glucocorticoids-antimetabolite azathioprine is used for the same goal. It is known that liver transplant is the only choice for advanced-stage liver disease thereby a great medical attention is made to this field. Some steroids with immunosuppressive activities demonstrate exciting results in preventing allograft rejection [39]. These are also effective in combination with cyclosporine and azathioprene in the treatment of acute organ rejection. Consequently, they are used in patients with advanced renal, liver, heart, and pancreas transplant-related medical problems [40].

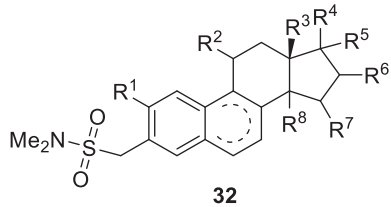

32

However, an excessive use of corticosteroids is harmful and may cause hyperglycemia, insulin resistance, diabetes, osteoporosis, anxiety, depression, gastritis, colitis, ictus, hypogonadism, hypothyroidism, and amenorrhoea [41].

Anabolic steroids: Anabolic-androgenic steroids (AASs) are related to testosterone. They function by increasing the synthesis of proteins in cells. This process helps to form better cellular tissue in muscles. Medicinally, they help to stimulate bone growth [42] and appetite. They also stimulate puberty in men and treat complex diseases, such as diverse cancers and AIDS [43]. The fluoxymesterone is active androgenically and is recommended for hypogonadism and breast neoplasma. It also demonstrates *anti*cancer activity through interaction with prolactin and ERs [44]. Some countries allow using gestrinone **34** for the control of endometriosis [45]. This molecule is also called dimetriose, dimetrose, and nemestran.

Anabolic steroids are helpful to build strong muscles and their growth (e.g., desoxymethyltestosterone **35** also called Madol or DMT). However, health risks are associated with long-term use or excessive amounts of anabolic steroids [46]. In extreme cases, permanent testosterone replacement therapy (TRT) is required [47].

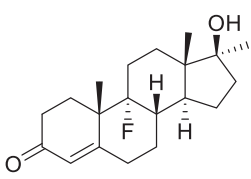

Halostestin
33

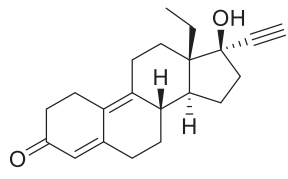

Gestrinone
34

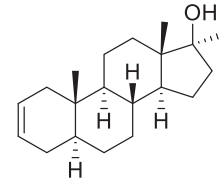

Desoxymethyltestosterone
35

Sterols: Sterols are important ingredients for the eukaryotes since these functions on membrane structures [48]. Cholesterol is present in the blood, liver, spinal cord, brain, heart, and in many other organs. It regulates numerous biochemical pathways that include the maintenance of cell membranes and the synthesis of hormones [49]. The cholesterol-derived compounds were investigated to identify molecules that have antioxidant properties [50] and follow cell signaling pathways in biochemical methods [51].

The 7α and 7β-spermidinyl cholesterols **36** are examined for their antibacterial and cytotoxic properties [52]. 7-Hydroxysterol **37** from a soft coral is active against testosterone-5α-reductase [53]. The radioactive iodine in 19-iodocholesterol **38** is useful as a contrast agent for patients [54].

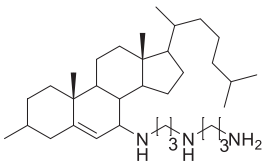

36

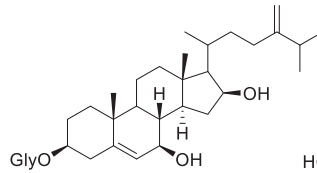

37

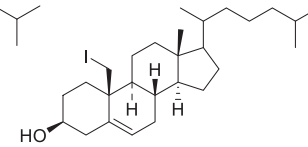

38

Neurosteroids: This type of steroids is recommended against peripheral neuropathy (e.g., aging, cancer, sugar problems, and physical injury) [55]. The neurosteroids alter neuronal excitability through interaction with neurotransmitter-gated ion channels. These compounds can act as allosteric modulators of neurotransmitter receptors, such as GABA(A), NMDA, and sigma receptors. Pregnenolone and progesterone are common representatives of neurosteroids. Neurosteroids play an important role in the development of nervous system and myelination, inhibition of neuronal toxicity, ischemia and have potential to be an effective therapy for Niemann Pick-type C disease (human childhood fatal neurodegenerative disease) and other lysosomal storage diseases. Progress of aging deeply influences morphological and functional parameters of peripheral nerves due to deterioration of myelin in PNS. The neuroactive steroids are able to reduce aging associated morphological abnormalities of myelin and aging associated myelin fiber loss in sciatic nerves as well. Althesin is an intravenous anesthetic drug popular for its short duration of action. It is composed of a mixture of two neurosteroids, alphadolone and alphaxalone (also known as alfaxalone). Alphadolone is responsible for the hypnotic effect of althesin whereas alfaxalone is responsible for the anesthetic effect and is used in veterinary practice as anesthetic for dogs and cats and has the advantage of less side effects and low plasma elimination half-life in these animals. Alfaxalone drug has been withdrawn from the market because of its severe side effects it, however, has now been re-branded as “Saffan” for veterinary anesthesia [56].

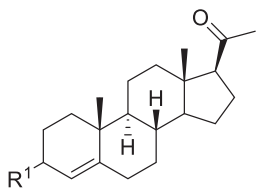

39 R^1=OH
40 R^1=O

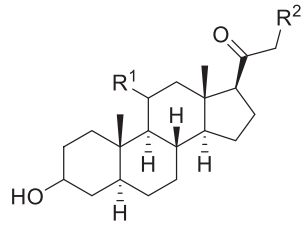

41 R^1=O, R^2=OH
42 R^1=O, R^2=H
43 R^1=R^2=H

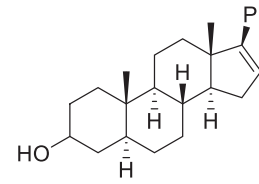

44

Another neurosteroid called allopregnanolone (3α,5α-tetrahydroprogesterone or THP) is responsible for neurogenesis and has been found to reverse neuron creation and cognitive deficits in a mouse model of Alzheimer's disease [57]. The sedative effects of neurosteroids are counteracted by another steroid called 17-phenylandrostenol (17-PA) which binds to GABA(A) receptors; however, 17-PA does not block the effects of benzodiazepines or barbiturates.

Vitamin D and secosteroids: Vitamin D is classified as a secosteroid in which the 9,10-C/C bond of ring B is broken. Several forms of vitamin D exist that include vitamin-D_1, D_2, D_3, D_4, and D_5. The two major forms are vitamin-D_2 (ergocalciferol) and vitamin-D_3 (cholecalciferol). Vitamin D plays an important role in the maintenance of a physiological system, for example, it regulates the Ca and P levels in the blood, which is necessary for a healthy skeleton system and promotes immunosuppression. These are currently being used for the treatment of cancer, tumor, hearing disorder, psoriasis, rickets, asthma, allergy, epilepsy, Fanconi syndrome [58], osteomalacia and osteoporosis. Physalins, a group of vitamin D isolated from *Physalis angulate* have been found to have in vitro antiinflammatory action [59].

12.4.2 Plant steroids

Plant steroids are of two broad categories: phytosterols and brassinosteroids (BRs).

Phytosterols (also called plant sterols): These are a group of steroid alcohol that occur naturally in plants. They are white powders with mild, characteristic odor, insoluble in water and soluble in alcohols. They have many applications as food additives and in medicine and cosmetics. Phytosterols (e.g., ergosterol) have cholesterol-lowering properties [60] and can reduce cholesterol level in human subjects up to 15% [61] and may act in cancer prevention. These are widely marketed as a dietary supplement [62].

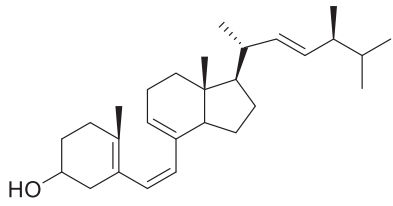

45

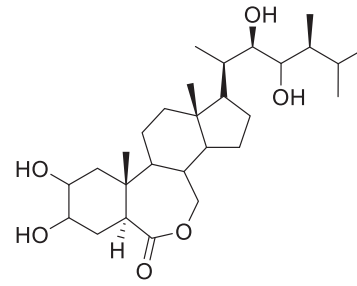

46

Brassinosteroids: Brassinosteroids (BRs), such as brassinolide, have been shown to elicit a broad spectrum of responses including the promotion of cell elongation and cell division, repression of light-regulated genes in the dark and repression of stress-regulated genes [58]. In view of their structural similarities with animal steroids, it has been proposed that BRs might interact with a soluble receptor in order to regulate the expression of specific genes [63]. The BRs tend to counter biotic as well as abiotic stress in plants [64]. Application of BRs to cucumbers results in increased metabolism and removal of pesticides. This property of BRs is beneficial for reducing the human ingestion of residual pesticides from nonorganically grown vegetables. The 24-epibranssinolide (EBL), a brassinolide isolated from *Aegle marmelos* Correa (Rutaceae), has been found to significantly reduce the maleic hydrazide (MH) induced genotoxicity in *Allium cepa* chromosomal aberration assay, and protect neuronal PC12 cells from 1-methyl-4-phenylpyridinium (MPP+)-induced oxidative stress and apoptosis in dopaminergic neurons [65].

Some 5α-hydroxy-6-ketopregnanes **47** have been examined [66] as analogs of BR plant growth regulators. The 17-substituted pregnadienes **48** have been prepared [67] as potential inhibitors of testosterone-5α-reductase. An unusual Δ^{20}-pregnene which was obtained from an octocoral, has been shown to be an inhibitor of the mitochondrial respiratory chain [68].

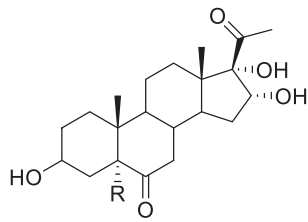

47

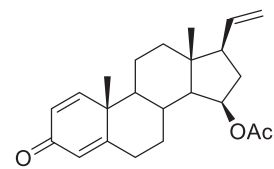

48

The steroidal alkaloids represent an important class of alkaloids that contain a perhydro-1,2-cyclopentanophenenthrene nucleus. This class of alkaloids invariable

occurs in plant kingdom as glycosidal combination with carbohydrate moieties. The steroidal alkaloids like dihydroplakinamine K **49** from marine sponge *Corcium niger* have been screened for cytotoxic activity [69]. Another unique class of steroidal alkaloids batrachotoxins **50** isolated from the skins of poison arrow frogs (genus *Phyllobates*) as well as from the skins and feathers of New Guinea birds (genus *Pitohui* and *Iflita*) is extremely potent neurotoxins [70]. Samandarin **51** isolated from the skin glands of fire salamander (*Salamandra salamandra*) causes muscle convulsions, high blood pressure, and hyperventilation in vertebrates [71].

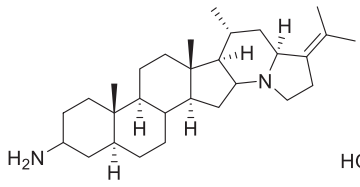

49

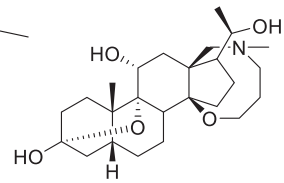

50

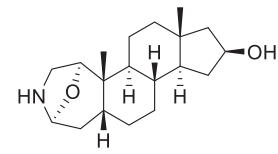

51

The bile acids are the steroid acids found predominantly in the bile of mammals. These bile acids are made by the cytochrome P450-mediated oxidation of cholesterol in the liver from where these are stored in gallbladder conjugated with sulfates or amino acid glycine. Bile acids and their salts are mainly responsible for the emulsification of fats and also regulate the level of cholesterol in the body and regulate the population of bacteria in the small intestine and in biliary tract. The cholic acid **52** and chenodeoxycholic acid **53** are the most important human bile acids.

Endogenous bile acids act as activators of farnesol receptor and play a variety of physiological roles related to the modulation of gene transcription. Some bile acid analogs of mifepristone **55** have been synthesized as liver selective glucocorticoid antagonists for the treatment of type II diabetes [72].

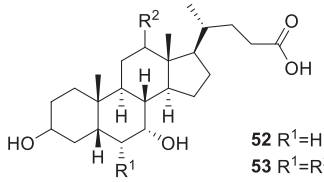

52 R^1=H, R^2=OH
53 R^1=R^2=H
54 R^1=Et, R^2=H

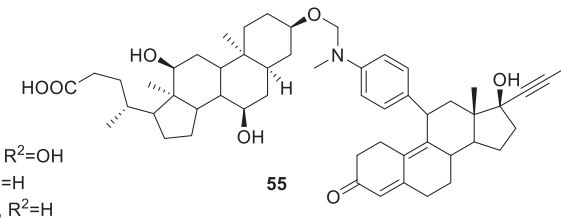

55

Certain steroidal derivatives have found their use as fluorescent detector for polyaromatic hydrocarbon (PAH), for example, **56** was derived from cholic acid which has a tweezer-like structure and has been screened for its use for the detection of PAHs [73]. The cholesteryl benzoate **57** forms cholesteric liquid crystals with helical structures and has applications in thermochromic liquid crystals. Cholesterol benzoate is also used in hair color, make-ups, and in cosmetic preparations [74].

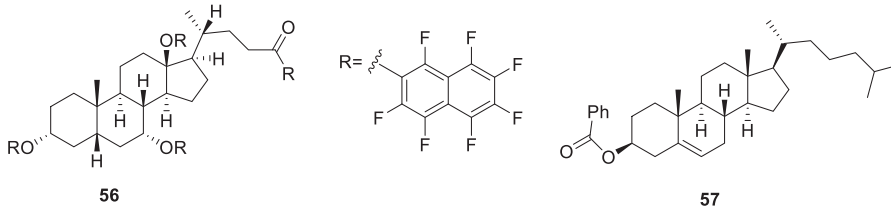

12.5 Different classical synthetic methods

A combination of Heck reaction and SmI_2-HMPA-induced cyclization was used for the synthesis of azasteroids **59** with unnatural *cis-cis* annulation of rings B, C, and D by Kang and his group (Scheme 12.7). The Heck reactions of quinolyl nonaflate (nonafluorobutanesulfonate, Nf) with 2-vinylcycloalkan-1-ols followed by oxidation and hydrogenation, smoothly give the desired heteroaryl substituted ketones substrates to SmI_2HMPA promoted cyclization. The major products of Heck reactions were unsaturated alcohols which were transformed into the desired ketones by oxidation with the $PySO_3$ complex in DMSO followed by hydrogenation [75].

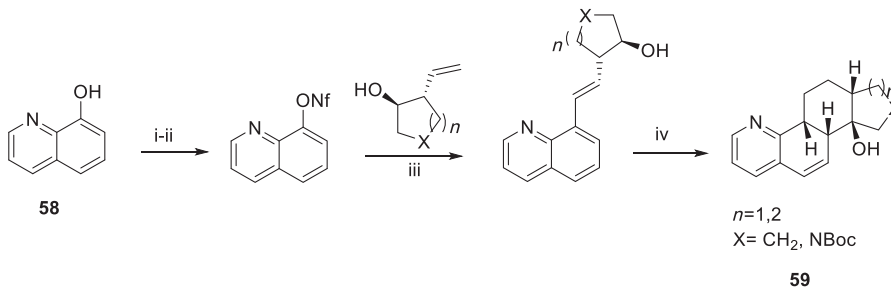

Scheme 12.7 *Reagent and conditions:* (i) NaH, THF, rt. (ii) NF, THF, rt. (iii) H_2, Pd/C, Py SO_3, DMSO, Et_3N, SmI_2, HMPA, tBuOH, THF, rt.

Riccardis et al. described the synthesis of steroidal derivatives containing a quinone moiety. Their strategy involved the synthesis of Grundmann's ketone, which is readily available by ozonolysis of vitamin D3, was converted to the vinyl triflate under kinetic control, the latter then converted to the 1,3-diene by Stille coupling with vinyl tributyltin, catalyzed by tetrakis(triphenylphosphine)-palladium(0). This diene had already been converted to the 1,4-dioxocholestane **61** by Diels-Alder cycloaddition with *p*-benzoquinone and to several moderately cytotoxic steroid-anthraquinone hybrids **62** by cycloaddition/oxidation with naphthoquinones presented by De Riccardis (Scheme 12.8) [76].

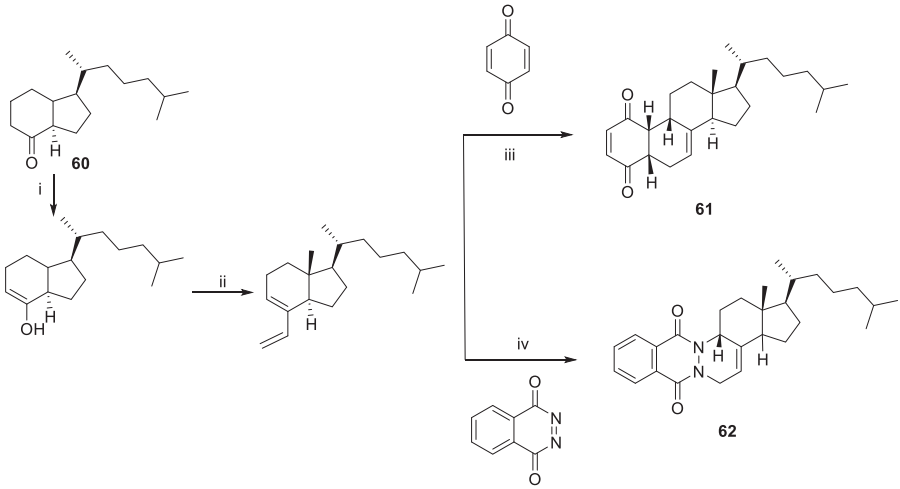

Scheme 12.8 *Reagents and conditions:* (i) Sodium bis(trimethylsilyl)amide, THF, 78°C, 1 h, then *N*-phenyl-bis(trifluoromethanesulfonimide), 78°C to r.t., 2.2 h (67%); (ii) $(PPh_3)_4Pd$, LiCl, vinyl tributyltin, THF, 75°C, 2 h (98%); and (iii) *p*-benzoquinone, toluene, 120°C, 12 h (36%).

Szarkaa et al. described hydrazinocarbonylation of 17-iodo-androst-16-ene **63** in the presence of palladium catalyst, a base and acetic or benzoic hydrazide. The desired N-acetamido-carbamoyl **64** was obtained without any problems. A few of these compounds were used for the preparation of steroidal 1, 3, 4-oxadiazoles (Scheme 12.9) [77].

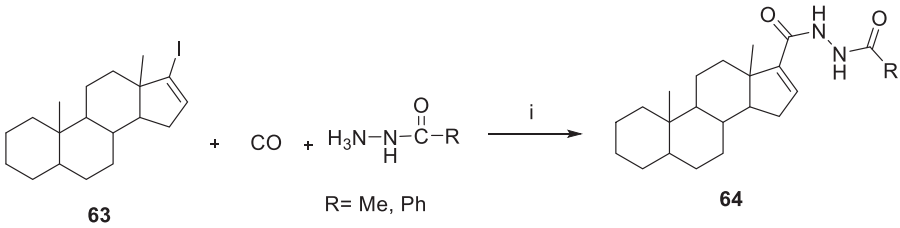

Scheme 12.9 *Reagent and conditions:* (i) $Pd(OAc)_2$, PPh_3, Et_3N, DMF, 60°C.

Tietze et al. explored Suzuki and Heck's reaction for the synthesis of the B-norestradiol **67** related compounds. They used boronic ester **66** and ortho-2-bromobenzylchloride **65** as reactants (Scheme 12.10) [78].

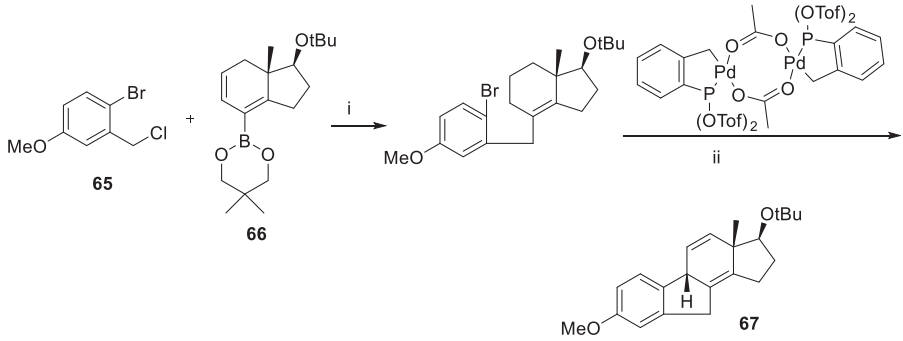

Scheme 12.10 *Reagent and conditions:* (i) $Pd(OAc)_2PPh_3$, nBu_4NOAc, DMF, 70°C, 7 h and (ii) nBu_4NOAc, DMF, 115°C, 4.5 h.

Wang et al. synthesized 3-*O*-glycosyl steroid derivatives **71** using a polyhydroxysteroid 3,5,6-trihydroxypregn-16-en-20-one **68** with peracetylated 1-bromo products of D-glucose (Scheme 12.11). A protection with acetic anhydride in pyridine produced the 6-*O*-acetylated glycosides of steroids. Deprotection of the acetylated steroid glycosides was performed with dibutyltin oxide. However, the acetyl group of the steroid system part was unaffected [79].

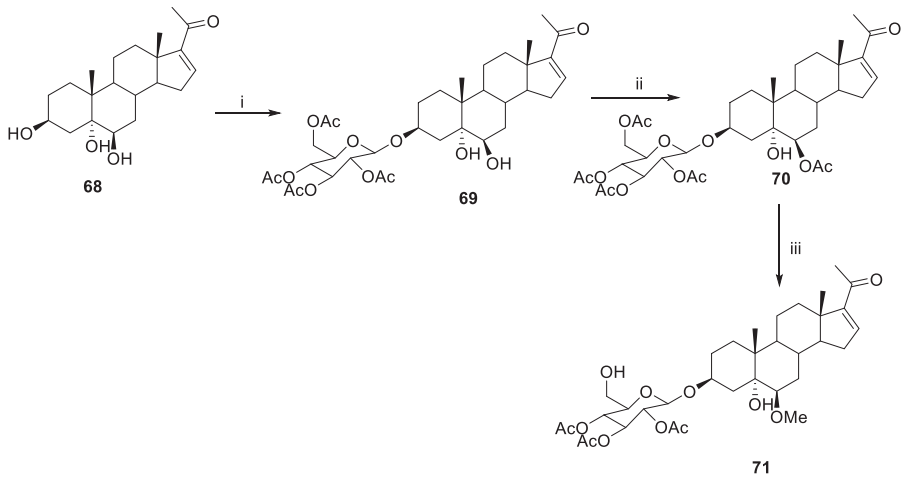

Scheme 12.11 *Reagents and conditions:* (i) 2, 3,4,6-Tetra-*O*-acetyl-D-glucopyranosyl bromide, Ag_2CO_3/diatomite (1:1), $CaSO_4$, CH_2Cl_2; (ii) Ac_2O, DMAP, pyridine; and (iii) Bu_2SnO, MeOH.

Saraber et al., described a procedure for the synthesis of C17-substituted steroids **74** and D homo steroids using a $ZnBr_2$-catalyzed coupling reaction of silyl enol ether with a Torgov type of reagent and subsequent acid-catalyzed cyclization of the intermediates to (D-homo) steroids (Scheme 12.12) [80].

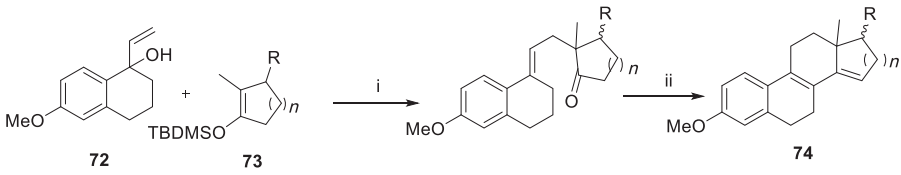

Scheme 12.12 *Reagent and conditions:* (i) $ZnBr_2$ and (ii) pTsOH.

Chowdhury et al. studied the regioselective preparation of steroidal antiinflammatory drug analogs **76**. These were prepared by the reaction of 16-dehydropregnenolone acetate with numerous aldoximes in the presence of chloramine-T (Scheme 12.13) [81].

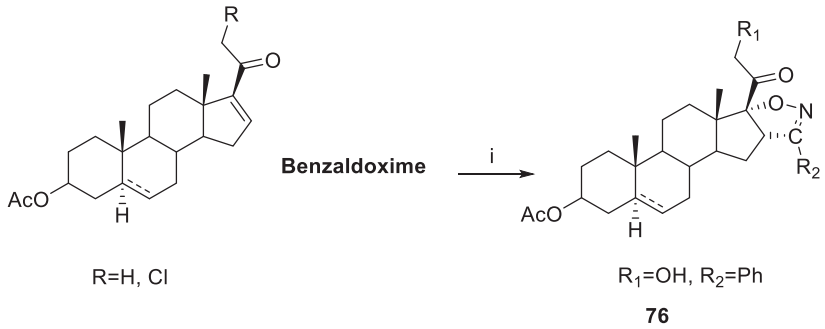

Scheme 12.13 *Reagent and conditions:* (i) Chloramine-T.

Sünnemann et al. investigated a method for the synthesis of optically pure steroidal D-amino acids **78** (Scheme 12.14) [82].

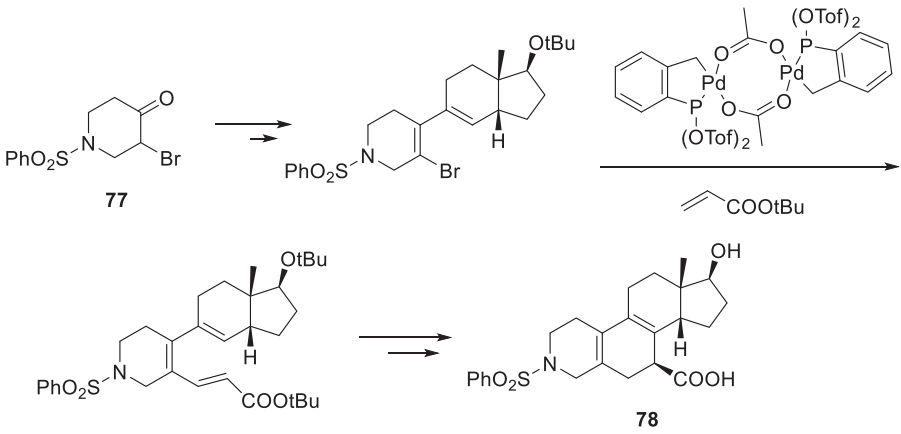

Scheme 12.14 *Reagent and conditions:* (i) dppb, Et_3N, DMF, H_2O, 100°C.

Bazzini et al. investigated the functionalization at the C-11 position of many steroids **80** (Scheme 12.15). It is important to note that the C-11 position of the steroid system is very crucial for the biological activities of a number of steroids, for example, corticoid activities [83].

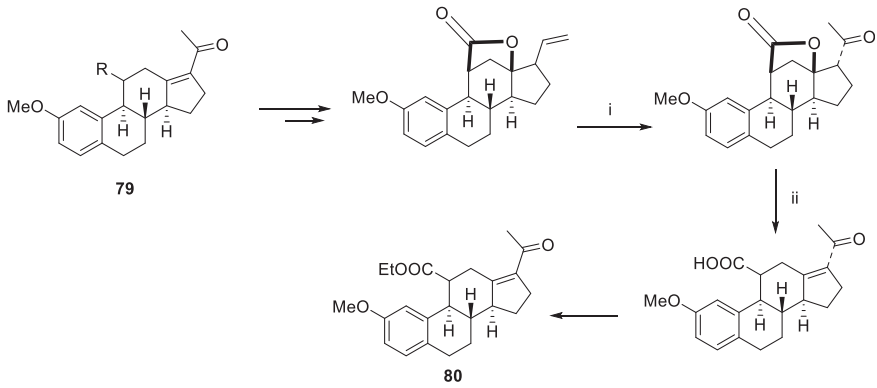

Scheme 12.15 *Reagent and conditions:* (i) $Pd(OAc)_2$, benzoquinone, $HClO_4$, 0.3m, MeCN, H_2O, (ii) K_2CO_3, EtOH, D, and (iii) $(COCl)_2$, EtOH.

Yan et al. synthesized pyridine rings fused steroids **82** and **83**. These pyridine compounds were synthesized by a reaction of propargylamine with 17-hydroxyandrost-4-en-3-one, 17methyl-17-hydroxyandrost-4-and en-3-one, 17-hydroxyestr-4-en-3-one **81** in the presence of Cu(II) (Scheme 12.16) [84].

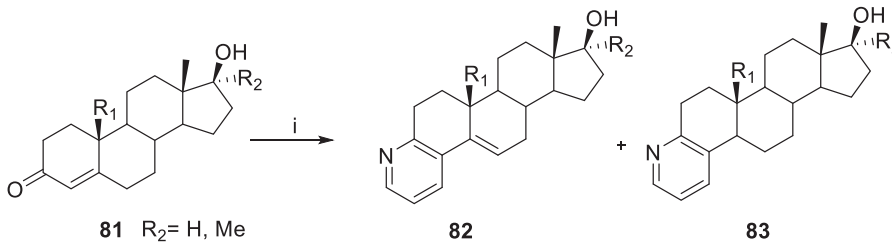

Scheme 12.16 *Reagent and conditions:* (i) $Cu(NO_3)_2{\cdot}3H_2O$, C_2H_5OH.

Sakac et al. investigated the preparation of triazoles **87** via intramolecular 1,3-dipolar cycloaddition of a steroidal 16,17-seco-17-diazo-16-nitrile **85** (Scheme 12.17). In vitro antiproliferative activity of the resulting triazoles against three tumor cell lines was investigated [85].

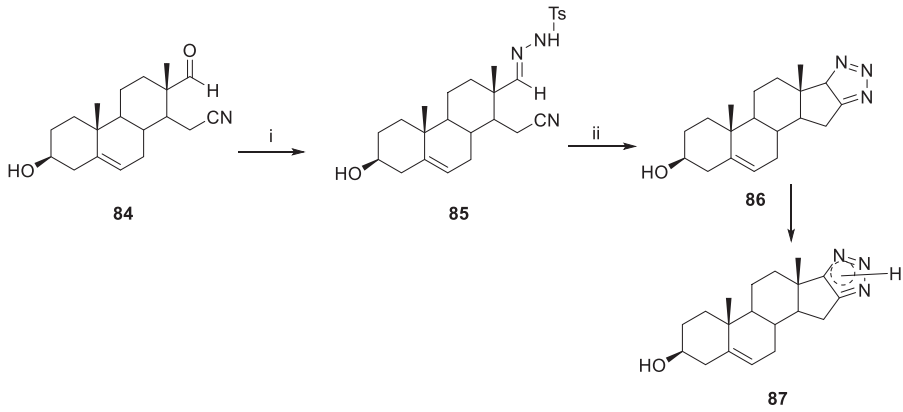

Scheme 12.17 *Reagent and conditions:* (i) $TsNHNH_2$, EtOH, reflux., 2 h, (ii) NaOH, dioxane/H_2O, reflux, and (iii) H_2, 10% Pd/C, MeOH, CH_2Cl_2, rt.

Linclau et al. reported an enantioselective synthesis of estrone **89** following Heck's reaction. In this procedure, a steroid system was constructed using three stereogenic centers (C8, C13, and C14) on the D ring through a three-component conjugate addition/alkylation reaction, followed by cyclizations of the C- and B-ring (Scheme 12.18). The C was constructed by RCM reaction using Hoveyda-Grubbs catalyst. The C9–C11 alkene group was ideally located for the B-ring closure [86].

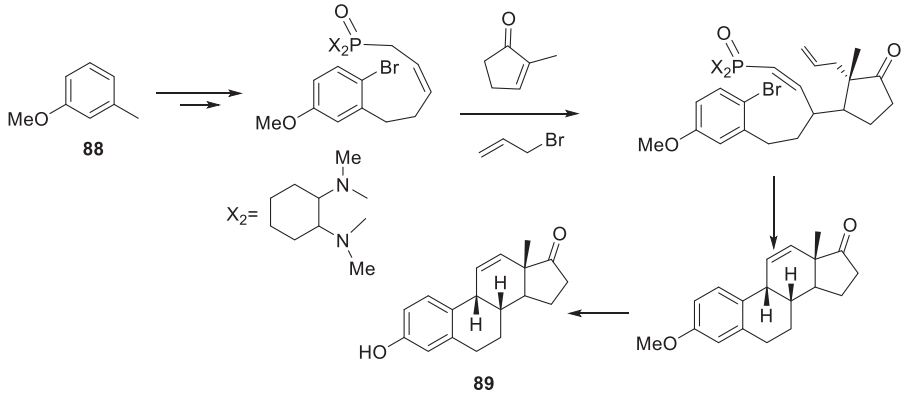

Scheme 12.18 *Reagent and conditions:* (i) NBS, hv, (ii) Et_2O/THF, (iii) LDA, THF, CH_2O, (iv) Zn, EtOH, $BrCH_2CH_2Br$, (v) $Cl_3C(CO)CCl_3$, PPh_3, CH_2Cl_2, (vi) $P(OEt)_3$, NaI, (vii) Bu_4NOAc, CH_3CN, (viii) Pd/C, cyclohexadiene, EtOH, and (ix) $AlCl_3$, NaI.

Richmonda et al. reported a method for the preparation of disodium 2β, 3α-disulfoxy-5α-cholestan-6-one disulfate **91** using cholesterol **90** (Scheme 12.19). Sulfation was accomplished using trimethylamine-sulfur trioxide complex in DMF [87].

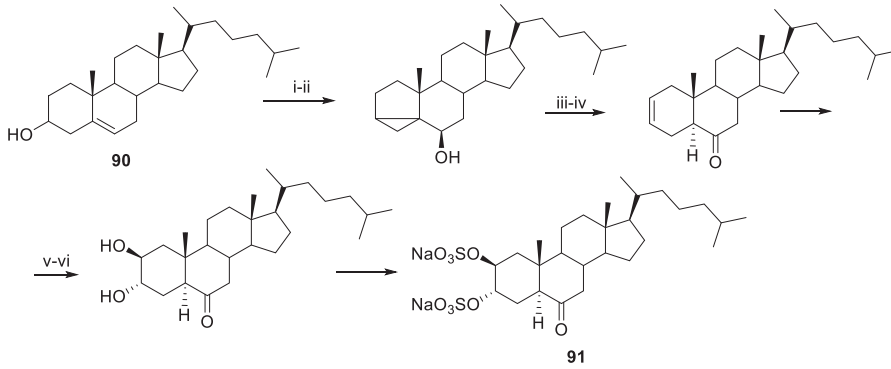

Scheme 12.19 *Reagent and conditions:* (i) MsCl, TEA, MEK, (ii) $NaHCO_3$, (iii) CrO_3, H_2SO_4, MEK, (iv) LiBr, p-TsOH, DMF, (v) m-CPBA, Na_2CO_3, H_2O-Cl_2CH_2, (vi) H_2SO_4, THF, and (vii) Et_3NSO_3, DMF, Amberlite CC-120, MeOH.

Huang et al. synthesized numerous 6-substituted steroidal lactams **95** following Beckman rearrangement using cholesterol **93**. These compounds demonstrated anticancer activities against MGC 7901, HeLa, and SMMC 7404 cancer cells lines (Scheme 12.20) [88].

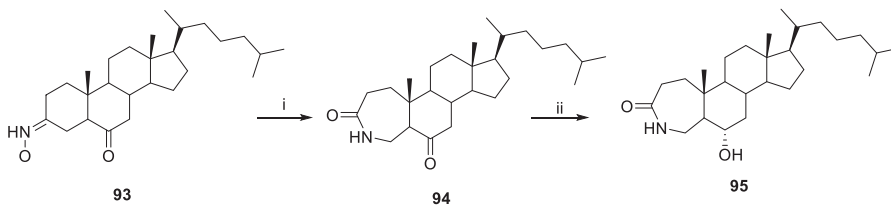

Scheme 12.20 *Reagents and conditions:* (i) $SOCl_2$/THF, 0°C; (ii) $NaBH_4$/MeOH, rt.; (iii) $H_2NOHCl/Na_2Ac_3H_2O$/EtOH, reflux; (iv) $H_2NC(S)NHNH_2$/EtOH, 60°C; and (v) $H_2NC(O)NHNH_2$/EtOH.

Shawakfeh et al. described the synthesis of symmetrical *bis*-steroidal pyrazines **97**. These were prepared by condensation of amino ketones with diosgenin **96** (Scheme 12.21) [89].

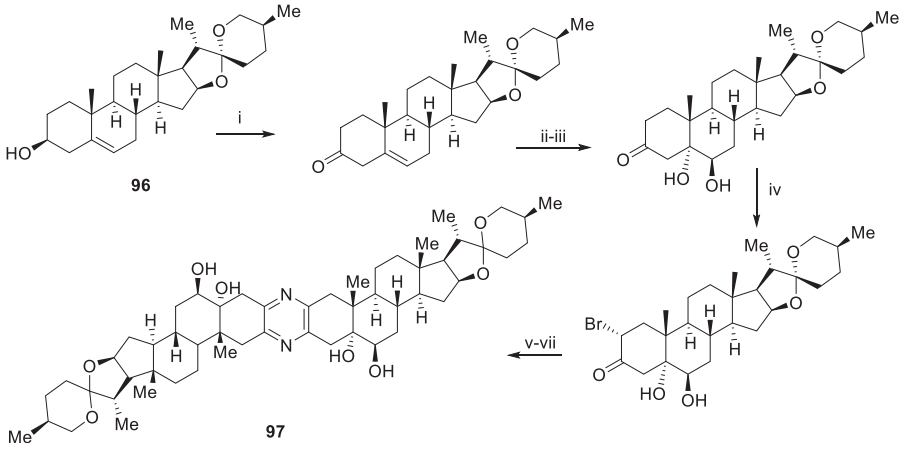

Scheme 12.21 *Reagent and conditions:* (i) PCC, $CaCO_3$, CH_2Cl_2, 1.5 h, (ii) MCBPA, CH_2Cl_2, 2 h, (iii) $HClO_4$, acetone, (iv) PTAB, THF, rt., 10 min, (v) NaN_3, DMF, KI, 50°C, (vi) PPh_3, THF, H_2O, 24 h, and (vii) Ethanol, TsOH, 24 h.

Khan et al. reported a procedure for the synthesis of steroidal oxazolo compounds **99** that demonstrates antibacterial properties (Scheme 12.22). The antibacterial properties of these steroids were examined by the disk diffusion method against two Gram-positive and two Gram-negative bacteria. The minimum inhibitory concentration (MIC) of these molecules was identified [90].

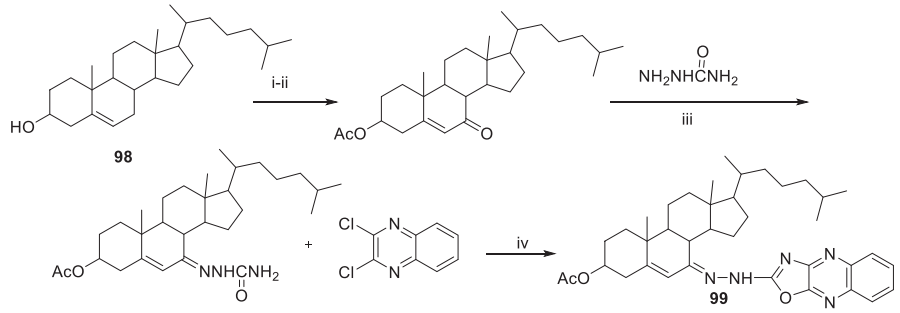

Scheme 12.22 *Reagent and conditions:* (i) Acetic anhydride, pyridine, (ii) t-butyl chromate, (iii) CH_3COONa, C_2H_5OH, and (iv) C_2H_5OH.

Ibrahim et al. explored pentacyclic steroids **101** through an epoxidation and subsequent epoxide opening reactions (Scheme 12.23) [91].

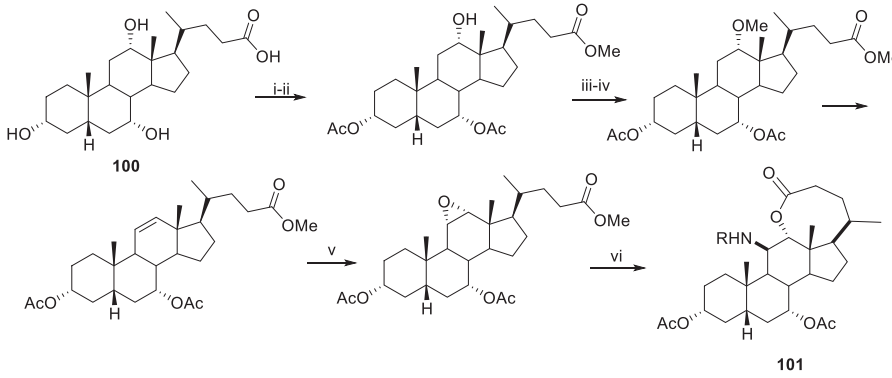

Scheme 12.23 *Reagent and conditions:* (i) MeOH, PTSA, (ii) Ac_2O, pyridine, DMAP, (iii) MeCl, pyridine, (iv) AcOK, HMPT, (v) m-CPBA, CH_2C_{12}, and (vi) RNH_2, EtOH/toluene, 24 h.

Fernandez-Herrera et al. studied the preparation of glycoconjugates of steroids **103**. The preparation of glucosamines diosgenin and hecogenin was performed by reacting the N-phthaloyl protected trichloroacetimidate of D-glucosamine and TMSOTf as a catalyst (Scheme 12.24). The glycoconjugates were then converted to acetamido derivatives. Some of these compounds were tested against HeLa, CaSki, and ViBo cervicouterine cancer cell lines. However, these molecules demonstrated low cytotoxicity against tumor cells and human lymphocytes, confirming that the cell death process is not through necrosis process. Interestingly, the antiproliferative properties of these molecules against cancer cells had no influence on the proliferative potential of peripheral blood lymphocytes [92].

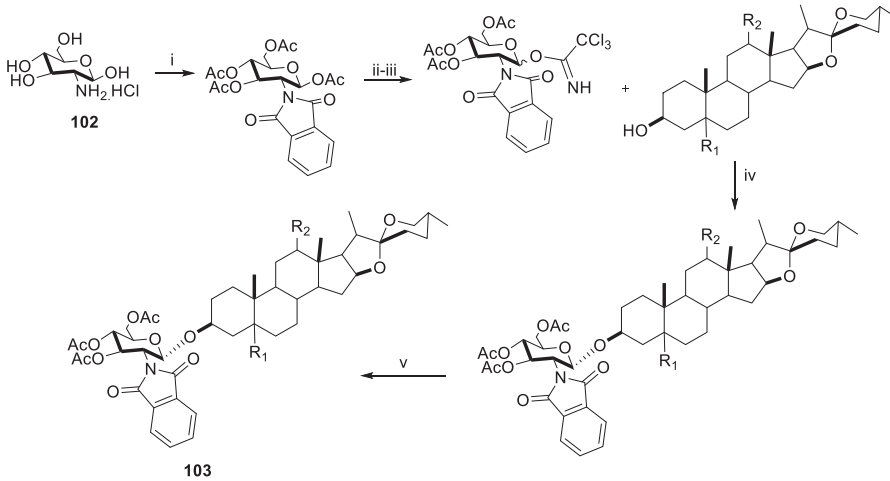

Scheme 12.24 *Reagent and conditions:* (i) NaOMe/MeOH, phthalic anhydride, Ac_2O, pyridine, (ii) hydrazine acetate, DMF, (iii) CCl_3CN, DBU, CH_2Cl_2, and (iv) TMSOTf, CH_2Cl_2.

Ibrahim et al. studied an efficient strategy to functionalize 3 and 11 positions of the steroid **105** with nitrogen (Scheme 12.25). The strategy used for this was an intramolecular Diels-Alder reaction of *o*-quinodimethanes. These starting materials were prepared from 3-azabicyclo[4.2.0]octa-1,3,5-trien-7-one [93].

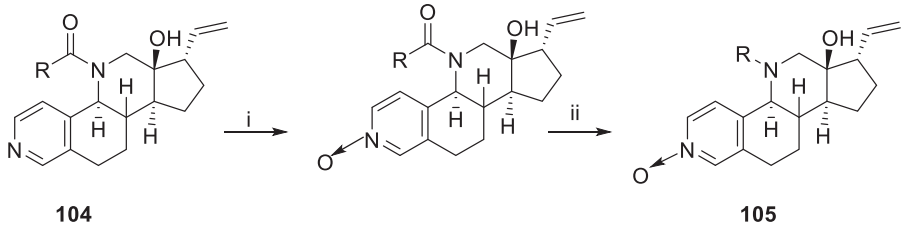

Scheme 12.25 *Reagent and conditions:* (i) m-CPBA, THF, 0°C and (ii) LAH, THF.

Wolfing et al. prepared 16-spiro-1,3,2-dioxaphosphorinanes **108** and **109** through the phosphorylation reaction of 16,16-bis(hydroxymethyl)androst-4-ene-3,17-dione **107** (Scheme 12.26). The dioxaphosphorinane system exists as chair conformation. The antiproliferative properties of the analogs were estimated in vitro using the MTT assay on three human cancer cell lines (HeLa, MCF7, and A431) [94].

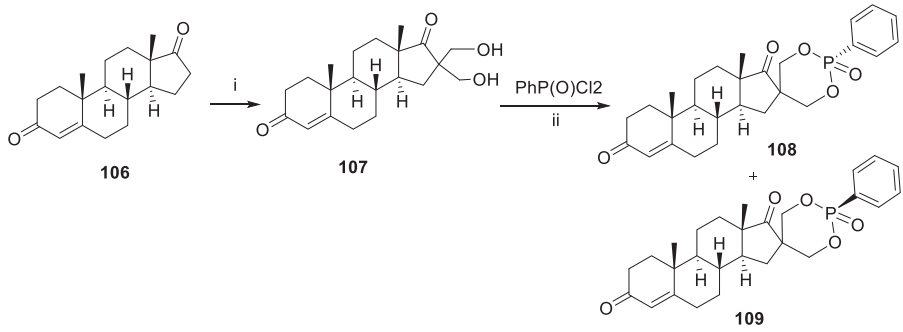

Scheme 12.26 *Reagent and conditions:* (i) CH_2O/H_2O, dioxane, NaOH and (ii) Et_3N, CH_2Cl_2, reflux.

Bansal et al. reported a method for the preparation of 16-imidazolyl-substituted steroids **111** (Scheme 12.27). These molecules exhibited cytotoxic properties in 60 cancer cell lines [95].

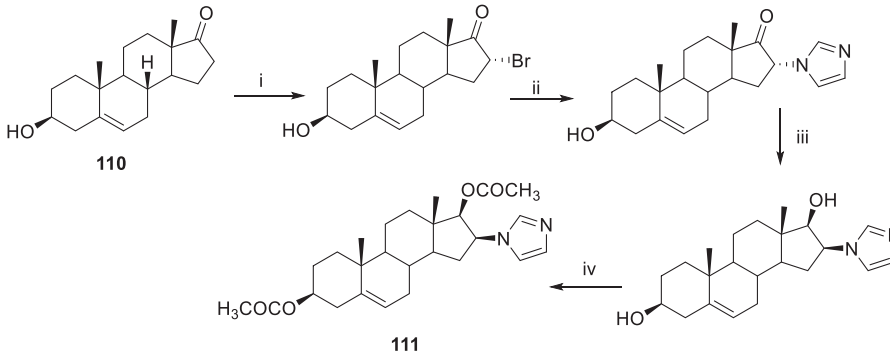

Scheme 12.27 *Reagent and conditions:* (i) Cupric bromide, MeOH, benzene, (ii) thermal fusion, imidazole, (iii) $NaBH_4$, MeOH, and (iv) acetic anhydride in dry pyridine.

Nickisch et al. described the synthesis of 17-fluorinated steroids **116** (Scheme 12.28). These molecules may have potential benefits in controlling estrogen and progesterone-related medical disorders. The cytotoxicity of these compounds in T47D breast cancer cells was investigated with respect to known antiprogestins. In addition, these molecules were analyzed against receptor-binding assays in vitro. The impressive antiprogestational activity and lack of antiglucocorticoid activity demonstrate that these compounds can probably be used against leiomyoma, endometriosis, and breast cancer [96].

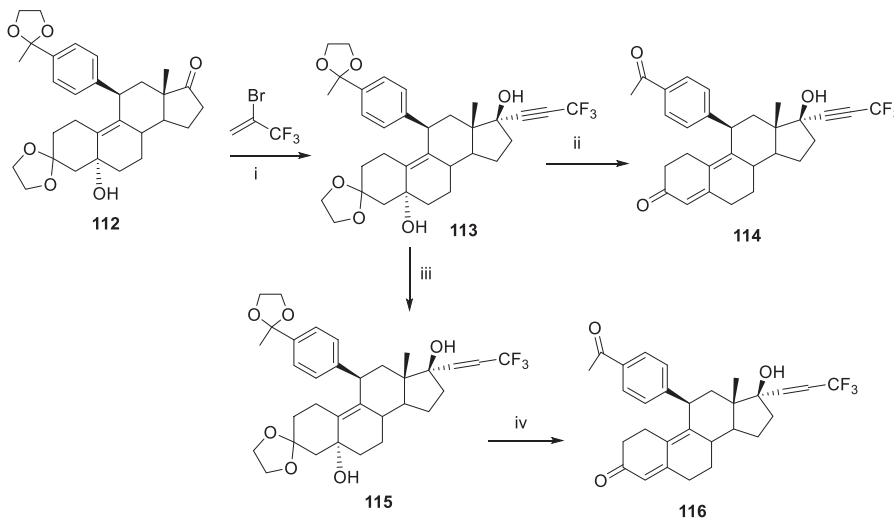

Scheme 12.28 *Reagent and conditions:* (i) LDA, (ii) H_2SO_4, MeOH, H_2O, (iii) Red-Al, and (iv) H_2SO_4, MeOH, H_2O.

Zhang et al. investigated the synthesis of steroids that have D-ring fused with heterocycles (pyridine imidazo [2,1-*b*]thiazoles or substituted thiazole imines **120**) using

dehydroepiandrosterone **117** (Scheme 12.29). The cytotoxicity of the synthesized compounds against EC-109 (human esophageal carcinoma), EC-9706 (human esophageal carcinoma), MGC-803 (human gastric carcinoma) was investigated [97].

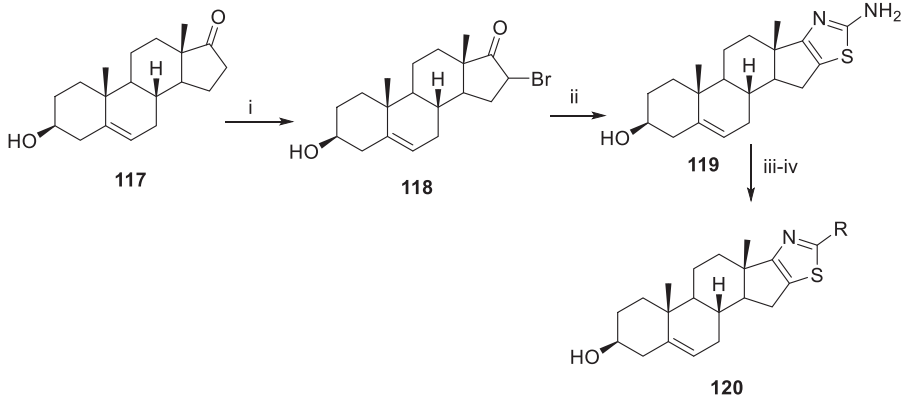

Scheme 12.29 *Reagent and conditions:* (i) $CuBr_2$, MeOH, reflux, (ii) thiourea, triethylamine, MeOH, (iii) aromatic aldehyde, K_2CO_3, EtOH/THF, and (iv) $NaBH_4$, MeOH, rt.

Shamsuzzaman et al. studied steroid-based compounds as anticancer agents. For example, 20-amino-30-cyanocholest-6-eno[5,7-de]4Hpyrans was used **122** (Scheme 12.30) [98].

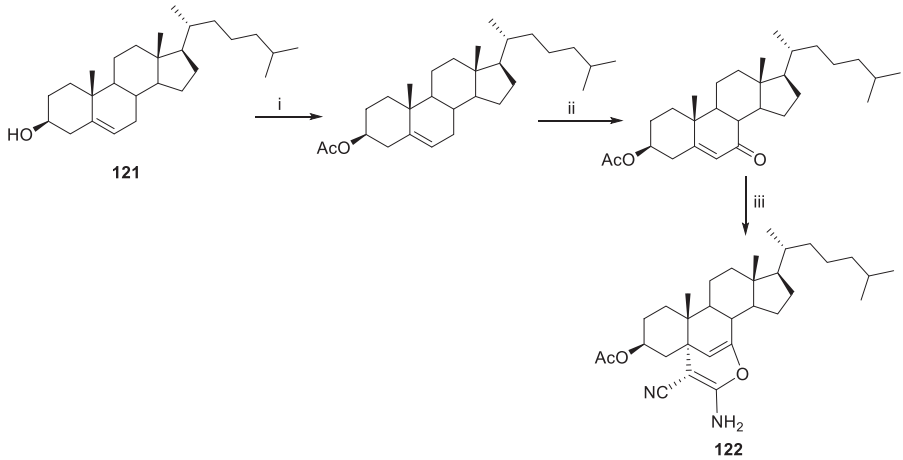

Scheme 12.30 *Reagent and conditions:* (i) Acetic anhydride, pyridine, (ii) t-butyl chromate, Ac_2O, CCl_4, and (iii) $CNCH_2CN$, piperidine, EtOH.

Ning-Juan et al. demonstrated the preparation of 21*E*-benzylidene-pregn-1,4-diene-3,20-dione **127** and 21*E*-benzylidene-4-chloro-pregn-1,4-diene-3,20-dione **126** derivatives from progesterone **123** (Scheme 12.31). These molecules were

screened for their anticancer activity against brine shrimp (*Artemia salina*) and murine Lewis lung carcinoma cells (LLCs) [99].

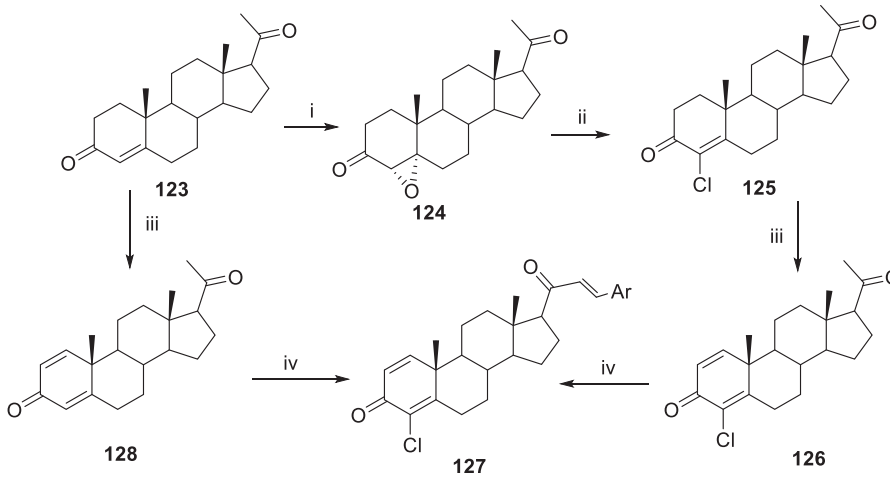

Scheme 12.31 *Reagent and conditions:* (i) H_2O_2, NaOH, MeOH-$CHCl_2$, (ii) conc. HCl, acetone, reflux, (iii) DDQ, TBDMSCl, dioxane, reflux, and (iv) benzaldehyde, EtOH-KOH.

Fan et al. prepared numerous steroidal C-17 pyrazolinyls **128** from progesterone **127** and tested their cytotoxic activity against brine shrimp and three human cancer cell lines (NCI-H460, HeLa, and HepG2) (Scheme 12.32) [100].

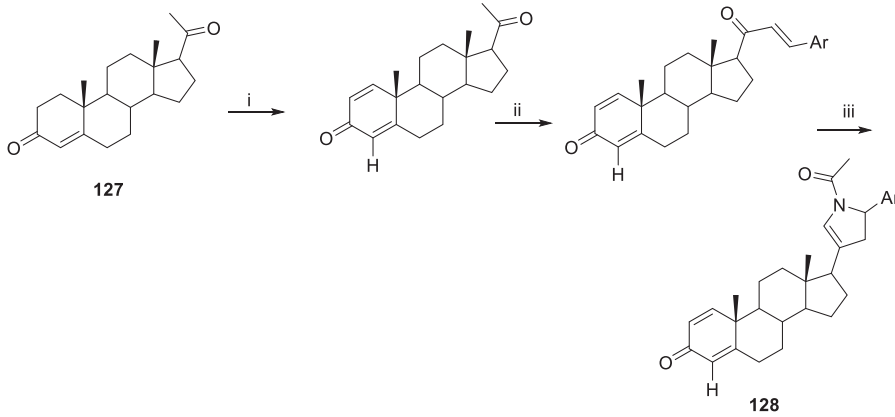

Scheme 12.32 *Reagent and conditions:* (i) H_2O_2/NaOH, MeOH/CH_2Cl_2, (ii) conc HCl/ acetone, reflux, 1 h, (iii) DDQ/TMDMSCl, dioxane, reflux, 2 h, (iv) ArCHO, KOH, EtOH, (v) NH_2NH_2, H_2O, ACOH, reflux, 2 h.

Carrilho et al. studied steroid dimers **130** by catalytic diaminocarbonylation of 17-iodo-5a-androst-16-ene **129** (Scheme 12.33). The dimeric molecules containing 17,17 0-dicarboxamide spacers were prepared through chemoselective processes [101].

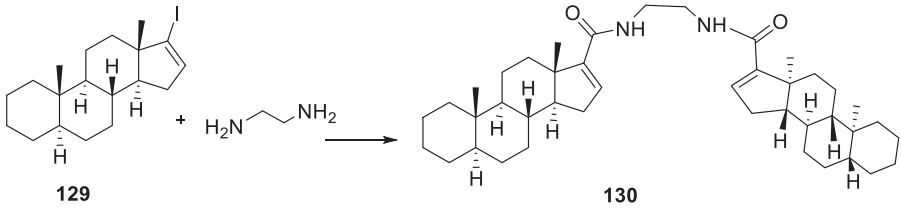

Scheme 12.33 *Reagent and conditions:* (i) CO, $Pd(OAc)_2/PPh_3$.

Shamsuzzaman et al. reported a simple method for the synthesis of ZnO nanoparticles for the preparation of steroidal pyrazolines **132** (Scheme 12.34). The synthesized ZnO nanoparticles were characterized by different types of spectroscopy [102].

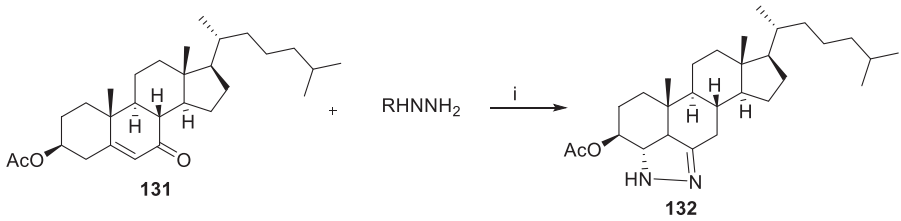

Scheme 12.34 *Reagent and conditions:* (i) ZnO nano, EtOH, reflux.

Waller et al. described a method for the preparation of steroid sulfates **134** (Scheme 12.35). These steroid sulfates are a type of metabolite [103].

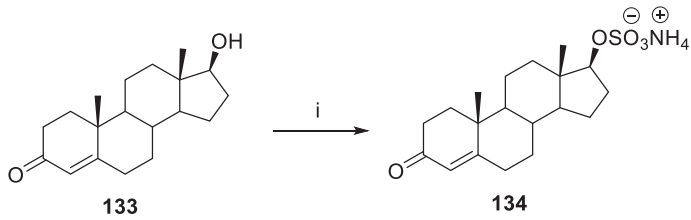

Scheme 12.35 *Reagent and conditions:* (i) SO_3.py, DMF, 1,4-dioxane, rt., 4 h and (ii) SPE.

Romero-Lopez et al. investigated an attractive method for the preparation of fused, substituted, and spiro pyrazoline steroids **137** and **138** via cycloaddition reaction (Scheme 12.36) [104].

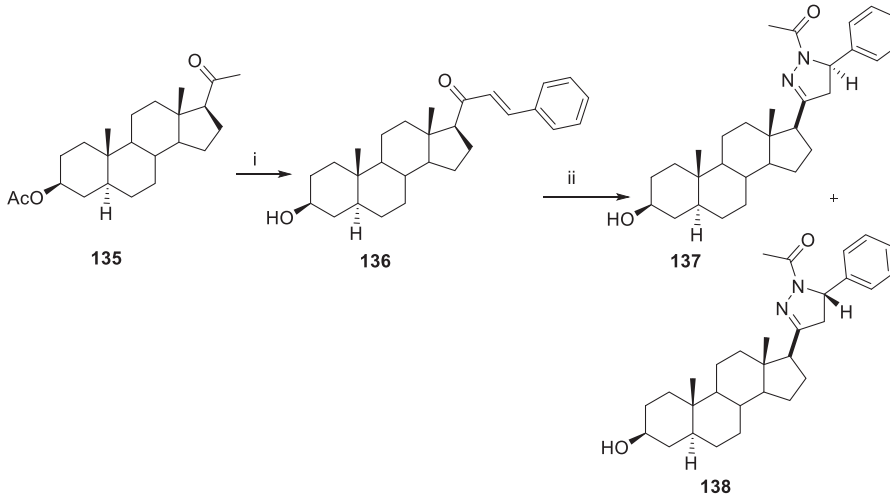

Scheme 12.36 *Reagent and conditions:* (i) EtOH, KOH, benzaldehyde and (ii) AcOH, hydrazine acetate, reflux.

Fustero et al. reported the Sonogashira cross-coupling method for the preparation of aminosteroids **140**. The Sonogashira reaction proceeded between haloaldehyde and trimethylsilylacetylene in the presence of Pd(dppf)Cl_2 and CuI as catalysts (Scheme 12.37). It was followed by the addition of an allyl zinc reagent to tert-butylsulfinimine. It was then completed through a Pauson-Khand reaction [105].

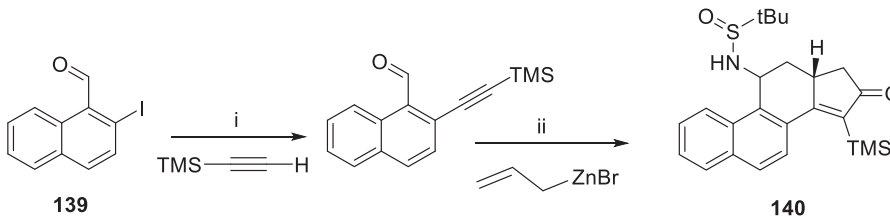

Scheme 12.37 *Reagent and conditions:* (i) $Pd(dpp)_2Cl_2$, CuI, Et_3N, THF, 80°C.

Zhang et al. reported a cascade reaction to prepare steroidal aniline derivatives **142** (Scheme 12.38). This method reported the creation of an aromatic ring and three continuous C—C bonds in a single step [106].

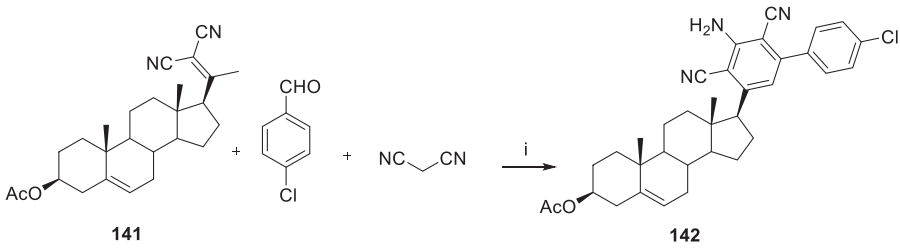

Scheme 12.38 *Reagent and conditions:* (i) (0.1 mmol), aldehydes (0.1 mmol), malononitrile (0.1 mmol), base (0.1 mmol), in solvent (3 mL) at r.t. for about 36 h.

Zhang et al. explored the preparation of steroidal 3-cyano-2-aminopyridines **145** by reacting enaminonitriles and amines (Scheme 12.39) [107].

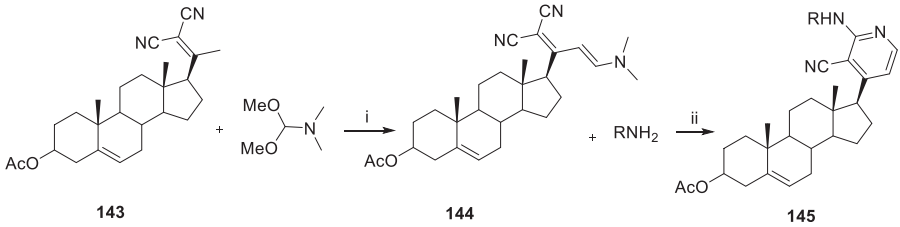

Scheme 12.39 *Reagent and conditions:* (i) Solvent free, rt., 2 h and (ii) solvent free, heat.

Arenas-González et al. prepared a number of steroidal [1,2,4]triazolo[1,5-*a*]pyrimidines (TPs) **150** (Scheme 12.40). These compounds were synthesized using α,β-unsaturated carbonyl compounds and 3-amino-1,2,4-triazole [108].

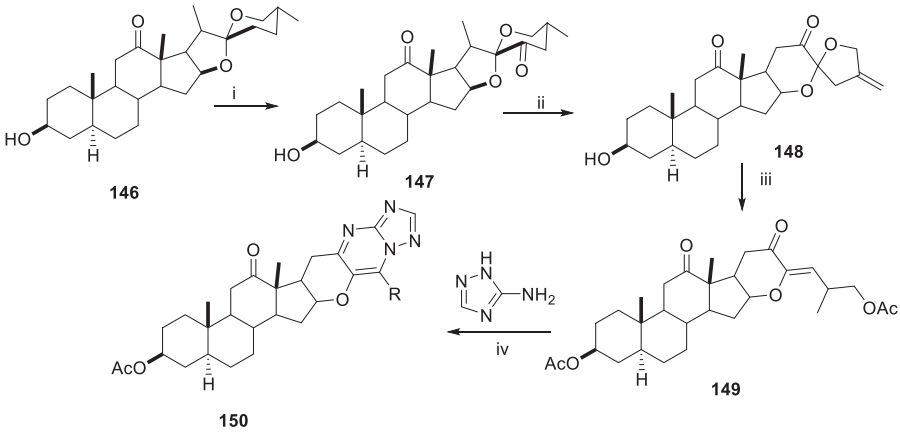

Scheme 12.40 *Reagent and conditions:* (i) CH_2COOH, BF_3 Et_2O, $NaNO_2$, Al_2O_3, (ii) TiCl4, CH_2Cl_2, (iii) Ac_2O, BF_3, Et_2O, CH_2Cl_2, and (iv) tBuOK, *n*-BuOH.

Gavaskar et al. developed a one-pot procedure for the synthesis of steroidal dispiroindenoquinoxaline pyrrolidines **151** using multicomponent [3+2] reaction of azomethine ylides in ionic liquid (Scheme 12.41) [109].

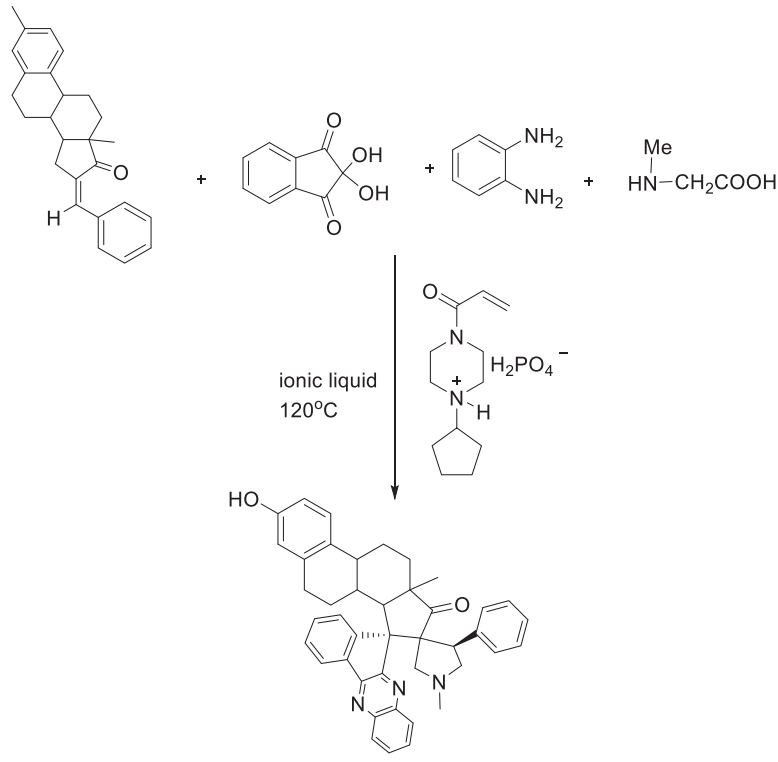

151

Scheme 12.41 Synthesis of steroidal spiro-indenoquinoxaline-pyrrolidines.

Rassokhina et al. reported the synthesis of steroidal imidazo[1,2-*a*]pyridine hybrids **153**. Thus, androstene and estrane series containing imidazo[1,2-*a*]pyridine motifs were synthesized from 17-ethynyl steroids **152** by copper-catalyzed cascade aminomethylation/cycloisomerization with imines **151** (Scheme 12.42). The resulting molecules were tested for cytotoxicity against numerous human breast (MCF-7, MDA-MB-231, HBL-100, MDA-MB-453) and prostate (LNCaP-LN3, PC-3, DU 145) cancer cell lines. Most of the compounds demonstrated activities at μM level [110].

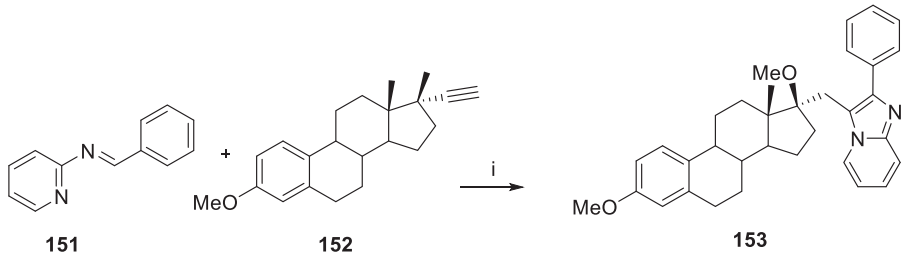

Scheme 12.42 *Reagent and conditions*: (i) $Cu(OTf)_2$, CuOTf, C_6H_6, toluene, 120°C.

Mayorquín-Torres et al. investigated the preparation of benzannulated steroid spiroketals **158**, **159** following Sonogashira coupling as one of the key steps (Scheme 12.43) [111].

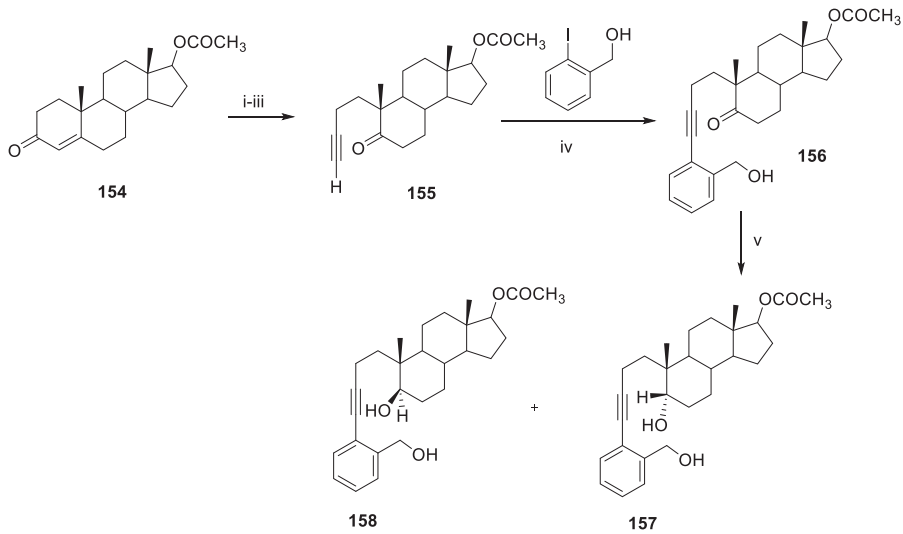

Scheme 12.43 *Reagent and conditions:* (i) H_2O_2, NaOH, CH_2Cl_2/MeOH, (ii) Ac_2O/Py, (iii) NH_2NHTS, CH_2Cl_2/AcOH, (iv) $Pd(PPH_3)_4$, Et_3N, CuI, and (v) $NaBH_4$, MeOH, $Pd(CH_3CN)_2Cl_2$, CH_3CN, rt. 24 h.

Enríquez et al. reported the preparation of steroid dimers **161**, **162** by $BF_3{\cdot}Et_2O$-induced aldol condensation of 2-formyl-estradiol diacetate **160** and sapogenins **161** (Scheme 12.44). The reaction proceeded through an exocyclic alkene group present in C-23 or through a spiro present in C-22 [112].

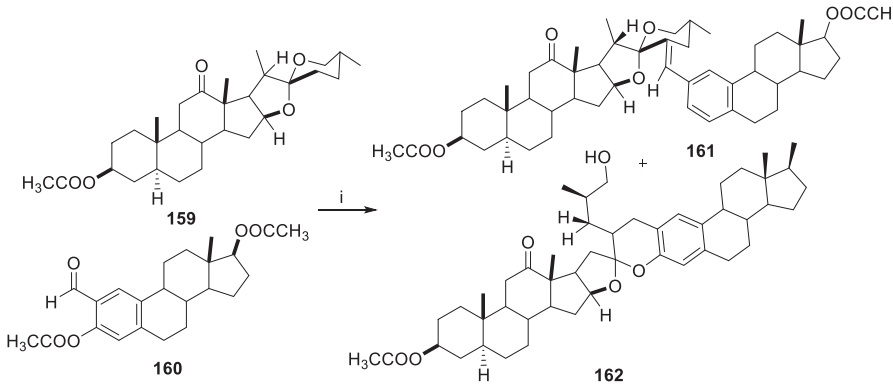

Scheme 12.44 *Reagent and conditions:* (i) $BF_3.Et_2O$, CH_2Cl_2.

Joppa et al. reported the Suzuki-Miyaura process of 16-*E*-(triflyloxymethylidene)-3-methoxy-estrone **163** for the preparation of 16-*E*-(arylidene)-3-methoxy-estrones **164** (Scheme 12.45) [113].

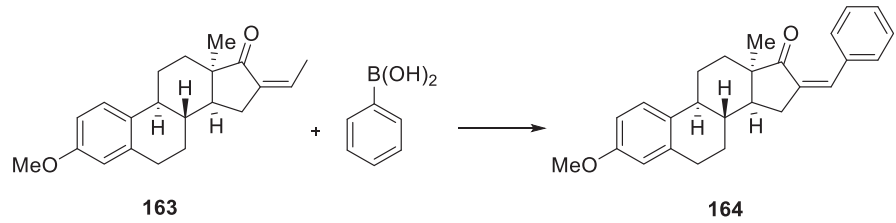

Scheme 12.45 *Reagents and conditions:* $Pd(OAc)_2$, *n*$BuPAd_2$, K_3PO_4, phenylboronic acid, toluene.

Song et al. studied pyridine heterocycles and their antitumor activity by molecular docking software (Scheme 12.46). The molecules were prepared in a one-pot multicomponent process and the resulting compounds were tested in vitro for their anticancer properties [114].

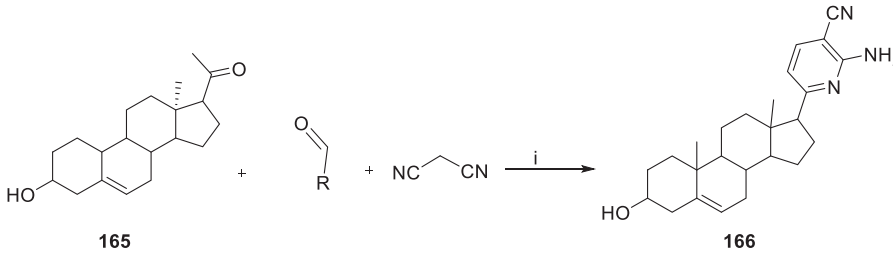

Scheme 12.46 *Reagent and conditions*: (i) CH_3COONH_4, EtOH.

Dara et al. prepared steroidal imidazolidinthiones **168** from steroidal thiosemicarbazones **167** (Scheme 12.47) [115].

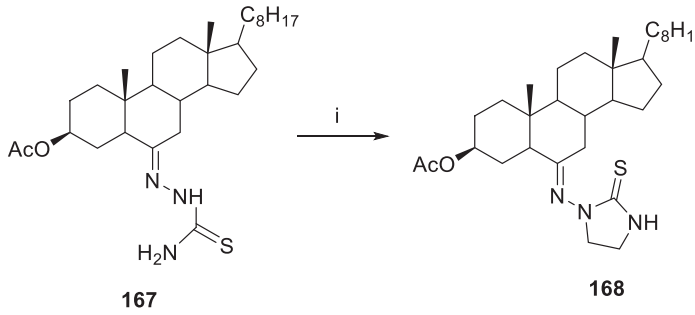

Scheme 12.47 *Reagent and conditions:* (i) CH_2ClCH_2Cl, AcONa, EtOH, reflux.

Sethi et al. reported *N*-methyl-2-pyrolidonehydrogensulphate (NMP + HSO_4-)-catalyzed synthesis of diosgenin prodrugs **170** (Scheme 12.48). The yield of the process was high. Diosgenin along the prodrugs were tested against anticancer activity and apoptosis by MTT assay and ethidium bromide/acridine orange (EB/AO). These compounds were active against prostate cancer [116].

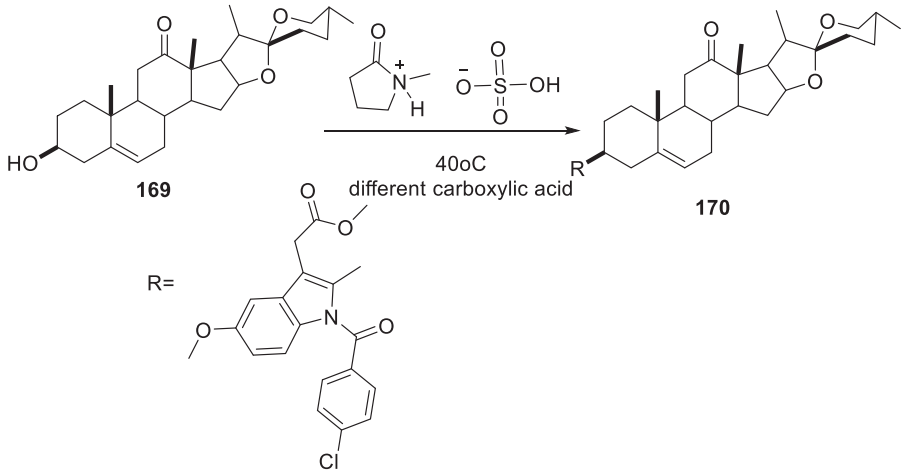

Scheme 12.48 Synthesis of diosgenin prodrugs.

Hryniewicka prepared steroid-based imidazolium salts which have demonstrated interesting biological activities including antitumor and antimicrobial properties (Scheme 12.49). The activity was against *Candida albicans* was very good. A few of these salts exhibited antifungal activities against phytopathogenic organisms: *Botrytis cinerea* and *Cercospora beticola* [117].

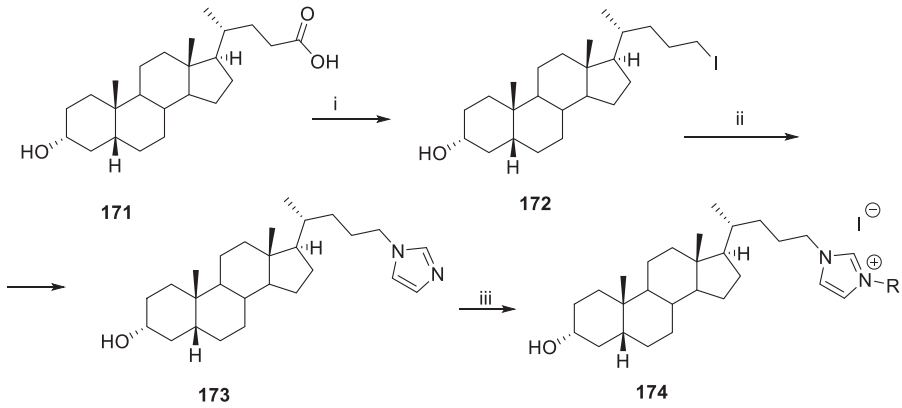

Scheme 12.49 *Reagent and conditions:* (i) $LiAlH_4$, P-TsCl, Et_3N, THF, NaI, acetone, (ii) imidazole, MaH, THF, and (iii) RI.

Hanson et al. investigated fluorescent imaging agents for the preparation of steroidal antiestrogens, 11β-(4-oxyphenyl)estradiol **180** (Scheme 12.50). The molecules were anticipated based on the affinity and selectivity of 11β-[4-(dimethylethoxy) phenyl]estradiol (RU39411) as an ER antagonist. The 5-(dimethylamino) naphathalene-

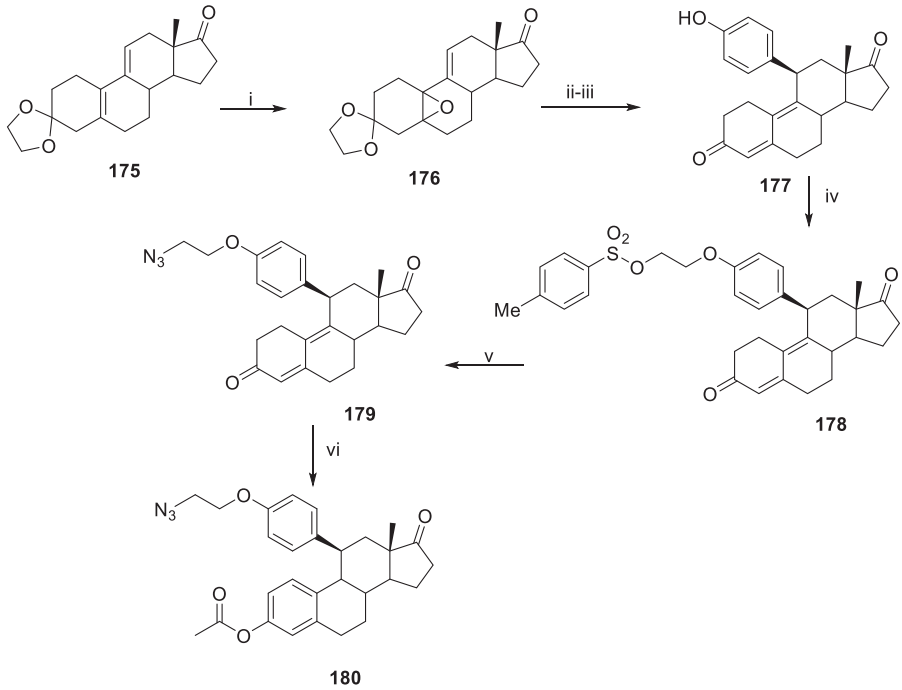

Scheme 12.50 *Reagent and conditions:* (i) CF_3COCF_3, H_2O_2, pyridine, CH_2Cl_2, (ii) 4-bromophenoxy trimethylsilane, Mg, CuI, THF, rt., NH_4Cl, (iii) $CH_3CO_2H.H_2O$, (iv) $TsOCH_2CH_2OTs$, Cs_2CO_3, CH_3CN, (v) NaN_3, ethanol, reflux, and (vi) acetic anhydride, CH_3COBr, CH_2Cl_2, rt.

1-sulfonyl (dansyl) and 7-nitrobenzo[*c*][1,2,5] oxadiaol-4-yl (NBD) components were chosen because of their fluorescent and physicochemical characteristics. A convergent preparation was performed through [3+2] copper(I)-assisted alkyne-azide cycloaddition reaction of the steroidal and fluorescent compounds. The steroid part may be used to evaluate their ER affinity and selectivity [118].

12.6 Conclusion

In this chapter, the authors have updated the knowledge of important biologically active steroids through their facile green synthetic route. Many of the synthesis described herein are convergent and highly efficient. The synthetic steps require necessary reagents and solvents to prepare these molecules with complete stereo control. Importantly, this chapter suggests the vast importance of steroids in medicinal chemistry and clinical science. Clearly, the medical benefits of these steroids are so significant that one can extrapolate their properties in diverse health disorders. Although many claims that drug discovery should be performed by modern techniques (e.g., computer-based drug design). However, many of the molecules described here were chosen without advancing any modern concepts. Nevertheless, important molecules were prepared. Probably, steroid skeletons have something special that many scientists ignore. It is believed that additional sustainable approaches will be undertaken to prepare steroids that may demonstrate clinically useful medicinal agents.

Acknowledgments

Bimal Krishna Banik (BKB) is grateful to the USA NIH, USA NCI, and USA Private Research Foundation. BKB also thanks Prince Mohammad Bin Fahd University for encouragement. PB acknowledges support from the Director of CSIR-Central Scientific Instruments Organization, Chandigarh.

References

[1] H. Rosen, V. Glukhman, T. Fildmann, E. Lichtstein, D. Lichtstein, Mol. Biol. Cell 15 (2004) 1044.
[2] R.A. Hill, H.L. Makin, D.N. Kirk, G.M. Murphy, Dictionary of Steroids, Chapman and Hall, London, GBR, 1991. ISBN 978-0412270604, Retrieved 20 June 2015.
[2a] A. Rasheed, M. Qasim, A review of natural steroids and their applications, Int. J. Pharm. Sci. Res. 4 (2) (2012) 520–531.
[3] D.S. Bhakuri, D.S. Rawat, Bioactive Marine Natural Products, Anamaya Publishers, 2005.
[4] (a) J.P. Guthrie, S. O'Leary, Can. J. Chem. 53 (1975) 2150. (b) H. Dugas, I.O. Malika, L. Rocheblave, Steroids 73 (2008) 375.
[5] (a) J.W. Morzycki, I. Wawer, A. Gryszkiewicz, I. Maj, L. Siergiejczyk, A.B. Zaworska, Steroids 67 (2002) 621. (b) J.W. Morzycki, Polish J. Chem. 69 (1995) 321.
[6] M.P. St-Onge, B. Lamarche, J.F. Mauger, P.J. Jones, Consumption of a functional oil rich in phytosterols and medium-chain triglyceride oil improves plasma lipid profiles in men, J. Nutr. 133 (2003) 1815–1820.

[7] R.C. Melcangi, I. Azcoitia, M. Ballabio, I. Cavarretta, L.C. Gonzalez, Neuroactive steroids influence peripheral myelination: a promising opportunity for preventing or treating age-dependent dysfunctions of peripheral nerves, Prog. Neurobiol. 71 (2003) 57–66.
[8] R. Bucourt, L. Nedelec, J.C. Gasc, J. Weill-Raynal, Symmetry, Bull. Soc. Chim. Fr. 561 (1969).
[9] R. Aav, T. Kanger, T. Pehk, M. Lopp, Unexpected reactivity of ethyl 2-(diethylphosphono) propionate toward 2,2-disubstituted-,3-cyclopentanediones, Phosphorus Sulfur Silicon Relat. Elem. 180 (2005) 1739–1748.
[10] W.E. Bachmann, W. Cole, A.L. Wilds, Total synthesis of the sex hormone equilenin and its stereoisomers, J. Am. Chem. Soc. 62 (4) (1940) 824–839.
[11] R.B. Woodward, F. Sondheimer, D. Taub, K. Heusler, W.M. McLamore, The total synthesis of steroids, J. Am. Chem. Soc. 74 (17) (1952) 4223–4251.
[12] R.J. Chein, E.J. Corey, Conversion of Torgov's synthesis of estrone into a highly enantioselective and efficient process, J. Am. Chem. Soc. 129 (34) (2007) 10346–10347.
[13] M. Weimar, G. Dürner, J.W. Bats, M.W. Göbel, Enantioselective synthesis of (+)-estrone exploiting a hydrogen bond-promoted Diels-Alder reaction, J. Org. Chem. 75 (8) (2010) 2718–2721.
[14] L.H. Sarett, G.E. Arth, R.M. Lukes, R.E. Beyler, G.I. Poos, W.F. Johns, J.M. Constantin, Stereospecific total synthesis of cortisone, J. Am. Chem. Soc. 74 (19) (1952) 4974–4976.
[15] P. Morgan, S.M. Melinda, Kirk Othmer Encyclopedia of Chemical Technology, vol. 4, John Wiley & Sons, 1997, p. 2000.
[16] IUPAC Nomenclature of Steroids Revised Tentative Rules, Arch. Biochem. Biophys. 136 (1967) 13.
[17] International Union of Biochemistry, Biochemical Nomenclature and Related Documents, The Biochemical Society, London, 1978.
[18] Rene L, Karine C, Salwa R, Stanislas V, Anne-Sophie F, et al. (2014) US2014309203A1.
[19] IUPAC, Nomenclature of Organic Chemistry, Sections A, B, C, D, E, F and H, 1979 ed., Pergamon Press, Oxford, 1979.
[20] K.B.G. Torrsell, Natural Product Chemistry, second ed., Apotekarsocieteten Ed, Kristianstads Boktryckeri/Stockholm, 1997, p. 292.
[21] W.L. Miller, Med. Prin. Pract. 14S (2005) 158.
[22] C.S. Thummel, J. Chory, Steroid signaling in plants and insects-common themes, different pathways, Genes Dev. 16 (2002) 3113–3129.
[23] N.S. Chermnykh, N.L. Shimanovskia, G.V. Shutko, V.N. Syrov, The action of methandrostenolone and ecdysterone on the physical endurance of animals and on protein metabolism in the skeletal muscles, Farmakol. Toksikol. 51 (1988) 57–60.
[24] D.S. Trenin, V.V. Volodin, 20-hydroxyecdysone as a human lymphocyte and neutrophil modulator: in vitro evaluation, Arch. Insect Biochem. Physiol. 41 (1999) 156–161.
[25] R.A. Werner, Massage Therapist's Guide to Pathology, third ed., Lippincott Williams & Wilkins, PA, USA, 2005.
[26] M.B. Ranke, J.R. Bierich, Treatment of growth hormone deficiency, Clin. Endocrinol. Metab. 15 (1986) 495–510.
[27] J.R. Berger, L. Pall, C.D. Hall, D.M. Simpson, P.S. Berry, Oxandrolone in AIDS-wasting myopathy, AIDS 10 (1996) 1657–1662.
[28] E.T. Schroeder, A.F. Vallejo, L. Zheng, Y. Stewart, C. Flores, Six-week improvements in muscle mass and strength during androgen therapy in older men, J. Gerontol. A Biol. Sci. Med. Sci. 60 (2005) 1586–1592.

[29] R.E. Olson, Discovery of the lipoproteins, their role in fat transport and their significance as risk factors, J. Nutr. 128 (1998) 439S–443S.
[30] G.D. Brown, The biosynthesis of steroids and triterpenoids, Nat. Prod. Rep. 15 (1998) 653–696.
[31] F. Lebideau, A. Percz, J. Marrot, M.N. Rager, E. Stephan, Tetrahedron 57 (2001) 3939.
[32] A. Murugkar, B. Unnikrishnan, S. Padhye, R. Bhonde, S. Teat, Hormone anchored metal complexes. 1. Synthesis, structure, spectroscopy and in vitro antitumor activity of testosterone acetate thiosemicarbazone and its metal complexes, Metal-Based Drugs 6 (1999) 177–182.
[33] U. Leuscher, Falk Symp. (Immunol. Liver) 114 (2000) 338.
[34] M. de la Torre, E. Peña, M. Calvin, C. Miguélez, D. González, et al., Basiliximab in lung transplantation: preliminary experience, Transplant. Proc. 37 (2005) 1534–1536.
[35] A. Jackson, J. Davis, R.J. Pither, A. Rodger, M.J. Hannon, Estrogen-derived steroidal metal complexes: agents for cellular delivery of metal centers to estrogen receptor-positive cells, Inorg. Chem. 40 (2001) 3964–3973.
[36] D. Bassler, Inhalation or instillation of steroids for the prevention of bronchopulmonary dysplasia, Neonatology 107 (2015) 358–359.
[37] L.L. Smith, Another cholesterol hypothesis: cholesterol as antioxidant, Free Radic. Biol. Med. 11 (1991) 47–61.
[38] M.S. Chadha, J. Biol. Phys. 20 (1994) 95.
[39] D.M. Harrison, Nat. Prod. Rep. 2 (1985) 543.
[40] S. Coopman, H. Degreef, A. Dooms-Goossens, Identification of cross-reaction patterns in allergic contact dermatitis from topical corticosteroids, Br. J. Dermatol. 121 (1989) 27–34.
[41] T.H. Haines, Do sterols reduce proton and sodium leaks through lipid bilayers? Prog. Lipid Res. 40 (2001) 299–324.
[42] G. Pinna, E. Costa, A. Guidotti, Fluoxetine and norfluoxetine stereospecifically and selectively increase brain neurosteroid content at doses that are inactive on 5-HT reuptake, Psychopharmacology 186 (2006) 362–372.
[43] S. Roberts, Anabolic Pharmacology (2009).
[44] S.N. Roy, S. Bhattacharya, Drug Safety: Int. J. Med. Toxicity Drug Exp. 27 (2004) 75.
[45] P. Diel, A. Friedel, H. Geyer, M. Kamber, U. Laudenbach-Leschowsky, Characterisation of the pharmacological profile of desoxymethyl testosterone (Madol), a steroid misused for doping, Toxicol. Lett. 169 (2007) 64–71.
[46] R.E. Ostlund, S.B. Racette, W.F. Stenson, Inhibition of cholesterol absorption by phytosterol-replete wheat germ compared with phytosterol-depleted wheat germ, Am. J. Clin. Nutr. 77 (2003) 1385–1389.
[47] E. De Stefani, P. Boffetta, A.L. Ronco, P. Brennan, H. Deneo-Pellegrini, Plant sterols and risk of stomach cancer: a case-control study in Uruguay, Nutr. Cancer 37 (2000) 140–144.
[48] M. Szekeres, K. Nemeth, Z. Koncz-Kalman, J. Mathur, A. Kauschmann, Brassinosteroids rescue the deficiency of CYP90, a cytochrome P450, controlling cell elongation and de-etiolation in Arabidopsis, Cell 85 (1996) 171–182.
[49] S. Takatsuto, J. Chromatogr. 658 (1994) 3.
[50] R. Liu, L.W. Faming, Shoumingshu ZSG 1 (2002) 167.
[51] D.B. Gower, in: H.J.L. Makin (Ed.), Biochemistry of Steroid Hormones, Blackwell Scientific Publications, London, 1984, p. 117.
[52] R.E. Counsell, V.V. Ranade, R.J. Blair, W.H. Beierwaltes, P.A. Weinhold, Steroids (1970) 317.

[53] G. Silvia, R. Simone, P. Marzia, C. Gaia, M. Nico, Neuroactive steroids and the peripheral nervous system: an update, Steroids (2015).
[54] Blizzard TA, Gude CM, Jerry A. (2005) WO 5,972.
[55] K. Fotherby, in: H.J.L. Makin (Ed.), Biochemistry of Steroid Hormones, vol. 207, Blackwell Scientific Publications, London, 1984.
[56] J. Dopseso, E. Quinoa, R. Riguera, C. Debitus, P.R. Bergquist, Tetrahedron 50 (1994) 3818.
[57] H. He, P. Kulanthaivel, B.J. Baker, K. Kalter, J. Darges, Tetrahedron 51 (1995) 51.
[58] Schwarz S, Mueller G, Osemund D, Richter M, Petus O, (2003) US 65,83,130.
[59] A. Migliuolo, V. Piccialli, D. Sica, Two new 9, 11-secosterols from the marine sponge *Spongia officinalis*. Synthesis of 9, 11-seco-3 beta, 6 alpha, 11-trihydroxy-5 alpha-cholest-7-en-9-one, Steroids 57 (1992) 344–347.
[60] D.V. Banthorpe, Natural Products: Their Chemistry and Biological Significance, first ed., Longman Scientific and Technical, Essex 289, 1994.
[61] A.T. Vieira, V. Pinho, L.B. Lepsch, C. Scavone, I.M. Ribeiro, Mechanisms of the anti-inflammatory effects of the natural secosteroids physalins in a model of intestinal ischaemia and reperfusion injury, Br. J. Pharmacol. 146 (2005) 244–251.
[62] M.T. Delvin, Text Book of Biochemistry With Clinical Correlations, fifth ed., Oxford University Press, Oxford, UK, 2002.
[63] P. Sharma, R. Bhardwaj, H.K. Arora, N. Arora, Biol. Plant. 52 (2008) 767.
[64] X.J. Xia, Y. Zhang, J.X. Wu, J.T. Wang, Y.H. Zhou, Brassinosteroids promote metabolism of pesticides in cucumber, J. Agric. Food Chem. 57 (2009) 8406–8413.
[65] N. Sondhi, R. Bhardwaj, S. Kaur, B. Singh, N. Kumar, Plant Growth Regul. 54 (2008) 217.
[66] Biggadike K, Morton GE, (2003) WO 0362,259.
[67] S. Mellon, W. Gong, L.D. Griffin, Niemann pick type C disease as a mode for defects in neurosteroidogenesis, Endocr. Res. 30 (2004) 727–735.
[68] E. Meggers, Exploring biologically relevant chemical space with metal complexes, Curr. Opin. Chem. Biol. 11 (2007) 287–292.
[69] V.S. Enev, J. Mohr, M. Harre, K. Nikisch, Tetrahedron Asymmetry 9 (1998) 2693.
[70] C. Schopf, K. Koch, Liebigs Ann. Chem. 552 (1942) 37.
[71] V. Philomin, A. Vessieres, M. Gruselle, G. Jaouen, Synthesis of cobalt carbonyl complexes of cortisol and testosterone. Study of their recognition by specific polyclonal antibodies, Bioconjug. Chem. 4 (1993) 419–424.
[72] L. Cano-Lerida, P. Walton, M. Rose, J. Tarbin, PCT Int. Appl. 1 (2005) 74.
[73] M. Simon, K.J. Harwood, J. Toyne, W. Goodby, P. Michael, The synthesis of 3α/3β-cholesteryl and cholestanyl esters and ethers—an assessment of their mesogenicity, Mol. Cryst. Liq. Cryst. 332 (1999) 485–495.
[74] L.G. Sevillano, E. Caballero, F. Tome, M. Medarde, A. San Feliciano, Tetrahedron 58 (2002), 10103.
[75] S.K. Kang, K.Y. Jung, C.H. Park, E.Y. Namkoong, T.H. Kim, Palladium-catalyzed arylation of allylic diols-highly selective synthesis of phenyl-substituted allylic diols, Tetrahedron Lett. 36 (1995) 6287–6290.
[76] F. De Riccardis, I. Izzo, C. Tedesco, G. Sodano, Synthesis and cytotoxic activity of steroid-anthraquinone hybrids, Tetrahedron 53 (1997) 10871–10882.
[77] Z. Szarkaa, R. Skoda-Foldesa, J. Horvath, Z. Tuba, L. Kolla, Synthesis of steroidal diacyl hydrazines and their 1,3,4-oxadiazole derivatives, Steroids 67 (2002) 581–586.
[78] L.F. Tietze, J.M. Wiegand, C. Vock, Synthesis of enantiopure B-nor-steroids by multiple Pd-catalyzed transformations, J. Organomet. Chem. 687 (2003) 346–352.

[79] S.M. Wang, W.Z. Gea, H.M. Liu, D.P. Zoua, X.B. Yan, Syntheses of acetylated steroid glycosides and selective cleavage of O-acetyl groups in sugar moiety, Steroids 69 (2004) 599–604.
[80] C.E. Saraber, A. Groot, New flexible synthesis of (D-homo) steroids florence, Tetrahedron Lett. 45 (2004) 9431–9433.
[81] P. Chowdhury, A.M. Das, P. Goswami, Synthesis of some new steroidal [16,17-d]-isoxazolines, Steroids 70 (2005) 494–498.
[82] H.W. Sünnemann, A. Hofmeister, J. Magull, A. de Meijere, An efficient access to novel enantiomerically pure steroidal D-amino acids, Chem. Eur. J. 12 (2006) 8336–8344.
[83] P. Bazzini, M.I. Ouali, H. Pellissier, M. Santelli, Efficient synthesis of C-11 functionalized steroids, 71 (2006) 459–468.
[84] J.Z. Yan, J. Li, G.W. Rao, One-pot synthesis of new A-ring fused steroidal pyridines, Steroids 72 (2007) 736–739.
[85] M.N. Sakac, A.R. Gakovic, J.J. Csanádi, E.A. Djurendic, O. Klisuric, V. Kojic, G. Bogdanovic, K.M.P. Gasi, An intramolecular one-pot synthesis of steroidal triazoles via 1,3-dipolar cycloadditions of in situ generated diazo compounds, Tetrahedron Lett. 50 (2009) 4107–4109.
[86] V. Foucher, B. Guizzardi, M.B. Groen, M. Light, B. Linclau, A novel, versatile D BCD steroid construction strategy, illustrated by the enantioselective total synthesis of estrone, Org. Lett. 12 (2010) 680–683.
[87] V. Richmonda, G.A. Garrido Santosa, A.P. Murray, M.S. Maier, Synthesis and acetylcholinesterase inhibitory activity of 2β, 3α-disulfoxy-5α-cholestan-6-one, Steroids 76 (2011) 1160–1165.
[88] Y. Huang, J. Cui, S. Chen, C. Gan, A. Zhou, Synthesis and antiproliferative activity of some steroidal lactams, Steroids 76 (2011) 1346–1350.
[89] K.Q. Shawakfeh, N.H. Al-Said, Synthesis of new symmetrical bis-steroidal pyrazine analogues from diosgenin, Steroids 76 (2011) 232–237.
[90] S.A. Khan, A.M. Asiri, Synthesis of novel steroidal oxazolo quinoxaline as antibacterial agents, Arab. J. Chem. 4 (2011) 349–354.
[91] M. Ibrahim-Ouali, E. Romero, K. Hamze, Stereoselective synthesis of pentacyclic steroids functionalized at C-11, Steroids 77 (2012) 1092–1100.
[92] M.A. Fernández-Herrera, H. López-Muñoz, J.M.V. Hernández-Vázquez, L. Sánchez-Sánchez, M.L. Escobar-Sánchez, B.M. Pinto, J. Sandoval-Ramírez, Synthesis and selective anticancer activity of steroidal glycoconjugates, Eur. J. Med. Chem. 54 (2012) 721–727.
[93] M. Ibrahim-Ouali, E. Romero, Synthesis and characterization of (±)-13-hydroxy-3, 11-diaza steroids, Steroids 77 (2012) 157–167.
[94] P.J. Wölfling, I. Kovács-Pénzes, G. Zupko, S.E. Frank, Synthesis, stereochemistry and cytotoxic activity of novel steroidal 16-spiro-1,3,2-dioxaphosphorinanes, J. Mol. Struct. 1013 (2012) 39–44.
[95] R. Bansal, S. Guleria, S. Thota, S.L. Bodhankar, M.R. Patwardhan, C. Zimmer, R. W. Hartmann, A.L. Harvey, Design, synthesis and evaluation of novel 16-imidazolyl substituted steroidal derivatives possessing potent diversified pharmacological properties, Steroids 77 (2012) 621–629.
[96] K. Nickisch, B. Hareesh, N. Nair, B. Kesavaram, R. Das, S.Q. Garfield, S.S. Shi, S. L. Bhaskaran, D.P. Grimm Edwards, Synthesis and antiprogestational properties of novel 17-fluorinated steroids, Steroids 78 (2013) 909–919.
[97] B.L. Zhang, E. Zhang, L.P. Pang, L.X. Song, Y.F. Li, B. Yu, H.M. Liu, Design and synthesis of novel D-ring fused steroidal heterocycles, Steroids 78 (2013) 1200–1208.

[98] A.M. Shamsuzzaman, D.Y. Khan, A. Sohail, Synthesis and biological studies of steroidal pyran based derivatives, J. Photochem. Photobiol. B Biol. 129 (2013) 36–47.
[99] F. Ning-Juan, B. Yu-Bin, Z. Fei-Yu, L. Bo, T. Jiang-Jiang, Z. Qiang-Zhe, G. Jin-Ming, Synthesis and cytotoxicity of some novel 21E-benzylidene steroidal derivatives, Steroids 78 (2013) 874–879.
[100] N.J. Fan, J.J. Tang, H. Li, X.J. Li, B. Luo, J.M. Gao, Synthesis and cytotoxic activity of some novel steroidal C-17 pyrazolinyl derivatives, Eur. J. Med. Chem. 69 (2013) 182–190.
[101] R.M.B. Carrilho, M.M. Pereira, M.J.S.M. Moreno, A. Takácsc, L. Kollár, A new facile synthesis of steroid dimers containing 17,170-dicarboxamide spacers, Tetrahedron Lett. 54 (2013) 2763–2765.
[102] Shamsuzzaman, A. Mashrai, H. Khanam, R.N. Aljawfi, Biological synthesis of ZnO nanoparticles using *C. albicans* and studying their catalytic performance in the synthesis of steroidal pyrazolines, Arab. J. Chem. 10 (2013) S1530–S1536.
[103] C.C. Waller, M.D. McLeod, A simple method for the small scale synthesis and solid-phase extraction purification of steroid sulphates, Steroids 92 (2014) 74–80.
[104] A. Romero-Lopez, S. Montiel-Smith, S. Meza-Reyes, P. Merino-Montiel, J.L. Vega-Baez, Synthesis of steroidal derivatives containing substituted, fused and spiro pyrazolines, Steroids 87 (2014) 86–92.
[105] S. Fustero, R. Lázaro, N. Aiguabella, A. Riera, A. Simon-Fuentes, P. Barrio, Asymmetric allylation/Pauson Khand reaction: a simple entry to polycyclic amines. Application to the synthesis of aminosteroid analogues, Org. Lett. (2014) 161224–161227.
[106] Y.L. Zhang, Y.F. Li, Y.K. Shi, B. Yu, G.C. Zhang, P.P. Qi, D.J. Fu, L.H. Shan, H.M. Liu, Efficient three-component one-pot synthesis of steroidal polysubstituted anilines, Steroids 104 (2015) 1–7.
[107] Y.L. Zhang, Y.F. Li, X.L. Shi, B. Yu, Y.K. Shi, H.M. Liu, Solvent-free synthesis of novel steroidal 2-aminopyridines, Steroids 115 (2016) 147–153.
[108] A. Arenas-González, L. Antonio Mendez-Delgado, P. Merino-Montiel, J.M. Padron, S. Montiel-Smith, J.L. Vega-Báez, S. Meza-Reyes, Synthesis of monomeric and dimeric steroids containing [1,2,4]triazolo [1,5a]pyrimidines, Steroids 116 (2016) 13–19.
[109] D. Gavaskar, A.R. Suresh Babu, R. Raghunathan, M. Dharani, S. Balasubramanian, An expedient sequential one-pot four component synthesis of novel steroidal spiro-pyrrolidine heterocycles in ionic liquid, Steroids 109 (2016) 1–6.
[110] I.V. Rassokhina, Y.A. Volkova, A.S. Kozlov, A.M. Scherbakov, O.E. Andreeva, V. Z. Shirinian, I.V. Zavarzin, Synthesis and antiproliferative activity evaluation of steroidal imidazo[1,2-a]pyridines, Steroids 113 (2016) 29–37.
[111] M.C. Mayorquín-Torres, M. Flores-Álamo, M.A. Iglesias-Arteaga, Synthesis of benzannulated steroid spiroketals by palladium-catalyzed spirocyclization of steroid alkynediols, Tetrahedron Lett. 58 (2017) 2073–2076.
[112] M.A. Ramos-Enríquez, M.A. Iglesias-Arteaga, Synthesis of novel hybrid steroid dimers by $BF_3{\cdot}Et_2O$-catalyzed aldol condensation of 2-formyl-estradiol diacetate and steroid sapogenins, Steroids 128 (2017) 46–49.
[113] S. Joppa, M. Lieseganga, P. Ehlersa, E. Frank, G. Schneider, J. Wolfling, P. Langer, Synthesis of novel 16-E-(arylidene)-3-methox-a-estrones via a palladium catalysed Suzuki-Miyaura reaction, Tetrahedron Lett. 59 (2017) 26–28.
[114] Y.L. Song, C.-P. Tian, Y. Wu, L.H. Jiang, L.Q. Shen, Design, synthesis and antitumor activity of steroidal pyridine derivatives based on molecular docking, Steroids 143 (2019) 53–61.

[115] A. Mahmood Dara, R. Nabic, S. Mird, M. Ahmad Gatooe, Shamsuzzamana, S.H. Lonef, Synthesis of steroidal imidazolidinthiones as potential apoptotic agents: investigation by theoretical and experimental studies, Bioorg. Chem. 79 (2018) 190–200.
[116] A. Sethi, P. Singh, N. Yadav, P. Yadav, M. Banerjee, R.P. Singh, Greener approach for synthesis of novel steroidal prodrugs using ionic liquid, their DFT study and apoptosis activity in prostate cancer cell line, J. Mol. Struct. 1180 (2019) 733–740.
[117] A. Hryniewicka, M. Malinowska, K. Hauschild, T. Pieczul, J.W. Morzyckia, Synthesis and antimicrobial properties of steroid-based imidazolium salts, J. Steroid Biochem. Mol. Biol. 189 (2019) 65–72.
[118] R.N. Hanson, N. Gajadeera, Design and synthesis of fluorescently labeled steroidal anti-estrogens, Steroids 145 (2019) 39–46.

Further reading

[119] Bijoy P, Naik RG, Shivakumar U, Rao GSRS Total synthesis of ring-A aromatic steroids, J. Indian Inst. Sci. 74, (1994) 519.

Reactions in water: Synthesis of biologically active compounds

13

Bimal Krishna Banik[a], *Biswa Mohan Sahoo*[b,*]
[a]Department of Mathematics and Natural Sciences, College of Sciences and Human Studies, Deanship of Research Development, Prince Mohammad Bin Fahd University, Al Khobar, Kingdom of Saudi Arabia, [b]Roland Institute of Pharmaceutical Sciences, Berhampur, India
[*]Corresponding author. e-mail address: drbiswamohansahoo@gmail.com

Abbreviation

Al_2O_3	aluminium oxide
°C	degree centigrade
CH_3CN	acetonitrile
CH_3OH	methanol
DBSA	4-dodecylbenzenesulfonic acid
DKPs	2,5-diketopiperazines
DMF	dimethylformamide
EtOH	ethanol
H_2O	water
HTW	high-temperature liquid water
INH	isoniazid
MIC	minimum inhibitory concentration
mL	millilitre
MWI	microwave irradiation
MeCN	acetonitrile
MTB	*Mycobacterium tuberculosis*
MDRTB	multidrug resistant *Mycobacterium tuberculosis*
Na_2CO_3	sodium carbonate
NaI	sodium iodide
NaOH	sodium hydroxide
NEt3	triethylamine
PSSA	polystyrene sulfonic acid
μg	microgram
$SnCl_2$	tin dichloride
THF	tetrahydrofuran
W	watt

13.1 Introduction

Green or sustainable chemistry provides intensive research areas which led to the design of clean and benign chemical reactions with the development of new technologies. For this purpose, attempt is made to replace the use of toxic and volatile organic

Green Approaches in Medicinal Chemistry for Sustainable Drug Design. https://doi.org/10.1016/B978-0-12-817592-7.00013-7
© 2020 Elsevier Inc. All rights reserved.

solvents with their safe alternate solvent like water. Water is considered as suitable solvent for various chemical reactions due to its low cost, safety, and environmental friendly nature [1]. With the help of green technologies such as microwave, ultrasound, UV-visible, milling, and grinding, the utilization of water as solvent in chemical reactions provides numerous advantages such as high product yield, better purity of the products, enhanced rate of reaction, and shorter reaction times. In case of water, the dipole arises due to the different affinities of oxygen and hydrogen atoms for the available electron density and the angular shape of water molecule. As the electron density is concentrated more on the electronegative oxygen atom, the net dipole moment is increased for the water molecule.

The use of water as solvent provides several benefits such as improvement in reactivity and selectivity toward chemical reactions, simple workup procedures, enable recycling of the catalyst and mild reaction conditions and protecting group free drug synthesis [2]. Hydrophobic interactions of water with organic substrates are responsible for the origin of selectivity and rate enhancements of organic reactions in water or even in suspensions. Many organic solvents like benzene, toluene, chlorobenzene, and halogenated solvents are carcinogenic, harmful to human health, and also cause environmental pollution. So, the replacement of volatile and nonvolatile organic solvents in organic reactions and drug development process is essential to avoid these problems. The protocol of using water as solvent in organic synthesis is considered as one of the powerful tool of green chemistry because it reduces the release of toxic chemicals in the environment thereby reducing pollution [3]. It exhibits powerful hydrogen bonding and remains in liquid state in wide range of temperature (Fig. 13.1). First, organic syntheses was carried out in water are Wohler's urea synthesis and Baeyer and Drewsen's indigo synthesis.

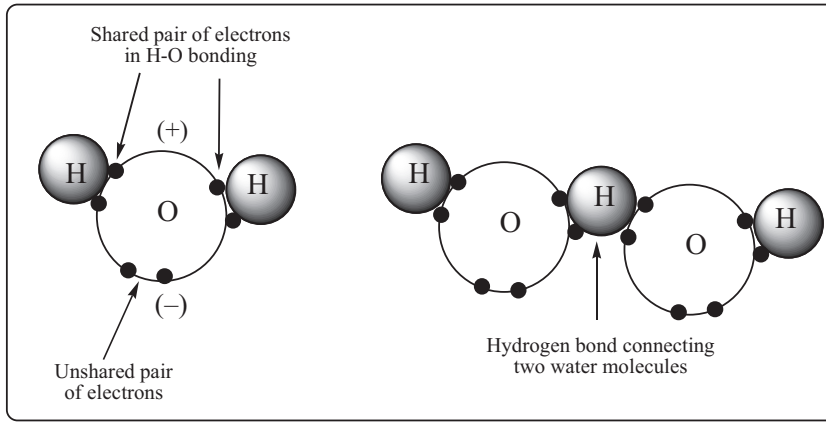

Fig. 13.1 Structure of water molecule and hydrogen bonding.

13.2 Properties of water as solvent in synthesis

- Water is the universal solvent in nature.
- Water shows high dielectric constant and hydrogen bonding at normal condition. But it changes its high polar nature to nonpolar at high temperature and pressure.
- Water has dielectric constant of 78 at 25°C and decrease to 20 at 300°C and at elevated temperature. So, it acts as the pseudo-solvents.
- Water exhibits high activity and low density at high temperature and pressure.
- In case of microwave synthesis, water has critical temperature (T_c) of 374°C and critical pressure (P_c) of 218 atm which is equivalent to 3204 psi or 221 bar.
- High-temperature (200–350°C) liquid water (HTW) is used as reaction medium for conducting acid and base-catalyzed organic synthesis.
- Water has high heat capacity of 4.184 J/g.
- Very high heat of fusion of 334 J/g and very high heat of vaporization of water, that is, 2.259 J/g.
- Water has surface tension of 71.97 at 25°C.

13.3 Synthesis of biologically active compounds in water

Water is the nature's solvent and many syntheses are carried in aqueous medium. Water possesses unique structural feature which distinguishes its physical and chemical properties. So, there is an increase in demand to perform various chemical reactions in water such as oxidation, reduction, cycloaddition, condensation, rearrangement, and coupling reaction (Fig. 13.2). The introduction of polar functional groups on reactant molecules enhances the water solubility to promote the reaction faster. The organic reactions can also be conducted in aqueous medium in either heterogeneous or homogeneous phase in which volume of water may differ from moderate to large quantity [2].

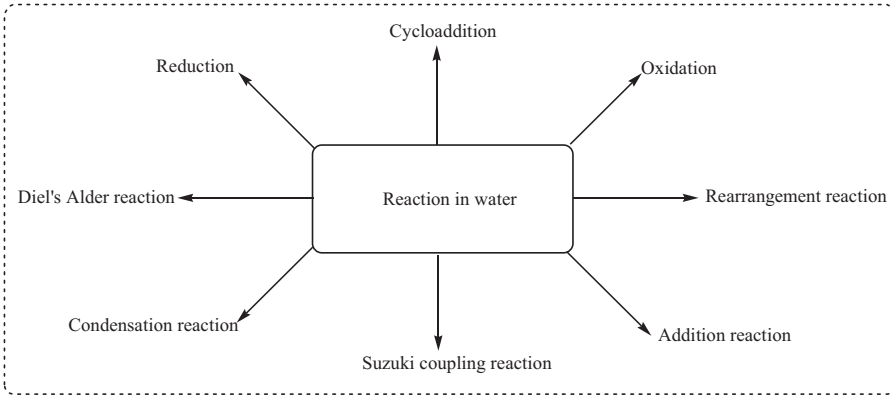

Fig. 13.2 Various chemical reactions in water.

Raju et al. synthesized substituted thiophenes via Pd/C-mediated Sonogashira coupling in the presence of water. A series of 2-alkynyl-thiophenes were synthesized by coupling 2-iodothiophene (1) with acetylinic compounds (2) using 0.026 equivalent of 10% Pd/C, PPh_3, CuI, and ethanolamine in water (Scheme 13.1). Some of the alkynylthiophenes were screened for their activity against three cancer cell lines (LoVo, H460, and HT-29) (Table 13.1) [1].

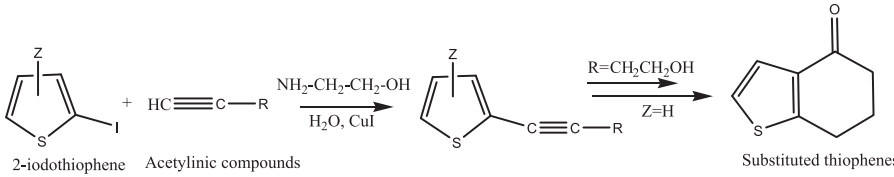

Scheme 13.1 Synthesis of substituted thiophenes in the presence of water.

Table 13.1 In vitro anticancer activity of substituted thiophenes.

Compound	Structure	Percentage growth at 100 µM in cell lines		
		LoVo	H460	HT-29
3a	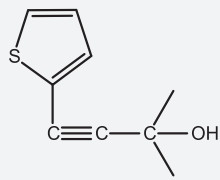	78	105	95
3b	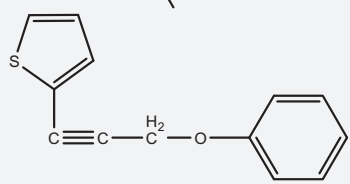	47	88	63
3c	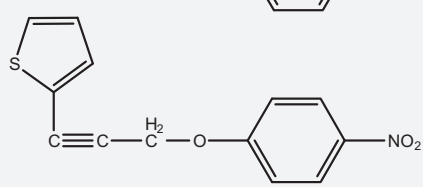	26	48	44

Shi et al. reported the green chemoselective synthesis of thiazolo[3,2-*a*]pyridine derivatives (7, 8) in the presence of water via microwave-assisted three-component reactions of malononitrile (4), aromatic aldehyde (5), and 2-mercaptoacetic acid (6) with molar ratios of 2:1:1.5 and 2:2.2:1, respectively, at 90–100°C and 250 W (Scheme 13.2). These compounds were subjected to cytotoxicity studies against

carcinoma HCT-116 cells and mice lymphocytes. In addition, most of these compounds showed cytotoxicity to HCT-116 cells and mice lymphocytes with no selectivity (Table 13.2). Cytotoxicity was represented as percentage of inhibition (mean ± SD, $n = 3$) of HCT-116 and lymphocyte. The concentration of tested compound was 1 mg/mL [4].

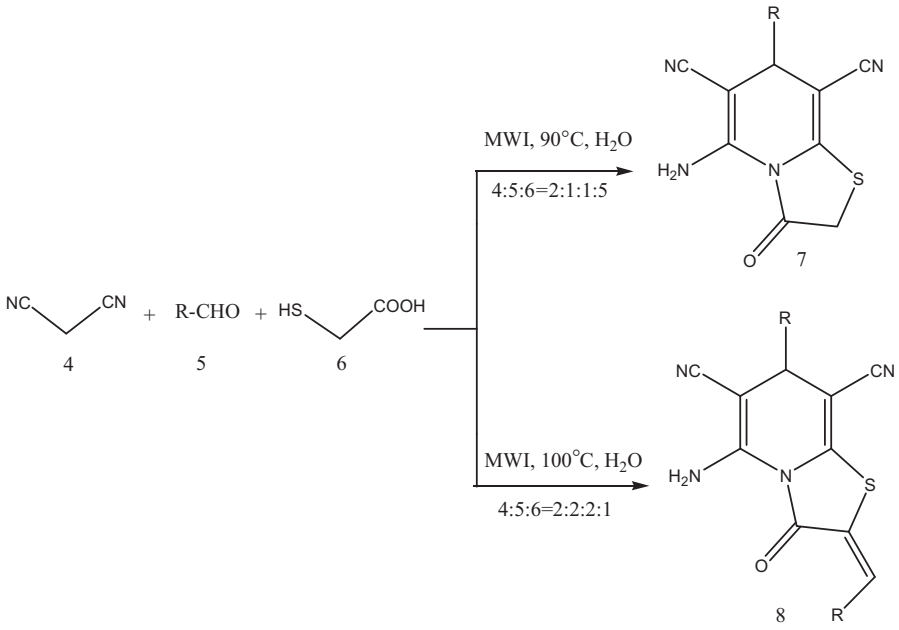

Scheme 13.2 Synthesis of thiazolo[3,2-*a*]pyridine derivatives (7, 8) in the presence of water.

Table 13.2 Cytotoxic activity of thiazolo[3,2-*a*]pyridine derivatives (7, 8).

Compound code	R	Inhibition rate on cell lines (%)	
		HCT-116	Lymphocyte
7a	4-F-C_6H_4	47.77 ± 2.85	66.88 ± 0.88
7b	4-Br-C_6H_4	43.55 ± 0.88	69.59 ± 3.57
7c	2-Cl-C_6H_4	54.06 ± 2.54	60.36 ± 3.81
7d	2,4-Cl_2-C_6H_3	29.93 ± 4.66	55.35 ± 6.79
7e	C_6H_5	50.84 ± 1.92	64.84 ± 2.97
7f	4-OCH_3-C_6H_4	50.17 ± 2.61	70.60 ± 2.08
7g	3,4-OCH_2O-C_6H_3	51.78 ± 2.57	62.02 ± 3.35
7h	4-CH_3-C_6H_4	47.42 ± 2.35	63.77 ± 4.76
8a	4-NO_2-C_6H_4	35.45 ± 1.87	51.69 ± 1.83
8b	4-Br-C_6H_4	56.65 ± 2.07	71.28 ± 0.84
8c	4-OH-3-NO_2-C_6H_3	52.99 ± 1.61	60.35 ± 4.40

Benzo[e][1,4]thiazepin-2(1H,3H,5H)-ones were synthesized via a microwave-assisted chemoselective multicomponent reaction in aqueous media (Scheme 13.3) [5]. This protocol had the advantages of better yields, less cost, and reduced environmental pollution.

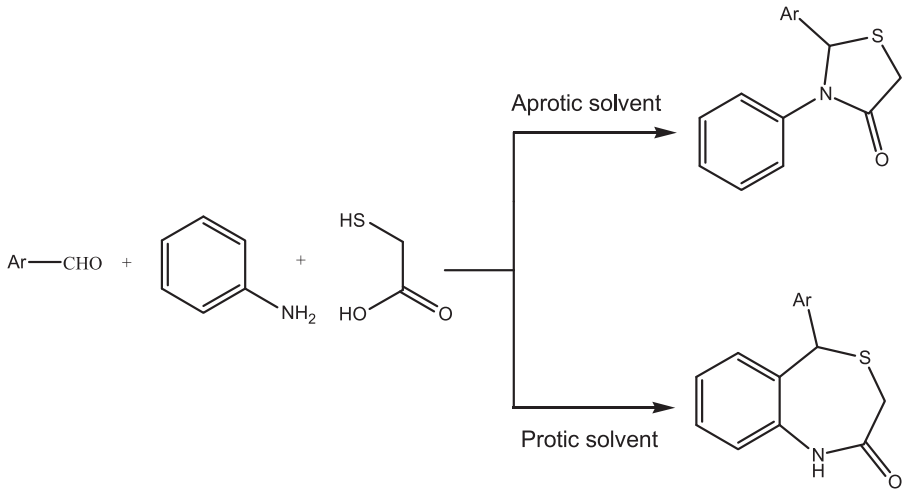

Scheme 13.3 Synthesis of benzo[e][1,4]thiazepin-2(1H,3H,5H)-ones.

Manjashetty et al. reported the synthesis of novel isoniazid (INH) analogs by microwave-assisted one-pot reaction of INH, various benzaldehydes and dimedone in water with catalytic amount of DBSA (Scheme 13.4) [6]. The synthesized compounds were evaluated for their anti-TB activity against *Mycobacterium tuberculosis* H37Rv (MTB) and multidrug-resistant *Mycobacterium tuberculosis* (MDRTB) (Table 13.3).

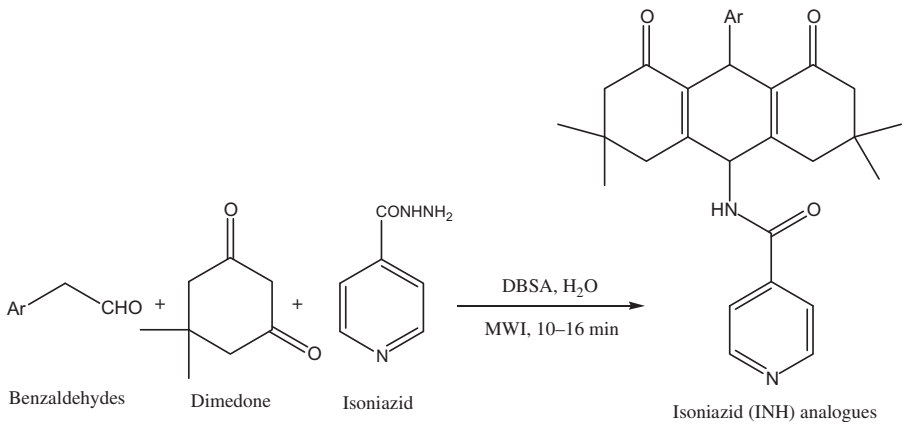

Scheme 13.4 Microwave-assisted one-pot synthesis of novel isoniazid analogs.

Table 13.3 Antitubercular activity against MTB and MDRTB.

Entry	Ar	MIC in μM	
		MTB	MDR-TB
1	-C_6H_5	6.66	–
2	2-CH_3-C_6H_4	3.22	–
3	3-CH_3-C_6H_4	6.44	–
4	4-CH_3-C_6H_4	6.44	–
5	2-OH-C_6H_4	>12.87	–
6	3-OH-C_6H_4	>12.87	–
7	4-OH-C_6H_4	12.87	–
8	2-OCH_3-C_6H_4	12.51	–
9	4-OCH_3-C_6H_4	12.51	–
10	4-$N(CH_3)_2$-C_6H_4	6.10	–
11	4-$CH(CH_3)_2$-C_6H_4	1.52	–

A series of furo[3,4-b][4,7]phenanthroline and indeno[2,1-b][4,7]phenanthroline derivatives were synthesized via a three-component reaction of aromatic aldehydes, 6-aminoquinoline, and either tetronic acid or 1,3-indanedione in water under microwave irradiation (MWI) without use of any catalyst (Scheme 13.5) [7].

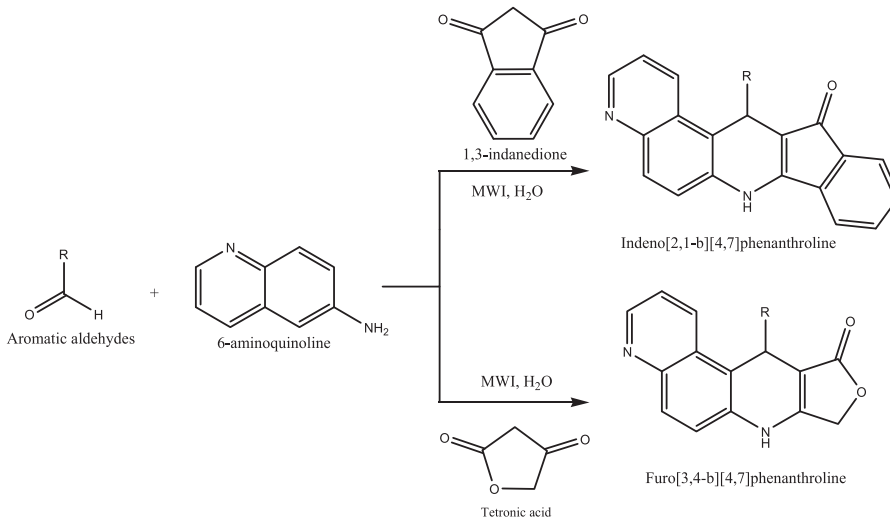

Scheme 13.5 Synthesis of furo[3,4-b][4,7]phenanthroline and indeno[2,1-b][4,7] phenanthroline derivatives.

Eco-friendly, one-pot three-component syntheses of 2-(3H-imidazo[4,5-*b*]pyridine-2-yl)-N-arylbenzamides (4) was developed by combining phthalic anhydride (1) with anilines (2) and pyridine-2,3-diamine (3) in water without any catalyst (Scheme 13.6). These reactions proceeded with an easy workup method and provided good yields [8].

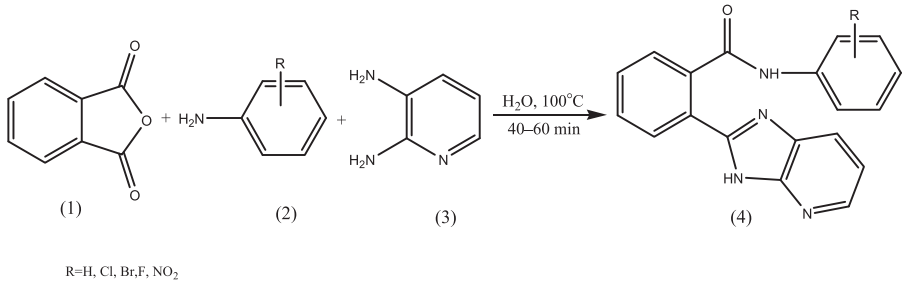

Scheme 13.6 Syntheses of 2-(3H-imidazo[4,5-*b*]pyridine-2-yl)-N-arylbenzamides.

Banik et al. reported an efficient microwave-induced iodine-catalyzed method for the synthesis of quinoxalines via condensation of 1,2-diamines with 1,2-dicarbonyl compounds (Scheme 13.7). It involved reaction between o-phenylenediamine and phenylglyoxal monohydrate in the presence of iodine as catalyst under MWI. EtOH/H_2O (1:1) was used as solvents to perform these reactions [9].

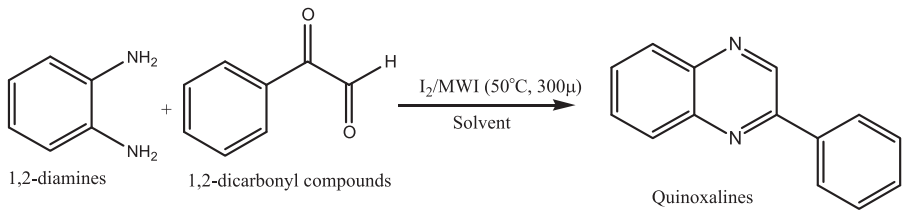

Scheme 13.7 Microwave-induced synthesis of quinoxalines.

Singhal et al. reported an efficient, simple, and environmentally clean synthesis of 3,4-dihydro-pyrimidinones with excellent yields in the presence of water without using solvents or acid catalyst under conventional heating, MWI, or ultrasound. MWI method involved the reaction between aldehyde (2 mmol), urea (2 mmol), and β-dicarbonyl compound (2 mmol) in the presence of water (three to four drops) at power level 750 W for 2 min (Scheme 13.8). A similar reaction condition was maintained to carry out the reaction by using ultrasound irradiation (25 kHz). In the case of conventional heating method, the same synthesis required longer reaction time, that is, 2 h (Table 13.4). The presence of water was found to be vital and the reactions were carried out faster with high products yield under microwave or ultrasound irradiation as compared to conventional heating method [10].

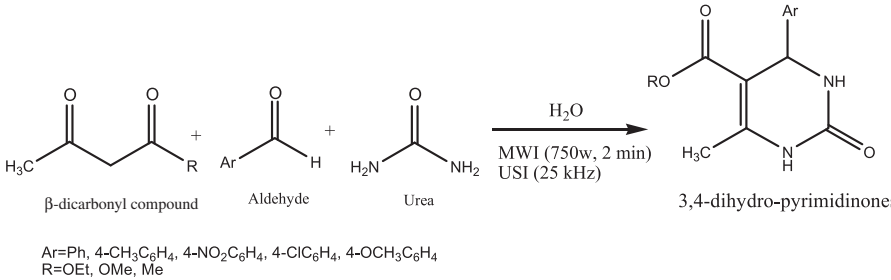

Scheme 13.8 Synthesis of 3,4-dihydro-pyrimidinones.

Table 13.4 Synthesis of 3,4-dihydro-pyrimidinones and optimization data.

Compound	Conventional		Microwave		Ultrasound	
	Time (min)	Yield (%)	Time (min)	Yield (%)	Time (min)	Yield (%)
2a	45	92	2	98	30	96
2b	45	94	2	96	30	95
2c	50	90	2	96	35	92
2d	60	89	2	97	40	92
2e	65	90	2	96	40	94
2f	60	90	2	95	40	94
2g	55	80	2	88	35	85
2h	60	80	2	90	35	90
2i	75	92	2	90	50	82

Varma et al. described green chemistry technique like microwave (MW) irradiation method to synthesize various heterocycles in aqueous medium. Dihydropyrimidinones were synthesized by following environmentally benign aqueous Biginelli protocol using polystyrene sulfonic acid (PSSA) as a catalyst (Scheme 13.9). This reaction under MWI proceeded efficiently in water without using any organic solvents [11].

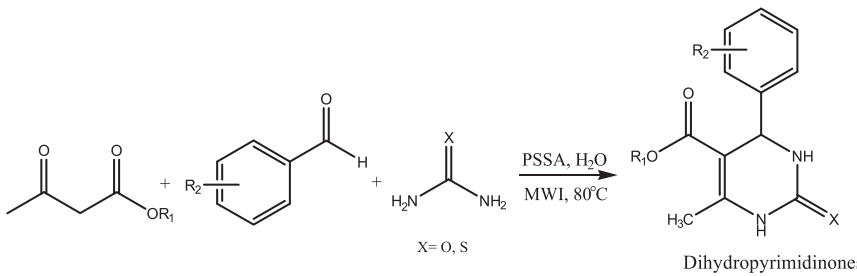

Scheme 13.9 Microwave-assisted synthesis of dihydropyrimidinones in aqueous medium.

A series of furo[3,4-*e*]pyrazolo[3,4-b]pyridine analogs of podophylloxin were synthesized via three-component reaction of aldehydes, 3-methyl-1-phenyl-1H-pyrazol-5-amine, and tetronic acid in the presence of water under MWI without using catalyst (Scheme 13.10). This method provided economical and green synthetic strategy to generate titled compounds under microwave-assisted synthesis in aqueous medium [12].

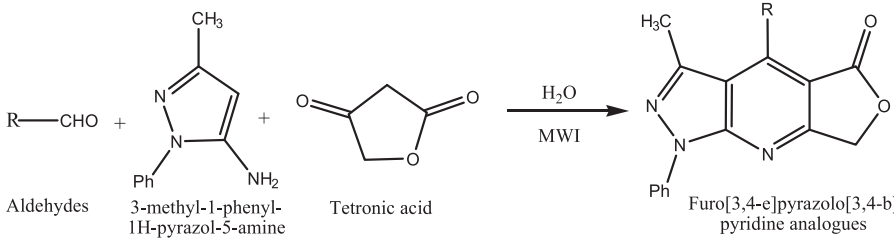

Scheme 13.10 Synthesis of furo[3,4-*e*]pyrazolo[3,4-b]pyridine analogs in aqueous medium.

Jiang et al. described the reaction of 2,6-diaminopyrimidin-3H-4-one with arylaldehydes and barbituric acids in water at 100°C for 6–9 min under MWI to produce 6-spirosubstituted pyrido[2,3-*d*]pyrimidines with good product yield (79%–90%) (Scheme 13.11). The product was found to be a mixture of diastereomers in which *cis*-isomer is the major product [13].

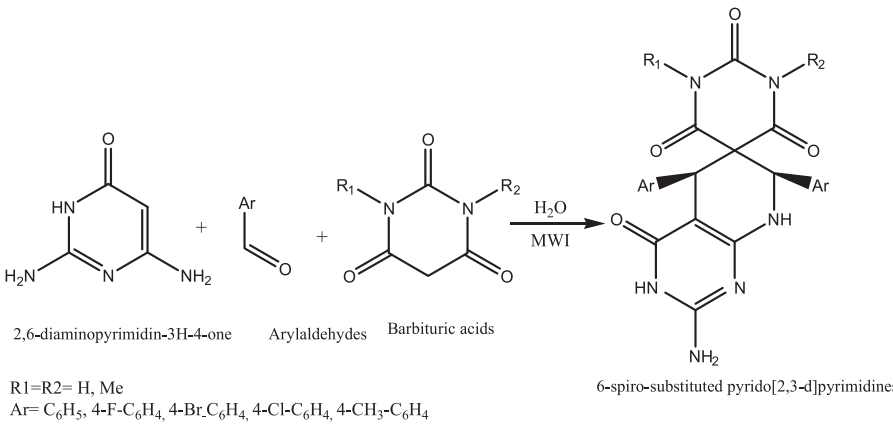

Scheme 13.11 Synthesis of 6-spirosubstituted pyrido[2,3-*d*]pyrimidines in water under MWI.

Dehbi et al. reported an efficient and eco-friendly method for the synthesis of disubstituted 5-aminopyrimidines from vinyl azides and urea or thiourea (Scheme 13.12). This reaction was carried out in the presence of water as a solvent under MWI conditions (Table 13.5). The significant features observed in this new protocol were faster conversion of starting materials to products, shorter reaction times, cleaner reactions, and simpler workup procedure.

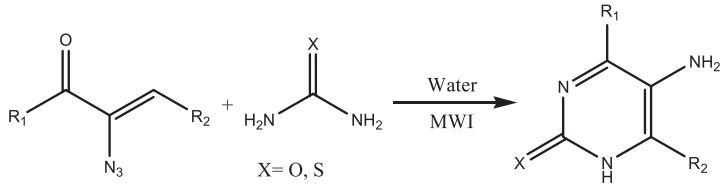

Scheme 13.12 Synthesis of disubstituted 5-aminopyrimidines in the presence of water.

Table 13.5 Synthesis of disubstituted 5-aminopyrimidines in presence of water under MWI.

Product	R_1	R_2	X	Microwave irradiation conditions	
				Time (min)	Yield (%)
3a	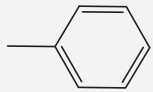	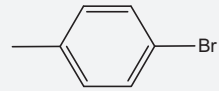	O	10	97
3b	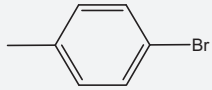	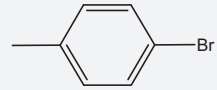	O	10	88
3c	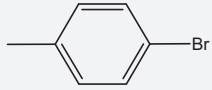		O	20	71
3d	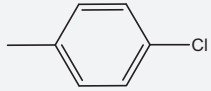	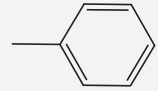	O	20	79
3e	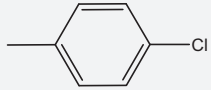		O	76	20
3f	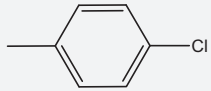		O	97	10
3g	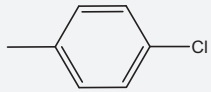		O	96	10
3h	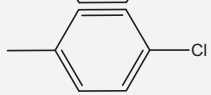		O	94	10
3i	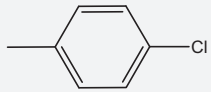	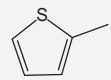	O	70	20

To optimize the reaction conditions, the coupling of 2-azido-3-(4-bromophenyl)-1-phenylprop-2-en-1-one with urea was carried out in the presence of different solvents such as methanol (CH_3OH), acetonitrile (CH_3CN), tetrahydrofuran (THF), dimethylformamide (DMF), toluene, dioxane, and water under MWI for 10 min (Scheme 13.13). From this reaction, it was observed that water is the most efficient solvent to carry out this reaction to produce the products in an excellent yield (97%) (Table 13.6) [14].

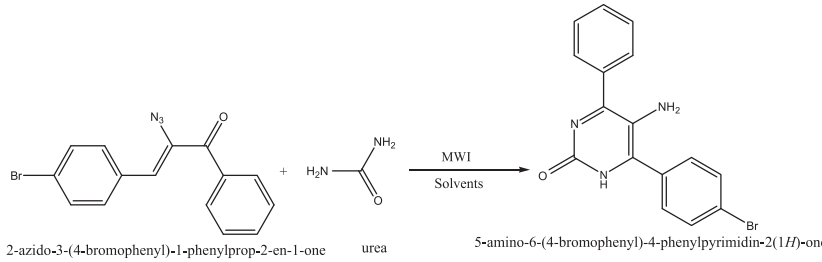

2-azido-3-(4-bromophenyl)-1-phenylprop-2-en-1-one urea 5-amino-6-(4-bromophenyl)-4-phenylpyrimidin-2(1*H*)-one

Scheme 13.13 Synthesis of 5-amino-6-(4-bromophenyl)-4-phenylpyrimidin-2(1H)-one.

Table 13.6 Optimization of reaction conditions using different solvents.

Entry	Solvents	Reaction time (min)	Yield (%)
1	CH_3OH	10	36
2	CH_3CN	10	12
3	THF	10	79
4	DMF	10	82
5	Toluene	10	53
6	Dioxane	10	46
7	Water	10	97

Sanghvi et al. reported one-pot microwave-assisted synthesis of substituted guanidine derivatives using green chemistry approach in water. Various substituted guanidine derivatives were prepared by reacting symmetrical and asymmetrical thioureas with different amines under alkaline condition using water as solvent under MWI (100 W) with moderate yield within 10–95 min (Scheme 13.14). To reduce the chemical hazards produced by organic solvents, water is used as a solvent. Sodium hydroxide was used to catalyze the reaction and to trap the evolved H_2S gas. Microwave synthesizer was used to reduce reaction time and to make the reactions eco-friendly [15].

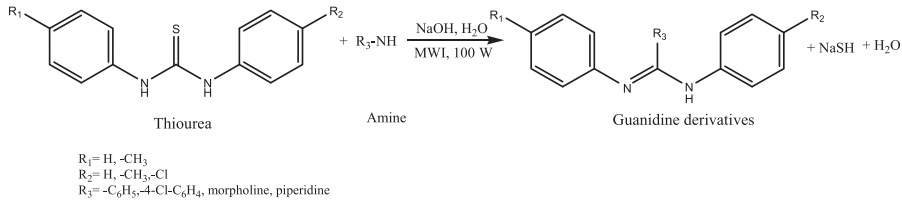

Scheme 13.14 Synthesis of substituted guanidine derivatives under MWI.

María et al. carried out efficient synthesis of 2,5-diketopiperazines (DKPs) from Nα-Boc-dipeptidyl methyl esters and tert-butyl esters under MWI at 250 W for 10 min with excellent yields (Scheme 13.15). This protocol provided rapid, safe, environmental friendly, and highly efficient technique to get the final products (Table 13.7) [16].

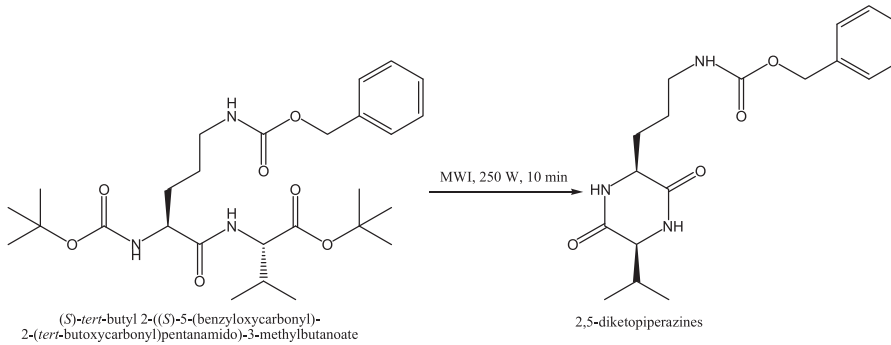

Scheme 13.15 Synthesis of 2,5-diketopiperazines under MWI.

Table 13.7 Optimization study on synthesis of 2,5-diketopiperazines under MWI.

Entry	Solvents	Temp (°C)	Power (W)	Time (min)	Yield (%)
1	Toluene	170	160	10	No reaction
2	Xylene	200	300	10	No reaction
3	DMF	200	300	5	61
4	H_2O	200	250	1	22
5	H_2O	200	250	2.5	85
6	H_2O	200	300	5	89
7	H_2O	250	250	10	86

Sharma et al. developed a simple, clean, rapid, efficient, and green protocol for the synthesis of coumarin-3-carboxylic acids [17]. It involved the reaction of 2-hydroxybenzaldehydes with Meldrum's acid (2,2-dimethyl-1,3-dioxan-4,6-dione) in aqueous medium under MWI for 2 min (Scheme 13.16). This protocol was eco-friendly because it avoids the use of hazardous organic solvents throughout the reaction (Table 13.8).

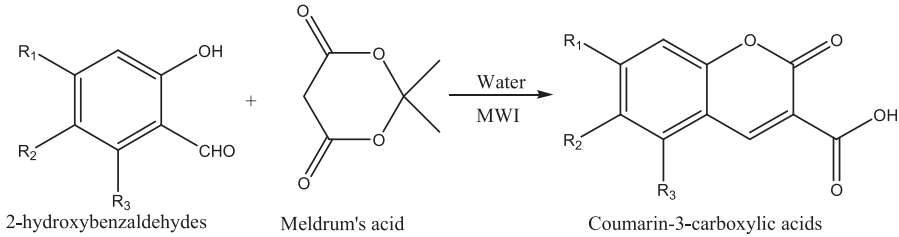

Scheme 13.16 Green synthesis of coumarin-3-carboxylic acids.

Table 13.8 Reaction time and yield of coumarin-3-carboxylic acids.

Compounds	R_1	R_2	R_3	Reaction time (min)	Yield (%)
a	H	H	H	2	85
b	H	Br	H	2	90
c	H	Cl	H	2	89
d	H	CH_3	H	2	88
e	H	—OCH_3	H	2	86
f	—OCH_3	H	H	2	85
g	—OCH_3	H	—OCH_3	2	80

Gutierrez et al. reported microwave-assisted one-pot synthesis of carbonylpyrazolo [3,4-*b*]pyridine derivatives catalyzed by $InCl_3$ in the presence of water (Scheme 13.17). It involved in the sonochemical or microwave-assisted condensation of aldehydes with formaldehyde (as paraformaldehyde) and β-diketones to obtain pyrazolopyridine derivatives. This technique was advantageous because of simple operation, higher yields, low cost with environmentally benign procedure [18].

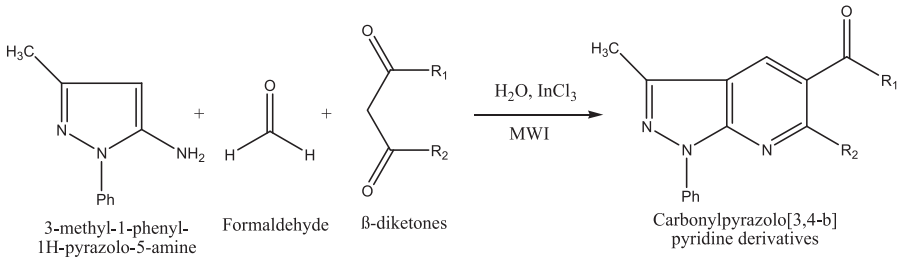

Scheme 13.17 Microwave-assisted synthesis of carbonylpyrazolo[3,4-*b*]pyridine derivatives.

Guirong et al. reported microwave-assisted synthesis of 6-substituted aminopurine analogs in water [19]. It involved in the amination of 6-chloropurine with various amine under MWI at power level 200 W for 10 min (Scheme 13.18). The products were obtained with moderate to high purity in much less reaction time (Table 13.9).

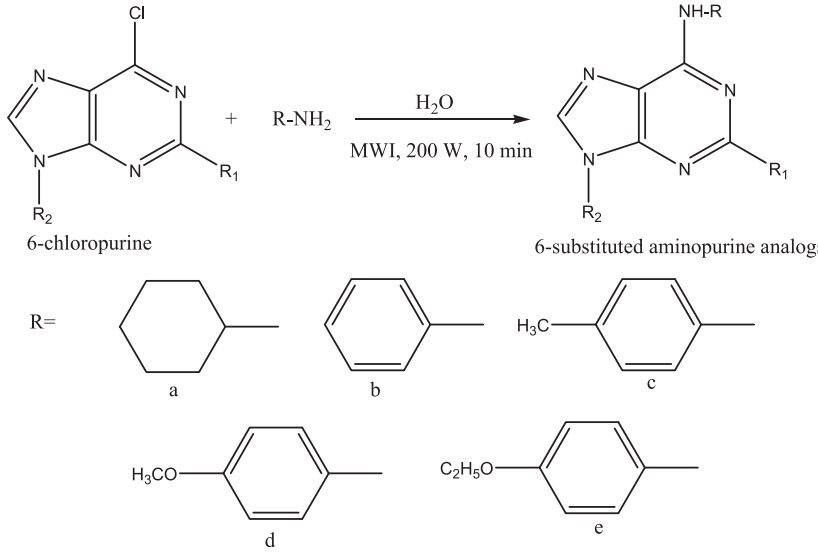

Scheme 13.18 Microwave-assisted synthesis of 6-substituted aminopurine analogs in water.

Table 13.9 Influence of different irradiation time on the yields of compound 1b in water.

Entry	Aniline equiv.	Irradiation time (min)	Yield (%)
1	3	5	72
2	3	8	85
3	3	10	87
4	3	13	84

Wei et al. carried out the base-free, ultrasound-accelerated one-pot synthesis of 2-sulfonylquinolines in water (Scheme 13.19). While comparing with conventional heating method, the use of ultrasound technique not only improves the efficiency of chemical reaction but also enhances the rate of reaction, simplifies scale-up and minimizes any side reactions or by-product formation. This reaction process followed green protocol as it provides good product yields (61%–91%) with chemo- and regioselectivity, high energy efficiency, and atom economy of 70.7%, *E*-factor of 1.17, and eco-scale score of 71 [20].

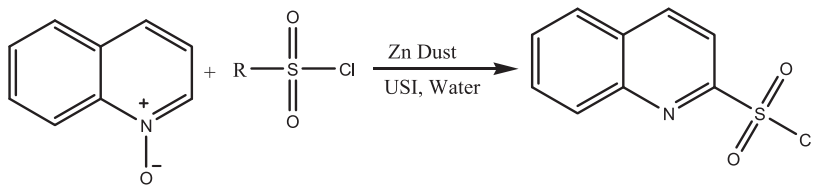

Scheme 13.19 Ultrasound-accelerated one-pot synthesis of 2-sulfonylquinolines in water.

Bagher et al. reported green and efficient method for the synthesis of 5-aryl-4-hydroxy-2-methyl-1*H*-pyrrole-3-carboxylic acid esters (3) and 6-aryl-3-methylpyridazine-4-carboxylic acid esters (4) via a three-component reaction of arylglyoxal hydrates (1) with β-dicarbonyl compounds (2) in the presence of ammonium acetate and hydrazine hydrate using water as solvent under ultrasonic irradiation (Scheme 13.20). This methodology was advantageous in terms of simple operation, high yields, short reaction times, mild reaction conditions without using any catalysts, economic, and environmental friendly [21].

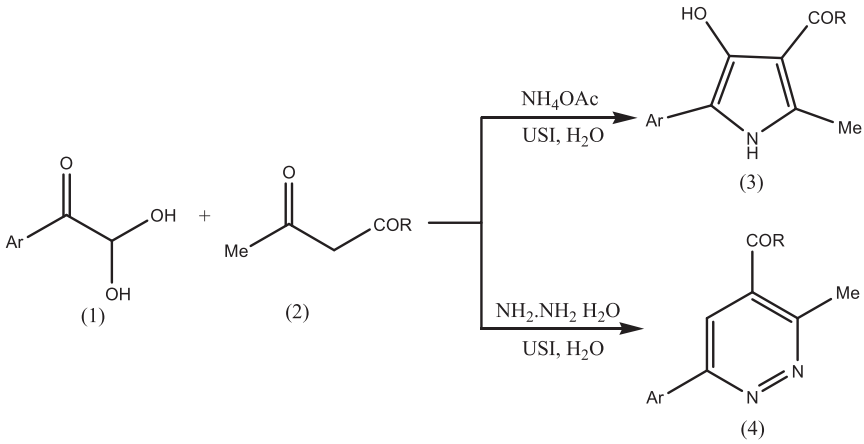

Scheme 13.20 Synthesis of pyrroles (3) and pyridazines (4) using water as solvent under USI.

Sapkal et al. developed a highly efficient and green protocol for the synthesis of various structurally diverse 2,2′-arylmethylene bis(3-hydroxy-5,5-dimethyl-2-cyclohexene-1-one) (3) and 2-substituted-1H-benzimidazole derivatives (5) (Scheme 13.21). This reaction was performed under ultrasound irradiation, using BiOCl nanoparticles as a catalyst in the presence of water. It was observed that the nanocatalyst is reusable for seven subsequent reactions without loss in catalytic activity. This green methodology provided mild reaction conditions with easy workup in short reaction time [22].

Koorosh et al. accomplished a simple and efficient synthesis of the spirooxindoles (4) via a three-component reaction between isatins (1), 4-hydroxy-2H-quinolin-2-one (2), and malononitrile or ethylcyanoacetate (3) in aqueous medium under ultrasound irradiation (Scheme 13.22). This reaction gained importance due to simple operation, faster rate of reaction, good yield, and easy workup (Table 13.10) [23].

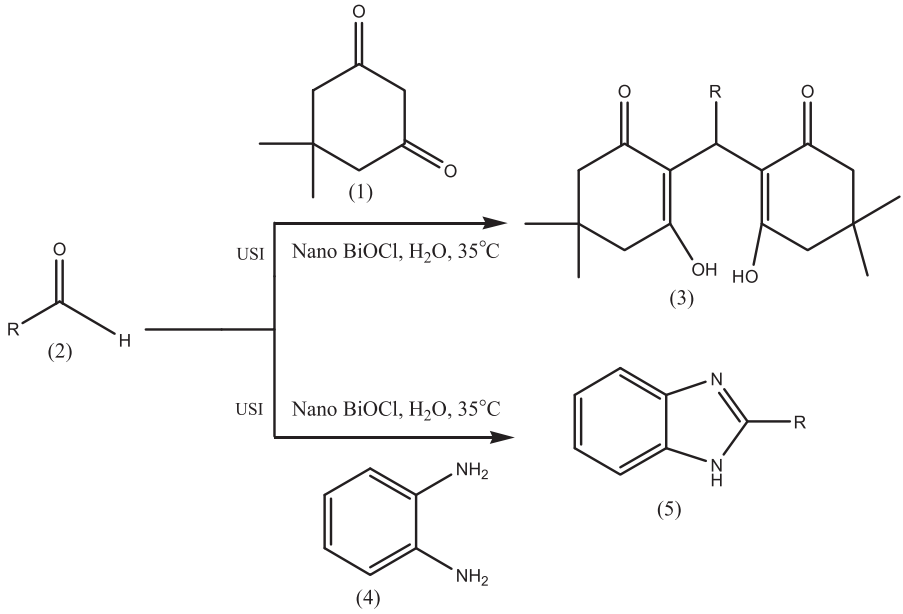

Scheme 13.21 Green protocol for the synthesis of compounds (3) and (5).

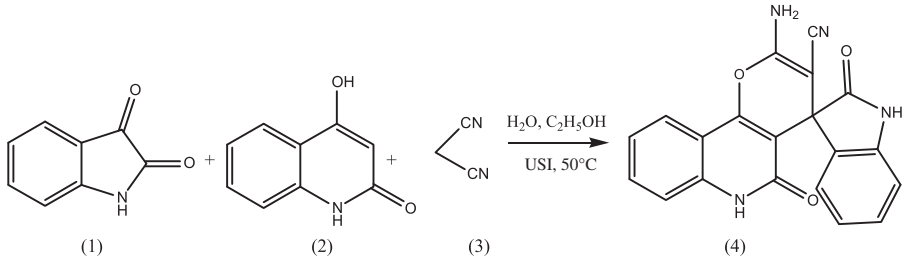

Scheme 13.22 Ultrasound-assisted three-component synthesis of spirooxindoles in water.

Table 13.10 Synthesis of the spirooxindoles in aqueous medium under ultrasound irradiation.

Entry	Catalyst	Time (min)	Yield (%)
1	Piperidine	10	79
3	NEt_3	10	78
3	KBr	45	48
4	Al_2O_3	45	32
5	Na_2CO_3	45	80
6	L-Proline	20	77

Pal et al. performed ultrasound-assisted rapid synthesis of 2-substituted quinoline derivatives (4) in the presence of $SnCl_2{\cdot}2H_2O$ as a catalyst in water [24]. The reaction involved in a one-pot, three-component reaction of aniline (1), aldehyde (2), and ethyl 3,3-diethoxypropionate (3) to produce the desired products in good yields (Scheme 13.23).

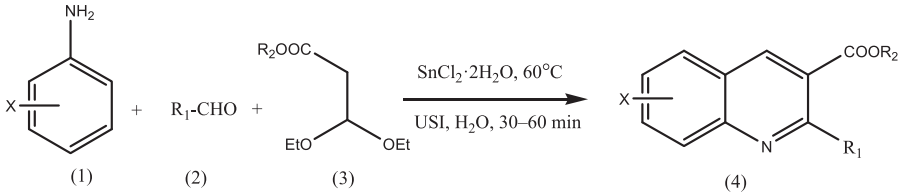

Scheme 13.23 Ultrasound-assisted rapid synthesis of 2-substituted quinoline derivatives.

Sadegh et al. described a green, efficient, rapid, high-yielding, catalyst-free method for the synthesis of rhodanines in water using ultrasonic radiation [25]. It involved in the one-pot, three-component reaction between dimethyl acetylene-dicarboxylate (1), benzylamine (2), and carbon disulfide (3) in the presence of water as the solvent under ultrasonic irradiation for 3–5 min with the highest yield of 94% (Scheme 13.24, Table 13.11).

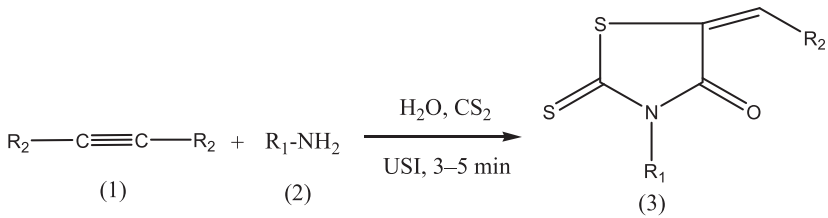

Scheme 13.24 Ultrasound-mediated synthesis of rhodanines in water.

Table 13.11 Synthesis of rhodanines in water using ultrasonic radiation.

Products	R1	R2	Time (min)	Yield (%)
3a	$PhCH_2$	CO_2Me	3	94
3b	4-Cl-C_6H_4-CH_2	CO_2Me	4	93
3c	2-Cl-C_6H_4-CH_2	CO_2Me	4	91
3d	2-Cl-C_6H_4-CH_2	CO_2Et	4	92
3e	PhCH(Me)	CO_2Me	3	92
3f	i-Bu	CO_2Me	5	88
3g	Allyl	CO_2Me	5	90
3h	i-pro	CO_2Me	5	86

Vanelle et al. reported microwave-assisted synthesis of new quinazoline derivatives in aqueous medium as anticancer agent precursors [26]. The reaction proceeded via *S*-alkylation or $S_{RN}1$ reaction of 2-chloromethyl-3-methylquinazolin-4(3*H*)-one derivatives with different benzenesulfinic acids and nitronate anions (Scheme 13.25).

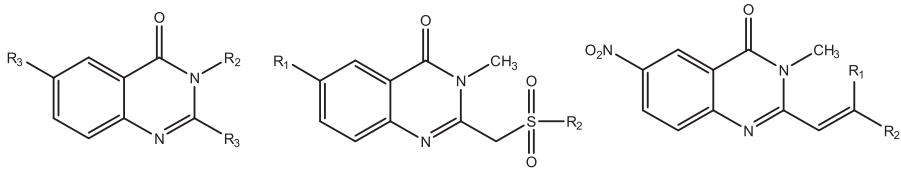

Scheme 13.25 Microwave-assisted synthesis of new quinazoline derivatives in aqueous medium.

Yildirim et al. developed a green procedure to prepare a new series of thiazolo [3,2-*c*]pyrimidine derivatives through Mannich reactions under MW-irradiation. This method involved in a multicomponent cyclization of 2-(nitromethylene) thiazolidine, various aliphatic or aromatic amines and formaldehyde in water (Scheme 13.26). The use of MW radiation promoted the high product yields and considerably reduced the reaction times in relation to conventional heating. This green protocol did not require any organic solvents to carry out the reaction or purification of final compounds [27].

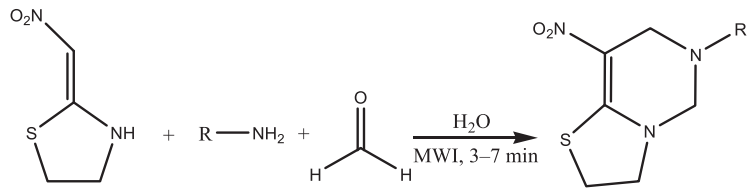

Scheme 13.26 Green protocol for synthesis of thiazolo[3,2-*c*]pyrimidine derivatives.

Varma et al. described an elegant protocol for synthesis of substituted 3,4-dihydropyrimidin-2(1H)-ones (4) under MW-irradiation [28]. This involved in the condensation of substituted benzaldehyde (1), acetoacetate (2), and urea or thiourea (3) using PSSA as a catalyst (Scheme 13.27). The reaction proceeded efficiently in water in the absence of any organic solvent.

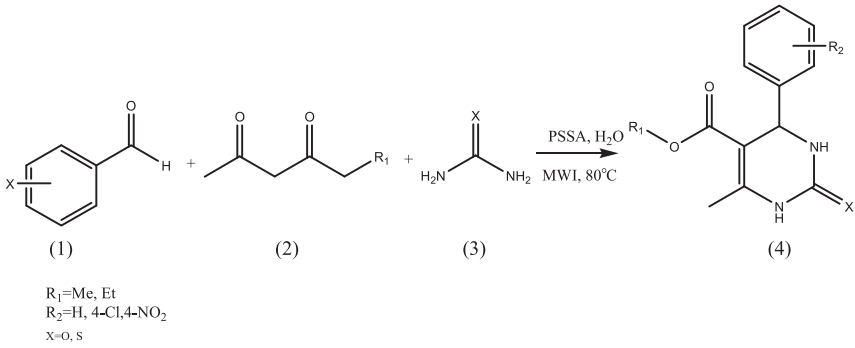

Scheme 13.27 Synthesis of 3,4-dihydropyrimidin-2(1H)-ones in aqueous media under MWI.

A series of new polycyclic-fused isoxazolo[5,4-*b*]pyridines were produced by one-pot synthesis under MWI in water (Scheme 13.28). Without using any additional reagent or catalyst, this synthetic process followed green protocol and makes this methodology suitable for generating compound library during drug development [29].

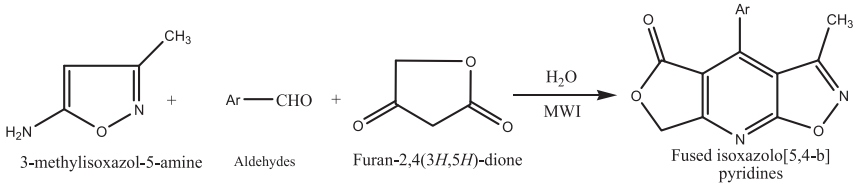

Scheme 13.28 Synthesis of new polycyclic-fused isoxazolo[5,4-*b*]pyridines.

The reaction of 8-acetyl-7-hydroxy-4-methyl coumarin (1) with 2-bromo-1-(4-bromophenyl)ethanone (2) in the presence of potassium carbonate, acetone produced new furocoumarin,4-(p-bromobenzoyl)-3,10-dimethyl-5.13-dioxatricyclo[7.4.0.02,6] trideca-1(9),2(6),3,7,10-pentaen-12-one (3). Compound 3 underwent Suzuki coupling reaction with different aryl boronic acids (4a–i) to produce 4-[(4-biphenylyl)-carbonyl]-3,10-dimethyl-5.13-dioxatricyclo[7.4.0.02,6] trideca-1(9),2(6),3,7,10-pentaen-12-one analogs (5a–i) (Scheme 13.29). The reaction was carried out under MWI using water as solvent. It provided eco-friendly process, accelerated rate of reaction with high yield, and followed green chemistry approach [30].

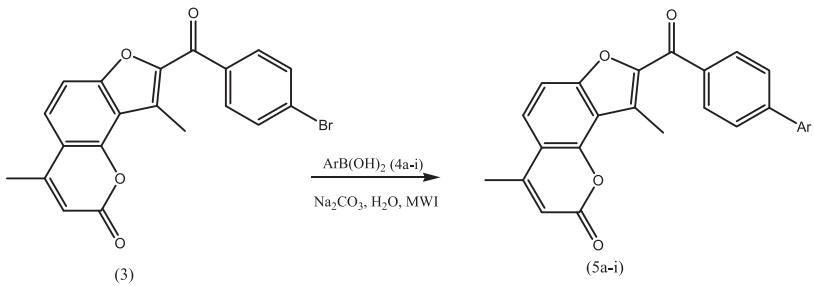

Scheme 13.29 Synthesis of compound 5(a–i) under microwave irradiation using water as solvent.

Dawood et al. reported microwave-assisted synthesis of 2-acetyl-5-arylthiophenes and 4-(5-arylthiophen-2-yl)thiazoles via Suzuki coupling reaction in water. 2-Acetyl-5-bromothiophene and 4-(5-bromothiophen-2-yl)-2-methyl-1,3-thiazole were prepared and used for Suzuki cross-coupling reactions with a number of aryl(hetaryl) boronic acids in water or DMF as solvents. The cross-coupling reactions were carried out under thermal heating as well as microwave irradiating conditions using benzothiazole-based Pd(II)-precatalyst (Scheme 13.30). The use of water as green solvent provided a clean, safe, and environmentally benign chemical process (Table 13.12) [31].

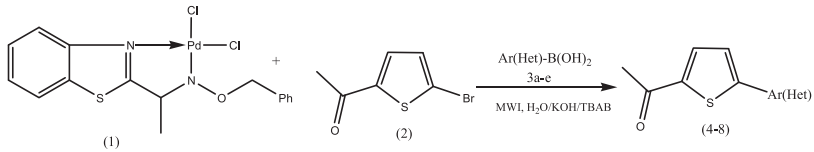

Scheme 13.30 Microwave-assisted synthesis of compound 4–8.

Table 13.12 Synthesis of compound 4–8 under and MW thermal heating.

Products	Structures	Thermal heating		MW heating	
		Time (h)	Yield (%)	Time (min)	Yield (%)
4	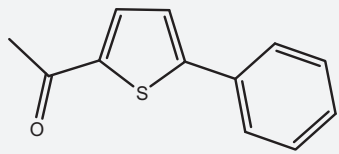	1	93	1	95
5	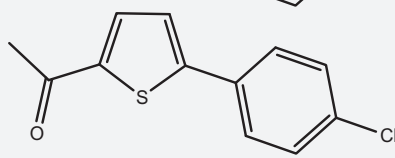	5	97	7	92
6	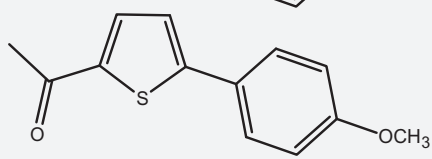	5	90	7	98
7	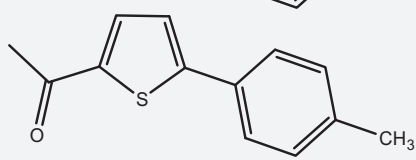	7	89	9	93
8	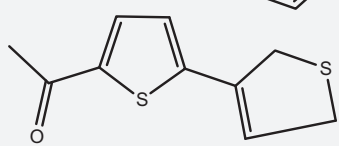	10	91	9	95

Deependra et al. described microwave-accelerated cyclocondensation reaction for the synthesis of pyrazolo[1,5-*c*]quinazolines derivatives (Scheme 13.31). It involved in the reaction of 2-(3-aryl-1H-pyrazol-5-yl)anilines with different aryl aldehydes/triethyl orthoformate in water or MeCN under MWI. 5-(2-Aminophenyl)-4,5-dihydro-3-arylpyrazole-1-carbaldehyde in methanol underwent an internal cyclocondensation and aromatization when heated under MW (Table 13.13). Quinazolines are condensed ring aromatic organic compounds of the heterocyclic series containing benzene ring fused to pyrimidine nucleus. A wide range of biologically active compounds containing quinazoline ring system were also synthesized by atom efficient, environmental friendly, and green methods such as MWI reactions [32].

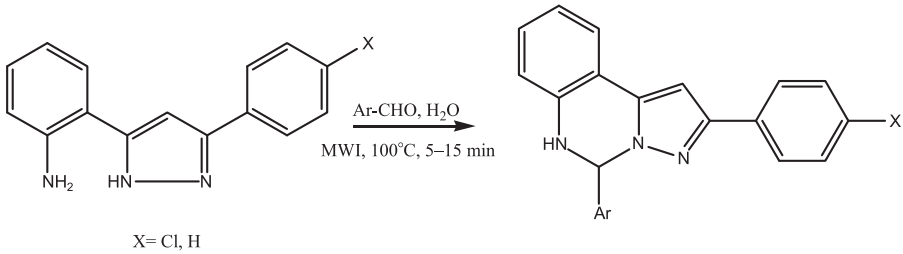

Scheme 13.31 Synthesis of pyrazolo[1,5-*c*]quinazolines derivatives under MWI.

Table 13.13 Synthesis of pyrazolo[1,5-*c*]quinazolines derivatives.

Entry	Ar-CHO	X	Yield (%)
1	4-Hydroxy-3-methoxy benzaldehyde	H	93
2	2-Nitrobenzaldehyde	H	91
3	3-Nitrobenzaldehyde	H	92

A series of warfarin analogs, β-aminomethyl-hydroxyl coumarins, were obtained in good yields by Mannich reaction of 4-hydroxycoumarin, aromatic aldehydes, and secondary amines in water under MWI at 100°C (Scheme 13.32). The salient features of the synthesis are: catalyst-free protocol, green solvent (water), complete avoidance of organic solvents in the synthesis, facile workup, and high yields [33].

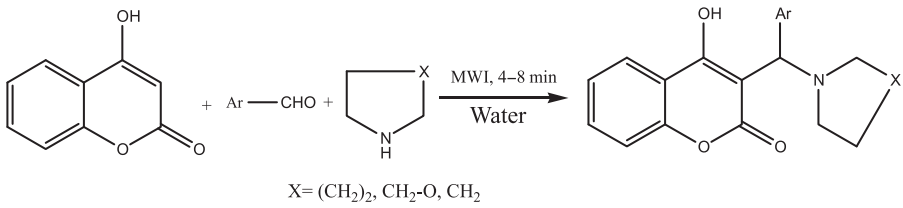

Scheme 13.32 Synthesis of warfarin analogs in the presence of water under MWI.

Remaily et al. developed a simple, fast, cost-effective environmentally benign protocol for the synthesis of guanidinyltetrazoles and 5-substituted 1*H*-tetrazoles derivatives via [2,3]cycloaddition reaction of nitriles and azide derivatives in water under MWI (Scheme 13.33). All the synthesized products are screened for their in vitro antimicrobial activity [34]. The synthesized compounds were obtained in an excellent yield (85%–98%).

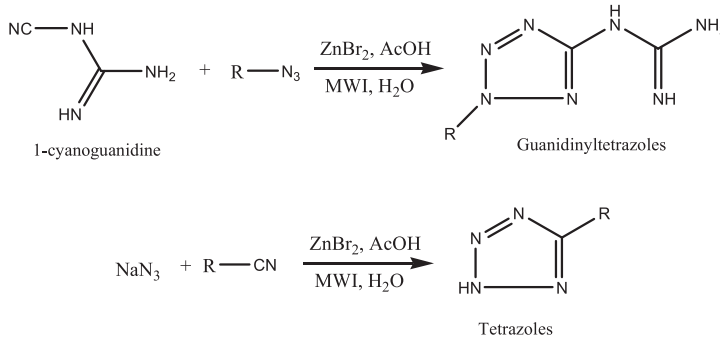

Scheme 13.33 Synthesis of guanidinyltetrazoles and 5-substituted 1*H*-tetrazoles derivatives.

An efficiently green protocol was developed for the synthesis of methyl-7-amino-4-oxo-5-phenyl-2-thioxo-2,3,4,5-tetrahydro-1H-pyrano[2,3-*d*]pyrimidine-6-carboxylates (4a–4k). This synthesis was performed through a one-pot three-component condensation reaction between various benzaldehydes (1), methylcyanoacetate (2), and thiobarbituric acid (3) in the presence of water under MWI (Scheme 13.34). This methodology offered several advantages such as high yields (78%–94%), short reaction time (3–6 min), safety, and eco-friendly without using any catalyst (Table 13.14). The synthesized compounds (4a–4k) demonstrated excellent *in vitro* antimicrobial and antifungal activities against different strains. The compounds 4a, 4b, 4c, 4d, 4e, and 4f exhibited significant antimicrobial activity against *Staphylococcus aureus*, *Bacillus cereus* (Gram-positive bacteria), *Escherichia coli*, *Klebshiella pneumonia*, *Pseudomonas aeruginosa* (Gram-negative bacteria). The synthesized compound 4f showed maximum antifungal activity against *Aspergillus niger* and *Penicillium chrysogenum* strains (Table 13.15). Streptomycin and Mycostatin were used as standard drug for antibacterial and antifungal studies, respectively [35].

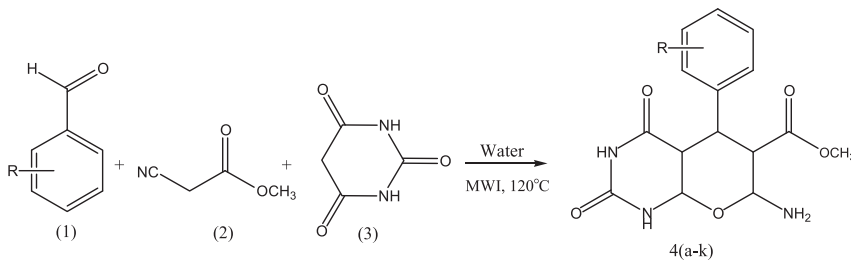

Scheme 13.34 Synthesis of pyrimidine derivatives (4a–4k) under microwave irradiation.

Table 13.14 Synthesis of compound (4a-4k) under conventional (4°C, 60°C), MW heating (120°C) and at room temperature.

Products	Room Temperature		Conventional heating				MW irradiation	
			48°C		60°C			
	Time (h)	Yield (%)	Time (h)	Yield (%)	Time (h)	Yield (%)	Time (min)	Yield (%)
4a	2	82	2	73	1	71	4	82
4b	3	78	3	78	2	83	6	87
4c	4	76	3	79	2	81	5	91
4d	4	81	3	83	3	81	4	84
4e	7	79	6	82	4	82	6	77
4f	4	82	3	86	1	87	5	94
4g	6	78	5	83	2	86	3	83
4h	6	72	4	81	3	76	4	89
4i	3	67	2	78	1	73	5	86
4j	4	78	3	69	2	75	4	78
4k	3	81	2	83	1	79	5	82

Pyrimidines and their oxo-derivatives exhibit various biological activities such as analgesic, antiinflammatory, antimicrobial, antifungal, antiviral, and anticancer. Therefore, pyrimidine derivatives with diverse structures were synthesized to build up compound libraries for the development of new drug candidates. Synthesis of 2,6-diaryl-4-(3H)-pyrimidinones and 2,6-diaryl-4-aminopyrimidines was carried out in two steps using ethanol as solvent and triethylamine as base. An alternative synthetic method was developed to carry out multicomponent one-step reaction between aromatic aldehydes (4a–j), ethyl cyanoacetate (5), and benzamidine hydrochloride (6) in an aqueous media with potassium carbonate as base under MWI for 40 min to produce 2,6-diaryl-4-(3H)-pyrimidinones (7a–j) in moderate yields (Table 13.16). Similarly, aromatic aldehydes (4a–j) were allowed to react with malononitrile (8) and benzamidine (6) under the same reaction conditions to obtain 2,6-diaryl-4-aminopyrimidines (9a–j) (Scheme 13.35). This new method was advantageous due to improvement in product yield, eco-friendly nature, reduced usage of organic solvents, and less harmful residues. Pyrimidine derivatives were evaluated for antinociceptive activity satisfactorily [36].

Table 13.15 Antibacterial and antifungal activities of compounds (4a-4k).

Comp.	MIC (μg/mL)[a]					MIC (μg/mL)[b]	
	Gram-positive			Gram-negative		Fungi	
	S. aureus	*B. cereus*	*E. coli*	*K. pneumoniae*	*P. aeruginosa*	*A. niger*	*P. chrysogenum*
4a	12	18	17	21	19	++	–
4b	15	12	16	19	21	+++	+++
4c	16	19	15	18	16	–	++
4d	17	21	17	17	20	+++	++
4e	13	15	16	14	12	+	++
4f	21	18	21	22	18	+++	+++
Std. Drug[c]	28	28	28	28	28	29	29

[a] Zone of inhibition for antibacterial activity: 18–28 mm (very strong activity), 11–17 mm (strong activity), 6–16 mm (moderate activity), 0–5 mm (weak activity), dash (–) denotes no activity.
[b] Zone area for antifungal activity: +++ (23–32 mm), ++ (12–22 mm), + (0-11 mm), dash (–) denotes no activity.
[c] Streptomycin and Mycostatin are used as standard drug for antibacterial and antifungal activity.

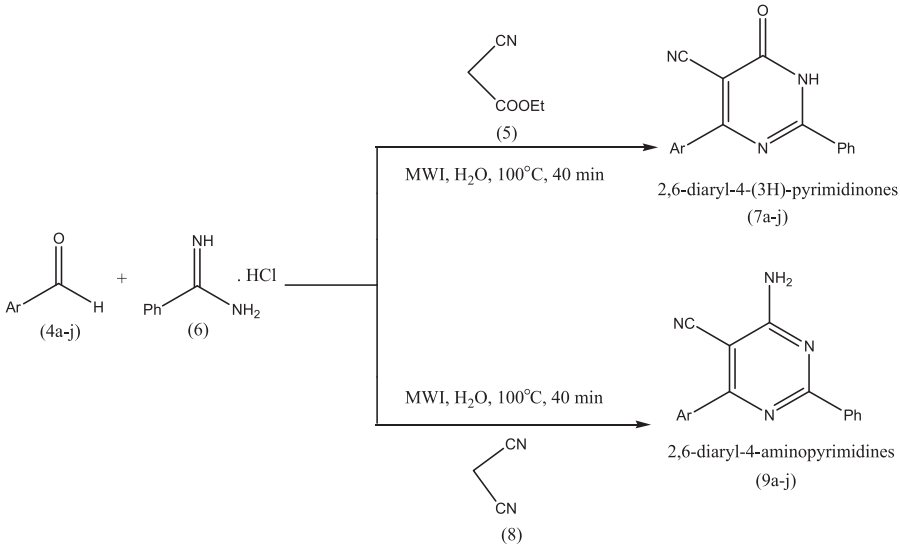

Scheme 13.35 Synthesis of 2,6-diaryl-4-(3H)-pyrimidinones (7a–j) and 2,6-diaryl-4-aminopyrimidines (9a–j).

Table 13.16 Microwave assisted multicomponent reaction of compound (7a-j) and (9a-j).

2,6-diaryl-4-(3H)-pyrimidinones			2,6-diaryl-4-aminopyrimidines		
Compounds	**Ar**	**Yield (%)**	**Compounds**	**Ar**	**Yield (%)**
7a	Ph	42	9a	Ph	56
7b	m-Tolyl	47	9b	m-Tolyl	36
7c	p-Tolyl	33	9c	p-Tolyl	47
7d	p-Cl-Ph	49	9d	p-Cl-Ph	70
7e	p-Br-Ph	46	9e	p-Br-Ph	48
7f	p-F-Ph	45	9f	p-F-Ph	27
7g	p-OCH_3-Ph	41	9g	p-OCH_3-Ph	48
7h	m-NO_2-Ph	20	9h	m-NO_2-Ph	40
7i	p-NO_2-Ph	43	9i	p-NO_2-Ph	67
7j	3,4-Cl_2-Ph	51	9j	3,4-Cl_2-Ph	22

A green approach was described for one-pot four-component sonochemical synthesis of 5-methyl-7-aryl-4,7-dihydrotetrazolo[1,5-*a*]pyrimidine-6-carboxylic esters (5) from the reaction of 2-cyano-guanidine (1), sodium azide (2), various aromatic aldehydes (3), and methyl or ethyl acetoacetate (4) in the presence of catalyst (Scheme 13.36). This method involved in an ultrasound-irradiated synthesis of the biologically and pharmaceutically important heterocyclic compounds in water. This novel sono-catalysis protocol offered several advantages such as high product yields,

short reaction times, environment-friendly reaction medium, easy isolation of the products, and simple preparation of the compounds [37].

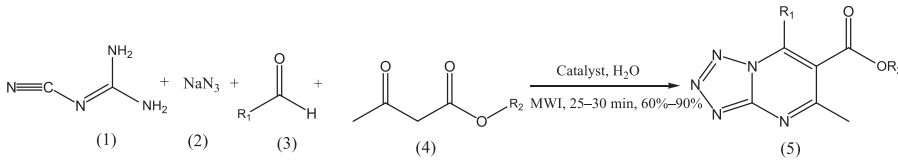

Scheme 13.36 Sonochemical synthesis of 5-methyl-7-aryl-4,7-dihydrotetrazolo[1,5-*a*] pyrimidine-6-carboxylic esters.

The first synthesis of ziprasidone (atypical antipsychotic agent) was not suitable for pilot plant scale-up. Initially, the two fragments were joined by alkylation of compound (1) with (2) in the presence of NaI and Na_2CO_3 in organic solvent to produce ziprasidone with 20% yield. In contrast, the reaction proceeded highly efficiently in water. The solubility of the reagents were improved in water and that leads to increase in the yield (90%–94%) (Scheme 13.37) [38].

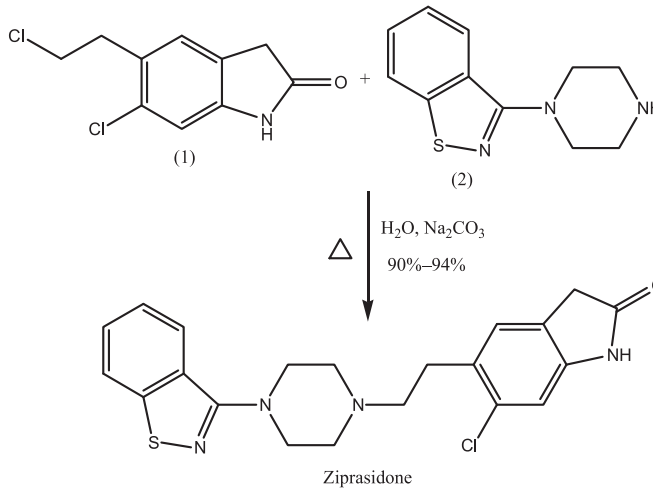

Scheme 13.37 Synthesis of ziprasidone (atypical antipsychotic agent) in water.

13.4 Advantage of using water as a solvent [39, 40]

- Water is the world's cheapest solvent.
- It is safety to handle any reaction in water than in organic solvents.
- It is having no smell, nontoxic, and nonflammable.
- It is available abundantly than organic solvents.
- Most of the chemical reactions are performed better in water.
- Water possesses high surface tension due to hydrogen bonding. So, it increases surface contact between reactants.

- Water is transparent to visible light to enable photosynthesis.
- It does not produce any chemical hazards during reaction.
- The use of water as solvent in chemical reaction follows green chemistry approach because it reduces environmental pollutions by reducing the formation of waste materials.

13.5 Limitations of using water as a solvent [41, 42]

- The use of water as solvent is not suitable in some of the chemical reactions.
- Most organic compounds are not soluble in water.
- Reaction range is narrower as compared to organic solvents. But the scope can be increased in the near future as can be seen from the description mentioned in this book chapter.
- Solubility may be increased by using organic cosolvents, pH control, surfactants, and hydrophilic auxiliaries.
- It may cause corrosion of the heat sink.
- It expands in freezing condition.
- It has large heat of evaporation.
- It forms chelation with metals thereby may prevent catalysis. But, this has been overcome in many chemical reactions.
- Instability of several intermediates and catalysts in water.

13.6 Conclusion

The use of water as solvent in various organic synthesis follows green chemistry approach because it reduces the release of toxic chemicals in the environment and thereby reduces the pollution. The reactions is carried out under mild conditions in the presence of water so as to minimize the formation of chemical waste with easy workup procedure and also enable the recycling of the catalyst. Microwave and other green technologies like ultra-sonication, UV-visible irradiation assist many organic reactions in the presence of water to improve product yields in less reaction time by minimizing unwanted side reaction or the formation of by-product. These green protocols are useful for rapid generation of lead molecules and their optimization to produce the new chemical entities with diverse biological activities such as antimicrobial and antifungal, analgesic, antiinflammatory, antiviral, and anticancer. It can be concluded that the use water as environmentally benign green solvent plays a major role in new drug development in future.

Acknowledgment

Bimal K. Banik is grateful to Prince Mohammad Bin Fahd University.

References

[1] S.J. Tauro, J.B. Gawad, Green chemistry: a boon to pharmaceutical synthesis, Int. J. Sci. Res. 2 (7) (2013) 67–69.
[2] M.-O. Simon, C.-J. Li, C.I. Abstract, Green chemistry oriented organic synthesis in water, Chem. Soc. Rev. 41 (4) (2012) 1415–1427.

[3] S. Madhvi, J. Smita, K.R. Desai, A brief review on microwave assisted organic reactions, Arch. Appl. Sci. Res. 4 (1) (2012) 645–661.
[4] F. Shi, C. Li, M. Xia, K. Miao, Y. Zhao, S. Tu, W. Zheng, G. Zhang, N. Ma, Green chemoselective synthesis of thiazolo[3,2-a]pyridine derivatives and evaluation of their antioxidant and cytotoxic activities, Bioorg. Med. Chem. Lett. 19 (2009) 5565–5568.
[5] S.-J. Tu, X.-D. Cao, W.-J. Hao, X.-H. Zhang, S. Yan, S.-S. Wu, Z.-G. Han, F. Shi, An efficient and chemoselective synthesis of benzo[e][1,4]thiazepin-2-(1H,3H,5H)-ones via a microwave-assisted multicomponent reaction in water, Org. Biomol. Chem. 7 (2009) 557–563.
[6] T.H. Manjashetty, P. Yogeeswari, D. Sriram, Microwave assisted one-pot synthesis of highly potent novel isoniazid analogues, Bioorg. Med. Chem. Lett. 21 (7) (2011) 2125–2128.
[7] F. Shi, D. Zhou, S. Tu, Q. Shao, C. Li, L. Cao, An efficient microwave assisted synthesis furo[3,4-b]-[4,7]phenanthroline and indeno[2,1-b][4,7]phenanthroline derivatives in water, J. Heterocycl. Chem. 45 (2008) 1065–1070.
[8] Y. Dathu Reddy, P. Praveen Kumar, B. Rama Devi, C.V.R. Reddy, P.K. Dubey, Top of form catalyst-free, eco-friendly, one pot syntheses of 2-(3H-imidazo[4,5-b]pyridine-2-yl)-N-arylbenzamides in water, Lett. Org. Chem. 11 (10) (2014) 768–773.
[9] D. Bandyopadhyay, S. Mukherjee, R.R. Rodriguez, B.K. Banik, An effective microwave-induced iodine-catalyzed method for the synthesis of quinoxalines via condensation of 1,2-diamines with 1,2-dicarbonyl compounds, Molecules 15 (2010) 4207–4212.
[10] S. Singhal, J.K. Joseph, S.L. Jain, B. Sain, Synthesis of 3,4-dihydro-pyrimidinones in the presence of water under solvent free conditions using conventional heating, microwave irradiation/ultrasound, Green Chem. Lett. Rev. 3 (1) (2010) 23–26.
[11] V. Polshettiwar, R.S. Varma, Greener and expeditious synthesis of bioactive heterocycles using microwave irradiation, Pure Appl. Chem. 80 (4) (2008) 777–790.
[12] F. Shi, S. Tu, B. Jiang, C. Li, D. Zhou, Q. Shao, L. Cao, Q. Wang, J. Zhou, A green and efficient synthesis of furo[3,4-*e*]pyrazolo[3,4-*b*]-pyridine derivatives in water under microwave irradiation without catalyst, J. Heterocycl. Chem. 45 (4) (2008) 1103–1108.
[13] B. Jiang, L.J. Cao, S.J. Tu, W.R. Zheng, H.Z. Yu, Highly diastereoselective domino synthesis of 6-spirosubstituted-pyrido[2,3-d]pyrimidine derivatives in water, J. Comb. Chem. 11 (2009) 612–616.
[14] O. Dehbi, E.A. Ishak, M.A. Bakht, M.H. Geesi, M.B. Alshammari, V. Chagnault, A. Kaiba, S. Lazar, Y. Riadi, Water-mediated synthesis of disubstituted 5-aminopyrimidines from vinyl azides under microwave irradiation, Green Chem. Lett. Rev. 11 (2) (2018) 62–66.
[15] K.P. Sanghvi, J.M. Amin, D.K. Sureja, A.P. Shah, M.T. Chhabria, One pot microwave assisted synthesis of various substituted guanidine derivatives using water as solvent: a green chemistry approach, J. Chem. Pharm. Res. 8 (7) (2016) 722–727.
[16] L. Perez-Picaso, J. Escalante, H.F. Olivo, M.Y. Rios, Efficient microwave assisted syntheses of 2,5-diketopiperazines in aqueous media, Molecules 14 (2009) 2836–2849.
[17] D. Sharma, S. Kumar, J.K. Makrandi, Water mediated green synthesis of coumarin-3-carboxylic acids under microwave irradiation condition, Chem. Sci. Trans. 2 (2) (2013) 403–406.
[18] M. Gutierrez, E. Polo, K. Ferrer-Pertuz, J. Trilleras, J. Quiroga, Microwave-assisted one-pot synthesis in water of carbonylpyrazolo[3,4-b]pyridine derivatives catalyzed by InCl3 and sonochemical assisted condensation with aldehydes to obtain new chalcone derivatives containing the pyrazolopyridinic moiety, RSC Adv. 7 (2017) 50044–50055.
[19] G. Qu, S. Han, Z. Zhang, M. Geng, F. Xue, Microwave assisted synthesis of 6-substituted aminopurine analogs in water, J. Braz. Chem. Soc. 17 (5) (2006) 915–922.

[20] W.-M. He, L.-Y. Xie, Y.-J. Li, J. Qu, Y. Duan, J. Hu, K.-J. Liu, Z. Cao, A base-free, ultrasound accelerated one-pot synthesis of 2-sulfonylquinolines in water, Green Chem. 19 (2017) 5642–5646.
[21] B. Eftekhari-Sis, S. Vahdati-Khajeh, Ultrasound-assisted green synthesis of pyrroles and pyridazines in water via three-component condensation reactions of arylglyoxals, Curr. Chem. Lett. 2 (2013) 1–8.
[22] B.M. Sapkal, P.K. Labhane, J.R. Satam, In water–ultrasound-promoted synthesis of tetraketones and 2-substituted-1H-benzimidazoles catalyzed by BiOCl nanoparticles, Res. Chem. Intermed. 43 (2017) 4967–4979.
[23] S. Gholizadeh, K. Radmoghadam, Ultrasound-assisted three-component synthesis of spiro [4H-pyrano[3,2-c]quinolin-4,3′-indoline]-2′,5(6H)-diones in water, Orient. J. Chem. 29 (4) (2013) 1637–1641.
[24] M. Pal, A.S.G. Prasad, T.B. Rao, D. Rambabu, M.V.B. Rao, Ultrasound assisted synthesis of quinoline derivatives in the presence of $SnCl_2.2H_2O$ as a precatalyst in water: evaluation of their antibacterial activities, Mini Rev. Med. Chem.y 18 (10) (2018) 895–903.
[25] S. Rostamnia, K. Lamei, A rapid, catalyst-free, three-component synthesis of rhodanines in water using ultrasound, Synthesis (19) (2011) 3080–3082.
[26] P. Vanelle, Y. Kabri, A. Gellis, Microwave-assisted synthesis in aqueous medium of new quinazoline derivatives as anticancer agent precursors, Green Chem. 11 (2009) 201–208.
[27] M. Yildirim, D. Celikel, Y. Durust, D.W. Knight, B.M. Kariuki, A rapid and efficient protocol for the synthesis of novel nitrothiazolo[3,2-c]pyrimidines via microwave-mediated Mannich cyclisation, Tetrahedron 70 (2014) 2122–2128.
[28] V. Polshettiwar, R.S. Varma, Biginelli reaction in aqueous medium: a greener and sustainable approach to substituted 3,4-dihydropyrimidin-2(1H)-ones, Tetrahedron Lett. 48 (2007) 7343–7346.
[29] S.-J. Tu, X.-H. Zhang, Z.-G. Han, X.-D. Cao, S.-S. Wu, S. Yan, W.-J. Hao, G. Zhang, N. Ma, Synthesis of isoxazolo[5,4-b]pyridines by microwave-assisted multi-component reactions in water, J. Comb. Chem. 11 (3) (2009) 428–432.
[30] D. Ashok, B.V. Lakshmi, M. Sarasija, An efficient microwave-assisted Suzuki cross-coupling on coumarin derivatives in water and evaluation of antimicrobial activity, Lett. Org. Chem. 13 (1) (2016) 76–84.
[31] K.M. Dawood, M.B. Elamin, A.M. Farag, Microwave-assisted synthesis of 2-acetyl-5-arylthiophenes and 4-(5-arylthiophen-2-yl)thiazoles via Suzuki coupling in water, Arch. Org. Chem. 7 (2015) 50–62.
[32] D. Kumar, R. Kumar, Microwave-assisted synthesis of pyrazolo[1,5-c]quinazolinesand their derivatives, Tetrahedron Lett. 55 (2014) 2679–2683.
[33] S. Muthusaravanan, E.T.A. Thangamani, A greener and microwave-mediated synthesis and spectral studies of β-aminomethyl-hydroxyl coumarins, Chem. Data Collect. 20 (2019) 100–199.
[34] M.A.E.A.A.A. El Remaily, K.M. Shaaban, Eco-friendly synthesis of guanidinyltetrazole compounds and 5-substituted 1*H*-tetrazoles in water under microwave irradiation, Tetrahedron 70 (2) (2014) 270–275.
[35] A.R. Bhat, A.H. Shalla, R.S. Dongre, Microwave assisted one-pot catalyst free green synthesis of new methyl-7-amino-4-oxo-5-phenyl-2-thioxo-2,3,4,5-tetrahydro-1H-pyrano [2,3-d]pyrimidine-6-carboxylates as potent in-vitro antibacterial and antifungal activity, J. Adv. Res. 6 (2015) 941–948.
[36] A.L. Xavier, A.M. Simas, E.P.d.S. Falcao, J.V. dos Anjos, Antinociceptive pyrimidine derivatives: aqueous multicomponent microwave assisted synthesis, Tetrahedron Lett. 54 (26) (2013) 3462–3465.

[37] A. Maleki, J. Rahimi, O.M. Demchuk, A.Z. Wilczewska, R. Jasińskid, Green in water sonochemical synthesis of tetrazolopyrimidine derivatives by a novel core-shell magnetic nanostructure catalyst, Ultrason. Sonochem. 43 (2018) 262–271.
[38] P. Bowles, Pfizer Inc., USA, Process for preparing aryl piperazinyl-heterocyclic compounds, US Patent 5206366, April 27, 1993.
[39] D. Dallinger, C.O. Kappe, Microwave-assisted synthesis in water as solvent, Chem. Rev. 107 (6) (2007) 2563–2591.
[40] P.T. Anastas, J.C. Warner, Green Chemistry: Theory and Practice, Oxford University Press, New York, 1998.
[41] J. Clark, D.M.A. Macquarrie, Handbook of Green Chemistry and Technology, Blackwell, Oxford, 2002.
[42] P.A. Grieco, Organic Synthesis in Water, Blackie Academic and Professional, London, 1998.

Solvent-less reactions: Green and sustainable approaches in medicinal chemistry

14

Biswa Mohan Sahoo[a,*], *Bimal Krishna Banik*[b]
[a]Roland Institute of Pharmaceutical Sciences, Berhampur, India, [b]Department of Mathematics and Natural Sciences, College of Sciences and Human Studies, Deanship of Research Development, Prince Mohammad Bin Fahd University, Al Khobar, Kingdom of Saudi Arabia
[*]Corresponding author. e-mail address: drbiswamohansahoo@gmail.com

Abbreviations

cm	centimeter
DHPMs	dihydropyrimidinones
EPA	Environmental Protection Agency
$FeCl_3$	ferric chloride
g	gram
GHz	gigahertz
Hz	hertz
ZSM	Zeolite Socony Mobil
HCl	hydrochloric acid
HSVBM	high-speed vibratory ball milling
IR	infrared
KF	potassium fluoride
kHz	kilohertz
KOH	potassium hydroxide
MCM	Mobil Composition of Matter
min	minute
$Mn(OAc)_3$	manganese(III) acetate
mL	milliliter
mm	millimeter
MHz	megahertz
MAOS	microwave assisted organic synthesis
MWI	microwave irradiation
NSAID	nonsteroidal anti-inflammatory drugs
PMA	phosphor molybdic acid
PZT	piezoelectric
%	percent
RFTA	riboflavin tetraacetate
$SnCl_2$	stannous chloride
TsOH	p-toluene-sulfonic acid

Green Approaches in Medicinal Chemistry for Sustainable Drug Design. https://doi.org/10.1016/B978-0-12-817592-7.00014-9
© 2020 Elsevier Inc. All rights reserved.

TEBA	triethyl-benzyl-ammonium chloride
UV/Vis	ultraviolet-visible
USI	ultrasound irradiation
W	watt

14.1 Introduction

Green chemistry is defined as environmentally benign chemical synthesis. It is also termed as sustainable chemistry, clean chemistry, benign by design chemistry, or atom economy. It involves the set of principles which reduces or eliminates the use of hazardous substances during design, manufacture, and application of chemical products. This approach plays an important role in controlling the environmental pollution by using safer solvents, catalysts, suitable reaction conditions and thereby increases the atom economy and energy efficiency [1].

But a dry media reaction or solid-state reaction or solvent-less reaction is a reaction system which can be carried out in the absence of solvent. It includes the neat methodologies for the development of various drug substances by synthesizing the new chemical entities without solvents consumption [2]. So, the solvent-less reactions minimize the formation of by-products or waste by avoiding the use of conventional volatile organic solvents. A solvent-free reaction is achieved by using the reactants alone or by incorporating them in clays, zeolites, silica, alumina, etc. to get the stereoselective products as well as enhance the rate of reaction [3].

14.1.1 Principles of green chemistry

Organic chemist, Anastas working in the Office of Pollution Prevention and Toxins at the EPA, and John C. Warner developed the 12 principles of green chemistry in 1991 (Fig. 14.1). The green chemistry principles provide the following steps [4]:

1. Prevention of waste or by-products: It is essential to carry out the synthesis in such a way that the formation of waste or by-products is less or absent. It is mainly significant because in most of the cases, the cost involved in the treatment and disposal of waste adds to the overall production cost.
2. Atom economy or efficiency: It represents the design of synthetic methods to maximize the incorporation of reactants (starting materials and reagents) to get the final products. If the product yield of a chemical reaction is 90%, then the reaction is considered to be good. The percentage yield is calculated by the following formula:

$$\%\text{yield} = \frac{\text{Actual yield of the product}}{\text{Theoretical yield of the product}} \times 100$$

If 1 mol of a starting material is utilized to produce 1 mol of the product, then the yield is 100%. So, the percentage atom utilization can be determined by using the following equation:

$$\%\text{Atom utilization} = \frac{\text{Mol.wt.of desired product}}{\text{Mol.wt.of (Desired product + Waste product)}} \times 100$$

The concept of atom economy was developed by Trost. It represents how much the reactants end up in the final product. Similarly, the percentage atom economy was determined by Sheldon as follows:

$$\%\text{Atom economy} = \frac{\text{Final product of atoms utilized}}{\text{Final product of reactants}} \times 100$$

3. Use of less hazardous and toxic chemicals: Various synthetic methods should be designed properly so that the use and generation of substances have less or no toxic effect on human health and the environment. In case of chemical reaction, risk can be defined as a function of hazard and exposure. So, risk can expressed as follows:

$$\text{Risk} = f\,(\text{hazard, exposure})$$

4. Designing of safer chemicals: Chemical products should be designed to affect their desired function while minimizing their toxicity.
5. Selection of most appropriate solvents: Avoid the use of auxiliary materials (solvents and extractants) if possible, or otherwise make them innocuous.
6. Energy efficiency by design: Energy requirements should be minimized and the synthesis should be performed at ambient temperature and pressure.
7. Use of renewable raw materials or starting materials: The raw material or feedstock should be renewable rather than depleting whenever technically and economically practicable.
8. Shorter syntheses (avoid derivatization): Unnecessary derivatization (use of blocking groups, protection or deprotection, and modification of physical or chemical processes) should be minimized or avoided if possible, because these steps require supplementary reagents and generate waste materials.
9. Catalytic rather than stoichiometric reagents: Catalytic reagents are superior to stoichiometric reagents.
10. Products obtained should be biodegradable: Chemical products should be designed in such a way that these can be degradable to innocuous products when disposed.
11. Strengthening of analytical techniques to control hazardous compounds: Analytical methodologies need to be further developed to allow for real-time, in-process monitoring, and control prior to the production of hazardous substances.
12. Hazard and accident prevention: The manufacturing plants should be designed so as to eliminate the possibility of accidents (explosions and fires) during operations.

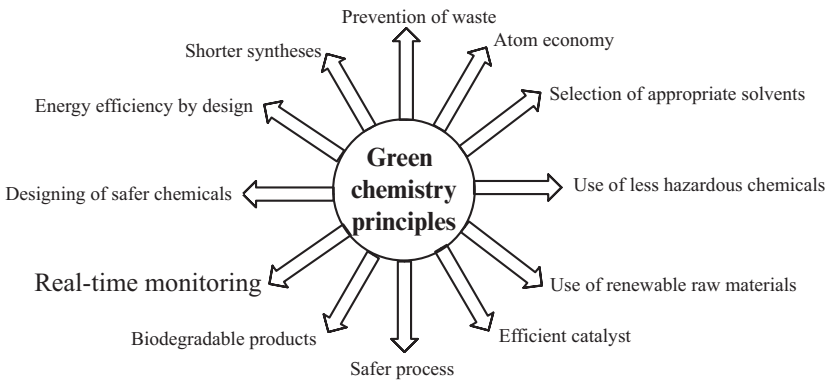

Fig. 14.1 Principles of green chemistry.

14.1.2 Green chemistry approaches

There are various approaches of green chemistry to carry out solvent-less organic reactions as given below. By using these technologies, the solvent-less reactions become efficient and economic by increasing the rate of reaction with reduced reaction time and high product yield [5].

a. Microwave (MW) technology
b. Ultrasonication
c. Photocatalysis [ultraviolet, visible, and infrared (IR) irradiation]
d. Grinding technique
e. Milling technique

14.1.2.1 MW technology

This technology utilizes the microwave irradiation (MWI) as heating source to carry out various chemical reactions. MW is an alternative energy source to carry out chemical transformations in minutes, instead of hours or even days. In the early 1990s, various laboratories focused on MW-expedited approach under solvent-free conditions using MW oven in open reaction vessels [6]. MWs are the electromagnetic radiation with wavelengths ranging from 1 m to 1 mm with frequencies between 300 MHz (1 m) and 300 GHz (1 mm). MWs with high-frequency electric fields are applied to heat the reactants of a chemical reaction with electric charges. In case of polar solvents, these are heated due to their dipolar rotation with the field and loose energy during collisions between molecules. By using MW heating methods, the rate of organic reactions can be accelerated and the products can be produced selectively by using suitable MW parameters [7].

Thus, microwave-assisted organic synthesis (MAOS) offers several advantages such as instantaneous and rapid heating, high temperature, homogeneity, and selective heating in comparison with conventional heating method. MW-accelerated chemical reactions are mainly depending on the capacity of the reaction mixture to absorb MW energy efficiently and also it depends on selection of solvents for conducting a chemical reaction [8]. So, the ability of a specific solvent or material to convert MW energy to heat is called loss tangent (δ). If the value of tan δ is higher, then the solvent is suitable for absorption of MW radiation that causes efficient heating [9].

An efficient synthesis of 3,4-dihydropyrimidinones (DHPMs) using sulfamic acid as catalyst from an aldehyde, β-keto ester, urea, or thiourea under the conventional heating and solvent-free MWIs is depicted. The solvent-free MW-assisted green procedure offers advantages such as shorter reaction times, simple workup, and excellent yield over the conventional heating [10] (Table 14.1).

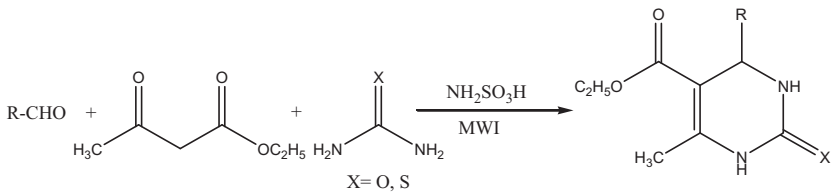

Table 14.1 Conventional heating and solvent-free microwave irradiations for synthesis of 3,4-dihydropyrimidinones.

Product	R	X	Conventional heating		Microwave irradiation	
			Time (h)	Yield (%)	Time (min)	Yield (%)
4a	C_6H_5	O	6	72	2	93
4b	4-OCH_3—C_6H_4	O	6	75	2.5	87
4c	2-furyl	O	7	65	2	88
4d	C_6H_5—CH═CH—	O	6	80	3	86
4e	4-OH—C_6H_4	O	6	67	3	92
4f	2-OH—C_6H_4	O	6	66	3	91
4g	2-Cl—C_6H_4	O	6	72	3	90
4h	3-NO_2—C_6H_4	O	6	68	3.5	90
4i	C_6H_5	S	6	70	3	90
4j	4-OH—C_6H_4	S	6	65	3	92
4k	C_6H_5—CH═CH—	S	7	64	3	84

Pinacol coupling reaction involves the formation of carbon-carbon covalent bond between the carbonyl groups of an aldehyde or a ketone in the presence of an electron donor via free radical process. The product obtained is called vicinal diol [11].

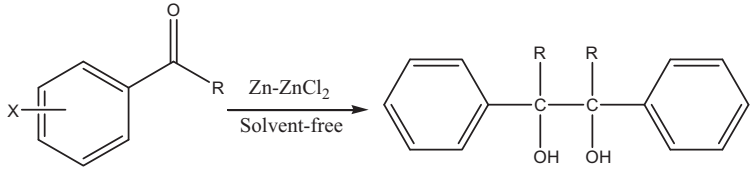

The synthesis of blockbuster anticancer drug, imatinib is based on MW-mediated solid-phase reactions. It involves the expeditious, high yield, and convenient synthesis of imatinib on an aldehydic, super acid-sensitive resin, through an efficient, MW-assisted synthetic protocol [12].

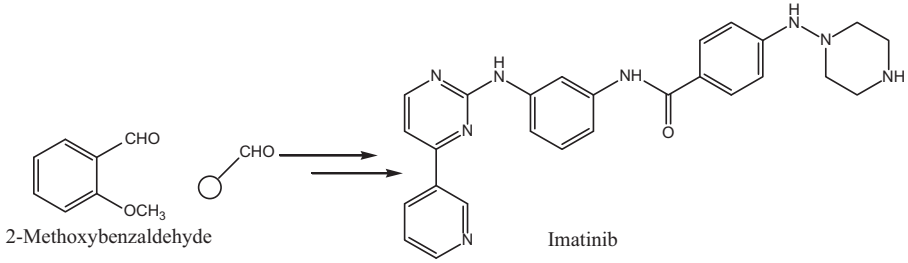

Kidwai and coworkers have carried out the MW synthesis of N-acetylated cephalosporin without using solvents. The cephalosporic acid is a carboxylic acid which gets adsorbed on the basic alumina and then it is brought in contact with MW radiation only for 2 min. The time required is very less with high yield under MWI as compared to the conventional method [13].

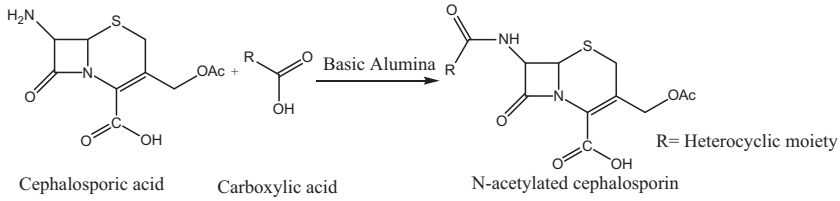

Heck, Suzuki, and Stille reactions involve the use of palladium catalyzed reactions under MWI. These are having more usefulness to produce new drug molecule during drug discovery process. The use of MW radiation for organic synthesis was established in June 1888 by Mills and coworker at Glaxo London. The following reaction was carried out between iodobenzene and 1-decane and the reaction was completed in 10 min, whereas the conventional method requires 14 h to complete the reaction [14].

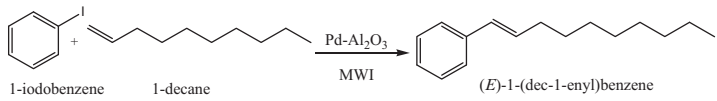

The solvent-free synthesis of 4-(substituted phenyl)-6-phenyl-3-cyano-2-pyridones is carried out by the treatment of ethyl 2-cyano-3-(substituted phenyl)acrylates with acetophenone using powdered potassium hydroxide (KOH) in the modified domestic MW oven (300 W, 5 min). It leads to the formation of final product with better yields in comparison to conventional procedure. It involves one-pot synthesis via three-component cyclo-condensation under solvent-free conditions [15] (Table 14.2).

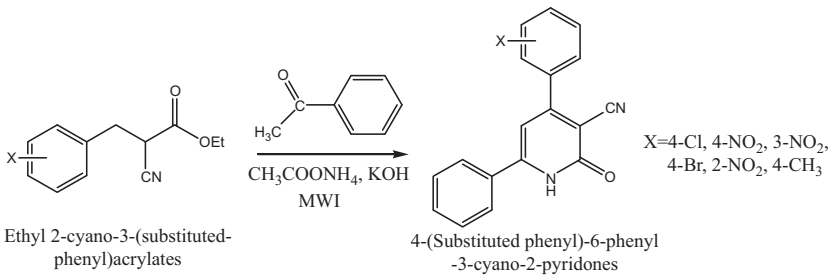

Table 14.2 Conventional and microwave synthesis of 4-(substituted phenyl)-6-phenyl-3-cyano-2-pyridones.

Sl. No.	X	Yield (%)	
		Conventional synthesis	Microwave synthesis
1	H	35	34
2	4-CH_3	40	32
3	4-OCH_3	30	34
4	4-Cl	32	33
5	4-NO_2	No product	23
6	4-Br	14	20
7	3-NO_2	35	40
8	3-Cl	26	29
9	2-NO_2	12	16

It has been reported that 1,3-dipolar cycloaddition of organic azides to acetylenic amides under solvent-free MWI produces the corresponding N-substituted-1,2,3-triazoles with excellent yields [16].

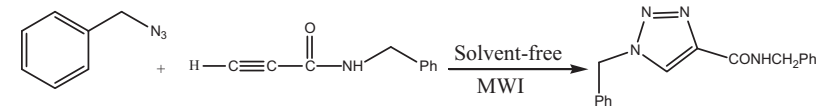

1-(Azidomethyl)benzene *N*-Benzylpropiolamide N-Substituted-1,2,3-triazoles

The synthesis of quinoline is carried out by reacting the substrates like 2-nitro-benzaldehyde and enolizable ketones in the presence of $SnCl_2$ under MWI without using any solvent [17].

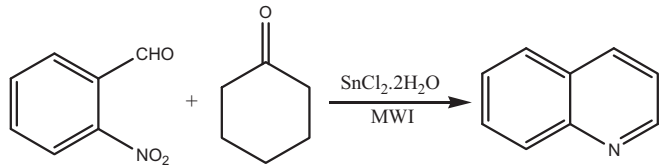

2-Nitrobenzaldehyde Cyclohexanone Quinoline

Beckmann rearrangement of oxime of a ketone (acetophenone) is mixed with montmorillonite and irradiated for 7–10 min in MW oven to give corresponding anilide (acetanilide) with 91% yield [18].

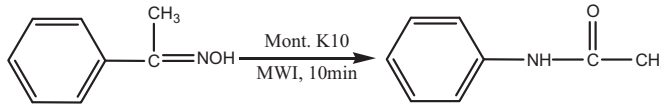

Acetophenone oxime Acetanilide

Green synthesis of 2-(2-methyl-3-trifluoromethylanilino)nicotinic acid is carried out by reaction of 2-methyl-3-trifluoromethylaniline with 2-chloronicotinic acid under solvent-free conditions in the presence of catalytic amount of boric acid [19].

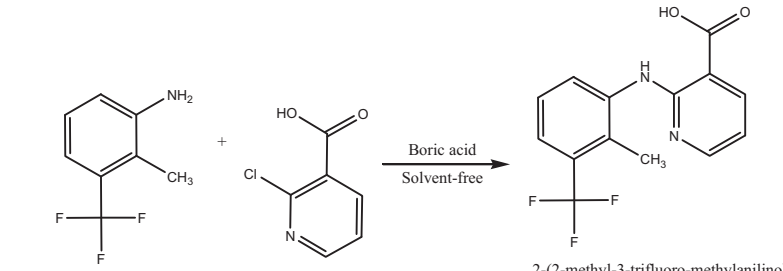

2-methyl-3-trifluoromethylaniline 2-chloronicotinic acid 2-(2-methyl-3-trifluoro-methylanilino) nicotinic acid

A series of salicylaldimines with high yield is produced by condensation reaction of salicylaldehyde and aryl amines under solvent-free MWI [20].

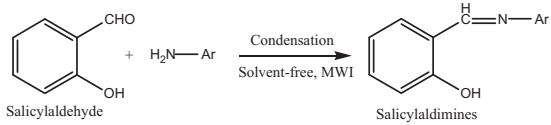

Salicylaldehyde Salicylaldimines

The synthesis of 2,4,5-triarylimidazoles is carried out by three-component, one-pot cyclo-condensation reaction of 1,2-diketones, aryl aldehydes, and ammonium acetate under solvent-free conditions. It provides clean, safe, cost-effective, efficient, and environmentally benign protocol for the synthesis of 2,4,5-triarylimidazoles with good product yield [21].

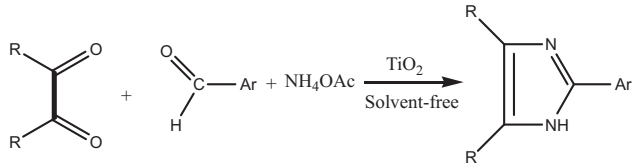

R=Ph, O-Furyl

4-methoxyphenyl chalcones are synthesized by crossed-aldol condensation of equimolar quantities of 4-methoxy-acetophenone and substituted benzaldehydes in the presence of $FeCl_3$/bentonite catalyst under solvent-free MWI [22].

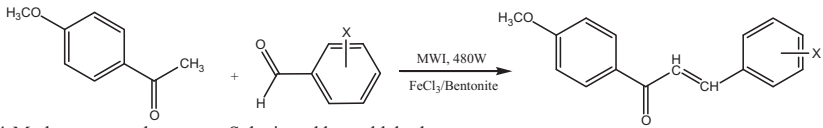

4-Methoxy-acetophenone Substituted benzaldehydes 4-Methoxyphenyl chalcones

X= H, 3-Cl, 4-Cl, 4-F, 2-OCH_3, 4-OCH_3, 4-CH_3, 3-NO_2, 4-NO_2

14.1.2.2 Ultrasonication

Ultrasonic irradiation leads to the acceleration of various catalytic reactions including both homogeneous and heterogeneous systems. The utilization of ultrasound to accelerate the chemical reactions is called as sonochemistry [23]. The use of ultrasound in organic synthesis involves specific activation based on the physical phenomenon, i.e., acoustic cavitation. Cavitation is a process in which mechanical activation destroys the attractive forces of molecules in the liquid phase. By applying ultrasound, the compression of the liquid is made followed by rarefaction (expansion), in which a sudden pressure drop forms small, oscillating bubbles of gaseous substances. These bubbles expand with each cycle of the applied ultrasonic energy until they reach an unstable size. Finally, they can collide or violently collapse as depicted in Fig. 14.2 [24].

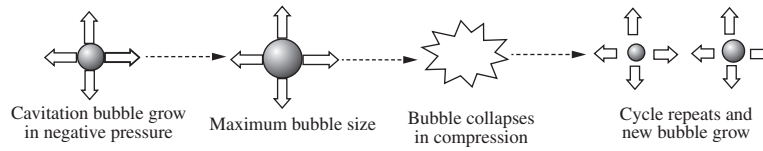

Fig. 14.2 Process of reaction by ultrasonication.

Various chemical reactions can be conducted by using ultrasonic cleaning bath. The amount of energy which reaches the reaction medium is only between 1 and 5 W cm^{-2} and temperature control is not proper. The first commercial application of ultrasonics was made by Langevin in 1917. Richards and Loomis first reported the effects of ultrasound in chemical reaction in 1927 [25].

The source of the ultrasound is a piezoelectric (PZT) materials such as lead-zirconate-titanate ceramic or quartz. These materials are subjected to high-voltage alternating current with an ultrasonic frequency (15 kHz–10 MHz). The PZT material expands and contracts in this electric field and is attached to the walls of the cleaning bath and converts electrical energy into sound energy. In most applications, the sonicators operate at a fixed frequency in the range of 20–35 kHz. In cleaning baths, the acoustic field is continuous, whereas it is in the pulsed form in probes [26]. So, the large-scale reactions can be conducted using immersible ultrasonic probes that circulate the transfer of the energy throughout water and the reaction vessel. Luche proposed an empirical classification of sonochemical reactions into three types as follows:

Type-1: Homogeneous systems which proceed *via* radical or radical-ion intermediates. This implies that sonication is able to affect reactions proceeding through radicals and further that it is unlikely to affect ionic reactions.

Type-2: Heterogeneous systems proceeding via ionic intermediates. Here, the reaction is influenced primarily through the mechanical effects of cavitation such as surface cleaning, particle size reduction and improved mass transfer. This is what has sometimes been referred to as "false sonochemistry."

Type-3: Heterogeneous reactions which include a radical pathway or a mixed mechanism, i.e., radical and ionic. Radical reactions will be chemically enhanced by sonication but the general mechanical effect referred to above may well still apply. If the radical and ionic mechanisms lead to different products, ultrasound should favor the radical pathway and this could lead to a switch in the nature of the reaction products.

There are two types of effects mediated by ultrasound such as physical and chemical. For example, when ultrasound is applied to an Ullmann reaction that normally requires a 10-fold excess of copper and 48 h of reaction time, this can be reduced to a fourfold excess of copper and a reaction time of 10 h. The particle size of the copper shrinks from 87 to 25 μm, but the increase in the surface area cannot fully explain the increase in reactivity. It was suggested that sonication also assists in the breakdown of intermediates and desorption of the products from the surface [27].

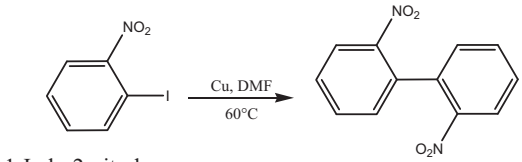

1-Iodo-2-nitrobenzene Biphenyl compound

The application of sonochemistry for the synthesis of different coumarins from active methylene compounds and 2-hydroxybenzaldehydes or resorcinol is very effective on a multigram scale with a higher yield of crystalline product in a shorter reaction time as compared to the compounds produced by conventional methods [28].

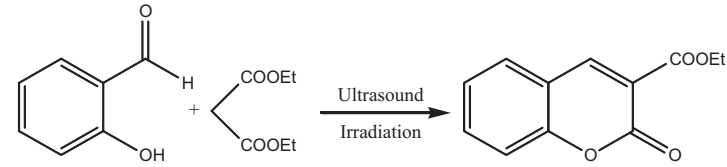

2-Hydroxybenzaldehydes Diethyl malonate Coumarin

Ultrasound irradiation (USI) promoted the cyclo-condensation of β-keto esters and amidines with an excellent yield to produce substituted 4-pyrimidinols. Finally, ultrasound promoted the tosylation followed by a Suzuki-Miyaura cross-coupling reaction to produce 4-aryl-pyrimidines [29].

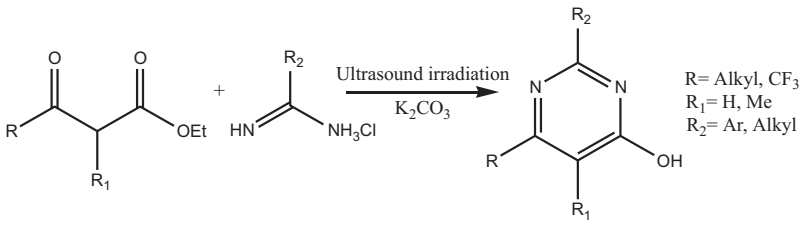

He et al. proposed USI method to prepare 1,4-diaza butadiene by the condensation of an α-diketone and an amine. This process has advantages like less reaction time, environment-friendly conditions, low temperature, high yields, etc. [30].

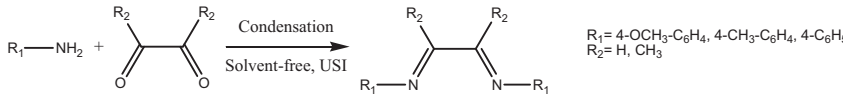

1,2,3-Benzotriazole derivatives are synthesized with moderate to good yields in the range of 71%–82% under ultrasonic and solvent-free conditions and their anthelmintic activities are determined against adult earthworms (*Pheretima posthuma*) [29].

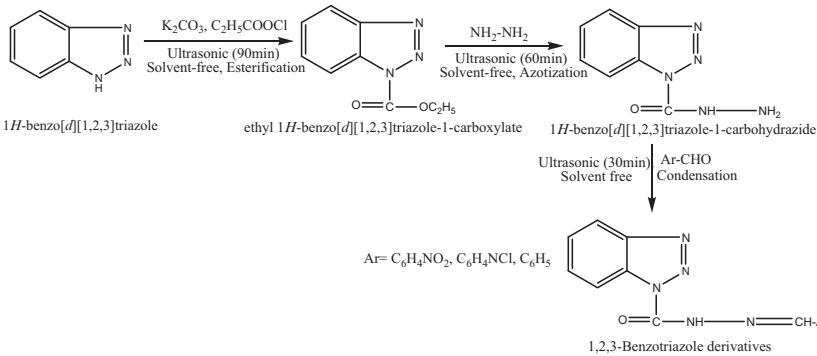

Puri et al. synthesized 4-substituted 2H-chromen-2-ones via von Pechmann condensation of substituted phenols and β-keto esters in solvent-less media with excellent yields using USI [31].

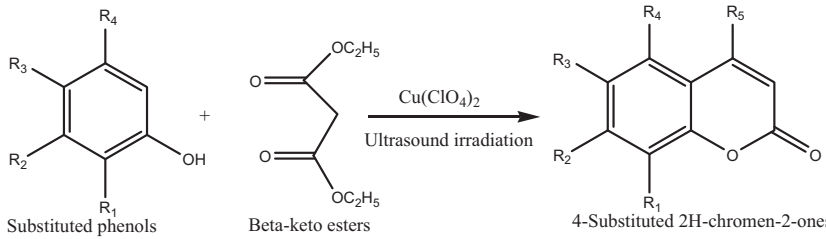

Zhang et al. accomplished a straightforward synthesis of substituted pyrroles using zirconium chloride-catalyzed modified Paal-Knorr method under USI. Compared to conventional methods, this new method provides as easy access to various substituted pyrroles in good to excellent yields with short reaction times [32].

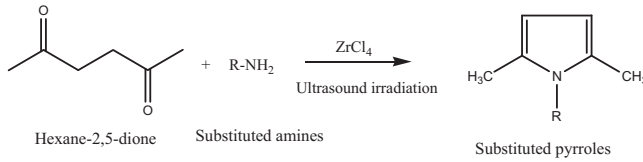

14.1.2.3 Photocatalysis (ultraviolet, visible, and IR irradiation)

Photocatalysis involves the use of ultraviolet, visible light, and IR radiation to generate new pharmaceutically active compounds with diverse structures. Before performing a photochemical reaction, UV/Vis spectrum of the photoactive compound is recorded. The photoactive compound is the molecule which can be electronically excited and undergoes chemical reaction from its excited state [33].

Photochemical alkene pericyclic reactions are capable of occurring in the solid state in the absence of solvents. When (E)-cinnamic acid is irradiated with visible light for 1 week a photochemical [2+2]cycloaddition occurs to form regioselectively and stereoselectively truxillic acid stereoisomer. Truxillic acid is known as a "head-to-tail" dimer in this reaction [34].

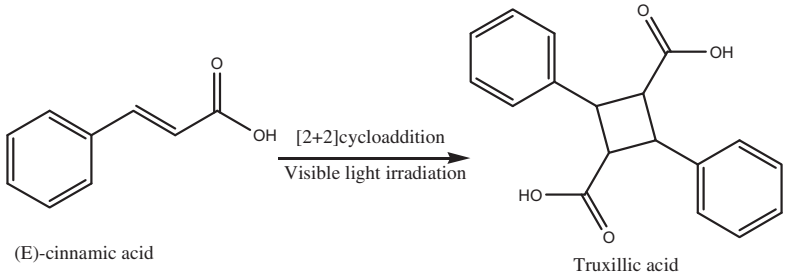

The oxidation of 4,4′-dimethoxybenzhydrol to 4,4′-dimethoxybenzophenone is carried out under solvent-free photocatalytic reaction in the presence of riboflavin tetraacetate (RFTA) as photocatalyst. RFTA is a well-known blue-light absorbing photocatalyst [35].

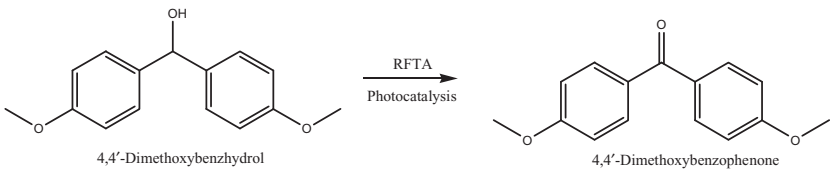

1,4-Dihydropyridine and their derivatives are synthesized by reaction between four components such as aldehyde, Dione, Meldrum acid, and ammonium acetate in the presence of solid support montmorillonite KSF under solvent-free IR irradiation. It is a greener method which involves multicomponent one-pot synthesis with higher yield in less reaction time [36].

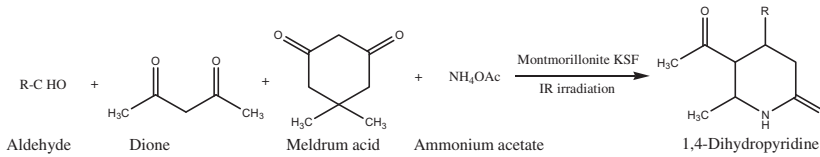

14.1.2.4 Grinding technique

Grinding technique is considered as an essential methodology to carry out the synthetic reactions under solvent-free condition with high product yield. Grinding of the reactants for a chemical reaction can be carried out by using mortar and pestle or by using high-speed vibrating mill. Due to collision between the reacting molecules, the chemical reaction is carried forward [37]. So, this makes the molecule to collide which leads to formation of the final products. The time required to complete the reaction is less as compared in the conventional heating techniques (Fig. 14.3).

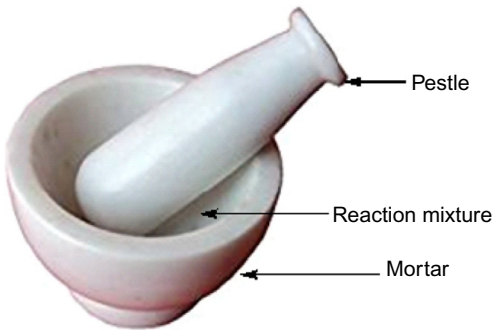

Fig. 14.3 Chemical reaction by grinding technique.

The grinding process for the chemical reaction can be performed out at room temperature also. Various organic reactions are carried out by using grinding technique under solvent-free conditions are Grignard reaction, Knoevenagel condensation, Aldol condensation, Dieckman reaction, Reformatsky reaction, oxidation, reduction, rearrangement reaction, etc. as presented in Fig. 14.4 [38].

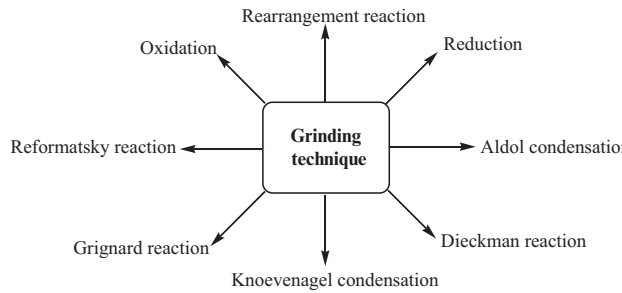

Fig. 14.4 Organic reactions performed by using grinding technique.

Knoevenagel condensation of aromatic aldehyde with active methylene compound is performed by using grinding technology. Ren et al. have reported the synthesis of α-cyanocinnamate using calcium oxide based on grinding method [39].

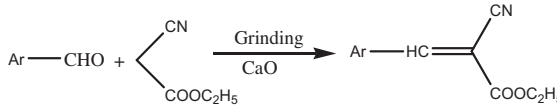

Rong et al. carried out Knoevenagel condensation using triethyl-benzyl-ammonium chloride (TEBA) as catalyst under grinding technique [40].

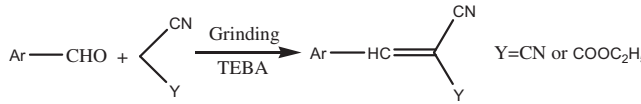

The synthesis of the 5-arylidene barbituric acid derivatives is performed by reacting aryl aldehydes with pyrimidine-2,4,6-trione catalyzed by amino-sulfonic acid under grinding condition [41].

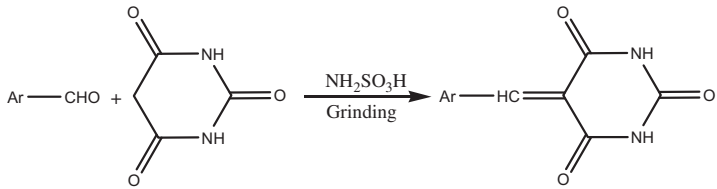

Pyrimidine-2,4,6-trione

Shingare et al. reported the synthesis of polyhydroquinolines at room temperature using MCM-41 catalyst (a mesoporous material/silica anchored with organic basic moieties) via four-component coupling reaction using the grinding technique [42].

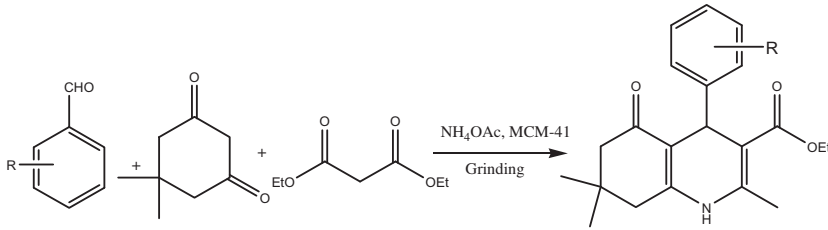

A series of 2,4,5-triaryl substituted imidazoles have been synthesized with high yield under solvent-free conditions by grinding 1,2-diketones, aromatic aldehydes, and ammonium acetate in the presence of molecular iodine as catalyst [43].

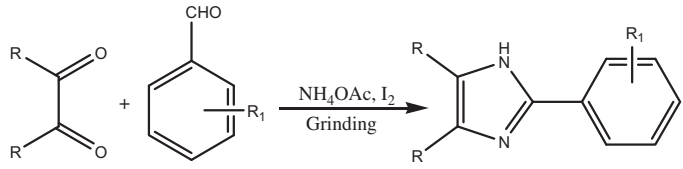

The synthesis of 4H-pyrans is performed by grinding aryl aldehydes, malononitrile with 3-methyl-2-phenyl-2-pyrazolin-5-one in the presence of potassium fluoride (KF) $2H_2O$ [44].

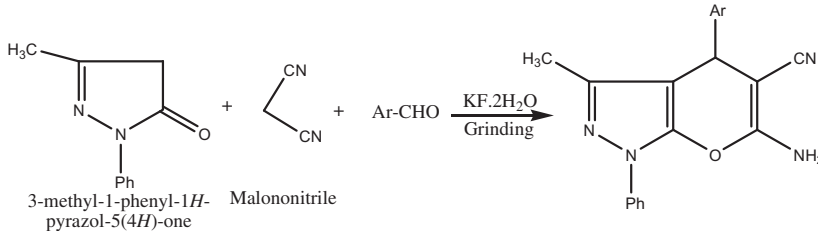

The solid-state etherification reaction is of an utmost prebiotic importance, since ethers are not easy to make under the aqueous conditions. The use of p-toluene-sulfonic acid (TsOH) as a catalyst can probably be substituted by various acidic clays [45].

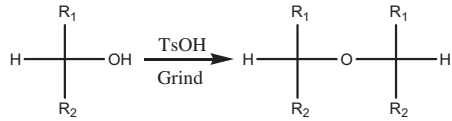

Leung and Angel described the preparation of (Z) and (E)-(4-bromophenyl)styrene by a solvent-less Wittig reaction. The reaction involves grinding of 4-bromobenzaldehyde, benzyl-triphenyl-phosphonium chloride, and tribasic potassium phosphate by using mortar and pestle for 20 min [46].

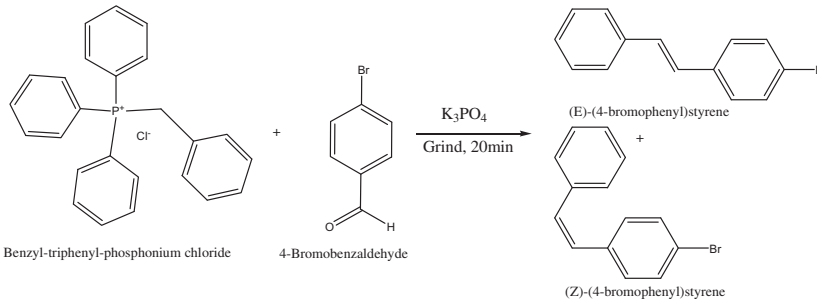

Palleros demonstrated a range of chalcone products can be synthesized by following grinding procedure in excellent yields. Substituted chalcone synthesis by a crossed-aldol condensation [47].

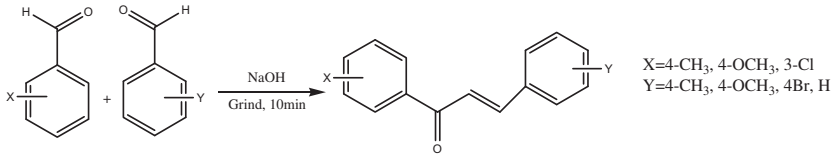

The synthesis of hydrazones catalyzed by citric acid is performed via reaction of hydrazine hydrate with different carbonyl compounds (o-hydroxy acetophenone) in 1:2 molar ratios by employing grinding technique [48].

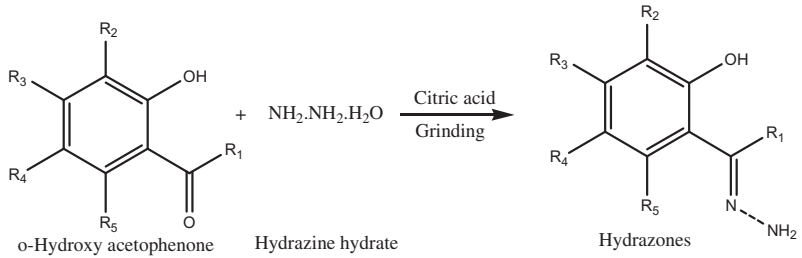

A series of (E)-3-[4-(difluoromethoxy)-3-hydroxyphenyl]-1-phenylprop-2-en-1-ones is synthesized by using solvent-free grinding technique. It involves reaction between acetophenones and 4-difluoro-methoxy-3-hydroxy-benzaldedye in the presence of base (sodium hydroxide). Mortar with pestle is used for grinding the above reactants for 5 min and left to harden at room temperature for 30 min. The solid is dissolved in cold water and acidified with dilute HCl and kept aside for overnight. The separated solid product is filtered, dried, and recrystallized from ethanol [48] (Table 14.3).

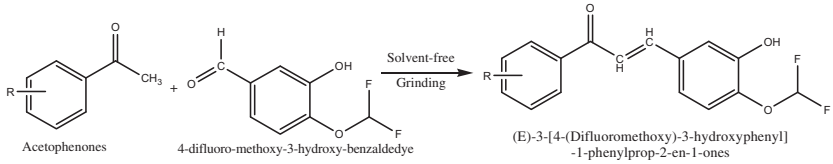

Table 14.3 Comparative data of conventional and grinding technique.

Entry	R	Yield (%)	
		Conventional	Grinding
1	H	70	86
2	F	75	88
3	Cl	80	90
4	—OCH_3	85	92
5	—$2NO_2$	50	85
6	Br	82	90
7	—CH_3	78	88

An efficient eco-friendly synthesis of flavones and 2-styrylchromones via cyclo-dehydration of corresponding 1-(2-hydroxyaryl)-3-aryl/styryl-1,3-propanediones is carried out under solvent-free conditions using grinding technique. Mortar with pestle is used for grinding the above reactants for 10–15 min. The reaction mixture was diluted with ice-cold water and the separated solid product is filtered at vacuum, washed with water, and recrystallized from methanol to afford flavones/2-styryl-chromones, respectively [49].

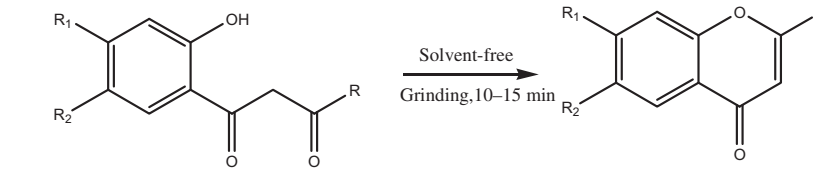

The synthesis of 2-pyrazoline derivatives is achieved by reacting 2′-hydroxy chalcones with hydrazine hydrate under solvent-free grinding technique. Mortar with pestle is used for grinding the above reactants at room temperature for 2–3 min. The obtained solid product is diluted with cold water, filtered, and recrystallized from ethanol to produce 2-pyrazoline derivatives [50] (Table 14.4).

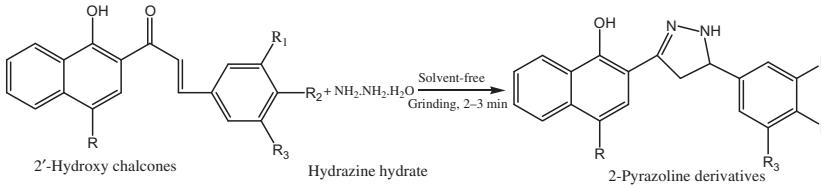

Table 14.4 Synthesis of 2-pyrazoline derivatives under solvent-free conditions using grinding technique.

Product	R	R_1	R_2	R_3	Grinding technique	
					Time (min)	Yield (%)
3a	H	—OCH_3	—OCH_3	—OCH_3	8	94
3b	I	—OCH_3	—OCH_3	—OCH_3	6	88
3c	H	—OCH_3	—OCH_3	H	9	92
3d	H	H	Cl	H	6	83
3e	I	H	Cl	H	5	89
3f	I	—OCH_3	—OCH_3	H	7	84
3g	Br	—OCH_3	—OCH_3	—OCH_3	10	91
3h	H	H	F	H	12	78

Electrophilic aromatic substitution of anisole can be achieved by solvent-less acylation with a mixed acid anhydride generated in situ. Reaction of trifluoroacetic anhydride with acetic acid on acidic alumina generates ethanoic trifluoroethanoic anhydride, which reacts with anisole at room temperature to form 4-methoxy-acetophenone [49].

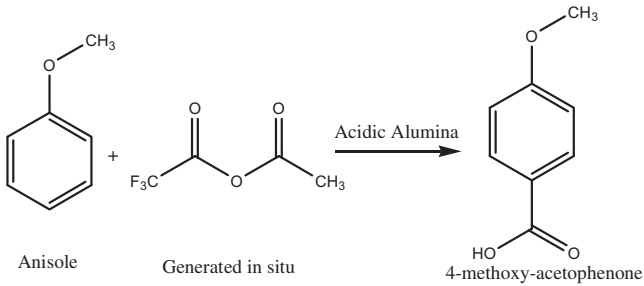

Synthesis of thiocarbonyl-imidazolide derivatives is carried out by reaction between alcohol and thiocarbonyl-diimidazole under grinding technology [51].

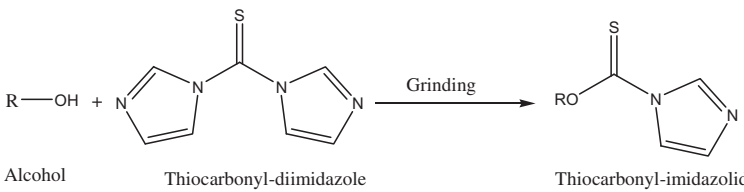

14.1.2.5 Milling technique

Ball milling is considered as one of the automated form of mortar and pestle. Electricity is applied as energy source to operate the ball mill. In case of ball mill, reacting materials are placed in reaction vessel attached with grinding balls and covered with lid. Vessel is allowed to shake at high speed to carry out the reaction. Based on the type of chemical reactions, different ball mills are used such as Wig-L-Bug mill, Retsch mixer mill, and planetary ball mill. Wig-L-Bug mill involves back and forth motion, whereas Retsch mixer mill utilizes side-to-side motion. In case of planetary ball mill, it provides planetary motion [52].

Ball milling is a mechanical method, used in organic synthesis to prepare various heterocyclic compounds [53]. It is an economical and eco-friendly method applied during synthesis and reactions of organic compounds as follows (Fig. 14.5).

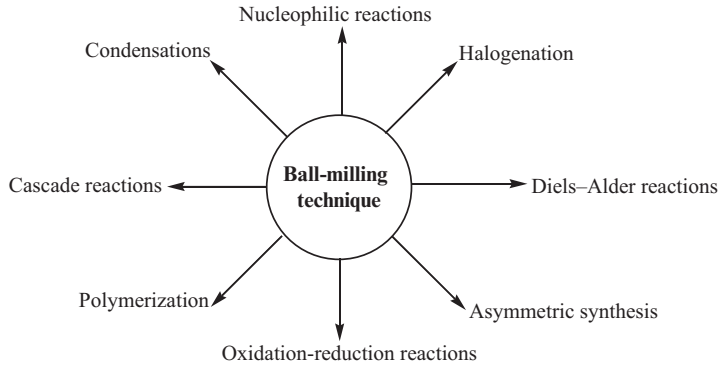

Fig. 14.5 Various chemical reaction performed by ball milling.

Ball milling involves mechanochemical reaction in which the chemical reaction is induced by the direct absorption of mechanical energy by reacting molecules [54]. The reaction process carried in ball milling involves various steps such as mechanical activation of solids, mechanical alloying, and reactive milling of solids (Fig. 14.6).

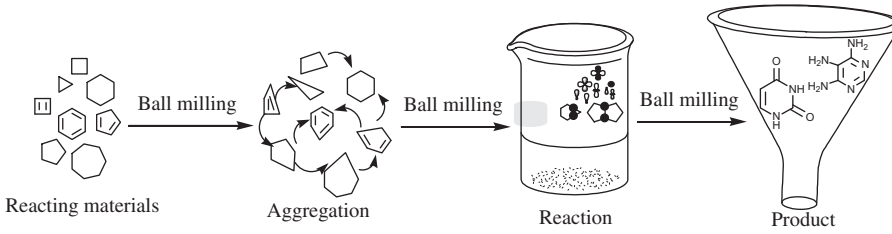

Fig. 14.6 Reaction process involved in ball milling.

Three-component one-pot synthesis of DHPMs derivatives is performed by reaction of β-keto ester derivatives, aldehyde, and urea or thiourea in the presence of alkali-treated H-ZSM-5 zeolite by using sustainable green technology, i.e., ball milling [55].

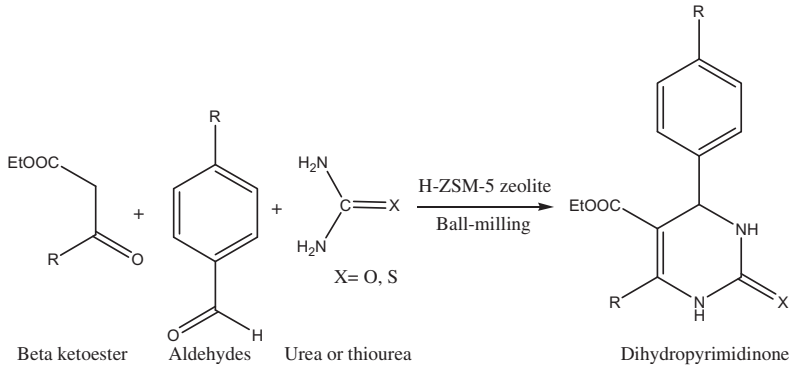

Dibenzo[a,c]phenazine is synthesized by reacting equimolar ratio of 9,10-phenanthrenequinone with 1,2-*o*-phenylenediamine by using solvent-free solid-state grinding technology. Ball mill is used for grinding the reacting materials and follows the principles of green chemistry [56].

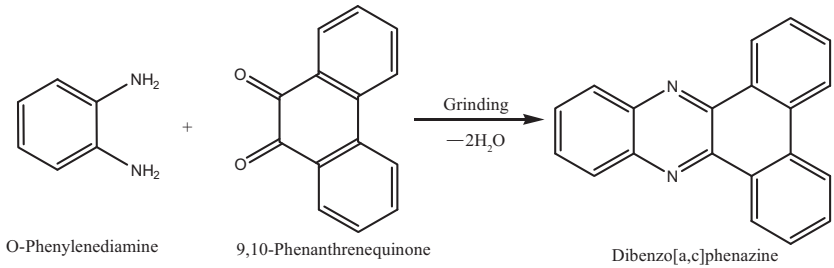

The one-pot synthesis of pyrano[2,3-d]pyrimidine-2,4(1*H*,3*H*)-diones is performed in good to excellent yields by reaction of aldehyde, malononitrile, and barbituric acid without using any catalyst or solvent. Ball milling is used to carry out the reaction [57].

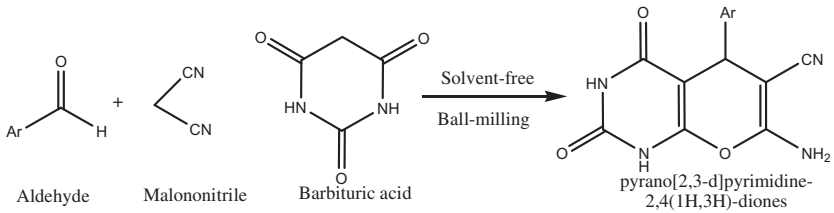

High-speed vibratory ball milling (HSVBM) green method is applied for synthesis of *cis*-2,4-disubstituted tetrahydro-quinolines with good to excellent yields (56%–76%). This process involves the mechanochemical activation of aniline and *N*-vinyl acetamide in the presence of phosphor-molybdic acid (PMA) as catalyst [58]. The reaction is carried out in Wig-L-Bug mixer mill at a frequency of 80 Hz using a 2.5-mL stainless steel grinding jar and a single ball ($d = 10$ mm, 1.05 g) (Table 14.5).

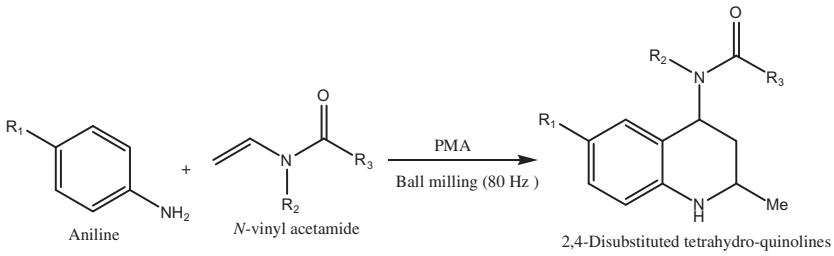

Table 14.5 Synthesis of *cis*-2,4-disubstituted tetrahydro-quinolines ball milling green method.

Entry	R_1	R_2	R_3	Yield (%)
1	COMe	H	Me	63
2	OMe	H	Me	61
3	H	H	Me	89
4	OMe	H	H	60
5	COMe	—$(CH_2)_2$	–	74
6	H	—$(CH_2)_2$	–	55

Zeng et al. demonstrated mechanochemical and solvent-free synthesis for preparing series of 2,5-dimethylpyrrole-3,4-dicarboxylates and 3,4-diphenylpyrroles in moderate to excellent yields from various amines and acetoacetate or 2-phenylacetaldehyde, respectively, in the presence of $Mn(OAc)_3$ as mediator [59].

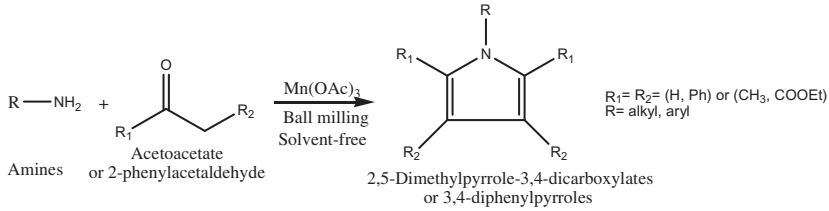

Paveglio et al. determined the mechanical parameters suitable for synthesis of 1H-pyrazole derivatives in the presence of para-toluenesulfonic acid (p-TSA) as catalyst by using ball mill. The optimum conditions maintained to operate ball mill is 450 rpm with five balls (10 mm) for 3 min [57].

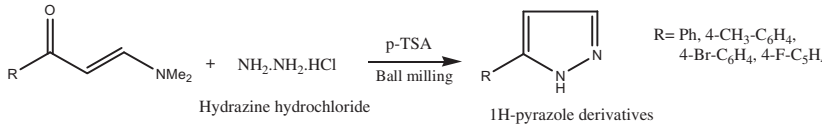

Ze et al. demonstrated one-pot and solvent-free synthesis of 3,5-diphenyl-1H-pyrazoles in an excellent yield under mechanochemical ball-milling conditions using sodium persulfate as the oxidant [60].

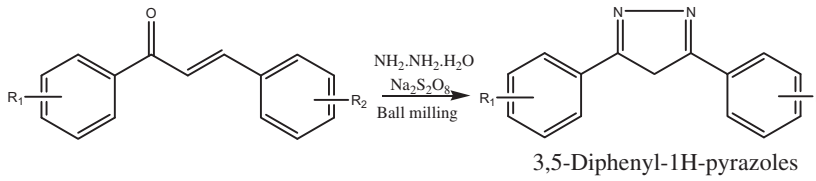

Ould et al. carried out the condensation reaction of an equimolar amount of aldehyde, malononitrile, and thiourea/urea by ball milling in 40 min to produce 2-thioxo or 2-oxo-1,2,3,4-tetrahydropyrimidine-5-carbonitrile derivatives [61]. The reaction is completed effectively without using any catalyst or solvent to get the final products with excellent yields (up to 98%).

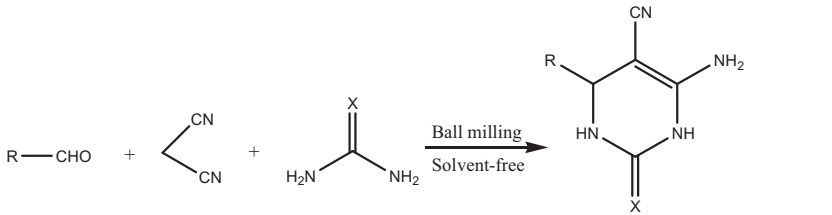

Aldehyde Malononitrile Urea/thiourea 2-thioxo or 2-oxo-1,2,3,4-tetrahydro-pyrimidine-5-carbonitrile derivatives

R= p-CH_3-O-C_6H_4, p-OH-C_6H_4, p-Cl-C_6H_4, Ph

X= O, S

14.1.3 Experimental conditions for solvent-free reaction

There are two experimental conditions employed to carry out the chemical reactions under solvent-free conditions such as (a) reaction on solid support and (b) reaction without any solvent, solid support, or catalyst [62].

In case of reaction on solid support, the reactants are initially adsorbed either on mineral support (alumina, silica clays) or polymer support (polystyrene, polyethylene glycol) or via their solution in an appropriate organic solvent of low boiling. Then, the solvent is removed and the reaction is carried out in dry media between adsorbed reactants either by MW heating technology or by grinding method. Finally, the products are obtained by elution using diethyl ether or dichloromethane and filtered to eliminate the insoluble solid support [63].

While the reaction without any solvent, solid support or catalyst can be carried out between neat reactants in quasi-equivalent amount without any adduct. In the case of solid-liquid mixture, the reaction involves either solublization of the solid in the liquid phase or adsorption of liquid on the solid surface as an interfacial reaction. When all the reactants are in solid state, then they require proper mixing or homogeneity which can be achieved by using grinding technology or MW heating methods. Various reactions such as condensation, cycloaddition, rearrangement reactions, oxidation and reduction, etc. are carried out based on this principle [64].

Advantages of solvent-free reaction

a. There is no reaction medium to collect, purify, and recycle, thus eco-friendly.
b. Product purity is high, so avoids extensive purification using chromatography, only recrystallization is required in some cases.
c. Reactions are facile, regioselective.
d. High yield and less time for the completion of reaction.

e. Process is cost effective.
f. Simple workup procedure and no need for specialized equipments.
g. Functional group protection-deprotection can be avoided.
h. Low energy consumption.
i. Solvent-free reactions are economic because organic solvents are expensive.
j. Solvent-free reactions are less or no hazardous but in case of reactions under solvents, solvents are volatile, flammable, toxic, and carcinogenic.
k. More efficient with more selectivity as compared to reactions carried out in solvents.

Limitations
a. Homogenous reactants should mix to a reaction system.
b. Solvents are required during workup (e.g., extraction).
c. Unsuitable for solvent-assisted chemical reactions.
d. High viscosity in reaction system.

14.2 Conclusion

The solvent-less or solvent-free chemical reaction is carried out either using the reactant materials or incorporating them into clays, zeolites, silica, alumina, or other matrices. Green and sustainable approaches are followed to utilize external heating source such as UV-visible, MW, ultrasound, IR irradiation and grinding, milling technique, etc. These techniques are employed to make the reactions environmental friendly due to the toxicity and volatile nature of most of the organic solvents. Various organic reaction are carried out by using these techniques are solvent-free conditions are Grignard reaction, Knoevenagel condensation, Aldol condensation, Dieckman reaction, Reformatsky reaction, oxidation, reduction, rearrangement reaction, etc. Thus, in current scenario, the design of solvent-less catalytic reaction has received tremendous attention in the field of green synthesis.

Acknowledgment

Bimal K. Banik is grateful to Prince Mohammad Bin Fahd University.

References

[1] P.T. Anastas, J.C. Warner, Green Chemistry, Theory and Practice, Oxford University Press, New York, 1998.
[2] R.A. Sheldon, Green solvents for sustainable organic synthesis: state of the art, Green Chem. 7 (2005) 267.
[3] M.S. Singh, S. Chowdhury, Recent developments in solvent-free multicomponent reactions: a perfect synergy for eco-compatible organic synthesis, RSC Adv. 2 (2012) 4547–4592.
[4] J. Clark, D. Macquarrie (Eds.), Handbook of Green Chemistry and Technology, Blackwell Science, Oxford, 2002.
[5] R.B. Nasir Baig, R.S. Varma, Alternate energy input: mechanochemical, microwave and ultrasound-assisted organic synthesis, *Chem. Soc. Rev.* 41 (2012) 1559–1584.

[6] B. Alimenla, A. Kumar, L. Jamir, D. Sinha, U.B. Sinha, Microwave-induced reactions: an alternative route for chemical synthesis, Rad. Eff. Def. Sol. 161 (2006) 687–693.
[7] C.R. Strauss, R.W. Trainor, Developments in microwave assisted organic chemistry, Aust. J. Chem. 48 (1995) 1665–1692.
[8] J.L. Krstenansky, I. Cotterill, Recent advances in microwave-assisted organic syntheses, Curr. Opin. Drug Discov. Devel. 4 (2000) 454–461.
[9] M. Larhed, A. Hallberg, Microwave-assisted high-speed chemistry: a new technique in drug discovery, Drug Discov. Today 6 (2001) 406–416.
[10] N. Pai, K. Waghmode, D. Khandekar, Microwave promoted solvent-free biginelli reaction for the one pot synthesis of dihydropyrimidin-2-(1*H*)-ones catalyzed by sulfamic acid, Asian J. Chem. 23 (12) (2011) 5217–5219.
[11] D.J. Upadhyaya, S.D. Samant, A facile and efficient pinacol–pinacolone rearrangement of vicinal diols using ZnCl2 supported on silica as a recyclable catalyst, Appl. Catal. A Gen. 340 (1) (2008) 42–51.
[12] F. Leonetti, C. Capaldi, A. Carotti, Microwave-assisted solid phase synthesis of Imatinib, a blockbuster anticancer drug, Tetrahedron Lett. 48 (19) (2007) 3455–3458.
[13] M. Kidwai, P. Mothsra, Neat reaction technology: a green tool, Indian J. Chem. 45B (2006) 2330–2336.
[14] D. Gangrade, S.D. Lad, A.L. Mehta, Overview on microwave synthesis—important tool for green chemistry, Int. J. Res. Pharm. Sci. 5 (2) (2015) 37–42.
[15] A. Marinkovic, D.Z. Mijin, J. Mirkovic, C. Oliver Kappe, A microwave approach to the synthesis of certain 4-substituted phenyl-6-phenyl-3-cyano-2-pyridones, J. Serbian Chem. Soc. 79 (7) (2014) 759–765.
[16] A.R. Katritzky, S.K. Singh, Synthesis of C-carbamoyl-1,2,3-triazoles by microwave-induced 1,3-dipolar cycloaddition of organic azides to acetylenic amides, J. Org. Chem. 67 (25) (2002) 9077–9079.
[17] M.K. Chaudhuri, S. Hussain, An efficient synthesis of quinolines under solvent-free conditions, J. Chem. Sci. 118 (2) (2006) 199–202.
[18] L.G. Donaruma, W.Z. Heldt, The Beckmann rearrangement. (Review), Org. React. 11 (1960) 1–156.
[19] M. Yarhosseini, S. Javanshir, Z. Dolatkhah, M.G. Dekamin, An improved solvent-free synthesis of flunixin and 2-(arylamino) nicotinic acid derivatives using boric acid as catalyst, Chem. Cent. J. 11 (2017) 124.
[20] H. Yang, W.-H. Sun, Z. Li, L. Wang, Solvent-free syntheses of salicylaldimines assisted by microwave irradiation, Synth. Commun. 32 (15) (2002) 2395–2402.
[21] S.E. Wolkenberg, D.D. Wisnoski, W. Leister, Y. Wang, Efficient synthesis of imidazoles from aldehydes and 1,2-diketones using microwave irradiation, Org. Lett. 6 (9) (2004) 1453–1456.
[22] G. Brahmachari, S. Das, A simple and straightforward method for one-pot synthesis of 2,4,5-triarylimidazoles using titanium dioxide as an eco-friendly and recyclable catalyst under solvent free conditions, Indian J. Chem. 52 (3) (2013) 387–393.
[23] G. Thirunarayanan, S. Vijayakumar, Solvent-free synthesis and antimicrobial potential of some (2*E*)-4-methoxyphenyl chalcones, Der Pharma Chem. 10 (10) (2018) 43–47.
[24] R. Miethchen, Selected applications of sonochemistry in organic chemistry, Ultrasonics 30 (3) (1992) 173–179.
[25] S. Puri, B. Kaur, A. Parmar, H. Kumar, Applications of ultrasound in organic synthesis—a green approach, Curr. Org. Chem. 17 (2013) 1790–1828.
[26] W. Bonrath, Ultrasound supported catalysis, Ultrason. Sonochem. 12 (2005) 103–106.
[27] Z. Yiyun, B. Cikuang, F. Ruo, New advances in applied research of sonochemistry, Chin. J. Chem. 8 (2014) 26–29.

[28] L. Pinto, M.V.N. de Souza, Sonochemistry as a general procedure for the synthesis of coumarins including multigram synthesis, Synthesis 49 (12) (2017) 2677–2682.
[29] M. Vidal, M. García-Arriagada, M.C. Rezende, M. Domínguez, Ultrasound-promoted synthesis of 4-pyrimidinols and their tosyl derivatives, Synthesis 48 (2016) 4246–4252.
[30] T.J. Mason, D. Peters, Practical Sonochemistry: Power Ultrasound Uses and Applications, 165 p,second ed., 2003.
[31] S. Puri, B. Kaur, A. Parmar, H. Chopra, Ultrasound-promoted greener synthesis of 2H-chromen-2-ones catalyzed by copper perchlorate in solventless media, Ultrason. Sonochem. 16 (6) (2009) 705–707.
[32] Z.-H. Zhang, J.-J. Li, T.-S. Li, Ultrasound-assisted synthesis of pyrroles catalyzed by zirconium chloride under solvent-free conditions, Ultrason. Sonochem. 15 (5) (2008) 673–676.
[33] B. König, Photocatalysis in organic synthesis—past, present, and future, Eur. J. Org. Chem. (2017) 1979–1981.
[34] M. Obst, B. König, Solvent-free, visible-light photocatalytic alcohol oxidations applying an organic photocatalyst, Beilstein J. Org. Chem. 12 (2016) 2358–2363.
[35] M.S. Sudhir, R. Venkata Nadh, Evaluation of in vitro anthelmintic activities of novel 1,2,3-benzotriazole derivatives synthesized in ultrasonic and solvent free conditions, J. Pharm. Res. 7 (2013) 47–52.
[36] P. Bansal, One pot synthesis of 1, 4 dihydropyridine derivatives by IR irradiation, Int. J. Innov. Eng. Technol. 5 (2) (2013) 274–281.
[37] L.-J. Geng, J.-T. Li, S.-X. Wang, Application of grinding method to solid-state organic synthesis, Chin. J. Org. Chem. 25 (5) (2005) 608–613.
[38] A. Kumar, S. Sharma, A grinding-induced catalystand solvent-free synthesis of highly functionalized 1,4-dihydropyridines via a domino multicomponent reaction, Green Chem. 13 (8) (2011) 2017–2020.
[39] Y. Lu, Z. Ren, W. Cao, W. Tong, M. Gao, Solvent-free synthesis of ethyl-cyanocinnamate in the presence of CaO, Synth. Commun. 34 (2003) 2047–2051.
[40] L. Rong, X. Li, H. Wang, D. Shi, S. Tu, Q. Zhuang, Efficient green procedure for the Knoevenagel condensation under solvent-free conditions, Synth. Commun. 36 (2006) 2407–2412.
[41] J.-T. Li, H.-.G. Dai, D. Liu, T.-S. Li, Efficient method for synthesis of the derivatives of 5-arylidene barbituric acid catalyzed by aminosulfonic acid with grinding, Synth. Commun. 36 (6) (2006) 789–794.
[42] V.M. Markhele, S. Sadaphal, M.S. Shingare, An efficient one-pot synthesis of polyhydroquinolines at room temperature using MCM-41 catalyst under solvent-free conditions, Bull. Catal. Soc. India 6 (2007) 125–131.
[43] A. Parveen, M.R.S. Ahmed, K.A. Shaikh, S.P. Deshmukh, R.P. Pawar, Efficient synthesis of 2,4,5-triaryl substituted imidazoles under solvent free conditions at room temperature, ARKIVOC (16) (2007) 12–18.
[44] Z. Ren, W. Cao, W. Tong, Z. Jin, Solvent free, one pot synthesis of pyrano[2,3-c]pyrazole derivatives in the presence of $KF{\cdot}2H_2O$ by grinding, Synth. Commun. 35 (19) (2005) 2509–2513.
[45] B. Baghernejad, Application of p-toluenesulfonic acid (PTSA) in organic synthesis, Curr. Org. Chem. 15 (17) (2011) 3091–3097.
[46] S.H. Leung, S.A. Angel, Solvent-free Wittig reaction: a green organic chemistry laboratory experiment, J. Chem. Educ. 81 (10) (2004) 1492.
[47] M.Z. Ahmed, N.T. Patel, K.A. Shaikh, M.A. Baseer, S. Shahid, V.A. Patil, Atom efficient grinding technique for the synthesis of hydrazones catalyzed by citric acid, Elixir Org. Chem. 43 (2012) 6583–6585.

[48] G. Senthilkumar, K. Neelakandan, H. Manikandan, A convenient, green, solvent free synthesis and characterization of novel fluoro chalcones under grind-stone chemistry, Der Chem. Sinica 5 (2) (2014) 106–113.
[49] D. Sharma, J.K. Makrandi, A green synthesis of 2-phenyl/2-styrylchromones under solvent-free conditions using grinding technique, Green Chemistry Letters and Reviews 2 (3) (2009) 157–159.
[50] S.B. Zangade, S.S. Mokle, A.T. Shinde, Y.B. Vibhute, An atom efficient, green synthesis of 2-pyrazoline derivatives under solvent-free conditions using grinding technique, Green Chem. Lett. Rev. 6 (2) (2012) 123–127.
[51] S.B. Zangade, S.S. Mokle, A.T. Shinde, Y.B. Vibhute, An atom efficient, green synthesis of 2-pyrazoline derivatives under solvent-free conditions using grinding technique, Green Chemistry Letters and Reviews 6 (2) (2013) 123–127.
[52] A. Stolle, T. Szuppa, S.E.S. Leonhardt, B. Ondruschka, Ball milling in organic synthesis: solutions and challenges, *Chem. Soc. Rev.* 40 (2011) 2317–2329.
[53] B. Ranu, Ball milling towards green synthesis: applications, projects, challenges, Johnson Matthey Technol. Rev. 60 (2) (2016) 148–150.
[54] M.O. M'hamed, Ball milling for heterocyclic compounds synthesis in green chemistry: a review, Synth. Commun. 45 (22) (2015) 2511–2528.
[55] A. Shahid, N. Ahmed, T.S. Saleh, M. Mokhtar, Solvent free Biginelli reactions catalyzed by hierarchical zeolite utilizing a ball mill technique: a green sustainable process, Catalysts 7 (3) (2017) 1–18.
[56] L. Carlier, M. Baron, A. Chamayou, G. Couarraze, Greener pharmacy using solvent-free synthesis: investigation of the mechanism in the case of dibenzophenazine, Tetrahedron Lett. 52 (2011) 4686–4689.
[57] S. Mashkouri, M. Reza Naimi-Jamal, Mechanochemical solvent-free and catalyst-free one-pot synthesis of pyrano[2,3-d]pyrimidine-2,4(1H,3H)-diones with quantitative yields, Molecules 14 (1) (2009) 474–479.
[58] V.V. Kouznetsov, D.R. Merchán-Arenas, C.A. Martínez-Bonilla, M.A. Macías, P. Rousseld, G.H. Gauthier, Grinding and milling: two efficient methodologies in the solvent-free phosphomolybdic acid-catalyzed and mechanochemical synthesis of *cis*-4-amido-*N*-yl-2-methyl-tetrahydroquinolines, J. Braz. Chem. Soc. 27 (12) (2016) 2246–2255.
[59] J.-C. Zeng, H. Xu, F. Yu, Z. Zhang, Manganese (III) acetate mediated synthesis of polysubstituted pyrroles under solvent-free ball milling, Tetrahedron Lett. 58 (2017) 674–678.
[60] Z. Zhang, Y.-J. Tan, C.-S. Wang, One-pot synthesis of 3,5-diphenyl-1H-pyrazoles from chalcones and hydrazine under mechanochemical ball milling, Heterocycles 89 (2014) 103–112.
[61] R.S. Varma, Solvent free organic syntheses using supported reagents and microwave irradiation, *Green Chem.* 1 (1999) 43–55.
[62] K. Tanaka, F. Toda, Solvent-free organic synthesis, Chem. Rev. 100 (3) (2000) 1025–1074.
[63] E.A.A. Hafez, S.M. Al-Mousawi, S.M. Moustafa, K.U. Sadek, M.H. Elnagdi, Green methodologies in organic synthesis: recent developments in our laboratories, Green Chem. Lett. Rev. 6 (3) (2013) 189–210.
[64] T. Deligeorgiev, N. Gadjev, A. Vasilev, S. Kaloyanova, J.J. Vaquero, J. Alvarez-Builla, Green chemistry in organic synthesis, Mini-Rev. Org. Chem. 7 (1) (2010) 44–53.

Versatile thiosugars in medicinal chemistry

15

Aparna Das[a,*], *Bimal Krishna Banik*[b,*]
[a]Department of Mathematics and Natural Sciences, College of Sciences and Human Studies, Prince Mohammad Bin Fahd University, Al Khobar, Kingdom of Saudi Arabia, [b]Department of Mathematics and Natural Sciences, College of Sciences and Human Studies, Deanship of Research Development, Prince Mohammad Bin Fahd University, Al Khobar, Kingdom of Saudi Arabia
[*]Corresponding author. e-mail address: adas@pmu.edu.sa; bimalbanik10@gmail.com; bbanik@pmu.edu.sa

15.1 Introduction

The displacement of the ring oxygen in a carbohydrate by other heteroatoms such as sulfur, nitrogen, phosphorus, or selenium leads to pronounced changes in the physicochemical and biological properties of carbohydrate. The modified carbohydrate entities can lead to useful applications as a diagnostic or therapeutic agent. Sugar analogs with sulfur or nitrogen instead of oxygen in the ring have attracted considerable attention due to their pronounced biological activities compared to their parent oxygen counterparts. But the introduction of phosphorus or selenium into oxygen position has had lesser impact on carbohydrate chemistry because of the additional challenges associated with their synthesis.

Among these sugar analogs, sulfur-containing carbohydrate acquired special attention because its close resemblance with oxygen, as sulfur is positioned next to oxygen in periodic table. Sulfur possess four different oxidation states (−2, +2, +4, and +6) that make organosulfur compounds to exhibit a wide range of properties. However, it is also important to note that sulfur atom is larger than oxygen, the carbon-sulfur bond is longer, the bond is weaker, and less polar than the carbon-oxygen bond. The endocyclic C-S-C angle is more acute than that for a cyclic oxygen system. Sulfur-in-the-ring sugar analogs demonstrate properties different than their oxygen counterparts, which include anomeric effect, chemical reactivity, conformational behavior, molecular recognition by proteins, and metabolic stability. Owing to these properties, sulfur-containing molecules have attracted considerable interest in organic and medicinal chemistry.

Thiosugars and their derivatives have shown potent inhibitory activities toward glycosidases and some thiosugars have good specificity [1] due to the stronger hydrophobic interaction between the sulfur-containing carbohydrates and the enzyme [2] inhibitory activities. Thiosugars are used as potential therapeutical agents such as antineoplastic [3, 4], antidiabetic [5], antiviral [6–8], and antithrombotic agents [9, 10]. Also they are important precursors for the preparation of inositol and aminocyclitol derivatives [5]. Codeé et al. have reported that the thiosugars and thio-oligosaccharides are moderately

Green Approaches in Medicinal Chemistry for Sustainable Drug Design. https://doi.org/10.1016/B978-0-12-817592-7.00015-0
© 2020 Elsevier Inc. All rights reserved.

active glycosidase inhibitors, with activity in the micro- to millimolar range [11]. Many techniques are now available for the preparation of thiosugars, including chemical and biochemical transformations [12–14] owing to their diverse biological activities and use in organic synthesis. Two kinds of thiosugars were considered for this study: thiosugars with sulfur atom as heteroatom or a disaccharide linked via a sulfur bridge.

15.2 Thiosugars with sulfur as a ring heteroatom: Synthesis and medicinal activity

As the sulfur atom can participate in a variety of reactions and rearrangements, the chemistry of thiosugars with sulfur in the ring is of particular interest. Several groups had reported the synthesis of a considerable number of thiosugars and its derivatives containing sulfur as a ring heteroatom [15–17]. A few examples are 4′-thiopentofuranosyl nucleosides [18], and 5-thiopyranoses of the D-*gluco*, D-*ribo*, and D-*xylo* configuration [17, 19–21]. In this section we describe the synthesis and biological activities of different thiosugar derivatives.

Perlin et al. have reported the synthesis of 5-thio-D-galactoses in the form of its crystalline anomeric methyl glycopyranosides [22]. The study also examined the possible influences of a ring-sulfur atom on the reactivity of the enzymes: D-galactose oxidase [23] and α- and β-D-galactosidase [24].

Gonzalez et al. have described the applications of cyclic sulfates of *vic*-diols in the synthesis of thiosugars (thiofuranoses and thiopyranoses) [25]. The *vic*-diols are widely used as precursors and easily transformed into thiiranes and olefins via cyclic sulfates in an efficient and expeditious form: *vic*-diol → cyclic sulfite → cyclic sulfate → acyclic sulfate potassium salt → thiirane or olefin. All the reactions produced good to high yields. The synthesis of different four- and five-membered thiosugars was not only performed by conventional opening of the episulfide ring with sodium acetate but also by direct hydride reduction of the thiocyanate sulfate potassium salt. 5-Thio-L-fucose and 2,5-dideoxy-4-thiofuranose were efficiently synthesized using this method.

A series of enantiomerically pure thiosugars such as 1,6-dideoxy-l,6-thio-D-mannitol or L-iditol, 1,5-dideoxy-l,5-thio-L-gulitol or D-glucitol and 2,5-dideoxy-2,5-thio-L-iditol or D-mannitol, and their corresponding sulfoxide or sulfone were synthesized by Merrer et al. via thiocyclization of C_2-symmetric bis-epoxides [26]. Thiocyclization of L-iditol bis-epoxides is shown in Scheme 15.1.

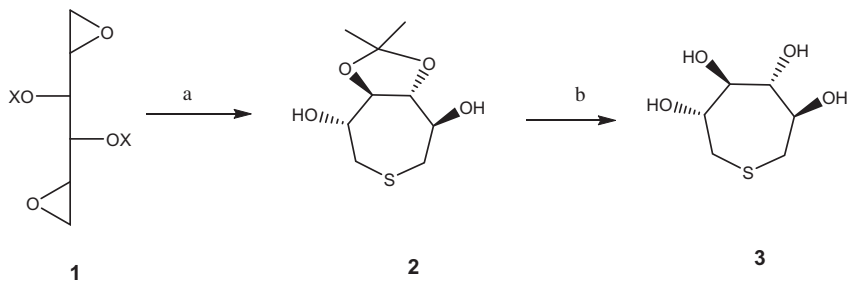

Scheme 15.1 Thiocyclization of L-iditol bis-epoxides. Reagents and conditions: (a) $Na_2S{\cdot}9H_2O$ (2 equiv), EtOH, Δ anh. KOH, MeOH; (b) CF_2CO_2, H_2O, 20°C, 80%.

Crystalline thiepane **2** was prepared from 1,2:5,6-dianhydro-3,4-*O*-methylidene-L-iditol **1** by using proper reaction conditions ($Na_2S{\cdot}9H_2O$, EtOH). Thus, thiocyclization of L-ido bis-epoxide **1**, in which the 3,4-diol is protected in a *trans*-dioxolane, gave only corresponding thiepane **2** in 90% yield. All other compounds were prepared in the similar way with appropriate reaction conditions.

The obtained thiosugars and their oxidative derivatives were evaluated as inhibitors of different glycosidases: α- and β-D-glucosidases, α-D-mannosidase, and α-L-fucosidase. All the thiosugar compounds were found to be weak inhibitors of glycosidases. The results also showed that the oxidation of the thiosugar into sulfoxide and sulfone reduce or abolish their inhibition activity.

Haudrechy et al. have reported a new thiosubstituted "D-arabino"-type derivative obtained from an open carbohydrate via a cascade of four consecutive transformations in a single reaction process [27]. This thiosugar **6** was formed as a side product during the synthesis of α-*C*-(alky-nyl)-galactosides [28, 29]. An unexpected rearrangement, which depends exclusively on reaction conditions, occurred during the synthesis of epoxydithio compound **5** and resulted in compound **6** as shown in Scheme 15.2 [30].

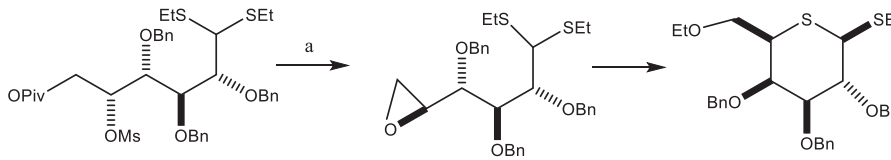

4 **5** **6**

Scheme 15.2 Synthesis of thiosugar 6. Reagents and conditions: (a) anh. KOH, MeOH.

Muraoka et al. have isolated a new class of α-glucosidase inhibitors, neoponkoranol, and neosalaprinol from the water extracts of salacia genus plants [31]. Along with that they synthesized epimers of neoponkoranol and neosalaprinol and studied their inhibitory activities against rat small intestinal aglucosidases. Among them, isolated sulfonium salts (**10**) showed potent inhibitory activity against three enzymes, and 3′-epimer of **10** was the most active molecules [32], and revealed as potent as currently used antidiabetics, voglibose, and acarbose. The synthesis of neoponkoranol (**10**) and 3′-epi-neoponkolanol (3′-epi-**10**) is shown in Schemes 15.3 and 15.4.

Eskandri et al. have reported the synthesis of **10** and its 5′-epimer (5′-epi-**10**) and commented that 5′-epi-**10** was more active than **10** itself, and was the most active inhibitor in this class of molecules [33]. For the synthesis of neoponkoranol (**10**), benzyl 2,3,4-tri-*O*-benzyl-b-D-glucopyranoside [34] (**7**) was derived from D-glucose on treatment with Tf_2O in dichloromethane in the presence of 2,6-lutidine produced **8**. Triflate (**8**) is then treated with thiosugar to get the desired sulfonium salt, 2,3,5-tri-*O*-benzyl-1,4-dideoxy-1,4-[(S)-(1,2,3,4-tetra-*O*-benzyl-6-deoxy-b-D-glucopyranos-6-yl)episulfoniumylid-ene]-D-arabinitol trifluoromethanesulfonate (**9**). Sulfonium salt **9** was then converted to **10** by hydrogenolysis over Pd-C, followed by the treatment with IRA 400J and finally by $NaBH_4$ reduction.

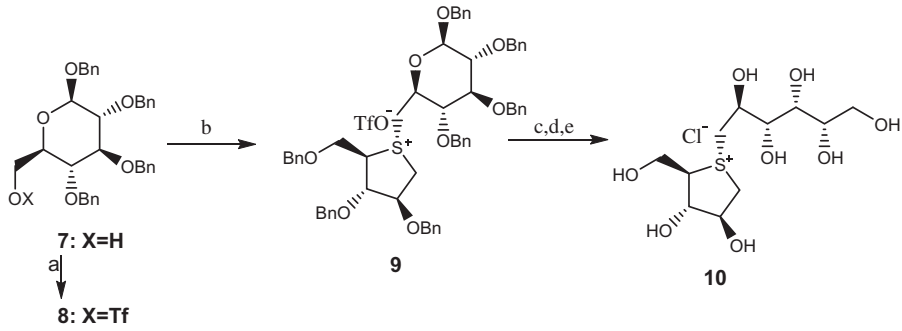

Scheme 15.3 Synthesis of neoponkoranol. Reagents and conditions: (a) Tf_2O, 2,6-lutidine, −20°C to 0°C; (b) thiosugar, THF, 40°C; (c) H_2, 10% Pd-C, 80% aq AcOH, 60°C; (d) IRA 400J (Cl form), CH_3OH, rt; (e) $NaBH_4$, H_2O, 0°C.

Commercially available 1,2:3,4-di-*O*-isopropylidene-a (α)-D-galactopyranose (**11**) was treated with trifluoromethanesulfonic anhydride (Tf_2O) in dichloromethane in the presence of 2,6-lutidine to produce 1,2:3,4-di-*O*-isopropyli-dene-6-*O*-trifluoromethanesulfonyl-a-D-galactopyranose (**12**). Triflate (**12**) was then treated with thiosugar to get the desired coupled product, 2,3,5-tri-*O*-benzyl-1,4-dideoxy-1,4-[(S)-(1,2:3,4-di-*O*-isopropyl-idene-6-deoxy-a-D-galactopyranos-6yl)ep-isulfoniumylidene]-D-arabinitol trifluoromethanesulfonate (**13**). Product **13** was then converted to **14** by hydrogenolysis over Pd-C, followed by the treatment with IRA 400J and finally by $NaBH_4$ reduction.

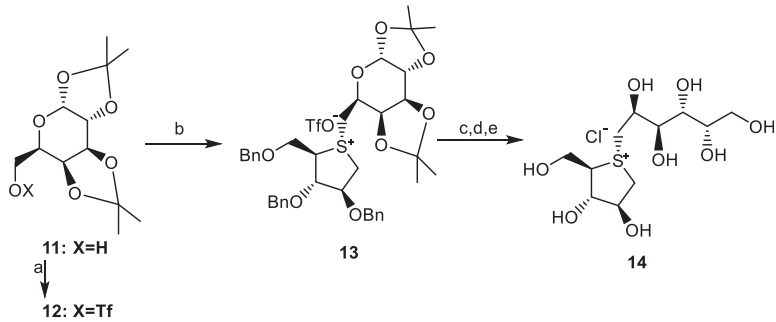

Scheme 15.4 Synthesis of 3′-epi-neoponkoranol. Reagents and conditions: (a) Tf_2O, 2,6-lutidine, −20°C to 0°C; (b) thiosugar, THF, 40°C; (c) H_2, 30% Pd-C, 30% aq TFA, 1,4-dioxane, 50°C; (d) IRA 400J (Cl form), CH_3OH, rt; (e) $NaBH_4$, H_2O, 0°C.

Ye et al. have reported one-pot synthesis of polyoxygenated tetrahydrothiopyrans and thiepanes from alditol derivatives with xylo, ribo, manno, gluco, galacto, and fuco configurations [35]. Scheme 15.5 shows the synthesis of tetrahydrothiopyrans and thiepanes from diols. The "one-pot" synthesis was started from diols, which were

synthesized from natural sugars or alditols [36]. The activation of two hydroxyl groups was done by mesylation, treated with $Na_2S{\cdot}9H_2O$ in DMF for cyclization. The two reactions were performed in one flask, and the final products were acquired in high isolated yields.

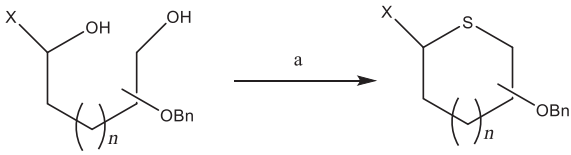

15 16

X=H, CH_3, CH_2OBn; *n*=1 or 2

Scheme 15.5 Synthesis of tetrahydrothiopyrans and thiepanes. Reagents and conditions: (a) MsCl, TEA, DMAP, $Na_2S{\cdot}9H_2O$, DMF.

Chandrasekaran et al. have reported a short and efficient method for the synthesis of biologically potent and novel 1-deoxythiosugars [37]. The group described benzyltriethyl ammonium tetra thiomolybdate $[BnEt_3N]_2MoS_4$ [38–43] as an efficient sulfur transfer reagent for the synthesis of biologically active deoxythiosugars and derivatives [44, 45] starting from aldonolactones [46, 47].

The presence of *cis*-hydroxy groups at C_2 and C_3 was not required for this method and this enhanced the scope of tetrathiomolybdate-mediated synthesis of deoxythiosugars from easily available carbohydrates. As a result, through selective ditosylation of aldonolactones the synthesis of appropriate substrate/s for the sulfur transfer reaction with tetrathiomolybdate was done easily. Scheme 15.6 shows the synthesis of the thiosugar, 1,4-anhydro-4-thio-D-arabinitol **20**, the core part of the many natural products such as salaprinol, salacinol, ponkoranol, kotalanol, and de-*O*-sulfonated kotalanol. The treatment of xylonolactone **17** with TsCl/pyridine in acetone at 0°C afforded xylonoditosylate **18**. The reaction of xylonoditosylate **18** with benzyltriethylammonium tetrathiomolybdate in DMSO at room temperature provided the expected bicyclic thiosugar lactone, 1-deoxy-4-thio-D-lyxono-2,5-lactone **19**. Further reduction of lactone **19** with borohydride exchange resin (BER) in methanol produced the desired 1-deoxythiosugar, 1,4-dideoxy-1,4-epithio-D-arabinitol **20** in good yield.

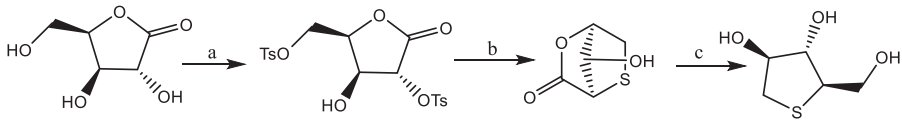

17 18 19 20

Scheme 15.6 Synthesis of 1,4-dideoxy-1,4-epithio-D-arabinitol **20**. Reagents and conditions: (a) TsCl/pyridine:acetone, 0°C, 5 h, 28%; (b) $[BnEt_3N]_2MoS_4$, DMSO, rt, 16 h, 53%; (c) BER, MeOH, 0°C—rt, 7.5 h, 65%.

To further illustrate the usefulness of this method 1,4-anhydro-4-thio-D-lyxitol **24**, a pentose sugar was also synthesized by the same group (Scheme 15.7). Tosylation of ribonolactone **21** with tosyl chloride/pyridine afforded ribono ditosylate **22** [48]. Further treatment of ribono ditosylate **22** with benzyltriethylammonium tetrathiomolybdate generated the 1-deoxy-4-thio-D-arabino-2,5-lactone **23**. Thiosugar 1,4-anhydro-4-thio-D-lyxitol **24** was obtained by the reduction of 1-deoxy-4-thio-D-arabino-2,5-lactone **23** with borohydride exchange resin in methanol.

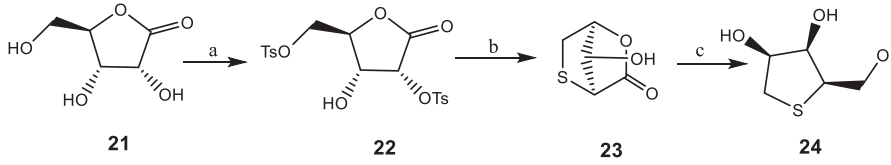

Scheme 15.7 Synthesis of 1,4-anhydro-4-thio-D-lyxitol. Reagents and conditions: (a) TsCl/pyridine:acetone, 0°C, 5 h, 63%; (b) $[BnEt_3N]_2MoS_4$, DMSO, rt, 12 h, 68%; (c) BER, MeOH, 0°C—rt, 10 h, 67%.

Scanlan et al. have reported a versatile synthetic approach for the preparation of a wide range of thiosugars and thioglycals by using the intramolecular thiol-ene and thiol-yne cyclization reactions with intense control over regioselectivity and diastereoselectivity [49, 50]. The endocyclic sulfur atom is introduced into the thiosugar backbone via thiyl radical-mediated cyclization. Utilizing the intramolecular thiol-ene cyclization pathway, both thiofuranose and thiopyranose products were attained from a single acyclic starting material [51]. During the synthesis, multistep process involving Wittig olefination, S_N2 displacement of OTf with KSAc, and base-catalyzed hydrolysis of the thioester to the thiol were used to modify the commercially available *O*-benzyl-protected arabinose into the corresponding alkene-glycosyl thiol derivatives suitable for thiol-ene cyclization. As shown in Scheme 15.8 the intramolecular

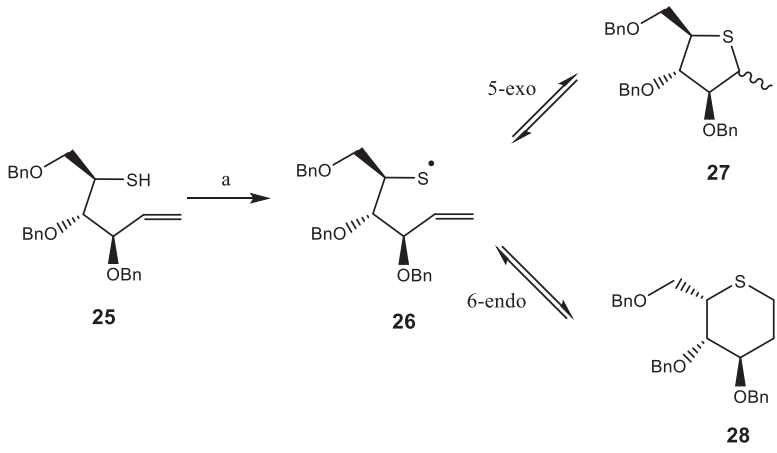

Scheme 15.8 Intramolecular thiol-ene cyclization onto terminal alkene. Reagents and conditions: (a) DPAP(2,2-dimethoxy-2-phenyl-acetophenone), $h\nu$.

cyclization of a thiyl radical onto a terminal alkene produced 6-*endo* thiosugar **28** as a major product [51]. These findings were in agreement with those reported by Surzur [52].

Both C-5 epimers **29** and **32** of the alkyne-glycosyl thiol derivative of *O*-benzyl-protected arabinose were also investigated for intramolecular thiol-yne cyclization process (Scheme 15.9). For D-sugar **29**, the intramolecular thiol-yne reaction produced 5-*exo* glycal **31** as the major product (58%) and L-sugar **32** gave a separable mixture of both 5-*exo* and 6-*endo* glycals, **34** and **35**, respectively, in a combined yield of 55 % [53]. These results were in contrast with the unsubstituted pent-4-yne-1-thiol substrate where 6-*endo* cyclization was favored, as reported by Surzur [52]. The study concluded that the regioselectivity of the cyclization process is significantly influenced by the stereochemistry of the substituents on the carbohydrate backbone.

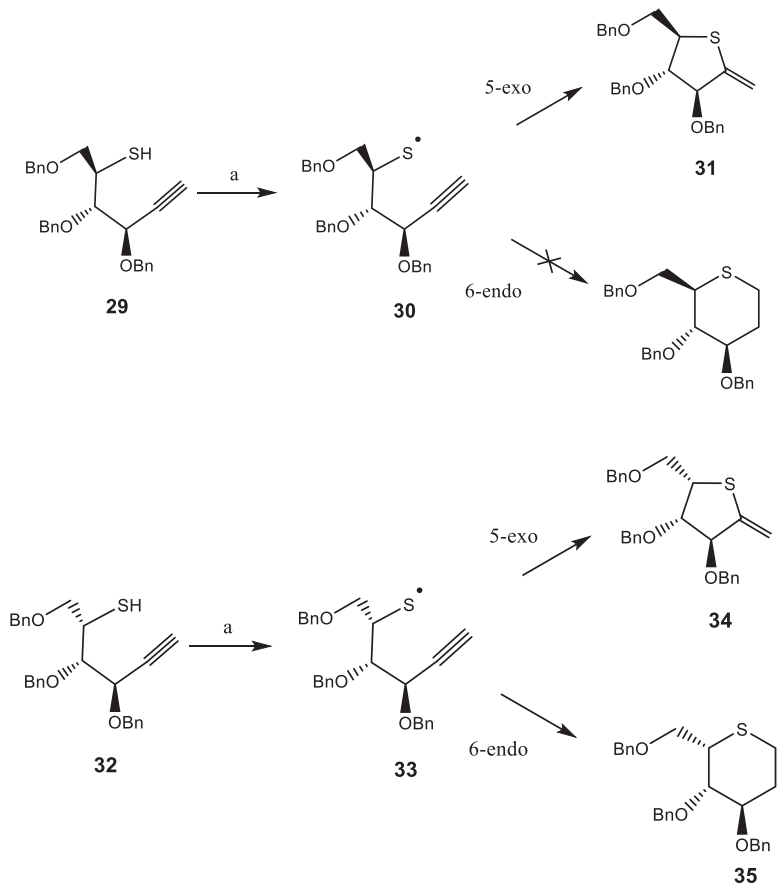

Scheme 15.9 Intramolecular thiol-yne cyclization on terminal alkyne.

Yoshimura et al. have reported the synthesis of 4′-thionucleosides as antitumor and antiviral agents [54]. To achieve the synthesis, they developed the Pummerer-type thioglycosylation reaction and the reaction was successfully applied for the synthesis of dihydrothiopyranonucleosides as well as 4′-thionucleosides. A series of nucleosides were synthesized and tested for biological activity. Most of the nucleosides were active against tumors or viruses. Among them, 4′-thioFAC, a 2′-fluoro analog of 4′-thiocytidine, showed prominent antitumor activity in an in vivo assay. The study demonstrated the significance of 4′-thionucleosides for drug development and their promise as drug candidates for antitumor and antiviral agents.

The synthesis of 4′-thioribonucleosides [55] by constructing the skeleton of 4-thioribose via a ring-contraction reaction under reductive conditions from 2-mesylate **37** procured from **36** was developed (Scheme 15.10). As depicted, first the episulfonium ion **38** was formed which is then triggered by intramolecular S_N2 reaction at the 5-position by sulfur atom. Next ring contraction from thiopyranose to thiofuranose occurred to produce 5-aldehyde **40**. Finally, hydride reduction of **40** resulted in 4-thiofuranose derivative **41**. The Pummerer-type glycosylation reaction of 5-*O*-silylated sulfoxide **42**, by further treatment with 2,4-bis(trimethylsilyl) uracil (**43**) and excess diisopropylethylamine (DIPEA) in the presence of TMSOTf, gave 4′-thiouridine derivative **44** in good yield. The reaction was proceeded stereoselectively and due to steric hindrance of the 2,3-di-*O*-isopropyli-dene group the predominant β-anomer was formed.

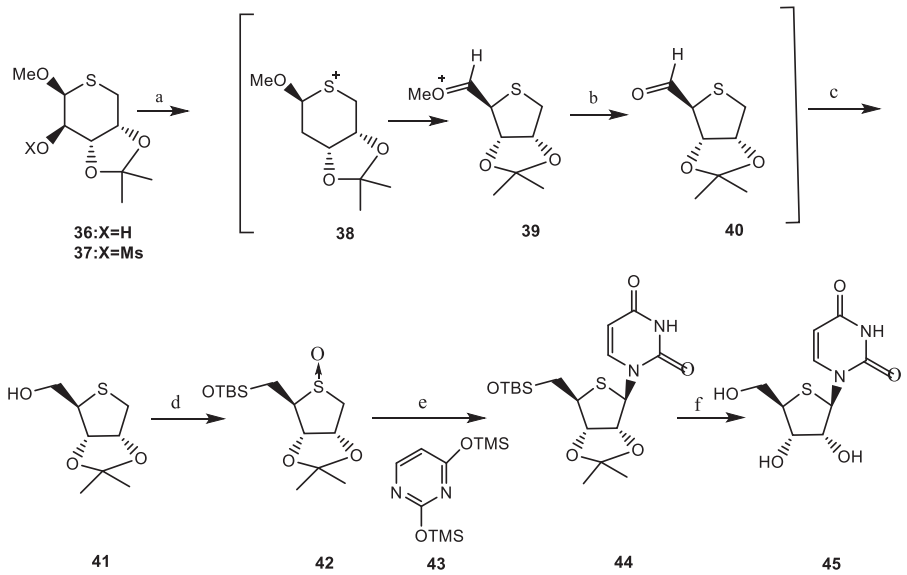

Scheme 15.10 Synthesis of 4′-thioribonucleosides. Reagents and conditions: (a) MsCl, Et_3N, $NaBH_4$; (b) H_2O; (c) —BH_4; (d) TBSCI, mCPBA; (e) TMSOTf, iPr_2NEt; (f) Dowex 50W (H^+ form).

Due to their increased chemical stability [56], 4-thiofuranoside and its derivatives showed biological activities such as antiviral, [57, 58] antibiotic, [59], and anticancer [59, 60] activities. Codee et al. have reported the synthesis, reactivity, and stereoselectivity of 4-thiofuranosides [61].

The synthesis of 4-thiofuranosyl donors is shown in Scheme 15.11 [62]. The synthesis of the 4-thio ribosyl donor **52** is started from D-ribose. On the protecting group manipulations method, 2,3,5-tri-*O*-benzyl ribose **46** was produced in 88% yield in over three steps. The corresponding ribitol was obtained after the reduction of the lactol with sodium borohydride in methanol in which both hydroxyl functionalities were mesylated to provide dimesylate **47**. For the formation of thio-ribofuranosyl donor **52**, a double inversion of the C-4-mesylate was required. Thus, both mesylates in **47** were substituted by bromines in a Finkelstein-type reaction. Also a second substitution and concomitant ring closure were considered to produce thioether **51** in 63% yield. To produce the required acetyl donor **52**, thioether **51** was oxidized with m-CPBA to give the corresponding sulfoxide, which then has undergone a series of transformations through a Pummerer rearrangement. For the construction of 4-thio lyxofuranosyl donor **49**, dimesylate **47** was also used. Compound **47** was then exposed to the sodium sulfide substitution/ring closure conditions to provide 4-thio L-lyxitol **48**. This compound was then oxidized to obtain, after a Pummerer rearrangement, 4-thio lyxosyl donor **49**.

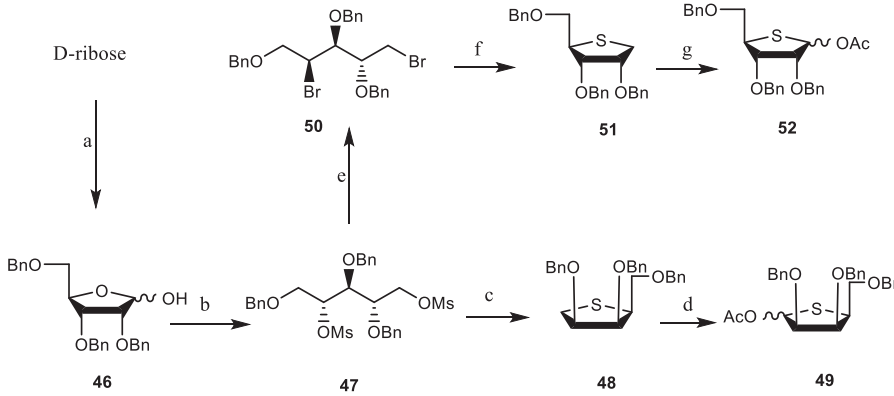

Scheme 15.11 Synthesis of 4-thiofuranosyl donors. Reagents and conditions: (a) three steps: 1. MeOH, AcCl, 2. DMF, BnBr, NaH, 3. H_2O, HCOOH; (b) 1. MeOH, $NaBH_4$, 2. DCM, MsCl, Et_3N; (c) DMF, Na_2S; (d) 1. DCM, m-CPBA, 2. Ac_2O; (e) 2-butanone, LiBr; (f) DMF, Na_2S; (g) 1. DCM, m-CPBA, 2. Ac_2O.

15.3 Thiosugars with sulfur outside the ring: Synthesis and medicinal activity

Deoxy sugars have hydroxyl groups instead of hydrogen atoms. Numerous naturally occurring, biologically active compounds, including the anticancer agents mithramycin, chromomycin A3, and olivomycin A as well as many of the cardiac glycosides

such as digitoxin and digoxin, contain 2,6-dideoxy sugar system. Hence it is important to synthesize more effective and less toxic analogs of these compounds.

Tatsuta et al. have described the synthesis of 2,6-dideoxy sugars by using 2,6-anhydro-2-thio sugars [63]. The group stereospecificaily synthesized L-cladinose, L-mycarose, L-oleandrose, L-olivose, and all of their C-3 epimers, 2,6-dideoxy-3-C-methyl-3-*O*-methyl-L-*arabino*-hexopyranose, 2,6-dideoxy-3-C-methyl-L-*arabino*-hexopyranose (L-olivomycose), 2,6-dideoxy-3-*O*-methyl-L-*ribo*-hexopyranose (L-cymarose), and 2,6-dideoxy-L-*ribo*-hexopyranose (L-digitoxose). The preparation of 2,6-anhydro-2-thio sugars is shown in Scheme 15.12.

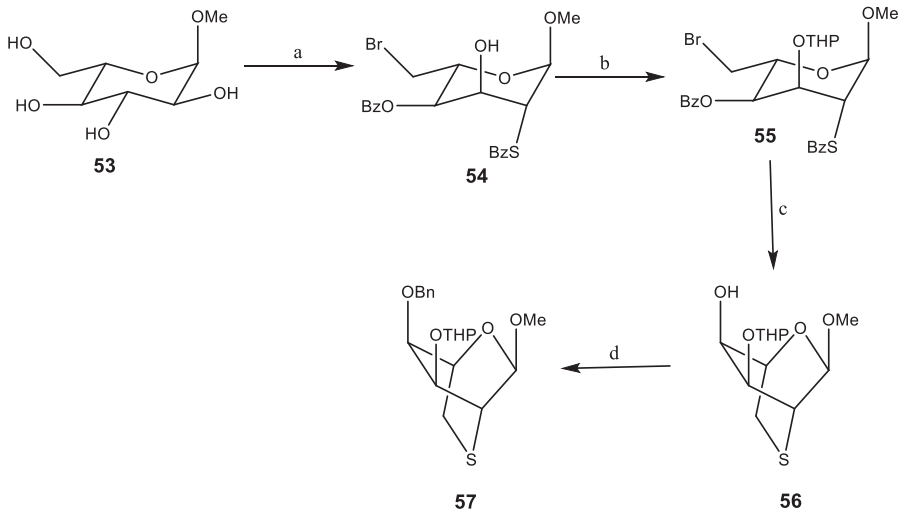

THP=tetrahydropyran-2-yl

Scheme 15.12 Synthesis of 2,6-anhydro-2-thio sugars. Reagents and conditions: (a) five steps: Refs. [64, 65]; (b) 3,4-dihydro-2*H*-pyran, 4A mol. sieves 10-dl-camphorsulfonic acid, CH_2Cl_2; (c) NaOMe, MeOH; (d) BnBr, NaH.

The synthesis started with the conversion of methyl α-L-glucopyranoside (**53**) into compound **54** in five steps [64, 65]. Reaction of **54** with 3,4-dihydro-2*H*-pyran in the presence of catalyst gave **55**. Basic hydrolysis of **55** with methanolic sodium methoxide led to the formation of a 2,6-anhydro-2-thio bridge (**56**) with deprotection of benzoyl groups. Standard benzylation of **56** produced **57**. All the 2,6-dideoxy sugars and their C-3 epimers were synthesized from this common intermediate **57**.

Vasodilators are used to open or widen blood vessels. They affect the muscles in the walls of arteries and veins, preventing the muscles from tightening.

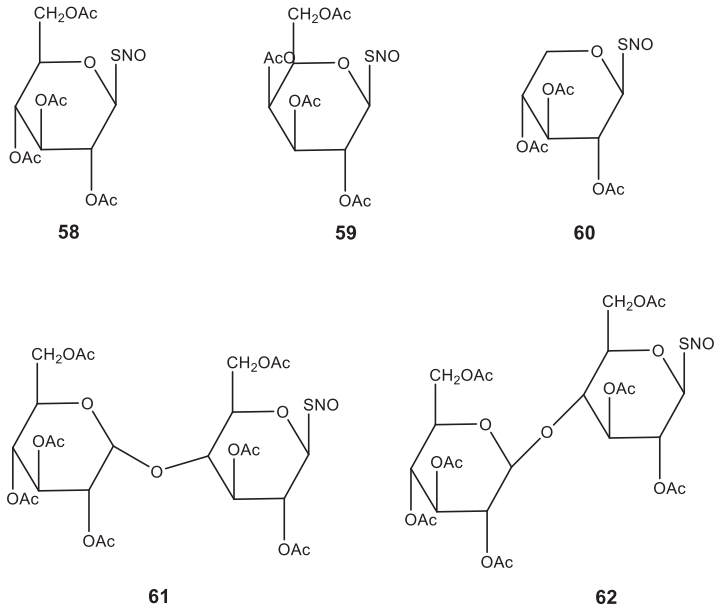

Scheme 15.13 *S*-nitroso derivatives of 1-thiosugars.

Butler et al. have reported the synthesis of *S*-nitroso derivatives of 1-thiosugar and its activity as vasodilator [66]. They synthesized a number of *S*-nitroso derivatives (Scheme 15.13) from 1-thiosugar (glucose, galactose, xylose, maltose, and lactose), 1-thioglucose tetraacetate (**58**), 1-thiogalactose tetraacetate (**59**), 1-thioxylose triacetate (**60**), 1-thiomaltose heptaacetate (**61**), and 1-thiolactose heptaacetate (**62**). But most of the compounds were unstable except *S*-nitroso-1-thio-2,3,4,6-tetra-*O*-acetylglucopyranose (**58**), which was stable enough to be examined as a vasodilator. It also showed effectiveness in human cutaneous vascular smooth muscle relaxation when delivered transdermally.

α-L-Fucosidase is an enzyme that can breaks down fucose and plays an important role in the cleaning of the nature by degrading hemicellulose and cellulose. It is also helpful for the normal functioning of cells along with its roles in antibacterial defense mechanisms and viral pathogenesis, and its deficiency leads to various metabolic disorders. Hence, α-l-fucosidases are clinically important targets and the synthesis of potent and selective inhibitors is a highly essential task.

Witczak et al. have designed and synthesized S-linked fucoside analogs, which were tested for the inhibition of α-L-fucosidases [67]. The group used 2,3,4,-tri-*O*-acetyl-l-thiofucose (**63**) as a starting material. A condensation of **63** with bromonitromethane in the presence of a catalytic amount of triethylamine produced thiosugar **64**. The reduction of the terminal nitro group was achieved efficiently with sodium borohydride/cobalt chloride complex (Scheme 15.14).

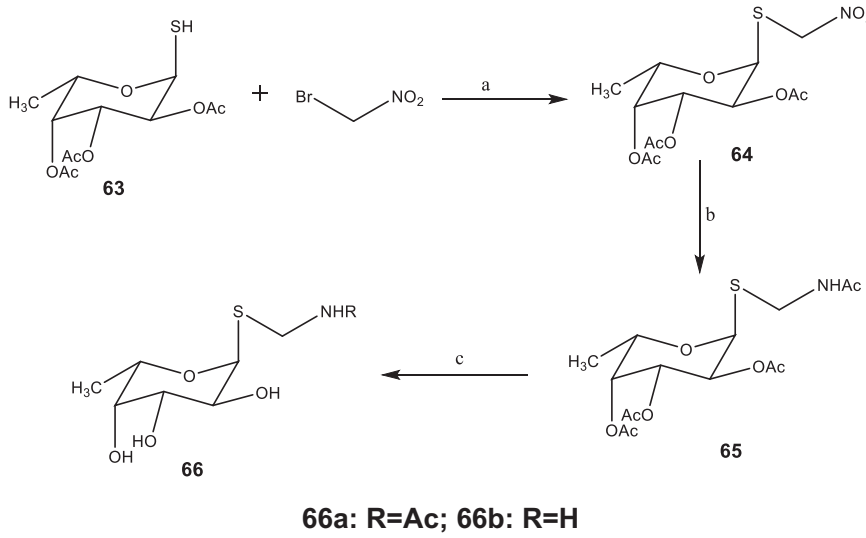

Scheme 15.14 Synthesized S-linked fucoside analogs.

The acetylation of the reduction product **64** produced an acetamido derivative **65**. The cleavage of ester groups of **65** was carried out with an aqueous/methanolic solution of triethylamine to produce **66a**. The removal of the acetamido function was performed with triethyloxonium fluoroborate to produce free amino derivative **66b**.

Compounds **66a** and **66b** were tested for the inhibition of α-L-fucosidases from bovine kidney, bovine epididymis, and human placenta. At pH 6.5, compound **66a** showed mixed/competitive inhibition against all fucosidases with the dissociation constant of 4.4, 5.6, and 3.9 μM respectively. Similarly, at pH 6.5 compound **66b** showed mixed/competitive inhibition against all fucosidases with the dissociation constant of 5.9, 6.8, and 6.1 μM, respectively. The result shows that free amino function does not have significance on the inhibitory activity against all the fucosidases.

Node et al. have reported the synthesis of thiosugars and thioglycosides using new odorless organosulfur reagents, *p*-octyloxyphenylmethanethiol and *p*-dodecylbenzenethiol [68]. *p*-Octyloxyphenylmethanethiol was prepared from the *p*-hydroxybenzaldehyde and *p*-dodecylbenzenethiol was prepared from *p*-alkylphenols. These odorless reagents were then used for the synthesis of thiosugars and thioglycosides.

Auranofin (AF) is a gold-containing drug and is largely used as an antiarthritic agent. It consists of a gold(I) center linearly coordinated to triethylphosphine and to a thiosugar (3,4,5 triacetyloxy-6-(acetyloxymethyl) oxane-2-thiolate). Molecular structure of AF is shown in Scheme 15.15. Along with antiarthritic activity, auranofin revealed a wide range of pharmaceutical applications [69–73]. Studies also show that the gold(I) center of AF exhibit a high affinity for dithiol motifs, often present in the active site of some crucial parasitic enzymes. Consequently, AF can act as an effective antiparasitic agent.

Colotti et al. have described the antiparasitic activity of AF against *Leishmania infantum* [74]. To test its ability, auranofin was challenged in vitro against

trypanothione reductase, a key enzyme of *L. infantum* and the result showed a pronounced enzyme inhibition. Gold has the ability to bind to the two active sites of TR, while the thiosugar moiety of AF binds to the trypanothione binding site. Thus, auranofin appeared to inhibit TR through a dual mechanism.

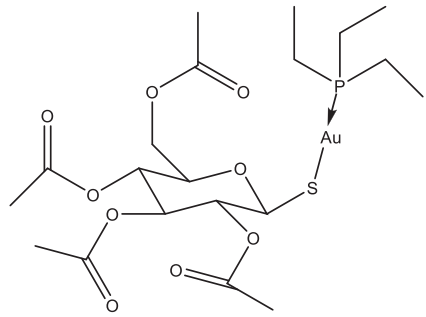

67

Scheme 15.15 Chemical structure of auranofin (AF).

Witczak et al. have synthesized (1–4)-*S*-thiodisaccharides, **68**–**71** and assessed their cytotoxicity and apoptosis against human cancer cell lines [75]. The molecular structure of the compounds is shown in Scheme 15.16.

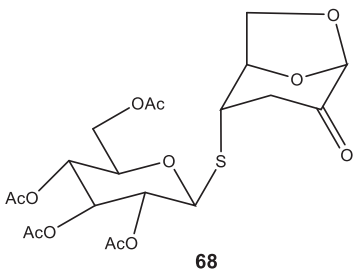

68

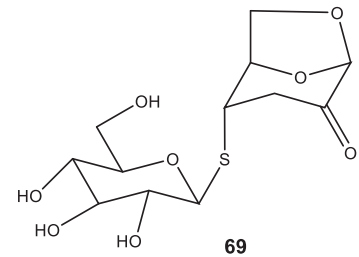

69

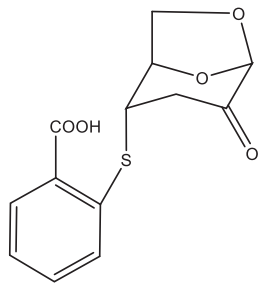

70

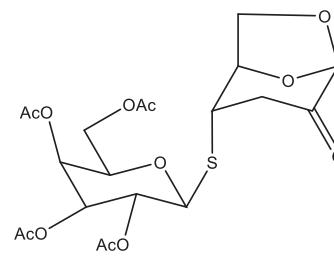

71

Scheme 15.16 (1–4)-*S*-thiodisaccharides.

The cytotoxicity of functional CARB-pharmacophore **68**–**71** was tested at nine different concentrations on four cell lines: lung (A549), cervix (HeLa), mammary gland-breast (MCF-7), and colon carcinoma (LoVo). The result is illustrated in Table 15.1. It shows that FCP **68** was more active against breast cancer line (IC_{50} 47.1 μM) compared with other studied cancer cell lines.

FCP **68** has four hydroxyl groups in the sugar ring protected by acetyl groups. A study showed that the hydroxyl group deprotection by removing the acetyl groups (FCP **69**) and/or substitution of glucose with galactose (FCP **71**) did not increase the cytotoxicity of compounds.

Table 15.1 The cytotoxicity of studied functional Carb-pharmacophores on A549, MCF7, HeLa and LoVo cells.

Compound	68	69	70	71
A549 (μM)	$IC_{50}=119.4$	$IC_{50}=691.5$	$IC_{50}=310.9$	$IC_{50}=466.6$
MCF-7 (μM)	$IC_{50}=47.1$	$IC_{50}=365.9$	$IC_{50}=217.5$	$IC_{50}=343.9$
HeLa (μM)	$IC_{50}=91.4$	$IC_{50}=1077.7$	$IC_{50}=434.0$	$IC_{50}=676.4$
LoVo (μM)	$IC_{50}=165.8$	$IC_{50}=771.9$	$IC_{50}=640.7$	$IC_{50}=623.7$

Borbas et al. have demonstrated the importance of free-radical hydrothiolation of alkenyl sugars bearing an exocyclic double bond, which resulted in stable carbon-sulfur-bridges glycomimetics. Photo-induced addition of thiols to exoglycal is shown in Scheme 15.17 [76].

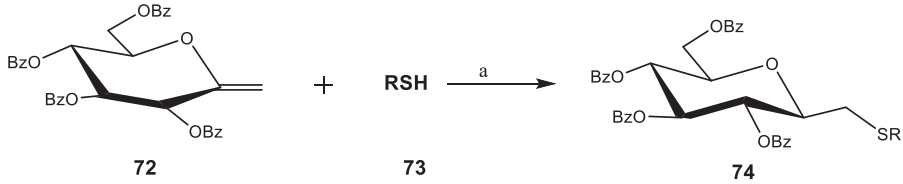

72 73 74

Scheme 15.17 Photo-induced addition of thiols to exoglycal. Reagents and conditions: (a) DPAP (2,2-dimethoxy-2-phenylacetophenone), *hν*, 15 min.

Enzyme thioredoxin reductase (TrxR) is essential in normal cells for protection against oxidative damage, mutation, and for redox homeostasis. TrxR supports tumor growth and progression when transformed into malignant cells. Gold(I) complexes containing stabilizing ligands such as phosphines or *N*-heterocyclic carbenes (NHCs) are known to be inhibitors of TrxR and therefore can act as potential apoptosis-inducing anticancer drugs.

Zhu et al. have reported the synthesis, characterization, and biological activity of four novel *N*-heterocyclic carbene-gold(I)-thiosugar complexes derived from lactose, glucose, and galactose. Synthesis of two selected NHC-Au(I)-SR complexes is shown in Schemes 15.18 and 15.19 [77].

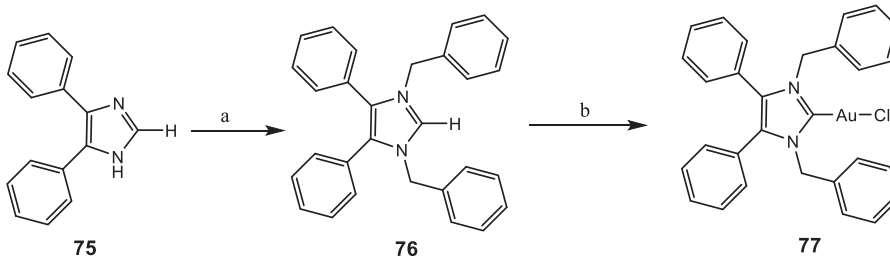

Scheme 15.18 Synthesis of NHC-Au(I) chloride. Reagents and conditions: (a) BnCl, K_2CO_3, CH_3CN; (b) 1. Ag_2O, CH_2Cl_2, 2. $(Me_2S)AuCl$.

Commercially available 4,5-diphenylimidazole **75** was first dibenzylated with BnCl in the presence of K_2CO_3 to give imidazolium chloride **76**. Chloride **76** was then treated with Ag_2O in CH_2Cl_2 under the exclusion of light at room temperature to generate NHC-Ag(I) chloride complex, which was in situ subjected to metal exchange with chloro(dimethylsulfide)gold(I) to give NHC-Au(I) chloride **77**. Chloride **77** then served as the precursor to all other target molecules.

Appropriate thio-containing sugars **78** and **80** were prepared following different procedures [78–82]. α-Thioglucose **78** was first coupled with chloride **77** in the presence of Et_3N in CH_2Cl_2 to produce compound **79**. α-Anomeric thiol, which was known to be less nucleophilic than its corresponding β-counterpart [83], showed fairly

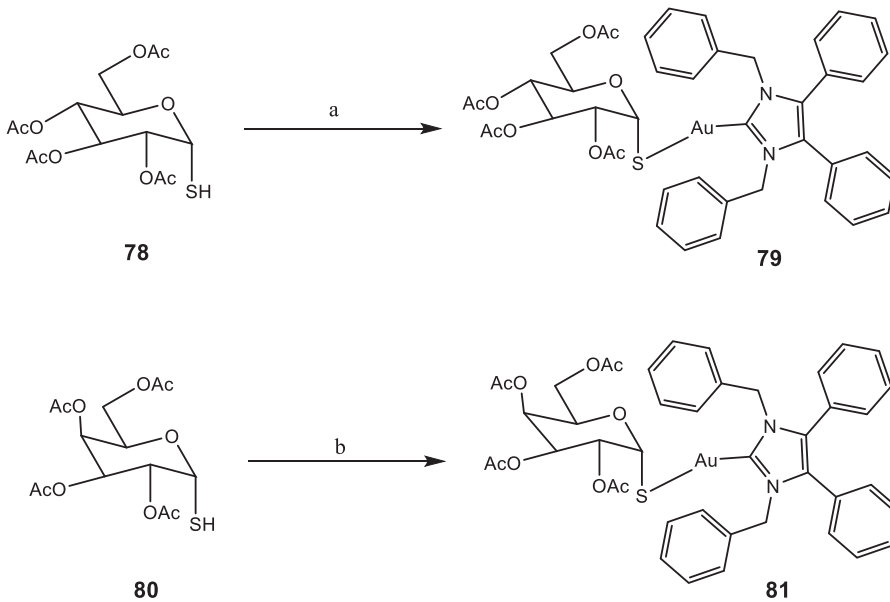

Scheme 15.19 Synthesis of NHC-Au(I)-SR complexes. Reagents and conditions: (a) **77**, Et_3N, CH_2Cl_2, rt, 6 h; (b) **77**, K_2CO_3, $EtOAc/H_2O$, rt, 24 h.

good reactivity toward the NHC-Au(I) chloride. A mixture of **80** and **77** in EtOAc was treated with an aqueous solution of K_2CO_3 to produce complex **81**.

All the complexes were tested against the NCI-60 cancer cell line panel for cytotoxicity. All compounds showed good activity against a wide range of cancer cell lines. Among them, complex **79** showed the best overall activity and exhibited better activity than its β-counterpart. The study indicated that appropriate substitution of the sugar moiety on the NHC-gold(I) complex can improve the activity against certain cancer cells.

Komor et al. have reported the synthesis of 1-thiosugar with α-configuration [84]. The group also synthesized and tested biological activity of glycoconjugates analogs of acyclic uridine derivatives. The synthesis of 1-thiosugars and the corresponding 1-thioglycosides is shown in Scheme 15.20.

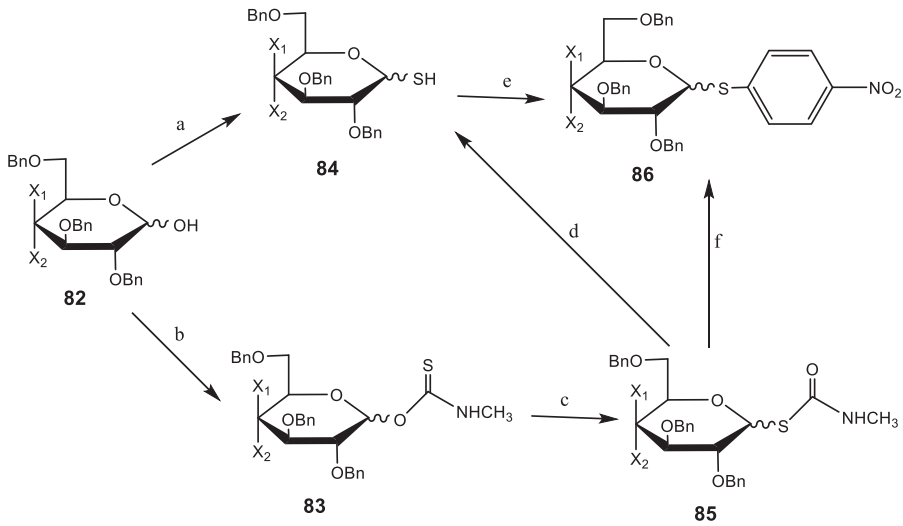

82a: X_1=H, X_2=OBn; 82b: X_1= OBn, X_2= H

83a: X_1=H, X_2=OBn; 83b: X_1= OBn, X_2= H

84a: X_1=H, X_2=OBn; 84b: X_1= OBn, X_2= H

85a: X_1=H, X_2=OBn; 85b: X_1= OBn, X_2= H

86a: X_1=H, X_2=OBn; 86b: X_1= OBn, X_2= H

Scheme 15.20 Synthesis of 1-thiosugars and the corresponding 1-thioglycosides. Reagents and conditions: (a) Lawesson reagent, 1,4-dioxane, reflux; (b) S=C=NCH_3, K_2CO_3, toluene, sonication; (c) TMSOTf, toluene, rt; (d) 1 M MeONa, THF/MeOH 1:1; (e) 2-chloro-5-nitropyridine, K_2CO_3, acetone, rt; (f) 2-chloro-5-nitropyridine, K_2CO_3, acetone, MeOH, sonication.

In this method *N*-methyl thiolcarbamates was used for the synthesis of glycosyl thiols (Scheme 15.20). Corresponding glycosylthiols were easy to obtain by alcoholysis and used for the preparation of heteroaryl 1-thioglycosides. For the synthesis of (5-nitro-2-pyridyl)-1-thioglycosides, the procedure of aromatic substitution of nucleophilic halogen in negatively substituted aryl derivatives was used. The treatment of 2,3,4,6-tetra-*O*-benzyl-1-thio-D-gluco- or 2,3,4,6-tetra-*O*-benzyl-1-thio-D-galactopyranose with 2-chloro-5-nitropyridine gave corresponding heteroaryl thioglycosides. Under the influence of ultrasound, the key step in the substitution of the chlorine atom in 2-chloro-5-nitropyridine molecule was carried out. After purification by column chromatography on silica gel, (5-nitro-2-pyridyl) 2,3,4,6-tetra-*O*-benzyl-1-thio-D-glucopyranoside **86** (79% yield) or (5-nitro-2-pyridyl) 2,3,4,6-tetra-*O*-benzyl-1-thio-D-galactopyranoside **87** (77% yield) were obtained as mixtures.

The first step to obtain glycoconjugate structure was the synthesis of the 1-thiosugar with the α-configuration, which was then converted into the 1-thioglycoside by a reaction with the corresponding nitropyridine derivative, followed by a reduction of the nitro group to the amino group. The next step was the synthesis of acyclic derivatives of uridine containing a carboxyl group in the terminal position. Condensing the intermediates to form an amide bond and removing protecting groups result in the formation of final glycoconjugates. The biological activity of the synthesized compounds was determined on the basis of their ability to inhibit the action of β-1,4-galactosyltransferase enzyme from bovine milk.

Heteroaryl-glycosides are commonly found in many compounds of enormous practical importance, ranging from natural compounds to pharmaceutical agents [85–88]. *N*-glycosyl quinolin-2-ones, in which a glycosyl unit is attached to a quinolin-2-one core, is one of the most important members of heteroaryl-*N*-glycosides family, because of its biological activity. Several studies have presented quinolin-2-ones as biologically active compounds and pharmaceutical agents [89–95]. Thus, the coupling of thiosugar derivatives with *N*-glycosyl quinolin-2-one nucleus had caused several changes in their features, including their chemical, physical, biochemical, and biological properties.

Messaoudi et al. have synthesized successfully various *N*,*S*-bis-glycosyl quinolin-2-ones via the palladium-catalyzed coupling of α- or β-mono-, di-, and poly-thiosugar derivatives with α- or β-3-iodo-*N*-glycosylquinolin-2-ones [96]. Coupling reaction of structurally diverse mono-, di-, and tri-thiosugar derivatives (**87a**–**f**) with various α- or β-*N*-lucosylquinolinones (**86a**–**d**) is shown in Scheme 15.21. The thiosugar derivatives, O-acetylated 1-thio-β-D-galactopyranose **87a**, O-acetylated 1-thio-β-D-glycopyranose **87b**, O-acetylated *N*-Ac-1-thio-β-D-glucopyranose **87c**, and O-benzoylated 1-thio-β-D-glucopyranose **87d**, were coupled easily with both glucosylquinolinones **β-86a** and **β-86d** to give β-*N*,*S*-bis-glycosyl quinolin-2-ones (**88**) without any loss of reactivity.

Thioglycosides are biologically important molecules [97–104] and more stable than their *O*-glycosides analogs to both chemical and enzymatic degradations. Different methods are available to synthesize thioglycosides [105–112]. Among them

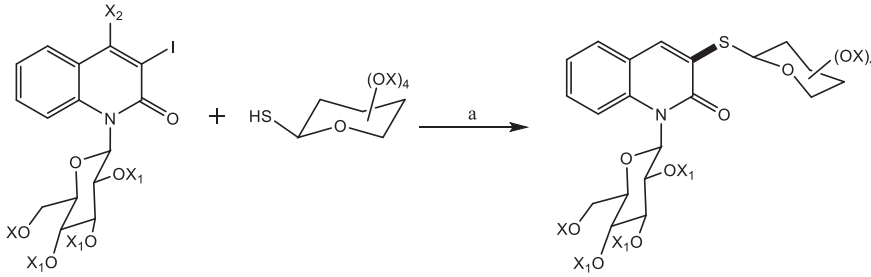

86 **87a–f** **88**

β-86a: X_1=OAc, X_2=H; **α-86b**: X_1=OAc, X_2=H; **β-86c**: X_1=OAc, X_2=4-OMePh; **β-86d**: X_1=X_2=H

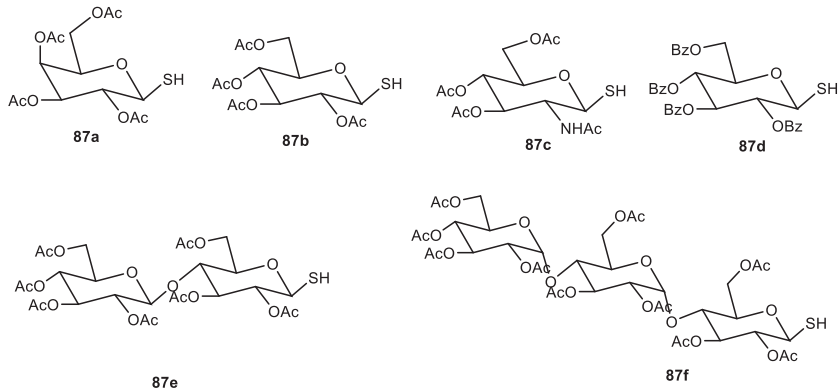

Scheme 15.21 Coupling of the quinolones **86a–d** with thiosugars **87a–f** under the optimized conditions. Reagents and conditions: (a) Pd G3-Xantphos (5 mol%) Et3N (1.5 equiv), THF (or THF:H_2O), rt, 3 h.

metal-catalyzed coupling of thiosugars with halogenated electrophiles was a superior and highly versatile approach to the synthesis of thioglycosides. Copper-catalyzed functionalization of 1-thiosugars for the synthesis of thioglycosides is shown in Scheme 15.22 [113].

The reaction appeared to be suitable for both α- and β-anomeric configurations and was conducted with per-O-acetylated 1-thio-β-D-glucose, galactose, *N*-acetyl-α-D-glucosamine to give the corresponding products (**91a–d**). The reaction was also influenced by the substituents on the iodoaryl triazenes moieties such as ester and acyl. This methodology was extended to the construction of bivalent *S*-glycoclusters (**91c**) by treating *O*,*O*′-dihaloaryl triazenes (1 equiv) with per-O-acetylated sugar mercaptans (2.2 equiv) under similar reaction conditions. This method also allowed the preparation of symmetrical and unsymmetrical 1,3-bis(glycopyranosylthio)benzene derivatives.

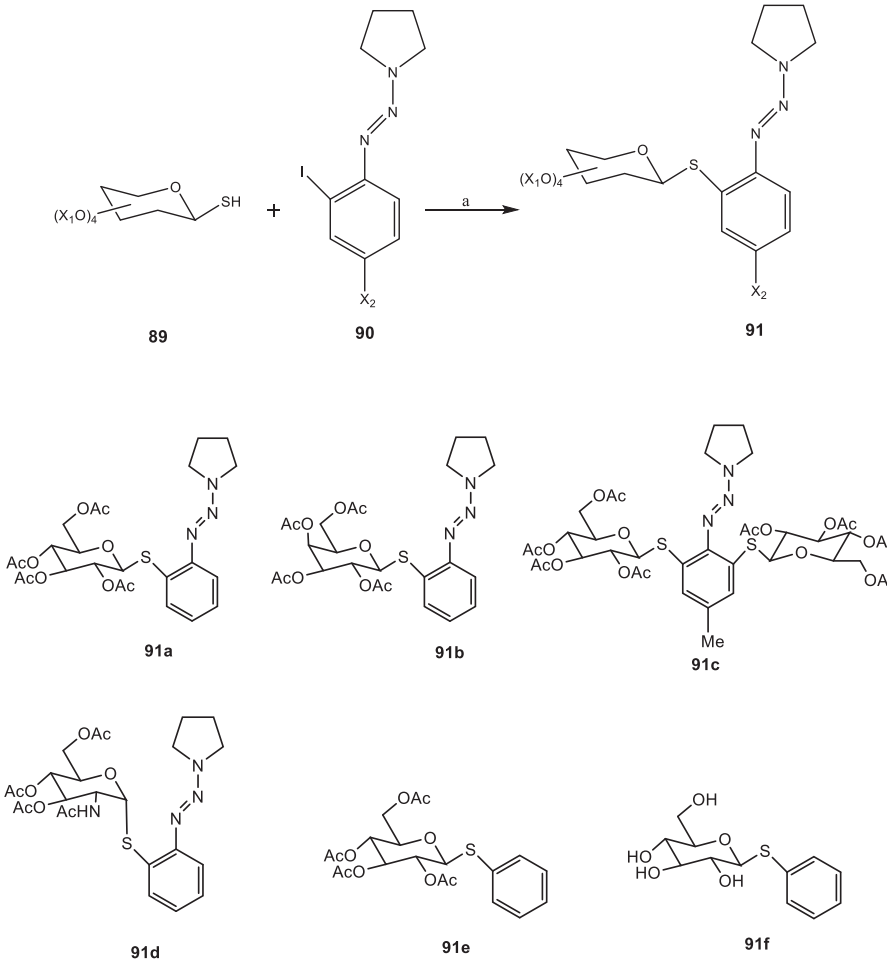

Scheme 15.22 Copper catalyzed functionalization of 1-thiosugars. Reagents and conditions: (a) CuI (1 equiv), K_2CO_3 (2 equiv), Pyridine (3 equiv), MeCN, 80°C, 24 h.

Metal complexes with *N*-heterocyclic carbene (NHC) ligands has a wide range of applications, such as in catalysis [114], as metal-based drugs [115, 116], and as materials [117]. In order to serve as a lipophilic part in drug-like molecules, NHC ligands are easily chemically modified, like 1,3-dibenzyl-4,5-diphenylimidazol-2-ylidene. Several groups have reported the potential antibiotic or anticancer activity of metal NHC complexes [118–120].

The synthesis of anticancer drug candidate 1,3-dibenzyl-4,5-diphenyl-imidazol-2-ylidene gold(I) chloride (NHC*-AuCl) and its derivative 2′,3′,4′,6′-tetra-*O*-acetyl-β-D-glucopyranosyl-1′-thiolate (NHC*-AuSR) [121–123] is shown in Scheme 15.23 [124].

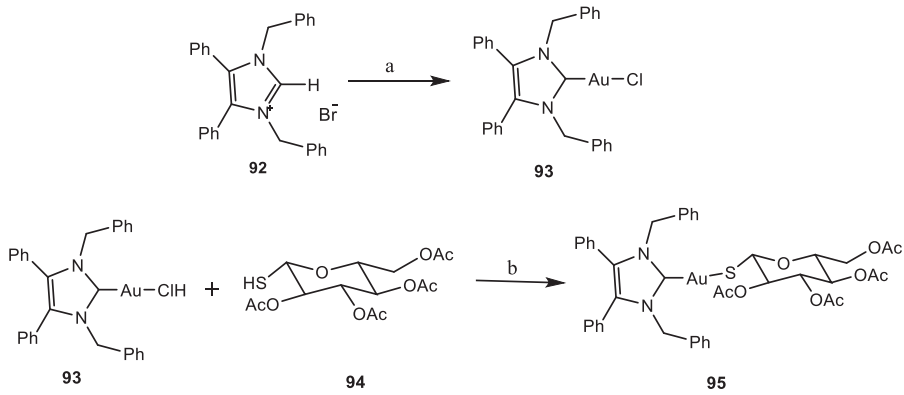

Scheme 15.23 Synthesis of 1,3-dibenzyl-4,5-diphenyl-imidazol-2-ylidene gold(I) chloride (NHC*-Au-Cl) and its 2′,3′,4′,6′-tetra-*O*-acetyl-β-D-glucopyranosyl-1′-thiolate derivative.

NHC*-AuCl and NHC*-AuSR were tested in vitro against NCI-60 cancer cell panel and both compounds showed very good activity against a wide range of human cancer cell lines, including renal cancer cell with similar average GI50 values of 1.78 and 1.95 μM, respectively.

15.4 Naturally occurring thiosugars: Medicinal activity

Many functionalized thiosugars occur naturally. A few examples are salacinol and kotalanol, tagetitoxin, thiolactomycin and analogs, mycothiol and analogs, and *S*-nitrosothiols. Among them many are used as a potential target for the development of carbohydrate-based therapeutics. 5-Thio-D-mannose is the first naturally occurring free thiosugar, which was isolated from the marine sponge *Clathria pyramida* in 1987 [125]. Molecular structure of 5-thio-D-mannose (**96**) is shown in Scheme 15.24. The other classes of naturally occurring thiosugars are 1,4-thioanhydrosugars (salacinol and kotalanol) and thioglycosides (glucosinolates and lincomycins). 1,4-Thioanhydrosugar, salacinol and kotalanol, is a class of thiosugar that possess potent sucrase inhibition, which bear a sulfonium salt-containing heterocycle in their skeleton [126].

Yoshikawa et al. have synthesized α-glucosidase inhibitor salacinol with unique thiosugar sulfonium sulfate structure [127]. It was extracted from the water-soluble fraction from the dried roots of *Salacia reticulata* by silica gel column chromatography and repeated various HPLC. The molecular structure of salacinol (**97**) is shown in Scheme 15.24. Yoshikawae et al. have isolated also kotalanol (**98**), another potent α-glucosidase inhibitor from the roots and stems of *S. reticulate* [128]; its molecular structure is shown in Scheme 15.24.

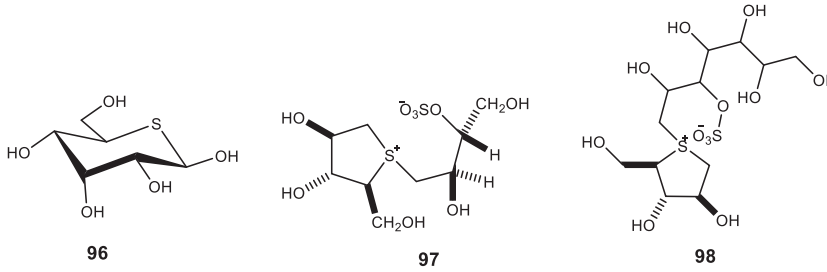

Scheme 15.24 Molecular structure of 5-thio-D-mannose, salacinol, and kotalanol.

Salacinol (**97**) was tested in vitro against intestinal α-glucosidase and showed competitive inhibition and IC_{50} values observed were 3.2 μg/mL to maltase, 0.84 μg/mL to sucrase, and 0.59 μg/mL to isomaltase. The inhibitory activity against isomaltase was much more potent than that of acarbose (Table 15.2). The inhibitory activities of **97** against maltase and sucrase were nearly equal to those of acarbose. It was also observed that this compound inhibited more strongly the increase of serum glucose levels in sucrose-loaded rats than acarbose. Thus, salacinol (**97**) is a most important α-glucosidase inhibitor isolated from natural medicine and is a significant constituent of Kotala himbutu, traditional antidiabetic Ayurvedic medicine. Kotalanol (**98**) was found to have more potent inhibitory activity against sucrase than salacinol and acarbose (Table 15.2) when tested against intestinal α-glucosidases.

Table 15.2 K_i values of salacinol, kotalanol, and acarbose for rat intestinal disaccharidase.

		***Ki* (μg/mL)**		
Substrate	**K_m (M)**	**Salacinol**	**Kotalanol**	**Acarbose**
Isomaltose	4.5×10^{-3}	0.47	1.8	75
Sucrose	2.0×10^{-2}	0.32	0.18	0.37
Maltose	2.7×10^{-3}	0.31	0.23	0.12

4-*O*-Acetyl-3-amino-1,6-anhydro-3-deoxy-D-gulose 2-phosphate commonly known as Tagetitoxin (**99**) is a bacterial phytotoxin [129]. Tagetitoxin is produced by the plant pathogenic bacteria, *Pseudomonas syringae pv. tagetis*. By specifically inhibiting chloroplast RNA polymerase, tagetitoxin induces chlorosis in the apex of the host plant making it potentially useful as herbicide [130].

Oishi et al. have isolated thiolactomycin (**100**) from *Nocardia sp.* [131]. It has a unique pharmacological activity against parasitic and bacterial organisms. In vitro studies showed that thiolactomycin is active against a wide range of *Mycobacterium tuberculosis* strains. It selectively inhibited the mycobacterial acyl carrier protein-dependent type II FAS (FAS-II) but not the multifunctional type I FAS (FAS-I) present in mammals [132, 133].

The low molecular weight thiol found in most actinomycetes, including mycobacteria and streptomycetes, is the mycothiol (**101**) [134]. It was isolated first in 1996 and is a conjugate of *N*-acetylcysteine, glucosamine, and myo-inositol, produced by most of the actinomycetes but not by other bacteria or eukaryotes [135]. Lee et al. have reported the first total synthesis of mycothiol and its disulfide [136]. Different methods and protocols are now available to synthesize mycothiol [137–139]. Mycothiol has the ability to mimic glutathione function in Gram-positive bacteria and thus instigated an interest in studying bacterial enzyme activity. Molecular structure of tagetitoxin (**99**), thiolactomycin (**100**), and mycothiol (**101**) are shown in Scheme 15.25.

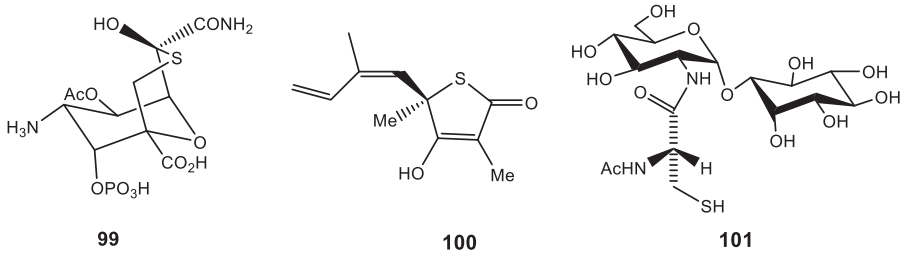

Scheme 15.25 Molecular structure of tagetitoxin, thiolactomycin, and mycothiol.

15.5 Conclusions

Many aspects of synthesis as well as biological activities associated with thiosugars are extensively reviewed in this chapter. Thiosugars with sulfur atom as heteroatom or a disaccharide linked via a sulfur bridge were treated separately and the data were taken from recent literatures. New methodologies and techniques to synthesize almost all representatives of functionalized analogs of thiosugars, oligosaccharides including thiodisaccharides and simple functionalized thiosugars, were illustrated. The chemistry and biology of oxygen sugars are enormously popular. Oxygen sugar-containing molecules are much more reactive than the thiosugars. The reactivity differences should be helpful to use intermediate or final thio compounds for the preparation of many other products even in relatively drastic conditions. The stability of thiosugars in the presence of electrophilic and nucleophilic reagents helps to maintain the sugar-containing ring without damage, rearrangement, and epimerization. From the past literature, it is known that sulfur-based compounds have diverse medicinal effects. Because of the stable nature, the metabolism of sulfur compounds may become slow and half-life of these molecules may also become high compared to their oxygen analogous. Therefore, this subject is integrated with biomedical research and should provide enormous opportunities for developing future research directions in this area. The current developments in the area of thiosugars will ensure that this rapidly developing field of carbohydrate chemistry remains a rich area of investigation for many years to come.

Acknowledgments

BKB is grateful to the USA NIH, USA NCI and USA Private Research Foundation. BKB and AD also thank Prince Mohammad Bin Fahd University for encouragement.

References

[1] T. Kajimoto, K.K.-C. Liu, R.L. Pederson, Z. Zhong, Y. Ichikaw, J.A. Porco Jr., C.-H. Wong, J. Am. Chem. Soc. 113 (1991) 6187.
[2] H. Yuasa, Y. Nakano, H. Hashimoto, Carbohydr. Lett. 2 (1996) 23.
[3] Y. Yoshimura, M. Endo, S. Sakata, Tetrahedron Lett. 40 (1999) 1937.
[4] S. Miura, Y. Yoshimura, M. Endo, H. Machida, A. Matsuda, M. Tanaka, T. Sasaki, Cancer Lett. 129 (1998) 103.
[5] T. Hudlicky, J.D. Price, F. Rulin, T. Tsunoda, J. Am. Chem. Soc. 112 (1990) 9439.
[6] R.F. Schinazi, C.K. Chu, A. Peck, A. McMillan, R. Mathis, D. Cannon, L.S. Jeong, J. W. Beach, W.B. Choi, S. Yeola, Antimicrob. Agents Chemother. 36 (1992) 672.
[7] J.A. Coates, N. Cammack, H.J. Jenkinson, A.J. Jowett, M.I. Jowett, B.A. Pearson, C.R. Penn, P.L. Rouse, K.C. Viner, J.M. Cameron, Antimicrob. Agents Chemother. 36 (1992) 733.
[8] J.W. Beach, L.S. Jeong, A.J. Alves, D. Pohl, H.O. Kim, C.N. Chang, S.L. Doong, R.F. Schinazi, Y.C. Cheng, C.K. Chu, J. Org. Chem. 57 (1992) 2217.
[9] E. Bozo, S. Boros, J. Kuszmann, Carbohydr. Res. 311 (1998) 191.
[10] E. Bozo, T. Gati, A. Demeter, J. Kuszmann, Carbohydr. Res. 337 (2002) 1351.
[11] S. Mohan, B.M. Pinto, Carbohydr. Res. 342 (2007) 1551.
[12] H. Yuasa, Y. Izukawa, H. Hashimoto, Curr. Top. Med. Chem. 9 (2009) 76.
[13] I. Robina, P. Vogel, Z. Witczak, J. Curr. Org. Chem. 5 (2001) 1177.
[14] I. Robina, P. Vogel, Curr. Org. Chem. 6 (2002) 471.
[15] D. Horton, D.H. Hijtson, Adv. Carbohydr. Chem. 18 (1963) 123.
[16] H. Paulsen, K. Todt, Adv. Carbohydr. Chem. 23 (1968) 115.
[17] R.L. Whittier, W.-C. Lake, Methods Carbohydr. Chem. 6 (1972) 286.
[18] E.J. Reist, L.V. Fisher, L. Goodman, J. Org. Chem. 33 (1968) 189.
[19] M.J. Pitts, M. Chemielewski, M.S. Chen, M.M. el-Rahman, R.L. Whistler, Arch. Biochem. Biophys. 169 (1975) 384.
[20] M.S. Chen, R.L. Whistler, Arch. Biochem. Biophys. 169 (1975) 392.
[21] C.J. Clayton, N.A. Hughes, Carbohydr. Res. 27 (1973) 89.
[22] J.E. Nam Shin, A.S. Perlin, Carbohydr. Res. 76 (1979) 165.
[23] (a) A. Maradufu, G.M. Cree, A.S. Perlin, Can. J. Chem. 49 (1971) 3429. (b) A. Maradufu, A.S. Pewn, Carbohydr. Res. 32 (1974) 93.
[24] J. E. N. Shin, Ph.D. Thesis, McGiil University, Montreal, Canada, 1978.
[25] F.G. Calvo-Flores, P.G. Mendoza, F.H. Mateo, J.I. Garcıa, F.S. Gonzalez, J. Org. Chem. 62 (1997) 3944.
[26] Y.L. Merrer, M. Fuzier, I. Dosbaa, M.-J. Foglietti, J.-C. Depezay, Tetrahedron 53 (1997) 16731.
[27] A. Martinez, E. Hénon, C. Coiffier, A. Banchet, D. Harakat, J.-M. Nuzillard, A. Haudrechy, Carbohydr. Res. 345 (2010) 1088.
[28] S. Guillarme, K. Plé, A. Haudrechy, J. Org. Chem. 71 (2006) 1015.
[29] S. Guillarme, A. Haudrechy, Tetrahedron Lett. 46 (2005) 3175.
[30] A. Banchet, S. Guillarme, A. Haudrechy, Synlett (2007) 1467.

[31] W. Xie, G. Tanabe, J. Akaki, T. Morikawa, K. Ninomiya, T. Minematsu, M. Yoshikawa, X. Wu, O. Muraoka, Bioorg. Med. Chem. 19 (2011) 2015.
[32] B.D. Johnston, H.H. Jensen, B.M. Pinto, J. Org. Chem. 71 (2006) 1111.
[33] R. Eskandari, D.A. Kuntz, D.R. Rose, B.M. Pinto, Org. Lett. 12 (2010) 1632.
[34] L. Wallach, N. Latifeh, D.T. Scott, Carbohydr. Res. 340 (2005) 1213.
[35] J. Zhang, Y. Niu, X. Cao, X.-S. Ye, Tetrahedron 68 (2012) 4242.
[36] M. Violante de Paz Banez, J.A.A. Moreno, J.A.J. Galbis, Carbohydr. Chem. 27 (2008) 120.
[37] T. Gunasundari, S. Chandrasekaran, Carbohydr. Res. 382 (2013) 30.
[38] Benzyl triethylammonium Tetrathiomolybdate: e-EROS Encyclopedia of Reagents for Organic Synthesis, **John Wiley and Sons Ltd, Chichester, UK, 2001.
[39] T.-L. Ho, M. Fieser, L. Fieser, Benzyltriethylammonium Tetrathiomolybdate: Fieser and Fieser's Reagents for Organic Synthesis, John Wiley and Sons, 2006.
[40] K.R. Prabhu, N. Devan, S. Chandrasekaran, Synlett (2002) 1762.
[41] D. Sureshkumar, K. Srinivasa Murthy, S. Chandrasekaran, J. Am. Chem. Soc. 127 (2005) 12760.
[42] D. Sureshkumar, T. Gunasundari, V. Ganesh, S. Chandrasekaran, J. Org. Chem. 72 (2007) 2106.
[43] P. Ramu Sridhar, K.R. Prabhu, S. Chandrasekaran, Eur. J. Org. Chem. (2004) 4809.
[44] T. Gunasundari, S. Chandrasekaran, J. Org. Chem. 75 (2010) 6685.
[45] T. Gunasundari, S. Chandrasekaran, Eur. J. Org. Chem. (2012) 6986.
[46] I. Lundt, Top. Curr. Chem. 187 (1997) 117.
[47] N.M. Xavier, A.P. Rauter, Y. Queneau, Top. Curr. Chem. 295 (2010) 19.
[48] I. Lundt, R. Madsen, Synthesis (1992) 1129.
[49] E.M. Scanlan, V. Corce, A. Malone, Molecules 19 (2014)19137.
[50] L. McSweeney, F. Dénès, E.M. Scanlan, Eur. J. Org. Chem. (2016) 2080.
[51] A. Malone, E.M. Scanlan, Org. Lett. 15 (2013) 504.
[52] J.M. Surzur, React. Intermed. 2 (1982) 121.
[53] V. Corce, L. McSweeney, A. Malone, E.M. Scanlan, Chem. Commun. (2015) 8672.
[54] Y. Yoshimura, Y. Saito, Y. Natori, H. Wakamatsu, Chem. Pharm. Bull. 66 (2018) 139.
[55] Y. Yoshimura, H. Wakamatsu, Y. Natori, Y. Saito, N. Minakawa, J. Org. Chem. 14 (2018) 1595.
[56] M.I. Elzagheid, M. Oivanen, R.T. Walker, J.A. Secrist, Nucleosides Nucleotides 18 (1999) 181.
[57] M. Bobek, A. Bloch, R.L. Whistler, J. Med. Chem. 15 (1972) 168.
[58] M.R. Dyson, P.L. Coe, R.T. Walker, J. Chem. Soc. Chem. Commun. (1991) 741.
[59] J.A. Secrist, K.N. Tiwari, J.M. Riordan, J.A. Montgomery, J. Med. Chem. 34 (1991) 2361.
[60] N. Ototani, R.L. Whistler, J. Med. Chem. 17 (1974) 535.
[61] J.M. Madern, T. Hansen, E.R. van Rijssel, H.A.V. Kistemaker, S. van der Vorm, H.S. Overkleeft, G.A. van der Marel, D.V. Filippov, J.D.C. Codeé, J. Org. Chem. 84 (2019) 1218.
[62] N. Minakawa, D. Kaga, Y. Kato, K. Endo, M. Tanaka, T. Sasaki, A. Matsuda, J. Chem. Soc. Perkin Trans. 1 (2002) 2182.
[63] K. Toshima, T. Yoshida, S. Mukaiyama, K. Tatsuta, Carbohydr. Res. 222 (1991) 173.
[64] L. Kocourek, Carbohydr. Res. 3 (1967) 502.
[65] A.B. Foster, J.M. Duxbury, T.D. Inch, J.M. Webber, Chem. Commun. (1967) 881.
[66] A.R. Butler, R.A. Field, I.R. Greig, F.W. Flitney, S.K. Bisland, F. Khan, J.J.F. Belch, Nitric Oxide 1 (1997) 211.
[67] Z.J. Witczak, D. Boryczewski, Bioorg. Med. Chem. Lett. 8 (1998) 3265.

[68] J. Hasegawa, M. Hamada, T. Miyamoto, K. Nishide, T. Kajimoto, J. Uenishi, M. Node, Carbohydr. Res. 340 (2005) 2360.
[69] P.N. Fonteh, F.K. Keter, D. Meyer, Biometals 23 (2) (2010) 185.
[70] R.E. Kast, Cent. Eur. Neurosurg. 71 (2010) 139.
[71] W.F. Kean, I.R. Kean, Inflammopharmacology 16 (2008) 112.
[72] M. Navarro, C. Gabbiani, L. Messori, D. Gambino, Drug Discov. Today 15 (2010) 1070.
[73] S. Prast-Nielsen, M. Cebula, I. Pader, E.S. Arner, Free Radic. Biol. Med. 49 (2010) 1765.
[74] A. Ilari, P. Baiocco, L. Messori, A. Fiorillo, A. Boffi, M. Gramiccia, T. Di Muccio, G. Colotti, Amino Acids 42 (2012) 803.
[75] Z.J. Witczak, J. Sarnik, A. Czubatka, E. Forma, T. Poplawski, Bioorg. Med. Chem. Lett. 24 (2014) 5606.
[76] L. Lazar, M. Csavas, M. Toth, L. Somsak, A. Borbas, Chem. Pap. 69 (2015) 889.
[77] O. Dada, G.S. Sanz, M. Tacke, X. Zhu, Tetrahedron Lett. 59 (2018) 2904.
[78] X. Zhu, R.T. Dere, J. Jiang, L. Zhang, X. Wang, J. Org. Chem. 76 (2011) 10187.
[79] H. Wang, X. Zhu, Org. Biomol. Chem. 12 (2014) 7119.
[80] M.B. Haque, B.P. Roberts, D.A. Tocher, J. Chem. Soc. Perkin Trans. 1 (1998) 2881.
[81] D.A. Fulton, J.F. Stoddart, J. Org. Chem. 66 (2001) 8309.
[82] M. Cerny, J. Vrkoc, J. Stanek, Collect. Czechoslov. Chem. Commun. 24 (1959) 64.
[83] R. Smith, H. Müller-Bunz, X. Zhu, Org. Lett. 18 (2016) 3578.
[84] R. Komor, G.P. Gawolek, E. Krol, W. Szeja, Molecules 23 (2018) 2017.
[85] R.A. Dwek, Chem. Rev. 96 (1996) 683.
[86] A.A.-H. Abdel-Rahman, S.H. El Ashry, R.S. Richard, Carbohydr. Res. 315 (1999) 106.
[87] J. Ren, C. Bailly, J.-B. Chaires, FEBS Lett. 470 (2000) 355.
[88] M. Rajesh, J. Pengei, S. Rohit, S. Dmitri, B. Ila, N. Natsuko, C. Ying, P. Sandra, Int. J. Nanomedicine 8 (2013) 3991.
[89] P. Hewawasam, N. Chen, M. Ding, J.T. Natale, C.G. Boissard, S. Yeola, V.K. Gribkoff, J. Starrett, S.I. Dworetzky, Bioorg. Med. Chem. Lett. 14 (2004) 1615.
[90] K.H. Raitio, J.R. Savinainen, J. Vepsäläinen, J.T. Laitinen, A. Poso, T. Järvinen, T. Nevalainen, J. Med. Chem. 49 (2006) 2022.
[91] P. Hewawasam, W. Fan, M. Ding, K. Flint, D. Cook, G.D. Goggings, R.A. Myers, V.K. Gribkoff, C.G. Boissard, S.I. Dworetzky, J. Med. Chem. 46 (2003) 2819.
[92] P. Hewawasam, W. Fan, J. Knipe, S.L. Moon, C.G. Boissard, V.K. Gribkoff, J.E. Starret, Bioorg. Med. Chem. Lett. 12 (2002) 1779.
[93] A.A. Cordi, P. Desos, J.C. Randle, J. Lepagnol, Bioorg. Med. Chem. 3 (1995) 129.
[94] P. Desos, J.M. Lepagnol, P. Morain, P. Lestage, A.A. Cordi, J. Med. Chem. 39 (1996) 197.
[95] R.W. Carling, P.D. Leeson, K.W. Moore, J.D. Smith, C.R. Moyes, I.M. Mawer, S. Thomas, T. Chan, R. Baker, A. Foster, J. Med. Chem. 36 (1993) 3397.
[96] W. Redjdal, N. Ibrahim, B. Benmerad, M. Alami, S. Messaoudi, Molecules 23 (2018) 519.
[97] C.S. Rye, S.G. Withers, Carbohydr. Res. 339 (2004) 699.
[98] B.B. Metaferia, B.J. Fetterolf, S. Shazad-ul-Hussan, M. Moravec, J.A. Smith, S. Ray, M.-T. Gutierrez-Lugo, C.A. Bewley, J. Med. Chem. 50 (2007) 6326.
[99] F. Castaneda, A. Burse, W. Boland, R.K.-H. Kinne, Int. J. Med. Sci. 4 (2007) 131.
[100] J. Rodrigue, G. Ganne, B. Blanchard, C. Saucier, D. Giguere, T.C. Shiao, A. Varrot, A. Imberty, R. Roy, Org. Biomol. Chem. 11 (2013) 6906.
[101] G.H. Elgemeie, A.B. Farag, K.M. Amin, O.M. El-Badry, G.S. Hassan, Med. Chem. 4 (2014) 814.
[102] M.R. Aouad, Nucleosides Nucleotides Nucleic Acids 35 (2016) 1.

[103] E. Kato, H. Nagano, S. Yamamura, M. Ueda, Tetrahedron 59 (2003) 5909.
[104] M. Schnabelrauch, A. Vasella, S.G. Withers, Helv. Chim. Acta 77 (1994) 778.
[105] R. Furneaux, R. Ferrier, Methods Carbohydr. Chem. 8 (1980) 251.
[106] K.C. Nicolaou, J.L. Randall, G.T. Furst, J. Am. Chem. Soc. 107 (1985) 5556.
[107] S.K. Das, J. Roy, K.A. Reddy, C. Abbineni, Carbohydr. Res. 338 (2003) 2237.
[108] C.-A. Tai, S.S. Kulkarni, S.-C. Hung, J. Org. Chem. 68 (2003) 8719.
[109] G. Agnihotri, P. Tiwari, A.K. Misra, Carbohydr. Res. 340 (2005) 1393.
[110] E. Fischer, K. Delbruek, Ber. Dtsch. Chem. Ges. 42 (1909) 1476.
[111] M. Blanc-Muesser, J. Defaye, H. Driguez, Carbohydr. Res. 67 (1978) 305.
[112] M. Apparu, M. Blanc-Muesser, J. Defaye, H. Driguez, Can. J. Chem. 59 (1981) 314.
[113] N. Ibrahim, M. Alami, S. Messaoudi, Asian J. Org. Chem. 7 (2018) 2026.
[114] D. Zhao, L. Candish, D. Paul, F. Glorius, ACS Catal. 6 (2016) 5978.
[115] W. Liu, R. Gust, Coord. Chem. Rev. 329 (2016) 191.
[116] T. Zou, C.T. Lum, C.-N. Lok, J.-J. Zhang, C.-M. Che, Chem. Soc. Rev. 44 (2015) 8786.
[117] L. Mercs, M. Albrecht, Chem. Soc. Rev. 39 (2010) 1903.
[118] M. Tacke, J. Organomet. Chem. 782 (2015) 17.
[119] S.A. Patil, S.A. Patil, R.S. Keri, S. Budagumpi, G. Balakrishna, M. Tacke, Future Med. Chem. 7 (2015) 1305.
[120] F. Hackenberg, M. Tacke, Dalton Trans. 43 (2014) 8144.
[121] S. Patil, A. Deally, B. Gleeson, H. Müller-Bunz, F. Paradisi, M. Tacke, Metallomics 3 (2011) 74.
[122] F. Hackenberg, H. Müller-Bunz, R. Smith, W. Streciwilk, X. Zhu, M. Tacke, Organometallics 32 (2013) 5551.
[123] M. Tacke, O. Dada, C. O'Beirne, X. Zhu, H. Müller-Bunz, Acta Cryst C72 (2016) 857.
[124] M. Tacke, NHC*-Gold(I) Bioconjugated to Carbohydrates and Peptides as Targeted Anticancer Drugs, Slovak Chemical Society, Bratislava, 2019.
[125] R.J. Capon, J.K. MacLeod, J. Chem. Soc. Chem. Commun. 15 (1987) 1200.
[126] H. Matsuda, T. Morikawa, M. Yoshikawa, Pure Appl. Chem. 74 (2002) 1301.
[127] M. Yoshikawa, T. Murakami, H. Shimada, H. Matsuda, J. Yamahara, G. Tanabe, O. Muraoka, Tetrahedron Lett. 38 (1997) 8367.
[128] M. Yoshikawae, T. Muraksmi, K. Yashiro, H. Matsuda, Chem. Pharm. Bull. 46 (1998) 1339.
[129] R.E. Mitchell, R.D. Durbin, Physiol. Plant Pathol. 18 (1981) 157.
[130] D.E. Mathews, R.D. Durbin, J. Biol. Chem. 265 (1990) 493.
[131] H. Oishi, T. Noto, K. Suzuki, T. Hayashi, H. Okazaki, K. Ando, M. Sawada, J. Antibiot. 35 (1982) 391.
[132] R.A. Slayden, R.E. Lee, J.W. Armour, A.M. Cooper, I.M. Orme, P.J. Brennan, G.S. Besra, Antimicrob. Agents Chemother. 40 (1996) 2813.
[133] L. Kremer, J.D. Douglas, A.R. Baulard, C. Morehouse, M.R. Guy, D. Alland, L.G. Dover, J.H. Lakey, W.R. Jacobs Jr., P.J. Brennan, D.E. Minnikin, G.S. Besra, J. Biol. Chem. 275 (2000)16857.
[134] G.M. Nicholas, C.A. Bewley, Curr. Med. Chem. Anti-Infect. Agents 3 (2004) 221.
[135] G.L. Newton, K. Arnold, M.S. Price, C. Sherrill, S.B. delCardayre, Y. Aharonowitz, G. Cohen, J. Davies, R.C. Fahey, C. Davis, J. Bacteriol. (1996) 178.
[136] S. Lee, J.P.N. Rosazza, Org. Lett. 6 (2004) 365.
[137] M.P. Patel, J. Am. Chem. Soc. 120 (1998) 11538.
[138] M.A. Jardine, H.S.C. Spies, C.M. Nkambule, D.W. Gammon, D.J. Steenkamp, Bioorg. Med. Chem. 10 (2002) 875.
[139] G.M. Nicholas, P. Kovac, C.A. Bewley, J. Am. Chem. Soc. 124 (2002) 3492.

Implementing green chemistry for synthesis of cholesterol-lowering statin drugs

16

Ajoy Basak[a,b,*], *Sarmistha Basak*[c]
[a]Pathology and Laboratory Medicine, Ottawa, ON, Canada, [b]Ottawa Hospital Research Institute, The Ottawa Hospital, Ottawa, ON, Canada, [c]Formerly of Kidney Research Center, Ottawa Hospital Research Institute, Ottawa, ON, Canada
[*]Corresponding author. e-mail address: abasa2@uottawa.ca

Abbreviations

CFC	chloro-fluoro carbon
CVD	cardiovascular disease
CYP	cytochrome P450
DERA	deoxy ribose 5-phosphate aldolase
DHP	3,4-dihydro-2H-pyran
DMAP	dimethylaminopyridine
DMB-S-MMP	2,2-dimethylbutyryl-S-methyl mercapto propionate
DMF	*N*,*N*′-dimethylformamide
ee	enantiomeric excess
EPA	Environment Protection Agency
Et3N	triethylamine
GDH	glucose dehydrogenase
HHDH	halohydrin dehydrogenase
HMG CoA	3-hydroxy 3-methylglutaryl coenzyme A
HN	hydroxy nitrile
KPB	potassium phosphate buffer
KRED	keto-reductase
LDA	lithium di-isopropyl amide
LDKS	noniterative lovastatin diketide synthase
LDL-C	low-density lipoprotein cholesterol
LNKS	iterative lovastatin nonketide synthase
NADP	nicotinamide adenine dinucleotide phosphate
PKS	polyketide synthase
Py	pyridine
Py-Py	pyridyl pyridine
RP-HPLC	reversed phase high-performance layer chromatography
RT	room temperature
SAM	S-adenosyl methionine
Stat	stirred
TBDMS	tertiary butyl dimethyl silyl
THF	tetrahydrofuran

Green Approaches in Medicinal Chemistry for Sustainable Drug Design. https://doi.org/10.1016/B978-0-12-817592-7.00016-2
© 2020 Elsevier Inc. All rights reserved.

16.1 Introduction

Green chemistry also known as sustainable chemistry is defined as a chemical process that is environmentally friendly with minimum or no toxicological and harmful impacts on the surrounding environments [1, 2]. The rationale of green chemistry is based on the elimination or minimization of the use or creation of hazardous materials during the process of design, manufacture, and application of chemical agents. It is applicable to life cycle of a chemical product, including its design, manufacturing method, and subsequent use. Chemical production and purification of most agents of high pharmaceutical, medicinal, biological, or agricultural significance are typically associated with the use of environmentally hostile and unfriendly conditions such as nonaqueous organic solvent, harsh chemical reagent, catalytic agent, high temperature, increased pressure, and/or high-energy associated methods [3, 4]. In simple plain term, the main objective of green chemistry is to minimize or prevent pollution, reduce toxic wastes, use renewable feedstocks, and least amount of energy for most efficient reaction process. In fact, there are 12 basic principles that govern the green chemistry platform. These are (i) waste prevention (minimize waste production); (ii) atom economy (maximize incorporation of all materials into the desired product); (iii) less hazardous chemicals production (with little or no toxicity); (iv) developing safer chemicals (preserve efficacy of function reducing toxicity); (v) safer solvents (minimum use of organic solvents and auxiliary substances); (vi) energy-efficient process (ambient temperature and pressure recommended); (vii) renewable feedstocks (raw materials should be renewable rather than depleting); (viii) reduce derivatizations (avoid unnecessary protection/deprotection steps); (ix) catalysis (use harmless catalytic agents with selectivity); (x) design for degradation (chemical products should degradable into benign materials after the function); (xi) real-time pollution prevention (in real-time monitoring and control prior to hazardous material formation), and (xii) safer chemistry (to prevent accident) [5]. The United States Environment Protection Agency (US EPA) (www.epa.gov/greenchemistry/basics-green-chemistry) and the American Chemical Society (ACS) Green Chemistry Institute (www.acs.org/content/acs/en/green chemistry/what-is-green chemistry/examples.html) both played major roles in encouraging and promoting research and education on the development of environmental safe and most efficient sustainable methodologies [6–9] (www.warner babcock.com/green-chemistry/a-historical-perspective/). There is now an increased level of awareness and interest in the field. Scientists and researchers in pharmaceutical, chemical, and academic sectors are gradually embracing clean, sustainable, economically sound, and renewable energy policy [10]. Owing to this shift in thought, significant achievements have been made possible on the development and incorporation of green chemistry technology in many industrial and manufacturing processes. In fact, this has now become a new norm and culture in all pharmaceutical, chemical, and household processes. The significance of "green science" concept in every aspect of society is well recognized through the award of prestigious Nobel Prize in 2005 to Richard R. Schrock, Robert H. Grubbs, and Yves Chauvin

for their contributions in the discovery of catalytic chemical process termed as "metathesis" [11, 12] which uses significantly less energy and reduces greenhouse gas emission [13].

Until now significant advancement has been achieved on the application of green technology in the fields of computer chips [14, 15], medicine [16] (also see University of Nottingham, UK, report "Using Green Chemistry to Deliver Cutting-edge Drugs," Science Daily, 14 September 2007), paint and coating industry [17, 18], agriculture [19, 20], and biomaterials [21, 22]. Since mid-20th century, the long-term negative impacts of technological advancement in health science, medicine, energy, and industry sectors were gradually realized. The implications of many environmental chemicals in causing diseases such as cancer, neurological dysfunction, cardiovascular, diabetes, and others could not be ignored [23]. As a consequence, several countries have imposed new regulations in dealing with the production and disposal of chemical and industrial wastes. In addition, environmental watch dog agencies like EPA were established to overlook and enforce environmental regulations and laws in order to protect our environment and health. In particular, pressure was exerted on industry and pharmaceutical sectors for adoption of greener cleaner technology for synthesis of their products [24]. Thus, the drug industry is constantly making efforts to find new ways for generating medicines with minimum harmful and toxic impacts on the environment [25]. This led to improved and more economical process conditions for synthesis of drugs and their intermediate products. Currently, it becomes an integral part of Research and Development program of all pharma industries. Maximum reduction or complete elimination of toxic solvents and chemicals as well as incorporation of biocatalyst-based aqueous chemistry wherever possible became an important part of commercial green chemistry technology. In order to inspire and encourage for adoption of green chemistry methodology, the US EPA has created annual Presidential Green Challenges Awards for Pharmaceutical companies [26]. This initiative has led to successful synthesis of a number of drugs and/or their key intermediates via newly developed energy-efficient and environment benign green methodologies [27].

These developments encouraged us to write a review on the progress of green chemistry application in manufacture of drugs. In this chapter, we focus our attention only on one particular family of drugs approved for reducing low-density lipoprotein-cholesterol (LDL-C) [28]. High level of LDL-cholesterol in the blood is a key risk factor for developing cardiovascular disease (CVD) and stroke [29]. This chapter provides a summary of our progress toward adoption of green chemistry for synthesis of cholesterol-lowering drugs which are crucial for managing CVD—now the number one killer disease in the globe [30]. So far the advancement in this field is unfortunately quite limited unlike in other disease areas, where significant progress has been achieved in incorporating green chemistry for drug manufacturing process [31–33]. In this review, we first provide a brief summary of the progress made in incorporating green chemistry in drug synthesis. Later on, we focus specifically on green chemistry technology for commercial synthesis of cholesterol-lowering statin drugs followed by the challenges and future directions.

16.2 Green chemistry in drug synthesis

The first successful application of green chemistry in industry was accomplished in 1996 by Dow Chemical Company when they manufactured polystyrene foam by using carbon dioxide as the blowing agent [34, 35]. The carbon dioxide here is reused from another process where it is generated as a by-product. In addition, the foam produced by this method can be recycled after use mostly in packaging industry [36]. This replaced chloro-fluoro carbons (CFCs) which are known to destroy ozone in the atmosphere. Since that time green chemistry technology caught the attention of industry primarily because of its various beneficial and economic outcomes.

An excellent example of success story for inclusion of green chemistry in drug industry is the synthesis of Sitagliptin, the active ingredient of Januvia (a potent inhibitor of dipeptidyl peptidase IV enzyme) by Mark and Codexis companies for treatment of type 2 diabetes [37]. In this third-generation process, a newly designed bioengineered transaminase biocatalyst (consisting of 27 mutations in the wild type) was used for reductive amination step where a 99.95% enantiomeric excess (ee) selectivity was achieved compared to 95% ee in the second-generation method. In addition, this process improved the overall yield (13%), productivity (53%), and on the amount of waste generated (19%) compared to the second-generation method. Moreover like the second-generation method, it completely eliminated the aqueous waste streams (reviewed in Ref. [38]). This impressive accomplishment became an eye opener to other industries about the efficacy of green energy and the economic power of bioengineered catalysts in drug manufacturing process.

Other examples include (i) the green chemistry approach by Eli Lilly Company for synthesis of their drug Tradipitant (LY686017) formerly VLY686 from Vanda Pharmaceuticals (Neurokinin-1 receptor antagonist) for treatment of alcoholism and chronic pruritus (itchiness) in atopic dermatitis [39, 40] (https://newdrugapprovals.org/); (ii) green synthesis of Montelukast, an intermediate for anti-asthma drug Singulair (leukotriene inhibitor) using a newly engineered biocatalyst (keto-reductase or KRED) (with 19 mutations and 3000-fold activity compared to wild type) for asymmetric reduction [41, 42]; (iii) development of greener route for manufacturing Darunavir (intermediate of Prezista) for treatment of HIV thereby reducing waste, raw materials, solvent, and eliminating hydrogen gas formation [43, 44]; (iv) greener chemistry for synthesis of antiretroviral drug Raltegravir (intermediate of Isentress) where methyl iodide reagent is substituted by trimethyl-sulfoxonium iodide [44] thereby significantly improving the green parameter "E-factor" (defined as Kg waste per Kg product) [45]; (v) green chemistry method for synthesis of anti-inflammatory pyridinyl-imidazole-based drugs by Roche Company reducing chemical wastes and pollution [44, 46].

The above description is just a snap shot of progress made in adopting green chemistry in drug manufacture. In order to facilitate more use of green chemistry technology in drug industry, Glaxo Smith Kline did an excellent job in producing a kit called

"Eco design tool kit" that summarizes modern day knowledge about green chemistry, the necessary guidelines and protocols while highlighting the potential challenges [47].

16.3 Cholesterol-lowering drugs

Cholesterol-lowering drugs are prescribed routinely for treatment of hypercholesterolemia, where the level of LDL-C in blood serum is kept within normal level. For people suffering with this condition, there is a higher than normal level of LDL-C in circulation in the blood. Continued accumulation of LDL-C can lead to the formation of plaque in the artery thereby creating obstruction for normal flow of blood. This results in high blood pressure and hypertension that may ultimately cause stroke leading to permanent disability or death [48, 49]. Thus, high level of LDL-C in the blood is considered as the most crucial risk factor for stroke and cardiovascular disease. Owing to this reason, it is essential that one maintains serum cholesterol level within normal limit using cholesterol-lowering drugs like statins, originally developed more than a decade ago (reviewed in Ref. [50]). Today, these drugs are considered as most effective agents for prevention of stroke and heart attack.

16.4 Statins

Statins are small organic compounds with molecular weights <1000 Da (Dalton) that inhibit the key enzyme in the liver known as HMG-CO-A reductase (3-hydroxy-3-methylglutaryl-coenzyme A reductase) which is responsible for synthesis of cholesterol [51]. A wide variety of statins have been approved and currently in use. This is listed in Table 16.1. In general, they are of three types based on their manufacturing process, namely (i) *fermentation type such as lovastatin* (*derived from microorganisms by biotechnology*), (ii) *semisynthetic type that includes simvastatin and pravastatin* (*obtained via partly synthetic route*), or (iii) *synthetic type such as fluvastatin, cerivastatin, atorvastatin, rosuvastatin, and pitavastatin* (*obtained by complete chemical synthesis*) [52, 53]. Fluvastatin is the first fully synthetic statin drug reported by Sandoz AG. This was followed by synthetic atorvastatin. Statins can also be classified based on the type of ring structure present. Thus statins may contain a partially reduced naphthalene ring (lovastatin, simvastatin, and pravastatin) or a heterocyclic ring system such as a pyrrole ring (atorvastatin), an indole ring (fluvastatin), a pyrimidine ring (rosuvastatin), a pyridine ring (cerivastatin), or a quinolone ring (pitavastatin). It is noteworthy to point out that, while fluvastatin is marketed as a racemic mixture, both atorvastatin and rosuvastatin are marketed as single pure enantiomeric form. It is also noted that both simvastatin and pravastatin are, respectively, methyl and hydroxyl derivatives of lovastatin and, therefore, they all are structurally related to one another. Finally, a new extended or slow-releasing form of lovastatin called altocor (or altoprev) [54] (https://www.rxlist.com/altocor-drug.

Table 16.1 List of all statin drugs which are approved worldwide.

No.	Name	Type of origin	Commercial name	Type of ring structure	Property
1	Lovastatin	Fungal	Mevacor/ Altoprev	P.R. Naph.	Lipophilic
2	Simvastatin	Semisynthetic	Zocor	P.R. Naph.	Lipophilic
3	Pravastatin	Semisynthetic/ Fungal	Pravachol	P.R. Naph.	Hydrophilic
4	Pitavastatin	Synthetic	Livalo	Quinoline	Hydrophilic
5	Cerivastatin	Synthetic	Baycol (WD)	Pyridine	Hydrophilic
6	Atorvastatin	Synthetic	Lipitor	Pyrrole	Lipophilic
7	Rosuvastatin	Synthetic	Crestor	Pyrimidine	Hydrophilic
8	Fluvastatin	Synthetic	Lescol/Lescol XL	Indole	Lipophilic

Note: P.R. Naph.: Partly reduced naphthalene or decalin; WD: Withdrawn (in 2001 due to reports of death from severe rhabdomyolysis or muscle pain); Fungal statins are also called Type 1 statins; Semisynthetic statins are called Type II statins.

htm#clinpharm) has been described and approved but it was later withdrawn due to serious side effects with reported fatality [55].

Despite side effects and potential safety issue in about 10%–12% of patients, statins continue to dominate the field of cholesterol management [56]. Chemical syntheses of statins involved multiple steps which are often expensive, energy inefficient, and environmental non-friendly. Therefore, efforts have been made to develop synthetic methods that are cost effective, energy efficient, and less toxic to the environment. This can be accomplished by deploying green chemistry technology which will generate less waste, reduce toxic substance, organic solvent, and improve reaction conditions [57, 58]. So far several attempts have been made to incorporate green chemistry for manufacture of statin drugs. There was successful outcome for simvastatin, lovastatin, atorvastatin, and rosuvastatin [59], while for others such as pravastatin efforts are still ongoing [60]. These will be first discussed with respect to their historical background, common manufacturing process, and the adoption of green chemistry technology.

16.5 Lovastatin and simvastatin

Since lovastatin and simvastatin are the most popular and effective cholesterol-lowering drugs that were approved before the others, they will be discussed first in terms of their historical background, common manufacturing process, and green chemistry adoption. Later on we focus on other statins.

16.5.1 Background

Lovastatin (also termed as synvinolin, mevacor, or mevinolin) (Fig. 16.1) is the first statin to be approved and commercialized by Marck in 1987 [61, 62]. It was isolated by Alfred Albert et al. in 1979 from the culture of *Aspergillus terreus* and they termed it as mevinolin [63]. In the same year, A. Endo et al. from the Tokyo Noko University also isolated a statin-like compound called monacolin K from *Monascus ruber* [64] which was later found to be identical with mevinolin. In subsequent years, both were called lovastatin. Earlier on, Endo while working with Sankyo Company in Japan isolated from the culture of *Penicillium citrinum* Pen-51 a potent cholesterol-lowering agent which he named compactin. It exhibited strong HMG CoA reductase inhibitory activity [65–67]. Unfortunately, the program was discontinued by Sankyo owing to adverse reports and inconsistent results in clinical trials in selected species, despite the observed cholesterol lowering results in hen, dog and monkey, and in humans [52]. The chemical structure of compactin was found to be similar to that of lovastatin. A detail historical background of lovastatin was elegantly presented by A. Endo in a review article published in 2010 [50]. It is now established that besides *Aspergillus* (*A. terreus*), various other fungi species such as *Monascus* (*M. ruber, M. purpureus, M. pilosus, M. vitreus, M. pubigerus*, and *M. anka*), *Paecilomyces viridis*, *Pleurotus ostreatus*, and *Pencillium citrinum* also produce lovastatin during fermentation [68]. Lovastatin is also present naturally in oyster mushroom and red yeast rice [69, 70].

Simvastatin was the second statin drug introduced by Merck under the brand name Zocor in 1987. Currently, it is the most prescribed cholesterol-lowering drug in the

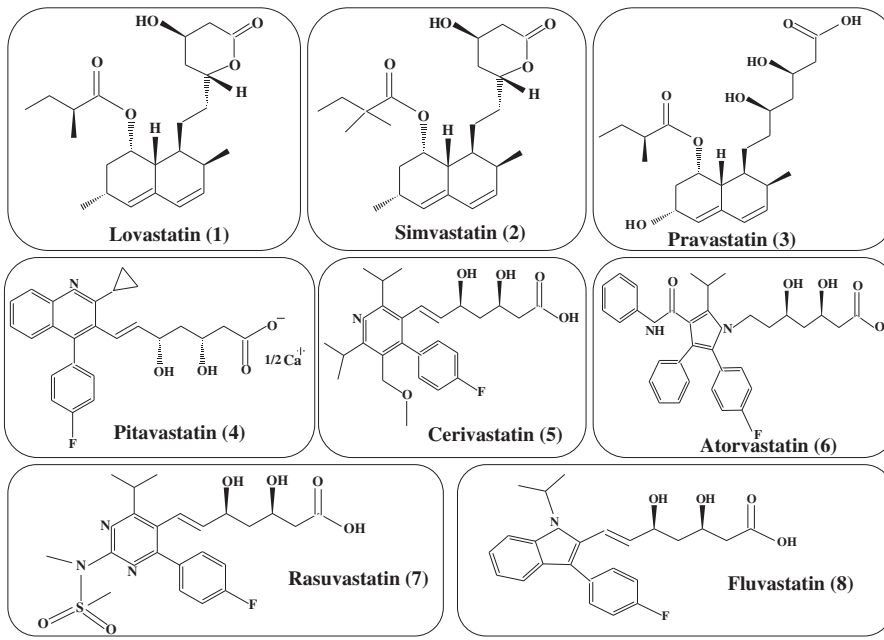

Fig. 16.1 Chemical structures of statin drugs.

world. Chemically, it is the 2′-methylated derivative of lovastatin (Fig. 16.1). Simvastatin is a semisynthetic product of lovastatin, where an additional methyl group has been inserted into its side chain. This subtle change resulted in enhanced cholesterol-lowering activity of simvastatin compared to lovastatin with advantage of reduced toxicity to the hepatocytes and side effects. Both lovastatin and simvastatin act in a similar manner but there are some important differences between the two [71, 72]. Thus, while lovastatin is prescribed for administration only with meal which enhances its absorption, simvastatin can be taken with or without food which does not exert any effect on its absorption. Also, the effect of lovastatin has been found to be more rapid, whereas simvastatin takes a much longer time for its effect to be observed [73]. A slow-releasing form of these drugs called altocor (altoprev) (https://www.rxlist.com/altocor-drug.htm) has been developed which found more useful and lasting effect on cholesterol reduction [72, 73].

16.5.2 Common production methods

16.5.2.1 Lovastatin

Large-scale production of lovastatin has been achieved by fermentation technology where its biosynthesis takes place in multiple steps involving endogenous biocatalysts as displayed in Fig. 16.2 (reviewed in Ref. [73]). Despite successful outcome, this

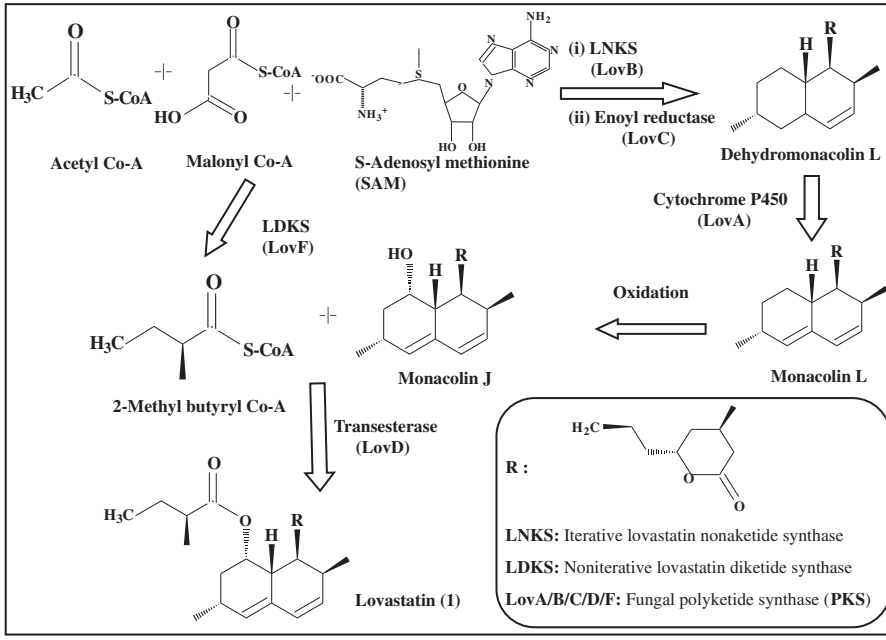

Fig. 16.2 Biosynthetic pathway for production of lovastatin within the cell system.

method has been found to be expensive. Therefore, efforts were made to produce lovastatin by chemical synthesis with the expectation of saving cost. The majority of this work was done in the early 1980s by Hirama et al. who reported the first full chemical synthesis of lovastatin from a synthetic intermediate trans-octalone [74, 75]. A few other chemical routes were also reported [76]. However, none of these methods proved less expensive and as a result the chemical synthesis of lovastatin could not be useful commercially and never explored further. Later on a semisynthetic route was developed by Yang et al. in 1997, where immobilized lipase enzyme was used for a key esterification reaction with 2-methyl butyric acid in an efficient and specific manner [77].

16.5.2.2 Simvastatin

Simvastatin, the more potent semisynthetic version of modified lovastatin became more useful than lovastatin itself. Chemically speaking, simvastatin is butanoic acid, 2,2-dimethyl, (1S,3R,7S,8S,8aR)-1,2,3,7,8,8a-hexahydro-3,7-dimethyl-8-(2-[(2R,4R)-tetrahydro-4-hydroxy-6-oxo-2H-pyran-2-yl)ethyl]-1-naphthalenyl ester (Fig. 16.1). It has been obtained via chemical synthesis from lovastatin [78–80]. However, despite success on laboratory scale, most were found to be unsuitable for large-scale production due to poor yield, high cost, too many chemical steps, or low conversion of the alkylation process.

The most pressing challenge in chemical synthesis of simvastatin is to remove the last trace of unreacted lovastatin from the final product [81]. Among all the chemical methods, two are now currently used commercially [82–84]. In the most traditional route originally developed in 1991 by Askin et al. [79], lovastatin was first deacetylated to dihydric alcohol which is then esterified with 2,2-dimethyl butyric acid via partial protection with tert-butyldimethylsilyl group, producing a monosilylated derivative. This product is subsequently acylated with 2,2-dimethylbutyryl chloride in the presence of base 4-pyrrolidino pyridine (py-py) in pyridine solvent. It was then deprotected to furnish the final material [82].

In a minor modification of this method, researchers from Reddy's Laboratory (India) used 3,4-dihydro-2H-pyran (DHP) as the protecting group instead of tert-butyldimethylsilyl group for free hydroxyl group of lovastatin that is generated following opening of the lactone ring with *n*-$BuNH_2$. This key intermediate is then subjected to alkylation reaction [83].

In an alternate protocol, simvastatin was also obtained by direct methylation at 2′ position of lovastatin [84]. Herein, the synthesis is based on the observation that the intermediate delta-lactone carbonyl is deactivated to enolization following derivatization with bis[(tert-butyl-dimethylsilyl)oxy] butylamide. This ester enolate is then alkylated almost quantitatively with 2,2-dimethylbutyryl chloride. The last few steps involved desilylation, intramolecularly assisted hydrolysis, and lactonization leading to the final product simvastatin in good yield (Fig. 16.3).

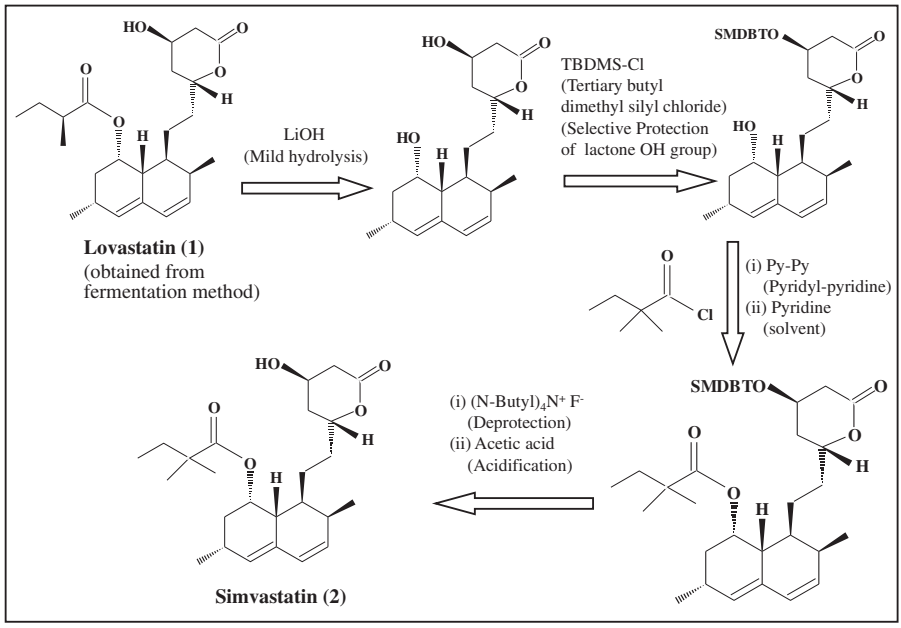

Fig. 16.3 Chemical synthesis of simvastatin from lovastatin using various reagents.

16.5.3 Adoption of green technology

Despite widespread use, the above chemical methods were all accompanied by huge waste of expensive organic solvents. They also required chemicals and reagents that were already known to be toxic to environment and hazardous to human health. Therefore, the pharmaceutical industries felt the need for better, greener, energy, and cost-efficient methodology for synthesis of lovastatin and simvastatin with minimum impact on environment. Thus, they started investing a significant part of their time, energy, and budget to engage in research on green chemistry in the field. This not only protected the environment but also benefitted their own revenue interests.

The first successful commercial application of green chemistry for statin production was reported for simvastatin, where a novel biocatalyst-mediated reaction was employed instead of chemical agents requiring multiple steps. Owing to this reason, we will discuss first the green chemistry application for simvastatin production. Later on we will review the literature on green synthesis of lovastatin and other statin drugs.

16.5.3.1 Green process for simvastatin

(i) *Recombinant biocatalyst approach*: The adoption of green chemistry for simvastatin synthesis was made possible when Prof. Yi Tang from the University of California in Los Angeles (USA) designed a novel bioengineered enzyme and a less costly feedstock. In this method, his team first produced an enzyme called *LovD acyltransferase* via cloning and used it for large-scale production of simvastatin from lovastatin in a most economical and

environmental friendly manner [85]. Basically, the method consists of three simple steps as depicted in Fig. 16.4A, where lovastatin (**1**) obtained from fermentation method was hydrolyzed to produce water-soluble ammonium salt of a trihydric alcohol known as monacolin J (**1a**). This trihydric alcohol was then selectively mono-acylated in the

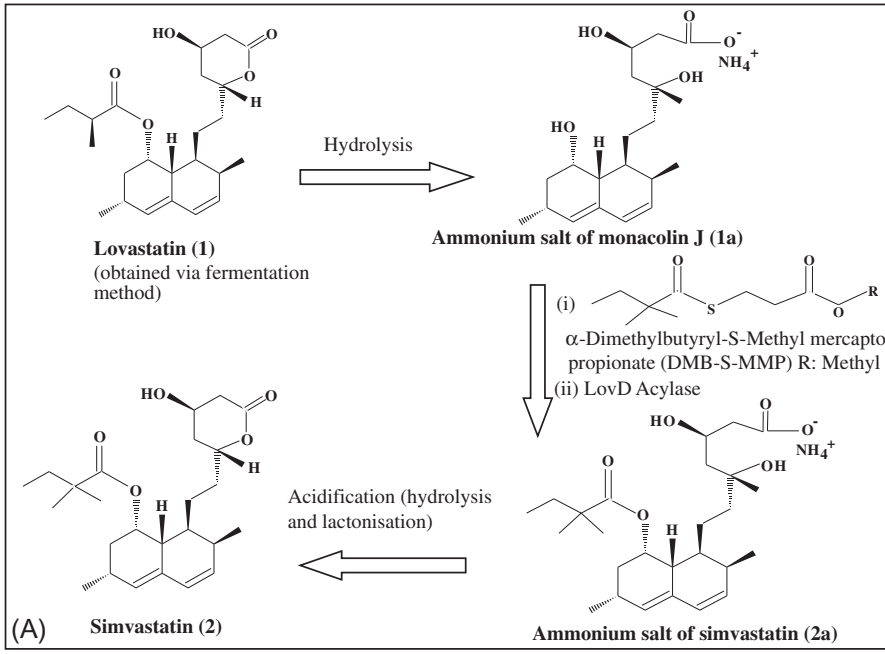

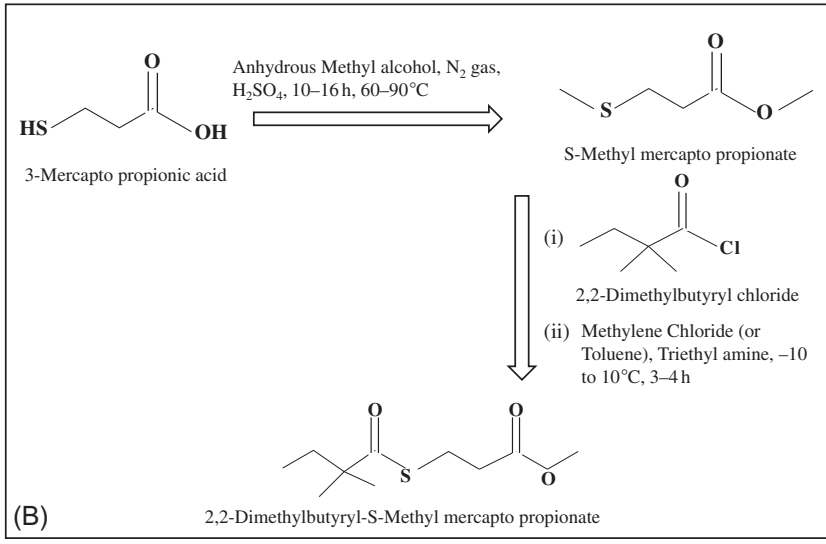

Fig. 16.4 (A) Green synthesis of simvastatin from lovastatin. (B) Chemical synthesis of simvastatin side chain acyl donor, 2,2-dimethylbutyryl-*S*-methyl mercapto propionate (DMB-S-MMP).

presence of recombinant *LovD acyl transferase enzyme* at the secondary hydroxyl group located in the decalin ring system. For this reaction 2,2-dimethyl butyryl-*S*-methyl mercapto propionate (DMB-S-MMP) was developed as the most efficient substrate which acts as the acyl donor for the enzyme *LovD* [86]. This led to the formation of water-soluble ammonium salt of simvastatin (**2a**). The only by-product of this reaction is methyl 3-mercaptopropionic acid which is recovered and subsequently recycled for making more DMB-S-MMP. DMB-S-MMP is easily synthesized in two simple chemical steps starting from 3-mercaptopropionic acid as described in Fig. 16.4B. Finally, (**2a**) was acidified to hydrolyze the ammonium salt. The resulting hydroxy acid was cyclized in the same reaction to produce six-membered lactone ring leading to simvastatin (**2**). This is a sustainable energy efficient and cost-effective green synthesis of simvastatin with minimum impact on the environment as it eliminates the use of hazardous chemicals such as tert-butyl dimethyl silyl chloride, methyl iodide, and n-butyl lithium [86].

(ii) *Cellular biocatalysis*: Tang's group also developed the whole cell biocatalysis method for efficient conversion of monacolin J to simvastatin. In this protocol, they first generated a novel *Escherichia coli* strain that overexpress *LovD enzyme* and used it with previously described acyl donor membrane-permeable substrate, DMB-S-MMP. Such bioconversion using high-cell-density fermentation with batchwise fed method proved to be extremely efficient and green friendly [86].

(iii) *Improved bioengineered catalysis:* The biocatalyst-mediated green method for synthesis of simvastatin as outlined above was significantly enriched by protein engineering expertise of pharmaceutical company Codexis, Redwood City, CA, USA (https://www.codexis.com). Codexis [87] in collaboration with Tang's group [88] optimized both the enzyme in terms of its aqueous solubility and catalytic activity as well as the reaction protocol. First, they developed via selective mutations a new variant of *LovD* (a 413 amino acids long protein) with high degree of catalytic efficiency. The resulting LovD variant with modified method greatly reduced the amount of hazardous and waste products providing a much cleaner and greener chemistry. As a result, it became even more cost effective and environmentally safe, while meeting the needs of customers. Among several LovD variants, the one with double **Cys^{40}/Ala** and **Cys^{60}/Ala** mutations caught the initial attention [89]. Additional mutagenesis experiments revealed that substituting these two **Cys** residues, respectively, by **Ala** and **Asn** in combination, improved the enzyme solubility and the whole cell enzyme activity by nearly 50% [86, 87]. Tang's group then produced mutant libraries in an effort to improve catalytic efficiency, solubility, and thermal stability of the enzyme. Their efforts yielded a variant with seven mutations which showed an ~11-fold enhancement in transferase activity based on *E. coli* expression system [90]. The seven key mutations are: **$A^{86}V$, $D^{12}G$, $A^{190}T$, $G^{275}S$, $K^{26}E$, $H^{161}Y$**, and **$V^{334}F$**. Some manufacturers in Europe and India immediately embraced this modified enzyme to make simvastatin [91], while other nations followed through in years much later. Most of the credit for this accomplishment should go to the US EPA and ACS Green Chemistry Institute who have been campaigning vigorously for pollution prevention and reduction of toxic wastes for a cleaner, more sustainable earth with economic and social benefits [92]. The above modified process for synthesis of simvastatin is considered as one of the best examples of the adoption of green and clean chemistry in statin synthesis.

16.5.3.2 Green process for lovastatin

Following successful adoption of green chemistry for synthesis of simvastatin, similar efforts were directed toward synthesis of lovastatin. As mentioned, lovastatin is a

natural metabolite of *A. terreus* produced during its fermentation. It requires 11 molecules of malonyl-co-enzyme A, one molecule of *S*-adenosyl *S*-methionine, and 5 enzymes, of which *LovD acyl transferase* is the most critical enzyme involved in the last step of biosynthesis (Fig. 16.2). The recombinant form of this enzyme (as described for simvastatin green synthesis) is currently in use for faster, cleaner, and efficient green synthesis of lovastatin, where methyl butyryl-*S*-methyl (or ethyl) mercapto propionate (MB-S-MMP) is employed as the acyl substrate. This substrate is synthesized separately by chemical route similar to that described in Fig. 16.4B. This method has now replaced the in vivo use of endogenous enzyme within the culture system [93, 94] as well as the long multistep and expensive chemical route as described in Fig. 16.5. Furthermore, immobilization of this recombinant enzyme on a solid matrix and green synthesis of a building block allowed faster and more efficient production of lovastatin with minimum use of buffer and reagents. This method not only saved cost but also the environment by enhancing more recycling [95].

16.6 Adoption of green chemistry for other statins

Following great progress in adopting green methods for the production of lovastatin and simvastatin, attention was drawn to develop similar technology for other statins. In fact, these efforts led to successful green synthesis of key intermediates of atorvastatin and rosuvastatin, where specific biocatalysts were designed via mutations to perform important chiral reactions. These are discussed below in more detail.

16.6.1 Green process for atorvastatin

The key chiral intermediate ethyl 4-cyano-3-hydroxybutyrate (known as hydroxyl nitrile or HN) for atorvastatin was prepared via green chemistry using three biocatalytic enzymes namely the *keto-reductase* (*KRED*), *glucose dehydrogenase* (*GDH*), and *halohydrin dehalogenase* (*HHDH*). First, ethyl 4-chloro acetoacetate was reduced by KRED in the presence of glucose and nicotinamide adenine dinucleotide phosphate (NADP)-dependent *GDH*. The product, ethyl-4-chloro 3-hydroxybutyrate thus produced is then transformed to corresponding ethyl 4-cyano 3-hydroxybutyrate by reacting with HCN in the presence of the enzyme *HHDH* (cyanation reaction) [96] (Fig. 16.6). The wild-type *HHDH* enzyme which is less efficient for the above reaction was later bioengineered to create a new variant which is ~2500-fold more potent than the natural enzyme. The use of this enzyme improved the yield and reduced the amount of waste produced by significant levels (E-factor reduced by ~ three fold) thereby making the reaction more environment friendly. The adoption of enzymes eliminated a number of unit operations from the earlier processes. In addition, it also abolished the fractional distillation step for the product, reduced by-products as well as the amount of solvents used, avoided the formation of hydrogen gas, and the use of purification instruments. This unique achievement earned a green chemistry award for Codexis Inc. in 2006 from the US EPA [97].

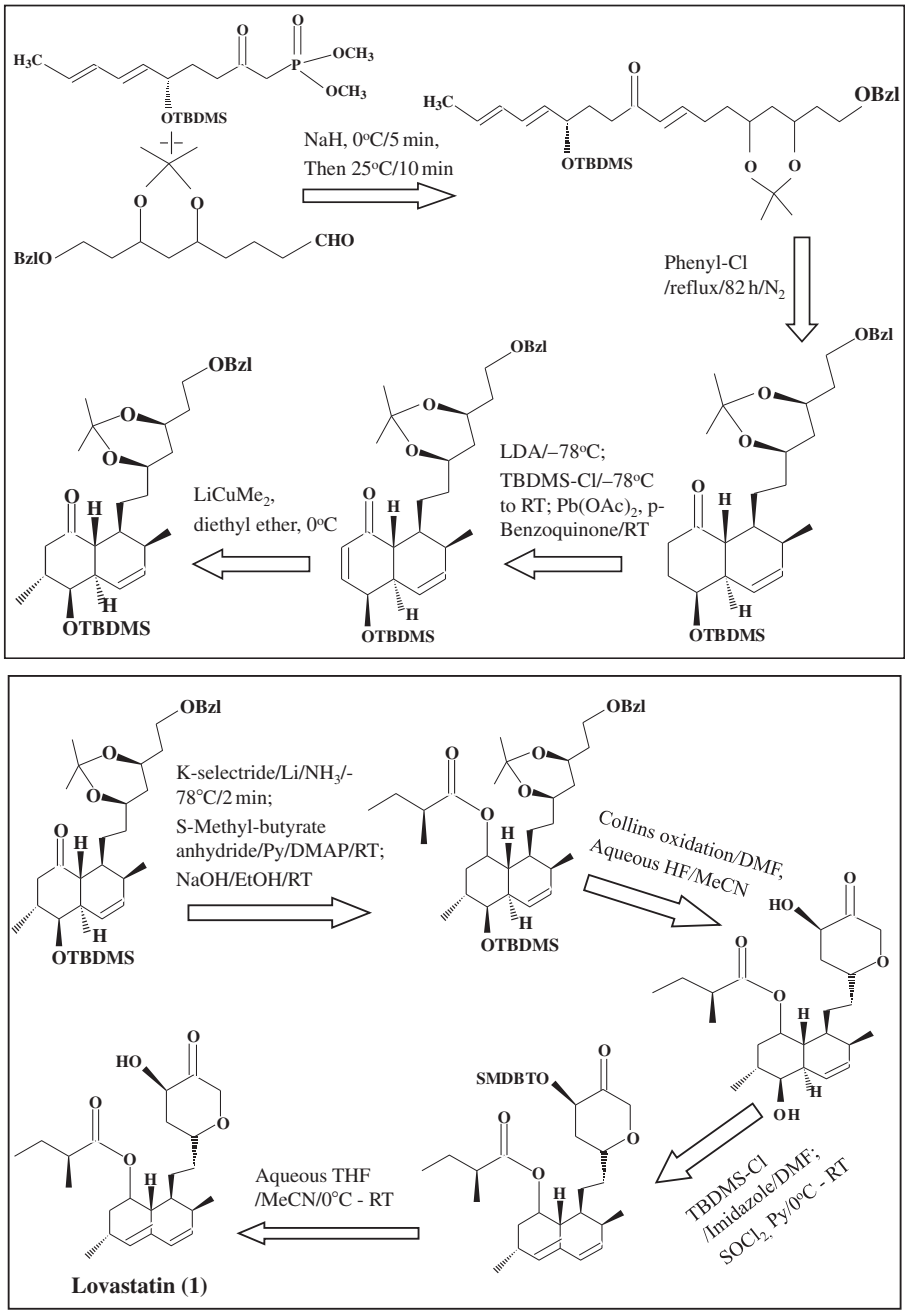

Fig. 16.5 Total chemical synthesis of lovastatin.

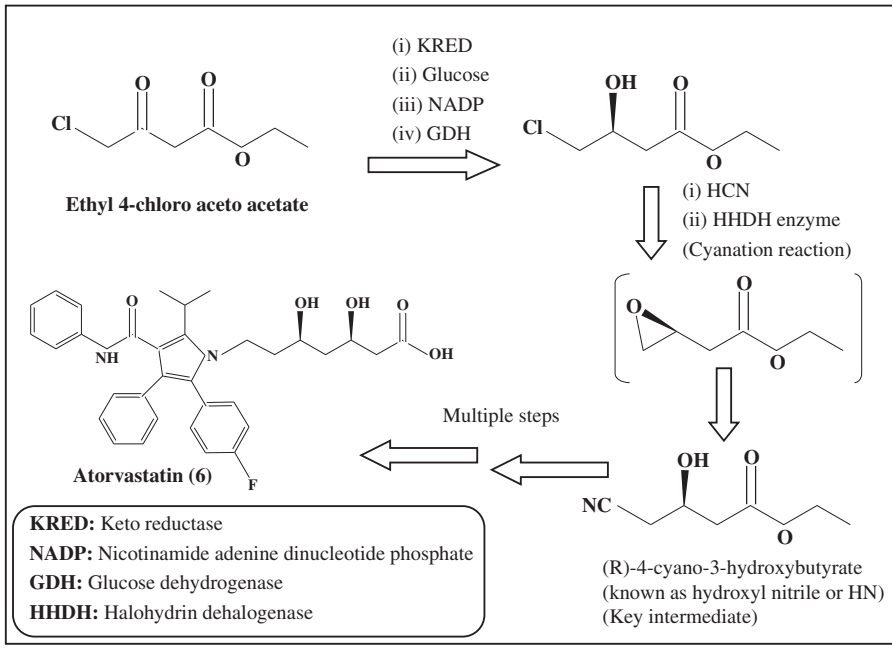

Fig. 16.6 Green synthesis of key atorvastatin intermediate.

In 2004, Liu et al. successfully synthesized atorvastatin by adopting green chemistry mediated by a bioengineered enzyme DERA (deoxy ribose 5-phosphate aldolase) with $Ser^{238}Asp$ mutation [98]. This enzyme allowed a clean and green synthesis of tert-butyl [(4R, 6R)-6-aminoethyl-2,2-dimethyl-1,3-dioxn-4-yl] acetate, a key chiral intermediate for manufacture of atorvastatin. Overall this enzyme catalyzes the sequential aldol condensation reaction between an amino aldehyde (1 equiv) and acetaldehyde (2 equivalents) to form a lactol with high enantiomeric excess (98%) and yield (97%). This was then converted to the side chain of atorvastatin upon oxidation, protection, and esterification. This new chemoenzymatic route has been found to be much shorter and efficient compared to the previous syntheses due to high catalytic efficiency and enantioselectivity of mutant enzyme [98, 99].

16.6.2 Green process for rosuvastatin

One of the most exciting achievement in green chemistry is the discovery by Wong and coworkers who first reported that the key chiral side chains of statins can be synthesized in pure enantiomeric form in a single step by using the enzyme DERA mentioned above [100, 101]. This avoids the typical multiple chemical steps that require protection and deprotection steps. DERA was produced and purified via recombinant technology using the expression system of *E. coli* strain DH5α [102]. The side-chain

intermediate for rosuvastatin (brand name Crestor®) was successfully prepared by using in vitro the recombinant DERA enzyme. The detail steps highlighting the application of DERA in stereospecific synthesis of side chain of rosuvastatin were depicted in Fig. 16.7 (reviewed in Ref. [103]). This enzyme catalyzes the formation of carbon-carbon bond under mild condition generating two chiral centers in a highly enantioselective manner. Research revealed that suitable mutation in DERA can generate variant that can be as much as 10-fold more enzymatically active than the wild type [104]. Significant improvement in efficiency in terms of cost, reaction kinetics, green chemistry, and environment safety have been accomplished with variant DERA enzyme. This allowed large-scale production and commercialization of rosuvastatin in green friendly manner. Since both rasuvastatin and fluvastatin contain same type of side chain, the above green chemistry-based synthesis of chiral side chain may also be adopted for fluvastatin synthesis.

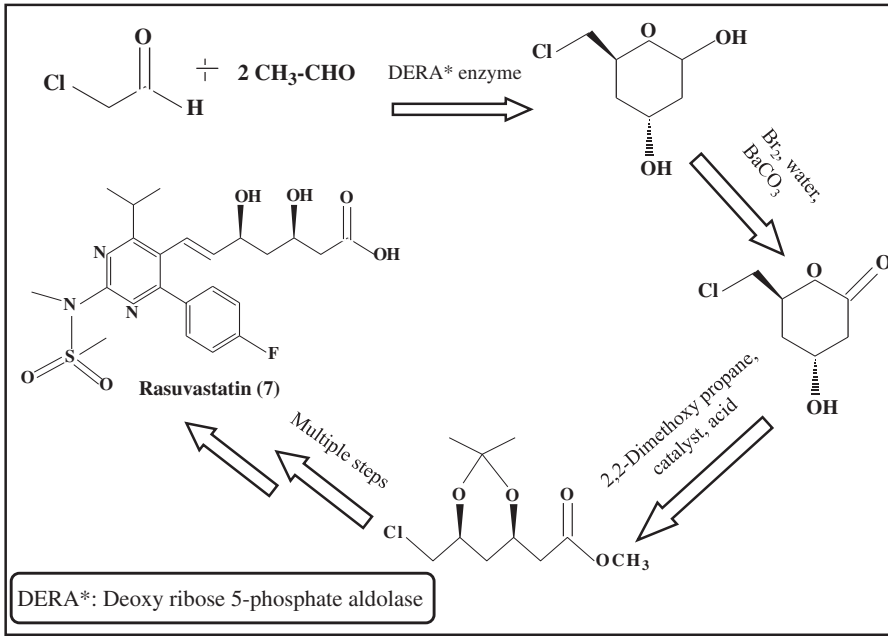

Fig. 16.7 Green synthesis of key rosuvastatin intermediate using DERA enzyme.

Earlier Metzner et al. reported the synthesis of chiral side chain of rosuvastatin via seven steps using two biocatalysts without isolating any of the intermediates. The two biocatalysts used in this process were *α-chymotrypsin* and *cephalosporin C-acetyl esterase*. Here, α-*chymotrypsin* causes desymmetrization of racemic 3-acetyloxy diethyl pimelate leading to enantiomeric pure 3-β-acetyloxy diethyl pimelate. *Cephalosporin C-acetyl esterase* then acts as a deacetylase to selectively

remove the acetyl group (Fig. 16.8). This led to the formation of optically active (R) diethyl ester of β 3-hydroxy pimelic acid—the key chiral side-chain intermediate for rosuvastatin [105]. This alternative method of rosuvastatin synthesis can be considered as partly green to environment because of the adoption of environment-friendly biocatalysts in two important reaction steps and elimination of purification processes for the intermediate products. These help to minimize the use of toxic organic solvents, production of wastes and by-products, thereby making the chemistry more environment friendly.

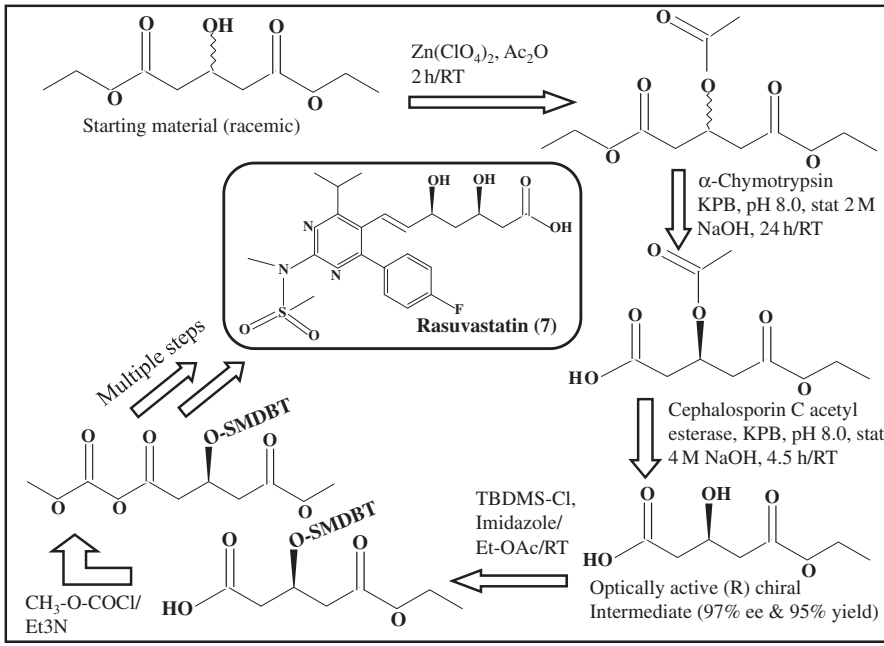

Fig. 16.8 Combination of two biotransformations for the production of the chiral unprotected monoester.

16.6.3 Partial green process for pravastatin

In the recent years, efforts were made to transform classical fermentation method for pravastatin synthesis into a much greener, environmental friendly, rapid, and cost-effective process. In this regard, partial success has been achieved when a new cytochrome P450 (CYP) from *Amycolatopsis orientalis* (CYP105AS1) was developed and later optimized via mutation. This CYP variant has been found to be efficient for catalytic conversion of compactin into pravastatin via enantiomeric hydroxylation. Subsequently, this new cytochrome mutant form, termed as $P450_{Prava}$ has been confirmed to be a perfect compactin hydroxylase which allows development of single-step fermentative production process for pravastatin. This new strain now replaces the classical two steps fermentation protocol for pravastatin [106].

16.7 Green chemistry in statin analysis

The detection and quantitative analysis of statin drugs in biological samples like serum were usually conducted by reverse-phase high-performance layer chromatography (RP-HPLC) analysis which utilizes environmentally toxic organic solvent such as acetonitrile. A large volume of this solvent and its mixture is dumped in the environment as waste. In 2015, Assassi et al. developed a much greener analytical tool by developing octadecyl grafted silica gel as the solid matrix for the column. This allowed the use of larger particle size (~2 μm) in the column, higher flow rate minimizing the solvent use and environmentally safer ethanol as the organic solvent substituting acetonitrile [107]. Thus, a rapid green analytical HPLC technique was developed for analyses of pravastatin, lovastatin, and atorvastatin. For this, the best HPLC condition consisted of using a flow rate of 1 mL/min with solvent ethanol/formic acid (pH 2.5, 25 mM) (50:50, v/v) and a steady temperature of 40°C [107].

16.8 Future direction of green chemistry for statins

It is highly satisfying to note that green chemistry technology has now become an important part and parcel of drug manufacturing process. Thus, there is an increased awareness especially within the industrial and pharmaceutical communities about the enormous benefit of green chemistry in drug manufacture. The present review is able to demonstrate this aspect using the case of statin drugs. Among the six most commonly used statin drugs, at least four have been successfully manufactured either completely or in part by safer and cleaner green chemistry. This has saved the environment from pollution and health hazard by a significant extent. Efforts are ongoing for synthesis of other statin drugs using green technology. Clearly in this journey, properly designed and bioengineered catalysts based on studies involving molecular modeling and structure activity relationships, play a huge contributory role. This is due to the fact that most crucial aspect of statin synthesis is the production of key chiral side chain in a highly stereospecific and enantioselective manner and its subsequent coupling to the appropriate ring system. This reaction has been accomplished by the action of enzyme in toxic-free medium under the conditions of green technology in a highly efficient and cost-effective manner [108–111]. It is now well established that the practice and embodiment of green science in industry and in other aspects of life is a key factor for future human survival as rightly envisioned almost a decade ago by Nobel Laureate Professor and Scientist Ryoji Noyori [112].

16.9 Summary

Thus far there have been significant accomplishment and progress made on the application of green chemistry in statin industry in terms of manufacture, detection, and analysis. This is a great first step by the pharmaceutical sectors in the battle to make our environment safe, clean, and less health hazardous. This advancement was

possible by dedicated scientists, protein chemists, enzymologists, system biologists, and bioengineers through their designs of new biocatalysts and energy-efficient variants with extremely high potency of catalytic activity with regio and stereoselectivity that require no or less organic solvents or toxic chemicals [113]. Besides they allow the use of ambient temperature for the reaction that generates less or no toxic products or organic wastes. In addition, it requires no protection and deportation steps of chemistry. Such enzyme-based processes minimize pollution and are more economical. It is reassuring to note that the pharmaceutical companies are becoming increasingly energy and environmental conscious and have realized the need for adoption of green methods in their manufacturing practice. They have already seen the economic benefits of green energy and are willing to invest a part of their budget in research and development section focusing on new green technology for synthesis of drugs like statins. Finally, this review showed the power and efficacy of biocatalysts and their engineered variants in green chemistry process over the normal regular chemistry.

Acknowledgment

We thank Prof. John P. Veinot, Chairman, Pathology and Laboratory Medicine, Faculty of Medicine, the University of Ottawa for his encouragement and interest in our work.

References

[1] A. Matlack, Introduction to Green Chemistry, second ed., CRC Press, 2010.
[2] P.T. Anastas, Introduction: green chemistry, Chem. Rev. 107 (6) (2007) 2167–2168.
[3] D. Pleissner, K. Kümmerer, Green chemistry and its contribution to industrial biotechnology, Adv. Biochem. Eng. Biotechnol. (2018), https://doi.org/10.1007/10_2018_73.
[4] C.-J. Li, B.M. Trost, Green chemistry for chemical synthesis, Proc. Natl. Acad. Sci. U. S. A. 105 (36) (2008) 13197–13202.
[5] P.T. Anastas, J.C. Warner, Green Chemistry Theory and Practice, Oxford University Press, Oxford, 1998.
[6] P.J. Dunn, The importance of green chemistry in process research and development, in: M.T. Williams, J. Blacker (Eds.), Pharmaceutical Process Development: Current Chemical and Engineering Challenges, Royal Society of Chemistry, 2011.
[7] J. Płotka-Wasylka, A. Kurowska-Susdorf, M. Sajid, M. de la Guardia, J. Namieśnik, M. Tobiszewski, Green chemistry in higher education: state of the art, challenges, and future trends, ChemSusChem 11 (17) (2018) 2845–2858.
[8] M. Lancaster, Green Chemistry: An Introductory Text, The Royal Society of Chemistry, Cambridge, United Kingdom, 2002.
[9] T. Welton, Solvents and sustainable chemistry, Proc. Math. Phys. Eng. Sci. 471 (2015) 20150502.
[10] C. Oji, O. Weber, Renewable Energy Projects for Sustainable Development: Financing Options and Policy Alternatives, Centre for International Governance Innovation (CIGI) Papers No. 122. 2017.
[11] V. Dragutan, I. Dragutan, A.T. Balaban, 2005 Nobel Prize in Chemistry awarded for the development of the metathesis reaction in organic synthesis, Platin. Met. Rev. 50 (1) (2006) 35–37.

[12] C.P. Casey, 2005 Nobel Prize in Chemistry. Development of the olefin metathesis method in organic synthesis, J. Chem. Educ. 83 (2) (2006) 192.
[13] Z. Tan, Air Pollution and Green House Gases, Springer, Singapore, 2014.
[14] S.N. Khot, J.J. LaScala, E. Can, S.S. Morye, G.I. Williams, G.R. Palmese, S.H. Kusefoglu, R.P. Wool, Development and application of triglyceride-based polymers and composites, J. Appl. Polym. Sci. 82 (3) (2001) 703–723.
[15] W. Wang, W. Liu, I.-Y. Chang, L.A. Wills, L.N. Zakharov, S.W. Boettcher, P.H.-Y. Cheong, C. Fang, D.A. Keszler, Electrolytic synthesis of aqueous aluminum nanoclusters and in situ characterization by femtosecond Raman spectroscopy & computations, Proc. Natl. Acad. Sci. U. S. A. 110 (46) (2013) 18397–18401.
[16] B.W. Cue, J. Zhang, Green process chemistry in the pharmaceutical industry, Green Chem. Lett. Rev. 2 (4) (2009) 193–211.
[17] J.A. Restrepo, Green Chemistry in Paintings, Inpra Latina, 2008.
[18] M.P.S.C. de Sousa, L.C.M. Freire, R.L.F. Oliveira, Green chemistry: principles and applications in the paint industry, Paint Coat. Ind. 3 (2014) 72–84.
[19] Azo Cleantech (Ed.), Development of Green Chemicals for the Agricultural Industry, 2015.
[20] W.M. Nelson (Ed.), Agricultural Applications in Green Chemistry, Oxford University Press, UK, 2004.
[21] H. Jahangirian, L.E. Ghasemian, R. Rafiee-Moghaddam, T.J. Webster, A review of using green chemistry methods for biomaterials in tissue engineering, Int. J. Nanomedicine 13 (2018) 5953–5969.
[22] G.K. Gupta, S. De, A. Franco, A.M. Balu, R. Luque, Sustainable biomaterials: current trends, challenges and applications, Molecules 21 (1) (2016) 48, https://doi.org/10.3390/molecules21010048.
[23] L.I. Simenov, M.A. Hassanien (Eds.), Exposure and Risk Assessment of Chemical Pollution—Contemporary Methodology, NATO Science for Peace and Security Series C: Environmental Security, Springer Science, 2009. https://doi.org/10.1007/978-90-481-2335-3.
[24] K. Betts, How Industrial Applications in Green Chemistry Are Changing Our World, American Chemical Society, 2015, pp. 1–27.
[25] V. Sharma, Applicability of Green Chemistry in Pharmaceutical Processes, Pharma Bio World, 2015, pp. 34–36.
[26] Environmental Protection Agency, Green Chemistry Challenge Agency Awards Program: Summary of 2009 Award Entries and Recipients, EPA, Washington DC, 2009. www.epa.gov/greenchemistry.
[27] V.R. Veleva, C.W. Berkeley Jr., S. Todorova, Benchmarking green chemistry adoption by the global pharmaceutical supply chain, ACS Sustain. Chem. Eng. 6 (1) (2018) 2–14.
[28] M. Viigimaa, S. Heinsar, D. Lovic, A. Katsimardou, A. Piperidou, D. Duishvili, New horizons in the pathogenesis, pathophysiology and treatment of familial hypercholesterolaemia, Curr. Pharm. Des. (2018), https://doi.org/10.2174/1381612824666181009105305. (Epub ahead of print).
[29] A. Gómez-Outes, M.L. Suárez-Gea, J.M. García-Pinilla, When are the cardiovascular and stroke risks too high? Pharmacotherapy for stroke prophylaxis, Expert. Opin. Pharmacother. 19 (13) (2018) 1427–1440.
[30] WHO, A Global Brief on Hypertension: Silent killer, Global Public Health Crisis: World Health Day 2013, WHO Reference number: WHO/DCO/WHD/2013.2, (2013), pp. 1–40.
[31] J.A. Restrepo, Ecology and VOCs: developing environmentally friendly products, Inpra Latina 11 (4) (2006) 34–36.

[32] N. Menges, The Role of Green Solvents and Catalysts at the Future of Drug Design and of Synthesis, Chapter 5, Intech, 2018.
[33] F. Roschangar, J. Colberg, P.J. Dunn, F. Gallou, J.D. Hayler, S.G. Koenig, M.E. Kopach, D.K. Leahy, I. Mergelsberg, J.L. Tucker, R.A. Sheldonk, C.H. Senanayake, A deeper shade of green: inspiring sustainable drug manufacturing, Green Chem. 19 (2017) 281–285.
[34] G.C. Welsh. Polystyrene Foam Made With Only Carbon Dioxide as a Blowing Agent and a Process for Making the Same. Patent: US 5250577A, Dow Chemical Company, 1989.
[35] E.J. Beckman, Green chemical processing using CO_2, Ind. Eng. Chem. Res. 42 (8) (2003) 1598–1602.
[36] M.E. Reedy, E.W. Rider, Jr. Process for Producing Polystyrene Foam. Patent: US5302624A, Current Assignee: Genpak Corp Reedy International Corp, 1992.
[37] K.B. Hansen, Y. Hsiao, F. Xu, N. Rivera, A. Clausen, M. Kubryk, S. Krska, T. Rosner, B. Simmons, J. Balsells, N. Ikemoto, Y. Sun, F. Spindler, C. Malan, E.J.J. Grabowski, J.D. Armstrong III, Highly efficient asymmetric synthesis of sitagliptin, J. Am. Chem. Soc. 131 (25) (2009) 8798–8804.
[38] A.A. Desai, Sitagliptin manufacture: a compelling tale of green chemistry, process intensification, and industrial asymmetric catalysis, Angew. Chem. Int. Ed. Engl. 50 (9) (2011) 1974–1976.
[39] J. Tauscher, W. Kielbasa, S. Iyengar, F. Vandenhende, X. Peng, D. Mozley, D.R. Gehlert, G. Marek, Development of the 2nd generation neurokinin-1 receptor antagonist LY686017 for social anxiety disorder, Eur. Neuropsychopharmacol. 20 (2) (2010) 80–87.
[40] D.T. George, J. Gilman, J. Hersh, A. Thorsell, D. Herion, C. Geyer, X. Peng, W. Keilbasa, R. Rawlings, J.E. Brandt, D.R. Gehlert, J.T. Tauscher, S.P. Hunt, D. Hommer, M. Heilig, Neurokinin 1 receptor antagonism as a possible therapy for alcoholism, Science 319 (5869) (2008) 1536–1539.
[41] J. Liang, J. Lalonde, B. Borup, V. Mitchell, E. Mundorff, N. Trinh, D.A. Kochrekar, R.N. Cherat, G.G. Pai, Development of a biocatalytic process as an alternative to the (−)-DIP-Cl-mediated asymmetric reduction of a key intermediate of montelukast, Org. Process. Res. Dev. 14 (1) (2010) 193–198.
[42] A.S. Bommarius, B.R. Bommarius, Enhancing enzymatic performance via restricted sequence space approach, in: G. Williams, M. Hall (Eds.), Modern Biocatalysis: Advances towards synthetic biological systems, The Royal Society of Chemistry, 2018, Chapter 7. pp. 178–204.
[43] C.L. King, Howard University, Novel, Green Chemistry Syntheses of the HIV-1 Protease Inhibitor Darunavir and Malaria Drugs Including Artemisinin, ProQuest Dissertations Publishing, 2014.
[44] EPA, The Presidential Green Chemistry Challenge Awards Program: Summary of 2008 Award Entries and Recipients (Washington, DC), 2008. Web: http://www.epa.gov/greenchemistry/pubs/docs/award_entries_and_recipients2008.pdf.
[45] R.A. Sheldon, E factors, green chemistry and catalysis: an odyssey, Chem. Commun. (Camb.) 29 (2008) 3352–3365.
[46] B. Wallmark, C. Briving, J. Fryklund, K. Munson, R. Jackson, J. Mendlein, E. Rabon, G. Sachs, Inhibition of gastric H+,K+-ATPase and acid secretion by SCH 28080, a substituted pyridyl(1,2a)imidazole, J. Biol. Chem. 262 (1987) 2077–2084.
[47] F. Vallet, B. Eynard, D.M. Stéphanie, G. Mahut, B. Tyl, G. Bertoluci, Using eco-design tools: an overview of experts' practices, Des. Stud. 34 (3) (2013) 345–377.

[48] B. Ivanovic, M. Tadic, Hypercholesterolemia and hypertension: two sides of the same coin, Am. J. Cardiovasc. Drugs 15 (6) (2015) 403–414.
[49] S.J. Kopp, J.T. Barron, J.P. Tow, Cardiovascular actions of lead and relationship to hypertension: a review, Environ. Health Perspect. 78 (1988) 91–99.
[50] A. Endo, A historical perspective on the discovery of statins, Proc. Jpn. Acad. Ser. B Phys. Biol. Sci. 86 (5) (2010) 484–493.
[51] C.G. Mihos, J. Salas, O. Santana, The pleiotropic effects of the hydroxy-methyl-glutaryl-CoA reductase inhibitors in cardiovascular disease: a comprehensive review, Cardiol. Rev. 18 (6) (2010) 298–304.
[52] A. Endo, The discovery and development of HMG-CoA reductase inhibitors, J. Lipid Res. 33 (1992) 1569–1582.
[53] A. Endo, A gift from nature: the birth of the statins, Nat. Med. 14 (2008) 1050–1052.
[54] Covis Pharma, Altoprev Prescribing Information, Zug, Switzerland, https://www.accessdata.fda.gov/drugsatfda_docs/label/2017/021316s034lbl.pdf, 2017.
[55] Anonymous, Three new drugs for hyperlipidemia, Med. Lett. Drugs Ther. 45 (1151) (2003) 17–19.
[56] S. Ramkumar, A. Raghunath, S. Raghunath, Statin therapy: review of safety and potential side effects, Acta Cardiol. Sin. 32 (6) (2016) 631–639.
[57] M. Schürmann, M. Wolber, S. Pank, H. Kierkels, Chpter 6. in: P.J. Dunn, A.S. Wells, M.T. Williams (Eds.), The Development of Short, Efficient, Economic, and Sustainable Chemoenzymatic Processes for Statin Side Chains, Wiley, 2010.
[58] P.A.C. McPherson, From fungus to pharmaceuticals—the chemistry of statins, Mini-Rev. Med. Chem. 12 (12) (2012) 1250–1260.
[59] P.J. Dunn, A.S. Wells, M.T. Williams, Green Chemistry in the Pharmaceutical Industry, Wiley-VCH Verlag GmbH & Co. KgaA, 2010.
[60] K.J. McLeana, M. Hansb, B. Meijrink, W.B. van Scheppingen, A. Vollebregt, K.L. Teea, J.-M. van der Laan, D. Leys, A.W. Munroa, M.A. van den Berg, Single-step fermentative production of the cholesterol lowering drug pravastatin via reprogramming of *Penicillium chrysogenum*, Proc. Natl. Acad. Sci. U. S. A. 112 (9) (2015) 2847–2852.
[61] P.R. Vagelos, Are prescribing drug prices high? Science 252 (1991) 1080–1084.
[62] P.R. Vagelos, L. Galambos, Medicine, Science and Merck, Cambridge University Press, Cambridge, United Kingdom, 2004, pp. 1–301.
[63] A.W. Alberts, J. Chen, G. Kuron, V. Hunt, J. Huff, C. Hoffman, et al., Mevinolin: a highly potent competitive inhibitor of hydroxymethylglutaryl-coenzyme A reductase and a cholesterol-lowering agent, Proc. Natl. Acad. Sci. U. S. A. 77 (1980) 3957–3961.
[64] A. Endo, Monacolin K, a new hypocholesterolemic agent produced by a Monascus species, J. Antibiot. 32 (1979) 852–854.
[65] A. Endo, M. Kuroda, Y. Tsujita, ML-236A, ML-236B, and ML-236C, new inhibitors of cholesterogenesis produced by Penicillium citrinum, J. Antibiot. (Japan) 29 (1976) 1346–1348.
[66] A. Endo, Chemistry, biochemistry, and pharmacology of HMG-CoA reductase inhibitors, Klin. Wochenschr. 66 (1988) 421–427.
[67] A. Endo, T. Tsujita, M. Kuroda, K. Tanzawa, Inhibition of cholesterol synthesis in vitro and in vivo by ML-236A and ML-236B, competitive inhibitors of 3-hydroxy-3-methylglutarylcoenzyme A reductase, Eur. J. Biochem. 77 (1977) 31–36.
[68] M. Manzoni, M. Rollini, Biosynthesis and biotechnological production of statins by filamentous fungi and application of these cholesterol-lowering drugs, Appl. Microbiol. Biotechnol. 58 (2002) 555–564.

[69] M. Tsukahara, N. Shinzato, et al., Red yeast rice fermentation by selected *Monascus sp*. With deep-red color, lovastatin production but no citrinin, and effect of temperature-shift cultivation on lovastatin production, Appl. Biochem. Biotechnol. 158 (2) (2009) 476–482.
[70] J. Alarcon, S. Aguila, P. Arancibia-Avila, O. Fuentes, E. Zamorano-Ponce, M. Hernandez, Production and purification of statins from Pleurotus ostreatus (Basidiomycetes) strains, Z. Naturforsch. 58c (2003) 62–64.
[71] E.J. Schaefer, J.R. McNamara, T. Tayler, J.A. Daly, J.L. Gleason, L.J. Seman, A. Ferrari, J.J. Rubenstein, Comparisons of effects of statins (atorvastatin, fluvastatin, lovastatin, pravastatin, and simvastatin) on fasting and postprandial lipoproteins in patients with coronary heart disease versus control subjects, Am. J. Cardiol. 93 (1) (2004) 31–39.
[72] J.A. Farmer, L.C. Washington, P.H. Jones, D.R. Shapiro, A.M. Gotto Jr., G. Mantell, Comparative effects of simvastatin and lovastatin in patients with hypercholesterolemia. The simvastatin and lovastatin multicenter study participants, Clin. Ther. 14 (5) (1992) 708–717.
[73] S. Goswami, A.S. Vidyarthi, B. Bhunia, T.J. Mandal, A review on lovastatin and its production, J. Biochem. Technol. 4 (1) (2012) 581–587.
[74] M. Hirama, M. Vet, A chiral total synthesis of compactin, J. Am. Chem. Soc. 104 (15) (1982) 4251.
[75] M. Hirama, M. Iwashita, Synthesis of (+)-Mevinolin starting from naturally occurring building blocks and using an asymmetry inducing reaction, Tetrahedron Lett. 24 (17) (1983) 1811–1812.
[76] K.C.L. Mulder, F. Mulinari, O.L. Franco, M.S.F. Soares, B.S. Magalhães, N.S. Parachin, Lovastatin production: from molecular basis to industrial process optimization, Biotechnol. Adv. 33 (6) Part 1. (2015) 648–665.
[77] F. Yang, T.W. Weber, J.L. Gainer, G. Carta, Synthesis of lovastatin with immobilized Candida rugose lipase in organic solvents: effects of reaction conditions on initial rates, Biotechnol. Bioeng. 56 (6) (1997) 671–680.
[78] W.F. Hoffman, A.W. Alberts, P.S. Anderson, J.S. Chen, R.L. Smith, A.K. Willard, 3-Hydroxy-3-methylglutaryl-coenzyme A reductase inhibitors. 4. Side chain ester derivatives of mevinolin, J. Med. Chem. 29 (1986) 849–852.
[79] D. Askin, T.R. Verhoeven, T.M.-H. Liu, I. Shinkai, Synthesis of synvinolin: extremely high conversion alkylation of an ester enolate, J. Org. Chem 56 (1991) 4929–4932.
[80] D. Askin, T.R. Verhoeven, T.M.-H. Liu, I. Shinkai, Simvastatin introduction, J. Org. Chem 56 (1991) 4929–4932.
[81] I. Forgas; V. Keri. A Process for Purifying Lovastatin and Simvastatin With Reduced Levels of Dimeric Impurities. Patent EP 1265884A1. Current Assignee: Plus Chemical, B.V. Original Assignee: Teva Gyogyszergyar Zrt, 2000.
[82] A.W. Alberts, Lovastatin and simvastatin—inhibitors of HMG CoA reductase and cholesterol biosynthesis, Cardiology 77 (1990) 14–21.
[83] R.K. Singamsetty, S.K. Vujjini, N.M. Manne, B. Rao, M.V. Naga, V. Himabindu, A. Bhattacharya, M.R. Ghanta, R. Bandichhor, New synthesis of simvastatin, Synth. Commun. 38 (24) (2008) 4452–4459.
[84] K. Dabak, H. Keskin, A convenient procedure for the methylation of lovastatin: synthesis of simvastatin, Heterocycl. Commun. 10 (1) (2011) 29–34.
[85] X. Xie, K. Watanabe, W.A. Wojcicki, C.C. Wang, Y. Tang, Biosynthesis of lovastatin analogs with a broadly specific acyltransferase, Chem. Biol. 13 (2006) 1161–1169.
[86] X. Xie, Y. Tang, Efficient synthesis of simvastatin by use of whole-cell biocatalysis, Appl. Environ. Microbiol. 73 (7) (2007) 2054–2060.

[87] L. Gilson, S.J. Collier, J. Sukumaran, W.L. Yeo, O. Alvizo, E.L. Teo, R.J. Wilson, J. Xu, Variant LovD Polypeptides and Their Uses. United States Patent Application 20180187225. Assignee: Codexis Inc, 2018.
[88] X. Xie, I. Pashkov, X. Gao, J.L. Guerrero, T.O. Yeates, Y. Tang, Rational improvement of simvastatin synthase solubility in Escherichia coli leads to higher whole-cell biocatalytic activity, Biotechnol. Bioeng. 102 (2009) 20–28.
[89] X. Xie, M.J. Meehan, W. Xu, P.C. Dorrecstein, Y. Tang, Acyltransferase mediated polyketide release from a fungal megasynthase, J. Am. Chem. Soc. 131 (2009) 8388–8389.
[90] X. Gao, X. Xie, I. Pashkov, M. Sawaya, J. Laidman, W. Zhang, W. Zhang, R. Cacho, T.O. Yeates, Y. Tang, Directed evolution and structural characterization of simvastatin synthase, Chem. Biol. 16 (10) (2009) 1064–1074.
[91] N. Savage, Chemistry: greener pastures, Nature 501 (2013) 125–127.
[92] B. Torok, T. Dransfield, Green Chemistry: An Inclusive Approach, Elsevier Inc, 2018.
[93] H. Hajjaj, P. Niederberger, P. Duboc, Lovastatin biosynthesis by *Aspergillus terreus* in a chemically defined medium lovastatin, Appl. Environ. Microbiol. 67 (6) (2001) 2596–2602.
[94] A. Liljeblad, A. Kallinen, L.T. Kanerva, Biocatalysis in the preparation of the statin side chain, Curr. Org. Synth. 6 (2009) 362–370.
[95] N.P. Money, Fungi and biotechnology, in: S.C. Watkinson, L. Boddy, N.P. Money (Eds.), The Fungi, third ed., Academic Press, Chapter 12. 2016, pp. 401–424.
[96] S.K. Ma, J. Gruber, C. Davis, L. Newman, D. Gray, A. Wang, J. Grate, G.W. Huisman, R.A. Sheldon, A green-by-design biocatalytic process for atorvastatin intermediate, Green Chem. 12 (2010) 81–86.
[97] Codexis, Inc, Presidential Green Chemistry Challenge: 2006 Greener Reaction Conditions Award, US EPA, 2006. https://www.epa.gov/greenchemistry/presidential-green-chemistry-challenge-2006-greener-reaction-conditions-award.
[98] J. Liu, C.-C. Hsu, C.-H. Wong, Sequential aldol condensation catalyzed by DERA mutant Ser238Asp and a formal total synthesis of atorvastatin, Tetrahedron Lett. 45 (2004) 2439–2441.
[99] N. Ran, L. Zhao, Z. Chen, J. Tao, Recent applications of biocatalysis in developing green chemistry for chemical synthesis at the industrial scale, Green Chem. 10 (2008) 361–372.
[100] L. Chen, D.P. Dumas, C.-H. Wong, Deoxyribose 5-phosphate aldolase as a catalyst in asymmetric aldol condensation, J. Am. Chem. Soc. 114 (1992) 741–748.
[101] H.J.M. Gijsen, C.-H. Wong, Unprecedented asymmetric aldol reactions with three aldehyde substrates catalyzed by 2-deoxyribose-5-phosphate aldolase, J. Am. Chem. Soc. 116 (1994) 8422–8423.
[102] C.-H. Wong, E. Garcia-Junceda, L. Chen, O. Blanco, H.J.M. Gijsen, D.H. Steensma, Recombinant 2-deoxyribose-5-phosphate aldolase in organic synthesis: use of sequential two-substrate and three-substrate aldol reactions, J. Am. Chem. Soc. 117 (1995) 3333–3339.
[103] P.J. Dunn, The importance of green chemistry in process research and development, Chem. Soc. Rev. 41 (4) (2012) 1452–1461.
[104] S. Jennewein, M. Schuermann, M. Wolberg, I. Hilker, R. Luiten, M. Wubbolts, D. Mink, Directed evolution of an industrial biocatalyst: 2-deoxy-D-ribose 5-phosphate aldolase, Biotechnol. J. 1 (2006) 537–548.
[105] R. Metzner, W. Humme, F. Wetterich, B. König, H. Gröger, Integrated biocatalysis in multistep drug synthesis without intermediate isolation: a de novo approach toward a rosuvastatin key building block, Org. Process. Res. Dev. 19 (2015) 635–638.

[106] K.J. McLeana, M. Hans, B. Meijrink, W.B. van Scheppingen, A. Vollebregt, K.L. Teea, J.-M. van der Laan, D. Leys, A.W. Munro, M.A. van den Bergb, Single-step fermentative production of the cholesterollowering drug pravastatin via reprogramming of Penicillium chrysogenum, Proc. Natl. Acad. Sci. U. S. A. 112 (9) (2015) 2847–2852.
[107] A.L. Assassi, C.E. Roy, P. Perovitch, J. Auzerie, T. Hamon, K. Gaudin, Green analytical method development for statin analysis, J. Chromatogr. A 1380 (2015) 104–111.
[108] T. Junhua (Alex), K. Romas, Reaction efficiencies and green chemistry matrices of biotransformations, in: Biocatalysis for Green Chemistry and Chemical Process Development, John Wiley & Sons, 2011.
[109] R.N. Patel, Biocatalysis: synthesis of key intermediates for development of pharmaceuticals, ACS Catal. 1 (9) (2011) 1056–1074.
[110] G.W. Huisman, S. Collier, The development of new biocatalytic processes for practical pharmaceutical synthesis, Curr. Opin. Chem. Biol. 17 (2) (2013) 284–292.
[111] Z.-J. Zhang, J. Pan, B.-D. Ma, J.-H. Xu, Efficient biocatalytic synthesis of chiral chemicals, Adv. Biochem. Eng. Biotechnol. 155 (2016) 55–106.
[112] R. Noyori, Insight: green chemistry: the key to our future, Tetrahedron 66 (2010) 1028.
[113] C.M. Clouthier, J.N. Pelletier, Expanding the organic toolbox: a guide to integrating biocatalysis in synthesis, Chem. Soc. Rev. 41 (2012) 1585–1605.

Sustainable release of nanodrugs: A new biosafe approach

17

*Prasun Patra, Dhrubajyoti Chattopadhyay**
Amity Institute of Biotechnology, Amity University, New Town, Kolkata, West Bengal, India
*Corresponding author. e-mail address: dhrubajyotic@gmail.com

17.1 Introduction

Drug delivery is the method or process of administering a pharmaceutical compound to achieve a therapeutic effect in humans or animals. It may involve scientific site targeting within the body, or it might involve facilitating systemic pharmacokinetics. It is typically concerned with both quantity and duration of drug presence. Drug delivery is often approached via a drug's chemical formulation, but it may also involve medical devices or drug-device combination products. The development of a new drug molecule is expensive and time consuming. Improving safety efficacy ratio of conventional drugs has been attempted using different methods such as individualizing drug therapy, dose titration, and therapeutic drug monitoring. Delivering drugs at a controlled rate, slow delivery, targeted delivery are other very attractive methods and have been pursued vigorously. Developments with other compounds have produced a plethora of new devices, concepts, and techniques that have together been termed controlled-release technology (CRT). A drug delivery system that is capable of achieving a prolonged therapeutic effect by slow release of the therapeutic substance over an extended duration (days or months) after administration of a single dose is termed as a sustained-release delivery system. Conventional drug administration methods, while widely utilized, have many problems that may be potentially overcome by this method. There are several advantages of sustained release dosage forms which include:

i. lesser frequency of administration
ii. reduced side effects
iii. stable drug absorption levels in blood and plasma
iv. better patient compliance [1].

This advancement may appear attractive relative to the costs of new drug development. Within the past few decades, nanotechnology, in particular, manufacturing of nanoparticles has found unprecedented attention in broad areas of science [2]. The smart use of nanoparticles has revolutionized how drugs are formulated and delivered. Nanotechnology is a multidisciplinary scientific field applying engineering and manufacturing principles at the molecular level [3]. Nanoparticles are solid, colloidal particles with a size range from 10 to <1000 nm; however, for nanomedical applications, the preferential size is <200 nm [4]. The major goals in designing nanoparticles

Green Approaches in Medicinal Chemistry for Sustainable Drug Design. https://doi.org/10.1016/B978-0-12-817592-7.00017-4
© 2020 Elsevier Inc. All rights reserved.

as a delivery system are to control particle size, surface properties, and release of pharmacologically active agents in order to achieve the site-specific action of the drug at the therapeutically optimal rate and dose regimen. It is notable that the efficiency of most drug delivery systems is directly related to particle size (excluding intravenous and solution). Due to their small size and large surface area, drug nanoparticles show increase solubility and thus enhanced bioavailability, additional ability to cross the blood-brain barrier (BBB), enter the pulmonary system, and be absorbed through the tight junctions of endothelial cells of the skin [5].

17.2 Problems of conventional drug delivery

An ideal dosage regimen in the drug therapy of any disease is one which immediately attains the desired therapeutic concentration of drug in plasma and maintains its constant for the entire duration of treatment. This is possible through the administration of conventional dosage forms in a particular dose and at a particular frequency. The frequency of administration or dose interval of any drugs depends on its half-life or mean residence time and its therapeutic index. In most cases, dosing interval is much shorter than the half-life of the drug, resulting in number of limitations associated with such a conventional dosage form which are:

i. Poor patient compliance; increased chances of missing the dose of a drug with short half-life for which frequent administration is necessary.
ii. A typical peak valley plasma concentration-time profile is obtained which makes attainment of steady-state condition difficult.
iii. The unavoidable fluctuation in the concentration may lead to under medication or over medication. The fluctuating drug level may lead to precipitation of adverse effect especially of a drug with a small therapeutic index whenever over medication occurs.

To overcome the above discussed limitations of conventional dosage forms, nanoparticles-based drugs have been developed. The major focus of the research and development of nanoparticles is to exploit their enhanced cellular penetration. The second reason for using nanoparticles is to increase blood circulation lifetimes, which facilitates passive targeting of tissue. The other use of nanoparticles is to improve the solubility of highly hydrophobic drugs such as paclitaxel while retaining the injectability of the formulation. Sustained delivery is warranted for many chronic conditions to achieve better patient compliance and safety. Currently, sustained release is achieved with some success by using nanospheres injected intramuscularly or subcutaneously [6].

17.3 Why sustainable drug delivery is important?

The basic rationale for sustained/controlled drug delivery system is to alter the pharmacokinetics and pharmacodynamics of pharmacologically active moieties by using novel drug delivery system or by modifying the molecular structure and or physiological parameter inherent in a selected route of administration.

i. reduction in fluctuation of drug blood levels about the mean
ii. reduce the dosage frequency

iii. to improve patients compliance
iv. to ensure safety and improve efficacy of drugs
v. more consistent and prolonged therapeutic effect
vi. decreased incidence and intensity of adverse effects and toxicity
vii. better drug utilization
viii. a greater selectivity of pharmacological activity
ix. delivery of drug at site at predicted time

17.4 Why nanomaterials are promising as nanodrug?

There is increasing optimism that nanotechnology, as applied to medicine, will bring significant advances in the diagnosis and treatment of disease. Anticipated applications in medicine include drug delivery, both *in vitro* and *in vivo* diagnostics, nutraceuticals, and production of improved biocompatible materials [7–9]. The reason why these nanoparticles (NPs) are attractive for medical purposes is based on their important and unique features, such as their surface to mass ratio that is much larger than that of other particles, their quantum properties, and their ability to adsorb and carry other compounds. NPs have a relatively large (functional) surface which is able to bind, adsorb, and carry other compounds such as drugs, probes, and proteins. However, many challenges must be overcome if the application of nanotechnology is to realize the anticipated improved understanding of the pathophysiological basis of disease, bring more sophisticated diagnostic opportunities, and yield improved therapies. Although the definition identifies nanoparticles as having dimensions below 0.1 μm or 100 nm, especially in the area of drug delivery relatively large (size $>$ 100 nm) nanoparticles may be needed for loading a sufficient amount of drug onto the particles. In addition, for drug delivery not only engineered particles may be used as carrier, but also the drug itself may be formulated at a nanoscale, and then function as its own "carrier" [10, 11]. One of the strategic advantages of NPs for drug delivery is their versatile modification possibilities, acting as platforms for the assembly of well-defined multifunctional structures. These structures once prepared still retain efficient solubility and colloidal properties for use in complex environments (e.g., blood, tissues, etc.). Slight variations in composition, surface coating, and ligand choice can lead to a wealth of possibilities for drug delivery in biological systems The primary interest to use nanoparticles is both drug and drug delivery agent including:

i. more specific drug targeting and delivery,
ii. reduction in toxicity while maintaining therapeutic effects,
iii. greater safety and biocompatibility, and
iv. faster development of new safe medicines.

17.5 Different nanoparticles as nanodrug and advantages

17.5.1 Liposomal nanocarriers

A number of nanoparticles have been evaluated over the years to improve loading and sustained delivery of drugs, including liposomal nanoparticles, polymer nanoparticles, and nanosuspensions. Among the nanoparticles studied, liposomes have

been the most successful drug delivery carriers [12]. Liposomes nanoparticles are used for the rational delivery of chemotherapeutic drugs in the treatment of cancer. Their use offers improved pharmacokinetic properties, sustained release of drugs, and lower systemic toxicity. The commercial availability of liposomal nano-formulations (Doxil and Abraxane) has focused attention on this field [13]. Recent advances in liposome technology also offer better treatment of multidrug-resistant cancers and lower cardiotoxicity. The liposome bilayer can be composed of either synthetic or natural phospholipids. Drug loading into liposomes can be achieved through

i. liposome formation in an aqueous solution saturated with soluble drug;
ii. the use of organic solvents and solvent exchange mechanisms;
iii. the use of lipophilic drugs; and
iv. pH gradient methods.

Liposomes generally reach their site of action by extravasation into the interstitial space from the bloodstream. Liposomes can target specific tissues through both active and passive targeting strategies. One of the most interesting developments in this field is the potential of liposomes to combat the increasing problem of multidrug resistance (MDR) acquired by cancers, which drastically reduces chemotherapeutic efficacy. Proposed mechanisms underlying MDR at the cellular level include:

i. increased metabolism of drugs due to increased enzyme expression, especially of glutathione *S*-transferase,
ii. drug transporters and efflux proteins, and
iii. point mutations in proteins that are therapeutic or drug targets.

17.5.2 Polymer-based NPs in drug delivery

Polymer-based NPs have been extensively investigated as drug nanocarriers. Their designs are very similar, with a polymeric backbone—usually formed from a biodegradable monomer based on a simple organic molecule that is biocompatible—and functional moieties for active targeting intercalated into the structure. Drug loading is achieved either by (i) entrapment of an aqueous drug phase using the polymer to form nanoscale structures such as cages and capsules or (ii) chemical linking of the drug molecules to the polymer backbone by means of a simple ester or amide bond that can be hydrolyzed *in vivo*. More complex polymeric NPs use polar groups to create hydrophobic and hydrophilic regions enabling the drug to adsorb onto the NP and facilitate delivery to the target site [14, 15].

The most widely researched synthetic polymers include polylactide (PLA), poly (D,L-lactide-*co*-glycolide) (PLGA), and PEG. All three polymers are hydrolyzed *in vivo* and are biodegradable. Other polymers based on biological polysaccharides have been extensively investigated, including chitosan, cyclodextrin, and dextrans. Different polymers can be combined to form copolymers. PLA-*block*-PEG copolymers harness the properties of both polymers, especially the antiopsonization of PEG. Ligands can be attached to the NP to facilitate active targeting. Ligands can be intercalated into the structure either by direct covalent linkage to the polymeric backbone or through the use of biologically inert spacer groups [14, 15].

17.5.3 Albumin NPs in drug delivery

Albumin, a plasma protein with a molecular weight of 66 kDa, has been extensively investigated as a drug carrier, with promising results. It is soluble in both water and ethanol, two viable solvents for intravenous administration. Because albumin is found in the circulating plasma of the human body at concentrations of 50 g L^{-1} of serum, it is nontoxic and well tolerated by the immune system. Albumin has favorable pharmacokinetics owing to its long half-life in circulating plasma, which makes it particularly attractive as a drug carrier for passive targeting. Albumin can be derived from human plasma and blood products. Alternatively, recombinant human serum albumin can be produced in genetically engineered yeast cells. Albumin NPs are prepared by desolvation or coacervation. Abraxane1, also known as nab-paclitaxel, is the first drug based on an albumin NP approved for human use by the US Food and Drug Administration. The chemotherapy drug paclitaxel is bound to 130-nm human albumin NPs. Abraxane1 has advantages over free paclitaxel in terms of its longer circulation half-life and lack of the hypersensitivity-inducing Cremophor EL1 solvent. Clinical trials have confirmed the efficacy of Abraxane1 in the treatment of metastatic breast cancer, for which it is routinely used. In addition, Abraxane1 is currently being investigated with other taxanes in the treatment of hormone-refractory prostate cancer. Albumin is transported across the endothelium into the extravascular space by transcytosis via caveolae, initiated by the albumin receptor gp60. Tumor tissues have a high metabolic demand and actively transport plasma proteins into their cells for anabolic processes. It has been proposed that this mechanism would explain why Abraxane1 targets and preferentially accumulates in cancer tissues *in vivo* via the excessive vascular network associated with cancers. There is also speculation that Abraxane1 is transported into tumor cells by secreted protein acidic rich in cysteine (SPARC) or osteonectin [16–20].

17.5.4 Magnetic nanoparticles in drug delivery

Due to their unique physical properties and ability to function at the cellular and molecular level of biological interactions, magnetic nanoparticles (MNPs) have been actively investigated as the next generation of targeted drug delivery. The greatest therapeutic potential is probably associated with applications involving "intelligent" particles with a magnetic core (to direct the particles to the vicinity of the target and also for hyperthermia or for temperature-enhanced release of the drug), a recognition layer (to which suitable receptors are attached), and a therapeutic load (adsorbed inside the pores or hosted within internal cavities of the particles). Cancer treatment is that most are nonspecific. Therapeutic (generally cytotoxic) drugs are administered intravenously leading to general systemic distribution. The nonspecific nature of this technique results in the well-known side effects of chemotherapy as the cytotoxic drug attacks normal, healthy cells in addition to its primary target, tumor cells [21, 22]. To overcome this great disadvantage MNP can be used. Nanoparticles can be used to treat tumors in three different ways:

i. specific antibodies can be conjugated to the MNPs to selectively bind to related receptors and inhibit tumor growth;

ii. targeted MNPs can be used for hyperthermia for tumor therapy; and
iii. drugs can be loaded onto the MNPs for targeted therapy [23–25].

The targeted delivery of antitumor agents adsorbed on the surface of MNPs is a promising alternative to conventional chemotherapy. The particles, loaded with the drug, are concentrated at the target site with the aid of an external magnet. The drugs are then released in the desired area.

17.5.5 Silicon dioxide in drug delivery

Common silicon dioxides (MSNs) including MCM-41, SBA-15, etc. exhibited a range of pore sizes (2–10 nm) are very promising in drug delivery. The advantages of MSNs are the following:

i. a large surface area and pore volume provides great potential for drug adsorption and loading within the pore channels,
ii. excellent mesoporous structure and an adjustable pore size enable better control of drug loading and release kinetics,
iii. an easily modified surface for controlled and targeted drug delivery enhances the drug therapeutic efficacy and reduces toxicity,
iv. the *in vivo* biosafety evaluations of cytotoxicity, biodegradation, biodistribution, and excretion, have yielded satisfactory results,
v. combinations with magnetic and luminescent compounds allow simultaneous drug delivery and bioimaging, and
vi. those with excellent surface properties and porosity have proved to be attractive candidates as bioactive materials for bone regeneration.

Many hydrophobic drugs have limited applications due to poor water solubility that results in poor absorption in the gastrointestinal tract after oral dosing. Mesoporous silica improves the dissolution rate and bioavailability of hydrophobic drugs after oral administration. Drug loading methods based on MSNs mainly involve physical adsorption and solvent evaporation. MSNs soak in a drug-containing solution until equilibrium is reached, and most drugs penetrate deeply into the pore channels of the carrier. MSNs have unique features compared with other types of carriers. The large surface area and high pore volume enable the encapsulation of drugs with a high payload. The mesoporous channels keep drugs in the amorphous or noncrystalline state within the pores, which facilitates drug dissolution. Additionally, the marked chemical stability and inert behavior allow for better control of drug loading and release [26–28].

17.5.6 Zinc oxide in drug delivery

ZnO is a conventional wide band-gap semiconductor that has been highly explored in multiple areas of science. One of the primary advantages for considering ZnO nanoparticles for use in cancer is the inherent preferential cytotoxicity against cancer cells *in vitro*. It is anticipated that their cancer cell selectivity may be even further improved by engineering design to minimize harmful effects to normal body cells,

which has been observed to occur at very high concentrations of ZnO nanoparticles, particularly those in the smaller size range of 4–20 nm. In this regard, the surface chemistry of ZnO nanoparticles readily lends them to functionalization with targeting proteins or chemical groups and may be a key to rendering them benign to normal cells while still retaining their cancer targeting and killing properties. Several studies have suggested an increase in *in vitro* cytotoxicity with nanophase ZnO compared to micron-sized ZnO for several types of cancers including glioma, breast, bone, colon, and leukemias and lymphomas [29–31]. In most of these studies, however, a systematic review of cancer cell cytotoxicity compared to relevant nonimmortalized cell types was not performed. Perhaps the most compelling evidence of ZnO preferential toxicity comes from controlled studies comparing nanoparticle susceptibility of cancerous cells to primary nonimmortalized cells of identical lineage. These studies showed that cancerous cells of lymphocytic lineage were ~28–35 times more susceptible to ZnO nanoparticles induced cytotoxicity compared to their normal counterparts. This high degree of selective cancer cell killing exceeds the ex vivo therapeutic indices of $\leq$10 reported for commonly used chemotherapeutic drugs such as doxorubicin and carboplatin against a variety of leukemias, lymphomas, and solid tumors using similar biological assays. The preferential cytotoxicity was found to be dependent on the proliferation status of cells, with rapidly dividing cells being the most susceptible. Based on a growing body of evidence, ROS production is proposed as a key cytotoxic mechanism of ZnO nanoparticles leading to cell death via an apoptotic mechanism. Recently, the use of ZnO quantum dots loaded with doxorubicin has proved to be an effective drug carrier characterized by an initial rapid drug release followed by a controlled release *in vitro*. In this study, ZnO nanoparticles were encapsulated with chitosan to enhance the nano-material stability due to its hydrophilicity and cationic charge characteristics [32]. Although ZnO nanomaterials have only recently been investigated for using drug delivery system, the feasibility of this approach has been demonstrated in related metal oxide systems.

17.5.7 Selenium in drug delivery

Selenium, an essential micronutrient obtained from dietary sources, is reported to have chemopreventative and therapeutic properties. Colloidal selenium has been developed for use as conventional cancer drug carriers. Studies indicate that selenium could reduce systemic toxicities associated with conventional chemotherapeutic drugs while working synergistically to improve efficacy. Low toxicity, high bioavailability, and biocompatibility are just some of the properties that make selenium an attractive drug carrier. Bioactivity coupled with a reported higher selectivity to cancer cells promises a targeted delivery with reduced chemotherapy side effects.

The drug can be physically dispersed or chemically bound to the colloidal system. The strategic use of drug-containing selenium nanocapsules, formed when a layer of polymer acting as a reservoir surrounds the nanoparticle, can incorporate drugs at a higher concentration than their intrinsic solubility while conferring protection from degradation and systemic toxicities. More recently, selenium-containing polymers have emerged as potential drug delivery systems for controlled release.

Stimulus responsive selenium polymers make ideal cancer drug delivery vehicles with various stimuli such as temperature, pH, light, and redox state, being able to trigger the breakdown of these polymers leading to a collapse in the structure of the polymer and release of therapeutic agent. A weak Se—Se bond (172 kJ mol^{-1}), compared with S—S (240 kJ mol^{-1}), C—C (346 kJ mol^{-1}), and C—Se (244 kJ mol^{-1}) bonds, coupled with its atomic radius (120 pm) and electronegativity, makes it favorable as a drug release agent, and readily cleavable in an oxidative environment [33–36].

17.5.8 Dendrimers in drug delivery

Dendrimers are three-dimensional, immensely branched, well-organized nanoscopic macromolecules (typically 5000–500,000 g mol^{-1}), possess a low polydispersity index and have displayed an essential role in the emerging field of nanomedicine. Dendrimers have received considerable attention in biological applications due to their high-water solubility, biocompatibility, polyvalency, and precise molecular weight [37–39]. These features make them an ideal carrier for drug delivery and targeting applications. For investigating dendrimers as drug delivery vehicles, their biopermeability across the biological membranes should be considered. The permeability of the cationic PAMAM-NH_2 (G0–G4) dendrimers has been evaluated across Caco-2 cell monolayers as a function of dendrimer generation, concentration, and incubation time, for oral drug delivery. Various parameters, viz., transepithelial electrical resistance, ^{14}C-mannitol permeability, and leakage of lactate dehydrogenase enzyme were studied and it was suggested that these amine-terminated PAMAM dendrimers could cross the biological membranes possibly by paracellular and endocytosis pathways. Moreover, by optimizing the size and surface charge, these dendritic platforms can be developed into oral delivery systems [40–43].

17.5.9 Carbon nanotube in drug delivery

The requirement of new drug delivery systems is to improve the pharmacological profiles by decreasing the toxicological effects of the delivered drugs. Carbon nanotubes (CNTs) have been envisaged as one of the potential cargos for the cancer therapy. CNTs belong to the fullerene family of carbon allotropes with cylindrical shape. The unique physicochemical properties [3, 44] of CNTs include easy surface modifications that have led to a surge in the number of publications in this interesting field. Apart from their uses in cellular imaging with diagnostic effects in nanomedicine, CNTs are promising drug carriers in the target drug delivery systems for cancer therapies [45–47].

17.5.10 Graphene oxide in drug delivery

Several drug delivery systems based on graphene and graphene oxide (GO) which are responsive to environmental stimulations have been recently reported [48, 49]. When the drugs are attached onto the drug carriers such as GO via pH-sensitive linkers, it is possible to control the release of the drug by manipulating the pH value of

environments. Using a DOX-GO system, this simple method can be effective to avoid undesired drug release during the drug transportation in blood circulation and to improve the effective release of the antitumor drugs in the tumor tissue or within tumor cells. However, a number of other and more complex pH-sensitive drug carriers have been designed using graphene derivatives. A phospholipid monolayer membrane functionalized graphene has been prepared which presents pH-controlled drug release behavior with a high drug loading capacity of 70% [50–52].

17.6 Stimuli-responsive drug delivery by nanoparticles: A new dimension in drug delivery

17.6.1 pH-induced drug release

The use of different pH environments *in vivo* has been a promising avenue for NP-based drug delivery. pH-sensitive polymers are readily available, which is especially important for encapsulation-based NP drug delivery vectors. The controlled triggered release is governed by the difference in physiological (pH 7.4) from that of endosomes and lysosomes (pH 5–6). Furthermore, tumor tissues are known to have a lower pH than regular tissues, which is especially helpful for cancer-specific drug delivery [53–55].

17.6.2 Temperature-induced drug delivery

The use of temperature-sensitive nanocomposites has been heavily explored for controlled drug delivery. Three distinctive areas of thermoresponsive drug delivery schemes have been reported: (a) diffusion from temperature-sensitive hydrogels, (b) induced breakage of encapsulate drugs, and (c) thermal-induced release from NP platforms. The roles of inorganic NPs, and more specifically metal and magnetic NPs, are to provide both a means of thermal excitation through external stimuli and a scaffold to build upon. Here, we review each of the three methodologies through a survey of the literature. Thermally induced drug delivery based on polymer-NP composites is popular, and there are many different polymers available for optimization. Changes to water-polymer interactions (i.e., hydrophilic or hydrophobic interactions) through heating allow the encapsulated drug to diffuse out of the matrix and into the target. Once thermally stimulated, the nanocomposite can release drugs by either swelling (positive mechanism based on the upper critical solution temperature UCST) or shrinkage (negative mechanism based on the lowest critical solution temperature LCST) of the polymer coating [56, 57].

17.6.3 Ultrasound-triggered drug delivery

Ultrasounds represent an effective method for attaining spatiotemporal control of drug release at the desired site, thus preventing harmful side effects to healthy tissues. The use of ultrasounds is also appealing because of their noninvasiveness, the absence of

ionizing radiations, and the facile regulation of tissue penetration depth by tuning frequency, duty cycles, and time of exposure. Ultrasound waves can trigger the release of the drug from a variety of nanocarriers through the thermal and/or mechanical effects generated by cavitation phenomena or radiation forces. Indeed, it has been shown that physical forces associated with cavitation can induce nanocarrier destabilization, drug release, and transient increase in vessel permeability, leading to the cellular uptake of therapeutic molecules [58–60].

17.7 Conclusion

Nanomedicine is one of the most rapidly growing fields of translational medicine and has made marked impacts in terms of alleviation of toxicity and enhancement of efficacy for therapies. The convergence of chemistry and nanomedicine may allow the development of patient-individualized treatments (e.g., on-demand drug delivery and self-regulated drug delivery) and provide new therapeutic modalities (e.g., new therapeutic formulations and imaging modalities). Progress in this field will depend on the fundamental understanding of organic and polymer chemistry, materials engineering, biology, and clinical practice to allow for rational design and creation of new smart chemistry. Incorporation of this chemistry will eventually impact the outcome of developed therapies in many aspects, including efficacy, targeting, biodistribution (pharmacokinetics), and NP penetration into diseased tissues. But improvement must be needed in some areas. New design strategies for nanovectors as nanomedicines should be developed in order to move these systems into the clinic for more effective treatment. Novel techniques for the effective loading of active molecules and surface activation (i.e., antibodies and functional groups) for active targeting are essential to improve the therapeutic effectiveness. Biocompatibility and toxicity will remain important issues when designing smart chemistry for medical application. The next generation of intelligent nanomaterials for sustained drug delivery are being intensively investigated and developed.

References

[1] J.V. Natarajan, C. Nugraha, X.W. Ng, S. Venkatraman, Sustained-release from nanocarriers: a review, J. Control. Release 193 (2014) 122–138.
[2] D. Bhattacharyya, S. Singh, Nanotechnology, big things from a tiny world: a review, Int. J. u- and e- Serv. Sci. Technol. 2 (3) (2009) 29–38.
[3] D.F. Emerich, C. Thanos, The pinpoint promise of nanoparticle-based drug delivery and molecular diagnosis, Biomol. Eng. 23 (2006) 171–184.
[4] A.K. Biswas, M.R. Islam, et al., Nanotechnology based approaches in cancer therapeutics, Adv. Nat. Sci. Nanosci. Nanotechnol. 5 (2014) 043001.
[5] D.S. Kohane, Microparticles and nanoparticles for drug delivery, Biotechnol. Bioeng. 96 (2) (2007) 203–209.
[6] A.A. Attama, C.E. Umeyo, The use of solid lipid nanoparticles for sustained drug release, Ther. Deliv. 6 (6) (2015) 669–684.
[7] R. Duncan, The dawning era of polymer therapeutics, Nat. Rev. Drug Discov. 2 (5) (2003) 347–360.

[8] W.H. De Jong, R.E. Geertsma, B. Roszek, Nanotechnology in medical applications: possible risks for human health, Report 265001002/2005, National Institute for Public Health and the Environment (RIVM), Bilthoven, 2005.
[9] M. Ferrari, Cancer nanotechnology: opportunities and challenges, Nat. Rev. Cancer 5 (3) (2005) 161–171.
[10] J.E. Kipp, The role of solid nanoparticle technology in the parenteral delivery of poorly water-soluble drugs, Int. J. Pharm. 284 (1–2) (2004) 109–122.
[11] M.G. Cascone, L. Lazzeri, C. Carmignani, Z. Zhu, Gelatin nanoparticles produced by a simple W/O emulsion as delivery system for methotrexate, J. Mater. Sci. Mater. Med. 13 (5) (2002) 523–526.
[12] T.M. Allen, P.R. Cullis, Liposomal drug delivery systems: from concept to clinical applications, Adv. Drug Deliv. Rev. 65 (2013) 36–48.
[13] Y. Barenholz, Doxil(r)—the first FDA-approved nano-drug: lessons learned, J. Control. Release 160 (2012) 117–134.
[14] F. Danhier, E. Ansorena, J.M. Silva, R. Coco, A.L. Breton, V. Préat, PLGA-based nanoparticles: an overview of biomedical applications, J. Control. Release 161 (2012) 505–522.
[15] U.B. Kompella, N. Bandi, S.P. Ayalasomayajula, Poly (lactic acid) nanoparticles for sustained release of budesonide, Drug Deliv. Technol. 1 (2001) 1–7.
[16] A.O. Elzoghby, W.M. Samy, N.A. Elgindy, Albumin-based nanoparticles as potential controlled release drug delivery systems, J. Control. Release 157 (2012) 168–182.
[17] E.S. Lee, Y.S. Youn, Albumin-based potential drugs: focus on half-life extension and nanoparticle preparation, J. Pharm. Investig. 46 (2016) 305–315.
[18] R. Tong, L. Yala, T.M. Fan, The formulation of aptamer-coated paclitaxel-polylactide nanoconjugates and their targeting to cancer cells, Biomaterials 31 (2010) 3043–3053.
[19] M. Karimi, S. Bahrami, S.B. Ravari, Albumin nanostructures as advanced drug delivery systems, Expert Opin. Drug Deliv. 13 (2016) 1609–1623.
[20] Q. Chen, Z. Liu, Albumin carriers for cancer theranostics: a conventional platform with new promise, Adv. Mater. 28 (2016) 10557–10566.
[21] J. Dobson, Magnetic nanoparticles for drug delivery, Drug Dev. Res. 67 (2006) 55–60.
[22] C. Sun, J.S.H. Lee, M.Q. Zhang, Magnetic nanoparticles in MR imaging and drug delivery, Adv. Drug Deliv. Rev. 60 (2008) 1252–1265.
[23] X.H. Peng, X.M. Qian, H. Mao, A.Y. Wang, Z. Chen, S.M. Nie, Targeted magnetic iron oxide nanoparticles for tumor imaging and therapy, Int. J. Nanomedicine 3 (2008) 311–321.
[24] R. Fernandez-Pacheco, C. Marquina, J.G. Valdivia, M. Gutierrez, M.S. Romero, R. Cornudella, Magnetic nanoparticles for local drug delivery using magnetic implants, in: 6th International Conference on the Scientific and Clinical Applications of Magnetic Carriers, Elsevier Science B.V, 2006, pp. 318–322.
[25] K. Subramani, H. Hosseinkhani, A. Khraisat, M. Hosseinkhani, Y. Pathak, Targeting nanoparticles as drug delivery systems for cancer treatment, Curr. Nanosci. 5 (2009) 135–140.
[26] M. Colilla, M. Manzano, I. Izquierdo-Barba, M. Vallet-Regí, C. Boissiére, C. Sanchez, Advanced drug delivery vectors with tailored surface properties made of mesoporous binary oxides submicronic spheres, Chem. Mater. 22 (2009) 1821–1830.
[27] Q. He, J. Shi, M. Zhu, Y. Chen, F. Chen, The three-stage *in vitro* degradation behavior of mesoporous silica in simulated body fluid, Microporous Mesoporous Mater. 131 (2010) 314–320.
[28] A. Garcia, M. Colilla, I. Izuierdo barba, M. Vallet Regi, Incorporation of phosphorus into mesostructured silicas: a novel approach to reduce the SiO_2 leaching in water, Chem. Mater. 21 (2009) 4135–4145.

[29] K.M. Reddy, K. Feris, J. Bell, et al., Selective toxicity of zinc oxide nanoparticles to prokaryotic and eukaryotic systems, Appl. Phys. Lett. 90 (2007) 213902–213903.
[30] N. Lewinski, V. Colvin, R. Drezek, Cytotoxicity of nanoparticles, Small 4 (2008) 26–49.
[31] P. Patra, S. Mitra, A. Das Gupta, S. Pradhan, S. Bhattacharya, M. Ahir, S. Mukherjee, S. Sarkar, S. Roy, S. Chattopadhyay, A. Adhikary, A. Goswami, D. Chattopadhyay, Simple synthesis of biocompatible biotinylated porous hexagonal ZnO nanodisc for targeted doxorubicin delivery against breast cancer cell: in vitro and in vivo cytotoxic potential, Colloids Surf. B: Biointerfaces 133 (2015) 88–98.
[32] Q. Yuan, S. Hein, R.D. Misra, New generation of chitosan-encapsulated ZnO quantum dots loaded with drug: synthesis, characterization and in vitro drug delivery response, Acta Biomater. 6 (2010) 2732–2739.
[33] T. Chen, Y.S. Wong, W. Zheng, Y. Bai, L. Huang, Selenium nanoparticles fabricated in *Undaria pinnatifida* polysaccharide solutions induce mitochondria-mediated apoptosis in A375 human melanoma cells, Colloids Surf. B: Biointerfaces 67 (1) (2008) 26–31.
[34] Y. Huang, L. He, W. Liu, et al., Selective cellular uptake and induction of apoptosis of cancer-targeted selenium nanoparticles, Biomaterials 34 (29) (2013) 7106–7116.
[35] W. Liu, X. Li, Y.S. Wong, et al., Selenium nanoparticles as a carrier of 5-fluorouracil to achieve anticancer synergism, ACS Nano 6 (8) (2012) 6578–6591.
[36] F. Gao, Q. Yuan, L. Gao, et al., Cytotoxicity and therapeutic effect of irinotecan combined with selenium nanoparticles, Biomaterials 35 (31) (2014) 8854–8866.
[37] D.L. Patton, Y.T. Cosgrove Sweeney, T.D. McCarthy, S.L. Hillier, Preclinical safety and efficacy assessments of dendrimer-based (SPL7013) microbicide gel formulations in a nonhuman primate model, Antimicrob. Agents Chemother. 50 (2006) 1696–1700.
[38] P. Singh, Dendrimers and their applications in immunoassays and clinical diagnostics, Biotechnol. Appl. Biochem. 48 (2007) 1–9.
[39] J.B. Wolinsky, M.W. Grinstaff, Therapeutic and diagnostic applications of dendrimers for cancer treatment, Adv. Drug Deliv. Rev. 60 (2008) 1037–1055.
[40] B.K. Nanjwade, H.M. Bechra, G.K. Derkar, F.V. Manvi, V.K. Nanjwade, Dendrimers: emerging polymers for drug-delivery systems, Eur. J. Pharm. Sci. 38 (2009) 185–196.
[41] R. Duncan, L. Izzo, Dendrimer biocompatibility and toxicity, Adv. Drug Deliv. Rev. 57 (2005) 2215–2237.
[42] D.A. Tomalia, Birth of a new macromolecular architecture: dendrimers as quantized building blocks for nanoscale synthetic polymer chemistry, Prog. Polym. Sci. 30 (2005) 294–324.
[43] K.M. Kitchens, M.E. El-Sayed, H. Ghandehari, Transepithelial and endothelial transport of poly(amidoamine) dendrimers, Adv. Drug Deliv. Rev. 57 (2005) 2163–2176.
[44] B. Dinesh, A. Bianco, et al., Designing multimodal carbon nanotubes by covalent multifunctionalization, Nanoscale 8 (44) (2016) 18596–18611.
[45] S. Murugesan, S.A. Mousa, et al., Carbon inhibits vascular endothelial growth factor- and fibroblast growth factor-promoted angiogenesis, FEBS Lett. 581 (2007) 1157–1160.
[46] V. Rastogi, P. Yadav, et al., Carbon nanotubes: an emerging drug carrier for targeting cancer cells, J. Drug Deliv. 2014 (2014) 670815.
[47] A. Sanginario, B. Miccoli, et al., Carbon nanotubes as an effective opportunity for cancer diagnosis and treatment, Biosensors (Basel) 7 (1) (2017) 9.
[48] H. Kim, R. Namgung, K. Singha, I.K. Oh, W.J. Kim, Graphene oxide–polyethylenimine nanoconstruct as a gene delivery vector and bioimaging tool, Bioconjug. Chem. 22 (2011) 2558–2567.

[49] J. Liu, S. Guo, L. Han, T. Wang, W. Hong, Y. Liu, et al., Synthesis of phospholipid monolayer membrane functionalized graphene for drug delivery, J. Mater. Chem. 22 (2012) 20634–20640.
[50] H.Y. Wen, C.Y. Dong, H.Q. Dong, A.J. Shen, W.J. Xia, X.J. Cai, et al., Engineered redoxresponsive PEG detachment mechanism in PEGylated nano-graphene oxide for intracellular drug delivery, Small 8 (2012) 760–769.
[51] H. Bai, C. Li, X.L. Wang, G.Q. Shi, A pH-sensitive graphene oxide composite hydrogel, Chem. Commun. 46 (2010) 2376–2378.
[52] D. Ma, J.T. Lin, Y.Y. Chen, W. Xue, L.M. Zhang, In situ gelation and sustained release of an antitumor drug by graphene oxide nanosheets, Carbon 50 (2012) 3001–3007.
[53] N. Murthy, J. Campbell, N. Fausto, A.S. Hoffman, P.S. Stayton, Design and synthesis of pH-responsive polymeric carriers that target uptake and enhance the intracellular delivery of oligonucleotides, J. Control. Release 89 (2003) 365–374.
[54] K. Na, K.H. Lee, Y.H. Bae, pH-sensitivity and pH-dependent interior structural change of self-assembled hydrogel nanoparticles of pullulan acetate/oligo-sulfonamide conjugate, J. Control. Release 97 (2004) 513–525.
[55] H. Peng, R. Dong, S. Wang, Z. Zhang, M. Luo, C. Bai, et al., A pH-responsive nano-carrier with mesoporous silica nanoparticles cores and poly(acrylic acid) shell-layers: fabrication, characterization and properties for controlled release of salidroside, Int. J. Pharm. 446 (2013) 153–159.
[56] J. Zhang, H. Chen, L. Xu, Y. Gu, The targeted behavior of thermally responsive nanohydrogel evaluated by NIR system in mouse model, J. Control. Release 131 (2008) 34–40.
[57] K.J. Chen, H.F. Liang, H.L. Chen, Y. Wang, P.Y. Cheng, H.L. Liu, Y. Xia, H.W. Sung, A thermo responsive bubble-generating liposomal system for triggering localized extracellular drug delivery, ACS Nano 7 (2013) 438–446.
[58] S.A. Stanley, J.E. Gagner, S. Damanpour, M. Yoshida, J.S. Dordick, J.M. Friedman, Radio-wave heating of iron oxide nanoparticles can regulate plasma glucose in mice, Science 336 (2012) 604–608.
[59] A. Schroeder, R. Honen, K. Turjeman, A. Gabizon, J. Kost, Y. Barenholz, Ultrasound triggered release of cisplatin from liposomes in murine tumors, J. Control. Release 137 (2009) 63–68.
[60] A. Kheirolomoom, L.M. Mahakian, C.Y. Lai, H.A. Lindfors, J.W. Seo, E.E. Paoli, K.D. Watson, E.M. Haynam, E.S. Ingham, L. Xing, R.H. Cheng, A.D. Borowsky, R.D. Cardiff, K.W. Ferrara, Copper-doxorubicin as a nanoparticle cargo retains efficacy with minimal toxicity, Mol. Pharm. 7 (2010) 1948–1958.

Further reading

[61] V.J. Mohanraj, Y. Chen, Nanoparticles—a review, Trop. J. Pharm. Res. 5 (1) (2006) 561–573.

Stimuli-responsive sugar-derived hydrogels: A modern approach in cancer biology

18

Santu Maity[a,*], *Aroni Chatterjee*[b], *Jhuma Ganguly*[a]
[a]Department of Chemistry, Indian Institute of Engineering Science and Technology, Shibpur, Howrah, India, [b]Virus Research Laboratory, National Institute of Cholera and Enteric Diseases, ID & BG Hospital Campus, Kolkata, India
[*]Corresponding author. e-mail address: santumaity77@gmail.com

18.1 Introduction

Till now malignancy happens to be among the most feared ailments affecting the global human populace. In 2018, almost 15.2 million cases have been clinically recognized, and more than 8.8 million of these cancer patients died [1, 2]. Multiple factors have been linked with efficient cancer prognosis including the type of cancer, genetic predisposition if any of the patient, family history, stage of prognosis, gender and age, tumor microenvironment, available therapeutics, and response of the patient to the therapy [2–4]. To orchestrate essential research in cancer biology and generate viable treatment for cancer therapy, an assortment of techniques is utilized that incorporate examinations of clinical examples, *in vitro* cell culture models, and *in vivo* animal models. Although *in vivo* models may provide a suitable route toward personalized medicine for patients with cancer, these models are low throughput, cost intensive, and difficult to scale up [5–8]. Hydrogels on the other hand offer a much better alternative in this scenario. A hydrogel is essentially a network of chemically/physically cross-connected polymer molecules that is filled with an aqueous medium [9]. Hydrogels can be engineered with different biophysical properties, range of compositions, and biological functions [10]. Along these lines, they have exceptionally encouraging applications both for facilitating cancer research and for anticancer drug screening. Protein-based biohydrogels, for example, collagen, matrigel, or fibrin are normally utilized for three-dimensional (3D) malignant growth cell culture attributable to their particular biophysical and cell-cement properties [11]. Matrigel is perceived as a "brilliant standard" platform for multicellular cancer spheroids (MCS) development *in vitro*. These 3D models using hydrogels empower the investigation of a wide scope of factors that influence tumor development, metastasis, and tissue invasion [11]. They give the ability of high-throughput anticancer drug screening that is quite impossible with human clinical samples and *in vivo* animal models. The use of formulations dependent on hydrogels as a delivery system of antiproliferative drugs in case of malignancy has a few points of interest over other drug delivery networks and

Green Approaches in Medicinal Chemistry for Sustainable Drug Design. https://doi.org/10.1016/B978-0-12-817592-7.00018-6
© 2020 Elsevier Inc. All rights reserved.

conventional treatments [12]. A biomechanical architect can accurately plan and synthesize hydrogels with command over structures even at the molecular level, for example, cross-connecting density and with custom-fitted properties, biodegradation, the rate of biodegradation, pore size, mechanical quality, and biological response to different stimuli, like pH, proteins, and temperature [12]. Another vital advantage of the hydrogel is their low cost contrasted with the other polymeric formulations, for example, microparticles, nanoparticles, and dendrimers. In this manner, the modifiable and exceedingly tunable properties of hydrogel settle on it as a strictly favored decision in case of malignancy treatment. In the future, it is important to make additional changes, based on the concentration of antineoplastic drugs applied keeping in focus the particular phase of malignant growth [13]. This review lists out the different possibilities with which hydrogels can be made applicable to research in cancer biology and medicine with a detailed focus on hydrogel-based drug delivery in cancer cells.

18.2 Basic concepts of hydrogels

Hydrogels, belong to a class of cross-linked polymeric materials, are good examples of a continuous technological development due to its ability to harness chemical innovation to meet environmental and economic goals simultaneously [14, 15]. The first appearance of synthetic hydrogels dates back more than 50 years, when Wichterle et al. (1955–60) prepared and inspected a hydrogel based on poly(2-hydroxyethyl methacrylate) (PHEMA) for the applications in contact lens [16, Fig. 3]. As a kind of rapidly developing materials, smart hydrogels developed from simply inert to complex stimuli-responsive materials such as pH, temperature, light, magnetic field, ultrasound, electric, redox, metal ions, etc. [17]. The research area for the hydrogels has expanded enormously in the last few decades with focus on the preparation, characterization, and applications of hydrogels [17–19]. Hydrogels are characterized as soft material having good biocompatible properties and have been exploited in many fields such as agriculture, catalysis, water purification, food additives, pharmaceuticals, cell culture, drug delivery, and biomedical implants [20–22]. More than 30,000 papers (published in the last 50 years, being c. 80% in the last decade) can be found by searching in the Journal of Citation Reports database under the topic “hydrogel.” This exhibits the significance of such smart hydrogels in both academic and industrial points of view [23–26].

Hydrogels (Fig. 18.1) are 3D networks fabricated by hydrophilic polymers cross-linked via covalent bonds or held together via physical interactions [27]. Hydrogels can swell readily without dissolving by absorbing large quantity of water or biological fluids, from 20% up to several thousand percent [28]. On the molecular level, water molecules, present in the hydrogel, are either bind to polar hydrophilic groups such as amino, carboxyl, amide, and hydroxyl groups as “bound water” and/or filling the open space between the network chains, pores as “free water” and this is the reason for the high hydrophilicity of the hydrogels [29]. Basically, hydrogels achieve equilibrium swelling when a balance occurs between the osmotic driving forces, which support the water or biological fluids to enter the hydrophilic network and the cohesive forces applied by the polymer strands. These cohesive forces lead to resist the hydrogel expansion and the magnitude of these forces depends mostly on the cross-linking

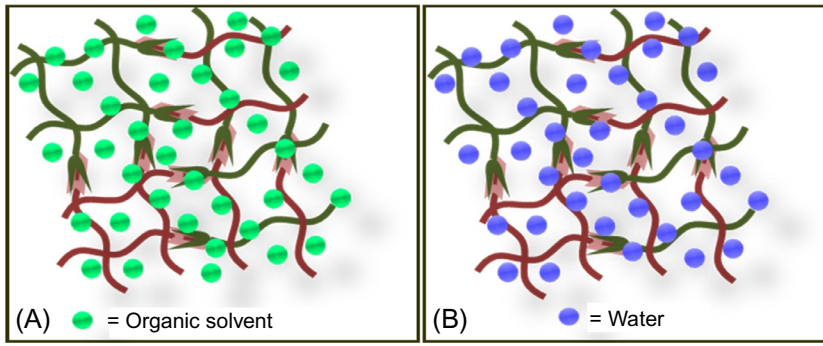

Fig. 18.1 Schematic representation of (A) organogel and (B) hydrogel.
Copyright taken from "Macroscopic Organohydrogel Hybrid from Rapid Adhesion between Dynamic Covalent Hydrogel and Organogel."

density. However, higher the extent of cross-linking for a particular hydrogel, lower is the degree of the gel hydration [30].

The hydrogels in their dry state with unhindered shrinkage forms are commonly known as xerogels [31]. When some techniques are applied for drying, such as freeze-drying or drying using solvent extraction, the resulting hydrogels become extremely porous. These porous dried hydrogels are referred to aerogels [31].

18.3 Classifications of hydrogels

Sugar-derived hydrogels can be classified (Fig. 18.2) into different categories depending on their sources, physical properties, configuration, nature of swelling, method of preparation, ionic charges, sources, physical appearance, rate of biodegradation, and observed nature of cross-linking [15, 29]. Depending on their sources of starting materials; they can be classified into natural polymeric hydrogels, synthetic polymeric hydrogels, and combinations of the two classes (hybrid) as shown in Fig. 18.2 [29]. Hydrogels can be divided as "physical gel" and "chemical gel" (Fig. 18.3). In "physical gel," the polymeric networks are held together by physical interactions, like ionic, H-bonding, or hydrophobic forces and they are thermoreversible and obtained when the solutions are cooled. While "chemical gel" consists of covalently cross-linked networks which are thermally irreversible [32, 33].

18.3.1 Chemically cross-linked hydrogels

Chemically cross-linked hydrogels can be prepared through covalent interaction of cross-linker with sugar backbone which produces irreversible hydrogel networks [34, 35]. Sugar can be cross-linked with various cross-linkers by the reaction of their functional groups like OH, COOH, and NH_2 [36–38]. There are several procedures reported in the literature by which chemically cross-linked hydrogels can be obtained [39–41]. In the following section, some of the major procedure to obtain chemically cross-linked sugar-based hydrogels is discussed.

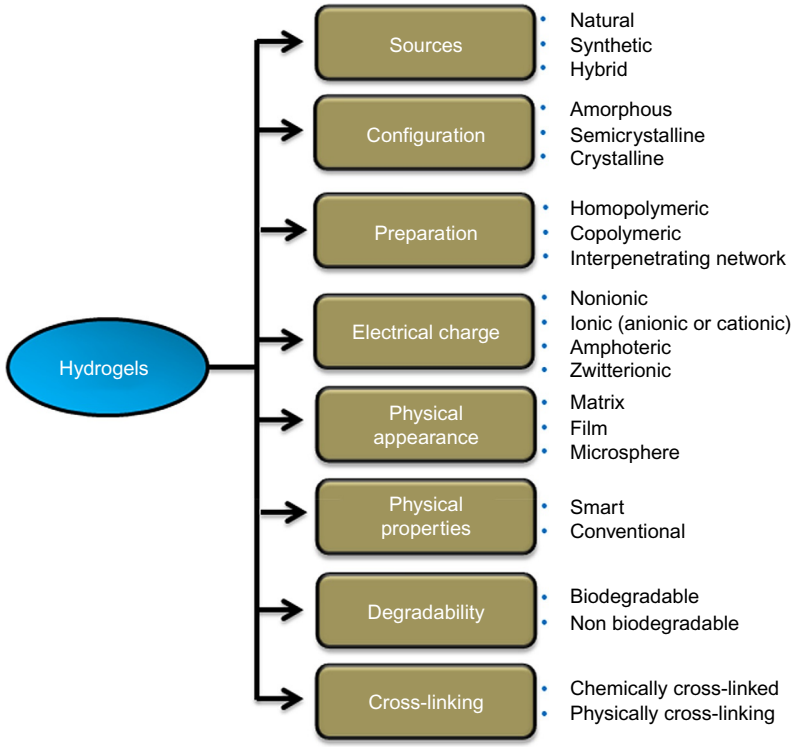

Fig. 18.2 Classification of hydrogels based on the different properties.
Authors own art work.

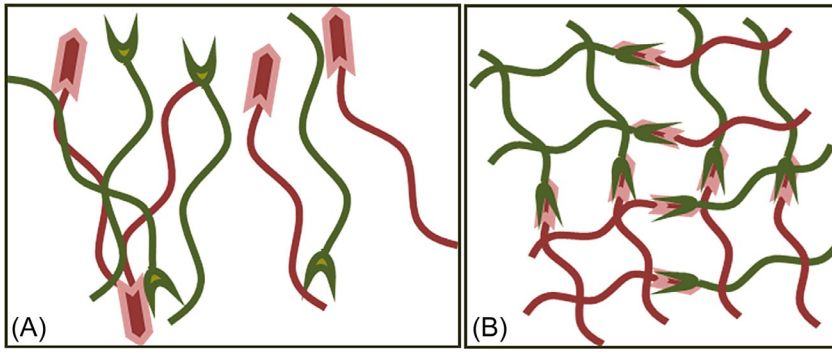

Fig. 18.3 Types of hydrogel representation: (A) physically cross-linked network and (B) chemically cross-linked network.
Authors own art work.

18.3.1.1 Small-molecule cross-linking

These types of cross-linked hydrogels are prepared by using a polymeric unit and one small cross-linker molecule in suitable reaction condition. Cross-linkers are the molecules containing one or more reactive functional groups and these active groups help to form new bonds between polymeric chains [38]. Till now, the most commonly used cross-linkers to achieve chitosan-based hydrogels are aldehydes, such as glutaraldehyde, glyoxal, formaldehyde, ethylene glycol di-glycidyl ether (EGDE), genipin, and others [42, 43]. The amino groups of chitosan are mainly responsible to form Schiff base linkage with the aldehyde groups [44, 45]. Sometimes, dialdehydes are more advantageous as it reacts directly with chitosan in aqueous environment under mild conditions without the addition of any auxiliary molecules to form cell compatible hydrogels [46].

The disadvantage of dialdehydes (e.g., glutaraldehyde) as a cross-linker is their cytotoxicity and even they show their toxicity at low doses. The polymerization of glutaraldehyde can release its residues during storage or sterilization [47–50]. Glutaraldehyde is hazardous for human health as it is neurotoxic [50]. Consequently, the presence of free unreacted dialdehydes in hydrogels may induce toxicity and the biocompatibility of the hydrogels gets affected [51, 52]. Therefore, researchers are trying to discover nontoxic cross-linking agents for controlling drug release and pharmaceutical applications [53, 54].

18.3.1.2 Photo-cross-linking

The photo-cross-linking is performed in the presence of ultraviolet (UV) light and a chemical photo-initiator (PI) [55, 56]. Several natural and synthetic macromers sometimes need to be modified for hydrogels preparation by photoactivation techniques in the presence of photo-initiators, for example, methacrylate or aryl azide-modified macromers [57]. The degree of cross-linking reaction depends on the UV exposure time [58]. With the increase in time of irradiation, photo-cross-linking of the hydrogel increases and as a result mechanical property increases and swelling ratio decreases [55, 59].

18.3.1.3 Polymer-polymer cross-linking or hybrid polymer networks

The cross-linking reaction in hybrid polymer networks (HPN) takes place between two monomeric units of two different polymeric chains [60]. Therefore, polymers should be functionalized with reactive functional groups before gelation. In this process, different types of covalent bonds can be obtained depending on the rate of cross-linking, variation of the reactive functional groups, and biocompatibility of the so-formed hydrogels network [60]. Michael type of addition reaction between a nucleophile and a vinyl group is the most commonly used for in situ cross-linking [38]. The HPN polymerization affords the formation of flexible bonds and eventually fast

formation of hydrogel [61]. Another method of this type for rapid cross-linking is the hydrazone-bond formation between an aldehyde and a hydrazide [62]. The main benefits of HPN polymerization are the reduction of hazardous cross-linker and rapid one-pot synthesis of hydrogels [63, 64]. The major disadvantages of this approach are the necessity of substantial polymeric modification to form a linkage between the functional group and a polymeric chain [38]. Moreover, the reactant polymers are seen to be toxic in the living body though they are prepared from natural polymer. Wang et al. synthesized hybrid hydrogel based on 2-hydroxypropyl methacrylamide copolymer backbone cross-linked noncovalently by coiled protein [46].

18.3.1.4 Interpenetrating networks

An interpenetrating network (IPN) is a kind of hydrogel which includes two or more polymeric units in the network in which the polymers are cross-linked with each other [65, 66]. IPNs are treated as "alloys" of cross-linked polymers and these networks are indivisible until the chemical bonds are broken [67, 68]. The polymers should have following criteria for the preparation of IPN hydrogel. First, there should be one polymer which can be synthesized and/or cross-linked with other. Second, the polymers should have similar reaction rate. Lastly, there should not be any phase separation between/among the polymers [69]. An IPN is advantageous over other type of polymer due to its viscoelastic property and easy swelling behavior without dissolving in any solvent [69]. There are two methods of IPNs: (i) by chemistry and (ii) by structure [67, 70].

(i) *Depending on the chemistry of preparation*, IPN hydrogels can be divided into following categories:
- **(a)** *Simultaneous IPN*: In this case, both the networks are prepared simultaneously from the precursors by independent, noninterfering routs that will not interfere with one another.
- **(b)** *Sequential IPN*: In this type of IPN, a network is made of a single-network hydrogel by swelling into a solution comprising of the mixture of monomer, initiator, and activator, with or without a cross-linker.

(ii) *Depending on the structure*, IPN hydrogels can be categorized into following types:
- **(a)** *Full IPNs*: This kind of IPN is composed of two networks which are ideally juxtaposed, with many entanglements and interactions between the networks.
- **(b)** *Homo-IPNs*: These types of IPNs are belonging to a special category of full IPN, where the two polymers used in the networks are the same.
- **(c)** *Semi- or pseudo-IPNs*: Semi-IPNs is a way of blending of two polymers, where one is cross-linked in the presence of other to produce a mixture of fine morphology, additional noncovalent interaction between two polymers can influence the surface morphology and the thermal properties of the semi-IPN gel.
- **(d)** *Latex IPNs*: These types of IPNs are resulted from emulsion polymerization. The morphology of the latex IPN depends on the polymerization techniques of the IPN components.
- **(e)** *Thermoplastic IPNs*: These kinds of IPNs can be moldable, extruded, and recycled. At least one component is generally a block copolymer.

18.3.1.5 Enzymatic cross-linking

This is a modern technique to prepare hydrogel in situ using enzyme as catalyst for the cross-linking between polymer chains via, for example, radical polymerization, chemical reaction of complementary groups [71]. A number of enzymes including copper-containing amine oxidases (CuAOs), transglutaminases (TG), peroxidases, tyrosinase, phosphopantetheinyl transferase, lysyl oxidase, plasma amine oxidase, and phosphatases are very well known [71–76]. Gelatin-chitosan-based gels have been synthesized using both transglutaminases and tyrosinase enzyme and following results were established; (i) for transglutaminase-catalyzed gel formation, chitosan was not essential though gel formation becomes faster with high mechanical strength, (ii) this gel lost thermo-reversibility, and (iii) TG-catalyzed gels were remarkably stronger than tyrosinase-catalyzed gelatin-chitosan gels [77]. The enzymatic cross-linking reaction has many advantages such as rapid gelation time, use of mild aqueous reaction conditions (at neutral pH and moderate temperature), no side reactions due to the substrate specificity of the enzyme, switchable physicochemical properties, and low viscous nature of precursors solutions which enable their administration on the tissue site [78]. However, external enzyme causes sudden biological changes and a foreign body reaction when used *in vivo* and, therefore, it is very necessary to select the appropriate enzyme [49].

18.3.2 Physically cross-linked (reversible hydrogels)

Physically cross-linked hydrogels have drawn special attention owing to the absence of chemical cross-linker [79]. Generally, chemical cross-linking agents are toxic in nature which can't be easily separated from the prepared hydrogels before further applications. The chemical cross-linking agents are able to change the nature of the desired product [80]. The major drawbacks of physical gels are their low mechanical strength, instability, and difficulty in controlling the pore size [81, 82]. Some of the well-known methods for physical cross-linked chitosan-based hydrogel are described below.

18.3.2.1 Cross-linking via hydrophobic interaction

Hydrophobic polymers can cross-link in water by reversible thermal gelation which is known as "sol-gel" chemistry [83]. The hydrophobic part is attached with a hydrophilic polymer segment by postpolymerization grafting or by direct synthesis of a block copolymer to produce a polymer amphiphile. These amphiphiles are soluble in water at low-temperature range [76]. However, with the increase in temperature, hydrophobic domains fused to minimize the hydrophobic surface area contacting the bulk water, minimizing the amount of structured water, and maximizing the solvent entropy. The gelation temperature depends on the polymer concentration, the length of the hydrophobic chain, and the chemical structure of the polymer [83].

18.3.2.2 Cross-linking via ionic complexes

This type of ionic complexes can be formed by chitosan without any cross-linking agent. The cationic amino groups of chitosan are typically present at low pH which enables ionic cross-linking with negatively charged molecules [76, 84].

18.3.2.3 Cross-linking via polyelectrolyte complexes

Polyelectrolyte complexes (PECs) are developed by ionic interaction between the cationic and anionic polymeric mixtures with large molecular weight [85]. Ionic interactions in PECs are stronger than H-bonding and van der Waals interactions and there is no need of organic precursors, catalysts, or covalent cross-linkers for the preparation of PECs [86]. This consequences in easy formation of PECs and, therefore, minimize the issues of their biocompatibility [84].

18.4 Benefits of sugar-derived hydrogel for biological applications

In the recent past, sugar-derived hydrogel has drawn special interest in both academic and industrial fields [87, 88]. Sugar-derived hydrogel is extensively studied for several application (Fig. 18.4) especially biological applications such as self-healing, sensing,

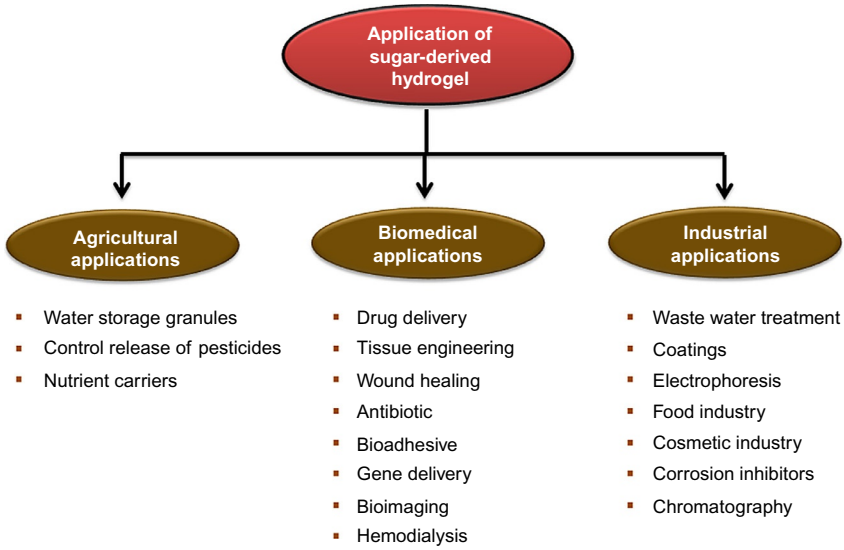

Fig. 18.4 Some important applications of sugar-derived hydrogels. Authors own art work.

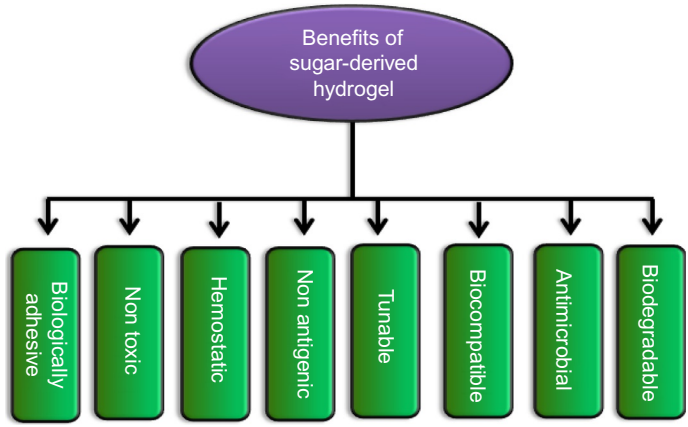

Fig. 18.5 Some important properties of sugar-derived hydrogels.
Authors own art work.

3D cell culture, drug delivery, and tissue regeneration for a number of reasons (Fig. 18.5) [87, 89–91]:

- **(i)** They have inherent biocompatibility, biodegradability, and bioadhesive benefits and inflammation, and can mimic natural biological processes.
- **(ii)** They are derived from abundant natural resources, exist in several repeat units (i.e., monosaccharides, oligosaccharides, and polysaccharides), and possess functional groups acquiescent to a several chemical modifications. Besides, biological molecules can be covalently incorporated into hydrogel structures using a range of well-established chemistries.
- **(iii)** They offer appropriate semiwet, 3D environments for molecular-level biological interactions.
- **(iv)** The presence of sugar conjugation and modification also facilitate several desirable properties, e.g., reduced cytotoxicity and immunogenicity, improving serum stability, and depressing freezing point.
- **(v)** They have enriched in hydrophilic functional groups, which allow them to interact with biological tissues.
- **(vi)** Such type of carriers has protracted residence time in certain tissues and, therefore, raises the absorbance of loaded drugs.
- **(vii)** Sugar functionalization can camouflage delivery systems, increasing circulation time in the bloodstream, allows cellular entry, which is highly desirable for delivery applications.
- **(viii)** Polymeric delivery systems bearing pendant sugars with appropriate spatial arrangements can induce remarkable binding affinity enhancement for proteins due to multivalent interactions, known as cluster glycoside effects, which is one of the underlying merits of sugars as active targeting ligands.
- **(ix)** Such hydrogels are highly tunable and can be prepared into different formulations (e.g., micelles, nanoparticles, vesicles, liposome, etc.), presenting a versatile platform for bioactive delivery.
- **(x)** Some hydrogels afford inert surfaces that prevent nonspecific adsorption of proteins.

(xi) They have tunable mechanical properties as their elasticity can be tuned by modifying cross-link densities.

(xii) Hydrogels can be designed to change properties (e.g., swelling/collapse or solution-to-gel transitions) in response to various environmental stimuli, such as pH, temperature, ionic strength, solvent polarity, electric/magnetic field, ultrasound, light, or small biomolecules.

18.5 Characteristic of stimuli-responsive sugar-derived hydrogels

Hydrogel can be defined as a 3D polymeric network composed of a polar and hydrophilic natural and/or synthetic polymer that is physically or chemically cross-linked and can hold a huge amount of water within its network. If one element within the hydrogel network can act as a receptor unit or is spectroscopically active, this gel is named as stimuli-responsive or smart material [91]. The influence of external stimuli induces some changes in shape and size of the hydrogel network on a macroscopic scale and/or it can change its optical, wettability, mechanical, and electrical properties [92].

Stimuli-responsive delivery systems are designed to release bioactive materials at a particular place in response to some physical, chemical, and biochemical parameters. Generally, these stimuli can be divided into three major categories (Fig. 18.6) [23, 93, 94]:

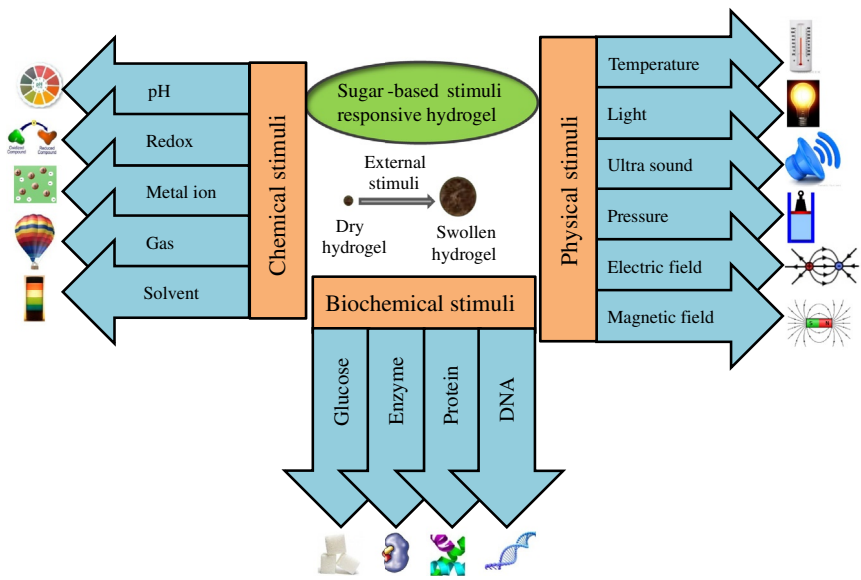

Fig. 18.6 Schematic representation of various stimuli-responsiveness of sugar-derived hydrogels.
License Number: 4580211231684, Licensed Content Title Hydrogel: preparation, characterization, and applications: a review.

(i) Physical stimuli which contains temperature, ultrasound, pressure, electric field, magnetic field, and light.
(ii) Chemical stimuli consist of pH, redox (oxidation-reduction), ionic strength, metal ions, and gas.
(iii) Biochemical stimuli comprise glucose, enzyme, protein, DNA, etc.

During the change of some environmental stimuli, a modification in the hydrogel occur which results in the release of bioactive materials. This response can arise via some variations in chemical composition of the hydrogel [15] or certain variations in the physical or conformational properties of the hydrogel [93, 95]. Some specific examples are that changes in chemical composition may be promoted by conjugation of the sugar to biomaterials, similar to a prodrug, by a stimuli-cleavable bond for local release of the free drug upon stimuli exposure. These stimuli-responsive changes are highly dependent on pH of the medium or enzymes [94]. Physical changes consist of stimuli-triggered changes in the morphology, swelling properties, and polymer folding conformation of the hydrogel [23, 95].

Stimuli-responsive delivery systems can reduce the cytotoxicity associated with systemic exposure by releasing the biomaterials at the targeted site. This method decreases the amount of drug required during administration to elicit a therapeutic effect, as the localized release mechanism causes a higher concentration at the desired location. A large number of hydrogels display stimuli-triggered release; but the sugar-based hydrogels have inherent ability to release the bioactive agents depending upon external stimuli [96, 97]. Therefore, this chapter will focus on sugar-based hydrogel systems, where stimuli-responsive properties are a direct result of the sugar components. The stimuli-responsiveness is not a necessary condition to the sugar for delivery systems that contains sugars as a core of the system [98]. Table 18.1 represents various hydrogel and their stimuli-responsive nature.

Table 18.1 Various stimuli-responsive sugar-derived hydrogels.

Stimulus	Name/abbreviation	Response	Ref.
pH	DA-PEG/CMC	pH-Induced sol-gel transitions	[99]
Redox	Methoxyl poly(ethylene glycol) (mPEG) and poly(3-benzyloxycarbonyl-L-lysine) (PZLL)	α-Helix (thioether) to random coil (sulfone) conformational transition	[100]
Protein	Mannose-6-phosphate glycopolypeptides (M6P-GPs)	Selectively target the lysosome	[101]
Temperature	Poly(*N*-isopropylacrylamide)-cellulose nanocrystals	Volume phase transition and release of drug	[102]
pH, temperature	Carboxymethyl chitosan/poly(*N*-isopropylacrylamide) semi-IPN	Release of coenzyme A	[103]

Table is authors original for this publication.

18.5.1 Temperature-responsive hydrogels

Among numerous possible external and internal stimuli, temperature changes are easy and safe for many applications, especially for biomedical applications. Temperature-responsive hydrogels are defined by their capability to swell and shrink when the temperature variations in the surrounding fluid, which means discontinuous volume changes, are observed depending on the surrounding temperature [104]. Thermal-responsive behavior of hydrogels is usually governed by the balance of hydrophilic and hydrophobic moieties on the polymer chain [105].

Some of the temperature-sensitive hydrogels undergo sudden decrease in solubility in response to the increase of environmental temperature called the lower critical solution temperature (LCST) [106]. This type of hydrogels will show a swelling behavior when the temperature is lower than the LCST and shrink when the temperature rises above the LCST. The LCST can be changed by mixing a small quantity of ionic copolymer in the gels or by altering the solvent composition and, therefore, this is the most important parameter for negative temperature-sensitive hydrogels. Generally, the LCST of a hydrogel with more hydrophobic constituent moves to lower-temperature region [105]. The LCST of a hydrogel will automatically alter if the ratio of hydrophobic to hydrophilic content of the structure of hydrogels is changed. These kinds of hydrogels contain two parts; the first is the hydrophilic part —CONH—, and the second is hydrophobic alkyl (—R—) part [105, 107]. At temperatures lower than the LCST, water or fluid interacts with the hydrophilic part by forming hydrogen bonds with the hydrogel and due to of these hydrogen bonds formation, the dissolution and swelling will increase. Above LCST, the hydrogen bonding interaction becomes weaker and at same time the hydrophobic interaction with the hydrophobic part will be stronger. Thus, the absorbed liquid will go out through a de-swelling process and the hydrogel will shrink owing to the interpolymer chain association [53]. The phase separation is directed by the balance of hydrophilic and hydrophobic on the sugar moieties and on the Gibbs free energy of mixing [105–107].

The effect of enthalpy (H), entropy (S), and temperature (T) on the Gibbs free energy of association (G) can be defined by the second law of thermodynamics [$\Delta G = \Delta H - T\Delta S$]. As the temperature increases, $T\Delta S$ also increases and considering that the enthalpy (ΔH) term is positive and often smaller than the entropy term (ΔS). Therefore, with the increase in temperature ΔG becomes negative and favors polymer chain association process. Besides, the temperature dependence also influences certain molecular interactions, for example, hydrophobic forces and, hydrogen bonds which contribute to the phase separation. At LCST, hydrogen bonds among sugar molecules and water molecules are unfavorable compared to sugar-sugar and water-water interactions. Thus, a sudden transition in the 3D matrix happens: water-solvated supramolecule rapidly dehydrates and changes to a more hydrophobic structure [108, 109].

Positive temperature sugar-derived hydrogels are generally known as the upper critical solution temperature (UCST) [107]. This type of hydrogels shrinks and releases fluids or solvents from the hydrogel matrix at the temperature below UCST.

At temperatures above UCST swelling of hydrogel occurs. From this, it can be summarized that these types of hydrogels are regressive at negative temperatures region. Positive temperature hydrogels contract at low temperatures owing to the formation of a complex structure by forming hydrogen bonds. However, the structure dissociates at a high temperature due to the breaking of the hydrogen bonds, and the maximum possible extent of swelling of the hydrogel will take place rapidly above the UCST [29, 110].

18.5.2 pH-Responsive hydrogels

pH-Sensitive hydrogels are a class of biomaterials that responds to the pH of the environment. In case of intracellular drug release, the pH of cellular microenvironment related with uptake mechanisms is used (e.g., endocytosis) [111, 112]. During endocytosis progresses, the pH of the endosome decreases from pH 5–6 in the early endosome to pH 4–5 when the endosome fuses with the lysosome [113]. Drug release prior to lysosomal fusion is promising to avoid cargo degradation. Moreover, certain tissues vary in pH compared to circulation; cancerous tumors have a slightly lower pH, that is, more acidic extracellular pH (pH 6–7) than normal tissues [112, 113]. This variation is mainly owing to the Warburg effect and increased glycolysis rate, which exports acidic molecules to the extracellular environment [114, 115, Fig. 4C]. Alternatively, the pathway taken by oral delivery systems involves a gradual increase in pH, culminating in the basic environment of the colon (pH 7.4–8.0). Therefore, the principle of such type of hydrogel is a structure that either shrinks or swells in response to the pH of the microenvironment [116]. pH-Responsive hydrogels contain acidic or basic groups are bonded to the polymer backbone that may accept or release the proton with respect to the change in the neighboring pH [117, 118] The acidic groups deprotonate at high pH, however, the basic groups protonate at low pH. The association, dissociation, and binding of various ions to polymer backbones result in swelling of the hydrogel in aqueous environment [23].

18.5.3 Light-responsive hydrogels

Light-sensitive hydrogels are smart functional materials that have widely used in several biotechnological applications such as photo-triggered targeted drug/gene delivery systems, micro lenses, light-controlled enzymatic bioprocessing system, sensors, and photo-controlled separation/recovery systems in biological microelectromechanical system (bioMEMs) formats, etc. due to the activation process via light can be remote and noninvasive [119–121]. These hydrogels are very promising to deliver the light in a controlled manner with accuracy. Thus, the light-responsive hydrogel is applied for fabrication of optical switches, display unit, and especially in optical drug delivery system [120, 122].

18.5.4 Electric current responsive hydrogels

Electric current responsive hydrogel are generally composed of polyelectrolyte complex and shrinks or swells in response to an applied electric field [123, 124]. The hydrogels with large number of the ionizable group on their backbone chain could be sensitive toward both pH and electricity [123]. There are some reported literature about the usage of electric current *in vivo* in the form, for instance, iontophoresis and electroporation in the application of dermal and transdermal drug delivery [125, 126].

18.5.5 Sound responsive hydrogels

Though conventional gelation is usually attained by a heating-cooling process, the application of ultrasound may induce gelation in some cases. The kinetics of gelation triggered by sonication is commonly much rapid compared to that of the heating-cooling process [127, 128]. Ultrasound-responsive hydrogel is promising to deliver the drug in an "on-off switch" manner. For such type of system, sound acts as a permeation enhancer which assists the drug to cross the biological barrier [129].

18.5.6 Redox-responsive hydrogels

Redox (reduction-oxidation)-responsive hydrogels are valuable strategy for rapid and effective drug release in tumor cells [19, 130]. For intracellular drug delivery, the high redox potential gradient between the extracellular and intracellular surroundings, as well as between tumorous and normal tissues favors drug release. The high reducing potential in cells is mostly owing to the abundance of a tripeptide, glutathione (GSH) [131]. Recently, reactive oxygen species (ROS) have attracted greater attention due to their close connection with many diseases [132]. That is why much effort has been given to the design and synthesis of redox-responsive sugar-derived hydrogel because of their potential applications in gene and drug delivery, particularly in cancer therapy.

18.5.7 Solvent-responsive hydrogels

Solvent-responsive hydrogels are also a very important aspect on stimuli hydrogels. Generally, the change in solvent from hydrophilic to hydrophobic (or the reverse) is a simple technique to induce the shrinking or swelling of a 3D hydrogel network [133, 134].

18.5.8 Glucose-responsive hydrogels

In the past few decades, there is growing impetus to the development of mimicking the natural response of the pancreas in a diabetic patient via glucose-sensitive hydrogels involves the appropriate delivery of insulin in response to the variation of glucose level in the body [93, 135]. Such hydrogels can continuously and automatically release insulin in response to the elevated level of blood glucose of diabetic patients with minimal patient intervention [136]. Among the numerous hydrogels, sugar-derived

hydrogel-based delivery systems are superior to others owing to their high biocompatibility and biodegradability. The strategy behind the controlled release of insulin from the system to maintain its level in a diabetic patient includes an enzyme-substrate reaction where glucose reacts with glucose oxidase forming gluconic acid, resulting in a decrease in the pH of the environment [137, 138]. With the variation in pH, the hydrogel shrinks or swells depending on the natures of that gel. Therefore, pores size of the hydrogels changes and insulin is released from the system [138]. Two different techniques have been employed for the synthesis of glucose-sensitive hydrogels [93, 138, 139] by (i) incorporation of phenylboronic acid (PBA) moieties into the hydrogel backbone, which is recognized as an intelligent saccharide receptor owing to its unique reversible six member cyclic boronic ester chelate complex forming ability with cis-diols and (ii) insertion of pH-responsive or oxidation-sensitive units that can recognize glucose indirectly; that is, glucose oxidase (GOD) converts glucose into gluconic acid triggering a decrease in local pH, which in turn affects pH-responsive units.

18.6 Hydrogels as *in vitro* cell culture models

To carry out certain exploratory investigations under physiological settings, different 3D *in vitro* culture models have been generated, with the sole point of reproducing the physiology of cell-to-cell contact and the microenvironment encompassing cancer cells. Additional advancements have also been made to reciprocate hypoxic-necrotic regions within the tumor mass, thereby conceivably adding to the understanding of tumor progression, metabolism, and metastasis [140]. They additionally give the capacity for high-throughput drug screening that is unimaginable with clinical samples and *in vivo* animal models. Diverse sorts of scaffolds ranging from polymers (froths and hydrogels) to nonwoven fiber ECM-determined materials have been explored. Among these, natural or synthetic hydrogels offer a few distinct preferences, for example, high water content, great bioactivity, biocompatibility, effective transportation of nutrients and oxygen because of the reticulated structure of cross-connected polymer chains [141]. In particular, hydrogels have been utilized every now and again to test the microenvironment effect on cell function, as their mechanical properties can be finely tuned so as to acquire dependability in reality [141].

Alginate has a decent possibility for the achievement of a 3D structure being stable over a long time which is fundamental for the acknowledgment of an *in vitro* model as a platform for carrying out pharmacological tests [142, 143]. Alginate can be quite effectively arranged in a 3D gel-like structure and the mechanical properties of the resultant gel can be decisively tuned by means of cross-linking with calcium ions. In a previous report, scientists have compared the organization form, proliferation rate, and viability of breast cancer cells when implanted in 3D alginate gels with variable rigidity, finally characterizing the most appropriate measures of alginate and calcium to improve cell activity [144]. This alginate-based model worked fine for less aggressive cells that both in two-dimensional (2D) and in 3D keep up a round

morphology and a cluster-like association, but for substantially more aggressive and invasive cells a much more tolerant environment becomes necessary [145].

Matrigel is a dissolvable and sterile concentrate of cellular basement membrane proteins extracted from the EHS tumor that frames a 3D gel at 37°C, known to upgrade biological events within the cells and also to permit cells reflecting some key highlights mirroring their internal malignant nature [144, 145]. The basic disadvantage of this gel is its structural weakness rendering it to be utilized only as monolayer or thin gel adaptations, chiefly for intrusion assays.

18.7 Biomimetic hydrogels in the study of MCS

MCS developed in biomimetic hydrogels reiterate numerous highlights of tumors formed *in vivo* and it is helpful *in vitro* model for crucial research in malignant biology. Commendable use of MCS models is in the investigation of the angiogenic capacity of malignant cells [145]. MCSs formed by oral squamous cell carcinoma cells in 3D alginate-based hydrogels have been utilized to investigate the angiogenic limit of malignant cells in a particular environment [145, 146]. MCSs from primary cancer cells and numerous other cancer cell lines have been developed in fibrin hydrogels. Matrigel paves the way for *in vitro* development of MCSs from cell lines and primary cells. Matrigel has been utilized for MCS development from colorectal cancer, breast cancer, prostate cancer cell lines, etc. Collagen, the most plenteous fibrous protein component of ECM in homeotherms, assumes a significant role in tumor invasion, progression, and metastasis by advancing cell attachment and migration [146, 147]. In this way, 3D collagen gels are broadly used to imitate ECMs. Collagen type I hydrogels have been utilized to develop MCSs from osteosarcoma, human colorectal cancer cells, breast cancer cells, primary cancer cells from patients with colorectal cancer, and prostate cancer cell lines. Polysaccharide hydrogels formed by agarose, alginate, and hyaluronic acid (HA) have helpful biophysical properties; notwithstanding, they require extra chemical adjustment with arginylglycylaspartic acid (RGD) peptides to present adhesion ports for mammalian cells [148]. Interestingly, in comparison with matrigel or collagen, polysaccharide hydrogels give controllable and stable physical and chemical conditions for MCS development, in light of the fact that their degradation is free of cell-secreted proteolytic enzymes. In view of their mechanical rigidity, agarose and alginate hydrogels were utilized to decide the impact of stress forced by developing MCSs on the hydrogels. Composite hydrogels with an interpenetrating system structure framed by polysaccharides and proteins offered command over mechanical properties of the hydrogel and gave cell-adhesion ligands, accordingly encouraging MCS development [149]. Alginate has additionally been joined with matrigel to explore the harmful movement of ordinary mammary epithelium intervened by changing the rigidity of hydrogel. Biopolymer hydrogels offer an expansive scope of biochemical and biophysical properties for cell morphogenesis and functional capacity. Synthetic hydrogel platforms conveying suitable cell adhesive ligands and biodegradable cross-linkers may overcome these impediments by providing command over arrangement, composition, and properties of the hydrogel [150]. Engineered hydrogels prepared synthetically have been prepared from ethylene

glycol or PEG molecules, which were cross-connected by photopolymerization of acrylate-PEG. Hydrogels made from PEG have likewise been modified with matrix metalloproteinase degradable sites and integrin-restricting RGD peptide sites. These have been used to develop MCSs from ovarian, lung, and brain cancer cell lines. Hybrid hydrogels prepared from natural and engineered constituents consolidate the better of the two universes: the benefits of organic polymers and synthetic polymers (i.e., control of the biochemical and mechanical properties) [151]. For instance, hydrogels have been framed from modified HA molecules. Another intriguing case of hybrid platforms for MCS development is a nanofibrillar hydrogel framed by rod-like cellulose nanocrystals (CNCs) like those of collagen nanofibrils conveying end-grafted molecules of an engineered polymer like poly(*N*-isopropylacrylamide) [152]. These hydrogels were utilized to culture breast cancer cells, with the MCS development profiles being like those acquired in matrigel.

18.8 Hydrogels as engineered tissue microenvironment

Tumor microenvironments, with their multifaceted nature, diversity, complexity, and dynamic nature assume a basic role in cancer growth and metastasis. In this way, numerous scientists have attempted to make artificial tumor microenvironments summarizing natural tumors by utilizing differently designed biomaterials. Advances in engineering and materials designing have empowered the utilization of different polymeric hydrogels as engineered 3D lattices that summarize the pathological tumor ECM to permit investigations of fundamental malignant growth science and screening of the adequacy of anticancer specialists [153]. Scientists have used biomimetic 3D breast cancer growth models containing collagen hydrogels encapsulating multicellular spheroids to assess the anticancer therapeutic impact of paclitaxel-stacked polymeric nanoparticles [154]. HA hydrogels have likewise been used as a stage for examining varieties in the matrix rigidity, the concentration of cell-adhesion locales and MMP sensitivity during the invasion of breast cancer. Scientists have been able to fabricate HA hydrogels with independently varying cross-linking (mechanical) and ligand (chemical) densities to study the effects of each factor on breast cancer invasion. Polyethylene glycol (PEG)-based hydrogels have been utilized by some scientists to investigate the effect of biochemical and biophysical matrix properties on fibrosarcoma cell migration. They prepared peptide-functionalized PEG hydrogels through thiolene photopolymerization [155]. Different approaches have been made to reiterate and model glioblastoma multiforme (GBM) tumor microenvironments *in vitro* so as to acquire a superior comprehension of the molecular and systemic functioning of GBMs. Utilizing PEG-based hydrogels, bioengineered 3D brain tumor models were made to explore the impacts of matrix rigidity on GBM cells. The hydrogels were made through photopolymerization and upheld 3D cell growth and lattice remodeling. Numerous scientists have used advanced hydrogel-based platforms to understand the hidden mechanism of growth and metastasis of prostate cancer. HA hydrogel-based 3D models utilizing prostate tumors from potential patients have been used for drug screening. 3D ovarian cancer models have likewise been created by utilizing GelMA hydrogels encapsulating a human epithelial ovarian cancer cell line

isolated from a patient [156]. The analysts examined the impact of matrix rigidity, matrix debasement, and consolidation of ECM fragments on the formation of ovarian cancer spheroids.

18.9 Role of hydrogels as drug delivery systems in cancer cells

New types of medicinal strategies are required to relentlessly target cancer cells, while at the same time diminishing the effects it has on normal healthy cells. To nullify the possible side effects, encapsulated transdermal drug delivery systems show up as a promising elective methodology to carry antineoplastic drugs (Fig. 18.7) [157]. Encapsulated antineoplastic drugs offer many advantages which include increased bioavailability and solubility of the drug, high stability, delayed half-life, controlled drug release, selective tissue distribution, and reduction of the total amount required as the dose. Together, every one of the advantages sketched out above can help limit the antagonistic side effects to a sensational degree [158]. Among these numerous sorts of drug delivery techniques, the improvement of hydrogels dependent on natural and engineered polymers as the drug transporters has received some unique consideration. These biomaterials present an energizing opportunity for planning new strategies for anticancer therapeutics [159]. These frameworks have special properties to improve the adequacy of the therapeutic operators and limit unwanted side effects [160]. Presently, hydrogels have exhibited various preferences compared to the customary forms of treatment. This is because of modifiable/tunable hydrogels, where it is conceivable to control properties of the hydrogel, including long-term discharge, degradation rate,

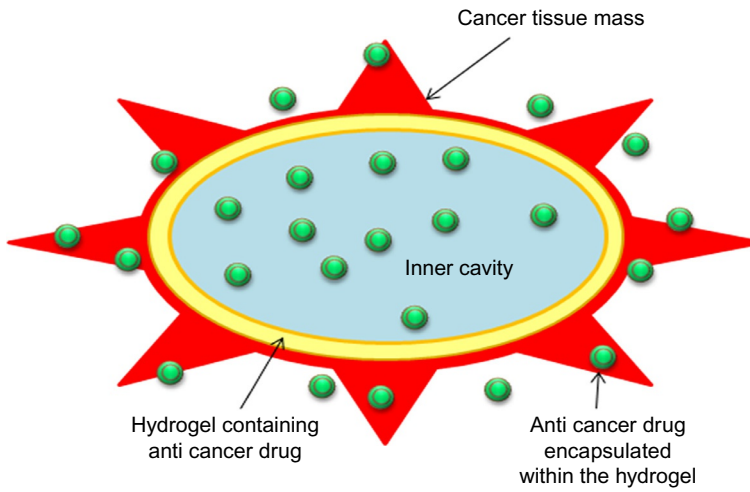

Fig. 18.7 Hypothetical diagram illustrating the binding and drug release by hydrogels in specific cancer tissues.
Authors own art work.

and tunable pore size [161]. Because of the tenability of hydrogels dependent on the previously mentioned properties, it is advantageous to examine hydrogels more intricately to discover ideal hydrogel formulations with explicit properties to treat malignancy.

18.10 Recent advancements in anticancer drug delivery

Alginate has been utilized to ensnare PLGA-PTX microspheres in a strong hydrogel grid so as to maintain a strategic distance from initial burst impact and control the drug discharge from the carriers. This hydrogel has been structured, characterized, and validated both *in vivo* and *in vitro* for its cytotoxicity, kinetics, and stability demonstrating promising outcomes [162]. Vesicular phospholipid gels were stacked with cytarabine and characterized as local delivery depots for GBM treatment, producing satisfactory results [163, 164]. In another study, scientists synthesized a thermosensitive gel (PEG-PLGA nanocomposite) loaded with TMZ and PTX [165]. This gel presents ideal rheological and gelation properties for a local application in the brain and possesses a lot higher restraining impact on cancer growth and apoptosis instigating rate in C6 and U87 glioma cells contrasted with the controls [166]. A few scientists utilized the TPG as a novel medication conveyance framework for the nearby treatment of GBM. TPG (thermoreversible gelation polymer) hydrogel commonly called as MebiolTMGel is a noncytotoxic, biocompatible, and totally pathogen free which when stacked with encapsulated DOX (in PLGA microspheres or liposomes) demonstrates huge restraint in GBM tumor growth [167]. In one more investigation a camptothecin (CPT)-stacked PLGA microspheres-containing TPG hydrogel was developed and its helpful viability was assessed in a resection model and C6 rat glioma model [168, 169] (Fig. 18.8).

Dynamic targeting can include both hyperproliferative tumor cells and ligand receptor or antigen-antibody interceded endocytosis pathways dependent on recognition at the molecular level [170]. In this manner, injectable hydrogels can be marked with specific biomolecules, for example, with monoclonal antibodies (mAb) and suitable activating ligands [171, 172]. Breast cancer cells widely express integrin αvβ3 receptors and estrogen receptors (ER) required largely for metastasis, tissue invasion, and angiogenesis [173]. Thus, both Arg-Gly-Asp (RGD) peptide, which exhibits a high affinity for integrin αvβ3 and estrogen (Et), which specifically binds to the ER on the surface of these cancer cells, can have a key role in the process of targeted drug delivery. For the advancement of the targeted delivery and anticancer effect of taxol, researchers proposed a hydrogel comprising: (i) Et and RGD peptide; (ii) taxol; and (iii) a self-assemble peptide hydrogel as a nanoscale carrier [174]. MCF-7 breast cancer cells effectively took up Et-peptide-taxol by virtue of the synergistic effect of both targeted Et and the RGD peptide. Besides, the dual modification promoted the necrotic and apoptotic impact of taxol-loaded hydrogels. *In vivo* proof-of-principle experiments also confirmed that the Et-peptide-taxol hydrogel could selectively target breast cancer tumors and was also metabolized to biocompatible materials [175]. To increase the half-life of a peptide drug and improve its antitumor activity, condensed

Fig. 18.8 Schematic illustration of the main concerns to contemplate for the development of anticancer drug-loaded hydrogels.
Authors own art work.

peptide-gelatin complex NPs were prepared through electrostatic interactions between alkalized gelatin and the peptide. Eventually, EGFR-lytic peptide was initially prepared [176] and its selective antitumor and cytotoxic activities were enhanced by substitution of the second histidine (H) with arginine (R). Avastin and vitamin D have also been used as biorelevant sources of marker biomolecules against colorectal cancer because both can positively impact chemotherapy and their level has been identified to associate with survival in lymphoma, colorectal, and breast cancers.

A couple of more alternatives as drug delivery frameworks have also been generated in the last few years [177]. Scientists have been able to develop a new form of chitosan-based injectable hydrogel scaffold to deliver live cytotoxically functional T-lymphocyte cultures into melanoma cells. A combinatorial approach was followed using phosphate buffer and sodium hydrogen carbonate as gelling agents, to create these chitosan-based biocompatible thermogels (CTGels). These gels showed excellent cyto-compatibility and mechanical stability along with superior functionality *in vitro* [178]. Table 18.2 represents some anticancer loaded sugar-derived hydrogel-based drug delivery system.

Table 18.2 Active targeting anticancer loaded sugar-derived hydrogel-based drug delivery system.

Sugar-derived hydrogel matrix	Active agent	Model of study	Ref.
Poly(lactide-*co*-glycolide): plasticizers (40:60)	Temozolomide	C6 rat glioma resection model	[177]
Polyvinyl alcohol hydrogel with sulfonate groups and 0.6% alginate solution	Doxorubicin	9L rat orthotopicglioma model	[178]
Chitosan/β-glycerophosphate hydrogel	Ellagic acid	*In vitro*	[160]
PEG-*g*-chitosan hydrogel	T lymphocytes	*In vitro*	[179]
Monomethoxy polyethylene glycol-poly(lactide-*co*-glycolide) hydrogel	Paclitaxel and temozolomide	*In vitro*	[180]
Chitosan hydrogel	Doxorubicin, vaccinia virus	Cervical carcinoma	[181]
Chitosan/β-glycerophosphate	Cisplatin	*In vitro* studies on HCT-116 (colon cancer) and MCF-7 (breast cancer)	[182]
Chitosan/β-glycerophosphate	Ellagic acid	*In vitro* studies on U87, C6 cell lines	[183]
Succinated chitosan/oxidized alginate	Doxorubicin	*In vitro* studies on MCF-7 cell and *in vivo* on breast cancer	[184]
β-Cyclodextrin-modified polyaldehyde dextran/carboxymethyl chitosan	Adamantane-modified doxorubicin	Hela (cervical carcinoma)	[185]

Table is authors original for this publication.

18.11 Conclusion and future perspectives

Nature always motivated us with a variety of ideas of creating and maintaining a balance among the cellular processes to sustain life to develop novel structures and to mimic natural properties. The current research on the development of "stimuli-responsive" smart materials to understand the structure-property relationship of naturally occurring sugar for cancer biology has brought us a step closer to the direction of understanding how the complex processes take place inside the living body. Sugar-derived hydrogels are very significant due to the set of properties not found in other class of materials. The number of publications in the field of novel sugar-based hydrogel has enormously increased year by year. Stimuli-responsive sugar-derived smart hydrogels occupy significant position owing to descent biocompatibility,

biodegradability, and bio-mimicking properties. Moreover, different functionalities can be incorporated easily to the hydrogel backbone as well as side chains that can recognize small biomolecules and certain stimuli. Yet, there is a long way to go in producing synthetic sugar-derived materials on a large scale for real field applications, partly because, to obtain tissue mimicking properties in the stimuli-responsive sugar-derived materials, precise control over the higher-order structure is required. With the current synthetic strategies for obtaining such hydrogels, sequence control and monodispersity of the synthetic biomaterials become difficult to achieve. Besides costly reagents, extensive and tedious synthetic procedures for preparation and careful handling of moisture-sensitive reagents which requires strictly anhydrous reaction conditions for generating such hydrogels with high purity are analytical barriers. However, more comprehensive studies with a better understanding and by adopting economical pathways will develop synthetic stimuli-responsive sugar-derived hydrogels for application in cancer treatment, in a fast fashion, for the next decades.

References

[1] J.T. Patterson, The Dread Disease Cancer and Modern American Culture, Harvard University Press, England, 2009. ISBN 0-674-21625-3.
[2] M.J. Bissell, D. Radisky, Putting tumours in context, Nat. Rev. Cancer 1 (2001) 46–54.
[3] K. Kourou, T.P. Exarchos, K.P. Exarchos, M.V. Karamouzis, D.I. Fotiadis, Machine learning applications in cancer prognosis and prediction, Comput. Struct. Biotechnol. J. 13 (2015) 8–17.
[4] D. Yang, A. Hendifar, C. Lenz, K. Togawa, F. Lenz, G. Lurje, A. Pohl, T. Winder, Y. Ning, S. Groshen, H.J. Lenz, Survival of metastatic gastric cancer: significance of age, sex and race/ethnicity, J. Gastrointest. Oncol. 2 (2011) 77–84.
[5] Y. Li, E. Kumacheva, Hydrogel microenvironments for cancer spheroid growth and drug screening. Sci. Adv. 4 (2018) eaas8998, https://doi.org/10.1126/sciadv.aas8998.
[6] T.G. Meijer, K.A.T. Naipal, A. Jager, D.C. Gent, Ex vivo tumor culture systems for functional drug testing and therapy response prediction, Future Sci. OA 3 (2) (2017), FSO190 https://doi.org/10.4155/fsoa-2017-0003.
[7] Y.S. DeRose, K.M. Gligorich, G. Wang, A. Georgelas, P. Bowman, S.J. Courdy, A.L. Welm, B.E. Welm, Patient-derived models of human breast cancer: protocols for in vitro and in vivo applications in tumor biology and translational medicine, Curr. Protoc. Pharmacol. (2013), (Chapter 14: Unit 14.23). https://doi.org/10.1002/0471141755.ph1423s60 .
[8] J. Cohen, L. Pivodic, G. Miccinesi, B.D. Onwuteaka-Philipsen, W.A. Naylor, D.M. Wilson, M. Loucka, A. Csikos, K. Pardon, L.V. Block, M. Ruiz-Ramos, M. Cardenas-Turanzas, Y. Rhee, R. Aubry, K. Hunt, J. Teno, D. Houttekier, L. Deliens, International study of the place of death of people with cancer: a population-level comparison of 14 countries across 4 continents using death certificate data, Br. J. Cancer 113 (2015) 1397–1404.
[9] W. Hu, Z. Wang, Y. Xiao, S. Zhanga, J. Wang, Advances in crosslinking strategies of biomedical hydrogels, Biomater. Sci. 7 (2019) 843–855.
[10] V. Drinberg, R. Bitcover, W. Rajchenbach, D. Peer, Modulating cancer multidrug resistance by sertraline in combination with a nanomedicine, Cancer Lett. 354 (2014) 290–298.

[11] F. Pampaloni, E.G. Reynaud, E.H.K. Stelzer, The third dimension bridges the gap between cell culture and live tissue, Nat. Rev. Mol. Cell Biol. 8 (2007) 839–845.
[12] D.W. Hutmacher, Biomaterials offer cancer research the third dimension, Nat. Mater. 9 (2010) 90–93.
[13] O.M. Benavides, A.R. Brooks, S.K. Cho, J.P. Connell, R. Ruano, J.G. Jacot, In situ vascularization of injectable fibrin/poly(ethylene glycol) hydrogles by human amniotic fluid-derived stem cells, J. Biomed. Mater. Res. A 103A (2015) 2645–2653.
[14] J. Shang, X. Le, J. Zhang, T. Chen, P. Theato, Trends in polymeric shape memory hydrogels and hydrogel actuators, Polym. Chem. 10 (2019) 1036–1055.
[15] E.M. Ahmed, Hydrogel: preparation, characterization, and applications: a review, J. Adv. Res. 6 (2015) 105–121.
[16] O. Wichterle, D. Lim, Hydrophilic gels for biological use, Nature 185 (1960) 117–118.
[17] S.J. Buwalda, K.W.M. Boere, P.J. Dijkstra, J. Feijen, T. Vermonden, W.E. Hennink, Hydrogels in a historical perspective: from simple networks to smart materials, J. Control. Release 190 (2014) 254–273.
[18] H.K. Lau, K.L. Kiick, Opportunities for multicomponent hybrid hydrogels in biomedical applications, Biomacromolecules 16 (2015) 28–42.
[19] S.J. Buwalda, T. Vermonden, W.E. Hennink, Hydrogels for therapeutic delivery: current developments and future directions, Biomacromolecules 18 (2017) 316–330.
[20] S. Rattan, L. Li, H.K. Lau, A.J. Crosby, K.L. Kiick, Micromechanical characterization of soft, biopolymeric hydrogels: stiffness, resilience, and failure, Soft Matter 14 (2018) 3478–3489.
[21] A. Sannino, C. Demitri, M. Madaghiele, Biodegradable cellulose-based hydrogels: design and applications, Materials 2 (2009) 353–373.
[22] A. Sosnik, K.P. Seremeta, Polymeric hydrogels as technology platform for drug delivery applications, Gels 3 (2017) 25, https://doi.org/10.3390/gels3030025.
[23] Q. Chai, Y. Jiao, X. Yu, Hydrogels for biomedical applications: their characteristics and the mechanisms behind them, Gels 3 (2017) 6, https://doi.org/10.3390/gels3010006.
[24] J.T. Zhang, S. Petersen, M. Thunga, E. Leipold, R. Weidisch, X. Liu, A. Fahr, K.D. Jandt, Micro-structured smart hydrogels with enhanced protein loading and release efficiency, Acta Biomater. 6 (2010) 1297–1306.
[25] Y. Shi, C. Ma, L. Peng, G. Yu, Conductive "smart" hybrid hydrogels with PNIPAM and nanostructured conductive polymers, Adv. Funct. Mater. 25 (2015) 1219–1225.
[26] A. Richter, G. Paschew, S. Klatt, J. Lienig, K.F. Arndt, H.J.P. Adler, Review on hydrogel-based pH sensors and microsensors, Sensors 8 (2008) 561–581.
[27] S. You, J. Li, W. Zhu, C. Yu, D. Mei, S. Chen, Nanoscale 3D printing of hydrogels for cellular tissue engineering, J. Mater. Chem. B 6 (2018) 2187–2197.
[28] E.P. Silva, M.R. Guilherme, F.P. Garcia, C.V. Nakamura, L. Cardozo-Filho, C.G. Alonso, A.F. Rubira, M.H. Kunita, Drug release profile and reduction in the *in vitro* burst release from pectin/HEMA hydrogel nanocomposites by crosslinking of titania, RSC Adv. 6 (2016) 19060–19068.
[29] F. Ullah, M.B.H. Othman, F. Javed, Z. Ahmad, H.M. Akil, Classification, processing and application of hydrogels: a review, Mater. Sci. Eng. C 57 (2015) 414–433.
[30] R.S.H. Wong, M. Ashton, K. Dodou, Effect of crosslinking agent concentration on the properties of unmedicated hydrogels, Pharmaceutics 7 (2015) 305–319.
[31] C. Tomasini, N. Castellucci, Peptides and peptidomimetics that behave as low molecular weight gelators, Chem. Soc. Rev. 42 (2013) 156–172.

[32] K. Varaprasad, G.M. Raghavendra, T. Jayaramudu, M.M. Yallapu, R. Sadiku, A mini review on hydrogels classification and recent developments in miscellaneous applications, Mater. Sci. Eng. C 79 (2017) 958–971.
[33] S.R. Raghavan, J.F. Douglas, The conundrum of gel formation by molecular nanofibers, wormlike micelles, and filamentous proteins: gelation without cross-links? Soft Matter 8 (2012) 8539–8546.
[34] M.D. Konieczynska, M.W. Grinstaf, Designing hydrogels for on-demand therapy, Acc. Chem. Res. 50 (2017) 151–160.
[35] F. Ahmadi, Z. Oveisi, S.M. Samani, Z. Amoozgar, Chitosan based hydrogels: characteristics and pharmaceutical applications, Res. Pharm. Sci. 10 (2015) 1–16.
[36] S. Dimida, C. Demitri, V.M.D. Benedictis, F. Scalera, F. Gervaso, A. Sannino, *In situ* synthesis of cabbage like polyaniline@hydroquinone nanocomposites and electrochemical capacitance investigations, J. Appl. Polym. Sci. 132 (2015) 42256, https://doi.org/10.1002/APP.42290.
[37] M. Rizwan, R. Yahya, A. Hassan, M. Yar, A.D. Azzahari, V. Selvanathan, F. Sonsudin, C.N. Abouloula, pH sensitive hydrogels in drug delivery: brief history, properties, swelling, and release mechanism, material selection and applications, Polymers 9 (2017) 137, https://doi.org/10.3390/polym9060225.
[38] L. Chen, X. Wang, W. Lu, X. Wu, J. Li, Molecular imprinting: perspectives and applications, Chem. Soc. Rev. 45 (2016) 2137–2211.
[39] L. Hu, Y. Sun, Y. Wu, Advances in chitosan-based drug delivery vehicles, Nanoscale 5 (2013) 3103–3111.
[40] S. Mavila, O. Eivgi, I. Berkovich, N.G. Lemcof, Intramolecular cross-linking methodologies for the synthesis of polymer nanoparticles, Chem. Rev. 116 (2016) 878–961.
[41] M.C.G. Pellá, M.K.L. Tenório, E.T.T. Neto, M.R. Guilherme, E.C. Muniz, A.F. Rubira, Chitosan-based hydrogels: from preparation to biomedical applications, Carbohydr. Polym. 196 (2018) 233–245.
[42] H. Tan, K.G. Marra, Injectable, biodegradable hydrogels for tissue engineering applications, Materials 3 (2010) 1746–1767.
[43] L. Marin, I. Stoica, M. Mares, V. Dinu, B.C. Simionescu, M. Barboiu, Antifungal vanillin-imino-chitosan biopolymeric flims, J. Mater. Chem. B 1 (2013) 3353–3358.
[44] C. Liu, E. Thormann, P.M. Claesson, E. Tyrode, Surface grafted chitosan gels. Part II. Gel formation and characterization, Langmuir 30 (2014) 8878–8888.
[45] F. Croisier, C. Jérôme, Chitosan-based biomaterials for tissue engineering, Eur. Polym. J. 49 (2013) 780–792.
[46] M. Dasha, F. Chiellini, R.M. Ottenbrite, E. Chiellini, Chitosan—a versatile semisynthetic polymer in biomedical applications, Prog. Polym. Sci. 36 (2011) 981–1014.
[47] R.A.A. Muzzarelli, Genipin-crosslinked chitosan hydrogels as biomedical and pharmaceutical aids, Carbohydr. Polym. 77 (2009) 1–9.
[48] C. Ghobril, M.W. Grinstaf, The chemistry and engineering of polymeric hydrogel adhesives for wound closure: a tutorial, Chem. Soc. Rev. 44 (2015) 1820–1835.
[49] W.H. Chang, Y. Chang, Y.C. Chen, H.W. Sung, Hemoglobin polymerized with a naturally occurring crosslinking agent as a blood substitute: in vitro and in vivo studies, Artif. Cells Blood Substit. Immobil. Biotechnol. 32 (2004) 243–262.
[50] J. Berger, M. Reist, J.M. Mayer, O. Felt, N.A. Peppas, R. Gurny, Structure and interactions in covalently and ionically crosslinked chitosan hydrogels for biomedical applications, Eur. J. Pharm. Biopharm. 57 (2004) 19–34.

[51] S.C. Chen, Y.C. Wu, F.L. Mi, Y.H. Lin, L.C. Yu, H.W. Sung, A novel pH-sensitive hydrogel composed of N,O-carboxymethyl chitosan and alginate cross-linked by genipin for protein drug delivery, J. Control. Release 96 (2004) 285–300.
[52] Y. Li, J. Rodrigues, H. Tomas, Injectable and biodegradable hydrogels: gelation, biodegradation and biomedical applications, Chem. Soc. Rev. 41 (2012) 2193–2221.
[53] C.M. Valmikinathan, V.J. Mukhatyar, A. Jain, L. Karumbaiah, M. Dasari, R.V. Bellamkonda, Photocrosslinkable chitosan based hydrogels for neural tissue engineering, Soft Matter 8 (2012) 1964–1976.
[54] J.V. Hoorick, P. Gruber, M. Markovic, M. Tromayer, J.V. Erps, H. Thienpont, R. Liska, A. Ovsianikov, P. Dubruel, S.V. Vlierberghe, Cross-linkable gelatins with superior mechanical properties through carboxylic acid modification: increasing the two-photon polymerization potential, Biomacromolecules 18 (2017) 3260–3272.
[55] C.C. Lin, Recent advances in crosslinking chemistry of biomimetic poly(ethylene glycol) hydrogels, RSC Adv. 5 (2015) 39844–398583.
[56] A. Das, P. Theato, Activated ester containing polymers: opportunities and challenges for the design of functional macromolecules, Chem. Rev. 116 (2016) 1434–1495.
[57] C.F. Nostrum, Covalently cross-linked amphiphilic block copolymer micelles, Soft Matter 7 (2011) 3246–3259.
[58] H. Hamedi, S. Moradi, S.M. Hudson, A.E. Tonelli, Chitosan based hydrogels and their applications for drug delivery in wound dressings: a review, Carbohydr. Polym. 199 (2018) 445–460.
[59] S. Czarnecki, T. Rossow, S. Seiffert, Hybrid polymer-network hydrogels with tunable mechanical response, Polymers 8 (2016) 82, https://doi.org/10.3390/polym8030082.
[60] C. Hiemstra, L.J. Aa, Z. Zhong, P.J. Dijkstra, J. Feijen, Novel in situ forming, degradable dextran hydrogels by Michael addition chemistry: synthesis, rheology, and degradation, Macromolecules 40 (2007) 1165–1173.
[61] P. Bulpitt, D. Aeschlimann, New strategy for chemical modification of hyaluronic acid: preparation of functionalized derivatives and their use in the formation of novel biocompatible hydrogels, J. Biomed. Mater. Res. 47 (1999) 152–169.
[62] M. Jaspers, S.L. Vaessen, P. Schayik, D. Voerman, A.E. Rowan, P.H.J. Kouwer, Nonlinear mechanics of hybrid polymer networks that mimic the complex mechanical environment of cells, Nat. Commun. 8 (2017) 15478, https://doi.org/10.1038/ncomms15478.
[63] S. Khan, A. Ullah, K. Ullah, N. Rehman, Insight into hydrogels, Des. Monomers Polym. 19 (2016) 456–478.
[64] C. Wang, R.J. Stewart, J. KopeCek, Hybrid hydrogels assembled from synthetic polymers and coiled-coil protein domains, Nature 397 (1999) 417–420.
[65] L. Racine, I. Texier, R.A. Velty, Chitosan-based hydrogels: recent design concepts to tailor properties and functions, Polym. Int. 66 (2017) 981–998.
[66] E.S. Dragan, Design and applications of interpenetrating polymer network hydrogels. A review, Chem. Eng. J. 243 (2014) 572–590.
[67] D. Myung, D. Waters, M. Wiseman, P.E. Duhame, J. Noolandi, C.N. Ta, C.W. Frank, Progress in the development of interpenetrating polymer network hydrogels, Polym. Adv. Technol. 19 (2008) 647–657.
[68] N. Naseri, B. Deepa, A.P. Mathew, K. Oksman, L. Girandon, Nanocellulose-based interpenetrating polymer network (IPN) hydrogels for cartilage applications, Biomacromolecules 17 (2016) 3714–3723.
[69] A.K. Bajpai, S.K. Shukla, S. Bhanu, S. Kankane, Responsive polymers in controlled drug delivery, Prog. Polym. Sci. 33 (2008) 1088–1118.

[70] E.L. Bakota, L. Aulisa, K.M. Galler, J.D. Hartgerink, Enzymatic cross-linking of a nanofibrous peptide hydrogel, Biomacromolecules 12 (2011) 82–87.
[71] M.A. Silva, F. Bode, A.F. Drake, S. Goldoni, M.M. Stevens, C.A. Dreiss, Enzymatically cross-linked gelatin/chitosan hydrogels: tuning gel properties and cellular response, Macromol. Biosci. 14 (2014) 817–830.
[72] J.J. Sperinde, L.G. Griffith, Control and prediction of gelation kinetics in enzymatically cross-linked poly(ethylene glycol) hydrogels, Macromolecules 33 (2000) 5476–5480.
[73] S. Kobayashi, H. Uyama, S. Kimura, Enzymatic polymerization, Chem. Rev. 101 (2001) 3793–3818.
[74] K.H. Bae, L.S. Wang, M. Kurisawa, Injectable biodegradable hydrogels: progress and challenges, J. Mater. Chem. B 1 (2013) 5371–5388.
[75] Y.P. Singh, J.C. Moses, N. Bhardwaj, B.B. Mandal, Injectable hydrogels: a new paradigm for osteochondral tissue engineering, J. Mater. Chem. B 6 (2018) 5499–5529.
[76] T. Chen, H.D. Embree, L.Q. Wu, G.F. Payne, In vitro protein–polysaccharide conjugation: tyrosinase-catalyzed conjugation of gelatin and chitosan, Biopolymers 64 (2002) 292–302.
[77] L.S.M. Teixeira, J. Feijen, C.A. Blitterswijk, P.J. Dijkstra, M. Karperien, Enzyme-catalyzed crosslinkable hydrogels: emerging strategies for tissue engineering, Biomaterials 33 (2012) 1281–1290.
[78] D.F. Coutinho, S.V. Sant, H. Shin, J.T. Oliveira, M.E. Gomes, N.M. Neves, A. Khademhosseini, R.L. Reis, Modified Gellan Gum hydrogels with tunable physical and mechanical properties, Biomaterials 31 (2010) 7494–7502.
[79] W.E. Hennink, C.F. van Nostrum, Novel crosslinking methods to design hydrogels, Adv. Drug Deliv. Rev. 64 (2012) 223–236.
[80] M. Patenaude, N.M.B. Smeets, T. Hoare, Designing injectable, covalently cross-linked hydrogels for biomedical applications, Macromol. Rapid Commun. 35 (2014) 598–617.
[81] G. Song, L. Zhang, C. He, D.C. Fang, P.G. Whitten, H. Wang, Facile fabrication of tough hydrogels physically cross-linked by strong cooperative hydrogen bonding, Macromolecules 46 (2013) 7423–7435.
[82] T.R. Hoare, D.S. Kohane, Hydrogels in drug delivery: progress and challenges, Polymer 49 (2008) 1993–2007.
[83] J.D. Schiffman, C.L. Schauer, Cross-linking chitosan nanofibers, Biomacromolecules 8 (2007) 594–601.
[84] X. Shen, J.L. Shamshina, P. Berton, G. Gurau, R.D. Rogers, Hydrogels based on cellulose and chitin: fabrication, properties, and applications, Green Chem. 18 (2016) 53–75.
[85] X. Ding, Y. Wang, Weak bond-based injectable and stimuli responsive hydrogels for biomedical applications, J. Mater. Chem. B 5 (2017) 887–906.
[86] A. Doring, W. Birnbaum, D. Kuckling, Responsive hydrogels–structurally and dimensionally optimized smart frameworks for applications in catalysis, micro-system technology and material science, Chem. Soc. Rev. 42 (2013) 7391–7420.
[87] S. Datta, S. Bhattacharya, Multifarious facets of sugar-derived molecular gels: molecular features, mechanisms of self-assembly and emerging applications, Chem. Soc. Rev. 44 (2015) 5596–5637.
[88] J.H. Jung, G. John, M. Masuda, K. Yoshida, S. Shinkai, T. Shimizu, Self-assembly of a sugar-based gelator in water: its remarkable diversity in gelation ability and aggregate structure, Langmuir 17 (2001) 7229–7232.
[89] L.H. Fu, C. Qi, M.G. Ma, P. Wan, Multifunctional cellulose-based hydrogels for biomedical applications, J. Mater. Chem. B 7 (2019) 1541–1562.

[90] Q. Huang, Y. Zou, M.C. Arno, S. Chen, T. Wang, J. Gao, A.P. Dove, J. Du, Hydrogel scaffolds for differentiation of adipose-derived stem cells, Chem. Soc. Rev. 46 (2017) 6255–6275.
[91] Q. Li, Intelligent Stimuli-Responsive Materials: From Well-Defined Nanostructures to Applications, John Wiley & Sons, 2013 Technology & Engineering.
[92] E.M. White, J. Yatvin, J.B. Grubbs III, J.A. Bilbrey, J. Locklin, Advances in smart materials: stimuli-responsive hydrogel thin films, J. Polym. Sci. B Polym. Phys. 51 (2013) 1084–1099.
[93] K. Bauri, M. Nandi, P. De, Amino acid-derived stimuli-responsive polymers and their applications, Polym. Chem. 9 (2018) 1257–1287.
[94] Y. Lu, W. Sun, Z. Gu, Stimuli-responsive nanomaterials for therapeutic protein delivery, J. Control. Release 194 (2014) 1–19.
[95] C.G. Wiener, R.A. Weiss, B.D. Vogt, Overcoming confinement limited swelling in hydrogel thin films using supramolecular interactions, Soft Matter 10 (2014) 6705–6712.
[96] E.R. Ruskowitz, M.P. Comerford, B.A. Badeau, C.A. DeForest, Logical stimuli-triggered delivery of small molecules from hydrogel biomaterials, Biomater. Sci. 7 (2019) 542–546.
[97] F. Li, J. He, M. Zhang, K.C. Tam, P. Ni, Injectable supramolecular hydrogels fabricated from PEGylated doxorubicin prodrug and α-cyclodextrin for pH-triggered drug delivery, RSC Adv. 5 (2015) 54658–54666.
[98] Y. Zhang, J.W. Chan, A. Moretti, K.E. Uhrich, Designing polymers with sugar-based advantages for bioactive delivery applications, J. Control. Release 219 (2015) 355–368.
[99] J. Huang, X. Jiang, Injectable and degradable pH-responsive hydrogels via spontaneous amino–Yne click reaction, ACS Appl. Mater. Interfaces 10 (2018) 361–370.
[100] J.X. Ding, J.J. Chen, D. Li, C.S. Xiao, J.C. Zhang, C.L. He, X.L. Zhuang, X.S. Chen, Biocompatible reduction-responsive polypeptide micelles as nanocarriers for enhanced chemotherapy efficacy in vitro, J. Mater. Chem. B 1 (2013) 69–81.
[101] D. Pati, A.Y. Shaikh, S. Das, P.K. Nareddy, M.J. Swamy, S. Hotha, S. Sen Gupta, Controlled synthesis of O-glycopolypeptide polymers and their molecular recognition by lectins, Biomacromolecules 13 (2012) 1287–1295.
[102] K. Zubik, P. Singhsa, Y. Wang, H. Manuspiya, R. Narain, Thermo-responsive poly (*N*-isopropylacrylamide)-cellulose nanocrystals hybrid hydrogels for wound dressing, Polymers 9 (2017) 119, https://doi.org/10.3390/polym9040119.
[103] B.L. Guo, Q.Y. Gao, Preparation and properties of a pH/temperature-responsive carboxymethyl chitosan/poly(*N*-isopropylacrylamide)semi-IPN hydrogel for oral delivery of drugs, Carbohydr. Res. 342 (2007) 2416–2422.
[104] J. Liu, Y. Yin, Temperature responsive hydrogels: construction and applications, Polym. Sci. 1 (2015), https://doi.org/10.21767/2471-9935.100003.
[105] E. Mah, R. Ghosh, Thermo-responsive hydrogels for stimuli-responsive membranes, Processes 1 (2013) 238–262.
[106] H.P. James, R. John, A. Alex, K.R. Anoop, Smart polymers for the controlled delivery of drugs—a concise overview, Acta Pharm. Sin. B 4 (2014) 120–127.
[107] L. Klouda, A.G. Mikos, Thermoresponsive hydrogels in biomedical applications—a review, Eur. J. Pharm. Biopharm. 68 (2008) 34–45.
[108] M. Mihajlovic, H.M. Wyss, R.P. Sijbesma, Effects of surfactant and urea on dynamics and viscoelastic properties of hydrophobically assembled supramolecular hydrogel, Macromolecules 51 (2018) 4813–4820.
[109] J.R. Dorvee, A. Veis, Water in the formation of biogenic minerals: peeling away the hydration layers, J. Struct. Biol. 183 (2013) 278–303.

[110] V.K. Thakur, M.K. Thakur, Polymer Gels: Synthesis and Characterization, Gels Horizons: From Science to Smart Materials, (2018). ISBN 978-981-10-6083-0, https://doi.org/10.1007/978-981-10-6083-0.

[111] J. Kydd, R. Jadia, P. Velpurisiva, A. Gad, S. Paliwal, P. Rai, Targeting strategies for the combination treatment of cancer using drug delivery systems, Pharmaceutics 9 (2017) 46, https://doi.org/10.3390/pharmaceutics9040046.

[112] W. Guo, L. Deng, J. Yu, Z. Chen, Y. Woo, H. Liu, T. Li, T. Lin, H. Chen, M. Zhao, L. Zhang, G. Li, Y. Hu, Sericin nanomicelles with enhanced cellular uptake and pH-triggered release of doxorubicin reverse cancer drug resistance, Drug Deliv. 25 (2018) 1103–1116.

[113] A. Madhusudhan, G.B. Reddy, M. Venkatesham, G. Veerabhadram, D.A. Kumar, S. Natarajan, M.Y. Yang, A. Hu, S.S. Singh, Efficient pH dependent drug delivery to target cancer cells by gold nanoparticles capped with carboxymethyl chitosan, Int. J. Mol. Sci. 15 (2014) 8216–8234.

[114] Y. Chen, R. Cairns, I. Papandreou, A. Koong, N.C. Denko, Oxygen consumption can regulate the growth of tumors, a new perspective on the Warburg effect, PLoS ONE 4 (2009) e7033, https://doi.org/10.1371/journal.pone.0007033.

[115] N. Hammad, M.R. Lemus, S.U. Carvajal, M. Rigoulet, A. Devin, The Crabtree and Warburg effects: do metabolite-induced regulations participate in their induction? Biochim. Biophys. Acta 1857 (2016) 1139–1146.

[116] S. Maity, A. Datta, S. Lahiri, J. Ganguly, Selective separation of ^{152}Eu from a mixture of ^{152}Eu and ^{137}Cs using a chitosan based hydrogel, RSC Adv. 5 (2015) 89338–89345.

[117] A.R. Hibbins, P. Kumar, Y.E. Choonara, P.P.D. Kondiah, T. Marimuthu, L.C. Toit, V. Pillay, Design of a versatile pH-responsive hydrogel for potential oral delivery of gastric-sensitive bioactives, Polymers 9 (2017) 474, https://doi.org/10.3390/polym9100474.

[118] S. Maity, A. Chatterjee, N. Chakraborty, J. Ganguly, A dynamic sugar based bio-inspired, self-healing hydrogel exhibiting ESIPT, New J. Chem. 42 (2018) 5946–5954.

[119] I. Tomatsu, K. Peng, A. Kros, Photoresponsive hydrogels for biomedical applications, Adv. Drug Deliv. Rev. 63 (2011) 1257–1266.

[120] L. Li, J.M. Scheiger, P.A. Levkin, Design and applications of photoresponsive hydrogels, Adv. Mater. (2019)1807333 https://doi.org/10.1002/adma.201807333.

[121] H. Kang, H. Liu, X. Zhang, J. Yan, Z. Zhu, L. Peng, H. Yang, Y. Kim, W. Tan, Photoresponsive DNA-crosslinked hydrogels for controllable release and cancer therapy, Langmuir 27 (2011) 399–408.

[122] S. Kazakov, Hydrogel films on optical fiber core: properties, challenges, and prospects for future applications, in: New Polymers for Special Applications, (Chapter: 2). InTech, 2012 https://doi.org/10.5772/48371 .

[123] G.S. Longo, M.O. Cruzbc, I. Szleifer, Controlling swelling/deswelling of stimuliresponsive hydrogel nanofilms in electric fields, Soft Matter 12 (2016) 8359–8366.

[124] S.J. Kim, S.G. Yoon, K.B. Lee, Y.D. Park, S.I. Kim, Electrical sensitive behavior of a polyelectrolyte complex composed of chitosan/hyaluronic acid, Solid State Ionics 164 (2003) 199–204.

[125] P. Verbrugghe, J. Verhoeven, W. Coudyzer, E. Verbeken, P. Dubruel, E. Mendes, F. Stam, B. Meuris, P. Herijgers, An electro-responsive hydrogel for intravascular applications: an in vitro and in vivo evaluation, J. Mater. Sci. Mater. Med. 26 (2015) 264, https://doi.org/10.1007/s10856-015-5598-9.

[126] N. Jackson, F. Stam, Optimization of electrical stimulation parameters for electro-responsive hydrogels for biomedical applications, J. Appl. Polym. Sci. 132 (2015) 41687, https://doi.org/10.1002/APP.41687.
[127] X. Yu, Q. Liu, J. Wu, M. Zhang, X. Cao, S. Zhang, Q. Wang, L. Chen, T. Yi, Sonication-triggered instantaneous gel-to-gel transformation, Chem. Eur. J. 16 (2010) 9099–9106.
[128] Y. Sang, M. Liu, Nanoarchitectonics through supramolecular gelation: formation and switching of diverse nanostructures, Mol. Syst. Des. Eng. 4 (2019) 11–28.
[129] L. Geng, X. Yu, Y. Li, Y. Wang, Y. Wu, J. Ren, F. Xue, T. Yi, Instant hydrogel formation of terpyridine-based complexes triggered by DNA via non-covalent interaction, Nanoscale 11 (2019) 4044–4052.
[130] X. Guo, Y. Cheng, X. Zhao, Y. Luo, J. Chen, W.E. Yuan, Advances in redox-responsive drug delivery systems of tumor microenvironment, J. Nanobiotechnology 16 (2018) 74, https://doi.org/10.1186/s12951-018-0398-2.
[131] G. Hermann, P. Heffeter, K. Kryeziu, W. Berger, S. Hann, G. Koellensperger, Studying reduced versus oxidized glutathione in cancer cell models employing isotopically labelled standards, Anal. Methods 6 (2014) 3086–3094.
[132] A.T. Dharmaraja, Role of reactive oxygen species (ROS) in therapeutics and drug resistance in cancer and bacteria, J. Med. Chem. 60 (2017) 3221–3240.
[133] P. Matricardi, F. Alhaique, T. Coviello, Polysaccharide Hydrogels: Characterization and Biomedical Applications, Taylor & Francis Group, 2015. ISBN 9789814613613.
[134] J.K. Chen, C.J. Chang, Fabrications and applications of stimulus-responsive polymer films and patterns on surfaces: a review, Materials 7 (2014) 805–875.
[135] A. Matsumoto, M. Tanaka, H. Matsumoto, K. Ochi, Y. Moro-oka, H. Kuwata, H. Yamada, I. Shirakawa, T. Miyazawa, H. Ishii, K. Kataoka, Y. Ogawa, Y. Miyahara, T. Suganami, Synthetic "smart gel" provides glucose-responsive insulin delivery in diabetic mice, Sci. Adv. 3 (2017) eaaq0723.
[136] M.J. Abdekhodaie, X.Y. Wu, Modeling of a glucose sensitive composite membrane for closed-loop insulin delivery, J. Membr. Sci. 335 (2009) 21–31.
[137] D. Bruen, C. Delaney, L. Florea, D. Diamond, Glucose sensing for diabetes monitoring: recent developments, Sensors 17 (2017) 1866, https://doi.org/10.3390/s17081866.
[138] B. Mishra, M. Upadhyay, S.K.A. Reddy, B.G. Vasant, M.S. Muthu, Hydrogels: an introduction to a controlled drug delivery device, synthesis and application in drug delivery and tissue engineering, Austin J. Biomed. Eng. 2381-9081, 4 (2017) 1037.
[139] T. Elshaarani, H. Yu, L. Wang, Z. ul-Abdin, R.S. Ullah, M. Haroon, R.U. Khan, S. Fahad, A. Khan, A. Nazir, M. Usman, K. ur Rahman, Synthesis of hydrogels-bearing phenylboronic acid moieties and their applications in glucose sensing and insulin delivery, J. Mater. Chem. B 6 (2018) 3831–3854.
[140] D.B. Stein, Handbook of Hydrogels—Properties, Preparation & Applications, Nova Science Publishers, Inc., New York, 2009.
[141] S. Rimmer, Biomedical Hydrogels–Biochemistry, Manufacture and Medical Applications, Woodhead Publishing in Materials, 2011. ISBN 978-0-85709-138-3.
[142] R.A. Caminero, L.P. Herrera, C.A.R. Martinez, J. Almodovar, Polymeric scaffolds for three-dimensional culture of nerve cells: a model of peripheral nerve regeneration, MRS Commun. 7 (2017) 391–415.
[143] S. Reakasame, A.R. Boccaccini, Oxidized alginate-based hydrogels for tissue engineering applications: a review, Biomacromolecules 19 (2018) 3–21.
[144] T. Andersen, P.A. Emblem, M. Dornish, 3D cell culture in alginate hydrogels, Microarrays 4 (2015) 133–161.

[145] A.S. Hoffman, G. Schmer, C. Harris, W.G. Kraft, Covalent binding of biomolecules to radiation-grafted hydrogels on inert polymer surfaces, Trans. Am. Soc. Artif. Intern. Organs 18 (1972) 10–18.
[146] B.D. Ratner, A.S. Hoffman, Synthetic hydrogels for biomedical applications, in: Hydrogels for Medical and Related Applications, ACS Symposium Series vol. 31, 1976, pp. 1–36.
[147] A.W. Holle, J.L. Young, J.P. Spatz, In vitro cancer cell–ECM interactions inform in vivo cancer treatment, Adv. Drug Deliv. Rev. 97 (2016) 270–279.
[148] N.A. Peppas, Hydrogels in medicine and pharmacy, Polym. Int. 21 (1989), https://doi.org/10.1002/pi.4980210223.
[149] J. Kondo, H. Endo, H. Okuyama, O. Ishikawa, H. Iishi, M. Tsujii, M. Ohue, M. Inoue, Retaining cell–cell contact enables preparation and culture of spheroids composed of pure primary cancer cells from colorectal cancer, Proc. Natl. Acad. Sci. U. S. A. 108 (2011) 6235–6240.
[150] K.E. Sung, D.J. Beebe, Microfluidic 3D models of cancer, Adv. Drug Deliv. Rev. 79–80 (2014) 68–78.
[151] C.L. Scott, M.A. Becker, P. Haluska, G. Samimi, Patient-derived xenograft models to improve targeted therapy in epithelial ovarian cancer treatment, Front. Oncol. 3 (2013) 295, https://doi.org/10.3389/fonc.2013.00295.
[152] H.J. Kong, D.J. Mooney, Microenvironmental regulation of biomacromolecular therapies, Nat. Rev. Drug Discov. 6 (2007) 455–463.
[153] S.R. Caliari, J.A. Burdick, A practical guide to hydrogels for cell culture, Nat. Methods 13 (2016) 405–414.
[154] J. Thiele, Y. Ma, S.M.C. Bruekers, S. Ma, W.T.S. Huck, Designer hydrogels for cell cultures: a materials selection guide, Adv. Mater. 26 (2014) 125–148.
[155] K.M. Tevis, Y.L. Colson, M.W. Grinstaff, Embedded spheroids as models of the cancer microenvironment, Adv. Biosyst. 1 (2017)1700083.
[156] W. Zhang, C. Li, B.C. Baguley, F. Zhou, W. Zhou, J.P. Shaw, Z. Wang, Z. Wu, J. Liu, Optimization of the formation of embedded multicellular spheroids of MCF-7 cells: how to reliably produce a biomimetic 3D model, Anal. Biochem. 515 (2016) 47–54.
[157] T. Arai, O. Benny, T. Joki, L.G. Menon, M. Machluf, T. Abe, R.S. Carroll, P.M. Black, Novel local drug delivery system using thermoreversible gel in combination with polymeric microspheres or liposomes, Anticancer Res. 30 (2010) 1057–1064.
[158] T. Arai, T. Joki, M. Akiyama, M. Agawa, Y. Mori, H. Yoshioka, T. Abe, Novel drug delivery system using thermoreversible gelation polymer for malignant glioma, J. Neurooncol. 77 (2006) 9–15.
[159] N. Qi, C. Cai, W. Zhang, Y. Niu, J. Yang, L. Wang, B. Tian, X. Liu, X. Lin, Y. Zhang, Y. Zhang, H. He, K. Chen, X. Tang, Sustained delivery of cytarabine-loaded vesicular phospholipid gels for treatment of xenografted glioma, Int. J. Pharm. 472 (2014) 48–55.
[160] S. Kim, S.K. Nishimoto, J.D. Bumgardner, W.O. Haggard, M.W. Gaber, Y. Yang, A chitosan/beta-glycerophosphate thermo-sensitive gel for the delivery of ellagic acid for the treatment of brain cancer, Biomaterials 31 (2010) 4157–4166.
[161] T. Ozeki, K. Hashizawa, D. Kaneko, Y. Imai, H. Okada, Treatment of rat brain tumors using sustained-release of camptothecin from poly(lactic-co-glycolic acid) microspheres in a thermoreversible hydrogel, Chem. Pharm. Bull. 58 (2010) 1142–1147.
[162] S.H. Ranganath, I. Kee, W.B. Krantz, P.K. Chow, C.H. Wang, Hydrogel matrix entrapping PLGA-paclitaxel microspheres: drug delivery with near zero-order release and implantability advantages for malignant brain tumour chemotherapy, Pharm. Res. 26 (2009) 2101–2114.

[163] N. Qi, X. Tang, X. Lin, P. Gu, C. Cai, H. Xu, H. He, Y. Zhang, Sterilization stability of vesicular phospholipid gels loaded with cytarabine for brain implant, Int. J. Pharm. 427 (2012) 234–241.
[164] A. Vashist, A. Vashist, Y.K. Gupta, S. Ahmad, Recent advances in hydrogel based drug delivery systems for the human body, J. Mater. Chem. B 2 (2014) 147–166.
[165] C. Shu, R. Li, Y. Yin, D. Yin, Y. Gu, L. Ding, W. Zhong, Synergistic dual-targeting hydrogel improves targeting and anticancer effect of Taxol *in vitro* and *in vivo*, Chem. Commun. 50 (2014) 15423–15426.
[166] P.Z. Elias, G.W. Liu, H. Wei, M.C. Jensen, P.J. Horner, S.H. Pun, A functionalized, injectable hydrogel for localized drug delivery with tunable thermosensitivity: synthesis and characterization of physical and toxicological properties, J. Control. Release 208 (2015) 76–84.
[167] B. Xue, V. Kozlovskaya, F. Liu, J. Chen, J.F. Williams, J.C. Gomez, M. Saeed, E. Kharlampieva, Intracellular degradable hydrogel cubes and spheres for anti-cancer drug delivery, ACS Appl. Mater. Interfaces 7 (2015) 13633–13644.
[168] S.D. Steichen, M.C. Moore, N.A. Peppas, A review of current nanoparticle and targeting moieties for the delivery of cancer therapeutics, Eur. J. Pharm. Sci. 48 (2013) 416–427.
[169] T. Ozeki, D. Kaneko, K. Hashizawa, Y. Imai, T. Tagami, H. Okada, Improvement of survival in C6 rat glioma model by a sustained drug release from localized PLGA microspheres in a thermoreversible hydrogel, Int. J. Pharm. 427 (2012) 299–304.
[170] R. Würth, S. Thellung, A. Bajetto, M. Mazzanti, T. Florio, F. Barbieri, Drug-repositioning opportunities for cancer therapy: novel molecular targets for known compounds, Drug Discov. Today 21 (2015) 190–199.
[171] S.R. Paliwal, R. Paliwal, H.C. Pal, A.K. Saxena, P.R. Sharma, P.N. Gupta, G.P. Agrawal, S.P. Vyas, Estrogen-anchored pH-sensitive liposomes as nanomodule designed for site-specific delivery of doxorubicin in breast cancer therapy, Mol. Pharm. 9 (2011) 176–186.
[172] M. Kohno, T. Horibe, M. Haramoto, Y. Yano, K. Ohara, O. Nakajima, K. Matsuzaki, K. Kawakami, A novel hybrid peptide targeting EGFR-expressing cancers, Eur. J. Cancer 47 (2011) 773–783.
[173] A. Gaowa, T. Horibe, M. Kohno, K. Sato, H. Harada, M. Hiraoka, Y. Tabata, K. Kawakami, Combination of hybrid peptide with biodegradable gelatin hydrogel for controlled release and enhancement of anti-tumor activity *in vivo*, J. Control. Release 176 (2014) 1–7.
[174] N. Ferrara, K.J. Hillan, W. Novotny, Bevacizumab (Avastin), a humanized anti-VEGF monoclonal antibody for cancer therapy, Biochem. Biophys. Res. Commun. 333 (2005) 328–335.
[175] J. Summers, M.H. Cohen, P. Keegan, R. Pazdur, FDA drug approval summary: bevacizumab plus interferon for advanced renal cell carcinoma, Oncologist 15 (2010) 104–111.
[176] A.L.Z. Lee, V.W.L. Ng, S. Gao, J.L. Hedrick, Y.Y. Yang, Injectable biodegradable hydrogels from vitamin D-functionalized polycarbonates for the delivery of avastin with enhanced therapeutic efficiency against metastatic colorectal cancer, Biomacromolecules 16 (2015) 465–475.
[177] U. Akbar, T. Jones, J. Winestone, M. Michael, A. Shukla, Y. Sun, C. Duntsch, Delivery of temozolomide to the tumor bed via biodegradable gel matrices in a novel model of intracranial glioma with resection, J. Neuro-Oncol. 94 (2009) 203–212.
[178] S.V. Petit, D. Jarnet, S. Michalak, A. Lewis, J.P. Benoit, P. Menei, Local implantation of doxorubicin drug eluting beads in rat glioma, Int. J. Pharm. 402 (2010) 184–189.

[179] C.T. Tsao, F.M. Kievit, A. Ravanpay, A.E. Erickson, M.C. Jensen, R.G. Ellenbogen, M. Zhang, Thermoreversible poly(ethylene glycol)-*g*-chitosan hydrogel as a therapeutic T lymphocyte depot for localized glioblastoma immunotherapy, Biomacromolecules 15 (2014) 2656–2662.
[180] Y. Xu, M. Shen, Y. Sun, P. Gao, Y. Duan, Polymer nanocomposites based thermo-sensitive gel for paclitaxel and temozolomide co-delivery to glioblastoma cells, J. Nanosci. Nanotechnol. 15 (2015) 9777–9787.
[181] H.D. Han, C.K. Song, Y.S. Park, K.H. Noh, J.H. Kim, T. Hwang, T.W. Kim, B.C. Shin, A chitosan hydrogel-based cancer drug delivery system exhibits synergistic antitumor effects by combining with a vaccinia viral vaccine, Int. J. Pharm. 350 (2008) 27–34.
[182] H.M. Abdel-Bar, A.Y. Abdel-Reheem, R. Osman, G.A.S. Awad, N. Mortada, Defining cisplatin incorporation properties in thermosensitive injectable biodegradable hydrogel for sustained delivery and enhanced cytotoxicity, Int. J. Pharm. 477 (2014) 623–630.
[183] S. Kim, S.K. Nishimoto, J.D. Bumgardner, W.O. Haggard, M.W. Gaber, Y. Yang, A chitosan/β-glycerophosphate thermo-sensitive gel for the delivery of ellagic acid for the treatment of brain cancer, Biomaterials 31 (2010) 4157–4166.
[184] J. Shi, W. Guobao, H. Chen, W. Zhong, X. Qiu, M.M.Q. Xing, Schiff based injectable hydrogel for in situ pH-triggered delivery of doxorubicin for breast tumor treatment, Polym. Chem. 5 (2014) 6180–6189.
[185] L. Xiong, Q. Luo, Y. Wang, X. Li, Z. Shen, W. Zhu, An injectable drug-loaded hydrogel based on a supramolecular polymeric prodrug, Chem. Commun. 51 (2015) 14644–14647.

Further reading

[186] R. Parhi, Cross-linked hydrogel for pharmaceutical applications: a review, Adv. Pharm. Bull. 7 (2017) 515–530.
[187] Y. Sun, L. Du, Y. Liu, X. Li, M. Li, Y. Jin, X. Qian, Transdermal delivery of the in situ hydrogels of curcumin and its inclusion complexes of hydroxypropyl-β-cyclodextrin for melanoma treatment, Int. J. Pharm. 469 (2014) 31–39.
[188] C.M.G. Marques, S. MacNeil, Use of a tissue engineered human skin model to investigate the effects of wounding and of an anti-inflammatory on melanoma cell invasion, PLoS ONE 11 (2016) e0156931, https://doi.org/10.1371/journal.pone.0156931.
[189] J. Liu, C. Qi, K. Tao, J. Zhang, J. Zhang, L. Xu, X. Jiang, Y. Zhang, L. Huang, Q. Li, H. Xie, J. Gao, X. Shuai, G. Wang, Z. Wang, L. Wang, Sericin/dextran injectable hydrogel as an optically trackable drug delivery system for malignant melanoma treatment, ACS Appl. Mater. Interfaces 8 (2016) 6411–6422.
[190] L. Zhao, L. Zhu, F. Liu, C. Liu, S. Dan, Q. Wang, C. Zhang, J. Li, J. Liu, X. Qu, Z. Yang, pH triggered injectable amphiphilic hydrogel containing doxorubicin and paclitaxel, Int. J. Pharm. 410 (2011) 83–91.
[191] G. Landskron, M.L. Fuente, P. Thuwajit, C. Thuwajit, M.A. Hermoso, Chronic inflammation and cytokines in the tumor microenvironment, J. Immunol. 2014 (2014)149185, https://doi.org/10.1155/2014/149185.
[192] M. Redpath, C.M.G. Marques, C. Dibden, A. Waddon, R. Lalla, S. MacNeil, Ibuprofen and hydrogel-released ibuprofen in the reduction of inflammation-induced migration in melanoma cells, Br. J. Dermatol. 161 (2009) 25–33.

[193] A. Monette, C. Ceccaldi, E. Assaad, S. Lerouge, R. Lapointe, Chitosan thermogels for local expansion and delivery of tumor-specific T lymphocytes towards enhanced cancer immunotherapies, Biomaterials 75 (2016) 237–249.
[194] B. Al-Lazikani, U. Banerji, P. Workman, Combinatorial drug therapy for cancer in the post-genomic era, Nat. Biotechnol. 30 (2012) 679–692.
[195] D.S. Rigel, J.A. Carucci, Malignant melanoma: prevention, early detection, and treatment in the 21st century, CA Cancer J. Clin. 50 (2000) 215–236.

Green synthesis and biological evaluation of anticancer drugs

19

Bimal Krishna Banik[a], *Biswa Mohan Sahoo*[b,*]
[a]Department of Mathematics and Natural Sciences, College of Sciences and Human Studies, Deanship of Research Development, Prince Mohammad Bin Fahd University, Al Khobar, Kingdom of Saudi Arabia, [b]Roland Institute of Pharmaceutical Sciences, Berhampur, India
[*]Corresponding author. e-mail address: drbiswamohansahoo@gmail.com

Abbreviations

%	percent
CDER	Center for Drug Evaluation and Research
DMA	dimethyl acetal
DMF	dimethyl formamide
DNA	deoxyribonucleic acid
EPA	Environmental Protection Agency
GI_{50}	concentration exhibiting 50% inhibition of growth
IC_{50}	inhibitory concentration
MAOS	microwave-assisted organic synthesis
min	minute
mL	milliliter
MTT	3-(4,5-dimethylthiazol-2-yl)-2,5-diphenyl tetrazolium bromide
MWI	microwave irradiation
ND	not determined
USFDA	U.S. Food and Drug Administration
USI	ultrasound irradiation
W	watt
μM	micrometer

19.1 Introduction

Cancer is a group of diseases which cause abnormal cell growth and spread to different parts of the body. According to the American Cancer Society, 7.6 million people died from cancer in the world during 2007. Cancer is the second leading cause of death globally and is responsible for an estimated 9.6 million deaths in 2018. Globally, about 1 in 6 deaths is due to cancer. Around one-third of deaths from cancer are due to five major behavioral and dietary factors such as high body mass index, low fruits and vegetables intake, lack of physical activity, consumption of tobacco and alcohol. In 2017, the World Health Assembly passed the resolution related to cancer prevention and control through an integrated approach and has also accelerated the action to achieve

Green Approaches in Medicinal Chemistry for Sustainable Drug Design. https://doi.org/10.1016/B978-0-12-817592-7.00019-8
© 2020 Elsevier Inc. All rights reserved.

the targets specified in the global action plan and 2030 UN agenda for sustainable development to reduce premature mortality from cancer [1].

The cancerous cells may produce a mass called as tumor. Tumor is categorized into two types such as cancerous or benign. Cancerous tumor is considered as malignant because it grows and spreads to other parts of the body whereas benign tumor can grow but it will not spread throughout the body as outlined in Fig. 19.1. The bloodstream or lymphatic systems carry the cancer cells to other parts of the body and the process is called as metastasis. The occurrence of different types of cancer is influenced by several factors such as age, gender, race, environment, diet, and genetics. The sign and symptoms of cancer depend on the type and grade of cancer which include fatigue, weight loss, pain, skin changes, change in bowel movement or bladder function, unusual bleeding, persistent cough, fever, and lumps. According to the type and stage of cancer, various treatment protocols are followed such as surgery, chemotherapy, radiation therapy, hormonal, gene, and immune therapy [2].

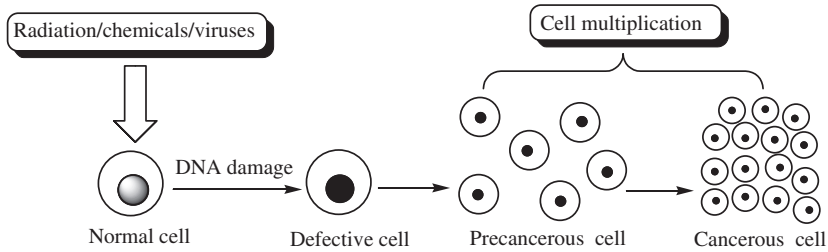

Fig. 19.1 Stages of cancer development.

19.1.1 Types of cancer

The different types of cancers are named for the area in which they begin and the type of cell they are made of, even if they spread to other parts of the body. For example, a cancer that starts in the lungs and spreads to the liver is termed as lung cancer [3]. Several terms used clinically for various types of cancer are as follows.

a. **Carcinomas:** It begins in the skin which covers the surface of internal organs and glands. Examples of carcinomas include prostate cancer, breast cancer, lung cancer, and colorectal cancer.
b. **Sarcomas:** It begins in the tissues that support and connect the body. It grows in fat, muscles, nerves, tendons, joints, blood vessels, lymph vessels, cartilage, and bone.
c. **Leukemias:** It is a cancer of the blood. There are four types of leukemia such as acute lym phocytic leukemia, chronic lymphocytic leukemia, acute myeloid leukemia, and chronic myeloid leukemia.
d. **Lymphomas:** It is a cancer which begins in the lymphatic system. There are two types of lymphomas such as Hodgkin lymphoma and non-Hodgkin lymphoma.
e. **Brain and spinal cord cancers:** Cancer starts in the cells of the brain or spinal cord. These are known as central nervous system cancers.

19.1.2 Major features of cancer

In 2000, as per the article by Hanahan and Weinberg, the major features of tumor cells are summarized as follows [4]:

- Acquisition of self-sufficiency in growth signals which leads to uncontrolled growth.
- Loss of sensitivity to antigrowth signals also leads unchecked growth.
- Loss of sensitivity to growth signals.
- Loss of capacity for apoptosis in order to allow growth despite genetic errors and external antigrowth signals.
- Loss of capacity for senescence which leads to limitless replicative potential (immortality).
- Acquisition of sustained angiogenesis that allows tumor to grow beyond the limitations of passive nutrient diffusion.
- Ability to invade neighboring tissues.
- Ability to generate metastasis at distant sites.
- Loss of capacity to repair genetic errors that cause an increased mutation rate (genomic instability) and thereby accelerate all the other changes.

19.1.3 Signs and symptoms

The various sign and symptom of cancer can be divided into the following three groups [5].

- Local symptoms: Unusual lumps, swelling (tumor), hemorrhage (bleeding), pain, ulceration, and jaundice.
- Symptoms of metastasis (spreading): Enlarged lymph nodes, cough, hemoptysis, hepatomegaly (enlarged liver), bone pain, fracture of affected bones, and neurological symptoms.
- Systemic symptoms: Weight loss, poor appetite, fatigue and cachexia (muscle atrophy, fatigue), excessive sweating (night sweats), anemia, thrombosis, and hormonal changes.

19.1.4 Etiology of cancer

Cancer is a diverse class of diseases which differ widely in their causes and biology. Research on the pathogenesis of cancer can be divided into three broad areas of focus [6].

- The first area of research focuses on the agents and events which cause or facilitate genetic changes in cells destined to become cancer.
- Second, it is important to uncover the precise nature of the genetic damage, and the genes which are affected by it.
- The third focus is on the consequences of those genetic changes on the biology of the cell, both in generating the defining properties of a cancer cell, and in facilitating additional genetic events, leading to further progression of cancer.

The various causes of cancer are

(i) Carcinogens
(ii) Ionizing radiation
(iii) Dysfunction of immune system
(iv) Heredity
(v) Infectious disease
(vi) Hormonal imbalances

19.1.5 Treatment of cancer

Cancer can be treated by surgery, chemotherapy, radiation therapy, immunotherapy, monoclonal antibody therapy, or other methods. The choice of therapy depends on the location and grade of the tumor and the stage of the disease, as well as the general state of the patient. A number of experimental cancer treatments are also under development. Complete removal of cancer without damage to the rest of the body is the goal of treatment. The effectiveness of chemotherapy is often limited by toxicity to other tissues in the body [7].

Chemotherapy is the treatment of cancer with drugs (anticancer drugs) that can destroy cancer cells. In current usage, the term "chemotherapy" usually refers to cytotoxic drugs which affect rapidly dividing cells. Most forms of chemotherapeutic agents target all rapidly dividing cells and are not specific for cancer cells. The following chemotherapeutic agents are used clinically for the treatment of various types of cancer (Fig. 19.2). These drugs produce their anticancer activities either by killing or inhibiting or modifying the growth of cancer cells [8].

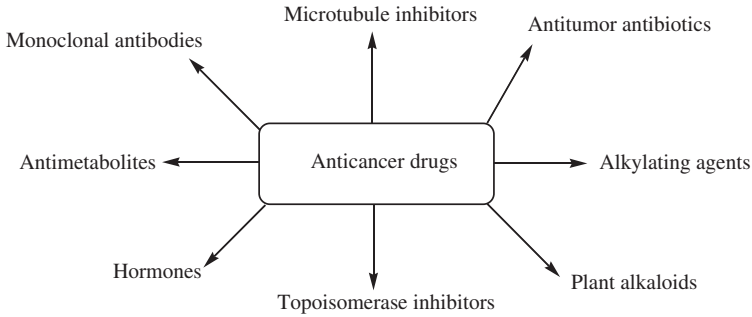

Fig. 19.2 Classification of anticancer drugs.

19.1.6 Chemistry, MOA, and uses anticancer drugs

a. Alkylating agents: These agents are mainly active in the resting phase of the cell cycle. The several types of alkylating agents used in chemotherapy are given below [2, 9–11].

(i) Nitrogen mustards: These are cytotoxic chemotherapy agents and derived from mustard gas. They form an adduct with the DNA that involves a cross-linking between guanine N-7 of one strand of DNA with the other. The generated cross-linking is irreversible and leads to cell apoptosis. Examples: mechlorethamine, cyclophosphamide, ifosfamide, chlorambucil, and melphalan (Fig. 19.3). Chlorambucil and cyclophosphamide were approved for treatment of cancer in United States during 1957 and 1959, respectively.

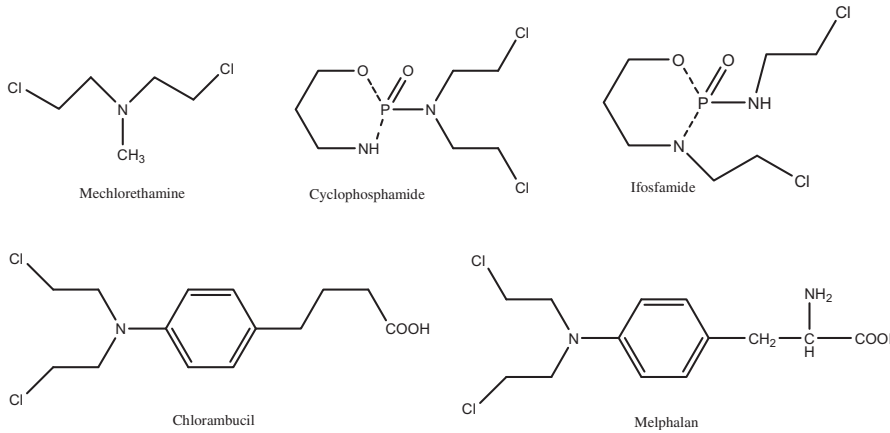

Fig. 19.3 Structures of nitrogen mustards.

(ii) Aziridines: Thiotepa is an organo-phosphorus compound with molecular formula $SP(NC_2H_4)_3$ as presented in Fig. 19.4. It is prepared by heating aziridine with thiophosphoryl chloride. On January 29, 2007, the European Medicines Agency designated thiotepa as an orphan drug. On April 2, 2007 the U.S. Food and Drug Administration (FDA) designated thiotepa as a conditioning treatment for use prior to hematopoietic stem cell transplantation. It is also used in the treatment of adenocarcinoma of the breast, adenocarcinoma of the ovary, papillary thyroid cancer, and bladder cancer. Thiotepa inhibits tumor growth by cross-linking guanine nucleobases in DNA double-helix strands.

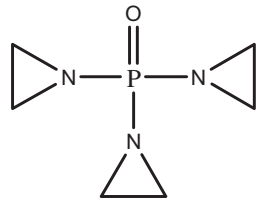

Thio-TEPA

Fig. 19.4 Structure of thiotepa.

(iii) Alkylsulfonates: Busulfan is a cell-cycle nonspecific alkylating antineoplastic agent (Fig. 19.5). It is chemically designated as 1,4-butanediol-dimethane-sulfonate. It was approved by the US FDA for the treatment of chronic myeloid leukemia (CML) in 1999. It is also used in pediatrics and adults in combination with cyclophosphamide or clofarabine as a conditioning agent prior to bone marrow transplantation.

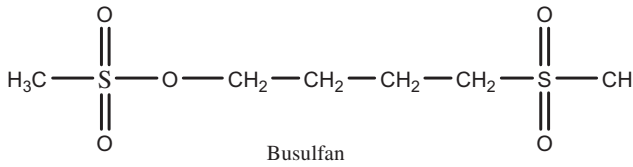

Fig. 19.5 Structure of busulfan.

(iv) Triazines and hydrazines: Dacarbazine and procarbazine are triazine and hydrazine derivative, respectively (Fig. 19.6). Dacarbazine is not cell cycle phase specific and is used for the treatment of metastatic malignant melanoma. Procarbazine is used for the treatment of Hodgkin's lymphoma and brain cancers. Dacarbazine was approved for medical use in United States in 1975. Procarbazine was approved for medical use in the United States in 1969. Metabolism of procarbazine yields azo-procarbazine and hydrogen peroxide which results breaking of DNA strands that lead to cell death.

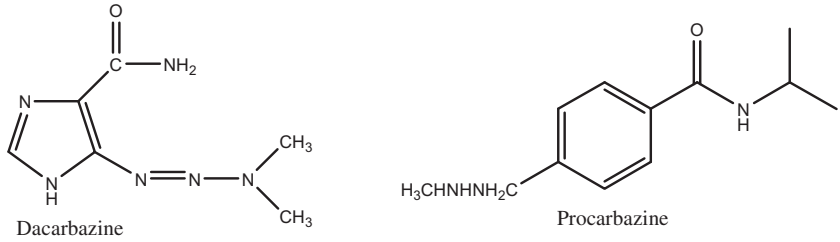

Fig. 19.6 Structures of dacarbazine and procarbazine.

(v) Nitrosureas: It is a class of compounds which include a nitroso (R-NO) group and a urea. They are lipophilic and can cross the blood-brain barrier (BBB). So, these are useful in the treatment of brain tumors. Example: carmustine and lomustine. Chemically, carmustine is 1,3-bis(2-chloroethyl)-1-nitrosourea whereas lomustine is 1-(2-chloroethyl)-3-cyclohexyl-1-nitrosourea (Fig. 19.7). Carmustine causes cross-links in DNA and RNA that leads to inhibition of DNA synthesis, RNA production, and RNA translation (protein synthesis). This leads to cell death.

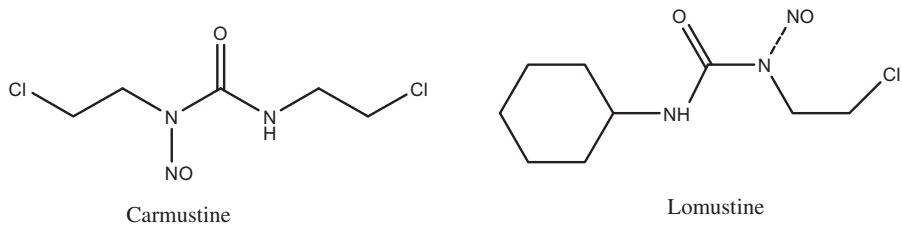

Fig. 19.7 Structures of carmustine and lomustine.

(vi) Metal salts: Cisplatin possess square planar coordination complex *cis*-$[Pt(NH_3)_2Cl_2]$ (Fig. 19.8). It was discovered in 1845 and licensed for medical use in the year 1978.

Cisplatin is administered intravenously as a short-term infusion in normal saline for treatment of solid and hematological malignant tumors. Similarly, carboplatin was patented in 1972 and approved for treatment of cancer in 1986. It is used to treat a number of forms of cancer such as ovarian cancer, lung cancer, brain cancer, and neuroblastoma. Whereas, oxaliplatin was patented in 1976 and approved in 1996 for its medical use. It is used for treatment of colorectal cancer.

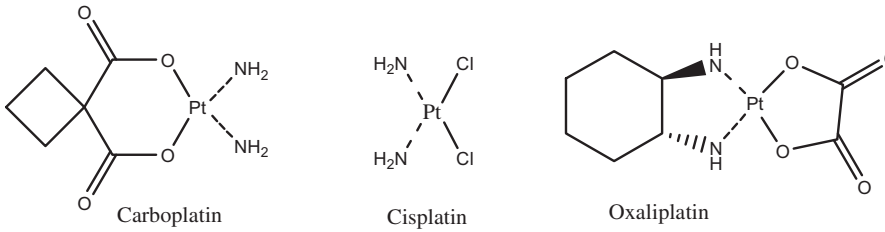

Fig. 19.8 Structures of carboplatin, cisplatin, oxaliplatin.

b. Plant-derived drugs: The following chemotherapeutic agents are derived from certain types of plants. The plant alkaloids are cell-cycle specific. They attack the cells during various phases of divisions [12–14].

(i) Taxanes: These are a class of diterpenes and produced from plants of the genus Taxus (yews). Paclitaxel (Taxol) and docetaxel (Taxotere) are widely used as chemotherapeutic agents (Fig. 19.9). The primary mechanism of action of the taxane class of drugs is the disruption of microtubule function. Microtubules are essential to cell division. So, these drugs inhibit the process of cell division.

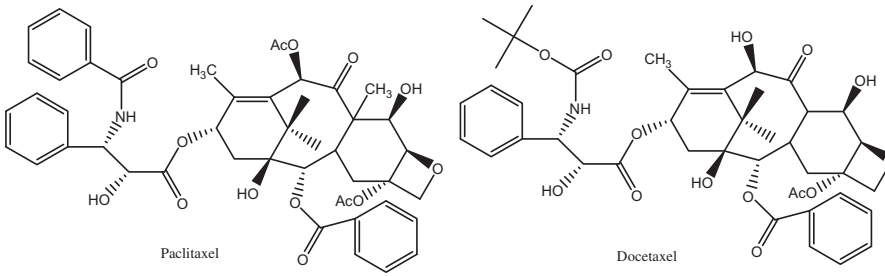

Fig. 19.9 Structures of paclitaxel (taxol) and docetaxel (taxotere).

(ii) Podophyllotoxins: It is extracted from the roots and rhizomes of *Podophyllum* species. Etoposide and teniposide are semisynthetic derivatives of podophyllotoxin (Fig. 19.10). Etoposide is the topoisomerase inhibitor and produces its action by re-ligation of the DNA strands that causes breaking of DNA strands. Etoposide was first synthesized in 1966 and US FDA approval was granted in 1983. It is used for the treatment of lung cancer, testicular cancer, lymphoma, etc. Teniposide causes dose-dependent single- and double-stranded breaks in DNA and DNA-protein cross-links. It used in the treatment of childhood acute lymphocytic leukemia (ALL), Hodgkin's lymphoma, and certain brain tumors.

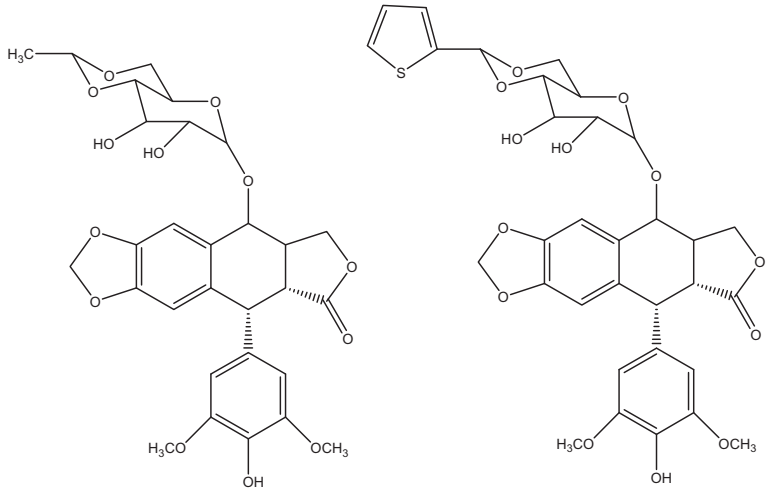

Fig. 19.10 Structures of podophyllotoxins (etoposide and teniposide).

(iii) Camptothecin analogs: It was discovered in 1966 by M.E. Wall and M.C. Wani in systematic screening of natural products for anticancer drugs. It was isolated from the bark and stem of *Camptotheca acuminate*. Camptothecin analogs such as irinotecan and topotecan have been approved for cancer chemotherapy (Fig. 19.11). Irinotecan was

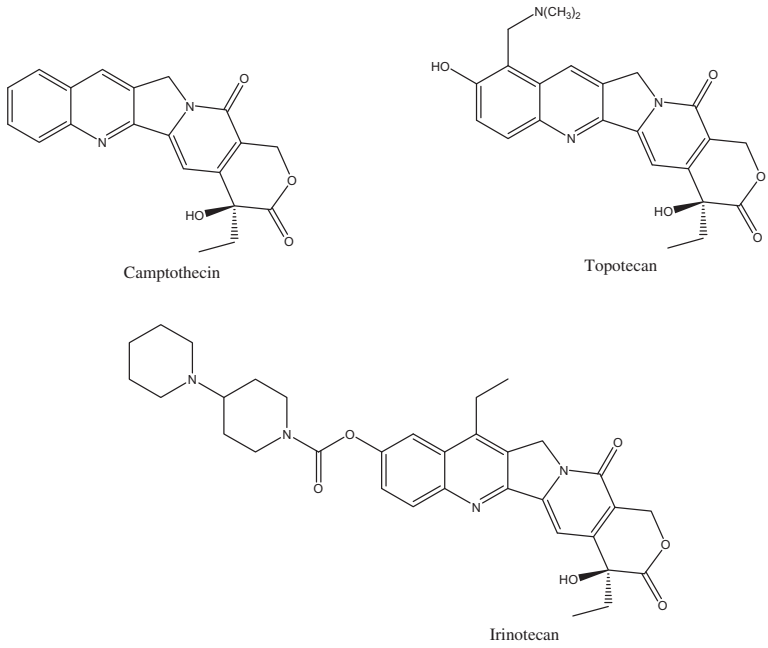

Fig. 19.11 Structures of camptothecin analogs.

approved in the United States in 1996 for treatment of colon cancer, and small cell lung cancer. Topotecan is a synthetic, water-soluble analog of camptothecin. After GlaxoSmithKline received final FDA approval for Hycamtin Capsules on October 15, 2007, topotecan became the first topoisomerase I inhibitor for oral use. It is used to treat ovarian cancer and lung cancer.

(iv) **Vinca alkaloids:** These are isolated from *Catharanthus roseus* which contain chemical constituents such as vincristine, vinblastine, vinorelbine, and vindesine (Fig. 19.12). Vinca alkaloid binds to specific sites of microtubular protein (tubulin) and prevents its polymerization and assembly into microtubules, which results in disruption of mitotic spindle. They are cell-cycle specific and act in mitotic phase (M-phase) of cell division.

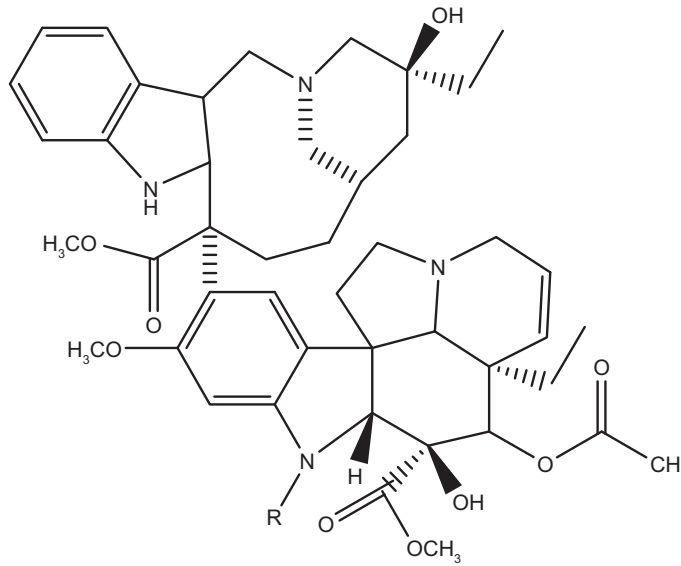

Vincristine (R=CHO)

Vinblastine (R=CH_3)

Fig. 19.12 Structure of vinca alkaloids.

c. **Antitumor antibiotics:** Antitumor antibiotics are produced by species of the soil fungus Streptomyces. These drugs act during multiple phases of the cell cycle and are considered as cell-cycle specific [15].
   - Anthracyclines: doxorubicin, daunorubicin, epirubicin, and mitoxantrone (Fig. 19.13).
   - Chromomycins: dactinomycin and plicamycin.

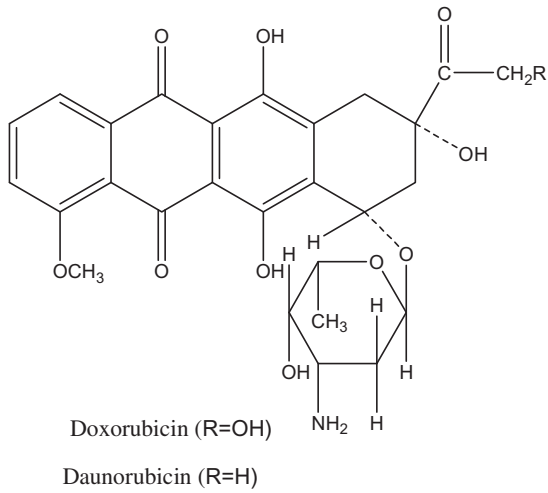

Fig. 19.13 Structures of anthracyclines (doxorubicin, daunorubicin).

d. Antimetabolites: These drugs are cell-cycle specific. They attack cells at very specific phases in the cell cycle. These are classified according to the substances with which they interfere [16–18].

(i) Folic acid antagonist: Methotrexate is an antimetabolite of the antifolate type (Fig. 19.14). For cancer, methotrexate competitively inhibits dihydrofolate reductase (DHFR), an enzyme responsible for the synthesis of tetrahydrofolate. DHFR catalyzes the conversion of dihydrofolate to the active tetrahydrofolate. Folic acid is required for synthesis of the nucleoside thymidine which is essential for DNA synthesis. Folate is essential for purine and pyrimidine base biosynthesis. Therefore, methotrexate inhibits the synthesis of DNA, RNA, thymidylates, and proteins.

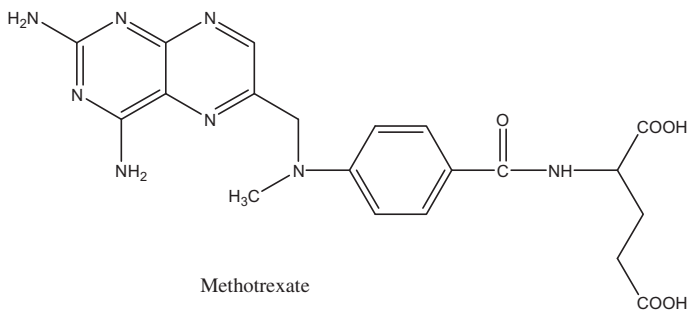

Fig. 19.14 Structure of folic acid antagonist (methotrexate).

(ii) Pyrimidine antagonist: 5-Fluorouracil (5-FU) is the antimetabolite and pyrimidine analog which interferes with DNA and RNA synthesis (Fig. 19.15). Fluorouracil was patented in 1956 and used clinically in 1962. It is used for the treatment of anal, breast, colorectal, esophageal, stomach, pancreatic, and skin cancers. Cytarabine is an anti-metabolic agent with the chemical name of 1β-arabinofuranosylcytosine. It works by blocking the function of DNA polymerase. Cytarabine was first synthesized by Richard

Walwick, Walden Roberts, and Charles Dekker in 1959 at University of California, Berkeley. It was approved by the US FDA in June 1969. Decitabine acts as nucleic acid synthesis inhibitor and used for treatment of acute myeloid leukemia (AML). Gemcitabine is chemically 2′,2′-difluoro-2′-deoxycytidine and works by blocking DNA synthesis. Gemcitabine was first synthesized in Larry Hertel's lab at Eli Lilly Company during 1980s. It was approved by the FDA in 1996 for treatment of pancreatic cancers. Capecitabine was patented in 1992 and approved for medical use in 1998. It is used to treat breast cancer, gastric cancer, and colorectal cancer. Capecitabine is metabolized to 5-FU which in turn is a thymidylate synthase inhibitor. Hence it inhibits the synthesis of thymidine monophosphate (ThMP), the active form of thymidine which is required for the de novo synthesis of DNA.

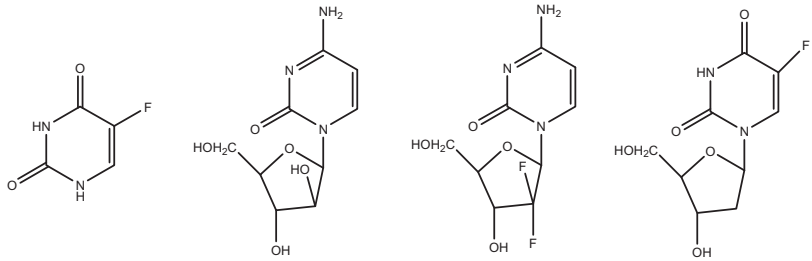

Fig. 19.15 Structure of pyrimidine antagonists.

(iii) Purine antagonist: Mercaptopurine was approved for medical use in the United States in 1953 (Fig. 19.16). 6-MP was discovered by Nobel Prize winning scientists Gertrude B. Elion and George H. Hitchings at Burroughs Wellcome in Tuckahoe, New York. It inhibits purine nucleotide synthesis and metabolism by inhibiting an enzyme called phosphoribosyl pyrophosphate amido transferase (PRPP amido transferase). It is used to treat acute lymphocytic leukemia (ALL), chronic myeloid leukemia (CML). 6-Thioguanine (6-TG) is a purine analog of guanine and works by disrupting DNA and RNA. It is a medication used to treat acute myeloid leukemia (AML), acute lymphocytic leukemia (ALL), and chronic myeloid leukemia (CML). Tioguanine was developed between 1949 and 1951. Cladribine is a purine analog and chemical name is 2-chloro-2′-deoxyadenosine. It is a medication used to treat hairy cell leukemia. Azathioprine inhibits purine synthesis and purines are needed to produce DNA and RNA.

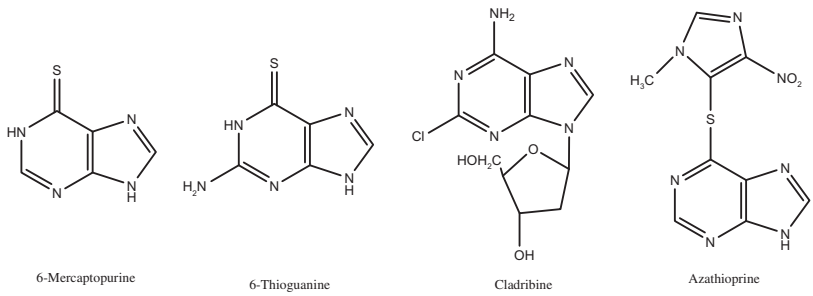

Fig. 19.16 Structure of purine antagonists.

e. **Topoisomerase inhibitors:** These drugs that interfere with the action of topoisomerase enzymes (topoisomerase I and II). Topoisomerase enzymes control the manipulation of the DNA structure necessary for replication [19].
   - Topoisomerase I inhibitors: ironotecan, topotecan.
   - Topoisomerase II inhibitors: amsacrine, etoposide, and teniposide.

f. **Hormonal therapy:** Hormone therapy is used to reduce or prevent symptoms of cancer [20]. This therapy stops hormones being made or prevents hormones from making cancer cells grow and divide. Estrogen antagonist, e.g., tamoxifen (Fig. 19.17).

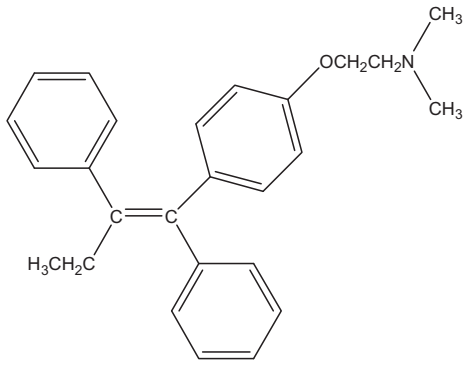

Fig. 19.17 Structure of estrogen antagonist (tamoxifen).

19.1.7 Adverse effects and toxicities of anticancer drugs

Chemotherapeutic agents can cure cancer because it either kills or inhibits the growth cancer cells as well as normal cells. So, the killing of normal cells can cause several side effects. The side effects vary from one drug to another and also from person to person. The common side effects of chemotherapy include anemia, mouth soreness, nausea, vomiting, loss of appetite, constipation or diarrhea, hair loss, skin changes or reactions, pain or nerve changes, changes in fertility and sexuality. Clinically useful anticancer agents exhibit selective toxicity toward malignant cells. The common toxicities observed are hematological, gastrointestinal, skin and hair follicle toxicity, nervous system toxicity, metabolic abnormalities, hepatic toxicity, urinary tract toxicity, cardiac toxicity, pulmonary toxicity, and gonadal toxicity [21].

19.1.8 Synthesis of commonly used anticancer drugs [22]

a. **Synthesis of chlorambucil**

The starting material for the synthesis of chlorambucil is 4-phenylbuanoic acid. First 4-phenylbuanoic acid undergoes nitration in the presence of Conc. HNO_3 in acidic condition produces 4-(4-nitrophenyl)butanoic acid. Then 4-(4-nitrophenyl)butanoic acid undergoes reduction in the presence of $Pd/CaCO_3$ to yield 4-(4-aminophenyl)butanoic acid which on reaction with 2 mol of ethylene oxide or oxirane to get 4-(4-(bis(2-hydroxyethyl) amino)phenyl)butanoic acid. Later the chlorination of compound in the presence of thionyl chloride yields the desired product of chlorambucil (Scheme 19.1).

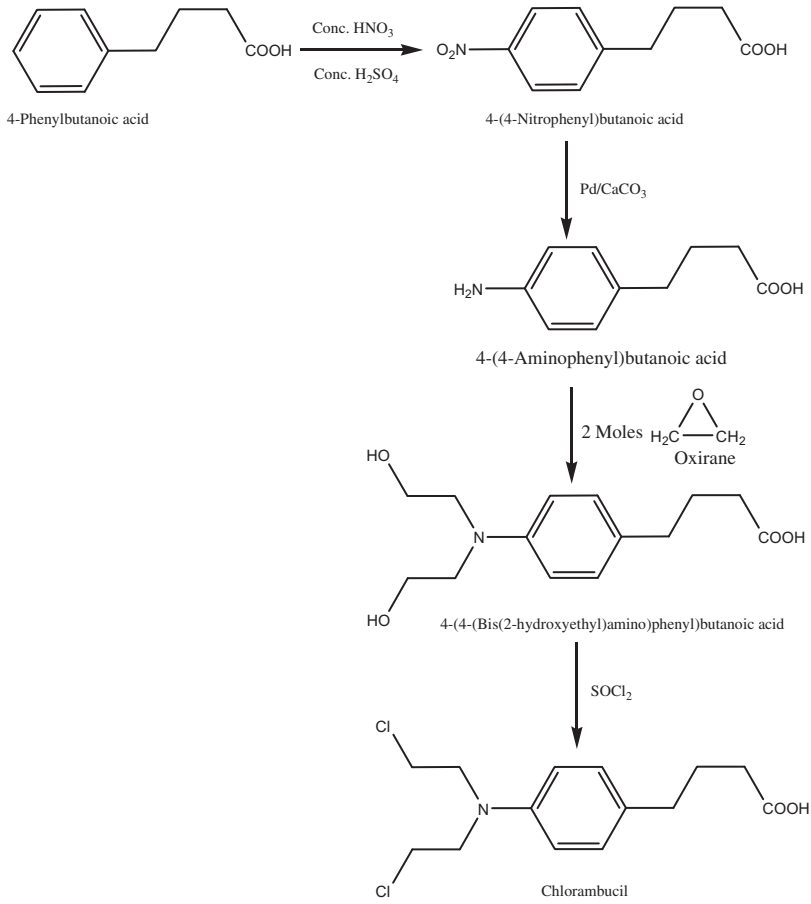

Scheme 19.1 Synthetic route of chlorambucil.

b. Synthesis of mechlorethamine

Methylamine reaction with 2 mol of ethylene oxide to produce Bis(2-hydroxyethyl) methylamine which on further chlorination in the presence of thionyl chloride ($SOCl_2$) yields mechlorethamine (Scheme 19.2).

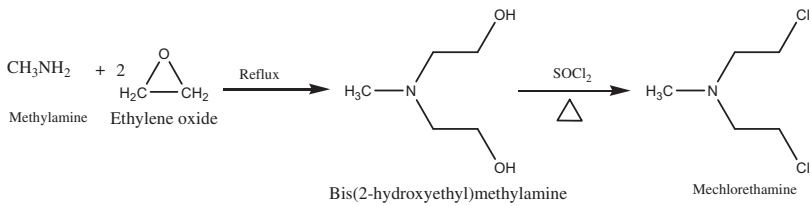

Scheme 19.2 Synthesis of mechlorethamine.

c. Synthesis of cyclophosphamide

Bis(2-chloroethyl)amine undergoes reaction with phosphorous oxychloride to obtain Bis (2-chloroethyl)phosphoroamidoyl dichloride which on heating in the presence of 3-aminopropan-1-ol produces cyclophosphamide (Scheme 19.3).

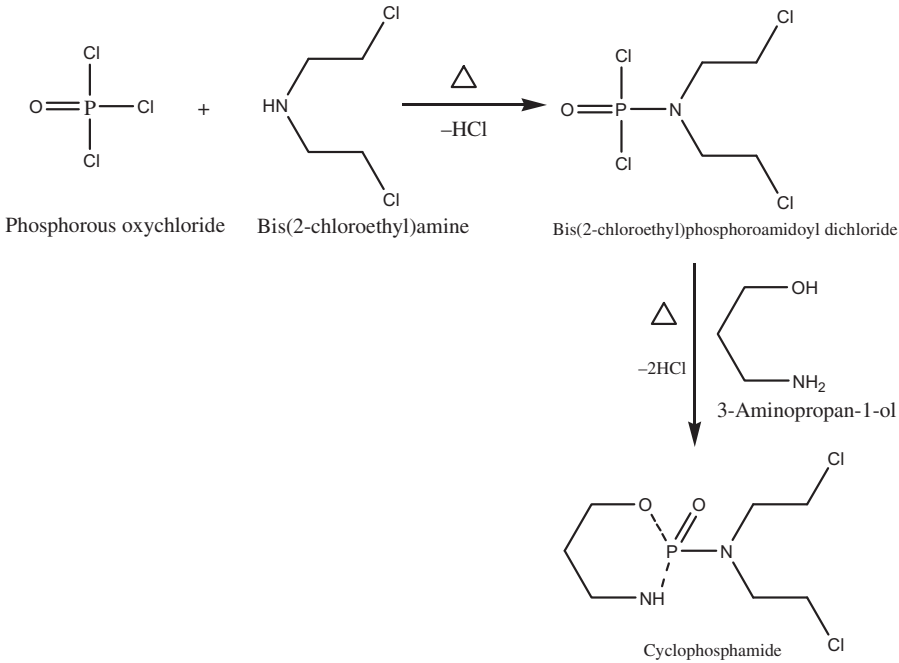

Scheme 19.3 Synthesis of cyclophosphamide.

d. Synthesis of carmustine

Carmustine is produced from 1,3-bis(2-chloroethyl)urea in the presence of $NaNO_2$ and formic acid (HCOOH) as given in Scheme 19.4.

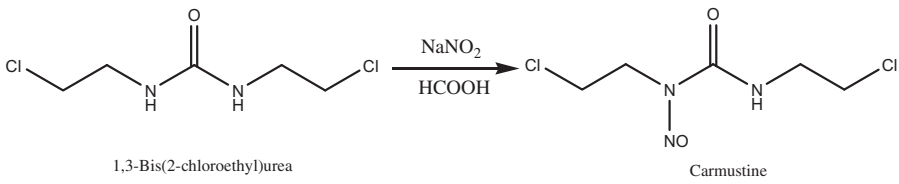

Scheme 19.4 Synthesis of carmustine.

e. Synthesis of lomustine

1,3-Bis(2-chloroethyl)urea reacts with 2 mol of cyclohexanamine to get 1-(2-chloroethyl)-3-cyclohexylurea which on further treatment with $NaNO_2$ and formic acid (HCOOH) produces lomustine (Scheme 19.5).

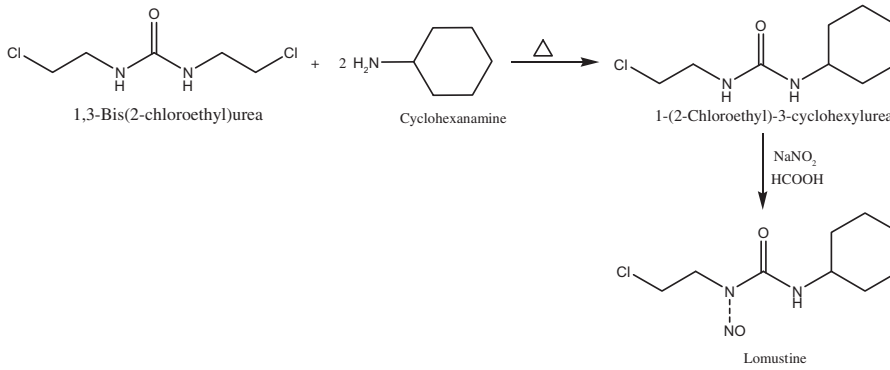

Scheme 19.5 Synthesis of lomustine.

f. Synthesis of busulfan

Busulfan is obtained by reaction of butane-1,4-diol with 2 mol of methanesulfonyl chloride in the presence of pyridine (Scheme 19.6).

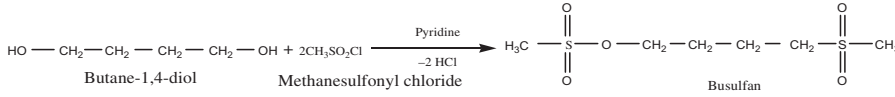

Scheme 19.6 Synthesis of busulfan.

g. Synthesis of 5-fluoro-uracil

5-Fluoro-uracil is produced by fluorination pyrimidine-2,4(1*H*,3*H*)-dione or uracil of in the presence of fluoroxy trifluoromethane (CF_3OF) as presented in Scheme 19.7.

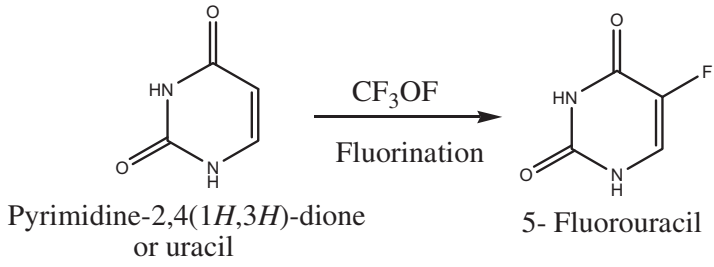

Scheme 19.7 Synthesis of 5-fluoro-uracil.

h. Synthesis of methotrexate

Pyrimidine-2,4,5,6-tetra-amine, 2,3-dibromo-propanal, and 2-(4-(methylamino) benzamido)pentanedioic acid undergo cyclization followed by dehydration in the presence of sodium hydroxide (NaOH) and acetic acid (CH_3COOH) to produce methotrexate (Scheme 19.8).

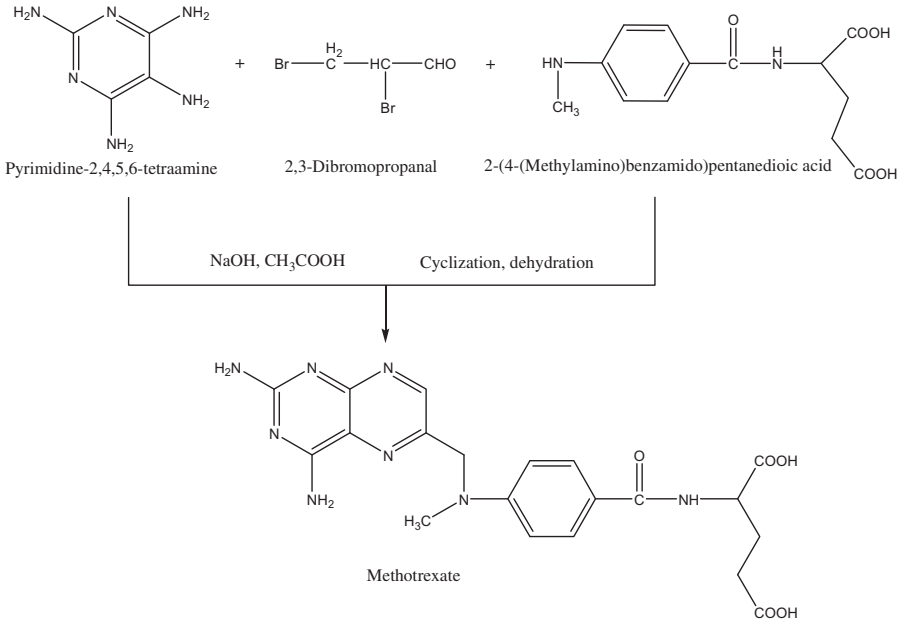

Scheme 19.8 Synthesis of methotrexate.

i. Synthesis of azathioprine

Azathioprine was synthesized by George Herbert Hitchings and Gertrude Elion in 1957. It is synthesized from 5-chloro-1-methyl-4-nitro-1*H*-imidazole and 6-mercaptopurine in the presence of dimethyl sulfoxide (DMSO). The synthesis of 5-chloro-1-methyl-4-nitro-1*H*-imidazole is obtained by carrying out the reaction between methylamine and diethyl oxalate followed by chlorination in the presence of phosphorus pentachloride (PCl_5) and subsequent nitration in the presence of nitric and sulfuric acid (Scheme 19.9).

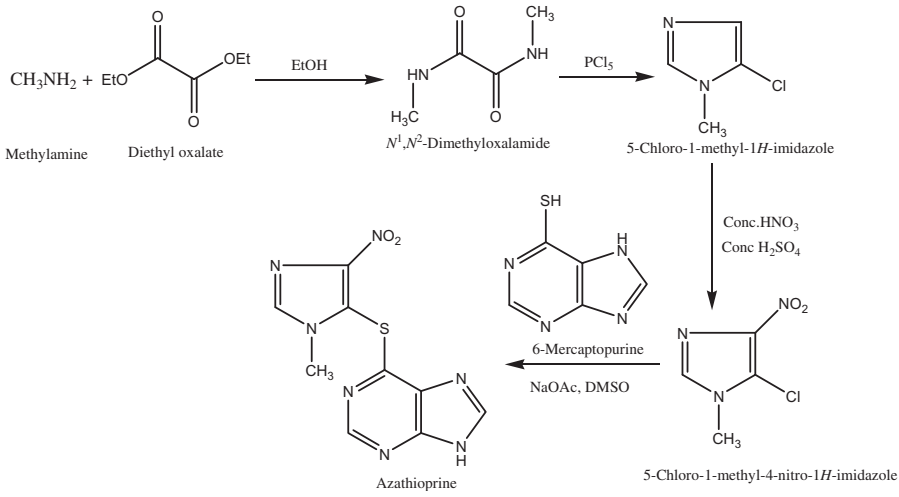

Scheme 19.9 Synthesis of azathioprine.

19.1.9 Conventional synthesis of anticancer drugs

Various heterocyclic compounds exhibit medicinal properties like anticancer activity. Some of the clinically useful drugs containing heterocyclic moiety include 5-fluorouracil, methotrexate, doxorubicin, daunorubicin, vinblastine, and vincristine, etc. [23]. The following novel anticancer drugs with different heterocyclic core are synthesized to expand the area of cancer research. These newly designed and prepared scaffolds with diverse molecular structures play a major role in drug discovery process which exhibits anticancer activity against different cancer cell lines.

A series of *N′*-(substituted)-4-(butan-2-ylidene-amino)benzohydrazides (1–21) is synthesized (Scheme 19.10) and screened for their in vitro anticancer activity against human colon (HCT116) cancer cell line by using 3-(4,5-dimethylthiazol-2-yl)-2,5-diphenyl tetrazolium bromide (MTT) assay method [24]. Among the tested compounds, some of the compounds have appreciable anticancer potential than the standard drug carboplatin (Table 19.1).

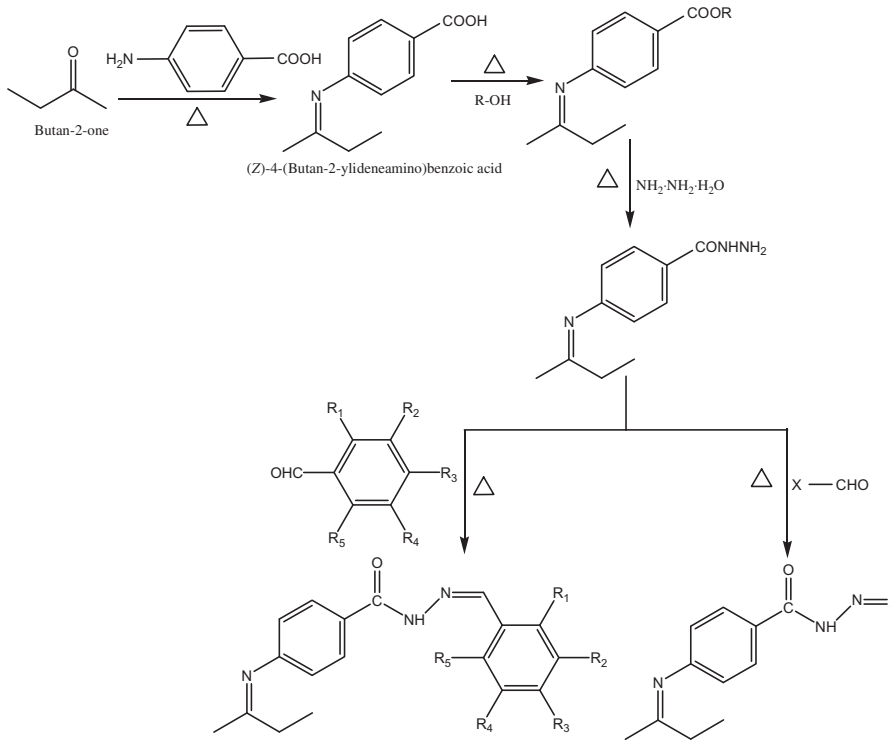

Scheme 19.10 Synthesis of *N′*-(substituted)-4-(butan-2-ylidene-amino)benzohydrazides (1–21).

Table 19.1 Anticancer activity (IC_{50} in μM) of the synthesized *N′*-(substituted)-4-(butan-2-ylidene-amino)benzohydrazides.

Compound	R_1	R_2	R_3	R_4	R_5	X	IC_{50} (HCT116, μM)
1	H	H	CH_3	H	H	–	96.64
2	H	OCH_3	OCH_3	H	H	–	74.59
3	H	Cl	H	H	H	–	243.64
4	H	H	$N(CH_3)_2$	H	H	–	163.69
5	H	OCH_3	OCH_3	OCH_3	H	–	209.08
6	H	H	Br	H	H	–	79.06
7	H	H	OCH_3	H	H	–	216.72
8	H	H	Cl	H	H	–	152.91
9	H	H	H	H	H	–	178.6
10	H	H	OCH_3	OH	H	–	141.59
11	H	H	OC_2H_5	OH	H	–	173.74
12	H	H	OH	H	H	–	89.55
13	H	NO_2	H	H	H	–	60.15
14	Cl	H	H	H	H	–	37.71
15	H	Br	H	H	H	–	88.71
16	OH	H	H	H	H	–	184.47
17	–	–	–	–	–		156.74
18	–	–	–	–	–	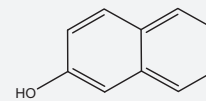	158.77
19	–	–	CHO	–	–	–	87.23
20	–	–	–	–	–	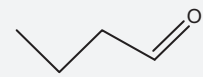	95.23
21	–	–	–	–	–	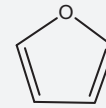	181.38
Tetrandrine	–	–	–	–	–	–	1.53
Doxorubicin	–	–	–	–	–	–	0.70
Camptothecin	–	–	–	–	–	–	0.15
Carboplatin	–	–	–	–	–	–	>100

A new series of quinazoline derivatives are synthesized. Treatment of 2-amino-5-methylbenzoic acid with butyl isothiocyanate results in the formation of new 2-thioxoquinazolin-4-one (3) [25]. Alkylation and hydrazinolysis of the inherent thioxo group in (1–3) afforded the corresponding thioethers (4–23) and hydrazine derivatives (24 and 25). Then compound 24 is further transformed into tricyclic derivative (26) via cyclocondensation reaction (Scheme 19.11). The cytotoxicity of all compounds is evaluated in vitro against the HeLa and MDA-MB-231 cancer cell lines using MTT assay. The treatment of the cells is performed with the synthesized

compounds and gefitinib at 0, 1, 5, 10, 25, and 50 μM and incubated for 24 h in 50% DMSO. The IC_{50} values of the target compounds are reported in μM using gefitinib as a standard. The results indicated that all the tested compounds exhibited significant in vitro cytotoxicity. Compounds 21–23 are found to be potential anticancer agents with IC_{50} values ranging from 1.85 to 2.81 μM in relation to Gefitinib ($IC_{50} = 4.3$ and 28.3 μM against HeLa and MDA-MB-231 cells, respectively) (Table 19.2).

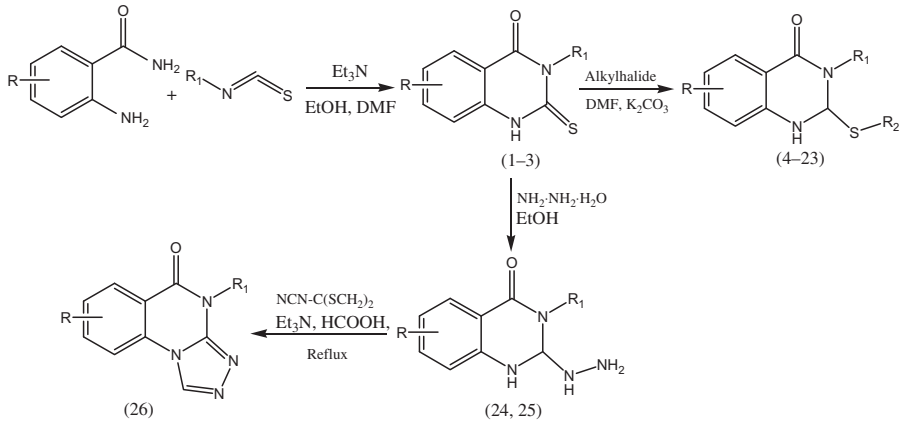

Scheme 19.11 Synthetic routes for compounds 1–26.

Table 19.2 Anticancer activity of the target compounds (1–26) (IC_{50}, μM).

Comp. no.	R	R_1	R_2	IC_{50} (μM)	
				HeLa	MDA-MB-231
1	Methyl	Benzyl	–	10.63	3.2
2	Methoxy	Benzyl	–	2.7	4.85
3	Methyl	Butyl	–	3.73	2.73
4	Methyl	Butyl	Ethyl	4.14	3.8
5	Methyl	Butyl	Allyl	5.65	3.77
6	Methyl	Butyl	2-Methyl-benzyl	6.3	4.44
7	Methyl	Butyl	3-Methyl-benzyl	4.45	5.0
8	Methyl	Butyl	4-Cl-benzyl	3.7	4.13
9	Methyl	Butyl	4-NO2-benzyl	4.56	4.12
10	Methyl	Butyl	2-CN-benzyl	3.7	4.26
11	Methyl	Butyl	3-CN-benzyl	6.1	95.97
12	Methyl	Butyl	4-CN-benzyl	7.5	5.1
13	Methyl	Butyl	3-Methoxy-benzyl	6.79	5.18
14	Methyl	Butyl	(1*H*-benzoimidazol-2-yl) methyl	7.8	4.97

Continued

Table 19.2 Continued

Comp. no.	R	R_1	R_2	IC_{50} (μM)	
				HeLa	MDA-MB-231
15	Methyl	Butyl	Morphilinoethyl	4.11	17.57
16	Methyl	Butyl	3-(Phthalimido-2-yl)-propyl	5.75	6.19
17	Methyl	Benzyl	4-CN-benzyl	3.9	2.93
18	Methyl	Benzyl	3-Methyl-benzyl	3.04	4.96
19	Methyl	Benzyl	4-NO2-benzyl	5.6	3.23
20	Methyl	Benzyl	7-NO2-benzoxadiazole	4.14	3.5
21	Methyl	Benzyl	3-(Phthalimido-2-yl) propyl	1.85	2.33
22	Methoxy	Benzyl	3-(Phthalimido-2-yl)-propyl	2.5	2.56
23	Methoxy	Benzyl	Morphilinoethyl	2.6	2.81
24	Methyl	Butyl	Hydrazine	5.39	2.74
25	Methyl	Benzyl	Hydrazine	4.77	5.6
26	Methyl	Butyl	–	5.03	5.74
Gefitinib	–	–	–	4.3	28.33

The synthesis of different series of 6-iodo-2-phenoxymethyl-3-substituted quinazolin-4(3*H*)-ones is described [26]. The reaction of 2-phenoxyacetyl chloride (1) with 5-iodo methyl anthranilate (2) in dry benzene afforded methyl 5-iodo-2-(2-phenoxyacetamido)benzoate (3). Then the mixture of compound (3) and hydrazine hydrate is refluxed in the presence of *n*-butanol to produce 3-amino-6-iodo-2-(phenoxymethyl)quinazolin-4(3*H*)-one (4). Further, the reaction of compound (4) with acetic anhydride or various acid anhydrides "namely maleic and phthalic" in glacial acetic acid afford the corresponding 3-substituted-6-iodo-2-(phenoxymethyl)quinazolin-4(3*H*)-one (5a–c). Meanwhile, the condensation of compound (4) with aromatic aldehydes (benzaldehyde, 4-chlorobenzldehyde, anisaldehyde, and 4-fluorobenzaldehyde) in glacial acetic acid produces the corresponding Schiff's bases (6a–d). Finally, the reduction of compound (6a–d) with sodium borohydride in absolute ethanol yield benzylamino derivatives (7a–d) as depicted in Scheme 19.12. In vitro antitumor activity of the synthesized compounds against MCF-7 breast cell line is carried out by using doxorubicin (IC_{50}: 5.46 μmol/mL) as a reference drug using sulforhodamine B (SRB) colorimetric assay method. Sulforhodamine B is a bright pink aminoxanthene anionic dye with two sulfonic acid groups that bind electrostatically to protein basic amino acid residues of trichloroacetic acid. Compound 5b exhibited a remarkable antitumor activity (IC_{50}: 5.49 μmol/mL) almost similar to that expressed by the reference drug, whereas compounds 7d, 12b, and 6c (IC_{50}: 6.23, 6.55, and 6.80 μmol/mL, respectively) showed a considerable antitumor activity (Table 19.3).

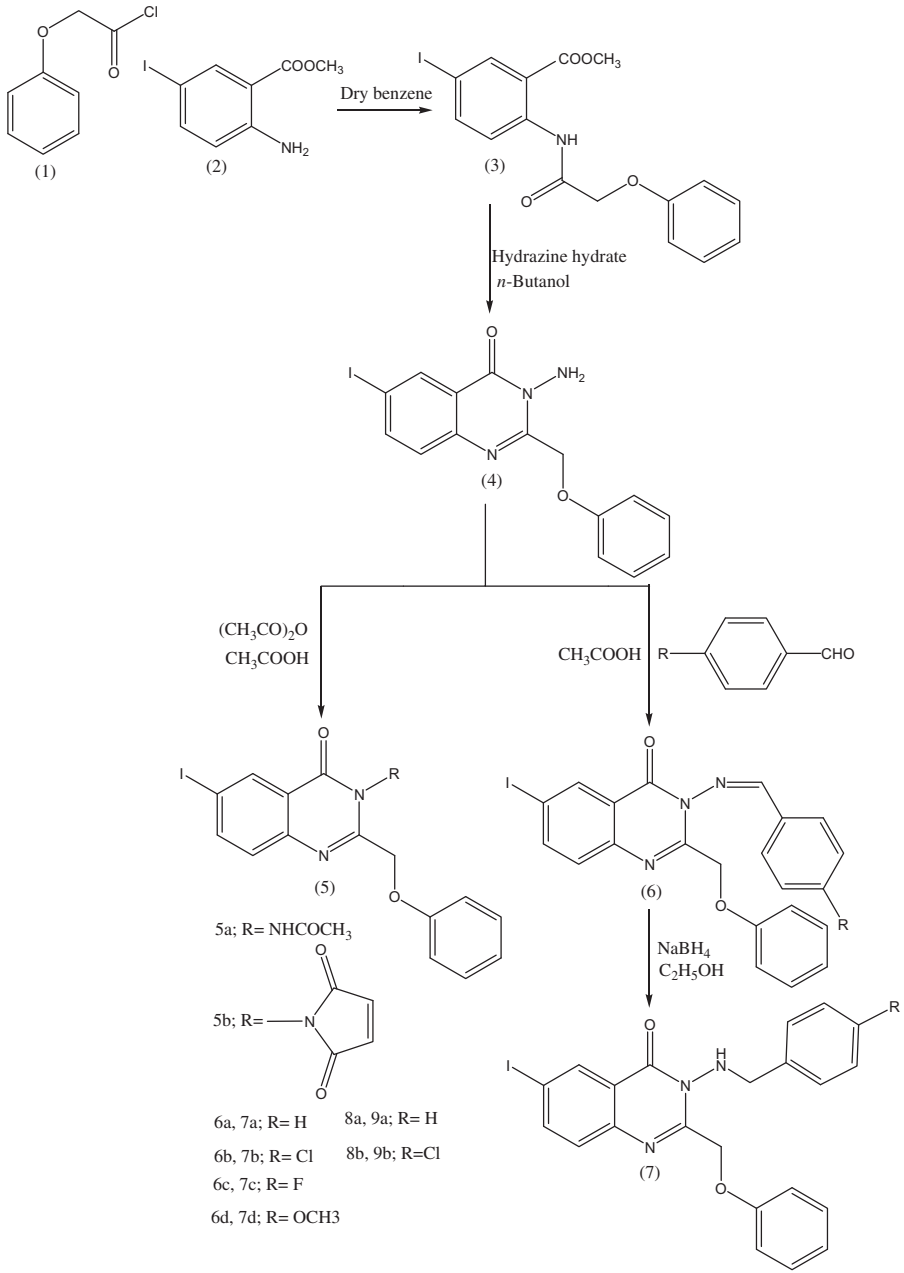

Scheme 19.12 Synthesis of 6-iodo-2-phenoxymethyl-3-substituted quinazolin-4(3*H*)-ones.

Table 19.3 Antitumor activity of the newly synthesized compounds.

Compound	IC_{50} (μmol/mL)	Compound	IC_{50} (μmol/mL)
4	24.92	7a	15.31
5a	21.59	7b	28.58
5b	5.49	7c	42.69
5c	27.51	7d	6.23
6a	13.29	12a	16.01
6b	8.14	12a	8.58
6c	6.80	12b	6.55
6d	19.55	Doxorubicin	5.46

Benzothiazole derivatives are synthesized and investigated for their probable anticancer activity [27]. First, 4-substitued benzaldehyde derivatives (1a–e) are afforded by the reaction of appropriate secondary amine and 4-fluorobenzaldehyde in the presence of DMF. Equimolar quantity of 5-substituted benzothiazole-2-thiol and ethyl chloroacetate in the presence of K_2CO_3 are refluxed in acetone to obtain 2-((5-substitutedbenzothiazol-2-yl)thio)acetate derivatives (2a,2b), which reacted with an excess of hydrazine hydrate to get 2-((5-substitutebenzothiazol-2-yl)thio)acetohydrazides (3a,3b). In the last step, 2-((5-substitutedbenzothiazol-2-yl)thio)-*N*′-(4-substituted benzylidene)acetohydrazide derivatives (4a–4j) are synthesized by the reaction of (1a–1e) and 3a–3b in the presence of EtOH (Scheme 19.13). The anticancer activity of target compounds is evaluated in three steps. First, an MTT test (3-(4,-5-dimethylthiazol-2-yl)-2,5-diphenyl tetrazolium bromide) is performed to observe cytotoxic activity of the compounds against carcinogenic C6 (rat brain glioma cell line), A549 (human lung adenocarcinoma epithelial cell line), MCF-7 (human breast adenocarcinoma cell line), and HT-29 (human colorectal adenocarcinoma cell line) cancer cell lines. Healthy NIH3T3 (mouse embryo fibroblast cell line) cells are also subjected to MTT assay to determine selectivity of the compounds toward carcinogenic cell lines (Table 19.4). Secondly, inhibitory effects of selected compounds 4d, 4e, and 4h on DNA synthesis of C6 cells are investigated. Finally, flow cytometric analysis is performed to identify the death pathway of the carcinogenic cells.

A series of some new 2,3-disubstituted-6-iodo-3*H*-quinazolin-4-one derivatives is prepared [28]. 5-Iodo-anthranilic acid is allowed to react with allyl, benzyl, and phenyl isothiocyanates to produce the 2-mercapto-3-substituted-6-iodo-3*H*-quinazolin-4-ones (1a–c). The 2-mercapto function of compound (1a–c) is then alkylated with some selected a-halo ketones as well as some alkyl halides to afford the corresponding S-alkylthioether derivatives (2–19). Oxidation of the thioether derivatives (17 and 19) using potassium permanganate afforded the corresponding sulfonyl derivatives

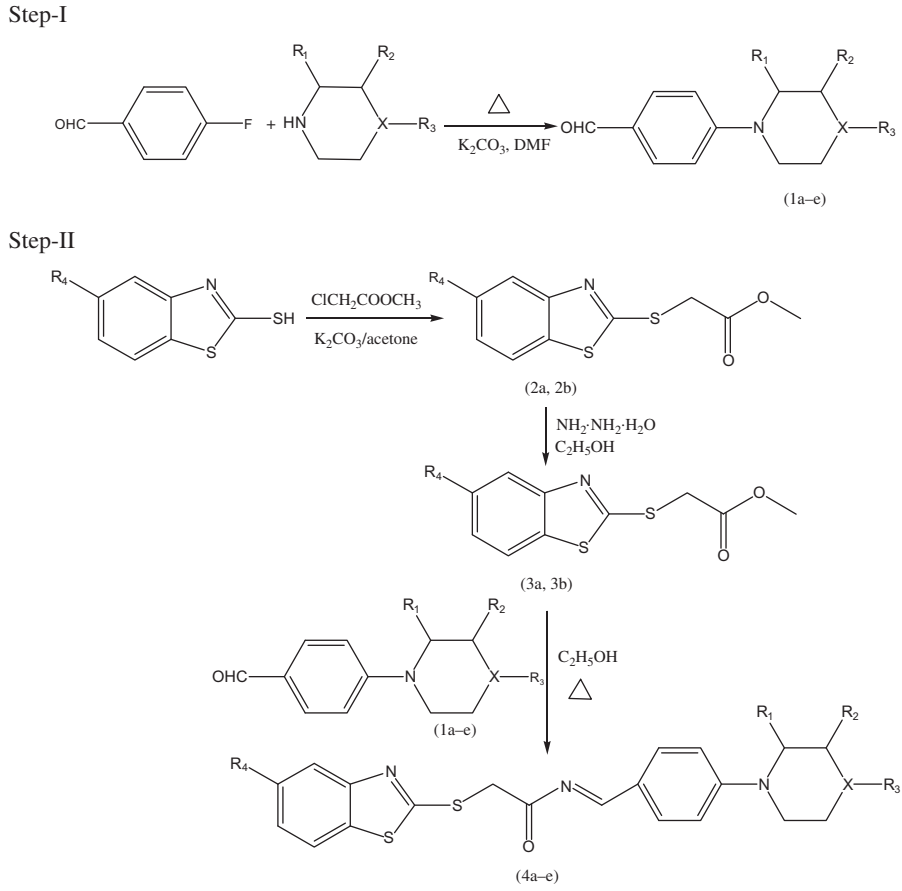

Scheme 19.13 Synthesis of benzothiazole derivatives.

(20 and 21), respectively (Scheme 19.14). The synthesized compounds are screened for their in vitro antitumor activity against the human breast cancer cell line (MCF-7), human cervix carcinoma cell line (HeLa), human liver cancer cell line (HepG2), and human colon cancer cell line HCT-8 using sulforhodamine B assay method. Five compounds exhibited broad spectrum antitumor activity in comparison to the standard drug doxorubicin (CAS-23214-92-8) against the four tested cell lines. The best cytotoxic results are obtained with compounds having allyl and/or benzyl moiety at positions 2 and/or 3 of the quinazoline nucleus (Table 19.5).

Table 19.4 Cytotoxic activity of the compounds against A549, C6, MCF-7, HT-29, and NIH3T3 cell lines.

Comp. code	R_1	R_2	R_3	R_4	X	IC_{50} (mM)				
						A549	C6	MCF-7	HT-29	NIH3T3
4a	—H	—H	—H	—Cl	—CH	1<	0.10	0.49	0.52	0.10
4b	—CH_3	—H	—H	—Cl	—CH	1	0.10	1<	1	0.10
4c	—H	—CH_3	—H	—Cl	—CH	0.52	0.10	0.10	0.30	0.03
4d	—H	—H	—CH_3	—Cl	—CH	1<	0.03	0.10	0.30	1<
4e	—H	—H	4-Methoxy phenyl	—Cl	—N	0.03	0.03	0.30	1<	0.01
4f	—H	—H	—H	—OCH_3	—CH	1<	1<	1<	1<	0.03
4g	—CH_3	—H	—H	—OCH_3	—CH	1<	1<	1<	1<	0.10
4h	—H	—CH_3	—H	—OCH_3	—CH	1<	0.03	1<	1<	0.10
4i	—H	—H	—CH_3	—OCH_3	—CH	0.49	0.10	0.30	1	0.03
4j	—H	—H	4-Methoxy phenyl	—OCH_3	—N	1<	1<	1<	1<	1<
Cisplatin	–	–	–	–	–	0.06	0.03	0.05	0.06	1<

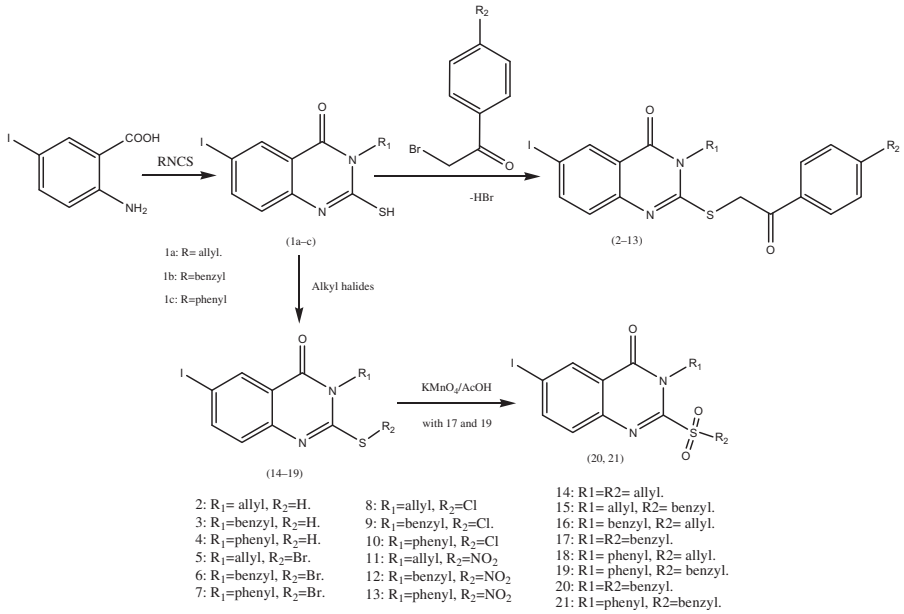

Scheme 19.14 Synthesis of 2,3-disubstituted-6-iodo-3*H*-quinazolin-4-one derivatives.

Table 19.5 In vitro antitumor activity of the designed quinazoline derivatives.

	IC_{50} (μg/mL)			
Compound	**MCF7**	**HeLa**	**HepG2**	**HCT-8**
2	4.95	4.60	7.12	10.25
3	5.39	4.73	9.21	6.03
4	9.98	10.0	11.95	12.6
5	3.37	4.63	4.72	6.02
6	3.78	4.75	7.0	9.20
7	12.60	10.14	12.0	9.0
8	3.56	4.72	23.1	4.52
9	3.76	4.98	4.17	9.5
10	16.1	16.2	9.60	10.5
11	5.59	5.18	12.1	8.4
12	5.39	5.19	18.4	8.41
13	11.18	13.3	11.1	9.50
14	3.25	3.31	3.70	4.0
15	3.65	3.98	4.39	4.35
16	3.64	3.97	4.40	4.78
17	5.16	4.30	6.84	11.0
18	13.0	13.76	9.37	16.1
19	8.03	9.66	23.9	9.0
20	9.35	9.39	15.59	16.3
21	9.46	9.25	9.04	15.3
Doxorubicin	4.84	4.09	4.65	5.26

A series of new coumarin containing compounds are synthesized from 4-bromomethyl-coumarin derivatives (2a, b) and different heteroaromatic systems (4a–e, 6a–d, 8, 10) via methylene thiolinker [29]. Twenty-four compounds are screened for their anticancer activity against two human tumor cell lines, breast carcinoma MCF-7, and hepatocellular carcinoma HePG-2, using 5-fluorouracil as standard drug. Compounds 5h, 7d, 7h, 9a, 13a, and 13d exhibit strong anticancer activity against both MCF-7 and HepG-2 cell lines. Among the tested compounds, compound 13a is the most active HepG-2 and MCF-7 with IC_{50} values of 5.5 mg/mL and 6.9 mg/mL, respectively (Fig. 19.18). Docking study is performed with protein 1KE9 to study the binding interaction of the designed compounds.

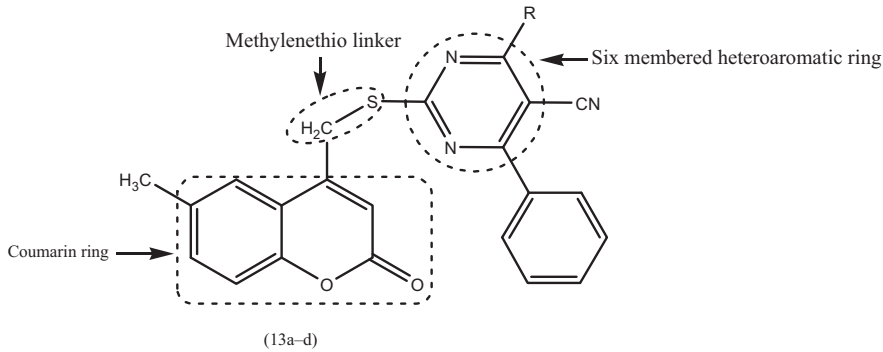

Fig. 19.18 Structures of coumarin derivatives (13a–d).

19.1.10 Green synthesis for development of new anticancer agents

The use of chemotherapeutic agents for the treatment of cancer produces various side effects and toxicities. So, it creates major problems to treat cancer patients effectively. Hence, it is necessary to design and develop new anticancer drug molecules with improved efficacy and reduced side effects to meet the demands of currently available chemotherapeutic agents. For this purpose, green synthetic protocols or technologies are applied to generate a large number of anticancer agents with diverse chemical structures to improve their therapeutic potentials (Fig. 19.19) [30].

Green synthesis is considered as a tool for the invention, design, and application of chemical products and processes to reduce or eliminate the use and generation of chemical hazardous and utilization of renewable raw materials. There are 12 principles of green chemistry approach to be followed while using the raw materials, solvents, and catalysts to carry out any chemical reactions. The selection of solvents plays a key role for the synthesis of new drug molecules because it allows the compounds to react efficiently in solution to yield pure product. The Center for Drug Evaluation and Research (CDER) of the USFDA categorized the solvents into four classes based on patient safety and environmental considerations. Class-I solvents include benzene, carbon tetrachloride, 1,2-dichloroethane, 1,1-dichloroethylene, and 1,1,

1-trichloroethane. These solvents are not suitable due to their undesirable toxicity or environmental pollution whereas Class-II solvents are organic solvents such as acetonitrile, methanol, methylene chloride, tetrahydrofuran, toluene, and hexane. Similarly, acetic acid, acetone, ethanol, ethyl acetate, heptane, and dimethyl sulfoxide are listed under Class-III solvents and these solvents have the lowest toxic effect. Class-IV solvents include isooctane, isopropyl ether, petroleum ether, and 2-methyl-tetrahydrofuran [31].

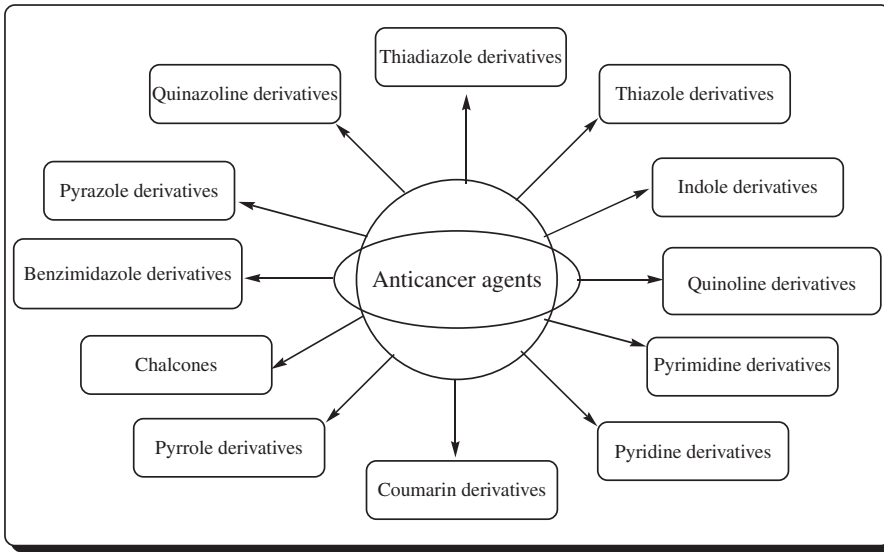

Fig. 19.19 Heterocyclic compounds as anticancer agents.

19.1.10.1 Quinoline derivatives as anticancer agents

Microwave-assisted synthesis of novel 4-aryl(alkyl)amino-3-nitroquinoline (1a) and 2,4-diaryl(dialkyl)amino-3-nitroquinolines (2a) via regioselective and nucleophilic substitution of 2,4-dichloro-3-nitroquinoline (4) with aryl(alkyl) amine, respectively, in water was presented (Scheme 19.15). The newly synthesized compounds were evaluated for their antiproliferative activity against EGFR over expressing human lung (A-549 and H-460) and colon (HCT-116-wild type and HCT-116-p53 null) cancer cell lines. Compounds 2e, 2f, and 2j exhibited excellent anticancer activity as compared with standard drug Erlotinib (Table 19.6) [32].

A simple and efficient synthesis of 6-fluoro-4-oxopyrido[2,3-*a*]carbazole-3-carboxylic acids (13a–e) and a structurally related 6-fluoro-4-oxothieno [20,30,4,5]pyrrolo[3,2-*H*]quinoline (13f) was achieved via Stille arylation of 7-chloro-6-fluoro-8-nitro-4-oxoquinoline-3-carboxylate and a subsequent microwave-assisted phosphite-mediated Cadogan reaction (Scheme 19.16). The newly synthesized

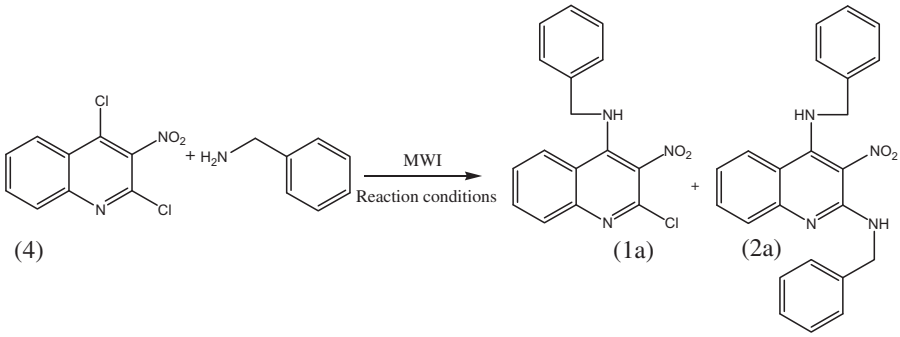

Scheme 19.15 Microwave-assisted synthesis of novel 4-aryl(alkyl)amino-3-nitroquinoline (1a) and 2,4-diaryl(dialkyl)amino-3-nitroquinolines (2a).

Table 19.6 Anticancer activity of the target compounds (1a–j, 2a–2j, and 3a).

Comp.	IC_{50} values (μM)			
	A-549 (lung cancer)	**H-460 (lung cancer)**	**HCT-116-wild type (colon carcinoma)**	**HCT-116-p53 null (colon carcinoma)**
1a	58.2	60.1	52.8	67.4
1b	56.1	51.3	49.7	69.1
1c	53.8	48.2	51.1	64.4
1d	38.2	42.9	43.1	52.1
1e	36.8	38.7	40.1	>70
1f	37.2	45.3	36.3	48.7
1g	32.9	42.7	33.3	34.6
1h	34.1	39.5	39.1	48.9
1i	53.4	59.2	49.7	>70
1j	57.2	51.1	54.3	>70
2a	40.2	43.1	50.6	>70
2b	45.2	41.7	43.9	69.3
2c	46.6	44.1	42.3	66.2
2d	19.2	25.5	26.3	61.0
2e	16.1	21.7	15.3	5.1
2f	6.5	5.4	20.1	19.8
2g	18.3	20.2	17.3	>70
2h	22.3	29.6	20.2	>70
2i	15.2	17.4	20.6	46.1
2j	11.2	7.1	24.1	52.3
3a	>70	15.8	>70	4.8
Erlotinib	12	8.30	7	–

compounds were tested for their in vitro antiproliferative activity [33]. The ability of 13a–f to inhibit the activity of DNA gyrase and topoisomerase IV was also investigated. Compounds 13a, 13c–f exhibited growth inhibition against MCF-7 breast tumor and A549 nonsmall cell lung cancer cells coupled with an absence of cytotoxicity toward normal human-derm fibroblasts (HuDe). Compound 13e was found to be active against MCF-7 cancer cells with high potency in comparison with standard drug Ellipticine with IC_{50} 0.8 and 1.6 l μM respectively (Table 19.7).

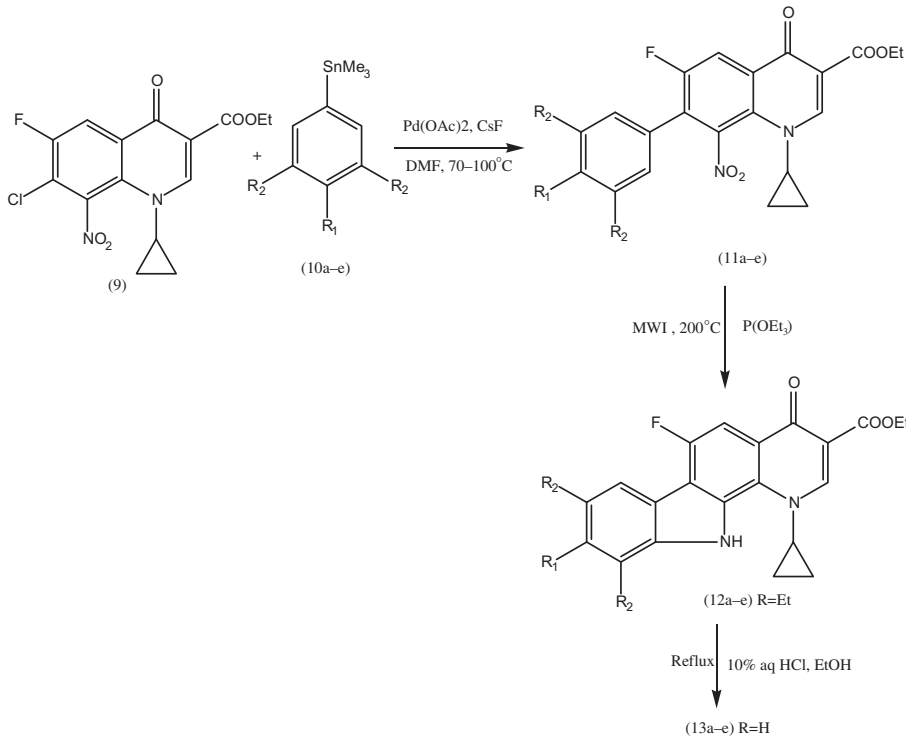

Scheme 19.16 Synthesis of tetracyclic fluoroquinolones derivatives.

Table 19.7 In vitro antiproliferative activity of titled compounds.

Comp.	R_1	R_2	IC_{50} (μM) MCF-7	IC_{50} (μM) A-549	IC_{50} (μM) HuDe
13a	H	H	3.6 ± 1.09	6.4 ± 1.02	>10
13b	Me	H	>10	>10	>10
13c	OMe	H	2.4 ± 1.05	4.9 ± 1.01	>10
13d	OMe	Me	1.7 ± 1.04	3 ± 1.03	>10
13e	F	H	4.4 ± 1.09	3.5 ± 1.07	>10
Ellipticine	–	–	1.6 ± 1.16	3.4 ± 1.04	>10

A new class of pyrano[3,2-*c*]quinoline analogs are synthesized in moderate to good yields by using microwave heating conditions. For enhancing the yield of products, multicomponent one-pot synthesis is developed. The cytotoxicity of these compounds is also evaluated against MCF-7 breast and A549 lung cancer cell lines. Most of the compounds displayed moderate-to-good anticancer activity against these cell lines (Scheme 19.17) [34].

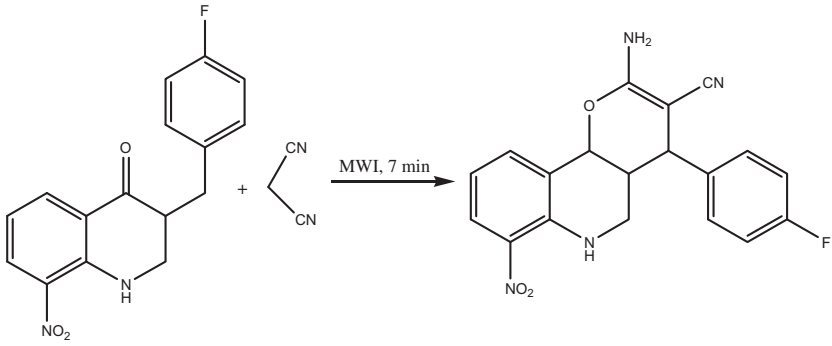

Scheme 19.17 Synthesis of quinoline analogs.

An efficient method for the synthesis of quinolines with good yields using microwave irradiation was developed [35]. The reaction was carried out between 4-bromoaniline (1a), benzaldehyde (2a) and styrene (3) in the presence of p-sulfonic acid calyx arene as catalyst under microwave irradiation (Scheme 19.18). The synthetic procedures were environmentally friendly, convenient, mild, and easy workup. Cell proliferation was determined by using the MTT assay with absorbance measurements at 540 nm. All synthesized quinolines (Q1–Q8) were evaluated in vitro against the various cancer cell lines such as NCI-H226 (lung), TOV-21G (ovary), and Hep-2c (HeLa contaminant). The concentrations of quinolines which caused cell growth inhibition by 50% (IC_{50} values) are summarized in Table 19.8.

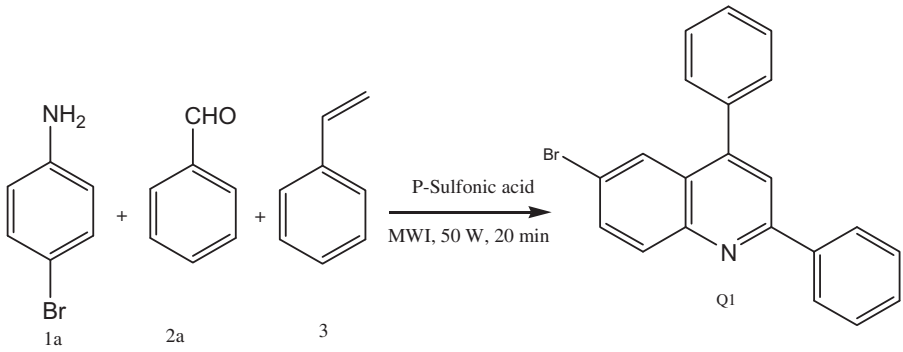

Scheme 19.18 Synthesis of quinoline (Q1).

Table 19.8 Concentration of quinolines required to inhibit the proliferation of tumor cells by 50% (IC_{50}).

Quinolines	IC_{50} (μM)		
	NCI-H226 (lung)	**TOV-21G (ovary)**	**Hep-2c**
Q1	43.4	530.7	128.1
Q2	1.58	ND	269.0
Q3	ND	570.4	5.0

ND, not determined.

19.1.10.2 Coumarin derivatives as anticancer agents

An efficient and rapid synthesis of coumarin derivatives was achieved via reactions of 3-(3-(4-methoxyphenyl)acryloyl)-2*H*-chromen-2-one (3) with different carbon nucleophiles such as ethyl acetoacetate, ethyl cyanoacetate, malononitrile, and ethyl benzoylacetate (Scheme 19.19). Both conventional heating and microwave irradiation conditions were used to perform the reactions (Table 19.9). The newly synthesized compounds were tested for in vitro cytotoxicity [36]. The preliminary screening results showed that most of the compounds have moderate cytotoxic activity against HCT-116 and MCF-7 cell lines as compared with the standard drug 5-fluorouracil (Table 19.10).

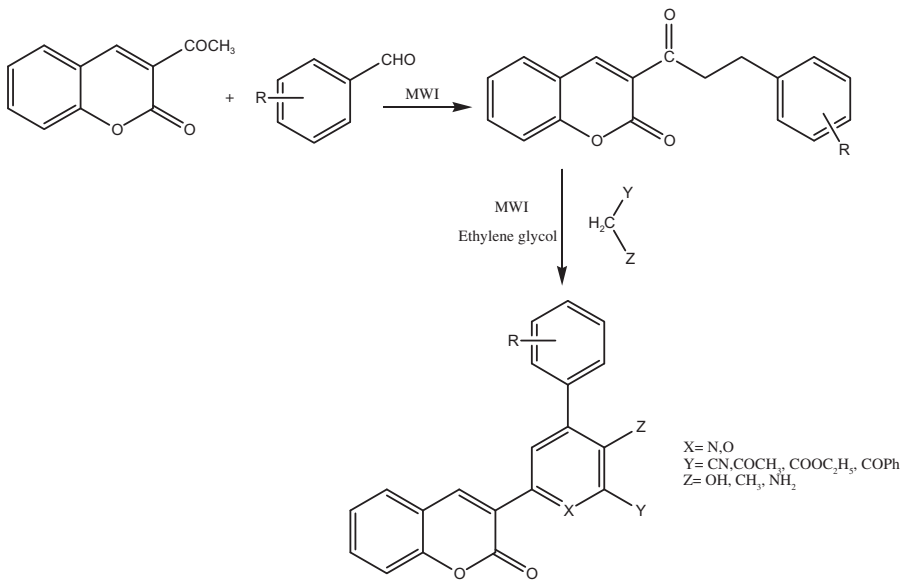

Scheme 19.19 Synthesis of coumarin derivatives.

Table 19.9 Comparison between conventional and microwave irradiation method.

Comp.	R	X	Y	Z	Time (min)		Yield (%)	
					C	M	C	M
4	*p*-C_6H_4-OCH_3	O	OH	$COCH_3$	360	3	59	85
5	*p*-C_6H_4-OCH_3	N	CH_3	$COOC_2H_5$	480	4	69	93
6	*p*-C_6H_4-OCH_3	O	OH	$COOC_2H_5$	420	3	57	86
7	*p*-C_6H_4-OCH_3	N	OH	CN	480	4	68	91
8	*p*-C_6H_4-OCH_3	N	NH_2	$COOC_2H_5$	360	4	63	89

C, conventional; *M*, microwave.

Table 19.10 Cytotoxic activity of some compounds against human tumor cells.

Compounds	In vitro cytotoxicity IC_{50} (μg/mL)	
	HCT-116	MCF-7
4	58.8 ± 3.10	41.4 ± 3.05
5	31.3 ± 2.37	27.4 ± 1.97
6	26.3 ± 2.28	50.5 ± 3.62
7	46.3 ± 2.58	42.5 ± 2.04
8	86.8 ± 4.15	72.9 ± 3.76
5-FU	40 ± 0.21	38.4 ± 0.17

1–10 (very strong), 11–20 (strong), 21–50 (moderate), 51–100 (weak), and >100 (noncytotoxic).

3-(Bromoacetyl)coumarin (3) is synthesized via two-step procedure. In the first step, the cyclocondensation of salicylaldehyde (1) with ethyl acetoacetate under microwave irradiation utilizing piperidine as a catalyst was involved to produce 3-acetylcoumarin (2). In the second step, compound (2) underwent bromination in the presence of chloroform to yield the bromoketone (3) with 63% yield (Scheme 19.20). Then, 2-arylidenehydrazinocarbothioamides (4a–t) were synthesized through condensation of the aromatic aldehydes and thiosemicarbazide in ethanol under microwave irradiation. Microwave irradiation technology was followed to react compounds (4a–t) and bromoketone (3) in ethanol by addition of ammonium hydroxide 5% to furnish the desired thiazolyl-coumarin hybrids (5a–t) in moderate to good yields (62%–89%) (Scheme 19.21). The new hybrid compounds were tested for in vitro antitumor efficacy over cervical (HeLa) and kidney fibroblast (COS-7) cancer cells. Compounds 5f, 5h, 5m, and 5r displayed promising efficacy toward HeLa cell line. In addition, 5h and 5r are found to be the most active candidates toward COS-7 cell line as presented in Table 19.11 [37].

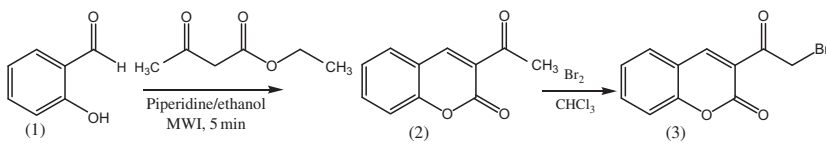

Scheme 19.20 Synthesis of 3-(bromoacetyl)coumarin (3).

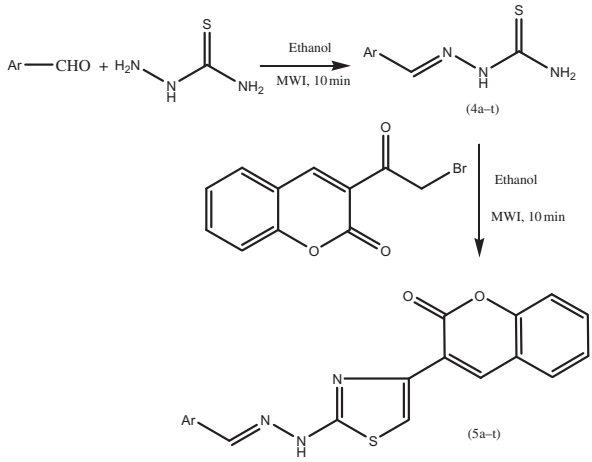

Scheme 19.21 Synthesis of thiazolyl-coumarin hybrids (5a–t).

Table 19.11 In vitro antitumor activity of 5a–j against HeLa and COS-7 cancer cell lines.

Comp. no.	Ar	IC_{50} (μg/mL)	
		HeLa	COS-7
5a	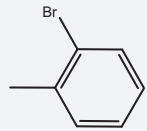	>50	>50
5b	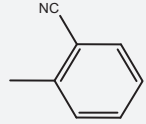	>50	>50
5c	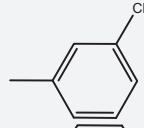	>50	>50
5d	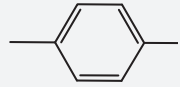	>50	>50
5e	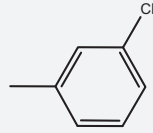	>50	>50
5f	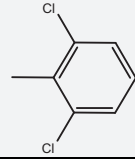	1.90	>50

Continued

Table 19.11 Continued

Comp. no.	Ar	IC_{50} (μg/mL)	
		HeLa	COS-7
5g	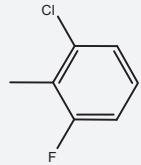	>50	>50
5h	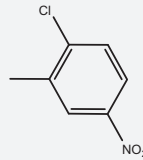	1.42	1.96
5i	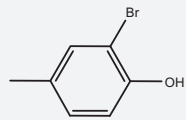	>50	>50
5j	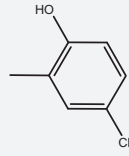	>50	>50
Doxorubicin	–	2.05	3.04

Microwave-assisted efficient and rapid synthesis of new fluorinated coumarin-pyrimidine hybrids (1a–1l) as potent anticancer agents was described (Scheme 19.22, Table 19.12). All the newly synthesized compounds (1a–1l) were evaluated for their anticancer activity against two human cancer cell lines *such as* A-549 (human lung carcinoma) and MDA-MB-231 (human adenocarcinoma mammary gland). From the results, it was revealed that some of the synthesized compounds exhibit significant cytotoxicity against the two tested cancer cell lines with $IC_{50} < 10$ μM (Table 19.13). Among the tested compounds, compound (1j) exhibited potent activity against the

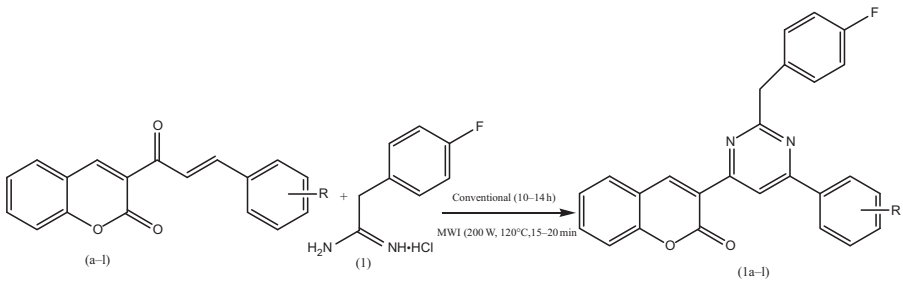

Scheme 19.22 Synthesis of new fluorinated coumarin-pyrimidine hybrids (1a–1l).

A-549 cell line in comparison with standard drug *Cisplatin*, whereas compound (1b) was found to be active against the MDA-MB-231 cell line as compared with standard drug *Cisplatin*. DNA cleavage study by the gel electrophoresis method revealed that compounds (1b), (1e), (1g), and (1j) inhibit the growth of the pathogenic organism by cleaving the genome [38].

Table 19.12 Comparative study of conventional and microwave irradiation method.

Products	R	Time (min)		Yield (%)	
		C	M	C	M
1a	*p*-CH_3	630	16	64	88
1b	*p*-OCH_3	600	15	67	91
1c	*m*-CH_3	680	16	61	81
1d	*m*-OCH_3	740	16	63	82
1e	*o*-CH_3	800	17	56	74
1f	*o*-OCH_3	820	19	54	76
1g	*p*-Br	730	16	61	83
1h	*m*-Br	750	18	57	79
1i	*o*-Br	840	20	54	74
1j	*p*-Cl	610	15	62	85
1k	*m*-Cl	650	16	59	81
1l	*o*-Cl	750	17	53	76

C, conventional; *M*, microwave.

Table 19.13 Anticancer activity of coumarin-pyrimidine hybrids (1a–1l).

Products	Cytotoxicity (IC_{50}) in μM	
	A-549	MDA-MB-231
1a	16.73 ± 1.42	4.16 ± 0.37
1b	16.11 ± 1.21	2.23 ± 0.19
1c	24.31 ± 2.38	16.42 ± 1.42
1d	22.41 ± 2.51	8.42 ± 0.73
1e	25.63 ± 2.58	4.62 ± 0.59
1f	21.72 ± 2.11	16.16 ± 1.31
1g	4.32 ± 0.53	24.43 ± 2.56
1h	8.43 ± 0.64	26.79 ± 2.79
1i	8.73 ± 0.84	28.57 ± 2.43
1j	2.15 ± 0.12	16.53 ± 1.61
1k	4.64 ± 0.59	8.31 ± 0.83
1l	8.56 ± 0.76	16.74 ± 1.82
Cisplatin	1.89 ± 0.09	3.5 ± 0.21

19.1.10.3 Synthesis of Imatinib as anticancer agents

An expeditious, high yield, and convenient synthesis of Imatinib was carried out on an aldehydic, super acid-sensitive resin, through an efficient, microwave-assisted synthetic protocol (Scheme 19.23). The high versatility of the reaction scheme enabled the straightforward preparation of libraries of potential protein kinase inhibitors endowed with large molecular diversity [39].

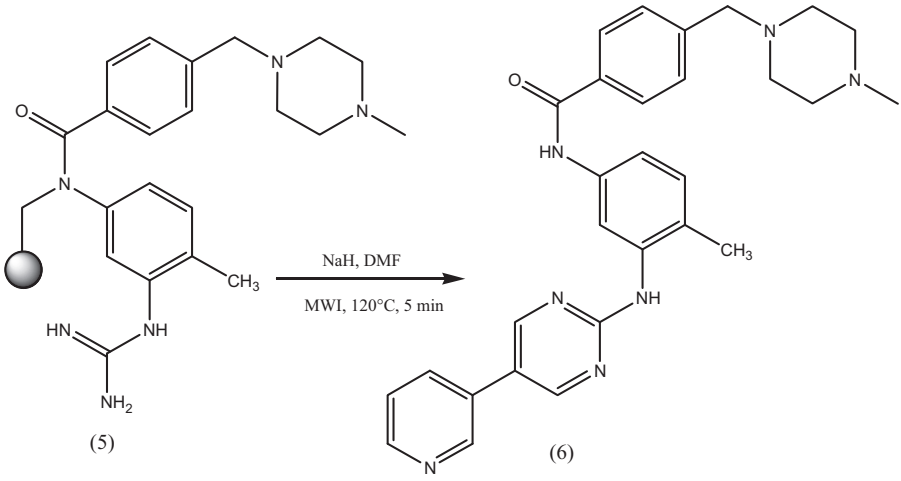

Scheme 19.23 Solid-phase synthesis of Imatinib.

19.1.10.4 Synthesis of thiadiazole derivatives as anticancer agent

A series of *S*-alkyl derivatives of 3-(substituted-(1,1′-biphenyl)-3-yl)[1,2,4]triazolo [3,4-*b*][1,3,4]thiadiazole-6-thiol (4a–j) were synthesized by both conventional and microwave irradiation methods (Scheme 19.24). Microwave irradiation method provided a rapid reaction rate with better yield as compared with conventional method [40]. The synthesized compounds were screened for their in vitro anticancer activity by MTT assay (Table 19.14). Among the tested compounds, the compound 4c was the most promising anticancer agent with IC_{50} value 12 μM in HT29 cell line.

A facile, solvent-free synthesis of a series of novel *N*-((5-(substituted methylene amino)-1,3,4-thiadiazol-2-yl)methyl)benzamide (7a–l) was carried out under microwave irradiation (Scheme 19.25, Table 19.15). All the synthesized hybrids were evaluated for their in vitro anticancer activity against a panel of four human cancer cell lines such as SK-MEL-2 (melanoma), HL-60 (leukemia), HeLa (cervical cancer), MCF-7 (breast cancer) and normal breast epithelial cell (MCF-10A) based on 3-(4,5-dimethythiazol-2-yl)-2,5-diphenyl tetrazolium bromide (MTT) assay method (Table 19.16). Most of the synthesized compounds exhibited promising anticancer activity as compared with standard drug adriamycin. The compounds 7k, 7l, 7b, and 7a were found to be the most promising anticancer agents in this study. A molecular docking study was performed to predict the probable mechanism of action and computational study of the synthesized compounds [41].

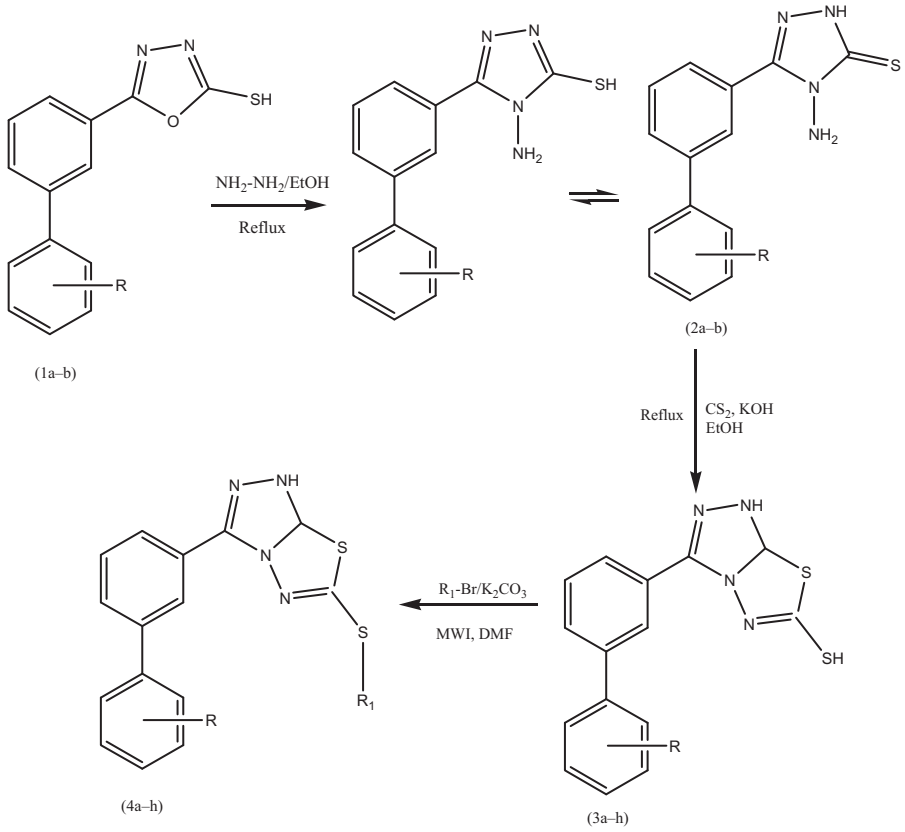

Scheme 19.24 Synthesis of *S*-alkyl derivatives of 3-(substituted-(1,10-biphenyl)-3-yl)[1,2,4] triazolo[3,4-*b*][1,3,4]thiadiazole-6-thiol.

Table 19.14 In vitro cytotoxicity data (IC_{50}, μM) of compounds 3a–b and 4a–j against cancer cell lines by MTT assay.

Comp.	R	R1	IC_{50} (μM)		
			HT29	K293	MDA231
4a	5′-F, 2′-OMe	$—(CH_2)_3CO_2Me$	20	50	35
4b	2′-F	$—(CH_2)_3CO_2Me$	24	55	38
4c	5′-F, 2′-OMe	$—(CH_2)_4F$	12	33	23
4d	2′-F	$—(CH_2)_4F$	15	36	25
4e	5′-F, 2′-OMe	$—(CH_2)_3CN$	24	53	38
4f	2′-F	$—(CH_2)_3CN$	28	57	40
4g	5′-F, 2′-OMe	$—(CH_2)_3NH_2$	19	67	31
4h	2′-F	$—(CH_2)_3NH_2$	26	71	39
4i	5′-F, 2′-OMe	$—(CH_2)_2OH$	24	69	34
4j	2′-F	$—(CH_2)_2OH$	31	75	45
Doxorubicin	–	–	08	25	16

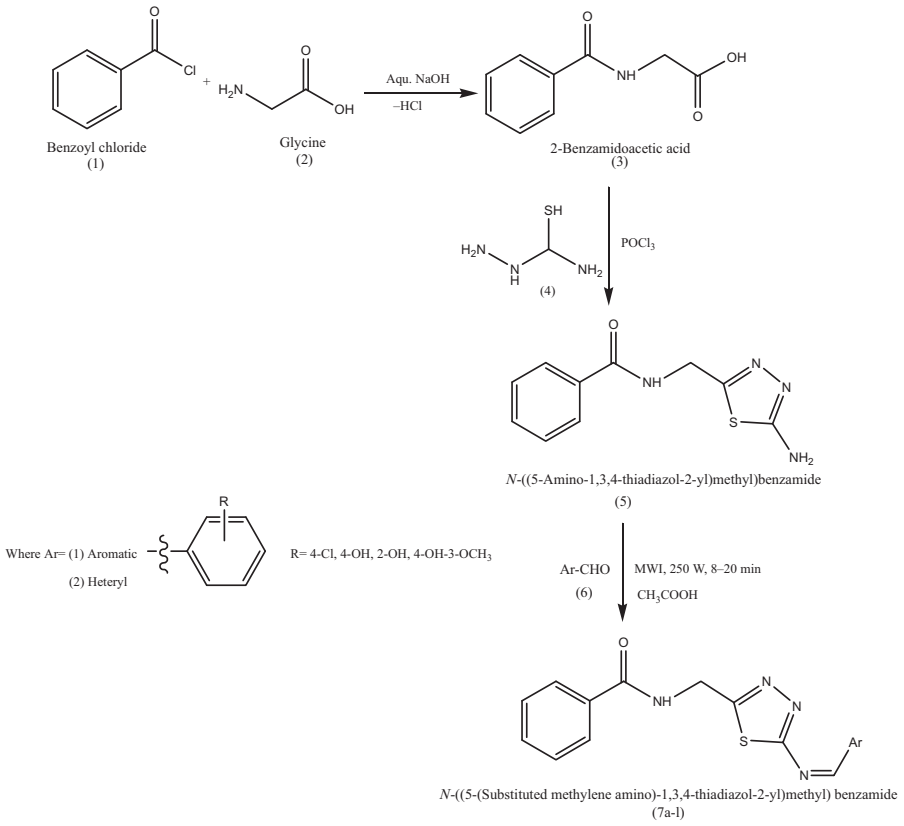

Scheme 19.25 Synthesis of *N*-((5-(substituted methylene amino)-1,3,4-thiadiazol-2-yl)methyl) benzamide (7a–l).

Table 19.15 Synthesis of compounds (7a–l) under microwave irradiation and conventional method.

Entry	Conventional method		Microwave method	
	Time (h)	Yield (%)	Time (min)	Yield (%)
7a	3.30	78	8	95
7b	5.10	77	12	92
7c	5.00	78	12	94
7d	7.20	66	15	94
7e	7.25	52	15	92
7f	8.00	48	18	92
7g	5.25	76	12	95
7h	7.30	66	15	88
7i	8.00	68	20	86
7j	8.00	48	20	88
7k	4.15	44	10	85
7l	4.25	56	10	84

Table 19.16 In vitro anticancer activity of compounds (7a–l).

Entry	GI_{50} (μM)				
	MCF-7	**HeLa**	**SKMEL-2**	**HL-60**	**MCF-10A**
7a	22.9	32.8	21.9	21.7	>100
7b	28.7	39.0	22.9	28.2	86.1
7c	32.4	41.1	27.5	33.3	ND
7d	36.7	52.4	34.0	40.2	ND
7e	35.2	46.8	28.1	39.6	ND
7f	38.4	49.2	30.0	37.5	ND
7g	41.0	66.1	46.4	42.4	ND
7h	46.2	71.7	49.1	48.2	ND
7i	49.0	78.0	52.6	45.8	ND
7j	51.4	78.8	55.7	49.9	ND
7k	11.7	23.8	19.6	35.5	>100
7l	19.0	28.8	22.0	29.9	>100
Adriamycin	<10	<10	<10	<10	ND

GI_{50}, concentration exhibiting 50% inhibition of growth; *ND*, not determined.

A series of 3-(5′-fluoro-2′-methoxybiphenyl-3-yl)-6-(substituted)[1,2,4]-triazolo [3,4-*b*][1,3,4]-thiadiazole (3a–j) were synthesized by conventional and microwave irradiation methods (Scheme 19.26). Microwave method provided a rapid rate of reaction with better yield as compared with conventional method (Table 19.17).

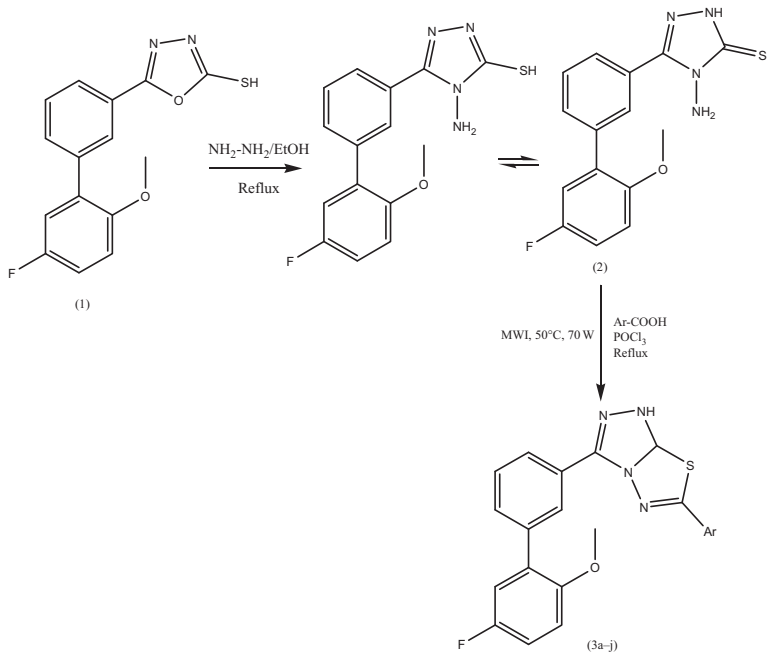

Scheme 19.26 Synthesis of thiadiazole derivatives (3a–j) by conventional and microwave irradiation methods.

These novel compounds were screened for their anticancer activity against cancer cell lines HT29 (human adenocarcinoma), K293 (human kidney cancer) and MDA231 (human breast cancer) by using the MTT assay (Table 19.18). Among the tested compounds, compounds 3b and 3g had promising anticancer activity [42].

Table 19.17 Determination of percentage yield of Thiadiazole derivatives (3a–j).

Comp. code	Ar	Yield (%)	
		Conventional	Microwave
3a	2-F-C_6H_4	65	79
3b	4-F-3-CF_3-C_6H_4	61	78
3c	4-I-C_6H_4	66	81
3d	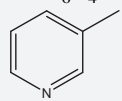	68	77
3e	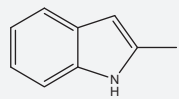	70	82
3f	2-Cl-6-F-C_6H_3	60	73
3g	2-F-5-NO_2-C_6H_3	62	72
3h	4-F-3-NO_2-C_6H_3	61	81
3i	2,4-Cl_2-5-F-C_6H_2	60	77
3j	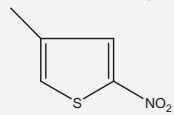	62	75

Table 19.18 In vitro cytotoxicity data (IC_{50}, μM) of compounds (3a–j) by using the MTT assay.

Comp. code	In vitro cytotoxicity (IC_{50}, μM)		
	HT29 ± SD	K293 ± SD	MDA231 ± SD
3a	83 ± 1.8	153 ± 1.2	94 ± 1.8
3b	10 ± 1.2	20 ± 1.1	9 ± 1.3
3c	81 ± 1.1	145 ± 1.2	78 ± 1.3
3d	86 ± 1.5	120 ± 1.4	87 ± 1.4
3e	75 ± 1.7	180 ± 1.8	90 ± 1.5
3f	81 ± 1.8	170 ± 1.8	75 ± 1.8
3g	13 ± 1.5	25 ± 1.1	13 ± 1.6
3h	21 ± 1.1	36 ± 1.4	28 ± 1.2
3i	52 ± 1.3	68 ± 1.3	75 ± 1.1
3j	15 ± 1.5	27 ± 1.8	17 ± 1.8
5-FU	8.5 ± 1.5	41 ± 1.1	10.1 ± 1.1

SD, standard deviation.

19.1.10.5 Benzimidazole derivatives as anticancer agents

Kayagil et al. performed the synthesis of 1,3-diarylpyrazino[1,2-*a*]benzimidazole derivatives and investigated their anticancer activities [43]. First of all, 2-aryloyl-benzimidazole derivatives (1a–c) were reacted with 2-bromo-acetophenones in acetone to produce 1-(2-aryl-2-oxoethyl)-2-aryloylbenzimidazoles (2a–e). The resulting materials were reacted with ammonium acetate in the presence of acetic acid to get titled compounds (3a–e) as presented in Scheme 19.27. Microwave irradiation method was applied to complete the reaction. The obtained compounds were investigated for their anticancer activities. It was observed that some of the compounds demonstrated significant anticancer activities (Table 19.19).

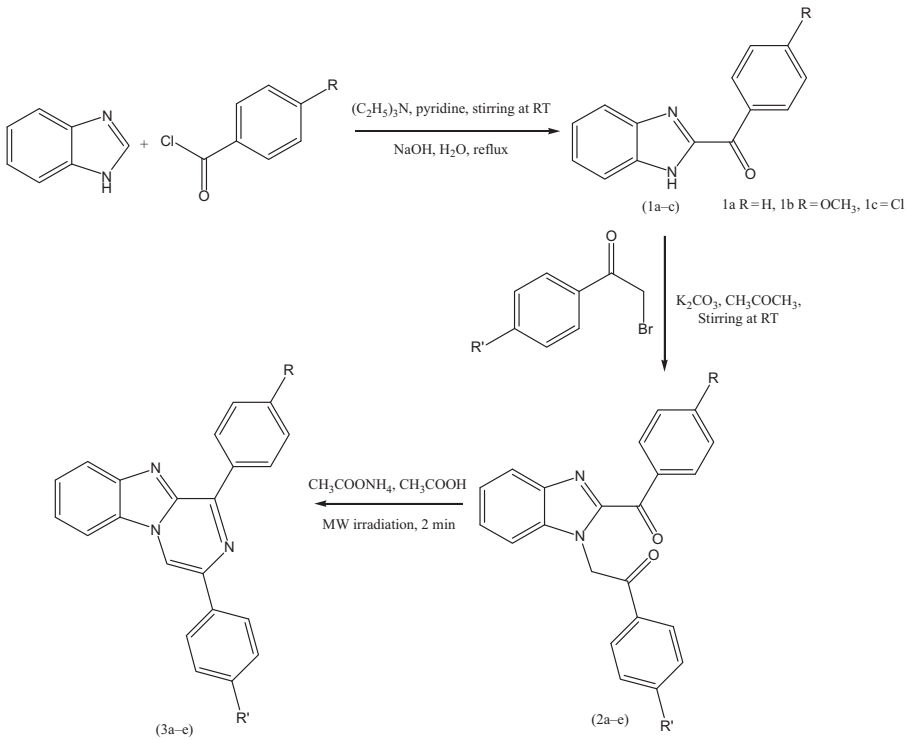

Scheme 19.27 Synthesis of titled compounds (2a–e, 3a–e).

Table 19.19 Anticancer activity (% growth) of titled compounds (2a–e, 3a–e).

Comp. code	R	R′	NSCLC	CNSC	OC	RC
2a	H	H	82.55	82.33	87.00	86.38
2b	H	CH_3	91.01	101.15	80.45	85.16
2c	H	OCH_3	36.00	25.38	30.25	38.60

Continued

Table 19.19 Continued

Comp. code	R	R′	NSCLC	CNSC	OC	RC
2d	H	F	70.39	65.49	65.25	71.58
2e	H	Cl	52.44	37.17	44.33	45.13
3a	H	H	100.25	62.17	61.50	101.17
3b	H	CH_3	100.38	77.00	85.17	103.00
3c	H	OCH_3	95.39	103.74	102.35	96.67
3d	H	F	92.59	91.16	91.34	91.75
3e	H	Cl	79.33	67.50	64.50	84.14

A series of new benzimidazole bearing thiazolidinedione derivatives was designed and synthesized by using conventional as well as microwave-assisted methods (Fig. 19.20). Microwave-assisted synthesis caused a significant reduction in the reaction times and improvement in the yields of all the derivatives. All the new synthesized compounds were evaluated for their in vitro cytotoxic potential against selected human cancer cell lines such as breast (MDA-MB-231), prostate (PC-3), cervical (HeLa), lung (A549), and bone (HT1080) along with normal kidney cells (HeK-293T). The compounds 17n, 17p, and 17q were found to be potent cytotoxic with IC_{50} values in the range of 0.096–0.63 μM on PC-3, HeLa, A549, and HT1080 cells. Most of the compounds were safe on normal HeK-293T kidney cells in comparison with cancer cells [44].

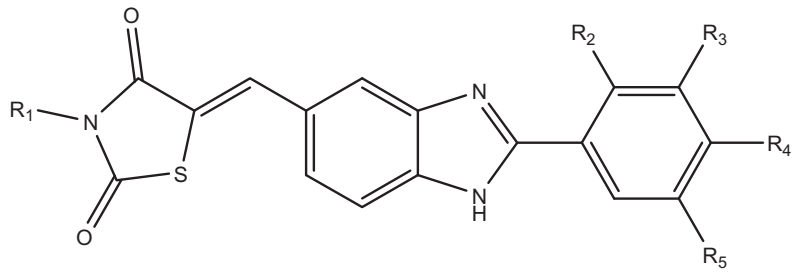

Fig. 19.20 Structure of benzimidazole bearing thiazolidinedione derivatives.

New 2-quinolizinyl-benzimidazole and 2-naphthalyl-benzimidazole derivatives with various 5- and 6-positioned substituents (aza, H, CH_3, Cl, NO_2, NH_2, OCH_3), were synthesized in moderate to excellent yields via the condensation of 4-oxo-4*H*-quinolizine-carbaldehyde or naphthalene-carbaldehyde with substituted *o*-phenylenediamines, *o*-nitroaniline, and 2,3-pyridinediamine using sodium metabisulfite or sodium hydrosulfite under microwave irradiation. These compounds were tested for cytotoxicity against human breast cancer cell line MCF-7. The results showed that some of the tested compounds are found to be as active as compared with standard drug tamoxifen (Scheme 19.28) [45].

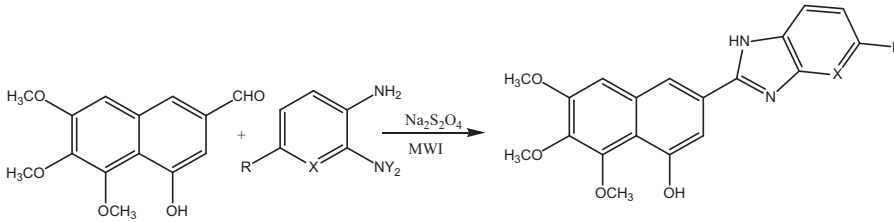

Scheme 19.28 Synthesis of benzimidazole derivatives.

19.1.10.6 *Pyrrole derivatives as anticancer agents*

A series of novel *N*-substituted pyrrole derivatives were designed and synthesized by reacting 2,5-dimethoxy-tetrahydrofuran with diverse amines under ultrasound-assisted condition in presence of $Bi(NO_3)_3{\cdot}5H_2O$ as catalyst (Scheme 19.29). This method provided eco-friendly route to prepare diverse varieties of *N*-substituted pyrroles with less nucleophilic polyaromatic amines. Cytotoxicity of some selected *N*-substituted pyrrole derivatives was evaluated in vitro in a panel of mammalian cancer cell lines which includes liver cancer cell lines (HepG2 and Hepa1-6), colon cancer cell lines (HT-29 and Caco-2), a cervical cancer cell line (HeLa) and NIH3T3 cells. Two compounds, 5-(1*H*-pyrrol-1-yl)-1,10-phenanthroline, and 1-(phenanthren-2-yl)-1*H*-pyrrole demonstrated good cytotoxicity against some cancer cell lines. Furthermore, these compounds exhibited cytotoxic specificity against liver cancer cell lines in vitro when compared with normal cultured primary hepatocytes [46].

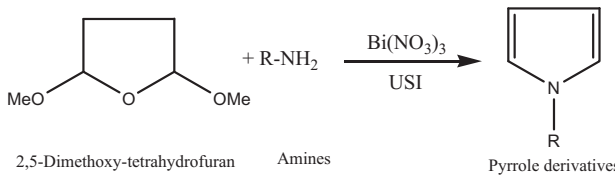

Scheme 19.29 Synthesis of pyrrole derivatives.

19.1.10.7 *Ferulic acid amide derivatives as anticancer agents*

Various amide derivatives of ferulic acid were synthesized under solvent-free conditions by using microwave-assisted reaction (Scheme 19.30). These compounds were found to exhibit in vitro anticancer activity against breast (MDA-MB-231 and MCF-7), cervical (HeLa), lung (A549), and liver (HepG2) human cancer cell lines [47].

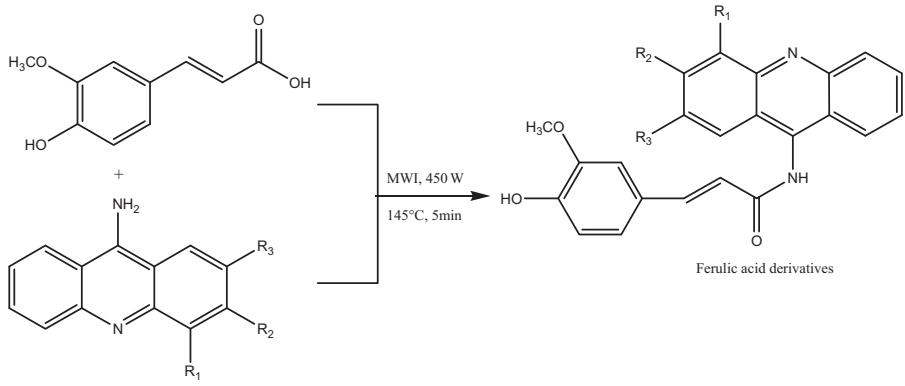

Code	R1	R2	R3
a	H	H	H
b	CH_3	H	H
c	H	CH_3	H
d	H	H	CH_3
e	OCH_3	H	H
f	H	CH_3	H
g	H	H	OCH_3

Scheme 19.30 Synthesis of ferulic acid derivatives.

19.1.10.8 Pyridine derivatives as anticancer agents

Novel tricyclic 5*H*-thiochromeno-pyridine and 5*H*-chromenopyridine analogs were designed and synthesized to evaluate the cytotoxic activity against human melanoma and glioma cell lines [48]. All of the 5*H*-thiochromenopyridines were achieved in good yields (89%–93%) via single-step, three-component cyclization under MWI (Scheme 19.31). All newly prepared 5*H*-thiochromenopyridines exhibited good to moderate cytotoxicity against three melanoma and two glioma cell lines (3–15 μM) (Table 19.20).

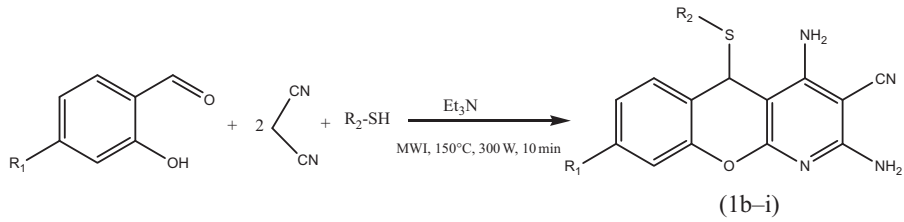

Scheme 19.31 Synthesis of pyridine analogs under MWI.

Table 19.20 Antiproliferative activity of pyridine analogs.

Comp. code	R1	R2	IC_{50} value (μM) ± SEM		
			A375	WM164	MT330
1a	—OCH_3	C_6H_5	6.4 ± 0.8	7.5 ± 1.2	>30
1b	—OCH_3	4-F-C_6H_5	6.7 ± 1.5	3.5 ± 1.2	6.1 ± 1.9
1c	—OCH_3	4-Fluoro-naphthalene	6.3 ± 0.7	3.6 ± 0.6	4.6 ± 0.1
1d	—OCH_3	4-OCH_3-C_6H_5	7.0 ± 0.9	6.6 ± 1.0	4.5 ± 0.9
1e	—OCH_3	Naphthalene	5.3 ± 0.7	5.7 ± 1.4	5.2 ± 0.0
1f	—OCH_3	$(CH_3)_2NH$-C_6H_5	5.7 ± 0.4	5.6 ± 0.6	5.4 ± 0.0
1g	$(CH_3)_2NH_2$-	4-OCH_3-C_6H_5	7.2 ± 1.4	9.7 ± 2.7	8.3 ± 0.0
Colchicine	–		0.02 ± 0.01	0.03 ± 0.02	–

Based on this green chemistry approach, two novel series of 2-amino cyanopyridine series (5a–g) and 2-oxocyanopyridine series (6a–g) were synthesized (Scheme 19.32). All of the newly synthesized compounds were evaluated for their in vitro anticancer activity against a panel of three cell lines such as liver cancer cell

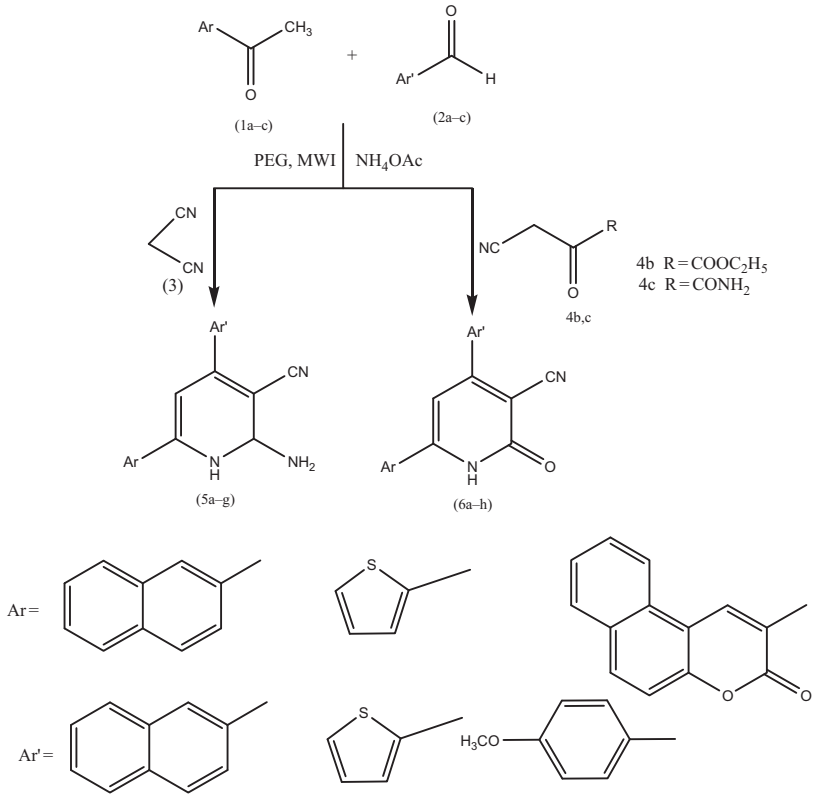

Scheme 19.32 Synthesis of 3-cyano pyridine derivatives under MWI condition.

line (HepG2), colon cancer cell line (HCT-116), and the breast cancer cell line (MCF-7). Most of the compounds exhibited good to moderate antiproliferative activity against HepG2 and HCT-116 cell lines while only a few compounds showed significant cytotoxic activity against MCF-7 cell line. Further, the Pim-1 kinase inhibitory activity for the two series is evaluated where most of the tested compounds showed marked Pim-1 kinase inhibitory activity (26%–89%) as presented in Table 19.21 [49].

Table 19.21 In vitro anticancer activity of compounds 5(a–g) and 6(a–g).

Comp.	Structure	HepG2 (μM)	HCT-116 (μM)	MCF-7 (μM)	% inhibition of Pim-1 kinase	Pim-1 kinase IC_{50} (μM)
5a	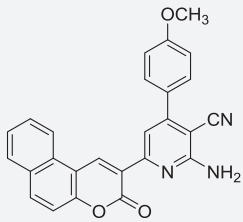	299.83	NA	NA	26.00	–
5b	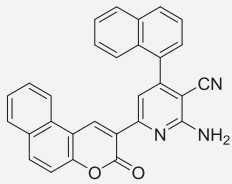	45.80	30.61	80.73	61.55	25.5
5c	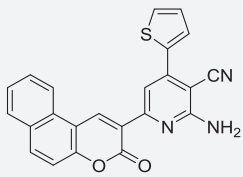	35.7	80	59.1	69.23	19.25
5d	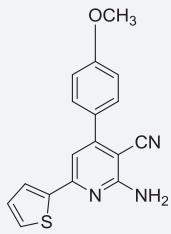	103.58	122.00	88.27	76.92	–

Table 19.21 Continued

Comp.	Structure	HepG2 (μM)	HCT-116 (μM)	MCF-7 (μM)	% inhibition of Pim-1 kinase	Pim-1 kinase IC_{50} (μM)
5e	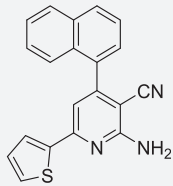	180.73	66.67	38.83	58.53	–
5f	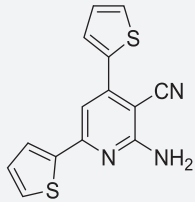	28.27	91.17	72.08	85.03	7.52
5g	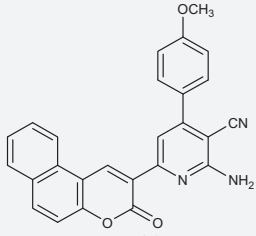	11.9	20.51	19.23	86.50	1.16
6a	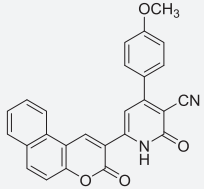	36.26	24.89	36.73	83.07	10.6
6b	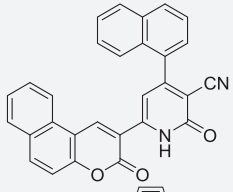	15.28	25.91	25.23	79.54	1.47
6c	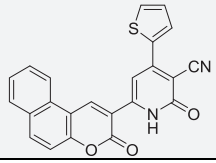	30.5	36.18	20.60	89	0.94

Continued

Table 19.21 Continued

Comp.	Structure	HepG2 (μM)	HCT-116 (μM)	MCF-7 (μM)	% inhibition of Pim-1 kinase	Pim-1 kinase IC_{50} (μM)
6d	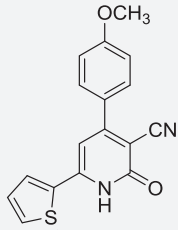	15.48	28.70	21.93	72.95	6.70
6e	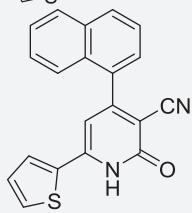	35.87	28.6	27.1	77.85	4.8
6f	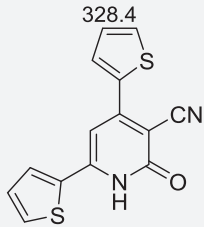	41.60	187.06	248.60	84.82	3.16
6g	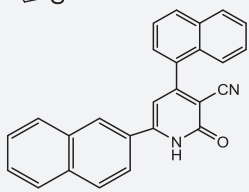	220	228	236	81.05	10.04
5-FU	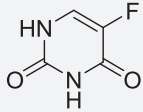	8.1	9.9	7.9	–	–

Carboethoxy/carbomethoxy pyridine derivatives were synthesized by both conventional and microwave irradiation method via one-pot three-component reaction mixture which consists of alkyl acetoacetate, aldehyde, and ammonium acetate (Scheme 19.33). The synthesized products were evaluated for their cytotoxic activity against MDA-MB (breast) and HT-29 (colon) human cancer cell lines. Few compounds exhibited some degree of cytotoxicity [50].

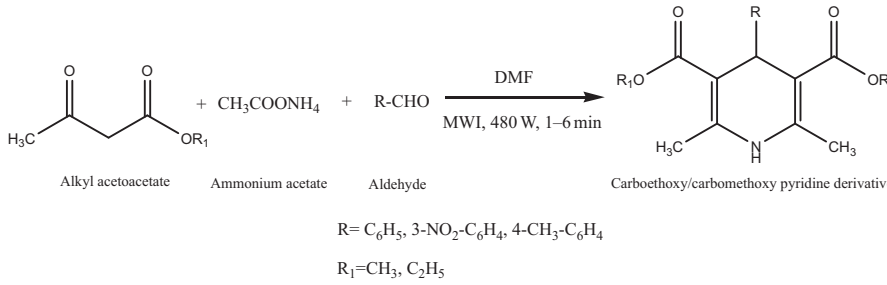

Scheme 19.33 Synthesis of carboethoxy/carbomethoxy pyridine derivatives.

19.1.10.9 Thiazoles as anticancer agents

A series of novel 2-aminothiazole (1,3,5,7,9) and 2-aminooxazole (2,4,6,8,10) derivatives were synthesized by using microwave-assisted method as a green chemistry approach (Scheme 19.34). The newly synthesized were screened for their anticancer activity against HeLa cell lines by MTT assay. Compound 9, 5, and 2 showed marked binding scores in the docking studies and exhibited anticancer activity with an IC_{50} value of 19.5, 31.20, and 52.43, respectively [51].

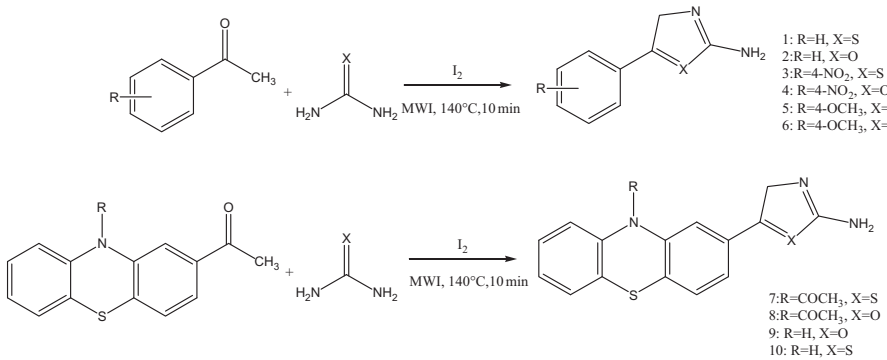

Scheme 19.34 Microwave-assisted synthesis of 2-aminothiazole derivatives.

The microwave-promoted cyclization method was used for the synthesis of a series of novel substituted 2,4-diarylthiazoles from α-halo ketones and thioamides using ethanol as solvent (Scheme 19.35). This rapid method produced compounds in good yield within 1 min in comparison with the conventional heating method. The synthesized molecules were evaluated for their antiproliferative effects against five different cancer cell lines [52].

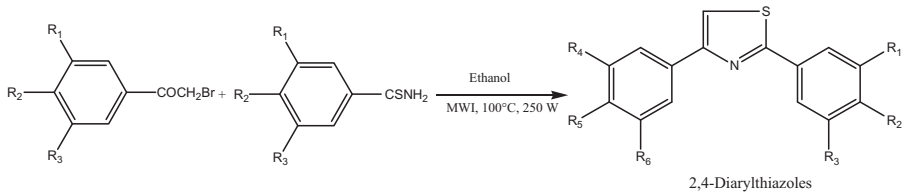

Scheme 19.35 Microwave-promoted synthesis of substituted 2,4-diarylthiazoles.

19.1.10.10 Quinazoline as anticancer agents

Novel series of imidazolo-quinazoline-4-one derivatives analogs (Fig. 19.21) are synthesized and screened for antitumor activity. The compounds showed significant in vitro antitumor action in selective cancer cell lines [53]. MTT assay confirmed the anticancer nature of the compounds tested against A-549, Vero, and HBL-500 cell lines (Table 19.22).

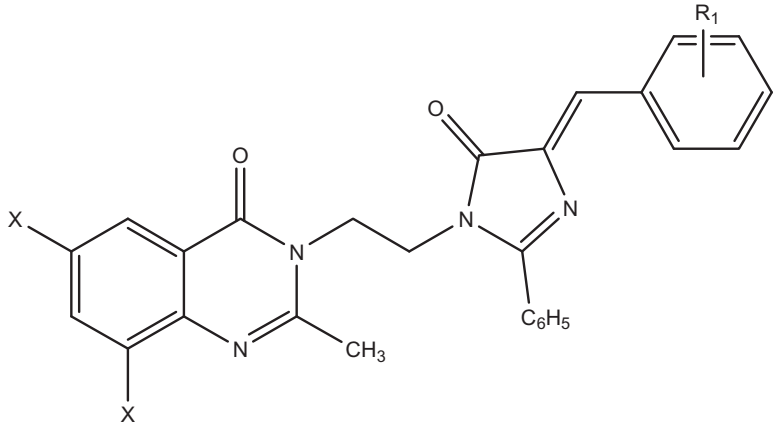

Fig. 19.21 Structure of imidazolo-quinazoline-4-one derivatives analogs.

Table 19.22 Antitumor activity of quinazolin-(3*H*)-ones.

Entry	X	R1	IC_{50} value (μM)		
			Vero	A-549	HBL-100
1	H	C_6H_5	40.11	22.97	51.87
2	H	C_6H_4OH	39.99	23.12	48.31
3	H	$C_6H_4N(CH3)_2$	71.9	35.33	152
4	Br	C_6H_5	28.87	12.22	53.19

19.1.10.11 Pyrazole as anticancer agents

Multicomponent reaction of acetyl pyrazole (1), dimethylformamide dimethylacetal (DMF-DMA) (2), and nitrileimine (4a–d) (generated in situ from 3a–d with triethylamine) in toluene under conventional heating for 10–15 h or under microwave irradiation at 150°C for 4–10 min afforded novel pyrazole-based azoles (6a–d) as presented in Scheme 19.36 and Table 19.23. All the newly synthesized compounds were evaluated for their in vitro anticancer activity against human lung cancer and human hepatocellular carcinoma cell lines using MTT assay [54]. The results obtained exploring the high potency of six of the tested compounds were compared with standard antitumor drug cisplatin (Table 19.24).

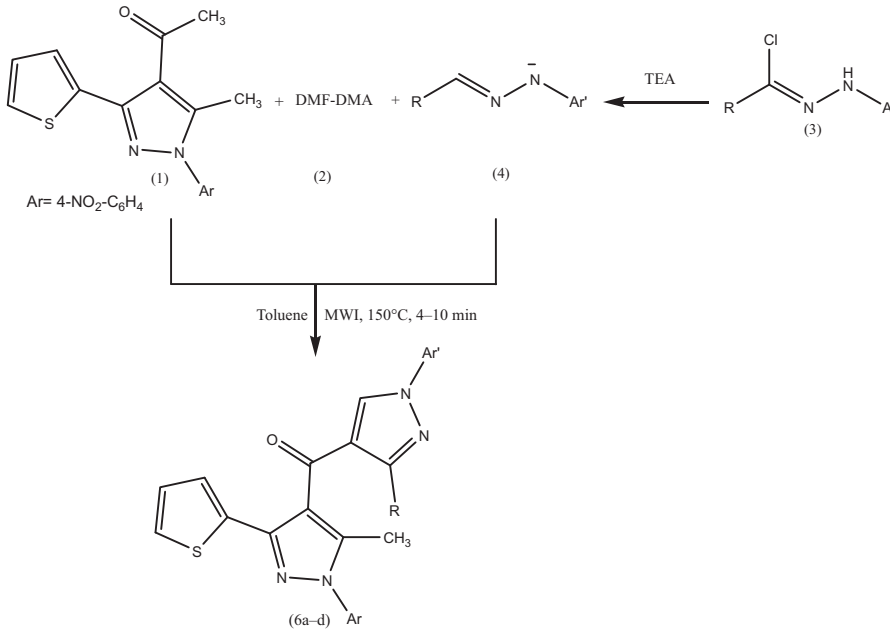

Scheme 19.36 Conventional and MWI methods for the synthesis pyrazole-based azoles (6a–d).

Table 19.23 Comparative data of conventional and MWI methods for the synthesis of compounds 6a–d.

	Conventional method		MWI method	
Comp.	**Time (h)**	**Yield (%)**	**Time (min)**	**Yield (%)**
6a	12	66	4	84
6b	15	68	10	85
6c	10	70	8	88
6d	8	69	5	90

Table 19.24 In vitro inhibitory activity of test compounds (6a–d) against tumor cell lines.

Test compound	R	Ar′	IC_{50} value (μM) ± SEM	
			A-549	Hepg2
6a	$COCH_3$	Ph	22.9 ± 0.9	5.60 ± 0.8
6b	$COCH_3$	4-Me-C_6H_4	38.5 ± 1.2	44.4 ± 1.3
6c	COC_2H_5	Ph	23.3 ± 0.9	22.4 ± 0.9
6d	2-Thienyl	4-NO_2-C_6H_4	30.6 ± 1.1	35.9 ± 1.4

A series of compounds having the pyranopyrazole pharmacophore were synthesized via four-component reaction between ethyl-3-oxobutanoate, hydrazine hydrate, malononitrile, and aldehydes by using both traditional method and microwave-assisted method (Scheme 19.37). The microwave strategy involved rapid rate of reaction with high product yield as compared with the traditional method (Table 19.25). The synthesized molecules were tested in vitro for their cytotoxic activity against the Hep3B cancer cell lines (Table 19.26). The activity results were subsequently rationalized for a quick structure-activity relationship leading to the conclusion that the presence of certain heteroatom substituents at a 3-position of the pharmacophore may be vital for anticancer potency [55].

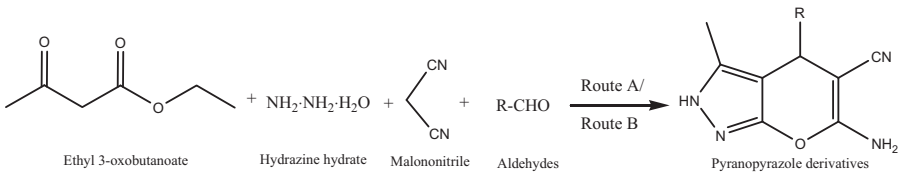

Scheme 19.37 Synthesis of pyranopyrazole pharmacophore under MWI. Route A: Et_3N, EtOH, 1–2 h, rt, average yields 85%. Route B: MWI reaction, EtOH, Et_3N, 3–5 min, average yields 81%.

Table 19.25 Synthesis of pyranopyrazole pharmacophore via Route A or B.

Entry	R	Route A		Route B	
		Time (min)	Yield (%)	Time (min)	Yield (%)
1	3′-OH-C_6H_4	100	88	4	82
2	4′-Br-C_6H_4	130	82	3	80
3	3′-Br-C_6H_4	110	80	5	77
4	3′-NO_2-C_6H_4	140	86	5	81
5	3′-Thiophenyl	90	88	4	80
6	2′-Pyrroyl	90	85	4	80
7	3′-Indolyl	110	81	5	79

Table 19.26 In vitro cytotoxic activity of test compounds against cancer cell lines.

Entry	IC_{50} value (mg/mL)
1	32
2	16
3	4–16
4	32
5	16–32
6	128
7	64

The fluorinated chalcone and pyrazoline derivatives were successfully synthesized by reacting 1-acetylnaphthalene (5 mmol) and 2-fluorobenzaldehyde (5 mmol) in the presence of ethanol (2.5 mL) under microwave irradiation condition at 180 W for 3 min (Scheme 19.38). Docking studies were performed to evaluate the effects of compound 1 and compound 2 against breast cancer. Docking study and MD simulation showed the binding affinity of two pyrazoline chalcone derivatives (compounds 1 and 2) to be within the enzyme binding pockets with relatively constructed hydrogen bond and van der Waals interaction. These compounds were used as potential drug candidates for anticancer activity [56].

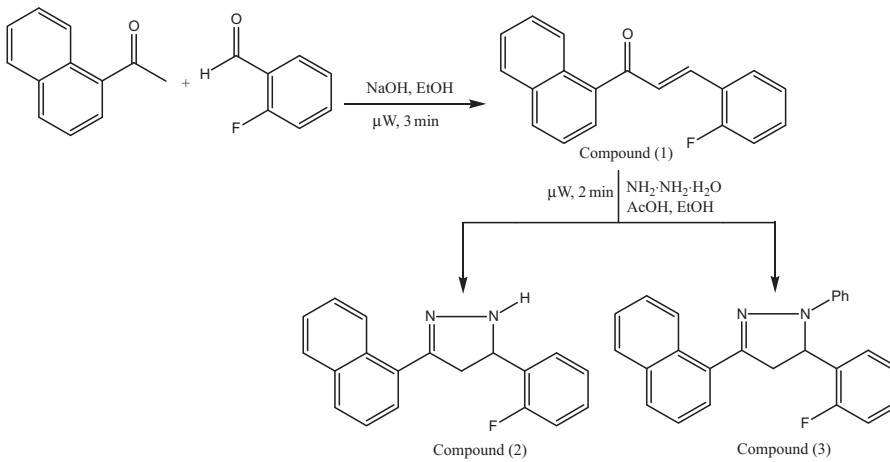

Scheme 19.38 Synthesis of fluorinated chalcone and pyrazoline analogs.

A series of novel pyrazole derivatives bearing pyran (4a, b), pyridine (5a, b), pyrazole (6) were synthesized under microwave irradiation (Scheme 19.39, Table 19.27). All the synthesized compounds screened for the anticancer activity against three tumor cell lines using doxorubicin as standard drug. Compounds 5b ($IC_{50} = 0.36, 0.28, 0.32$ μmol L^{-1}) was observed as good cytotoxic agents against the three tumor cell lines in comparison with the activity of doxorubicin (Table 19.28) [57].

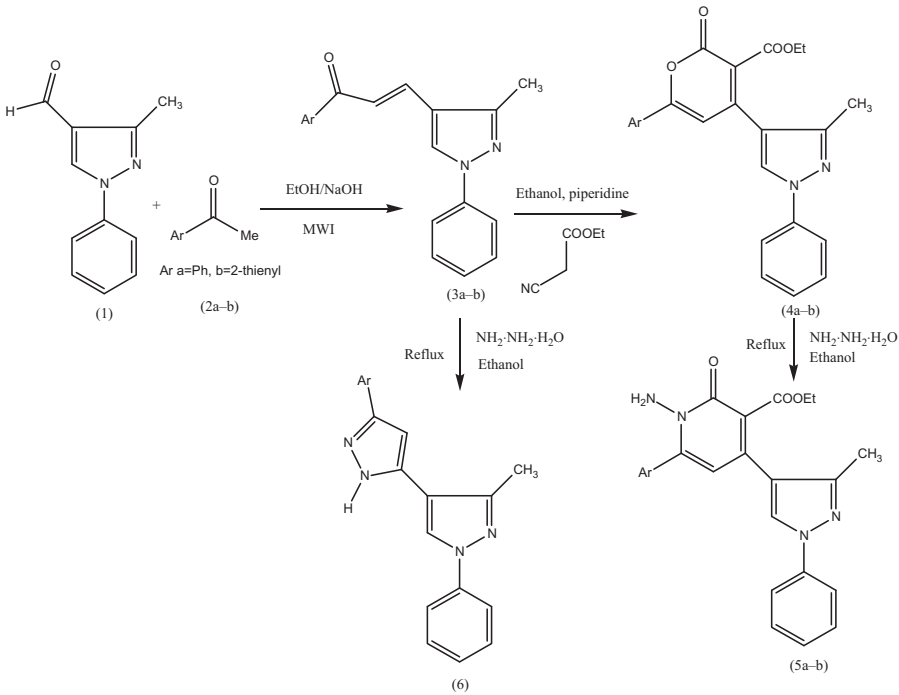

Scheme 19.39 Synthesis of 4-substituted-3-methyl-1-phenyl-1*H*-pyrazole derivatives.

Table 19.27 Comparison of yield of compound 3a–b with or without MWI.

Comp.	Method	Time	Temp. (°C)	Yield (%)
3a	No-MWI	16 h	rt	60
3b	No-MWI	19 h	rt	65
3a	MWI	180 s	70	89
3b	MWI	300 s	90	91

Table 19.28 In vitro anticancer activity of tested compounds against tumor cell lines.

Comp.	Tumor cell lines, IC_{50} value (μmol L^{-1}) ± SEM		
	MCF-7	HepG2	HT 29
4a	22.40 ± 0.20	29.11 ± 0.21	25.42 ± 0.21
4b	29.41 ± 0.07	23.42 ± 0.21	20.1 ± 0.12
5a	4.35 ± 0.47	5.59 ± 0.37	4.06 ± 0.38
5b	0.36 ± 0.22	0.28 ± 0.09	0.32 ± 0.01
6	10.71 ± 0.27	15.72 ± 0.24	13.71 ± 0.28
Doxorubicin	0.46 ± 0.21	0.42 ± 0.22	0.38 ± 0.025

19.1.10.12 Indole derivatives as anticancer agents

The novel pyrido[3,4-*b*]indoles are synthesized by using both conventional and microwave irradiation method [58]. First, tryptamine derivative (0.524 mmol) and aldehyde (0.63 mmol) are dissolved in THF (20 mL). The reaction mixture was cooled to 0°C and then CF_3COOH (0.2 mL) was added at 0°C and the reaction mixture is stirred at 0°C for 1 h to obtain tetrahydro-β-carboline product. Under microwave irradiation method, tryptamines (0.62 mmol) and aldehydes (0.75 mmol) are allowed to react in the presence of 10% Pd/C and 500 mg of montmorillonite K-10 and irradiated at 100 W for 60 min at 150°C to obtain tetrahydro-β-carbolines (Scheme 19.40). These compounds were screened for their antiproliferative activity against a broad range of human cancer cell lines, comprising HCT116 colon, HPAC, MIA PaCa-2 and Panc-1 pancreatic, MCF-7 and MDA-MB-468 breast, A375 and WM164 melanoma, A549 lung, and LNCaP, DU145, and PC3 prostate cancer lines (Table 19.29).

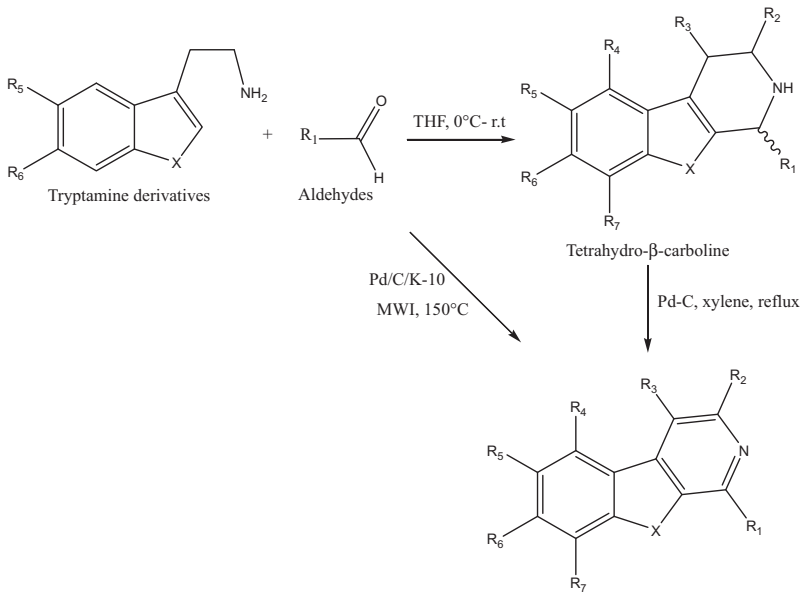

Scheme 19.40 Synthesis of new pyrido[3,4-*b*] indole (β-carboline) derivatives.

Table 19.29 Antiproliferative activity of pyrido[3,4-*b*]indoles.

Entry	R_1	R_2	R_3	R_4	IC_{50} value (μM)	
					MCF-7	MDA-MB-468
1	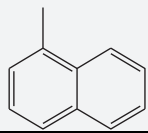	OCH_3	H	H	0.26	0.08

Continued

Table 19.29 Continued

Entry	R_1	R_2	R_3	R_4	IC_{50} value (μM)	
					MCF-7	MDA-MB-468
2	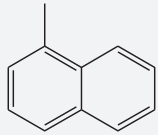	H	H	H	1.42	0.80
3	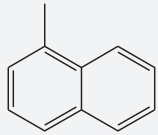	OCF_3	H	H	7.61	4.99
4	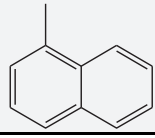	H	H	CH_3	50.80	14.23

19.1.10.13 Pinostrobin as anticancer agent

Pinostrobin (5-hydroxy-7-methoxyflavanone) (1) was produced in large amounts from finger root (*Boesenbergia pandurata*) and was further converted to its C-6 (2) and C-8 (3) prenylated derivatives based on efficient microwave-assisted synthesis (Fig. 19.22) [59]. The Mitsunobu reaction, europium (III)-catalyzed Claisen-Cope rearrangement, and Claisen reaction coupled with cross-metathesis were used as the key steps. By using a sealed-vessel microwave reactor, the Mitsunobu and Claisen/Cope reactions proceeded smoothly with short reaction times and satisfactory yields. The target compounds and five new intermediary substances showed cytotoxic activity toward SK-BR-3, MCF-7, PC-3, and Colo-320DM human tumor cell lines, and all of them had significantly lower IC_{50} (μM) values than pinostrobin.

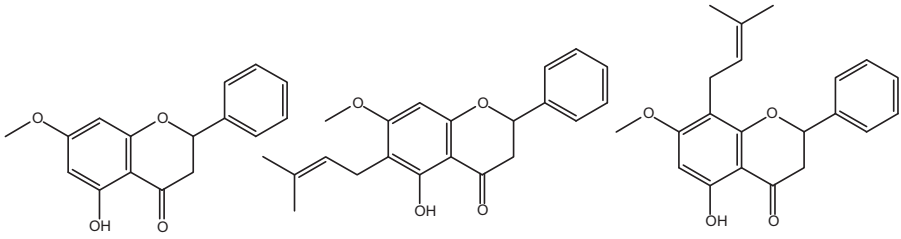

Fig. 19.22 Pinostrobin (1) and its prenylated derivatives (2 and 3).

19.1.10.14 Pyrimidine derivatives as anticancer agents

Green synthetic approach was followed for the synthesis 5-amino-2-(4-chlorophenyl)-7-substituted-phenyl-8,8a-dihydro-7*H*-(1,3,4)thiadiazolo(3,2-α)pyrimidine-6-carbonitrile (Scheme 19.41). It involved ultrasound mediated one-pot, three-component reaction between 5-(4-chlorophenyl)-1,3,4-thiadiazol-2-amine, malononitrile, and aldehydes in the presence of sodium hydroxide and ethanol. This green protocol was advantageous in terms of using eco-friendly catalyst, reduced reaction time, simple work-up process, ease of isolation, and high yield of product. The in vitro anticancer activities of these compounds were evaluated against four human tumor cell lines. Among all the tested compounds, compound 4i, which has substituent 3-hydroxy-4-methoxyphenyl was found to have the highest GI_{50} value of 32.7 μM, 55.3 μM, 34.3 μM, 28.9 μM for MCF-7, K562, HeLa, and PC-3 cancer cell lines, respectively [60].

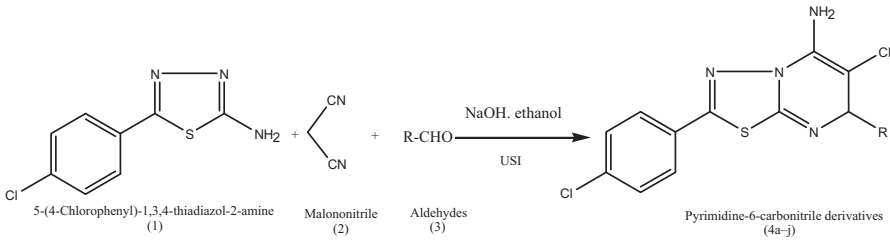

Scheme 19.41 Synthesis of pyrimidine-6-carbonitrile derivatives.

19.1.10.15 Miscellaneous

Dibenzo[*a*,*h*]anthracene derivatives were synthesized via a one-pot synthetic protocol with three-component reaction of 2-hydroxy-1,4-naphthoquinone, aromatic aldehydes, and 2-naphthol using $InCl_3$ as catalyst under solvent-free condition (Scheme 19.42). These *o*-quinonic adducts showed strong cytotoxicity against MCF-7 and HEL tumoral cell lines [61].

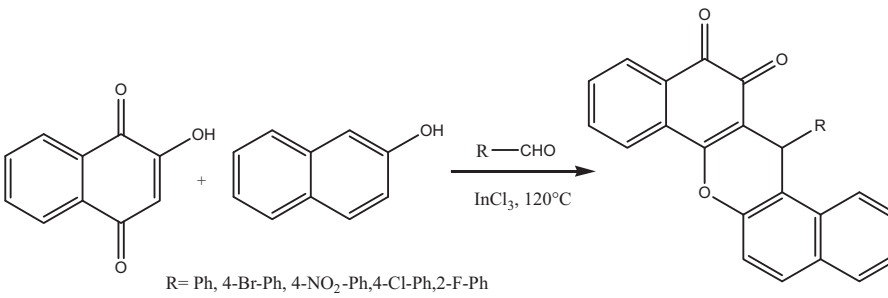

Scheme 19.42 Synthesis of *o*-quinonic adducts.

A series of 1-hydroxynaphthalene-2-carboxanilides were designed based on the fragment-based approach and are synthesized based on the microwave-assisted protocol (Scheme 19.43). The biological activity of all of the compounds was tested on human colon carcinoma cell lines. Some of the compounds revealed a good to excellent activity as compared with the standard anticancer drugs [62].

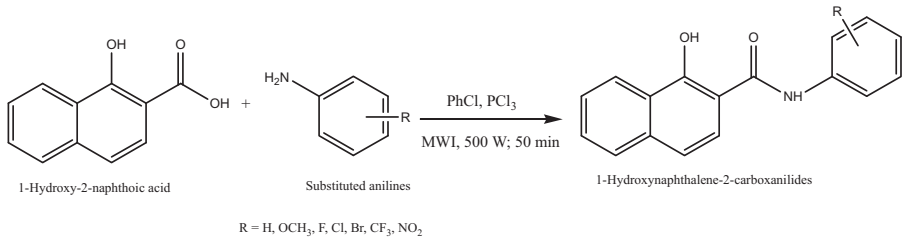

Scheme 19.43 Synthesis of ring-substituted 1-hydroxynaphthalene-2-carboxanilides.

4-Aryl-2-amino-4*H*-chromenes possessing *N*,*N*-dimethylamino group were reported as potential anticancer drugs. One-pot condensation of *N*,*N*-dimethyl-3-aminophenol, aromatic aldehydes, and (*E*)-*N*-methyl-1-(methylthio)-2-nitro-ethenamine was carried out by using MW irradiation to get the 4-aryl-2-methylamino-3-nitro-4*H*-chromenes under catalyst-free conditions (Scheme 19.44). The significant features of this reaction included catalyst-free, solvent-free, no column chromatographic purification, short reaction time, and good yields [63].

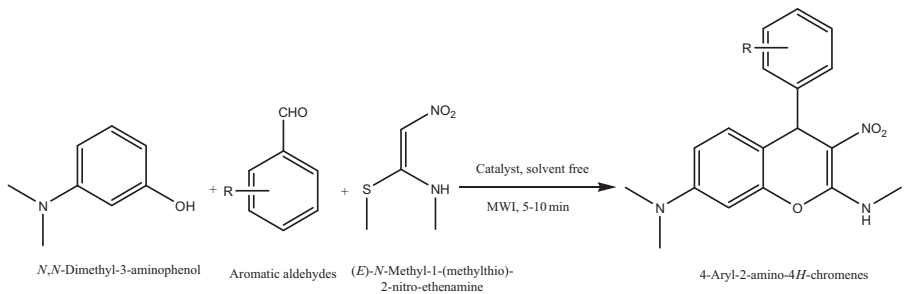

Scheme 19.44 MW irradiated synthesis of 4-aryl-2-amino-4*H*-chromenes.

19.2 Conclusion

Green synthesis is an efficient protocol for the synthesis of various biologically active compounds with diverse molecular structures. The chemical reactions under microwave, ultrasound irradiation follows a green chemistry approach by reducing reaction time, improvement in product yield, enhancement in rate of reaction, and reducing formation of waste. This technology is environment-friendly by eliminating the use

and generation of chemical hazardous and utilization of renewable raw materials. Various anticancer drugs are available clinically for treatment of cancer but most of them are associated with side effects and toxicity. And also there is development of resistance to chemotherapeutic agents that creates problem to treat cancer effectively. Hence, green technologies are applied to generate a variety of anticancer agents with diverse chemical structures to increase their therapeutic potentials with less or no side effects and toxicity.

Acknowledgment

Bimal K. Banik is grateful to Prince Mohammad Bin Fahd University.

References

[1] D.E. Thurston, Chemistry and Pharmacology of Anticancer Drugs, first ed., CRC Press, 2006.
[2] E. Izbicka, A.W. Tolcher, Development of novel alkylating drugs as anticancer agents, Curr. Opin. Investig. Drugs 5 (2004) 587–591.
[3] J. Carmen Avendano, C. Menendez, Medicinal Chemistry of Anticancer Drugs, second ed., Elsevier, 2015.
[4] D. Hanahan, R.A. Weinberg, The hallmarks of cancer, Cell 100 (2000) 57–70.
[5] A.J. Trevor, B.G. Katzung, M. Kruidering-Hall, Cancer chemotherapy, in: Katzung & Trevor's Pharmacology: Examination & Board Review, 11th ed., McGraw-Hill, 2015, pp. 440–451 (Chapter 54).
[6] J.H.M. Schellens, H.L. McLeod, D.R. Newell, Cancer Clinical Pharmacology, Oxford University Press, 2005.
[7] A. Urruticoechea, R. Alemany, J. Balart, A. Villanueva, F. Viñals, G. Capellá, Recent advances in cancer therapy: an overview, Curr. Pharm. Des. 16 (1) (2010) 3–10.
[8] S.S. Kadam, K.G. Bothara, Anti-neoplastic agents, in: Principles of Medicinal Chemistry, 22nd ed., vol. I, Nirali Prakashan, 2015.
[9] A. Gilman, The initial clinical trial of nitrogen mustard, Am. J. Surg. 105 (1963) 574–578.
[10] O.M. Colvin, An overview of cyclophosphamide development and clinical applications, Curr. Pharm. Des. 5 (8) (1999) 555–560.
[11] M.J. Maanen, C.J. Smeets, J.H. Beijnen, Chemistry, pharmacology and pharmacokinetics of N,N′,N″-triethylenethiophosphoramide (ThioTEPA), Cancer Treat. Rev. 26 (2000) 257–268.
[12] A.L. Demain, P. Vaishnav, Natural products for cancer chemotherapy, Microb. Biotechnol. 4 (6) (2011) 687–699.
[13] E.K. Rowinsky, R.C. Donehower, Paclitaxel (taxol), N. Engl. J. Med. 332 (1995) 1004–1014.
[14] I.S. Johnson, J.G. Armstrong, M. Gorman, J.P. Burnett, The vinca alkaloids: a new class of oncolytic agents, Cancer Res. 23 (1963) 1390–1427.
[15] T. Takeuchi, Anti-tumor antibiotics discovered and studied at the Institute of Microbial Chemistry, J. Cancer Res. Clin. Oncol. 121 (9–10) (1995) 505–510.
[16] W.B. Parker, Enzymology of purine and pyrimidine antimetabolites used in the treatment of cancer, Chem. Rev. 109 (2009) 2880–2893.
[17] G.H. Hitchings, G.B. Elion, The chemistry and biochemistry of purine analogs, Ann. N. Y. Acad. Sci. 60 (1954) 195–199.

[18] D.B. Longley, D.P. Harkin, P.G. Johnston, 5-Fluorouracil: mechanisms of action and clinical strategies, Nat. Rev. Cancer 3 (2003) 330–338.
[19] Y. Pommier, Topoisomerase I inhibitors: camptothecins and beyond, Nat. Rev. Cancer 6 (10) (2006) 789–802.
[20] H.S. Feigelson, B.E. Henderson, Estrogens and breast cancer, Carcinogenesis 17 (1996) 2279–2284.
[21] K.J. Schimmel, D.J. Richel, R.B. van den Brink, H.J. Guchelaar, Cardiotoxicity of cytotoxic drugs, Cancer Treat. Rev. 30 (2004) 181–191.
[22] K. Ilango, P. Valentina, Antineoplastic agents, in: Text Book of Medicinal Chemistry, second ed., vol. II, Keerthi Publishers, 2017, pp. 226–267 (Chapter 12).
[23] I. Ali, M.N. Lone, Z.A. Al-Othman, A. Al-Warthan, M.M. Sanagi, Heterocyclic scaffolds: centrality in anticancer drug development, Curr. Drug Targets 16 (7) (2015) 711–734.
[24] M. Saini, P. Kumar, M. Kumar, K. Ramasamy, V. Mani, R.K. Mishra, A.B.A. Majeed, B. Narasimhan, Synthesis, in vitro antimicrobial, anticancer evaluation and QSAR studies of N'-(substituted)-4-(butan-2-lideneamino)benzohydrazides, Arab. J. Chem. 7 (2014) 448–460.
[25] H.A. Abuelizz, M. Marzouk, H. Ghabbour, R. Al-Salahi, Synthesis and anticancer activity of new quinazoline derivatives, Saudi Pharm. J. 25 (2017) 1047–1054.
[26] S.E. Abbas, F.F. Barsoum, H.H. Georgey, E.R. Mohammed, Synthesis and antitumor activity of certain 2,3,6-trisubstituted-quinazolin-4(3H)-one derivatives, Bull. Fac. Pharm. Cairo Univ. 51 (2013) 273–282.
[27] D. Osmaniye, S. Levent, A.B. Karaduman, S. Ilgın, Y. Özkay, Z.A. Kaplancık, Synthesis of new benzothiazole acylhydrazones as anticancer agents, Molecules 23 (2018) 1054.
[28] A.M. Alafeefy, Some new quinazolin-4(3H)-one derivative, synthesis and antitumor activity, J. Saudi Chem. Soc. 15 (2011) 337–343.
[29] S.A. Morsy, A.A. Farahat, M.N.A. Nasr, A.S. Tantawy, Synthesis, molecular modeling and anticancer activity of new coumarin containing compounds, Saudi Pharm. J. 25 (2017) 873–883.
[30] S. Perveen, A.M. Al-Taweel, Green chemistry and synthesis of anticancer molecule, in: Green Chemistry, 2018, pp. 52–72 (Chapter 4).
[31] M. Salihu, Application of green chemistry in pharmaceutical industry, Int. J. Pharm. Sci. Res. 3 (1) (2018) 24–28.
[32] M. Chauhan, A. Rana, J.M. Alex, A. Negi, S. Singh, R. Kumar, Design, microwave-mediated synthesis and biological evaluation of novel 4-aryl(alkyl)amino-3-nitroquinoline and 2,4-diaryl(dialkyl)amino-3-nitroquinolines as anticancer agents, Bioorg. Chem. 58 (2015) 1–10.
[33] S.A. Al-Trawneh, J.A. Zahra, M.R. Kamal, M.M. El-Abadelah, F. Zani, M. Incerti, A. Cavazzoni, R.R. Alfieri, P.G. Petronini, P. Vicini, Synthesis and biological evaluation of tetracyclic fluoroquinolones as antibacterial and anticancer agents, Bioorg. Med. Chem. 18 (2010) 5873–5884.
[34] A. Thangaraj, M. Sadasivam, G. Subashini, S. Selvaraj, A. Athar, S.M. Palathurai, Biologically active perspective synthesis of heteroannulated 8-nitroquinolines with green chemistry approach, Bioorg. Med. Chem. Lett. 27 (2017) 1538–1546.
[35] N.A. Liberto, J.B. Simoes, S.d.P. Silva, C.J. da Silva, L.V. Modolo, A. de Fátima, L.M. Silva, M. Derita, S. Zacchino, O.M.P. Zuniga, G.P. Romanelli, S.A. Fernandes, Quinolines: microwave-assisted synthesis and their antifungal, anticancer and radical scavenger properties, Bioorg. Med. Chem. 25 (2017) 1153–1162.
[36] A.M. El-Naggar, M.M. Hemdan, S.R. Atta-Allah, An efficient one-pot synthesis of new coumarin derivatives as potent anticancer agents under microwave irradiation, J. Heterocyclic Chem. 54 (6) (2017) 3519–3526.

[37] M.T. Gabr, N.S. El-Gohary, E.R. El-Bendary, M.M. El-Kerdawy, N. Ni, Microwave-assisted synthesis and antitumor evaluation of a new series of thiazolylcoumarin derivatives, EXCLI J. 16 (2017) 1114–1131.
[38] K.M. Hosamani, D.S. Reddya, H.C. Devarajegowda, Microwave-assisted synthesis of new fluorinated coumarin–pyrimidine hybrids as potent anticancer agents, their DNA cleavage and X-ray crystal studies, RSC Adv. 5 (2015) 11261–11271.
[39] F. Leonetti, C. Capaldi, A. Carotti, Microwave-assisted solid phase synthesis of imatinib, a blockbuster anticancer drug, Tetrahedron Lett. 48 (2007) 3455–3458.
[40] G.C. Rama Prasad, B.K. Kalluraya, B. Sunil Kumar, Microwave-assisted synthesis of triazolothiadiazole analogs as anticancer agents, Med. Chem. Res. (2014), https://doi.org/10.1007/s00044-014-0944-x.
[41] S.V. Tiwari, S. Siddiqui, J.A. Seijas, M. Pilar Vazquez-Tato, A.P. Sarkate, D.K. Lokwani, A.P.G. Nikalje, Microwave-assisted facile synthesis, anticancer evaluation and docking study of N-((5-(substituted methylene amino)-1,3,4-thiadiazol-2-yl)methyl)benzamide derivatives, Molecules 22 (2017) 1–14.
[42] G.C. Ramaprasad, B. Kalluraya, B. Sunil Kumar, S. Mallya, Microwave assisted synthesis of triazolothiadiazole analogues as anticancer and antibacterial agents, Der Pharm. Chem. 4 (3) (2012) 1026–1032.
[43] S. Demirayak, I. Kayagil, L. Yurttas, Microwave supported synthesis of some novel 1,3-diarylpyrazino[1,2-a]benzimidazole derivatives and investigation of their anticancer activities, Eur. J. Med. Chem. 46 (2011) 411–416.
[44] P. Sharma, T.S. Reddy, N.P. Kumar, K.R. Senwar, S.K. Bhargava, N. Shankaraiah, Conventional and microwave-assisted synthesis of new 1H-benzimidazole-thiazolidinedione derivatives: a potential anticancer scaffold, Eur. J. Med. Chem. 138 (29) (2017) 234–245.
[45] T.B.B. Hue, T.K.H. Quy, K.O. Won, D.V. Duy, N.T.C. Yen, T.K.T. Cuc, C.P. Em, T.T. Phuong, T.T. Loan, V.M. Hieu, Microwave assisted synthesis and cytotoxic activity evaluations of new benzimidazole derivatives, Tetrahedron Lett. 57 (2016) 887–891.
[46] D. Bandyopadhyaya, S. Mukherjee, J.C. Granados, J.D. Short, B.K. Banik, Ultrasound-assisted bismuth nitrate-induced green synthesis of novel pyrrole derivatives and their biological evaluation as anticancer agents, Eur. J. Med. Chem. 50 (2012) 209–215.
[47] K. Naresh, K. Sandeep, A. Sheenu, N. Kumar, M.S. Sham, V.B. Prasad, R. Partha, P. Vikas, Ferulic acid amide derivatives as anticancer and antioxidant agents: synthesis, thermal, biological and computational studies, Med. Chem. Res. 25 (2016) 1175–1192.
[48] S. Banerjee, J. Wang, S. Pfeffer, D. Ma, L.M. Pfeffer, S.A. Patil, W. Li, D.D. Miller, Design, synthesis and biological evaluation of novel 5*H*-chromenopyridines as potential anti-cancer agents, Molecules 20 (2015) 17152–17165.
[49] A.M.A. Khaled, H.A. Ghada, M.E. Abeer, Eco-friendly synthesis of novel cyanopyridine derivatives and their anticancer and PIM-1 kinase inhibitory activities, Eur. J. Med. Chem. 134 (2017) 357–365.
[50] N.A. Srinivas, P. Mahendar, A. Sadanandam, G. Achaiah, R.V. Malla, Synthesis, anticancer and MRP1 inhibitory activities of 4-alkyl/aryl-3,5-bis(carboethoxy/carbomethoxy)-1,4-dihydro-2, 6-dimethylpyridines, Med. Chem. Res. 22 (2013) 147–155.
[51] R.K.S. Ravi, K. Sundaram, S. Venkatachalapthi, S.A. Muhammad, Conventional and microwave assisted synthesis of 2-aminothiazoles and oxazoles and their anti-cancer activity, Indo Am. J. Pharm. Res. 5 (01) (2015) 550–560.
[52] R. Romagnoli, P.G. Baraldi, O.C. Lopez, M.D. Carrion, C.L. Cara, D. Preti, M.A. Tabrizi, J. Balzarini, Microwave-assisted synthesis of substituted 2,4-diarylthiazoles and their evaluation as anticancer agents, Lett. Drug Des. Discov. 4 (2007) 464–466.

[53] V.R. Reddy, N.R. Rao, R. Raja Reddy, R. Suthakaran, Microwave assisted synthesis, characterization and pharmacological evaluation of imidazolo quinazoline-4-one derivatives, Int. J. Pharm. Sci. Rev. Res. 29 (2) (2014) 1–4.
[54] S.M. Gomha, M.M. Edrees, R.A.M. Faty, Z.A. Muhammad, Y.N. Mabkhot, Microwave assisted one pot three component synthesis of some novel pyrazole scaffolds as potent anticancer agents, Chem. Central J. 11 (37) (2017) 1–12.
[55] A. Sharma, R. Chowdhury, S. Dash, B. Pallavia, P. Shuklaa, Fast microwave assisted synthesis of pyranopyrazole derivatives as new anticancer agents, Curr. Microw. Chem. 3 (2016) 78–84.
[56] J. Jasril, I. Ikhtiarudin, A. Zamri, H.Y. Teruna, N. Frimayanti, New fluorinated chalcone and pyrazoline analogs: synthesis, docking, and molecular dynamic studies as anticancer agents, TJPS 41 (3) (2017) 93–98.
[57] H.N. Hafez, Microwave-assisted synthesis and cytotoxicity evaluation of some novel pyrazole containing imidiazoles, pyrazoles, oxazoles, thiadiazoles and benzochromene derivatives, Egypt. J. Chem. 60 (6) (2017) 1015–1028.
[58] S.A. Patil, J.K. Addo, H. Deokar, S. Sun, J. Wang, W. Li, D.P. Suttle, W. Wang, R. Zhang, J.K. Buolamwini, Synthesis, biological evaluation and modeling studies of new pyrido [3,4-b]indole derivatives as broad spectrum potent anticancer agents, Drug Des. 6 (1) (2017) 1–14.
[59] H. Poerwono, S. Sasaki, Y. Hattori, K. Higashiyam, Efficient microwave-assisted prenylation of pinostrobin and biological evaluation of its derivatives as antitumor agents, Bioorg. Med. Chem. Lett. 20 (7) (2010) 2086–2089.
[60] V.T. Shailee, A.S. Julio, M.P. Vazquez-Tato, P.S. Aniket, K.L. Deepak, P.G.N. Anna, Ultrasound mediated one-pot, three component synthesis, docking and ADME prediction of novel 5-amino-2-(4-chlorophenyl)-7-substituted-phenyl-8,8a-dihydro-7H-(1,3,4)-thiadiazolo(3,2-α) pyrimidine-6-carbonitrile derivatives as anticancer agents. Molecules 21 (8) (2016), https://doi.org/10.3390/molecules21080894 pii: E894.
[61] H.F. Idaira, A. Angel, M. Patricia, L. Matias, F. Leandro, E. Ana, Indium catalyzed solventfree multicomponent synthesis of cytotoxic dibenzo[*a,h*]anthracenes from aldehydes, 2-hydroxy-1,4-naphthoquinone and 2-naphthol, Tetrahedron 70 (2014) 8480–8487.
[62] T. Kauerova, J. Kos, T. Gonec, J. Jampilek, P. Kollar, Antiproliferative and pro-apoptotic effect of novel nitro-substituted hydroxynaphthanilides on human cancer cell lines, Int. J. Mol. Sci. 17 (2016) 1219.
[63] P. Nagaraju, P. Padmaja, P.N. Reddy, Microwave-assisted one-pot synthesis of 7-dimethylamino-4-aryl-2-methylamino-3-nitro-4H-chromenes, Lett. Org. Chem. 16 (6) (2019) 468–473.

Green chemistry and synthetic approaches in the development of antidepressant and antipsychotic agents

20

Bimal Krishna Banik[a,*], *Biswa Mohan Sahoo*[b], *B.V.V. Ravi Kumar*[b], *Jnyanaranjan Panda*[b], *Anjan Kumar*[b]
[a]Department of Mathematics and Natural Sciences, College of Sciences and Human Studies, Deanship of Research Development, Prince Mohammad Bin Fahd University, Al Khobar, Kingdom of Saudi Arabia, [b]Roland Institute of Pharmaceutical Sciences, Berhampur, India
[*]Corresponding author. e-mail address: bimalbanik10@gmail.com; bbanik@pmu.edu.sa

20.1 Introduction

Depression and psychosis are brain disorders. Depression is a mood disorder which causes a persistent feeling of sadness and loss of interest and can interfere with daily functioning. Antidepressants are drugs used for the treatment of major depressive disorder by correcting chemical imbalances of neurotransmitters in the brain. Chemical imbalances of neurotransmitters in the brain may be responsible for changes in mood and behavior [1]. The various classes of antidepressants drugs are categorized as follows [2].

20.1.1 Selective serotonin reuptake inhibitors

These drugs increase the extracellular level of the neurotransmitter serotonin by limiting its reabsorption into the presynaptic cell and thereby increase the level of serotonin in the synaptic cleft available to bind to the postsynaptic receptor. Example: Citalopram, Escitalopram, Fluoxetine, Paroxetine, Sertraline, and Fluvoxamine.

20.1.2 Serotonin-norepinephrine reuptake inhibitors

They inhibit the reuptake of both serotonin and norepinephrine neurotransmitters. Example: Duloxetine, venlafaxine, Desvenlafaxine, and Levomilnacipran.

20.1.3 Monoamine oxidase inhibitors

This class of drugs inhibit the activity of one or both monoamine oxidase enzymes such as monoamine oxidase A and monoamine oxidase B. Example: Phenelzine, Selegiline,

Green Approaches in Medicinal Chemistry for Sustainable Drug Design. https://doi.org/10.1016/B978-0-12-817592-7.00020-4
© 2020 Elsevier Inc. All rights reserved.

Tranylcypromine. Nialamide, Isocarboxazid, Hydracarbazine, Tranylcypromine, Moclobemide, Bifemelane, Pirlindole, Toloxatone, Rasagiline, and Safinamide.

20.1.4 Tricyclic antidepressant

These drugs increase the level of Norepinephrine, Serotonin, and block the action of acetylcholine. Example: Amitriptyline, Imipramine, Desipramine, Nortriptyline, Clomipramine, Trimipramine, Protriptyline, and Doxepin.

20.1.5 Norepinephrine-dopamine reuptake inhibitor

This drug acts as a reuptake inhibitor for the neurotransmitters norepinephrine and dopamine by blocking the action of the norepinephrine transporter and the dopamine transporter, respectively. Example: Bupropion.

Norepinephrine reuptake inhibitor with serotonin receptors antagonism: Example: Maprotiline.
Serotonin receptors antagonist with serotonin reuptake inhibition: Example: Trazodone, Nefazodone, and Vortioxetine.
Serotonin 5-HT_{1A} autoreceptor partial agonist with serotonin reuptake inhibition: Example: Vilazodone.

Psychosis is a mental disorder which causes abnormal thinking and perceptions. Various symptoms of psychosis include delusions (false beliefs) and hallucinations (sees, hears, smells, tastes, or feels things that do not exist outside), catatonia (unresponsiveness). Psychosis may have different characteristics such as functional disorders (Schizophrenia), mood or affective disorders (mania), and cognitive disorders [3]. Antipsychotics are the medications used to reduce or relieve symptoms of psychosis such as delusions, hallucinations, and paranoia or disordered thought. Antipsychotics are also called as neuroleptics or major tranquilizers and categorized into first generation (typical antipsychotic) and second generation (atypical antipsychotic) (Table 20.1). Both first- and second-generation drugs produce their action by blocking dopamine receptors in the brain and periphery. Typical antipsychotic drugs block mainly D_2, D_3, and D_4 receptors in the mesolimbic system of the brain whereas atypical antipsychotic block $5HT_{2A}$ and D_2 receptors. The first atypical antipsychotic drug, clozapine was discovered in the 1950s, and introduced in clinical practice in the 1970s. During the 1990s, olanzapine, risperidone, and quetiapine were introduced for treatment of psychosis. The newest atypical antipsychotic drug, paliperidone was approved by FDA in the year 2006 [4].

Green chemistry is also called as sustainable chemistry or environmentally benign chemistry which involves utilization of a set of principles that reduces or eliminates the use or generation of hazardous substances in the design, manufacture, and application of chemical products. It is necessary to design new synthetic methods so as to use and generate substances that are not toxic to human

Table 20.1 List of antipsychotic drugs.

First-generation or typical antipsychotics		Second-generation or atypical antipsychotics	
Class	**Drugs**	**Class**	**Drugs**
Butyrophenones	Benperidol, Bromperidol, Droperidol, Haloperidol, Timiperone	Benzamides	Amisulpride, Sultopride, Remoxipride
Diphenylbutyl-piperidines	Fluspirilene, Penfluridol, Pimozide	Benzisoxazoles/ benzisothiazoles	Lurasidone, Risperidone, Ziprasidone
Phenothiazines	Chlorpromazine, Cyamemazine, Dixyrazine, Fluphenazine, Perphenazine	Phenylpiperazines/ quinolinones	Aripiprazole, Cariprazine, Brexpiprazole
Thioxanthenes	Chlorprothixene, Clopenthixol, Flupentixol, Thiothixene, Zuclopenthixol	Tricyclics	Clozapine, Olanzapine, Quetiapine, Zotepine

health [5]. The concept of atom economy is considered to carry out organic syntheses in which most of the atoms of the reactants become incorporated into reaction medium to get desired final products with high yield by lowering the formation of waste or by-products. Conventional catalysts are hazardous, corrosive, and toxic in nature. So, it is essential to use green catalyst which is environmentally friendly and more selective for the formation of products. Organic solvents are toxic and volatile in nature and harmful to human health. The use of those solvents in chemical synthesis creates environmental pollution [6]. Therefore, it is necessary to replace these solvents by green solvents such as ionic liquids, supercritical CO_2 or water and also solvent-free synthetic methods which utilize the surfaces of clay, zeolites, silica, alumina, etc. Hence, various green technologies such as ultrasound mediated organic synthesis (USMOS), microwave-assisted eco-friendly organic synthesis (MAEOS) are applied to generate new drug molecules related to antidepressant and antipsychotic activity [7].

A series of novel 3-[5-substituted phenyl-1,3,4-thiadiazole-2-yl]-2-styryl quinazoline-4(3*H*)-ones (Fig. 20.1) were synthesized and evaluated for anticonvulsant, sedative-hypnotic, and CNS depressant activities. After i.p. injection to mice at doses of 30, 100, and 300 mg/kg body weight 2-styrylquinazolin-4(3*H*)-one derivatives were examined in the maximal electroshock-induced seizures (MES) and subcutaneous pentylenetetrazole (scPTZ)-induced seizure models in mice. The neurotoxicity was assessed using the rotorod method. Out of 18 compounds only 4a, 4d, 4e, 4j, and 4k exhibited anticonvulsant activity in one or more test models. All except 4e and 4f exhibited significant sedative-hypnotic activity via

actophotometer screen. CNS depressant activity screened with the help of the forced swim pool method resulted into some potent compounds. From the experimental observation it was concluded that synthesized compounds exhibit relatively better sedative-hypnotic and CNS depressant activities [8].

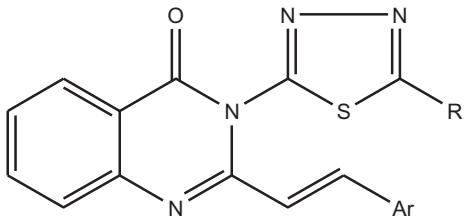

Fig. 20.1 Structure of 3-[5-substituted phenyl-1,3,4-thiadiazole-2-yl]-2-styryl quinazoline-4 (3*H*)-ones.

A number of new imine derivatives of 5-amino-1,3,4-thiadiazole-2-thiol were synthesized (Fig. 20.2), and their antidepressant activity was tested using imipramine as reference drug. Two compounds namely 5-{[1-(4-chlorophenyl)-3-(4-methoxy-phenyl)prop-2-en-1-ylidene]-amino}-5-benzylthio-1, 3,4-thiadiazole 4i(b), and 5-{[1-(4-chlorophenyl)-3-(4-dimethyl-aminophenyl)-prop-2-en-1-ylidene] amino}-5-benzylthio-1,3,4-thiadiazole 4i(c) showed significant antidepressant activity, which decreased immobility time by 77.99% and 76.26% compared to the standard imipramine (82%). All the compounds in the series passed neurotoxicity tests [9].

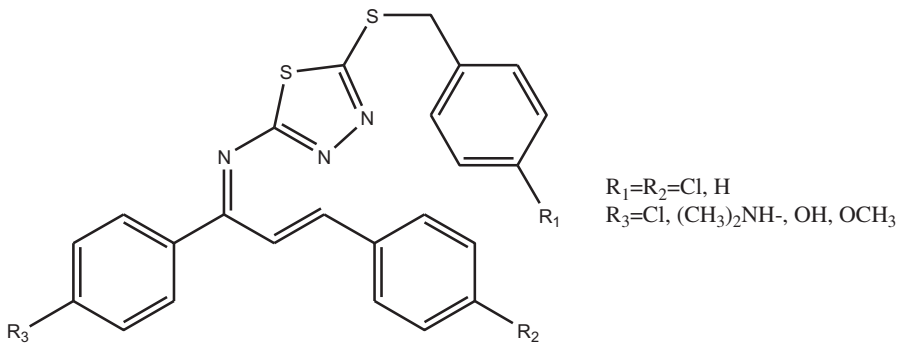

Fig. 20.2 Structure of imine derivatives of 5-amino-1,3,4-thiadiazole-2-thiol.

A novel series of quinoxalin-2-carboxamides were designed based on the ligand-based approach via three-point pharmacophore model which consists of an aromatic residue and a linking carbonyl group and basic nitrogen (Scheme 20.1). The target new chemical entities were synthesized from the key intermediate, quinoxalin-2-carboxylic acid, by coupling it with various amines in the presence of 1-(3-dimethylaminopropyl)-3-ethylcarbodiimide hydrochloride (EDC·HCl) and 1-hydroxybenzotriazole (HOBt). The target new chemical entities were evaluated for their 5-HT_3 receptor antagonisms in longitudinal muscle myenteric plexus preparation from guinea pig ileum. All the synthesized compounds showed antagonism towards 5-HT_3 receptor. Based on this result, a structure-activity relationship is derived, which reveals that the aromatic residue in 5-HT_3 receptor antagonists may have hydrophobic interaction with 5-HT_3 receptor. Regardless of their antagonistic potentials, all the synthesized molecules were screened for their antidepressant potentials by using forced swim test in mice model. Interestingly, none of the tested compounds affects the locomotion of mice in the tested dose levels. Compounds with significant pA_2 values exhibited good antidepressant-like activity as compared to the vehicle-treated group [10].

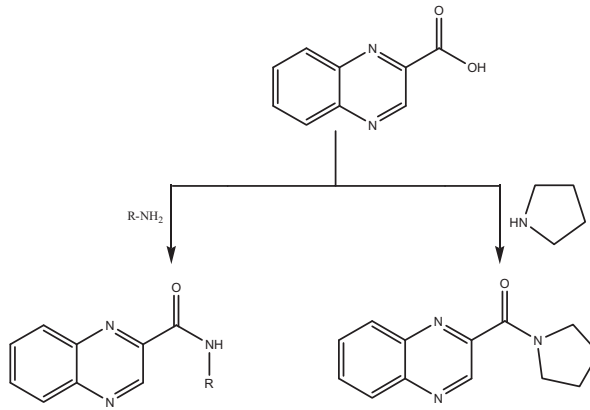

Scheme 20.1 Synthesis of quinoxalin-2-carboxamides.

A series of 7-chloro-3-[substituted (amino/phenylamino)]-2-phenyl quinazolin-4(3*H*)-one/thione derivatives and 1-(7-chloro-4-oxo/-2-phenylquinazoline-3(4*H*-yl)) substituted urea derivatives were prepared. The reaction proceeded through the intermediate 7-chloro-2-phenyl-4*H*-benzo[d][1,3]oxazin-4-one. The anticonvulsant and CNS depressant activity was investigated by maximum electroshock (MES) seizure test and porsolt's behavioral despair test (forced swimming), respectively. The rotarod test was performed to evaluate any probable changes in motor coordination

induced by the test compounds. Among the tested compounds, six compounds (IIc, IIg, IIj, IIIc, IIIg, IIIj) exhibited a good activity profile in CNS depressant activity (Table 20.2). The quinazoline derivatives obtained from this research work indicated that the methyl/methoxy group in phenyl ring, amine, and thiourea substitution at third position of quinazoline derivatives are essential for CNS depressant activity [11] (Scheme 20.2).

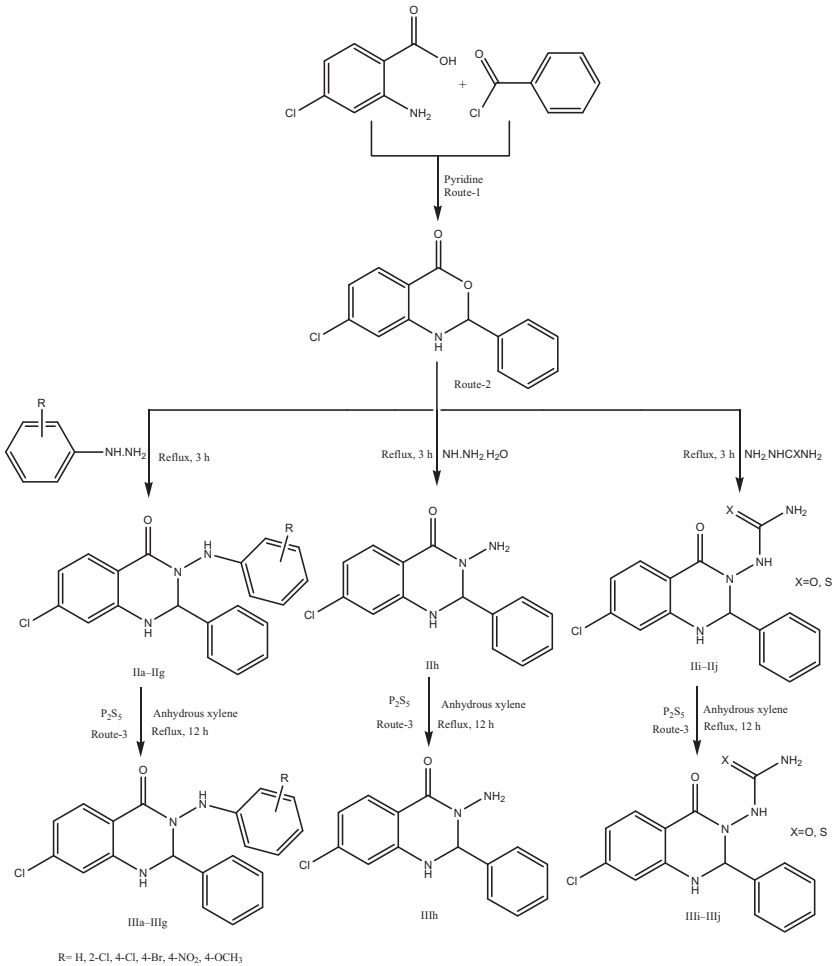

Scheme 20.2 Synthesis of 7-chloro-3-[substituted (amino/phenyl amino)]-2-phenyl quinazolin-4 (3*H*)-one/thione derivatives and 1-(7-chloro-4-oxo/-2-phenylquinazoline-3(4*H*-yl)) substituted urea.

Table 20.2 CNS depressant activity of compounds IIa–IIIj.

Compounds	Substitutions	Immobility times(s) mean ± SEM
IIa	H	175 ± 11.34
IIb	2-Cl	180 ± 10.23
IIc	2-CH_3	236 ± 10.45
IId	4-Cl	192 ± 12.54
IIe	4-Br	198 ± 17.56
IIf	4-NO_2	187 ± 11.19
IIg	4-OCH_3	245 ± 16.12
IIh	NH_2	192 ± 15.28
IIi	O	212 ± 14.23
IIj	S	255 ± 16.78
IIIa	H	178 ± 12.15
IIIb	2-Cl	195 ± 13.18
IIIc	2-CH_3	261 ± 12.35
IIId	4-Cl	188 ± 11.27
IIIe	4-Br	191 ± 14.32
IIIf	4-NO_2	182 ± 15.75
IIIg	4-OCH_3	254 ± 17.85
IIIh	NH_2	212 ± 16.64
IIIi	O	210 ± 18.92
IIIj	S	253 ± 16.01
PEG (control)	–	155 ± 10.54
Carbamazepine	–	260 ± 15.24

The use of central nervous system (CNS) acting drugs in the management of neurodegenerative and psychiatric problems cannot be overemphasized. Therefore, the chemical structure of piroxicam was modified to yield new CNS stimulants and depressants that can be of great benefit to human beings. The conversion of piroxicam to CNS acting drugs was done by desulfation, methylation, dehydrogenation, carboxylation, and carbonylation [12] (Scheme 20.3).

Shukla et al. reported the synthesis of 2-oxo-3[4′-*p*(subst/unsubst)-phenyl-2′-thiazolyl/oxazolyl]morpholino-*N*-acetyl-indoles. Various thiazolyl/oxazolyl imino indoles were produced by condensation of different heterocyclic moieties with isatin in ethanol containing few drops of glacial acetic acid. These imino indoles were condensed with chloro acetyl chloride in the presence of K_2CO_3 to yield *N*-chloroacetyl-indole derivatives which on further treatment with morpholino in benzene to produce titled compounds (Scheme 20.4). Among all the synthesized compounds, selected compounds were screened for their CNS activity. Chlorpromazine hydrochloride was used as the reference standard. From the results, it was concluded that, tested compounds show more depressant activity as compared to reference standard [13].

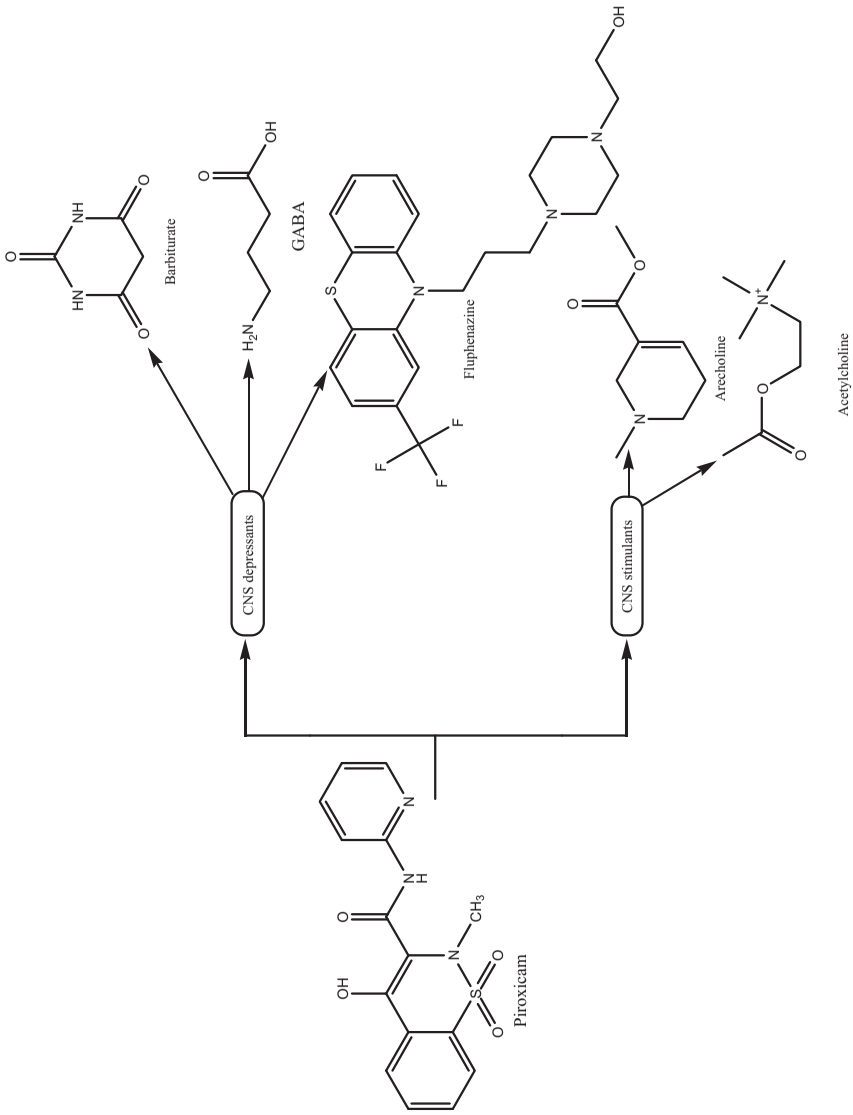

Scheme 20.3 Synthesis of modified piroxicam as CNS stimulants and depressants.

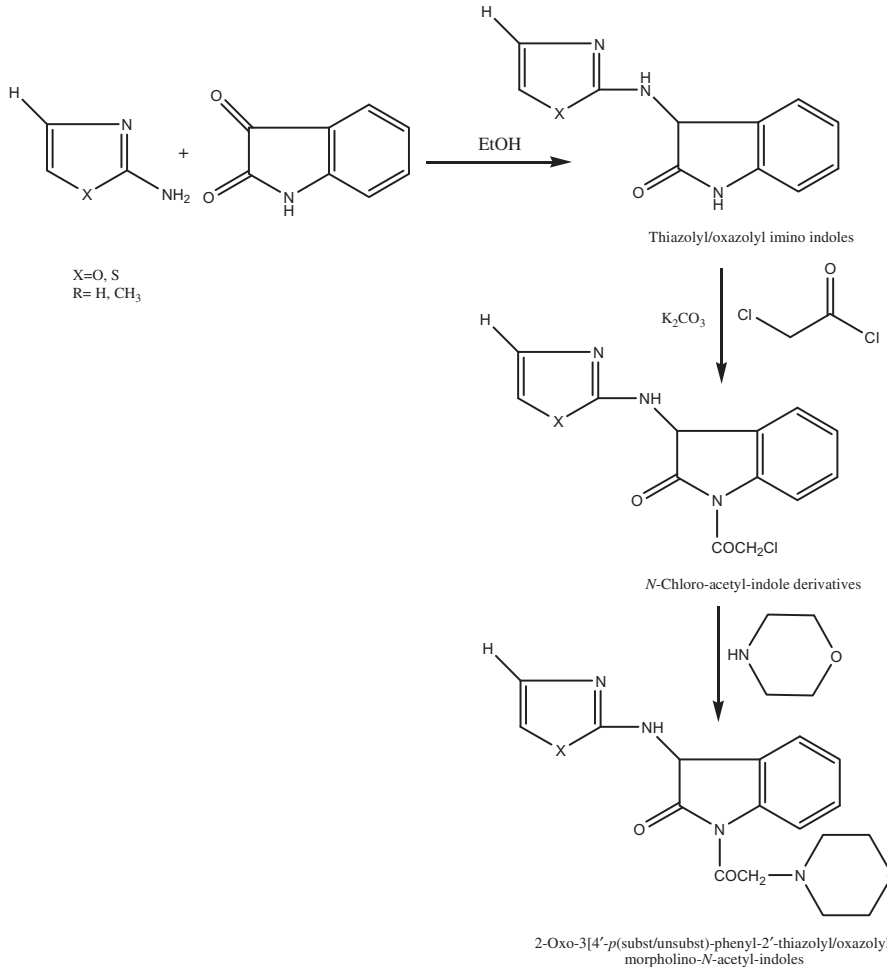

Scheme 20.4 Synthesis of 2-oxo-3[4′-*p*(subst/unsubst)-phenyl-2′-thiazolyl/oxazolyl] morpholino-*N*-acetyl-indoles.

Diazotization of substituted anilines with $NaNO_2$ and concentrated hydrochloric acid at 0°C produced diazonium chlorides. The substituted aryl diazonium chlorides underwent coupling with ethyl-acetoacetate in methanol yield ethyl-2-aryl-hydrazono-3-oxobutyrates (2a–h). Then the reaction of (2a–h) with naphthoic carbo-hydrazide (3) produced the title compounds of pyrazolone derivatives (4a–h) (Scheme 20.5). The newly synthesized compounds were screened for their *in vivo* antidepressant activity by tail suspension test and forced swimming test. Some of the tested compounds 4f, 4g showed very good activity when compared to the standard drug imipramine [14].

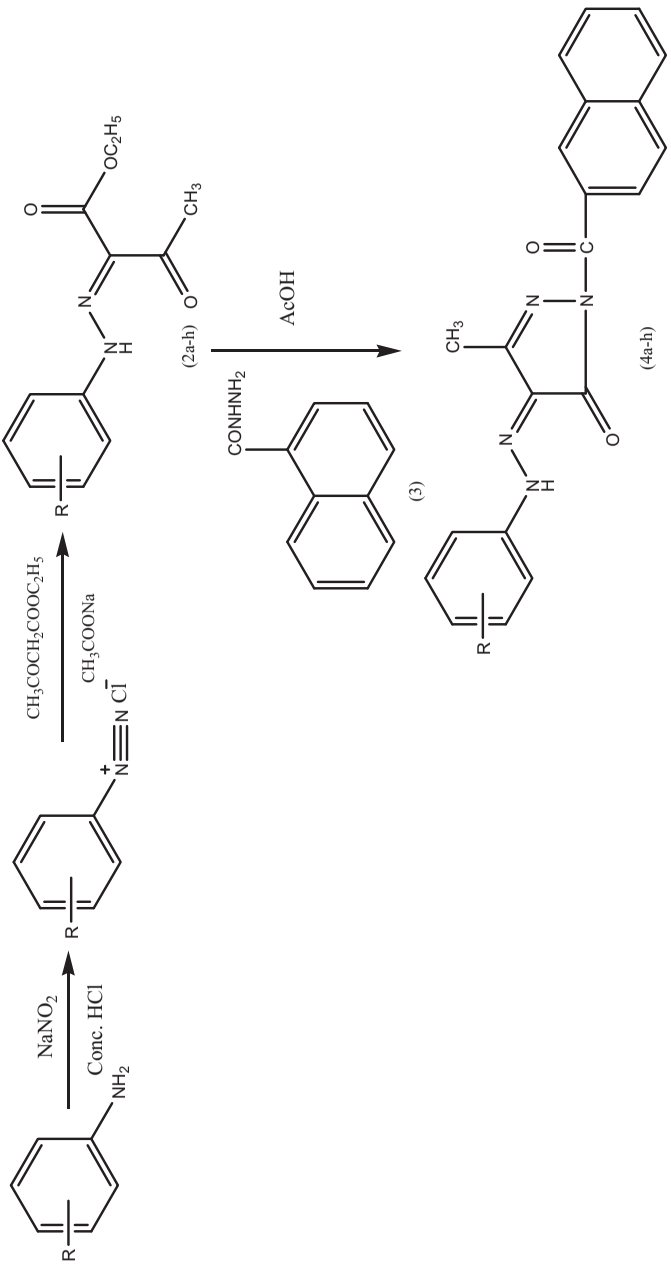

Scheme 20.5 Synthesis of pyrazolone derivatives (4a–h).

A series of 1,3,5-triphenyl-2-pyrazoline derivatives were synthesized through microwave-assisted condensation of 1,3-diphenyl-2-propene-1-one (chalcones) with phenylhydrazine using dry acetic acid as a cyclizing agent and evaluated for antidepressant activity (Scheme 20.6). The antidepressant activity of these compounds was screened by porsolt behavioral despair test using imipramine as a reference drug. Among tested compounds, 2-pyrazoline derivatives were found to possess significant antidepressant activity. It was observed that 1,5-diphenyl-3-(4-methoxyphenyl)-2-pyrazoline showed maximum antidepressant activity, comparable with imipramine. The presence of methoxy group on the phenyl ring at position 3 of the pyrazoline ring was found to enhance antidepressant activity. The replacement of the methoxy group by methyl and any other electron-withdrawing group decreased antidepressant activity [15].

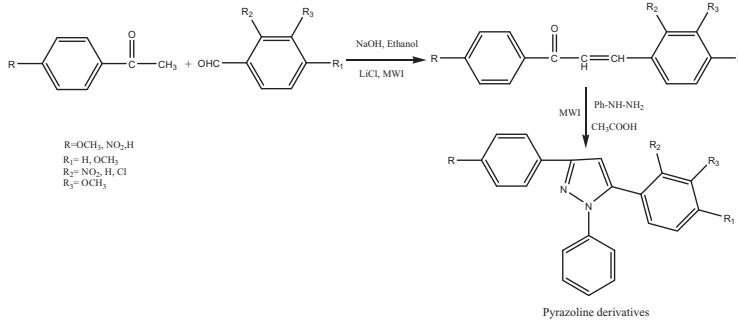

Scheme 20.6 Synthesis of 1,3,5-triphenyl-2-pyrazoline derivatives.

Nikalje et al. reported facile, eco-friendly microwave-assisted solvent-free synthesis of coupled heterocyclic system 2-(1Hindol-3-yl)-4-substitued-2,3-dihydrobenzo[1,5] thiazepine derivatives (Scheme 20.7 and Table 20.3). These compounds were obtained by cyclo-condensation of 1-substituted-3(1*H*-indolyl)-2-propen-1-ones with 2-aminothiophenol in the presence of eco-friendly catalyst zirconium (IV)oxychloride under solvent-free conditions. The reaction was completed in 3–6 min and produced better yields than the conventional synthesis which requires 6–8 h. The activity was measured as the digital score using actophotometer with the i.p. administration of test drugs (30 mg/kg) to mice [16] (Tables 20.4 and 20.5).

(*S*)-Duloxetine was prepared from 3-chloro-1-(2-thienyl)-1-propanone in good yield with an excellent enantioselectivity via asymmetric borane reduction catalyzed by the spiroborate ester. The nucleophilic aromatic substitution of (*S*)-3-(methylamino)-1-(thiophen-2-yl)propan-1-ol with 1-fluoronaphthalene in the presence of sodium hydride and DMSO afforded (*S*)-duloxetine with 78% yield (Scheme 20.8). The mild reaction conditions and operational simplicity of this method were attractive for a practical synthesis of (*S*)-duloxetine as potent dual inhibitor of serotonin and norepinephrine reuptake. Currently, (*S*)-duloxetine was used for the treatment of major depressive disorder and stress-related urinary incontinence under the name of Cymbalta [17].

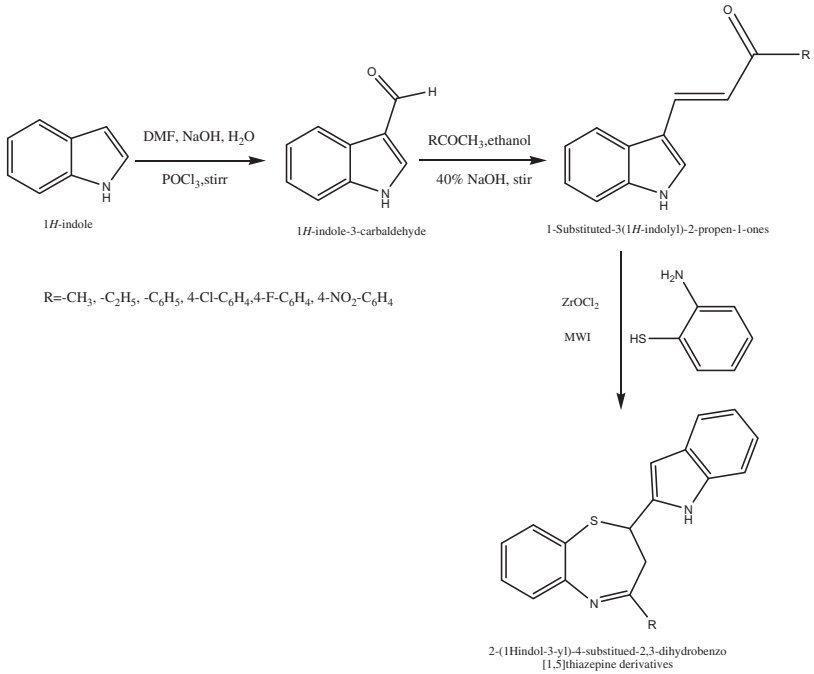

Scheme 20.7 Synthesis of 2-(1hindol-3-yl)-4-substitued-2,3-dihydrobenzo[1,5]thiazepine derivatives.

Table 20.3 Microwave-assisted solvent-free synthesis thiazepine derivatives.

Comp. code	R	Time (min)	Yield (%)
4a	CH_3	3.5	75
4b	C_2H_5	3	82
4c	C_6H_5	5	65
4d	4-ClC_6H_4	4	65
4e	4-FC_6H_4	3.5	74

Table 20.4 Evaluation of CNS depressant activity using actophotometer after 30 min.

Comp. code	Mean changes in locomotor activity ± SEM			Percentage inhibition in locomotor activity		
	I	II	III	I	II	III
4a	73 ± 6.221*	59.4 ± 13.422**	25.6 ± 1.965***	50	70.60	77.73
4b	73 ± 8.626**	87.6 ± 4.434*	24.4 ± 1.939***	68.52	38.08	78.78
4c	41.2 ± 5.490***	89.6 ± 5.240*	98.2 ± 2.354 ns	64.17	22.08	14.60
4d	78.4 ± 12.205**	102.8 ± 3.39 ns	23.4 ± 0.8602***	31.82	10.60	79.65
4e	71 ± 10.232***	64±4.517***	54.6 ± 2.561***	38.68	44.34	52.52
D	30.2 ± 2.922			47		
C	115 ± 7.791					

Each value represents the mean_SEM significantly different from the control at $P < .05$; ns denotes not significant at $P < .05$ (Student's *t*-test); $^{*}P < .05$, $^{**}P < .01$, $^{***}P > .05$ locomotor activity score was measured for 10 min. *D*, diazepam; *C*, control; *I* = 30 mg/kg, *II* = 100 mg/kg, *III* = 300 mg/kg.

Table 20.5 Evaluation of CNS depressant activity using actophotometer after 4 h.

Comp. code	Mean changes in locomotor activity ± SEM			Percentage inhibition in locomotor activity		
	I	II	III	I	II	III
4a	40 ± 9.965***	33.8 ± 1.655***	26 ± 2.168***	46.14	54.50	44.21
4b	75.2 ± 11.608*	46.8 ± 5.324***	54.8 ± 10.017***	39.54	62.37	55.94
4c	36.8 ± 6.094***	58.2 ± 5.161***	64 ± 4.231***	39.53	43.56	42.28
4d	84 ± 7.817*	138.2 ± 4.432 ns	19 ± 1.414***	32.47	11.09	43.24
4e	133 ± 13.657 ns	98 ± 3.347 ns	51.8 ± 12.212***	6.91	21.22	58.36
D	75 ± 11.150			47.42		
C	124.4 ± 5.758					

Each value represents the mean_SEM significantly different from the control at $P < .05$; ns denotes not significant at $P < .05$ (Student's *t*-test); $^{*}P < .05$, $^{**}P < .01$, $^{***}P > .05$ locomotor activity score was measured for 10 min. *D*, diazepam; *C* control; *I* = 30 mg/kg, *II* = 100 mg/kg, *III* = 300 mg/kg.

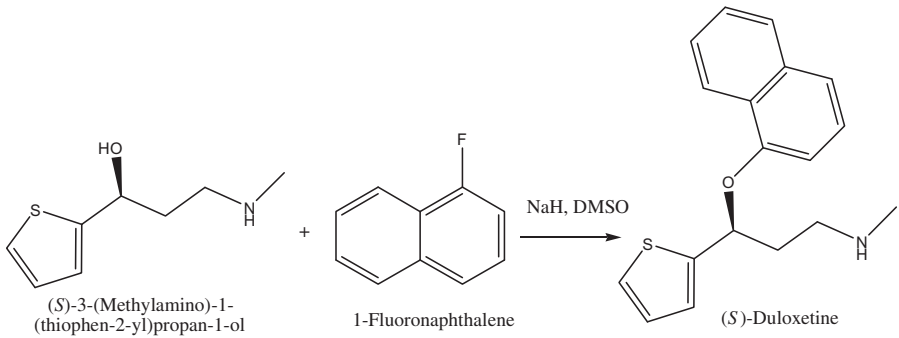

Scheme 20.8 Synthesis of (*S*)-duloxetine.

Trazodone was widely used as antidepressant drug and works as a 5-hydroxytryptamine (5-HT_2) and α1-adrenergic receptor antagonist and serotonin reuptake inhibitor. In conventional methods of the synthesis of trazodone and its derivatives, organic and toxic solvents were used and the synthesis was completed in several hours. But the synthesis of trazodone and its derivatives was performed successfully in the presence of potassium carbonate as a reaction medium under microwave irradiation within a few minutes [18] (Scheme 20.9).

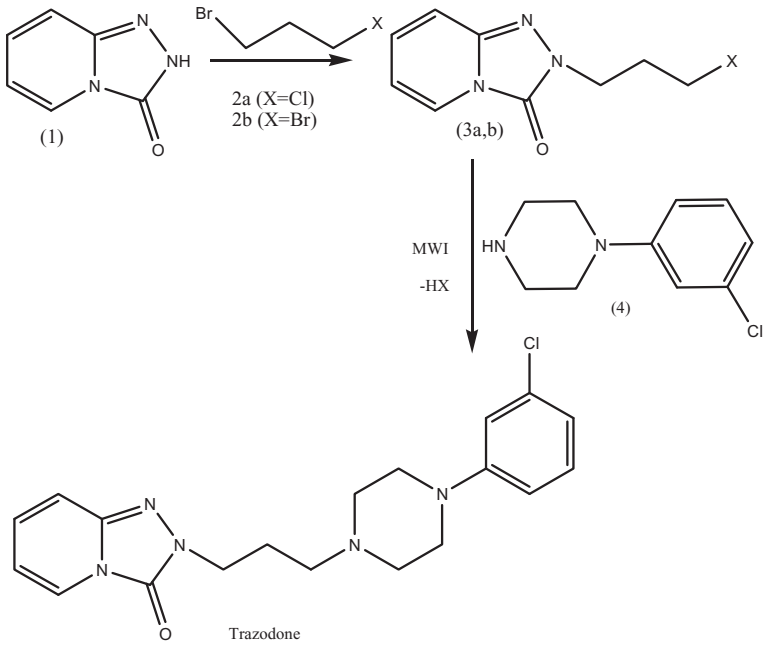

Scheme 20.9 Synthesis of trazodone under MWI.

A series of new substituted 5-(1*H*-Indol-3-yl)-3-(phenyl)-4,5-dihydropy-razoline derivatives (2a–m) were synthesized with good yield by microwave-assisted synthesis (Scheme 20.10). The synthesized compounds were screened for their antidepressant and anticonvulsant potentialities in mice by a forced swim test and subcutaneous pentylenetetrazole (scPTZ) test, respectively. Neuro-toxicities were determined by using the rotarod test in albino mice. The results revealed that compounds 2b, 2e, and 2k are found to be potent antidepressant molecules of the series at 20 mg/kg dose level as compared to reference drugs imipramine and fluoxetine. In contrast, compounds 2c and 2d were found to be potent anticonvulsant molecules of this series, when compared with the reference drug diazepam. None of the synthesized compounds showed neurotoxicity [19].

A series of new substituted *N*-11-(40-*N*-aryl carboxamido/*N*-(aryl)-a-phenyl-acetamido-piperazinyl)-dibenz[b,f][1,4]-oxazepine derivatives were designed. All the compounds (MJ1–MJ12) were synthesized by the economical route (Scheme 20.11). The antipsychotic potentialities of the synthesized derivatives were evaluated in mice by catalepsy and foot sock induced aggression. The present study demonstrated significant antipsychotic activity for most of the compounds from the series. Compounds MJ1, MJ3, and MJ4 were found to be potent antipsychotic compounds of the series at 5 mg/kg dose level as compared to the reference drug clozapine [20].

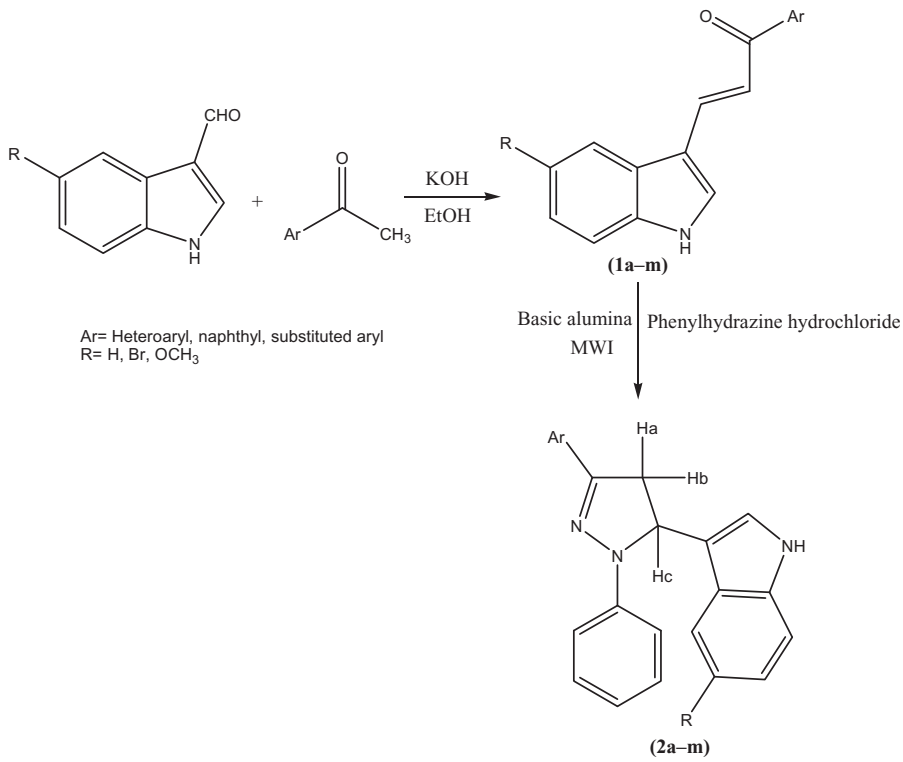

Scheme 20.10 Synthesis of 3-(1,3-diphenyl-4,5-dihydro-1*H*-pyrazol-5-yl)-1*H*-indole derivatives (2a–m) under microwave irradiation.

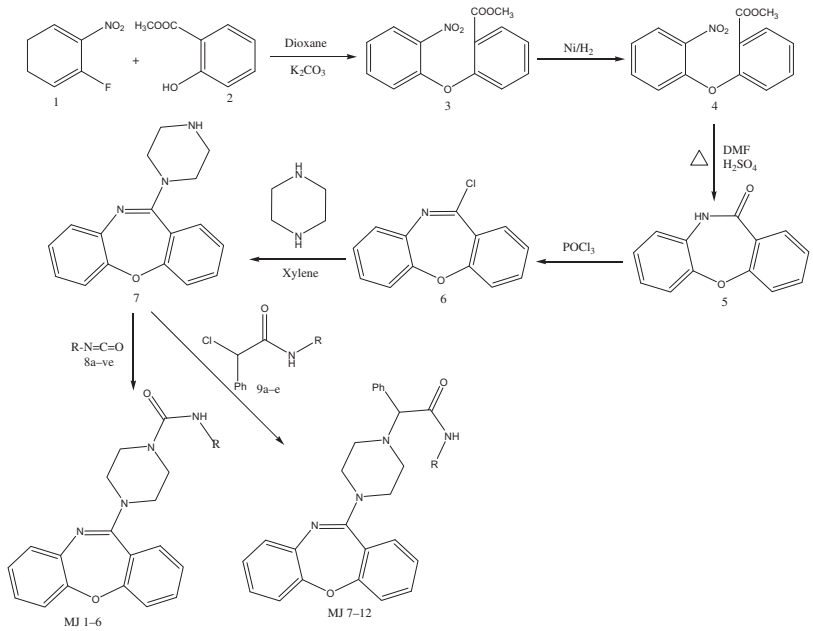

Scheme 20.11 Synthetic pathway for synthesis of dibenz-[b,f][1,4]-oxazepine derivatives (MJ1–MJ12).

A series of thienopyrimidines and related heterocycles were synthesized by refluxing related imidoyl chloride with primary and secondary amines under microwave irradiation and classical heating. The imidoyl chlorides are synthesized from corresponding cyclic imides with phosphorus oxychlorides under microwave irradiation and classical heating (Scheme 20.12). The synthesized compounds were screened for antipsychotic activity [21].

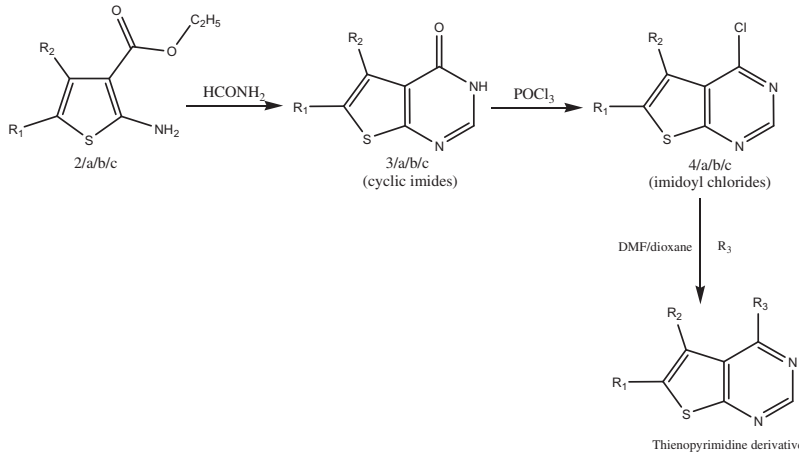

Scheme 20.12 Synthesis of thienopyrimidines derivatives under microwave irradiation and classical heating.

A series of 1-(quinoliloxypropyl)-4-aryl-piperazines was synthesized and the target compounds were evaluated for atypical antipsychotic activity in apomorphine-induced mesh climbing and stereotypic behavior in mice (Scheme 20.13). The 8-hydroxyquinoline ether derivative (14) emerged as an important lead compound showing a potential atypical antipsychotic profile. Employing appropriate physicochemical properties, the similarity of the compounds was assessed with respect to some atypical antipsychotic drugs as clozapine, ketanserine, ziprasidone, and risperidone [22].

The prototypical dopamine and serotonin antagonist (±)-7-chloro-9-(4-methylpiperazin-1-yl)-9,10-dihydropyrrolo[2,1-*b*][1,3]benzothiazepine was resolved into its *R* and *S*-enantiomers via crystallization of the diastereomeric tartaric acid salts (Fig. 20.3). Binding studies confirmed that the (*R*)-(−)-enantiomer was a more potent D_2 receptor antagonist than the (*S*)-(+)-enantiomer. (*S*)-(+)-enantiomer increases the extracellular levels of dopamine in the rat striatum after subcutaneous administration. Based on the structure-activity relationship study and molecular modeling, a novel series of potential atypical antipsychotics was developed [23].

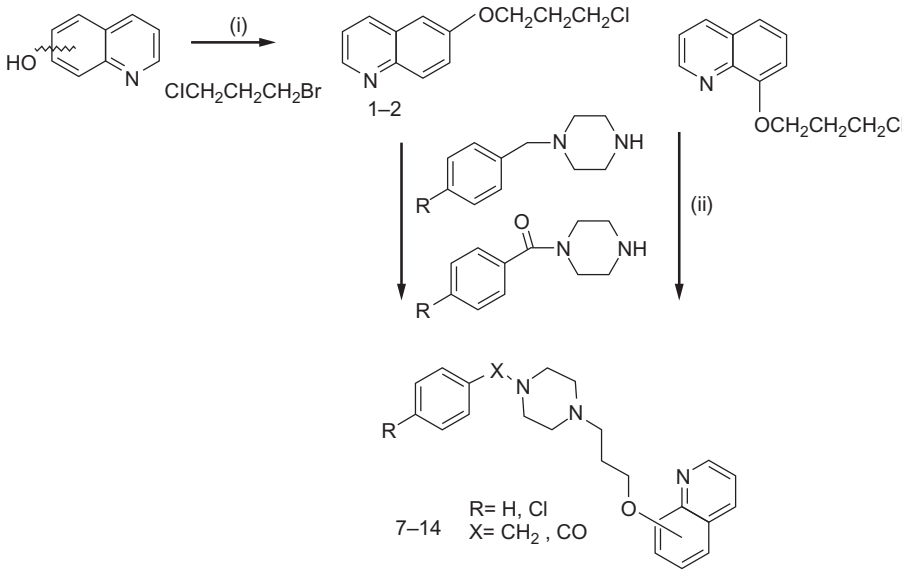

Scheme 20.13 Reagents and conditions: (i) Na, EtOH, 20–24 h; (ii) DMF, 18–20 h reflux.

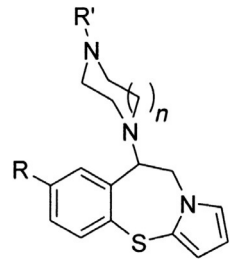

Fig. 20.3 Structure of (±)-7-chloro-9-(4-methylpiperazin-1-yl)-9,10-dihydropyrrolo[2,1-*b*][1,3]benzothiazepine.

A series of substituted phenethyl derivatives of 3-benzisothiazolylpiperazine incorporating potent D_2 and 5-HT_{2A} antagonist activity was investigated as an approach to generate novel atypical antipsychotic agent (Scheme 20.14). The in vitro profile of compound **8e** from this series was a combination of D_2 receptor affinity as compared to the typical antipsychotic agent haloperidol and a 5-HT_{2A}/D_2 ratio as compared to the atypical agent clozapine. The *in vivo* results indicated that the compound **8e** had efficacious antipsychotic activity with fewer tendencies to induce extrapyramidal side effects in human [24].

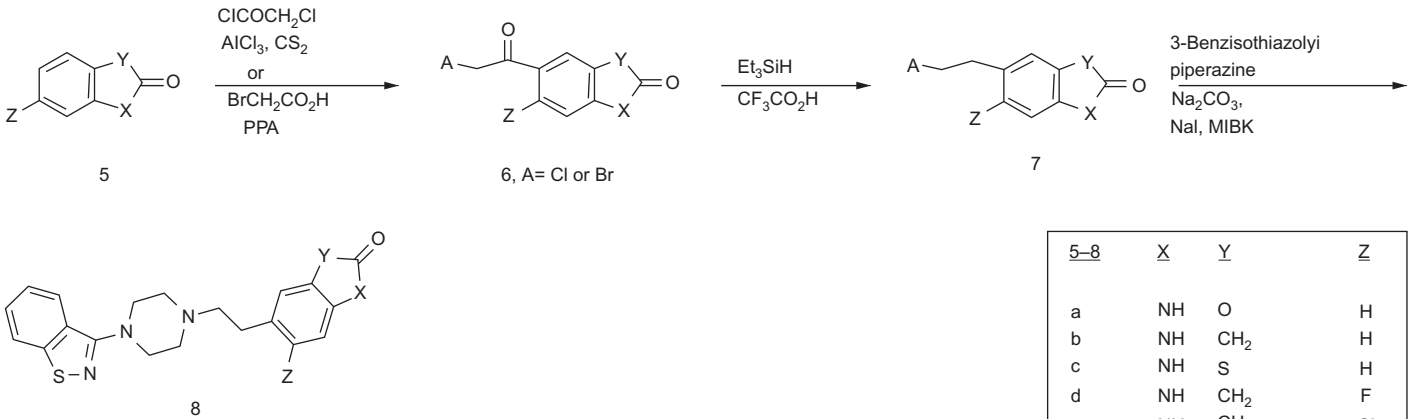

5–8	X	Y	Z
a	NH	O	H
b	NH	CH_2	H
c	NH	S	H
d	NH	CH_2	F
e	NH	CH_2	Cl
f	NEt	CH_2	H
g	NH	$C(CH_3)_2$	H
h	NH	$C((CH_2)_4)$	H

Scheme 20.14 Synthesis of 3-benzisothiazolylpiperazine derivatives.

Aripiprazole is a widely used antipsychotic drug approved by the FDA (Food and Drug Administration) in 2002. Methods for preparation of aripiprazole mainly involved the use of expensive and toxic solvents, and the reaction time can be even several hours long. But the green method was applied to get aripiprazole with high yield (70%–80%) in few minutes using solvent-free conditions in the presence of PTC (Phase Transfer Catalysts) and microwave radiation [25] (Schemes 20.15 and 20.16).

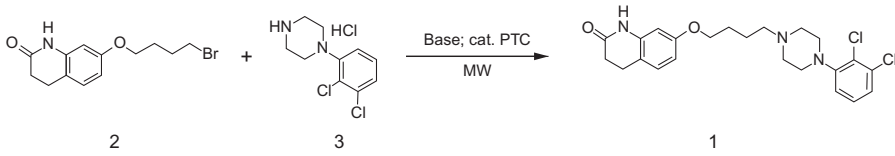

Scheme 20.15 Synthesis of aripiprazole (**1**).

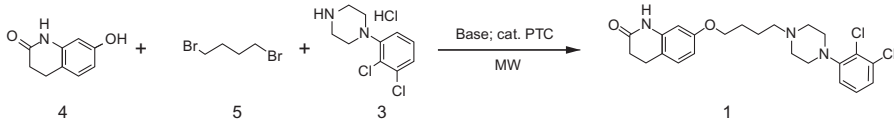

Scheme 20.16 One-pot synthesis of aripiprazole (1).

Heterocyclic analogs of 1192U90, 2-amino-*N*-(4-(4-(1,2-benzisothiazol-3-yl)-1-piperazinyl)butyl)benzamide hydrochloride (1), was prepared and evaluated as potential antipsychotic agents (Fig. 20.4). These analogs were evaluated in vitro for their binding to the dopamine D_2, serotonin 5-HT_2, and serotonin 5-HT_{1a} receptors and *in vivo* for their ability to antagonize the apomorphine-induced climbing response in mice. Nine different types of heterocyclic carboxamides were studied in this investigation (i.e., pyridine-, thiophene-, benzothiophene-, quinoline-, 1,2,3,4-tetrahydroquinoline-, 2,3-dihydroindole-, indole-, benzimidazole-, and indazolecarboxamides). Furthermore,

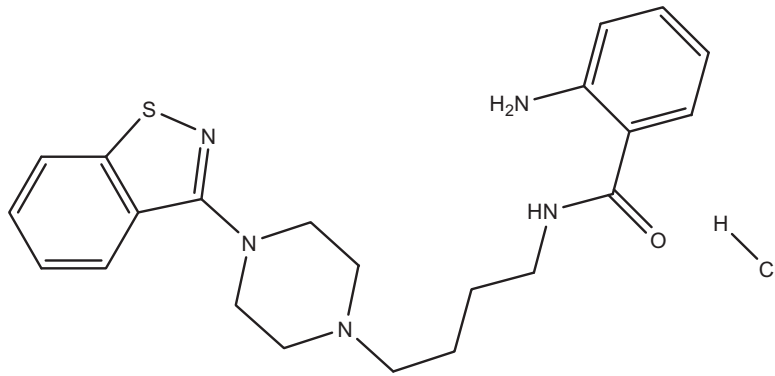

Fig. 20.4 Structure of heterocyclic analogs of 1192U90.

these derivatives were found to be less active in behavioral models predictive of extrapyramidal side effects than in the mouse climbing assay, which predicts antipsychotic activity [26].

The target compounds 2-[4-(aryl substituted) piperazin-1-yl]-*N*-phenylacetamides (3a–j) were synthesized by reacting aniline (**1**) with chloroacetyl chloride in the presence of 2*N* sodium hydroxide and dichloromethane to obtain 2-chloro-*N*-phenylacetamide (2) and subsequently treating with appropriate phenylpiperazine in acetonitrile in the presence of K_2CO_3 and KI (Scheme 20.17). The compounds were evaluated for antipsychotic activity using three animal models. All the newly synthesized arylpiperazines showed variable antipsychotic activity with compound 3h being the least effective in the induction of catalepsy. Their effect may involve interaction with 5-HT_{2A} and D_2 receptors [27].

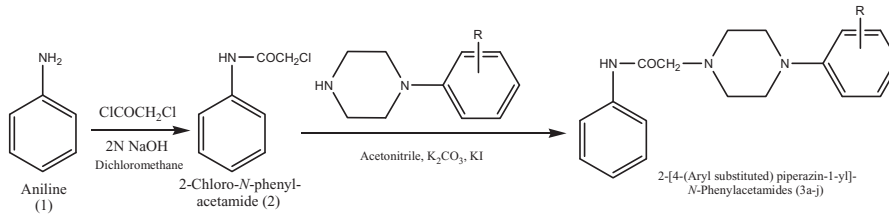

Scheme 20.17 Synthesis of 2-[4-(aryl substituted) piperazin-1-yl]-*N*-phenylacetamides (3a–j).

A series of tetrahydro-pyrido-pyrimidinone derivatives, possessing potent dopamine D_2, serotonin 5-HT_{1A} and 5-HT_{2A} receptors properties, were synthesized and evaluated as potential antipsychotics (Scheme 20.18). Among them, 3-(2-(4-(benzo[*b*]thiophen-4-yl)piperazin-1-yl)ethyl)-9-hydroxy-2-methyl-6,7,8,9-tetrahydro-4*H*-pyrido[1,2-*a*]pyrimidin-4-one (10d) had the best pharmacological profile. It not only exhibited potent and balanced activities for D_2, 5-HT_{1A}, and 5-HT_{2A} receptors, but also endowed with low activities for α_{1A}, 5-HT_{2C}, H_1 receptors, and hERG channels, suggesting a low propensity for inducing orthostatic hypotension, weight gain, and QT prolongation. In animal models, compound 10d reduced phencyclidine-induced hyperactivity with a high threshold for catalepsy induction. On the basis of its robust in vitro potency and *in vivo* efficacy in preclinical models of schizophrenia, coupled with a good pharmacokinetic profile, 10d was selected as a candidate for further development [28].

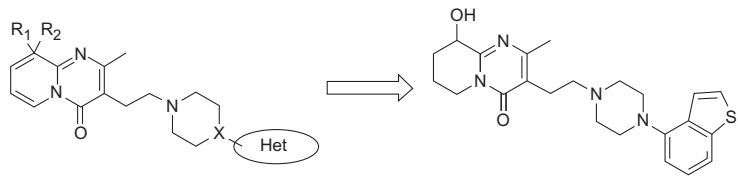

Scheme 20.18 Synthesis of tetrahydro-pyridopyrimidinone derivatives.

The synthesis of novel, potential antipsychotic coumarin derivatives combining potent dopamine D_2, D_3 and serotonin 5-HT_{1A}, 5-HT_{2A} receptors properties were reported (Scheme 20.19). The unique pharmacological features of compound **27** are a high affinity for dopamine D_2, D_3 and serotonin 5-HT_{1A}, 5-HT_{2A} receptors, together with a low affinity for H_1 receptor (to reduce the risk of obesity under chronic treatment). In animal models, compound **27** inhibited apomorphine-induced climbing and MK-801-induced hyperactivity without observable catalepsy at the highest dose tested. In particular, compound **27** was more potent than clozapine [29].

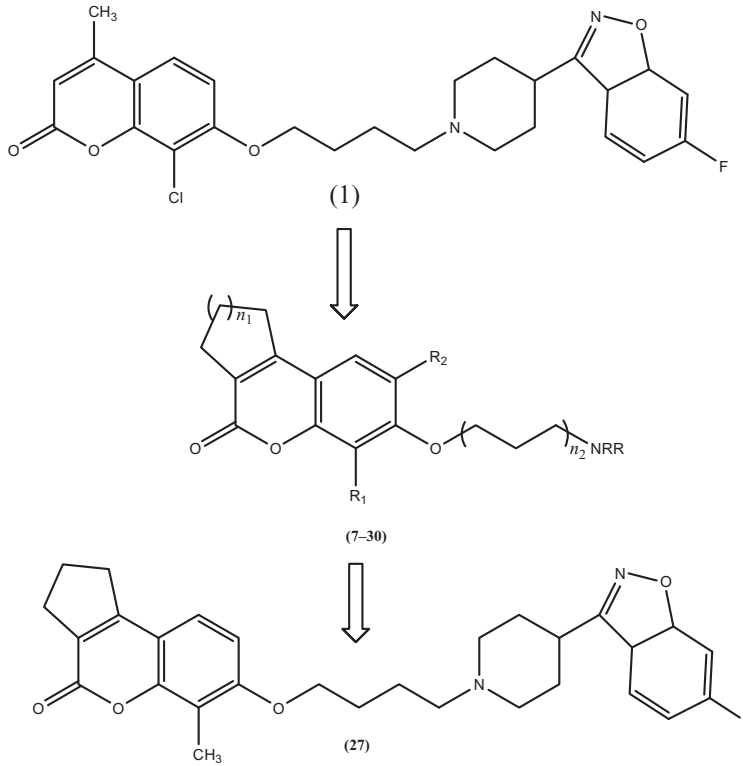

Scheme 20.19 Synthesis of coumarin derivatives.

A series of benzamides was identified as potent antipsychotic agents (Fig. 20.5). As a continuation of the program to discover novel antipsychotics, the evaluation of a series of pyridine-carboxamide derivatives was performed. The most promising compound **7**h had good activities on dopamine D_2, serotonin 5-HT_{1A}, and 5-HT_{2A} receptors. They also exhibited low potency for α_{1A}, H_1, and 5-HT_{2C} receptors, indicating a low propensity of side effects like orthostatic hypotension and weight gain. Furthermore, **7**h exhibited more potent antipsychotic-like effect than aripiprazole in behavioral studies. The preliminary results were promising enough for further research around this scaffold [30].

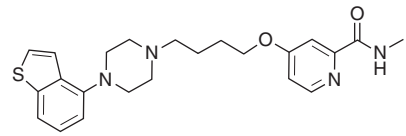

7h

IC_{50} (D_2R) = 24.0 nM, EC_{50} (5-$HT_{1A}R$) = 1.2 nM, IC_{50} (5-$HT_{2A}R$) = 154 nM
low potency for α_{1A}, H_1 and 5-HT_{2C} receptors
potent antipsychotic-like effect in mice

Fig. 20.5 Structure of benzamide derivatives.

A series of novel benzoxazole-piperidine (piperazine) derivatives combining high dopamine D_2 and serotonin 5-HT_{1A}, 5-HT_{2A} receptor affinities were reported. Of these derivatives, the pharmacological features of compound 29 exhibited high affinities for D_2, 5-HT_{1A}, and 5-HT_{2A} receptors, but low affinities for the 5-HT_{2C} and histamine H_1 receptors. Furthermore, compound 29 reduced apomorphine-induced climbing and 1-(2,5-dimethoxy-4-iodophenyl)-2-aminopropane (DOI)-induced head twitching without observable catalepsy, even at the highest dose tested. Thus, compound 29 was a promising candidate as a multitarget antipsychotic treatment [31] (Scheme 20.20).

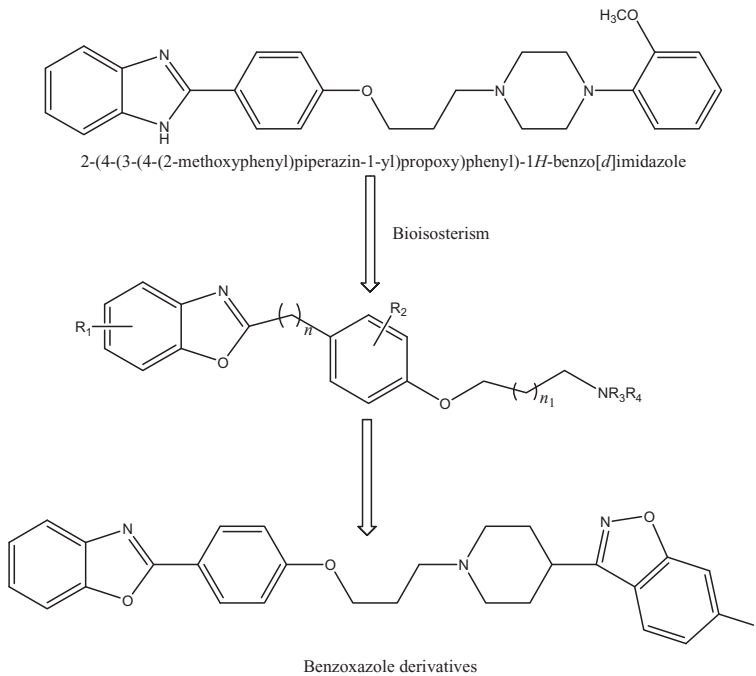

Scheme 20.20 Synthesis of benzoxazole-piperidine (piperazine) derivatives

20.2 Conclusion

There is an urgent need to establish green technologies for synthesis of drug molecules which will minimize the use of chemicals or solvents and that will help towards sustainable development. Green chemistry approach must be implemented successfully to carry out environmentally friendly chemical processes and design of new products. The synthetic schemes should be designed in such a way that there will be least pollution to the environment. Therefore, attempts have been made to design synthesis for manufacturing new antidepressant and antipsychotic agents.

Acknowledgments

Bimal K. Banik is grateful to Prince Mohammad Bin Fahd University.

References

[1] L. Jennings, Antidepressants, in: G.T. Grossberg, L.J. Kinsella (Eds.), Clinical Psychopharmacology for Neurologists: A Practical Guide, Springer, 2018, pp. 45–71 (Chapter 4).
[2] R.W. Pies, Antidepressants, J. Clin. Psychopharmacol. 36 (1) (2016) 1–4.
[3] F.S.K. Barar, Essentials of Pharmacotherapeutics, New Edition, 2005, p. 139.
[4] P. Devender, D. Rajiv, P. Kamla, D. Sunita, New generation antipsychitics—a review, Indian J. Pharm. Educ. Res. 40 (2) (2006) 123–125.
[5] R. Ametha, C. Ametha, T. Paras, S. Benzamin, S. Ametha, Green chemistry: a step towards clean and sustainable development, J. Indian Chem. Soc. 89 (2012) 999.
[6] B.V. Badami, Concept of Green Chemistry, Resonance (2008) 1041–1048.
[7] J.B. Devhade, M.J. Devade, S.S. Kalwaghe, Green chemistry for chemical synthesis, Int. Res. J. Sci. Eng. 2 (3) (2014) 100–103.
[8] V. Jatav, P. Mishra, S. Kashaw, J.P. Stables, Synthesis and CNS depressant activity of some novel 3-[5-substituted 1,3,4-thiadiazole-2-yl]-2-styryl quinazoline-4(3H)-ones, Eur. J. Med. Chem. 43 (1) (2008) 135–141.
[9] M. Yusuf, R.A. Khan, B. Ahmed, Syntheses and anti-depressant activity of 5-amino-1,3,4-thiadiazole-2-thiol-imines and thiobenzyl derivatives, Bioorg. Med. Chem. 16 (17) (2008) 8029–8034.
[10] R.K. Mahesha, T. Devadoss, D.K. Pandey, S. Bhatt, S.K. Yadav, Design, synthesis and structure–activity relationship of novel quinoxalin-2-carboxamides as 5-HT3 receptor antagonists for the management of depression, Bioorg. Med. Chem. Lett. 20 (22) (2010) 6773–6776.
[11] B. Dash, S. Dash, D. Laloo, Design and synthesis of 4-substituted Quinazoline derivatives for their anticonvulsant and CNS depressant activities, Int. J. Pharm. Pharm. Sci. 9 (1) (2017) 165–172.
[12] S.A. Saganuwan, Piroxicam: source for synthesis of central nervous system (CNS) acting drugs, Cent. Nerv. Syst. Agents Med. Chem. 17 (2) (2017) 135–140.
[13] S.K. Shukla, B.S. Rawat, Synthesis and evaluation of heterocyclic derivatives of morpholino-N-acetylindoles for central nervous system depressant activity, Int. J. Sci. Res. 5 (9) (2016) 111–115.
[14] V.K. Merugumolu, R.B. Chandrashekarappa, Synthesis and anti-depressant evaluation of novel pyrazolone derivatives, Bangladesh J. Pharmacol. 11 (2016) 558–563.
[15] P.O. Patil, D.P. Belsarea, S.B. Kosalge, R.A. Fursule, Microwave assisted synthesis and antidepressant activity of some 1,3,5-triphenyl-2-pyrazolines, Int. J. Chem. Sci. 6 (2) (2008) 717–725.

[16] A.P.G. Nikalje, M.S. Ghodke, F.A.K. Khan, J.N. Sangshetti, Microwave assisted facile synthesis and biological evaluation of novel 2-indolyl-1, 5-benzothiazepines, Open Pharm. Sci. J. 3 (2016) 117–130.
[17] S.-A. Lee, V.S. Sadu, N.-J. Park, I.-T. Hwang, K.-I. Lee, A practical synthesis of the antidepressant (S)-duloxetine, Bull. Kor. Chem. Soc. 35 (6) (2014) 1894–1896.
[18] J. Jaśkowska, P. Zaręba, P. Śliwa, E. Pindelska, G. Satała, Z. Majka, Microwave-assisted synthesis of trazodone and its derivatives as new 5-HT_{1A} ligands: binding and docking studies, Molecules 24 (2019) 1–19 1609.
[19] P.O. Patil, S.B. Bari, Synthesis, characterization and screening for antidepressant and anticonvulsant activity of 4,5-dihydropyrazole bearing indole derivatives, Arab. J. Chem. 9 (2016) 588–595.
[20] M.S. Jain, S.J. Surana, Synthesis and evaluation of antipsychotic activity of 11-(40-(N-aryl-carboxamido/N-aryl-a-phenylacetamido)-piperazinyl)-dibenz[b,f][1,4]-oxazepine derivatives, Arab. J. Chem. 10 (2017) S2032–S2039.
[21] C. Sharma, S. Yerande, R. Chavan, A.V. Bhosale, Synthesis of thienopyrimidines and their antipsychotic activity, E-J. Chem. 7 (2) (2010) 655–664.
[22] A. Bali, S. Malhotra, H. Dhir, A. Kumar, A. Sharma, Synthesis and evaluation of 1-(quinoliloxypropyl)-4-aryl piperazines for atypical antipsychotic effect, Bioorg. Med. Chem. Lett. 19 (2009) 3041–3044.
[23] G. Campiani, S. Butini, S. Gemma, V. Nacci, C. Fattorusso, B. Catalanotti, G. Giorgi, A. Cagnotto, M. Goegan, T. Mennini, P. Minetti, M.A. Di Cesare, D. Mastroianni, N. Scafetta, B. Galletti, M.A. Stasi, M. Castorina, L. Pacifici, O. Ghirardi, O. Tinti, P. Carminati, Pyrrolo[1,3]benzothiazepine-based atypical antipsychotic agents. synthesis, structure-activity relationship, molecular modeling, and biological studies, J. Med. Chem. 45 (2002) 344–359.
[24] H.R. Howard, J.A. Lowe, T.F. Seeger, P.A. Seymour, S.H. Zorn, P.R. Maloney, F. E. Ewing, M.E. Newman, A.W. Schmidt, J.S. Furman, G.L. Robinson, E. Jackson, C. Johnson, J. Morrone, **3-**Benzisothiazolylpiperazine derivatives as potential atypical antipsychotic agents, J. Med. Chem. 39 (1996) 143–148.
[25] J. Jaśkowska, A.K. Drabczyk, D. Kułagaa, P. Zaręba, Z. Majka, Solvent-free microwave-assisted synthesis of aripiprazole, Curr. Chem. Lett. 7 (2018) 81–86.
[26] M.H. Norman, F. Navas, J.B. Thompson, G.C. Rigdon, Synthesis and evaluation of heterocyclic carboxamides as potential antipsychotic agents, J. Med. Chem. 39 (24) (1996) 4692–4703.
[27] S. Kumar, A.K. Wahi, R. Singh, Synthesis and preliminary pharmacological evaluation of 2-[4-(arylsubstituted)piperazin-1-yl]-Nphenylacetamides: potential antipsychotics, Trop. J. Pharm. Res. 10 (3) (2011) 265–272.
[28] H. Xiamuxi, Z. Wang, J. Li, Y. Wang, C. Wu, F. Yang, X. Jiang, Y. Liu, Q. Zhao, W. Chen, J. Zhang, Y. Xie, T. Hu, M. Xu, S. Guo, H. Akber Aisa, Y. He, J. Shen, Synthesis and biological investigation of tetrahydropyridopyrimidinone derivatives as potential multireceptor atypical antipsychotics, Bioorg. Med. Chem. 25 (17) (2017) 4904–4916.
[29] Y. Chen, Y. Lan, S. Wang, H. Zhang, X. Xu, X. Liu, M. Yu, B.F. Liu, G. Zhang, Synthesis and evaluation of new coumarin derivatives as potential atypical antipsychotics, Eur. J. Med. Chem. 74 (3) (2014) 427–439.
[30] M. Xu, Y. Wang, F. Yang, C. Wu, Z. Wang, B. Ye, X. Jiang, Q. Zhao, J. Li, Y. Liu, J. Zhang, G. Tian, Y. He, J. Shen, H. Jiang, Synthesis and biological evaluation of a series of novel pyridine-carboxamides as potential multi-receptor antipsychotic drugs, Bioorg. Med. Chem. Lett. 28 (4) (2018) 606–611.
[31] L. Huanga, W. Zhang, X. Zhang, L. Yin, B. Chen, J. Song, Synthesis and pharmacological evaluation of piperidine (piperazine)-substituted benzoxazole derivatives as multi-target antipsychotics, Bioorg. Med. Chem. Lett. 25 (22) (2015) 5299–5305.

Natural spices in medicinal chemistry: Properties and benefits

21

Shibani Basu[a,*], *Bimal Krishna Banik*[b,*]
[a]Department of Chemistry and Biochemistry, Boise State University, Boise, ID, United States, [b]Department of Mathematics and Natural Sciences, College of Sciences and Human Studies, Deanship of Research Development, Prince Mohammad Bin Fahd University, Al Khobar, Kingdom of Saudi Arabia
[*]Corresponding author. e-mail address: meetbasu.shibani@gmail.com; bimalbanik10@gmail.com; bbanik@pmu.edu.sa

21.1 Introduction

Since ancient civilization, plant spices have been added to enrich the taste and zest of the foods. Currently, >85,000 plant species have been documented for therapeutic use worldwide. This indicates that natural products from plant present a broad range for research and development of new medicines in diverse clinical trials [1–3]. This further involves many medicines from plants that have been extensively used clinically. Traditional natural products from plants have been significantly contributing to the improvement of contemporary medicines [4–6]. Further study indicates that about 80%–85% of the world's population depends on these traditional medicines from plant products for health care [7, 8]. Therefore, the principal object of this paper is to present studies which have been completed on the different medicinally important spices.

21.2 General features of spices

Spices originate from numerous portions of the plant such as flowers, fruits, leaves, buds, bark, stigmas, and styles or seeds [9, 10]. These include flowers such as cloves, fruits such as cayenne pepper and cumin, leaves such as mint, buds such as onion and garlic, bark such as cassia and cinnamon, stigma such as saffron, seeds such as black pepper and fennel, and root and rhizomes such as ginger and turmeric [11–13]. Plant produces spices through secondary metabolism, some components as complex molecular structures. Plants produce metabolites such as flavonoids, isoflavonoids, alkaloids, glycosides, tannins, phenolic compounds, coumarins, and terpenes which give the spices their characteristics as aroma, antioxidant, and antimicrobial activity [14, 15]. Spices are acknowledged due to their medicinal approach but in recent times they have been used to enhance flavor and color instead of preserving shelf-life of food. Spices are frequently dried up [16]. The spices have distinct assets that mark them valuable for numerous practices. Some exceptional features that provide them diversity are illustrated in Table 21.1.

Green Approaches in Medicinal Chemistry for Sustainable Drug Design. https://doi.org/10.1016/B978-0-12-817592-7.00022-8
© 2020 Elsevier Inc. All rights reserved.

Table 21.1 General property and importance of the Apiaceae family membered spices.

Biological name	Common name	Other names	Active constituents	Pharmacological activities
Trachypermum ammi	Ajwain, Bishop's weed	Yamani, Javan, Ajma, Juani, Omam	6-*O*-β-glucopyranosyloxythymol, thymol, para-cymene, α- and β-pinene	Antimicrobial, antioxidant, antilithiasis, antiinflammatory, antifilarial, antiseptic, antispasmodic, digestive
Cuminum cyminum	Jeera, Cumin	Kamun, Safed jeeraa	Cuminaldehyde, *b*-pinene, *g*-terpinene, *p*-cymene	Antibacterial, astringent, analgesic, carminative, cough remedy and eupeptic
Foeniculum vulgare	Fennel, sweet cumin	Fenikel, Perum jeerakam, fenicol, fenkel, fenkhel, fenkoli, fennel, saunf, shamaar	α-pinene, Anethole, β-pinene, β-myrcene, camphene, fenchone, fenchone, estragole, limonene, *p*-cymen	Antimicrobial, antioxidant, anticancer, cold, cough and cattle condiment, carminative

21.3 General and chemical features of spices

Chemical properties of spices make them distinctive such as aroma, color, and to be used as food preservatives. Chemical components of spices also represent the antimicrobial activity against several pathogenic bacteria [17]. Table 21.1 illustrates the chemical components that are responsible for many characteristic properties of spices. Spices are the rich source of flavonoids, terpenes, and phenolic compounds which provide spices color, flavor, and medicinal value [18]. For example, curcuminoids such as curcumin and demethoxycurcumin in turmeric represent antimicrobial activity and pinene in clove provides antioxidant activity [19]. Different spices show medicinal activity as antimicrobial and antioxidant based on their chemical components with the ability to inhibit microorganisms or the responsible constitutes [20, 21]. Ajwain, cumin, and fennel belong to the family of Apiaceae. The Apiaceae family is a group of plants that contains hollow stems and aromatic compounds. Other important plants of this family are caraway, celery, coriander, anise, parsley, and parsnip. Plants of this family have achieved levels of medicinal value as well as food value due to their chemical constituents such as curcumin, thymol, and several volatile oils.

Trachyspermum ammi (Linn) Sprague (Ajwain) is an inherent from Egypt and mostly cultivated in India, Iraq, Iran, and Afghanistan. Ajwain is a highly valued medicinal plant which belongs to the Apiaceae family [22]. The seeds of this plant contain 2%–5% oil which possesses aphrodisiac properties. The ajwain seed oil mainly consists of thymol which plays a significant role in the treatment of bronchial problems, gastrointestinal problems, and loss of appetite [23]. The oil of ajwain exhibits antimicrobial and fungicidal properties on humans. Ajwain is a traditional medicinal herb, extensively used for curing numerous diseases in humans and animals. Ajwain seeds comprise an essential oil with about 50% thymol content which could potentially be used as fungicide, germicide, and antispasmodic [24].

Cuminum cyminum (Cumin) is a popular spice and is used in folk medicine from the ancient time. The presence of aromatic substances makes this spice very significant in medical application as well as culinary spice [21]. Cumin has been highly popular since ancient times and was frequently used as a medicinal plant for long time. Cumin seed is a slight fusiform, grayish in color, obtained from liner fashioned seed plant that have a pungent flavor and slightly bitter in test [25, 26]. Cumin is an astringent and an aromatic herb that provides assistance to the digestive system. It has been widely used to cure mild gastric disorders as a eupeptic and carminative, as an analgesic and as an astringent in bronco pulmonary illnesses [27]. The essential oil from cumin seeds has revealed a potential antibacterial activity against *Klebsiella pneumoniae* in vitro [28].

Foeniculum vulgare (Fennel) is a popular spice that has been used in traditional medicine for a wide variety of diseases associated with endocrine, digestive, respiratory, and reproductive system [29]. Phytochemical findings of fennel seeds have revealed the existence of abundant valuable compounds such as flavonoids, volatile compounds, phenolic compounds, amino acids, and fatty acids [30]. Based on the study, fennel remains to be the most commonly used herbal plant. Experimental data

indicates their efficacy in several in vitro and in vivo pharmacological properties such as antitumor, antiinflammatory, antimicrobial, antithrombotic, apoptotic, antipyretic, chemomodulatory, cardiovascular, hypoglycemic, and hepatoprotective [31, 32]. Fennel seed has appeared as a decent cause of traditional medicine and delivers a remarkable source in medicinal chemistry/biology for the discovery of new drugs and upcoming experimental practices [33].

21.4 Phytochemical composition

Analysis of ajwain seed has shown that it comprises carbohydrate (38%), fiber (11.9%), fat (18%), protein (15%), tannins and glycosides (9%), and flavonoids and minerals (7%). Essential oil of ajwain exhibited 26 recognized constituents which account for 96.3% of the total amount. Ajwain seed contains thymol (39%), terpinene (23%), *p*-cymene (31%), terpinene-4-ol (0.8%), and pinene (1.7%) [34]. On the other hand, acetone extract of ajwain seed contains thymol (40%), linoleic acid (10%), oleic acid (10.4%), palmitic acid (1.6%), xylene (0.1%), and cymene (1.6%). Alcoholic extract of ajwain contains a highly hygroscopic saponin [35]. A yellow, crystalline flavone and steroid-like constituent have been isolated from the fruits, which also contain glucosides, 6-*O*-β-glucopyranosyloxythymol, and volatile oil (thymol, α- and β-pinene) [36].

Cumin seeds hold amino acids, flavonoids, aldehydes, fats, glycosides, and volatile oil containing cuminaldehyde as its principal constituents. The main compounds occurring in cumin are α- and β-pinene, α- and γ-terpinene, cuminaldehyde, 1,8-cineole, limonene, *o*-and *p*-cymene, linalool, and safranal. The cumin fruit contains protein, fat, resin, gum, lignin, salts, and volatile oil. The conformation of the seeds specifies that they comprise protein, sugar, cellulose, oil (approximately 10%), volatile oil (1%–5%), and mineral elements [37]. Cumin fruits contain abundance of phenolic compounds including flavonoids, diterpenes, and phenolic acids. Phenolic compounds present in cumin play a significant role in presenting antioxidant activity, lipid peroxidation, and several types of oxidizing enzymes [38]. The organic acids present in cumin are citric, ascorbic, malic, oxalic, tartaric, oxalic, aspartic, fumaric, and propionic acids. The phenols present are cinnamic acid, gallic acid, rutin, salicylic acid, hydroquinone, coumarine, *p*-hydroxybenzoic acid, resorcinol, quercetin, and anethole. Essential oils present in cumin are thymol, vanillin, benzoic acid, octanol, limonene, and anisyl alcohol which imparts aroma to cumin seed oil and used in cosmetic industry [39].

All parts of the fennel plant including seeds, fruit, roots, and leaves are being used for medicinal purposes. Fennel seed comprises 42% carbohydrates, 18% fibers, 13% minerals, 10% fat, 10% protein, and 6% water [40]. Fruits contain almost 10%–12% oil which consists of 22% palmitic acid, 14% linoleic acid, 6% petrocyclic acid, and 4% palmitic acid. Leaves contain vitamin C, riboflavin, thiamine, calcium, iron, sodium, phosphorus, and potassium [41]. The aromatic property of fennel comes from the compound present in the essential oil. There are >30 types of terpenes, most importantly 50%–80% transanethole, 5% limonene, and 8% fenshon are present in

the essential oil of fennel seed [42]. The herb comprises flavonoids, phenolic compounds, hydroxycinnamic acid, tannin, and coumarin. Flavonoids include rosmarinic acid, quercetin-3-rutinoside, and eriodictyol-7-rutinoside. Phenolic acids consist of 1,3-*O*-di-caffeoylquinic acid, 1,4-*O*-di-caffeoylquinic acid, and 1,5-*O*-di-caffeoylquinic acid [43].

21.5 Pharmacological activities of ajwain

Ajwain has a distinguishing aromatic aroma and strong taste which is why it is commonly used in cooking as spice. In Indian folk medication, ajwain seeds are used for the treatment of asthma, stomach disorders, and colic pains. Ajwain seed has been found to retain antimicrobial, antihypertensive, antispasmodic, antiinflammatory, antifilarial, broncho-diating, diuretic, digestive stimulant, and detoxification effects. Beneficial uses of *T. ammi* fruits include antimicrobial, antiseptic, amoebiasis, carminative, and expectorant activities.

21.5.1 Antimicrobial activity

Ajwain shows the antimicrobial activities in the preservation of foods against microbial decay, directing laboratory analyses of antimicrobial potentiality in vitro. The constituents assumed to be accountable to the antimicrobial action of ajwain were thymol and carvacol. Thymol can destroy the microorganisms resistant to the established third-generation multidrug resistant bacteria pathogens and therefore works as a plant-based antibiotic agent. Volatile constituents of ajwain seed show antifungal activity on several fungi such as *Acrophialophora fusispora*, *Alternaria grisea, Curvularia lunata*, *Drechslera tetramera*, *Fusarium chlamydosporum*, and *Rhizoctonia solani* [44].

21.5.2 Antiinflammatory activity

Antiinflammatory activity of the aqueous extract and alcohol extract of the ajwain seeds was experimentally proved. Aqueous extract and alcohol extract were found to possess substantial ($P < 0.001$) antiinflammatory activity in animal models [45].

21.5.3 Antifilarial activity

In vitro antifilarial activity of the fruits of ajwain against *Setaria digitate* was studied. Both the active fraction and the crude extract of ajwain exhibited substantial action against *S. digitate* by both 3-(4,5-dimethylthiazole-2-yl)-2,5-diphenyltetrazolium bromide (MTT) reduction assays and worm motility. In vivo antifilarial activity of the active phenolic monoterpene against human filarial worm *Brugia malayi* exhibited macrofilaricidal action. On the other hand, in vivo antifilarial activity of crude extract of ajwain against female worm *B. malayi* presented macrofilaricidal activity. The active fraction of 2-isopropyl-5-methyle phenol showed IC_{50} values of 0.024 and

0.002 mg/mL at the incubation periods of 24 and 48 h, respectively. The in vivo effect against the *B. malayi* parasite in a *Mastomys coucha* model of the active fraction of 2-isopropyl-5-methyle phenol was estimated [46].

21.5.4 Antilithiasis and diuretic activities

In vivo experiment of ajwain seed for antilithiasis and diuretic activities to inhibit oxalate urolithiasis has shown potential effects in rats. In an advance revision of a promising diuretic effect, it was established that ajwain seed was not effective in increasing the 24-h urine production. The results of this trial determined that the use of ajwain in the cure of kidney stones could not be justified by their investigational confirmation [47].

21.5.5 Antitussive effects

The antitussive effects of ajwain, codeine, and saline were tested by calculating the amount of coughs formed. The results indicated a substantial decrease in cough in the presence of ajwain extracts ($P < 0.001$) and codeine ($P < 0.01$) [48].

21.5.6 Anthelmintic activity

Anthelmintic activity of ajwain indicates its potential action against various helminths such as *Haemonchus contortus* in sheep and *Ascaris lumbricoides* in human. Anthelmintic activity of ajwain extracts inhibits helminths by interfering with the energy metabolism of parasites over ATPase activity which causes loss of energy reserves. The ajwain plant has also been described to have cholinergic activity with peristaltic association in the gut [49].

21.5.7 Antihypertensive, antispasmodic, and broncho-dilating activities

The antihypertensive effect of ajwain seed was shown in vivo. The broncho-dilating and antispasmodic activities in vitro exhibited that calcium channel facilitates the spasmolytic effects of plant materials. It is being considered that this mechanism justified the antihypertensive effect to their experiential result and sustained the clinical use of ajwain in hyperactive disease of the gut as diarrhea and colic [50].

21.5.8 Antiplatelet-aggregatory

The extract of ajwain seeds has shown the antiplatelet-aggregatory effect in in vitro trial with blood taken from human participants. Clinical trial displayed that ajwain seeds are highly efficient to block platelet aggregation by induced epinephrine, arachidonic acid, and collagen [51].

21.5.9 Hepatoprotective activity

The hepatoprotective activities in vivo exhibited that ajwain was 70%–80% defensive in mice compared to normal lethal dose of paracetamol (1 g/kg). Ajwain seeds show potential to inhibit the CCl_4-induced elongation of pentobarbital sleeping time in mice. Ajwain seed also has the ability to control high serum levels of liver enzymes produced by CCl_4-tempted liver injury in rats [51].

21.5.10 Ameliorative effect

Ameliorative effects of ajwain extract on hexachlorocyclohexane-induced oxidative stress and effects in rats were examined. Pre-feeding with ajwain extract caused higher GSH-peroxidase, GSH, G-6-PDH, SOD, glutathione S-transferase, and reduced levels of lipid peroxides. It was established that treatment with hexachlorocyclohexane resulted in hepatic-free radical stress, which could be reduced by the ajwain seed extract [52].

21.5.11 Antiflatulant

Conventionally ajwain is used to treat flatulence and gas. People use ajwain in a very classic way from ancient time to treat digestion problems. One popular way is to take 20 g of the rock salt and table salt and 500 g of ajwain seed and mix with lemon juice. This preparation of ajwain is an outstanding medication to cure nausea, vomiting, travel sickness, and abdominal gas [53].

21.5.12 Detoxification of aflatoxins

The ajwain seed extract exhibited aflatoxin G1 (AFG1) degradation. The detoxification of aflatoxin by ajwain seed extract was markedly decreased upon a heat treatment. Ajwain seed extract also showed significant amount of degradation of other aflatoxins such as AFB1, AFB2, and AFG2. AFG1 detoxification by dialyzed ajwain extract revealed that 78% of degradation happened within 6 h of incubation and about 91% degradation happened at 24 h [54].

21.5.13 Hypolipidemic action in vivo

Ajwain seed extract showed antihyperlipidemic effect in albino rabbits. It was considered that ajwain seed powder at 2 g/kg body weight dose rate is significantly effective in reducing lipid action by decreasing LDL cholesterol, total cholesterol, triglycerides, and total lipids [55].

21.5.14 Nematicidal activity

Nematicidal activity of ajwain oil components such as carvacrol, thymol, camphene, limonene, pinene, myrcene, terpinene, and terpinen showed potential activity against pinewood nematode (PWN) [56]. Target sites of methyl isothiocyanate in nematodes are proposed as amino and hydroxyl groups. Essential oils of ajwain was described to inhibit the GABA-gated chloride channels or neuromodulator octopamine of insect pests [57]. Further research have confirmed that the nematicidal activity of ajwain oil mainly ascribed to the activity of carvacrol and thymol [54].

21.6 Pharmacological activities of cumin

Cumin seeds are used as a spice in cooking to flavor and texture the food. The constituents of cumin usually have antibacterial, antioxidant, and anticancer properties. Cumin seeds are also used to reduce seizures, strengthen bones, and lower blood sugar. Traditionally cumin is used to increase urine volume, inhibit gas, decrease inflammation, and defeat muscle tremors [58]. Cumin is also used to treat diarrhea, indigestion, jaundice, and poultice and taken orally. Cumin has been used as an aromatic element in perfumes, creams, and lotions. Cumin also is considered astringent, antiseptic, antihypertensive, stimulant, carminative, and galactagogue. The taste of cumin is strong and pungent and can be used as tonic to treat respiratory, gastrointestinal, and gynecological disorders and also to cure diarrhea, epilepsy, and toothache [28].

Cumin and its essential elements was used as antibacterial, antiinflammatory, antioxidant, antifungal agents, astringent, for atherosclerosis, for improving bone density, as blood thinner, for cancer, cataracts, cardiovascular disease, cavities, diabetes, dental plaque, digestion, ear infections, gastrointestinal disorders, general stimulant, general health maintenance, high cholesterol, insect repellant, insecticidal, low blood sugar, menstrual flow stimulant, relaxation, seizures/epilepsy, ulcers, and weight loss [59]. The pharmacological activities or uses of cumin are discussed below:

21.6.1 Antimicrobial activity

Cumin seed oil and aqueous extract both showed significant antimicrobial activity against a broad variety of pathogenic Gram-positive and Gram-negative strains [60]. Cumin seeds are used to prevent biofilm formation of many bacteria like *Streptococcus pyogenes* and *Streptococcus mutans* [61, 62]. Alcoholic extract of cumin seeds and cumin seed oil prevented the growth of *K. pneumoniae* and its experimental isolates [63]. Cumin seeds are also used in to improve capsule expression, cell morphology, and to reduce urease activity [64]. Cumin seeds have also exhibited antifungal activity against several human pathogens [65–70].

21.6.2 Antioxidant activity

The cumin seed oils have shown significant antioxidant activity [25, 71]. Antioxidant activity of cumin was due to the presence of active components such as flavonoids, monoterpene alcohols, poly-phenolic components, and essential aromatic components [72, 73].

21.6.3 Anticarcinogenic/antimutagenic

Cumin seeds have shown the activity to inhibit the occurrence of colon cancer in rat. Cumin also reduces the probability of induction of colon-specific carcinogen as well as lowers the activity of mucinase enzymes and β-glucuronidase [74]. It has been experimentally proven that the levels of 3-methylglutaryl CoA reductase and cholesterol/phospholipids ratio have considerably decreased in colon cancer of rat after treatment with cumin. Cumin also inhibited the activities of 3-methylcholanthrene-induced uterine cervix tumorigenesis, stomach tumorigenesis induced by benzopyrene, and 3-methyle-4-dimethyaminoazobenzene-induced hepatomas [75].

21.6.4 Antidiabetic activity

Cumin showed hypoglycemic effect in rabbit causing substantial reduction in the glucose tolerance curve of hyperglycemic peak. The bioactive component of cumin such as cuminaldehyde inhibited alpha glucosidase and aldose reductase isolated from rat [76]. It was proved to encounter hyperlipidemia in alloxan-induced diabetic rats; the oral administration of cumin decreased the plasma and tissue cholesterol, free fatty acids and triglycerides, and phospholipids. Cumin also decreased the alkaline phosphatase, aspartate transaminase, and γ-glutamyl transferase activities and reduced the tissue levels of triglyceride, cholesterol, and phospholipids [77].

21.6.5 Immunomodulatory activity

The oral administration of cumin induced the Th1 cytokines expression and T cells (CD4, CD8) in normal cells and also in the cyclosporine-induced immune suppressed cells. Cumin also reduced the corticosterone levels, and blocks the activity of T lymphocytes [78].

21.6.6 Antiosteoporotic/estrogenic activity

Cumin has shown the antiosteoporotic effect. The active component present in cumin such as phytoestrogens helps to decrease the accumulation of calcium, urinary calcium excretion, and increase the mechanical strength of bones [79].

21.6.7 Central nervous system

Cumin seed oil has shown the potential to decrease the rate of impulsive activity induced by pentylenetetrazol and maximal electroshock in mice [80]. Experimental study of the concentration of cumin seed oil in a time-dependent manner revealed the activity of cumin seeds (cuminaldehyde) to inhibit the tyrosinase. This inhibited the oxidation of I-3,5- dihydroxyphenylalanine activity [81].

21.6.8 Bioavailability enhancer

Cumin seeds have been used to develop rifampicin rate in rat plasma by improving the concentration and area of rifampicin by 35% and 53%, respectively [82]. It has been found that the bioactive flavonoid components such as 7-*O*-β-galacturonide, glycoside 3,5-dihydroflavone, and 4-*O*-β-D-glucopyranoside are the main precursors of this mechanism [83].

21.7 Pharmacological activities of fennel

The pharmacological activities of fennel are described below.

21.7.1 Antibacterial activity

Fennel has shown activity against many bacterial, mycobacterial, and fungal infective diseases [84]. Fennel contains compounds like 1,3-benzenediol, linoleic acid, undecanal, undecadienal, and oleic acid, which trigger the antibacterial activity against several pathogenic bacteria [40]. Fennel seeds contain 5-hydroxy-furanocoumarin which has a significant role against microorganisms and also shows potential antibacterial activity. Aqueous extract of fennel seeds plays a significant role against *Escherichia coli, Enterococcus faecalis, Salmonella typhi, Staphylococcus aureus, Pseudomonas aeruginosa, Shigella flexneri*, *and Salmonella typhimurium* [85, 86]. Several experimental studies have revealed that aqueous and alcoholic extracts of fennel seeds show MIC in the range of 20–80 mg/mL and 5–15 mg/mL, respectively [87]. The potential activity of fennel plant represented very broad range of pathogens such as *E. coli, S. typhimurium*, and *S. aureus* in food [88]. Fennel seeds also show strong activity against *Campylobacter jejuni, Acinetobacter baumannii*, and *Helicobacter pylori* strains. The experimental results proved that the fennel seed extract can be used to treat several pathogenic bacteria [89].

21.7.2 Antifungal activity

Fennel seed extract showed significant antifungal activity against several fungal species such as *Aspergillus* sp., dermatophytes, and *Candida albicans* [90]. Several experimental studies of the fennel showed substantial antifungal activity against

Fusarium oxysporum and *Aspergillus niger* in food waste [91]. The MIC of fennel seeds against *F. oxysporum* and *A. niger* was shown to be 250 and 750 μg per mL, respectively [92]. The phenyl propanoid which is an active derivative of fennel stack showed antimicrobial activity against *Aladosporium cladosporioides, A. niger*, and *Bacillus subtilis*. Another experiment proved that the fennel has antifungal activity against *Sclerotinia sclerotiorum* [93]. On the other hand, it has been demonstrated that nitric oxide production has significantly improved in peritoneal macrophages after administration of fennel seed extract at a concentration of 10 mg/mL. Toxicity study also demonstrated that treatment of fennel at concentrations of 10–20 mg/mL with macrophages showed antifungal effects more than the control group. Studies demonstrated that the anethole possesses the strongest antifungal activity among other chemical precursors in the fennel plant extracts [94].

21.7.3 Antioxidant activity

Fennel is well known as an excellent source of antioxidants. Fennel plant contains high amount of flavonoids and polyphenol which can reduce free radicals in a broad range. Rosmarinic acid, quercetin 3-*O*-galactoside, eriodictyol-7-orutinoside, kaempferol-3-*O*-glucoside, and caffeoylquinic acid are the active phenolic compounds present in fennel which play the major role in antioxidant activity [95]. Volatile oil of fennel has also strong antioxidant activity over several free radicals. It was shown that the aqueous extract and methanol extract of fennel seeds could reduce free radicals and provide primary antioxidant activity [96]. The antioxidant activity of fennel seeds (aqueous and ethanol extracts) was determined using different types of chemical methods such as hydrogen peroxide scavenging, metal chelating activity, DPPH free radical scavenging, and superoxide anion radical scavenging. Antioxidant activities of aqueous and ethanol extracts of fennel seeds were compared to standard antioxidant component such as alpha-tocopherol and butylated hydroxyanisole (BHT) [97]. It was proved that the fennel seed extracts could be a prospective source of natural antioxidants for clinical trials. The antioxidant activity of the aqueous extract and methanol extract of fennel seeds exhibited 77% and 90%, respectively, which is higher than the activity of standard antioxidant agent alpha-tocopherol (36.1%) at the same dose [98].

21.7.4 Antiinflammatory activity

Fennel fruits show inhibitory effects on acute and subacute inflammatory reaction and type 4 allergic responses. It was shown that fennel seeds reduce the activities of catalase (CAT) and superoxide dismutase (SOD) [99]. Fennel seeds considerably improve the plasma levels of HDL cholesterol. This seed also decrease the rate of malondialdehyde (MDA) to the measure of lipid peroxidation. These experimental studies indicated that the methanol extract of fennel seeds is effective in reducing inflammation [100].

21.7.5 Antianxiety activity

Crude extract of fennel was reported as a potential agent for anxiolytic activity. Fennel contains phytoestrogens which was significant in clinical use for the treatment of estrogen deficiency abnormalities [101, 102]. Estrogens hormones trigger anxiety through the GABA-A receptor molecule. Several experimental studied have revealed that the administration of fennel seeds over an extended time period showed substantial anxiolytic effect. Tamoxifen and picrotoxin (GABA receptor antagonist) present in fennel seeds inhibited anxiolytic effect [103, 104]. Based on several experimental studies it was established that fennel seeds significantly reduce the stress and anxiety.

21.7.6 Gastro-protective activity

It was demonstrated that fennel seeds play an important role in treating gastrointestinal disorders [105, 106]. It was also revealed that the oral administration of fennel oil emulsions has reduced colic in infants by 60%. It was also experimentally shown that the fennel seeds can reduce gastric ulcer as well as mucosal lining of the stomach [107, 108].

21.7.7 Estrogenic activity

Fennel seeds have shown importance as an estrogenic agent since ancient times. It was reported that fennel seeds decrease menstrual pain, induce milk secretion, simplify birth, and increase sexual desire [109]. Fennel seeds contain anatole as an active component which interferes with estrogenic secretion and other hormonal actions. In many research it was recognized that active polymers of anthole such as photoanatole and dianthole are pharmaceutically very significant agents with less side effects than the usual drug [110, 111]. Oral administration of dose-dependent fennel extract has been shown to considerably reduce the contractions rate of prostaglandins and oxytocin induction. On the other hand, mild dose of fennel increases the secretion of the mammary gland but decreases the endometrium, cervix, and oviduct level at a higher dose. Fennel seeds have estrogenic effects and have been used to treat infertile women from a long time [112].

21.7.8 Antidiabetic activity

In a study it was revealed that the aqueous extracts of fennel seeds have effects such as reducing blood sugar as well as demonstrating antidiabetic activities [113]. Several clinical trials have shown that a regular consumption of fennel seeds could be beneficial to reduce the blood glucose level in diabetic patients [114]. Also regular consumption of fennel seeds has shown noticeable activity in decreasing chronic symptoms associated with diabetes [115].

21.7.9 Anticancer activity

Fennel seeds have demonstrated anticancer activity on several clinical trials. It was found that TNF-α-dependent reactions are directly involved in cancer and inflammation. It was found that fennel seeds contain anethol which induces TNF-α through transcription factor named NF-KB [116]. The experimental data proved that anethole plays a principal role in suppressing cancer by reducing cellular responses induced by cytokines. It also indicated that the fennel seeds inhibit prostate tumor xenograft due to its antiangiogenic mechanisms [117]. Several experiments have proven that methanol extracts of fennel seeds had significant effects on cytotoxic and antitumor activities in cancer treated mice. It also has been indicated that the methanol extracts of fennel seeds extensively increase the MDA levels and considerably reduce the CAT activity [118]. The experimental data validated that the methanol extracts of fennel seeds possess substantial anticancer activity against liver cancer (Hepg) cells and breast cancer cells (MCF-7) by increasing the antioxidant defense system, by modulating lipid peroxidation, and by exhibiting inhibitory effects on free radicals [119].

21.8 Conclusions

The spices are extremely useful for human health because they contain a number of medicinally active organic compounds. Isolation of these natural products takes time, but follows mostly a green and sustainable approach. A few scientists may argue that the extracts obtained from the spices may not be structurally pure and therefore the cause of bioactivity is not established. But, the benefits of these extracts and the pure components are all have been established by numerous studies. Therefore, the future goal of spice research may take a new dimension so that the production of these agents can be increased.

Acknowledgments

SB is grateful to Dr. Koustav Sinha for his constructive comments and thoughtful suggestion on this review. BKB is thankful to Prince Mohammad Bin Fahd University for providing academic support and encouragement.

Conflict of interest

The authors confirm that this paper's content has no conflict of interests.

References

[1] M. Ekor, The growing use of herbal medicines: issues relating to adverse reactions and challenges in monitoring safety, Front. Pharmacol. 4 (2013) 177.
[2] K. Platel, K. Srinivasan, Studies on the influence of dietary spices on food transit time in experimental rats, Nutr. Res. 21 (2001) 1309–1314.

[3] S. Basu, H.S. Samanta, J. Ganguly, Green synthesis and swelling behavior of Ag-nanocomposite semi-IPN hydrogels & its drug delivery using *Dolichos biflorus* Linn, Soft Mater. 16 (1) (2018) 7–19, https://doi.org/10.1080/1539445X.2017.1368559.
[4] S. Basu, P. Maji, J. Ganguly, Biosynthesis, characterization and antimicrobial activity of silver and gold nanoparticles by *Dolichos biflorus Linn* seed extract, J. Exp. Nanosci. 11 (8) (2016) 660–668, https://doi.org/10.1080/17458080.2015.1112042.
[5] S. Basu, P. Maji, J. Gangul, Rapid green synthesis of silver nanoparticles by aqueous extract of seeds of Nyctanthes arbor-tristis. J. Appl. Nanosci. 6 (2016) 1, https://doi.org/10.1007/s13204-015-0407-9.
[6] S. Basu, B.K. Banik, Versatile natural products as antioxidants, Contemp. Chem. 1 (2017) 001–003.
[7] G.J. Kaur, D.S. Arora, Antibacterial and phytochemical screening of Anethum graveolens, Foeniculum vulgare and *Trachyspermum ammi*, BMC Complement. Altern. Med. 9 (2009) 30.
[8] D.R.L. Caccioni, M. Guizzardi, D.M. Biondi, A. Renda, G. Ruberto, Relationship between volatile components of citrus fruit essential oils and antimicrobial action on *Penicillium digitatum* and *Penicillium italicum*, Int. J. Food Microbiol. 43 (1998) 73–79.
[9] M. Bajpai, A. Pande, S.K. Tewari, D. Prakash, Phenolic contents and antioxidant activity of some food and medicinal plants, Int. J. Food Sci. Nutr. 56 (4) (2005) 287–291.
[10] P. Khajehdehi, Turmeric: reemerging of a neglected Asian traditional remedy, J. Nephropathol. 1 (1) (2012) 17–22.
[11] L.D. Kapoor, Handbook of Ayurvedic Medicinal Plants, CRC Press, Boca Raton, 1990, p. 172.
[12] K.S. Bhat, K. Vivek, Biocidal potential of clove oils against Aede albopictus—a comparative study, Afr. J. Biotechnol. 8 (24) (2009) 6933–6937. 15.
[13] A. Szallasi, Piperine: researchers discover new flavor in an ancient spice, Trends Pharmacol. Sci. 26 (9) (2005) 437–439.
[14] D.S. Fabricant, N.R. Farnsworth, The value of plants used in traditional medicine for drug discovery, Environ. Health Perspect. 109 (1) (2001) 69–75.
[15] D.J. Newman, G.M. Cragg, Natural products as sources of new drugs over the 30 years from 1981 to 2010, J. Nat. Prod. 75 (2012) 311–335.
[16] B. Prakash, P. Singh, A. Kedia, N.K. Dubey, Assessment of some essential oils as food preservatives based on antifungal, antiaflatoxin, antioxidant activities and in vivo efficacy in food system, Food Res. Int. 49 (2012) 201–208.
[17] M. Getasetegn, Y. Tefera, Biological activities and valuable compounds from five medicinal plants, Nat. Prod. Chem. Res. 4 (2016) 220, https://doi.org/10.4172/2329-6836.1000220.
[18] S. Demissew, N. Asfaw, Aframomum corrorima (Braun) Jansen, in: Aromatic Plants of Ethiopia, Shama Books, Addis Ababa, 2009, pp. 178–180.
[19] C.A. Rice-Evans, N.J. Miller, G. Paganga, Structure-antioxidant activity relationships of flavonoids and phenolic acids, Free Radic. Biol. Med. 20 (1996) 933–956.
[20] J. Seidemann, World Spice Plants, Springer, 2005, pp. 115–253.
[21] L. Jirovetz, G. Buchbauer, A.S. Stoyanova, E.V. Georgiev, S.T. Damianova, Composition, quality control and antimicrobial activity of the essential oil of cumin (Cuminum cyminum L.) seeds from Bulgaria that had been stored for up to 36 years, Int. J. Food Sci. Technol. 40 (2005) 305–310.
[22] S. Basu, J. Ganguly, A comparative bioefficacy of aqueous and methanolic extract of *Trachyspermum ammi* towards the antioxidant potentiality and electrochemical

behaviour, Asian J. Org. Med. Chem. 1 (2016) 17–21, https://doi.org/10.14233/ajomc.2016.AJOMC-P9.
[23] G. Singh, S. Maurya, C. Catalan, M.P. de Lampasona, Chemical constituents, antifungal and antioxidative effects of ajwain essential oil and its acetone extract, J. Agric. Food Chem. 52 (2004) 3292–3296.
[24] J. Minija, J.E. Thoppil, Essential oil composition of *Trachyspermum ammi* (L.) sprague from South India, Indian J. Pharm. Sci. 64 (2002) 250–251.
[25] A. Najda, J. Dyduch, N. Brzozowski, Flavonoid content and antioxidant activity of caraway roots (Carum carvi L.), Veg. Crop. Res. Bull. 68 (1) (2008) 127–133.
[26] M. Razzaghi-Abyaneh, M. Shams-Ghahfarokhi, M.B. Rezaee, K. Jaimand, S. Alinezhad, R. Saberi, Chemical composition and anti-aflatoxigenic activity of Carum carvi L., Thymus vulgaris and Citrus aurantifolia essential oils, Food Control 20 (11) (2009) 1018–1024.
[27] M. El-Kani, G. Fereshteh, M. Mehdi, R. Soosan, Extraction of volatile oil from cumin (Cuminum cyminum L.) with superheated water, J. Food Process. Eng. 30 (2) (2007) 255–266.
[28] S. Derakhshan, M. Sattari, M. Bigdeli, Effect of subinhibitory concentrations of cumin (Cuminum cyminum L.) seed essential oil and alcoholic extract on the morphology, capsule expression and urease activity of Klebsiella pneumoniae, Int. J. Antimicrob. Agents 32 (2008) 432–436.
[29] B. Muckensturm, D. Foechterlen, J.P. Reduron, P. Danton, M. Hildenbrand, Phytochemical and chemotaxonomic studies of *Foeniculum vulgare*, Biochem. Syst. Ecol. 25 (4) (1997) 353–358.
[30] A. Dua, G. Garg, R. Mahajan, Polyphenols, flavonoids and antimicrobial properties of methanolic extract of fennel (*Foeniculum vulgare* Miller), Eur. J. Exp. Biol. 3 (4) (2013) 203–208.
[31] H. Ozbek, S. Uğraş, H. Dülger, et al., Hepatoprotective effect of *Foeniculum vulgare* essential oil, Fitoterapia 74 (3) (2003) 317–319.
[32] N.A. El-Soud, N. El-Laithy, G. El-Saeed, et al., Antidiabetic activities of *Foeniculum vulgare* mill. Essential oil in streptozotocin-induced diabetic rats. Macedonian, J. Med. Sci. 4 (2) (2011) 139–146.
[33] I.E. Orhan, B. Özçelik, M. Kartal, Y. Kan, Antimicrobial and antiviral effects of essential oils from selected Umbelliferae and Labiatae plants and individual essential oil components, Turk. J. Biol. 36 (3) (2012) 239–246.
[34] S. Basu, M. Ghosh, R.K. Bhunia, J. Ganguly, B.K. Banik, Polysaccharides from Dolichos biflorus Linn and Trachyspermum ammi Linn seeds: isolation, characterization and remarkable antimicrobial activity, Chem. Cent. J. 11 (1) (2017) 118, https://doi.org/10.1186/s13065-017-0349-2.
[35] D.B. Singh, S.P. Singh, R.C. Gupta, Antifungal effect of volatiles from seeds of some Umbelliferae, Trans. Br. Mycol. Soc. 73 (1979) 349–350.
[36] P.J. Christie, K. Atmakuri, V. Krishnamoorthy, S. Jakubowski, E. Cascales, Biogenesis, architecture and function of bacterial Type IV secretion systems, Annu. Rev. Microbiol. 59 (2005) 451–485.
[37] H. Fadel, F. Marx, A. El-Sawy, A. El-Ghorab, Effect of extraction techniques on the chemical composition and antioxidant activity of Eucalyptus camaldulensis var. brevirostris leaf oils, Z. Lebensm. Unters. Forsch. 208 (1999) 212–216.
[38] R. Li, Z.T. Jiang, Chemical composition of the essential oil of Cuminum cyminum L. from China, Flavour Fragr. J. 19 (2004) 311–313.

[39] M. Gallo, R. Ferracane, G. Giulia, A. Ritieni, V. Fagliano, Microwave assisted extraction of phenolic compounds from four different spices, Molecules 15 (3) (2010) 6366–6374.
[40] M.H.H. Roby, M.A. Sarhan, K.A. Selim, K.I. Khalel, Antioxidant and antimicrobial activities of essential oil and extracts of fennel (*Foeniculum vulgare* L.) and chamomile (*Matricaria chamomilla* L.), Ind. Crop. Prod. 44 (2013) 437–445.
[41] M. Faudale, F. Viladomat, J. Bastida, F. Poli, C. Codina, Antioxidant activity and phenolic composition of wild, edible, and medicinal fennel from different Mediterranean countries, J. Agric. Food Chem. 56 (6) (2008) 1912–1920.
[42] I. Parejo, O. Jauregui, F. Sánchez-Rabaneda, F. Viladomat, J. Bastida, C. Codina, Separation and characterization of phenolic compounds in fennel (*Foeniculum vulgare*) using liquid chromatography-negative electrospray ionization tandem mass spectrometry, J. Agric. Food Chem. 52 (12) (2004) 3679–3687.
[43] M.T.M. Ghanem, H.M.A. Radwan, E.M. Mahdy, Y.M. Elkholy, H.D. Hassanein, A. A. Shahat, Phenolic compounds from *Foeniculum vulgare* (Subsp. *Piperitum*) (Apiaceae) herb and evaluation of hepatoprotective antioxidant activity, Pharm. Res. 4 (2) (2012) 104–108.
[44] A.P. Saxena, K.M. Vyas, Antimicrobial activity of seeds of some ethno-medicinal plants, J. Econ. Taxon. Bot. 8 (1986) 291–299.
[45] S. Basu, S. Mandal, T. Maiti, J. Ganguly, In-vivo anti-inflammatory effect of purified aqueous and methanol extract of *Trachyspermum ammi* (Linn.) and *Dolichos biflorus* Linn on albino rats, Asian J. Org. Mater. Chem. (2017), https://doi.org/10.14233/ajomc.2017.AJOMC-P82.
[46] N. Mathew, S. Misra-Bhattacharya, V. Perumal, K. Muthuswamy, Antifilarial lead molecules isolated from *Trachyspermum ammi*, Molecules 13 (2008) 2156–2168.
[47] S.K. Ahsan, M. Tariq, A.M. Ageel, M.A. Al-Yahya, A.H. Shah, Studies on some herbal drugs used in fracture healing, Int. J. Crude Drug Res. 27 (1989) 235–239.
[48] M.H. Boskabady, S. Kiani, P. Jandaghi, L. Hasanzadeh, Antitussive effect of *Carum copticum* in guinea pigs, J. Ethnopharmacol. 97 (2005) 79–82.
[49] A. Jabbar, Z. Iqbal, M.N. Khan, *In vitro* anthelmintic activity of *Trachyspermum ammi* seeds, Pharmacogn. Mag. 2 (2006) 126–129.
[50] A.H. Gilani, Q. Jabeen, M.N. Ghayur, K.H. Janbaz, M.S. Akhtar, Studies on the antihypertensive, antispasmodic, bronchodilator and hepatoprotective activities of the *Carum copticum* seed extract, J. Ethnopharmacol. 98 (2005) 127–135.
[51] K.C. Srivastava, Extract of a spice-Omum (*Trachyspermum ammi*)-shows antiaggregatory effects and alters arachidonic acid metabolism in human platelets, Prostaglandins Leukot. Essent. Fatty Acids 33 (1988) 1–6.
[52] K.R. Panel, V. Anilakumar, F.M. Saritha, A.S. Bawa, Ameliorative effect of ajwain extract on hexachlorocyclohexane-induced lipid peroxidation in rat liver, Food Chem. Toxicol. 47 (2) (2009) 279–282.
[53] J.A. Hawrelak, T. Cattley, S.P. Myers, Essential oils in the treatment of intestinal dysbiosis: a preliminary *in vitro* study, Altern. Med. Rev. 14 (2009) 380–384.
[54] C.M. Priestley, E.M. Williamson, K.A. Wafford, D.B. Sattelle, Thymol, a constituent of thyme essential oil, is a positive allosteric modulator of human $GABA_A$ receptors and a homo-oligomeric GABA receptor from *Drosophila melanogaster*, Br. J. Pharmacol. 140 (2003) 1363–1372.
[55] I.M. Javed, T. Akhtar, M.Z. Khaliq, G. Khan, M. Muhammad, Antihyperlipidaemic effect of *Trachyspermum ammi* (Ajwain) in rabbits, in: Proceedings of the 33rd All Pakistan Science Conference, December 25–28, 2002, pp. 80–81.

[56] I.K. Park, J. Kim, S.G. Lee, S.C. Shin, Nematicidal activity of plant essential oils and components from ajowan (*Trachyspermum ammi*), allspice (*Pimenta dioica*) and litsea (*Litsea cubeba*) essential oils against pine wood nematode (*Bursaphelenchus xylophilus*), J. Nematol. 39 (2007) 275–279.
[57] J.O. Kong, S.M. Lee, Y.S. Moon, S.G. Lee, Y.J. Ahn, Nematicidal activity of plant essential oils against *Bursaphelenchus xylophilus* (Nematoda: Aphelenchoididae), J. Asia Pac. Entomol. 9 (2006) 173–178.
[58] C. Hanif, T. Ayesha, S. Adila, M. Saeed, A. Tanveer, M. Ashfaq, Physico-chemical investigation and antimicrobial activity of essential oil of Cuminum cyminum L, World Appl. Sci. J. 19 (3) (2012) 330–333.
[59] M. De, A.K. De, R. Mukhopadhvay, A.B. Banerjee, M. Micro, Antimicrobial activity of Cuminum cyminum L, Ars Pharmaceutica 44 (2003) 257–269.
[60] M.L. De, F.V. De, F. Fratianni, F. Nazzaro, Chemistry, antioxidant, antibacterial and antifungal activities of volatile oils and their components, Nat. Prod. Commun. 4 (2009) 1741.
[61] S. Derakhshan, M. Sattari, M. Bigdeli, Effect of cumin (Cuminum cyminum L.) seed essential oil on biofilm formation and plasmid integrity by Klebsiella pneumoniae, Pharmacog. Mag. 6 (2010) 57–61.
[62] S. Shayegh, I. Rasooli, M. Taghizadeh, S.D. Astaneh, Phytotherapeutic inhibition of supragingival dental plaque, Nat. Prod. Res. 22 (2008) 428–439.
[63] H. Hajlaoui, H. Mighri, E. Noumi, M. Snoussi, N. Trabelsi, R. Ksouri, Chemical composition and biological activities of Tunisian Cuminum cyminum L. essential oil: a high effectiveness against Vibrio spp. strains, Food Chem. Toxicol. 48 (2010) 2186–2192.
[64] N. Boyraz, M. Ozcan, Antifungal effect of some spice hydrosols, Fitoterapia 76 (2005) 661–665.
[65] R.S. Farag, Z.Y. Daw, S.H. Abo-Raya, Influence of some spice essential oils on Aspergillus parasiticus growth and production of aflatoxins in a synthetic medium, J. Food Sci. 54 (1989) 74–76.
[66] R.S. Farag, Z.Y. Daw, F.M. Hewedi, G.S. El Baroty, Antimicrobial activity of some Egyptian spice essential oils, J. Food Prot. 52 (1989) 665–667.
[67] A.A.I. Hammad, B.M. Youssef, Growth inhibition of some pharmacological molds by garlic and cumin essential oils, Egypt J. Microbiol. 29 (1995) 115–120.
[68] M. Razzaghi-Abyaneh, M. Shams-Ghahfarokhi, M.B. Rezaee, K. Jimand, S. Alinezahad, R. Saberi, Chemical composition and antiaflatoxigenic activity of Carum carvi L, Thymus vulgaris and Citrus aurantifolia essential oils, Food Control 20 (2009) 1018–1024.
[69] C. Romagnoli, E. Andreotti, S. Maietti, R. Mahendra, D. Mares, Antifungal activity of essential oil from fruits of Indian Cuminum cyminum, Pharm. Biol. 48 (2010) 834–848.
[70] M.M. Skrinjar, A.I. Mandi, A.C. Misan, M.B. Sakac, L.C. Saric, M.M. Zec, Effect of mint (Mentha piperita L.) and Caraway (Carum carvi L.) on the growth of some toxicogenic Aspergillus species and aflatoxin B1 production, Proc. Nat. Sci. Matica Srpska. Novi. Sad. (116) (2009) 131–139.
[71] I. Samojlik, N. Lakic, N. Mimica-Dukic, K. Dakovic-Svajcer, B. Bozin, Antioxidant and hepatoprotective potential of essential oils of coriander (Coriandrum sativum L.) and caraway (Carum carvi L.) (Apiaceae), J. Agric. Food Chem. 58 (2010) 8848–8853.
[72] G. Ruberto, M.T. Baratta, Antioxidant activity of selected essential oil components in two lipid model systems, Food Chem. 69 (2000) 167–174.
[73] V. Rodov, Y. Vinokur, N. Gogia, I. Chkhikvishvili, Hydrophilic and lipophilic antioxidant capacities of Georgian spices for meat and their possible health implications, Georgian Med. News 179 (2010) 61–66.

[74] N. Nalini, K. Sabitha, P. Vishwanathan, V.P. Menon, Influence of spices on the bacterial (enzyme) activity in experimental colon cancer, J. Ethnopharmacol. 62 (1998) 15–24.
[75] N. Nalini, V. Manju, V.P. Menon, Effect of spices on lipid metabolism in 1,2-dimethylhydrazine-induced rat colon carcinogenesis, J. Med. Food 9 (2006) 237–245.
[76] R. Roman-Ramos, J.L. Flores-Saenz, F.J. Alarcon-Aguilar, Antihyperglycemic effect of some edible plants, J. Ethnopharmacol. 48 (1995) 25–32.
[77] H.S. Lee, Cuminaldehyde: aldose reductase and alpha glucosidase inhibitor derived from Cuminum cyminum L. seeds, J. Agric. Food Chem. 53 (2005) 2446–2453.
[78] P.S. Chauhan, N.K. Satti, K.A. Suri, M. Amina, S. Bani, Stimulatory effects of Cuminum cyminum and flavonoid glycoside on cyclosporine-A and restraint stress induced immune-suppression in swiss albino mice, Chem. Biol. Interact. 185 (2010) 66–72.
[79] T. Malini, G. Vanithakumari, Estrogenic activity of Cuminum cyminum in rats, Indian J. Exp. Biol. 25 (1987) 442–444.
[80] I. Kubo, I. Kinst-Hori, Tyrosinase inhibitors from cumin, J. Agric. Food Chem. 46 (1998) 5338–5341.
[81] M. Sayyah, A. Mahboubi, M. Kamalinejad, Anti-convulsant effect of the fruit essential oil of Cuminum cyminum in mice, Pharm. Biol. 40 (2002) 478–480.
[82] B.S. Sachin, S.C. Sharma, S. Sethi, S.A. Tasduq, M.K. Tikoo, A.K. Tikoo, Herbal modulation of drug bioavailability: enhancement of rifampicin levels in plasma by herbal products and a flavonoid glycoside derived from Cuminum cyminum, Phytother. Res. 21 (2007) 157–163.
[83] B.S. Sachin, P. Monica, S.C. Sharma, N.K. Satti, M.K. Tikoo, A.K. Tikoo, Pharmacokinetic interaction of some antitubercular drugs with caraway: implications in the enhancement of drug bioavailability, Hum. Exp. Toxicol. 28 (2009) 175–184.
[84] R. Manonmani, V.M. Abdul Khadir, Antibacterial screening on *Foeniculum vulgare* Mill, Int. J. Pharm. Bio Sci. 2 (4) (2011) 390–394.
[85] M.M. Özcan, J. Chalchat, D. Arslan, A. Ateş, A. Ünver, Comparative essential oil composition and antifungal effect of bitter fennel (*Foeniculum vulgare* ssp. *piperitum*) fruit oils obtained during different vegetation, J. Med. Food 9 (4) (2006) 552–561.
[86] M.R. Martins, M.T. Tinoco, A.S. Almeida, J. Cruz-Morais, Chemical composition, antioxidant and antimicrobial properties of three essential oils from Portuguese flora, J. Pharmacogn. 3 (3) (2012) 39–44.
[87] S.H. Park, I. Seong, Antifungal effects of the extracts and essential oils from *Foeniculum vulgare* and *Illicium verum* against *Candida albicans*, Korean J. Med. Mycol. 15 (4) (2010) 157–164.
[88] F. Anwar, M. Ali, A.I. Hussain, M. Shahid, Antioxidant and antimicrobial activities of essential oil and extracts of fennel (*Foeniculum vulgare* Mill.) seeds from Pakistan, Flavour Fragr. J. 24 (4) (2009) 170–176.
[89] N. Thakur, N. Sareen, B. Shama, K. Jagota, Studies on *in vitro* antifungal activity of *Foeniculum vulgare* Mill. against spoilage fungi, Global J. Bio Sci. Biotechnol. 2 (3) (2013) 427–430.
[90] N. Mimica-Dukić, S. Kujundžić, M. Soković, M. Couladis, Essential oils composition and antifungal activity of F. vulgare Mill. obtained by different distillation conditions, Phytother. Res. 17 (4) (2003) 368–371.
[91] G. Singh, S. Maurya, L.M.P. De, C. Catalan, Chemical constituents, antifungal and antioxidative potential of *F. vulgare* volatile oil and its acetone extract, Food Control 17 (9) (2006) 745–752.

[92] Y.S. Kwon, W.G. Choi, W.J. Kim, W.K. Kim, M.J. Kim, W.H. Kang, et al., Antimicrobial constituents of Foeniculum vulgare, Arch. Pharm. Res. 25 (2) (2002) 154–157.
[93] S. Soylu, H. Yigitbas, E. Soylu, Ş. Kurt, Antifungal effects of essential oils from oregano and fennel on Sclerotinia sclerotiorum, J. Appl. Microbiol. 103 (4) (2007) 1021–1030.
[94] A. Naeini, M. Naseri, M. Kamalinejad, F. Khoshzaban, T. Rajabian, H. Nami, et al., Study on anti-candida effects of essential oil and extracts of Iranian medicinal plants, in vitro, J. Med. Plants 2 (38) (2011) 163–172.
[95] A. Scalbert, C. Manach, C. Morand, C. Remesy, Dietary of polyphenols and the prevention of diseases, Rev. Food Sci. Nutr. 45 (4) (2005) 287–306.
[96] A.A. Shahat, A.Y. Ibrahim, S.F. Hendawy, et al., Chemical composition, antimicrobial and antioxidant activities of essential oils from organically cultivated fennel cultivars, Molecules 16 (2) (2011) 1366–1377.
[97] M.C. Díaz-Maroto, I.J. Díaz-Maroto Hidalgo, E. Sánchez-Palomo, M.S. Pérez-Coello, Volatile components and key odorants of fennel (*Foeniculum vulgare* Mill.) and thyme (*Thymus vulgaris* L.) oil extracts obtained by simultaneous distillation-extraction and supercritical fluid extraction, J. Agric. Food Chem. 53 (13) (2005) 5385–5389.
[98] M. Oktay, İ. Gülçin, Ö.İ. Küfrevioğlu, Determination of in vitro antioxidant activity of fennel (Foeniculum vulgare) seed extracts, LWT- Food Sci. Technol. 36 (2) (2003) 263–271.
[99] E. Choi, J. Hwang, Antiinflammatory, analgesic and antioxidant activities of the fruit of *Foeniculum vulgare*, Fitoterapia 75 (6) (2004) 557–565.
[100] H. Kataoka, S. Horiyama, M. Yamaki, et al., Anti-inflammatory and anti-allergic activities of hydroxylamine and related compounds, Biol. Pharm. Bull. 25 (11) (2002) 1436–1441.
[101] S. Pourabbas, M. Kesmati, A. Rasekh, Study of the anxiolytic effects of fennel and possible roles of both gabaergic system and estrogen receptors in these effects in adult female rat, Physiol. Pharmacol. 15 (1) (2011) 134–143.
[102] M. Mesfin, K. Asres, W. Shibeshi, Evaluation of anxiolytic activity of the essential oil of the aerial part of Foeniculum vulgare Miller in mice, BMC Complement. Altern. Med. 14 (1) (2014) 310.
[103] S. Koppula, H. Kumar, Foeniculum vulgare Mill (Umbelliferae) attenuates stress and improves memory in Wister rats, Trop. J. Pharm. Res. 12 (4) (2013) 553–558.
[104] P. Padma, R.L. Khosa, Anti-stress agents from natural origin, J. Nat. Remedies 2 (1) (2002) 21–27.
[105] F.M. Birdane, M. Cemek, Y.O. Birdane, I. Gülçin, E. Büyükokuroğlu, Beneficial effects of vulgare ethanol-induced acute gastric mucosal injury in rat, World J. Gastroenterol. 13 (4) (2007) 607–611.
[106] I. Chakŭrski, M. Matev, A. Koĭchev, I. Angelova, G. Stefanov, Treatment of chronic colitis with an herbal combination of Taraxacum officinale, Hipericum perforatum, Melissa officinaliss, Calendula officinalis and Foeniculum vulgare, Vutr. Boles. 20 (6) (1980) 51–54.
[107] I. Alexandrovich, O. Rakovitskaya, E. Kolmo, T. Sidorova, S. Shushunov, The effect of fennel (Foeniculum vulgare) seed oil emulsion in infantile colic: a randomized, placebo-controlled study, Altern. Ther. Health Med. 9 (4) (2003) 58–61.
[108] I. Al-Mofleh, M. Al-Sobaihani, S. Alqasoumi, M. Al-Said, M. Al-Dosari, M. Al-Yahya, et al., Fennel "Foeniculum vulgare" treatment protects the gastric mucosa of rats against chemically-induced histological lesions, Int. J. Pharm. 9 (3) (2013) 182.

[109] S. Ostad, M. Soodi, M. Shariffzadeh, N. Khorshidi, H. Marzban, The effect of fennel essential oil on uterine contraction as a model for dysmenorrhea, pharmacology and toxicology study, J. Ethnopharmacol. 76 (3) (2001) 299–304.
[110] T. Malini, G. Vanithakumari, D. Nmsak, V. Fiango, Effect of Foeniculum vulgare Mill. seed extract on the genital organs of male and female rats, Indian J. Physiol. Pharmacol. 29 (1) (1985) 21–26.
[111] F. Myrseyed, A. Shiravi, M. Nasr-Abadi, The effect of intraperitoneal injection of alcoholic extract Foeniculum vulgare seed on gonadotropic and testosterone hormones in male Wistar rats, J. Anim. Sci. 1 (1) (2008) 49–56.
[112] G. Mirabolghasemi, F. Alizadeh, The effect of hydroalcoholic extract of fennel (Foeniculum vulgare) seed on serum levels of sexual hormones in female Wistar rats with polycystic ovarian syndrome (PCOS), Arak. Med. Univ. J. 17 (5) (2014) 70–78.
[113] K. Sushruta, S. Satyanarayana, S. Srinivas, J.R. Sekhar, Evaluation of the blood-glucose reducing effects of aqueous extracts of the selected umbelliferous fruits used in culinary practices, Trop. J. Pharm. Res. 5 (2) (2007) 613–617.
[114] N. El-Soud, N. El-Laithy, G. El-Saeed, M. Wahby, M. Khalil, F. Morsy, et al., Antidiabetic activities of Foeniculum vulgare Mill. essential oil in streptozotocin-induced diabetic rats, Maced J. Med. Sci. 4 (2) (2011) 139–146.
[115] V. Dongare, A. Arvindekar, C. Magadum, Hypoglycemic effect of Foeniculum vulgare Mill. fruit on dexamethasone induced insulin resistance rats, Res. J. Pharmacogn. Phytochem. 2 (2) (2010) 163–165.
[116] C. Garga, S. Khan, S. Ansari, A. Suman, M. Garg, Chemical composition, therapeutic potential and perspectives of Foeniculum vulgare, Pharmacogn. Rev. 3 (6) (2009) 346–352.
[117] A. Bogucka-Kocka, H. Smolarz, J. Kocki, Apoptotic activities of ethanol extracts from some Apiaceae on human leukaemia cell lines, Fitoterapia 79 (7) (2008) 487–497.
[118] M. Pradhan, S. Sribhuwaneswari, D. Karthikeyan, et al., In-vitro cytoprotection activity of *Foeniculum vulgare* and *Helicteres isora* in cultured human blood lymphocytes and antitumour activity against B16F10 melanoma cell line, Res. J. Pharm. Technol. 1 (4) (2008) 450–452.
[119] M.M. Al-Harbi, S. Qureshi, M. Raza, M.M. Ahmed, A.B. Giangreco, A.H. Shah, Influence of anethole treatment on the tumour induced by Ehrlich ascites carcinoma cells in paw of Swiss albino mice, Eur. J. Cancer Prev. 4 (4) (1995) 307–318.

Further reading

[120] Y. Qurishi, A. Hamid, M.A. Zargar, S.K. Singh, A.K. Saxena, Potential role of natural molecules in health and disease: importance of boswellic acid, J. Med. Plant Res. 4 (2010) 2778–2785.

Medicinal plants and their compounds with anticancer properties

22

Preetismita Borah[a,*], *Bimal Krishna Banik*[b,*]
[a]CSIR-Central Scientific Instruments Organization, Chandigarh, India, [b]Department of Mathematics and Natural Sciences, College of Sciences and Human Studies, Deanship of Research Development, Prince Mohammad Bin Fahd University, Al Khobar, Kingdom of Saudi Arabia
[*]Corresponding author. e-mail address: preetiboradu@gmail.com; bimalbanik10@gmail.com; bbanik@pmu.edu.sa

22.1 Introduction: Background of medicinal plants

Medicinal plants have been investigated with greatest interest in many countries since herbal medicine is active, less toxic, and safe as compared with the synthetic drug molecules. Globally, herbal medicines have been promoted as a potential source of new and effective drugs. Humans have been using the plants for medicinal benefits for more than a century around the world including in India, Pakistan, and Bangladesh [1]. Based on this and realizing green and sustainable approaches of drug development, it is necessary to study medicinal plants which may become extremely rewarding. Medicinal plant contains immunomodulatory and antioxidant properties and several phytochemicals with diverse anticancer activities [2, 3]. The antioxidant compounds protect the cells from oxidative damage. Although, approximately 1500 anticancer drugs are known while more than 500 are in clinical trials, it is necessary to develop many useful and effective drugs using plants. India is the largest place for medicinal plants and is called the "Botanical garden of the World." More than 8000 species of medicinal plants of 400 families are available in India [4]. But only a few of them with medicinal properties have been identified. According to the World Health Organization (WHO), three-quarters of the world's population use traditional medicine or herbs for the treatment of diseases. Since the last two decades, the use of plants and phytomedicines has increased [5]. Modern drugs (approximately 50%) in clinical therapy have originated from natural products. Many of them have the ability to include apoptosis in various human cancer cells [6]. Currently, cancer is perhaps the most critical diseases to tackle. The most common cancers are lung, stomach, colorectal, liver, blood, prostate, ovary, cervix, pancreas, brain, and breast. It is important to note that all cancers within a particular form are also different in nature and obviously, their treatment become different. Lung cancer is recognized as the most common cancer diagnosed in men and breast cancer in women. In general, it is believed

Green Approaches in Medicinal Chemistry for Sustainable Drug Design. https://doi.org/10.1016/B978-0-12-817592-7.00023-X
© 2020 Elsevier Inc. All rights reserved.

that cancer is incurable, and may start at any age in the body. Perhaps, cancer represents the largest cause of death. A results from the International Agency for Research on Cancer in 2012 found 8.2 million cancer deaths [7]. Many million (17 million) cancer deaths per year is expected by 2030 [8].

Natural products have considerable expectations because of their numerous therapeutic properties [9, 10]. More than 60% of anticancer agents have been isolated from natural sources, including from plants, marine organisms, and microorganisms [11, 12]. These include taxus diterpenes, camptotheca alkaloids, vinca alkaloids, and podophyllum lignans. Currently, 16 new molecules isolated from plants have been tested in clinical trials and among them 13 are in phase I or II and the rest are in phase III trial [13]. The compounds, flavopiridol, derived from the Indian tree *Dysoxylum binectariferum*, and meisoindigo, which is isolated from the Chinese plant *Indigofera tinctoria*, have demonstrated anticancer activity with acceptable profile and bioavailability than the commercial drugs [14].

It is assumed that more than 3000 plants have anticancer properties [15]. The scheme to find anticancer agents from plants was initiated by the US National Cancer institute (NCI) in 1957. NCI program has explored more than 35,000 plant species and found important anticancer drugs like vincristine, vinblastine, taxol, indicine-N-oxide, etoposide analogs, camptothecin, and various other drug candidates [16]. Many of the important and effective drugs derived from higher plants were vinca alkaloids viz Vinblastine and Vincristine drugs derived from *Catharanthus roseus* are used to treat leukemia, bladder, and testicular cancer. Paclitaxol (Taxol TM) originally derived from *Taxus brevifolia* was used in the treatment of ovarian and breast cancers which was assumed to bind the tubulin subunit of microtubules and stabilize the microtubule to normal disassembly [17]. Traditionally plants with known therapeutics potential have long been used to cure several diseases. Potentially curative plants might be particularly significant for their uses as medicinal herbs. Thus the discovery of new drug or drug intermediate from plant source is a better option for medicinal chemist in the present time.

22.2 Value of medicinal plants

Medicinal plants have long been an abundant source of promise for the treatment of cancer, which is a crucial source of major causes of death in this century. However, it is essential to discover new anticancer drugs, drug therapy, and chemotherapy techniques. Worldwide more than 250,000 species of plants are available; among them nearly 3000 plants have shown anticancer properties. Many compounds obtained from the nature have shown pharmaceutical properties and many molecules have been identified by the medicinal chemists. Plants have been used for medical purposes long before prehistoric period. Ancient Unani manuscripts, Egyptian papyrus, and Chinese literature have described the use of herbs. Evidence exist that Unani Hakims, Indian Vaids, and European and Mediterranean cultures were using herbs as medicines for over 4000 years. Indigenous cultures like Egypt, Rome, Africa, Iran, and America recommended herbs in their healing rituals. In many developed traditional medical systems (Unani, Ayurveda, and Chinese Medicine) herbal therapies were shown to be highly attractive and useful.

High population, lack of active drugs, high cost of treatment procedures, several side effects of commercial synthetic medicines, and discovery of resistance to modern/old drugs for infectious diseases have led to great attention on the use of plant compounds as source of medicines for the treatment of a wide range of human medical problems. Among ancient civilizations, India has high repository of medicinal plants. The forest in India is the principal source of numerous medicinal plants. These are collected mainly as raw substances for the discovery of drugs. Ayurveda and Unani medicines are most common and widely cultured in India. Recently, the WHO has discovered that 80% people in the world depend on herbal medicines as a part of their medical care. The WHO has stated that 21,000 plant species have beneficial effects against medical problems. The United States have used plant drugs in much lesser amount (25%) compared to other countries like India and China. For example, India and China have used 80% plant-based medicines or medicinally active raw materials. Medicinal plants like *aloe*, *neem*, *tulsi*, *turmeric*, and *ginger* have several applications for improving the health in human. These plants are also treated as remedies in other countries. Numerous pharmaceutical and ayurvedic practitioners have been using *tulsi* for preparing medicines. Moreover, a few of these plants are considered as important sources of nutrition.

Importance of some herbs with medicinal properties

- As stated above, many herbs like black pepper, cinnamon, myrrh, aloe, sandalwood, ginseng, red clover, burdock, bayberry, and safflower have the abilities to heal infections, wounds, sores, and boils.
- These plants have antibacterial properties. Turmeric is used against germs, cut, wounds, microbes, and bacteria.
- A few antipyretic herbs like *Chirata*, black pepper, sandal wood, and safflower have been used in the treatment of fever.
- Ginger and cloves have the ability to reduce cough because they have expectorant activity. This property promotes the thinning and ejection of mucus from the lungs, trachea, and bronchi. Eucalyptus, cardamom, and cherry have also expectorants properties.
- Chamomile, calamus, ajwain, tulsi, cardamom, fennel, chrysanthemum, peppermint coriander, spearmint, cinnamon, ginger, and turmeric have the abilities to improve blood circulation. Often, they are treated as chest stimulants.

22.3 Medicinal plants with anticancer properties

Plants are the chief source of natural medicine. It has been shown that populations who take natural herbal products have a reduced incidence of various diseases including cancers. For example, Soybean is the major dietary source of saponins that reduce the growth of cancer cells [18]. Some medicinally crucial plants are discussed below.

22.3.1 Solanum nigrum

S. nigrum has numerous medicinal properties such as antimicrobial, antioxidant, anticancer, and antiulcerogenic activities. *S. nigrum* is found to be effective against cancer. Diosgenin present in this plant is responsible for the medicinal activity.

22.3.2 Cynodon dactylon

C. dactylon possess medicinal activities. This has antihelmintic, antidiuretic, antiinflammatory, and hepatoprotective activities. It has been used for diabetes, jaundice disorder, kidney problem, urinary diseases, gastrointestinal disorder, constipation malfunction, and abdominal pain. Interestingly, the entire plant has been used for diuretics, dropsy, and syphilis.

22.3.3 *Tinospora cordifolia*

Giloy is an important ayurvedic herb which acts as tonic, anthelmintic, antiarthritic, antipyretic, blood purifier carminative, digestive, diuretic, expectorant, rejuvenating, appetizing, and antiinflammatory agents. It is believed that giloy can increase the lifespan of humans by preventing numerous chronic diseases. Starch obtained from the roots of giloy has been recommended to use for diarrhea and dysentery. The juice from this herb has medicinal applications in the treatment of chronic fever, gout, vomiting, cardiac problem, skin problem, leprosy, anemia, cough, asthma, jaundice, seminal malfunction, cancer, high cholesterol, has antiaging, and liver protection properties. The principal chemical agents responsible for the medicinal benefits of this plant are tinosporin, perberillin, palmarin, and berberine. The stem barks have giloin, gilonin, gilosterol, and phenolic lignins [19].

22.3.4 *Momordica dioica*

M. dioica is known as spiny gourd, teasel gourd, small bitter gourd, kankro, kartoli, kantola, kantroli, ban karola, or janglee karela. It has many medicinal properties that include antitumorigenic, analgesic, antidiabetic, antiinflammatory, and antiallergic activities. MTT assay was investigated to identify the antiproliferative activity of *M. dioica* against breast and lung carcinoma cell lines. Importantly, the results showed good inhibition of cancer cell growth in these two cell lines [20].

22.3.5 *Barleria grandiflora*

B. grandiflora (Family-Acanthaceae) is used for treating the mouth ulcer. The main constituents of leaf and stem are composed of glycosides (Shanzhiside methyl ester) [21].

22.3.6 Moringa oleifera

M. oleifera is found in Thailand, India, Philippines, and Pakistan. This is used as food and traditional medicine. The leaves have amino acids, vitamins, minerals, and beta-carotene. This plant is used against rheumatism, ascites, infection, hiccough, influenza, internal abscess, hyperglycemia, and dyslipidemia [22].

22.3.7 Cucurbita maxima

C. maxima (pumpkin) is used as vegetable and medicine. *Cassia auriculata* may have wound healing and antioxidant activities. The flower of *Cassia auriculata* is used against rheumatism. This vegetable has antipyretic, hepatoprotective, antidiabetic, antiperoxidative, antihyperglycemic, and microcidal activities [23].

22.3.8 Terminalia chebula

T. chebula is a medicinal herb which is used against many diseases [24] (Table 22.1).

Table 22.1 Medicinal plants with anticancer activity.

Plant name/family	Active constituent
Aegle marmelos Rutaceae	Lupeol [25]
Aglaila sylvestre Meliaceae	Silvesterol
Allium cepa, Allicinalliin, diallyldisulphide	Liliaceae/Alliaceae quarcetin, flavonoids, vitamin C and E [25]
Allium sativum Liliaceae	Alliin, allicin alliin, alliinase, *S*-allylcysteine (SAC), diallyldisulphide
Aloe ferox, Aloe barbadenis	Aloe-emodin, emodin, aloin, Acemannan [26, 27]
Andrographis paniculata, Acanthaceae	Andrographolide [25]
Annona species Annonaceae	Acetogenins [27]
Angelica sinensis Umbelliferae	Polysaccharide fraction "AR-4"
Agapanthus africanus Agapanthaceae	Isoliquiritigenin
Aglaila sylvestre Meliaceae	Silvesterol
Azadirecta indica Meliaceae	Swainsonine [28]
Arctium lappa, Compositae	Potent anticancer factors
Astragalus membranaceus Papilionaceae	Swainsonine
Betula utilis Betulaceae	*Betulin*
Catharanthus roseus Apocynaceae	Vinblastine, Vincristine, Alstonine, Ajmalicine, and Reserpine [11, 29]
Camellia sinensis Theaceae	Epigallocatechin gallate
Chlorella pyrenoidosa Oocystaceae	Lysine
Cleistanthus collinus Euphorbiaceae	Cleistanthin, Collinusin [30]
Colchicum luteum Liliaceae	Colchicines demecolcine [31]
Combretum caffrum Combritaceae	Combretastatin
Corcus sativus Iridaceae	Safranal, Crocetin, Crocin
Curcuma longa Linn. Zinziberaceae	Tumerone, curcumine [32–34]

Continued

Table 22.1 Continued

Plant name/family	Active constituent
Dysoxylum binectariferum Meliaceae	Rohitukine
Echinacea angustifolia Asteraceae	Arabinogalactan
Ginkgo biloba Ginkoaceae	Ginkgolide-B, A, C, and J
Fagopyrum esculentum, Polygonaceae	Amygdalin, Rutin [35]
Glycine max Leguminosae	Zinc, selenium, vitamins, isoflavones, protease inhibitors, saponins and phytosterols [36]
Glycyrrhiza glabra Leguminosae	Glycyrrhizin [37]
Gossypium barbadense Malvaceae	Gossypol
Gyrophora esculenta Umbilicariaceae	Polysaccharides β-glucans, α-glucans
Lentinus edodes Agaricaceae	Lentinan
Linum usitatissimum Linaceae	Cynogenetic glycosides, lignans
Justicia procumbens Acanthaceae	Justicidin A, B
Linum usitatissimum Linaceae	Cynogenetic glycosides, lignans [38, 39]
Mentha species Labiateae	Monoterpene ketones [40, 41]
Nigella sativa linn	Thymoquinone, dithymoquinone [25]
Ranunculaceae, Ocimum sanctum linn, lamiaceae	Eugenol, orientin and vicenin [25]
Panax ginseng Aralaceae	Ginsenosides, panaxosides
Picrorrhizia kurroa Scrophulariaceae	Picrorrhizia (kutki) Picrosides I, II, III and kutkoside [42]
Podophyllum emodii Berberidaceae	Epipodophyllotoxin
Podophyllum hexandrum Berberidaceae	Podophyllin, astragalin [43]
Psoralea corylifolia linn, fabaceae	Bavachinin and psoralen, psoralidin [25]
Rubia cordifolia linn Rubiaceae	Rubidianin, rubiadin, rosemary acids, purpurin, alizarin, xanthopurpurin [25]
Solanum nigrum linn Solanaceae	Solamargine, solasonine, solanin, quercetin
Taxus brevifolia Taxaceae	Taxanes, taxol cepholomannine [44]
Tinospora cordifolia (*willd*)	Berberin, tinosporin, giloin, giloinin
Withania somnifera Solanaceae	Withanolides, *Withaferin* [34, 45–49]
Zingiber officinale Zingiberaceae	Curcumin, gingerenoneA, gingeols, shogaols, zingerone [50, 51]

22.4 Plant-derived anticancer agents in clinical use

In the mid of 1950s, the anticancer activity from medicinal plants has been started and found to develop many agents such as in 1960 NCI has started the plant collection program which is based only on temperate region. This program discovered many novel chemotypes of cytotoxic activities, such as taxanes and camptothecins, but the development of this agent to clinically effective stage took 30 years. In 1986, the development of new screening technologies led to the revival of the collection of medicinal plants. Plant-derived drugs are required for anticancer treatment since they are natural and easily available. They can be readily administered orally as part of patient's dietary intake. [52]

Also, being naturally derived compounds from plants they are generally more tolerated and nontoxic to normal human cells [53]. Also, there are some exceptions such as cyanogenetic glycosides, saponins, lectins, lignans, and some taxanes [53, 54].

However, the compounds isolated from plants are generally tolerable and nontoxic to human cells. As the plant-derived drugs are nontoxic to human cells and show cytotoxicity in cancer cell lines, these drugs are ideal leads for clinical trials for further therapeutic applications. Plant-derived drugs are classified into four categories with the following activities: methyltransferase inhibitor, DNA damage preventive drugs or antioxidants, histone deacetylase inhibitors, and mitotic disruptors [55]. Fig. 22.1 shows some plant-derived anticancer agents in clinical use [11].

Semisynthetic derivatives of natural products, viz, epipodophyllotoxin, etoposide (VM 26), and teniposide (VP 16-213) were used for the treatment of cancers. The Podophyllum species (Podophyllaceae) and *Podophyllum peltatum* Linnaeus obtained from the Indian subcontinent had medicinal use (skin cancers and warts). The podophyllotoxin was first discovered in 1880. But the correct structure was elucidated after many years (1950s). Podophyllotoxin-related lignans were also found in nature. Clinical trials were conducted on some of them. Extensive research identified etoposide and teniposide as clinically effective drugs which are used against lymphomas, bronchial, and testicular malignancies. The most important plant-derived chemotherapeutic agents are the Taxanes. Paclitaxel was obtained from the bark of a tree Pacific Yew, *T. brevifolia* Nutt. Some portions of *T. brevifolia* and other Taxus species were used by several Native American tribes for the treatment of noncancerous disorders. The leaves of *Taxus baccata* were beneficial to Ayurvedic medicine. Paclitaxel and other key medicinally active compounds were isolated from the leaves of Taxus species. Paclitaxel was used in the treatment of diverse cancers including breast, ovarian, and nonsmall cell lung cancer. Docetaxel was effective against breast and lung cancers. Paclitaxel was effective against multiple sclerosis, psoriasis, and rheumatoid arthritis. Importantly, numerous taxanes are in the development stage against deadly diseases.

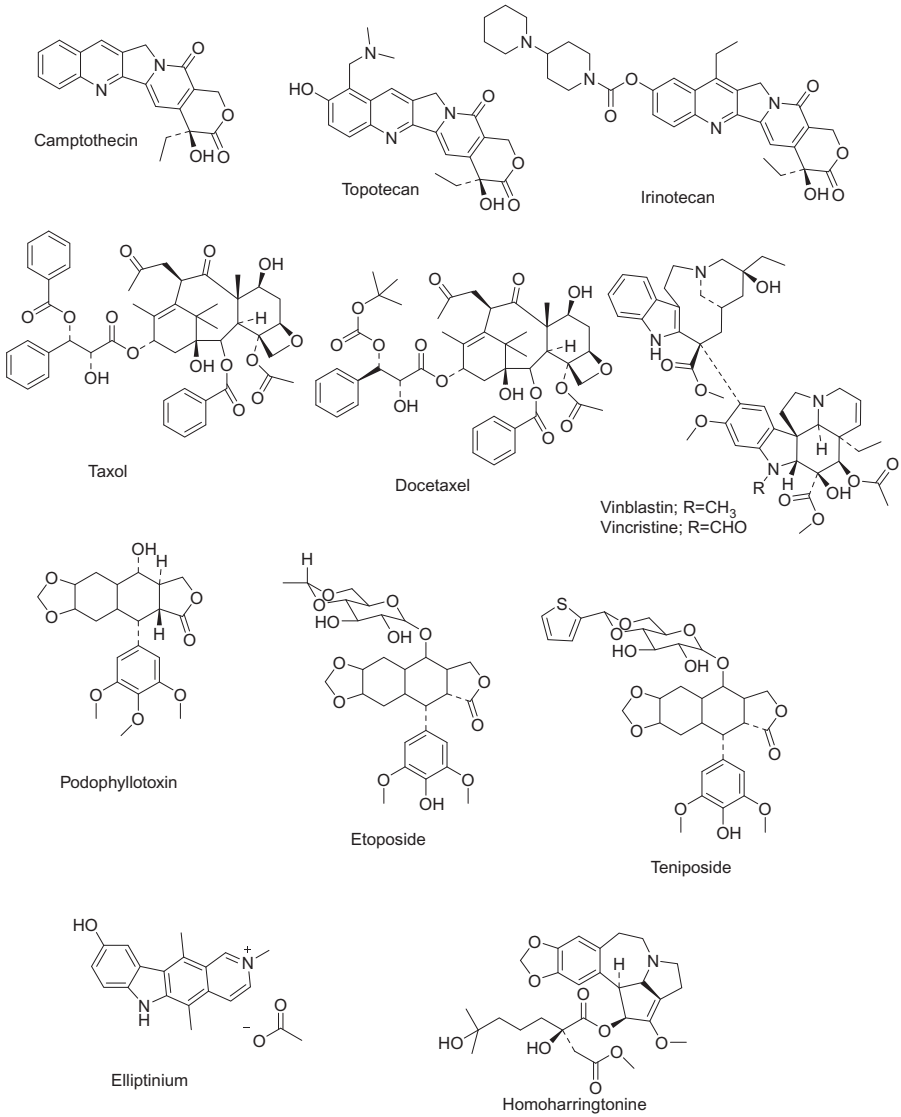

Fig. 22.1 Plant-derived anticancer agents in clinical use.

Camptothecin was discovered from the Chinese ornamental tree, *Camptotheca acuminata* Decne [56]. Highly effective derivatives in this series were discovered (topotecan and irinotecan). Topotecan was effectively used against ovarian and lung cancers. Irinotecan was helpful for the treatment of colorectal cancer. Homoharringtonine, cephalotaxaceae [57], and elliptinium were also effective against diverse cancers.

22.5 Plant-derived anticancer drugs

(a) Vinca alkaloids: Vinca alkaloids are the first organic compounds developed for clinical purposes. The agents were vinblastine (VLB) and vincristine (VCR). These were isolated from the plant *Catharanthus roseus* G. Don belonging to the family Apocynaceae. These compounds were identified during an investigation on hypoglycemic agents. It was amazing to note that the plant extracts is able to reduce white blood cell counts and bone marrow depression in rats. Moreover, the extracts were effective against lymphocytic leukemia in mice [58]. Semisynthetic products of vinca alkaloids, vinorelbine (VRLB), and vindesine (VDS) were also prepared. These were found to be effective alone or in combination with various chemotherapeutic molecules to combat different types of cancers. VLB was used for the treatment of lymphoma, leukemia, and different types of cancers (breast, testes, lymphocytic leukemia, and lung) [59].

(b) Podophyllotoxin derivatives: These compounds belong to Podophyllaceae family such as *Podophyllum peltatum* Linn. These are used for different therapeutic disorders including the treatment of skin cancer and warts. *Podophyllum peltatum* has been used by the Native Americans for the treatment of cancers [60]. The interest in these plants was established by the observation in the 1940s that an alcohol extract of the dried roots known as podophyllin cures venereal. The cytotoxic therapeutic components were identified as podophyllotoxins and were first isolated in 1880, but the correct structure of these natural compounds was confirmed in 1950. [61]

(c) *Allium sativum* (Allicin): *A. sativum* is used to treat a large variety of diseases. Allicin is a major component in garlic and ajoene is a rearrangement product of allicin. The cytotoxic effects of this species have been determined using human primary fibroblasts, non-tumorgenic cell line, and tumorgenic lymphoid cell line. The cell growth inhibition was in the range 2–50 μg/mL [62]. Organo-sulfur compounds from garlic, like *S*-allylcysteine, are reported to retard the growth of chemically induced and transplantable tumors in several animal models [63]. The administration of garlic (250 mg/kg, p.o., thrice a week) in male wistar rats has been used to suppress 4-nitroquinoline-1-oxide-induced tongue carcinogenesis. This is confirmed by the absence of carcinomas in the initiation phase and their reduced incidence afterwards [64]. Therefore, the consumption of garlic may protect human from cancer.

(d) *A. paniculata*: Phytochemical analyses of the ethanol extracts of *A. paniculata* have revealed the isolation of 14 molecules. A majority of them are flavonoids and labdane-types of terpenoids. The anticancer activities of these compounds have been studied against numerous cancer cell lines. The results indicate that these molecules have a tumor inhibitory activity against many cell lines [65]. The extract of *A. paniculata* was fractionated and specific portion of these fractions exhibited cytotoxic and immunostimulating activities [66]. However, some side effects were also detected which include gastric disorder, headache, taste disorder, and fatigue. High doses of *A. paniculata* also affect the normal functions of the liver [67].

(e) *Annona muricata*: The crucial medicinal agents found in fruits, seeds, leaves, and barks of *A. muricata* are acetogenins. Research demonstrated that acetogenins block the synthesis of adenosine triphosphate inhibiting the pump to remove cancer medicines from the components of the cell. This allowed effective chemotherapy. Importantly, research indicated that acetogenins have chemotherapeutic properties, especially against cancers that are resistant to other drugs [68]. However, Parkinson symptom was the side effects observed [69]. A few acetogenins were identified as toxic against cancer cell lines (e.g., human-breast cancer, pancreatic carcinoma, prostatic adenocarcinoma, colonic

adenocarcinoma, human lymphoma, liver cancer, and multidrug-resistant human-breast adenocarcinoma).

(f) *Apis mellifera*: *A. mellifera* is the scientific name of honey bee. Honey is useful in the treatment of skin wounds, ulcerations, and burns. But, a protein of the honeybee *A. mellifera* is shown to enhance proliferation of rat hepatocytes and diminish apoptosis [70]. It has also demonstrated cytotoxicity against human lymphocytes and HL-60 cancer cells.

(g) *Bidens pilosa*: *B. pilosa* is a folk medicine and contains polyacetylenes, flavonoids, terpenoids, and phenylpropanoids. An extensive research work has on various extracts of *B. pilosa* identified phenyl-1,3,5-heptatriyne. This compound has revealed toxicity on normal blood cells. Different extracts (hexane, chloroform, and methanol) of *B. pilosa* and their fractions were examined against cancer cell lines and hexane extracts were found to have antitumor activity [71].

(h) *Bolbostemma paniculatum*: The triterpenoid saponin tubeimoside-V was obtained from Chinese herb *B. paniculatum*. A systematic investigation on tubeimoside-V confirmed apoptotic killing properties on glioblastoma cells. A few tubeimosides like molecules (tubeimodes-I, tubeimoside-II, and tubeimoside-III) demonstrated cytotoxic effects. This was due to the inhibition of DNA synthesis and induction of phenotypic reverse transformation of tumor cells [72].

(i) *Cannabis sativa*: The major constituents of *C. sativa* inhibited human breast tumor cells *in vitro* experiments. The survival of animals has increased when marijuana was injected into malignant brain tissues. The potent portions of *C. sativa* are cannabinoid molecules. Cannabinoids and the products obtained from them have palliative properties in cancer patients. These molecules have shown anticancer activity in cell cultures and animal models through the modulation of cell-signaling mechanisms [73].

(j) *Daphne mezereum*: The alcoholic extract of *D. mezereum* exhibit antileukemic activity against lymphocytic leukemia. A fractionation studies on the extracts identified mezerein as an effective antileukemic molecule [74].

(k) *Gossypium hirsutum*: *G. hirsutum* known as Gossypol or cottonseed oil is used as a contraceptive. This is also used in the treatment of metastatic carcinoma of endometrium and ovary. A few in vivo and in vitro studies suggested the antitumor activities of gossypol on cytosolic and mitochondrial enzymes. These enzymes are crucial against the growth of many tumor cells including melanoma, endometrial, colon, lung, prostate, breast, brain, and adrenocortical cancers [75, 76].

(l) *Nervilia fordii*: The petroleum ether and ethyl acetate extracts of *N. fordii* have been examined for antitumor activities in mice models. These extracts have demonstrated excellent antitumor effects. However, further research is necessary to isolate the active components present in the systems [77].

(m) *Salvia miltiorrhiza*: Tanshinone-I isolated from *S. miltiorrhiza* has effects on the expression of intercellular adhesion. Experiments have demonstrated the anticancer properties of tanshinone-I against breast cancer cells [78]. Tanshinone II-A obtained from *S. miltiorrhiza* killed cells through apoptosis and this pathway was through proteolytic cleavage [79].

(n) *T. chebula*: *T. chebulais* is a source of hydrolysable tannis and its antimutagenic activity in *Salmonella typhimurium* has been documented [80]. Phenols like chebulinic acid, tannic acid, and ellagic acid are the cancer growth inhibitors found in the fruits of *T. chebula* [47]. The acetone extract of *T. chebula* fruit powder and its bark have been reported with promising antimutagenic and anticarcinogenic activities [81].

(o) *Zingiber officinale*: The ethanol extract of *Z. officinale* was identified for its antitumor effects in skin tumorigenesis model. The preapplication of *Z. officinale* ethanol extract

onto the skin of mice resulted in the significant inhibition of 12-0-tetradecanoylphorbol-13-acetate (TPA)-caused induction of epidermal ODC, cyclooxygenase, and lipoxygenase activities and ODC mRNA expression in a dose-dependent manner. The preapplication of ethanol extract of *Z. officinale* onto mouse skin also resulted in a significant inhibition of TPA-caused epidermal edema and hyperplasia. In long-time studies, topical application of *Z. officinale* ethanol extract 30 min prior to that of each TPA application to 7,12-dimethylbenz(a)anthracene-initiated mice resulted in a marked protection against skin tumor incidence and its multiplicity [82]. Ginger's natural bioactives, specifically ginger extract and 6-gigerol, have also been investigated for their in vitro inhibition of two key aspects of colon cancer biology, cancer cell proliferation, and angiogenic potential of endothelial cell tubule formation. These active ginger constituents have been linked to a direct effect on cancer cells. Among other compounds, 6-gingerol was found more effective even at lower doses and resulted in the inhibition of endothelial cell tube formation [81]. The ginger extract suppresses the growth of colon cancer cells, arrest the G0/G1-phase, reduce DNA synthesis, and induce apoptosis.

22.5.1 Apoptosis

Apoptosis is a special form of programmed cell death that occurs in multicellular organisms in a systematic way [83]. Biochemical events lead to a series of characteristic cell changes and finally to death. Some of these changes include blebbing, cell shrinkage, nuclear fragmentation, chromatin condensation, chromosomal DNA fragmentation, and global mRNA decay. The average adult human loses between 50 and 70 billion cells each day because of apoptosis [84]. In an average human child between the ages of 8 and 14 approximately 20–30 billion cells die per day.

The initiation of apoptosis process is tightly regulated by numerous activation mechanisms, because once apoptosis starts, it inevitably leads to the death of the cell. The two best-understood activation mechanisms are the intrinsic pathway (also called the mitochondrial pathway) and the extrinsic pathway. The intrinsic pathway is activated by intracellular signals generated when cells are stressed and depends on the release of proteins from the intermembrane space of mitochondria. The extrinsic pathway is activated by extracellular ligands binding to cell-surface death receptors, which leads to the formation of the death-inducing signaling complex (DISK) [85].

A cell initiates intracellular apoptotic signaling in response to a stress, which may bring about cell suicide. The binding of nuclear receptors by glucocorticoids [86], heat [86], radiation [86], nutrient deprivation [86], viral infection [86], hypoxia [86], increased intracellular concentration of free fatty acids, [87] and increased intracellular calcium concentration [88, 89], for example, by damage to the membrane, can all trigger the release of intracellular apoptotic signals by a damaged cell. A number of cellular components, such as poly ADP ribose polymerase, may also help regulate apoptosis. Single cell fluctuations have been observed in experimental studies of stress-induced apoptosis [90].

Before the actual process of cell death is precipitated by enzymes, apoptotic signals must cause regulatory proteins to initiate the apoptosis pathway. This step allows those signals to cause cell death, or the process to be stopped, should the cell no longer need to die. Several proteins are involved, but two main methods of regulation have been identified: the targeting of mitochondria functionality [91], and directly

transducing the signal via adaptor proteins to the apoptotic mechanisms. An extrinsic pathway for initiation identified in several toxin studies is an increase in calcium concentration within a cell caused by drug activity, which also can cause apoptosis via calcium-binding protease calpain.

22.5.2 Enzyme inhibitor

An enzyme inhibitor is a molecule that binds to an enzyme and decreases its activity. Since blocking an enzyme's activity can kill a pathogen or correct a metabolic imbalance, many drugs are enzyme inhibitors. These inhibitors modify key amino acid residues needed for the enzymatic activity.

Enzyme inhibitors are found in nature and are also designed and produced as part of pharmacology and biochemistry. Natural poisons are often enzyme inhibitors that have evolved to defend a plant or animal against predators. These natural toxins include some of the most poisonous compounds known. Artificial inhibitors are often used as drugs, but can also be insecticides such as malathion, herbicides such as glyphosate, or disinfectants such as triclosan. Other artificial enzyme inhibitors block acetylcholinesterase, an enzyme which breaks down acetylcholine, and are used as nerve agents in chemical warfare.

The binding of an inhibitor can stop a substrate from entering the enzyme's active site and/or hinder the enzyme from catalyzing its reaction. Inhibitor binding is either reversible or irreversible. Irreversible inhibitors usually react with the enzyme and change it chemically (e.g., via covalent bond formation). These inhibitors modify key amino acid residues needed for enzymatic activity. In contrast, reversible inhibitors bind noncovalently and different types of inhibition are produced depending on whether these inhibitors bind to the enzyme, the enzyme-substrate complex, or both.

Many drug molecules are enzyme inhibitors, so their discovery and improvement is an active area of research in biochemistry and pharmacology. A medicinal enzyme inhibitor is often judged by its specificity (its lack of binding to other proteins) and its potency (its dissociation constant, which indicates the concentration needed to inhibit the enzyme). A high specificity and potency ensure that a drug will have few side effects and thus low toxicity.

Enzyme inhibitors also occur naturally and are involved in the regulation of metabolism. For example, enzymes in a metabolic pathway can be inhibited by downstream products. This type of a negative feedback slows the production line when products begin to build up and is an important way to maintain homeostasis in a cell. Other cellular enzyme inhibitors are proteins that specifically bind to and inhibit an enzyme target. This can help control enzymes that may be damaging to a cell, like proteases or nucleases. A well-characterized example of this is the ribonuclease inhibitor, which binds to ribonucleases in one of the tightest known protein-protein interactions. Natural enzyme inhibitors can also be poisons and are used as defenses against predators or as ways of killing prey [92].

Chemotherapy [93, 94], antibiotics [95], metabolic control, [96] and pesticides [97] are working as enzyme inhibitor in human and animals.

22.6 Conclusions

In conclusion we can demonstrate that nature is mankind's greatest chemist. More than 50% of drugs are derived from medicinal plants so it is clear that natural resources, especially plants could be drastically used to find effective drugs for cancer treatment. Cancer is becoming a high profile disease in developed and developing countries. Although, chemically derived drugs have been developed, other cancer treatments also preexist. However, current methods such as chemotherapy have their limitations due to their toxic effects on nontargeted tissues furthering human health problems. Therefore, there is a demand for alternative treatments with naturally derived anticancer agents with plants being the desired source.

Acknowledgments

PB acknowledges the support from the director of CSIR-Central Scientific Instruments Organization, Chandigarh. BKB is grateful to the USA NIH, USA NCI, and USA Private Research Foundation. BKB also thanks Prince Mohammad Bin Fahd University for encouragement.

References

[1] O. Said, K. Khalil, S. Fulder, H. Azaizeh, Ethnopharmacological survey of medicinal herbs in Israel, the Golan Heights and the West bank region, J. Ethnopharmacol. 83 (2002) 251–265.
[2] (a) P. Govind, S. Madhur, Medicinal plants: better remedy for neoplasm, Indian Drugs 43 (2006) 869–874. (b) S.K. Agrawala, S. Chatterjee, S.K. Misra, Immunepotentiation activity of a polyherbal formulation Immu-21, Phytomedica 2 (2001) 1–22.
[3] A.K. Gupta, N. Tandon, Reviews on Indian Medicinal Plants, vol. 2, Indian Council of Medical Research, New Delhi, 2004.
[4] R.K. Goel, K. Sairam, Anti-ulcer drugs from indigenous sources with emphasis on Musa sapientum, Tamrabhasma, Asparagus racemosus and Zingiber officinale, Indian J. Pharm. 34 (2002) 100–110.
[5] C.V. Rao, K. Sairam, R.K. Goel, Experimental evaluation of Bacopa monniera on rat gastric ulceration and secretion, Indian J. Physiol. Pharmacol. 44 (2000) 435.
[6] S. Coseri, Natural products and their analogues as efficient anticancer drugs, Mini-Rev. Med. Chem. 9 (5) (2009) 560–571.
[7] Cancer Research UK, Available at: http://www.cancerresearchuk.org/about-cancer/what-is-cancer, 2014. (Accessed 23 January 2015).
[8] M. Gordaliza, Natural products as leads to anticancer drugs, Clin. Transl. Oncol. 9 (12) (2007) 767–776.
[9] A. Saklani, S.K. Kutty, Plant-derived compounds in clinical trials, Drug Discov. Today 13 (3–4) (2008) 161–171.
[10] G.M. Cragg, D.J. Newman, Plants as a source of anti-cancer agents, J. Ethnopharmacol. 100 (2005) 72–79.
[11] D.J. Newman, G.M. Cragg, K.M. Snader, Natural products as sources of new drugs over the period 1981–2002, J. Nat. Prod. 66 (2003) 1022–1037.

[12] R. Gerson-Cwillich, A. Serrano-Olvera, A. Villalobos-Prieto, Complementary and alternative medicine (CAM) in Mexican patients with cancer, Clin. Transl. Oncol. 8 (3) (2006) 200–207.
[13] M. Tascilar, F.A. de Jong, J. Verweij, R.H.J. Mathijssen, Complementary and alternative medicine during cancer treatment: beyond innocence, Oncologist 11 (7) (2006) 732–741.
[14] B.M. Molassiotis, L. Milovics, V. Panteli, E. Patiraki, P. Fernandez-Ortega, Complementary and alternative medicine use in patients with gynecological cancers in Europe, Int. J. Gynecol. Cancer 16 (Suppl. 1) (2006) 219–224.
[15] R. Kaur, H. Kaur, The antimicrobial activity of essential oil & plant extracts of Woodfordia fruticosa, Arch. Appl. Sci. Res. 2 (2010) 302–309.
[16] W. Fan, K.R. Johnson, M.C. Miller, In vitro evaluation of combination chemotherapy against human tumor cells, Oncol. Rep. 5 (5) (1998) 1035–1042.
[17] S. Belman, Onion and garlic oils inhibit tumor promotion, Carcinogenesis 4 (1983) 1063–1065.
[18] R. Ahmad, A.N. Shrivastava, M. Ali, Khan, Evaluation of in-vitro anticancer activity of stem of Tinospora cordifolia against human breast cancer and vero cell lines, J. Med. Plant Stud. 3 (4) (2015) 33–37.
[19] R. Asirwatham, A.J.M. Christina, A. Murali, In-vitro antioxidant and anticancer activity studies on Drosera indica L. (Droseraceae), Adv. Pharm. Bull. 3 (1) (2013) 115–120.
[20] G. Sukumar, D. Divyalaxmi, S. Mithula, S. Rupachandra, In-vitro anticancer effect of methanolic seed coat extracts of Momordica Dioica against human carcinoma cell lines, Int. J. ChemTech Res. 9 (2) (2016) 284–289.
[21] N. Manglani, S. Vaishnava, P. Dhamodaran, H. Sawarkar, In-vitro and in-vivo anticancer activity of leaf extract of Barleria grandiflora, Int J Pharm Pharm Sci 6 (3) (2014) 70–72.
[22] S. Charoensin, Antioxidant and anticancer activities of Moringa oleifera leaves, J. Med. Plant Res. 8 (7) (2014) 318–325.
[23] G. Bupesh, E. Manikanandan, K. Thanigaiarul, S. Magesh, Enhanced antibacterial, anticancer activity from Terminalia chebula medicinal plant rapid extract by phytosynthesis of silver nanoparticles core-shell structures, J. Nanomed. Nanotechnol. 7 (1) (2016) 1000355.
[24] N. Murganatham, S. Solomon, M.M. Senthamilselvi, Anticancer activity of Cucurbita maxima flowers (Pumpkin) against human liver cancer, Int. J. Pharma Sci. 6 (1) (2016) 1356–1359.
[25] L. Wasserman, S. Avigad, E. Beery, J. Nordenberg, E. Fenig, The effect of aloe-emodin on the proliferation of a new merkel carcinoma cell line, Am. J. Dermatopathol. 24 (1) (2002) 17–22.
[26] T. Pecere, M.V. Gazzola, C. Micignat, Aloe-emodin is a new type of anticancer agent with selective activity against neuro-ectodermal tumors, Cancer Res. 60 (2000) 2800–2804.
[27] J. Wang, H. Ito, K. Shimura, The Wealth of India A Dictionary of Indian Raw Materials and Industrial Products, i (ab) (1985) 80, 109 pp.
[28] J. Bruneton, Pharmacognosy, Phytochemisty Medicinal Plants, Lavoisier, France, 1993, p. 832.
[29] H.M. Kantrajian, M. Talpaz, T.L. Smith, J. Cortes, F.J. Giles, Homoharringtonine and low-dose cytarabine in the management of late chronic-phase chronic myelogenous leukemia, J. Clin. Oncol. 18 (2000) 3513–3521.
[30] J. Bruneton, Pharmacognosy, Phytochemisty Medicinal Plants, Lavoisier, France, 1993, pp. 771–777.
[31] M. Nagabhushan, S.V. Bhide, Curcumin as an inhibitor of cancer, J. Am. Coll. Nutr. 11 (1992) 192–198.
[32] M.M. Chan, D. Fong, Anti-inflammatory and cancer-preventive immunomodulation through diet: effects of curcumin on t-lymphocytes, Am. Chem. Soc. (1994) 222–230.

[33] H. Kikuzaki, N. Nakatani, Antioxidant effects of some ginger constituents, J. Food Sci. 58 (1993) 1407–1410.
[34] J. Bruneton, Pharmacognosy, Phytochemisty Medicinal Plants, Lavoisier, France, 1993, p. 281.
[35] J. Kleijnen, P. Knipschild, Gingko biloba, Lancet 340 (1992) 1136–1139.
[36] S.P. Ambasta (Ed.), The Useful Plant of India, fourth ed., National Institution of Science Communication, Delhi, 2000, p. 239.
[37] M. Serraino, L.U. Thompson, The effect of flaxseed supplementation on early risk markers for mammary carcinogenesis, Cancer Lett. 60 (1991) 135–142.
[38] M. Serraino, L.U. Thompson, The effect of flaxseed supplementation on the initiation and promotional stages of mammary tumorigenesis, Nutr. Cancer 17 (1992) 153–159.
[39] T.K. Yun, S.Y. Choi, A case-control study of ginseng intake and cancer, Int. J. Epidemiol. 19 (1990) 871–876.
[40] T.K. Yun, Experimental and epidemiological evidence of the cancer-preventive effects of panax ginseng C.A. Meyer, Nutr. Rev. 54 (1996) 71–81.
[41] S.K. Chakraborti, B.K. De, T. Bandyopadhyay, Variations in the antitumor constituents of withania somnifera, Exp. Dermatol. 30 (8) (1974) 852–853.
[42] P.U. Devi, A.C. Saradana, F.E. Soloman, Antitumor and radiosensitizing effects of *withania somnifera* (ashwagandha) on a transplantable mouse tumor, sarcoma-180, Indian J. Exp. Biol. 31 (7) (1993) 607–611.
[43] P.U. Devi, K. Akagi, V. Ostapenko, Y. Tanaka, T. Sugahara, A. Withaferin, A new radiosensitizer from the indian medicinal plant withania somnifera, Int J Radiat Boil. 69 (2) (1996) 193–197.
[44] J.M. Romero, S.J. Campos, M. Analla, A. Munoz-Serrano, M.A. Alonso, Genotoxicity and anti-genotoxicity of some traditional medicinal herbs, Mutat. Res. 585 (2005) 147–155.
[45] T.W. Yu, M. Xu, R.H. Dashwood, Antimutagenic activity of spearmint, Environ. Mol. Mutagen. 44 (2004) 387–393.
[46] P.U. Devi, *Withania somnifera* dunal (ashwagandha): potential plant source of a promising drug for cancer chemotherapy and radiosensitization, Indian J. Exp. Biol. 34 (1996) 927–932.
[47] S.K. Katiyar, R. Agarwal, H. Mukhtar, Inhibition of tumor promotion in sencar mouse skin by ethanol extract of *zingiber officinale* rhizome, Cancer Res. 56 (5) (1961) 1023–1030.
[48] H.J. Dorman, M. Kosar, K. Kahlos, Y. Holm, R. Hiltunen, Antioxidant properties and composition of aqueous extracts from *mentha* species, hybrids, varieties and cultivars, J. Agric. Food Chem. 51 (2003) 4563–4569.
[49] K.M. Nadkarni, Indian Materia Medica, Indian Materia Medica: With Ayurvedic, Unani-Tibbi, Siddha, Allopathic, Homeopathic, Naturopathic & Home Remedies, Appendices & Indexes, Volume 1, 1996.
[50] C.K. Kokate, A.P. Purohit, S.B. Gokhale, Text Book of Pharmacognosy, thirty-fifth ed., Nirali Prakashan, Pune, 2006, pp. 410–412.
[51] J.M. Cassady, J.D. Douros, Anticancer Based on Natural Products Models, Academic Press, New York, 1980.
[52] S. Unnati, S. Ripal, A. Sanjeev, A. Niyati, Novel anticancer agents from plant sources, Chin. J. Nat. Med. 11 (1) (2013) 0016–0023.
[53] J.D. Phillipson, Medicinal plants, J. Biol. Educ. Soc. Biol. 31 (2) (1999) 109.
[54] A. Amin, H. Gali-Muhtasib, M. Ocker, R. Schneider-Stock, Overview of major classes of plant-derived anticancer drugs, Int. J. Biomed. Sci. 5 (1) (2009) 1–11.
[55] B. F, A. Rahier, B. Camara, Biogenesis, molecular regulation and function of plant isoprenoids, Prog. Lipid Res. 44 (6) (2005) 357–429.

[56] I. Takano, I. Yasuda, N. Motohiro, Y. Hitotsuyanagi, T. Koichi, H. Itokawa, New Cephalotaxus alkaloids from Cephalotaxus harringtonia var. Drupacea, J. Nat. Prod. 59 (10) (1996) 965–967.
[57] T.L. Lemkeb, D.A. Williams, V.F. Roche, Z.S. William, Foye's Principles of Medicinal Chemistry, sixth ed., Lippincott Williams & Wilkins, Philadelphia, 2008, pp. 1147–1148.
[58] Z. Hilal, S. Michael, B.-A. Eran, S. Bashar, Greco-Arab and Islamic herbal-derived anticancer modalities: from tradition to molecular mechanisms, Evid. Based Complement. Alternat. Med. 2012 (2012) 349040 p. 13.
[59] (a) T. Wen, L. Jinjian, H. Mingqing, Y. Li, C. Meiwan, W. Guosheng, G. Jian, Z. Zhangfeng, X. Zengtao, D. Yuanye, G. Jiajie, C. Xiuping, W. Yitao, Anti-cancer natural products isolated from chinese medicinal herbs, Chinas Med. 6 (2011) 27. (b) R. Prema, S. D. Sekar, K.B. Chandra Sekhar, Review on: herbs as anticancer agents, Int. J. Pharma & Ind. Res 1 (2011) 105.
[60] K. Scharfenberg, R. Wagner, K.G. Wagner, The cytotoxic effect of adjoin, a natural product from garlic, investigated with different cell lines, Cancer Lett. 53 (3) (1990) 103.
[61] M. Thomson, M. Ali, Garlic (Allium sativum): a review of its potential use as an anticancer agent, Curr. Cancer Drug Targets 3 (1) (2003) 67.
[62] S. Banasenthil, C.R. Ramachandran, S. Nagini, Prevention of 4-nitroquinoline-1-oxide induced rat tongue carcinogenesis by garlic, Fitoterapia 72 (2001) 524.
[63] M. Geethangili, Y.K. Rao, S.H. Fang, Y.M. Tzeng, Cytotoxic constituents from *Andrographis paniculata* induce cell cycle arrest in jurkat cells, Phytother. Res. 22 (10) (2008) 1336.
[64] R.A. Kumar, K. Sridevi, V.N. Kumar, S. Nanduri, S. Rajagopal, Anticancer and immunostimulatory compounds from *Andrographis paniculata*, J. Ethnopharmacol. 92 (2–3) (2004) 291.
[65] Zhion *http://www.zhion.com/herb/Andrographis.html*, July 28, 2011.
[66] J.M. Muriel, Herbs or natural products that decrease Cancer growth, Oncol. Nurs. Forum 31 (4) (2004) 75.
[67] A. Lannuzel, P.P. Michel, L.D. Caparros, J. Abaul, R. Hocquemiller, M. Ruberg, Toxicity of Annonaceae for dopaminergic neurons, potential role in atypical parkinsonism in Guadeloupe, Mov. Disord. 17 (2002) 84.
[68] T.A. Khwaja, C.B. Dias, S. Pentecost, Recent studies on the anticancer activities of mistletoe (Viscum album) and its alkaloids, Oncology 43 (1986) 42–50.
[69] M. Kamakura, T. Sakaki, A hypopharyngeal gland protein of the worker honeybee *Apis mellifera* L. enhances proliferation of primary-cultured rat hepatocytes and suppresses apoptosis in the absence of serum, Protein Expr. Purif. 45 (2) (2006) 307.
[70] Y.J. Lee, S.J. Kang, B.M. Kim, Y.J. Kim, H.D. Woo, H.W. Chung, Cytotoxicity of honeybee *(Apis mellifera)* venom in normal human lymphocytes and HL-60 cells, Chem. Biol. Interact. 169 (3) (2007) 189.
[71] I. Hamzaoglu, K. Saribeyoglu, H. Durak, T. Karahasanoglu, I. Bayrak, T. Altug, Protective covering of surgical wounds with honey impedes tumor implantation, Arch. Surg. 135 (2002) 1414.
[72] S.M. Kupchan, R.L. Baxter, Mezerein: anti leukemic principle isolated from Daphne mezereum, Life Sci. 187 (4177) (1975) 652.
[73] N.E. Gilbert, J.E. Reilly, C.J. Chang, Y.C. Lin, R.W. Brueggemeier, Antiproliferative activity of gossypol and gossypolone on human breast cancer cells, Life Sci. 57 (1995) 61.
[74] D. Wu, An overview of the clinical pharmacology and therapeutic potential of gossypol as a male contraceptive agent and in gynaecological disease, Drugs 38 (1989) 333.

[75] H.S. Zhen, Study of anticancer effect in vivo of active fraction from Nervillia fordii, Zhong, Yao Cai 30 (9) (2007) 1095.
[76] I.T. Nizamutdinova, G.W. Lee, J.S. Lee, M.K. Cho, K.H. Son, S.J. Jeon, Tanshinone -I suppresses growth and invasion of human breast cancer cells, MDA- MB- 231, through regulation of adhesion molecules, Carcinogenesis 29 (10) (2008) 1885.
[77] Y. Yoon, Y. Kim, W.K. Jeon, H.J. Park, H.J. Sun, Tanshinone IIA isolated from *Salvia miltiorrhiza* B. induced apoptosis in HL60 human premyelocytic leukemia cell line, J. Ethno Pharmacol. 68 (1) (1999) 121.
[78] S. Kaur, I.S. Grover, M. Singh, S. Kaur, Antimutagenesity of hydrolysable tannins from Terminalia chebula in Salmonella typhimerium, Mutat. Res. 419 (3) (1998) 169.
[79] S. Arora, K. Kaw, S. Kaur, Indian medicinal plants as reserver of protective phytochemicals, Teratog. Carcinog. Mutagen. 23 (1) (2003) 295.
[80] M. Saleem, M. Hushum, P. Harkonen, K. Pihlaja, Inhibition of cancer cell growth by crude extract and phenolics of Terminalia chebula fruit, J. Ethno Pharmacol. 81 (2002) 327.
[81] A.C. Brown, Ginger's inhibition of rat colonic adenocarcinoma cells proliferation angiogenesis in vitro, Photother. Res. 32 (2008).
[82] S. Abdullah, S.A.Z. Abidin, N.A. Murad, M. Suzana, W.Z.W. Ngah, Y.A.M. Yusof, Ginger extract (*Zingiber officinale*) triggers apoptosis and G0/G1 cells arrest in HCT 116 and HT 29 colon cancer cell lines, Afr. J. Biochem. Res. 4 (4) (2010) 134.
[83] D. Green, Means to an End: Apoptosis and Other Cell Death Mechanisms, Cold Spring Harbor Laboratory Press, Cold Spring Harbor, NY, ISBN: 978-0-87969-888-1, 2011.
[84] ScienceDirect, www.sciencedirect.com. Retrieved 19 March 2019.
[85] I. Böhm, H. Schild, Apoptosis: the complex scenario for a silent cell death, Mol. Imaging Biol. 5 (1) (2003) 2–14.
[86] R.S. Cotran, C. Kumar, Robbins Pathologic Basis of Disease, W.B Saunders Company, Philadelphia, ISBN: 978-0-7216-7335-6, 1998.
[87] S. Hardy, W. El-Assaad, E. Przybytkowski, E. Joly, M. Prentki, Y. Langelier, Saturated fatty acid-induced apoptosis in MDA-MB-231 breast cancer cells. A role for cardiolipin, J. Biol. Chem. 278 (34) (2003) 31861–31870.
[88] M.P. Mattson, S.L. Chan, Calcium orchestrates apoptosis, Nat. Cell Biol. 5 (12) (2003) 1041–1043.
[89] A.C. Uğuz, M. Naziroğlu, J. Espino, I. Bejarano, D. González, A.B. Rodríguez, J. A. Pariente, Selenium modulates oxidative stress-induced cell apoptosis in human myeloid HL-60 cells through regulation of calcium release and caspase-3 and -9 activities, J. Membr. Biol. 232 (1–3) (2009) 15–23.
[90] J.K. Lee, S. Lu, A. Madhukar, Real-time dynamics of Ca^{2+}, caspase-3/7, and morphological changes in retinal ganglion cell apoptosis under elevated pressure, PLoS One 5 (10) (2010) e13437.
[91] I. Bejarano, J. Espino, D. González-Flores, J.G. Casado, P.C. Redondo, J.A. Rosado, C. Barriga, J.A. Pariente, A.B. Rodríguez, Role of calcium signals on hydrogen peroxide-induced apoptosis in human myeloid HL-60 cells, Int. J. Biomed. Sci. 5 (3) (2009) 246–256.
[92] R. Shapiro, B.L. Vallee, Interaction of human placental ribonuclease with placental ribonuclease inhibitor, Biochemistry 30 (8) (1991) 2246–2255.
[93] M. Maggi, S. Filippi, F. Ledda, A. Magini, G. Forti, Erectile dysfunction: from biochemical pharmacology to advances in medical therapy, Eur. J. Endocrinol. 143 (2) (2000) 143–154.
[94] J.J. McGuire, Anticancer antifolates: current status and future directions, Curr. Pharm. Des. 9 (31) (2003) 2593–2613.

[95] A.H. Katz, C.E. Caufield, Structure-based design approaches to cell wall biosynthesis inhibitors, Curr. Pharm. Des. 9 (11) (2003) 857–866.
[96] D.A. Okar, A.J. Lange, Fructose-2,6-bisphosphate and control of carbohydrate metabolism in eukaryotes, Biofactors 10 (1) (1999) 1–14.
[97] S.O. Duke, Overview of herbicide mechanisms of action, Environ. Health Perspect. 87 (1990) 263–271.

Further reading

[98] P. Govind, Some important anticancer herbs: a review, Int. Res. J. Pharm. 2 (2) (2011) 45–52.
[99] B.S. Cornblatt, L. Ye, A.T. Dinkova-Kostova, M. Erb, J.W. Fahey, K. Singh, M.A. Chen, T. Stierer, E. Garrett-Mayer, P. Argani, N.E. Davidson, P. Talalay, T.W. Kensler, K. Visvanathan, Preclinical and clinical evaluation of sulforaphane for chemoprevention in the breast, Carcinogenesis 28 (7) (2007) 1485–1490.

Microwave-assisted synthesis of antitubercular agents: A novel approach

23

Biswa Mohan Sahoo[a,*], *Bimal Krishna Banik*[b,*], *Arun Kumar Mahato*[c], *C. Nithya Shanthi*[c], *Bibhash C. Mohantad*[d]

[a]Roland Institute of Pharmaceutical Sciences, Berhampur, India, [b]Department of Mathematics and Natural Sciences, College of Sciences and Human Studies, Deanship of Research Development, Prince Mohammad Bin Fahd University, Al Khobar, Kingdom of Saudi Arabia, [c]Department of Pharmaceutical Sciences, Sardar Bhagwan Singh University, Dehradun, India, [d]Seemanta Institute of Pharmaceutical Sciences, Mayurbhanj, Odisha, India

[*]Corresponding author. e-mail address: drbiswamohansahoo@gmail.com; bimalbanik10@gmail.com; bbanik@pmu.edu.sa

Abbreviations

AUC	area under the plasma drug concentration
Br	bromo
Cl	chloro
°C	degree centigrade
DMAP	4-dimethylaminopyridine
DMF	dimethylformamide
DMSO	dimethyl sulfoxide
DNA	deoxyribonucleic acid
GHz	gigahertz
GQSAR	group-based quantitative structure-activity relationship
H_2SO_4	sulfuric acid
HIV	human immunodeficiency virus
IC_{50}	half maximal inhibitory concentration
INH	isoniazid
K_2CO_3	potassium carbonate
LRP	luciferase reporter phage
MABA	microplate Alamar Blue assay
MDR	multi drug resistant
MIC	minimum inhibitory concentration
mL	milliliter
MLC	minimum lethal concentration
MOA	mechanism of action
Mtb	*Mycobacterium tuberculosis*
MTB	*Mycobacterium tuberculosis* bacteria
MTT	3-(4,5-Dimethylthiazol-2-yl)-2,5-diphenyl tetrazolium bromide
MW	microwave

Green Approaches in Medicinal Chemistry for Sustainable Drug Design. https://doi.org/10.1016/B978-0-12-817592-7.00024-1
© 2020 Elsevier Inc. All rights reserved.

NIAID	National Institute of Allergy and Infectious Diseases
OD	optical density
PZA	pyrazinamide
QSAR	quantitative structure-activity relationship
RLU	relative light units
SAR	structure-activity relationship
SD	standard deviation
SI	electivity index
STM	streptomycin
TAACF	tuberculosis antimicrobial acquisition and coordinating facility
TDR	totally drug resistant
TB	tuberculosis
TFA	trifluoro acetic acid
μg	microgram
μM	micrometer
%	percent
WHO	World Health Organization
XDR	extensively drug resistant

23.1 Introduction

23.1.1 Tuberculosis

Tuberculosis (TB) is an infectious disease, caused by a microbial pathogen, *Mycobacterium tuberculosis* (Mtb). It mainly affects the lungs (pulmonary TB) but can affect other organs or tissues as well (extrapulmonary TB). The disease is transmitted through the air when people with pulmonary TB expel bacteria by coughing [1]. In 1882, Mtb, the causative agent of tuberculosis (TB), was discovered by Dr. Robert Koch, for which he was later awarded the Nobel Prize in 1905. Mtb is an acid-fast, nonmotile, nonsporulating, weak Gram-positive bacillus. TB is considered as one of the most chronic communicable diseases in the world. It is also one of the major causes of morbidity and mortality in most of the developing countries mainly in Africa and Asia [2]. As per the global TB report 2014, 9 million people suffered from TB and 1.5 million died from the disease. TB is responsible for 9.6 million infections in 2015 with an estimated 1.5 million global deaths. In 2016, there were 600,000 new cases with resistance to most effective first-line drug rifampicin and 490,000 had multidrug-resistant TB [3].

According to the World Health Organization (WHO) report-2017, TB is the ninth leading cause of death globally. As per the WHO in the year 2011, antitubercular drugs were classified as group-I or first-line oral anti-TB drugs (e.g., Isoniazid, Rifampicin, Ethambutol, and Pyrazinamide), group-II or injectable anti-TB drugs (e.g., Streptomycin, Kanamycin, Amikacin, and Capreomycin), group-III drugs (Fluoroquinolones, Ofloxacin, Levofloxacin, and Moxifloxacin), group-IV or second-line anti-TB drugs (Ethionamide, Cycloserine, *p*- and Aminosalicylic acid). The WHO has recently approved a revision of the classification of new anti-TB drugs based on current evidence on each drug which will be safer and more effective for MDR- and XDR-TB treatment regimen. Antitubercular drugs mainly produce their action by inhibiting the synthesis of mycolic acid that results in disruption of the bacterial cell wall as presented in Table 23.1 and Fig. 23.1 [5].

Table 23.1 List of antitubercular drugs with MOA and mutated genes responsible for resistance toward antitubercular drugs [4].

Antitubercular drugs	Year of discovery	Mechanism of action	Mutated genes
Isoniazid	1951	Inhibition of cell wall mycolic acid	*Kat G*, *inhA, ndh*
Rifampicin	1972	Inhibition of bacterial DNA dependent RNA synthesis	*rpoB*
Pyrazinamide	1952	Disruption of membrane transport	*pncA*
Streptomycin	1943	Inhibition of protein synthesis	*rpsL*, *rrs*
Viomycin	1951	Inhibition of protein synthesis	*tlyA*, *rrs*
Kanamycin	1957	Inhibition of protein synthesis	*Rrs*
Capreomycin	1960	Inhibition of protein synthesis	*tlyA*, *rrs*
Quinolones Fluoroquinolones	1963	Inhibition of DNA replication and transcription	*yrA*, *gyrB, atpE*
Ethionamide	1956	Inhibition of mycolic acid synthesis	*inhA*, *etaA*or *ethA*
Ethambutol	1961	Inhibition of cell wall arabinogalactan synthesis	*Emb CAB* operon
Amikacin	1971	Inhibition of protein synthesis	*Rrs*
PAS	1944	Inhibition of folic acid and iron metabolism	*thyA*
Cycloserine	1952	Inhibition of peptidoglycan synthesis	*Unknown*

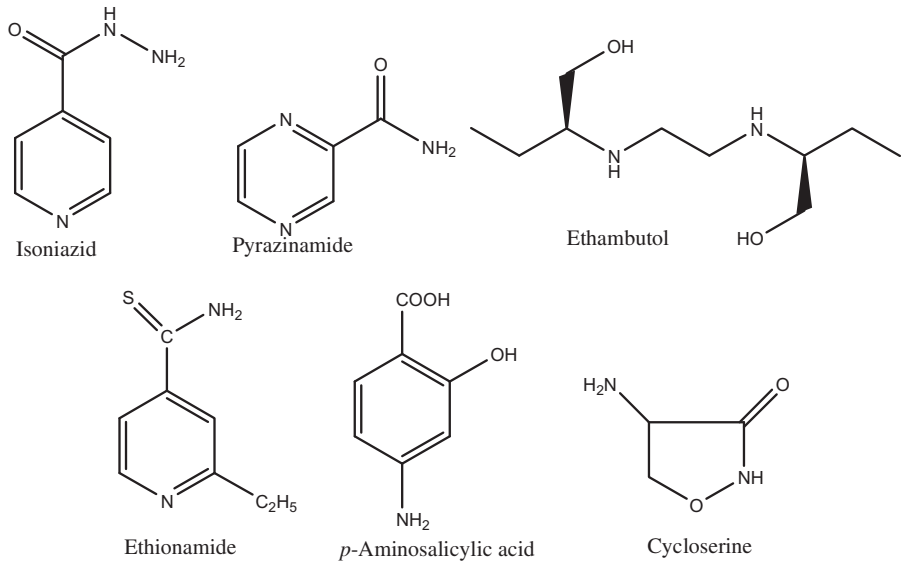

Fig. 23.1 Structures of anti-TB drugs.

The treatment of TB is mainly affected by various factors such as the development of multidrug resistant (MDR), extensively drug resistant (XDR), and totally drug resistant (TDR). The increase in resistance of *Mycobacterium tuberculosis* to currently available drug therapy and the large number of epidemic infections due to *Mycobacterium avium* complex are the stimulating factors to carry out the research for generating new active drug molecules [6]. Therefore, microwave-assisted synthesis as green technology is utilized to develop the novel alternative, safe, and potent drugs with a broader spectrum of antitubercular activity [7].

23.1.2 Microwave chemistry

Microwave irradiation is a versatile technology that can accelerate the chemical reactions and has shown great promise in the new drug development process. Microwave heating relies on two main principles such as dipolar polarization and conduction. Dipolar polarization is responsible for the generation of heat from polar molecules [8]. When an electromagnetic force is applied, polar molecules attempt to align themselves in the direction of the field. The applied frequency field must be in the microwave radiation region for heating to occur. Once the field is in the microwave radiation region (0.3–30 GHz), the dipoles will align themselves in one direction, but at that point, the field is already in the opposite direction, causing a phase difference. This difference gives way to an energy release from the molecular friction and dielectric loss of the dipole, thereby causing the reaction to heat. Conduction or ionic conduction is formed from ions in the reaction medium. They move through the solution with the electromagnetic field and thereby increasing the collision rate, and finally lead to the generation of heat. Apart from the electrical component, microwave heating is also dependent on the characteristics of the materials being heated [9]. A schematic diagram of a typical microwave instrument is provided in Fig. 23.2.

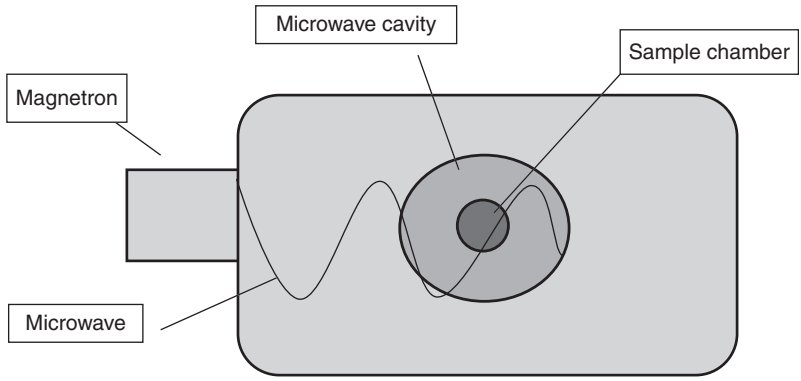

Fig. 23.2 Top view of a monomodal microwave.

The magnetron produces the microwave which is then sent through the cavity to the sample chamber. The microwave cavity absorbs the microwave on the other end, causing a single wave to be introduced into the sample chamber at a time. Materials can include anything in the reaction vessel, from solids to solvents [10]. Solvents have two values that impact microwave heating, the dielectric constant (which corresponds to the ability to absorb microwave energy) and the loss angle (which quantifies the efficiency of the absorbed energy to be translated to heat). The ability of a material to heat in a microwave is thus reported as the loss tangent, tan δ. Loss tangent is used to determine how easily microwaves heat a substance. The equation used is: $\tan\delta = \varepsilon'' / \varepsilon'$ where ε'' is the dielectric loss or the ability of the substance to convert electromagnetic radiation into heat, and ε' is the dielectric constant or the ability of the polar molecule to align itself with the electric field (Table 23.2) [12].

Table 23.2 Dielectric constants and loss tangent values for commonly used solvents [11].

Solvents	Dielectric constant	Loss tangent
Acetone	20.7	0.054
Acetic acid	6.2	0.174
Acetonitrile	37.5	0.062
1-Butanol	17.1	0.571
2-Butanol	15.8	0.447
Chlorobenzene	2.6	0.101
Chloroform	4.8	0.091
1,2-Dichloroethane	10.4	0.127
Dichloromethane	9.1	0.042
Dimethyl sulfoxide	45	0.825
Dimethylformamide	37.7	0.161
Ethanol	24.3	0.941
Ethyl acetate	6	0.059
Hexane	1.9	0.02
Methanol	32.6	0.659
Tetrahydrofuran	7.4	0.047
Toluene	2.4	0.04
Water	80.4	0.123

23.1.3 Importance of MW in the synthesis of new anti-TB entities

There are four widely accepted primary objectives for improving TB therapy: (1) shortening and simplifying the treatment for active, drug-sensitive TB, (2) improving treatment efficacy, safety, and duration for drug-resistant disease, (3) improving the safety of co-therapy for TB patients coinfected with HIV, and (4) establishing an effective therapy for latent, persistent TB. The solutions achieving each of these goals will have different features, but there are some overarching issues that complicate each area of concern. Microwave (MW) irradiation has proven to be a highly effective

heating source for driving chemical reactions in sealed vessels. Microwaves can accelerate the reaction rate, provide uniform and selective heating, achieve greater reproducibility of reaction outcome and help in developing cleaner and greener synthetic routes [13].

23.1.3.1 Pyrimidine derivatives as antitubercular agents

The manifestation of various drug-resistant *Mycobacterium tuberculosis* (Mtb) strains has necessitated the development of a new drug candidate so as to decrease the resistance of existing drug therapies. By screening the Med Chem Express bioactive compound library, Ceritinib was identified as a compound with antimycobacterial activity against Mtb H37Ra. Ceritinib had a MIC value of 9.0 μM in vitro and demonstrated in vivo efficacy in a BALB/c mouse model infected with autoluminescent H37Ra. Then, novel ceritinib derivatives were synthesized, and their antimycobacterial activities were evaluated in vitro. The antimycobacterial activities of the synthesized compounds were drastically affected by substitutions at position 4 of the pyrimidine nucleus and were enhanced by the presence of 2-isopropoxy-5-methyl-4-(piperidin-4-yl)aniline at position 2 of the pyrimidine nucleus. The in vivo antitubercular activities of the three most potent compounds were evaluated. 5-Chloro-N2-(2-isopropoxy-5-methyl-4-(piperidin-4-yl)phenyl)-N4-(naphthalen-1-yl)pyrimidine-2.4-diamine (16j) remarkably reduced the Mtb burden of mice. This result suggested the potential of 16j as a novel drug with superior antitubercular activities. The results of experiments on the combination of sulfamethoxazole with 16j and in silico modeling suggested that dihydrofolate reductase is the potential molecular target of 16j (Fig. 23.3) [14].

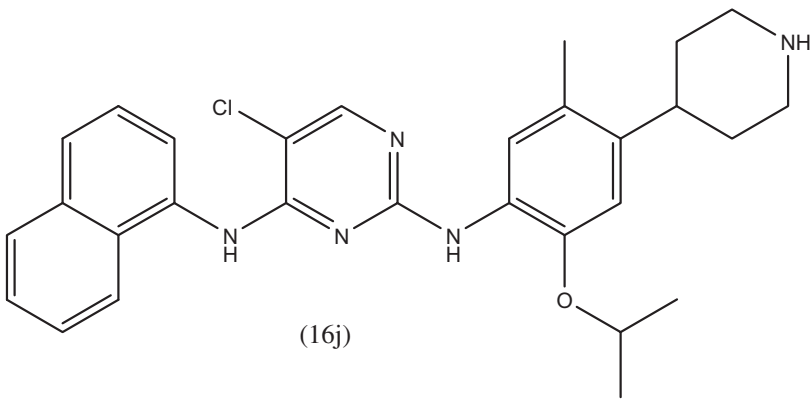

(16j)

Fig. 23.3 Structure of compound 16j.

A series of 1,2,3,4-tetrahydropyrimidine-5-carbonitrile derivatives was designed. The target compounds were synthesized by multicomponent reaction which involves one-pot organic reactions using ethyl cyanoacetate, urea/thiourea, and arylaldehydes

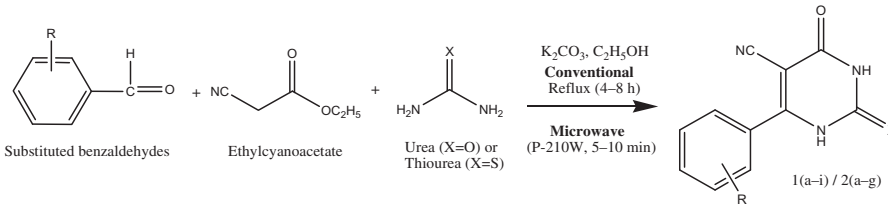

Scheme 23.1 Synthetic route for the preparation of 1,2,3,4-tetrahydropyrimidine-5-carbonitrile derivatives.

Table 23.3 Comparison between conventional and microwave-assisted synthesis.

Comp. code	Conventional method			Microwave-assisted method		
	Time (h)	Energy (temp. °C)	Yield (%)	Time (min)	Energy (power. watt)	Yield (%)
1a	4	98–100	61	5	210	82
1b	6	98–100	60	7	210	81
1c	6	98–100	59	7	210	80
1d	6	98–100	58	7	210	79
1e	6	98–100	61	7	210	82
1f	6	98–100	57	7	210	78
1g	6	98–100	58	7	210	79
1h	8	98–100	56	10	210	79
1i	8	98–100	56	10	210	77
2a	4	98–100	66	5	210	85
2b	6	98–100	65	7	210	85
2c	6	98–100	62	7	210	81
2d	6	98–100	60	7	210	79
2e	6	98–100	61	7	210	82
2f	6	98–100	57	7	210	78
2g	6	98–100	59	7	210	80

in the presence of ethanolic K_2CO_3 (Scheme 23.1 and Table 23.3). Two methodologies, conventional and microwave-assisted, were adopted for the synthesis. The later strategy gave high yields in <10 min as compared with long hours using the former approach. Molecular docking of the target compounds into the enzyme *Mycobacterium tuberculosis* enoyl reductase (InhA) revealed important structural information on the plausible binding interactions. Major binding interactions were found to be of dispersion type (residues Tyr158, Ile215, Met103, and Met199) and a hydrogen bond with Tyr158. Binding poses of all the compounds were energetically favorable and showed good interactions with the active site residues. Few selected compounds were also evaluated for antitubercular activity in vitro against drug-sensitive M. tuberculosis H37Rv strain and clinically isolated S, H, R, and E resistant M. tuberculosis by

luciferase reporter phage (LRP) assay method. Some compounds displayed promising antimycobacterial activity comparable to or less than the standard drugs isoniazid and rifampicin (Table 23.4). A compound was considered to be an antimycobacterial agent if a 50% reduction in the Relative Light Units (RLU) is observed when compared with the standard drug using luminometer [15].

Table 23.4 Antimycobacterial activity of the target compounds.

	% Reduction in RLU			
	M. tuberculosis H37Rv		Clinical isolate: S, H, R, and E resistant *M. tuberculosis*	
Compd. code	**100 µg/mL**	**500 µg/mL**	**100 µg/mL**	**500 µg/mL**
1b	46.49	44.20	38.38	47.86
1d	54.28	61.02	50.10	52.77
1i	33.40	48.72	25.47	33.49
2e	46.21	65.23	61.35	66.65
2g	75.73	82.04	38.03	74.91
Rifampicin (2 µg/mL)	82.58		29.19	
Isoniazid (0.5 µg/mL)	98.42		89.6	

A simple and efficient approach toward single-step synthesis of 6-amino-5-cyano-2-(hydroxy/mercapto)-4-substitutedpyrimidine derivatives was developed by three-component condensation of aromatic aldehydes, malononitrile, and urea or thiourea using conventional heating and microwave irradiation technique (Scheme 23.2). Some of these novel derivatives showed moderate to potent in vitro antitubercular activity (Table 23.5). The microwave-assisted synthesis was advantageous in simple reaction conditions and easy workup procedures, less time consuming, and eco-friendly which result in better yields over the conventional method. Both synthetic methods were compared in terms of percentage yield and reaction time (Table 23.6) [16].

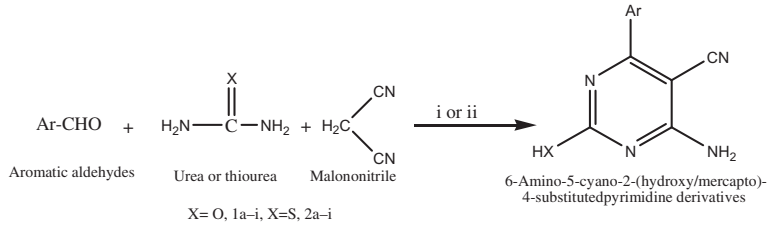

Reaction condition: i= Ethanol, Conc. HCl, Reflux, 1.5–3h (56%–81%) and ii= Ethanol, Conc. H_2SO_4, MWI, 2–3.5 min (64%–87%).

Scheme 23.2 Synthesis of 6-amino-5-cyano-2-(hydroxy/mercapto)-4-substituted-pyrimidine derivatives.

Table 23.5 Antitubercular activity of synthesized compounds (1a–1l and 2a–2l).

Compounds	Acid fast *M. tuberculosis* MIC (μg/mL)	Compounds	Acid fast *M. tuberculosis* MIC (μg/mL)
1a	>100	2a	>100
1b	>100	2b	>100
1c	<25	2c	>100
1d	>100	2d	>100
1e	>100	2e	>100
1f	>100	2f	>100
1g	>100	2g	>100
1h	>100	2h	>100
1i	>100	2i	>100
1j	<25	2j	50
1k	>100	2k	>100
1l	>100	2l	>100

Table 23.6 Comparison of microwave-assisted synthesis and conventional method in terms of percentage yield and reaction time.

Compounds	X	Ar	Conventional method		Microwave-assisted method	
			Time (h)	Yield (%)	Time (h)	Yield (%)
1a	O	C_6H_5-	3.0	78	3.5	84
1b	O	$C_6H_5CH{=}CH$-	2.5	60	3.0	67
1c	O	4-OHC_6H_4-	2.5	74	3.0	80
1d	O	2-Cl C_6H_4-	2.0	81	2.5	86
1e	O	4-Cl C_6H_4-	1.5	79	2.0	85
1f	O	4-$N(CH_3)_2$ C_6H_4-	1.5	74	2.0	81
1g	O	4-$OMeC_6H_4$-	1.5	77	2.0	83
1h	O	4-OH-3-OMe-C_6H_3-	2.5	62	3.0	69
1i	O	2-NO2C_6H_4-	1.5	81	2.0	87
1j	O	4-$NO_2C_6H_4$-	1.5	77	2.0	87
1k	O	3-OMe C_6H_4-	2.0	71	2.5	79
1l	O	3-NO_2 C_6H_4-	2.0	72	2.5	80
2a	S	C_6H_5-	3.0	75	3.5	83
2b	S	$C_6H_5CH{=}CH$-	2.5	56	3.0	64
2c	S	4-OHC_6H_4-	2.5	72	3.0	79
2d	S	2-Cl C_6H_4-	2.0	78	2.5	84
2e	S	4-Cl C_6H_4-	1.5	73	2.0	80
2f	S	4-$N(CH_3)_2$ C_6H_4-	1.5	76	2.0	83
2g	S	4-$OMeC_6H_4$-	1.5	71	2.0	78
2h	S	4-OH-3-OMe-C_6H_3-	2.5	64	3.0	70
2i	S	2-NO2C_6H_4-	1.5	79	2.0	85
2j	S	4-$NO_2C_6H_4$-	1.5	75	2.0	82
2k	S	3-OMe C_6H_4-	2.0	71	2.5	77
2l	S	3-NO_2 C_6H_4-	2.0	74	2.5	80

23.1.3.2 Thiadiazole derivatives as antitubercular agents

A series of imidazo[2,1-b][1,3,4]thiadiazole derivatives 5(a–j) were synthesized (Scheme 23.3). These compounds were evaluated for their in vitro antitubercular activity against *Mycobacterium tuberculosis* H37Rv strain using Alamar Blue susceptibility test as part of the TAACF TB screening program under the direction of the US National Institutes of Health, the NIAID division. Among the tested compounds, 2-(1-methyl-1H-imidazol-2-yl)-6-(4-nitrophenyl)imidazo[2,1-b][1,3,4]thiadiazole (5f) had shown the highest (98%) inhibitory activity with MIC of 3.14 μg/mL as compared with other tested compounds. Further, some potent compounds were also assessed for their cytotoxic activity against a mammalian Vero cell line using MTT assay. The results revealed that these compounds exhibit antitubercular activity at noncytotoxic concentrations as shown in Table 23.7 [17].

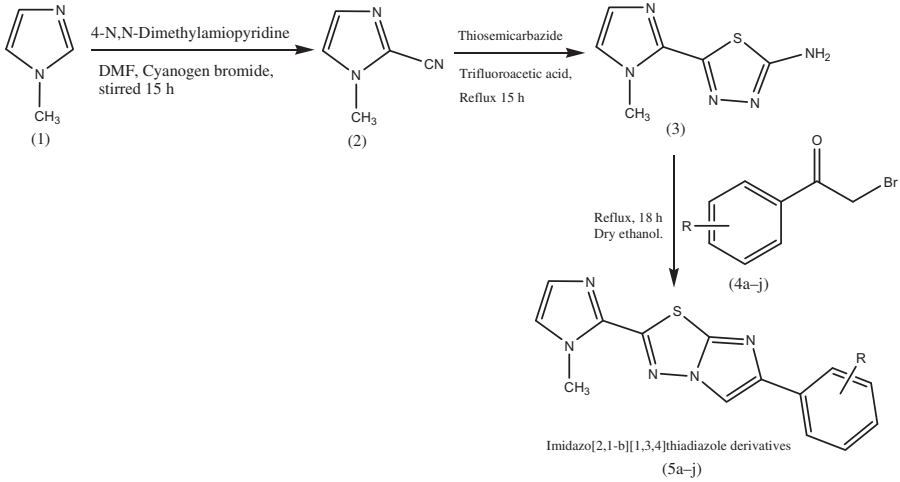

Scheme 23.3 Synthesis of imidazo[2,1-b][1,3,4]thiadiazole derivatives 5(a–j).

Table 23.7 In vitro anti-tubercular activity and cytotoxicity of compounds 5 (a–j).

Compounds	R	Inhibition (%)	Activity	MIC (μg/mL)	IC_{50}[a]	SI[b]
5a	3-Nitro	91	+	4.34	10.56	2.43
5b	4-Bromo	94	+	5.78	11.4	1.97
5c	4-Chloro	95	+	5.48	12.3	2.24
5d	4-Fluoro	90	+	4.86	8.5	1.74
5e	H	16	–	>6.25	–	–
5f	4-Nitro	98	+	3.14	9.8	3.12
5g	4-Methyl	18	–	>6.25	–	–
5h	5-Methyl	30	–	>6.25	–	–
5i	2,4-Dichloro	92	+	5.66	10.3	1.81
5j	2,4-Dihydroxy	35	–	>6.25	–	–

MIC Rifampicin: 0.125–0.25 μg/mL. SI (selectivity index) for Rifampicin >10.
[a]IC_{50} inhibition concentration (inhibited 50% of total cells in μM and converted into μg/mL for SI calculation).
[b]SI selectivity index (ratio between IC_{50} and *M. tuberculosis* MIC value).

23.1.3.3 Benzodiazepines derivatives as antitubercular agents

A series of 1,4-benzodiazepines derivatives were synthesized by condensation of *o*-phenylenediamines with 1,3-diketone (Dimedone) as illustrated in Scheme 23.4. Further, these synthesized derivatives were screened for their antitubercular property/activity. Among the tested compounds, potent activities were observed for compounds 9, 10 (MIC 1.6 μg/mL) followed by compound 11 (3.12 μg/mL), compound 04 (6.25 μg/mL) against *M. tuberculosis* H37Rv as summarized in Table 23.8 [18].

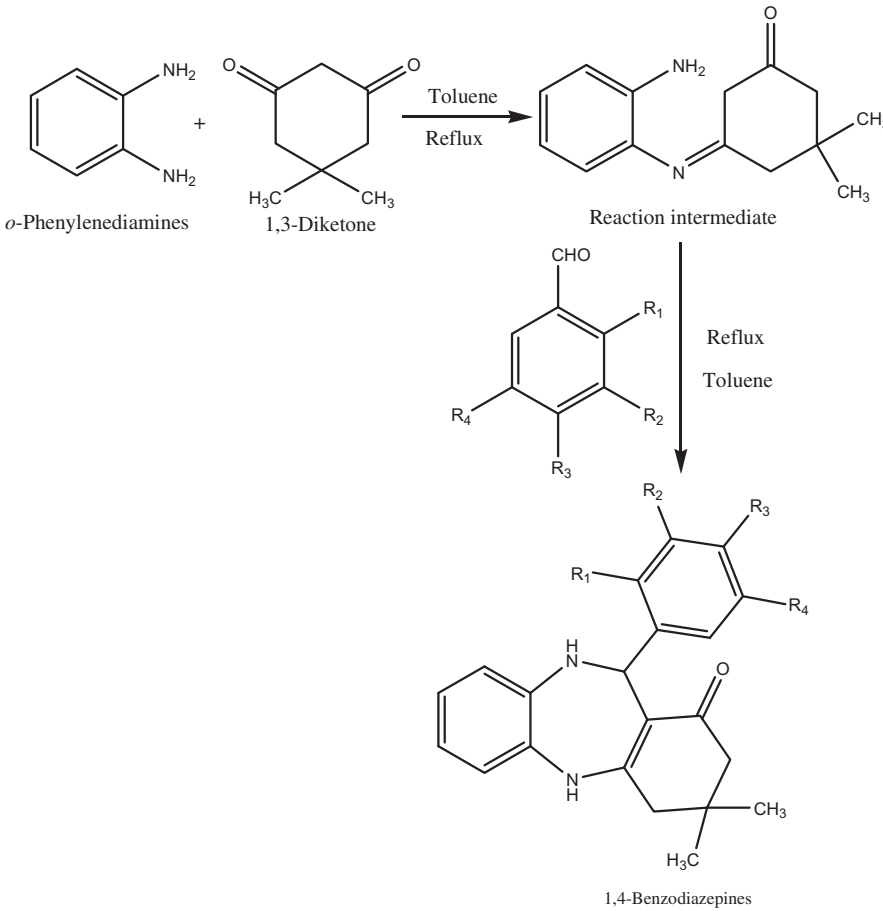

Scheme 23.4 Synthesis of 1,4-benzodiazepine derivatives (1–18).

Table 23.8 Anti-tubercular activity of 1,4-benzodiazepines derivatives.

Compound	R_1	R_2	R_3	R_4	MABA assay MIC (μg/mL)
1	H	H	H	H	12.5
2	H	H	$-OCH_3$	H	12.5
3	H	OH	H	H	25
4	H	H	-F	H	6.25
5	H	H	OH	H	100
6	H	H	-Br	H	50
7	$-OCH_3$	H	$-OCH_3$	H	25
8	H	H	$-NO_2$	H	25
9	H	$-OCH_3$	$-OCH_3$	H	1.6
10	H	H	$-N(CH_3)_2$	H	1.6
11	H	$-OC_2H_5$	OH	H	3.125
12	H	-F	-F	H	25
Pyrazinamide	–	–	–	–	3.125
Streptomycin	–	–	–	–	6.25
Ciprofloxacin	–	–	–	–	3.125

23.2 SAR study of 1,4-benzodiazepines derivatives

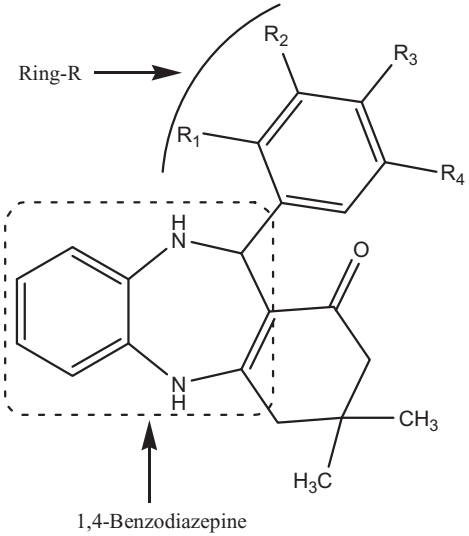

Based on the evaluation results obtained from antitubercular activity of 1,4-benzodiazepines derivatives, the following observations were made to determine the effect of structural features and the presence of substitution on the ring of 1,4-benzodiazepines derivatives.

- The substitution of electron-withdrawing groups like —F on the ring-R at para position increased anti-TB activity.
- Similarly the substitution of electron-donating groups at meta position like $-OC_2H_5$ on the ring-R slightly reduced anti-TB activity due to increase in alkyl chain.
- Substitution of electron-withdrawing groups like —Br, —Cl at ortho, meta, and para positions on the ring-R reduced anti-TB activity.
- The presence of benzodiazepine moiety was essential for antitubercular activity. The replacement of benzodiazepine with other heteronucleus diminished the activity.

23.2.1 Hydantoins as antitubercular agents

The synthesis of various 5-arylidene-2-thiohydantoins was carried out by condensation of 2-thiohydantoin with suitable aldehydes or ketones based on two methods. In the case of method-A, the reaction mixture was refluxed in the presence of acetic acid and anhydrous sodium acetate. In the case of method-B, the reaction was performed in the presence of toluene and ammonium acetate (Scheme 23.5). The synthesized compounds were screened for their antimycobacterial activity. Eight of those compounds exhibited >90% inhibition of *Mycobacterium tuberculosis* growth (Table 23.9) [19].

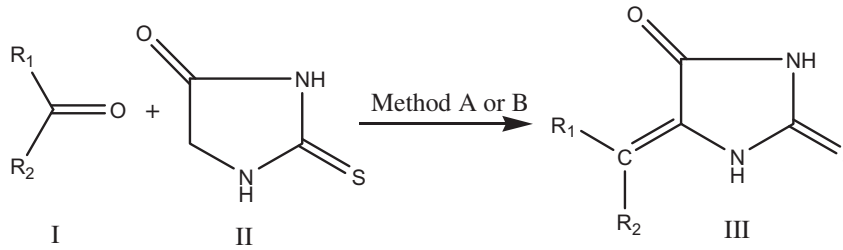

Scheme 23.5 Synthesis of 5-arylidene-2-thiohydantoins (III).

23.2.2 Chalcones as antitubercular agents

In order to develop relatively small molecules as antimycobacterial agents, 25 chalcones were synthesized (Fig. 23.4). The synthesis was based on the Claisen-Schimdt condensation reaction and the resultant compounds were tested for antitubercular activity by luciferase reporter phage (LRP) assay. Compound C_{24} was found to be the most active (~99%) in this series based on the percentage reduction in Relative Light Units at both 50 and 100 μg/mL levels. Four compounds at the 50 μg/mL and eight compounds at the 100 μg/mL showed activity above 90% level. QSAR model was developed between activity and spatial, topological, and

Table 23.9 Antimycobacterial activity of arylidene hydantoins.

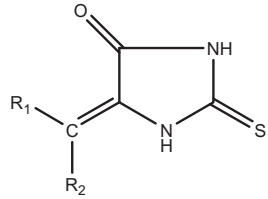

Comp.	R_1	R_2	% Inhibition at 6.25 µg/mL
33	H	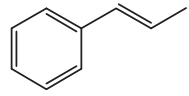	94
34	H	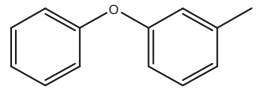	78
35	H	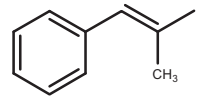	95
36	H	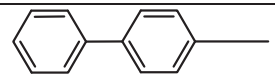	97
37	H	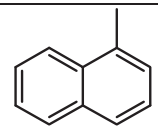	16
38	H	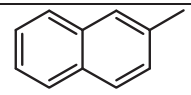	53
39	H	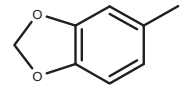	0
40	H	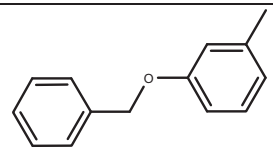	94

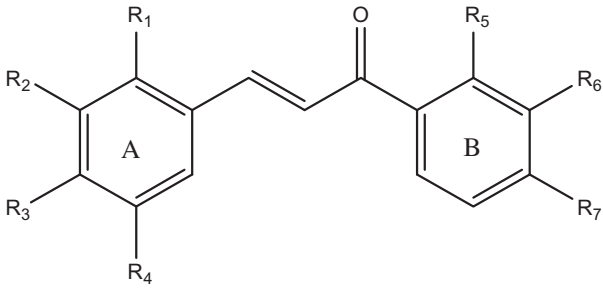

Fig. 23.4 Structure of chalcones.

ADME descriptors for the 50 μg/mL data. The statistical measures such as r, r2, q2, and F values obtained for the training set were in the acceptable range and hence this relationship was useful for the test set. The predictive ability of the model was satisfactory ($q2 = 0.56$) and it was used for designing a similar group of compounds [20].

Chalcones were synthesized by reacting substituted benzaldehydes and acetophenones in the presence of ethanolic sodium hydroxide (Scheme 23.6). These compounds were evaluated for antimycobacterial activity against *Mycobacterium tuberculosis* H37Rv. Ortho-chloro-substitutions at ring-A and -B favored the antitubercular activity. Compound 12 with chloro and hydroxyl substitution exhibited 98% reduction in relative light units at a concentration of 100 μg/mL. Methyl-sulfonyl chalcones also exhibited very good antitubercular activity (Scheme 23.7, Table 23.10). The requirements for the anti-infective activity were explored with 2D, 3D, and group-based QSAR studies. The 2D technique indicated the importance of volume, refractivity, and molecular weight of the compounds on the activity. The 3D-QSAR indicated less bulky at R_5 and more hydrophilic substituent groups at R_3 can improve the antitubercular activity. The GQSAR technique indicated that the presence of hydrophilic groups on R_3 or R_5 positions enhance the antitubercular activity. The oral bioavailability of all the molecules was between 30% and 70%. Compound 12 was mildly acidic, soluble in water, stable at $pH < 2$ and did not violate the Lipinski's rule of 5 [21].

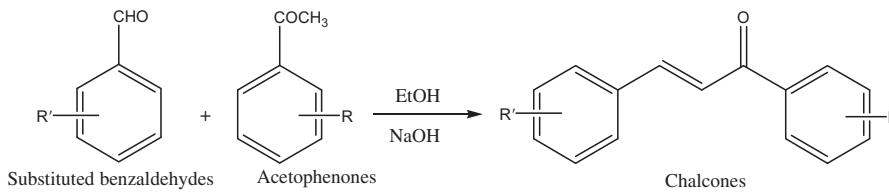

Scheme 23.6 Synthesis of chalcones.

Table 23.10 Antimycobacterial activity of chalcones.

Compd. no.	Percentage reduction in RLU	
	50 µg/mL	100 µg/mL
1	0	12.69
2	0	0
3	0	0
4	0	66.73
5	50.87	61.66
6	70.27	82.72
7	51.07	69.22
8	18.53	75.01
9	34.10	77.29
10	0	22.66
11	0	0
12	73.69	98.31
13	0	4.56
14	0	0
15	0	3.15

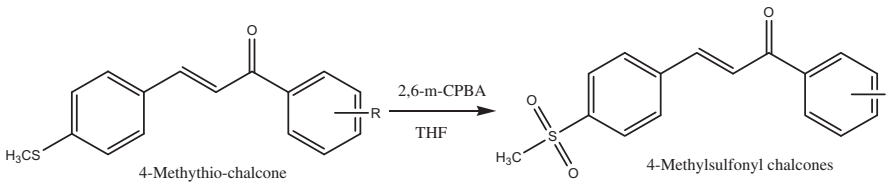

Scheme 23.7 Synthetic route for conversion of 4-methythiochalcone to 4-methylsulfonyl chalcones.

A series of chalcones (JC1–JC8) were synthesized by condensation of 9-anthraldehyde with various substituted acetophenones in the presence of ethanolic sodium hydroxide by using conventional and microwave heating method (Scheme 23.8). Better yield and decrease in reaction time were the advantages of the microwave when compared with the conventional methods (Table 23.11). These compounds (JC1–JC8) were evaluated for in vitro antitubercular activities. The antimycobacterial activity of compounds was determined by using the Microplate Alamar Blue assay (MABA) method. The final drug concentrations tested were 0.2–100.0 µg/mL and Streptomycin and Pyrazinamide were used as standards (Table 23.12). Among the tested compounds, compounds JC1 and JC3 showed promising antitubercular activity [22].

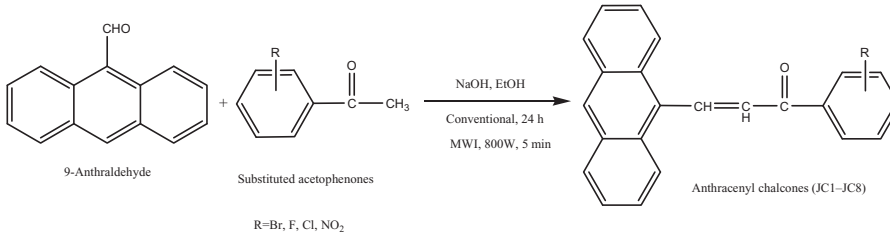

Scheme 23.8 Synthesis of chalcones (JC1–JC8).

Table 23.11 Reaction time and yield of conventionally and microwave-assisted synthesis.

Compounds	Conventional synthesis		Microwave-assisted synthesis	
	Time (h)	Yield (%)	Time (min)	Yield (%)
JC1–JC8	24	52–75	3–5	70–85

Table 23.12 Antitubercular activity of substituted chalcones (JC1–JC5).

Compound	R	MIC in µg/mL
JC1	4-Br	0.8
JC2	4-F	6.25
JC3	4-NO_2	0.8
JC4	4-Cl	50
JC5	4-NH_2	25
Pyrazinamide	–	3.125
Streptomycin	–	6.25

23.2.3 Quinoline derivatives as antitubercular agents

A series of styryl-quinoline derivatives (4a–j) was prepared by reacting quinaldic acid and a variety of aryl-benzaldehydes via Knoevenagel reaction in the presence of trifluoroacetic acid (TFA) as catalyst under eco-friendly conditions (Scheme 23.9). The final products were achieved in short reaction times with good yields. The synthesized compounds were evaluated for growth inhibitory activity toward *Mycobacterium tuberculosis* H37Rv (Mtb) through the National Institute of Allergy and Infectious Diseases (NIAID, USA) [23].

Microwave-assisted synthesis of 4-aminoquinoline-phthalimides was carried out in order to explore their antitubercular potential. Different reaction conditions were maintained by using both conventional and microwave heating. Synthesis of desired

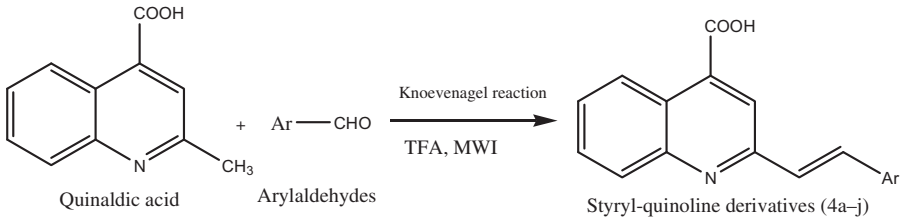

Scheme 23.9 Synthesis of styryl-quinoline derivatives (4a–j).

4-aminoquinoline-phthalimide (3a) was performed by the reaction between unsubstituted phthalic anhydride (1a) and 4-aminoquinoline-diamine (2a) as outlined in Scheme 23.10. The best results were obtained by microwave heating in DMSO at 160°C for 2 min to get the desired 4-aminoquinoline-phthalimides in quantitative yields (Tables 23.13 and 23.14). Antitubercular evaluation against mc^26230 strain of *Mycobacterium tuberculosis* revealed that compound 3e with octyl chain length as a spacer to be the most potent among synthesized compounds and exhibited MIC_{99} of 13.7 μM (Table 23.15). Most of the synthesized scaffolds exhibited good activity profiles with the activities being dependent on the nature of the substituent on the phthalimide ring as well as on the length of the alkyl chain [24].

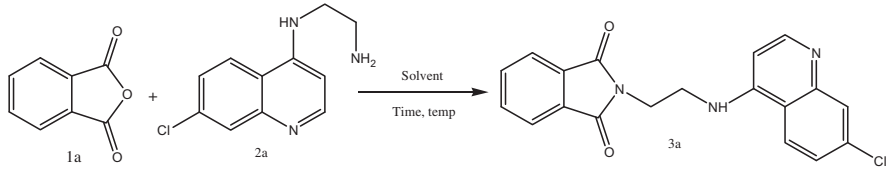

Scheme 23.10 Synthesis of 4-aminoquinoline-phthalimide (3a).

Table 23.13 Synthesis of 3a under both conventional and microwave heating.

Conventional heating				Microwave heating			
Solvent	**Time (h)**	**Temp. (°C)**	**Yield (%)**	**Solvent**	**Time (min)**	**Temp.**	**Yield (%)**
CH_3CN	6	80	22	CH_3CN	3	80	39
DMF	6	130	31	DMF	5	130	81
DMSO	8	160	51	DMSO	2	160	89
C_2H_5OH	6	80	34	AcOH	5	110	76
AcOH	6	110	50	NMP	5	140	88
NMP	7	150	50	–	–	–	–

Table 23.14 Synthesis of different 4-aminoquinoline-phthalimides (3b-y) under microwave heating.

Entry	R	*n*	Yield (%)	Entry	R	*n*	Yield (%)
3b	H	3	86	3n	4-F	6	84
3c	H	4	74	3o	4-F	8	88
3d	H	6	87	3p	3,4,5,6-Cl	2	92
3e	H	8	90	3q	3,4,5,6-Cl	3	91
3f	3-F	2	78	3r	3,4,5,6-Cl	4	90
3g	3-F	3	82	3s	3,4,5,6-Cl	6	85
3h	3-F	4	90	3t	3,4,5,6-Br	2	83
3i	3-F	6	79	3u	3,4,5,6-Br	3	81
3j	3-F	8	86	3v	3,4,5,6-Br	4	79
3k	4-F	2	89	3w	3,4,5,6-Br	6	74
3l	4-F	3	78	3x	3-NO_2	2	90
3m	4-F	4	77	3y	3-NO_2	6	82

Table 23.15 In vitro anti-tubercular activity of compounds (3a-y) against mc^26230 strain of *Mtb*.

Compound	$MIC_{99} \pm SD$ (μM)	Compound	$MIC_{99} \pm SD$ (μM)
3a	364	3n	66 ± 6
3b	329 ± 11	3o	31 ± 3
3c	158 ± 6	3p	>523
3d	34.3 ± 3	3q	270 ± 11
3e	13.7 ± 3	3r	232 ± 11
3f	692.3	3s	234.5
3g	354.3 ± 11	3t	192
3h	322	3u	188
3i	141 ± 6	3v	40.2 ± 3
3j	62 ± 3	3w	19.3 ± 3
3k	692.3	3x	>645.1
3l	354.3 ± 11	3y	132.4 ± 6
3m	302 ± 11	Isoniazid	0.14

23.2.4 Triazines as antitubercular agents

A series of triazines were synthesized starting from 5-alkyl-1,3,4-thiadiazole-2-thioles (1a–d). On reaction with ethyl bromoacetate in the presence of anhydrous K_2CO_3 under microwave irradiation (MWI), these yielded corresponding esters (2a–d) which on hydrazinolysis under MWI produced (5-alkyl-1,3,4-thiadiazol-2-yl sulfanyl) acetohydrazides (3a–d) as outlined in Scheme 23.11. The reaction of 3a–d with ω-bromoacetophenone under MWI yielded 6-aryl-3-[(5-alkyl-1,3,4-thiadiazol-2-yl-sulfanyl) methyl]-1.2,4-triazines (4a–h). All the synthesized triazines showed in vitro antitubercular activity and are summarized in Table 23.16 [25].

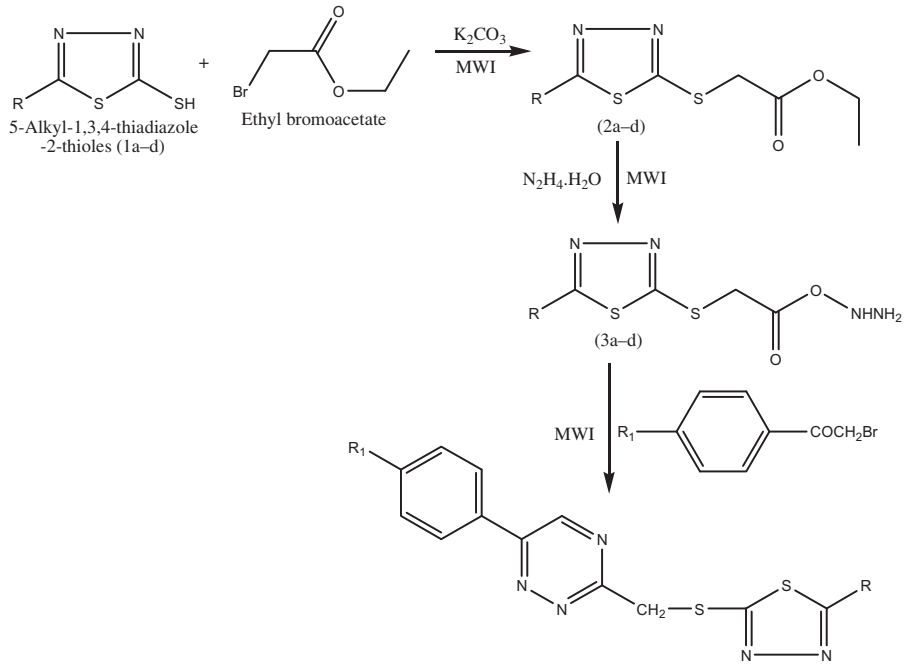

Scheme 23.11 Synthesis of 1,2,4-triazine derivatives (4a–h).

Table 23.16 Anti-tubercular activity data of compounds (4a-h).

Compound code	R	R_1	Minimum inhibitory concentrations (MIC) (μg/mL)
4a	CH_3	H	50
4b	C_7H_{15}	H	100
4c	C_9H_{19}	H	100
4d	$C_{11}H_{23}$	H	100
4e	CH_3	Cl	100
4f	C_7H_{15}	Cl	100
4g	C_9H_{19}	Cl	100
4h	$C_{11}H_{23}$	Cl	100

23.2.5 Phenothiazine analogs as antitubercular agents

A hybrid pharmacophore was designed containing phenothiazine moiety and the synthetic reaction conditions were optimized successfully with the help of a microwave synthesizer. First, phenothiazinyl-chalcones (2a–o) was obtained by reaction between

2-acetyl phenothiazine (1) with aryl aldehyde was placed in the presence of aqueous sodium hydroxide and a mixture of methanol: 1,4-dioxan. The reaction mixture was refluxed for 3–6 h to get the product. Then, pyrazolinyl-phenothiazines (3a–o) were produced by between phenothiazinyl-chalcone (2a–o), hydrazine hydrate and triethylamine in the presence of methanol. This reaction was performed by microwave heating in a Biotage initiator microwave synthesizer at 100°C for 5 min. As the reaction progresses to completion, the color of the reaction mixture changed from dark red to pale yellow. Similarly, microwave-assisted synthesis of phenyl pyrazolinyl-phenothiazines (4a–o) was carried out by reaction between phenothiazinyl-chalcone (2a–o), phenyl hydrazine, and DMAP in the presence of glacial acetic acid. The synthesis of isoxazolinyl-phenothiazines (5a–o) was preceded through a reaction between phenothiazinyl-chalcone (2a–o), hydroxylamine hydrochloride and DMAP in the presence of glacial acetic acid under Microwave irradiation (Scheme 23.12). Among all the synthesized compounds, 4b, 4e, 4i, and 4n exhibited potent in vitro antitubercular activity with MIC value 6.25 μg/mL and selectivity index >10 (Table 23.17) [26].

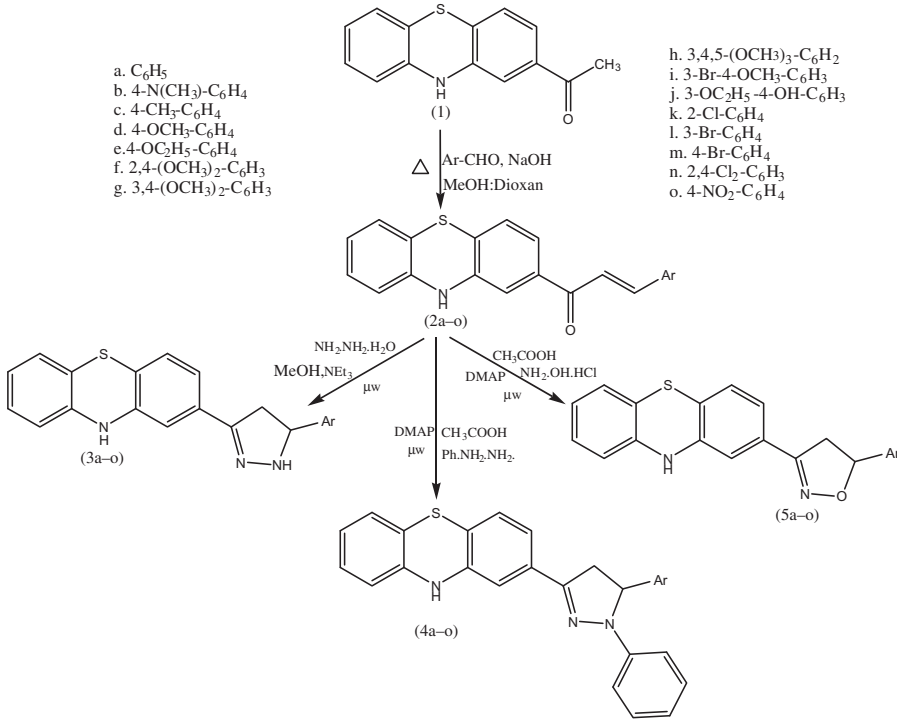

Scheme 23.12 Synthetic route for the preparation of series of phenothiazine analogs.

Table 23.17 Antimycobacterial activity of compounds in series.

Comp. code	C log P*	MIC** (μg/mL)	Comp. code	C log P*	MIC** (μg/mL)
2a	6.119	50	4d	7.925	12.5
2b	6.284	50	4e	8.454	6.25
2c	6.618	50	4f	8.014	12.5
2d	6.038	50	4g	7.664	12.5
2e	6.567	50	4h	7.306	12.5
2f	6.127	50	4i	8.698	6.25
2g	5.777	50	4j	7.717	25
3a	5.511	25	4k	8.719	12.5
3b	5.676	25	4l	8.869	12.5
3c	6.010	25	4m	8.869	12.5
3d	5.430	25	4n	9.432	6.25
3e	5.959	25	5a	6.385	25
3f	5.519	25	5b	6.55	12.5
3g	5.169	25	5c	6.844	12.5
4a	8.006	25	5d	6.304	12.5
4b	8.171	6.25	5e	6.833	12.5
4c	8.505	12.5	5f	6.393	12.5

*C log *P* values were calculated using Chem Draw Ultra 8.0 software; **MIC (μg/mL) for the standard drugs: Pyrazinamide-3.125; Streptomycin-6.25; Ciprofloxacin-3.125.

23.2.6 Benzocoumarin-benzothiazepine hybrids as antitubercular agents

An efficient and expeditious method was developed for the synthesis of benzocoumarin-benzothiazepine hybrids under microwave irradiation. The present methodology was cost effective in addition to other advantages like mild reaction condition, high yields of products in shorter reaction time and simple workup procedure (Scheme 23.13 and Table 23.18). All the newly synthesized compounds (2a–2j) were evaluated for their in vitro antitubercular and DNA cleavage study. Among all the screened compounds, 2 h showed the most pronounced activity against *Mycobacterium tuberculosis* (*Mtb*) obtaining MIC of 3.12 μg/mL (Table 23.19). The compounds

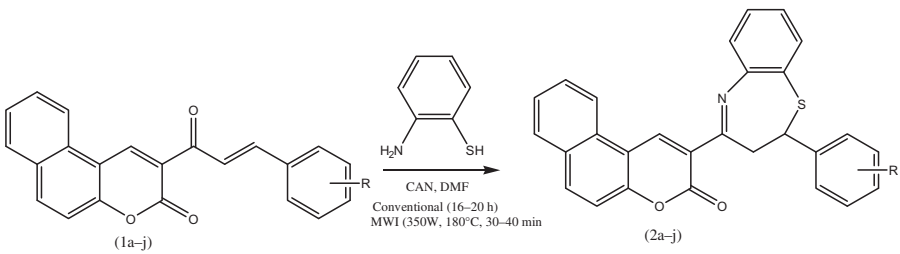

Scheme 23.13 Synthesis of benzocoumarin-benzothiazepine hybrids under MWI.

Table 23.18 Comparison between conventional and microwave irradiation method.

Products	R	Time (min)		Yield (%)	
		C[a]	M[b]	C	M
2a	*p*-CH_3	960	32	61	83
2b	*p*-OCH_3	960	30	63	85
2c	*m*-CH_3	980	37	58	77
2d	*m*-OCH_3	960	36	59	80
2e	*p*-Br	970	37	57	81
2f	*m*-Br	960	35	53	73
2g	*o*-Br	1200	40	43	69
2h	*p*-Cl	980	36	54	75
2i	*m*-Cl	1000	38	46	73
2j	*o*-Cl	990	37	45	72

[a]C, conventional.
[b]M, microwave.

Table 23.19 Tuberculosis inhibition test (Alamar).

Products	% Inhibition at 12.5 μg/mL	MIC (μg/ mL)
2a	54	960
2b	62	960
2c	51	980
2d	71	960
2e	90	970
2f	83	960
2g	77	1200
2h	97	980
2i	94	1000
2j	91	990
Isoniazid	–	0.03

were further subjected for DNA cleavage study by agarose gel electrophoresis method, which revealed that compound (2h) inhibits the growth of the pathogenic organism by cleaving the genome as no traces of DNA are found [27].

23.2.7 1,3,4-Oxadiazoles as antitubercular agents

A series of newer analogs of 5-(pyridine-4-yl)-1,3,4-oxadiazole-2(3H)-thione were designed and synthesized by incorporating 1,3,4-oxadiazole and bezo[*d*]thiazole by Mannich base reaction using conventional as well as microwave irradiation (Scheme 23.14). This process had considerable advantages such as milder reaction conditions, accelerated rate of reaction, less time consuming, and higher product yields as compared with the conventional heating methods (Table 23.20). The synthesized compounds were

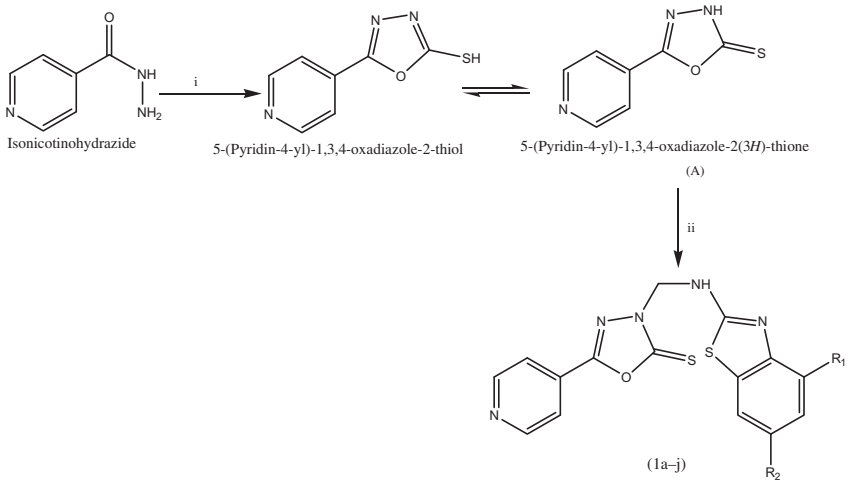

Reaction condition:

(i) Potassium-*o*-ethyldithicarbonate, IPA:MeOH, 80°C, 4 h.

(ii) Conventional: 37% HCHO, substituted-2-amino-benzo[*d*]thiazole, DMF:EtOH, 80°C, 8-9 h and Microwave: 37% HCHO, substituted-2-amino-benzo[*d*]thiazole, DMF:EtOH, 400 W, 10–12 min.

Scheme 23.14 Synthesis of 3-((substituted-benzo[*d*]thiazol-2-ylamino)methyl)-5-(pyridin-4-yl)-1,3,4-oxadiazole-2(3h)-thione.

Table 23.20 Comparison of conventional heating and nonconventional microwave technique.

Compound no.	R_1	R_2	Conventional method		Microwave irradiation	
			Reaction time (h)	Yield (%)	Reaction time (min)	Yield (%)
A	–	–	5	90	–	–
1a	H	H	8	63	10	85
1b	H	CH_3	8	66	10	82
1c	CH_3	H	8	59	10	80
1d	H	NO_2	9	58	12	75
1e	NO_2	H	9	55	12	78
1f	H	F	9	63	11	80
1g	F	H	8	60	10	75
1h	H	Br	8	58	10	78
1i	H	Cl	9	54	10	75
1j	H	OCH_3	8	60	10	80

evaluated for their antimycobacterial activity against *M. tuberculosis*. Among tested compounds, compound 1c containing methyl group at ortho-position on aromatic ring, showed better activity against M. tuberculosis H37Ra using MABA method (Table 23.21). So, the modification of substituents on bezo[*d*]thiazole ring with various electron-releasing and electron-withdrawing substituents affected the activity [28].

Table 23.21 In vitro antimycobacterium activity against *M. tuberculosis* H37Rv strain.

Compound no.	% Inhibition	MIC (μM)
A	0	>100
1a	66	>50
1b	6	>100
1c	100	>50
1d	65	>50
1e	10	>100
1f	21	>100
1g	3	>100
1h	16	>100
1i	0	>100
1j	30	>100
Isoniazide	99	0.25
Rifampicin	99	40

Benzofuran-oxadiazole derivatives 7(a–o) were designed, synthesized, characterized, and evaluated for antitubercular activity against *Mycobacterium tuberculosis* H37RV and *Mycobacterium phlei* using the Microplate Alamar Blue Assay (MABA) method. The structure-activity relationship (SAR) study results revealed that the compounds with chlorine (7j, 7k) and bromine (7l, 7m) on benzofuran ring exhibit excellent activity (Schemes 23.15 and 23.16). The MIC ranges were in between 1.56 and 100 μg/mL. The highest activity of 7m was superior to standard drug pyrazinamide and it was further supported by molecular docking results (Table 23.22) [29].

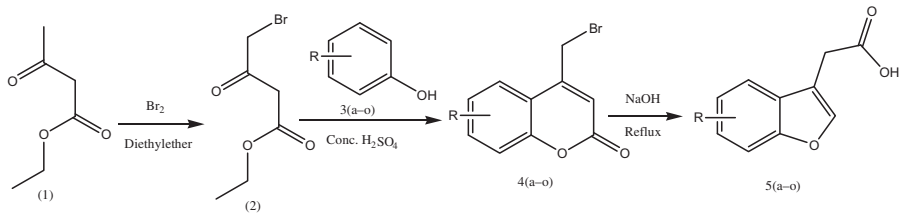

Scheme 23.15 Synthesis of benzofuran acetic acids 5(a–o).

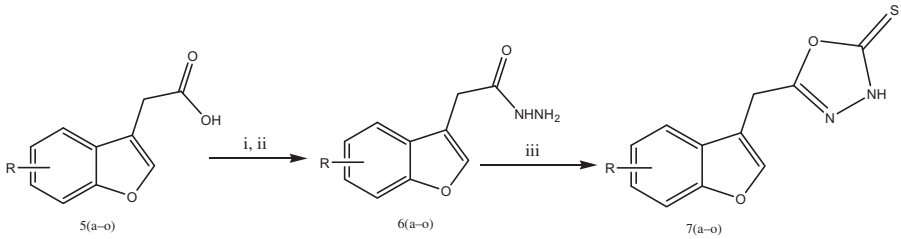

Scheme 23.16 Synthesis of benzofuran-oxadiazoles 7(a–o).

Table 23.22 Antitubercular activity of compounds 7(a-o).

Compounds	MICs (μg/mL)	
	***Mycobacterium tuberculosis* (H37RV)**	***Mycobacterium phlei***
7a	12.5	>100
7b	12.5	>100
7c	25	50
7d	12.5	50
7e	12.5	50
7f	12.5	50
7g	6.25	12.5
7h	6.25	25
7i	6.25	25
7j	3.125	3.125
7k	3.125	3.125
7l	3.125	3.125
7m	1.56	1.5
7n	25	50
7o	25	50
Pyrazinamide	3.125	3.125
Streptomycin	6.25	6.25

23.2.8 Benzothiazoles as antitubercular agents

Benzothiazole-2-carboxy-arylalkyl-amides were reported as a new class of potent antimycobacterial agents (Fig. 23.5). In all, target compounds were synthesized following a green synthetic strategy using water as the reaction medium to construct the benzothiazole scaffold followed by (i) microwave-assisted catalyst-free and (ii) ammonium chloride-catalyzed solvent-free amide coupling. The antimycobacterial potency of the compounds was determined against $H_{37}Rv$ strain.

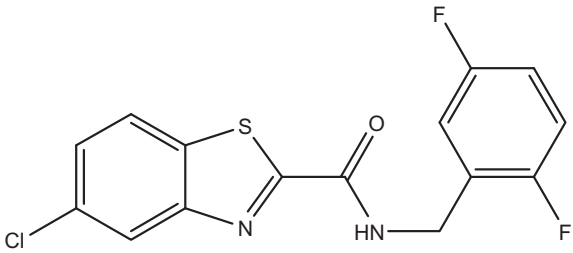

Fig. 23.5 Structure of N-(2,5-difluorobenzyl)-5-chlorobenzo[*d*]thiazole-2-carboxamide (5bf).

A total of 12 compounds exhibited promising anti-TB activity in the range of 0.78–6.25 μg/mL and were found to be nontoxic (<50% inhibition at 50 μg/mL) to HEK 293T cell lines with therapeutic index (TI) of 8–64. The most promising anti-TB compound 5bf showed MIC of 0.78 μg/mL (TI > 64). The molecular docking studies of 5bf predicted it to be a ligand for the *M. tuberculosis* HisG, the putative drug target for tuberculosis and could serve as a guiding principle for lead optimization [30].

23.2.9 Indole analogs as antitubercular agents

A rapid, efficient and environmentally benign synthesis of novel indole analogs bearing thiazolidinone attached to substituted thiazolyl coumarin scaffolds were synthesized (Scheme 23.17). Both conventional and microwave-assisted (MW)

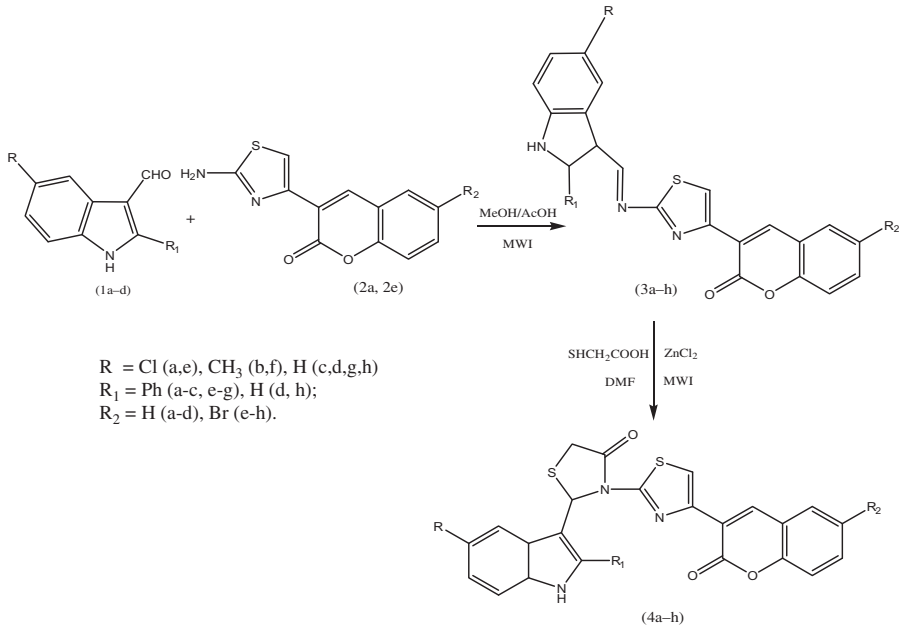

Scheme 23.17 Synthetic approach to new indole analogs.

approaches were studied. The newly synthesized compounds were evaluated for in vitro antitubercular activities against *M. tuberculosis* H37Rv strain (ATCC No-27294) using Alamar blue (MABA) minimum inhibitory concentration (MIC) assays. MIC for the compounds of highest activity was performed at different concentrations (0.8, 1.6, 3.12, 6.25, 12.5, 25, and 100 μg/mL). The results of MIC of the tested compounds revealed that the compound 4e substituted with the electron-withdrawing groups (Cl and Br) at C5 position of indole and C6 of coumarin moiety demonstrated MIC at the lowest concentration (12.5 μg/mL) against M. tuberculosis H37Rv as compared with the standards INH, PZA, STM, and CPF. Some of the screened compounds demonstrated promising anti-TB properties. The structure-activity relationship (SAR) study revealed that the compounds containing halogens are most potent. Docking of the potent compounds inside the active site of a target enzyme mycobacterial enoyl reductase (InhA) (PDB code 4TZK) was performed to determine their potentials [31].

23.2.10 Piperazines as antitubercular agents

Parallel solid-phase synthesis offers a unique opportunity for the synthesis and screening of large numbers of compounds and significantly enhances the prospect of finding new lead molecules. The synthesis and antitubercular activity of chiral 1,2,4-trisubstituted piperazines derived from resin-bound acylated dipeptides against Mycobacterium tuberculosis strain H37Rv were reported (Scheme 23.18). The minimum inhibitory concentration (MIC) of each compound was determined as the concentration required to prevent growth as measured by optical density (OD) of the culture [32].

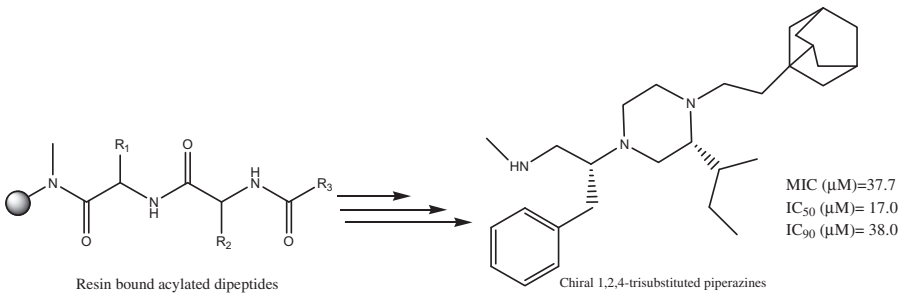

Scheme 23.18 Synthesis of chiral 1,2,4-trisubstituted piperazines.

23.2.11 Pyrazolines as antitubercular agents

Two new series of pyrazolines (3a–h and 4a–h) were synthesized starting from *p*-acetamidophenol (paracetamol) and evaluated for their antitubercular activity. Chalcones (2a–h) were prepared by condensation of 3-acetyl-4-hydroxyphenyl

acetamide (1) with different aromatic aldehydes. Finally, compounds (2a–h) underwent reaction with phenyl hydrazine and isonicotinic acid hydrazide to get phenylpyrazolines (3a–h) and isoniazid-pyrazolines (4a–h) respectively (Scheme 23.19). The results of antitubercular activity of the synthesized compounds against Mycobacterium tuberculosis H37Rv by the agar microdilution method were promising [27]. The results of the antitubercular activity of the titled compounds were presented in Table 23.23. Among the 16 tested compounds, three compounds, 4c, 4d, and 4g were found to be the most active compounds with MIC of 3.12 μg/mL as compared with

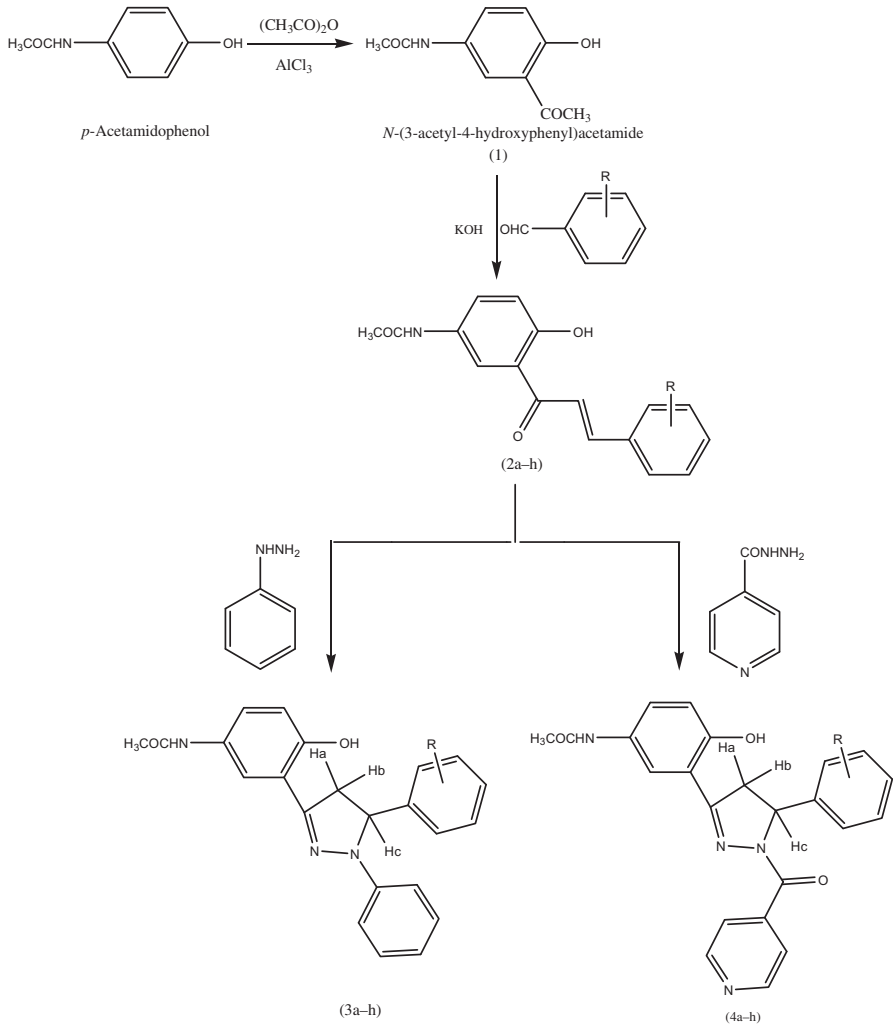

Scheme 23.19 Protocol for synthesis of pyrazoline derivatives (3a–h and 4a–h).

Table 23.23 Results of antitubercular activity of the pyrazoline compounds.

Compounds	R	*M. tuberculosis* MIC in μg/mL
3a	H	25
3b	-3-Cl	6.25
3c	-4-Cl	12.5
3d	-2,4-Cl_2	6.25
3e	2-OH	25
3f	2-NO_2	12.5
3g	4-NO_2	6.25
3h	3-OCH_3	12.5
4a	H	50
4b	-3-Cl	25
4c	-4-Cl	3.12
4d	-2,4-Cl_2	3.12
4e	2-OH	12.5
4f	2-NO_2	6.25
4g	4-NO_2	3.12
4h	3-OCH_3	6.25
Streptomycin	–	6.25

standard drug Streptomycin against M. tuberculosis bacteria (MTB). Five more compounds, 3b, 3d, 3g, 4f, and 4h showed excellent antitubercular activity with MIC 6.25 μg/mL [33].

23.2.12 Benzimidazoles as antitubercular agents

Aryl-benzimidazoles were synthesized as antimycobacterial agents. An efficient synthesis was developed for 2-arylbenzimidazoles from *o*-phenylenediamines and aromatic aldehydes in molecular sieves-methanol system. The methodology was straightforward to obtain 2-arylbenzimidazoles (3a–3z) in excellent yields with high chemo-selectivity over 2-aryl-1-benzyl-benzimidazoles (4a–4z) (Scheme 23.20). All these benzimidazole analogs were evaluated against *M. tuberculosis* in BACTEC radiometric assay. The compounds 4y and 4z exhibited potential antitubercular activity against *M. tuberculosis* $H_{37}R_V$ with MIC at 16 and 24 μM, respectively. Compound 4y was well tolerated by Swiss-albino mice in acute oral toxicity. Compound 4y with diaryl-benzimidazole core can be further optimized for better activity [34].

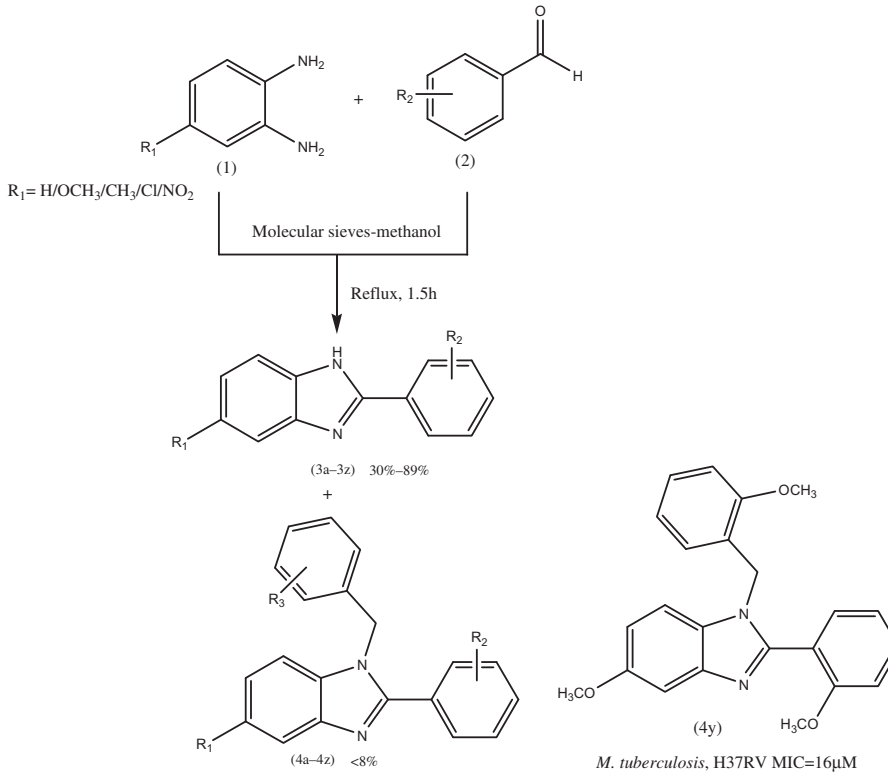

Scheme 23.20 Synthesis of benzimidazole derivatives.

A series of benzimidazole derivatives (1–20) were synthesized and evaluated for antitubercular activities (Scheme 23.21). The compounds which were active in in vitro evaluation against *M. tuberculosis* are further evaluated for their in vivo activity in mice (Table 23.24). It was observed that the dose of the compounds with 5.67 mg/kg in antitubercular evaluation is proved to be fatal and highly toxic to mice while lethal dose was varied from 1.82 mg/kg to 3.23 mg/kg body weight of the mice. The dose of 1.34 mg/kg was found to be safe for each of the compounds. All compounds inhibited the mycobacterial enzymes but to a lesser extent than streptomycin. Compound 19 exhibited inhibition of 67.56%, 53.45%, and 47.56% against isocitrate lyase, pantothenate synthetase, and chorismate mutase, respectively, and was found to be the most potent antitubercular compound among the synthesized benzimidazole derivatives [35].

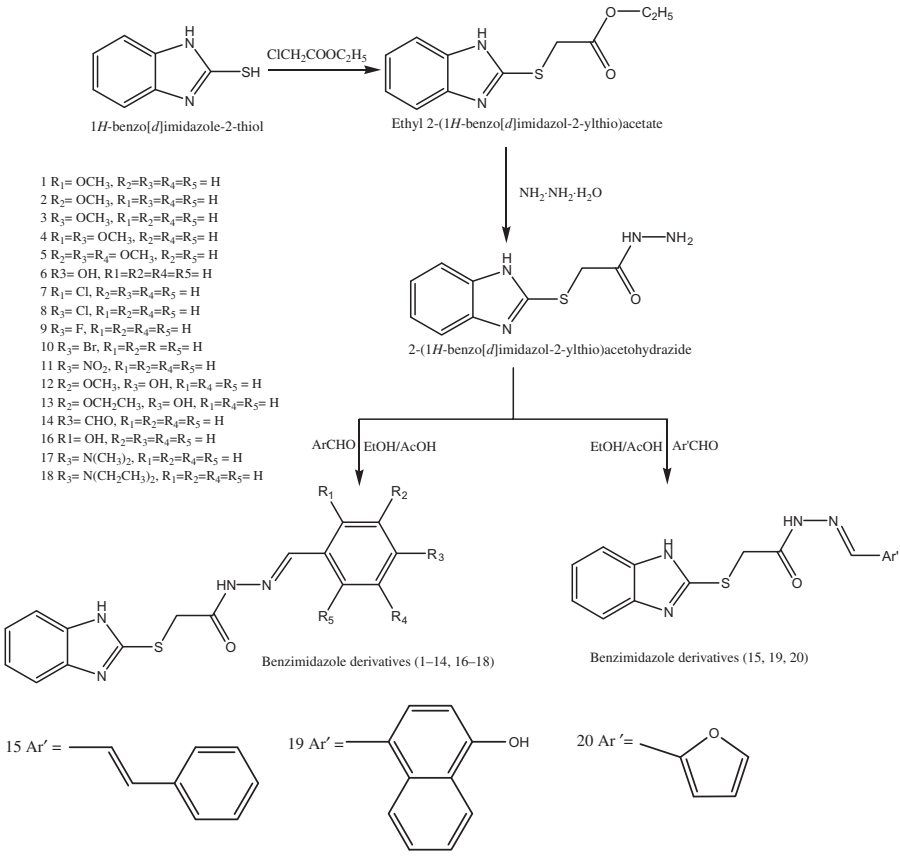

Scheme 23.21 Synthesis of benzimidazole derivatives (1–20).

Table 23.24 Antimycobacterial activity, MIC and MLC of synthesized compounds against M. tuberculosis H37Rv.

Compound no.	MIC in µg/mL	MLC in µg/mL
1	NA	NA
2	12.5	25
3	12.5	25
4	12.5	25
5	12.5	25
6	NA	NA
7	NA	NA
8	NA	NA
9	15	28
10	NA	NA
11	NA	NA

Table 23.24 Continued

Compound no.	MIC in μg/mL	MLC in μg/mL
12	12.5	25
13	12.5	25
14	15	25
15	NA	NA
16	NA	NA
17	12.5	25
18	12.5	25
19	12.5	25
20	NA	NA
Streptomycin	12.5	25

NA, not active.

23.3 Structure-activity relationship (SAR) study

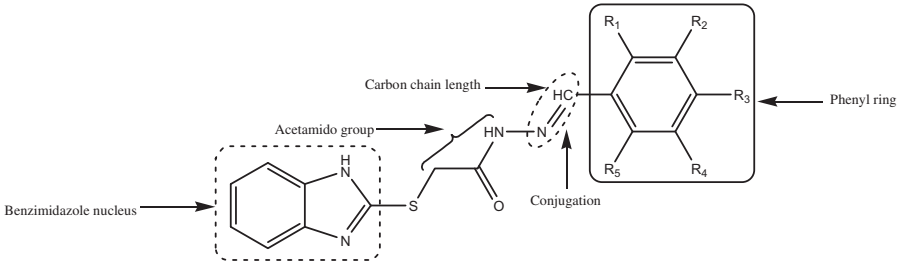

From the results of antitubercular activity of synthesized benzimidazole derivatives (1–20), the following points were considered for the SAR study.

- The synthesized benzimidazole derivatives had good binding interaction with target sites and thereby produce good activity.
- Replacement of phenyl ring with *p*-hydroxy-naphthol (compound 19) increased the antitubercular activity.
- There was a significant increase in antitubercular activity by increasing the chain length and conjugation as in the case of a compound synthesized using cinnamaldehyde.
- The substitution of hydroxyl group at ortho-position generated compound with better activity but di- and tri-substitution on phenyl ring decreased the activity.
- The substitution of electron-withdrawing groups like CF_3, NO_2, or halogens at para position of the phenyl ring (compound 10) enhanced the biological activity.

23.3.1 Pyridine derivatives as antitubercular agents

A series of reduced lipophilic N-benzylic-imidazo[1,2-*a*]pyridine-carboxamides (IPAs) with various side chains were designed and synthesized as new antitubercular agents. Five derivatives A2, A3, A4, B1, and B9 exhibited excellent in vitro activity (MIC: <0.035 μM) against Mycobacterium tuberculosis H37Rv strain and two clinically isolated multidrug-resistant strains. Compound B1 possessed cyclohexylmethyl piperazine moiety and the same side chain was also present in PBTZ169 and Q203 (Figs. 23.6 and 23.7). From the activity study, it was observed that compound B1 has greater $AUC_{0-\infty}$ and Cmax as compared with PBTZ169 and Q203. This result suggested that compound B1 may become a promising potential lead molecule for antitubercular drug development in the future [36].

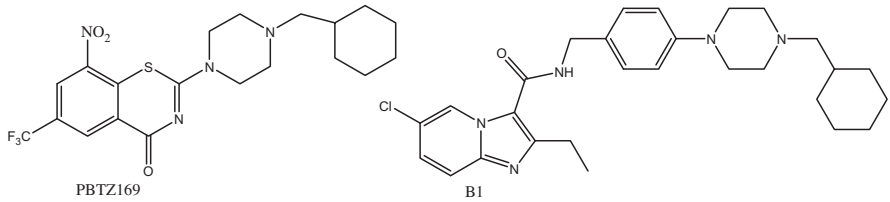

Fig. 23.6 Structure of PBTZ169 and compound B1.

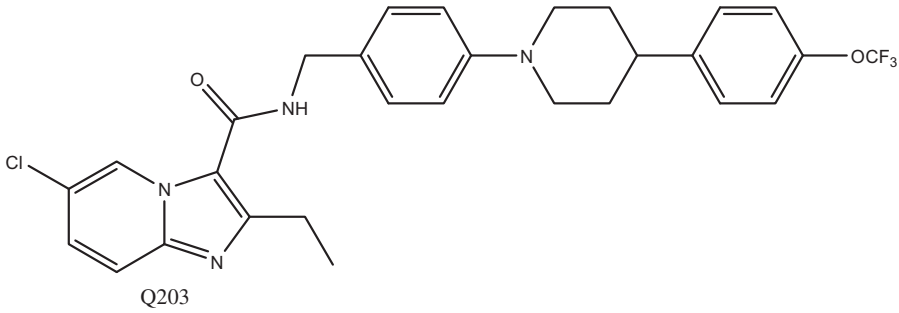

Fig. 23.7 Structure of Q203.

23.3.2 Thiazolidine derivatives as antitubercular agents

The green protocol has developed for the synthesis of 1,3-thiazolidin-4-ones in excellent yields. This method was highly efficient which involves solvent-free, one-pot, multicomponent reaction between aryl amines, aryl aldehydes, and 2-mercaptoacetic acid, catalyzed by $[Et_3NH][HSO_4]$ as outlined in Scheme 23.22. The synthesized compounds were evaluated in vitro for their antimycobacterial activity against *Mycobacterium tuberculosis* dormant *MTB H37Ra* and *Mycobacterium bovis BCG* strains. Among the tested compounds, mainly compounds 4c, 4d, 4e, 4f, 4h, 4i, and 4j exhibited promising antitubercular activity along with no significant cytotoxicity against the cell lines MCF-7, A549, and HCT-116 [37].

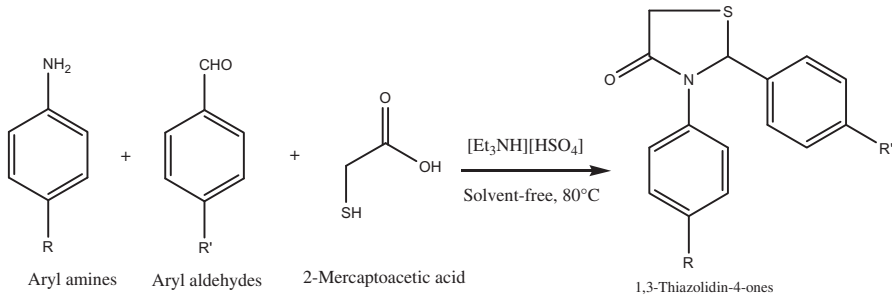

Scheme 23.22 Synthesis of 1,3-thiazolidin-4-ones.

23.3.3 1,3-Oxazole derivatives as antitubercular agents

Tuberculosis treatment remains a challenge that requires new antitubercular agents due to the emergence of multidrug-resistant Mycobacterium strains. A series of new 2,5-dimethyl-4-(aryl or heteroaryl) substituted-aniline-1,3-oxazole derivatives were synthesized by C-N coupling (Buchwald coupling) reaction. This reaction involved coupling of 4-(4-bromophenyl)-2,5-dimethyloxazole [obtained by the bromination reaction of 1-(4-bromophenyl)propan-1-one and further cyclization reaction with acetamide under microwave] with substituted aryl or heteroaryl-amine in the presence of Tris (dibenzylidene acetone) di-palladium, BINAP, and cesium carbonate in toluene (Scheme 23.23). All the compounds were screened for their in vitro antimycobacterial activity against mycobacterium tuberculosis (MTB) H37Rv. Isoniazid and thiacetazone were used as standard drugs. Some of the compounds exhibited significant antitubercular activity [38]. The results of the antitubercular studies are presented in Table 23.25.

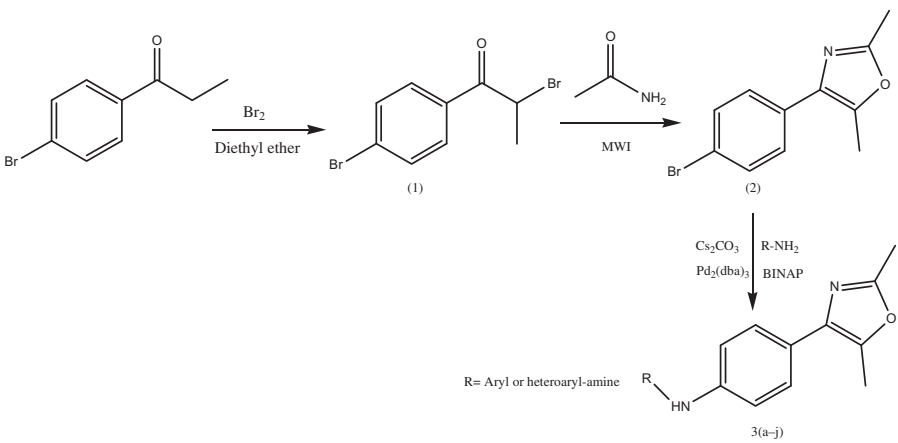

Scheme 23.23 Synthesis of 1,3-oxazole derivatives.

Table 23.25 In vitro antimycobacterial activity of titled compounds (3a–j).

Compounds	R	MIC(μg/mL)
3a	2,5-Dichloroaniline	11.1
3b	3-Amino-6-chloropyridazine	18.3
3c	2-Amino pyrazine	25.8
3d	2-Chloro-5-fluoroaniline	9.7
3e	2-Chloro-4-(trifluoromethyl) aniline	15.4
3f	4-Chloro-2-methylaniline	22.3
3g	2,4-Dichloroaniline	19.2
3h	2-Chloro-5-(trifluoromethyl) aniline	3.4
3i	2-Fluoroaniline	2.1
3j	3-Chloro-4-methylaniline	8.5
Isoniazid	–	0.125
Thiacetazone	–	0.138

23.3.4 Pyrazinamide-Mannich bases as antitubercular agents

A series of pyrazinamide (PAZ) Mannich bases were synthesized by reacting PAZ, formaldehyde, and various substituted piperazines using microwave irradiation with the yield ranging from 46% to 86% (Fig. 23.8). The synthesized compounds were evaluated for antimycobacterial activity in vitro and in vivo against *Mycobacterium tuberculosis* H37Rv (MTB). Among the tested compounds, compound **17** [1-cyclopropyl-6-fluoro-1,4-dihydro-8-methoxy-7-(3-methyl-4-((pyrazine-2-carboxamido)methyl)piperazin-1-yl)-4-oxoquinoline-3-carboxylic acid] was found to be the most active compound in vitro with MIC of 0.39 and 0.2 μg/mL against MTB and multidrug-resistant MTB, respectively. In the in vivo animal model **17** decreased the bacterial load in lung and spleen tissues with 1.86 and 1.66-log 10 protections, respectively [39].

Fig. 23.8 Structure of pyrazinamide (PAZ) Mannich bases.

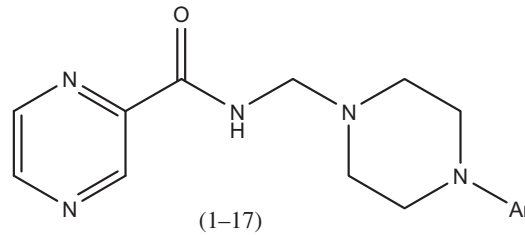

(1–17)

23.3.5 1,2,3-Triazoles as antitubercular agents

It was observed that antifungal azoles such as econazole and miconazole are active against Mtb through interactions with CYP130 in Mtb. In particular, econazole had encouraging activity profiles against Mtb and MDR-TB. Triazoles were also used very

often in the medicinal applications. For instance, a variety of 1H-1,2,3-triazole compounds had antitubercular activity. It was reported that enantiomerically pure 1H-1,2,3-triazole analogs tethered with imidazole are active against Mtb (Fig. 23.9). Encouraged by these results and the background information mentioned above, the feasibility of 1H-1,2,3-triazole compounds derived from econazole as a novel scaffold for antitubercular agents was designed [40].

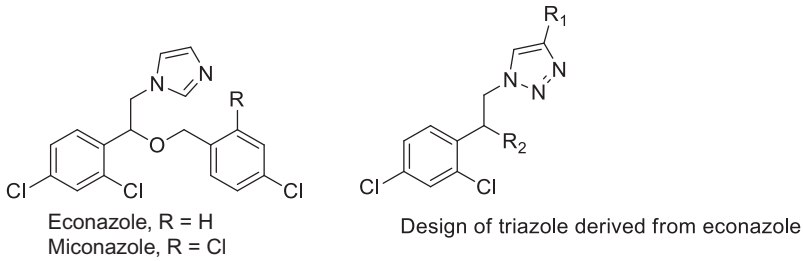

Fig. 23.9 Design of triazole from econazole.

23.4 Future perspective

The developments of drugs for the treatment of tuberculosis become emerged area in the drug discovery process. Several targets have been identified for different antitubercular drugs to treat M. tuberculosis. The mechanisms of action of drugs toward various targets are studied to inhibit the growth of mycobacterium. Various targets in the growth phase are GIgE (maltose metabolism), mycolic acid (mycolic acid metabolism), DprE1/DprE2 (cell wall metabolism), MshC (mycothiol ligase), HisG (histidine biosynthesis), and AtpE (ATP synthesis). Some targets of dormant phase are isocitrate lyase (energy metabolism), proteosome complex (protein processing), L,D-transpeptidase (peptidoglycan metabolism), DosR (DevR) (regulation of dormancy) and CarD (stringent response). Most of the advances in new TB target identification have been directed by the genome sequence of *M. tuberculosis*. However genome-derived target-based approach has less success rate. Currently, the global TB development pipeline has nine candidates in different stages of the clinical trial. These pipelines are: PNU 100480 (protein synthesis inhibitor), AZD 5847(protein synthesis inhibitor), SQ 109 (cell wall and multi-target inhibitor), OPC67683 (cell wall and multi-target inhibitor), PA824 (cell wall and multi-target inhibitor), gatifloxacin (DNA gyrase inhibitor), moxifloxacin (DNA gyrase inhibitor), and TMC 207 (ATP synthase inhibitor). Some of them are active in the latent stage and active form against MDR-TB and XD-TB. Most of current pipeline TB drugs were developed using molecular modification strategies. The fluorquinolones derivatives gatifloxacin and moxifloxacin were derivatized scaffolds from the parent nalidixic acid using the bioisosterism as a molecular modification. Molecular modification is an important tool to discover new compounds to treat

Mycobacterium tuberculosis infection. The use of this strategy has allowed identifying more active and safe compounds with broad-spectrum activity against MDR and XDR-TB.

23.5 Conclusion

Microwave has revolutionized the way of heating is now accomplished. This heating method improves cost-efficiency by completing transformations quickly with lower amounts of waste and recovered starting materials. This technology holds the potential to offer a cost-effective pathway for the production of drug molecules with diverse structures. During production processes, there is use of environmentally benign solvents, reduced volumes of solvents and reagents and reduced heating or energy costs. Modification of substituents on aryl rings with various electron-releasing and electron-withdrawing groups affect the antitubercular activity.

Acknowledgments

Bimal K. Banik is grateful to Prince Mohammad Bin Fahd University.

References

[1] C.J. Queval, R. Brosch, R. Simeone, Mycobacterium tuberculosis, Front. Microbiol. 8 (2017) 2284.
[2] J.A. Caminero, A. Scardigli, Classification of anti-tuberculosis drugs: a new proposal based on the most recent evidence, Eur. Respir. J. 46 (2015) 887–893.
[3] A. Rattan, A. Kalia, N. Ahmad, Multidrug-resistant Mycobacterium tuberculosis: molecular perspectives, Emerg. Infect. Dis. 4 (1998) 195.
[4] L.C. Santos, The molecular basis of resistance in Mycobacterium tuberculosis, Open J. Med. Microbiol. 2 (1) (2012) 24.
[5] J. Palomino, A. Martin, Drug resistance mechanisms in Mycobacterium tuberculosis, Antibiotics 3 (3) (2014) 317–340.
[6] A. Koul, E. Arnoult, N. Lounis, J. Guillemont, K. Andries, The challenge of new drug discovery for tuberculosis, Nature 469 (7331) (2011) 483.
[7] M. De Rosa, J. Gising, L.R. Odell, M. Larhed, Syntheses of new tuberculosis inhibitors promoted by microwave irradiation, Ups. J. Med. Sci. 119 (2) (2014) 181–191.
[8] M. Gaba, N. Dhingra, Microwave chemistry: general features and applications, Indian J. Pharm. Educ. Res. 45 (2) (2011) 175–183.
[9] R. Gedye, R. Smith, K. Westaway, H. Ali, L. Baldisera, et al., The use of microwave ovens for rapid organic synthesis, Tetrahedron Lett. 27 (1986) 279–282.
[10] S. Sadler, A.R. Moeller, G.B. Jones, Microwave and continuous flow technologies in drug discovery, Expert Opin. Drug Discovery 7 (12) (2012) 1107–1128.
[11] A.K. Mahato, B.M. Sahoo, B.K. Banik, B.C. Mohanta, Microwave-assisted synthesis: paradigm of green chemistry, J. Indian Chem. Soc. 95 (11) (2018) 1327–1339.
[12] C.O. Kappe, Controlled microwave heating in modern organic synthesis, Angew. Chem. Int. Ed. 43 (46) (2004) 6250–6284.

[13] R.J. Giguere, T.L. Bray, S.M. Duncan, G. Majetich, Application of commercial microwave-ovens to organic-synthesis, Tetrahedron Lett. 27 (1986) 4945–4948.
[14] P. Liu, Y. Yang, Y. Tang, T. Yang, Design and synthesis of novel pyrimidine derivatives as potent anti-tubercular agents, Eur. J. Med. Chem. 163 (2019) 169–182.
[15] S.B. Mohan, B.V.V. Ravi Kumar, S.C. Dinda, D. Naik, S. Prabu Seenivasan, V. Kumar, D.N. Rana, P.S. Brahmkshatriy, Microwave-assisted synthesis, molecular docking and antitubercular activity of 1,2,3,4-tetrahydropyrimidine-5-carbonitrile derivatives, Bioorg. Med. Chem. Lett. 22 (2012) 7539–7542.
[16] D.K. Sureja, S.P. Dholakia, K.R. Vadalia, Conventional and microwave assisted synthesis of novel pyrimidine derivatives as antimicrobial and antitubercular agent, Pharm. Lett. 8 (9) (2016) 181–186.
[17] H.M. Patel, M.N. Noolvi, N.S. Sethi, A.K. Gadad, S.S. Cameotra, Synthesis and antitubercular evaluation of imidazo[2,1-b][1,3,4]thiadiazole derivatives, Arab. J. Chem. 10 (2017) S996–S1002.
[18] M. Murali Krishna Kumar, T. Mohan, G. Krupa Mai, G.P.V. Sangeeta, K. Purna Nagasree, Synthesis, characterization and biological evaluation of novel 1,4-benzodiazepine derivatives as potent anti-tubercular agents, J. Young Pharm. 10 (3) (2018) 267–271.
[19] K. Kiec-Kononowicz, E. Szymanska, Anti-mycobacterial activity of 5-arylidene derivatives of hydantoin, Farmaco 57 (11) (2002) 909–916.
[20] P.M. Sivakumar, S.P. Seenivasan, V. Kumar, M. Doble, Synthesis, antimycobacterial activity evaluation, and QSAR studies of chalcone derivatives, Bioorg. Med. Chem. Lett. 17 (6) (2007) 1695–1700.
[21] P.M. Sivakumar, V. Kumar, S. Prabu Seenivasan, J. Mohana Priya, M. Doble, Experimental and theoretical approaches to enhance anti tubercular activity of chalcones, WSEAS Trans. Biol. Biomed. 2 (7) (2010) 51–61.
[22] P.J. Jainey, K. Ishwar Bhat, Antitumor and antitubercular activities, microwave assisted synthesis of some chalcones, Asian J. Biochem. Pharm. Res. 2 (3) (2013) 8–14.
[23] G.C. Muscia, S.E. Asis, G.Y. Buldain, Microwave-assisted synthesis of 2-styrylquinoline-4-carboxylic acids as anti-tubercular agents, Med. Chem. 13 (5) (2017) 448–452.
[24] A. Rani, A. Viljoen, Sumanjit, L. Kremer, V. Kumar, Microwave-assisted highly efficient route to 4-aminoquinoline-phthalimide conjugates: synthesis and anti-tubercular evaluation, Med. Chem. Drug Discov. 2 (2017) 10782–10785.
[25] M. Kidwai, R. Kumar, A. Srivastava, H.P. Gupta, Microwave assisted synthesis of novel 1,3,4-thiadiazolyl-substituted 1,2,4-triazines as potential anti-tubercular agents, Bioorg. Chem. 26 (1998) 289–294.
[26] R.V. Pemmadi, P.N. Kurre, P.V.S. Guruvelli, R.N. Jamullamudi, M.K.K. Muthyala, Microwave assisted synthesis and SAR studies of novel hybrid phenothiazine analogs as potential antitubercular agents, Indian J. Chem. 57B (2018) 556–566.
[27] K.M. Hosamani, D.S. Reddy, K.S. Rangappa, Microwave assisted synthesis of benzocoumarin-benzothiazepine hybrids as potent anti-tubercular agents and their DNA cleavage study, Eur. J. Biomed. Pharm. Sci. 2 (3) (2015) 576–592.
[28] V.M. Patel, N.B. Patel, Microwave irradiated synthesis, biological evaluation and molecular docking studies of 3-((substituted-benzo[d]thiazol-2-yl amino)methyl)-5-(pyridin-4-yl)-1,3,4-oxadiazole-2(3H)-thione, Int. J. Pharm. Sci. Res. 8 (9) (2017) 4021–4033.
[29] V.S. Negalurmath, S.K. Boda, O. Kotresh, P.V. Anantha Lakshmi, M. Basanagouda, Benzofuran-oxadiazole hybrids: design, synthesis, antitubercular activity and molecular docking studies, Chem. Data Collect. 19 (2019) 1–20.

[30] P. Shah, T.M. Dhameliya, R. Bansal, M. Nautiyal, D.N. Kommi, P.S. Jadhavar, J.P. Sridevi, P. Yogeeswari, D. Sriram, A.K. Chakraborti, N-Arylalkylbenzo[d] thiazole-2-carboxamides as anti-mycobacterial agents: design, new methods of synthesis and biological evaluation, Med. Chem. Commun. 5 (2014) 1489–1495.
[31] A.S. Rathoda, S.S. Godipurgea, J.S. Biradar, Microwave assisted, solvent-free, "Green" synthesis of novel indole analogs as potent antitubercular and antimicrobial agents and their molecular docking studies, Russ. J. Gen. Chem. 88 (6) (2018) 1238–1246.
[32] K.H. Rohde, H.A. Michaels, A. Nefzi, Synthesis and antitubercular activity of 1,2,4-trisubstitued piperazines, Bioorg. Med. Chem. Lett. 26 (9) (2016) 2206–2209.
[33] A. Ahmad, A. Husain, S.A. Khan, M. Mujeeb, A. Bhandari, Synthesis, antimicrobial and antitubercular activities of some novel pyrazoline derivatives, J. Saudi Chem. Soc. 20 (2016) 577–584.
[34] A.K. Chaturvedi, A.K. Verma, J.P. Thakur, S. Roy, A novel synthesis of 2-arylbenzimidazoles in molecular sieves-MeOH system and their antitubercular activity, Bioorg. Med. Chem. 26 (5) (2018) 4551–4559.
[35] S. Yadav, B. Narasimhan, S.M. Lim, K. Ramasamy, M. Vasudevan, S.A.A. Shah, A. Mathur, Synthesis and evaluation of antimicrobial, antitubercular and anticancer activities of benzimidazole derivatives, Egyptian J. Basic Appl. Sci. 5 (2018) 100–109.
[36] H. Wang, A. Wang, J. Gu, L. Fu, Synthesis and antitubercular evaluation of reduced lipophilic imidazo[1,2-a]pyridine-3-carboxamide derivatives, Eur. J. Med. Chem. 165 (2019) 11–17.
[37] D.D. Subhedar, M.H. Shaikh, M.A. Arkile, A. Yeware, Facile synthesis of 1,3-thiazolidin-4-ones as anti-tubercular agents, Bioorg. Med. Chem. Lett. 26 (7) (2016) 1704–1708.
[38] R.K. Singh, B.M. Sahoo, A. Bhatt, R. Kant, Synthesis, characterization and antitubercular activity of novel 2, 5-dimethyl-4-(aryl or hetero aryl) substituted aniline-1,3-oxazole derivatives, World J. Pharm. Res. 7 (1) (2018) 962–969.
[39] D. Sriram, P. Yoggeswari, S.P. Reddy, Synthesis of pyrazinamide mannich bases and its anti-tubercular properties, Bioorg. Med. Chem. Lett. 16 (2006) 2113–2116.
[40] S. Kim, S.-N. Cho, T. Oh, P. Kim, Design and synthesis of 1H-1,2,3-triazoles derived from econazole as antitubercular agents, Bioorg. Med. Chem. Lett. 22 (22) (2012) 6844–6847.

Microwave-induced synthesis of steroids and their chemical manipulations

24

Preetismita Borah[a], *Bimal Krishna Banik*[b,*]
[a]CSIR-Central Scientific Instruments Organization, Chandigarh, India, [b]Department of Mathematics and Natural Sciences, College of Sciences and Human Studies, Deanship of Research Development, Prince Mohammad Bin Fahd University, Al Khobar, Kingdom of Saudi Arabia
[*]Corresponding author. e-mail address: bimalbanik10@gmail.com; bbanik@pmu.edu.sa

This chapter provides an overview of the several strategies for the synthesis of the steroid skeleton by employing the classical method. As compared to classical reactions for the steroids synthesis microwave (MW) technology has become very important in the synthesis and it is reasonable to assert that there are now very few areas of synthetic organic chemistry that have not been shown to be enhanced using MW heating. It has been recognized that many chemical reactions, which require heating are likely to proceed more rapidly using this different form of heating. It is clear that MW chemistry can provide access to synthetic transformations, which may be prohibitively long or low yielding using conventional heating [1]. In 1969, Bucourt et al. achieved the synthesis of steroids from squalene using a sequential acid-mediated reaction of epoxide and subsequent formation of cationic unstable species in three steps [2]. In 1940, Bechmann et al. reported the synthesis of equilenin by utilizing the AB → ABC → ABCD strategy. In this approach, 1-naphthylamine-2-sulfonic acid was selected as the stating material that has the AB-ring of this steroid. Ring C ring was constructed on AB ring and then the D ring was prepared following a cyclization pathway [3]. In 1952, Woodward et al. reported a stereospecific approach to synthesize cholesterol [4]. Because of the medicinal activities of estrone, many synthetic chemists have focused to synthesize this complex molecule. In 1968, Kuo et al. applied an aldol-type reaction for the preparation of estrone through AAD → ABCD method [5]. In 2010, Weimar et al. reported the synthesis of estrone by using Dane's diene as AB- and a D-ring as dienophile [6]. Research on cortisone was challenging since it is a very useful medicine. In 1952, Sarrett et al. used an ABC → ABCD strategy; to synthesize the cortisone molecule [7]. A combination of Heck reaction and SmI_2-HMPA-induced cyclization was used for the synthesis of azasteroids with unnatural cis–cis annulation of rings B, C, and D by Kang and his group [8]. In 1997, Riccardis et al. described a synthesis of steroid-anthraquinone utilizing the Diels-Alder cycloaddition strategy. Grundmann's ketone, readily available by ozonolysis of vitamin D3, was converted into the vinyl triflate under kinetic control,

Green Approaches in Medicinal Chemistry for Sustainable Drug Design. https://doi.org/10.1016/B978-0-12-817592-7.00025-3
© 2020 Elsevier Inc. All rights reserved.

and the latter was then converted into the 1,3-diene by Stille coupling with vinyltributyltin, catalyzed by tetrakis(triphenylphosphine)palladium(0) [9]. An efficient synthesis of steroidal diacylhydrazines and their 1,3,4-oxadiazole derivatives was achieved by Szarkaa et al. via homogeneous catalytic hydrazinocarbonylation reaction in the presence of a palladium catalyst, a base and acetic or benzoic hydrazide as the nucleophilic reagent [10]. Tietze et al. used a combination of Suzuki and Heck reactions for the synthesis of the B-norestradiol analog [11]. In 2004, Wang et al. achieved the synthesis of acetylated steroid glycosides **by** the reaction of polyhydroxysteroid 3,5,6-trihydroxypregn-16-en-20-one with the peracetylated 1-bromo derivatives of D-glucose and D-galactose [12]. Chowdhury and his group developed the regioselective synthesis of novel steroidal antiinflammatory ante drug analogs, prepared by the reaction of 16-dehydropregnenolone acetate with various aldoximes in the presence of chloramine-T in refluxing ethanol [13]. In 2006, Sunnemann et al. assembled novel enantiomerically pure steroidal D-amino acids [14]. Due to the biological importance of the C-11 functionalization, Bazzini and coworkers developed an efficient method [15]. In 2007, Yan et al. designed and synthesized a novel series of pyridine rings fused steroidal derivatives [16]. In 2009, Sakac et al. reported the syntheses of triazoles via 1,3-dipolar cycloadditions reaction [17]. Recently, in 2010, Linclau et al. adapted the enantioselective synthesis of estrone [18]. In 2011, Huang et al. synthesized a series of 6-substituted steroidal lactams through Beckman rearrangement and condensation reaction starting from cholesterol. Later, they have found that these synthesized compounds displayed a distinct cytotoxicity against MGC 7901, HeLa, and SMMC 7404 cancer cells [19]. In 2011, Shawakfeh et al. reported symmetrical bis-steroidal pyrazine dimers which were obtained by classical, condensation of amino ketones [20]. In 2011, Khan and his group described an efficient method for the preparation of Steroidal oxazolo derivative and these compounds show antibacterial activity [21]. In 2012, Ibrahim et al. described pentacyclic steroids substituted at cholic acid via a stereoselective epoxidation and the epoxide opening as the key steps [22]. In 2012, Herrera et al. developed a method for the synthesis of steroidal glycoconjugates [23]. In 2012, Ibrahim et al. described an efficient strategy for introducing a nitrogen atom in positions 3 and 11 of the steroidal skeleton, which are key positions for biological purposes. Their strategy involves an intramolecular Diels-Alder cycloaddition of *o*-quinodimethanes which are generated from a 3-azabicyclo [4.2.0]octa-1,3,5-trien-7-one [24]. Wolfing and his research group synthesized the steroidal 16-spiro-1,3,2-dioxaphosphorinanes [25]. Another work in 2012 by Bansal and his group described an efficient method for the synthesis of 16-imidazolyl substituted steroidal derivatives [26]. In 2013, Zhang et al. described the synthesis of several steroid analogs possessing D-ring fused with heterocycles like pyridine, imidazo[2,1-*b*] thiazoles, or substituted thiazole imines using dehydroepiandrosterone as the starting material. They also investigated the cytotoxicity of the synthesized compounds against EC-109 (human esophageal carcinoma), EC-9706 (human esophageal carcinoma), MGC-803 (human gastric carcinoma) [27]. Shamsuzzaman and coworkers synthesized steroid-based cancer chemotherapeutic agents of the type 20-amino-30-cyanocholest-6-eno[5,7-de]4*H*pyrans [28]. In 2013, Fan et al. synthesized a series of novel derivatives of 21*E*-benzylidene derivatives from the readily available progesterone. These compounds were evaluated for their cytotoxic activity

against brine shrimp (*Artemia salina*) and murine Lewis lung carcinoma cells (LLC) [29]. Again in 2013, Fan et al. synthesized 14 novel steroidal C-17 pyrazolinyl derivatives from commercially available progesterone and tested for their cytotoxic activity against brine shrimp (*A. salina*) and three human cancer cell lines (NCI-H460, HeLa, and HepG2) [30]. In 2013, Shamsuzzaman et al. described a green and simple procedure for the biosynthesis of ZnO nanoparticles using *Candida albicans* as eco-friendly reducing and capping agents for the synthesis of steroidal pyrazolines [31]. In 2014, Waller et al. described the synthesis of steroid sulfates since the steroid sulfates are a major class of steroid metabolite that are of growing importance in fields such as antidoping analysis, the detection of residues in agricultural produce or medicine [32]. Again in 2014, Fustero and his group described the Sonogashira cross-coupling reaction for the synthesis of aminosteroid derivatives, an important subclass of steroids that display interesting biological properties that are mostly used in the area of anesthesia [33]. In 2014, Lopez et al. reported an efficient and facile synthesis of fused, substituted, and spiropyrazoline steroid derivatives through a cycloaddition reaction of different α,β-unsaturated ketones with hydrazine acetate in acetic acid [34]. In 2015, Zhang et al. described an efficient and practical base-promoted cascade reaction to synthesized steroidal polysubstituted anilines from simple precursors [35]. Again in another work, Zhang et al. established the synthesis of novel steroidal 3-cyano-2-aminopyridines using enaminonitrile and various primary amines under solvent-free condition [36]. Gonzalez and coworkers described the synthesis of several monomeric and dimeric steroidal [1,2,4]triazolo[1,5-*a*]pyrimidines steroids via Claisen-Schmidt condensation and rearrangement of the spiro moiety followed by a cycloaddition with 3-amino-1,2,4-triazole [37]. In 2016, Gavaskar et al. described a facile one-pot synthesis of novel steroidal dispiro-indenoquinoxaline pyrrolidines via multicomponent [3 + 2]-cycloaddition of azomethine ylides in ionic liquid [38]. In 2016, Rassokhina and his groups synthesized some steroidal imidazo[1,2-*a*]pyridines derivatives [39]. In 2017, Torres et al. described the Sonogashira coupling of 17β-acetoxy-4,5-secoandrost-3-yn-5-one with 2-iodobenzyl alcohol, followed by $NABH_4$ reduction followed by palladium-catalyzed spirocyclization to produce the corresponding benzannulated steroid spiroketals [40]. In 2017, Enríquez et al. have described the synthesis of novel hybrid steroid dimers by $BF_3{\cdot}Et_2O$ catalyzed aldol condensation of 2-formyl-estradiol diacetate and steroid sapogenins [41]. In 2017, Joppa and his group described the Suzuki-Miyaura reactions of 16-*E*-(triflyloxymethylidene)-3-methoxy-estrone for the synthesis of various 16-*E*-(arylidene)-3-methoxy-estrones in good to high yields and with excellent *E*-selectivity [42]. In 2018, Song et al. introduced a pyridine heterocycle on the D ring, a series of steroidal pyridine derivatives were designed and studied for their antitumor activity by molecular docking software [43]. In 2018, Dara et al. synthesized a group of steroidal imidazolidinthione derivatives from steroidal thiosemicarbazones and dichloroethane [44]. Recently, Sethi and coworkers described the use of ionic liquid (IL), *N*-methyl-2-pyrolidone hydrogen sulfate ($NMP + HSO_4^-$) as the green catalyst for the synthesis of novel biologically active diosgenin prodrugs [45]. Again in 2019, Hryniewickaa synthesized steroid-based imidazolium salts and these compounds reveal interesting biological properties, especially regarding antitumor and antimicrobial activities [46]. In 2019, Hanson et al. described the use of fluorescent imaging agents for the synthesis of steroidal antiestrogens [47].

24.1 Microwave background

The magic of MW heating technology, known as Bunsen burner of the 21st century, has emerged as potential alternatives in the synthesis of various types of organic compounds, polymers, as well as inorganic materials. Throughout the scientific history, the most fundamental obstacles in developing technologies are to minimize energy consumption and to eliminate/minimize the use of hazardous substances. In this scenario, the use of MW energy to bring about chemical transformations is a suitable alternative, as it takes care of two very essential criteria of synthesis: minimizing energy consumption required for heating and time required for the reaction [48]. In the electromagnetic spectrum, the MW radiation is located between infrared and radio waves, having a wavelength (1 mm–1 m), with corresponding frequencies from 0.3 to 300 GHz. The use of MW heating in organic synthesis was introduced in 1986 by the group of Gedye and Giguere, Majetich [49, 50]. MW technology has a potential impact on the fields of combinatorial chemistry, green chemistry, medicinal chemistry, and drug development. A large number of reviews have been published elaborating the accelerating effect of MWs in solvent-free reactions, cycloaddition reactions [51], the synthesis of radioisotopes [52], fullerene chemistry [53–55], polymers [56], heterocyclic chemistry [57, 58], carbohydrates [59, 60], homogeneous and heterogeneous catalysis [61, 62], medicinal and combinatorial chemistry [63, 64], and green chemistry [65–67]. One of the most fundamental obstacles in developing technologies is to minimize energy consumption and to minimize/eliminate the use of toxic and hazardous substances. In this regard, the application of MW energy to bring about a chemical reaction is a suitable alternative, as it takes care of two very necessary criteria of synthesis, viz., energy consumption for heating and the time required for the reaction. Therefore, during the last few years, the studies on the effect of MW irradiation in organic and macromolecules have become a subject of considerable interest [68–72]. Accelerating effect and efficient noncontact heating are the two important traits of MW irradiated reactions. The accelerating effects of MW irradiation have recently been demonstrated by Carsten et al. in their work on polymer chemistry [73]. A number of MW irradiated multicomponent reactions are reported by several workers in recent times [71]. Under the MW irradiation condition, the organic reaction can be expedited with high selectivity of the ensuing product by choosing an appropriate MW parameter and thus offering several advantages over conventional heating like instantaneous and rapid heating, high-temperature homogeneity, etc.

MW-prompted synthesis fulfills the promise of being a fast synthesis practice in organic synthesis. Since, the first reports of MW-assisted synthesis in 1986 [74], the use of this MW heating technique has become a powerful tool in all areas of synthetic organic chemistry including solvent-free and water-mediated reactions [75–80]. Fig. 24.1 depicts the application of MW energy in various types of organic synthesis.

Thus over the last decade, microwave-assisted organic synthesis (MAOS) has emerged as a promising field in organic synthesis [81]. The beauty of the MAOS technique is less energy intensive as well as less time-consuming [82]. Moreover, the growing emphasis on following the “green chemistry” protocols while developing

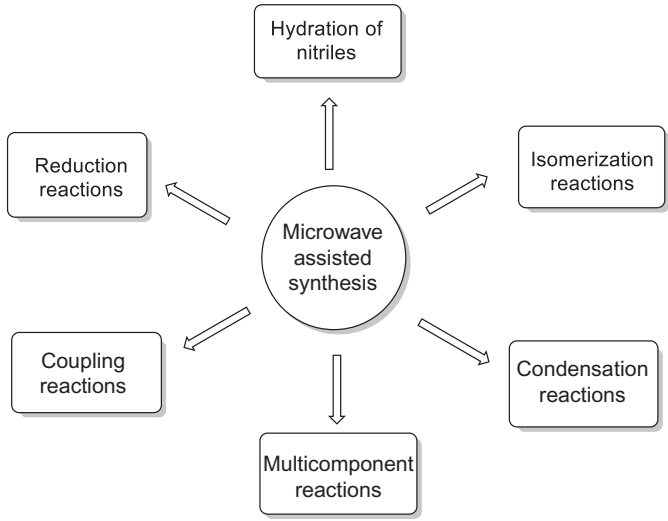

Fig. 24.1 Applications of microwave in various synthesis.

a synthetic technology have resulted in a characteristic swing in momentum from conventional heating methods toward MW heating chemistry, as it offers a rapid, clean, efficient, and economic alternative to carry out organic transformations. MW energy has found vast applications in a broad spectrum of areas such as organometallic chemistry, metal catalysis, coupling reaction, photochemistry, radical reactions, protection-deprotection reactions, cycloaddition reactions, heterocyclic chemistry, carbohydrate, peptide chemistry, and many more.

24.2 Microwave in steroid synthesis

Performing MW reactions is one of the major challenges in organic, combinational, and medicinal chemistry because they address both diversity and complexity in organic synthesis. With the development of MW energy in organic synthesis, the application of MW in steroids is gaining considerable importance to provide green technology.

An efficient synthesis of fluoropyridyl derivatives of [3,2-*c*]pyrazolo-corticosteroids was achieved by Khan et al. via MW-heating which have a high affinity for the glucocorticoid receptor (GR) and are highly active glucocorticoids. They are thus considered to be excellent candidates for PET imaging of GR containing tissues when labeled with fluorine-18 ($t1/2 = 110$ min). Previously reported syntheses of these fluorinated glucocorticoids were accomplished by conventional thermal nucleophilic halogen exchange reactions with chloropyridyl precursors. These reactions were found to proceed at rates too slow for feasible application to radiosynthesis

using fluoride. Khan and coworkers applied MW-heating methods to these reactions and found that significant rate enhancements can be realized (Scheme 24.1) [83].

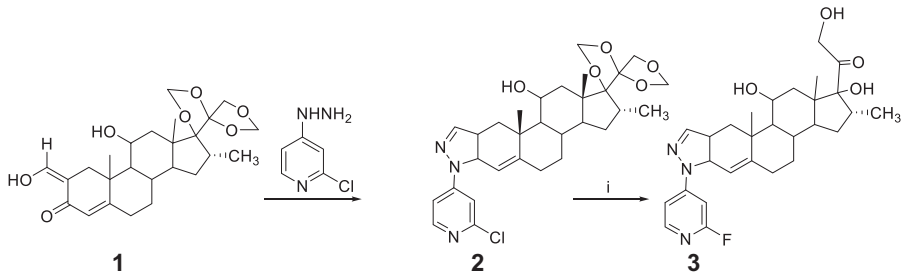

Scheme 24.1 *Reagent and conditions*: (i) KF, kryptofix, DMSO, Heat, 60% HCOOH, 90°C, 15 min.

An efficient formal approach toward the synthesis of steroidal thiosemicarbazone derivatives has been reported by Zhigang's research group by effectively utilizing the MW irradiation via the condensation of steroidal ketones and substituted thiosemicarbazides under solvent-free conditions. The yields obtained are in the range of 84%–96% using the MW method and 46%–62% using the conventional method. All the series compounds were evaluated for their antibacterial activity against and the results were compared with the standard drug Amoxicillin (Scheme 24.2) [84].

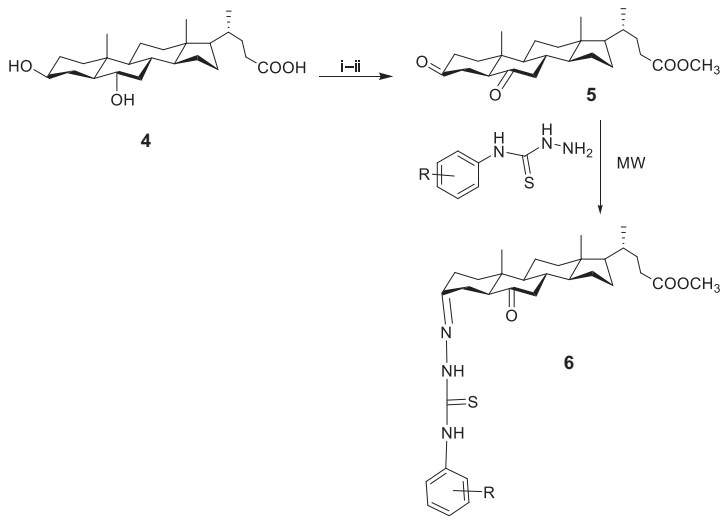

Scheme 24.2 *Reagent and conditions*: (i) CH_3OH, H_3PO_4; (ii) PCC, CH_2Cl_2.

In 2012, a recent report by Mahboob et al. describes the synthesis of solid-state synthesis of some reported steroidal pyrazolines by a novel eco-friendly route as in Scheme 24.3. The synthesized pyrazolines were compared with those obtained from conventional methods in terms of reaction time and overall yield. A substantial enhancement in reaction rate and yield was observed. The pyrazolines **8** was prepared by the reaction of α,β-unsaturated steroidal ketone **7** with thiosemicarbazide under MW energy. The antimicrobial activity and the subsequent molecular docking studies of the steroidal pyrazolines have also been carried out [85].

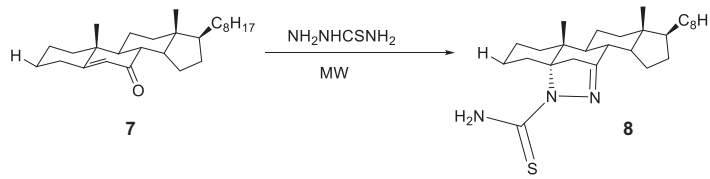

7 **8**

Scheme 24.3 *Reagent and conditions*: (i) Et_3N, 30 s–2 min.

In 2014, Kovács et al. achieved the synthesis of 17-*exo*-heterocycles **11** using MW-assisted condensation of 3α-hydroxy or 3α-acetoxyandrost-5-ene-17β-carbaldehyde **9** with different acylhydrazides **10** depicted in Scheme 24.4. The desired compounds **11** were subjected to in vitro pharmacological studies to investigate their antiproliferative activities on four malignant adherent cell lines (HeLa, MCF7, A2780, and A431), and exhibited the highest potency against HeLa cells, some of them revealing action comparable to that of the reference agent cisplatin [86].

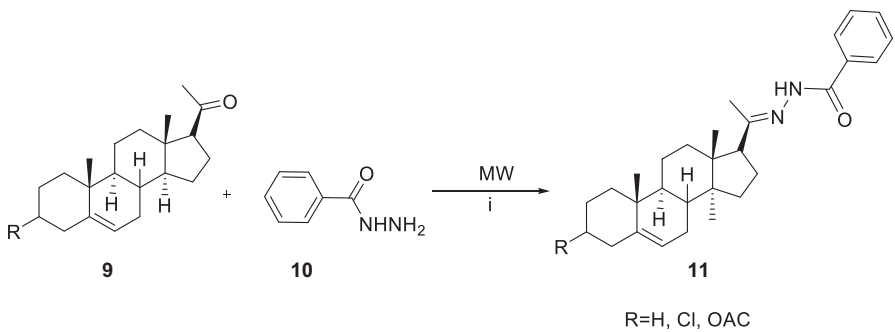

9 **10** **11**

R=H, Cl, OAC

Scheme 24.4 *Reagent and Conditions*: (i) PIDA, CH_2Cl_2.

In 1995, Dayal and coworkers reported the efficient syntheses of sarcosine conjugated bile acids **13** which were achieved in absolute ethanol in a domestic MW oven by the reaction of ursocholic acid, sarcosine ethyl ester hydrochloride, and *N*-ethoxycarbonyl-2-ethoxy-1,2-dihydroquinoline (Scheme 24.5) [87].

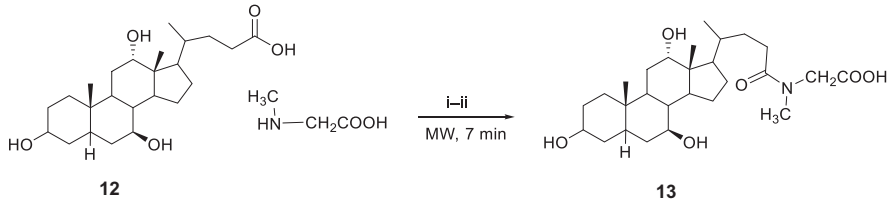

Scheme 24.5 *Reagent and conditions*: (i) EEDQ, C_2H_5OH, (ii) K_2CO_3/C_2H_5OH.

In 2013, Zhichuan et al. assembled the synthesis of chenodeoxycholic acid bisthiocarbazones **17** via the condensation of steroidal diketones and substituted benzaldehyde thiocarbohydrazones by means of MW irradiation (Scheme 24.6) [88].

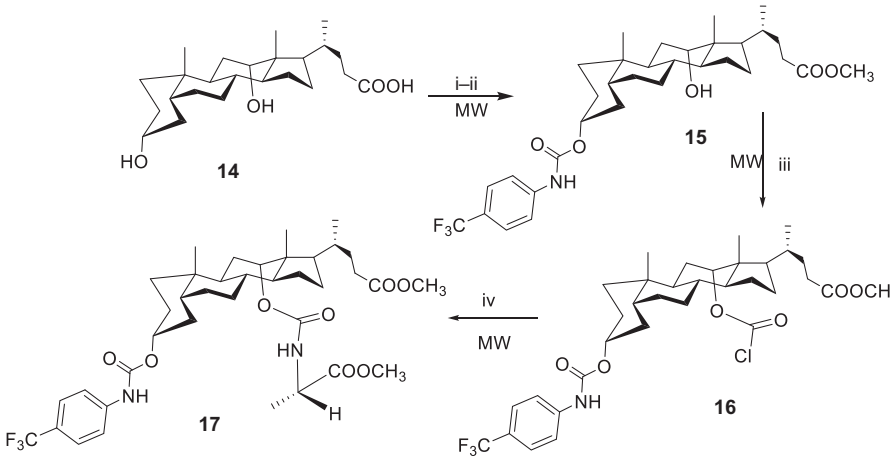

Scheme 24.6 *Reagent and conditions*: (i) CH_3OH, CH_3COCl, (ii) triphosgene, CH_2Cl_2, pyridine, 4-aminobenzotrifluoride, (iii) CH_2Cl_2, triphosgene, pyridine, (iv) amino acid methyl esters hydrochloride, pyridine.

Khan and his research group described the synthesis of 2-amino-5α-cholest-6-eno [6,7-*d*] thiazole derivatives **19** under MW irradiation using dry-media conditions. The additional advantage of this methodology includes a much faster reaction, easy workup, high yield, high purity of the products, and an environmentally friendly approach (Scheme 24.7) [89].

In 2011, Shi et al. developed an efficient and simple method for synthesis of new hyodeoxycholic acid thiosemicarbazone derivatives **22** under solvent-free conditions using MW. The preliminary results indicate that some of these compounds possess inhibitory effects against *Escherichia coli*. Steroidal thiosemicarbazones and their derivatives have attracted considerable interest due to their wide biological activities.

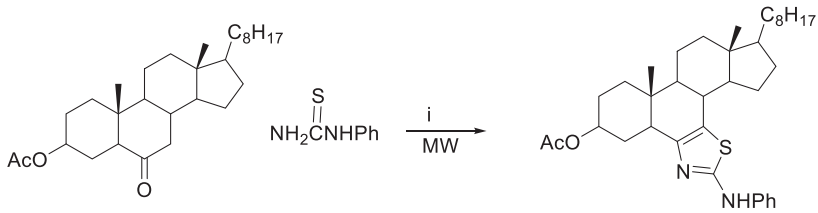

18 19

Scheme 24.7 *Reagent and conditions*: (i) I_2, isopropanol.

As far as we know, steroidal thiosemicarbazones showed in vitro inhibitory effect against bacteria such as *Staphylococcus aureus*, *Staphylococcus pyogenes*, *Salmonella typhimurium*, and *E. coli* (Scheme 24.8) [90].

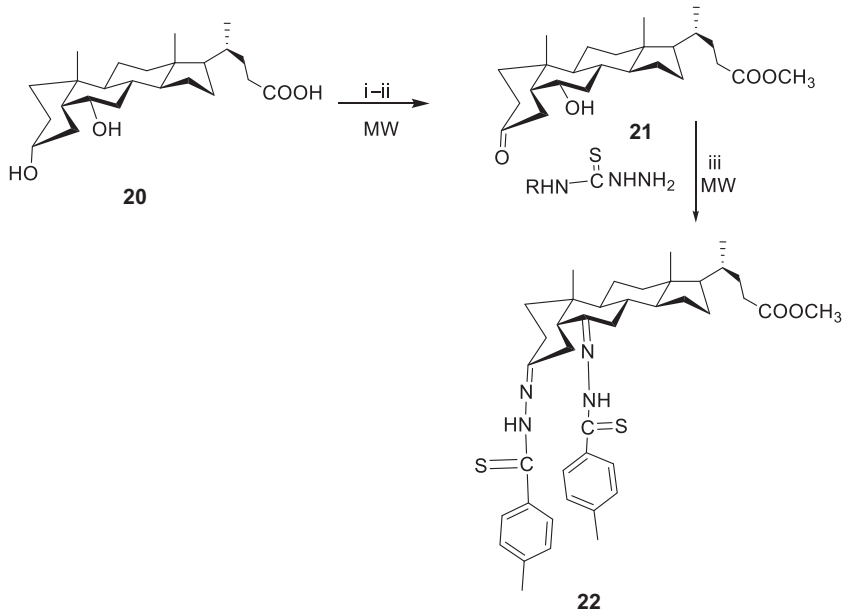

20 22

Scheme 24.8 *Reagent and conditions:* (i) CH_3OH, H_3PO_4, MW, (ii) PCC, CH_2Cl_2, rt, (iii) MW, solvent-free.

In 2012, Renmin et al. developed a pressured microwave-assisted hydrolysis (PMAH) technique for hydrolyzing the crude glycyrrhizic acid (GA) extracted from licorice root to prepare glycyrrhetinic acid (GRA) **24** (Scheme 24.9) [91].

In 2016, Baji et al. efficiently developed a novel D- and A-ring-fused quinolines in the estrone and 5α-androstane series were efficiently synthesized from the corresponding β-chlorovinyl aldehydes **26** with different arylamines in DMF under MW irradiation (Scheme 24.10) [92].

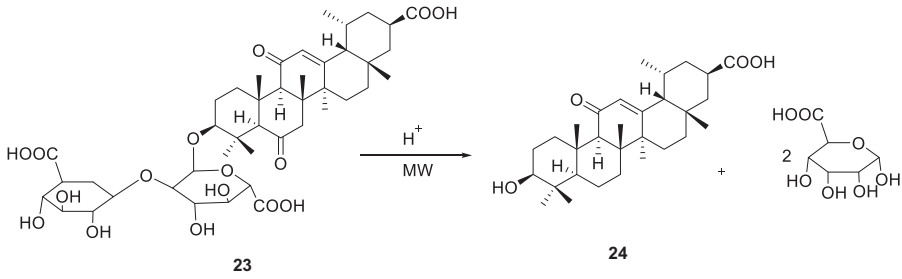

Scheme 24.9 *Reagent and conditions*: (i) CH_3CH_2OH, CH_3COOH, NH_4OAc, H_2SO_4, $CHCl_3$, 450 W, 5–10 min.

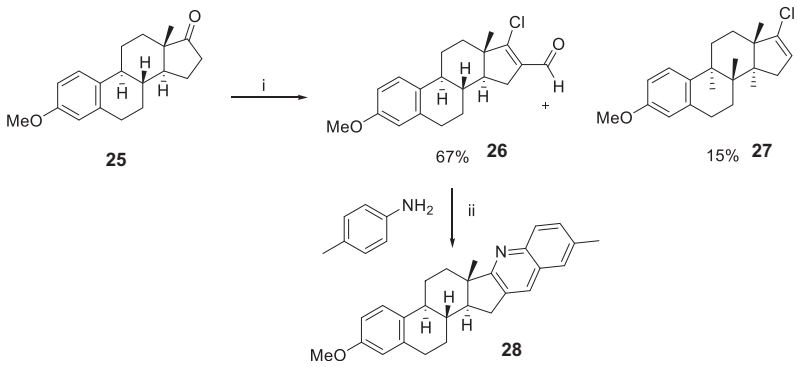

Scheme 24.10 *Reagent and conditions*: (i) $POCl_3$, DMF, $CHCl_3$, 0–60°C, 4 h, (ii) DMF, MW, 140°C.

Motyan and coworkers reported a synthetic route to synthesize a novel ring D-condensed 2-pyrazolines **30** were efficiently synthesized from 16-dehydropregnenolone **29** under MW irradiation (Scheme 24.11). The reactions are assumed to occur via hydrazone intermediates, followed by intramolecular 1,4-addition leading to the fused hetero ring stereoselectively with a 16a,17a-cis ring junction. The synthesized compounds were subjected to in vitro pharmacological studies of their antiproliferative activities against four human breasts (MCF7, T47D, MDA-MB-231, and MDA-MB-361) and three cervical (HeLa, C33A, and SiHA) malignant cell lines. Flow cytometry revealed that the most potent agent elicited a cell cycle disturbance [93].

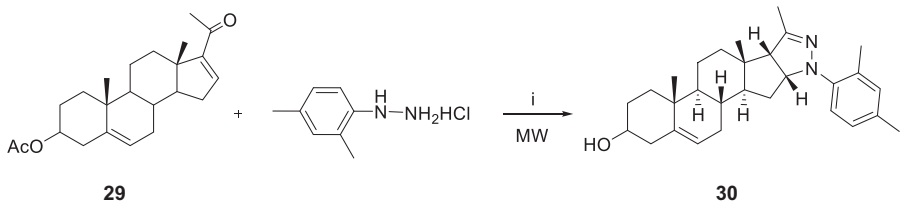

Scheme 24.11 *Reagent and conditions*: (i) PTSA, EtOH, 100°C, 20 min.

Dayal et al. reported an efficient synthetic procedure for the esterification, deformylation, and deacetylation of bile acids (Scheme 24.12). This is achieved by the addition of a catalytic amount of methanesulfonic acid or para-toluene sulfonic acid to a solution of bile acid in methanol in the domestic MW oven. All these reactions were completed in the MW oven within 1–3 min at 60% power (390 W) and the desired bile acids, namely trihydroxy-5-cholestanoic acid, (23*R*)-3ct,7,23-trihydroxy-5fS-cholan-24-oic acid, ursocholic acid, and 7-ketolithocholic acid were isolated in 86%–94% yield [94].

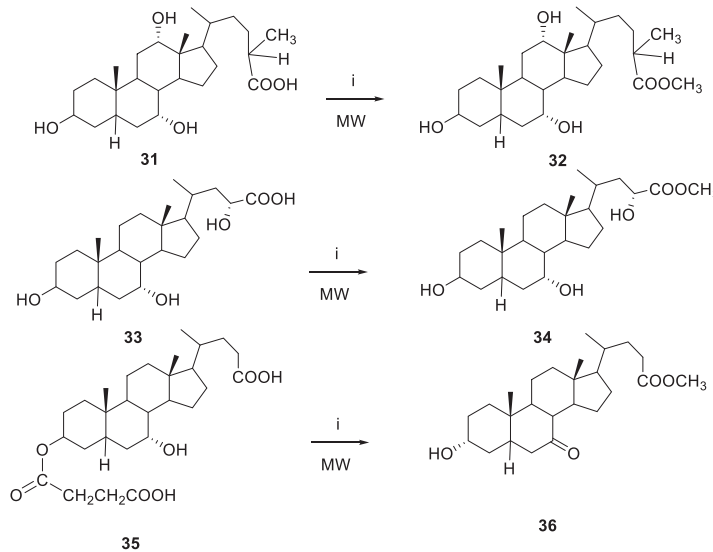

Scheme 24.12 *Reagent and conditions*: (i) MSA/MeOH, MW, 1–3 min, 390 W.

In another work Dayal and coworkers described the rapid hydrogenation of unsaturated sterols and bile alcohols in a domestic MW oven (Scheme 24.13). This has been achieved by the addition of catalytic amounts of Pd/C in methylene chloride/propylene glycol solvents in the presence of ammonium formate followed by MW irradiation. It is suggested that this methodology will be helpful in the identification of saturated and unsaturated sterols with different side-chain structures in rare diseases:

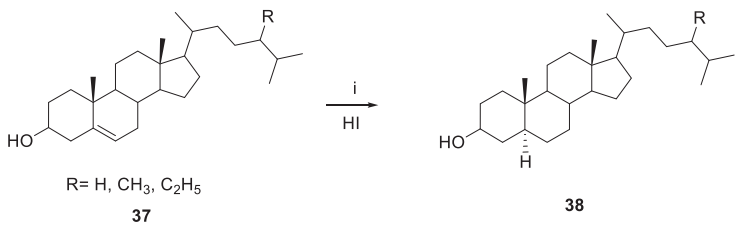

Scheme 24.13 *Reagent and conditions*: (i) Pd/C, CH_2Cl_2, NH_4HCO_2.

sitosterolemia, cerebrotendinous xanthomatosis (CTX), as well as atherosclerosis and diabetes mellitus. Sterols, such as cholesterol, campesterol, sitosterol, and bile alcohols with unsaturated side chains were converted to their reduced congeners with high yield and purity [95].

Skoda-Foldes et al. reported the synthesis of Steroidal dienes **40** by Stille-coupling of the corresponding alkenyl iodides with vinyltributyltin under MW irradiation in a domestic MW oven in good yield (Scheme 24.14). Rate acceleration was observed also in the one-pot Stille-coupling-Diels-Alder reaction of 17-iodo-5-androst-16-ene **39**. The stereoselectivity of cycloaddition was slightly improved with diethyl maleate as the dienophile, compared to that achieved with thermal heating [96].

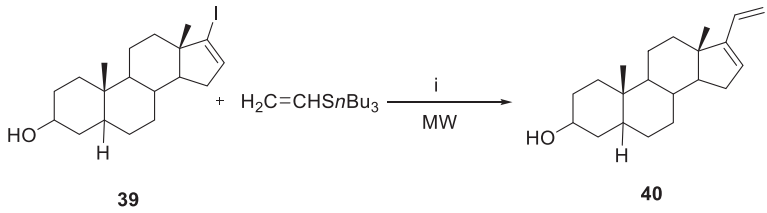

39 40

Scheme 24.14 *Reagent and conditions*: (i) $Pd(PPh_3)_4$.

In 2015, Penov Gasi developed MW-assisted synthesis and biomedical potency of salicyloyloxy **42** and 2-methoxybenzoyloxy androstane and stigmastane **43** derivatives (Scheme 24.15) [97].

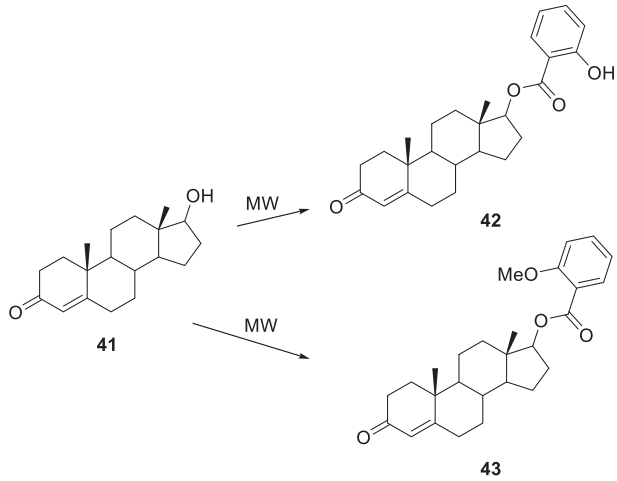

Scheme 24.15 *Reagent and conditions*: (i) $Pd(PPh_3)_4$.

In 2014, Boruah and his research group described a synthesis of a new class of steroidal and nonsteroidal epoxide ring-opening reaction by nitrogen-containing

heterocycles under MW irradiation. Their strategy involved the synthesis of epoxide **46** from commercially available cholesterol acetate **44** via allylic oxidation, acid-catalyzed elimination, and epoxidation pathway (Scheme 24.16). This epoxidation afforded only epoxide **46** due to the presence of angular methyl group at C-10 position of the steroid moiety. Finally, the MW irradiation of an equimolar mixture of epoxide **46** and imidazole in a closed vessel in a Synthos 3000 MW reactor at 600 W (140°C and 12 bar) for 6 min afforded compound 3-(1*H*-imidazol-yl)-4-hydroxy-5-en-cholest-7-one **47** in 69% yield. The antimicrobial activities of the epoxide ring-opening compounds and *N*-(1-cycloalkenyl) heterocyclic compounds were tested by agar diffusion assay [98].

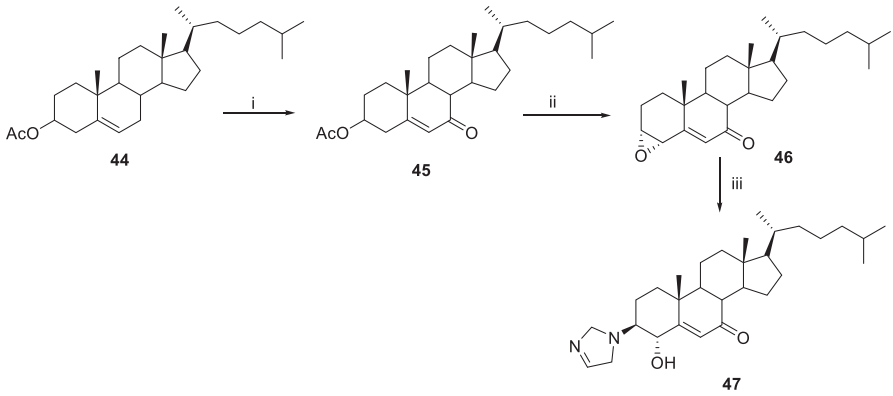

Scheme 24.16 *Reagent and conditions*: (i) t-BuOOH, $RuCl_3$, cyclohexane, rt, 4 h; (ii) HCl, MeOH, reflux, 1 h; mCPBA, $CHCl_3$, 5 h; (iii) N-heterocycles, MW, 600 W (140°C and 12 bar), 15 min.

In another work, Boruah et al. reported a new set of steroidal A, D-ring fused 5,6-disubstituted pyridines and nonsteroidal substituted pyridines **49** starting from steroidal β-halovinyl aldehyde **48**, alkyne, and benzylamine, using a $Pd(OAc)_2$ catalyzed multicomponent reaction under MW (Scheme 24.17) [99].

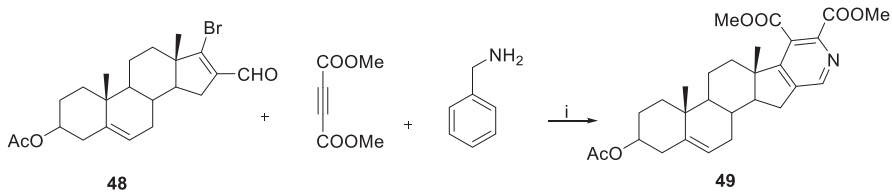

Scheme 24.17 *Reagent and conditions*: (i) $Pd(OA)_2$, PPh_3, Na_2CO_3, neutral alumina, 10 min, MW.

In 2013, Dutta et al. reported the synthesis of novel steroidal heterocycles containing 4,6-diaryl substituted pyridine moiety **52** fused to the 2,3- and 16,17-positions of

the steroid nucleus. The Michael reaction of steroidal ketones **50** with in situ generated chalcones provided the intermediates 3,5-diaryl-1,5-dicarbonyl steroidal derivatives **51**. Subsequently, the intermediates **51** were converted to the pyridine derivatives **52** by solid-phase reaction with urea in the presence of $BF_3{\cdot}OEt_2$ (Scheme 24.18) as the catalyst under MW irradiation [100].

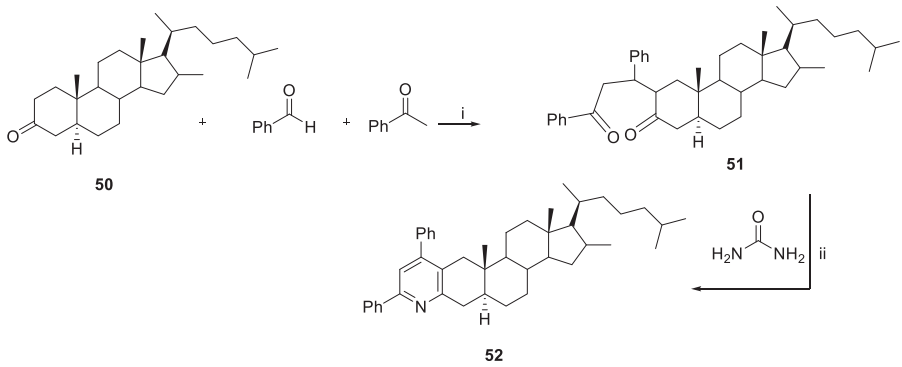

50 51 52

Scheme 24.18 *Reagent and conditions*: (i) KOH, toluene, rt; (ii) $BF_3{\cdot}OEt_2$, MW.

In 2013, Kakati et al. described the synthesis of a novel class of chalconoyl pregnenolones via Claisen-Schmidt condensation under MW activation and solvent-free reaction conditions (Scheme 24.19). The compounds were screened for antimicrobial activity against two bacterial strains *Bacillus subtilis* and *E. coli* and two fungal strains *Aspergillus niger* and *C. albicans*. Some of the compounds exhibited significant inhibitory activity against the microbial strains. Presence of the α,β-unsaturated carbonyl moiety in the synthesized compounds was found to be essential for the activity as manipulation of the same through epoxidation of the double bond diminished the activity [101].

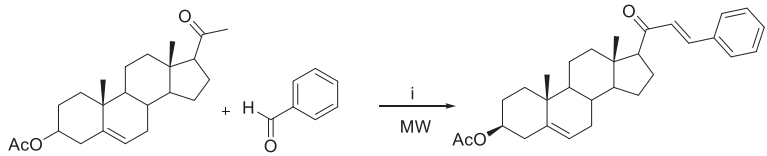

53 54

Scheme 24.19 *Reagent and conditions*: (i) I_2-Al_2O_3, 5–7 min.

In 2012, Boruah and his group described the synthesis of A-ring and D-ring fused steroidal quinolines from the one-pot reaction of steroidal β-bromovinyl aldehydes and arylamines in solvent-free and catalyst-free condition under MW irradiation (Scheme 24.20) [102].

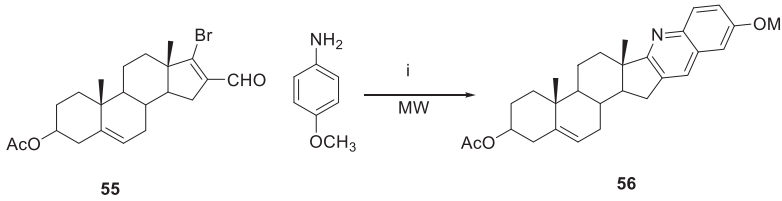

Scheme 24.20 *Reagent and conditions*: (i) 600 W, 10 min.

Hernández-Linares and his coworker developed an easy and fast procedure for one-pot synthesis of steroidal isoxazoles starting from 23-acetylsapogenins derivatives **58** in the presence of P_2O_5/SiO_2 in dry media under MWs irradiation [103] (Scheme 24.21).

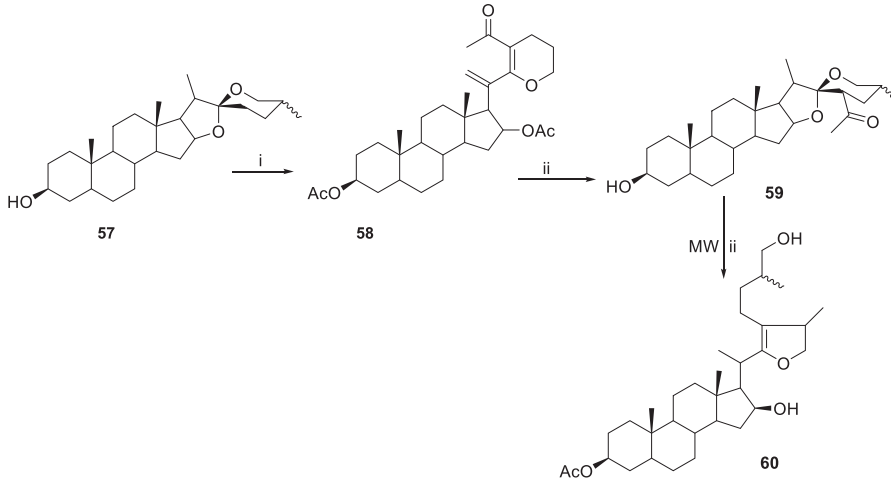

Scheme 24.21 *Reagent and conditions*: (i) BF_3-Et_2O, AC_2O, 10 min; (ii) KOH/EtOH 20%, 20 min; (iii) NH_2OH-HCl, P_2O_5/SiO_2, MW.

In 2011, Borah et al. described the application of Baeyer-Villiger (BV) reaction in the synthesis of natural products and steroid-peptide conjugates. Their strategy involves the BV oxidation of carbonyl compounds with special reference to steroidal ketones under MW irradiation justifying its accelerating effect [104] (Scheme 24.22).

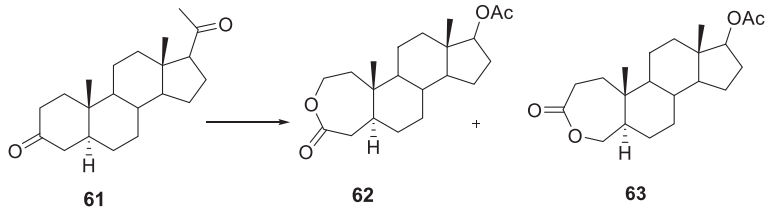

Scheme 24.22 *Reagent and conditions*: (i) m-CPBA, $CHCl_3$, MW, 3–5 min.

An efficient synthesis of 12-heterosteroids **69** was achieved by Ibrahim-Ouali et al. via a Baeyer-Villiger oxidation and photolysis as the key steps (Scheme 24.23) [105].

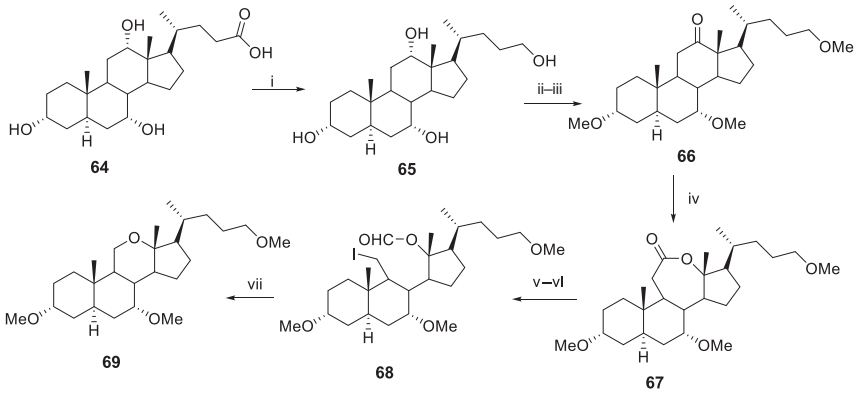

Scheme 24.23 *Reagent and conditions*: (i) $LiAlH_4$, THF, 0°C; (ii) CH_3I, NaH, THF, rt; (iii) PCC, MW; (iv) m-CPBA, PTSA, CH_2Cl_2; (v) DIBAL, CH_2Cl_2; (vi) HgO-I_2, pyridine, C_6H_6; (vii) MeLi, THF, −78°C.

In 2012, Ahonena et al. reported the MW-assisted synthesis and solid-state structural characterizations of novel lithocholyl amides of 2-, 3-, and 4-aminopyridine (Scheme 24.24). It is shown that the MW technique is a proper method in the preparation of *N*-lithocholyl amides of isomeric aminopyridines [106].

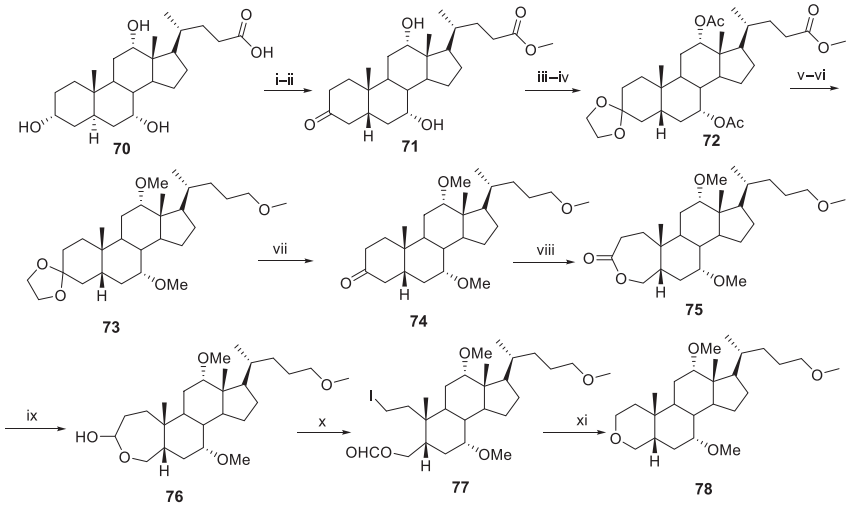

Scheme 24.24 *Reagent and conditions*: (i) MeOH, PTSA; (ii) Ag_2CO_3/celite, MW, 3 min; (iii) Ac_2O, pyridine, DMAP; (iv) $(CH_2OH)_2$, PTSA, C_6H_6; (v) $LiAlH_4$, Et_2O, rt; (vi) CH_3I, NaH, THF, rt; (vii) HCl, acetone; (viii) m-CPBA, PTSA, CH_2Cl_2; (ix) DIBAL, CH_2Cl_2; (x) HgO-I_2, py, C_6H_6; (xi) MeLi, THF, −78°C.

In 2010, Deb et al. synthesized fatty acid ester (FAE) derivatives of several steroids **80** under MW irradiation in an ionic liquid (Scheme 24.25) [107].

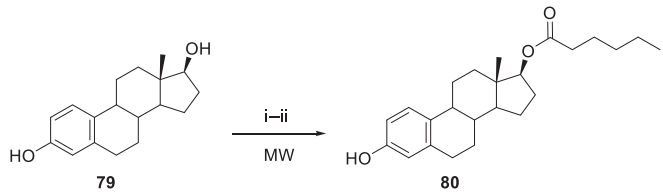

Scheme 24.25 *Reagent and conditions*: (i) Py, DMAP, fatty acid chloride, 40°C; (ii) KOH, MW, 1 min, 80°C.

In 2010, Barthakur et al. reported a facile strategy for the annulation of 2,6-dicyanoaniline **82** moiety to steroidal A/B-ring from base-catalyzed and MW-promoted reaction of steroidal 3-keto-2-hydroxymethylenes **81** with malononitrile in high yields Scheme 24.26 [108].

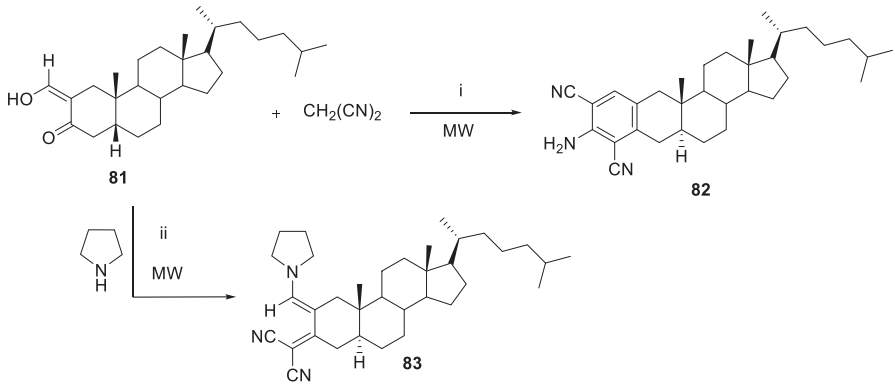

Scheme 24.26 *Reagent and conditions*: (i) NaOMe, Al_2O_3 (basic); (ii) $CH_2(CN)_2$.

In 2009, Boruah and his coworker described the fusion of a pyrimidine ring at 2,3 position of A-ring of steroid moiety (Scheme 24.27). Their strategy involved the solid-phase three-component reaction of 2-hydroxymethylene-3-keto steroids, arylaldehydes, and ammonium acetate under MW irradiation [109].

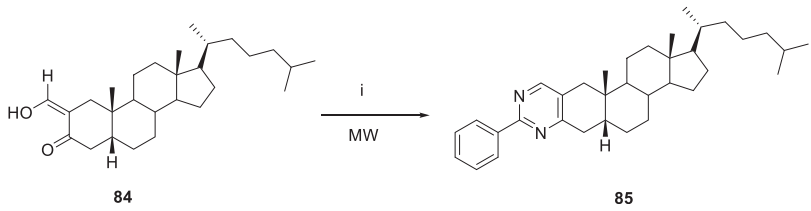

Scheme 24.27 *Reagent and conditions*: (i) PhCHO, NH_4OAc, 6 min.

Borthakur et al. described the preparation of 3-oxo-4-azasteroid **88** from A-nor-3,5-secosteroid-3-oic acid **87** in a solvent-less condition catalyzed by Lewis acid under MW irradiation (Scheme 24.28). They utilized urea as an environmentally benign source for the generation of ammonia for the aza cyclization reaction [110].

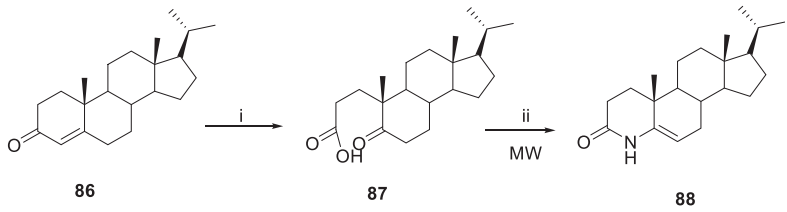

86 87 88

Scheme 24.28 *Reagent and conditions*: (i) $NaIO_4/KMnO_4$; (ii) $Urea/BF_3{\cdot}Et_2O$.

In 2006, Katritzky et al. described the synthesis of chiral *O*-(-protected dipeptidoyl) steroids under the MW irradiation in isolated yields of 65%–96%, with complete chirality retention (Scheme 24.29). Their strategy utilized readily available *N*-(*Z*-α-aminoacyl)benzotriazoles **90** and *Z*-dipeptidoylbenzotriazole, with naturally occurring steroidal alcohols **89** [111].

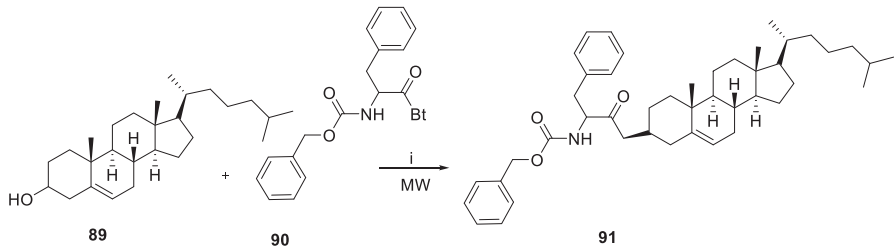

89 90 91

Scheme 24.29 *Reagent and conditions*: (i) 0.1 Eq. DMAP, THF, 65°C, 15 min.

Cravotto and his coworker exploited the MW irradiation for the synthesis of bile acid derivatives (Scheme 24.30). By using this MW energy, esterification, amidation, hydrolysis, oxidation, and reduction were investigated [112].

In 2014, Wang et al. converted steroid saponins into diosgenin **97** by the catalytic hydrolysis with an acid-functionalized ionic liquid under MW irradiation (Scheme 24.31). The typical acid-functionalized ionic liquid, 1-sulfobutyl-3-methylimidazolium hydrosulfate ($[BHSO_3MIm]\ HSO_4$), was used to evaluate the catalytic efficiency [113].

Asif and his coworker synthesized a series of steroidal thiazole derivatives by an efficient manner by one-step reaction methodology employing MW irradiation. The synthesis involves the reaction of steroidal ketones **98** with thiosemicarbazide and phenacyl bromide [114] (Scheme 24.32).

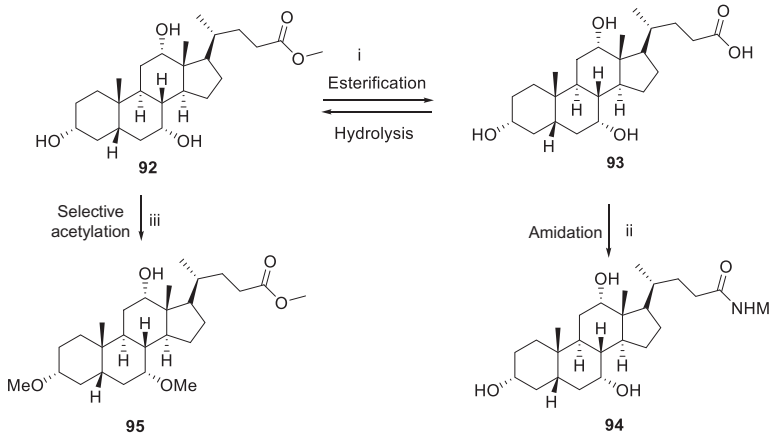

Scheme 24.30 *Reagent and conditions*: (i) PTSA, CH_3OH, anhyd. Na_2SO_4, THF, MW, 400 W, 3 min, (ii) imidazole, benzylamine, MW, 4 min, 400 W, (iii) Ac_2O, DMAP, MW, 350 W, 5 min.

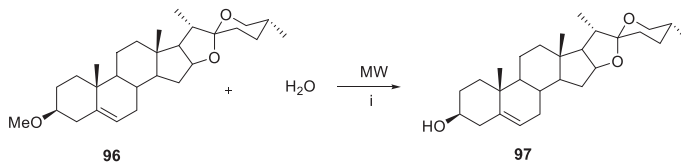

Scheme 24.31 *Reagent and conditions*: (i) $[BHSO_3MIm]$ HSO_4.

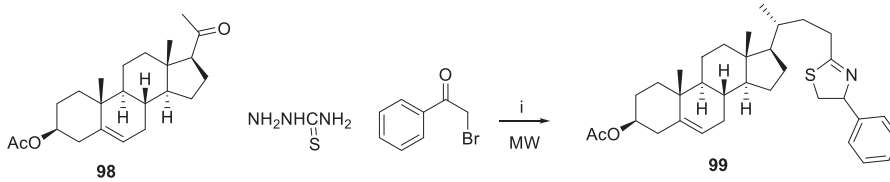

Scheme 24.32 *Reagent and conditions*: (i) EtOH, 35–40 min.

Baji and his research group synthesized a new, efficient MW-promoted steroidal isothiazole derivatives **102** from corresponding β-bromo-α,β-unsaturated aldehydes **101** that has been described using a sodium thiocyanateurea system (Scheme 24.33). The β-bromo-α,β-unsaturated aldehydes derivatives are efficiently synthesized from corresponding cyclic ketones **100** using Vilsmeier formylation reaction [115].

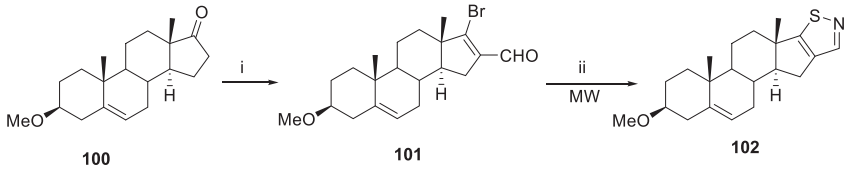

Scheme 24.33 *Reagent and conditions*: (i) PBr_3/DMF/$CHCl_3$; NaSCN/Urea/DMF, MW, 360 W, 10 bar.

In 2013, Gogoi et al. reported Pd-catalyzed protocol for the synthesis of fused steroidal pyrimidines **104** from β-halo-α,β-unsaturated aldehydes **103** under MW irradiation [116] (Scheme 24.34).

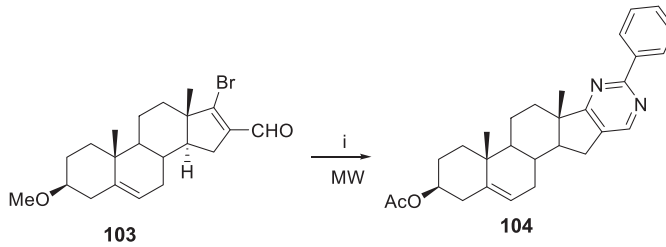

Scheme 24.34 *Reagent and conditions*: (i) Benzamidine hydrochloride, base, ligand, MW, 130 W, 8 bar, 140°C.

In 2014, Shekarrao et al. reported a facile method for the synthesis of steroidal D-ring fused pyrazolo[1,5-*a*]pyrimidines **106** through a MW-mediated reaction between steroidal β-bromovinyl aldehydes **105** and pyrazoloamines using palladium(II) catalyst (Scheme 24.35) [117].

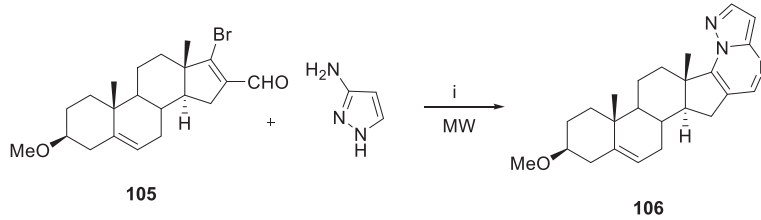

Scheme 24.35 *Reagent and conditions*: (i) $Pd(OAc)_2$, PPh_3, K_2CO_3, DMF, MW, 20 min.

In 2015, Saikia et al. synthesized a new and efficient synthesis of steroid fused pyrimidines [118]. Starting from steroidal α,β-unsaturated ketones **107** and amidine derivatives **108** with base-mediated reaction under MW irradiation as depicted in Scheme 24.36.

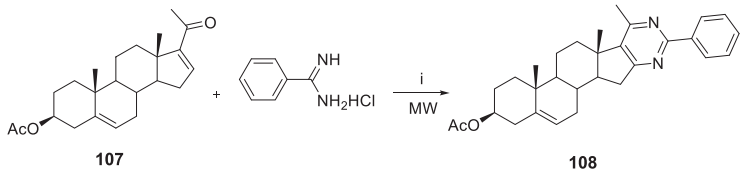

107 108

Scheme 24.36 *Reagent and conditions*: (i) Baes (2 mmol), 700 W, 10 min.

An efficient synthesis of ring D-condensed 2-pyrazolines in the D5-androstene was achieved by Motyan et al. in 2016, starting from a commercially 16-dehydropregnenolone or its acetate **109** with different arylhydrazines or methylhydrazine under MW irradiation via hydrazone intermediates, followed by intramolecular 1,4-addition as the key step (Scheme 24.37). The synthesized compounds were subjected to in vitro pharmacological studies of their antiproliferative activities against four human breast (MCF7, T47D, MDA-MB-231, and MDA-MB-361) and three cervical (HeLa, C33A, and SiHA) malignant cell lines [119].

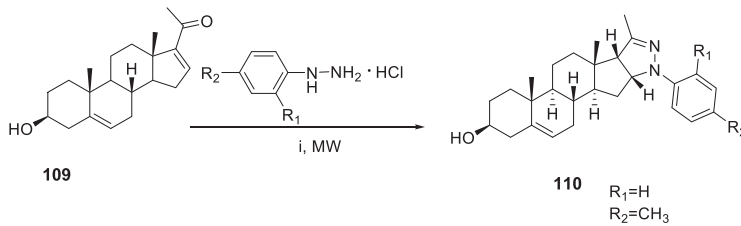

109 110

Scheme 24.37 *Reagent and conditions*: (i) PTSA, EtOH, 100°C, 20 min, MW.

In 2003, Marwah et al. reported under MW irradiation steroidal enones, more specifically, position three carbonyls were efficiently and selectively converted to the corresponding enol acetates **112** in the presence of additional enolizable carbonyl functions at other positions, using acetic anhydride and a catalytic amount of toluene-*p*-sulfonic acid. Acetylation of hydroxyl groups of the sterols, including those at the hindered positions, was near quantitative (Scheme 24.38). Strictly anhydrous conditions were not a prerequisite for acetylation and the reaction system easily tolerated up to 10% (v/v) moisture [120].

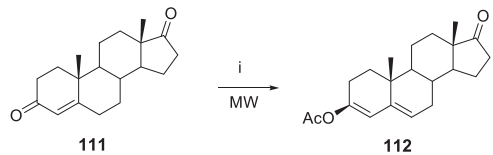

111 112

Scheme 24.38 *Reagent and conditions*: (i) Ac_2O, toluene-*p*-sulfonic acid.

In 2009, Edelsztein et al. reported a new approach to C—C bonded steroidal homodimers **114** derived from deoxycholic acid, pregnenolone, and progesterone **113** were synthesized by an olefin metathesis reaction assisted by MW heating (Scheme 24.39). Due to the bulky nature of the steroidal skeleton, the more favorable E-dimers were formed as the sole or major products depending on the linker length [121].

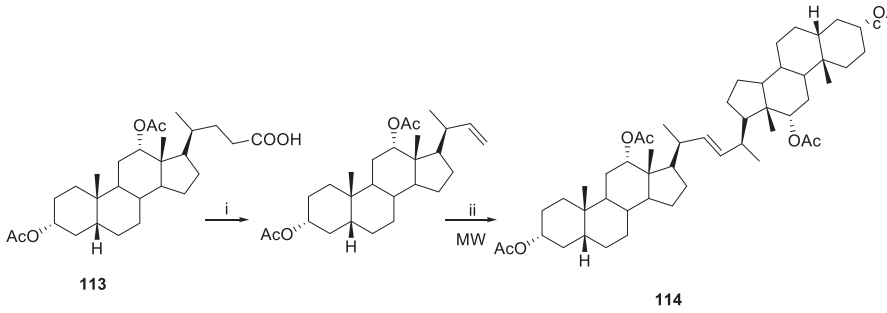

113 114

Scheme 24.39 *Reagent and conditions*: (i) DIB, py, Cu^{2+}, toluene; (ii) Grubbs cat second gen, 10 mol%, CH_2Cl_2, MW.

Sharma and coworkers synthesized steroid fused pyridines by the condensation of formyl enamides with cyanomethylenes under MW irradiation in the presence of basic alumina (Scheme 24.40) [122].

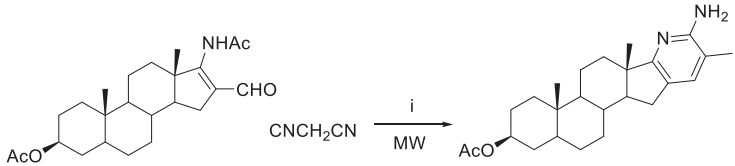

115 116

Scheme 24.40 *Reagent and conditions*: (i) Al_2O_3, 8–10 min.

Recently, Bautista-Hernández et al. reported the synthesis of a novel carbohydrate-lithocholic acid conjugate linked through 1,2,3-triazole rings (Scheme 24.41). The conjugate was synthesized via copper-catalyzed azide–alkyne cycloaddition (CuAAC) from methyl 4,6-*O*-benzylidene-2,3-di-*O*-propargyl-α-D-glucopyranoside **117** and methyl 3-azidolithocholate **118**. The 1,3-dipolar cycloaddition of dipropargyl ether (1.0 equiv.) to azide (2.0 equiv.) with Cu-Al mixed oxide heterogeneous catalyst and sodium ascorbate in EtOH-H_2O (3:1) was reacted under MW irradiation at 100°C to afford **119** in an excellent yield of 93% in just 5 min [123].

In 2017, Lopes et al. reported the regio- and stereoselective synthesis of novel chiral 4,5,6,7-tetrahydropyrazolo[1,5-*a*]pyridine-fused steroids **121** via [8π + 2π] cycloaddition of diazafulvenium methides with steroidal scaffolds (Scheme 24.42).

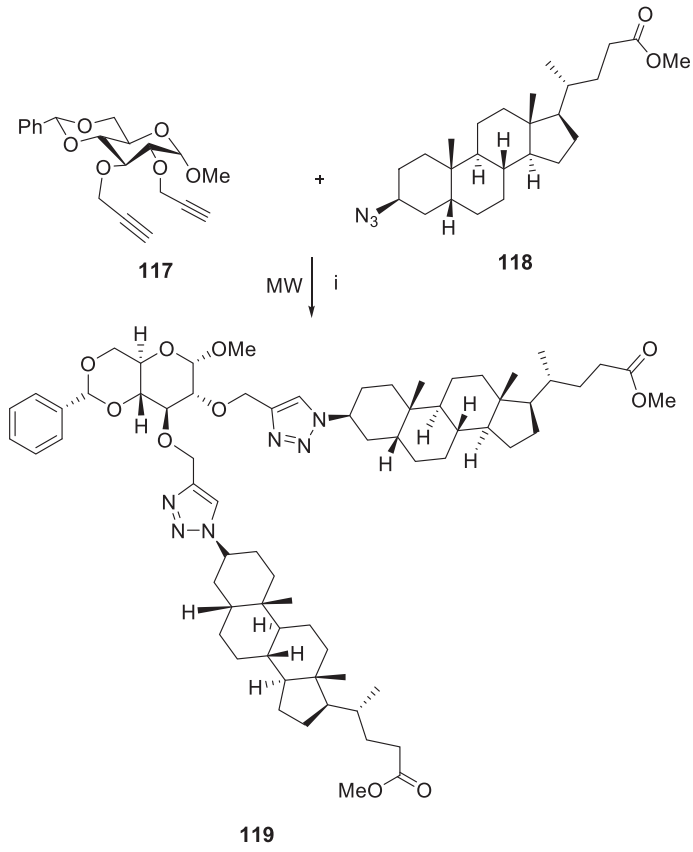

Scheme 24.41 *Reagent and conditions*: (i) Cu-Al mixed oxide, sodium ascorbate, EtOH, H_2O (3:1), MW, 30 W, 100°C, 5 min.

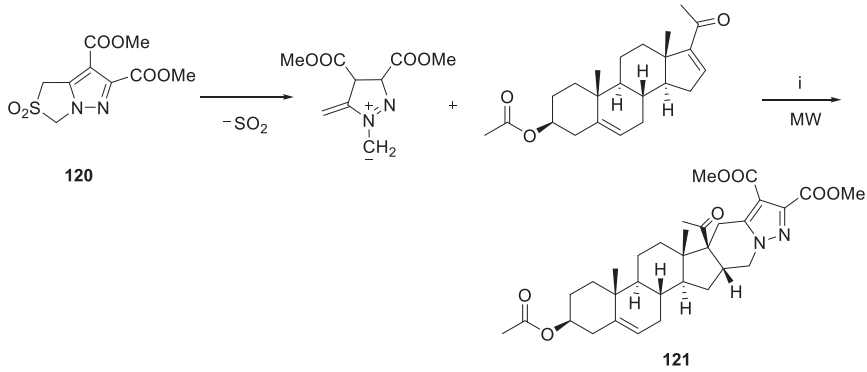

Scheme 24.42 *Reagent and conditions*: (i) TCB, MW, 250°C, 10 min.

The biological evaluation of the new family of hexacyclic steroids as anticancer agents was also carried out. Hexacyclic steroids bearing a benzyl group at C-22, derived from 16-dehydropregnenolone and 16-dehydroprogesterone, show considerable cytotoxicity against EL4 (murine T-lymphoma) in contrast with the corresponding C-22-unsubstituted derivatives showing low cytotoxicity. Thus, results indicate that the presence of the benzyl group is important to ensure cytotoxicity [124].

In 2006, Kiuru et al. reported an efficient synthesis for 2,4,16,16-D4-estrone palmitate, stearate, oleate, linoleate, and linolenate and the corresponding 2,4,16,16,17-D5-estradiol fatty acid 17-mono and 3,17-diesters using analogous fatty acid chlorides or fatty acid anhydrides and 4-(dimethylamino)pyridine under MW irradiation (Scheme 24.43) [125].

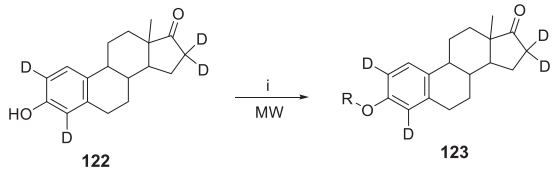

Scheme 24.43 *Reagents and conditions*: (i) Fatty acid chloride or anhydride, DMAP, pyridine. MW, 50 W, 50°C, 2 min.

Kovács et al. synthesized a novel types of 17-*exo*-heterocycles **126** in the Δ^5 androstene series carrying a 1,3,4-oxadiazolemoiety via aldehyde *N*-acylhydrazone intermediates, obtained from the MW-assisted condensation of 3β-hydroxy or 3β-acetoxyandrost-5-ene-17β-carbaldehyde **124** with different acylhydrazides **125** (Scheme 24.44). The subsequent phenyl iodonium diacetate-induced oxidative

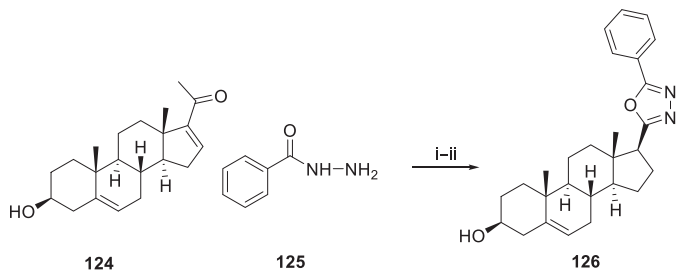

Scheme 24.44 *Reagents and conditions*: (i) EtOH, MW, 120°C, 10 min, (ii) PIDA, CH_2Cl_2.

cyclization proceeded under mild conditions. The synthesized compounds were subjected to in vitro pharmacological studies to investigate their antiproliferative activities on four malignant adherent cell lines (HeLa, MCF7, A2780, and A431), and exhibited the highest potency against HeLa cells, some of them revealing action comparable to that of the reference agent cisplatin [86].

In 2008, Zeng et al. reported a rapid and efficient method for the synthesis of novel molecular clefts based on deoxycholic acid **130** (Scheme 24.45) [126].

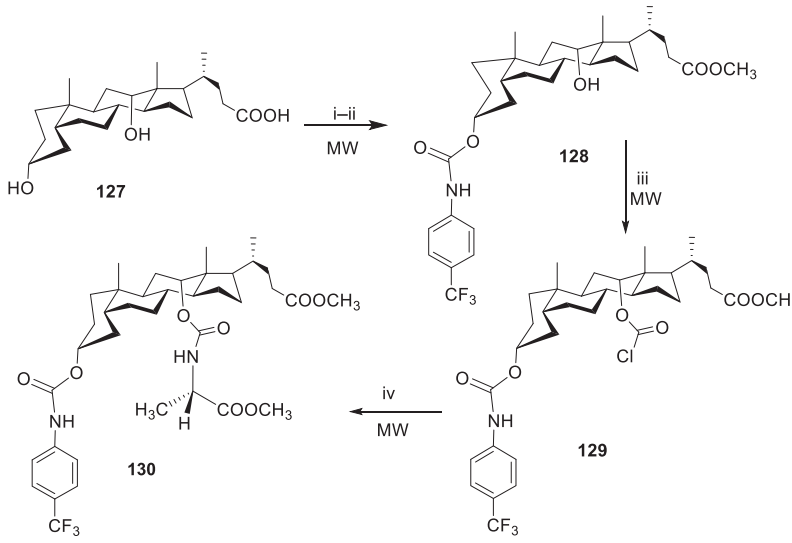

Scheme 24.45 *Reagents and conditions*: (i) CH_3OH, CH_3COCl; (ii) triphosgene, CH_2Cl_2, pyridine, 4-aminobenzotrifluride; (iii) CH_2Cl_2, triphosgene, pyridine; (iv) L-amino acid methyl ester hydrochloride, pyridine.

In 2005, Scho and his research group described an efficient Pd(0)-catalyzed method for the rapid and efficient preparation of 3-aminoestrone via 3-benzylaminoestrone from estrone-triflate (Scheme 24.46) [127].

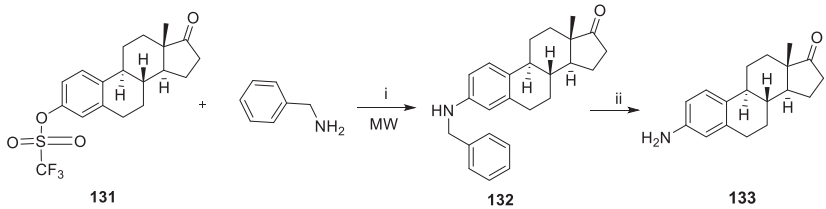

Estrone-triflate Amino benzyl estrone

Scheme 24.46 *Reagents and conditions*: (i) $Pd(OAc)_2$, MW, X-phos, Cs_2CO_3, 120–160°C; (ii) H_2, Pd/C.

In 2003, De Meijere and his coworker demonstrated that a sequence of Stille and Heck cross-coupling reactions and subsequent thermal 6p-electrocyclization provided easy access to the steroidal compounds by a convergent A + CD → ACD → ABCD strategy (Scheme 24.47). The highly chemoselective Stille couplings on the triflate moiety of several 2-bromo-cyclohex-1-enyl triflates **135** with cis- and transfused bicyclo[4.3.0]-nonenylstannanes **134** furnished the corresponding tricyclic bromobutadienes **136** in good to excellent yields (70%–97%). These were subjected to Heck reactions with *tert*-butyl acrylate to provide pentasubstituted tricyclic 1,3,5-hexatrienes. A significant increase in efficiency of the Heck coupling process could be achieved by applying a protocol with a precatalyst on the basis of Herrmann's palladacycle prepared from $Pd(OAc)_2$ and P(*o*-Tol)$_3$ with added triarylphosphines as co-ligands (73%–90% yield). Upon heating these hexatrienes cyclized to yield various unsaturated steroid analogs **138** [128].

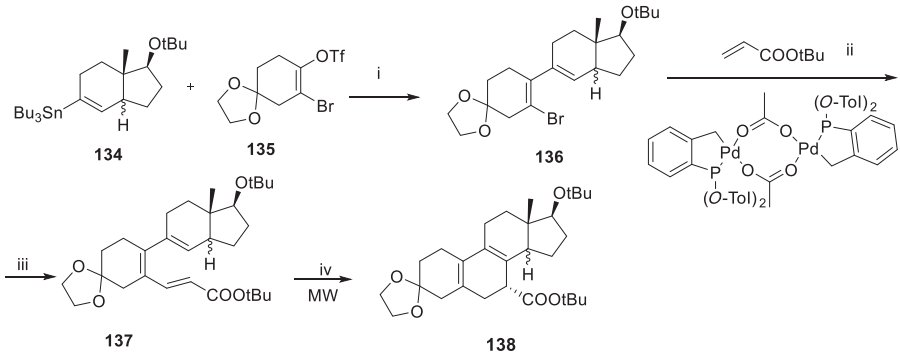

Scheme 24.47 *Reagent and condition*: (i) $Pd(dba)_2$, $AsPh_3$,CuI, LiCl, NMP, 60°C, (ii) nBu$_4$NOAc, DMF, MeCN, H_2O, 120°C, (iii) DMF/toluene, MW, 170°C (45 min)–200°C (2 min).

In 2013, Boruah and his research group reported the palladium-catalyzed multicomponent synthesis of steroidal A- and D-ring fused pyridines. Their strategy involved a solvent-free three-component reaction of steroidal β-halovinyl aldehyde, alkyne, and benzylamine in the presence of $Pd(OAc)_2$ under MW irradiation led to the target steroidal pyridine in high yield (Scheme 24.48). It is worth noting that all of the reactions of β-bromovinyl aldehydes **139** with unsymmetrical alkynes **140**

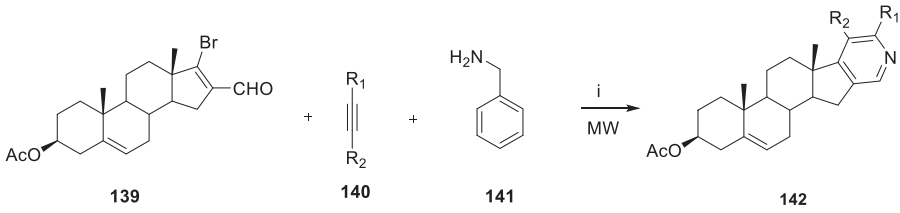

Scheme 24.48 *Reagent and Conditions*: (i) $Pd(OAc)_2$, PPh_3, Na_2CO_3, Al_2O_3, MW, 600 W, 10 min.

and benzylamine **141** afforded only one regioisomer of the pyridine derivative **142**. A wide variety of alkyl-, aryl-, and ester-substituted alkynes underwent this highly regioselective reaction to give good yields of the desired steroidal pyridines [99].

Our research group in 2015 reported an elegant synthetic strategy for the synthesis of a new class of peptidomimetic steroid-amino acid hybrid compounds **144** having diverse biological properties. We reported the synthesis of these compounds of alanine and valine methyl esters with seco-steroids (A, B, and D ring cleavage) in an expedited way by MW-promoted Ugi-four-component reaction (Ugi-4CR) (Scheme 24.49) [129].

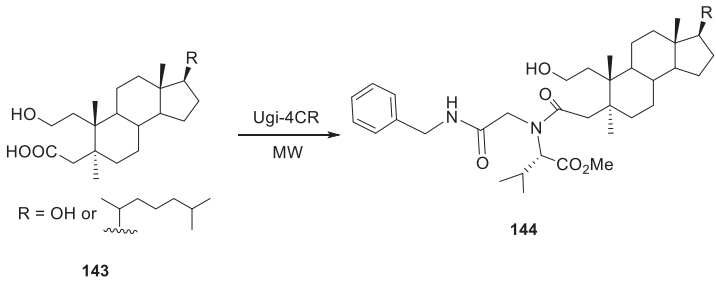

Scheme 24.49 *Reagent and conditions*: (i) L-Alanine methyl ester hydrochloride, paraformaldehyde, triethylamine, benzylisocyanide, MeOH, MW 400 W, 100°C, 15 bar, 10 min.

Recently, our group reported an efficient strategy to construct a sterylferulates (Scheme 24.50). Synthetic sterylferulates [3-*O*-(*trans*-4-feruloyl)-sterols] are currently gaining considerable importance in recent years to be used as nutraceuticals and food additives as well as in pharmaceutical applications substituting c-oryzanol—a class of naturally occurring sterylferulates having potent antioxidant and other organoleptic properties. Considering the importance of this class of compounds coupled with green technology associated with MW energy in organic synthesis, we report here an expedited and high yield synthesis of sterylferulates from abundant steroids, viz., cholesterol, cholestanol, stigmasterol, stigmastanol, β-sitosterol, β-campesterol, β-campestanol, and ergosterol applying MW energy in the crucial step of esterification process of sterols with *trans*-4-*O*-acetylferulic acid **146** to

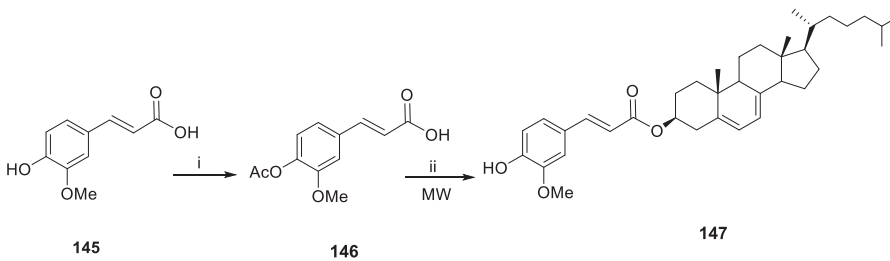

Scheme 24.50 *Reagent and conditions*: (i) TMSCl-NaI-Ac_2O, (ii) DCC, DMAP, 20 min, base.

furnish their esterified products, viz., 3-*O*-(*trans*-4-*O*-acetylferuloyl)-sterols **147** for their eventual deprotection to their respective sterylferulates [130].

Recently, our group developed an efficient method for the synthesis of MW-assisted peptidomimetic steroid–amino acid hybrid compounds based on steroidal amines by Ugi-four-component reaction (Ugi-4CR) (Scheme 24.51) [131].

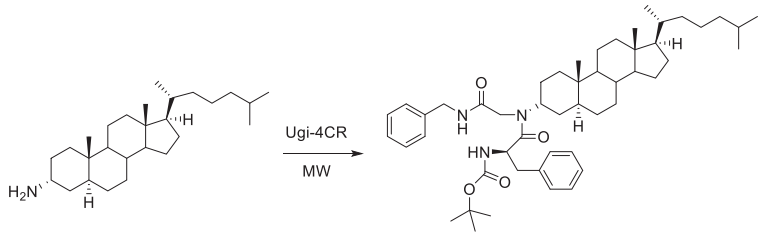

Scheme 24.51 *Reagent and conditions*: (i) Paraformaldehyde (ii) benzylisocyanide, (iii) *N*-(tert-butoxycarbonyl)-L-phenylalanine MW, 400 W, 100°C, 15 min, 82%–87%.

24.3 Microwave in the synthesis of compounds based on the properties (cholesterol, hormone, bile acid, vitamin, steroids links to other molecules, and other types)

The interest in the microwave-assisted organic synthesis has been growing during recent years. It results from an increasing knowledge of fundamentals of the dielectric heating theory, availability of equipment designed especially for the laboratory use as well as the discovery of the special techniques of the MW syntheses. The efficiency of MW flash-heating chemistry in dramatically reducing reaction times (reduced from days and hours to minutes and seconds) has recently been proven in several different fields of organic chemistry and this aspect is of great importance in high-speed combinatorial and medicinal chemistry.

In an ideal world, chemical transformations occur at room temperature, reach full conversion within a few minutes, and provide quantitative isolated product yields. The reality, however, is quite different. Many synthetically relevant processes necessitate an elevated temperature regime in order to proceed, with reaction times of several hours or even days to drive a reaction to completion not being uncommon. MW radiation is an alternative to conventional heating for introducing energy into reactions. MW heating uses the ability of some compounds (liquids or solids) to transform electromagnetic energy into heat. The use of MW irradiation has led to the introduction of new concepts in chemistry because the absorption and transmission of the energy are completely different from the conventional mode of heating. This method of heating associated with MW technology has applied a number of useful processes. These include the preparation for analysis, organic synthesis, application to waste treatment, polymer technology, drug release/targeting, ceramic,

and alkane decomposition [132]. The technique has also found use in a range of decomposition processes including hydrolysis of proteins and peptides [133]. The ability of MAOS to rapidly synthesize organic compounds is of significant benefit for library generation and its potential as a feature tool for drug-discovery programs has recently been recognized [134].

MW heating of foods may cause the formation of cholesterol oxidation products (COPs). COPs formation depend on the conditions of MW heating and the composition of the food matrix. The aim of this work was to study the formation of major COPs from cholesterol incorporated into palm, extra virgin olive, soybean, or fish oils during MW heating, and to monitor changes in peroxide value and fatty acid (FA) profiles. Model systems composed of mixtures of cholesterol and oil (2.5 mg of cholesterol/g oil), were heated for 20 min in multimode (900 W), unimode MW (≈300 W) ovens or convection oven at 180°C. Maximum total COPs contents largely varied (46.4–250.4 μg/g lipids), depending on the type of heating system and oil matrix. Multimode MW heating caused greater COPs formation than unimode MW. COPs formation trends in the conventional oven were similar to those of MW heating, except for fish oil. Results indicated that soybean oil, compared with the other oils tested, did not promote cholesterol oxidation during MW heating, while the opposite trend was observed for extra-virgin olive oil and palm oil. FA profile and natural antioxidants influenced cholesterol and surrounding media oxidation during MW heating [135]. The synthesis of cholesterol-based sterylferulate is exemplified in Scheme 24.50, in which MW irradiation played a crucial role in the esterification step with *trans*-4-*O*-acetylferulic acid [130].

In 2018, Motyan et al. described the synthesis of novel 17β-pyrazol-5′-ones in the Δ^5-androstane starting from available pregnenolone acetate. A steroidal 17-carboxylic acid was first synthesized as a norpregnene precursor by the bromoform reaction followed by subsequent acetylation. Its CDI-activated acylimidazole derivative was then converted to a β-ketoester containing a two carbon atom-elongated side chain than that of the starting material. A Knorr cyclization of the bifunctional 1,3-dicarbonyl compound with hydrazine and its monosubstituted derivatives in AcOH under MW heating conditions led to the regioselective formation of 17-*exo*-heterocycles in good to excellent yields (Scheme 24.52). The antiproliferative activities of the structurally related steroidal pyrazol-5′-ones and their deacetylated analogs were screened on three human adherent breast cancer cell lines (MCF7, T47D, and MDA-MB-231): the microculture tetrazolium assay revealed that some of the presented derivatives exerted cell growth inhibitory effects on some of these cell lines comparable to those of the reference compound, cisplatin [136].

Wang and coworker proposed a simple and fast sample pretreatment method for the determination of steroid hormones in fish tissues by coupling dynamic MW-assisted extraction with salting-out liquid-liquid extraction. The steroid hormones were successively extracted with acetonitrile and water under the action of MW energy. Subsequently, the extract was separated into an acetonitrile phase and an aqueous phase with ammonium acetate. The acetonitrile phase containing the target analytes was concentrated and determined by LC-MS/MS. The limits of detection for the steroid hormones were in the range of 0.03–0.15 ng/g. This method was successfully applied

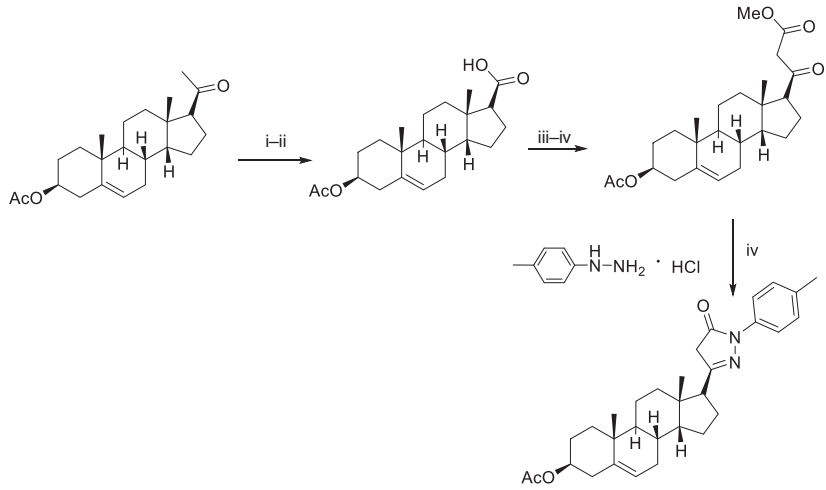

Scheme 24.52 *Reagent and conditions*: (i) Br_2/NaOH, dioxane, (ii) Ac_2O/Py, (iii) CDI, THF, (iv) $MgCl_2$, Et_3N, CH_3CN.

to analyze seven kinds of fish tissues, and the recoveries of the steroid hormones for the spiked samples were in the range of 75.3 ± 4.9% to 95.4 ± 6.2%. Compared with the traditional method, the proposed method could reduce the consumption of the organic solvent, shorten the sample preparation time, and increase the sample throughput [137].

In 2006, Pore et al. designed a novel bile acid conjugates via Cu(I) catalyzed intermolecular 1,3-dipolar cycloaddition. These new molecules showed good antifungal activity against Candida species [138] (Scheme 24.53).

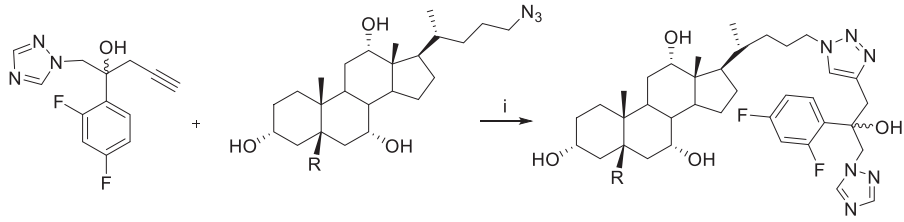

Scheme 24.53 *Reagent and conditions*: (i) $CuSO_4 \cdot 5H_2O$ (5 mol%), sodium ascorbate (40 mol%), DMF/H_2O (9:1), MW, 5 min.

In 2007, Aher and his group reported 1,3-dipolar cycloaddition of propargyl esters of bile acids to azide group attached at different positions of bile acids gave dimers, trimer, and tetramer linked with 1,2,3-triazole. These dimeric and oligomeric structures were able to solubilize hydrophilic dye-cresol red, in nonpolar solvent (Scheme 24.54) [139].

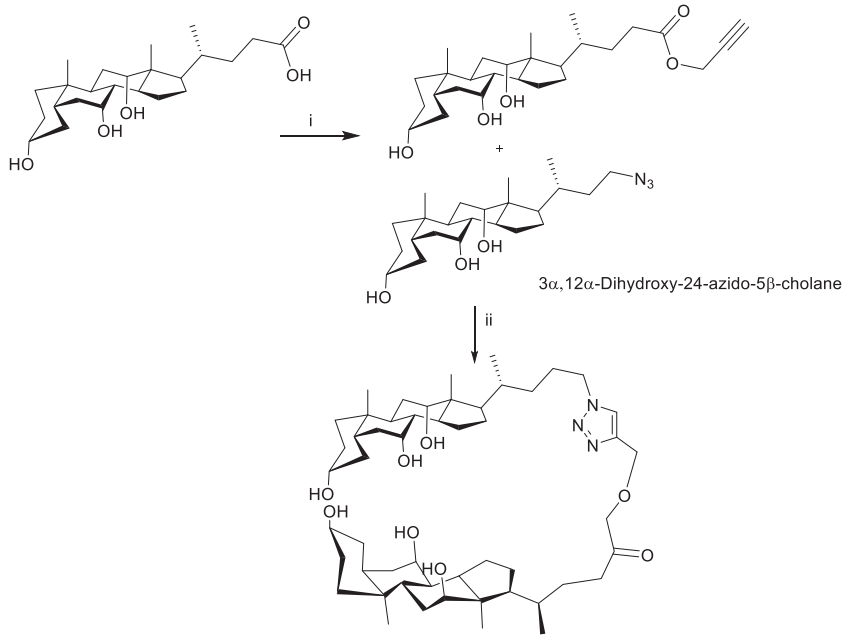

Scheme 24.54 *Reagents and conditions*: (i) PTSA (10 mol%), propargyl alcohol, 60°C (ii) $CuSO_4 \cdot 5H_2O$ (5 mol%), sodium ascorbate (40 mol%), DMF/H_2O (4:1), microwave, 5 min, 90%–96%.

24.4 Comparison of microwave vs classical method

MW technology is becoming exceedingly popular in the chemical industry because it gives an increased rate of conversion and yield in a short duration of time. MW energy couples with the polar molecules in the reaction system to generate vibrations that are independent of the temperature of the reaction. It leads to instant localized superheating due to ionic conduction [140]. MW combines two effects, that is, nonthermal and thermal [141]. MW irradiation leads to direct coupling of molecules of the reaction system which gives much better results compared to conventional heating as it leads to direct coupling of molecules by selective absorption [142]. Thus, some reactions which take hours to complete under conventional heating can be successful using the MW in a very short time. In the synthesis of lauric acid esters using Novozym 435, conventional heating required 24 h whereas, the reaction was completed in merely 8 min under the MW system [143]. Also, MW radiations improve the stability profile of enzymes by delaying denaturation. Enzymes like *Candida antarctica* lipase B have shown improved stability under MW system as compared to conventional heating [144, 145]. Specialty esters are chemical components that are used for their effect and performance. They can be categorized on the basis of their application and function. Based on the application they are used in agrochemicals, fragrance and flavors, personal care products, foods and

nutraceuticals, textiles, polymers, dyes, lubricants, etc. Specialty esters by function include emulsifiers, viscosity builders, antioxidants, synthetic dyes, fixatives, surfactants, synthetic intermediates, pesticide synergists, etc. [146, 147]. Chemical, as well as enzymatic routes, can be used for the synthesis of specialty esters. However, conventional enzymatic reactions are very slow [148, 149]. One of the approaches to intensify the enzymatic reactions is through the use of MW energy. MW heating and biocatalysis show the synergistic effect with augmentation of rate and final conversion [150]. In the enzyme-catalyzed esterification of adipic acid with various alcohols, low MW energy leads to an improvement in rate by a factor of up to 2.63 as compared to normal heating [151]. This effect was due to the higher collision frequency between the molecules under MW [152–154]. The synergism of MW energy and biocatalysis has shown good results in esterification [155] as well as transesterification reactions [156]. However, this synergistic approach in the synthesis of specialty esters is still in a nascent stage.

24.5 Conclusion

From the above discussion, it is clear that MW heating effects have a major impact on many areas of preparative science and particularly in the area of synthetic chemistry and medicinal chemistry. It is notable that the impact has probably been far greater than many other technological developments and that MW heating methods have become mainstream. Numerous laboratories have commercial instruments, particularly as they have become very reliable, safe, and relatively inexpensive. It has become clear that, unlike many new technologies, MWs have genuinely become an acceptable and routinely applied method for synthesis. Continued efforts by the suppliers of instruments should hopefully make the technology available to every bench chemist and perhaps even to every bench scientist who needs to heat a sample. Although costs have dramatically reduced in recent years, we have yet to see them reduce to a point where the instruments become viewed as a standard piece of individual laboratory equipment. If that does happen then we could see further dramatic developments in the uptake of this valuable technology. The size of instruments may also need to reduce a little such that every laboratory bench could readily accommodate an instrument. So, further developments from equipment suppliers could continue to enhance the field further. Scientifically, we can envisage still further attempts to speed up processes. One of the most exciting developments has probably been in peptide chemistry and the idea that we might at some point be able to make large-scale synthetic proteins in a day is an appealing prospect. Further, major impacts on sample preparation for biology, materials science, nanotechnology, and polymer science are all likely to result in the next 5–10 years. Although there have been exciting developments, there are still many opportunities for MW heating to revolutionize these areas.

Acknowledgments

Dr. Bimal is grateful to Prince Mohammad Bin Fahd University. Dr. Preetismita acknowledges support from the Director of CSIR-Central Scientific Instruments Organization, Chandigarh.

References

[1] A. De La Hoz, A. Diaz-Ortiz, A. Moreno, Selectivity in organic synthesis under microwave irradiation, Curr. Org. Chem. 8 (2004) 903–918.

[2] R. Bucourt, L. Nédélec, J.C. Gasc, J. Weill-Raynal, Some data on the asymmetric synthesis in the estradiol series, Bull. Soc. Chim. Fr. 2 (1967) 561–563.

[3] W.E. Bachmann, W. Cole, A.L. Wilds, Total synthesis of the sex hormone equilenin and its stereoisomers, J. Am. Chem. Soc. 62 (4) (1940) 824–839.

[4] R.B. Woodward, F. Sondheimer, D. Taub, K. Heusler, W.M. McLamore, The total synthesis of steroids, J. Am. Chem. Soc. 74 (17) (1952) 4223–4251.

[5] C.H. Kuo, D. Taub, N.L. Wendler, A synthesis of estrone via novel intermediates: mechanism of the coupling reaction of a vinyl carbinol with a diketone, J. Org. Chem. 33 (8) (1968) 3126–3132.

[6] M. Weimar, G. Dürner, J.W. Bats, M.W. Göbel, Enantioselective synthesis of (+)-estrone exploiting a hydrogen bond-promoted diels–alder reaction, J. Organomet. Chem. 75 (8) (2010) 2718–2721.

[7] L.H. Sarett, G.E. Arth, R.M. Lukes, R.E. Beyler, G.I. Poos, W.F. Johns, J.M. Constantin, Stereospecific total synthesis of cortisone, J. Am. Chem. Soc. 74 (19) (1952) 4974–4976.

[8] S.K. Kang, K.Y. Jung, C.H. Park, E.Y. Namkoong, T.H. Kim, Palladium-catalyzed arylation of allylic diols-highly selective synthesis of phenyl-substituted allylic diols, Tetrahedron Lett. 36 (1995) 6287–6290.

[9] F.D. Riccardis, I. Izzo, C. Tedesco, G. Sodano, Synthesis and cytotoxic activity of steroid-anthraquinone hybrids, Tetrahedron 53 (1997) 10871–10882.

[10] Z. Szarkaa, R. Skoda-Foldesa, J. Horvath, Z. Tuba, L. Kolla, Synthesis of steroidal diacyl hydrazines and their 1,3,4-oxadiazole derivatives, Steroids 67 (2002) 581–586.

[11] L.F. Tietze, J.M. Wiegand, C. Vock, Synthesis of enantiopure B-nor-steroids by multiple Pd-catalyzed transformations, J. Organomet. Chem. 687 (2003) 346–352.

[12] S.M. Wang, W.Z. Gea, H.M. Liu, D.P. Zoua, X.B. Yan, Syntheses of acetylated steroid glycosides and selective cleavage of O-acetyl groups in sugar moiety, Steroids 69 (2004) 599–604.

[13] P. Chowdhury, A.M. Das, P. Goswami, Synthesis of some new steroidal [16, 17-d]-isoxazolines, Steroids 70 (2005) 494–498.

[14] H.W. Sünnemann, A. Hofmeister, J. Magull, A. de Meijere, An efficient access to novel enantiomerically pure steroidal d-amino acids, Chem. Eur. J. 12 (2006) 8336–8344.

[15] P. Bazzini, M.I. Ouali, H. Pellissier, M. Santelli, Efficient synthesis of C-11 functionalized steroids, Steroids 71 (2006) 459–468.

[16] J.Z. Yan, J. Li, G.W. Rao, One-pot synthesis of new A-ring fused steroidal pyridines, Steroids 72 (2007) 736–739.

[17] M.N. Sakac, A.R. Gakovic, J.J. Csanadi, E.A. Djurendic, O. Klisuric, V. Kojic, G. Bogdanovic, K.M.P. Gasi, An intramolecular one-pot synthesis of steroidal triazoles via 1,3-dipolar cycloadditions of in situ generated diazo compounds, Tetrahedron Lett. 50 (2009) 4107–4109.

[18] V. Foucher, B. Guizzardi, M.B. Groen, M. Light, B. Linclau, A novel, versatile D → BCD steroid construction strategy, illustrated by the enantioselective total synthesis of estrone, Org. Lett. 12 (2010) 680–683.

[19] Y. Huang, J. Cui, S. Chen, C. Gan, A. Zhou, Synthesis and antiproliferative activity of some steroidal lactams, Steroids 76 (2011) 1346–1350.

[20] K.Q. Shawakfeh, N.H. Al-Said, Synthesis of new symmetrical bis-steroidal pyrazine analogues from diosgenin, Steroids 76 (2011) 232–237.

[21] S.A. Khan, A.M. Asiri, Synthesis of novel steroidal oxazolo quinoxaline as antibacterial agents, Arab. J. Chem. 4 (2011) 349–354.
[22] M. Ibrahim-Ouali, E. Romero, K. Hamze, Stereoselective synthesis of pentacyclic steroids functionalized at C-11, Steroids 77 (2012) 1092–1100.
[23] M.A. Fernández-Herrera, H. López-Muñoz, J.M.V. Hernández-Vázquez, L. Sánchez-Sánchez, M.L. Escobar-Sánchez, B.M. Pinto, J. Sandoval-Ramírez, Synthesis and selective anticancer activity of steroidal glycoconjugates, Eur. J. Med. Chem. 54 (2012) 721–727.
[24] M. Ibrahim-Ouali, E. Romero, Synthesis and characterization of (±)-13-hydroxy-3,11-diaza steroids, Steroids 77 (2012) 157–167.
[25] J. Wolfling, P. Kovács-Pénzes, I. Zupko, G. Schneider, É. Frank, Synthesis, stereochemistry and cytotoxic activity of novel steroidal 16-spiro-1,3,2-dioxaphosphorinanes, J. Mol. Struct. 1013 (2012) 39–44.
[26] R. Bansal, S. Guleria, S. Thota, S.L. Bodhankar, M.R. Patwardhan, C. Zimmer, R.W. Hartmann, A.L. Harvey, Design, synthesis and evaluation of novel 16-imidazolyl substituted steroidal derivatives possessing potent diversified pharmacological properties, Steroids 77 (2012) 621–629.
[27] B.L. Zhang, E. Zhang, L.P. Pang, L.X. Song, Y.F. Li, B. Yu, H.M. Liu, Design and synthesis of novel D-ring fused steroidal heterocycles, Steroids 78 (2013) 1200–1208.
[28] Shamsuzzaman, A.M. Dar, Y. Khan, A. Sohail, Synthesis and biological studies of steroidal pyran based derivatives, J. Photochem. Photobiol. B Biol. 129 (2013) 36–47.
[29] N.J. Fan, Y.-B. Bai, F.-Y. Zhang, B. Luo, J.-J. Tang, Q.-Z. Zhang, J.-M. Gao, Synthesis and cytotoxicity of some novel 21*E*-benzylidene steroidal derivatives, Steroids 78 (2013) 874–879.
[30] N.J. Fan, J.J. Tang, H. Li, X.J. Li, B. Luo, J.M. Gao, Synthesis and cytotoxic activity of some novel steroidal C-17 pyrazolinyl derivatives, Eur. J. Med. Chem. 69 (2013) 182–190.
[31] Shamsuzzaman, A. Mashrai, H. Khanam, R.N. Aljawfi, Biological synthesis of ZnO nanoparticles using *C. albicans* and studying their catalytic performance in the synthesis of steroidal pyrazolines. Arab. J. Chem. (2013). https://doi.org/10.1016/j.arabjc.2013.05.004.
[32] C.C. Waller, M.D. McLeod, A simple method for the small scale synthesis and solid-phase extraction purification of steroid sulphates, Steroids 92 (2014) 74–80.
[33] S. Fustero, R. Lázaro, N. Aiguabella, A. Riera, A. Simon-Fuentes, P. Barrio, Asymmetric allylation/Pauson Khand reaction: a simple entry to polycyclic amines. Application to the synthesis of aminosteroid analogues, Org. Lett. 16 (2014) 1224–1227.
[34] A. Romero-Lopez, S. Montiel-Smith, S. Meza-Reyes, P. Merino-Montiel, J.L. Vega-Baez, Synthesis of steroidal derivatives containing substituted, fused and spiro pyrazolines, Steroids 87 (2014) 86–92.
[35] Y.L. Zhang, Y.F. Li, Y.K. Shi, B. Yu, G.C. Zhang, P.P. Qi, D.J. Fu, L.H. Shan, H.M. Liu, Efficient three-component one-pot synthesis of steroidal polysubstituted anilines, Steroids 104 (2015) 1–7.
[36] Y.L. Zhang, Y.F. Li, X.L. Shi, B. Yu, Y.K. Shi, H.M. Liu, Solvent-free synthesis of novel steroidal 2-aminopyridines, Steroids 115 (2016) 147–153.
[37] A. Arenas-Gonzalez, L.A. Mendez-Delgado, P. Merino-Montiel, J.M. Padron, S. Montiel-Smith, J.L. Vega-Báez, S. Meza-Reyes, Synthesis of monomeric and dimeric steroids containing [1,2,4]triazolo [1,5 a]pyrimidines, Steroids 116 (2016) 13–19.
[38] D. Gavaskar, A.R. Suresh Babu, R. Raghunathan, M. Dharani, S. Balasubramanian, An expedient sequential one-pot four component synthesis of novel steroidal spiro-pyrrolidine heterocycles in ionic liquid, Steroids 109 (2016) 1–6.

[39] I.V. Rassokhina, Y.A. Volkova, A.S. Kozlov, A.M. Scherbakov, O.E. Andreeva, V.Z. Shirinian, I.V. Zavarzin, Synthesis and antiproliferative activity evaluation of steroidal imidazo[1,2-a]pyridines, Steroids 113 (2016) 29–37.
[40] M.C. Mayorquín-Torres, M. Flores-Álamo, M.A. Iglesias-Arteaga, Synthesis of benzannulated steroid spiroketals by palladium-catalyzed spirocyclization of steroid alkynediols, Tetrahedron Lett. 58 (2017) 2073–2076.
[41] M.A. Ramos-Enríquez, M.A. Iglesias-Arteaga, Synthesis of novel hybrid steroid dimers by BF_3•Et_2O-catalyzed aldol condensation of 2-formyl-estradiol diacetate and steroid sapogenins, Steroids 128 (2017) 46–49.
[42] S. Joppa, M. Lieseganga, P. Ehlersa, E. Frank, G. Schneider, J. Wolfling, P. Langer, Synthesis of novel 16-*E*-(arylidene)-3-methox-a-estrones via a palladium catalysed Suzuki-Miyaura reaction, Tetrahedron Lett. 59 (2017) 26–28.
[43] Y.L. Song, C.-P. Tian, W. Yan, L. Jiang, L.Q. Shen, Design, synthesis and antitumor activity of steroidal pyridine derivatives based on molecular docking, Steroids 143 (2018) 53–61.
[44] A. Mahmood Dar, R. Nabi, S. Mir, M. Ahmad Gatoo, Shamsuzzaman, S.H. Lone, Synthesis of steroidal imidazolidinthiones as potential apoptotic agents: investigation by theoretical and experimental studies, Bioorg. Chem. 79 (2018) 190–200.
[45] A. Sethi, P. Singh, N. Yadav, P. Yadav, M. Banerjee, R. Pratap Singh, Greener approach for synthesis of novel steroidal prodrugs using ionic liquid, their DFT study and apoptosis activity in prostate cancer cell line, J. Mol. Struct. 1180 (2019) 733–740.
[46] A. Hryniewickaa, M. Malinowskaa, T. Hauschildb, K. Pieczulc, J.W. Morzyckia, Synthesis and antimicrobial properties of steroid-based imidazolium salts, J. Steroid Biochem. Mol. Biol. 189 (2019) 65–72.
[47] R.N. Hanson, N. Gajadeera, Design and synthesis of fluorescently labeled steroidal antiestrogens, Steroids 145 (2019) 39–46.
[48] (a) R.J. Giguere, T.L. Bray, S.M. Duncan, G. Majetich, Tetrahedron Lett. 27 (1986) 4945. (b) R. Gedye, F. Smith, K. Westaway, H. Ali, L. Baldisera, L. Laberge, J. Rousell, Tetrahedron Lett. 27 (1986) 279.
[49] (a) C.O. Kappe, Controlled microwave heating in modern organic synthesis, Angew. Chem. Int. Ed. 43 (2004) 6250. (b) C. Oliver Kappe, A. Stadler, Microwaves in Organic and Medicinal Chemistry, Wiley-VCH, Weinheim, 2005.
[50] A. Loupy, G. Bram, J. Sansoulet, Thermolysis improvements in retro-diels–alder reactions of benzylamino alcohols under microwave irradiation, New J. Chem. 16 (1992) 233.
[51] R.S. Varma, Clay and clay-supported reagents in organic synthesis, Tetrahedron 58 (2002) 1235–1255.
[52] A. Diaz-Ortiz, F. Langa, A. de la Hoz, A. Moreno, Microwaves in organic synthesis. Thermal and non-thermal microwave effects, Eur. J. Org. Chem. 4 (2000) 3659.
[53] N. Elander, J.R. Jones, S.Y. Lu, S. Stone-Elander, Microwave-enhanced radiochemistry, Chem. Soc. Rev. 29 (2000) 239.
[54] F. Langa, P. de la Cruz, E. Espildora, J.J. Garcia, M.C. Perez, A. de la Hoz, Advances in organic synthesis: modern organofluorine chemistry-synthetic aspects, Carbon 38 (2000) 1641.
[55] A. Ali, A.U. Rahman, M. Ateeq, F. Ullah, U.R. Mughal, A. Wadood, Conventional versus microwave assisted synthesis, molecular docking studies and in vitro evaluation of benzohydrazide derivatives as new acetylcholinesterase and butyrylcholinesterase inhibitors, Med. Chem. 6 (2016) 583–592.
[56] L. Zong, S. Zhou, N. Sgriccia, M.C. Hawley, L.C. Kempel, Advances in organic synthesis: modern organofluorine chemistry-synthetic aspects, J. Microw. Power Electromagn. Energy. 38 (2003) 49.

[57] Y. Xu, Q.-X. Guo, Synthesis of fused heterocyclic compounds from arylidenerhodanines under microwave irradiation, Heterocycles 63 (2004) 903.
[58] N.N. Romanova, P.V. Kudan, A.G. Gravis, Y.G. Bundel, Advances in organic synthesis: modern organofluorine chemistry-synthetic aspects, Chem. Heterocycl. Compd. 36 (2000) 1130.
[59] S.K. Das, Application of microwave irradiation in the synthesis of carbohydrates, Synlett 35 (2004) 915.
[60] A. Corsaro, U. Chiacchio, V. Pistara, G. Romeo, Microwave-assisted chemistry of carbohydrates, Curr. Org. Chem. 8 (2004) 511.
[61] M. Larhed, C. Moberg, A. Hallberg, Microwave-accelerated homogeneous catalysis in organic chemistry, Acc. Chem. Res. 35 (2002) 717.
[62] H. Will, P. Scholz, B. Ondruschka, Advances in organic synthesis: modern organofluorine chemistry-synthetic aspects, Chem. Ing. Tech. 74 (2002) 1057.
[63] C. Oliver Kappe, Rapid parallel synthesis of polymer-bound enones utilizing microwave-assisted solid-phase chemistry, Comb. Chem. 6 (2002) 314.
[64] M. Lahred, A. Hallberg, M. Lahred, A. Hallberg, Microwave-assisted high-speed chemistry: a new technique in drug discovery, Drug Discov. Today 6 (2001) 406.
[65] A. Lew, P.O. Krutzik, M.E. Hart, A.R. Chamberlin, Increasing rates of reaction: microwave-assisted organic synthesis for combinatorial chemistry, J. Comb. Chem. 4 (2002) 95.
[66] B. Wathey, J. Tierney, P. Lidstrom, J. Westman, The impact of microwave-assisted organic chemistry on drug discovery, Drug Discov. Today 7 (2002) 373.
[67] R.S. Varma, Solvent-free organic syntheses on mineral supports using microwave irradiation, Clean Prod. Process. 1 (1999) 132.
[68] R.S. Varma, A. Zeneca, Microwave Assisted Solventless Synthesis of Melamines With Flexible Aromatic Substituents, Kavitha Printers, Bangalore, 2002.
[69] A.C. Metaxis, R.J. Meredith, Industrial Microwave Heating, Peregrinus, London, 1988.
[70] E. Bezdushna, H. Ritter, Microwave-assisted esterification of methacrylic acid and polymer analogous esterification of poly[ethylene-co-(acrylic acid)] with dissimilar phenols, Macromol. Rapid Commun. 28 (2007) 443–448.
[71] A. Loupy, L. Perreux, M. Liagre, K. Burle, M. Moneuse, Reactivity and selectivity under microwaves in organic chemistry relation with medium effects and reaction mechanisms, Pure Appl. Chem. 73 (2001) 161–166.
[72] K. Carsten, M. Iannelli, P. Kerep, M. Klink, S. Schmitz, S. Sinwell, Microwave-assisted polymer chemistry: heck-reaction, transesterification, Baeyer–Villiger oxidation, oxazoline polymerization, acrylamides, and porous materials, Tetrahedron 62 (2006) 4709–4714.
[73] S.B. Angelica de Fatima, O.E. Vercillo, C.Z. Andrade, Microwave-assisted Passerini reactions under solvent-free conditions, J. Braz. Chem. Soc. 22 (2011) 462–467.
[74] M.H. Hügel, Microwave multicomponent synthesis, Molecules 14 (2009) 4936–4972.
[75] S. Santra, P.R. Andreana, A one-pot, microwave-influenced synthesis of diverse small molecules by multicomponent reaction cascades, Org. Lett. 9 (2007) 5035–5038.
[76] V. Polshettiwar, M.N. Nadagouda, R.S. Varma, Microwave-assisted chemistry: a rapid and sustainable route to synthesis of organics and nanomaterials, Aust. J. Chem. 62 (2009) 16.
[77] J. Virkutyte, R.S. Varma, Green synthesis of metal nanoparticles: biodegradable polymers and enzymes in stabilization and surface functionalization, Chem. Sci. 2 (2011) 837.
[78] M.N. Nadagouda, T.F. Speth, R.S. Varma, Microwave-assisted green synthesis of silver nanostructures, Acc. Chem. Res. 44 (2011) 469–478.

[79] J.H. Kou, R.S. Varma, Beet juice-induced green fabrication of plasmonic AgCl/Ag nanoparticles, ChemSusChem 5 (2012) 2435–2441.
[80] B. Baruwati, R.S. Varma, High value products from waste: grape pomace extract-A three-in-one package for the synthesis of metal nanoparticles, ChemSusChem 2 (2009) 1041–1044.
[81] B. Baruwati, V. Polshettiwar, R.S. Varma, Glutathione promoted expeditious green synthesis of silver nanoparticles in water using microwaves, Green Chem. 11 (2009) 926–930.
[82] M.B. Gawande, V.D.B. Bonifacio, R. Luque, P.S. Branco, R.S. Varma, Benign by design: catalyst-free in-water, on-water green chemical methodologies in organic synthesis, Chem. Soc. Rev. 42 (2012) 5522–5551.
[83] G.C. Michael Kahn, K. Emmanuel, D. Francis, C.L. David, R.B. Hochberg, M.H. Robert, Microwave-enhanced nucleophilic fluorination in the synthesis of fluoropyridyl derivatives of [3,2-c]pyrazolo-corticosteroids, potential glucocorticoid receptor-mediated imaging agents, Bioorg. Med. Chem. Lett. 16 (2006) 3454–3458.
[84] Z. Zhigang, S. Zhichuan, L. Min, L. Xingli, Microwave-assisted synthesis and in vitro antibacterial activity of novel steroidal thiosemicarbazone derivatives, Bioorg. Med. Chem. Lett. 22 (2012) 7730–7734.
[85] A. Mahboob, A.A. Shahab, N.M. Parveen, L. Dong-Ung, S. Park, Microwave assisted synthesis and in silico screening of steroidal pyrazolines, Chin. Chem. Lett. 23 (2012) 1039–1042.
[86] D. Kovács, G. Mótyán, J. Wölfling, I. Kovács, I. Zupkó, É. Frank, A facile access to novel steroidal 17-2′-(1′,3′,4′)-oxadiazoles, and an evaluation of their cytotoxic activities in vitro, Bioorg. Med. Chem. Lett. 24 (5) (2014) 1265–1268.
[87] B. Dayal, K.R. Rapole, C. Patel, B.N. Pramanik, S. Shefer, G.S. Tint, G. Salen, Microwave-induced rapid synthesis of sarcosine conjugated bile acids, Bioorg. Med. Chem. Lett. 5 (12) (1995) 1301–1306.
[88] S. Zhichuan, Z. Zhigang, L. Min, W. Xiaohong, Solvent-free synthesis of novel unsymmetric chenodeoxycholic acid bis thiocarbazone derivatives promoted by microwave irradiation and evaluation of their antibacterial activity, C. R. Chim. 16 (2013) 977–984.
[89] A. Khan, M. Alam, M. Mushfiq, The synthesis of 20-amino-5a-cholest-6-eno [6,7-d] thiazole derivatives under microwave irradiation using dry-media conditions, Chin. Chem. Lett. 19 (2008) 1027–1030.
[90] Z.C. Shi, Z.G. Zhao, X.L. Liu, Y. Chen, Synthesis of new hyodeoxycholic acid thiosemicarbazone derivatives under solvent-free conditions using microwave, Chin. Chem. Lett. 22 (2011) 405–408.
[91] W. Renmin, L. Chan, L. Jingliang, Y. Fang, G. Jianpei, P. Xuejun, Pressured microwave-assisted hydrolysis of crude glycyrrhizic acid for preparation of glycyrrhetinic acid, Chin. J. Chem. Eng. 20 (1) (2012) 152–157.
[92] A. Baji, A. Gyovai, J. Wolfling, R. Minorics, I. Ocsovszki, I. Zupko, E. Frank, Microwave-assisted one-pot synthesis of steroid–quinoline hybrids and an evaluation of their antiproliferative activities on gynecological cancer cell lines, RSC Adv. 6 (2016) 27501–27516.
[93] G. Motyan, F. Kovacs, J. Wolfling, A. Gyovai, I. Zupko, E. Frank, Microwave-assisted stereoselective approach to novel steroidal ring D-fused 2-pyrazolines and an evaluation of their cell-growth inhibitory effects in vitro, Steroids 112 (2016) 36–46.
[94] B. Dayal, K. Rao, G. Salen, Microwave-induced organic reactions of bile acids: esterification, deformylation and deacetylation using mild reagents, Steroids 60 (1995) 453–457.

[95] B. Dayal, N.H. Ertel, K.R. Rapole, A. Asgaonkar, G. Salen, Rapid hydrogenation of unsaturated sterols and bile alcohols using microwaves, Steroids 62 (1997) 451–454.
[96] R. Skoda-Foldes, P. Pfeiffer, J. Horvath, Z. Tuba, L. Kollar, Microwave-assisted Stille-coupling of steroidal substrates, Steroids 67 (2002) 709–713.
[97] K.M. Penov Gasi, E.A. Djurendic, M. Szecsi, J. Gardi, J.J. Csanadi, O.R. Klisuric, S.V. Dojcinovic-Vujaskovic, A.R. Nikolic, M.P. Savic, J.J. Ajdukovic, A.M. Okljesa, V.V. Kojic, M.N. Sakac, S.S. Jovanovic-Santa, Microwave assisted synthesis and biomedical potency of salicyloyloxy and 2-methoxybenzoyloxy androstane and stigmastane derivatives, Steroids 94 (2015) 31–40.
[98] P. Saikia, P.P. Kaishap, J. Goswami, A.K. Singh, H.P. Deka Boruah, S. Gogoi, R.C. Boruah, Synthesis of steroidal and nonsteroidal vicinal heterocyclic alcohols, N-(1-cycloalkenyl)heterocycles and their antibacterial studies, Steroids 84 (2014) 36–45.
[99] K. Shekarrao, D. Nath, P.P. Kaishap, S. Gogoi, R.C. Boruah, Palladium-catalyzed multicomponent synthesis of steroidal A- and D-ring fused 5,6-disubstituted pyridines under microwave irradiation, Steroids 78 (2013) 1126–1133.
[100] M. Dutta, P. Saikia, S. Gogoi, R.C. Boruah, Microwave-promoted and Lewis acid catalysed synthesis of steroidal A- and D-ring fused 4,6-diarylpyridines, Steroids 78 (2013) 387–395.
[101] D. Kakati, R.K. Sarma, R. Saikia, N.C. Barua, J.C. Sarma, Rapid microwave assisted synthesis and antimicrobial bioevaluation of novel steroidal chalcones, Steroids 78 (2013) 321–326.
[102] S. Gogoi, K. Shekarrao, A. Duarah, T.C. Bora, S. Gogoi, R.C. Boruah, A microwave promoted solvent-free approach to steroidal quinolines and their in vitro evaluation for antimicrobial activities, Steroids 77 (2012) 1438–1445.
[103] M.G. Hernández-Linares, J. Sandoval-Ramírez, S. Meza-Reyes, S. Montiel-Smith, G. Guerrero-Luna, Stereospecific synthesis of new steroidal isoxazoles in dry media, Steroids 76 (2011) 1521–1526.
[104] J.M. Borah, P. Chowdhury, Expedited Baeyer–Villiger oxidation of steroidal ketones by microwave irradiation, Steroids 76 (2011) 1341–1345.
[105] M. Ibrahim-Ouali, K. Hamzea, L. Rocheblave, Synthesis of 12-oxa, 12-aza and 12-thia cholanetriols, Steroids 76 (2011) 324–330.
[106] K.V. Ahonena, M.K. Lahtinenb, A.M. Valkonena, M. Dracinsky, E.T. Kolehmainen, Microwave assisted synthesis and solid-state characterization of lithocholyl amides of isomeric aminopyridines, Steroids 76 (2011) 261–268.
[107] S. Deb, K. Wahala, Rapid synthesis of long chain fatty acid esters of steroids in ionic liquids with microwave irradiation: expedient one-pot procedure for estradiol monoesters, Steroids 75 (2010) 740–744.
[108] M.G. Barthakur, A. Hasib, J. Gogoi, R.C. Boruah, A convenient strategy for the annulation of aryl scaffold to A/B-ring steroids under microwave irradiation, Steroids 75 (2010) 445–449.
[109] M.G. Barthakur, S. Gogoi, M. Dutta, R.C. Boruah, A facile three-component solid phase synthesis of steroidal A-ring fused pyrimidines under microwave irradiation, Steroids 74 (2009) 730–734.
[110] M. Borthakur, R.C. Boruah, A microwave promoted and Lewis acid catalysed solventless approach to 4-azasteroids, Steroids 7 (3) (2008) 637–641.
[111] A.R. Katritzky, P. Angrish, Efficient microwave assisted access to chiral O-(protected-aminoacyl) steroids, Steroids 71 (2006) 660–669.

[112] G. Cravotto, L. Boffa, M. Turello, M. Parenti, A. Barge, Chemical modifications of bile acids under high-intensity ultrasound or microwave irradiation, Steroids 70 (2005) 77–83.
[113] P. Wang, C. Ma, S. Chen, S. Zhu, Z. Lou, H. Wang, Conversion of steroid saponins into diosgenin by catalytic hydrolysis using acid-functionalized ionic liquid under microwave irradiation, J. Clean. Prod. 79 (2014) 265–270.
[114] M. Asif, A. Ali, A. Zafar, M. Farhan, H. Khanam, S.M. Hadi, Shamsuzzaman, Microwave-assisted one pot synthesis, characterization, biological evaluation and molecular docking studies of steroidal thiazoles, J. Photochem. Photobiol. B 166 (2016) 104–115.
[115] A. Baji, T. Kiss, J. Wolfling, D. Kovacs, N. Igaz, M.K. Gopisetty, M. Kiricsi, É. Franka, Multicomponent access to androstano-arylpyrimidines under microwave conditions and evaluation of their anti-cancer activity in vitro, J. Steroid Biochem. Mol. Biol. 172 (2017) 79–88.
[116] J. Gogoi, P. Gogoi, P. Bezbaruah, R.C. Boruah, Microwave-assisted Pd-catalyzed synthesis of fused steroidal and non-steroidal pyrimidines from b-halo-a,b-unsaturated aldehydes, Tetrahedron Lett. 54 (2013) 7136–7139.
[117] K. Shekarrao, P.P. Kaishap, S. Gogoi, S. Gogoi, R.C. Boruah, A facile synthesis of steroidal D-ring fused pyrazolo[1,5-a]pyrimidines, Tetrahedron Lett. 55 (2014) 5251–5255.
[118] P. Saikia, S. Gogoi, R.C. Boruah, A facile synthesis of steroidal and nonsteroidal pyrimidines under microwave irradiation, Tetrahedron Lett. 56 (16) (2015) 2106–2109.
[119] G. Motyan, F. Kovacs, J. Wölfling, A. Gyovai, I. Zupko, E. Frank, Microwave-assisted stereoselective approach to novel steroidal ring D-fused 2-pyrazolines and an evaluation of their cell-growth inhibitory effects in vitro, Steroids 112 (2016) 36–46.
[120] P. Marwah, A. Marwah, H.A. Lardy, Microwave induced selective enolization of steroidal ketones and efficient acetylation of sterols in semisolid state, Tetrahedron 59 (2003) 2273–2287.
[121] V.C. Edelsztein, P.H. Di Chenna, G. Burton, Synthesis of C–C bonded dimeric steroids by olefin metathesis, Tetrahedron 65 (2009) 3615–3623.
[122] U. Sharma, S. Ahmed, R.C. Boruah, A facile synthesis of annelated pyridines fromformyl enamides under microwave irradiation, Tetrahedron Lett. 41 (2000) 3493–3495.
[123] C.I. Bautista-Hernández, G.E. Negrón-Silva, R. Santillán, B.I. Vergara-Arenas, D. Angeles-Beltran, L. Lomas-Romero, D. Pérez-Martínez, Design and synthesis of new carbohydrate-lithocholic acid conjugates linked via 1,2,3-triazole rings, Tetrahedron 74 (16) (2018) 2009–2019.
[124] S.M.M. Lopes, E.P. Sousa, L. Barreira, C. Marques, M.J. Rodrigues, T.M.V.D. Pinho E Melo, Synthesis and anti-cancer activity of chiral tetrahydropyrazolo[1,5-a]pyridine fused steroids, Steroids 122 (2017) 16–23.
[125] P.S. Kiuru, K. Wahal, Microwave-assisted synthesis of deuterium labelled estrogen fatty acid esters, Steroids 71 (2006) 54–60.
[126] B.T. Zeng, Z.G. Zhao, X.L. Liu, Y. Shi, Microwave assisted one-pot synthesis of novel molecular clefts with only one chiral arm based on deoxycholic acid, Chin. Chem. Lett. 19 (2008) 33–36.
[127] U. Scho, J. Messinger, M. Buchholz, U. Reinecker, H. Thole, M.K.S. Prabhu, A. Konda, An improved synthesis of 3-aminoestrone, Tetrahedron Lett. 46 (2005) 7111–7115.
[128] A. de Meijere, M. Schelper, M. Knoke, B. Yucel, H.W. Sünnemann, R.P. Scheurich, Palladium-catalyzed cross-coupling reactions and electrocyclizations/efficient combinations for new cascade reactions, J. Organomet. Chem. 687 (2003) 249–255.

[129] P. Borah, J.M. Borah, P. Chowdhury, Microwave (MW) irradiated Ugi four-component reaction (Ugi-4CR): expedited synthesis of steroid–amino acid conjugates—a novel class of hybrid compounds, Steroids 98 (2015) 49–57.
[130] A. Begum, P. Borah, P. Chowdhury, Microwave (MW) promoted high yield expedient synthesis of steryl ferulates—a class of novel biologically active compounds: a comparative study of their antioxidant activity with that of naturally occurring c-oryzanol, Steroids 107 (2016) 37–44.
[131] P. Borah, A. Begum, P. Chowdhury, Microwave energy in Ugi four-component reaction (Ugi-4CR): expedient synthesis of steroid-peptide conjugates based on aminosteroids-an important class of hybrid compounds, Curr. Org. Synth. 13 (2016) 1–7.
[132] S. Caddick, Microwave assisted organic reactions, Tetrahedron 51 (1995) 10403–10432.
[133] M.Y. Tse, M.C. Depew, J.K. Wan, Applications of high power microwave catalysis in chemistry, Res. Chem. Intermed. 13 (1990) 221–236.
[134] S.T. Chen, S.H. Chiou, Y.H. Chu, K.T. Wang, Rapid hydrolysis of proteins and peptides by means of microwave technology and its application to amino acid analysis, Int. J. Pept. Protein Res. 30 (1987) 572–576.
[135] E.J. Leal-Castañeda, J.A. Hernández-Becerra, M.T. Rodríguez Estrada, H.S. García, Formation of cholesterol oxides in lipid medium during microwave heating, Eur. J. Lipid Sci. Technol. 119 (4) (2016) 1–39.
[136] G. Motyan, L. Merai, M.A. Kiss, Z. Schelz, I. Sinka, I. Zupko, E. Frank, Microwave-assisted synthesis of biologically relevant steroidal 17-*exo*-pyrazol-5′-ones from a norpregnene precursor by a side-chain elongation/heterocyclization sequence, Beilstein J. Org. Chem. 14 (2018) 2589–2596.
[137] H. Wang, X. Zhou, Y. Zhang, H. Chen, G. Li, Y. Xu, Q. Zhao, W. Song, H. Jin, L. Ding, Dynamic microwave-assisted extraction coupled with salting-out liquid–liquid extraction for determination of steroid hormones in fish tissues, J. Agric. Food Chem. 60 (2012) 10343–10351.
[138] V.S. Pore, N.G. Aher, M. Kumar, P.K. Shukla, Design and synthesis of fluconazole/bile acid conjugate using click reaction, Tetrahedron 62 (2006) 11178–11186.
[139] N.G. Aher, V.S. Pore, S.P. Patil, Design, synthesis, and micellar properties of bile acid dimmers and oligomers linked with a 1,2,3-triazole ring, Tetrahedron 63 (2007) 12927–12934.
[140] P. Mazo, G. Restrepo, L. Rios, Biodiesel: feedstocks and processing technologies, in: M. Stoytcheva (Ed.), Alternative Methods for Fatty Acid Alkyl-Esters Production: Microwaves, Radio-Frequency and Ultrasound, 2011, pp. 269–288.
[141] C.O. Kappa, Controlled microwave heating in modern organic synthesis, Angew. Chem. Int. Ed. Engl. 43 (2004) 6250–6284.
[142] J.M. Collins, N.E. Leadbeater, Microwave energy: a versatile tool for the biosciences, Org. Biomol. Chem. 5 (2007) 1141–1150.
[143] V. Osuna, I.A. Rivero, Study of the influence of microwave and conventional heating on the lipase-catalyzed esterification of lauric acid with different alcohols, J. Mex. Chem. Soc. 56 (2012) 176–182.
[144] B. Rejasse, S. Lamare, M.D. Legoy, T. Besson, Stability improvement of immobilized *Candida antarctica* lipase B in an organic medium under microwave radiation, Org. Biomol. Chem. 2 (2004) 1086–1089.
[145] B. Rejasse, T. Bessonen, M.D. Legoy, S. Lamare, Influence of microwave radiation on free *Candida antarctica* lipase B activity and stability, Org. Biomol. Chem. 4 (2006) 3703–3707.

[146] A. Schumacher, O. Thum, Immobilized lipases in the cosmetics industry, Chem. Soc. Rev. 42 (2013) 6475–6490.
[147] O. Thum, Enzymatic production of care specialties based on fatty acid esters, Tenside Surfactant Deterg. 41 (2004) 287–290.
[148] S.M. Radzi, M. Basri, A.B. Salleh, A. Ariff, R. Mohammad, High performance enzymatic synthesis of oleyl oleate using immobilized lipase from *Candida antarctica*, Electron. J. Biotechnol. 8 (2005) 292–298.
[149] C.H. Kuo, H.H. Chen, J.H. Chen, Y.C. Liu, C.J. Shieh, High yield of wax ester synthesized from cetyl alcohol and octanoic acid by lipozyme RMIM and Novozym 435, Int. J. Mol. Sci. 13 (2012) 11694–11704.
[150] G.D. Yadav, A.D. Sajgure, Synergism of microwave irradiation and enzyme catalysis in synthesis of isoniazid, J. Chem. Technol. Biotechnol. 82 (2007) 964.
[151] G.D. Yadav, P.S. Lathi, Synergism of microwaves and immobilized enzyme catalysis in synthesis of adipic acid esters in nonaqueous media, Synth. Commun. 35 (2005) 1699–1705.
[152] T.J. Mason, C. Leonelli, Microwave and ultrasonic processing: now a realistic option for industry, Chem. Eng. Process. Process Intensif. 49 (2010) 885–900.
[153] P.N. Dange, V.K. Rathod, Equilibrium and thermodynamic parameters for heterogeneous esterification of butyric acid with methanol under microwave irradiation, Resour. Effic. Technol. 3 (2017) 64–70.
[154] A.D. Hoz, A.D. Ortiz, A. Moreno, Microwaves in organic synthesis: thermal and non-thermal microwave effects, Chem. Soc. Rev. 34 (2005) 164–178.
[155] G.D. Yadav, P.A. Thorat, Microwave assisted lipase catalyzed synthesis of isoamyl myristate in solvent-free system, J. Mol. Catal. B Enzym. 83 (2012) 16–22.
[156] G.D. Yadav, P.S. Lathi, Synergism between microwave and enzyme catalysis in intensification of reactions and selectivities: transesterification of methyl acetoacetate with alcohols, J. Mol. Catal. A Chem. 223 (2014) 51–56.

Microwave-induced synthesis as a part of green chemistry approach for novel antiinflammatory agents

25

Jnyanaranjan Panda[a], *Anjan Kumar*[a], *Ch. Niranjan Patra*[a], *Biswa Mohan Sahoo*[a,*], *Bimal Krishna Banik*[b,*]
[a]Roland Institute of Pharmaceutical Sciences, Berhampur, India, [b]Department of Mathematics and Natural Sciences, College of Sciences and Human Studies, Deanship of Research Development, Prince Mohammad Bin Fahd University, Al Khobar, Kingdom of Saudi Arabia
[*]Corresponding author. e-mail address: drbiswamohansahoo@gmail.com; bimalbanik10@gmail.com; bbanik@pmu.edu.sa

Abbreviation

ANOVA	analysis of variance
CADD	computer-aided drug design
COX	cyclooxygenase
DMF	dimethylformamide
DMAP	4-dimethylaminopyridine
°C	degree centigrade
GHz	gigahertz
H	hour
I.P.	Indian Pharmacopoeia
IKK2	inhibitor of nuclear factor kappa-B kinase subunit
IL-1β	interleukin-1-beta
LOXs	lipoxygenases
Min	minute
mg/kg	milligram/kilogram
μg/mL	microgram per microliter
%	percentage
QSAR	quantitative structure–activity relationships
SE	standard error
SD	standard deviation
SEM	standard error of mean
TNF	tumor necrosis factor
THF	tetrahydrofuran
W	watt

Green Approaches in Medicinal Chemistry for Sustainable Drug Design. https://doi.org/10.1016/B978-0-12-817592-7.00026-5
© 2020 Elsevier Inc. All rights reserved.

25.1 Inflammation

Inflammation is a part of the body's immune response. It is the response of organism to the pathogens. Inflammation is a local reaction of the vascular and supporting elements of a tissue to injury leading into the formation of protein-rich exudates. It is a protective response from nonspecific immune system to localize, neutralize, or to destroy an injurious agent in preparation for the process of healing. Symptoms of inflammation are calor (heat), dolor (pain), tumor (swelling), rubor (redness), and function laesa (loss of function). It is the complex biological response of vascular tissues to harmful stimuli, such as pathogens, damaged cells, or irritants. The symptoms of pain are redness, swelling, heat, and loss of function. By the help of inflammation, the organism gets rid of the injurious stimuli and to initiate the healing process. Inflammation is caused by physical agents, chemical agents, immunological reactions, and infection by pathogenic organism. Antiinflammatory refers to the property of a substance to treat and reduce inflammation. Nonsteroidal antiinflammatory drugs (NSAIDs) are useful tools in the treatment of acute and chronic inflammation, pain, and fever. Long-term usage of antiinflammatory drugs leads to side effects such as gastrointestinal lesions, bleeding, and nephrotoxicity[1].

The inflammatory response represents a generalized response to infection or tissue damage and is designed to remove cellular debris, to localize invading organisms and arrest the spread of infection. The inflammatory response is characterized by the following symptoms: reddening of the localized area, swelling, pain, and elevated temperature. Reddening results from capillary dilation that allows more blood to flow to the damaged tissue. Elevated temperature results from capillary dilation which permits increased blood flow through these vessels, with associated high metabolic activities of neutrophils and macrophages. The dilation of blood vessels is accompanied by increased capillary permeability causing swelling as fluid accumulates in the spaces surrounding tissue and cells. Pain in the case of inflammation is due to the lysis of blood cells that trigger the production of bradykinin and prostaglandins. The area of inflammation also becomes walled off as a result of the development of fibrinous clots. The deposition of fibrin isolates the inflamed area, cutting off normal circulation. The fluid in the inflamed area is known as inflammatory exudates, commonly called as pus. These exudates contain dead cells and debris in addition to body fluids. After the expulsion of the exudates, the inflammation may terminate and tissues may return to their normal state [2].

25.1.1 Acute inflammation

Acute inflammation is a short-term process which is characterized by the classic signs of inflammation which are: swelling, redness, pain, heat, and loss of function due to the infiltration of the tissues by plasma and leukocytes. It occurs as long as the injurious stimulus is present and ceases once the stimulus has been removed, broken down, or walled off by scarring (fibrosis). The first four characteristics have been known since ancient times and are attributed to Celsus. Loss of function was added to the definition of inflammation by Virchow in 1870. The process of acute inflammation is initiated by the blood vessels neighboring to the injured tissue. It allows the exudation of plasma proteins and leukocytes into the surrounding tissue. The increased flow of fluid into the tissue causes the characteristic swelling

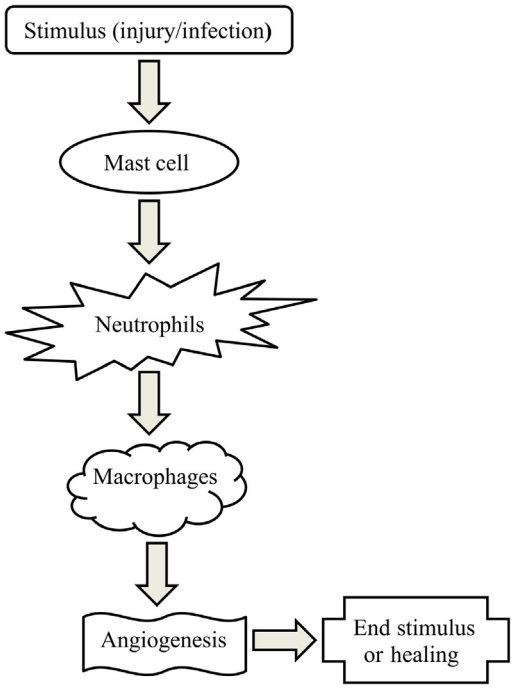

Fig. 25.1 Mechanism of acute inflammation.

associated with inflammation since the lymphatic system does not have the capacity to compensate for it, and the increased blood flow to the area causes the red color and increased heat [3]. The blood vessels also get altered permitting the movement of leukocytes through the endothelium and basal membrane constituting the blood vessel. Once in the tissue, the cells migrate along a chemotactic gradient to reach the site of injury, where they can attempt to remove the stimulus and repair the tissue (Fig. 25.1).

25.1.2 Chronic inflammation

Chronic inflammation is a pathological condition characterized by concurrent active inflammation, tissue destruction, and attempts at repair. Chronic inflammation is not characterized by the classic signs of acute inflammation listed above. Instead, chronically inflamed tissue is characterized by the infiltration of mononuclear immune cells (monocytes, macrophages, lymphocytes, and plasma cells) tissue destruction and attempts at healing, which include angiogenesis and fibrosis. Endogenous causes include persistent acute inflammation. Exogenous causes are varied and include bacterial infection, especially by *Mycobacterium tuberculosis*, prolonged exposure to chemical agents such as silica, tobacco smoke, or autoimmune reactions such as rheumatoid arthritis. In acute inflammation, removal of the stimulus halts the recruitment

of monocytes (which become macrophages under appropriate activation) into the inflamed tissue, and existing macrophages exit the tissue via lymphatics. However, in chronically inflamed tissue, the stimulus is persistent, and therefore, recruitment of monocytes is maintained, existing macrophages are tethered in place, and proliferation of macrophages is stimulated [4].

25.1.3 Mediators of inflammation

A variety of chemical mediators from circulation system, inflammatory cells, and injured tissue actively contribute to and adjust the inflammatory response. The released chemical mediators include (1) vasoactive amines such as histamine and serotonin, (2) peptide (e.g., bradykinin), and (3) eicosanoids (e.g., thromboxanes, leukotrienes, and prostaglandins).

Inflammation is produced by the release of chemicals, from tissues and migrating cells, induced by various reasons such as injuries. Most strongly implicated chemicals are the prostaglandins (PGs), leukotrienes (LTs), histamine, and bradykinin [5]. More recently, platelet-activating factor (PAF) and interleukin-1 also are included. Evidence for their involvement comes from the studies with competitive antagonists for their receptors and inhibitors of their synthesis (Fig. 25.2).

25.2 Importance of antiinflammatory drugs

Antiinflammatory drugs reduce pain caused by inflammation. It inhibits or blocks the effect of cyclooxygenase (COX) enzymes. COX enzymes produce the chemical called prostaglandin. At the side of injury or damage, some prostaglandins are

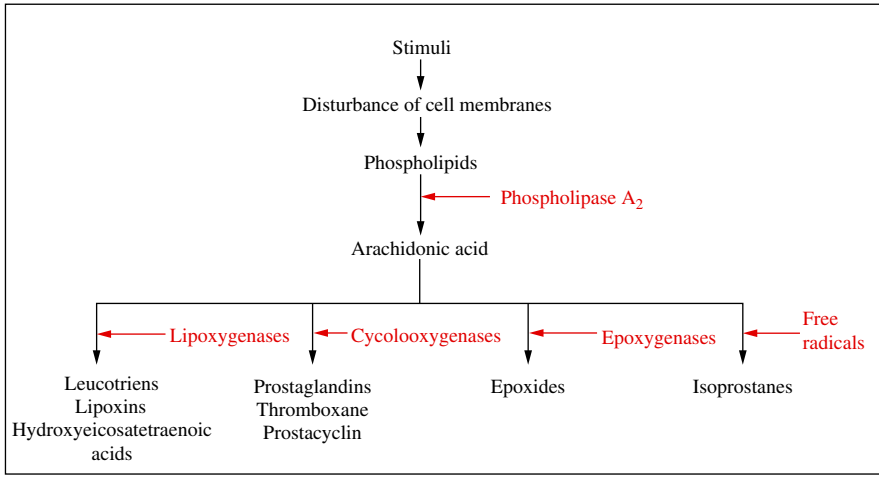

Fig. 25.2 Pathway of mediators released from arachidonic acid.

produced. These drugs block the production of prostaglandin and reduce pain. There are two types of COX enzymes—COX-1 and COX-2. COX-2 enzyme is responsible for the production of prostaglandins. To reduce the pain, anti-inflammatory compounds are used to ease up pain in various situations, including osteoarthritis, rheumatoid arthritis, joint pains, muscle and ligament pains (strains and sprains), dysmenorrhea (period pain), postoperative pain, headaches, migraines, etc. to reduce inflammation. This can further reduce pain and stiffness that occurs with inflammation condition such as rheumatoid arthritis [6]. The main antiinflammatory drugs are either steroidal [7] (e.g., betamethasone, prednisolone, and dexamethasone) or nonsteroidal [8] (e.g., aspirin, diclofenac, ibuprofen, indomethacin, naproxen, nimesulide, and celecoxib) used to treat both acute inflammatory condition and chronic inflammatory diseases such as osteoarthritis and rheumatoid arthritis [9]. However, their prolonged use is associated with various side effects; for example, steroidal drug causes adrenal atrophy [10], osteoporosis, suppression of response to infection or injury, euphoria, cataracts, glaucoma, and nonsteroidal drug [11] causes peptic ulcers and bronchospasm due to blockade of both the physiological and inflammatory prostaglandins and concurrent production of leukotrienes [12, 13].

Traditional NSAIDs such as aspirin (**1**), ibuprofen (**2**), and diclofenac (**3**) that exhibit nonselective COX inhibition represent the most widely prescribed NSAIDs to relieve short-term fever, pain, and inflammation [14, 15]. The characteristic feature of these traditional nonselective COX inhibitor NSAIDs was the presence of a carboxylic acid (COOH) functional group. Consequently, selective COX-2 inhibitors (coxibs) based on a diarylheterocyclic ring template as in celecoxib (**4**) and rofecoxib (**5**) were developed [16, 17]. These agents were characterized by the presence of a para-sulfonamide (SO_2NH_2) or a paramethane-sulfonyl (SO_2Me) pharmacophore present on one of the aryl rings (Fig. 25.3).

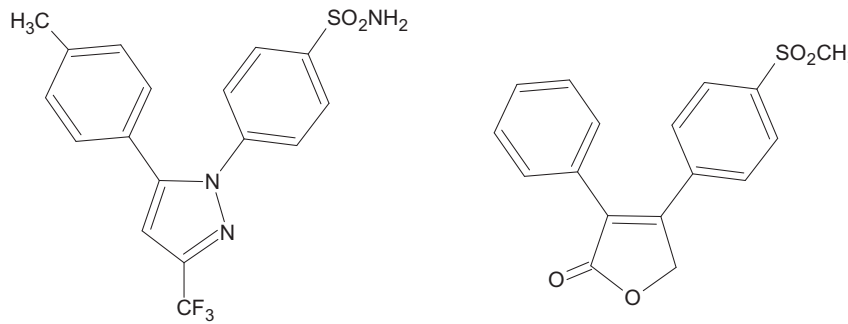

Celecoxib (**4**) Rofecoxib (**5**)

Fig. 25.3 Chemical structures of some nonselective and selective COX inhibitors.

25.2.1 Nitric oxide (NO)-donating NSAIDs (NO-NSAIDs)

The derivatives of nitric oxide-donating NSAIDs were principally developed to decrease the gastrointestinal toxicities associated with the use of traditional NSAID. In the GI tract, nitric oxide is known to exert its protective role by increasing the mucous secretion, mucosal blood flow, and inhibition of neutrophil aggregation. NO-NSAIDs based on the aspirin, naproxen, and diclofenac ring templates. These agents contain organic nitrates or nitrosothiols as the NO-donor moiety (Fig. 25.4) [18–20].

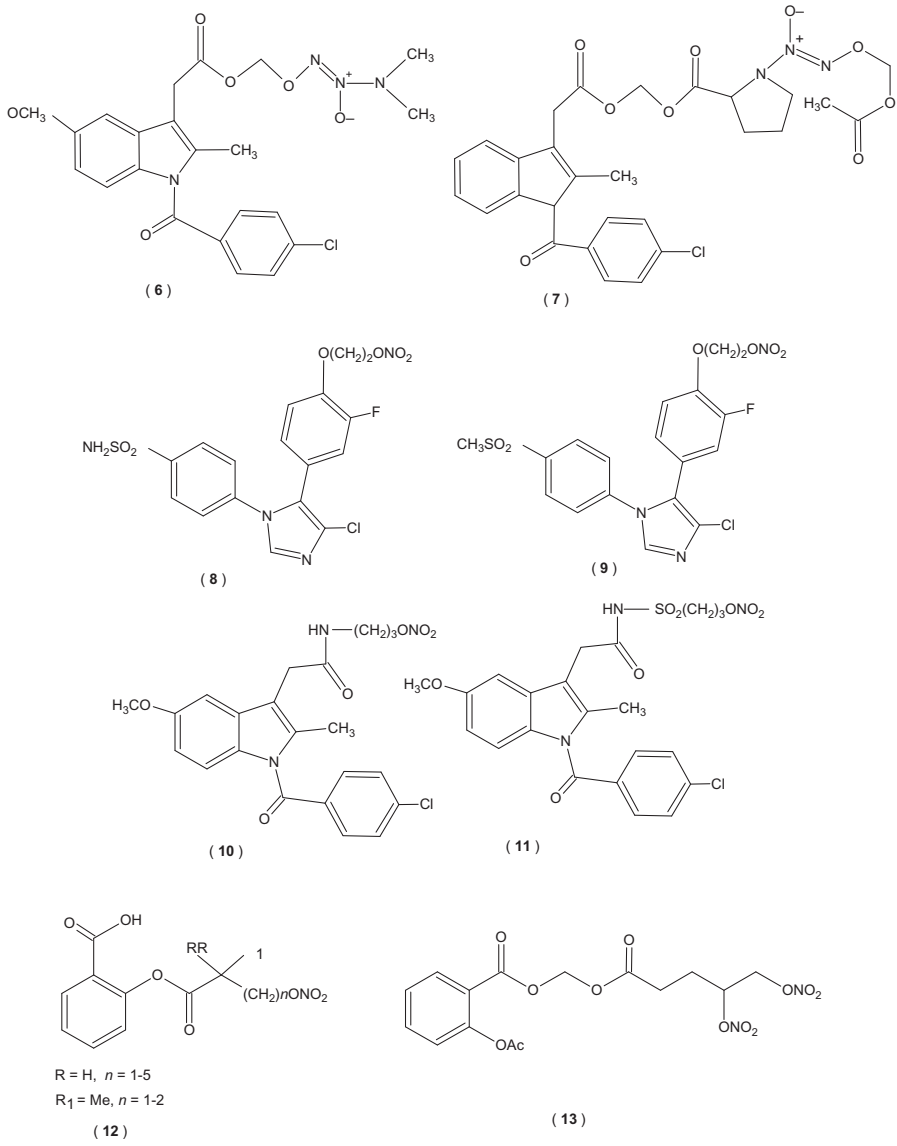

Fig. 25.4 Chemical structures of some representative NO-donor antiinflammatory agents.

25.2.2 Selective COX-2 inhibitors

The adverse cardiovascular events associated with selective COX-2 inhibitors led to a dramatic decline in selective COX-2 inhibitor pipeline. Due to this many approaches have done to develop some selective COX-2 inhibitor. Here, the chemical structures of some representative selective COX-2 inhibitors are represented (Fig. 25.5) [21–23].

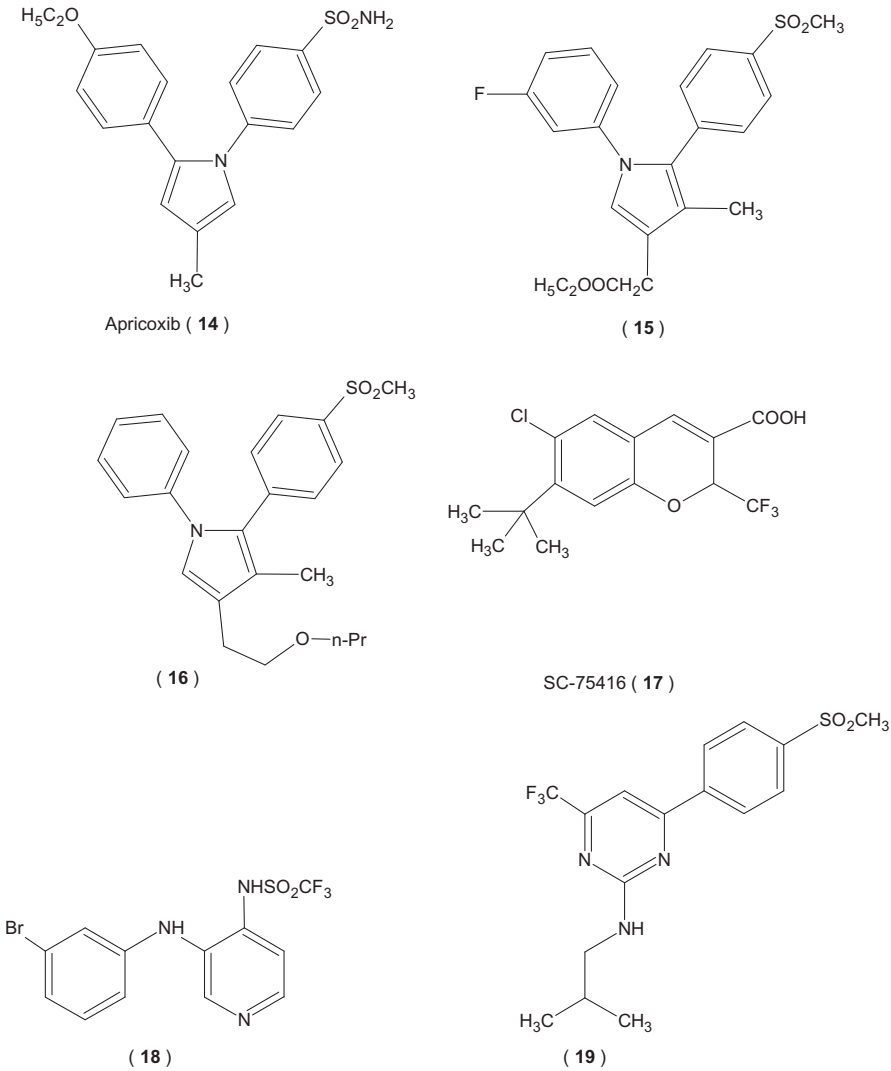

Fig. 25.5 Chemical structures of some representative selective COX-2 inhibitors.

25.2.3 Dual COX/LOX inhibitors

Currently, LOXs are potential targets in the treatment of various diseases such as asthma, atherosclerosis, cancer, and a variety of inflammatory conditions. It was hypothesized that blocking the arachidonic acid (AA) metabolism via COX inhibition by either traditional NSAIDs or selective COX-2 inhibitors could lead to the generation of pro-inflammatory leukotrienes and lipoxins via the LOX pathway (Fig. 25.2) partly accounting for the side effects seen with traditional NSAIDs and selective COX-2 inhibitors. To counter this, several dual small molecule COX/LOX inhibitors have been reported. Some representatives of dual COX/LOX inhibitors are given below (Fig. 25.6) [24–26].

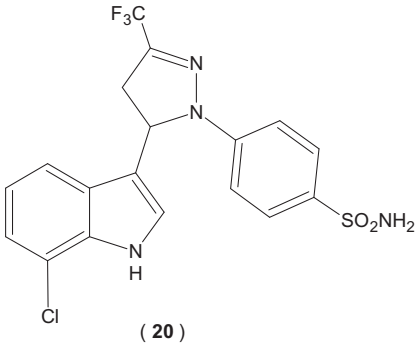

(**20**)

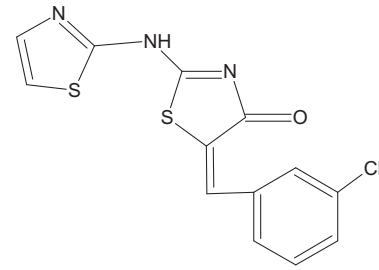

(**21**)

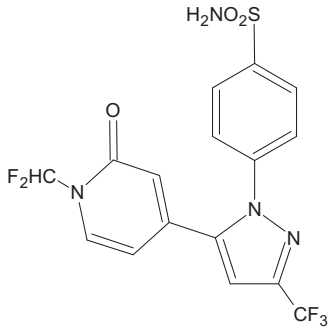

(**22**)

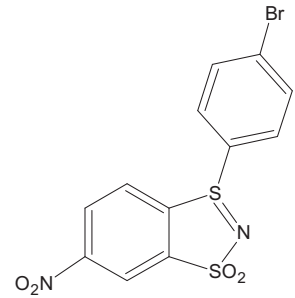

(**23**)

Fig. 25.6 Chemical structures of some representative dual COX/LOX inhibitors.

25.2.4 Ipoprotein-PLA2 inhibitors

The phospholipase A2 (PLA2) enzyme catalyzes the release of fatty acids such as AA, a critical rate-limiting step, by acting on membrane phospholipids (Fig. 25.2). The released AA gets converted to various pro-inflammatory mediators such as prostaglandins, leukotrienes, and platelet-activating factor (PAF) that are known to play

a major role in regulating the vascular tone [27]. Recent studies have indicated that Lp-PLA_2 is closely involved in the onset and progression of atherosclerosis [28–31]. In humans, Lp-PLA_2 is primarily produced from leukocytes and macrophages and is associated with circulating macrophages and low-density lipoproteins (LDL). It acts on polar phospholipids in oxidized LDL to form lysophosphatidylcholine and nonesterified phospholipids that are known to have proinflammatory properties by activating and recruiting macrophages/monocytes mediating plaque vulnerability, apoptosis, leading to onset and progression of atheroma [32,33]. Some derivatives of PLA_2 inhibitors are included here (Fig. 25.7).

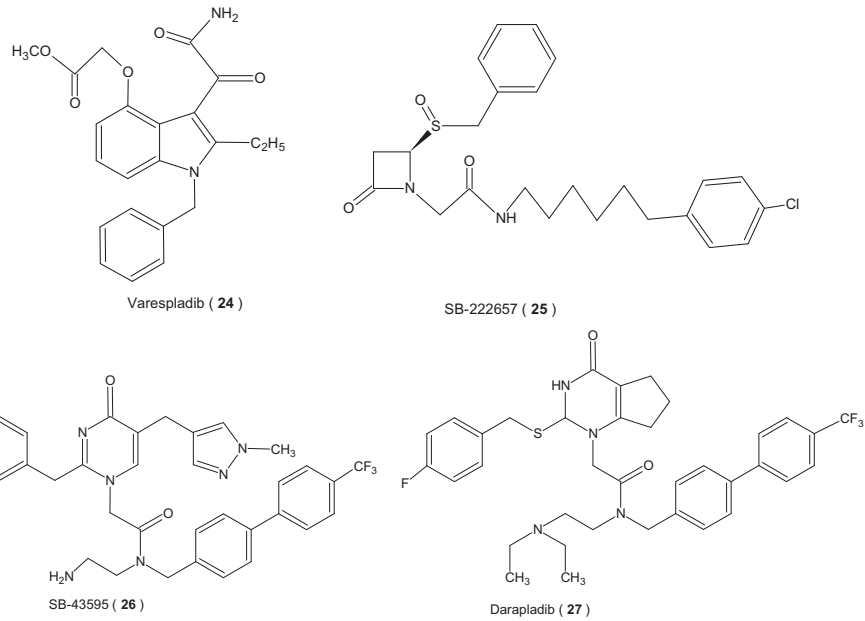

Fig. 25.7 Chemical structures of some representative PLA2 inhibitors.

25.2.5 Microsomal prostaglandin E_2 synthase inhibitors

In the prostaglandin biosynthesis pathway, formation of the prostaglandin E_2 (PGE_2), a major mediator of pain and inflammation from prostaglandin H_2 (PGH_2) is catalyzed by PGE synthase such as cytosolic PGES (cPGES) and microsomal PGE synthases-1 and -2 (mPGES-1 and mPGES-2). The membrane-associated protein mPGES-1 is an inducible enzyme under inflammatory conditions such as RA, OA, and atherosclerosis. Examples of some representatives of mPGES-1 inhibitors are given below (Fig. 25.8) [34–38].

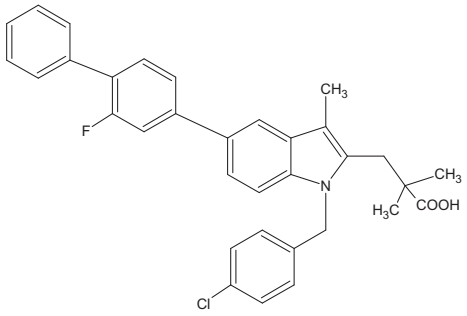

(**28**)

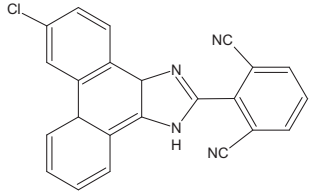

(**29**)

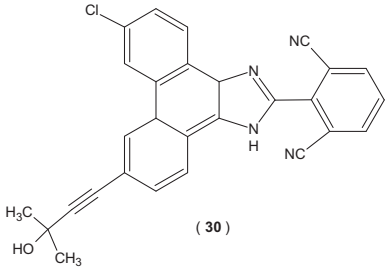

(**30**)

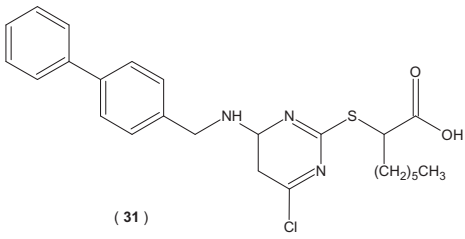

(**31**)

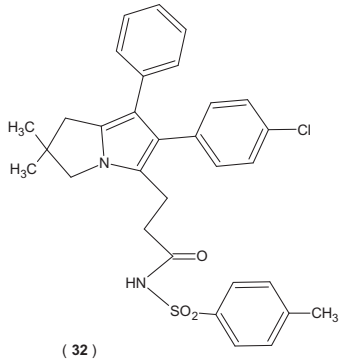

(**32**)

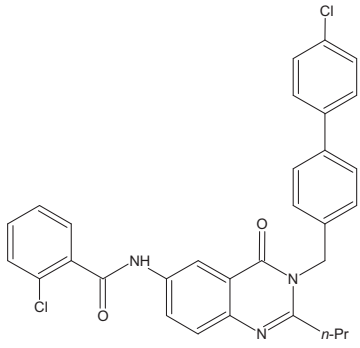

(**33**)

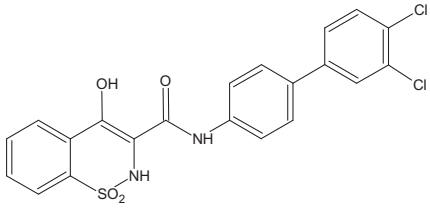

(**34**)

Fig. 25.8 Chemical structures of some representative mPGES-1 inhibitors.

25.2.6 TNF-α inhibitors

Treating RA with biological therapeutics that targets the pro-inflammatory cytokine TNF-α has been highly successful. In this regard, several small molecule agents that inhibit TNF-α indirectly have been reported below (Fig. 25.9) [39–41].

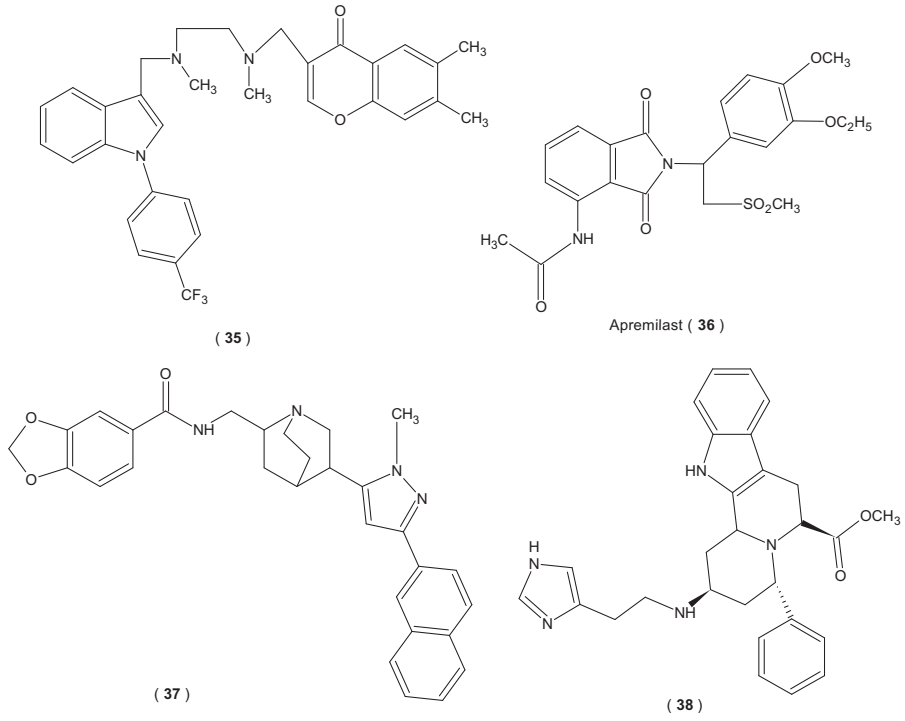

Fig. 25.9 Examples of some representative TNF-α inhibitors.

25.3 Introduction to microwave technique

Nowadays, microwave technique is considered as an important approach toward green chemistry, because this technique is more environmentally friendly. It has the potential to have a large impact on the fields of screening, combinatorial chemistry, organic chemistry, medicinal chemistry, and drug development. Conventional method of organic synthesis usually needs longer heating time, tedious apparatus setup, which result in higher cost of process and the excessive use of solvents or reagents lead to environmental pollution. This growth of green chemistry holds significant potential for a reduction of the by-product, a reduction in waste production, and a lowering of the energy costs. Due to its ability to couple directly with the reaction molecule and by passing thermal conductivity leading to a rapid rise in the temperature, microwave

irradiation is used to improve much organic synthesis. The application of alternative solvents such as water, fluorous, ionic liquids, and supercritical media is increasing rapidly. Catalysis remains one of the most important fields of green chemistry by providing atom-economical, selective, and energy efficient solutions to many industrially important problems. The utilization of inorganic solid-supported reagents attracted attention because of enhanced selectivity, milder reaction conditions, and associated ease of manipulation. Microwave heating attracted the attention of investigators in that it makes it possible to shorten the length of reactions significantly, to increase their selectivity, and to increase the product yields, which is particularly important in the case of high-temperature processes that take a long time [42–44].

25.3.1 Microwaves

Microwaves are in the form of electromagnetic energy which lie in electromagnetic spectrum corresponds to wavelength of 1 cm to 1 m and frequency of 30 GHz to 300 MHz. This places it between infrared radiations, which has shorter wavelength in the 1–25 cm range for radar, whereas remaining section is devoted to telecommunication. Microwave energy consists of both electric as well as magnetic field. Microwave moves with the speed of light and it has very less energy relative to the energy which is required to break the bond in the chemical molecule thus, microwaves are such a source of energy which will not hamper the structure of the chemical molecule. Microwaves are coherent and polarized in contrast to visible waves (apart from lasers). They obey the laws of optics and can be transmitted, absorbed, or reflected depending on the type of material [45].

25.3.2 Mechanism of microwave heating

Traditionally, organic reactions are heated using an external heat source (such as an oil bath), and therefore, heat is transferred by conductance. This is a comparatively slow and inefficient method for transferring energy into the system because it depends on the thermal conductivity of the various materials that must be penetrated, and results in the temperature of the reaction vessel being higher than that of the reaction mixture. By contrast, microwave irradiation produces efficient internal heating by direct coupling of microwave energy with the polar molecules (e.g., solvents, reagents, and catalysts) that are present in the reaction mixture [46].

25.3.3 Benefits of microwave-assisted synthesis

Microwaves can accelerate the rate of reaction, provide better yields and higher purity, uniform and selective heating with lower energy usage, achieve greater reproducibility of reactions, and help in developing convenient and cleaner synthetic routes. The main advantages of microwave-assisted organic synthesis are [47]:

- Faster reaction
- Better yield with higher purity
- Energy saving

- Uniform and selective heating
- Green synthesis
- Reproducibility.

25.3.4 Microwave synthesis apparatus

The apparatus for microwave-assisted synthesis includes single-mode microwave ovens and multimode microwave ovens [48].

25.3.4.1 Single-mode microwave apparatus

The important feature of a single-mode apparatus is its ability to create a standing wave pattern. This interface generates an array of nodes where microwave energy intensity is zero, and an array of antinodes where the magnitude of microwave energy is at its highest. One of the limitations of single-mode apparatus is that only one vessel can be irradiated at a time. However, the apparatus is user friendly. An advantage of single-mode apparatus is their high rate of heating. This is because the sample is always placed at the antinodes of the field, where the intensity of microwave radiation is the highest. These apparatus can process volumes ranging from 0.2 to about 50 mL under sealed-vessel conditions, and volumes around 150 mL under open-vessel conditions. Single-mode microwave ovens are currently used for small-scale drug discovery, automation, and combinatorial chemical applications.

25.3.4.2 Multimode microwave apparatus

An essential feature of a multimode apparatus is the deliberate avoidance of generating a standing wave pattern inside it. The goal is to generate as much chaos as possible inside the apparatus. The greater the chaos, the higher is the dispersion of radiation, which increases the area that can cause effective heating inside the apparatus. As a result, a multimode microwave heating apparatus can accommodate a number of samples simultaneously for heating, unlike single-mode apparatus where only one sample can be irradiated at a time. Owing to this characteristic, a multimode heating apparatus is used for bulk heating and carrying out chemical analysis processes such as ashing, extraction, etc. In large multimode apparatus, several liters of reaction mixture can be processed in both open and closed-vessel conditions. A major limitation of multimode apparatus is that heating samples cannot be controlled efficiently because of lack of temperature uniformity [49–51].

25.3.5 Applications of microwave-assisted synthesis

Microwave-enhanced synthesis results in faster reactions, higher yields, and increased product purity. In addition to this, due to the availability of high-capacity microwave apparatus, the yields of the experiments are now easily scaled up from milligrams to kilograms, without the need to alter reaction parameters. Microwave-assisted synthesis can be suitably applied to the drug discovery process [52].

Microwave-assisted organic synthesis is the foremost and one of the most researched applications of microwaves in chemical reactions. Literature survey reveals that scientists have successfully conducted a large range of organic reactions. These include Diels-Alder reaction, Ene reaction, Heck reaction, Suzuki reaction, Mannich reaction, hydrolysis, dehydration, esterification, cycloaddition reaction, epoxidation, reductions, condensations, cyclization reactions, protection and deprotection, etc. Based on the reaction conditions, organic synthesis reactions can be conducted in the following techniques [53].

25.3.6 Microwave-assisted synthesis of novel antiinflammatory agents

An efficient, rapid, eco-friendly, and cost-effective microwave-assisted protocol using fewer amounts of solvents was developed for the synthesis of 3,5-diaryl/heteryl substituted-2-pyrazolines by reaction of substituted prop-2-ene-1-ones with hydrazine hydrate in acetic acid. The synthesized compounds were tested for their antiinflammatory activity by using carrageenan-induced hind paw edema model in albino rats. Indomethacin was used as standard drug. All the synthesized pyrazoline derivatives except a few have shown significant activity. Among them compounds containing furan, methoxy phenyl, thiophene, *p*-amino phenyl, trimethoxy-phenyl, 3-methoxy-2-hydroxyphenyl, and 2-hydroxy-phenyl group exhibited equivalent potency with the standard drug indomethacin (Scheme 25.1; Table 25.1) [54].

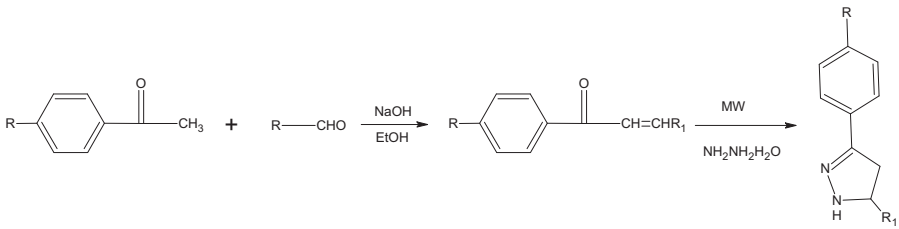

Scheme 25.1 Synthesis of 3, 5-diaryl substituted-2-pyrazolines.

Ipsita et al. have prepared some novel antiinflammatory agents using 4-aminoantipyrine, nicotinic acid, ethylisocyanoacetate, and substituted aldehydes via Ugi four-component reaction under microwave irradiation in the presence of fluorite as the catalyst (Scheme 25.2). All the synthesized molecules were examined in vivo antiinflammatory activity using Wistar Albino rats with a reference drug, indomethacin. In general, an increase in percentage inhibition of paw edema was observed as time interval increases for all the synthesized compounds (Table 25.2) [55].

Table 25.1 Antiinflammatory activity of 3,5-diaryl substituted-2-pyrazolines.

Compound code	R	R_1	Rat paw edema (in mL) (mean ± SE)			
			0 h	1 h	2 h	4 h
Control	–	–	3.75 ± 0.023	4.69 ± 0.075	5.10 ± 0.21	4.65 ± 0.23
Indomethacin	–	–	3.77 ± 0.143	3.85 ± 0.183	3.75 ± 0.17	3.75 ± 0.26**
1.	H		3.69 ± 0.15	4.57 ± 0.24	4.78 ± 0.19	3.80 ± 0.35*
2.	H	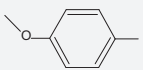	3.59 ± 0.14	4.73 ± 0.12	4.10 ± 0.15	3.64 ± 0.24**
3.	H	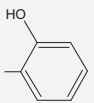	3.71 ± 0.06	4.74 ± 0.19	4.79 ± 0.11	3.75 ± 0.07*
4.	H	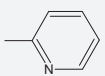	3.79 ± 0.13	4.64 ± 0.09	3.74 ± 0.09**	3.89 ± 0.11**
5.	H		3.52 ± 0.11	4.35 ± 0.17	4.50 ± 0.13	3.85 ± 0.10*
6.	H	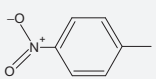	3.75 ± 0.07	4.20 ± 0.14	4.41 ± 0.52	3.87 ± 0.24**
7.	H	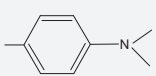	3.64 ± 0.11	4.40 ± 0.37	4.59 ± 0.41	3.75 ± 0.18*

Continued

Table 25.1 Continued

Compound code	R	R_1	Rat paw edema (in mL) (mean ± SE)			
			0 h	1 h	2 h	4 h
8.	H	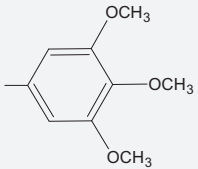	3.57 ± 0.12	4.41 ± 0.51	4.39 ± 0.34	3.75 ± 0.36*
9.	H	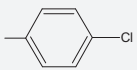	3.69 ± 0.15	4.58 ± 0.24	4.74 ± 0.19	3.80 ± 0.35*
10.	H	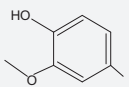	3.59 ± 0.14	4.70 ± 0.12	4.10 ± 0.15	3.82 ± 0.24**
11.	OH		3.72 ± 0.06	4.74 ± 0.19	4.77 ± 0.11	3.76 ± 0.07*
12.	OH	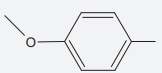	3.80 ± 0.13	4.63 ± 0.09	3.72 ± 0.09**	3.84 ± 0.11**
13.	OH	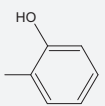	3.54 ± 0.11	4.40 ± 0.17	4.57 ± 0.13	3.77 ± 0.10*
14.	OH	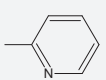	3.74 ± 0.07	4.25 ± 0.14	4.40 ± 0.52	3.81 ± 0.24**

15.	OH		3.67 ± 0.11	4.47 ± 0.37	4.54 ± 0.41	3.71 ± 0.18*
16.	OH	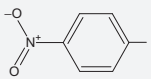	3.54 ± 0.12	4.50 ± 0.51	4.41 ± 0.34	3.65 ± 0.36*
17.	OH	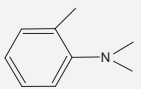	3.65 ± 0.15	4.55 ± 0.24	4.79 ± 0.19	3.75 ± 0.35*
18.	OH	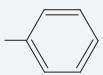	3.51 ± 0.14	4.72 ± 0.12	4.10 ± 0.15	3.62 ± 0.24**
19.	OH	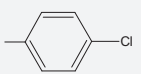	3.76 ± 0.06	4.74 ± 0.19	4.77 ± 0.11	3.82 ± 0.07*
20.	OH	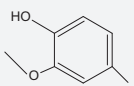	3.79 ± 0.13	4.63 ± 0.09	3.74 ± 0.09**	3.82 ± 0.11**

Results were expressed as mean ± SEM. *$P < .05$, **$P < .01$ as compared to control.

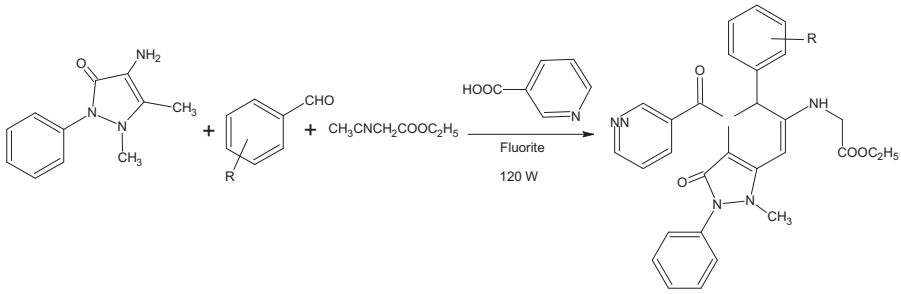

Scheme 25.2 Synthesis of Ugi-4CR under microwave irradiation.

2-(4′-Methylbiphenyl-2-yl)-5-aryl-1,3,4-oxadiazole analogs were designed and synthesized using microwave-assisted method by Sujit et al. (Scheme 25.3). The compounds were evaluated for antiinflammatory activity by in vivo models. Female Wistar rats (175–200 g) were used for the experiment. Diclofenac was used as standard drug. Carrageenan-induced paw edema method was used to carry out this study. Some of the compounds displayed prominent activity (Table 25.3) [56].

Aryl and heteroaryl-substituted dihydropyrimidinone has been achieved via initial Knoevenagel, subsequent addition, and final cyclization of aldehyde, ethylcyanoacetate, and guanidine nitrate in the presence of piperidine as a catalyst in solvent free under microwave irradiation. A mixture of aldehyde, ethyl cyanoacetate, guanidine nitrate, and—two to three drops of piperidine was subjected to microwave irradiation at 60% power in 600-W microwave oven for 5 min. The solid product was separated and recrystallized from ethanol to afford pure products in good yields (Scheme 25.4). The antiinflammatory activity was determined in vivo using the carrageenan-induced rat paw edema test. Indomethacin was used as the reference drug. Almost all of the tested compounds were shown moderate to good antiinflammatory activity (Table 25.4) [57].

The synthesis of 3-methyl-5-substituted-1H-pyrazol-1-yl-(3-substituted-benzofuran-2-yl)methanone derivatives are carried out by microwave-assisted organic synthesis at 100 W for 3 min (Scheme 25.5). Antiinflammatory activity is determined by the rat hind paw method. Albino rats of either sex weighing 175–185 g were selected and divided into six each and fasted for 24 h prior to experiment with water ad libitum. The edema was induced by injecting 1% carrageenan into the plantar surface of the hind paw of rats. The first group was given the acacia suspension (control) and the other group was administered with phenylbutazone as a standard (50 mg/kg I.P.). The paw edema was measured by plethysmometer. The pharmacological screening of the tested compounds showed antiinflammatory activity ranging from 38.33% to 78.11%, whereas the standard drug phenylbutazone showed 79.5% inhibition after 4 h. The presence of 3-methoxy group and further chloro substitution at fourth position increases the antiinflammatory activity (Table 25.5) [58].

Table 25.2 Antiinflammatory activity of compounds against carrageenin-induced paw edema in Wistar Albino rats.

Test comp.	R	% Inhibition of paw edema at different time (h) interval[a]							
		200 mg/kg				400 mg/kg			
		0 h	1 h	3 h	5 h	0 h	1 h	3 h	5 h
Control[b]	–	1.43 ± 0.15 (0.0)	1.46 ± 0.11 (0.0)	1.52 ± 0.14 (0.0)	1.48 ± 0.13 (0.0)	1.45 ± 0.12 (0.0)	1.47 ± 0.14 (0.0)	1.54 ± 0.15 (0.0)	1.46 ± 0.12 (0.0)
1.	3-NO_2	1.13 ± 0.04 (34.08)	1.16 ± 0.15 (26.81)	1.18 ± 0.08 (56.15)	1.17 ± 0.03* (65.28)	1.19 ± 0.02* (45.07)	1.15 ± 0.13 (71.08)	1.17 ± 0.11* (60.22)	1.16 ± 0.12 (74.21)
2.	2-NO_2	1.24 ± 0.14 (10.21)	1.25 ± 0.19 (16.12)	1.27 ± 0.21 (46.11)	1.23 ± 0.04 (55.13)	1.26 ± 0.01 (42.13)	1.28 ± 0.05 (32.06)	1.32 ± 0.09 (57.11)	1.25 ± 0.03* (54.03)
3.	4-N $(Me)_2$	1.34 ± 0.01* (16.27)	1.35 ± 0.04 (26.51)	1.38 ± 0.06* (33.17)	1.28 ± 0.06* (46.21)	1.33 ± 0.01* (23.12)	1.37 ± 0.02* (32.28)	1.40 ± 0.05 (54.17)	1.34 ± 0.03* (47.15)
4.	4-OMe	1.17 ± 0.04 (30.31)	1.18 ± 0.07 (56.27)	1.19 ± 0.03 (54.32)	1.16 ± 0.08 (64.52)	1.28 ± 0.03 (36.25)	1.34 ± 0.04 (60.21)	1.42 ± 0.02 (72.05)	1.38 ± 0.06 (76.18)
5.	2-OH	1.37 ± 0.04 (16.05)	1.38 ± 0.07 (23.07)	1.44 ± 0.13 (40.05)	1.35 ± 0.07 (55.13)	1.37 ± 0.01* (18.03)	1.39 ± 0.02* (35.07)	1.42 ± 0.04 (53.13)	1.38 ± 0.05* (24.16)
6.	4-OH	1.12 ± 0.02* (32.06)	1.14 ± 0.06 (34.13)	1.16 ± 0.09 (58.04)	1.15 ± 0.05 (67.05)	1.18 ± 0.12 (40.62)	1.21 ± 0.15 (70.21)	1.24 ± 0.03 (68.18)	1.20 ± 0.11 (74.08)
7.	2-Cl	1.31 ± 0.06 (13.09)	1.33 ± 0.04 (33.06)	1.42 ± 0.05 (40.02)	1.36 ± 0.06* (50.05)	1.28 ± 0.13* (38.02)	1.25 ± 0.014 (25.15)	1.42 ± 0.07 (36.17)	1.48 ± 0.15 (53.04)
8.	4-Cl	1.12 ± 0.16 (33.14)	1.14 ± 0.04 (47.23)	1.15 ± 0.06* (57.11)	1.13 ± 0.12 (70.21)	1.22 ± 0.01* (40.13)	1.25 ± 0.03* (71.32)	1.32 ± 0.13 (66.57)	1.30 ± 0.05 (75.31)

[a] Results are expressed as mean ± SEM and compared with Student's "*t*" test.
[b] The group was injected with 1 mL of 0.5% aqueous saline water.
* Significantly different from control at $P < .05$.

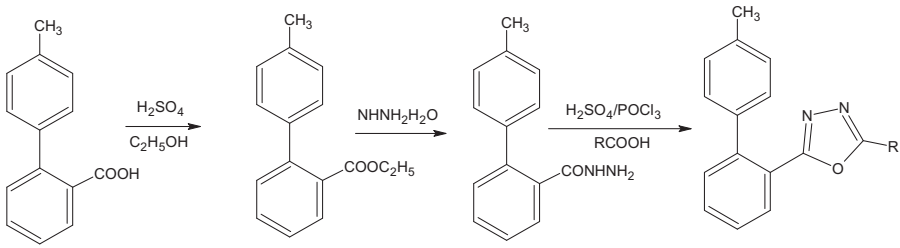

Scheme 25.3 Synthesis of 2-(4′-methylbiphenyl-2-yl)-5-aryl-1,3,4-oxadiazole analogs.

Table 25.3 Effect of carrageenan induced hind paw edema on rats.

Group	R	Difference in paw volume at hours (mean ± SEM) (% Inhibition)		
		1 h	3 h	5 h
Control	–	1.35 ± 0.05	1.59 ± 0.03	1.98 ± 0.03
Diclofenac	–	1.23 ± 0.03	1.12 ± 0.02***	0.91 ± 0.03***
1.	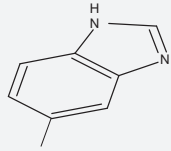	1.25 ± 0.02	1.29 ± 0.03***	1.27 ± 0.03***
2.		1.25 ± 0.03	1.17 ± 0.03***	0.97 ± 0.03***
3.	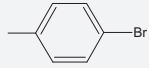	1.28 ± 0.05	1.46 ± 0.04*	1.66 ± 0.04***
4.		1.24 ± 0.03	1.26 ± 0.03***	1.17 ± 0.03***
5.	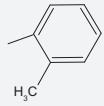	1.25 ± 0.02	1.22 ± 0.02***	1.06 ± 0.03***
6.	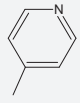	1.25 ± 0.02	1.32 ± 0.02***	1.41 ± 0.04***
7.	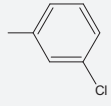	1.23 ± 0.02	1.22 ± 0.03***	1.06 ± 0.02***
8.		1.24 ± 0.04	1.26 ± 0.03***	1.24 ± 0.03***

Table 25.3 Continued

Group	R	Difference in paw volume at hours (mean ± SEM) (% Inhibition)		
		1 h	3 h	5 h
9.	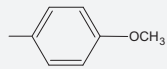	1.26 ± 0.04	1.35 ± 0.04***	1.48 ± 0.03***
10.	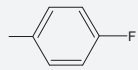	1.25 ± 0.04	1.17 ± 0.06***	0.96 ± 0.05***
11.	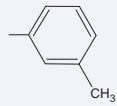	1.25 ± 0.03	1.20 ± 0.04***	1.00 ± 0.03***
12.	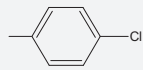	1.26 ± 0.04	1.44 ± 0.04**	1.59 ± 0.04***
13.	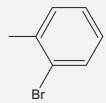	1.24 ± 0.01	1.24 ± 0.01***	1.11 ± 0.02***
14.	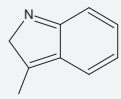	1.27 ± 0.03	1.45 ± 0.04**	1.64 ± 0.05***

Values are mean ± SEM., $n = 6$ in each group; Statistical analysis by Two-way ANOVA followed by post hoc Dunnett's test using Graphpad Instat software.
* P value < .05 compared with vehicle (gum acacia, 10 mL/kg) treated group.
** P value < .01 compared with vehicle (gum acacia, 10 mL/kg) treated group.
*** P value < .001 compared with vehicle (gum acacia, 10 mL/kg) treated group.

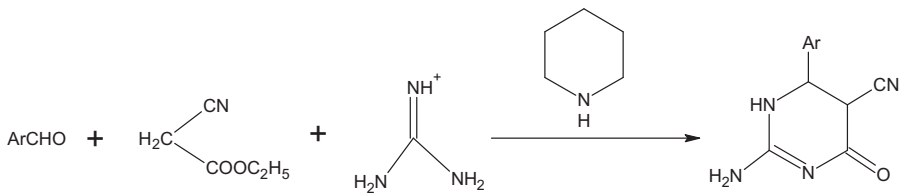

Scheme 25.4 Synthesis of 2-amino dihydropyrimidinone derivatives.

A series of ethyl 2-[2-arylamino-4-(thiophen-2-yl) thiazol-5-yl] acetates and ethyl 2-[2-(arylhydrazino)-4-(thiophen-2-yl) thiazol-5-yl] acetates were synthesized by Mahesh et al. Antiinflammatory activity was determined for all the synthesized compounds using the carrageenan-induced rat hind paw edema method with Wister rats. In vivo test results showed that the compounds with halogen substitution at the para position on the 2-aryl amino group exhibited good antiinflammatory activities, similar to that of indomethacin (Scheme 25.6). Further, a molecular docking study was performed to predict the possible binding modes on cyclooxygenase-1 (COX-1) and COX-2 for the tested compounds. Good correlation was observed between the antiinflammatory activity of the compounds and the results of the binding modes in COX-2 (Table 25.6) [59].

Table 25.4 Effects of compounds and indomethacin in the inhibition of carrageenan-induced rat paw edema.

Drug	Ar	Paw volume response at different time intervals in mean ± SEM				
		Dose	**1 h**	**2 h**	**3 h**	**4 h**
Control	–	10 mL/kg	0.5912 ± 0.005***	0.5930 ± 0.002***	0.6102 ± 0.002***	0.6303 ± 0.002***
Indomethacin	–	100 mg/kg	0.2700 ± 0.005**	0.3124 ± 0.005**	0.3133 ± 0.008**	0.3500 ± 0.005**
1.	4-NO_2-C_6H_4	20 mg/kg	0.4000 ± 0.005***	0.4300 ± 0.005**	0.4500 ± 0.011***	0.4711 ± 0.011***
2.		40 mg/kg	0.3533 ± 0.003**	0.3833 ± 0.003**	0.3967 ± 0.003**	0.4200 ± 0.010**
3.		20 mg/kg	0.4133 ± 0.003**	0.4433 ± 0.003**	0.4667 ± 0.008***	0.4933 ± 0.012***
4.	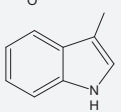	40 mg/kg	0.3567 ± 0.003**	0.3867 ± 0.003**	0.4133 ± 0.003**	0.4520 ± 0.005***
5.	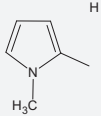	20 mg/kg	0.3833 ± 0.003**	0.4133 ± 0.003***	0.4433 ± 0.003**	0.4667 ± 0.008***

Values are expressed as mean ± SEM; $n = 6$ in each group, $^{***}P < .001$, $^{**}P < .01$, compared with control. Data was analyzed by one-way ANOVA followed by Duneet's test.

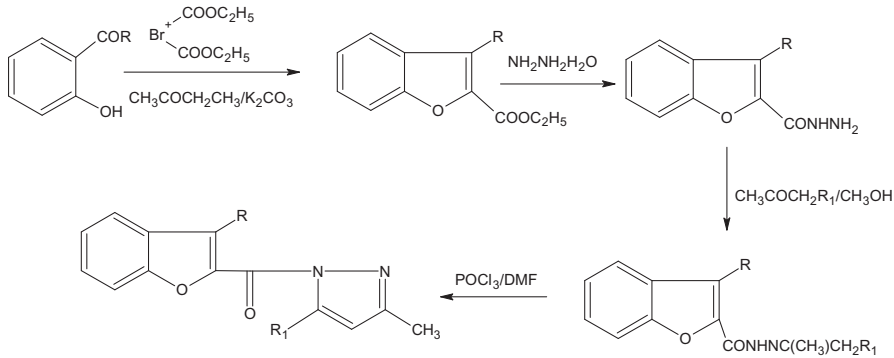

Scheme 25.5 Synthesis of 3-methyl-5-substituted-1H-pyrazol-1-yl-(3-substituted benzofuran-2-yl) methanone derivatives.

Table 25.5 Antiinflammatory activity of compounds on carrageenan induced rat paw edema.

Group	Compound	R	R_1	Admn. mg/kg	Antiinflammatory activity on carrageenan-induced rat paw edema					
					% of inhibition in hour					
					0 h	0.5 h	1 h	2 h	4 h	6 h
1.	Control	–	–	–	–	–	–	–	–	–
2.	Phenyl butazone	–	–	50	46.65	50.01	56.12	58.22	62.66	61.01
3.	1.	H	C_6H_5	200	38.3	41.17	44.43	46.42	49.34	48.14
4.	2.	H	$C_6H_4Cl(p)$	200	52.5	62.06	64.03	65.58	66.63	64.86
5.	3.	OCH_3	C_6H_5	200	48.61	57.41	59.25	60.65	61.05	60.34
6.	4.	OCH_3	$C_6H_4Cl(p)$	200	55.3	66.66	69.55	72.35	74.46	74.01

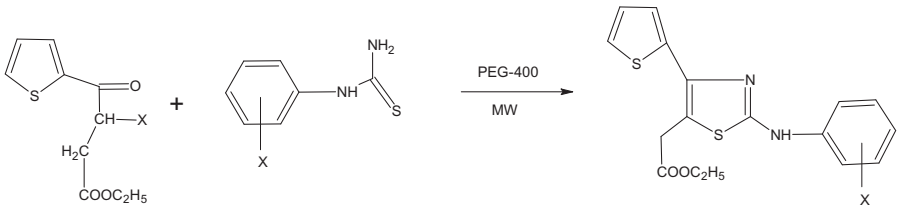

Scheme 25.6 Synthesis of ethyl 2-[2-arylamino-4-(thiophen-2-yl) thiazol-5-yl] acetates and ethyl 2-[2-(arylhydrazino)-4-(thiophen-2-yl) thiazol-5-yl] acetates.

Table 25.6 Antiinflammatory activity of titled compounds.

Compound	X	Mean paw volume ± SEM	% Antiinflammatory activity
1.	2-Cl	0.22 ± 0.060	66.6
2.	3-Cl	0.21 ± 0.074	68.1
3.	4-Cl	0.18 ± 0.069	72.7
4.	2-CH_3	0.28 ± 0.056	54.9
5.	3-CH_3	0.20 ± 0.079	69.6
6.	4-CH_3	0.24 ± 0.074	63.4
7.	4-Br	0.14 ± 0.068	78.8
8.	4-F	0.15 ± 0.070	77.2
9.	2,4-Cl_2	0.18 ± 0.07	72.7
10.	3-Cl-4-F	0.17 ± 0.047	74.3
11.	4-OCH_3	0.29 ± 0.072	50.1
12.	H	0.31 ± 0.076	53.3
13.	2-OH	0.35 ± 0.072	46.9
14.	2-Cl	0.30 ± 0.079	54.5
15.	4-Cl	0.32 ± 0.082	51.5
16.	4-NMe_2	0.40 ± 0.064	39.3
17.	4-OMe	0.48 ± 0.077	27.3
18.	4-OH-3-OMe	0.42 ± 0.083	36.36
Indomethacin	–	0.12 ± 0.051	82.6

A series of 1-(2-((18*Z*)-4-substituted benzylidene-4,5-dihydro-5-oxo-2-phenylimidazol-1-yl) ethyl)-1,2-dihydro-4-methyl-2-oxoquinolin-7-yl substitutes of imidazolo quinoline analogs were synthesized by condensation of substituted imidazole and substituted quinoline (Scheme 25.7). The title compounds were investigated for antiinflammatory activity using carrageenan-induced rat paw edema method using male albino rats weighing between 100 and 150 g. All the lead compounds were assessed by QSAR and molecular modeling (CADD) studies to predict best physicochemical, pharmacokinetic, toxicological properties, and best fit with targets like COX-1 and COX-2. The result indicates that the compounds show convincing activities against inflammation when compared with standard drug ibuprofen. The percent protection was measured and the activity was compared with standard drug ibuprofen. All the synthesized compounds exhibited antiinflammatory activity (Table 25.7) [60].

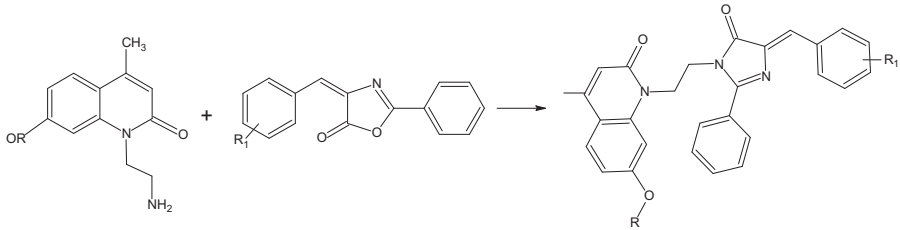

Scheme 25.7 Synthesis of 1-(2-((18*Z*)-4-substituted benzylidene-4,5-dihydro-5-oxo-2-phenylimidazol-1-yl) ethyl)-1,2-dihydro-4-methyl-2-oxoquinolin-7-yl substitutes of imidazolo quinoline analogs.

Table 25.7 Antiinflammatory activity of the synthesized compounds (in vitro).

Compound	R	R_1	% Protection[a]			
			30 min	1 h	2 h	3 h
1.	CH_3CO	H	35 ± 1.793	47 ± 1.444	49 ± 1.876	34 ± 1.414
2.	CH_3CO	4-OCH_3	39 ± 1.881	49 ± 1.643	53 ± 1.372	44 ± 1.424
3.	CH_3CO	4-$N(CH_3)_2$	44 ± 1.079	47 ± 1.377	52 ± 2.46	43 ± 1.762
4.	CH_3CO	2-OH	39 ± 2.198	49 ± 1.404	57 ± 1.729	39 ± 2.306
5.	C_6H_5CO	H	35 ± 1.472	47 ± 2.174	49 ± 1.752	39 ± 1.861
6.	C_6H_5CO	4-Cl	39 ± 2.66	48 ± 1.872	54 ± 1.4111	41 ± 1.472
7.	C_6H_5CO	4-OCH_3	39 ± 1.831	42 ± 1.472	49 ± 1.876	35 ± 1.876
8.	C_6H_5CO	4-$N(CH_3)_2$	35 ± 1.333	39 ± 2.357	47 ± 1.875	37 ± 3.246
9.	C_6H_5CO	2-OH	36 ± 1.831	39 ± 2.412	43 ± 1.163	32 ± 1.159
10.	$C_6H_5CH_2$	H	27 ± 1.362	34 ± 1.522	41 ± 1.476	29 ± 3.132
11.	$C_6H_5CH_2$	4-$N(CH_3)_2$	35 ± 3.214	37 ± 2.327	42 ± 1.874	36 ± 1.861
12.	$C_6H_5CH_2$	2-OH	38 ± 2.538	41 ± 1.781	46 ± 1.323	32 ± 1.672
Ibuprofen	–	–	46 ± 2.429	53 ± 2.16	65 ± 1.871	43 ± 1.871

Significant levels $P < .01$ as compared with the respective control. [a]Each value represents the means ± SD ($n = 6$).

Rishikesh et al. prepared various 4-(2-amino-6-(substituted)pyrimidin-4-yl)-3-methyl-1-(substituted)-1H-pyrazol-5(4H)-one derivatives and their Schiff bases in a microwave oven for the appropriate time in between 5 and 7 min at 30% power output (Scheme 25.8). Antiinflammatory activity of the synthesized compounds was evaluated by carrageenan-induced rat paw edema model, at equimolar doses, using groups of six animals each, using indomethacin as the standard drug. The pharmacological studies revealed that the presence of 4-hydroxy, 4-methoxy, 4-(*N*,*N*-dimethylamino), or 2-hydroxy groups on phenyl ring at C_6 of amino pyrimidine exhibited significant antiinflammatory activity (Table 25.8) [61].

Anand et al. prepared some novel, nonsteroidal antiinflammatory drug (NSAID), acetaminophen conjugates with amino acid linkers utilizing benzotriazole chemistry. The target compounds were prepared by coupling unprotected amino acid-acetaminophen conjugates with NSAID-benzotriazolides in the presence of K_2CO_3 in DMF under microwave irradiation at 50 W, 70°C for 2.5 h (Scheme 25.9). Biological data acquired for all the novel bisconjugates exhibited antiinflammatory activity than their parent drugs, and the potent bioactive compounds have no mortality rates or toxic symptoms at fivefold the applied antiinflammatory dosage. Antiinflammatory activity of compounds was determined in vivo by the acute carrageenan-induced paw edema standard method in rats taking indomethacin as the standard drug. Structure-activity relationships based on the observed results exhibit that the alkyl/arylalkyl function of the amino acid residue controls the antiinflammatory potency of the compounds. Generally, the benzyl group of the amino acid function affords more potent agents compared with alkyl functions (methyl, isopropyl, and isobutyl) (Table 25.9) [62].

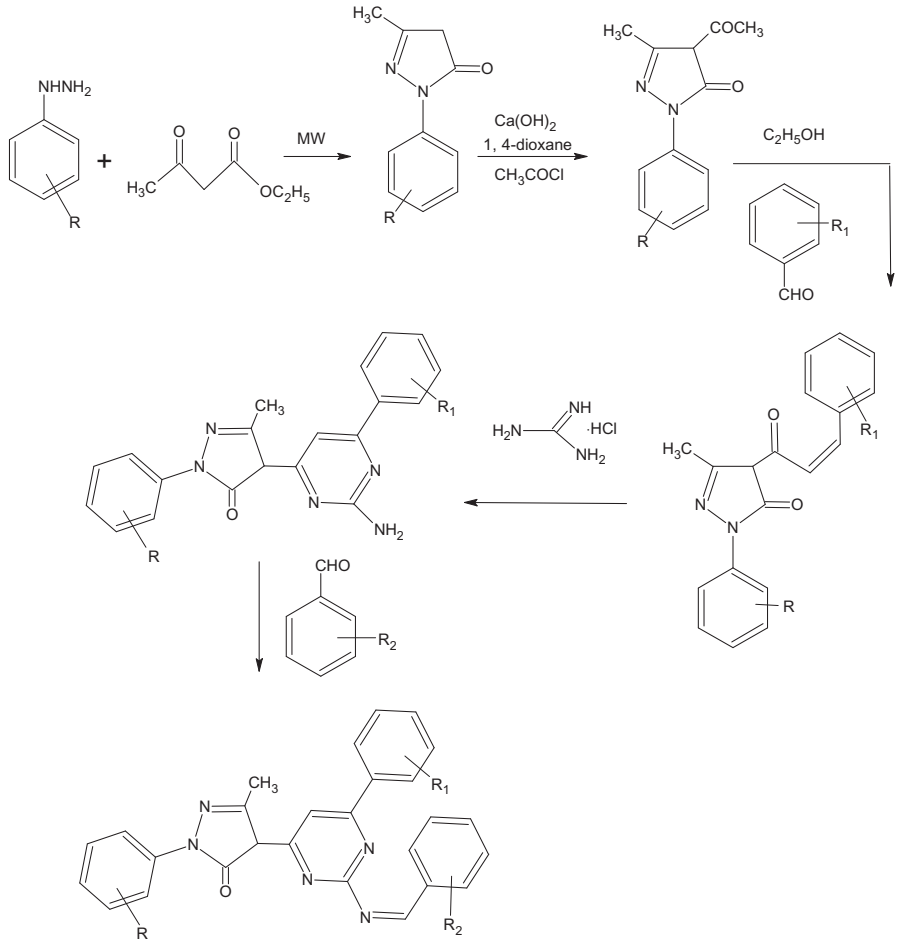

Scheme 25.8 Synthesis of 4-(2-(substituted)-6-(substituted)pyrimidin-4-yl)-3-methyl-1-phenyl-1H-pyrazol-5(4H)-one as Schiff bases.

Design and microwave-assisted synthesis of 2-aryl-5-(4-pyridyl)-1,3,4-oxadiazole derivatives are prepared by Biju et al., under microwave irradiation at 300 W internally at 30 s intervals for 4 min (Scheme 25.10). The antiinflammatory activity study was carried out by carrageenan-induced rat paw edema method using indomethacin as the standard drug. Some of the tested compounds showed good antiinflammatory activity (Table 25.10) [63].

Adriana et al. prepared some *p*-toluenesulfonyl-hydrazinothiazole derivatives by the Hantzsch condensation reaction of *p*-toluene-sulfonyl-thiosemicarbazide with a series of α-halogenocarbonyls such as chloroacetone, 1,3-dichloroacetone,

Table 25.8 Results of antiinflammatory activity of compounds against carrageenan induced rat paw edema model in rats.

Compounds	R	R1	R2	Mean volume in (mL) after drug treatment (mean ± SEM)		
				1 h	2 h	3 h
Control	–	–	–	1.525 ± 0.015	1.815 ± 0.022	1.95 ± 0.009
Indomethacin	–	–	–	0.875 ± 0.020	0.806 ± 0.007	0.718 ± 0.014
1.	H	4-OH-3-OCH_3	4-NO_2	0.915 ± 0.020	0.826 ± 0.016	0.756 ± 0.011
2.	H	4-NO_2	4-CH_3	1.325 ± 0.130	1.765 ± 0.019	1.518 ± 0.0154
3.	H	4-OCH_3	4-NO_2	0.93 ± 0.264	0.846 ± 0.031	0.76 ± 0.024
4.	H	2-OH	4-CH_3	0.924 ± 0.013	0.801 ± 0.042	0.744 ± 0.030
5.	H	4-(N,N-$(CH_3)_2$)	4-NO_2	0.903 ± 0.016	0.846 ± 0.018	0.741 ± 0.033
6.	(2,4-NO_2)	4-OH-3-OCH_3	4-Cl	0.891 ± 0.0210	****836 ± 0.013	0.731 ± 0.027
7.	(2,4-NO_2)	3-NO_2	4-Cl	1.29 ± 0.091	1.556 ± 0.176	1.793 ± 0.0
8.	(2,4-NO_2)	4-(N,N-$(CH_3)_2$)	4-Cl	0.921 ± 0.013	0.808 ± 0.042	0.74 ± 0.030
9.	(2,4-NO_2)	2-NO_2	4-Cl	1.351 ± 0.146	1.586 ± 0.137	1.803 ± 0.047
10.	(2,4-NO_2)	4-(N,N-$(CH_3)_2$)	4-CH_3	1.493 ± 0.021	1.798 ± 0.058	1.926 ± 0.030

Data analyzed by one-way ANOVA followed by Dunnett's test ($n = 6$).

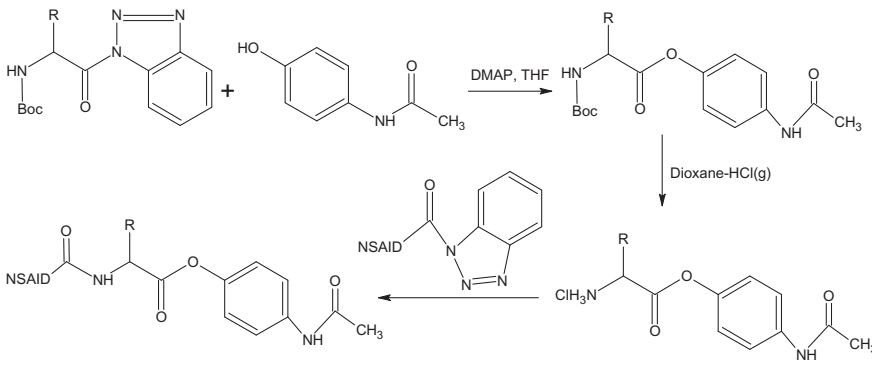

Scheme 25.9 Synthesis of NSAID bisconjugates with acetaminophen and amino acids.

α-bromoacetophenone, 3-chloroacetylacetone, ethyl α-bromoacetoacetate, and ethyl-γ-bromoacetoacetate by microwave-assisted reaction (Scheme 25.11). The synthesized derivatives were tested for potential antiinflammatory activity using rat hind paw edema induced with 10% kaolin, in order to evaluate the vascular phase of the inflammatory process. To compare the effectiveness of the tested compounds, phenylbutazone was used as the standard drug (Table 25.11) [64].

Table 25.9 Observed and predicated values of the tested antiinflammatory active agents according to the multilinear QSAR model[a].

Compounds	R	Observed % inhibition of edema at 3 h	Predicted % inhibition of edema at 3 h	Error
1.	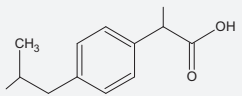	29.7	32.7	−3.0
2.	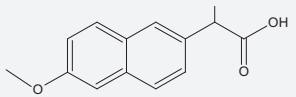	46.0	58.4	−12.4
3.	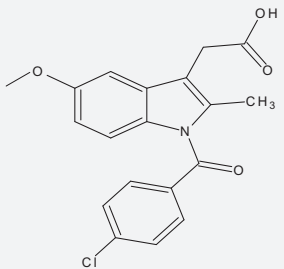	61.3	56.8	4.5
4.	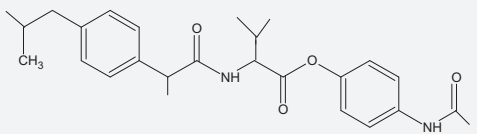	17.3	25.9	−8.6
5.	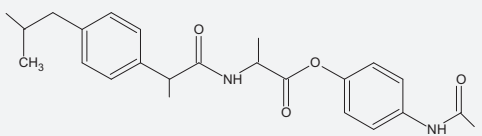	10.6	9.9	0.7

6.	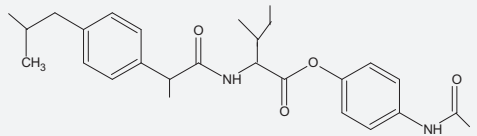	8.7	11.4	−2.7
7.	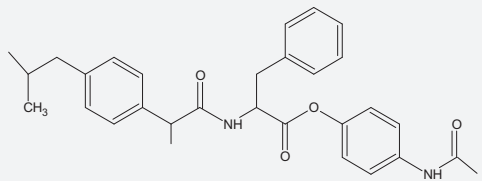	43.5	34.0	9.5
8.	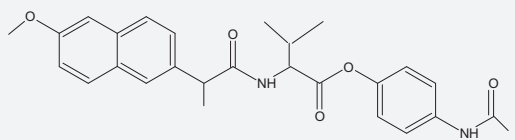	50.2	42.8	7.4
9.	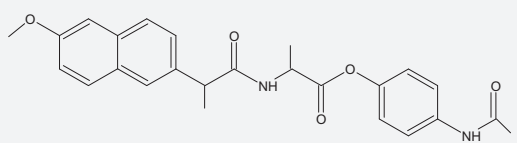	25.8	21.7	4.1
10.	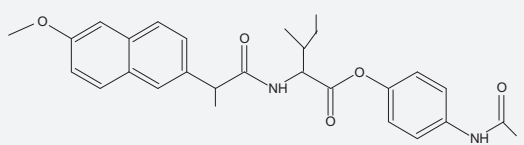	39.7	43.3	−3.6

Continued

Table 25.9 Continued

Compounds	R	Observed % inhibition of edema at 3 h	Predicted % inhibition of edema at 3 h	Error
11.	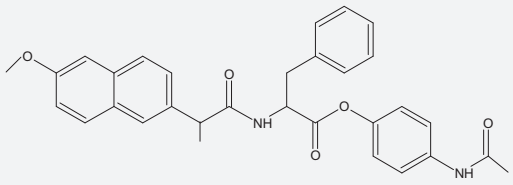	51.4	51.6	−0.2
12.	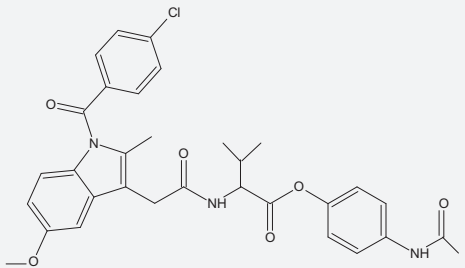	58.2	44.0	14.2
13.	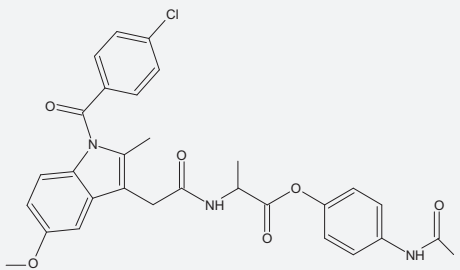	21.0	16.5	4.5

14.	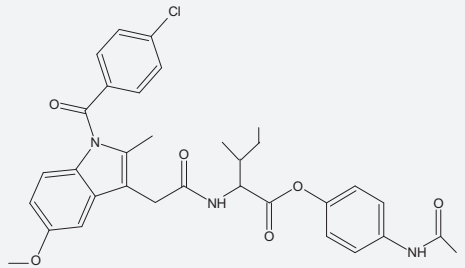	71.3	65.2	6.1
15.	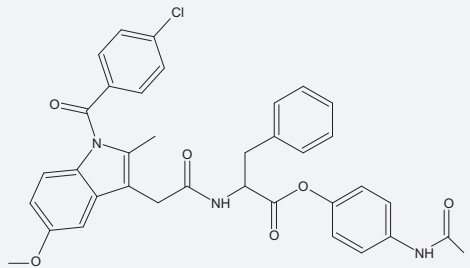	48.5	60.9	−12.4

[a] Activity was undertaken as percentage inhibition of edema for the tested compound sat 3 h effect.

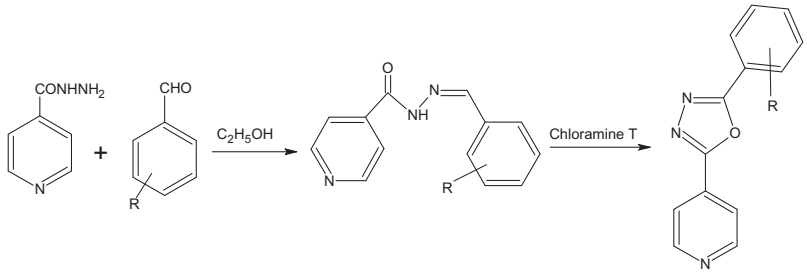

Scheme 25.10 Synthesis of 2-aryl-5-(4-pyridyl)-1,3,4-oxadiazole derivatives.

Table 25.10 Antiinflammatory activity by carrageenan-induced rat paw edema method.

Treatment	R	Dose (per kg)	Mean difference in paw thickness = SEM	Percentage inhibition of edema
Control	–	20 mg/kg	2.23 ± 0.09	–
Indomethacin	–	20 mg/kg	0.72 ± 0.08	67.71
1.	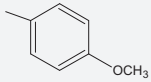	500 mg/kg	0.70 ± 0.03	68.60
2.	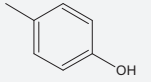	500 mg/kg	0.69 ± 0.04	69.05
3.	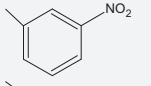	500 mg/kg	0.96 ± 0.03	56.95
4.	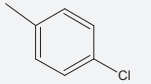	500 mg/kg	0.89 ± 0.02	60.08
5.	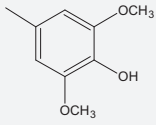	500 mg/kg	0.86 ± 0.04	61.43

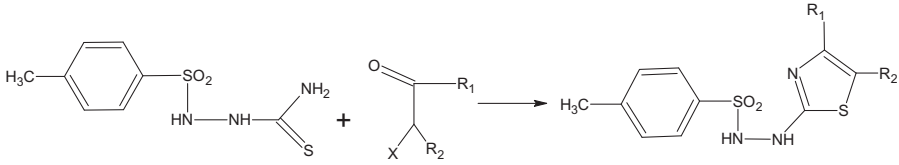

Scheme 25.11 Synthesis of *p*-toluenesulfonylthiosemicarbazide with some α-halogenocarbonyl derivatives.

Table 25.11 Inhibition of inflammatory edema induced by in rats with 10% kaolin.

Compounds	R1	R2	Dose (mg/kg)	% Inhibition of edema after		
				2 h	4 h	24 h
Phenylbutazone	–	–	50	44.66	39.68	23.07
1.	–	–	50	23.33	30.15	5.49
2.	CH_3	H	50	45.73	43.18	32.31
3.	CH_2Cl	H	50	50.00	53.96	−40.65
4.	C_6H_5	H	50	44.18	41.66	9.14
5.	CH_3	$COCH_3$	50	30.00	4.76	−20.17
6.	CH_3	$COOC_2H_5$	50	8.33	15.87	12.08
7.	$CH_2COOC_2H_5$	H	50	46.51	40.90	6.09
8.	CH_3	H	50	16.66	15.87	8.79
9.	CH_2Cl	H	50	53.48	50.00	7.92
10.	C_6H_5	H	50	51.93	51.51	12.80
11.	CH_3	$COCH_3$	50	35.00	22.22	−9.89
12.	CH_3	$COOC_2H_5$	50	60.46	62.12	13.41
13.	$CH_2COOC_2H_5$	H	50	47.28	57.57	9.14

An efficient and environmentally benign protocol was designed by Subramanyam et al. for the synthesis of pyrazole derivatives by the reaction of chalcones with phenyl hydrazine hydrochloride under solvent-free conditions at room temperature using microwave radiation at 490 W (Scheme 25.12). In vitro antiinflammatory activities of the tested compounds were evaluated with albumin denaturation method and membrane test methods. Phenyl butazone, flufenamic acid, and salicylic acid are used as standard reference drugs for the study. The tested compounds showed moderate to good antiinflammatory activity. Especially, the compounds bearing with 4-nitrophenyl moiety, 4-fluorophenyl moiety, and pyridinyl group showed potent antiinflammatory activity compared with other derivatives. It was observed that the position of the substituent on terminal benzene ring of pyrazole moiety has profound effect on the activity. The para position on the terminal benzene ring is the favorable site for the higher potency. Evidently, the compound with NO_2 and F at para position, exhibiting highest inhibitory activity in the two methods. The presence of pyridine as substituent also exhibits high inhibitory activity in the two methods when compared with standard drugs. The remaining compounds were found to have moderate to good activity (Tables 25.12 and 25.13) [65].

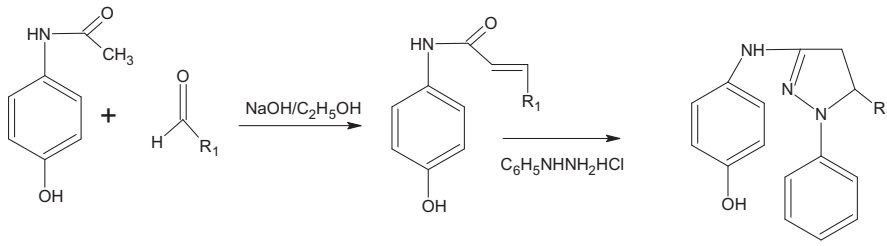

Scheme 25.12 Synthesis of pyrazole derivatives.

Table 25.12 In vitro antiinflammatory activity of the title compounds by inhibition of albumin denaturation method.

Compounds	R1	Dose (mg/mL)	Mean OD	SD	% Inhibition
NC	–	RO water	2.385	0.043	–
PC1	–	100	0.954[a]	0.010	60.432
PC2	–	200	0.504[a]	0.005	79.363
SC	–	0.2	1.045[a]	0.022	57.676
1.	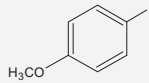	0.2	1.521[a]	0.009	39.235
2.	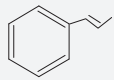	0.2	1.236[a]	0.005	43.242
3.	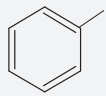	0.2	1.151[a]	0.006	54.474
4.	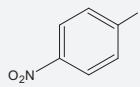	0.2	0.624[a]	0.025	75.328
5.	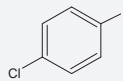	0.2	1.014[a]	0.008	62.743
6.	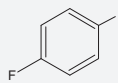	0.2	0.737[a]	0.010	74.137
7.	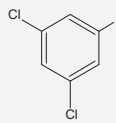	0.2	1.114[a]	0.009	56.948
8.	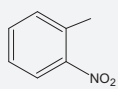	0.2	1.197[a]	0.019	53.754
9.	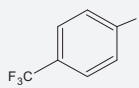	0.2	0.823[a]	0.007	68.203
10.		0.2	0.687[a]	0.015	74.272

NC = phenyl butazone; PC = flufenamic acid.
[a] $P < .05$.

Table 25.13 In vitro antiinflammatory activity of the title compounds by membrane stabilization test method.

Compounds	R1	Dose (mg/mL)	Mean OD	SD	% Inhibition
NC	–	RO water	2.430	0.133	–
PC1	–	100	0.912[a]	0.025	62.713
PC2	–	200	0.373[a]	0.042	85.253
SC	–	0.2	0.962[a]	0.076	61.921
1.	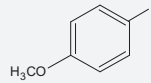	0.2	1.395[a]	0.008	41.045
2.	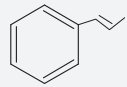	0.2	1.203[a]	0.011	45.933
3.	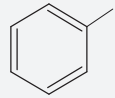	0.2	1.333[a]	0.324	42.152
4.	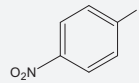	0.2	0.730[a]	0.015	76.625
5.	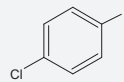	0.2	0.706[a]	0.016	70.964
6.	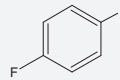	0.2	0.656[a]	0.026	79.720
7.	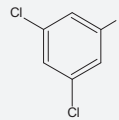	0.2	1.153[a]	0.010	52.898
8.	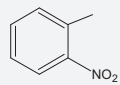	0.2	1.295[a]	0.007	47.701
9.	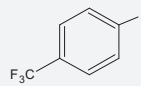	0.2	0.814[a]	0.026	66.545
10.		0.2	1.687[a]	0.040	77.042

NC = phenyl butazone; PC = salicylic acid.
[a] $P < .05$.

A series of pyrazolo[3,4-*b*]quinolines have been synthesized using one-pot water-mediated synthetic route under microwave irradiation involving the condensation of 2-chloroquinoline-3-carbaldehydes with semicarbazide or 2,4-dinitrophenyl hydrazine at 1000 W for 2–5 min (Scheme 25.13). The synthesized compounds were evaluated for their antiinflammatory activity using carrageenan-induced paw edema

method. Ibuprofen was used as a standard. The pharmacological evaluation showed that the compounds are good at inhibiting edema induced by carrageenan. Some of the tested compounds showed statistically significant antiinflammatory activity. Furthermore, the activity is higher in case of substitution with negative hydrophobic and electronic constants (methoxy substitution) as compared with that of the substitutions with both positive and negative hydrophobic and electronic constants; as was seen with the methyl and chloro substitution. However, the activity was found to decline in compounds with no substitution (Table 25.14) [66].

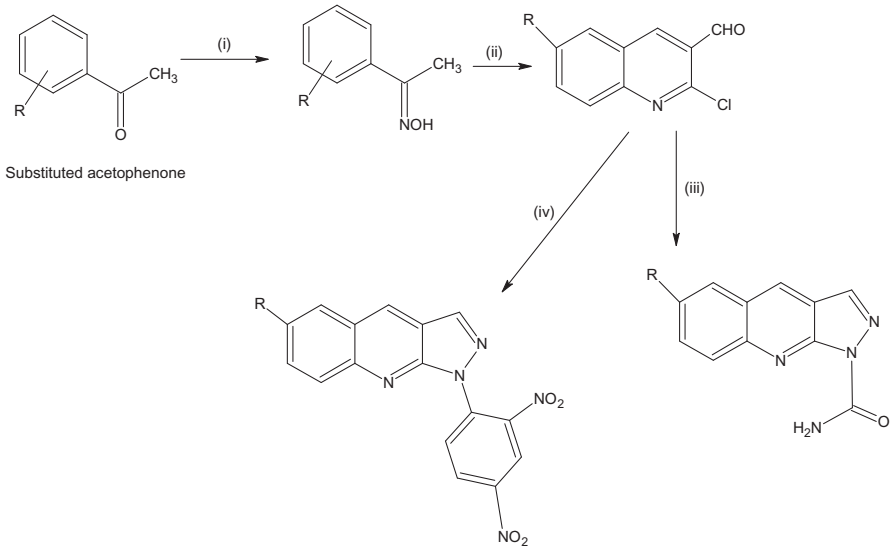

Scheme 25.13 Synthesis of pyrazolo[3,4-*b*]quinolines.

Table 25.14 Antiinflammatory activity of the synthesized compounds.

Compound	R	% Inhibition ± SEM[a]	
		After 2 h	After 3 h
Control	–	–	–
Ibuprofen	–	69.52 ± 1.26	78.04 ± 0.71
1.	H	33.09 ± 1.13***	50.00 ± 1.13***
2.	Cl	46.42 ± 2.01***	61.38 ± 1.62***
3.	OCH_3	54.52 ± 1.45***	67.07 ± 0.71***
4.	CH_3	28.57 ± 1.22***	44.51 ± 2.11***
5.	H	35.00 ± 1.32***	49.59 ± 1.12***
6.	Cl	38.09 ± 2.23***	56.50 ± 1.39***
7.	OCH_3	45.71 ± 1.52***	63.41 ± 1.41***
8.	CH_3	24.52 ± 2.00***	42.27 ± 1.43***

[a] Relative to their respective control and data were analyzed by one-way ANOVA followed by Tukey test for $n = 6$.
*** $P < .001$.

Parameshwar et al. have prepared a novel series of 1-(4-chlorophenyl)-3-(4-substituted phenyl)-5-(5-(4-nitrophenyl)furan-2-yl)-4,5-dihydro-1H-pyrazole derivatives and 3-(4-substitutedphenyl)-5-((5-(4-nitrophenyl)furan-2-yl)-4,5-dihydropyrazol-1-yl)(pyridin-4-yl)methanone derivatives by microwave irradiation method for time period of 5–8 min at a power level of 600 W in the presence of piperidine catalyst (Scheme 25.14). The compounds were screened for their in vivo antiinflammatory activity using the carrageenan-induced paw edema method by taking ibuprofen as the standard. The results of the antiinflammatory activity showed that the presence of pyridinoyl moiety on nitrogen of pyrazoline enhances the activity (Table 25.15) [67].

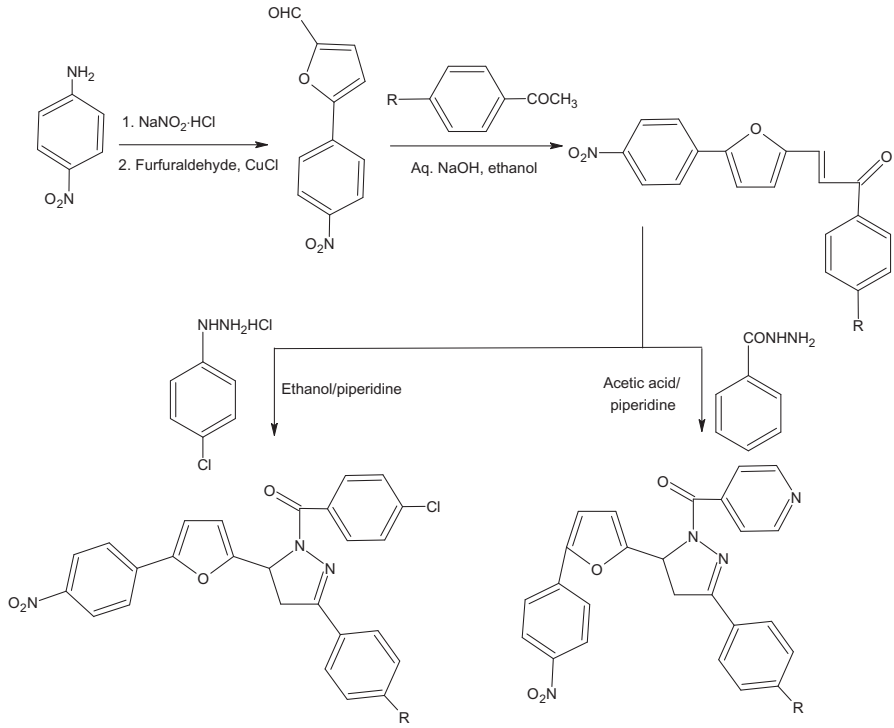

Scheme 25.14 Synthesis of 3-(4-substituted phenyl)-5-((5-(4-nitrophenyl)furan-2-yl)-4,5-dihydropyrazol-1-yl)(pyridin-4-yl)methanone derivatives.

Vyankatesh et al. carried out the synthesis of 2-amino-4,5-diphenyl-1-substituted-1H-pyrrole-3-carbonitrile derivatives by direct reaction of a heterocyclic compound with substituted anilines using microwave irradiation (Scheme 25.15). In vitro antiinflammatory activity of synthesized compounds was analyzed by using spectroscopic quantification by protein denaturation method. The synthesized pyrrole derivatives show promising in vitro antiinflammatory activity by taking diclofenac sodium as reference drug. The percentage inhibition of protein denaturation was calculated.

Table 25.15 Antiinflammatory activity of ibuprofen and synthesized compounds.

Compd.	R	0.5 h	1 h	2 h	3 h	% Inhibition after 3 h
Control	–	2.62 ± 0.02	3.81 ± 0.05	4.24 ± 0.06	4.68 ± 0.03	–
Ibuprofen	–	1.68 ± 0.03*	1.16 ± 0.02*	0.96 ± 0.02*	0.55 ± 0.04*	88.26
1.	H	1.95 ± 0.01*	2.15 ± 0.04*	1.97 ± 0.02*	1.68 ± 0.05*	64.05
2.	Cl	1.81 ± 0.03*	1.72 ± 0.06*	1.35 ± 0.03*	1.07 ± 0.03*	77.03
3.	CH_3	1.84 ± 0.02*	1.84 ± 0.05*	1.76 ± 0.04*	1.52 ± 0.03*	67.47
4.	OH	1.91 ± 0.06*	2.11 ± 0.04*	1.55 ± 0.03*	1.49 ± 0.04*	68.14
5.	OCH_3	1.80 ± 0.02*	1.69 ± 0.06*	1.48 ± 0.04*	1.19 ± 0.03*	74.58
6.	H	1.86 ± 0.02*	1.77 ± 0.07*	1.67 ± 0.03*	1.58 ± 0.05*	66.15
7.	Cl	1.80 ± 0.01*	1.72 ± 0.03*	1.28 ± 0.02*	0.92 ± 0.04*	80.19
8.	CH_3	1.85 ± 0.01*	1.75 ± 0.05*	1.68 ± 0.04*	1.39 ± 0.03*	70.31
9.	OH	1.76 ± 0.02*	1.68 ± 0.03*	1.48 ± 0.02*	1.22 ± 0.04*	73.83
10.	OCH_3	1.82 ± 0.01*	1.64 ± 0.02*	1.39 ± 0.02*	0.95 ± 0.02*	79.73

Each value represents mean ± SE of six animals.
* $P < .05$ as compared with control; using one-way ANOVA was done by Dunnett's *t*-test. Ibuprofen and test compounds were taken at a dose of 100 mg/kg body weight.

This antidenaturation effect was further supported by the change in viscosities. It has been reported that the viscosities of protein solutions increase on denaturation. The ability of pyrrole derivatives to bring down thermal denaturation of protein is possibly a contributing factor for its antiinflammatory activity (Table 25.16) [68].

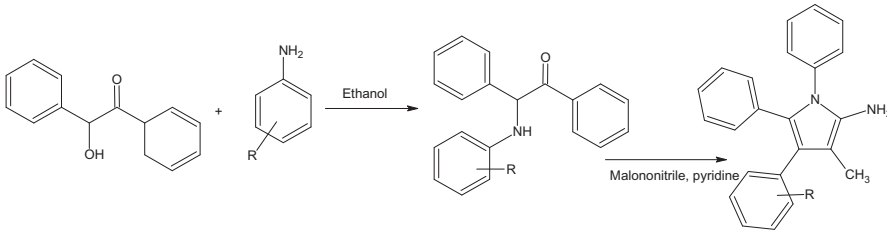

Scheme 25.15 Synthesis of 2-amino-4,5-diphenyl-1-substituted-1H-pyrrole-3 carbonitrile derivatives.

Table 25.16 The antiinflammatory activities of synthesized compounds.

Compounds	R	% of inhibition of protein denaturation	
		50 µg/mL	100 µg/mL
Diclofenac sodium	–	76.7	82.01
1.	*p*-Nitroacetanilide	70.12	70.25
2.	*N*,*N*-Dimethyl-aniline	50.79	52.95
3.	*o*-Anisidine	60.29	61.36
4.	Aniline	53.06	58

Venakata et al. synthesized some imidazolo quinazoline-4-one analogs by microwave irradiation method and are screened for antiinflammatory action by carrageenan-induced paw edema method (Scheme 25.16). Carrageenan-induced rat hind paw edema, the percentage inhibition and reduction in paw volume were significant as compared with indomethacin (Table 25.17) [69].

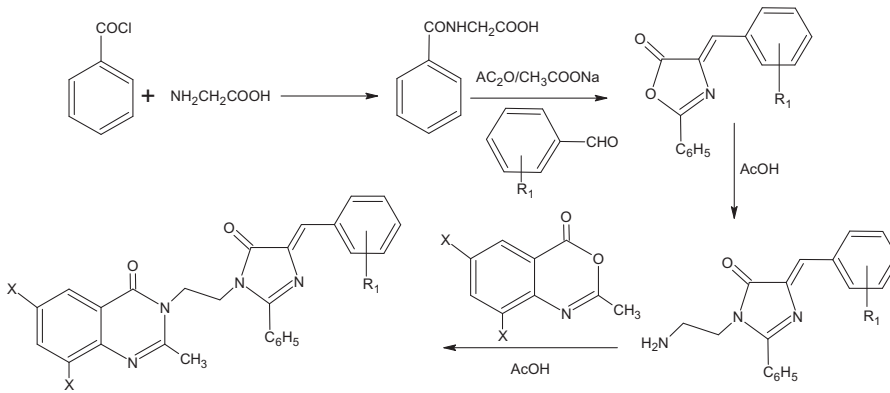

Scheme 25.16 Synthesis of Imidazolo quinazoline-4-one derivatives analogs.

Table 25.17 Percent protection antiinflammatory activity of quinazoline-4(3H)-one analogs.

Compounds	X	% Protection[a]			
		30 min	1 h	2 h	3 h
1.	H	36 ± 1.789	41 ± 1.414	44 ± 1.871*	34 ± 1.414
2.	Br	37 ± 2.098	49 ± 1.414	50 ± 1.789*	30 ± 2.366

*Significant levels $P < .01$ as compared with the respective control.
[a]Each value represents the means ± SD ($n = 6$).

Rakesh et al. have designed an efficient and rapid synthesis of (*E*)-1, 5-dimethyl-4-((2-((substituted-2-oxo-2H-chromen-4-yl)methoxy)naphthalen-1-yl) methyleneamino)-2-phenyl-1,2-dihydropyrazol-3-one derivatives containing Schiff bases under microwave irradiation under 200 W power at 35°C for 8–12 min (Scheme 25.17). The synthesized compounds were subjected to antiinflammatory effect against denaturation of hen's egg albumin method at the concentration with standard aceclofenac drug. The results suggested that an electron releasing group (—OCH_3) and hydrogen bonding group (—OH) increases the antiinflammatory potency (Table 25.18) [70].

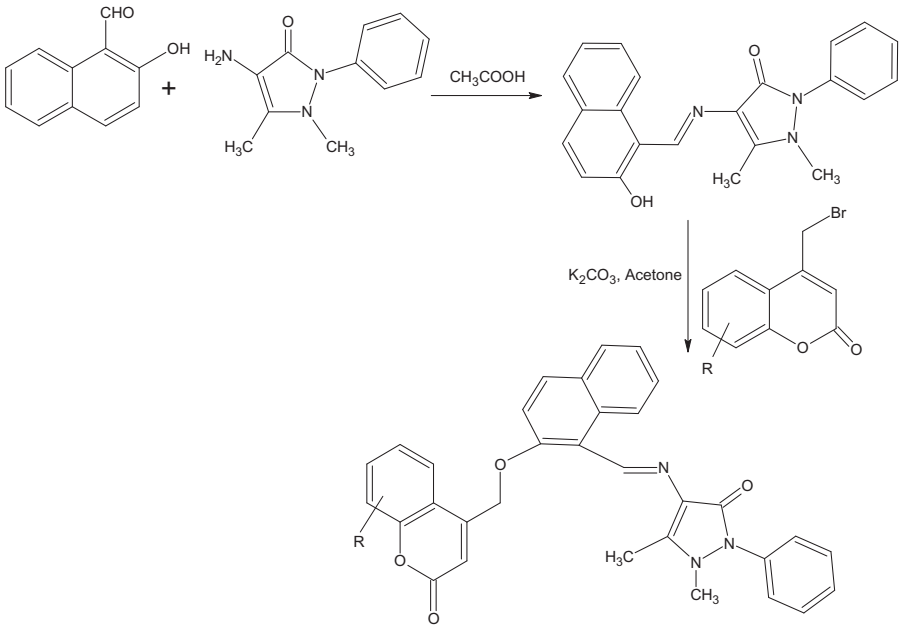

Scheme 25.17 Synthesis of (*E*)-1,5-dimethyl-4-((2-((substituted-2-oxo-2H-chromen-4-yl) methoxy) naphthalen-1-yl)methyleneamino)-2-phenyl-1,2-dihydropyrazol-3-one derivatives containing Schiff base.

Table 25.18 In vitro antiinflammatory activity in protein denaturation method of compounds.

Test compounds	R	Percentage of inhibition of egg albumin in 31.25 µg/mL
Control	–	–
1.	5,7-diCH_3	7.69 ± 0.03
2.	6-ter-butyl	40.59 ± 0.01
3.	6-OCH_3	53.65 ± 0.03
4.	6-CH_3	19.33 ± 0.04
5.	6-Cl	39.09 ± 0.03
6.	7-OH	67.27 ± 0.05
7.	7-CH_3	24.87 ± 0.01
8.	5,6-benzo	3.78 ± 0.05
9.	7,8-benzo	14.44 ± 0.02
Aceclofenac	–	5.50 ± 0.01

Values are mean ± SD, $n = 3$.

A series of 3, 5-disubstituted-4, 5-dihydro-1H-pyrazoles have been synthesized by Musarat et al. under solvent-free microwave irradiation method by the condensation of α, β-unsaturated ketones with hydrazine and its differently substituted derivatives (Scheme 25.18). All the synthetics were evaluated for their antiinflammatory activity under in vivo conditions using carrageenan-induced rat paw edema method. The results suggested that the tested compounds have antiinflammatory activity (Table 25.19) [71].

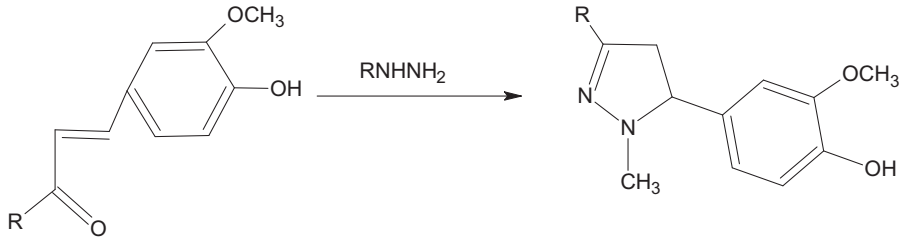

Scheme 25.18 Synthesis of 3, 5-disubstituted-4, 5-dihydro-1H-pyrazoles.

Table 25.19 Effect of compound 1–12 (5 mg/kg/body weight) and ibuprofen (100 mg/kg/body weight) on the oedema in the acute model of inflammation induced by carrageenan.

Groups	R	R1	Concentration (mg/kg)	Mean ± S. E.	Activity (%)
Control	–	–	–	1.58 ± 0.10	–
1.	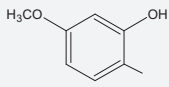	H	5	1.00 ± 0.09	36.70%↓
2.	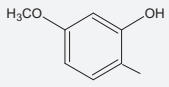	CH_3	5	0.95 ± 0.12	39.87%↓**
3.	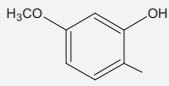	Ph	5	1.09 ± 0.11	31.01%↓*
4.	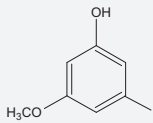	H	5	1.19 ± 0.16	24.68%↓
5.	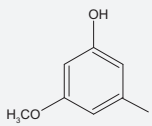	CH_3	5	1.32 ± 0.10	16.45%↓

Continued

Table 25.19 Continued

Groups	R	R1	Concentration (mg/kg)	Mean ± S. E.	Activity (%)
6.	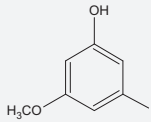	Ph	5	1.27 ± 0.19	19.62%↓
7.	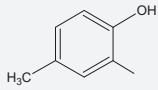	H	5	1.20 ± 0.09	24.05%↓
8.	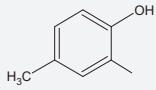	CH_3	5	1.31 ± 0.12	17.08%↓
9.	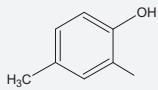	Ph	5	1.25 ± 0.13	20.88%↓
10.	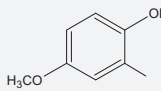	H	5	1.12 ± 0.11	29.11%↓*
11.	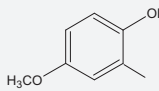	CH_3	5	1.05 ± 0.09	33.54%↓*
12.	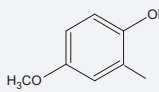	Ph	5	0.92 ± 0.15	41.77%↓**
Ibuprofen	–	–	100	0.78 ± 0.14	50.63%↓**

Values represented the mean ± S.E.M, which were analyzed by Student's *t*-test, $n = 6$.
* $P < .01$.
** $P < .001$.

Efficient approach for the synthesis of a series of triazolothiadiazole analogs of ibuprofen has been carried out by Sujith et al. using microwave energy (Scheme 25.19). Antiinflammatory activity was determined by carrageenan-induced paw edema method in Wistar albino rats using plethysmography. Diclofenac at an oral dose of 20 mg/kg served as the standard drug. The antiinflammatory activity data showed that the compound having furyl group at position 6 of triazolothiadiazole possesses highest activity. Similarly, other compounds possessing methyl, 4-bromophenyl, and 2-chlorophenyl showed an excellent antiinflammatory activity (Table 25.20) [72].

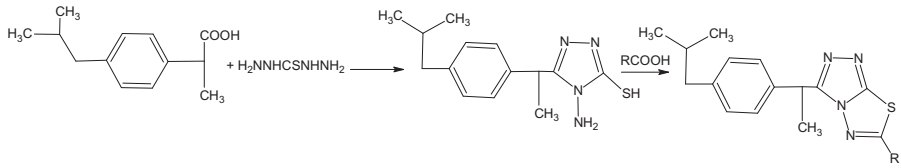

Scheme 25.19 Synthesis of triazolothiadiazole analogs of ibuprofen.

Table 25.20 Antiinflammatory activity of ibuprofen derivatives against carrageenan-induced rat paw edema model in rats.

Compounds	R	Change in paw volume in milliliter ± SEM[a] (% inhibition)					
		0.5 h	1 h	1.5 h	2 h	2.5 h	3 h
Diclofenac	–	0.2 ± 2.38 (82)*	0.5 ± 1.01 (65)*	0.6 ± 2.56 (80)**	0.8 ± 4.18 (76)	1 ± 3.9 (73)*	1 ± 0.89 (75)**
Ibuprofen	–	0.88 ± 4.31 (20)	1.15 ± 2.67 (18)**	2.17 ± 2.69 (25)*	2.11 ± 3.74 (36)*	2.19 ± 4.25 (39)	2.26 ± 2.35 (42)*
1.	CH_3	0.4 ± 1.13 (64)	0.8 ± 3.02 (43)*	1.1 ± 1.67 (62)*	1.4 ± 2.08 (58)	1.6 ± 3.27 (56)	1.5 ± 4.08 (62)*
2.	C_2H_5	1.05 ± 3.22 (5)	1.1 ± 1.14 (22)	1.5 ± 2.14 (49)**	1.8 ± 4.41 (45)	2 ± 1.71 (44)	1.75 ± 2.19 (55)*
3.	C_3H_7	1 ± 3.64 (10)	1.2 ± 1.79 (15)*	2.2 ± 1.74 (24)	2.4 ± 1.15 (28)	2.5 ± 4.99 (31)*	2.6 ± 4.19 (34)**
4.	4-Br-C_6H_5	0.8 ± 2.14 (28)	0.6 ± 1.64 (58)**	0.9 ± 3.37 (69)	1.2 ± 0.97 (64)*	1.15 ± 2.31 (68)*	1.3 ± 1.72 (67)*
5.	2-Cl-C_6H_4	0.4 ± 0.87 (64)	0.8 ± 1.48 (43)*	1.25 ± 3.05 (57)	1.35 ± 1.54 (59)**	1.5 ± 4.11 (58)**	1.6 ± 3.13 (59)*
6.	2-Cl-4-$NO_2C_6H_3$	2.0 ± 0.94 (−)	1.35 ± 1.71 (4)	1.2 ± 2.84 (59)*	1.1 ± 2.64 (67)	1.2 ± 5.14 (67)**	1.2 ± 4.28 (69)
7.		0.7 ± 3.16 (36)*	1.15 ± 3.26 (18)*	1.3 ± 1.44 (55)	1.35 ± 0.85 (59)*	1.4 ± 2.07 (61)	1.4 ± 1.56 (64)**

[a] Results are expressed as their mean values ($n = 6$).
[b] $P < .05$.
[c] $P < .01$; significant from the control.

Ashwani et al. prepared a series of 5-substituted imidazolones by the condensation of different 5-substituted oxazolones and substituted aromatic amines in anhydrous pyridine under solvent-free conditions in a microwave reactor (Scheme 25.20). The in vivo antiinflammatory activity of the synthesized compounds was determined using the carrageenin-induced paw edema method in rats. The antiinflammatory activity of the test compounds was compared with a standard drug indomethacin. Compounds containing chlorophenyl and *p*-methoxybenzene group demonstrated remarkable reduction in inflammation, after 4 h of carrageenan administration (Table 25.21) [73].

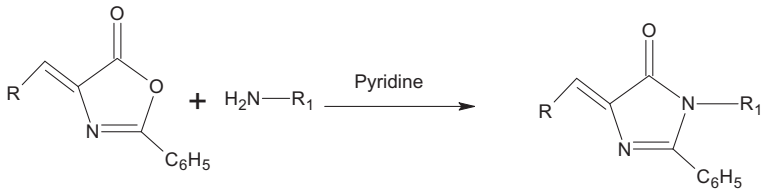

Scheme 25.20 Synthesis of 5-substituted imidazolones.

Table 25.21 Antiinflammatory potential of compounds on carrageenan-induced rat paw edema.

Tested substances	R	R1	Change in paw edema (mL) ± SEM[a,b]	% Protection
Control	–	–	0.94 ± 0.021	0.0
Indomethacin	–	–	0.24 ± 0.021 74.5	74.5
1.	3-Cl,4-*F*-phenyl	3-NO_2-phenyl	0.69 ± 0.028 26.6	26.6
2.	3-NO_2-phenyl	3-NO_2-phenyl	0.72 ± 0.023 23.4	23.4
3.	Napthyl	3-NO_2-phenyl	0.68 ± 0.029 27.6	27.6
4.	Pyridyl	2-Cl-phenyl	0.20 ± 0.019 78.7	78.7
5.	3-Cl,4-F-phenyl	2-*Cl*-Phenyl	0.27 ± 0.026 71.3	71.3
6.	Pyridyl	4-*F*-Phenyl	0.32 ± 0.024 65.9	65.9
7.	Cl,4-*F*-phenyl	4-*F*-Phenyl	0.36 ± 0.026 61.7	61.7
8.	2,5-Dimethylbenzene	4-*F*-Phenyl	0.27 ± 0.024 71.3	71.3
9.	Pyridyl	4-OH-phenyl	0.31 ± 0.027 67.0	67.0
10.	3-Cl,4-F-phenyl	4-OH-phenyl	0.26 ± 0.027 72.3	72.3
11.	Pyridyl	*p*-Methoxybenzene	0.19 ± 0.026 7	79.8
12.	3-Cl,4-F-phenyl	*p*-Methoxybenzene	0.42 ± 0.017 55.3	55.3

[a] SEM denotes the standard error of the mean.
[b] All data are significantly different from control ($P < .001$).

Frank et al. synthesized 5-substituted-2-(2-methyl-4-nitroimidazomethyl)-1, 3, 4-oxadiazoles containing the nitroimidazole moiety by microwave-assisted method (Scheme 25.21) and their antiinflammatory activity was reported [74].

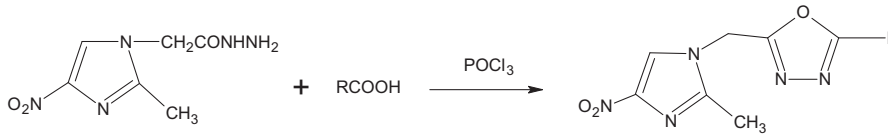

Scheme 25.21 Synthesis of 5-substituted-2-(2-methyl-4-nitroimidazomethyl)-1, 3, 4-oxadiazoles containing the nitroimidazole moiety.

Yashoda et al. synthesized a series of 1-substituted-2, 4, 5-triphenyl imidazoles by the reaction of equimolar mixture of 2, 4, 5 triphenyl imidazole with chloro compound in the presence of anhydrous potassium carbonate (Scheme 25.22). Antiinflammatory activity was screened by carrageenan-induced rat paw edema method. Some of the tested compounds showed highly significant activity [75].

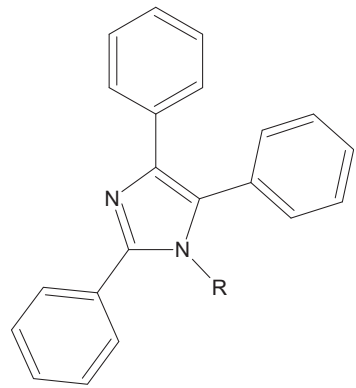

Scheme 25.22 Synthesis of 1-substituted-2, 4, 5-triphenyl imidazoles.

Anjna et al. reported a synthesis of 2-amino dihydropyrimidinone derivatives by three-component condensation of aldehydes, ethyl cyanoacetate, and guanidine nitrate in the presence of—two to three drops of piperidine under microwave irradiation (Scheme 25.23). The synthesized compounds were screened for their antiinflammatory activity using carrageenan-induced rat paw edema method. Most of the compounds were reported to have significant antiinflammatory activity. They observed that by increasing microwave power up to 600 W, there was an increase in the yield and shortened reaction time, but beyond 600 W there was no significant change in reaction time and yield [76].

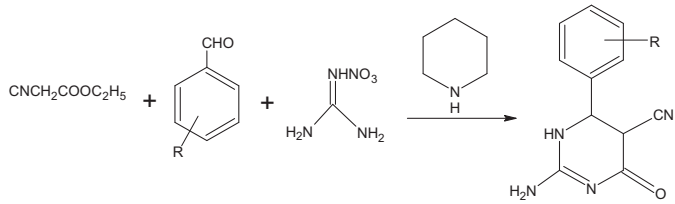

Scheme 25.23 Synthesis of 2-amino dihydropyrimidinone derivatives.

Chikhale et al. have presented the one-pot synthesis of a series of ethyl 6-methyl-2-methoxy-3-(substituted 1-phenylethanone)-4-(substituted phenyl)-1,2,3, 4-tetrahydropyrimidine-5-carboxylates via Biginelli-type condensation of aromatic aldehydes with urea (or thiourea) using as a catalyst (Scheme 25.24). Antiinflammatory activity was carried out by carrageenan-induced rat paw edema method [77].

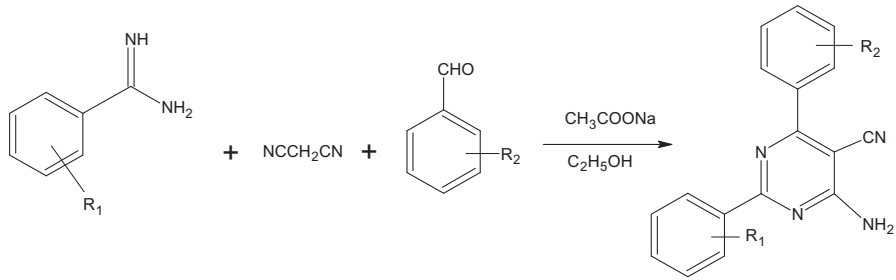

Scheme 25.24 Synthesis of 3-(substituted 1-phenylethanone)-4-(substituted phenyl)-1, 2, 3,4-tetrahydropyrimidine-5-carboxylates.

Naeem et al. have prepared 4-thiazolidinone derivatives by using 1,3-dipyridin-2-ylthiourea, chloroacetic acid, substituted benzaldehyde, and ionic liquids in water and irradiated under microwave irradiation (Scheme 25.25). The compound was synthesized and evaluated for antiinflammatory activity [78].

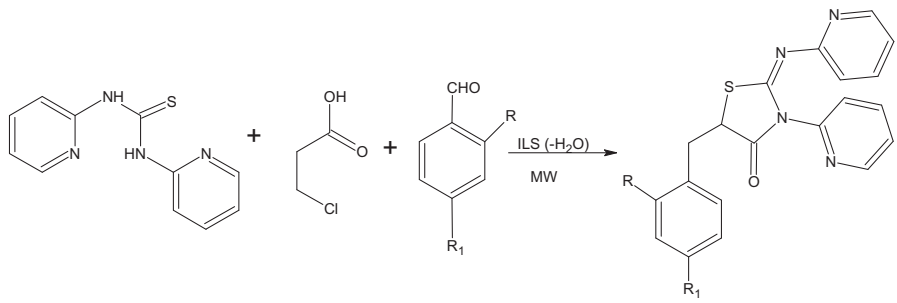

Scheme 25.25 Synthesis of 4-thiazolidinone derivatives.

Tripathy et al. have demonstrated one-pot synthesis of 1,2,4,5-tetra-substituted imidazoles by single-step four-component condensation reaction, wherein the cyclization occurs to form imidazole ring. The target molecule was obtained from benzil, ammonium acetate, aldehydes, and amine were triturated with silica under microwave irradiation (Scheme 25.26). The synthesized compound was screened for antiinflammatory activity by rat paw edema method [79].

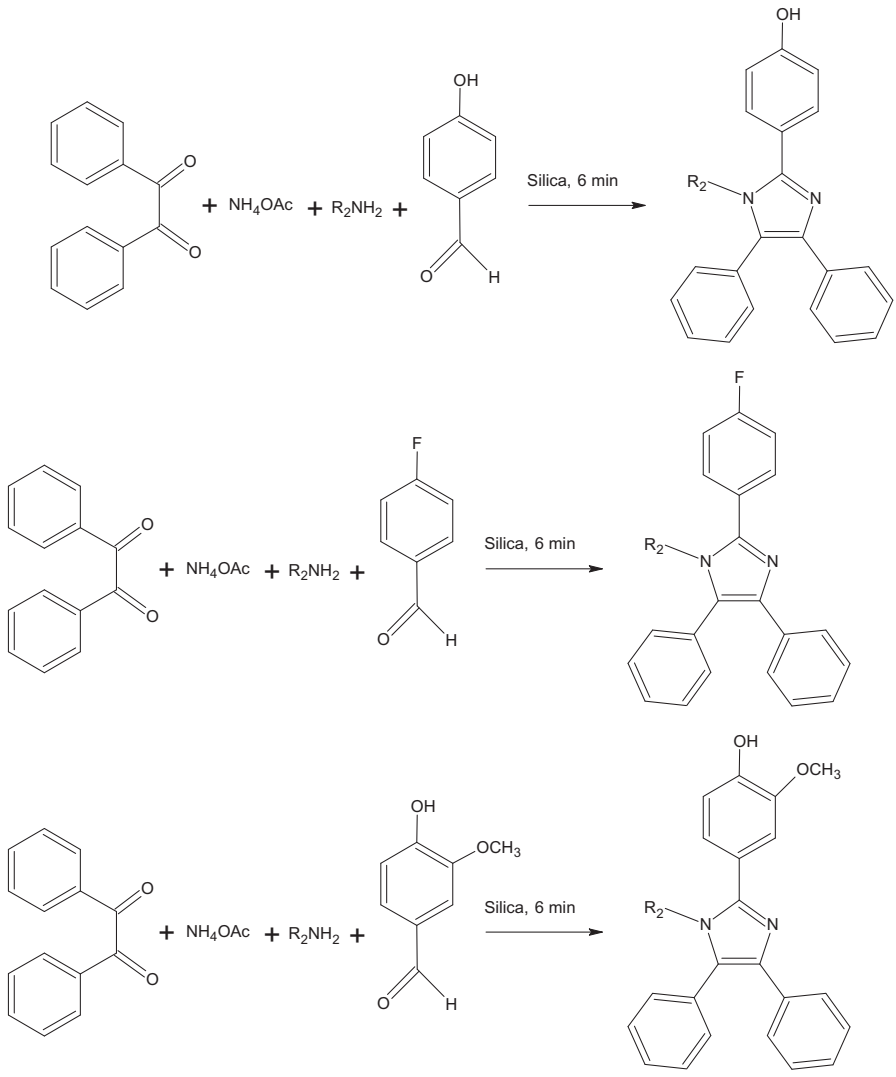

Scheme 25.26 Synthesis of 1,2,4,5-tetra-substituted imidazoles.

Tripathy et al. have synthesized trisubstituted imidazoles using synthetic microwave oven, which showed significant reduction in reaction time, increased yield, and synthesis of library of compounds in a very short time (Scheme 25.27). The synthesized compounds were screened for antiinflammatory activity by rat paw edema method and they showed good activity [80].

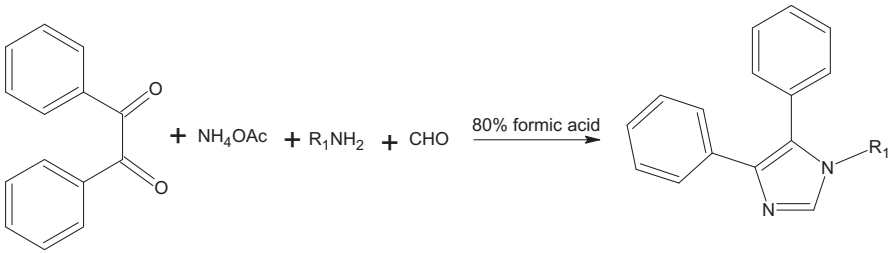

Scheme 25.27 Synthesis of trisubstituted imidazoles.

Condensed thieno-pyrimidines have shown some interesting biological activity as nonsteroidal antiinflammatory agents, and the drug design possibilities in this field led Prasad and Kishore to prepare an efficient microwave-assisted route for pyrimido [1,2-*c*]thieno[3,2-e]pyrimidine derivatives as antiinflammatory agents (Scheme 25.28). All reactions were performed under continuous internal temperature control [81].

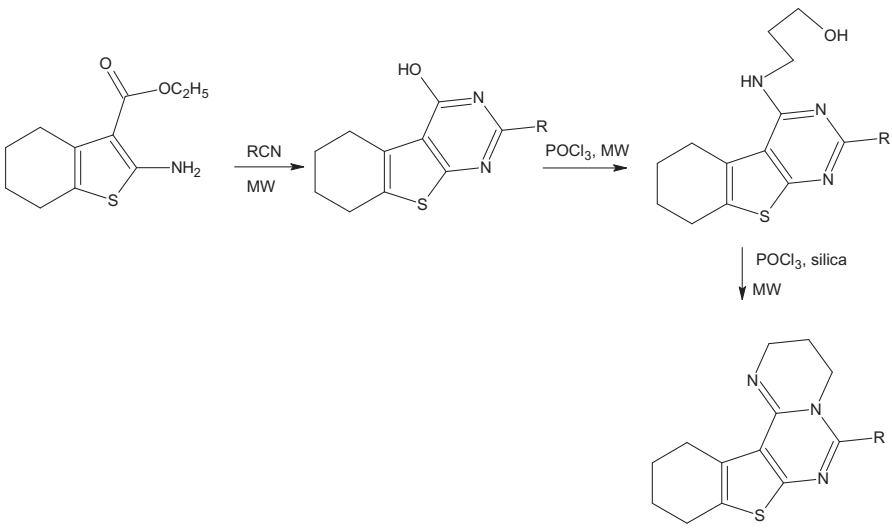

Scheme 25.28 Synthesis of condensed thienopyrimidine derivatives.

A solvent-free microwave-assisted method promoting cyclization of polycyclic benzimidazole derivatives was published by Sondhi et al. with the aim of identification of their antiinflammatory activity. The cyclization reactions were carried out by irradiating a mixture, previously mixed in a mortar, in a MW oven (4–8 min, 850 W). Various diamines were mixed with succinic acid to obtain tricyclic benzimidazole derivatives and with either 4-carboxyphenyl acetic acid or 2,3-pyrazinedicarboxylic acid to obtain tetracyclic derivatives (Scheme 25.29) [82].

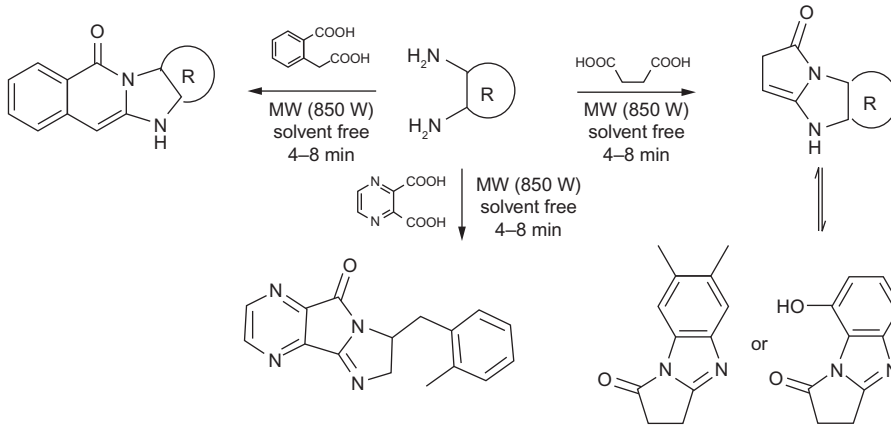

Scheme 25.29 Synthesis of polycyclic benzimidazole derivatives.

Burke et al. have reported the preparation of an imidazoquinoxaline-based inhibitor of IkB kinase 2 (IKK2) as an orally active therapeutic agent for the treatment of inflammatory diseases. Despite promising in vitro efficacy studies in both acute and chronic preclinical inflammation models, the compound has relatively weak potency in vivo. Thiophene and pyrazolopurine chemotypes revealed themselves to be potent and selective inhibitors of IKK2, but their preparation was tedious, and pharmacokinetic profiles and chemotype diversification were quite poor. Kempson et al. aimed to improve the low metabolic stability of the pyrazolopurine and thiophene tricycles and developed a new synthetic route to block their metabolism sites. To test this hypothesis, a series of oxazole and imidazole tricycles were prepared under MW irradiation in the cyclization step (Scheme 25.30) [83].

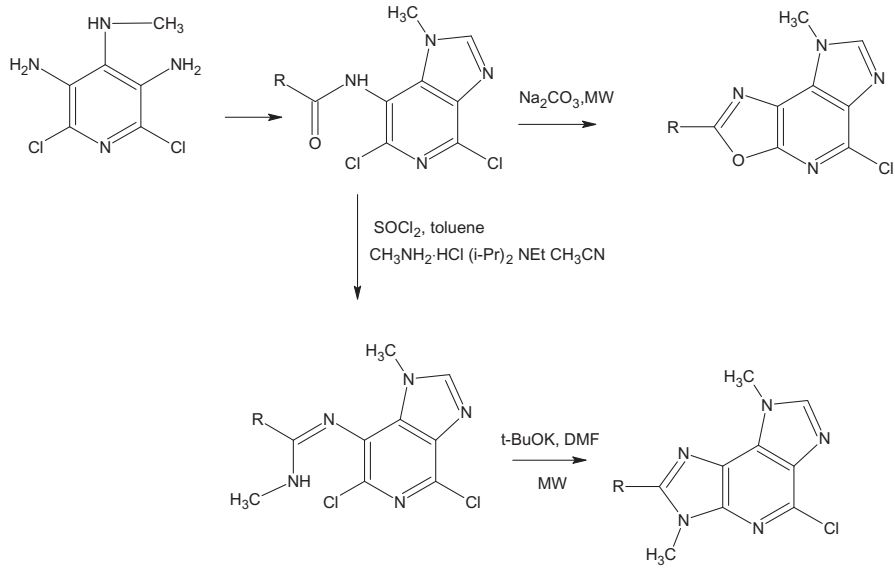

Scheme 25.30 Synthesis of imidazoquinoxaline-based inhibitor of IkB kinase 2.

Musarat et al. have prepared a series of 3,5-disubstituted-4,5-dihydro-1H-pyrazoles under solvent-free microwave irradiation method by the condensation of α, β-unsaturated ketones with hydrazine and its differently substituted derivatives (Scheme 25.31). All the synthetics were evaluated for their antiinflammatory activity under in vivo conditions using male Wistar rats. Their study describes the potential of these pyrazole ring containing scaffolds to assess the TNF-α and IL-1β inhibitory potential. TNF-α and IL-1β are inflammatory cytokines that are pro-inflammatory in nature and play a major role in inflammatory cascades of many pathologically dreadful diseases ranging from neurodegenerative disorders to autoimmune diseases such as rheumatoid arthritis. Their results revealed that the compounds have moderate to considerable activity when compared with the standard ibuprofen. The synthesized compounds showed antiinflammatory activity in the range of 20%–49%, whereas standard drug showed 50% inhibition in paw edema [71].

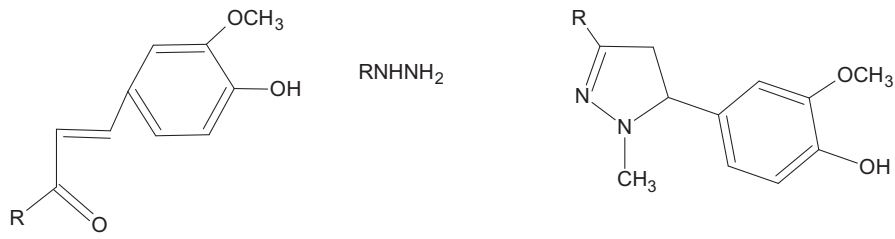

Scheme 25.31 Synthesis of 3,5-disubstituted-4,5-dihydro-1H-pyrazoles.

Anjna et al. reported a synthesis of 2-amino-dihydro-pyrimidinone derivatives by three-component condensation reaction between aldehydes, ethyl cyanoacetate, and guanidine nitrate in the presence of piperidine under microwave irradiation (Scheme 25.32). The synthesized compounds were screened for their antiinflammatory activity using carrageenan-induced rat paw edema method. Most of the compounds were exhibited significant antiinflammatory activity. The synthesized compounds were produced in an excellent yield within short period of time. They observed that by increasing microwave power up to 600 W, there was an increase in the yield and shortened reaction time, but beyond 600 W there was no significant change in reaction time and yield [84].

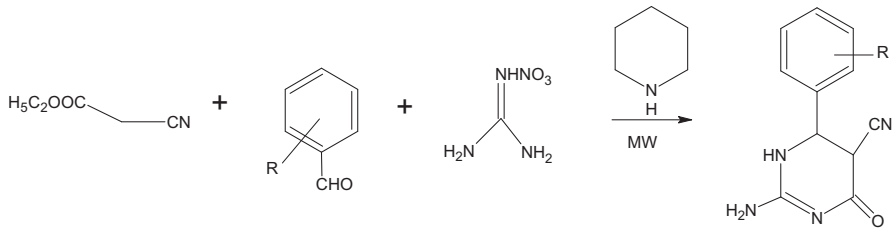

Scheme 25.32 Synthesis of 2-aminodihydropyrimidinone derivatives.

Hassan et al. reported the synthesis of 3-(4,6-disubtituted-2-thioxo-1,2,3,4-tetrahydropyrimidin-5-yl) propanoic acid derivatives. The compounds were synthesized by using Biginelli reaction, a condensation of thiourea, 5-(4-isobutylphenyl)-5-oxopentanoic acid and substituted aldehydes. Aryl acetic acid or propanoic acid derivatives have found to have major contribution in nonsteroidal antiinflammatory agents (Scheme 25.33). Acid side chain was frequently used to have more potent antiinflammatory agent. The synthesized compounds were obtained in good yield. All the newly synthesized compounds demonstrated antiinflammatory activity comparable to that of ibuprofen at the same dose [85].

Muhammad Naeem et al. prepared 4-thiazolidinone derivatives by using 1,3-dipyridin-2-ylthiourea, chloroacetic acid, substituted benzaldehyde, and ionic liquids in water and irradiated under microwave irradiation (Scheme 25.34). The compound was synthesized and evaluated for antiinflammatory activity [86].

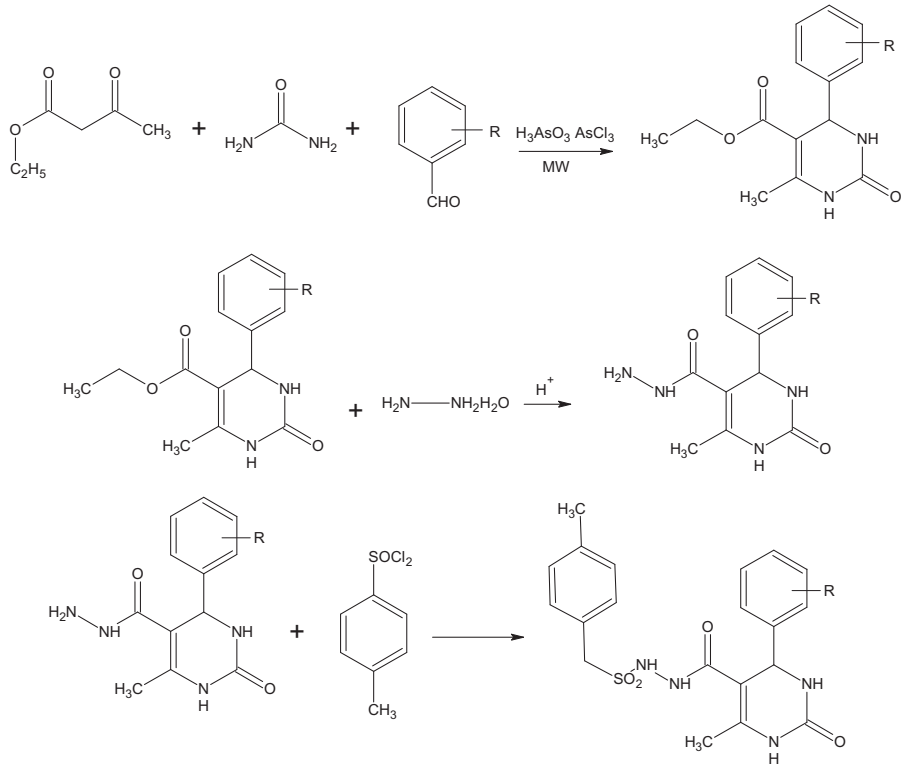

Scheme 25.33 Synthesis of 3-(4,6-disubtituted-2-thioxo-1,2,3,4-tetrahydropyrimidin-5-yl) propanoic acid derivatives.

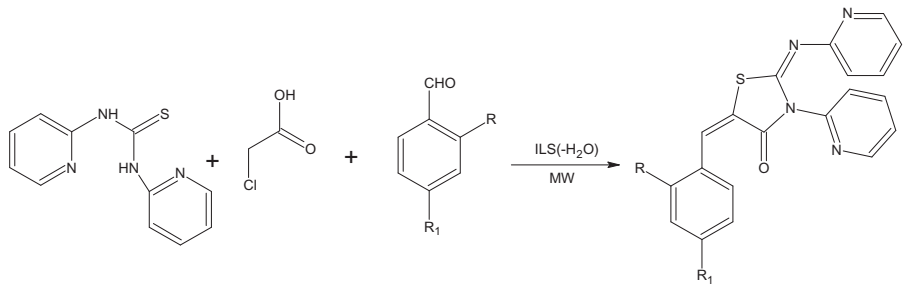

Scheme 25.34 Synthesis of 4-thiazolidinone derivatives.

Acknowledgments

Bimal K. Banik is grateful to Prince Mohammad Bin Fahd University.

References

[1] A.S. Bagad, J.A. Joseph, N. Bhaskaran, A. Agarwal, Comparative evaluation of anti-inflammatory activity of curcuminoids, turmerones, and aqueous extract of *Curcuma longa*, 2013Adv. Pharmacol. Sci. (2013) 1–7 Article ID 805756.

[2] M.A. Palladino, F.R. Bahjat, E.A. Theodorakis, L.L. Moldawer, Anti-TNF-α therapies: the next generation, Nat. Rev. Drug Discov. 2 (2003) 736–746.

[3] C.A. Dinarello, Reduction of inflammation by decreasing production of interleukin-1 or by specific receptor antagonism, Int. J. Tissue React. 14 (1992) 65–75.

[4] R. Medzhitov, Origin and physiological roles of in flammation, Nature 454 (7203) (2008) 428–435.

[5] B. Halliwell, J.M. Gutteridge, Free Radicals in Biology and Medicine, Oxford University Press, USA, 2015.

[6] C. Huerta, J. Castellsague, C. Varas-Lorenzo, L.A. Garcia Rodriguez, Nonsteroidal anti-inflammatory drugs and risk of ARF in the general population, Am. J. Kidney Dis. 45 (3) (2002) 531–539.

[7] T. Kawai, S. Akira, Toll-like receptors and their crosstalk with other innate receptors in infection and immunity, Immunity 34 (2011) 637–650.

[8] R. Van Furth, Mononuclear Phagocytes: Functional Aspects, Springer Science and Business Media, New York, 2013.

[9] H.J. Forman, J.M. Fukuto, M. Torres, Redox signaling: Thiol chemistry defines which reactive oxygen and nitrogen species can act as second messengers, Am. J. Physiol. Cell Physiol. 287 (2004) C246–C256.

[10] S. Phalitakul, M. Okada, Y. Hara, H. Yamawaki, Vaspin prevents TNF-α-induced intracellular adhesion Molecule-1 via inhibiting reactive oxygen species-dependent NF-κB and PKCθ activation in cultured rat vascular smooth muscle cells, Pharmacol. Res. 64 (2011) 493–500.

[11] C.R. Craig, R.E. Stitzel, Modern Pharmacology With Clinical Applications, Lippincott Williams & Wilkins, Philadelphia, PA, 2004.

[12] J. Burchum, L. Rosenthal, Lehne's Pharmacology for Nursing Care, Elsevier Health Sciences, St. Louis, 2014.

[13] K. Izuhara, S.T. Holgate, M. Wills-Karp, Inflammation and Allergy Drug Design, John Wiley & Sons, Chichester, 2011.

[14] A. Inotai, B. Hanko, A. Meszaro, Trends in the non-steroidal anti-inflammatory drug market in six central-eastern european countries based on retail information, Pharmacoepidemiol. Drug Saf. 19 (2010) 183–190.

[15] E.A. Meade, W.L. Smith, D.L. DeWitt, Differential inhibition of prostaglandin endoperoxide synthase (cyclooxygenase) isozymes by aspirin and other non-steroidal anti-inflammatory drugs, J. Biol. Chem. 268 (1993) 6610–6614.

[16] T.D. Penning, J.J. Talley, S.R. Bertenshaw, J.S. Carter, P.W. Collins, S. Docter, M.J. Graneto, L.F. Lee, J.W. Malecha, J.M. Miyashiro, R.S. Rogers, D.J. Rogier, S.S. Yu, G.D. Anderson, E.G. Burton, J.N. Cogburn, S.A. Gregory, C.M. Koboldt, W.E. Perkins, K. Seibert, A.W. Veenhuizen, Y.Y. Zhang, P.C. Isakson, Synthesis and biological evaluation of the 1,5-diarylpyrazole class of cyclooxygenase-2 inhibitors: identification of 4-[5-(4-methylphenyl)-3-(trifluoromethyl)-1H-pyrazol-1-yl]benzen-esulfonamide(SC-58635, celecoxib), J. Med. Chem. 40 (1997) 1347–1365.

[17] P. Prasit, Z. Wang, C. Brideau, C.C. Chan, S. Charleson, W. Cromlish, D. Ethier, J.F. Evans, A.W. Ford-Hutchinson, J.Y. Gauthier, R. Gordon, J. Guay, M. Gresser, S. Kargman,

B. Kennedy, Y. Leblanc, S. Léger, J. Mancini, G.P. O'Neill, M. Ouellet, M.D. Percival, H. Perrier, D. Riendeau, I. Rodger, R. Zamboni, The discovery of rofecoxib, [MK 966, Vioxx, 4-(4′-methylsulfonylphenyl)-3-phenyl-2(5H)-furanone], an orally active cyclooxygenase-2-inhibitor, Bioorg. Med. Chem. Lett. 9 (1999) 1773–1778.

[18] J.L. Wallace, L.J. Ignarro, S. Fiorucci, Potential cardioprotective actions of NO-releasing aspirin, Nat. Rev. Drug Discov. 1 (2002) 375–382.

[19] M.N. Muscara, W. McNight, P. Del Soldato, J.L. Wallace, Effects of a nitric oxide-releasing naproxen derivative on hypertension and gastric damage induced by chronic nitric oxide inhibition in the rat, Pharmacol. Lett. 62 (1998) 235–240.

[20] U.K. Bandarage, L. Chen, X. Fang, D.S. Garvey, A. Glavin, D.R. Janero, L.G. Letts, G.J. Mercer, J.K. Saha, J.D. Schroeder, M.J. Shumway, S.W. Tam, Nitrosothiol esters of diclofenac: synthesis and pharmacological characterization as gastrointestinal-sparing prodrugs, J. Med. Chem. 43 (2000) 4005–4016.

[21] M. Biava, G.C. Porretta, G. Poce, S. Supino, S. Forli, M. Rovini, A. Cappelli, F. Manetti, M. Botta, L. Sautebin, A. Rossi, C. Pergola, C. Ghelardini, E. Vivoli, F. Makovec, P. Anzellotti, P. Patrignani, M. Anzini, Cyclooxygenase-2 inhibitors. 1,5-diarylpyrrol-3-acetic esters with enhanced inhibitory activity toward cyclooxygenase-2 and improved cyclooxygenase-2/cyclooxygenase-1 selectivity, J. Med. Chem. 50 (2007) 5403–5411.

[22] M. Anzini, M. Rovini, A. Cappelli, S. Vomero, F. Manetti, M. Botta, L. Sautebin, A. Rossi, C. Pergola, C. Ghelardini, M. Norcini, A. Giordani, F. Makovec, P. Anzellotti, P. Patrignani, M. Biava, Synthesis, biological evaluation, and enzyme docking simulations of 1,5-diarylpyrrole 3-alkoxyethyl ethers as selective cyclooxygenase-2 inhibitors endowed with anti-inflammatory and antinociceptive activity, J. Med. Chem. 51 (2008) 4476–4481.

[23] M. Biava, G.C. Porretta, G. Poce, C. Battilocchio, F. Manetti, M. Botta, S. Forli, L. Sautebin, A. Rossi, C. Pergola, C. Ghelardini, N. Galeotti, F. Makovec, A. Giordani, P. Anzellotti, P. Patrignani, M. Anzini, Novel ester and acid derivatives of the 1,5-diarylpyrrole scaffold as anti-inflammatory and analgesic agents: Synthesis and in vitro and in vivo biological evaluation, J. Med. Chem. 53 (2010) 723–733.

[24] A.M. Fourie, Modulation of inflammatory disease by inhibitors of leukotriene A4 hydrolase, Curr. Opin. Investig. Drugs 10 (2009) 1173–1182.

[25] C. Charlier, C. Michaux, Dual inhibition of cyclooxygenase-2 (COX-2) and 5-lipoxygenase (5-LOX) as a new strategy to provide safer nonsteroidal anti-inflammatory drugs, Eur. J. Med. Chem. 38 (2003) 645–659.

[26] D. Poeckel, C.D. Funk, The 5-lipoxygenase/leukotriene pathway in preclinical models of cardiovascular disease, Cardiovasc. Res. 86 (2010) 243–253.

[27] J. Balsinde, M.A. Balboa, P.A. Insel, E.A. Dennis, Regulation and inhibition of phospholipase A_2, Annu. Rev. Pharmacol. Toxicol. 39 (1999) 175–189.

[28] M.L. Blank, T. Lee, V. Fitzgerald, F. Snyder, A specific acetylhydrolase for 1-alkyl-2-acetylsn-glycero-3-phosphocholine (a hypotensive and platelet-activating lipid), J. Biol. Chem. 256 (1981) 175–178.

[29] J.A. Berliner, G. Subbanagounder, N. Leitinger, A.D. Watson, Vora, D, evidence for a role of phospholipid oxidation products in atherogenesis, Trends Cardiovasc. Med. 11 (2001) 142–147.

[30] L.W. Tjoelker, C. Eberhardt, J. Unger, H.L. Trong, G.A. Zimmerman, T.M. McIntyre, D.M. Stafforini, S.M. Prescott, P.W. Gray, Plasma platelet-activating factor acetylhydrolase is a secreted phospholipase A2 with a catalytic triad, J. Biol. Chem. 270 (1995) 25481–25487.

[31] C.H. Macphee, J. Nelson, A. Zalewski, Role of lipoprotein-associated phospholipase A2 in atherosclerosis and its potential as a therapeutic target, Curr. Opin. Pharmacol. 6 (2006) 154–161.
[32] M.J. Caslake, C.J. Packard, Lipoprotein-associated phospholipase A2 as a biomarker for coronary disease and stroke, Nat. Rev. Cardiol. 2 (2005) 529–535.
[33] R.L. Wilensky, Y. Shi, E.R. Mohler, D. Hamamdzic, M.E. Burgert, J. Li, A. Postle, R.S. Fenning, J.G. Bollinger, B.E. Hoffman, D.J. Pelchovitz, J. Yang, R.C. Mirabile, C.L. Webb, L. Zhang, P. Zhang, M.H. Gelb, M.C. Walker, A. Zalewski, C.H. Macphee, Inhibition of lipoprotein-associated phospholipase A2 reduces complex coronary atherosclerotic plaque development, Nat. Med. 14 (2008) 1059–1066.
[34] P.J. Jakobsson, R. Morgenstern, J. Mancini, A. Ford-Hutchinson, B. Persson, Common structural features of MAPEG-A widespread superfamily of membrane associated proteins withhighly divergent functions in eicosanoid and glutathione metabolism, Protein Sci. 8 (1999) 689–692.
[35] P.J. Jakobsson, S. Thoren, R. Morgenstern, B. Samuelsson, Identification of human prostaglandin E synthase: a microsomal, glutathione-dependent, inducible enzyme, constituting a potential novel drug target, Proc. Natl. Acad. Sci. U. S. A. 96 (1999) 7220–7225.
[36] B. Samuelsson, R. Morgenstern, P.J. Jakobsson, Membrane prostaglandin E synthase-1: a novel therapeutic target, Pharmacol. Rev. 59 (2007) 207–224.
[37] R.W. Friesen, J.A. Mancini, Microsomal prostaglandin E2 synthase-1 (mPGES-1): a novel anti-inflammatory therapeutic target, J. Med. Chem. 59 (2008) 4059–4067.
[38] C. Jegerschoeld, S.C. Pawelzik, P. Purhonen, P. Bhakat, K.R. Gheorghe, N. Gyobu, K. Mitsuoka, R. Morgenstern, P.J. Jakobsson, H. Hebert, Structural basis for induced formation of the inflammatory mediator prostaglandin E_2, Proc. Natl. Acad. Sci. U. S. A. 105 (2009) 11110–11115.
[39] B. Foxwell, E. Andreakos, F. Brennan, M. Feldmann, C. Smith, M. Conron, Prospects for the development of small molecular weight compounds to replace anti-tumour necrosis factor biological agents, Ann. Rheum. Dis 62 (2003) ii90–ii93.
[40] J.A. Wells, C.L. McClendon, Reaching for high-hanging fruit in drug discovery at protein interfaces, Nature 450 (2007) 1001–1009.
[41] P.C. Taylor, The future of TNF-α antagonism, Future Rheumatol. 2 (2007) 233–236.
[42] A.B. Sebastian Sinnwell, A. Helmut Ritter, Recent advances in microwave-assisted polymer synthesis, Aust. J. Chem. 60 (2007) 729–743.
[43] C.O. Kappe, A. Stadler, Microwaves in Organic and Medicinal Chemistry, first ed., Wiley VCH, Weinheim, 2005.
[44] S.G. Ajmer, K. Karunesh, R. Sonika, B. Shashikant, Microwave-assisted synthesis: a green chemistry approach, Int. Res. J. Pharm. Appl. Sci. 3 (5) (2013) 278–285.
[45] R. Somani, S. Pawar, S. Nikam, Microwave assisted synthesis and antimicrobial activity of Schiff bases, Int. J. Chemtech Res. 2 (2010) 860–864.
[46] H. Rajak, P. Mishra, Microwave-assisted combinatorial chemistry: the potential approach for acceleration of drug discovery, J. Sci. Ind. Res. 63 (8) (2004) 641–654.
[47] J.L. Krstenansky, I. Cotterill, Recent advances in microwave-assisted organic syntheses, Curr. Opin. Drug Discov. Dev. 3 (4) (2000) 454–461.
[48] B.S. Sekhon, Microwave-assisted pharmaceutical synthesis: an overview, Int. J. Pharmtech Res. 2 (1) (2010) 827–833.
[49] M. Larhed, A. Hallberg, Microwave-assisted high-speed chemistry: a new technique in drug discovery, Drug Discov. Today 6 (8) (2001) 406–416.

[50] A. Lew, P.O. Krutzik, M.E. Hart, A.R. Chamberlin, Increasing rates of reaction: microwave-assisted organic synthesis for combinatorial chemistry, J. Comb. Chem. 4 (2) (2002) 95–105.
[51] S.V. Ley, I.R. Baxendale, New tools and concepts for modern organic synthesis, Nat. Rev. Drug Discov. 1 (8) (2002) 573–586.
[52] M.S. Charde, A. Shukla, V. Bukhariya, R.D. Chakole, A review on: a significance of microwave assist technique in green chemistry, Int. J. Phytopharm. 2 (2) (2012) 39–50.
[53] B.L. Hayes, Recent advances in microwave-assisted synthesis, Aldrichim. Acta 37 (2) (2004) 66–76.
[54] M. Pankaj, P. Shashikant, P.N. Anna, Microwave assisted synthesis and antiinflammatory activity of 3, 5-diaryl substituted-2-pyrazolines, Int. J. Pharm. Pharm. Sci. 2 (2) (2010) 21–26.
[55] M. Ipsita, M. Jyotsna, K. Bhavna, S. Ambareen, D. Shilpa, Synthesis of novel anti-inflammatory and antimicrobial agents via Ugi-4CR and its evaluation, J. Appl. Pharm. Sci. 3 (3) (2013) 57–61.
[56] G. Sujit, V. Bhansali, M. Kulkarni, Design, synthesis, docking, QSAR, ADME studies and pharmacological evaluation of biphenyl-2-oxadiazoles as anti-inflammatory agents, Der Pharma Chem. 7 (1) (2015) 156–173.
[57] B. Anjna, R.J. Srinivasa, K. Tanuja, P. Pradeep, J. Shubha, Microwave-assisted synthesis and biological evaluation of dihydropyrimidinone derivatives as anti-inflammatory, antibacterial and antifungal agents, Int. J. Med. Chem. (2013), https://doi.org/10.1155/2013/197612.
[58] D. Raghunandan, R.M. Bhagawan, S. Parameshwar, K.S.M. Shanth, S. Appalaraju, S.Y. Manjunath, Microwave-assisted synthesis and pharmacological activity of pyrazolyl benzofuran deravatives, Am. J. Chem. 2 (3) (2012) 115–120.
[59] V.A. Mahesh, A.K. Mohammed, E.A. Bandar, Microwave assisted synthesis, pharmacological activities and molecular docking studies of ethyl 2-[2-Substituted-4-(Thiophenyl) Thiazolyl] acetates, Iran. J. Pharm. Res. 16 (4) (2017) 1379–1395.
[60] P. Raghavendra, G. Veena, K.G. Arun, K.E. Raj, N. Sangeetha, B. Sirivennela, S. Smarani, K.H. Praneeth, R. Suthakaran, Microwave synthesis and anti-inflammatory evaluation of some new imidazolo quinoline analogs, Rasayan J. Chem. 4 (1) (2011) 91–102.
[61] V.A. Rishikesh, A. Cendilkumar, G. Divakar, S.A. Ganesh, J.O. Rajesh, Microwave assisted synthesis of novel pyrazolone derivatives attached to a pyrimidine moiety and evaluation of their anti-inflammatory, analgesic and antipyretic activities, Saudi Pharm. J. 19 (2011) 233–243.
[62] D.T. Anand, S.P. Siva, S.G. Adel, S. Sandhyamayee, F.G. Riham, M.S. Aladdin, L.S. Brian, M.A. Abdullah, H.C. Dennis, R.K. Alan, Microwave assisted synthesis and QSAR study of novel NSAID acetaminophen conjugates with amino acid linkers, Org. Biomol. Chem. 12 (2014) 7238–7249.
[63] C.R. Biju, K. Ilango, P. Manju, K. Rekha, Design and microwave-assisted synthesis of 1,3,4-oxadiazole derivatives for analgesic and anti-inflammatory activity, J. Young Pharm. 4 (1) (2012) 33–37.
[64] I. Adriana, Z. Valentin, C. Mogosan, P. Nicolae, C. Castelia, S. Luminiţa, Microwave assisted synthesis of some p-toluensulfonylhydrazinothiazoles with analgesic and anti-inflammatory activity, Farmacia 58 (3) (2010) 290–302.
[65] C. Subramanyam, B. Sujatha, K.D. Ravi, R.C. Naga, Microwave assisted synthesis and anti-inflammatory activity evaluation of pyrazole derivatives, Int. J. Res. Eng. Appl. Manag. (2018) 307–312 IMC18610.

[66] M.A. Mohammad, M. Akranth, A. Mymoona, H. Asif, S.Y. Mohammad, S. Mohammad, T. Om Prakash, S. Rikta, K. Suruchi, S. Syed, Microwave assisted one pot synthesis of some pyrazole derivatives as a safer anti-inflammatory and analgesic agents, Acta Pol. Pharm. Drug Res. 70 (3) (2013) 435–441.
[67] R. Parameshwar, B.V. Harinadha, P. Manichandrikab, C.N. Ramana, J.N.S. Chandra, Microwave assisted synthesis, biological evaluation and docking studies of novel pyrazoline derivatives as potent antiinflammatory and antibacterial agents, Int. J. Chem. Sci. 14 (2) (2016) 769–782.
[68] D. Vyankatesh, T. Swapnali, A. Rahul, M. Shrinivas, Chandrakant, M, microwave assisted synthesis of 2-amino-4,5-diphenyl-1-Substituted-1-H-pyrrole-3-carbonitrile for anti-inflammatory and antifungal activity, Pharm. Lett. 9 (12) (2017) 51–58.
[69] R.R. Venakata, R.R. Nadendla, R.R. Raja, R. Suthakaran, Microwave assisted synthesis, characterization and pharmacological evaluation of imidazolo quinazoline-4-one derivatives, Int. J. Pharm. Sci. Rev. Res. 29 (2) (2014) 1–4.
[70] R.C. Rakesh, M.H. Kallappa, Microwave-assisted synthesis, computational studies and antibacterial/anti-inflammatory activities of compounds based on coumarin-pyrazole hybrid, R. Soc. Open Sci. (2018) 1–15.
[71] A. Musarat, N.K. Satti, N.M. Al Musayeib, S. Bani, A. Touseef, TNF-α and IL-1β inhibitors, 3, 5-disubstituted-4, 5-dihydro-1H-pyrazoles, Biomed. Res. 28 (10) (2017) 4316–4323.
[72] K.V. Sujith, K. Balakrishna, A. Adithya, K. Vijayanarayana, Microwave-mediated synthesis of triazolothiadiazoles as anti-inflammatory, analgesic, and anti-oxidant agents, Med. Chem. Res. 21 (2012) 543–551.
[73] K.D. Ashwani, C. Bhawna, D. Rameshwar, K.M. Sanjeev, Synthesis, antimicrobial and anti-inflammatory activities of some novel 5-substituted imidazolone analogs, Chin. Chem. Lett. 27 (2016) 707–710.
[74] P.V. Frank, K.S. Girish, B. Kalluraya, Solvent-free microwave-assisted synthesis of oxadiazoles containing imidazole moiety, J. Chem. Sci. 119 (1) (2007) 41–46.
[75] A. Yasodha, A. Sivakumar, G. Arunachalam, A. Puratchikody, Synthesis and Biological evaluation of some 2, 4, 5 triphenyl imidazoles derivatives, J. Pharm. Sci. Res. 1 (4) (2009) 127–130.
[76] A. Bhatewara, S.J. Rao, T. Kadre, P. Paliwal, S. Jain, Microwave assisted synthesis and biological evaluation of dihydropyrimidin one derivatives as anti-inflammatory, antibacterial and antifungal agents, Int. J. Med. Chem. (2013) 1–5.
[77] R.V. Chikhale, R.P. Bhole, P.B. Khedekar, K.P. Bhusari, Synthesis and pharmacological investigation of 3-(substituted 1-phenylethanone)-4-(substituted phenyl)-1, 2, 3, 4-tetrahydropyrimidine-5-carboxylates, Eur. J. Med. Chem. 44 (2009) 3645–3653.
[78] N. Muhammad, M.N. Chadhury, A. Rana, S.R.K. Khan, Anti-inflammatory, anti-bacterial activity and structure-activity relationship of substitution on 4-thiazolidinone derivatives-Part-1, Pak. J. Pharm. Sci. 25 (4) (2012) 731–739.
[79] H. Tripathy, S.T. Krishnanand, L. Adhikary, J. Chandrashekar, Parallel synthesis of tetra substituted imidazoles by microwave irradiation and evaluation of their anti-inflammatory activity, Res. J. Pharm. Biol. Chem. Sci. 1 (4) (2010) 31–44.
[80] H. Tripathy, S.T. Krishnanand, L. Adhikary, J. Chandrashekar, Microwave assisted parallel synthesis of 1,4,5-trisubstituted imidazoles and their pharmacological evaluation, Res. J. Pharm. Biol. Chem. Sci. 1 (4) (2010) 23–30.
[81] M.R. Prasad, D.P. Kishore, Multistep, microwave assisted, solvent free synthesis and antibacterial activity of 6-substituted-2,3,4-trihydropyrimido[1,2-c]9,10,11,12-tetrahydrobenzo [b]thieno[3,2-e]pyrimidines, Chem. Pharm. Bull. 55 (2007) 776–779.

[82] S.M. Sondhi, R. Rani, J. Singh, P. Roy, S.K. Agrawal, A.K. Saxena, Solvent free synthesis, anti-inflammatory and anticancer activity evaluation of tricyclic and tetracyclic benzimidazole derivatives, Bioorg. Med. Chem. Lett. 20 (2010) 2306–2310.

[83] J.R. Burke, M.A. Pattoli, K.R. Gregor, P.J. Brassil, J.F. MacMaster, K.W. McIntyre, X. Yang, V.S. Iotzova, W. Clarke, J. Strnad, Y. Qiu, F.C. Zusi, BMS-345541 is a highly selective inhibitor of I kappa B kinase that binds at an allosteric site of the enzyme and blocks NF-kappa B-dependent transcription in mice, J. Biol. Chem. 278 (3) (2003) 1450–1456.

[84] M. Manal, K. Arul, A.K. Anjana, K. Remya, Synthesis, docking studies and pharmacological evaluation of imidazole analogues of arecoline, Int. J. Curr. Pharm. Res. 6 (1) (2014) 22–26.

[85] H.A. Osman, S.R. Shaikh, M.S. Pandharpatte, G.M. Nazeruddin, Synthesis, docking studies and pharmacological evaluation of imidazole analogues of arecoline, Arch. Sci. 66 (4) (2013) 503–511.

[86] N. Muhammad, M.N. Chadhury, A. Rana, S.R.K. Khan, Anti-inflammatory, anti-bacterial activity and structure-activity relationships of substitutional on 4-thiazolidinone derivatives-part-I, Pak. J. Pharm. Sci. 25 (4) (2012) 731–739.

Dipole moment in medicinal research: Green and sustainable approach

26

Aparna Das[a,*], *Bimal Krishna Banik*[b,*]
[a]Department of Mathematics and Natural Sciences, College of Sciences and Human Studies, Prince Mohammad Bin Fahd University, Al Khobar, Kingdom of Saudi Arabia, [b]Department of Mathematics and Natural Sciences, College of Sciences and Human Studies, Deanship of Research Development, Prince Mohammad Bin Fahd University, Al Khobar, Kingdom of Saudi Arabia
[*]Corresponding author. e-mail address: aparnadasam@gmail.com; bimalbanik10@gmail.com; bbanik@pmu.edu.sa

26.1 Background on dipole moment

Dipole is basically a system comprising two poles opposite in nature. Dipoles are characterized by their dipole moment (μ), a measure of the system's overall polarity, and a vector quantity. Two kinds of dipole moment are known in electromagnetism: electric dipole moment, which is the measure of the electrical polarity of a system of charges, and magnetic dipole moment, which is the measure of the magnetic polarity of a system of charges.

An electric dipole moment is established when a positive ($q+$) and a negative ($q-$) electrical charge with equal magnitude is separated by a distance (d). Dipole moment is equal to the distance between the charges multiplied by the magnitude of the charge.

$$\mu = qd$$

The SI unit for electric dipole moment is coulomb-meter (C m), however, the most convenient unit is Debye (D), 1 Debye is equal to 3.34×10^{-30} C m. The unit is named Debye in honor of physical chemist Peter J. W. Debye, who has first studied molecular dipoles extensively. The direction of electric dipole moment always, independent of the sides, points from the negative charge toward the positive charge. Electric dipole moment can be in different forms. The electric dipole moment associated with the transition between the two states is known as transition dipole moment, the electrical dipole moment in quantum mechanics. Molecular dipole moment is the electric dipole moment of a molecule due to nonuniform distributions of positive and negative charges on various atoms. The measure of the polarity of a chemical bond within a molecule is noted as bond dipole moment. Electron electric dipole moment is an intrinsic property of an electron, that is, the measure of the charge distribution within an electron.

Green Approaches in Medicinal Chemistry for Sustainable Drug Design. https://doi.org/10.1016/B978-0-12-817592-7.00021-6
© 2020 Elsevier Inc. All rights reserved.

Magnetic dipole moment is the measure of the magnetic polarity of a system of charges. It can be in two forms: electron magnetic moment and nuclear magnetic moment.

In this study, we have mainly described about molecular dipole moment, the dipole moment associated with a molecule that arise from the differences in electronegativity of atoms, that is, the measure of the polarity of the molecule. Three types of dipoles are observed in molecules: permanent dipoles, instantaneous dipoles, and induced dipoles. A molecule with a permanent dipole moment is called a polar molecule. Dipole moment values of the some of the common molecules are presented in Table 26.1.

Table 26.1 Dipole moment values of selected molecules.

Molecule	Dipole moment	Molecule	Dipole moment
CO_2	0	HF	1.82 D
CO	0.112 D	HCl	1.08 D
H_2O	1.85 D	C_6H_6	0
NaCl	9 D	CH_3Cl	1.87 D
NH_3	1.47 D	HCN	2.98 D
CH_2N_2	4.27 D	KBr	10.41 D

Potassium bromide (KBr) is an ionic compound and has one of the highest dipole moments. The overall dipole moment of a molecule can be estimated from the vector sum of bond dipole moments. Thus, it depends on the relative orientation of the bonds and based on the dipole moment information the geometry of the molecule is described. Fig. 26.1 shows the molecular geometry of carbon dioxide (CO_2), water (H_2O), and isomers of 1,2-dichloroethenemolecules. CO_2 has zero dipole which implies that two C═O bond dipole moments cancel each other out and therefore the molecule is linear. For H_2O the O—H bond moments do not cancel each other out and therefore the molecule is bent. The isomers of same molecule show different dipole moment, for example, dipole moment of *cis* and *trans* isomers of 1,2-dichloroethene is different. In *cis* isomer, the two polar C—Cl bonds are on the same side of the C═C double bond and the dipole moment is 1.90 D. In *trans* isomer, the two C—Cl bonds are on opposite sides of the C═C and cancel each other out and the dipole moment is zero.

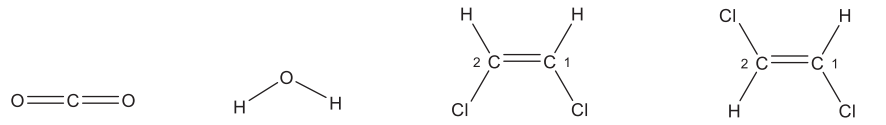

Fig. 26.1 Molecular geometry of (A) CO_2, (B) H_2O, (C) *cis* isomers of 1,2-dichloroethene, and (D) *trans* isomers of 1,2-dichloroethene.

The dipole moment values of numerous compounds and their implications on biological activity are discussed here based on the available data.

26.1.1 2-Pyrrolidone

2-Pyrrolidone is a compound consisting of a five-membered lactam. A lactam is a cyclic amide, which can be found in different forms: α-lactam (three-atom rings), β-lactam (four-atom rings), γ-lactam (five-atom rings), δ-lactam (six-atom rings), and ε-lactam (seven-atom rings). Lactam plays an important role in drug discovery. Many pharmaceutical drugs including povidone, cotinine, ethosuximide, piracetam, and doxapram are 2-pyrrolidone derivatives. Fig. 26.2 shows the molecular structure of 2-pyrrolidone. Several studies have been performed to calculate the dipole moment of the five-membered lactams, that is, 2-pyrrolidone [1].

Fig. 26.2 Molecular structure of 2-pyrrolidone.

Kumler et al. have observed dipole moment in the range 3.7–3.9 D for simple amides in dioxane at 30 degrees [2]. In dioxane, the dipole moment value calculated for 2-pyrrolidone at 30 degrees was 3.79 D. Fischer reported dipole moment value of 3.7 D for 2-pyrrolidone in benzene [3]. Huisgen et al. calculated a lower value of 3.55 D for 2-pyrrolidone in benzene at 25 degrees [4]. Prior to that, Devoto has observed a much lower value of 2.3 D for pyrrolidone in benzene [5]. A reduction in dipole moment was observed due to the formation of a pyrrolidone dimer [3], a value of 2.2 D was reported in benzene dimer at 25 degrees [4]. A rise in dipole moment was expected from the stabilized carbonyl resonance. But, the observed result was opposite due to the destabilization of the ring resonance by the small amount of s-character in the ring bonds, which resulted in a low moment [1].

26.1.2 Cholestanone

Cholestanone is a steroid ketone prepared from cholestanol. It is a biologically active organic compound and can be found in animals, plants, and fungi. Studies have shown that the biological activity of steroids could be increased by the substitution of fluorine for hydrogen on a carbon atom adjacent to the carbonyl group [6–11].

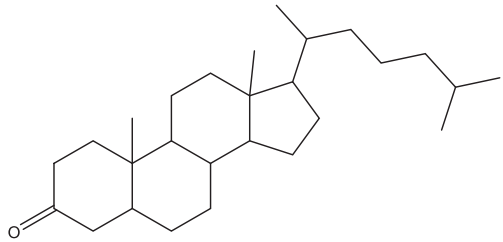

Fig. 26.3 Molecular structure of 3-cholestanone.

The dipole moment of 3-cholestanone was found to have a value of 3.01 D in benzene solution. The molecular structure of 3-cholestanone is shown in Fig. 26.3. Allinger et al. have calculated the dipole moment of 2-fluorocholestanone [12]. 2-Fluorocholestanone can be found in two forms: 2α-fluorocholestanone and 2β-fluorocholestanone. The calculated dipole moment of 2α-fluorocholestanone was 4.28 D and 2β-fluorocholestanone was 2.95 D. The experimentally measured dipole moment of the only known 2-fluorocholestanone was 4.39 D in benzene solution.

26.1.3 Purines, pyrimidines, and azines

Purines and pyrimidines are biologically important aromatic organic compounds. Both purines and pyrimidines are needed by the cell in approximately equal quantities in order to form DNA and RNA. Therefore, an important objective was to study the dipole moment of purines and pyrimidines.

Mishra et al. have calculated the dipole moment of ground and lowest singlet π-π^* and n-π^* excited states of biologically important azines, pyrimidines, and purines [13]. Findings showed that in going from the ground to the n-π^* excited state the dipole moment of pyridine changed by −2.3 D, pyridazine changed by −2.0 D, and pyrimidine changed by −2.1 D.

Experimentally obtained values of dipole moment changes for pyridine, pyridazine, and pyrimidine were −3.2 D, −2.84 D, and −2.7 D, respectively, following the corresponding π-π^* excitation [14]. No significant changes have been observed in the dipole moments of these molecules following the respective π-π^* excitations.

26.1.4 Thiophene and carboxamides

Thiophene is a five-membered heterocyclic compound. The substituted thiophenes and condensed thiophenes possess pharmacological activities like antiviral [15], antibacterial [16], anticancerous [17], antifungal [18], analgesic, and antiinflammatory [19].

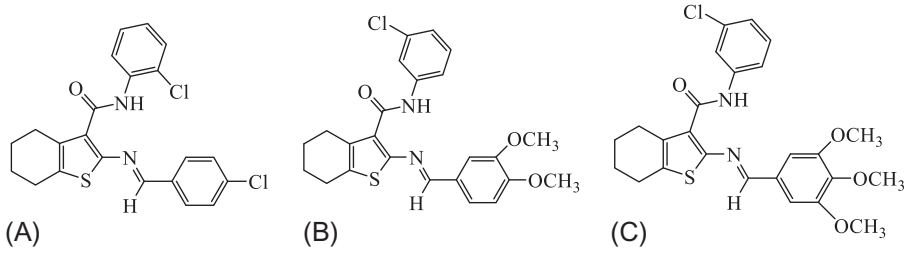

Fig. 26.4 Molecular structure of C_1 (A), C_2 (B), and C_3 (C).

Melavanki et al. have reported the ground and excited state dipole moment of three carboxamides: (*E*)-2-(4-chlorobenzylideneamino)-*N*-(2-chlorophenyl)-4, 5, 6, 7-tetrahydrobenzo[*b*]thiophene-3-carboxamide (C_1), (*E*)-*N*-(3-chlorophenyl)-2-(3, 4-dimethoxybenzylideneamino)-4, 5, 6, 7-tetrahydrobenzo[*b*] thiophene-3-carboxamide

(C_2), and (*E*)-*N*-(3-chlorophenyl)-2-(3, 4, 5-trimethoxybenzylideneamino)-4, 5, 6, 7-tetrahydrobenzo[*b*]thiophene-3-carboxamide (C_3) [20] (Fig. 26.4). Calculated dipole moment values are presented in Table 26.2. It indicates that the excited state dipole moment is higher compared to ground state.

Table 26.2 Calculated dipole moment values of ground state (μ_g), excited state (μ_e) and the change in dipole moment ($\Delta\mu$) for C_1, C_2, and C_3.

Compound	μ_g (D)	μ_e (D)	$\Delta\mu$ (D)
C_1	0.84	3.94	3.10
C_2	3.63	7.53	3.89
C_3	0.27	4.69	4.42

26.2 Dipole moment and anticancer activity

Cancer is ranked as the second most common cause of death after cardiovascular diseases. Different types of cancers are found in human, and it is affecting the humanity very aggressively. Therefore, it is important to develop more active cancer drugs with less side effects. This section describes different types of anticancer drugs and their dipole moment values.

26.2.1 Organometallic bismuth (III) compounds

Bismuth is the least toxic among the heavy metals, relatively cheap, and is easily available. These attractive features along with the green chemistry principles are responsible for the preparation of numerous organic and inorganic derivatives of bismuth. Organic compounds which contain at least one bond between a carbon atom and a metal atom are basically known as organometallics. Organometallic bismuth compounds and their derivatives are safely and broadly used in organic synthesis, catalysis, and medicine.

Studies on the biological activity of organobismuth (III) thiolates have shown the antimicrobial properties of the compounds [21–23], which were effective against various bacterial and fungal infections. It was also observed that derivatives of compounds were able to inhibit the growth of *Escherichia coli* bacteria and bacteria became elongated and filamentous [24] during the treatment, even at the concentrations as low as 1 μg/g. In 1988, Klapotke revealed the antitumor activity of organobismuth (III) thiolates [21] and the activity was similar to that of inorganic platinum compounds (cisplatin). Recently, heterocyclic organobismuth (III) compounds have shown anticancer activities in various human cancer cell lines and were more effective against leukemia cell lines.

One of the important parameter for the biological application of compounds is solubility in polar solvents. Thus the polar bismuth compound was much better than neutral derivatives for pharmaceutical benefits. It is obvious that higher dipole moment has a profound influence on the medicinal activity of these bismuth compounds.

26.2.2 Topovale

Topovale, also known as ARC-111, is a potent topoisomerase I inhibitor. Topoisomerase inhibitors are chemical compounds used to stop the action of topoisomerase I and II, an enzyme that controls the changes in DNA structure.

Studies have shown that ARC-111 (dibenzo[*c*,*h*]-[1,6]naphthyridin-6-one) is one of the effective topoisomerase I (top I) targeting agents and its analogs exhibit antitumor activities [25]. ARC-111 interrupts DNA replication in cancer cells, which results in cell death. A series of ARC-111 compounds were considered, by substituting X in compound **1** (Scheme 26.1), for cytotoxicity test against tumor cell lines in RPMI 8402 [26].

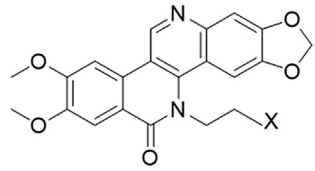

1

Scheme 26.1 Schematics of ARC-111 analogs.

The dipole moment data along with pIC_{50} data of the five selected compounds (**1a–1e**) are illustrated in Table 26.3. Three chemometric tools were used for calculation: multiple linear regression (MLR), partial least squares (PLS), and artificial neural network (ANN). The data from chemometric tools, PLS, and ANN indicated that the dipole moment of ARC-111 analogs have great impacts on antitumor activities.

Table 26.3 Dipole moment in Debye (D) and cytotoxicity data calculated using MLR, PLS, and ANN methods.

Compound	1a	1b	1c	1d	1e
Substituent X	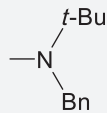	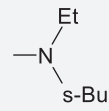	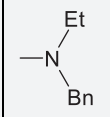	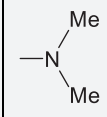	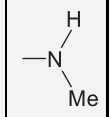
μ	0.9	1.0	1.2	1.4	1.5
pIC_{50} (MLR)	5.9	7.3	8.2	8.9	9.4
pIC_{50} (PLS)	6.0	6.8	7.9	8.9	9.1
pIC_{50} (ANN)	6.6	6.9	8.3	8.8	8.9

26.2.3 MDMA

MDMA (3,4-methyl-enedioxy-methamphetamine), commonly known as ecstasy, is a psychoactive drug. MDMA is an amphetamine derivative, a methylenedioxy group (—O—CH_2—O—) is attached to the aromatic ring, that makes it resemble the structure of the hallucinogenic drugs.

Riahi et al. have carried out studies on the effects of the novel drug MDMA as an anticancer drug on biologic receptor of DNA [27]. Density functional tight-binding (DFTB) and Hartree-Fock (HF) techniques were used for the quantum mechanical description of interactions between MDMA and DNA base pairs. For the computational studies, molecular geometries of MDMA and DNA bases (adenine, guanine, cytosine, and thymine) were optimized. Parameters like polarizability, atomic charges, geometrical values (bond lengths, bond angles, and dihedral angles), dipole moment, and energies of the frontier molecular orbitals (HOMO and lowest unoccupied molecular orbital (LUMO)) were calculated. Table 26.4 illustrates the dipole moment of the MDMA along with dipole moment of adenine (A), guanine (G), cytosine (C), thymine (T), base pairs adenine-thymine (AT), and base pair guanine-cytosine (GC). The dipole moment was varied from 0.89 to 7.97 D.

Table 26.4 Dipole moment calculated using HF and DFTB methods.

	Adenine (A)	**Thymine (T)**	**Guanine (G)**	**Cytosine (C)**	**Adenine-thymine (AT)**	**Guanine-cytosine (GC)**	**MDMA**
μ (DFTB)	2.4	3.8	2.7	6.1	1.2	2.5	0.9
μ (HF)	2.5	3.3	2.5	7.9	1.1	2.2	0.8

26.2.4 Efavirenz (EFZ)

Efavirenz (Sustiva or EFZ) is an anti-HIV drug that slows down the damage to the immune system and prevents the occurrence of AIDS-related illnesses. It belongs to a family of drugs known as nonnucleoside reverse transcriptase inhibitors, which converts single-stranded viral RNA into a double-stranded DNA.

The description of interactions between EFZ and DNA base pairs (*Watson-Crick base pairing*) using the DFTB method was reported [28]. Riahi et al. reported a dipole moment value of 4.68 D for EFZ. Before the calculation, in order to get the most stable equilibrium structure, all the structures were optimized at B3LYP level using the 6-31G* basis set. The dipole moment was derived with respect to their mass center for the charged species. The dipole moment was found to affect the medicinal activities of the compounds.

26.2.5 Adriamycin and daunomycin

Adriamycin (doxorubicin or 14-hydroxydaunomycin) and daunomycin (daunorubicin) are well-known chemotherapy drugs. They are used for the treatment of a wide range of cancers.

Scientific studies showed that adriamycin and daunomycin produce complexes with DNA and block the processes of transcription and replication [29, 30]. Even though Adriamycin showed only a slight difference in geometry with daunomycin

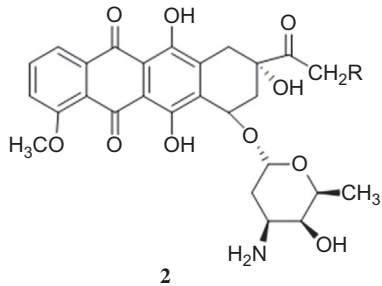

2

Scheme 26.2 Molecular structure of adriamycin (R = OH) and daunomycin (R = H).

(Scheme 26.2), its activities are different. Daunomycin is mainly used to treat leukemia, while adriamycin has a wide range of anticancer activities including acute lymphoblastic, malignant lymphomas of both Hodgkin and non-Hodgkin types, myeloblastic leukaemias, carcinoma of different parts of the body, like bladder, breast, thyroid, lung, and ovary [29, 31].

The dipole moment of optimal structures was calculated using HF and B3LYP computational methods [32]. Adriamycin showed dipole moment value of 5.74 D and daunomycin showed a value of 4.72 D [33]. As predicted the dipole moment of these two molecules are high enough for molecular and cell attraction to occur.

26.2.6 Methotrexate, temozolomide, carmustine, tamoxifen, and hydroxifen

Methotrexate is mainly used as chemotherapy drug either alone or in combination with other drugs. Different types of cancers in human including breast, lymphoma, head, lung, neck, leukemia, bladder, osteosarcoma, and trophoblastic neoplasms can be effectively treated with Methotrexate. Methotrexate disrupts the synthesis of DNA, RNA, thymidylates, and proteins [34–39] by inhibiting the production of folate. It is cytotoxic during the S-phase of the cell cycle. The cytotoxic prodrug temozolomide has shown a broad spectrum of antineoplastic activities [40] by preventing DNA replication and methylating nucleotide bases.

Carmustine (BiCNU) is one of the nitrosoureas, 1,3-bis(2-chloroethyl)-1-nitrosourea, used in the treatment of certain neoplastic diseases. Carmustine acts as an alkylating agent, and can form interstrand cross-links in DNA and RNA, which can prevent replication and transcription. Tamoxifen is mainly used to prevent and treat breast cancer in women and men. Hydroxytamoxifen is a metabolite of tamoxifen. Tamoxifen is characterized as a mixed agonist/antagonist, which acts as an estrogen-stimulating agent in cholesterol metabolism, bone density, and cell proliferation in the endometrium and acts as estrogen-inhibiting agent in the mammary tissue.

Theoretical calculations were done for anticancer drugs like methotrexate, carmustine, temozolomide, tamoxifen, and hydroxifen to study their physicochemical

and geometrical properties [41]. Dipole moments of methotrexate, carmustine, temozolomide, tamoxifen, and hydroxifen were calculated in density functional theory (DFT) and are presented in Table 26.5.

Table 26.5 Dipole moment (in Debye) of methotrexate, carmustine, temozolomide, tamoxifen, and hydroxifen.

	Methotrexate	Carmustine	Temozolomide	Tamoxifen	Hydroxifen
μ	7.1	1.8	5.8	1.4	1.8

26.2.7 Ruthenium azopyridine complex

Ruthenium azopyridine complexes are one of the promising organometallic compounds because of their high activity and less toxicity compared to platinum. The biological activities of ruthenium compounds are strongly controlled by ligand structure. Azopyridine ligands are organic compounds consisting of a pyridine and an aromatic ring (Scheme 26.3 and Table 26.6), linked by an azo bond, and can easily bind with ruthenium ion which provides metal with excellent stability.

Anticancer activity is also observed in ruthenium azopyridine complex [42, 43]. Bamba et al. have reported its anticancer activities against breast cancer (MCF-7), renal cancer (A498), ovarian cancer (IGROV), lung cancer (H226), and colon cancer (WIDR) [44]. The five isomers of $RuCl_2L_2$ complexes (α-, β-, γ-, δ-, and ε-) are shown in Scheme 26.4. Nine ruthenium azopyridine complexes were considered for cytotoxic activity test. The experimental anticancer activity data were correlated with dipole moment calculated by the DFT methods (Table 26.7). To quantify the relationships between dipole moment and cytotoxic activity, MLR was used. A strong correlation was reported between the experimental anticancer data and the predicted data.

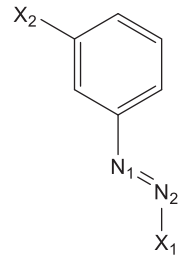

3

Scheme 26.3 Azopyridine ligand with different substituents X_1 and X_2.

Table 26.6 Different substituent for X_1 and X_2.

Compound	X_1 substituent	X_2 substituent	Ligand
3a		H	2-Phenylazopyridine
3b	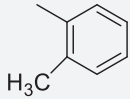	H	*o*-Tolylazopyridine
3c		CH3	4-Methyl-2-phenylazopyridine

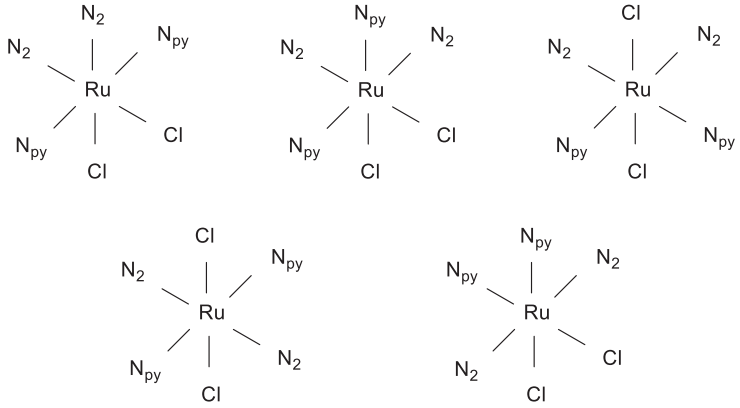

Scheme 26.4 Five isomers (α-, β-, γ-, δ-, and ε-) of $RuCl_2L_2$ complexes and L stands for all azopyridine ligands.

Table 26.7 Dipole moment (μ) and anticancer activity (pIC_{50}) of six selected $RuCl_2L_2$ complexes against different cell lines.

	3b-α	**3b-β**	**3b-γ**	**3c-α**	**3c-β**	**3c-γ**
μ	7.85	8.61	2.54	7.51	9.38	2.84
A498	6.44	4.13	5.92	5.95	4.36	6.30
H226	7.52	4.53	7.08	6.33	4.74	6.77
IGROV	8.05	4.52	7.11	6.65	4.85	6.85
MCF-7	7.67	4.49	7.03	6.37	4.82	7.10
WIDR	7.34	4.28	6.63	6.09	4.67	6.69

26.2.8 Glutamine

Glutamine is an α-amino acid with many functions in the body. It is used in the biosynthesis of proteins and is a critical part of the immune system. Glutamine has a special role in intestinal health since human body naturally produces this amino acid.

To know and detect novel anticancer agents with good selectivity to kill cancer cells and inhibit their proliferation without being toxic [45] is a very difficult task. Nonessential amino acids like glutamine (GLN) can supply its amide nitrogen atoms in the biosynthesis of other amino acids, amino sugars, purine, pyrimidine bases, and coenzymes [46, 47] via amide transferases [48]. Srikanth et al. have discussed the antitumor activities of GLN [49]. Elidrissia et al. have modeled different antitumor glutamines by substituting 5-*N*-substituted-2-(substituted benzenesulfonyl) glutamines with different substitutions (Scheme 26.5) [50]. The theoretical calculations from modeled structures showed that molecular descriptor like dipole moment is a useful tool for the prediction of more active antitumor 5-*N*-substituted-2-(substituted benzenesulfonyl) glutamine compounds. They also addressed the importance of quantitative structure-activity relationship (QSAR) studies for the prediction of new biological active glutamine compounds.

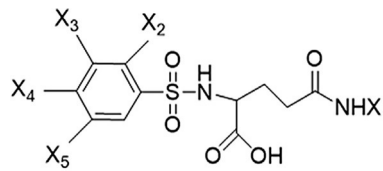

4

Scheme 26.5 Molecular structure of 5-*N*-substituted-2-(substituted benzenesulfonyl) glutamines.

26.2.9 Lantadenes

Lantadenes are bioactive compounds derived from the weed *Lantana camara*. It exhibited potent cytotoxic activity against a number of cancer cell lines and showed antitumor potential.

QSAR-based studies including dipole moment calculation were helpful in determining the anticancer activities of lantadenes against A549 cell lines [51]. A series of 40 compounds were considered for the study (Scheme 26.6). Substituents of four selected compounds and their anticancer activity are presented in Table 26.8.

26.2.10 Xanthone

Xanthone (9*H*-xanthene-9-one) is a naturally occurring oxygenated heterocyclic compound with interesting pharmaceutical properties. The compound has dibenzo-γ-pyrone as the main structure with molecular formula $C_{13}H_8O_2$, as shown in

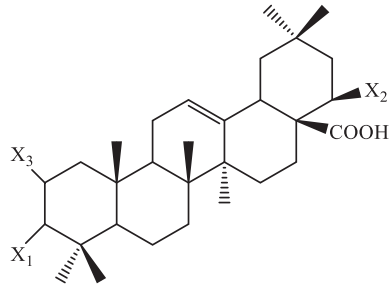

5

Scheme 26.6 Molecular structure of lantadenes.

Table 26.8 Substituent of four selected compounds and their anticancer activity against A549 cell lines.

Compound	X_1	X_2	X_3	pIC_{50}
5a	=O	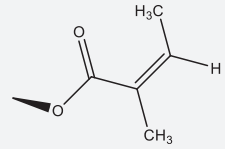	H	2.84
5b	=O	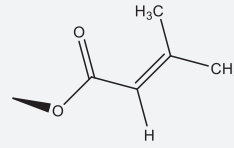	H	1.19
5c	—OH	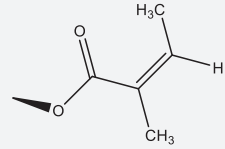	H	0.79
5d	—OH	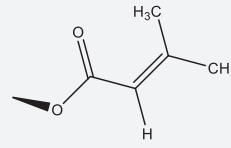	H	0.43

Scheme 26.7. It is prepared by heating phenyl salicylate. The most significant activities of xanthones include antibacterial, anticancer, antiviral, antiprotozoal, antimalarial, and antiinflammatory.

Xanthone compounds showed higher anticancer activity for colorectal cancer (WiDR cell line) [52]. Miladiyah et al. made QSAR analysis to predict their activity based on the biological activity of xanthones in WiDR cell lines and quantum

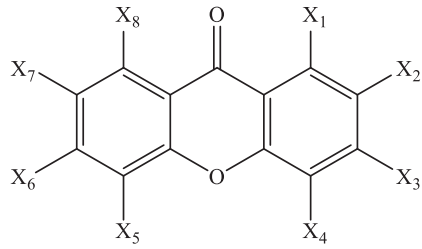

6

Scheme 26.7 Molecular structure of xanthone derivatives.

descriptors of the structures of xanthones. They have selected AM1 semiempirical method for the optimization of the structure because AM1 method is fast, requires no complex mathematical calculation [53], and is able to predict large molecules and multivalent compounds with good accuracy [54].

Miladiyah et al. considered a series of xanthone derivatives as cytotoxic agents against the WiDR cell line and the range for inhibitory concentration of compounds was between 9.23 and 286.4 μg/mL. One compound showed good activity with a selectivity index (SI) of 66.40. The study revealed that the parameters like dipole moment, log *P*, and descriptors of the net atomic charges were hypothetically most significant for the compound's cytotoxic activities.

26.2.11 Fullerene C_{60} and benzopyrene

Fullerene, an allotrope of carbon, consists of carbon atoms connected either by single bonds or by double bonds to form a partially closed or fully closed mesh and the fused rings are made with five to seven carbon atoms. The fullerene molecules were found in different shapes and sizes. Fullerene and its derivatives have enormous potential in various fields of science owing to their unique chemical and physical properties. Fullerene C_{60} (buckyballs or buckminsterfullerene) is the most famous member in the fullerene family. Fullerene C_{60} is nontoxic, biologically antioxidant, and has less solubility. Because of the numerous conjugated double bonds and low-level LUMO [55], fullerene can easily take up an electron, which makes it an apt antioxidant. Studies demonstrated the biological antioxidant potential of fullerenes [56] and its activity against carcinogenic agent [57, 58].

Benzo(α)pyrene (BaP) belongs to the family of polycyclic aromatic hydrocarbons with the formula $C_{20}H_{12}$. They are pentacyclic and are the fusion products of pyrene and a phenylene group. BaP is listed as a Group 1 carcinogen by the International Agency for Research on Cancer (IARC). BaP can be found in automobile exhaust fumes, coal tar, all smoke resulting from the combustion of organic material including tobacco smoke, and many foods, especially grilled and smoked meats [59, 60]. BaP destabilizes the genome by making covalent adducts to DNA [61] and eventually cause cancer [62–64]. In an enzymatic reaction, BaP turns into a toxic compound by forming benzo(α) pyrene-7, 8-dihydro diol-9, 10-epoxide [65]. Studies were done

to analyze the chemical reactivity of the carcinogenic BaP 7,8 diol 9,10 epoxide using semiempirical (PM3) and DFT methods [65].

Tavangar et al. have examined the interaction of fullerenes with benzo(α) pyrene 7, 8 epoxide (BaPe) molecule using the DFT method [58]. They have considered fullerene C_{60} and its derivatives (OH, COOH, $CONH_2$, and CH_2OH) for the reaction with BaP epoxide in two different positions: adjacent to the functional group and away from group. This study analyzed the effect of different chemical groups on the electronic structure of fullerene C_{60} and its anticancer activity. Results showed that the solubility of fullerene C_{60} could be improved by attaching to these chemical groups.

Table 26.9 Dipole moment for optimized structures.

Compound	C_{60}	$C_{60}OH$	$C_{60}CH_2OH$	$C_{60}COOH$	$C_{60}CONH_2$
Dipole moment	0	1.0	1.1	1.3	2.8
Compound	C_{60}-BaPe	$C_{60}OH$-7,8 BaPe	$C_{60}CH_2OH$-7,8 BaPe	$C_{60}COOH$-7,8 BaPe	$C_{60}CONH_2$-7,8 BaPe
Dipole moment	2.0	5.1	2.0	4.7	5.1

The dipole moment of all structures increased after the reaction (Table 26.9). Studies showed that the total charge of BaPe is positive in all the tested structures, which indicates a charge transfer from BaPe to C_{60} and functionalized C_{60} during reaction. BaPe had the lowest positive charge in $C_{60}CH_2OH$-7,8 BaPe complex and largest charge in $C_{60}CONH_2$-7,8 BaPe.

26.2.12 Coumarins

Coumarins are aromatic organic compound found in many plants. Coumarin has acquired attention because of its various therapeutic properties such as antiviral, antimicrobial, antitumor, antiinflammatory, antidiabetic, anticancer, antioxidant, and many others [66]. Coumarins, a molecule that has a benzene and a pyrone ring at the junction, can be derived from benzo-α-pyrones.

Ouattara et al. have considered QSAR method to correlate the structure of the compound and its anticancer activity, mainly for breast cancer [67]. A series of compounds described were obtained by C_4 substitution through thio-methyl linker. They have considered a series of 20 compounds, of which five selected compounds are shown in Scheme 26.8. Table 26.10 illustrates the dipole moment and anticancer activity of the selected compounds. The study revealed that dipole moment is the paramount descriptor for improving anticancer activity.

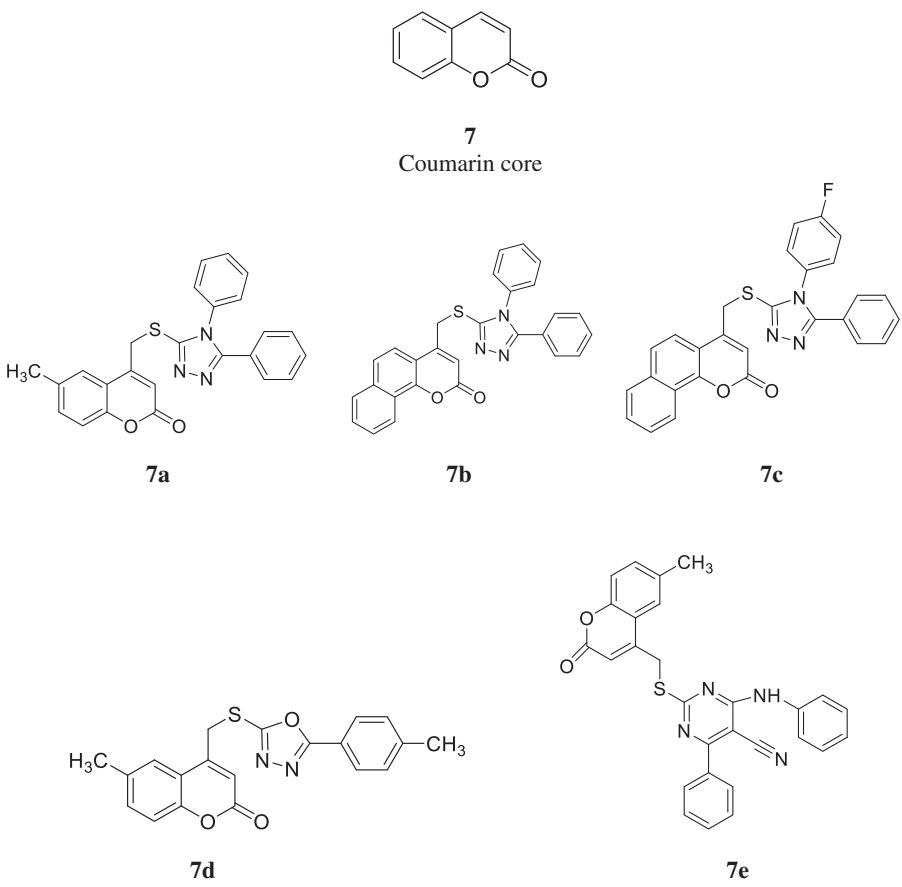

7
Coumarin core

7a **7b** **7c**

7d **7e**

Scheme 26.8 Molecular structure of coumarin core (**7**) and five selected coumarin derivatives (**7a**–**7e**).

Table 26.10 Dipole moment and biological activity of five selected compounds.

	7a	**7b**	**7c**	**7d**	**7e**
Dipole moment	6.6	8.4	7.1	4.5	4.2
IC50	47.7	83.8	58.7	21.1	6.9

26.3 Dipole moment and antifungal activity

There are a wide variety of fungi that cause infections in human. Fungus of the genus *Candida* cause serious illnesses, the frequency of which remains constant despite the development of new therapeutic means, especially in immunocompromised patients. Among the *Candida* kind, 54% of infections are due to *albicans* species. The thrush,

due to fungus of the genus *Candida*, is the most common opportunistic infection, and its frequency has doubled between the age of 80 and 90 years. Indeed, it represents more than 75% of infectious fungus. *Aspergillus* are mostly respiratory pathogens. For example, the genus *Aspergillus niger* causes not only mycoses such as keratitis, otomycoses, onyxis, cutaneous lesions but also otitis and sinusitis.

26.3.1 Thiosemicarbazide

Thiosemicarbazide is a biologically active compound; it is a white odorless crystalline powder.

Thiosemicarbazide is formed by a reaction between heterocarboxylic acid hydrazide and aryl isothiocyanate (Scheme 26.9). Thiosemicarbazide and its derivatives have a broad spectrum of therapeutic properties such as antiviral, antifungal, antibacterial, antimalarial, and antitumor. This compound is also effective for the control of bacterial leaf blight of rice.

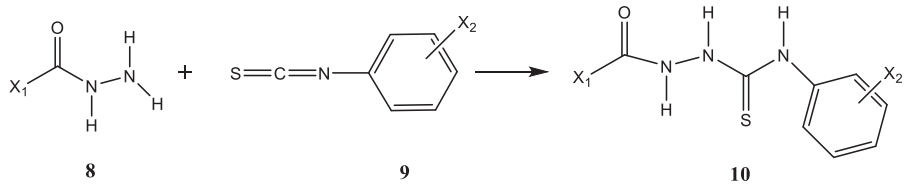

8 9 10

Scheme 26.9 Synthesis of 4-arylthiosemicarbazides.

Siwek et al. have described the antifungal effect of 4-arylthiosemicarbazides against *Candida* species [68]. They have considered six series of 4-arylthiosemicarbazides derivatives for the study. To provide a better understanding of the relationship between antifungal activity and structure of the compound, molecular modeling approach and docking studies were carried out. The 4-arylthiosemicarbazide compounds with isoquinoline ring and methyl or methoxy groups showed higher antifungal activity than other substituted groups. The active compounds are also distinguished by high dipole moment, highest occupied molecular orbital energy (E_{HOMO}), favorable binding energy (E_B), and an electron accepting heteroaromatic ring at N_1 position. No direct quantitative correlation was found between antifungal activity and LUMO localization. The study did not exhibit any relation between geometry and antifungal activity, rather demonstrated a direct relation between electronic property and biological activity.

26.3.2 Pyrazolopyridines

Pyrazolopyridines are a family of drugs, with nitrogen-containing fused heterocycles, that has unique pharmacological properties such as antidepressant, antiinflammatory, antihyperglycemic, antitumor, antibacterial, anxiolytic and are also used for the treatment of Alzheimer diseases, drugs addiction, and infertility [69–77].

Quiroga et al. have shown the synthesis and antifungal in vitro activity of pyrazolo [3,4-*b*] pyridines derivatives (Scheme 26.10) [78]. Microwave-assisted aza-Diels-

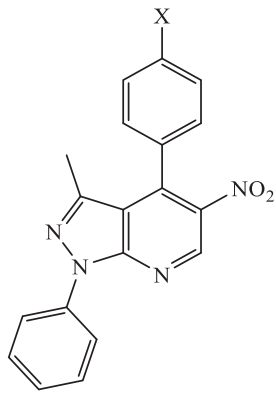

11

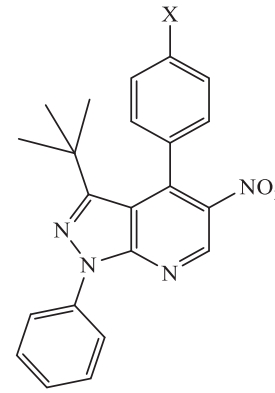

12

X = H, Cl, Br, CH_3, OCH_3

Scheme 26.10 Molecular structure of pyrazolo [3,4-*b*] pyridines derivatives: **11a** (X = H), **11b** (X = Cl), **11c** (X = Br), **11d** (X = CH_3), **11e** (X = OCH_3), **12a** (X = H), **12b** (X = Cl), **12c** (X = Br), **12d** (X = CH_3), and **12e** (X = OCH_3).

Alder reaction between pyrazolylformimidamides and *β*-nitrostyrenes method were used to prepare pyrazolo [3,4-*b*] pyridines derivatives. All these compounds were tested for antifungal properties against *Candida albicans* and *Candida neoformans* at a concentration range of 250–3.9 μg/mL. To find the correlation between structure and antifungal activity, theoretical calculations were done at semiempirical level using PM3 method and the quantitative parameters like dipole moment and Log *P* were calculated. Whereas dipole moment gives the polarity of compound, Log *P* determines its ability to penetrate fungal cell membranes and to reach the interacting sites [78, 79]. The data of the compounds is presented in Table 26.11. The result showed that the most active compounds (**11a**, **12a**, and **12c**) that reach 100% inhibition at 250 μg/mL have lower dipole moments values and highest Log *P*.

Table 26.11 The in vitro antifungal activity, dipole moment and Log *P* values of pyrazolo [3,4-*b*] pyridines derivatives.

	11a	**11b**	**11c**	**11d**	**11e**	**12a**	**12b**	**12c**	**12d**	**12e**
Inhibition percentages (%) of *Candida albicans at* 250 μg/mL	100	54.9	63.6	18.2	34.9	100	45.4	100	40.4	47.9
Inhibition percentages (%) of *Candida neoformans* at 250 μg/mL	100	32.5	67.3	11.8	33.6	100	35.4	100	42.6	44.7
μ	2.2	4.5	4.6	6.1	3.8	2.1	4.3	2.7	3.9	3.9
Log *P*	6.4	3.1	5.2	2.9	3.4	6.8	3.5	6.6	4.3	4.8

26.3.3 Oxadiazoles

Oxadiazoles are five-membered heterocyclic compounds containing a nitrogen atom and at least one other noncarbon atom in the ring. It belongs to azole family with molecular formula $C_2H_2N_2O$. Four isomers of oxadiazole are found. The three isomers 1,2,4-oxadiazole, 1,2,5-oxadiazole, and 1,3,4-oxadiazole have a wide range of pharmaceutical applications; they appear in a variety of drugs including butalamine, raltegravir, oxolamine, fasiplon, and pleconaril. The fourth isomer 1,2,3-oxadiazole is unstable.

Ashtekar et al. have studied the antifungal activity of 1,3,4-oxadiazole by QSAR approach [80] to design more potent antifungal oxadiazole derivatives. They have considered a series of 2-substituted phenyl-5-(1-(substituted piperidin-4-yl)-1*H*-1,2,3-triazol-4-yl)-1,3,4-oxadiazole derivatives (Scheme 26.11) to test against *Fusarium oxysporum*. The study suggested that molar refractivity and dipole moment show positive contribution toward the antifungal activity of oxadiazole.

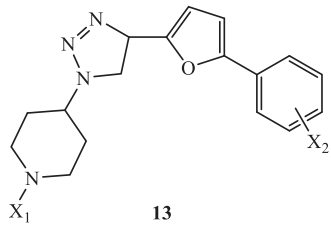

13

X_1 = H, CH_3, CH_2CH_3, SO_2CH_3, COC_6H_5, COC_6H_5, 4Cl, $COCH_3$

X_2 = H, Cl, OH, OCH_3, CH_3

Scheme 26.11 2,5-Disubstituted 1,3,4-oxadiazoles analogs.

26.3.4 Beta-pinene (β-pinene)

β-Pinene is a monoterpene, a class of terpene that consists of two isoprene units, commonly found in plants. β-pinene is one of the two isomers of pinene. It possesses biological activities like antibacterial, antidepressant, cytotoxic, and antimicrobial.

Gao et al. have investigated the synthesis of three series of β-pinene derivatives and their fungicidal activities against three important agricultural pathogens *Rhizoctonia solani*, *Fusarium graminearum*, and *Botrytis cinerea* [81]. The antifungal effect was determined from the inhibition of mycelia radial growth.

Most of the synthesized compounds exhibited moderate to significant fungicidal activity. Among them, acylthiourea derivatives from β-pinene showed better activity. The structure-activity relationship (SAR) analysis indicated that the compounds with more net positive charge possessed better fungicidal activity. The study showed that the most important factors affecting the activity were the geometry and charge distribution, which involved some descriptors such as HOMO, LUMO, and dipole moment.

26.3.5 Indol-4-one

Indole, consisting of a six-membered benzene ring fused to a five-membered pyrrole ring, is an aromatic heterocyclic organic compound that has a bicyclic structure.

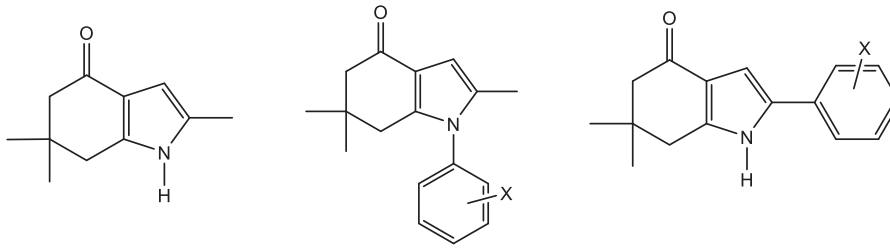

14 **15** **16**

X = H, 2-F,4-F, 2,4-diF, 2-Cl, 4-Cl,2,4-diCl

Scheme 26.12 Molecular structure of indol-4-one derivatives.

González et al. have designed, synthesized, and tested a series of indol-4-one derivatives with 1- and 2-(2,4-substituted phenyl) side chains (Scheme 26.12) [82]. The antifungal in vitro testing was done against *A. fumigatus*, *A. niger*, *Candida albicans*, *Candida glabrata*, *Candida parapsilosis*, *Candida krusei*, *Candida tropicalis*, and *Candida guilliermondii*. The results showed that the derivatives of compounds **15** and **16** possess antifungal activity. They have reported that a change in the position of the halophenyl regioisomers from N_1 to C_2 has increased the antifungal activity.

González-Chávez et al. have reported theoretical reactivity study of indol-4-ones derivatives and its correlation with antifungal activity [83]. The calculated dipole moment of the compounds is presented in Table 26.12. The calculated dipole moment of compound **14** was 5.9 D. The compounds with a 2-F substitution in the aromatic ring showed higher dipole moment.

Table 26.12 Dipole moment of indol-4-one derivatives.

Substitution (X)	Compound 15	Dipole moment	Compound 16	Dipole moment
H	a	6.7	a	5.4
2-F	b	7.2	b	6.6
4-F	c	4.8	c	5.3
2,4-diF	d	5.4	d	4
2-Cl	e	7.2	e	4.4
4-Cl	f	4.7	f	5.3
2,4-diCl	g	5.4	g	4.4

This study suggested that there is a correlation between the relative polarity of compounds and the antifungal activity [82, 83].

26.3.6 Aminobenzenesulfonamide Schiff bases

Sulphonamides (sulfonamides) are derivatives of para amino benzene sulfonamide. They are the first effective chemotherapeutic drugs used for bacterial infection. A wide range of pharmacological activities have been observed in sulfonamides derivatives, such as antibacterial, oral hypoglycemic, anticancer, antileprotic, antiinflammatory, antiepileptic, antihypertensive, antifungal, antiprotozoal, antiretroviral, and are used as diuretic.

Santosh et al. have synthesized a series of Schiff bases derivatives from 4-aminobenzenesulphonamide and tested against the fungi *A. niger* and *Candida albicans* [84]. Six selected compounds are shown in Scheme 26.13.

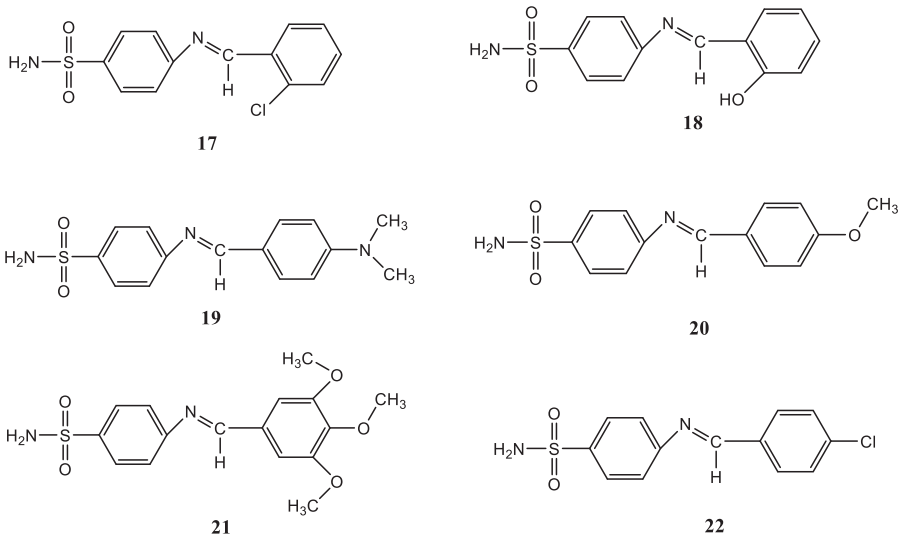

Scheme 26.13 Molecular structure of 4-aminobenzenesulphonamide Schiff bases.

Richard et al. have conducted an SAR study on identical series of compounds to predict more active antifungal agents [85]. The study described the relationship between the antifungal activity and quantum descriptors like dipole moment and electrophile index of the molecules (Table 26.13). It showed that the diameter inhibition of *A. niger* and *Candida albicans* may be improved with a low value of the dipole moment. In *A. niger*, the diameter inhibition may also be improved with a high value of the electrophilicity index, a useful tool to predict the reactivity of an electrophile.

Table 26.13 Dipole moment, electrophile index and experimental antifungal activities of the compounds.

Compound	*Candida albicans* inhibition diameters (mm)	*Aspergillus niger* inhibition diameters (mm)	Dipole moment (Debye)	Electrophile index (eV)
17	12	14	6.2	2.4
18	13	15	5.8	2.1
19	16	13	5.9	1.7
20	11	15	6.4	2
21	20	15	10.1	2.1
22	13	19	5.4	2.4

26.3.7 Chalcones and chromanes

Chalcones are natural compounds that belong to the flavonoid family [86]. These compounds have attracted great interest due to their wide range of pharmacological properties, including antiinflammatory, analgesic, antipyretic, antimutagenic, antileishmanial, antiproliferative, and antifungal effects [87–93].

Chromanes are small natural compounds, and fragments of complex natural products that are used in this manner. They have attracted intense interest because of their numerous biological activities such as antimicrobial, allergenic, plant growth inhibitory, antiherbivore, and antiproliferative effects against cancer cell lines [94, 95]. In addition, a structure known as dihydrochromane (or tetrahydropyran) is an important structural fragment of the molecules in many biologically active and natural compounds [96, 97]. In particular, antibiotic activity has been identified for this fragment [98].

A current trend in the discovery and development of highly active compounds is the hybridization of two or more active fragments that may present improved pharmacological activities [99, 100].

Mellado et al. have synthesized a series of chalcones and dihydrochromane-chalcones hybrids (Scheme 26.14) and the compounds were tested for antifungal activity against *Botrytis cinerea* and *Monilinia fructicola* [101]. QSAR study was used to elucidate the structural-activity relationship of these compounds. The study showed that the biological activity depends more significantly on the dipole moment and electron density on C_1 carbon and CO. The active compound exhibited a higher electron density on the oxygen atom due to the resonance effect of the dihydrochrome system and the dimethylamine group. The increased polarization of the carbonyl group led to an increased antifungal activity of the compound against *Monilinia fructicola*. This study also presented an increase in antifungal activity of chalcone for *Monilinia fructicola* with an electron donor substituent on the ortho position of C_1.

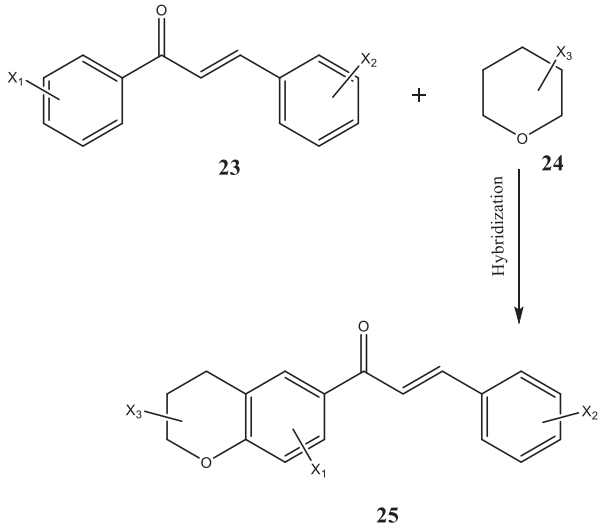

Scheme 26.14 Schematics of hybridization of chalcone and dihydrochromane fragments.

26.4 Dipole moment and antibacterial activity

Pathogenic bacteria cause diseases. Although most bacteria are harmless or often beneficial, some are pathogenic, with the number of species estimated as fewer than a hundred, that are seen to cause infectious diseases in humans. One of the bacterial diseases with the highest disease burden is tuberculosis, caused by *Mycobacterium tuberculosis* bacteria, which kills about 2 million people a year. This section introduces different antibacterial compounds and their structural-activity relationship.

26.4.1 Copper (II) complexes with quinolones and nitrogen-donor heterocycles

Quinolones shows a wide range of antibacterial activities. By targeting essential type II bacterial topoisomerases [102], quinolones inhibit DNA replication [103]. They act more effectively in the presence of certain metal ions like Cu^{2+}, Mg^{2+} [104, 105]. Several groups have reported the synthesis and antibacterial activity of metal compounds with quinolones [106–108].

Deng et al. have presented the QSAR of a series of copper (II) complexes with quinolones and nitrogen-donor heterocycles [109]. Specifically, they have investigated the electronic, hydrophobic, and steric property parameters of complexes with antibacterial activity and aimed to find the minimum inhibitory concentration against *Staphylococcus aureus*, a Gram-positive bacteria. Different descriptors relating to electronic characteristics, like dipole moment, HOMO, LUMO, energy difference, and net charges, were investigated in the correlation analysis. The theoretical

calculations indicated that net HOMO (Σ_{NHOMO}) and dipole moment are the most independent parameters affecting the antibacterial activity. They found a positive correlation, that is, antibacterial activity increases with dipole moment.

26.4.2 Thiourea derivatives

Thiourea derivatives and their transition metal complexes were studied extensively due to their wide range of pharmacological activities [110–113].

Soliman reported QSAR on five *N*-alkyl substituted thiourea ligands (L) and their $[ZnL_2Cl_2]$ complexes to investigate their antibacterial activity against *E. coli* and *Pseudomonas aeruginosa* [114]. This study considered *N*-alkyl-substituted thiourea derivatives (L), namely, diazinane-2-thione (DAT), *N*,*N*′-diethylthiourea (DETU), *N*,*N*′-dimethylthiourea (DMTU), *N*-methylthiourea (MTU), tetramethylthiourea (TMTU) (Scheme 26.15), and their zinc chloride complexes $[ZnL_2Cl_2]$. Among the different compounds, tetramethylthiourea (TMTU) showed better biological activity.

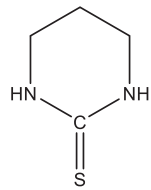

DAT

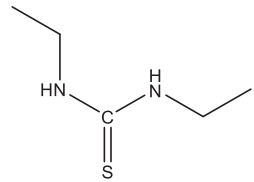

DETU

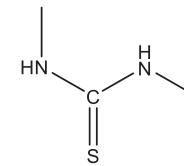

DMTU

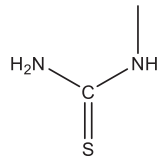

MTU

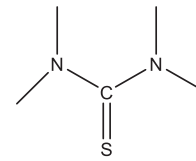

TMTU

Scheme 26.15 Structure of *N*-alkyl-substituted thiourea ligands.

Different quantum chemical descriptors were analyzed during this study. Table 26.14 illustrates the calculated dipole moment of the compounds. The compound tetramethylthiourea (TMTU) showed lowest dipole moment among the thiourea derivatives (L) and highest biological activity.

Table 26.14 Calculated dipole moment of *N*-alkyl substituted thiourea ligands and their $[ZnL_2Cl_2]$ complexes.

	DAT	DETU	DMTU	MTU	TMTU	ZnDAT	ZnDETU	ZnDMTU	ZnMTU	ZnTMTU
μ	6.4	4.9	5	5	4.8	2.4	2.5	3.3	2.63	4.65

The results indicated that the antibacterial activity of the thiourea derivatives (L) increases with an increase in *N*-alkyl substituents. The decrease in dipole moment, energy gap, and charge descriptors of these compounds as well as the increase in their molecular polarizabilities due to *N*-alkyl substituents enhanced the antibacterial activities of the thiourea derivatives (L). Interestingly, the antibacterial activities of $[ZnL_2Cl_2]$ complexes enhanced with a decrease in polarizability and charge descriptors as well as with the increase in energy gap.

26.4.3 Indolylpyrimidines

The pharmaceutical importance of pyrimidine compounds lies on the fact that they can be effectively used as analgesic, antiinflammatory, anticonvulsant, insecticidal, herbicidal, antitubercular, anticancer, and antidiabetic agents. The indole ring is known to exhibit antiinflammatory, antimicrobial, and antifungal activities. The fused ring system of substituted indolylpyrimidines displayed remarkably effective antitumor and antibacterial activities.

Datar made a QSAR analysis to predict the antibacterial activity of indolylpyrimidine derivatives against *Pseudomonas aeruginosa*, a Gram-negative pathogen and *Staphylococcus aureus*, a Gram-positive pathogen [115]. Dipole moment and antibacterial activity of nine selected derivatives (Scheme 26.16) are presented in Table 26.15.

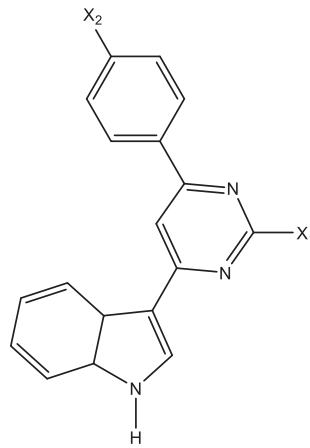

26

Scheme 26.16 Molecular structures of indolylpyrimidines.

The obtained data showed that dipole moment is highly correlated with the activity. The higher the dipole moment the higher the inhibitory activity for *Pseudomonas aeruginosa*.

Table 26.15 Dipole moment and antibacterial activity of nine selected derivatives.

Compounds	X_1	X_2	μ	Zone of inhibition against *Pseudomonas aeruginosa* in mm	Zone of inhibition against *Staphylococcus aureus* in mm
26a	OH	*p*-NH_2	3.5	24	26
26b	OH	*o*,*p*-OH	4.3	14	14
26c	OH	*p*-NO_2	14.3	23	22
26d	SH	H	4.2	12	13
26e	SH	*p*-Cl	6.1	16	17
26f	SH	*p*-CH_3	3.9	10	21
26g	NH_2	*p*-Br	6.3	17	23
26h	NH_2	*p*-F	6.7	23	22
26i	NH_2	*p*-OCH_3	5.9	25	29

26.4.4 Terpenes and phenylporpanes

Terpenes and phenylporpanes are the major constituents of different essential oils. Several groups have reported the antibacterial [116] and antimycobacterial activities of essential oils [117].

Chavira et al. have evaluated the antimycobacterial activity of 25 constituent molecules of essential oils against *Mycobacterium tuberculosis* H37Rv and *Mycobacterium bovis* AN5 [118]. Four selected terpenes compounds are shown in Scheme 26.17 and their dipole moment and antimycobacterial activities are illustrated in Table 26.16.

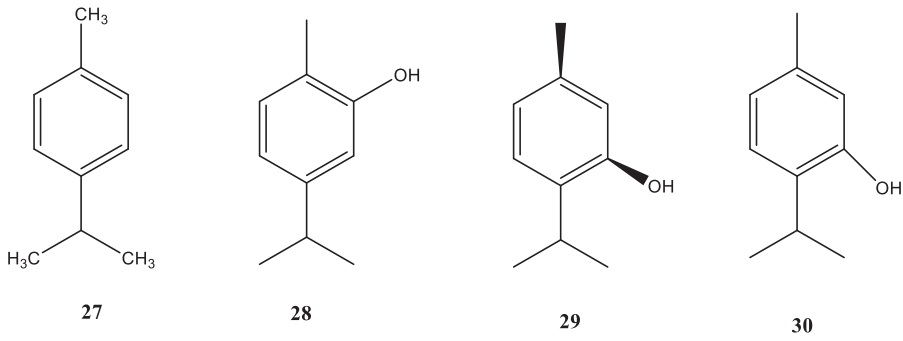

27 28 29 30

Scheme 26.17 Molecular strucure of *p*-cymene, carvacrol, menthol, and thymol.

All the 25 considered compounds showed antimicrobial activity against *Mycobacterium tuberculosis*. Carvacrol and thymol were the highly active terpenes. Cinnamaldehyde and cinnamic acid were the most active phenylpropanes (MIC values of 3.12 and 8.16 μg/mL, respectively, not shown in the table).

Table 26.16 Dipole moment and antimycobacterial activity of terpenes against *Mycobacterium tuberculosis* and *Mycobacterium bovis*.

Compound	Compound	*Mycobacterium tuberculosis* MIC (μg/mL)	*Mycobacterium bovis* MIC (μg/mL)	Dipole moment
27	*p*-Cymene	91.66 ± 14.43	91.66 ± 14.43	0.0890
28	Carvacrol	2.02 ± 0.88	5.20 ± 1.81	1.9475
29	Menthol	41.66 ± 14.43	83.33 ± 14.43	2.4083
30	Thymol	0.78 ± 0.01	2.02 ± 0.88	1.8865

Menthol has a higher dipole moment and cymene has the lowest dipole moment. Thymol and carvacrol are the compounds with lower free energy of solvation. The study demonstrated that the lipophilicity alone is not responsible for the antimycobacterial activity of the compounds, but this activity is linked to the electronic characteristics of the phenolic group.

26.4.5 Quinazolinone

The quinazolinone derivatives are biologically active compounds, which are intensively used as anticonvulsant, anticancer, antiinflammatory, antiulcer, antibacterial, and analgesic agents [119–121].

Irfan et al. have investigated the structural and electronic properties and the antibacterial activity of quinazolinone derivatives (Scheme 26.18) against Gram-positive (*Staphylococcus aureus*) and Gram-negative bacteria (*Klebsiella pneumonia*, *Proteus bacilli*, and *Shigella flexneri*) [122]. The same group have synthesized and characterized the quinazolinone derivatives as active compounds [123, 124].

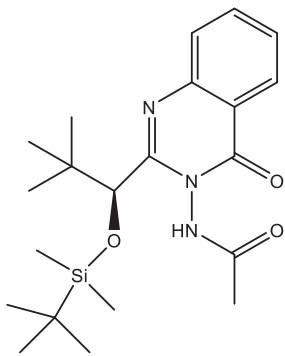

31

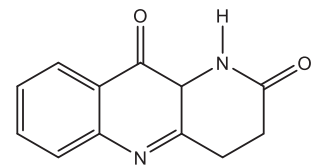

32

Scheme 26.18 Quinazolinone derivatives.

Compounds (**31** and **32**) showed activity against *Staphylococcus aureus*, *Klebsiella pneumonia*, *Proteus bacilli*, and *Shigella flexneri*. Compound **32** exhibited dipole moment (5.1 D) higher than compound **31** (3.6 D), revealing that this compound

has higher ability of interaction with the surrounding medium and more binding ability resulting in superior biological effects.

26.4.6 Azole-derived compounds

Azole-derived compounds are widely used as antifungal agents due to their properties like broad spectrum of action, chemical stability, and oral bioavailability. The activity of azoles against fungi is based on the inhibition of ergosterol [125]. Azoles also show antibacterial activity by inhibiting the enoyl acyl carrier protein reductase [126]. Among the azole derivatives, triazole compounds showed higher antifungal activity [127] and good antimicrobial [128] and antitumor [129] activities. Azoles derivatives in combination with metals are promising to develop new efficient drugs, even against drug-resistant pathogens [130–135].

Hurtado et al. have reported the synthesis and characterization of new chromium(III) and cobalt(II) complexes derived from triazole ligands and their antifungal, antibacterial, and cytotoxic activities [136]. The ligand was prepared using the phase-transfer-catalyzed reaction of 1,3-bis(bromomethyl) toluene and 1*H*-1,2,4-triazole (Scheme 26.19).

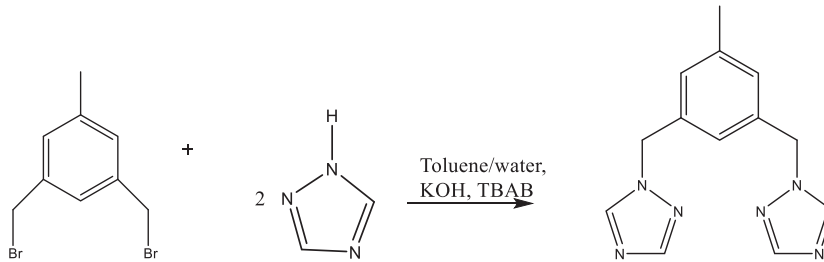

Scheme 26.19 Synthesis of the ligand.

They have considered three triazole chromium(III) complexes and three triazole cobalt(II) complexes for the study. The calculated molecular dipole moment showed values ranging from 2.22 to 12.97 D. For activities against *Candida tropicalis*, the compound with larger permanent dipole moments showed lowest MIC values. The same results were observed in other biological traits, which indicate that the dipole moment is a useful parameter to consider for developing better biologically active complexes.

26.4.7 Polyphenols

The main compound of many plant extracts are phenolic compounds. Besides their established antioxidant activity, many phenolic compounds have also shown antibacterial activity.

Bordes et al. have studied the antibacterial activity of 35 polyphenols against six foodborne pathogens, three Gram-positive bacteria (*Staphylococcus aureus*, *Bacillus*

subtilis, and *Listeria monocytogenes*) and three Gram-negative bacteria (*E. coli*, *Pseudomonas aeruginosa*, and *Salmonella enteritidis*) [137]. The study showed that the effects of phenolic compounds depend on bacterial strains and were highly heterogeneous ranging from bacterial growth stimulation to antibacterial activity. Different quantum descriptors like HOMO, LUMO, dipole moment, polarizability, the maximal and minimal atomic Mulliken charges, and the maximal and minimal atomic Hirshfeld charges were considered for QSAR analysis. The calculated data described that both electronic and electric charge (dipole moment, minimum atomic charge (Mulliken)) properties of polyphenols were important for the explanation of bacterial load difference with *E. coli*.

26.5 Dipole moment and various other medical disorders (antimicrobial, antimalarial, and antileishmanial)

26.5.1 Hydrazide analogs

Hydrazide analogs possess biological activities like antidepressant, anticonvulsant, antiinflammatory, antimycobacterial, antimalarial, anticancer, and antimicrobial. Narasimhan et al. have reported the synthesis, antimicrobial activity, and QSAR studies of the substituted benzoic acid benzylidene/furan-2-yl-methylene hydrazides [138]. A series of 20 compounds were synthesized (Scheme 26.20) and considered for the study. The in vitro antimicrobial activity was evaluated against two Gram-positive bacteria—*Staphylococcus aureus, Bacillus subtilis*; Gram-negative bacterium—*E. coli*, and a fungal strain—*A. niger*.

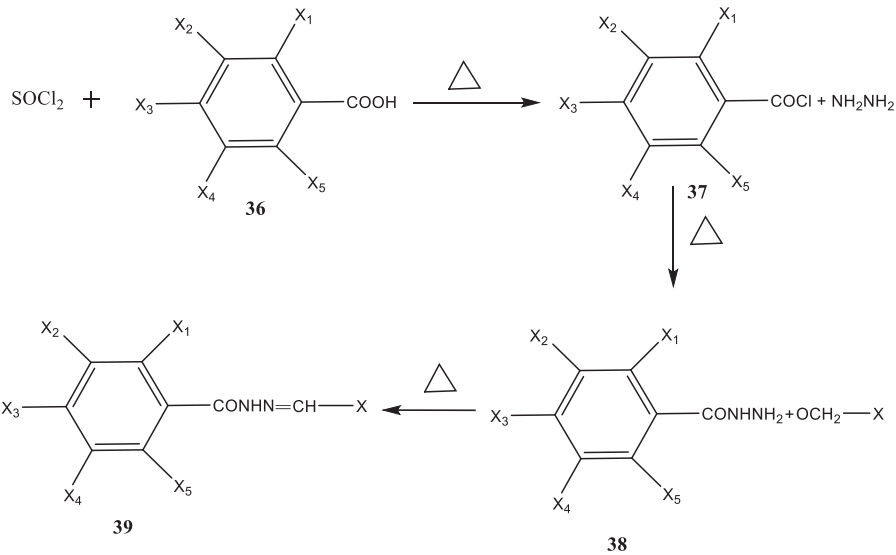

Scheme 26.20 Synthesis of substituted benzoic acid benzylidene/furan-2-yl-methylene hydrazides.

Table 26.17 illustrates the antimicrobial activity and dipole moment of eight selected compound. Compounds **38a** and **39d** were most effective against

Table 26.17 Dipole moment and antimicrobial activity of substituted benzoic acid benzylidene/furan-2-yl-methylene hydrazides.

Compound	X_1, X_2, X_3, X_4, X_5	X	pMICsa	pMICbs	pMICec	pMICan	μ
38a	X_1, X_2, X_4, $X_5 = H$; $X_3 = Cl$	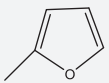	1.6	1.4	1.4	1.4	3.1
38b	X_1, X_3, $X_5 = H$; X_2X_4, $= NO_2$	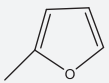	1.2	1.5	1.2	1.5	5.2
38c	X_2, X_3, $X_5 = H$; $X_1 = Cl$; $X_4 = NO_2$	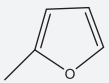	1.4	1.8	1.2	1.5	5.4
39a	X_1, X_2, X_4, $X_5 = H$; $X_3 = Cl$	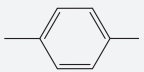	1.5	2.5	1.9	1.3	3.9
39b	X_2, X_3, X_4, $X_5 = H$; $X_1 = Br$	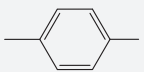	1.5	2.6	2.	1.4	3.5
39c	X_2, X_3, $X_5 = H$; $X_1 = Cl$; $X_4 = NO_2$	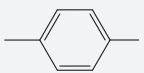	0.8	0.8	0.8	1.5	8.2
39d	X_2, X_3, X_4, $X_5 = H$; $X_1 = Br$	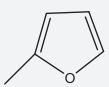	1.6	2.5	1.8	1.3	2.8
39e	X_1, X_2, X_4, $X_5 = H$; $X_3 = NH_2$	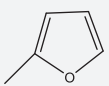	1.5	2.4	1.6	1.3	3.9

Staphylococcus aureus (pMICsa value of 1.60 and 1.67, respectively). Compounds **39a, 39b, 39d**, and **39e** showed better activity against *Bacillus subtilis*. Compounds **39a, 39b**, and **39d** were the most active ones against *E. coli* with pMICec value of 1.97, 2.03 and 1.80, respectively. These active antibacterial compounds exhibited very weak activity against *A. niger*. Thus, the structural requirements for antibacterial and antifungal activities were different for substituted hydrazides. The study also showed that the presence of electron-withdrawing groups (–NO_2, –Cl, –Br) on aromatic ring improved the antimicrobial activity of compounds.

Different quantum descriptors were used for QSAR analysis. Dipole moment was the best descriptor for antibacterial activity of substituted hydrazides against *Staphylococcus aureus*. Analysis showed that this is due to the presence of carbonyl group (C^+-O^-) and the permanent polarization results in a dipole-dipole interaction with antibacterial target. The study also demonstrated the importance of dipole moment in describing antibacterial activity of the compound against *Bacillus subtilis* and *E. coli* and its ineffectiveness in describing the antifungal activity.

26.5.2 Phenothiazine (PTZ)

Phenothiazine is a heterocyclic compound from thiazine family. The derivatives of phenothiazine are highly bioactive and have a wide spread use as antipsychotropic [139], antimalarial [140], antimicrobial [141], antitumor [142, 143], antitubercular [144, 145], and analgesic [146].

Bayoumy et al. have reported the synthesis, biological activity, and molecular modeling of phenothiazine derivatives [147]. All the compounds were tested against Gram-positive bacteria (*Staphylococcus aureus* and *Bacillus subtilis*), Gram-negative bacteria (*E. coli* and *Pseudomonas aeruginosa*), and fungal strain (*Candida albicans* and *F. oxysporum*). The biological activity along with dipole moment of three selected compounds (Scheme 26.21) is presented in Table 26.18.

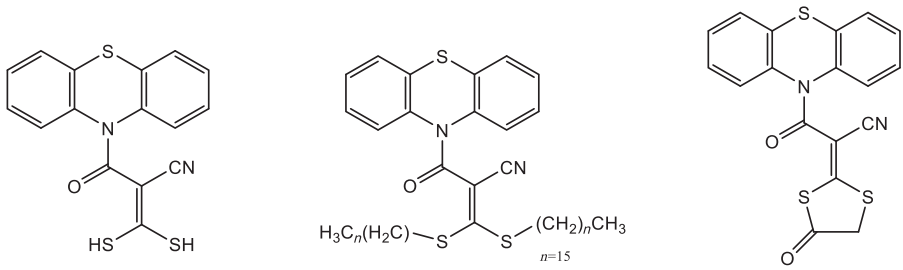

40 **41** **42**

Scheme 26.21 Molecular structure of phenothiazine derivatives.

SAR revealed that compound **40** containing cyanoacetamide moiety was equipotent to ampicillin in inhibiting the growth of *E. coli* and *Pseudomonas aeruginosa* (MIC = 125 μg/mL) and its activity was noted as 33% more than that of ampicillin

Table 26.18 Calculated dipole moment and biological activity of three selected compounds.

	μ	*Candida albicans* MIC in (μg/mL)	*F. axysporum* MIC in (μg/mL)	*Staphylococcus aureus* MIC in (μg/mL)	*Bacillus subtilis* MIC in (μg/mL)	*E. coli* MIC in (μg/mL)	*Pseudomonas aeruginosa* MIC in (μg/mL)
40	2.1	125	62.5	125	125	125	125
41	5.6	NA	NA	57.5	62.5	125	62.5
42	1.9	NA	NA	NA	NA	31.5	62.5
Colitrimazole		5.8	4.2	NA	NA	NA	NA
Ampicillin		NA	NA	187.5	125	125	125

against *Staphylococcus aureus* (MIC = 125 μg/mL). Compound **42** showed 75% more activity than ampicillin against *E. coli* (MIC = 31.5 μg/mL) and 50% more than that against *Pseudomonas aeruginosa* (MIC = 62.5 μg/mL). Compound **41** was 66% (MIC = 62.5 μg/mL) and 69% (MIC = 57.5 μg/mL), respectively, more potent than ampicillin against *Staphylococcus aureus.*

Compound **42** was most potent against Gram-negative bacteria and had lowest value of dipole moment compared to other compounds. The inverse correlation between the activity and the dipole moment of compound **42** revealed that a decrease in dipole moment decreases the polarity and increases the lipophilic nature of the compound and aids in its permeation more efficiently through the lipid layer of the microorganism [148].

26.5.3 Thiazolidine

Thiazolidine is a heterocyclic compound with five-membered saturated ring with a thioether group and an amine group in 1 and 3 positions of the ring. Thiazolidine-2,-4-dione (TZD) is an important derivative of thiazolidine with a sulfur and nitrogen atom in positions 1 and 3, and carbonyl in position 4 of the ring. These derivatives have a wide range of medicinal applications such as antiviral [149], antimicrobial [150, 151], anticonvulsant [152], antiinflammatory [153, 154], and antimalarial activities [155, 156].

Scientific reports showed that these types of compounds have activity against Gram-positive bacteria (*Staphylococcus aureus*, *Staphylococcus epidermis*, *Kocuria rhizophila*, *Bacillus cereus*, and *Bacillus subtilis*), Gram-negative bacteria (*E. coli*, *Pseudomonas aeruginosa*, and *Klebsiella pneumonia*), and fungi (*Candida maltosa*, *A. niger*, *A. fumigatus*, *Cryptococcus neoformans*, and *A. flavus*) [157, 158].

De Pavia et al. have reported the synthesis of 5-arylidene-thiazolidine-2,4-dione derivatives and evaluated their antimicrobial activity against *Staphylococcus aureus* ATCC 29213 [159]. Six selected derivatives are shown in Scheme 26.22.

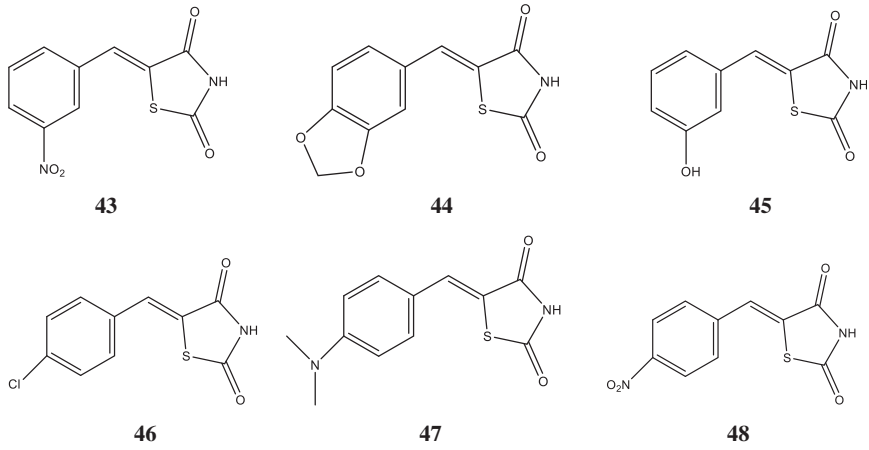

Scheme 26.22 Six selected 5-arylidene-thiazolidine-2,4-dione derivatives.

Table 26.19 Dipole moment and activity of 5-arylidene-thiazolidine-2,4-dione derivatives.

	43	**44**	**45**	**46**	**47**	**48**
Dipole moment	4.9826	3.8561	4.4923	1.6363	7.0838	3.1789
Activity	Inactive	Inactive	Inactive	Active	Inactive	Active

Different descriptors were considered for structural-activity analysis and the only selected descriptor that was not exclusively related to benzene ring was the dipole moment. The data showed that active compound have lower dipole moment values compared to inactive compounds (Table 26.19).

26.5.4 Cinchona alkaloids

The bark of *Cinchona*, *a* flowering plant from Rubiaceae family, is the source of a variety of alkaloids, the most familiar one is quinine. Cinchona alkaloids especially were used for treating *falciparum* malaria [160], which has evolved resistance to synthetic drugs. The bark contains different alkaloids, namely, laevorotatory (−) quinine (6′-methoxy cinchonan-9-ol) (Q), its diastereomer dextrorotatory (+) quinidine (QD), and their 9-epimers epiquinine (EQ) and epiquinidine (EQD), (−) cinchonidine (*des* methoxyquinine) (CD), its diastereomer (+) cinchonine (C) and their 9-epimers epicinchonidine (ECD) and epicinchonine (EC). In addition to the above alkaloids, *Cinchona* bark also produced analogous dihydro compounds of hydroquinine (HQ) and its diastereomer hydroquinidine (HQD) (Scheme 26.23).

Warhurst et al. have calculated the dipole moment of different amino alcohol alkaloids (Table 26.20) [161]. The calculated dipole moment of each active alkaloid was lower than that of its 9-epimer. In Q and QD, the positive electric field of the aliphatic N_1 proton was directed toward the quinolone ring, and the dipole moment was less, while in the 9-epimers EQ and EQD the field was directed toward the solvent and the dipole moment was higher.

26.5.5 Tetraoxanes

Tetraoxanes are biologically active compounds containing two peroxide groups. Different groups have reported the antimalarial activity of tetraoxanes [162–166].

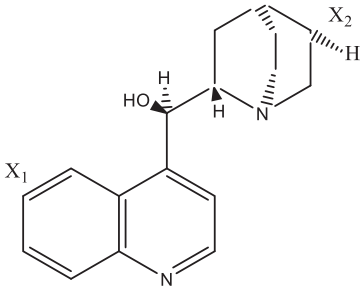

49

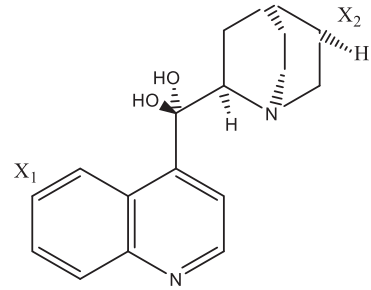

50

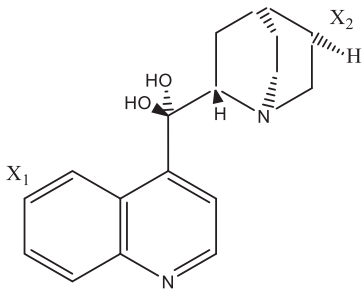

51

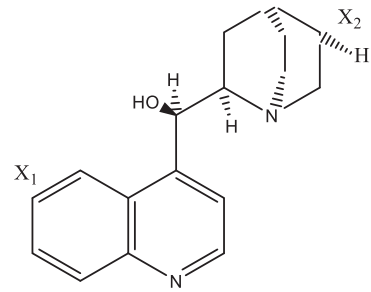

52

Scheme 26.23 Molecular structure cinchona alkaloids.

Table 26.20 Calculated the dipole moment of different cinchona alkaloids.

Compound		X_1	X_2	μ
49a	Q	$-OCH_3$	$-CH_2{:}CH_2$	1.88
50c	C	—H	$-CH_2{:}CH_2$	0.96
49b	HQ	$-OCH_3$	$-CH_2CH_3$	2.08
49c	CD	—H	$-CH_2{:}CH_2$	1.15
50a	QD	$-OCH_3$	$-CH_2{:}CH_2$	1.66
50b	HQD	$-OCH_3$	$-CH_2CH_3$	1.79
51	EQ			2.44
52	EQD			2.21
51	ECD			1.54
52	EC			1.27

Paula et al. have calculated the electron affinity, dipole moment, and log *P* 1,2,4,5-tetraoxanes and analyzed its correlation with activity against *Plasmodium falciparum* [167]. Six selected compounds are shown in Scheme 26.24.

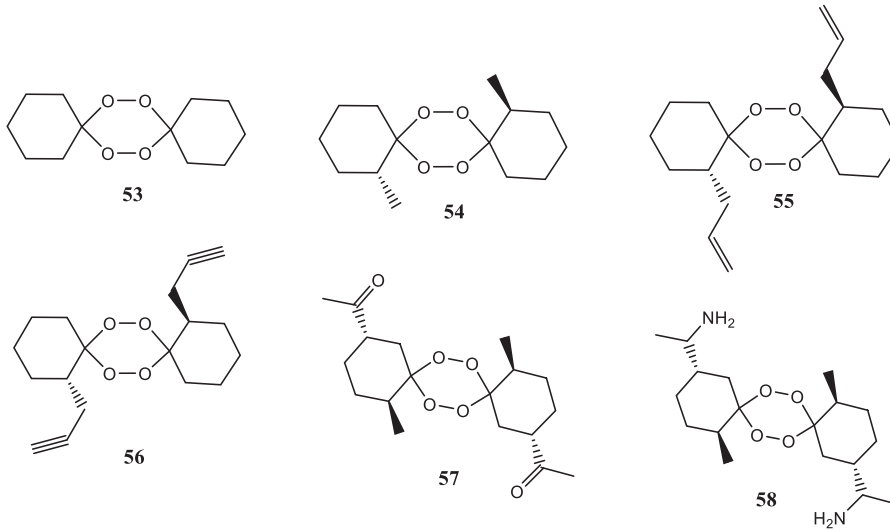

Scheme 26.24 Molecular structure of selected 1,2,4,5-tetraoxanes.

Table 26.21 Calculated molecular and experimental biological activity.

Compounds	Dipole	EA	Log *P*	pIC50
53	0.07	38.96	4.27	7.66
54	0.10	38.04	5.24	7.55
55	0.14	40.69	6.37	7.72
56	0.08	44.61	5.42	7.89
57	4.83	49.06	4.59	8.68
58	0.52	44.53	3.52	7.27

The results showed both dipole moment and EA have an important correlation with antimalarial activity. An increase in the dipole led to a higher activity (Table 26.21). Docking study suggested that a highly polarized molecule have stronger interaction with the heme, which leads to a stronger binding.

26.5.6 Chalcones

Chalcones, also known as chalconoids, are biologically important compounds. The central core of the compound is chalcone, aromatic ketone, and an enone. Researchers have reported the antiinflammatory [168], antibacterial [169], trypanocidal [170], antitumoral [171], antiviral [172, 173], and antileishmanial activities [174–177] of chalcones.

Souza et al. have described the effects of sulfonamide 4-methoxychalcones against *Leishmania amazonensis* [178, 179].

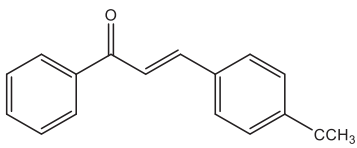

59

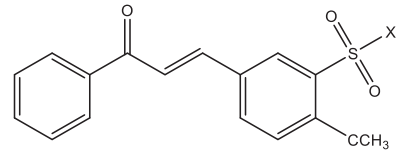

60

	60a	60b	60c
X	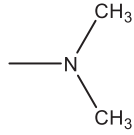	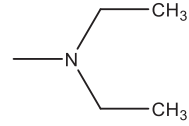	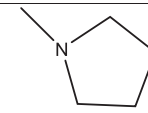
	60d	**60e**	**60f**
X	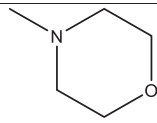	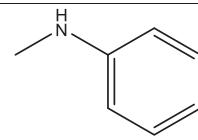	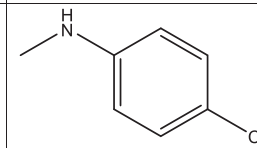
	60g	**60h**	**60i**
X	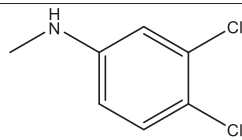	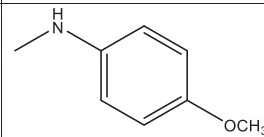	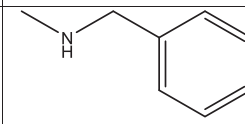

Scheme 26.25 4-Methoxychalcone and sulfonamide 4-methoxychalcone derivatives.

To determine structural and electronic features, a SAR analysis of sulfonamide 4-methoxychalcones was performed. The derivatives of sulfonamide 4-methoxychalcones are shown in Scheme 26.25. Different parameters including HOMO, LUMO, electron distribution, and dipole moment were calculated. Table 26.22 demonstrates dipole moment data and antileishmanial activity. No direct correlation was observed.

26.5.7 Cimetidine analogs

Cimetidine's activity against peptic ulcer has opened the research interest of H_2 receptor antagonists as clinically effective agents. The cimetidine derivatives like ranitidine [180] and tiotidine [181] showed a better H_2 antagonists activity.

Table 26.22 Dipole moment and biological activity against the intracellular infective form (amastigote) of *Leishmania amazonensis*.

	59	**60a**	**60b**	**60c**	**60d**	**60e**	**60f**	**60g**	**60h**	**60i**
μ	3.3	7.3	8.9	7.2	7.3	8.6	8.2	7.8	7.5	7.1
IC50 (μM)	>30	>30	12.5 ± 0.5	16.1 ± 3	>30	>30	2.0 ± 0.3	18.7 ± 5	18.5 ± 5.9	>30

Young et al. have considered a series of cimetidine analogs to investigate H_2 receptor histamine antagonist activity by replacing the cyanoguanidine moiety with other neutral and dipolar groups [182]. The study showed that there was no simple relationship between antagonist activity and dipole moment alone. But the combination of dipole moment and lipophilicity gave a reasonable correlation. The most active compound showed high dipole moment with high lipophilicity.

26.6 Conclusions

In this chapter, we have described the significance of dipole moment in determining the biological activity of diverse compounds. Many of the compounds have shown a direct correlation between dipole moment and biological activity. For example, a higher dipole moment is observed for a better potent compound compared to a relatively nonpotent compound in an identical series of molecules. A higher cellular interaction of the more polar molecule is offered as one of the causes for the superior medicinal activity. In contrast, some examples have demonstrated that a compound with lower dipole moment has better activity than a compound with higher dipole values. In these examples and in many others, a few authors have clearly suggested that dipole moment is not exclusively responsible for controlling biological activities. It is obvious that even if a compound has optimal dipole moment, the activity can be affected by other parameters like solubility, hydrophilicity, hydrophobicity, enzymatic reactions, cell and macromolecular interaction, cell membrane interaction, cell permeability, and molecular docking. Based on this, it is understandable that dipole moment calculation can be extremely valuable prior to the synthesis of a molecule of potential medicinal activity. An increase or decrease in dipole moment values can be achieved by modifying the core structure of a lead molecule. Electron-donating and electron-withdrawing groups along with the configuration of a molecule can increase or decrease the dipole moment of a molecule. In reality, such studies although seem to be useful, unfortunately no publications describe the alteration of chemical structures based on dipole moment values when medicinal chemistry of molecules are involved. Therefore, it is necessary to perform these types of modifications to prepare derivatives of the lead molecules so that scientists can identify molecules with high and low dipole moment (depending on the previous results or start without any prior knowledge) in that particular series and test them for enhanced biological activity. It is feasible to calculate the dipole moment of a projected structure prior to synthesis. Intra- and intercellular interactions of molecules with polar and nonpolar compounds are expected to cause significant differences in the medicinal properties of these molecules. An ionic or covalent molecule because of its intrinsic and extrinsic electrical charge distribution surely will affect numerous parameters of the diseased and nondiseased cells probably in a meaningful way.

Clearly, the research in dipole moment area in chemical biology is increasing very rapidly. Despite efforts we were unable to include all compounds and references. We are extremely sorry for this.

Acknowledgments

BKB is grateful to the USA NIH, USA NCI and USA Private Research Foundation. BKB and AD also thank Prince Mohammad Bin Fahd University for encouragement.

References

[1] C.M. Lee, W.D. Kumler, J. Am. Chem. Soc. 83 (1961) 4593.
[2] W.D. Kumler, C.W. Porter, J. Am. Chem. Soc. 56 (1934) 2549.
[3] E. Fischer, J. Chem. Soc. (1955) 1382.
[4] R. Huisgen, H. Waltz, Chem. Ber. 89 (1953) 2616.
[5] G. Devoto, Cazz. Chim. Ital. 63 (1933) 495.
[6] A.H. Nathan, B.J. Magerlein, J.A. Hogg, J. Org. Chem. 24 (1959) 1517.
[7] J.S. Mills, A. Bowers, C. Djerassi, H.J. Ringold, J. Am. Chem. Soc. 82 (1960) 3399.
[8] H.M. Kissman, A.M. Small, M.J. Weiss, J. Am. Chem. Soc. 82 (1960) 2312.
[9] A.H. Nathan, J.C. Babcock, J.A. Hogg, J. Org. Chem. 24 (1959) 1395.
[10] J. Edwards, H.J. Ringold, J. Am. Chem. Soc. 81 (1959) 5262.
[11] R.B. Gabbard, E.V. Jensen, J. Org. Chem. 23 (1958) 1406.
[12] N.L. Allinger, H.M. Blatter, M.A. DaRooge, L.A. Freiberg, J. Org. Chem. 26 (1961) 2550.
[13] M.K. Shukla, P.C. Mishra, J. Chem. Inf. Comput. Sci. 38 (1998) 678.
[14] P.C. Mishra, R.D. Tewari, Indian J. Pure Appl. Phys. 25 (1987) 387.
[15] D. Binder, C.R. Noe, W. Holzer, B. Rosenworth, Arch. Pharm. Weinheim Ger. 318 (1985) 48.
[16] A.A. El Maghraby, B. Haroun, N.A. Mohamed, Egypt J. Pharm. Sci. 23 (1982) 203–208.
[17] G. Karminshi-Aamola, M. Bajc, Heterocycles 23 (1985) 1497.
[18] J.C. Ramanathan, D.G. Namboothiri, J. Indian Chem. Soc. 55 (1978) 822.
[19] J. Svoboda, J. Paleki, Cesk Farm 38 (1989) 175.
[20] N.R. Patil, R.M. Melavanki, S.B. Kapatkar, N.H. Ayachit, J. Saravanan, J. Fluoresc. 21 (2011) 1213.
[21] T. Klapotke, Biol. Metals 1 (1988) 69.
[22] T. Klapotke, J. Organomet. Chem. 331 (1987) 299.
[23] T. Klapotke, P. Gowik, Z. Naturforsch. 42b (1987) 940.
[24] P. Kopf-Maier, T. Klapotke, Inorg. Chim. Acta 152 (1988) 49.
[25] A.L. Ruchelman, P.J. Houghton, N. Zhou, A. Liu, L.F. Liu, E.J. LaVoie, J. Med. Chem. 48 (2005) 792.
[26] Y. Yu, R. Su, L. Wang, W. Qi, Z. He, Med. Chem. Res. 19 (2010) 1233.
[27] S. Riahi, S. Eynollahi, M.R. Ganjali, Chem. Biol. Drug Des. 76 (2010) 425.
[28] S. Riahi, S. Eynollahi, M.R. Ganjali, P. Norouzi, Int. J. Electrochem. Sci. 5 (2010) 815.
[29] A. diMarco, F. Arcamone, F. Zunino, Antibiotics, Springer, Berlin, 1974, p.101.
[30] M.W. Viswamitra, O. Kennard, P.G. Jones, G.M. Sheldrick, S. Salisbury, L. Falvello, Z. Shakked, Nature 273 (1978) 687.
[31] M. Manfait, A.J.P. Alix, P. Jeannesson, J.-C. Jardillier, T. Theophanides, Nucleic Acids Res. 10 (1982) 3803.
[32] P.S. Kushwaha, P.C. Mishra, J. Mol. Struct. 636 (2003) 149.
[33] S. Bagheri, Z. Bayat, S.J. Mahdizadeh, E. Taghizadeh, J. Chem. Pharm. Res. 3 (2011) 370.
[34] M.R. Sawaya, J. Kraut, Biochemistry 36 (1997) 586.

[35] C.A. Fierke, K.A. Johnson, S.J. Benkovic, Biochemistry 26 (1987) 4085.
[36] P.J. Cayley, S.M. Dunn, R.W. King, Biochemistry 20 (1981) 874.
[37] C.E. Cameron, S.J. Benkovic, Biochemistry 36 (1997) 15792.
[38] D. Beckett, E. Kovaleva, P.J. Schatz, Protein Sci. 8 (1999) 921.
[39] G.P. Miller, D.C. Wahnon, S.J. Benkovic, Biochemistry 30 (2001) 867.
[40] K.M. Hvizdos, K.L. Goa, CNS Drugs 12 (1999) 237.
[41] S.M. Hassani1, S. Bagheri, H. Ghahremani, Ann. Biol. Res. 3 (2012) 2393.
[42] A.C.G. Hotze, A.H. Velders, F. Ugozzoli, M. Biagini-Cingi, A.M. Manotti-Lanfredi, J. G. Haasnoot, J. Reedijk, Inorg. Chem. 39 (2000) 3838.
[43] A.H. Velders, H. Kooijman, A.L. Spek, J.G. Haasnoot, D. De Vos, J. Reedijk, Inorg. Chem. 39 (2000) 2966.
[44] K.N. N'guessan, M. Guy-Richard Koné, K. Bamba, O.W. Patrice, N. Ziao, Comput. Mol. Biosci. 7 (2017) 19.
[45] A. Kamal, G. Balakishan, G. Ramakrishna, T.B. Shaik, K. Sreekanth, M. Balakrishna, Rajender, D. Dastagiri, S.V. Kalivendi, Eur. J. Med. Chem. 45 (2010) 3870.
[46] C. Costa, J.F. Huneau, D. Tome, Biochim. Biophys. Acta 1509 (2000) 95.
[47] M.A. Medina, J. Nutr. 131 (2001) 2539.
[48] J.L. Zalkin, J.L. Smith, Adv. Enzymol. Relat. Areas Mol. Biol. 72 (1998) 87.
[49] K. Srikanth, B. Debnath, T. Jha, Bioorg. Med. Chem. 10 (2002) 1841.
[50] B. Elidrissia, A. Ousaa, M.A. Ajana, T. Lakhlifi, M. Bouachrine, Int. J. Sci. Res. Environ. Sci. Toxicol. 3 (2018) 1.
[51] Monika, R. Dhingra, A. Gupta, A. Kaul, M. Sharma, N. Dhingra, Acta Sci. Pharm. Sci. 2 (11) (2018) 41.
[52] I. Miladiyah, J. Jumina, S. Mubarika Haryana, M. Mustofa, Drug Des. Devel. Ther. 12 (2018) 149.
[53] J.J.P. Stewart, J. Mol. Model. 19 (2013) 1.
[54] S. Gunasekaran, B. Anita, S. Seshadri, Indian J. Pure Appl. Phys. 48 (2010) 183.
[55] A. Hirsch, M. Brettreich, Fullerenes: Chemistry and Reactions, John Wiley & Sons, Wiley-VCH Verlag GmbH & Co. KGaA, Weinheim, 2006.
[56] R. Bakry, R.M. Vallant, M. Najam-Ul-Haq, M. Rainer, Z. Szabo, C.W. Huck, G.K. Bonn, Int. J. Nanomedicine 2 (2007) 639.
[57] S. Prylutska, A. Burlaka, Y.I. Prylutskyy, U. Ritter, P. Scharff, Exp. Oncol. 33 (2011) 162.
[58] Z. Hajiahmadia, Z. Tavangara, H. Behzadic, Polycycl. Aromat. Compd. 39 (2019) 1–10.
[59] T.H. Ueng, H.W. Wang, Y.P. Huang, C.C. Hung, Arch. Environ. Contam. Toxicol. 46 (2004) 4.
[60] International Agency for Research on Cancer, Certain Polycyclic Aromatic Hydrocarbons and Heterocyclic Compounds (IARC Monographs on the Evaluation of the Carcinogenic Risks of Chemicals to Man), vol. 3, International Agency for Research on Cancer, 1972.
[61] B.D. Jeffy, E.J. Chen, J.M. Gudas, D.F. Romagnolo, Neoplasia 2 (2000) 460.
[62] B. Sadikovic, D.I. Rodenhiser, Toxicol. Appl. Pharmacol. 216 (2006) 458.
[63] Q. Shi, L.-E. Wang, M.L. Bondy, A. Brewster, S.E. Singletary, Q. Wei, Carcinogenesis 25 (2004) 1695.
[64] International Agency for Research on Cancer, IARC Monogr. Eval. Carcinog. Risks Hum. 92 (2010) 1–853.
[65] P. Huetz, V. Poux, J. Mol. Struct. THEOCHEM 764 (2006) 167.
[66] Y. Garazd, M. Garazd, R. Lesyk, Saudi Pharm. J. 25 (2017) 214.
[67] L. Ouattara, K. Bamba, M. Guy-Richard Koné, J.S. N'dri, K.N. N'Guessan, O. P. Massapihanhoro, D. Fatogoman, Chem. Sci. Int. J. 26 (2019) 1.

[68] A. Siwek, J. Stefańska, K. Dzitko, A. Ruszczak, J. Mol. Model. 18 (2012) 4159.
[69] S. Huang, R. Lin, Y. Yu, Y. Lu, P.J. Connolly, G. Chiu, S. Li, S.L. Emanuel, S. A. Middleton, Bioorganic Med. Chem. Lett. 17 (2007) 1243.
[70] E.E. Elboray, R. Grigg, C.W.G. Fishwick, C. Kilner, M.A.B. Sarker, M.F. Aly, H. H. Abbas Temirek, Tetrahedron 67 (2011) 5700.
[71] S.-A. Thompson, P.B. Wingrove, L. Connelly, P.J. Whiting, K. Wafford, Mol. Pharmacol. 61 (2002) 861.
[72] T. El-Sayed Ali, Eur. J. Med. Chem. 44 (2009) 4385.
[73] L.R.S. Dias, M.B. Santos, S. de Albuquerque, H.C. Castro, A.M.T. de Souza, A.C. C. Freitas, M.A.V. DiVaio, L.M. Cabral, C.R. Rodrigues, Bioorganic Med. Chem. 15 (2007) 211.
[74] K. Chavva, S. Pillalamarri, V. Banda, S. Gautham, J. Gaddamedi, P. Yedla, C.G. Kumar, N. Banda, Bioorganic Med. Chem. Lett. 23 (2013) 5893.
[75] M.A. Gaston, L.R.S. Dias, A.C.C. Freitas, A.L.P. Miranda, E.J. Barreiro, Pharm. Acta Helv. 71 (1996) 213.
[76] F.E. Goda, A.A.M. Abdel-Aziz, O.A. Attef, Bioorganic Med. Chem. 12 (2004) 1845.
[77] P. Nagender, G. Malla Reddy, R. Naresh Kumar, Y. Poornachandra, C. Ganesh Kumar, B. Narsaiah, Bioorganic Med. Chem. Lett. 24 (2014) 2905.
[78] J. Quiroga, Y. Villareal, J. Gálvez, A. Ortíz, B. Insuasty, R. Abonia, M. Raimondi, S. Zacchino, Chem. Pharm. Bull. 65 (2017) 143.
[79] X. Wang, Y. Dong, L. Wang, S. Han, Chemosphere 44 (2001) 447.
[80] R.B. Nawale, S.S. Ashtekar, IJRPC 4 (2014) 26.
[81] J. Li, X. Tian, Y. Gao, S. Shang, J. Feng, X. Zhang, RSC Adv. 5 (2015) 66947–66955.
[82] R. González-Chávez, R. Martínez, M.E. Torre-Bouscoulet, M. Gallo, M.M. González-Chávez, Chem. Pharm. Bull. 62 (2014) 16.
[83] M.Á. Zermeño-Macías, M.M. González-Chávez, F. Méndez, R. González-Chávez, A. Richaud, Molecules 22 (2017) 427.
[84] K. Santosh, M.S. Niranjan, K.C. Chaluvaraju, C.M. Jamakhandi, K. Dayanand, J. Curr. Pharm. Res. 1 (2010) 39.
[85] N.J. Stéphane, K.M. Guy-Richard, K.C. Guillaume, A.S. Thomas, K.A. Landry Claude, O.Z. Adama, Z. Nahossé, IOSR J. Pharm. 7 (2017) 27.
[86] A. Agrawal, Int. J. Pharm. Sci. Nanotech. 4 (2011) 1394.
[87] V.R. Yadav, S. Prasad, B. Sung, B.B. Aggarwal, Int. Immunopharmacol. 11 (2011) 295.
[88] M. Pilatova, L. Varinska, P. Perjesi, M. Sarissky, L. Mirossay, P. Solar, A. Ostro, J. Mojzis, Toxicol. Int. 24 (2010) 1347.
[89] Y. Luo, R. Song, Y. Li, S. Zhang, Z.J. Liu, J. Fu, H.L. Zhu, Bioorg. Med. Chem. Lett. 22 (2012) 3039.
[90] A. Kamal, S. Prabhakar, M.J. Ramaiah, P.V. Reddy, C.R. Reddy, A. Mallareddy, N. Shankaraiah, T.L.N. Reddy, S.N.C.V.L. Pushpavalli, M. Pal-Bhadra, Eur. J. Med. Chem. 46 (2011) 3820.
[91] U.M. Kocyigit, Y. Budak, F. Eliguzel, P. Taslimi, D. Kilic, I. Gulcin, M. Ceylan, Arch. Pharm. 350 (2017) e1700198.
[92] U.M. Kocyigit, Y. Budak, M.B. Gurdere, F. Erturk, B. Yencilek, P. Taslimi, I. Gulcin, M. Ceylan, Arch. Physiol. Biochem. 124 (2018) 61.
[93] S. Burmaoglu, A.O. Yilmaz, M.F. Polat, R. Kaya, I. Gulcin, O. Algul, Bioorg. Chem. 85 (2019) 191.
[94] E. Romano, A.B. Raschi, A.M. Gonzalez, G. Jaime, M.A. Fortuna, L.R. Hernandez, H. Bach, A.M. Benavente, Plant Physiol. Biochem. 49 (2011) 671.
[95] C.S. Jeffrey, M.D. Leonard, A.E. Glassmire, C.D. Dodson, L.A. Richards, M.J. Kato, L. A. Dyer, J. Nat. Prod. 77 (2014) 148.

[96] M.A. Sanz, T. Voigt, H. Waldmann, Adv. Synth. Catal. 348 (2006) 1511.
[97] A.K. Ghosh, D.D. Anderson, Future Med. Chem. 3 (2011) 1181.
[98] C.F. Thompson, T.F. Jamison, E.N. Jacobsen, J. Am. Chem. Soc. 123 (2001) 9974.
[99] E. Otero, S. Vergara, S.M. Robledo, W. Cardona, M. Carda, I.D. Velez, C. Rojas, F. Otalvaro, Molecules 19 (2014) 13251.
[100] G. Singh, A. Arora, S.S. Mangat, S. Rani, H. Kaur, K. Goyal, R. Sehgal, I.K. Maurya, R. Tewari, D. Choquesillo-Lazarte, S. Sahoo, N. Kaur, Eur. J. Med. Chem. 108 (2016) 287.
[101] M. Mellado, L. Espinoza, A. Madrid, J. Mella, E. Chavez-Weisser, K. Diaz, M. Cuellar, Mol. Divers. 23 (2019) 1–13.
[102] K. Drlica, X.L. Zhao, Microbiol. Mol. Biol. Rev. 61 (1997) 377.
[103] H.C. Neu, Am. J. Med. America 82 (1987) 395.
[104] G. Palu, S. Valisena, G. Ciarrocchi, B. Gatto, M. Palumbo, Proc. Natl. Acad. Sci. 89 (1992) 9671.
[105] C. Sissi, M. Andreolli, V. Cecchetti, A. Fravolini, B. Gatto, M. Palumbo, Bioorg. Med. Chem. 6 (1998) 1555.
[106] I. Turel, A. Golobi, A. Klavžar, B. Pihlar, P. Buglyó, E. Tolis, et al., J. Inorg. Biochem. 95 (2003) 199.
[107] M.P. López-Gresa, R. Ortiz, L. Perelló, J. Latorre, M. Liu-González, S. García-Granda, et al., J. Inorg. Biochem. Spain 92 (2002) 65.
[108] M. Ruíz, L. Perelló, J. Server-Carrió, R. Ortiz, S. García-Granda, M.R. Díaz, et al., J. Inorg. Biochem. 69 (1998) 231.
[109] S. Deng, X. Zeng, W. Hu, X. Liu, International Conference on Biomedical Engineering and Biotechnology, 2012.
[110] F.-Y. Wu, L.-N. Zhang, Z.-J. Ji, X.-F. Wan, J. Lumin. 130 (2010) 1280.
[111] M.R. Malik, V. Vasylyeva, K. Merz, N. Metzler-Nolte, M. Saleem, S. Ali, A.A. Isab, K. S. Munawar, S. Ahmad, Inorg. Chim. Acta 376 (2011) 207.
[112] S.A. Khan, N. Singh, K. Saleem, Eur. J. Med. Chem. 43 (2008) 2272.
[113] U. El-Ayaan, J. Mol. Struct. 998 (2011) 11.
[114] S.M. Soliman, Asian J. Chem. 26 (2014) 1161.
[115] P.A. Datar, J. Comput. Med. 2014 (2014) 1–9.
[116] L. Hernández-Ochoa, C.A. Macias-Castañeda, G.V. Nevárez-Moorillón, E. Salas-Muñoz, F. Sandoval-Salas, CyTA J. Food 10 (2012) 85.
[117] S. Andrade-Ochoa, K.F. Chacón-Vargas, G.V. Nevárez-Moorillón, B.E. Rivera-Chavira, L.R. Hernández-Ochoa, Adv. Biol. Chem. 3 (2013) 480.
[118] S. Andrade-Ochoa, G.V. Nevárez-Moorillón, L.E. Sánchez-Torres, M.V. García, B.E. Sánchez-Ramírez, L.M. Rodríguez-Valdez, B.E. Rivera-Chavira, BMC Complement. Altern. Med. 15 (2015) 332.
[119] N.C. Desai, A. Dodiya, N. Shihory, J. Saudi Chem. Soc. 17 (2013) 259.
[120] K.P. Rakesh, H.M. Manukumar, D.C. Gowda, Bioorg. Med. Chem. Lett. 25 (2015) 1072.
[121] M.A. Mohamed, R.R. Ayyad, T.Z. Shawer, A.A.M. Abdel-Aziz, A.S. El-Azab, Eur. J. Med. Chem. 112 (2016) 106.
[122] A.G. Al-Sehemi, A. Irfan, S.A. Alrumman, A. El-Latif Hesham, Bull. Chem. Soc. Ethiop. 30 (2016) 307.
[123] A.G. Al-Sehemi, JKAU: Sci. 18 (2006) 47.
[124] A.G. Al-Sehemi, M.A.M. Al-Melfi, A. Irfan, Struct. Chem. 24 (2013) 499.
[125] M.K. Kathiravan, A.B. Salake, A.S. Chothe, P.B. Dudhe, R.P. Watode, M.S. Mukta, S. Gadhwe, Bioorg. Med. Chem. 20 (2012) 5678.
[126] D.J. Shrinivas, R.D. Sheshagiri, A.M. Uttam, A. Tejraj, H.K. Venkatrao, K. G. Andanappa, Mini Rev. Med. Chem. 14 (2014) 678.

[127] H. Bendaha, L. Yu, R. Touzani, R. Souane, G. Giaever, C. Nislow, C. Boone, S. El Kadiri, G.W. Brown, M. Bellaoui, Eur. J. Med. Chem. 46 (2011) 4117.
[128] K. Singh, D.P. Singh, M.S. Barwa, P. Tyagi, Y. Mirza, J. Enzyme Inhib. Med. Chem. 21 (2006) 557.
[129] B.S. Holla, K.N. Poojary, B.S. Rao, M.K. Shivananda, Eur. J. Med. Chem. 37 (2002) 511.
[130] O.A. El-Gammal, M.M. Bekheit, M. Tahoon, Spectrochim. Acta A Mol. Biomol. Spectrosc. 135 (2015) 597.
[131] J. Hurtado, L. Ibarra, D. Yepes, P. García-Huertas, M.A. Macías, O. Triana-Chavez, E. Nagles, L. Suescun, A. Muñoz-Castro, J. Mol. Struct. 1146 (2017) 365.
[132] A.-N.M.A. Alaghaz, R.A. Ammar, Eur. J. Med. Chem. 45 (2010) 1314.
[133] M.T.H. Tarafder, M.A. Ali, D.J. Wee, K. Azahari, S. Silong, K.A. Crouse, Transit. Met. Chem. 25 (2000) 456.
[134] G.G. Mohamed, M.A. Zayed, S.M. Abdallah, J. Mol. Struct. 979 (2010) 62.
[135] A.A.A. Emara, Spectrochim. Acta A Mol. Biomol. Spectrosc. 77 (2010) 117.
[136] R.A. Murcia, S.M. Leal, M.V. Roa, E. Nagles, A. Muñoz-Castro, J.J. Hurtado, Molecules 23 (2018) 2013.
[137] L. Bouarab-Chibane, V. Forquet, P. Lantéri, Y. Clément, L. Léonard-Akkari, N. Oulahal, P. Degraeve, C. Bordes, Front. Microbiol. 10 (2019) 1.
[138] P. Kumar, B. Narasimhan, D. Sharma, ARKIVOC 13 (2008) 159.
[139] G. Lin, K.K. Midha, E.M. Hawes, J. Heterocycl. Chem. 28 (1991) 215.
[140] J.N. Dominguez, S. Lopez, J. Charris, L. Iarruso, G. Lobo, A. Semenow, J.E. Olson, P. J. Rosenthal, J. Med. Chem. 40 (1997) 2726.
[141] J. Raval, K.K. Desai, ARKIVOC xiii (2005) 21.
[142] N. Motohasho, M. Kawase, S. Saito, H. Sakagami, Curr. Drug Target 1 (2000) 237.
[143] N. Motohashi, M. Kawase, S. Saito, T. Kurihara, K. Satoh, H. Nakashima, M. Premanathan, R. Arakaki, H. Sakagami, J. Molnar, Int. J. Antimicrob. Agents 14 (3) (2000) 203.
[144] M. Viveros, L. Amaral, Int. J. Antimicrob. Agents 17 (2001) 225.
[145] L. Amaral, J.E. Kristiansen, Int. J. Antimicrob. Agents 14 (2000) 173.
[146] P.A. Richter, M.P. Burk, J. Foot Surg. 31 (1992) 378.
[147] A.A. Fadda, A. Fekri and N.M. Bayoumy, RSC Adv. 5, (2015) 80844.
[148] R.N. Jones, A.L. Barry, T.L. Gavan, I.I.J.A. Washington, in: E.H. Lennette, A. Ballows, W.J. Hausler Jr., H.J. Shadomy (Eds.), Manual of Clinical Microbiology, (1972) fourth ed., American Society for Microbiology, Washington, DC, 1985.
[149] A. Verma, S.K. Saraf, Eur. J. Med. Chem. 43 (2008) 897.
[150] S.G. Alegaon, K.R. Alagawadi, Med. Chem. Res. 21 (2012) 816.
[151] M.J. Naim, M.J. Alam, S. Ahmad, F. Nawaz, N. Shrivastava, M. Sahu, O. Alam, Eur. J. Med. Chem. 129 (2017) 218.
[152] C.D. Barros, A.A. Amato, T.B. de Oliveira, K.B.R. Iannini, A.L. da Silva, T.G. da Silva, E.S. Leite, M.Z. Hernandes, M.C.A. de Lima, S.L. Galdino, Bioorg. Med. Chem. 18 (2010) 3805.
[153] L.C. Santos, F.T. Uchōa, A.R.P.A. Canas, I.A. Sousa, R.O. Moura, M.C.A. Lima, S. L. Galdino, I.R. Pitta, J. Barbe, Heterocycl. Commun. 11 (2005) 121.
[154] R. Maccari, A. del Corso, M. Giglio, R. Moschini, U. Mura, R. Ottana, Bioorg. Med. Chem. Lett. 21 (2011) 200.
[155] M.P. Anthony, J.N. Burrows, S. Duparc, J.J. Moehrle, T.N. Wells, Malar. J. 11 (2012) 316.
[156] R.K. Sharma, Y. Younis, G. Mugumbate, M. Njoroge, J. Gut, P.J. Rosenthal, K. Chibale, Eur. J. Med. Chem. 90 (2015) 507.
[157] S.K. Bharti, G. Nath, R. Tilak, S.K. Singh, Eur. J. Med. Chem. 45 (2010) 651.

[158] B.F. Abdel-Wahab, H.A. Abdel-Aziz, E.M. Ahmed, Eur. J. Med. Chem. 44 (2009) 2632.
[159] R.K.C. de Paiva, J.F. da Silva, H.A. Moreira, O.G. Pinto, L.T.F.M. Camargo, P.L. F. Naves, A.J. Camargo, L. Ribeirod, L.M. Ramos, J. Braz. Chem. Soc. 30 (2019) 164.
[160] H.M. Gilles, Management of Severe and Complicated Malaria, A Practical Handbook. World Health Organisation, Geneva (1991) pp. vi + 56 pp.
[161] C. Warhurst, J.C. Craig, I.S. Adagu, D.J. Meyer, S.Y. Lee, Malar. J. 2 (2003).
[162] J.L. Vennerstrom, H.N. Fu, W.Y. Ellis, A.L. Ager, J.K. Wood, S.L. Andersen, L. Gerena, W.K. Milhous, J. Med. Chem. 35 (1992) 3023.
[163] H. Atheaya, S.I. Khan, R. Mamgain, D.S. Rawat, Bioorg. Med. Chem. Lett. 18 (2008) 1446.
[164] G.L. Ellis, R. Amewu, C. Hall, K. Rimmer, S.A. Ward, P.M. O'Neill, Bioorg. Med. Chem. Lett. 18 (2008) 1720.
[165] N. Kumar, S.I. Khan, G. Beena Rajalakshmi, P. Kumaradhas, D.S. Rawat, Bioorg. Med. Chem. 17 (2009) 5632.
[166] F. Marti, J. Chadwick, R.K. Amewu, H. Burrell-Saward, A. Srivastava, S.A. Ward, R. Sharma, N. Berry, P.M. O'Neill, Med-Chem. Comm. 2 (2011) 661.
[167] M.C. de Paula, M.S. Valle, J.R. Pliego Jr., Med. Chem. Res. 23 (2014) 5197.
[168] H.K. Hsieh, T.H. Lee, J.P. Wang, J.J. Wang, C.N. Lin, Pharm. Res. 15 (1998) 39.
[169] L. Ni, C.Q. Meng, J.A. Sikorski, Expert Opin. Ther. Pat. 14 (2004) 1669.
[170] F. Lunardi, M. Guzela, A.T. Rodrigues, R. Correa, I. Eger-Mangrich, M. Steindel, E. C. Grisard, J. Assreuy, J.B. Calixto, A.R. Santos, Antimicrob. Agents Chemother. 47 (2003) 1449.
[171] T. Owa, T. Okauchi, K. Yoshimatsu, N.H. Sugi, Y. Ozawa, T. Nagasu, N. Koyanagi, T. Okabe, K. Kitoh, H. Yoshino, Bioorg. Med. Chem. Lett. 10 (2000) 1223.
[172] F. Uchiumi, T. Hatano, H. Ito, T. Yoshida, S.I. Tanuma, Antivir. Res. 58 (2003) 89.
[173] J.H. Wu, X.H. Wang, Y.H. Yi, K.H. Lee, Bioorg. Med. Chem. Lett. 13 (2003) 1813.
[174] G. Bhattacharya, J. Herman, D. Delfin, M.M. Salem, T. Barszcz, M. Mollet, G. Riccio, R. Brun, K.A. Werbovetz, J. Med. Chem. 47 (2004) 1823.
[175] P. Boeck, C.A.B. Falcão, P.C. Leal, R.A. Yunes, V. Cechinel Filho, V.E.C. Torres-Santos, B. Rossi-Bergmann, Bioorg. Med. Chem. 14 (2006) 1538.
[176] K. Chibale, H. Haupt, H. Kendrick, V. Yardley, A. Saravanamuthu, A.H. Fairlamb, S. L. Croft, Bioorg. Med. Chem. Lett. 11 (2001) 2655.
[177] S.F. Nielsen, T. Boesen, M. Larsen, K. Schonning, H. Kromann, Bioorg. Med. Chem. 12 (2004) 3047.
[178] C.R. Andrighetti-Fröhner, K.N. Oliveira, D. Gaspar-Silva, L.K. Pacheco, A.C. Joussef, M. Steindel, C.M.O. Simões, A.M.T. Souza, U.O. Magalhães, I.F. Afonso, C. R. Rodrigues, R.J. Nunes, H.C. Castro, Eur. J. Med. Chem. 44 (2009) 755.
[179] A.M.T. Souza, H.C. Castro, M.A. Brito, C.R. Andrighetti-Frohner, U. Magalhaes, K. N. Oliveira, D. Gaspar-Silva, L.K. Pacheco, A.C. Joussef, M. Steindel, C.M. O. Simoes, D.O. Santos, M.G. Albuquerque, C.R. Rodrigues, R.J. Nunes, Curr. Microbiol. 59 (2009) 374.
[180] J. Bradshaw, R.T. Brittain, J.W. Clitherow, M.J. Daly, D. Jack, B.J. Price, R. Stables, Br. J. Pharmacol. 66 (1979) 464P.
[181] T.O. Yellin, S.H. Buck, D.J. Gilman, D.F. Jones, J.M. Wardleworth, Life Sci. 25 (1979) 2001.
[182] R.C. Young, G.J. Durant, J.C. Emmett, C.R. Ganellin, M.J. Graham, R.C. Mitchell, H. D. Prain, M.L. Roantree, J. Med. Chem. 29 (1986).

Computational methods and tools for sustainable and green approaches in drug discovery

27

*Arindam Chatterjee**
Saint Louis University, School of Medicine, Department of Pharmacology and Physiology, St. Louis, MO, United States
*Corresponding author. e-mail address: arindam.chatterjee@health.slu.edu; chatterjee.arindam@yahoo.com

27.1 Introduction

In a recent study by Tuft's Institute to determine how much it costs to bring a drug molecule to the market, a staggering number came up [1]. It costs about 2.6 billion dollars to bring a single molecule to the market. With this increased price tag, the process of drug discovery is becoming more and more challenging and less sustainable. Modern-day drug discovery is getting challenged not only by the sustainability of the process but also by the increased requirements for the process to be more environmentally benign. Medicinal chemistry is a branch of drug discovery science which encompasses chemistry, structure-activity relationship (SAR), drug design, computational chemistry, pharmacology, and absorption, distribution, metabolism, excretion (ADME). In the preclinical drug discovery, medicinal chemistry is at the interface of multiple research-stages. Different stages include target identification, target to hit, hit to lead, lead optimization, and candidate selection. An estimate of the time and money involved in these different stages of the drug discovery processes is described in Fig. 27.1. The estimate was based on a study done in 2010 from data collected in various stages of discovery processes at Eli Lilly and Company [2].

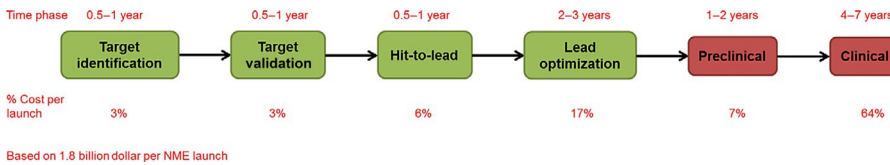

Fig. 27.1 Time required, and the money involved in each stage of a new molecular entity (NME) launch.

The complete drug discovery process is distributed in several stages to bring an NME to the market, namely, target identification, target validation, hit to lead, lead optimization, preclinical development, and clinical development [3]. The clinical part involves the most money, time, and a long elaborated process because it involves

Green Approaches in Medicinal Chemistry for Sustainable Drug Design. https://doi.org/10.1016/B978-0-12-817592-7.00027-7
© 2020 Elsevier Inc. All rights reserved.

patient dosing. It consists of the phases I, II, and III clinical trials. On the other hand, preclinical development requires intense biological, pharmacokinetic (PK), pharmacodynamics (PD), ADME, and pilot synthesis efforts. It is also associated with the correct selection of the dosage mode and parameters to determine if the drug is safe for human testing.

The remainders of the stages are the preclinical discovery research which involves medicinal chemistry. The medicinal chemistry effort takes about 3–6 years and roughly about one-third of the total cost (~29%) to bring out a new drug. The process starts with the identification of the biological target and molecule/s, which intensely involves the high-throughput biological screening of either the existing in-house or external molecular libraries. Once few target molecules are identified, different simple analogs were synthesized to validate the target/s and get template/s with a scope of patentability for the particular biological target. It was then followed by a more intense procedure of SAR effort, identification of secondary assays, in vivo testing, and ADME characterization. This stage is known as the hit to lead or identification of lead. Once a lead is identified, more intense chemistry, in vitro, in vivo biology, and ADME involvement occur. This is also a very rigorous stage associated with significant medicinal chemistry involvement. In this stage, the best candidate and backups are selected based on their in vivo efficacy, PK profiling, stability, initial safety study, and ease of scalability. Even with this elaborate effort, the failure to produce a candidate is often the case in any drug discovery program. The worst comes when a drug fails in the clinical trial. In 2008, the FDA approved 21 new drugs of which the large pharma developed only six of them. In 2009, the FDA approved 24 new drugs, and the large pharma discovered only 10. Additionally, it was estimated that one in twenty molecules that advanced to the clinic failed to advance. So with the soaring cost of bringing NME and decreased productivity measured by the lower number of drugs for the research money spent by the pharmaceutical companies raise the question of sustainability. The environmental stringency further adds to the pressure of improving research and discovery (R&D) productivity to bring in NME in lesser time and money.

One of the green approaches of increasing the R&D productivity is the introduction of computational algorithms, like QSAR, structure- and ligand-based drug discovery, virtual screening, ADME predictive tools, and statistical models like the rule of five, beyond the rule of five. With the introduction of the computational tools, the preclinical discovery time can be reduced by half and cost by one-third as described in Fig. 27.2 [1, 4, 5].

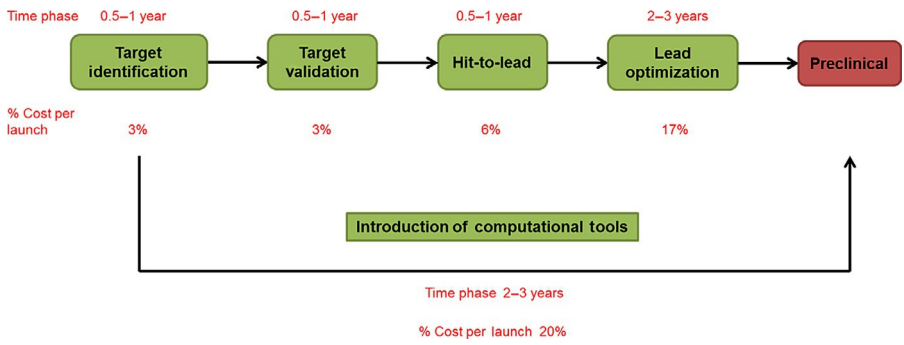

Fig. 27.2 Increased efficiency with the introduction of computational tools in early drug discovery.

SAR is a qualitative way to determine the biological activities of compounds based on the variation in their structural features. Whereas, quantitative structure-activity relationship (QSAR) [6] is a mathematical predictive model uses different parameters to speculate the biological activities of molecules based on their similarities in a structural cluster.

Structure-based drug discovery (SBDD) is the design of new drug molecules based on the crystal structure of enzyme-ligand complex [7–9]. If the X-ray structure of the target enzyme with a modulator is known, new SAR compounds can be designed using computational methods. This method of identifying and designing new drugs not only reduces the time for bringing a lead molecule but also provides a sustainable and green way of doing medicinal chemistry.

The ligand-based drug discovery approach is usually used to design SAR compounds when the X-ray structure of the receptor is unknown [10–12]. It is also known as three-dimensional (3D)-QSAR strategy. Based on a series of active ligands, SAR compounds are designed to find lead molecule.

In this modern day, the sustainable way of approaching drug discovery is the use of virtual screening strategy to find hit molecules which uses much faster and efficient techniques. Structure-based or ligand-based virtual screening is an alternate and efficient tool to the traditional high-throughput biological screening to identify hit molecule [8, 13–16]. In this paradigm, we use several efficient computational tools like metabolic, ADME, CNS permeability predictors, filters such as, ligand efficiency (LE), lipophilic ligand efficiency (LLE), rule of 5 and methods like SBDD, QSAR, and 3D QSAR to design new lead-like molecules. The main goal is to reduce the time and cost to bring new drug molecules more sustainably.

27.2 QSAR, 3D QSAR, and ligand-based drug design

QSAR is a mathematical way of finding a relationship between the variations of physicochemical properties and biological activities of molecular entities. Once a mathematical correlation is drawn, it can be used as a predictive tool for the biological activities of designed molecules to progress the course of drug discovery.

QSAR predictive design and pharmacophore approaches are the basis for making ligand-based drug discovery.

27.2.1 Why there is a need for QSAR?

Say we are planning to develop a medicinal chemistry approach of a drug containing a benzene ring. To find a potent compound, we will use 10 different substituents in three positions of the benzene ring with varied substitution pattern.

So, we have to synthesize 10^3 compounds to explore the variations.

But with the concept of QSAR, we can easily form a mathematical equation relating to the properties of the substituents and synthesize a handful of compounds. Analyze the biological activity of this small set of compounds and from this data-driven

model predict the activity of the compounds to be synthesized further to find potent compounds.

The basic steps of QSAR are as follows:

(1) Selection of the data set or the trial set which has known biological properties
(2) Finding of the structural or physicochemical parameters
(3) Variable or descriptor selection
(4) Model building
(5) Model validation
(6) Model application, prediction of the activity of the test set or predicted compound.

The concept of QSAR method was first started in the 19th century, back when Crum-Brown and Fraser postulated a relationship in 1868, correlating the physiological activities of molecules to their chemical composition [17]. The major drawback of the postulate was the lack of any quantitative representation of the structures. Later, Richardson [18], Mills [19], Richet [20], and Overton and Meyer [21, 22] also gave qualitative relationships in terms of describing physicochemical properties with biological activities.

The major breakthrough happened in the mid-1900s when Hammett postulated a quantitative equation defining linear free energy as a function of the substituent constant (σ) and rate or reaction constant (ρ), while studying the substitution effects for different meta (*m*-) and para (*p*-) substituted benzoic acids [23, 24]. In postulating the equation, he considered the effect of the substitutions on the dissociation of benzoic acid to the benzoate anion and proton. The free energy is related to the equilibrium constant as follows:

$$\Delta G = -RT \ln k$$

where

ΔG = change in Gibb's free energy for the reaction
R = universal gas constant 8.3145 J mol^{-1} K^{-1}
T = temperature in Kelvin
K = equilibrium constant.

Hammett equation is represented as follows:

$$\log \frac{K}{K^0} = \sigma\rho;$$

where

K = equilibrium constant for a substituted reactant
K^0 = equilibrium constant for the unsubstituted parent reactant.
σ (substituent constant) is a function of the substituent. It is a measure of the electronic and the inductive effects of the substituents. σ is positive for the electron-withdrawing substituents, whereas it is negative for the electron-donating substituents. It is "zero" for hydrogen by definition.
For nitro (—NO_2) group, σ is positive. Hence, it shows electron-withdrawing effect either through inductive (for *m*-) or through the combination of inductive and resonance effects (for *p*-). On the other hand, methoxy (—OCH_3) group could have both positive and negative

values. Depending on the position of the substitution, it could have electron-withdrawing inductive effect as in *m*- or electron-donating resonance effect as in *p*- substitution.
ρ (reaction constant) is a function of the nature of the reaction, temperature, and solvent.
Electron-withdrawing groups favor where $\rho > 0$
Electron-donating groups favor where $\rho < 0$
For unsubstituted benzoic acid $\rho = 1$ at 25°C and using water as the solvent.

Taft [25] was the first one who introduced the concept of steric factor (*Es*) into the equation by comparing the rate of hydrolysis of a substituted ester to that of the parent one. In his postulate, he separated the polar, steric, and resonance effects. The equation representing the steric factor (*Es*) was described as follows:

$$Es = \log k_R - \log k_0$$

where

k_R = rate of hydrolysis of a substituted ester
k_0 = rate of hydrolysis of the parent ester.

The next major contribution in the field of QSAR was by Hansch et al. with the introduction of the concept of lipophilicity or hydrophobicity in predicting the biological activity [26–28].

The term lipophilicity is defined by the affinity of a drug toward the lipid phase. It is an intrinsic property of drugs to get distributed in the lipid bilayer of different physiological environments to reach the targets like brain, gut, or tumor. It is defined by log P, where P is the partition coefficient of the drug distributed between octanol and water, where octanol represents the lipid phase.

$$P = \frac{[\text{concentration of the drug in octanol}]}{[\text{to the concentration of drug in water}]}$$

There is a linear relationship exists between the concentration and the lipophilicity. In general, higher binding to the lipid phase (octanol) is represented by increasing log *P* values. It is not feasible to determine the log *P* values of all the compounds. So the log *P* values are usually calculated computationally. The term "clog *P*" or *calculated* log *P* is used in most cases. In case for the drug molecules the term "log *D*" is used instead of log *P*, because the majority of the drug molecules contain ionizable groups. In an ideal situation, log *P* and log *D* are the same for nonionizable molecules.

The three primary physicochemical properties were used in Hansch's empirical design:

(1) Hydrophobic properties or parameters
(2) Electronic properties or parameters
(3) Steric properties or parameters.

Hansch equation is represented as follows:

$$^1/_c = k_1\pi - k_2\pi^2 + k_3\sigma + k_4E_s + k_5$$

$1/C$ = biological activity, where C = concentration of a drug for the given response
π = partition coefficient of the drug distributed between octanol and water and is the representation of the lipophilicity of the drug

σ = Hammett's substitution constant and it is a measure of the electronic effect of the substituent
Es = Taft's steric parameter
k_1, k_2, k_3, k_4, and k_5 are constants dependent on temperature and solvent.

Activity increases if the π value is positive, for hydrophobic substituents.

The activity also increases if the σ value is negative, for electron-donating groups.

Free and Wilson postulated an additive model where the biological activity was represented by the summation of the equally weighted molecular descriptors of different substituents [29].

The equation is represented as

$$\frac{1}{c} = \Sigma a_i + \mu$$

where

a_i = the activity contribution of substitution i
μ = activity of the parent molecule.

Each type of chemical group was assigned with the relative contribution to the activity depending on their type and position, e.g., *m*-, *p*- substitution.

Topliss was one of the pharmaceutical industry pioneers came up with a rational approach for QSAR. He designed a very logical approach for analog synthesis for drug design based on the electronic and hydrophobic effects of the substituents, which was known as Topliss tree approach [30]. There were two Topliss schemes, one for the aromatic substituents and one for the aliphatic substituents. This approach showed a grand promise for simple substitutions in SAR development.

The three primary statistical methods often used in the linear QSAR models are

(1) Multiple linear regression analysis (MLR) which uses multivariate linear regression to determine the drug property as the function of all the descriptors [31].
(2) Principal component analysis (PCA) is a data optimization technique utilizes the relationship among the independent variables [32].
(3) Partial least-square analysis (PLS). It is a regression method that uses the conversion of a large number of the original descriptors to orthogonal functions known as latent variables [33].

Even though there are lots of benefits of using two-dimensional (2D) QSAR for predicting biological activities of compounds, this classical QSAR approach is associated with a lot of shortcomings. The advantages of the method are relatively shorter time involved and the number of compounds to be synthesized in a SAR development.

The major sources of uncertainty of this method are the unreliability of the data, unavailability of appropriate physicochemical parameters, lack of knowledge of substituent constants beyond simple substitutions, and poor quality of the statistical method selection for model building and validation.

Overall, the classical QSAR is a good approach in predicting biological activities of molecules with simple substituents.

27.2.2 Ligand-based virtual screening

Ligand-based virtual screening is a technique where the future SAR can be developed for a biological target where no receptor crystal structure is available, but a lot of information is available for the ligands. In this approach, often a 3D QSAR method gets applied. The concept of "pharmacophore" is also critical. Since the 3D QSAR is derived from the exiting ligands from a biological target, it is somewhat limited to the similarity in structural features of the parent ligand. 3D QSAR uses the 3D structural elements of the ligands correlating with the noncovalent interactions surrounding the molecules in its model building.

The pharmacophores are defined as the descriptor of the molecular features responsible for biological activity [34, 35]. IUPAC defines pharmacophore as the additive representation of the steric and electronic effects to produce the necessary biological responses [35]. The pharmacophoric features are H-bonding, hydrophobic, and electrostatic interactions encompassing virtual points in the molecule. Say, for example, there is a phenyl ring in a molecule responsible for biological activity. The pharmacophore will not be represented by the phenyl ring but the nature of the generalized substitution pattern, that is, a hydrophobic substituent which would produce a similar effect.

Let us take an example of a CDK2 inhibitor [36] that has the following 2D structure (Fig. 27.3).

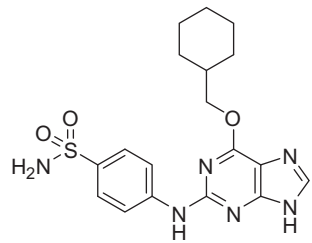

Fig. 27.3 CDK2 inhibitor [36].

The pharmacophoric representation is given in Fig. 27.4,

where H1, H2, H3, H4, and H5 are the hydrophobic substitutions; A1 is the H-bond acceptor region. In this example, the concept of pharmacophore dictates that similar hydrophobic groups can replace the purine or phenyl or the cyclohexyl rings. In addition to that, the acceptor O can be replaced by other H-bond acceptor atoms or groups.

A list of reviews describes different techniques used for developing the 3D QSAR studies over the time [10, 38–54]. Commonly used methods are comparative molecular field analysis (COMFA) [55], comparative molecular similarity indices (COMSIA) [56], genetically evolved receptor models (GERM) [57], comparative binding energy analysis (COMBINE) [58], and comparative residue interaction analysis (CORIA) [59]. All of these techniques use alignment-based methods. The result

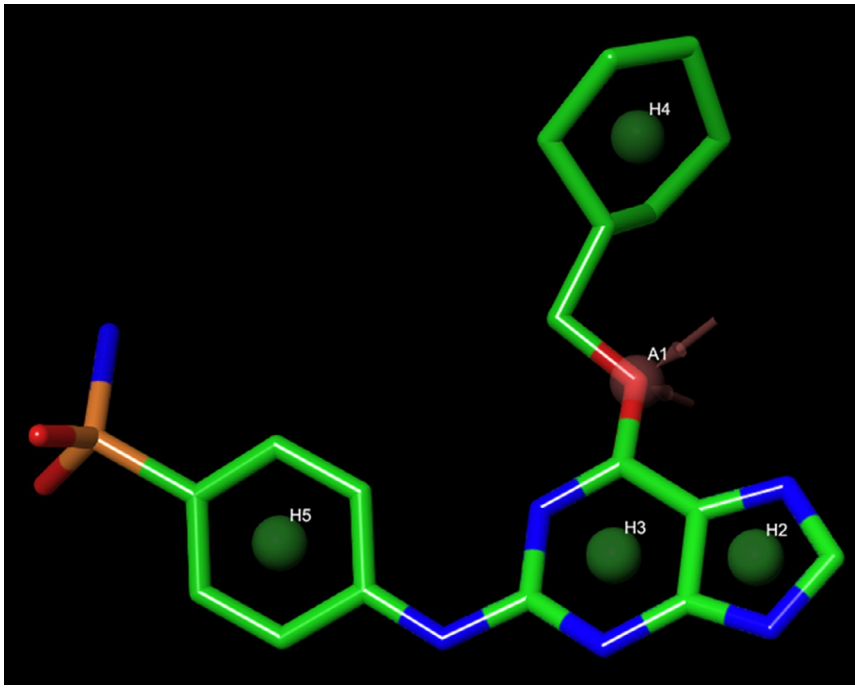

Fig. 27.4 Pharmacophoric representation of ligand for PDB ID 2C6O, generated by maestro [37].

varies depending on how the active conformations of all the molecules align to each other [60]. The problem arises from aligning highly flexible molecules.

COMFA is the most widely used methods in 3D QSAR model development. It correlates the steric and electrostatic properties the molecules to their biological activities. In this method, molecules are aligned in a 3D grid with their electrostatic and steric energies. The energies of each molecule are calculated at each grid points. Usually, the minimum energy conformers are assigned as the active conformer. With the energies of each grid points, partial least-square (PLS) statistics were used to develop the COMFA model. The effectiveness of the COMFA model in predicting activity is solely dependent on the selection of the active conformations of the molecules and proper alignment of these active conformers. The drawbacks of the COMFA methods are as follows:

(1) Flexible molecules produce poor alignments resulting in erroneous results.
(2) The energy functions do not properly accommodate hydrophobicity or H-bonding interactions.
(3) Uncertainty in the selection of trial and test sets.
(4) Practical issues with PLS.
(5) Unrealistic high values of the electrostatic and steric interactions because of the use of hyperbolic energy functions like Coulombic and Lennard-Jones potentials.
(6) Cut off values are used.

COMSIA is a similar technique as COMFA but much improved and eliminates some of its drawbacks. The major improvements can be depicted as

(1) It includes hydrophobic, H-bond donor, and acceptor interactions along with the steric and the electrostatic functions.
(2) Uses Gaussian distribution of similarity indices, which eliminates the steep slopes as in Lennard-Jones or Coulombic functions.
(3) It does not put an arbitrary cutoff limit.
(4) Similarity indices offer the molecular fields to define the ligand-binding interactions.
(5) Better accommodate flexible molecular alignments.

Some recent research on 3D QSAR studies using COMFA and COMSIA are referenced here [61–71].

Both COMFA and COMSIA are provided by Sybyl software developed by Tripos [72].

GERM is a 3D technique which incorporates the macromolecular binding site models in the absence of receptor structures. The primary requirement of this model is the presence of a chemical series with SAR with reasonable alignments. It uses a genetic algorithm to calculate the atomic-level models of the receptor site. The model shows a high level of correlation between the calculated intermolecular energies and the activities. The predicted binding energy also correlates very well with the biological activity of the test set. Genetic codes are used for each type of atoms usually found in protein structures, e.g., aliphatic or polar hydrogens, carbonyl or neutral carbon atoms, amide or amino nitrogen, etc. The energies are calculated by using Chemistry at HARvard Macromolecular Mechanics (CHARMM) force field. The model has a very high potential of successfully finding leads from a 3D-structural database. The limitation of GERM is that it considers only a single orientation of the ligand in the training set and in the binding site. Also, since the model is based on hypothetical receptors, these assumptions come with the shortcoming of the model building [73].

COMBINE is a 3D QSAR method uses structural data from the ligand-macromolecular complex. In this method, the free energy of activation is calculated by considering the ligand bound or unbound to the receptor [74]. The energies between the ligand and the receptor interactions are calculated using molecular mechanics force field. The electrostatic interactions are determined using the distance-dependent dielectric constants without assigning any arbitrary cutoff values. The limitation occurs for the prediction of the binding pattern of different ligand-receptor systems, because of the biasedness of this method to the positioning fragments to the binding sites and data-based searching. Some recent researches on 3D QSAR studies using COMBINE are referenced here [75–79].

CORIA is a 3D QSAR methodology based on the thermodynamic functions describing the ligand-receptor binding. In this method, both the qualitative and quantitative functions are included in the ligand interaction to the binding site. Initially, it was based on only the nonbonding interactions of the ligands to the different active-site residues of the receptor [59]. But later the method got expanded in two different variants, viz. reverse-CORIA (r-CORIA) and mixed-CORIA (m-CORIA). In the r-CORIA, the nonbonding interaction energies of the ligand are calculated

considering the receptor interaction as a whole, while in m-CORIA the energies are calculated considering the interaction with the individual active sites in the receptor. Some recent researches on 3D QSAR studies using CORIA are referenced here [80–82].

27.3 Structure-based drug design and virtual screening strategy

The primary requirement for a SBDD model is the presence of a defined X-ray structure of a ligand with the biological target of interest. SBDD is a well-known, green, and very effective procedure used by many in industry and academia for finding lead compounds in medicinal chemistry-driven drug discovery program [83–86]. Structure-based virtual screening strategy is often used as an alternative to the expensive and time consuming high-throughput biological screening strategies [8, 13, 87]. The computer-based drug discovery research at Merck in the early 1980s was considered as the pioneer of SBDD [88]. The popularity of this SBDD method lies to the fact that by knowing the structural information of the existing ligand-protein binding, new ligands can be easily predicted to improve the drug discovery program. The prediction can be drawn based on the known crystal structure by extracting the interaction pattern of the existing ligand to the active site of the protein and reproducing that for the new predicted ligands. The process for achieving it is called molecular docking [89]. In the structure-based virtual screening, hits can be identified from small molecules obtained from a database by docking the structures to the receptor active sites. Often this process of direct docking of small molecules to the active site to find the lead from a large database is very computer intensive and could take a month depending on the number of molecules to be docked. To avoid excessive computer time, often the ligand structure is converted to a structure-based pharmacophore model and screened through the database much quickly [90]. The pharmacophore model is described in Fig. 27.4, where the structure of the ligand from the crystal structure (PDB ID 2C6O) was converted to its pharmacophoric representation. The total process of SBDD can be represented by the following cartoon (Fig. 27.5).

The overall SBVS process is divided into three following stages:

(1) Binding site detection, protein, and ligand refinement
(2) Direct docking of ligands or shape screening for structure-based pharmacophores
(3) Analysis of the hits and identification of the lead

27.3.1 Binding site detection, protein, and ligand refinement

The binding site interaction can be determined easily if the ligand is co-crystallized with the target protein. The protein structure is then refined to eliminate the ambiguity in the binding mode. The process includes removing the nonparticipating water molecules (redundant water molecules for the protein-ligand interaction) [91], adding hydrogen atoms, setting up bond orders, and formal charges. It also selects the correct tautomeric

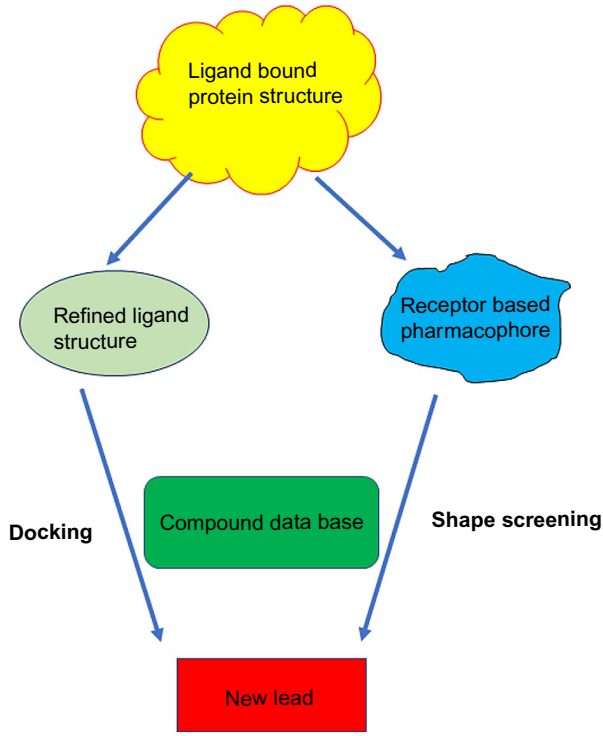

Fig. 27.5 Cartoon expressing structure-based virtual screening (SBVS).

form and the orientation of the hydroxyl or thiol groups of the protein fragments [92]. Once the protein is refined, the next is the ligand selection, and it is done from a database containing compounds. Among the common databases used for virtual screening, the most popular is the free ZINC database [93]. It contains over 120 million purchasable compounds [94]. The other data bases are ChemSpider [95], maintained by the Royal Society of Chemistry (RSC), ChemDB [96] and PubChem [97], which is maintained by the national center for biotechnology information (NCBI). Most large commercial chemical vendors also make their compound files available for virtual screening. The selected ligands are then minimized to get the lowest energy conformation and possible tautomer conformations. Once these ligand refinements are done, the next stage is finding the fit which matches the receptor interaction.

27.3.2 Direct docking

The selected ligands can be docked individually to the receptor grid to find the fit. The algorithm of the docking program has two jobs, viz. prediction of the correct binding modes of the ligands at the active site and subsequent ranking of these poses. The docking program treats the ligands flexibly, which are then minimized by three

different methods, viz., systematic methods (conformational search); random methods (Monte Carlo); and simulation methods (molecular dynamics and energy minimization) [98]. Some most commonly used docking programs are AutoDock [99], DOCK [100], Glide [101], and GOLD [102]. It is difficult to conclude which gives the best results and all can be used depending on the availability or need.

27.3.3 Structure-based pharmacophore screening

Structure-based pharmacophore modeling (SBPM) is based on identifying the complementary chemical features of the active site and their spatial relationship with the ligand. Subsequently, a pharmacophore model is generated from selected features. Here are few of the common software available commercially to generate pharmacophores—such as HipHop [103], HypoGen [104], DISCO [105], PHASE [106, 107], and MOE [108]. One of the major problems with SBPM is the generation of too many chemical features (not prioritized). Typically, a selection of three to five chemical features for virtual screening is an optimum approach. Since the purpose for SBPM-based virtual screening is to find hits with similar chemical features as the template, often the screening ends up with completely new molecular entity. But finding a *de novo* molecule might not always translate into biological activity. This is one of the major drawback of the model. But on the other hand, if the new molecular entity is active, it would produce the scope for a patentable template.

27.3.4 Analysis of the hits

In certain cases, some virtual screening ends up with a lot of hits. The introduction of various statistical methods can be used to prioritize these large number of hits. One of this method is clustering analysis with similarity search [109]. The similarity between molecular cluster often calculated using Tanimoto coefficient [110].

27.3.5 Similarity searching

Mathematically, Tanimoto coefficient can be described as follows:

The similarity between objects A and B can be described as

$$T_c(\mathrm{AB}) = \frac{c}{a+b-c}$$

where

T_c = Tanimoto coefficient between object A and B
a = number of features present in A but not in B
b = number of features present in B but not in A
c = number of features present in both.

27.3.6 Homology modeling

In certain cases, especially for the G-coupled receptor (GPCR), where there is hardly any X-ray structural information is available, a homology model can be used.

Homology model is developed by constructing an atomic-resolution model of the target protein, by comparing its protein sequence with the high-resolution X-ray structure of a homologous protein [111, 112]. The process of homology modeling is achieved through the following three steps:

- Alignment of the sequence between the target protein and an appropriate homologous protein.
- The building of homology model, refinement, and validation.
- Docking of ligands in the newly build receptor model.

Some recent studies using structure-based drug design and virtual screening are referenced here [113–133]. To elucidate several of the features of structure-based virtual screening, we will use the following example.

In our lab, we have developed a pharmacophore-based virtual screening approach to find CDK5-p25 inhibitors for Alzheimer's disease [134]. We were looking for compounds with selectivity in CDK5-p25 but not in CDK2 or other cell cycle kinases to avoid any side effects. We started with a ligand-bound crystal structure of CDK5-p25 (protein data bank or PDB ID 3O0G). The structure of the ligand is given in Fig. 27.6.

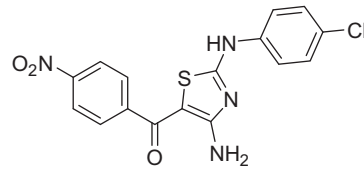

Fig. 27.6 Structure of the ligand from PDB ID 3O0G

The ligand binding in the protein space-filling structure is represented as follows (Fig. 27.7).

The overall receptor-ligand H-bonding interactions can be pictorially represented as follows.

In Fig. 27.8, the four different H-bonding interactions of the ligand with the receptor sites are shown as interactions with CYS 83, GLU 81, LYS 33, and a ternary water-mediated interaction with ASN 144. These interactions can be represented in the e-pharmacophore model, as in Fig. 27.9.

In Fig. 27.9, the maestro-generated e-pharmacophore models have two acceptor sites (A1 and A2), three donor sites (D3, D4, and D5), one hydrophobic pocket (H6), and two aromatic residues (R7 and R8). But as we were mentioning before, not all the chemical features are relevant to the H-bonding, donor, acceptor, or π stacking interactions. Selected features are used in the virtual screening workflow. The virtual screening workflow is described below.

Fig. 27.10 represents the workflow of computer-based screening strategy used in screening a database of 2.84 million compounds to end up with a hit of nine compounds. With further biological assays of these nine compounds, we were able to identify a single compound as the lead [134]. This is the shown benefit of virtual screening a huge database to come up with a lead in a short time and money with an efficient and green process.

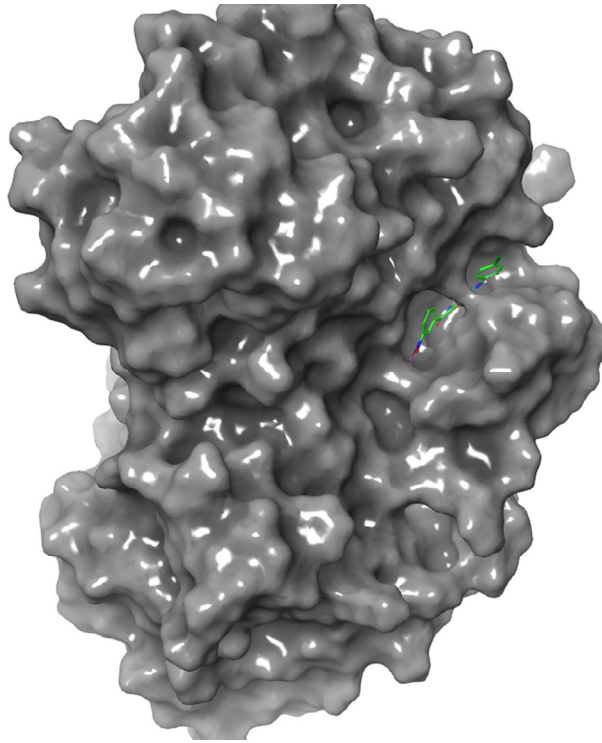

Fig. 27.7 Bound ligand in protein space-filling structure of CDK5-p25 (PDB ID 3O0G); generated by maestro [37].

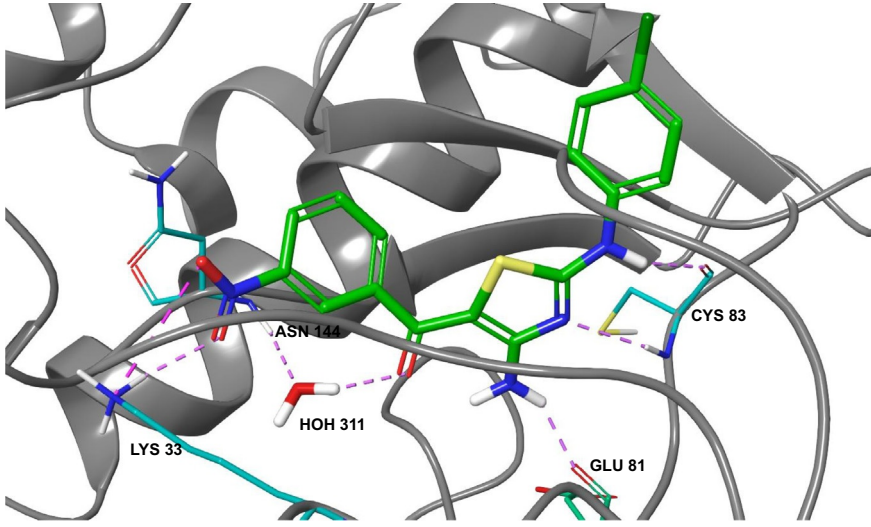

Fig. 27.8 H-bonding interaction of ligand in the active site (PDB ID 3O0G); generated by maestro [37].

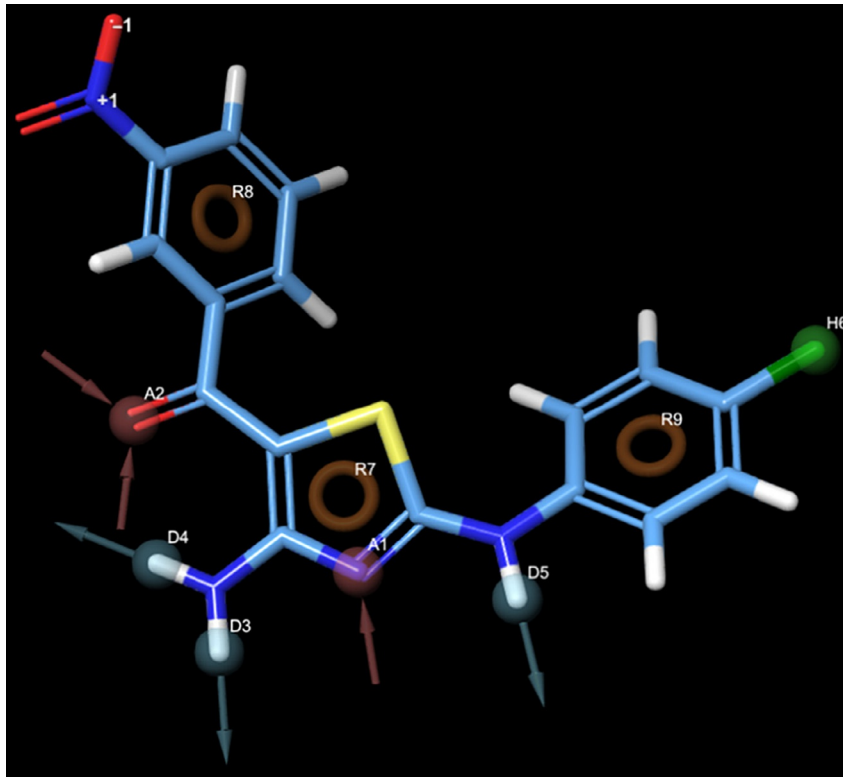

Fig. 27.9 *E*-Pharmacophore [107] representation of ligand (PDB ID 3O0G); generated by phase [106].

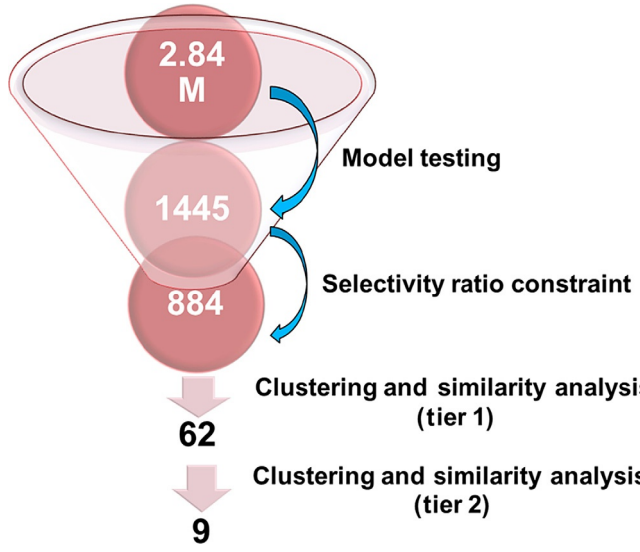

Fig. 27.10 Virtual screening workflow to identify hit [134].

27.4 Drugability

The concept of drugability or drug likeness goes back to a Pfizer scientist Cristopher Lipinski who formulated an empirical rule based on the physicochemical properties of oral drugs. The rule is known as Lipinski's rule of five [135, 136]. According to the rule, compounds will have good absorption and bioavailability, if

(1) Molecular weight is $\leq$500
(2) Log P or lipophilicity is $\leq$5
(3) Number of H-bond donor is $\leq$5
(4) Number of H-bond acceptor is $\leq$10

This concept was originally developed to predict orally active compounds but later had to be extended for central nervous system (CNS) drugs by including certain other features. For CNS drugs, blood-brain barrier (BBB) permeability is a major determinant beyond the physicochemical properties. For active CNS drugs, the standard rule of thumb is that the polar surface area (PSA) of the compound is $\leq$60–70 [137] and number of rotatable bonds $\leq$10. Two simple rules can be used to predict the physicochemical properties of CNS drugs [138].

First rule says N+ O $\leq$ 5; the molecule will have a good brain permeability.

Second rule says, log P − (N + O) = +ve; molecule will be CNS active.

There are several computational methods available to predict the CNS permeability [139].

In modern drug discovery, virtual screening techniques utilize several filters to refine the database to screen only drug-like compounds. This refinement increases the chance of getting a hit with drug-like properties. Few of the common in silico filters used for virtual screening are ADME prediction, solubility prediction, Lipinski rule of five, and BBB permeability (for CNS drugs). Two relatively newer concepts, like ligand efficiency (LE) [140, 141] and lipophilic ligand efficiency (LLE) often used in finding hit and lead molecules and in lead optimization strategies [142].

All these computational techniques described in this chapter made modern drug discovery more efficient and sustainable.

References

[1] J.A. DiMasi, H.G. Grabowski, R.W. Hansen, Innovation in the pharmaceutical industry: new estimates of R&Dcosts, J. Health Econ. 47 (2016) 20–33.
[2] S.M. Paul, D.S. Mytelka, C.T. Dunwiddie, C.C. Persinger, B.H. Munos, S.R. Lindborg, A.L. Schacht, How to improve R&D productivity: the pharmaceutical industry's grand challenge, Nat. Rev. Drug Discov. 9 (2010) 203–214.
[3] PhRMA, Biopharmaceutical R&D: The Process Behind New Medicines, 2015.
[4] www.switch-biotech.com/Drug%20Discovery.html.
[5] A. Gautam, X. Pan, The changing model of big pharma: impact of key trends, Drug Discov. Today 21 (3) (2016) 379–384.
[6] A. Cherkasov, E.N. Muratov, D. Fourches, A. Varnek, I.I. Baskin, M. Cronin, J. Dearden, P. Gramatica, Y.C. Martin, R. Todeschini, V. Consonni, V.E. Kuz'min, R. Cramer, R. Benigni, C. Yang, J. Rathman, L. Terfloth, J. Gasteiger, A. Richard, A. Tropsha, QSAR modeling: where have you been? Where are you going to? J. Med. Chem. 57 (2014) 4977–5010.

[7] A.S. Hauser, M.M. Attwood, M. Rask-Andersen, H.B. Schiöth, D.E. Gloriam, Trends in GPCR drug discovery: new agents, targets and indications, Nat. Rev. Drug Discov. 16 (2017) 829–842.
[8] E. Lionta, G. Spyrou, D.K. Vassilatis, Z. Cournia, Structure-based virtual screening for drug discovery: principles, applications and recent advances, Curr. Top. Med. Chem. 14 (2014) 1923–1938.
[9] X.-Y. Meng, H.-X. Zhang, M. Mezei, M. Cui, Molecular docking: a powerful approach for structure-based drug discovery, Curr. Comput. Aided Drug Des. 7 (2011) 146–157.
[10] C. Acharya, A. Coop, J.E. Polli, A.D. Mackerell Jr., Recent advances in ligand-based drug design: relevance and utility of the conformationally sampled pharmacophore approach, Curr. Comput. Aided Drug Des. 7 (2011) 10–22.
[11] M. Schenone, V. Dančík, B.K. Wagner, P.A. Clemons, Target identification and mechanism of action in chemical biology and drug discovery, Nat. Chem. Biol. 9 (2013) 232–240.
[12] J. Verma, V.M. Khedkar, E.C. Coutinho, 3D-QSAR in drug design—a review, Curr. Top. Med. Chem. 10 (2010) 95–115.
[13] A.D. Andricopulo, L.B. Salum, D.J. Abraham, Structure-based drug design strategies in medicinal chemistry, Curr. Top. Med. Chem. 9 (2009) 771–790.
[14] H. Geppert, M. Vogt, J. Bajorath, Current trends in ligand-based virtual screening: molecular representations, data mining methods, new application areas, and performance evaluation, J. Chem. Inf. Model. 50 (2010) 205–216.
[15] M.F.S.A. Nuno, D.G. Cerqueira, E.F. Oliveira, D. Santos-Martins, N.F. Bras, S.F. Sousa, P.A. Fernandes, M.J. Ramos, Receptor-based virtual screening protocol for drug discovery, Arch. Biochem. Biophys. 582 (2015) 56–67.
[16] P. Ripphausen, B. Nisius, J. Bajorath, State-of-the-art in ligand-based virtualscreening, Drug Discov. Today 16 (2011) 372–376.
[17] A. Crum-Brown, T.R. Fraser, On the connection between chemical constitution and physiological action. Part 1. On the physiological action of the ammonium bases, derived from Strychia, Brucia, Thebaia, Codeia, Morphia and Nicotia, Trans. R. Soc. Edinburgh 25 (1868) 151–203.
[18] B.J. Richardson, Physiological research on alcohols, Med. Times Gaz. 2 (1868) 703–706.
[19] E.J. Mills, On melting point and boiling point as related to composition, Philos. Mag. 17 (1884) 173–187.
[20] C. Richet, On the relationship between the toxicity and the physical properties of substances, C. R. Seances Soc. Biol. 9 (1893) 775–776.
[21] H. Meyer, On the theory of alcohol narcosis I. which property of anesthetics gives them their narcotic activity? Arch. Exp. Pathol. Pharmakol. 42 (1899) 109–118.
[22] E. Overton, Osmotic properties of cells in the bearing on toxicology and pharmacology, Z. Physik. Chem. 22 (1897) 189–209.
[23] L.P. Hammett, Some relations between reaction rates and equilibrium constants, Chem. Rev. 17 (1935) 125–136.
[24] L.P. Hammett, The effect of structure upon the reactions of organic compounds. Benzene derivatives, J. Am. Chem. Soc. 59 (1937) 96–103.
[25] R.W. Taft, Polar and steric substituent constants for aliphatic and o-benzoate groups from rates of esterification and hydrolysis of esters, J. Am. Chem. Soc. 74 (1952) 3120–3128.
[26] C. Hansch, Quantitative approach to biochemical structure-activity relationships, Acc. Chem. Res. 2 (1969) 232–239.
[27] C. Hansch, T. Fujita, ρ-σ-π analysis. A method for the correlation of biological activity and chemical structure, J. Am. Chem. Soc. 86 (1964) 1616–1626.
[28] C. Hansch, P.P. Maloney, T. Fujita, R.M. Muir, Correlation of biological activity of phenoxyacetic acids with hammett substituent constants and partition coefficients, Nature 194 (1962) 178–180.

[29] S.M. Free Jr., J.W. Wilson, A mathematical contribution to structure-activity studies, J. Med. Chem. 7 (1964) 395–399.
[30] J.G. Topliss, Utilization of operational schemes for analog synthesis in drug design, J. Med. Chem. 15 (1972) 1006–1011.
[31] R.A. Berk, The formalities of multiple regression, in: R.A. Berk (Ed.), Regression Analysis: A Constructive Critique, SAGE Publications Ltd, London, 2003, pp. 103–110.
[32] G.H. Dunteman, Basic concepts of principal components analysis, in: G.H. Dunteman (Ed.), Principal Components Analysis, SAGE Publications Ltd, London, 1989, pp. 15–22.
[33] S. Wold, M. Sjostrom, L. Eriksson, PLS: partial least squares projections to latent structures, in: H. Kubinyi (Ed.), 3D QSAR in Drug Design: Theory, Methods and Applications, ESCOM Science Publishers, Leiden, 1993, pp. 523–550.
[34] C. Chang, P.W. Swaan, Computational approaches to modeling drug transporters, Eur. J. Pharm. Sci. 27 (2006) 411–424.
[35] C.G. Wermuth, C.R. Ganellin, P. Lindberg, L.A. Mitscher, Glossary of terms used in medicinal chemistry (IUPAC recommendations 1998), Pure Appl. Chem. 70 (1998) 1129–1143.
[36] C.M. Richardson, D.S. Williamson, M.J. Parratt, J. Borgognoni, A.D. Cansfield, P. Dokurno, G.L. Francis, R. Howes, J.D. Moore, J.B. Murray, A. Robertson, A. E. Surgenor, C.J. Torrance, Triazolo[1,5-a]pyrimidines as novel CDK2 inhibitors: protein structure-guided design and SAR, Bioorg. Med. Chem. Lett. 16 (2006) 1353–1357.
[37] Schrödinger Release 2018-4: Maestro, Schrödinger, LLC, New York, NY, 2018.
[38] M. Arakawa, K. Hasegawa, K. Funatsu, The recent trend in QSAR modeling—variable selection and 3D-QSAR methods, Curr. Comput. Aided Drug Des. 3 (2007) 254–262.
[39] R.D. Clark, U. Norinder, Two personal perspectives on a key issue in contemporary 3D QSAR, Wiley Interdiscip. Rev. Comput. Mol. Sci. 2 (2012) 108–113.
[40] Y. Connolly Martin, 3D QSAR. Current state, scope, and limitations, in: H. Kubinyi, G. Folkers, Y.C. Martin (Eds.), 3D QSAR in Drug Design. Three-Dimensional Quantitative Structure Activity Relationships, vol. 3, Springer, 1998, pp. 3–23.
[41] G. Cruciani, E. Carosati, S. Clementi, Three-dimensional quantitative structure-property relationships, Elsevier, 2003, pp. 405–416. 8 plates.
[42] C. Fang, Z. Xiao, Receptor-based 3D-QSAR in drug design: methods and applications in kinase studies, Curr. Top. Med. Chem. 16 (2016) 1463–1477.
[43] I. Garcia, Y. Fall, G. Gomez, QSAR, docking, and CoMFA studies of GSK3 inhibitors, Curr. Pharm. Des. 16 (2010) 2666–2675.
[44] I. Garcia, Y. Fall, G. Gomez, Update of QSAR & docking studies of the GSK-3 inhibitors, Curr. Bioinform. 6 (2011) 215–232.
[45] J.C. Garro Martinez, E.G. Vega-Hissi, M.F. Andrada, M.R. Estrada, QSAR and 3D-QSAR studies applied to compounds with anticonvulsant activity, Expert Opin. Drug Discovery 10 (2015) 37–51.
[46] S.M. Green, G.R. Marshall, 3D-QSAR: a current perspective, Trends Pharmacol. Sci. 16 (1995) 285–291.
[47] T. Ginex, J. Vazquez, E. Gilbert, E. Herrero, F.J. Luque, Lipophilicity in drug design: an overview of lipophilicity descriptors in 3D-QSAR studies, Future Med. Chem. 11 (2019) 1177–1193.
[48] A. Leitao, A.D. Andricopulo, C.A. Montanari, 3D quantitative structure-activity relationships: the three-dimensional road to lead design, Curr. Methods Med. Chem. Biol. Phys. 1 (2007) 61–90.

[49] F.R. Makhouri, J.B. Ghasemi, In silico studies in drug research against neurodegenerative diseases, Curr. Neuropharmacol. 16 (2018) 664–725.
[50] G. Marzaro, A. Chilin, QSAR and 3D-QSAR models in the field of tubulin inhibitors as anticancer agents, Curr. Top. Med. Chem. 14 (2014) 2253–2262.
[51] S.Q. Pantaleao, D.G.V. Fujii, V.G. Maltarollo, D.d.C. Silva, G.H.G. Trossini, K.C. Weber, L.P.B. Scott, K.M. Honorio, The role of QSAR and virtual screening studies in type 2 diabetes drug discovery, Med. Chem. 13 (2017) 706–720.
[52] F. Prado-Prado, I. Garcia, Review of theoretical studies for prediction of neurodegenerative inhibitors, Mini-Rev. Med. Chem. 12 (2012) 452–466.
[53] S. Sen, N.A. Farooqui, T.S. Easwari, B. Roy, CoMFA -3D QSAR approach in drug design, Int. J. Res. Dev. Pharm. Life Sci. 1 (2012) 167–175.
[54] C. Silipo, A. Vittoria, Three-dimensional structure of drugs, in: C.A. Ramsden (Ed.), Quantitative Drug Design, vol. 4, Pergamon Press, Oxford, 1990, pp. 153–204.
[55] R.D. Cramer, D.E. Patterson, J.D. Bunce, Comparative molecular-field analysis (Comfa). 1. Effect of shape on binding of steroids to carrier proteins, J. Am. Chem. Soc. 110 (1988) 5959–5967.
[56] G. Klebe, U. Abraham, T. Mietzner, Molecular similarity indices in a comparative analysis (CoMSIA) of drug molecules to correlate and predict their biological activity, J. Med. Chem. 37 (1994) 4130–4146.
[57] D.E. Walters, R.M. Hinds, Genetically evolved receptor models: a computational approach to construction of receptor models, J. Med. Chem. 37 (1994) 2527–2536.
[58] A.R. Ortiz, M.T. Pisabarro, F. Gago, R.C. Wade, Prediction of drug binding affinities by comparative binding energy analysis, J. Med. Chem. 38 (1995) 2681–2691.
[59] P.A. Datar, S.A. Khedkar, A.K. Malde, E.C. Coutinho, Comparative residue interaction analysis (CoRIA): a 3D-QSAR approach to explore the binding contributions of active site residues with ligands, J. Comput. Aided Mol. Des. 20 (2006) 343–360.
[60] M. Akamatsu, Current state and perspectives of 3D-QSAR, Curr. Top. Med. Chem. 2 (2002) 1381–1394.
[61] M. Atabati, S. Sharifi, 3D-QSAR study on VEGFR kinase inhibition of aminopyrazolopyridine urea derivatives by CoMFA and CoMSIA, Med. Chem. Res. 23 (2014) 3539–3545.
[62] E. Hernandez-Vazquez, O. Mendez-Lucio, F. Hernandez-Luis, Activity landscape analysis, CoMFA and CoMSIA studies of pyrazole CB1 antagonists, Med. Chem. Res. 22 (2013) 4133–4145.
[63] S.V. Jain, M. Ghate, Atom-based pharmacophore modeling, CoMFA/CoMSIA-based 3D-QSAR studies and lead optimization of DPP-4 inhibitors for the treatment of type 2 diabetes, Med. Chem. Res. 23 (2014) 3436–3450.
[64] H.-C. Liu, S.-Z. Tang, S. Lu, T. Ran, J. Wang, Y.-M. Zhang, A.-Y. Xu, T. Lu, Y.-D. Chen, Studies on [5,6]-fused bicyclic scaffolds derivatives as potent dual B-RafV600E/KDR inhibitors using docking and 3D-QSAR approaches, Int. J. Mol. Sci. 16 (2015) 24451–24474.
[65] I. Mitra, A. Saha, K. Roy, Development of multiple QSAR models for consensus predictions and unified mechanistic interpretations of the free-radical scavenging activities of chromone derivatives, J. Mol. Model. 18 (2012) 1819–1840.
[66] C. Pan, H. Meng, S. Zhang, Z. Zuo, Y. Shen, L. Wang, K.-J. Chang, Homology modeling and 3D-QSAR study of benzhydrylpiperazine δ opioid receptor agonists, Comput. Biol. Chem. 83 (2019), 107109.
[67] P. Parikh, M. Ghate, V.K. Vyas, CoMFA and CoMSIA studies on 6,7-disubstituted-4-phenoxyquinoline derivatives as c-met kinase inhibitors and anticancer agents, Med. Chem. Res. 24 (2015) 4078–4092.

[68] J. Romero-Parra, H. Chung, R.A. Tapia, M. Faundez, C. Morales-Verdejo, M. Lorca, C.F. Lagos, V. Di Marzo, C. David Pessoa-Mahana, J. Mella, Combined CoMFA and CoMSIA 3D-QSAR study of benzimidazole and benzothiophene derivatives with selective affinity for the CB2 cannabinoid receptor, Eur. J. Pharm. Sci. 101 (1–10) (2017).
[69] O.A. Santos-Filho, D. Forge, L.V.B. Hoelz, G.B.L. Freitas, T.O. Marinho, J.Q. Araujo, M.G. Albuquerque, R.B. Alencastro, N. Boechat, CoMFA/CoMSIA 3D-QSAR of pyrimidine inhibitors of Pneumocystis carinii dihydrofolate reductase, J. Mol. Model. 18 (2012) 4061–4072.
[70] M. Singh, S.K. Singh, M.T. Chhabria, K. Vasu, D. Pandya, CoMFA and CoMSIA 3D QSAR models for a series of some condensed thieno[2,3-d]pyrimidin-4(3H)-ones with antihistaminic (H1) activity, Med. Chem. 9 (2013) 389–401.
[71] V.N. Telvekar, H.K. Chaudhari, 3D-QSAR and docking-based combined in silico study on C-5 methyl substituted 4-arylthio and 4-aryloxy-3-iodopyridin-2-(1H)-one as HIV-1 RT inhibitors, Med. Chem. Res. 21 (2012) 2032–2043.
[72] SYBYL 8.1, Tripos International, St. Louis, USA, 2009.
[73] D.E. Walters, T.D. Muhammad, Genetically evolved receptor models (GERM): a procedure for construction of atomic-level receptor site models in the absence of a receptor crystal structure, in: J. Devillers (Ed.), Genetic Algorithms in Molecular Modeling, Academic Press, London, 1996, pp. 193–210.
[74] G.H. Lushington, J.X. Guo, J.L. Wang, Whither combine? New opportunities for receptor-based QSAR, Curr. Med. Chem. 14 (2007) 1863–1877.
[75] D. Dai, L. Zhou, X. Zhu, R. You, L. Zhong, Combined multi-pharmacophore, molecular docking and molecular dynamic study for discovery of promising MTH1 inhibitors, J. Mol. Struct. 1137 (2017) 33–42.
[76] M.-h. Kim, J.Y. Chung, J.-S. Ryu, J.-M. Hah, Structure tuning of pyrazolylpyrrole derivatives as ERK inhibitors utilizing dual tools; 3D-QSAR and side-chain hopping, Bioorg. Med. Chem. Lett. 21 (2011) 4900–4904.
[77] P. Kumar Ojha, I. Mitra, S. Kar, R. Narayan Das, K. Roy, Lead hopping for PfDHODH inhibitors as antimalarials based on pharmacophore mapping, molecular docking and comparative binding energy analysis (COMBINE): a three-layered virtual screening approach, Mol. Inform. 31 (2012) 711–718.
[78] S. Nakamura, R. Ohmura, I. Nakanishi, An interaction-based approach for affinity prediction between antigen peptide and human leukocyte antigen using COMBINE analysis, Chem-Bio Inform. J. 17 (2017) 93–102.
[79] A. Weber, M. Boehm, C.T. Supuran, A. Scozzafava, C.A. Sotriffer, G. Klebe, 3D QSAR selectivity analyses of carbonic anhydrase inhibitors: insights for the Design of Isozyme Selective Inhibitors, J. Chem. Inf. Model. 46 (2006) 2737–2760.
[80] P.K. Ambre, R.R.S. Pissurlenkar, E.C. Coutinho, R.P. Iyer, Identification of new checkpoint kinase-1 (Chk1) inhibitors by docking, 3D-QSAR, and pharmacophore-modeling methods, Can. J. Chem. 90 (2012) 675–692.
[81] V.M. Khedkar, E.C. Coutinho, CoRILISA: a local similarity based receptor dependent QSAR method, J. Chem. Inf. Model. 55 (2015) 194–205.
[82] V.M. Khedkar, J. Joseph, R. Pissurlenkar, A. Saran, E.C. Coutinho, How good are ensembles in improving QSAR models? The case with eCoRIA, J. Biomol. Struct. Dyn. 33 (2015) 749–769.
[83] N. Drinkwater, S. McGowan, From crystal to compound: structure-based antimalarial drug discovery, Biochem. J. 461 (2014) 349–369.

[84] W. Feinstein, M. Brylinski, Structure-based drug discovery accelerated by many-Core devices, Curr. Drug Targets 17 (2016) 1595–1609.
[85] A. Gaurav, V. Gautam, Structure-based three-dimensional pharmacophores as an alternative to traditional methodologies, J. Recept. Ligand Channel Res. 7 (2014) 27–38.
[86] C.T. Supuran, Advances in structure-based drug discovery of carbonic anhydrase inhibitors, Expert Opin. Drug Discov. 12 (2017) 61–88.
[87] P.D. Lyne, Structure-based virtual screening: an overview, Drug Discov. Today 7 (2002) 1047–1055.
[88] J.H.V. Drie, Computer-aided drug design: the next 20 years, J. Comput. Aided Mol. Des. 21 (2007) 591–601.
[89] G.M. Morris, M. Lim-Wilby, Molecular docking, in: A. Kukol (Ed.), Molecular Modeling of Proteins. Methods Molecular Biology, Humana Press, 2008, pp. 365–382.
[90] S. Pirhadi, F. Shiri, J.B. Ghasemi, Methods and applications of structure based Pharmacophores in drug discovery, Curr. Top. Med. Chem. 13 (2013) 1036–1047.
[91] B.C. Roberts, R.L. Mancera, Ligand – protein docking with water molecules, J. Chem. Inf. Model. 48 (2008) 397–408.
[92] G.M. Sastry, M. Adzhigirey, T. Day, R. Annabhimoju, W. Sherman, Protein and ligand preparation: parameters, protocols, and influence on virtual screening enrichments, J. Comput. Aided Mol. Des. 27 (2013) 123–124.
[93] J.J. Irwin, T. Sterling, M.M. Mysinger, E.S. Bolstad, R.G. Coleman, ZINC: A free tool to discover chemistry for biology, J. Chem. Inf. Model. 52 (2012) 1757–1768.
[94] T. Sterling, J.J. Irwin, ZINC 15—ligand discovery for everyone, J. Chem. Inf. Model. 55 (2015) 2324–2337.
[95] H.E. Pence, A. Williams, ChemSpider: an online chemical information resource, J. Chem. Educ. 87 (2010) 1123–1124.
[96] J. Chen, S.J. Swamidass, J. Bruand, P. Baldi, ChemDB: a public database of small molecules and related chemoinformatics resources, Bioinformatics 21 (2005) 4133–4139.
[97] E.E. Bolton, Y. Wang, P.A. Thiessen, S.H. Bryant, Chapter 12—PubChem: Integrated platform of Small molecules and biological activities, Annu. Rep. Comput. Chem. 4 (2008) 217–241.
[98] G.L. Warren, C.W. Andrews, A.M. Capelli, B. Clarke, J. LaLonde, M.H. Lambert, M. Lindvall, N. Nevins, S.F. Semus, S. Senger, G. Tedesco, I.D. Wall, J.M. Woolven, C.E. Peishoff, M.S. Head, A critical assessment of docking programs and scoring functions, J. Med. Chem. 49 (2006) 5912–5931.
[99] R.T. Kroemer, Structure-based drug design: docking and scoring, Curr. Protein Pept. Sci. 8 (2007) 312–328.
[100] P.T. Lang, S.R. Brozell, S. Mukherjee, E.F. Pettersen, E.C. Meng, V. Thomas, R.C. Rizzo, D.A. Case, T.L. James, I.D. Kuntz, DOCK 6: combining techniques to model RNA–small molecule complexes, RNA 15 (2009) 1219–1230.
[101] R.A. Friesner, J.L. Banks, R.B. Murphy, T.A. Halgren, J.J. Klicic, D.T. Mainz, M.P. Repasky, E.H. Knoll, M. Shelley, J.K. Perry, D.E. Shaw, P. Francis, P.S. Shenkin, Glide: a new approach for rapid, accurate docking and scoring. 1. Method and assessment of docking accuracy, J. Med. Chem. 47 (2004) 1739–1749.
[102] M.L. Verdonk, J.C. Cole, M.J. Hartshorn, C.W. Murray, R.D. Taylor, Improved protein–ligand docking using GOLD, Proteins 52 (2003) 609–623.
[103] D. Barnum, J. Greene, A. Smellie, P. Sprague, Identification of common functional configurations among molecules, J. Chem. Inf. Comput. Sci. 36 (1996) 563–571.
[104] http://accelrys.com/products/datasheets/discovery-studio-overview.pdf.

[105] Y.C. Martin, DISCO: what we did right and what we missed, in: O.F. Güner (Ed.), Pharmacophore Perception, Development, and Use in Drug Design, International University Line, 2000, pp. 49–68.
[106] Schrödinger Release 2018-4: Phase, Schrödinger, LLC, New York, NY, 2018.
[107] N.K. Salam, R. Nuti, W. Sherman, Novel method for generating structure-based pharmacophores using energetic Analysis, J. Chem. Inf. Model. 49 (2009) 2356–2368.
[108] S. Vilar, G. Cozza, S. Moro, Medicinal chemistry and the molecular operating environment (MOE): application of QSAR and molecular docking to drug discovery, Curr. Top. Med. Chem. 8 (2008) 1555–1572.
[109] H. Kubinyi, Similarity and dissimilarity: a medicinal Chemist's view, Perspect. Drug Discov. Des. 9 (1998) 225–252.
[110] D. Bajusz, A. Rácz, K. Héberger, Why is Tanimoto index an appropriate choice for fingerprint-based similarity calculations? J. Cheminform. 7 (2015) 20.
[111] C.S. Tautermann, D.E. Gloriam, Editorial overview: new technologies: GPCR drug design and function-exploiting the current (of) structures, Curr. Opin. Pharmacol. 30 (8–10) (2016).
[112] M.A. Martí-Renom, A.C. Stuart, A. Fiser, R. Sánchez, F. Melo, A. Šali, Comparative protein structure modeling of genes and genomes, Annu. Rev. Biophys. Biomol. Struct. 29 (1) (2000) 291–325.
[113] N. Atatreh, S. Al Rawashdah, S.S. Al Neyadi, S.M. Abuhamdah, M.A. Ghattas, Discovery of new butyrylcholinesterase inhibitors via structure-based virtual screening, J. Enzyme Inhib. Med. Chem. 34 (2019) 1373–1379.
[114] E.F. Castro, J.J. Casal, M.J.E. de Marco, L. Battini, M. Fabiani, G.A. Fernandez, A.M. Bruno, L.V. Cavallaro, M. Bollini, Identification of potent bovine viral diarrhea virus inhibitors by a structure-based virtual screening approach, Bioorg. Med. Chem. Lett. 29 (2019) 262–266.
[115] R. Dash, M. Junaid, S. Mitra, M. Arifuzzaman, S.M.Z. Hosen, Structure-based identification of potent VEGFR-2 inhibitors from in vivo metabolites of a herbal ingredient, J. Mol. Model. 25 (2019) 1–15.
[116] X. Dou, H. Huang, Y. Li, L. Jiang, Y. Wang, H. Jin, N. Jiao, L. Zhang, L. Zhang, Z. Liu, Multistage screening reveals 3-substituted Indolin-2-one derivatives as novel and isoform-selective c-Jun N-terminal kinase 3 (JNK3) inhibitors: implications to drug discovery for potential treatment of neurodegenerative diseases, J. Med. Chem. 62 (2019) 6645–6664.
[117] M.A. Ghattas, N.A. Eissa, F. Tessaro, R. Perozzo, L. Scapozza, D. Obaid, N. Atatreh, Structure-based drug design and in vitro testing reveal new inhibitors of enoyl-acyl carrier protein reductases, Chem. Biol. Drug Des. 94 (2019) 1545–1555.
[118] X. Hu, Y.-Q. Zhang, O.W. Lee, L. Liu, M. Tang, K. Lai, M.B. Boxer, M.D. Hall, M. Shen, Discovery of novel inhibitors of human galactokinase by virtual screening, J. Comput. Aided Mol. Des. 33 (2019) 405–417.
[119] S. Huang, X. Wang, G. Lin, J. Cheng, X. Chen, W. Sun, R. Xiang, Y. Yu, L. Li, S. Yang, Discovery of human TyrRS inhibitors by structure-based virtual screening, structural optimization, and bioassays, RSC Adv. 9 (2019) 9323–9330.
[120] C.-S. Jiang, Y.-X. Ge, Z.-Q. Cheng, J.-L. Song, Y.-Y. Wang, K. Zhu, H. Zhang, Discovery of new multifunctional selective acetylcholinesterase inhibitors: structure-based virtual screening and biological evaluation, J. Comput. Aided Mol. Des. 33 (2019) 521–530.
[121] M. Jiang, L. Peng, K. Yang, T. Wang, X. Yan, T. Jiang, J. Xu, J. Qi, H. Zhou, N. Qian, Q. Zhou, B. Chen, X. Xu, L. Deng, C. Yang, Development of small-molecules targeting

receptor activator of nuclear factor-κB ligand (RANKL)-receptor activator of nuclear factor-κB (RANK) protein-protein interaction by structure-based virtual screening and hit optimization, J. Med. Chem. 62 (2019) 5370–5381.
[122] A.F. Kassem, E.M.H. Abbas, D.S. El-Kady, H.M. Awad, W.A. El-Sayed, Design, synthesis and anticancer activity of new Thiazole-Tetrazole or Triazole hybrid glycosides targeting CDK-2 via structure-based virtual screening, Mini Rev. Med. Chem. 19 (2019) 933–948.
[123] A.C. Kaushik, S. Kumar, D.Q. Wei, S. Sahi, Structure based virtual screening studies to identify novel potential compounds for GPR142 and their relative dynamic analysis for study of type 2 diabetes, Front. Chem. 6 (2018) 23/1–23/14.
[124] S.U. Khan, N. Ahemad, L.-H. Chuah, R. Naidu, T.T. Htar, Sequential ligand- and structure-based virtual screening approach for the identification of potential G protein-coupled estrogen receptor-1 (GPER-1) modulators, RSC Adv. 9 (2019) 2525–2538.
[125] A. Kumar, E. Rathi, S.G. Kini, E-pharmacophore modelling, virtual screening, molecular dynamics simulations and in-silico ADME analysis for identification of potential E6 inhibitors against cervical cancer, J. Mol. Struct. 1189 (2019) 299–306.
[126] A.F. Macarini, T.U.C. Sobrinho, G.W. Rizzi, R. Correa, Pyrazole-chalcone derivatives as selective COX-2 inhibitors: design, virtual screening, and in vitro analysis, Med. Chem. Res. 28 (2019) 1235–1245.
[127] M. Quintana, A. Bilbao, J. Comas-Barcelo, J. Bujons, G. Triola, Identification of benzo [cd]indol-2(1H)-ones as novel Atg4B inhibitors via a structure-based virtual screening and a novel AlphaScreen assay, Eur. J. Med. Chem. 178 (2019) 648–666.
[128] M.M. Rahman, M.B. Hosen, M. Zakir Hossain Howlader, Y. Kabir, Lead molecule prediction and characterization for designing MERS-CoV 3C-like protease inhibitors: an in silico approach, Curr. Comput. Aided Drug Des. (15) (2019) 82–88.
[129] M. Rambabu, S. Jayanthi, Virtual screening of National Cancer Institute database for claudin-4 inhibitors: synthesis, biological evaluation, and molecular dynamics studies, J. Cell. Biochem. 120 (2019) 8588–8600.
[130] K. Sharma, K. Patidar, M.A. Ali, P. Patil, H. Goud, T. Hussain, A. Nayarisseri, S.K. Singh, Structure-based virtual screening for the identification of high affinity compounds as potent VEGFR2 inhibitors for the treatment of renal cell carcinoma, Curr. Top. Med. Chem. 18 (2018) 2174–2185.
[131] S. Singh, G. Khare, R.K. Bahal, P.C. Ghosh, A.K. Tyagi, Identification of *Mycobacterium tuberculosis* BioA inhibitors by using structure-based virtual screening, Drug Des. Dev. Ther. 12 (2018) 1065–1079.
[132] Y. Wang, X. Dou, L. Jiang, H. Jin, L. Zhang, L. Zhang, Z. Liu, Discovery of novel glycogen synthase kinase-3α inhibitors: Structure-based virtual screening, preliminary SAR and biological evaluation for treatment of acute myeloid leukemia, Eur. J. Med. Chem. 171 (2019) 221–234.
[133] B. Waszkowycz, K.M. Smith, A.E. McGonagle, A.M. Jordan, B. Acton, E.E. Fairweather, L.A. Griffiths, N.M. Hamilton, N.S. Hamilton, J.R. Hitchin, C.P. Hutton, D.I. James, C.D. Jones, S. Jones, D.P. Mould, H.F. Small, A.I.J. Stowell, J.A. Tucker, I.D. Waddell, D.J. Ogilvie, Cell-active Small molecule inhibitors of the DNA-damage repair enzyme poly(ADP-ribose) Glycohydrolase (PARG): discovery and optimization of orally bioavailable Quinazolinedione sulfonamides, J. Med. Chem. 61 (2018) 10767–10792.
[134] A. Chatterjee, S.J. Cutler, R.J. Doerksen, I.A. Khan, J.S. Williamson, Discovery of thienoquinolone derivatives as selective and ATP non-competitive CDK5/p25 inhibitors by structure-based virtual screening, Bioorg. Med. Chem. 22 (2014) 6409–6421.

[135] C.A. Lipinski, Lead- and drug-like compounds: the rule-of-five revolution, Drug Discov. Today Technol. 1 (2004) 337–341.
[136] C.A. Lipinski, F. Lombardo, B.W. Dominy, P.J. Feeney, Experimental and computational approaches to estimate solubility and permeability in drug discovery and development settings, Adv. Drug Deliv. Rev. 23 (1997) 3–25.
[137] J. Kelder, P.D.J. Grootenhuis, D.M. Bayada, L.P.C. Delbressine, J.-P. Ploemen, Polar molecular surface as a dominating determinant for oral absorption and brain penetration of drugs, Pharm. Res. 1514–1519 (1999) 1514–1519.
[138] U. Norinder, M. Haeberlein, Computational approaches to the prediction of the blood–brain distribution, Adv. Drug Deliv. Rev. 54 (2002) 291–313.
[139] G.F. Ecker, C.R. Noe, In silico prediction models for blood–brain barrier permeation, Curr. Med. Chem. 11 (2004) 1617–1628.
[140] C. Abad-Zapatero, J.T. Metz, Ligand efficiency indices as guideposts for drug discovery, Drug Discov. Today 10 (2005) 464–469.
[141] I.D. Kuntz, K. Chen, K.A. Sharp, P.A. Kollman, The maximal affinity of ligands, Proc. Natl. Acad. Sci. 96 (1999) 9997–10002.
[142] P.D. Leeson, B. Springthorpe, The influence of drug-like concepts on decision-making in medicinal chemistry, Nat. Rev. Drug Discov. 6 (2007) 881–890.

Index

Note: Page numbers followed by *f* indicate figures, *t* indicate tables, and *s* indicate schemes.

B

N

Q

R

S

T

Advances in **Green and Sustainable Chemistry**

Green Approaches in Medicinal Chemistry for Sustainable Drug Design

Edited by Bimal Krishna Banik

A guide to understanding and implementing effective green medicinal chemistry for improved sustainability in the drug discovery process

Extensive experimentation and high failure rates are a well-recognized downside to the drug discovery process, with the resultant high levels of inefficiency and waste producing a negative environmental impact. ***Green Approaches in Medicinal Chemistry for Sustainable Drug Design*** reveals how medicinal chemistry can play a direct role in addressing this issue. After providing essential context to the growth of green chemistry in relation to drug discovery, the book goes on to identify a broad range of practical techniques and useful insights, revealing how medicinal chemistry techniques can be used to improve efficiency, mitigate failure and increase the environmental benignity of the entire drug discovery process.

Drawing on the knowledge of a global team of experts, ***Green Approaches in Medicinal Chemistry for Sustainable Drug Design*** encourages the growth of green medicinal chemistry, and supports medicinal chemists, drug discovery researchers, organic chemists, pharmacologists and all those in related fields across both academia and industry in integrating these approaches into their own work.

Key Features

- Highlights the need for adoption of sustainable and green chemistry pathways in drug development
- Reveals risk factors associated with the drug development process and the ways sustainable approaches can help address these
- Identifies novel and cost effective green medicinal chemistry approaches for improved efficiency and sustainability

Bimal Krishna Banik a Professor and Senior Researcher in the Department of Mathematics and Natural Sciences at Prince Mohammad Bin Fahd University, Kingdom of Saudi Arabia. In addition to receiving awards and recognitions for his work, Professor Banik has been awarded $7.25 million in grants from the US National Institutes of Health, US National Cancer Institute, and Kleberg Foundation. He has more than 400 publications to his name, and has held positions as editorial board member, editor-in-chief, associate editor and guest editor for internationally renowned journals. Furthermore, Professor Banik has presided over research sessions at top conferences, including at the Nobel Prize celebration in Germany.

ISBN 978-0-12-817592-7

9 780128 175927

ELSEVIER elsevier.com/books-and-journals